Neven Kresic

Hydrogeology 101

Introduction to Groundwater Science and Engineering

Hydrogeology 101

Introduction to Groundwater
Science and Engineering

Neven Kresic

BLUERIDGE Press

Hydrogeology 101
Introduction to Groundwater Science and Engineering

Front cover photo credit: Dinko Stopić, Speleological Club Karlovac, Croatia
Back cover photo credits: Late Dr. Gerald Seaburn, David Rhea, Global Underwater Explorers, Vojislav Ilić; Chris Legg, Branimir Jukić, Neven Kresic. Captions for all photos are provided in the text.

Foreword

This textbook was developed for an undergraduate level academic course in hydrogeology (also known as groundwater hydrology, geohydrology, and groundwater engineering) with two main goals in mind:

(1) To make it widely available, and free of charge. Many similar textbooks are often quite expensive, making them unaffordable for many students. The pdf file of the book is free for downloading, posting, and re-posting on any non-commercial, non-profit sites including all educational and academic institutions for use by their students.

(2) The second goal is to present this fascinating topic of groundwater science and engineering in sixteen manageable lectures (the duration of a typical one- to two-semester course at American universities), in a manner that will, hopefully, make it attractive to students wishing to continue onto higher-level or graduate courses such as Hydrogeology 505, or Groundwater Modeling.

The Hydrogeology 101 textbook is not overwhelmed by "heavy" differential equations which are typically crammed into classic hydrogeology books. These complicated equations sometimes overshadow the essential practical aspects of hydrogeology, including those that most if not all hydrogeologists will face at the beginning of their careers. At the same time, this textbook does introduce quantitative solutions to most common problems hydrogeologists will typically face throughout their professional life.

More complex quantitative problems described by differential equations including their step-by-step analytical solutions are presented in the advanced textbooks such as *Hydrogeology and Groundwater Modeling, Second Edition* by Neven Kresic (2007; CRC, Taylor & Francis Group). This textbook, and *Hydrogeological Conceptual Models: Data Analysis and Visualization* by Neven Kresic and Alex Mikszewski (2013; CRC, Taylor & Francis Group), also include practical applications of various groundwater-related computer programs (models) that are widely available today, user-friendly, and more efficient than most manual solutions of complex differential-equation problems which abound in theoretical hydrogeology textbooks. A typical example that comes to mind is designing a well field for water supply located near a large river. Calculating feasible and/or sustainable pumping rates at multiple wells, or influence of their combined pumping on the river (and vice-versa, i.e., groundwater – surface water interactions) would not be practicable or reasonably accurate without the use of a numeric groundwater flow model. In other words, analytical calculations and methods of classical hydrogeology would not suffice in this and many other cases from practice.

I am indebted to my colleagues and friends for many useful suggestions and review of the presented materials, and especially for the excellent color photographs without which this book would be just another "dry" thick textbook: Zoran Stevanović, Jeff Manuszak, Nick McMillan, Alex Mikszewski, Peter Thompson, Nenad Marić, Phil Lucas, William Bill Jones, John Ackerman, Timothy Bechtel, Ted Wilson, Mark Bauer, Dawit Yifru, Chris Legg, James Brode, Adrian Ezeagy, Gregg Eckhardt, Dinko Stopić, Avi Burg, Doron Nissim, Mohamed Chebaane. Vojislav Ilić, Qiang Wu, Francis Sowers, who kindly granted me use of photos by the late Georgia Institute of Technology Professor George Sowers, and many others.

The Author
Warrenton, Virginia

Dedicated to all my students, and my mentors, colleagues, and professors: Dr. William Back, Phillip LaMoreaux, Roger Pennifill, Dr. Gerald Seaburn, Dr. James Wallace, Larry Neal, Leonard Ledbetter, Robert Masters, Daniel Grogan, Dr. Michael Kavanaugh, Dr. Dragoljub Zogović, Vladimir Filipovski, Prof. Dr. Budimir Filipović, Prof. Dr. Nadežda Dimitrijević, Prof. Dr. Milorad Marković, and Prof. Dr. Radmila Pavlović.

About The Author

Neven Kresic, Ph.D., P.G. is an independent groundwater consultant with more than 40 years of experience focused on groundwater and surface water consulting, research, and teaching. He specializes in characterizing and analyzing complex groundwater systems for water supply and groundwater remediation projects and is an expert in the application of numerical models for simulating groundwater flow, and contaminant fate and transport in groundwater. Over the course of his career, Dr. Kresic served in lead technical roles at major national and international engineering and environmental consulting companies based in the United States.

Dr. Kresic has worked on numerous projects for a variety of U.S. and international clients including federal, state, and local agencies; industries such as water, transportation, and power utilities; and oil, petrochemical, chemical, mining, and construction companies. He was Senior Fulbright Scholar at the United States Geological Survey in Reston, Virginia, and the George Washington University, Washington, D.C., where he conducted novel research on characterizing and modeling groundwater flow and contaminant fate and transport in fractured rock and karst aquifers. Prior to coming to the United States in 1991, Dr. Kresic was professor of groundwater dynamics at the University of Belgrade, former Yugoslavia.

Dr. Kresic taught academic courses and professional workshops in hydrogeology, groundwater modeling, and groundwater remediation at universities, government agencies, and conferences around the World. He authored and co-authored numerous papers and seven books on the topic of groundwater. Dr. Kresic is a founding member of the Ground Water Modeling Interest Group sponsored by the National Ground Water Association, and former Co-chair of the Karst Commission of the International Association of Hydrogeologists. He is past Vice President for International Affairs of the American Institute of Hydrology and was committee member of the Groundwater Management and Remediation Specialty Group of the International Water Association. Dr. Kresic currently serves on the Board of Directors of Karst Waters Institute (KWI).

The author is grateful to the following organizations for hosting the electronic (pdf) version of *Hydrogeology 101: Introduction to Groundwater Science and Engineering* on their web sites for free download.

The National Ground Water Association is a not-for-profit professional society and trade association for the global groundwater industry. Our members around the world include leading public and private sector groundwater scientists, engineers, water well system professionals, manufacturers, and suppliers of groundwater-related products and services. The Association's vision is to be the leading groundwater association advocating for responsible development, management, and use of water. Visit us at

S.S. Papadopulos & Associates, Inc. (SSP&A) was established in 1979 to provide professional groundwater and hydrogeology consulting services. With that cornerstone, SSP&A developed an internationally recognized practice in contaminant studies, environmental engineering, remediation, geochemistry, and surface-water hydrology. SSP&A has led or contributed to the development of leading simulation and calculation software, in recent years distributed primarily as freeware or open source. SSP&A maintains close ties with professional organizations, research programs, national labs, academia, and other leading experts in the environmental field. This includes providing professional training courses, and authoring peer-reviewed articles and leading or contributing to books on the topics of contaminant transport and model calibration and uncertainty analysis, among other topics. Home page: www.sspa.com. For any questions: write matt@sspa.com or models@sspa.com

Environmental Simulations, Inc. (ESI) is a company specializing in groundwater modeling software, training, and consulting. ESI products include Groundwater Vistas for MODFLOW groundwater modeling and AquiferWin32 for analysis of aquifer test data and analytical modeling. For more information, please send email to support@groundwatermodels.com or visit our website at www.groundwatermodels.com

IGRAC, the International Groundwater Resources Assessment Centre, is an independent center working under the auspice of UNESCO and WMO and supported by the Government of The Netherlands.

IGRAC produces and disseminates evidence-based information on groundwater worldwide to support decision-making for a sustainable planet. It focuses on groundwater data and information acquisition and management, groundwater assessment and research, advocacy and awareness raising. Since 2003, IGRAC provides an independent content and process support, in particular on transboundary aquifer and groundwater monitoring. Visit us at www.un-igrac.org

GSI Environmental Inc. (GSI) is an engineering and environmental science consulting firm committed to investigating, analyzing, and solving complex environmental problems around the globe. Our work ranges from practical solutions for environmentally sound industrial operations and property development to toxicological analysis and management of chemical hazards, sustainable development of water and other natural resources, and protection of our rivers, bays, and estuaries. Our staff combines practical know-how with leading-edge research to deliver timely, innovative, and focused solutions to your environmental challenges. As a service to professional community, we have developed various freeware and open-source groundwater modeling programs. Visit us at www.gsienv.com

The Karst Waters Institute (KWI) is a 501 (c)(3) nonprofit institution whose mission is to improve the fundamental understanding of karst water systems for professionals and the public. KWI seeks to advance karst science through the engagement of professionals in small conferences and workshops, to increase the recognition and publication of karst science, to foster the development of karst professionals, and to communicate and disseminate information to the public. KWI supports these activities by acting as a coordinating agency for funding and personnel. The volunteers constituting the Board of Directors make an annual presentation of a Karst Award to an outstanding member of the cave and karst field, oversee an annual award of a graduate-student scholarship, and have convened 16 conferences and produced 20 special publications on various karst topics. The KWI website is a frequently accessed source of educational resources on the geology, hydrology, and biology of karst systems with implications for the protection water resources in karst terrains.

https://karstwaters.org/

CONTENTS

Lecture 1 Introduction to Hydrogeology

Traditionally, hydrogeology is defined as the area of geologic sciences, as well as engineering, that in its broadest sense deals with water below the land surface. *Hydro* is the Greek word for water, and *geology* is the science of Earth: *geo* being a prefix derived from the Greek word *gaia* (meaning the earth, but also *Gaia* – a primordial Earth goddess in Greek myth), whereas *logy* is derived from the Greek word *logos* which means word, thought, principle, or speech, but in modern times is most commonly understood to mean science. Thus, geology literally means the science of Earth.

The term *hydrogeology* (hydrogéologie in French) was first created by the French biologist and naturalist Jean-Baptiste Lamarck in 1802 in a publication with the same name published in Paris by the Museum of Natural History (Lamarck, 1802). Lamarck also introduced the term *biology*. Although an entire scientific and engineering field owes its name to the French scientist, Lamarck and hydrogeology have not had much in common since. Until recently, a global approach to the preservation of both the environment and humankind has not been endorsed widely. Like Werner and Humboldt (also prominent scientists of the time), Lamarck considered nature as a whole, emphasizing the close connections between its abiotic and biotic parts. He declared that there must be one integrative science – *Physique terrestre* (the physics of the Earth) which would be able to embrace the study of the atmosphere (*Météorologie)*, the study of Earth's crust (Hydrogéologie), and the study of living organisms (Biologie). (Ghilarov, 1998).

The definition of *Gaia* provided by the popular Merriam-Webster dictionary states that the word also refers to the hypothesis that the living and nonliving components of Earth function as a single system in such a way that the living component regulates and maintains conditions (such as the temperature of the ocean or composition of the atmosphere) suitable for life. This definition is greatly influenced by the proposition introduced in the 1970s by chemist James Lovelock and his research partner microbiologist Lynn Margulis that the earth is a living being, self-regulating the elements to sustain life. Lovelock and Margulis, in turn, picked up the idea from the Russian scientist Vernadsky (e.g., see Lovelock and Margulis, 1974; Vernadsky, 1926, 1929, 1997). At the time, this revolutionary hypothesis was discredited, but has since been accepted as a legitimate theory.

Hydrogeology evolved from the broadest definition of the study of Earth's crust at the beginning of the 19th century to the relatively narrow practice of studying the physical aspects of water below the land surface during the first half of the 20th century. This was followed by an added focus on the contamination and remediation of groundwater starting in late 1980s, continuing to the very question of sustainability of life on Earth we face today. Without groundwater many surface streams and freshwater bodies would cease to flow or exist, agriculture and food production would end as we know it, and public and individual drinking water supply would be severely restricted or non-existent in many parts of the world. Groundwater, of course, cannot simply vanish, but its availability and quality can and have been greatly impacted by many if not all human activities.

Importantly, compared to surface water, groundwater moves very slowly for the most part, and the negative anthropogenic impacts on it may last for a relatively long time. Contamination that happened years or decades ago may still be impacting groundwater quality today and may continue to do so for decades to come. In addition, as emphasized by the European Commission (2008), at large-scale contaminated sites it may be difficult or even impossible to rapidly clean up the groundwater contamination encountered. The experience of remediation of the past several decades has shown that the measures taken have in most cases not been able to completely remove all contaminants and that some contaminant sources, if partially left in the subsurface, continue to emit for long periods

of time (i.e., several or more generations). Therefore, an important focus in the European Union is on preventing groundwater contamination in the first place, as opposed to some other developed countries such as the United States and most developing countries around the World where such focus is lacking.

1.1 Hydrologic Cycle and Water Budget

Groundwater is an important part of Earth's hydrologic cycle, or the movement of water between oceans, atmosphere, and land (Figure 1.1). Groundwater is derived mostly from the percolation of precipitation and, to a lesser degree, from surface water streams and lakes (reservoirs) that lose water to underlying aquifers. Only minute quantities of groundwater have their origin from processes located in the deeper crust associated with magmatism (this water is often called *juvenile water*). Groundwater from aquifers and aquitards discharges to bodies of freshwater on land (streams, lakes, marshes) and to oceans. This discharge is either concentrated via springs and seeps, or directly into surface water bodies where it is normally not visible but can sometimes be quite spectacular (Figure 1.2). The volume of groundwater stored and moving through aquifers and aquitards in the upper portion of Earth's crust is much larger than any other form of mobile freshwater on Earth, excluding glaciers and ice caps (Figure 1.3).
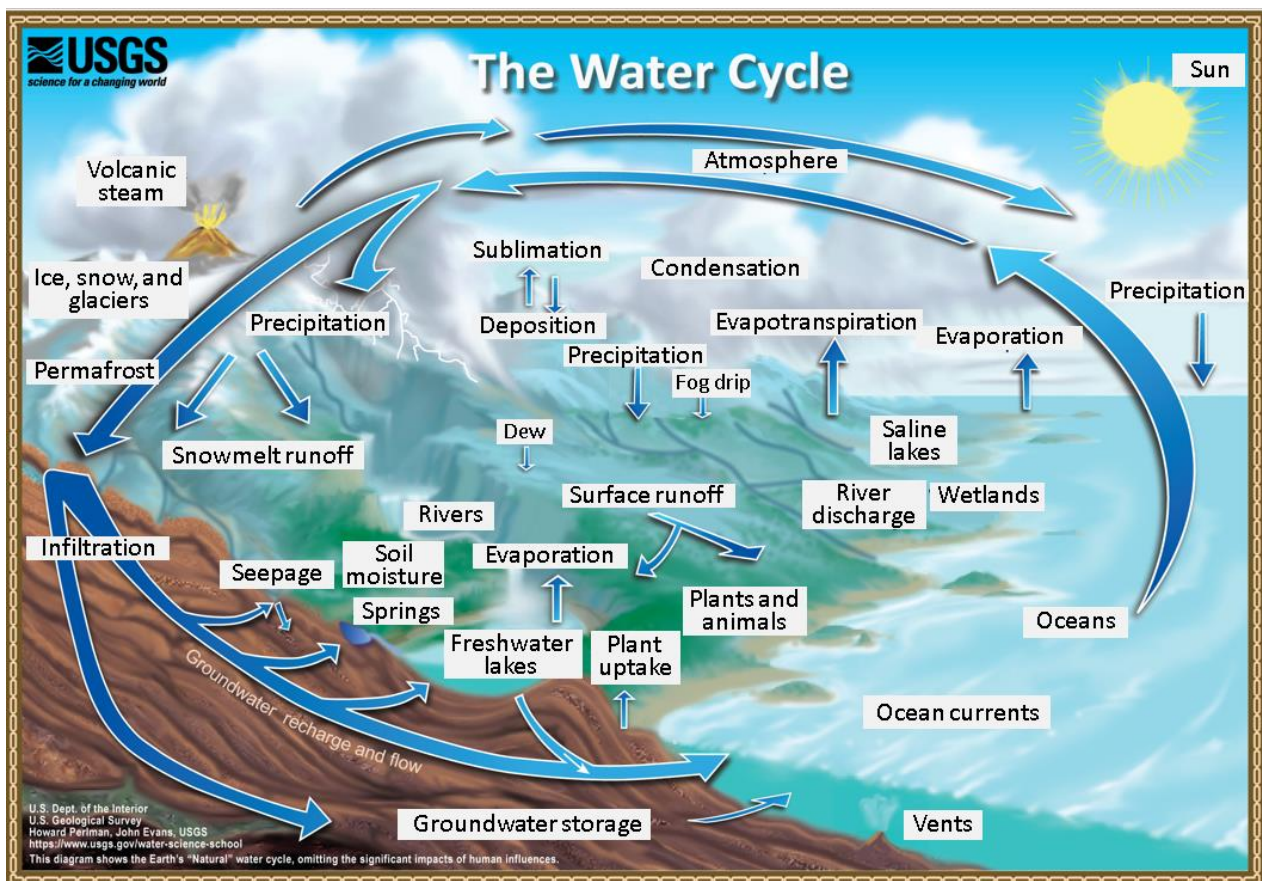
Figure 1.1 The water (hydrologic) cycle. Modified from the United States Geological Survey (USGS). In public domain, available at https://www.usgs.gov/media/images/water-cycle-natural-water-cycle)

Figure 1.2 Boiling Spring on Potts Creek, Alleghany County, Virginia. Photo courtesy of Phil Lucas.
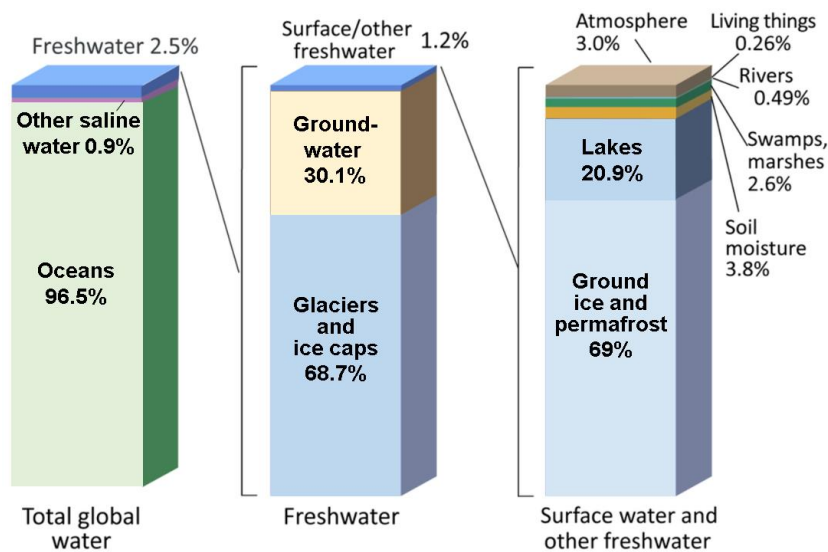
Figure 1.3 Distribution of water on Earth. Modified from USGS. In public domain; https://www.usgs.gov/media/images/
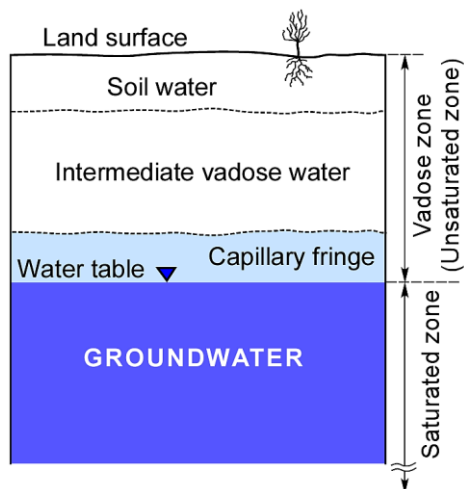
Figure 1.4 Hydrogeologic zones and types of water in the subsurface. Modified from Meinzer, 1923a. USGS; in public domain; available at

https://pubs.usgs.gov/wsp/0577/report.pdf.

Water in the subsurface, from a practical hydrogeologic perspective, can be divided into two major zones: water stored in the *unsaturated zone*, also called the *vadose zone* or *zone of aeration*, and water stored in the *saturated zone* (Figure 1.4). In either case, water is stored in pore spaces between solids of the soil and in spaces between solids (mineral grains) of all rocks in general, unconsolidated and consolidated ("hard") rocks alike (see Lecture 2).

Soil pore space in the vadose zone is filled with both air and water in varying proportions depending on the soil type, climate, and seasonal conditions. This zone may be divided with respect to the occurrence and circulation of water into the uppermost zone of *soil water*, the *intermediate zone*, and the *capillary fringe* immediately above the water table. The zone of *soil water* is the part of the lithosphere from which water is discharged into the atmosphere in perceptible quantities by the action of plants (transpiration) and by direct evaporation, jointly called evapotranspiration. It differs greatly in thickness with different types of soil and vegetation, being only a few feet thick where the surface is covered with grass or ordinary field crops, but much thicker in forests and in tracts that support certain deep-rooting desert plants. The soil water is of primary interest in agriculture because it is near enough to the land surface to be available to the roots of plants. The depths to which the roots of plants reach for water varies greatly with different types of plants and with different soil and moisture conditions. Grasses and most field crops draw water from depths of up to 7 feet. However, crops such as alfalfa, once well established in fine sandy soils derived from loess, may obtain groundwater from as much as 20 to 30 feet below land surface. Large trees and certain types of deep-rooted desert plants draw water from considerable depths. There is evidence that a certain type of mesquite obtains water from as much as 50 feet below the surface and that other perennials may send their roots to depths of 50 or even 60 feet. With respect to its availability to plants, soil water is referred to as being either available or not available for plant growth. The latter is so firmly held by adhesion or other forces that it cannot be taken up by plants rapidly enough to produce growth. More detail on various relationships between vegetative cover and water below the surface is given by Meinzer (1927).

Hygroscopic water is the water in the soil that is in equilibrium with atmospheric water vapor. It is essentially the water which molecular attraction of soil grains can hold against evaporation, or against downward drainage by gravity. It can be removed from the soil only after heating to about 100 to 110 degrees Celsius (i.e., after converting hygroscopic water back into vapor). It is also commonly referred to as *residual soil moisture*.

The *capillary fringe* is a zone directly above the water table and contains capillary interstices some or all of which are filled with water that is continuous with the water in the zone of saturation but is held above that zone by capillarity acting against gravity. Capillarity is a term that describes the joint action of two main molecular forces: *adhesion* (attraction between molecules of water and molecules of porous media), and *cohesion* (attraction between molecules of water). The capillary fringe moves upward and downward together with the water table due to seasonal patterns of aquifer recharge from the percolating precipitation.

The thickness of the capillary fringe depends on the texture of the rock or soil. The fringe is relatively thin if it consists of materials in which all the capillary interstices are large. Materials that have only *sub-capillary* interstices (such as fresh crystalline rocks) are not regarded as having any capillary fringe or as forming a functional part of such a fringe. In materials whose interstices are all *super-capillary,* the capillary fringe is practically absent, such as in uniform coarse gravels. The thickness of the capillary fringe in silty materials has frequently been observed to be about 8 feet; in very fine-grained materials (clay) it is even thicker, and in coarse sand it is considerably thinner (Figure 1.5). Knowing the characteristics of the capillary fringe is important when designing an irrigation system, estimating potential evapotranspiration from the water table, or when studying fate and transport (F&T) of certain groundwater contaminants that may be accumulating at the water table or in the unsaturated zone (see Lectures 12 and 13).
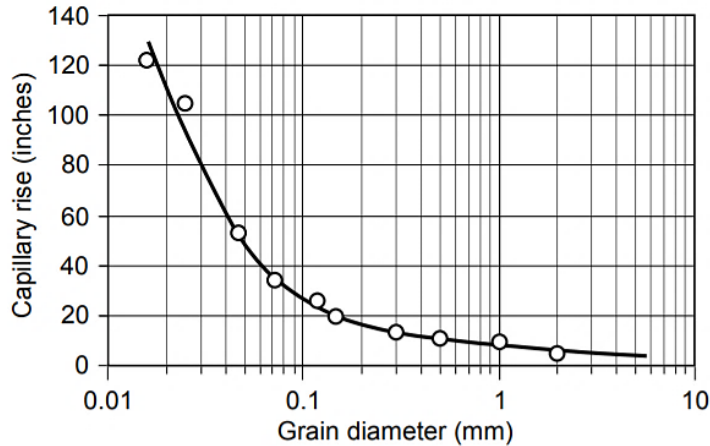
Figure 1.5 Capillary rise in porous materials of different grain sizes. From Meinzer, 1923a, after Hilgard, 1906. USGS, in public domain.

Water that percolates downward beyond the soil water zone enters the *intermediate vadose zone.* Here it is either drawn further downward by gravity to the underlying zone of saturation or is drawn by molecular attraction into the capillary and sub-capillary pores, where it may become stationary. Some of this "trapped" water may move downward if the newly percolated water provides enough pressure height to overcome capillary forces.

Whereas the zone of soil water and the capillary fringe are limited in thickness by local conditions, such as character of vegetation and texture of rock or soil, the intermediate zone is not limited in that respect. It is the residual part of the zone of aeration. It may be entirely absent or may attain a thickness of several hundred feet or more, depending on regional hydrogeologic and climatic conditions. In the arid and semi-arid regions, such as in the southwestern United States, when it is separated from rivers and groundwater discharge areas the unsaturated zone is commonly thicker than 100-150 feet.

Groundwater is water below the water table, completely filling all rock interstices (void or pore spaces) in the saturated zone. Groundwater may be divided with respect to the force by which it is controlled into water that can flow through the rock freely under the influence of gravity (*gravity groundwater*), and groundwater that is not under the control of gravity. The latter is held against gravity and retained in the capillary and sub-capillary pores and fissures within the host rock. (Note that term *rock* in geology refers to all types of unconsolidated sediments, sedimentary rocks, magmatic rocks, and metamorphic rocks, i.e., rocks of all origins.)

Gravity (mobile) groundwater in the saturated zone is constantly moving from areas where it is recharged to areas where it discharges at land surface or into surface water bodies. As mentioned earlier, this flow of groundwater is much slower compared to the flow of surface water (Figure 1.6). Some notable exceptions include groundwater flow in karst aquifers where it may be rather fast through karst conduits and cavities, and in very coarse unconsolidated deposits, such as clean glaciofluvial gravels, where groundwater velocity can be high as well.

As discussed by Kresic and Mikszewski (2013), typically only a few of the general water budget components shown in Figure 1.7 would be of interest at any specific site, or *project,* except for some groundwater availability studies at watershed scales. Common to most of them, including groundwater recharge, is that they cannot be measured directly and are estimated from measurements of related quantities, or *parameters*. Exceptions are direct measurements of precipitation, streamflow, spring discharge rates, and well pumping rates. Other important quantities that can be measured directly and that are used in water budget calculations as part of various equations are the hydraulic head, or *water level*, of both groundwater and surface water, and soil moisture content.

5
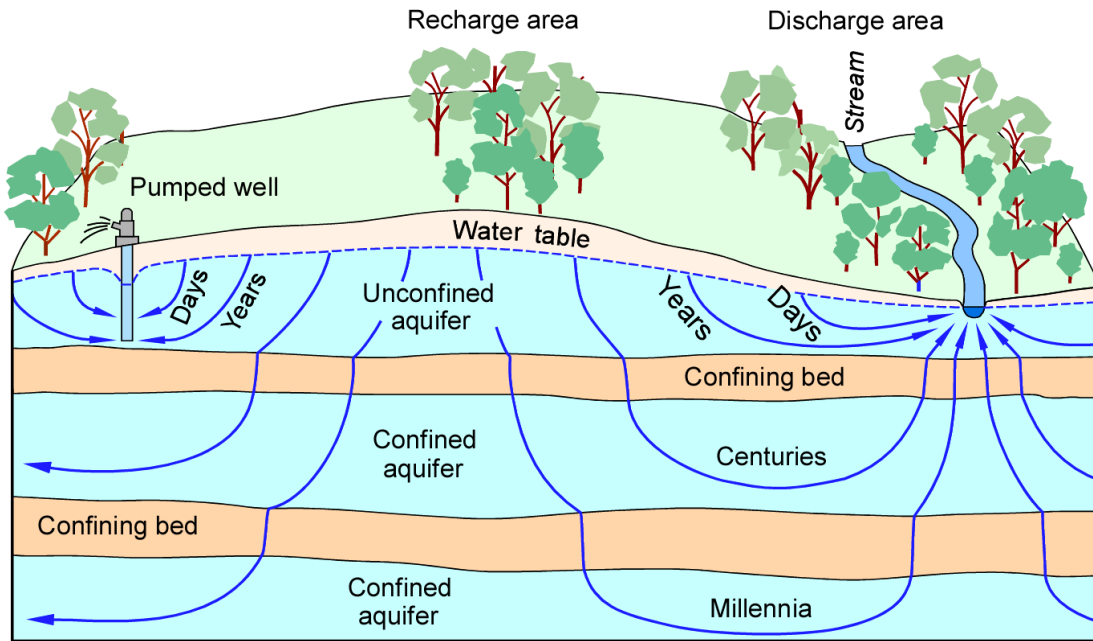
Figure 1.6 Groundwater flow paths vary greatly in length, depth, and travel time from points of recharge to points of discharge in the groundwater system. Modified from Healy et al., 2007. USGS, in public domain.

Water budget terms are often used interchangeably, sometimes causing confusion. In general, *infiltration* refers to any water movement from the land surface into the subsurface. This water is sometimes called *potential recharge* indicating that only a portion of it may eventually reach the water table, or *saturated zone* . The term *actual recharge* is being increasingly used to avoid any possible confusion; it is the portion of infiltrated water that reaches the aquifer, and it is confirmed based on groundwater studies. The most obvious confirmation that actual groundwater recharge is taking place is a rise in the water table. *Effective infiltration*, or *deep percolation*, refers to water movement below the root zone, and is often equated to actual recharge. In hydrologic studies, the term *effective rainfall* describes the amount of precipitation that reaches surface streams via direct overland flow or near-surface flow (*interflow*). *Rainfall excess* describes the component of rainfall that generates surface runoff without infiltrating into the subsurface. *Interception* is the amount of rainfall that is intercepted by vegetative cover before it reaches land surface, and it is not available for either infiltration or surface runoff.
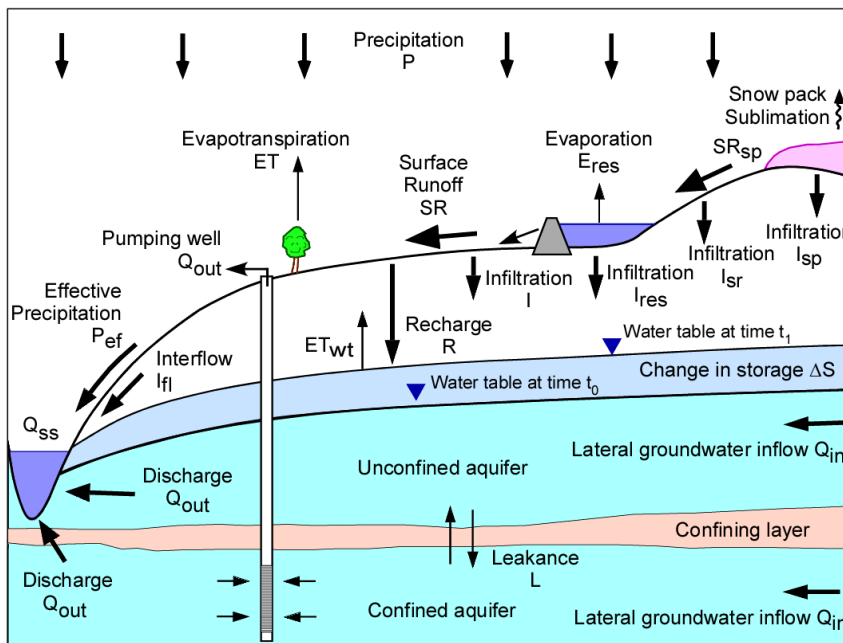
Figure 1.7 Elements of the water budget of a groundwater system. Modified from Kresic, 2009. Copyright McGraw Hill; permission is required for further use.

The term *net recharge* is being used to distinguish between the following two water fluxes: recharge reaching the water table due to vertical downward flux from the unsaturated zone, and evapotranspiration from the water table, which is an upward flux, or *negative recharge*. *Areal recharge* refers to recharge derived from precipitation and irrigation that occurs over large areas, whereas *concentrated recharge* refers to loss of stagnant water from playas, lakes and recharge basins or loss of flowing stream water to the subsurface via sinks and/or over well-defined stretches of the stream.

The complexity of the water budget determination depends on many natural and anthropogenic factors present in the general area of interest, such as:

- Climate
- Hydrography and hydrology
- Geologic and geomorphologic characteristics
- Hydrogeologic characteristics of the surficial soils and subsurface porous media
- Land cover and land use
- Presence and operations of artificial surface water reservoirs
- Surface water and groundwater withdrawals for consumptive use and irrigation
- Wastewater management

The most general equation of water budget that can be applied to any water system has the following form:

$$\text{Water Input - Water Output} \ = \ \text{Change in Storage} \qquad (1.1)$$

Water budget equations can be written in terms of volumes (for a fixed time interval), fluxes (volume per time, such as cubic meters per day or acre-feet per year), and flux densities (volume per unit area of land surface per time, such as millimeters or inches per day). Following are some of the relationships between the components shown in Figure 1.7 that can be utilized in quantitative water budget analyses of the unconfined aquifer (*ua*) in this case:

$$I = P - SR - ET$$

$$I = I_{sr} + I_{res} + I_{sp}$$

$$P_{ef} = SR + I_{fl}$$

$$Q_{ss} = P_{ef} + Q_{out}^{ua} + Q_{out}^{ca}$$

$$Q_{out}^{ua} = R + Q_{in}^{ua} - L$$

$$Q_{out}^{ca} = Q_{in}^{ca} \pm L - Q_{out}^{w}$$

$$\Delta S = R + Q_{in}^{ua} \pm L - Q_{out}^{ua} \qquad\qquad (1.2)$$

where *I* is infiltration in general, *SR* is surface water runoff, *ET* is evapotranspiration, I_{sr} is infiltration from surface runoff, I_{res} is infiltration from surface water reservoirs, I_{sp} is infiltration from snow pack and glaciers, *R* is groundwater recharge in general, ET_{wt} is evapotranspiration from the water table, P_{ef} is effective precipitation, I_{if} is interflow, Q_{ss} is surface stream flow, Q_{out} is direct discharge of the unconfined (*ua*) and confined (*ca*) aquifers, Q_{in} are lateral groundwater inflows to the unconfined (*ua*) and confined (*ca*) aquifers, *L* is leakance from the unconfined aquifer to the underlying confined aquifer and vice-versa, Q_{out} is well pumpage, and *ΔS* is change in storage of the unconfined aquifer. If the area is irrigated, two more components would be added to the list: infiltration and surface runoff of the irrigation water.

Ideally, all applicable relationships at a given site would have to be established to fully quantify the processes governing the water budget including volumes of water stored in and flowing between three general reservoirs – surface water, vadose zone, and saturated zone. By default, a change in one of the many water budget components causes a "chain reaction" and influences all other components. These reactions take place with a certain delay depending on both the actual physical movement of water and the hydraulic and hydrogeologic characteristics of the three general reservoirs.

1.2 Groundwater Use

Water use is a general term that refers to water used for a specific purpose, such as for domestic and public water supply, irrigation, or industrial processing. Water use pertains to human interaction with and influence on the hydrologic cycle. It includes elements such as water withdrawal from surface water and groundwater sources, water delivery to irrigated land, homes, and businesses, consumptive use of water, water released from wastewater treatment plants, water returned to the environment, and in-stream uses such as production of electricity in hydropower plants. *Consumptive use,* or consumed water, is that part of water withdrawn that is evaporated, transpired by plants, incorporated into products or crops, consumed by humans or livestock, or otherwise removed from the immediate water environment (USGS, 2007). It is very important to make a distinction between water withdrawal and water consumption during resource evaluation. For example, not all water withdrawn for irrigation purposes and applied to farmland will be consumed. Depending on the irrigation method, more or less diverted water will return to its original source or another body of water (e.g., surface streams and aquifers) due to drainage, runoff and infiltration. This portion of the withdrawn water, called *return flow*, becomes available for further use.

Following is a list of terms commonly used by the water industry and regulators in the United States (USGS, 2007; USEPA, 2007).

Public supply. Water withdrawn by public governments and agencies, such as a county water department, and by private companies that is then delivered to users. Public suppliers provide water for domestic, commercial, thermoelectric power, industrial, and public water users. Most household water is delivered by a public water supplier.

Municipal (public) water system. A water system that has at least five service connections (such as households, businesses, or schools) or which regularly serves 25 individuals for at least 60 days out of the year.

Water supply system. The collection, treatment, storage, and distribution of potable water from source to consumer.

Water purveyor. A public utility, mutual water company (including privately owned), county water district, or municipality that delivers drinking water to customers.

Potable water. Water that is safe for drinking and cooking.

Water quality criteria. Levels of water quality expected to render a body of water suitable for its designated use. Criteria are based on specific levels of pollutants that would make the water harmful if used for drinking, swimming, farming, fish production, or industrial processes.

Water quality standards. State-adopted and EPA-approved ambient standards for water bodies. The standards prescribe the use of the water body and establish the water quality criteria that must be met to protect designated uses.

Public water use. Water supplied from a public water supply and used for such purposes as firefighting, street washing, and municipal parks and swimming pools.

Domestic water use. Water used for household purposes, such as drinking, food preparation, bathing, washing clothes, dishes, pets, flushing toilets, and watering lawns and gardens. About 85% of domestic water is delivered to homes by a public-supply facility, such as a county water department. About 15% of the nation's population supplies its own water, mainly from wells.

Commercial water use. Water used for motels, hotels, restaurants, office buildings, commercial facilities, and institutions. Water for commercial uses comes both from public-supplied sources, such as a county water department, and self-supplied sources, such as local wells.

Industrial water use. Water used for industrial purposes in such industries as steel, chemical, paper, and petroleum refining. Nationally, water for industrial uses comes mainly (80%) from self-supplied sources, such as local wells or withdrawal points in a river, but some water comes from public-supplied sources, such as the county/city water department.

Irrigation water use. Water application on lands to assist in the growing of crops and pastures or to maintain vegetative growth in recreational lands, such as parks and golf courses.

Livestock water use. Water used for livestock watering, feedlots, dairy operations, fish farming, and other on-farm needs.

Sanitation. Control of physical factors in the human environment that could harm development, health, or survival.

Sanitary water (also known as *gray water*). Water discharged from sinks, showers, kitchens, or other non-industrial operations, but not from commodes.

Wastewater. The spent or used water from a home, community, farm, or industry that contains dissolved or suspended matter.

Water pollution. The presence in water of enough harmful or objectionable material to damage the water's quality.

Treated wastewater. Wastewater that has been subjected to one or more physical, chemical, and biological processes to reduce its potential of being health hazard.

Reclaimed wastewater. Treated wastewater that can be used for beneficial purposes, such as irrigating certain plants.

Publicly owned treatment works (POTWs). A waste-treatment works owned by a state, unit of local government, or Native American tribe, usually designed to treat domestic wastewaters.

Groundwater, about 93% of all water on the planet, is by far the most abundant and readily available source of freshwater on continents outside polar regions, followed by mountainous ice caps and glaciers, lakes, reservoirs, wetlands, and rivers (Figure 1.3). About 1.5 billion people depended upon groundwater for their drinking water supply at the end of the 20th century (WRI, 1998). The amount of total groundwater withdrawn annually was roughly estimated at about 20% of global water withdrawals at the end of the 20th century (WMO, 1997) and at 26% in 2010 (Margat and van der Gun, 2013). The three countries that withdraw the most groundwater annually are India (251 km^3/year in 2010), China (112 km^3/year) and the United States (also 112 km^3/year), with the next

two countries, Pakistan and Iran, using roughly one-half of what is extracted in the U.S. and China, or about 64-65 km³/year (Margat and van der Gun, 2013).

Agriculture consumes the most water worldwide. It accounted for 67% of the world's total freshwater withdrawal (surface water and groundwater), and 86% of its consumption in the year 2000 (UNEP, 2007). Similarly, groundwater used in agriculture was of disproportionally higher percentage compared to any other groundwater uses: 89% in India, 54% in China, 71% in the U.S., 94% in Pakistan, 72% in Mexico, 92% in Saudi Arabia, and 67% in Italy. By 2025, worldwide agriculture is expected to increase its water requirements by 1.2 times, and the world's irrigation areas are projected to reach about 330 million hectares, up from approximately 253 million hectares in 1995 (Shiklomanov, 1999).

In the United States, groundwater accounted for 26% of all freshwater withdrawals in 2015 (Table 1.1). After excluding withdrawals for thermoelectric power, the percentage of groundwater used for all other purposes was 44.5%. Irrigation was the second largest use of freshwater with a relatively even split: 48% was from groundwater and 52% from surface water. Domestic water supply was virtually all dependent on groundwater, whereas surface water was utilized more for public water supply than groundwater, 61% vs. 39%.

Table 1.1 Use and source of water in the United States in 2015, in millions of gallons per day. Data from Dieter et al., 2018, USGS (available at https://www.usgs.gov/media/images/source-and-use-water-us-2015).

Use	Groundwater	%	Surface water	%
Domestic supply	3,210	98.5	49,1	1.5
Public supply	15,200	39	23,800	61
Industrial	2,710	18	12,000	82
Irrigation	57,200	48	60,900	52
Thermoelectric	597	0.5	132,000	99.5
Mining	2,870	72	1,130	28
Livestock	1,240	62	760	38
Aquaculture	1,600	21	5,950	79
TOTAL	84,700	26	237,000	74

Figure 1.8 shows withdrawal of surface water and groundwater in the United States between 1950 and 2015 together with the population trend. The drop in total freshwater withdrawals in 2015 was primarily caused by significant decreases in withdrawals for thermoelectric power (28.8 billion gallons per day or Bgal/d), which accounted for 89 percent of the decrease in total withdrawals. The decrease in surface water withdrawals accounted for another 9 percent of the decline in total withdrawals. Groundwater withdrawals remained steady between 1975 and 2015. Categories of use where withdrawals increased from 2010-2015 were irrigation and mining.

The percentage of groundwater use for public supply increased from 26 percent for 1950 to 40 percent for 1985 and has remained at slightly less than 40 percent since 1985. Figure 1.9 shows that groundwater was an important source of public water supply for every state in 2015. Three States—California, Florida, and Texas—each withdrew more than 1,000 Mgal/d of groundwater for public supply in 2015 and accounted for 37 percent of total groundwater withdrawals for public supply. States that relied on groundwater for 75 percent or more of their public-supply withdrawals were Hawaii, Idaho, Florida, Mississippi, Iowa, and Nebraska.

Estimated withdrawals for self-supplied domestic use increased by 71 percent between 1950 and 2000. The self-supplied domestic population was 57.5 million people for 1950, or 38 percent of the total population. For 2000, 43.5 million people, or 15 percent of the total population, were self-supplied (Hutson et al., 2004). Data after 2000 is not readily available but it can be assumed that there was not a significant increase in the number of people relying on self-supply as population growth has been occurring mainly in urban areas and suburbs with public water supply systems.

Irrigation remained the largest use of freshwater in the U.S. Since 1950, it accounted for between 62 and 65 percent of total water withdrawals, excluding those for thermoelectric power. Historically, more surface water than groundwater has been used for irrigation. However, the percentage of total irrigation withdrawals from groundwater has continued to increase, from 23 percent in 1950 to 48 percent in 2015. Irrigated acreage more than doubled between 1950 and 1980, then remained constant before increasing nearly 7 percent between 1995 and 2000 in response to droughts in some states, especially in the Southwest. Recently, national irrigated area reached a plateau at about 55 million acres as continuing growth in eastern states has been offset by declines in western irrigation.
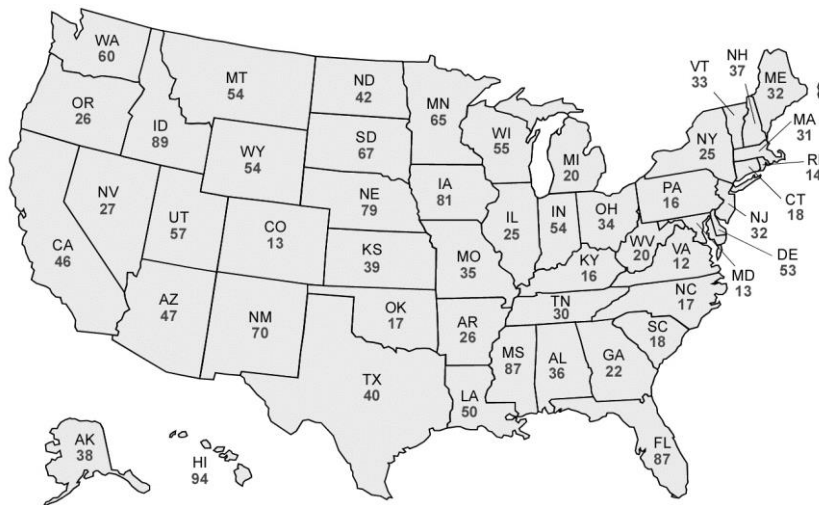
Figure 1.8 Groundwater as percentage of total public-supply water withdrawal in the United States in 2015 per state. Raw data from Dieter et al., 2018, USGS, in public domain.
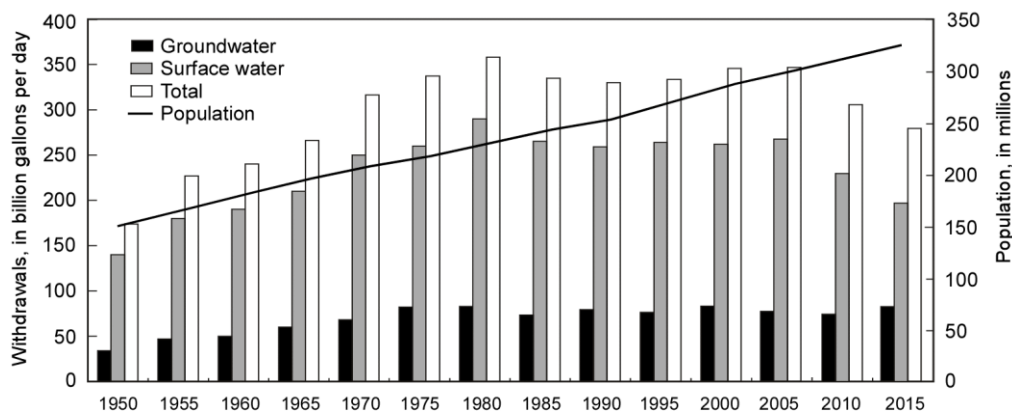
Figure 1.9 Trends in population and freshwater withdrawals in the United States by source, 1950–2015. Modified from Dieter et al., 2018. USGS, in public domain.

Figure 1.10 Distribution of irrigated land on farms in the United States. One dot represents 5,000 irrigated acres. From Gollehon and Quinby, 2006. U.S. Department of Agriculture, in public domain.

Figure 1.11 Center pivot irrigation on wheat growing in Yuma County, Colorado using LESA (Low Elevation Spray Application) system. This type of application uses the least water and reduces evaporation. Photo courtesy of Gene Alexander, USDA National Resources Conservation Service. In public domain.

In general, there is an increasing reliance on irrigation in the humid East, and a northward redistribution of irrigation in the West (Figure 1.10). In recent decades, large concentrations of irrigation have emerged in humid areas—Florida, Georgia, the Delmarva Peninsula (Eastern Delaware and Maryland) and especially in the Mississippi River Valley, primarily Arkansas and Mississippi (Gollehon and Quinby, 2006). Groundwater supplied most of the irrigation water in the eastern 37 states, the area that experienced the largest irrigation growth in the last decade of the 20th century. Most withdrawals occur in the arid Western States where irrigated production is concentrated (Figure 1.11). In 2000, about 85 percent of total agricultural withdrawals occurred in a 19-State area encompassing the Plains, Mountain, and Pacific regions. In the Mountain region, over 90 percent of the water withdrawn is used by agriculture, almost all of which (96 percent) is used for irrigation.

Water withdrawals are not the only measure of water use. Consumptive use—the water not returned to the immediate water environment—is much greater for agriculture than any other sector, both in total and as a share of water withdrawn. Estimates available from 1960 through 1995 show that agriculture accounts for over 80 percent of the United States' consumptive use, because a high share of applied irrigation water is used by plants for evapotranspiration (building of biomass), with little returning to surface water or groundwater. Water diverted for cooling thermoelectric plants tends to be used as a thermal sink, with much of it returned to rivers and streams.

Greater irrigation withdrawals do not necessarily translate into greater consumptive use per irrigated acre. The difference between withdrawals and consumptive use highlights the importance of losses, runoff, and return flows (Gollehon and Quinby, 2006).

1.3 Hydrogeology Professions

Hydrogeology professions are as diverse as the many aspects of groundwater science and engineering. Just like the name conveys, a hydrogeologist is at the crossroads of geology and water-related jobs, in their broadest sense. While a novice hydrogeologist may often be engaged in field data collection and general assessments (similarly to a "family practice" medical doctor), senior hydrogeologists tend to specialize. In either case, however, it is expected that practicing hydrogeologists have excellent quantitative skills including application of computer programs for solving various engineering and water resource management problems at hand. Moreover, since almost all problems in hydrogeologic engineering include calculations of groundwater flow and velocity, and increasingly the fate and transport of groundwater contaminants, the basic knowledge of fluid mechanics and an understanding and quantification of biochemical reactions in the subsurface are in many cases requirements for a successful hydrogeologic practice.

Although a few different job titles may be used in academic circles, the industry, and the regulatory community to describe groundwater-related jobs, such as hydrogeologist, groundwater hydrologist, hydrologist, or groundwater engineer, in every case the work must include dealing with groundwater in some way. At the same time, as discussed earlier, groundwater is inseparable from surface water as they both belong to the same hydrologic cycle and are best understood and managed when considered as one *integrated* water resource. Consequently, there is often an overlap between groundwater professions and surface water professions, and it is only to the benefit of both if the practitioners are cross trained to some extent, either formally or through professional practice.

Entry-level hydrogeologist jobs tend to involve more field work such as oversight of the installation of piezometers and wells (for water-supply, dewatering, monitoring, and sampling), groundwater sampling, borehole logging, hydrogeologic reconnaissance and mapping, field testing of wells (pumping tests, slug tests, packer tests), tracer testing, and others. This data collection effort is supplemented with a fair share of data entry, analysis, and visualization with the help of various maps, cross-sections, graphs, and schematics.

Mid-level hydrogeologists tend to spend equal or more time in the office designing the field investigations and analyzing the data collected from all sources (field, literature, laboratory, and others) with the goal of developing a conceptual site model (CSM) for their project. This CSM will be utilized to provide answers, both qualitative and quantitative, to a variety of questions key to the project decision-making process. A successful hydrogeologist will be well-versed in using a Geographic Information System (GIS) and several other industry-standard software programs for contouring, graphing, and otherwise presenting the data and key CSM elements in a visually pleasing and easily understood manner. They will be comfortable using various analytical programs and numeric groundwater models.

Traditionally, hydrogeologists are separated roughly into two major groups:

(1) Physical hydrogeologists focusing on water supply and non-contaminant groundwater engineering. Typical jobs include assessment, development (extraction), and management of groundwater resources and sources; groundwater dewatering at mines, construction, and transportation sites; agricultural drainage and irrigation; flood control; designing artificial reservoirs, dams, and levees; artificial groundwater recharge, and others.

(2) Contaminant hydrogeologists focusing on human health and the environmental risk assessment (i.e., environmental impacts caused by contaminated groundwater), and groundwater remediation, i.e., aquifer restoration to beneficial uses.

This division is somewhat artificial since all hydrogeologists, most of the time, work on same basic problems regardless of the final goal of any groundwater project. They also often work on both types of projects (non-contaminant and contaminant), especially if employed by larger engineering and environmental consultancy firms. And they all must provide answers to the following key questions (modified from Kresic and Mikszewski, 2013):

- Where is the groundwater flowing from and where is it flowing to?

- Through which type of porous media is it flowing?

- How much of it is there, and how fast is it flowing?

- How/where is it recharged and how/where it discharges?

- How did the groundwater system behave in the past, and how will it change in the future based on both natural and anthropogenic influences?

- When the groundwater is contaminated, a CSM (conceptual site model) also includes answers to similar general questions regarding the contaminant(s).

Specializations in hydrogeology are quite diverse, but still with a clear understanding that all basic hydrogeology knowledge listed above and typically acquired in college and/or through field work experience and on-the-job training is required by default. Senior practitioners may further focus on optimization of groundwater extraction (withdrawal) technologies and techniques, providing design specifications and drawings. Or they may specialize in the application and development of high-end numeric groundwater models and/or software programs and use them to provide quantitative simulations, predictions, and groundwater engineering or remediation design parameters. They may prefer working on a specific groundwater remediation technology such as efficient delivery of reactive fluids into the subsurface (aquifer) that will destroy or neutralize groundwater contaminants. They may specialize in developing strategies and specific plans for conjunctive use of surface water and groundwater for large utilities and municipalities. They may like the challenge of using renewable sources of energy and focus on utilization of geothermal energy. Or, sometimes, they like being expert witnesses in multi-million-dollar lawsuits involving adverse impacts of contaminated groundwater on human health and the environment, or a high-value groundwater resource (source).

The U.S. Bureau of Labor Statistics (BLS) predicts employment in hydrology (19-2043 Hydrologists) will grow by 5% until 2029, listing a median annual wage of $81,270 ($93,820 at management, scientific, and technical consulting services; the highest 10% earn more than $127,400.) A Geoscientist occupation (19-2042) had a median annual wage of $92,040 in 2019, driven largely by mining, quarrying, and oil and gas extraction, and the same growth rate of 5% until 2029. The job outlook for environmental engineers is estimated to increase by 3%; on average they earn about $7,000 more than hydrologists. Environmental scientists on average earn $10,000 less than hydrologists annually, but their job outlook is predicted to grow by 8% by 2029.

In the case of hydrogeologists, hydrologists, and environmental scientists, this above average job outlook is based on increased demands for water supply in many human activities including public drinking water supply, agriculture, food production, and mining, to name a few, as well as continuously increasing stress on the environment caused by human activities. In addition, environmental concerns related to global climate change and the potential rise in sea-level are also likely to increase demand for hydrologists, hydrogeologists, and environmental scientists in the U.S. and worldwide. It should be noted that BLS does not specifically recognize hydrogeology as an occupation for their statistical analyses, but their definition of "hydrologists" does include a groundwater aspect as well. More information about the wage distribution and employment prospects in different states in the United Sates, including detail statistics and maps, is available at www.bls.gov.

Top employers for hydrogeologists and hydrologists are the Federal Executive Branch; State Governments; Management, Scientific, and Technical Consulting Services; Architectural, Engineering, and Related Services; and Local Governments. The BLS reports that most jobs in these fields now require a master's degree. Although master's programs in geosciences are available at many universities, a relatively small number of universities in the U.S. offer a comprehensive graduate program in hydrogeology. Instead, undergraduate programs at larger universities typically feature a basic level course dedicated to hydrogeology and/or hydrology and may include lab or field experience. Consequently, professionals with hydrogeology degrees are in high demand.

.

Lecture 2 Porosity and Hydraulic Characteristics of Porous Media

2.1 Porosity and Effective Porosity

The nature of the *porosity* of porous media (sediments and all rocks in general) is the single most important factor in determining the storage and movement of groundwater in the subsurface. Many quantitative parameters describing "life cycle" of water and contaminants (when present) within a groundwater system directly or indirectly depend on porosity. Here are just a few: infiltration of precipitation into the subsurface, rock (sediment) permeability, groundwater velocity, volume of water that can be extracted from the groundwater system, and diffusion of contaminants into the porous media. The following discussion is based primarily on materials presented by Kresic (2007 and 2009) and various authors of the United States Geological Survey (USGS).

Porosity (*n*) is defined as the percentage of voids (empty space occupied by water or air) in the total volume of rock, which includes both solids and voids:

$$n = \frac{V_v}{V} \times 100\%$$

(2.1)

where V_v is the volume of all rock voids and V is the total volume of rock (in geologic terms, rock refers to soils, unconsolidated and consolidated sediments, magmatic and metamorphic rocks, or any type of rock in general). Assuming the specific gravity of water equals unity, the total porosity, as a percentage, can be expressed in four different ways (Lohman, 1972):

$$n = \frac{V_i}{V} = \frac{V_w}{V} = \frac{V - V_m}{V} = 1 - \frac{V_m}{V} \quad [\times 100\%]$$

(2.2)

where *n* is the porosity, in percent per volume; V is the total volume; V_i is the volume of all interstices (voids); V_m is the aggregate volume of mineral (solid) particles; V_w is the volume of water in a saturated sample. Porosity can also be expressed as:

$$n = \frac{\rho_m - \rho_d}{\rho_m} = 1 - \frac{\rho_d}{\rho_m} \quad [\times 100\%]$$

(2.3)

where ρ_m is the average density of mineral particles (grain density); ρ_d is the density of a dry sample (bulk density).

The shape, amount, distribution, and interconnectivity of voids influence the permeability of rocks. Voids, on the other hand, depend on the depositional mechanisms of unconsolidated and consolidated sedimentary rocks, and on various other geologic processes that affect all rocks during and after their formation. *Primary porosity* is the porosity formed during the formation of rock itself, such as voids between the grains of sand, voids between minerals in hard (consolidated) rocks, or bedding planes of sedimentary rocks. *Secondary porosity* is created after the rock formation, mainly due to tectonic forces (faulting and folding) which create micro and macro fissures, fractures, faults, and fault zones in solid rocks. Both the primary and secondary porosities can be successively

altered multiple times, thus completely changing the original nature of the rock porosity. These changes may result in porosity decrease, increase, or altering of the degree of void interconnectivity without a significant change in the overall void volume.

The following discussion by Meinzer (1923a), and the figure that accompanies it (Figure 2.1) is probably the most cited explanation of rock porosity, and one can hardly add anything to it.
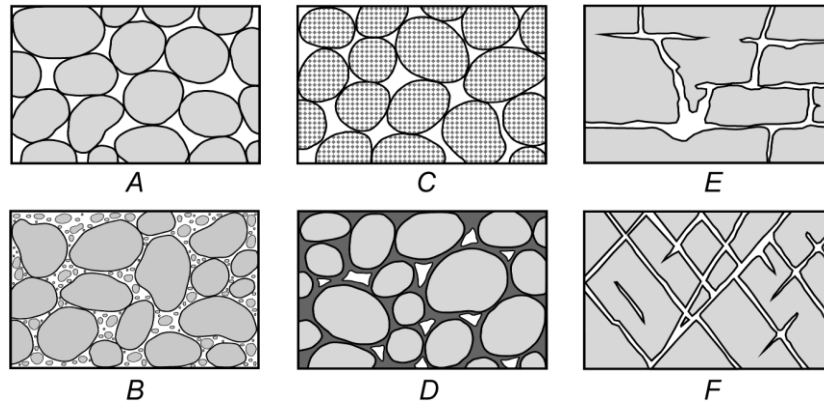
Figure 2.1. Diagram showing several types of rock interstices and the relation of rock texture to porosity. A: well-sorted sedimentary deposit having high porosity; B: poorly sorted sedimentary deposit having low porosity; C: well-sorted sedimentary deposit consisting of pebbles that are themselves porous, so that the deposit as a whole has a very high porosity; D: well-sorted sedimentary deposit whose porosity has been diminished by the deposition of mineral matter in the interstices; E: rock rendered porous by solution; F, rock rendered porous by fracturing. Modified from Meinzer, 1923a. USGS, in public domain.

"The porosity of a sedimentary deposit depends chiefly on (1) the shape and arrangement of its constituent particles, (2) the degree of assortment of its particles, (3) the cementation and compacting to which it has been subjected since its deposition, (4) the removal of mineral matter through solution by percolating waters, and (5) the fracturing of the rock, resulting in joints and other openings. Well-sorted deposits of uncemented gravel, sand, or silt have a high porosity, regardless of whether they consist of large or small grains. If, however, the material is poorly sorted small particles occupy the spaces between the larger ones, still smaller ones occupy the spaces between these small particles, and so on, with the result that the porosity is greatly reduced (Figure 2.1.A and B). Boulder clay, which is an unassorted mixture of glacial drift containing particles of great variety in size, may have a very low porosity, whereas outwash gravel and sand, derived from the same source but assorted by running water, may be highly porous. Well-sorted uncemented gravel may be composed of pebbles that are themselves porous, so that the deposit as a whole has a very high porosity (Figure 2.1.C). Well-sorted porous gravel, sand, or silt may gradually have its interstices filled with mineral matter deposited out of solution from percolating waters, and under extreme conditions it may become a practically impervious conglomerate or quartzite of very low porosity (Figure 2.1.D). On the other hand, relatively soluble rock, such as limestone, though originally dense, may become cavernous as a result of the removal of part of its substance through the solvent action of percolating water (Figure 2.1.E). Furthermore hard, brittle rock, such as limestone, hard sandstone, or most igneous and metamorphic rocks, may acquire large interstices through fracturing that results from shrinkage or deformation of the rocks or through other agencies (Figure 2.1.F). Solution channels and fractures may be large and of great practical importance, but they are rarely abundant enough to give an otherwise dense rock a high porosity."

The porosity of unconsolidated sediments (gravel, sand, silt, and clay) is often called *intergranular (interparticle) porosity* because the solids are loose grains (particles; see Figure 2.3). When such rocks become consolidated, the former intergranular porosity is called *matrix porosity*. In general, the term matrix porosity is applied to primary porosity of all consolidated (hard) rocks, such as porosity between mineral grains (minerals) in granite, gneiss, slate, or basalt. Some unconsolidated or loosely consolidated (semi-consolidated) rocks may contain fissures and fractures, in which case the non-fracture portion of the overall porosity is also called matrix porosity. Good examples are fractured clays and glacial till sediments, or residuum deposits which have preserved the fabric of the original bedrock in the form of fractures and bedding planes.

Sometimes, microscopic fissures in rocks are also considered part of the matrix porosity (Figure 2.2-*Right*) as opposed to larger fissures and fractures called *macroporosity*. In general, rocks that have both the matrix and the fracture porosity are referred to as *dual-porosity* media. This distinction is important in terms of groundwater flow, which has very different characteristics in fractures and conduits compared to the bulk of the rock. It is also important in contaminant fate and transport analysis, especially when contaminant concentrations are high causing its diffusion into the rock matrix where it can remain for long periods of time. Figures 2.2 through 2.8 help illustrate the very diverse nature of rock porosity at different scales. Average total porosity and porosity ranges for various rock types are shown in Figure 2.7. Raw data for this analysis, compiled by the USGS, include thousands rock samples from around the world and can be found in Wolff (1982) and Kresic (2007).
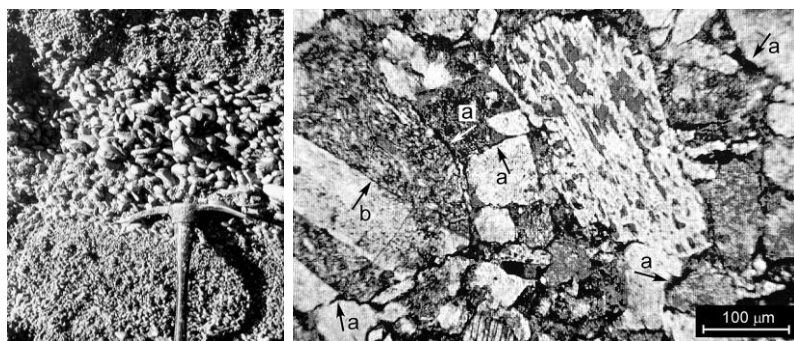
Figure 2.2 *Left*: Details of sorting in gravel of the Provo formation east of Springville. Utah County, Utah. Circa 1940. Courtesy USGS Photographic Library, 2007. (https://library.usgs.gov/photo/#/) *Right*: Photomicrograph of feldspar rich sandstone (arkose). a) arrows point to pore spaces between individual sandstone grains. b) arrow points to an intra-granular discontinuity between a feldspar crystal and surrounding ground mass. Note the scale of 100 microns. Courtesy of Jeff Manuszak.
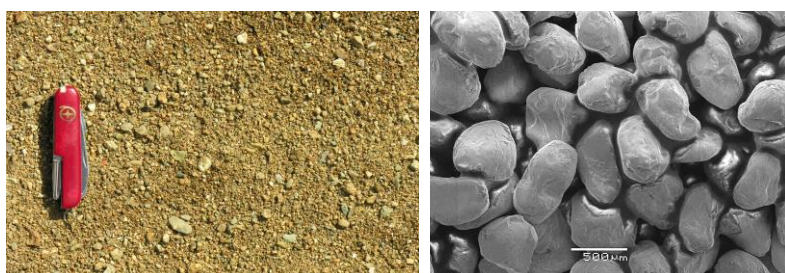
Figure 2.3 *Left*: photograph of coarse alluvial sand with gravel. *Right*: ESM (Electron Scanning Microscope) image of uniform, pure quartz sand. Photo courtesy of Dr. Scott Chumbley, Iowa State University.)
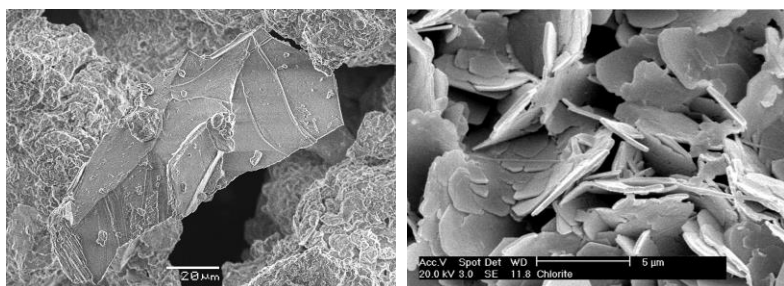
Figure 2.4 *Left*: ESM image of clay-rich residuum on top of metamorphic basalt, Piedmont, Virginia. Macropores (black areas) provide for moderate permeability, while clay minerals provide for high overall porosity. Courtesy of Dr. Scott Chumbley, Iowa State University. *Right*: Magnesium-rich chlorite, Rotliegend, Northern Germany. Photo courtesy of M. Roe, Macaulay Institute.

Figure 2.5 ESM images of two different types of sandstone. *Left*: quartz grains and maybe feldspar grains coated with clay minerals; the clay minerals are likely illite and/or chlorite. Photo courtesy of James Talbot; copyright 2000, James Talbot, K/T GeoServices, Inc.   *Right*: loosely cemented sandstone with high porosity. Photo courtesy of Dr. Fred Longstaffe, The University of Western Ontario, Canada.

Figure 2.6 *Upper left*: Honeycombed sandstone in Mesa Verde. *Upper right*: Coarse gravel. *Middle left*: Fractured marlstone. *Middle right*: very loosely cemented and stratified fine sand. *Lower left*: Stratified alluvial sediments, gravel, sand, and silt. *Lower right*: Massive fractured sandstone (top) underlined by layers of shale and siltstone. All lithologies shown have relatively high and similar overall porosity, with marlstone, shales, and silts being considerably less permeable because of the clay content.
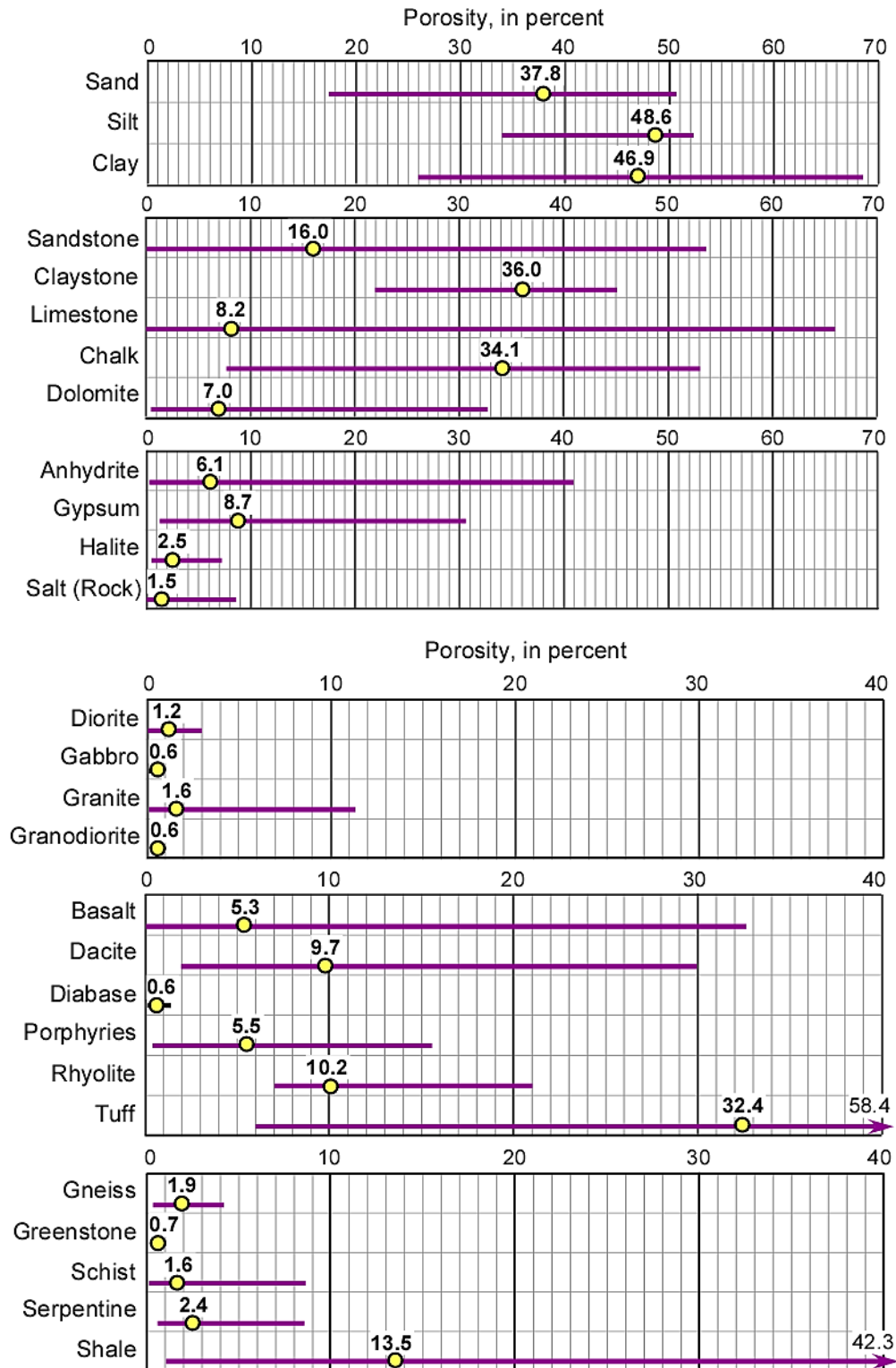
Figure 2.7 Porosity range (horizontal bars) and average total porosities (circles) of different types of rocks. Modified from Kresic, 2007. Copyright CRC Taylor & Francis; permission is required for further use. Raw data from Wolff, 1984. USGS, in public domain.

Lecture 2 Porosity and Characteristics of Porous Media

When studying and observing porosity from the hydrogeologic perspective, it is very important to make a very clear distinction between the total porosity and the *effective porosity* of the rock. It is, however, unfortunate that some widely used hydrogeology textbooks do not make such distinction and even hypothesize that there is no such thing as effective porosity since "water molecules are shown to be able to move through any pore size". The following discussion by Meinzer (1932) may help in explaining why using the appropriate "form of porosity" and the appropriate corresponding number in quantitative hydrogeologic analyses does matter:

"To determine the flow of ground water, however, a third factor, which has been called the effective porosity, must be applied. Much of the cross section is occupied by rock and by water that is securely attached to the rock surfaces by molecular attraction. The area through which the water is flowing is therefore less than the area of the cross section of the water-bearing material and may be only a small fraction of that area. In a coarse, clean gravel, which has only large interstices, the effective porosity may be virtually the same as the actual porosity, or percentage of pore space; but in a fine-grained or poorly assorted material the effect of attached water may become very great, and the effective porosity may be much less than the actual porosity. Clay may have a high porosity but may be entirely impermeable and hence have an effective porosity of zero. The effective porosity of very fine grained materials is generally not of great consequence in determinations of total flow, because in these materials the velocity is so slow that the computed flow, with any assumed effective porosity, is likely to be relatively slight or entirely negligible. The problem of determining effective porosity, as distinguished from actual porosity, is, however, important in studying the general run of water-bearing materials, which are neither extremely fine nor extremely coarse and clean. Hitherto not much work has been done on this phase of the velocity methods of determining rate of flow. No distinction has generally been made between actual and effective porosity, and frequently a factor of 33 1/3 per cent has been used, apparently without even making a test of the porosity. It is certain that the effective porosity of different water-bearing materials ranges between wide limits and that it must be at least roughly determined if reliable results as to rate of flow are to be obtained. It would seem that each field test of velocity should be supplemented by a laboratory test of effective porosity, for which the laboratory apparatus devised by Slichter (1905) could be used."

One of the reasons why some professionals today chose to ignore statements like this one by Meinzer, is that determining the effective porosity is not straightforward since there is no one "magic" method of doing so, and different methods yield different results (e.g., see Stephens et al., 1998). On the other hand, determining the total porosity of a rock specimen has been a routine procedure for more than a century, as it involves simple volumetric-gravimetric techniques, i.e., measurement of simple quantities listed in equations (2.2) and (2.3).

Effective porosity is often equated to *specific yield* of the porous material, or that volume of water in the pore space that can be freely drained by gravity due to change in the hydraulic head. Effective porosity is also defined as the volume of interconnected pore space that allows free gravity flow of groundwater. The volume of water retained by the porous media, which cannot be easily drained by gravity, is called *specific retention*. Since drainage of pore space by gravity may take long periods of time, especially in fine-grained sediments, values of specific yield determined by various laboratory and field methods during necessarily limited times are probably somewhat lower than the "true" effective porosity. Specific yield determined by aquifer testing in the field is a lumped hydrodynamic response to pumping by all porosity types (porous media) present in the aquifer. This value cannot be easily related to values of total porosity, which are always determined in the laboratory for small samples. More detail on aquifer specific yield is given in next section.

One important distinction between the specific yield and the effective porosity concepts is that the specific yield relates to <u>volume</u> of water that can be freely extracted from an aquifer, while the effective porosity relates to groundwater <u>velocity</u> and <u>flow</u> through the interconnected pore space. Unnecessary confusion is introduced by some professionals trying to distinguish between the effective porosity for groundwater flow, and the effective porosity for contaminant transport. If the contaminant is dissolved in groundwater, its advective transport will be governed by the same effective porosity since it moves with groundwater. Diffusive transport of the contaminant is its movement due to concentration gradient and is independent of the groundwater flow. Diffusion involves the entire (total) porosity: molecules of the contaminant (and water) can move through minute pores, which would otherwise not allow free gravity flow. In conclusion, there are no two different effective porosities, and it is sufficient to determine two values for any quantitative analysis of groundwater flow, or contaminant fate and transport: one for the effective porosity, and one for the total porosity.

Figure 2.8 Example of secondary fracture porosity in granite. Acadia National Park, Maine.

Most laboratory methods for determining effective porosity from the specific yield and specific retention involve a complete saturation of the undisturbed rock specimen with water (fluid), and then removal of the fluid by drainage. Alternatively, the fluid is first removed by forced drainage (e.g., by centrifuge), or by drying, and then completely saturated with the fluid. In either case, the volume of fluid used to fully saturate the sample at a given pressure, and the volume of fluid that can be drained are easily measured. Testing of low-permeable materials and hard-rock cores may involve application of vacuum and pressures higher than the atmospheric pressure and use of air or gasses such as helium. The pressures and procedures applied affect the degree or size of interconnections measured. Drying clay samples at temperatures close to 100 ºC and then fully saturating them may yield erroneously high values of effective porosity as such temperatures are high enough to remove significant volumes of otherwise immobile (hydrated) water stored between clay minerals that could not be removed by drainage alone.

For all these reasons, a list of determined values of the effective porosity for different types of rocks, including a clear explanation of what was exactly tested and how, does not exist to the best of author's knowledge. Unfortunately (again) some hydrogeology textbooks "offer" values for both the effective porosity and the specific yield for clays and some other low-permeable rocks as high as 35 percent or more, without providing an explanation of the unique method that discovered this amazing natural phenomenon. And some recent hydrogeology

publications available for free on the web list something even more amazing: the effective porosity of certain rock types is listed higher than their total porosity!

In any case, and regardless of the rock type, effective porosity is always smaller than total porosity.

To repeat this key fact: effective porosity of porous media (all sediments and all types of rocks in general) is always smaller than the total porosity.

ASTM (American Society for Testing and Materials) standard D2325 (now superseded by ASTM D6836) can be used to determine *effective drainage porosity* of medium to coarse grain sediments from *water retention* and *full saturation water content* (Figure 2.9).
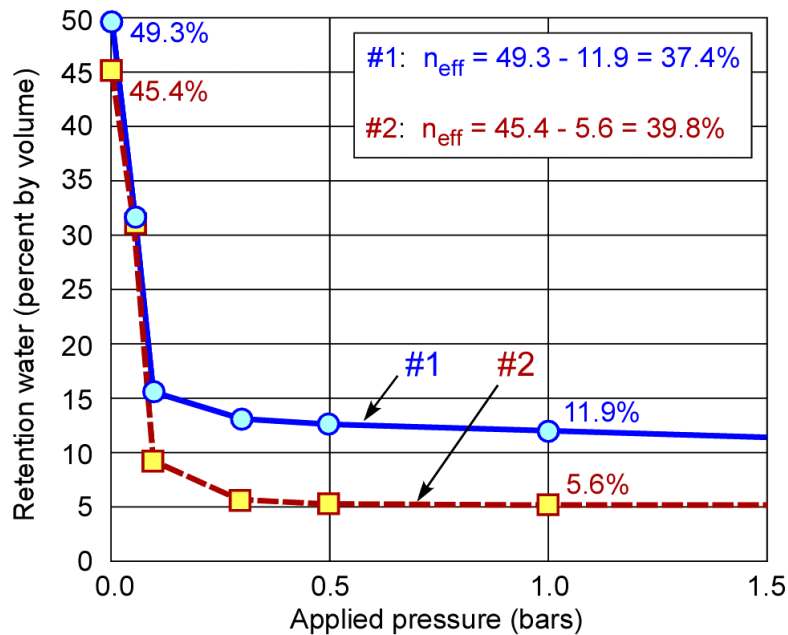
Figure 2.9 Typical graph of a water retention test by ASTM D2325, for two clean uniform beach sands. The *effective drainage porosity* is found for an applied pressure by subtracting the retained percent water (by volume) from the full saturation percent water. Applied pressure of 1 bar corresponds to free gravity drainage. From Kresic, 1998. Copyright Law Engineering and Environmental Services.

Total, and therefore effective porosity of consolidated rocks generally decreases with depth. Matrix porosity decreases mainly due to compaction, while decrease in the secondary fracture porosity is a combination of two main factors: 1) high fracture density near land surface and at shallow depths as the result of over-relaxation due to removal of the overlying solid matter by erosion, and 2) lower fracture density and smaller fracture aperture at greater depths due to high pressures exerted by the overlying rock mass. In addition to its general decrease with depth, the fracture porosity, even when fractures appear to be frequent and of notable size, is almost always much lower than the surrounding matrix porosity of compact blocks which make up the bulk of the overall rock volume. The following examples illustrate these two points:

1. Groundwater in the granites and gneisses of Connecticut occurs largely in vertical joints, which have an average spacing between 3 and 7 feet at the surface. At depths of more than 50 feet, the spacing is greater, owing to the dying out of subordinate joints. At still greater depths there appear to be very few water-bearing joints, 250 feet being the depth fixed as a limit beyond which is not advisable to drill for water. Of the horizontal joints, almost all are limited to the upper few feet of the rock, being generally above the water

table. While the joints may be half an inch or more in width at the surface, they rapidly narrow with depth, so that the common width in the upper 200 or 300 feet is 0.01 inch (Ellis, 1909).

2. In a rock cut by three sets of fractures, each set with fractures spaced 5 feet apart, if the average thickness of the void space in each fracture is 0.01 inch, the total void space represented by the fractures is only one-twentieth of 1 percent of the total volume of the rock (Meinzer, 1923a).

Carbonate and sandstone aquifers are the most important consolidated rock aquifers worldwide (see Lecture 7). However, the nature of porosity in these two rock types is notably different as shown in Table 2.1. Most importantly, in soluble carbonate rocks (such as limestone, dolomite, chalk, anhydrite, gypsum, marbles, and carbonate conglomerates) the matrix and secondary porosity are enhanced and enlarged by the process of *karstification* or dissolution of carbonate minerals by flowing water containing weak carbonic acid (Figures 2.10 and 2.11). As can be seen from the Figure 2.7, limestone, the principal rock of karst aquifers worldwide, has the widest porosity range of all rocks thanks to many different depositional environments and processes of its diagenesis (conversion of lose carbonate sediment into consolidated rock). Since major oil fields around the world are hosted in limestone and dolomite reservoirs, there is abundant literature on the porosity, diagenesis, and classification of carbonate sedimentary rocks with classic works by Folk (1959, 1980) and Bathurst (1975) still holding on their own. More on the process of karstification and karst aquifers is presented in Lecture 7.

Figure 2.10 Hydrogeology professor Dr. David Drew of Trinity College, Dublin, Ireland observing fractures enlarged by limestone dissolution in the famous karst area of Ireland called Burren.

Figure 2.11 Spectacular karren "jungle", limestones of Maganik Mountain, Montenegro. Photo courtesy of Dobrislav Bajović Bajone.

Aspect	Sandstone	Carbonate
Amount of primary porosity in sediments	Commonly 25%-40%	Commonly 40%-70%
Amount of ultimate porosity in rocks	Commonly half or more of initial porosity; 15%-30% common	Commonly none or only small fraction of initial porosity; 5%-15% common in reservoir facies
Type(s) of primary porosity	Almost exclusively interparticle	Interparticle commonly predominates, but intraparticle and other types are important
Type(s) of ultimate porosity	Almost exclusively primary interparticle	Widely varied because of post-depositional modifications
Size of pores	Diameter and throat sizes closely related to sedimentary particle size and sorting	Diameter and throat size commonly show little relation to sedimentary particle size or sorting
Shape of pores	Strong dependence on particle shape–a "negative" of particles	Greatly varied, ranges from strongly dependent "positive" or "negative" of particles to form completely independent of shapes of depositional or diagenetic components
Uniformity of size, shape, and distribution	Commonly fairly uniform within homogeneous body	Variable, ranging from fairly uniform to extremely heterogeneous, even within body made up of single rock type
Influence of diagenesis	Minor; usually minor reduction of primary porosity by compacxtion and cementation	Major; can create, obliterate, or completely modify porosity; cementation and solution important
Influence of fracturing	Generally not of major importance in reservoir properties	Of major importance in reservoir properties if present
Visual evaluation of porosity and permeability	Semiquantitative visual estimates commonly relatively easy	Variable; semiquantitative visual estimates range from easy to virtually impossible; instrument measurements of porosity, permeability and capillary pressure commonly needed
Adequacy of core analysis for reservoir evaluation	Core plugs of 1-in. diameter commonly adequate for "matrix" porosity	Core plugs commonly inadequate; even whole cores (~3-in. diameter) may be inadequate for large pores
Permeability-porosity interrelations	Relatively consistent; commonly dependent on particle size and sorting	Greatly varied; commonly independent of particle size and sorting

Table 2.1 Comparison of porosity in sandstone and carbonate rocks (Choquette and Pray, 1970; Copyright AAPG, 1970, reprinted by permission of the AAPG whose permission is required for further use).

2.2 Groundwater Storage, Specific Yield, and Coefficient of Storage

Groundwater is stored in and withdrawn from storage or pore spaces (voids) within porous media (rocks) of the saturated zone. An *aquifer* is a geologic formation, a group of formations, or a part of a formation that contains sufficient saturated permeable material to yield significant quantities of water to wells and springs. A water-table or unconfined aquifer is an aquifer whose upper water surface (water table or top of the saturated zone) is at atmospheric pressure, and thus can freely rise and fall. Groundwater in aquifers between layers of poorly permeable rock, such as clay or shale, is confined under pressure. If such a confined aquifer is tapped by a well, water will

rise above the top of the aquifer and may even flow from the well onto the land surface. Water confined in this way is said to be under artesian pressure, and the aquifer is called an artesian aquifer or a confined aquifer (USGS, 2022.)

Land surface

Root zone

Vadose zone

Available storage

High water table

Dynamic storage

Low water table

Saturated zone

Static storage

Base of aquifer

Confining layer
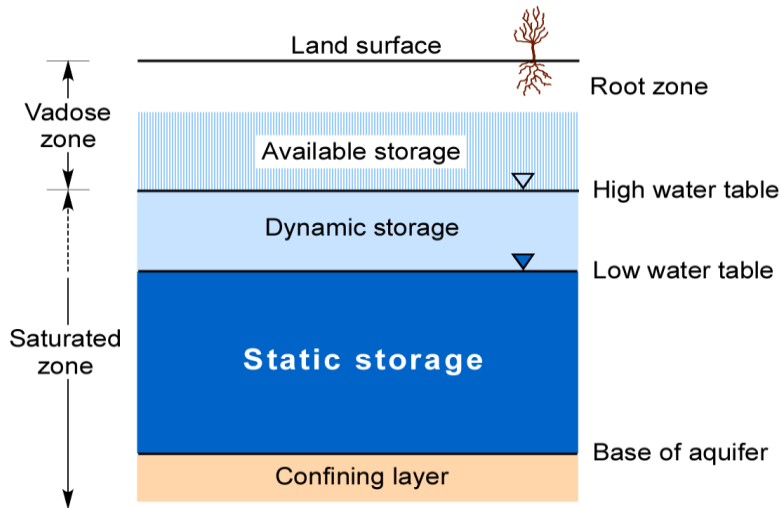
Figure 2.12 Schematic of different groundwater storage components in an unconfined aquifer. Note that groundwater is constantly flowing in both the dynamic and the static parts of the storage. Modified from Milojević, 1967. University of Belgrade; acknowledgment required for further use.

Figure 2.12 shows some key concepts of the natural groundwater storage. The portion of the saturated zone that changes its thickness in response to natural recharge patterns represents *dynamic storage*. This storage volume can vary widely in time depending on seasonal and long-term fluctuations of precipitation and other sources of groundwater (aquifer) recharge. Over a multiyear period spanning several natural cycles of wet and dry years, and in the absence of artificial (anthropogenic) groundwater withdrawals, this part of the storage can be considered as fully renewable. The portion of the saturated zone below the multiyear low water table has constant volume of stored groundwater and is therefore referred to as long-term or *static storage*, even though groundwater in it is constantly flowing. The static storage remains unchanged if the withdrawals equal the dynamic storage. In the presence of artificial groundwater withdrawals, the long-term static storage can decrease if the extracted volume of water exceeds the dynamic storage. This is called aquifer mining and is evidenced by the continuing excessive decline of the water table of unconfined aquifers, or hydraulic head (piezometric surface) of confined aquifers (see Lecture 5) or decrease of spring flows (Figure 2.13). When considering artificial aquifer recharge, the *available storage*, i.e., that part of the vadose zone that can be safely filled up, is one of the key design parameters to be characterized.

Examples of a catastrophic influence of aquifer pumping and mining on "groundwater reservoirs" (storage) that sustain aquatic life and the environment in general are numerous, both in the United States and around the world. One such example is Comanche Springs at Fort Stockton, Pecos County, Texas: "These artesian springs, issuing from a Comanchean limestone groundwater reservoir, formerly flowed as much as 66 ft^3/s, and served the Comanche and other Indians for uncounted hundreds of years. From 1875 on the springs were the basis for an irrigation district which supplied water to 6,200 acres of cropland. Heavy pumping of the aquifer lowered the water table so that the spring discharge began to fall off in May 1947. The irrigation district sought an injunction in 1954 to restrain pumping which interfered with the normal flow of Comanche Springs. The injunction was denied by the courts, and the springs ceased to flow in March 1961." (Gunnar Brune, 1975: *Major and Historical Springs of Texas*, Texas Water Development Board Report 189, Austin.)
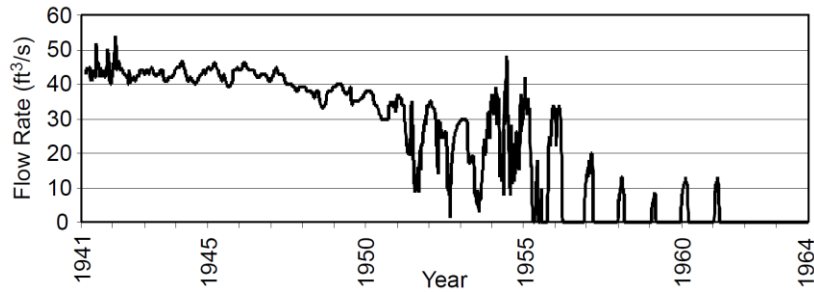
Figure 2.13 Top: Mean daily discharge hydrograph of Comanche Springs in Fort Stockton, Texas. USGS, 2008; in public domain. Aerial view of Comanche Springs pool in 1938, at the time a popular tourist destination in Fort Stockton, Texas. The springs ceased to flow due to excessive groundwater pumping for irrigation. Photo courtesy of Fort Stockton Historical Society.

Two very different mechanisms are responsible for groundwater release from storage in unconfined and confined aquifers. Respectively, they are explained with two quantitative parameters – specific yield and coefficient of storage.

Specific yield of the porous material is defined as the volume of water in the pore space that can be freely drained by gravity due to lowering of the water table. The volume of water retained by the porous media, which cannot be easily drained by gravity, is called *specific retention*. Together, the specific yield and the specific retention are equal to the total porosity of the porous medium (rock).

Since drainage of pore space by gravity may take long periods of time, especially in fine-grained sediments, values of specific yield determined by various laboratory and field methods are likely somewhat lower than the true values due to limited testing times. A long-term aquifer pumping test, or a continuous monitoring of the hydraulic head increase due to a known recharge, are arguably the most reliable methods of determining the value of specific yield, which is one of the key parameters for defining quantities of extractable groundwater. These tests provide a long-term lumped hydrodynamic response to pumping (or recharge) by all porous media present in the groundwater system. Consequently, the value of specific yield obtained from such tests cannot be explicitly related to values of effective porosity, even though these two parameters have been often equated by working professionals.

Values of specific yield are readily found in literature and as expected, vary widely due to inevitable heterogeneity of natural aquifers and different field-testing methods. Unfortunately, some hydrogeology textbooks "offer" values for both the effective porosity and the specific yield for clays and some other low-permeable rocks as high as 35 percent or more, without providing an explanation of the unique method that discovered this amazing natural phenomenon.

Figure 2.14 shows values of average total porosity of uniform unconsolidated sediments (clay through coarse sand) processed from data provided by Wolff (1982) and Kresic (2007), versus specific yield values listed by Johnson (1967). Total porosity values for gravel were not available, as it is usually not feasible to collect undisturbed gravel samples in the field. However, as first demonstrated by Slichter (1899), uniform sand and uniform gravel of the same grain packing (spatial arrangement of grains) have the same theoretical porosity regardless of the grain size. Professional judgment should be exercised when using this graph for site-specific calculations since it shows that the specific yield has a range of possible values, even for uniform materials. In general, presence of fine-grained sediments such as silt and clay, even in relatively small quantities, can greatly reduce specific yield (effective porosity) of sands and gravels. This is illustrated in Figure 2.15 which can be used to find specific yield (and effective porosity) for various heterogeneous mixtures of sand, silt, and clay. A very detail discussion of the specific yield concept, various methods of measurements, and case studies is given by Johnson (1967).
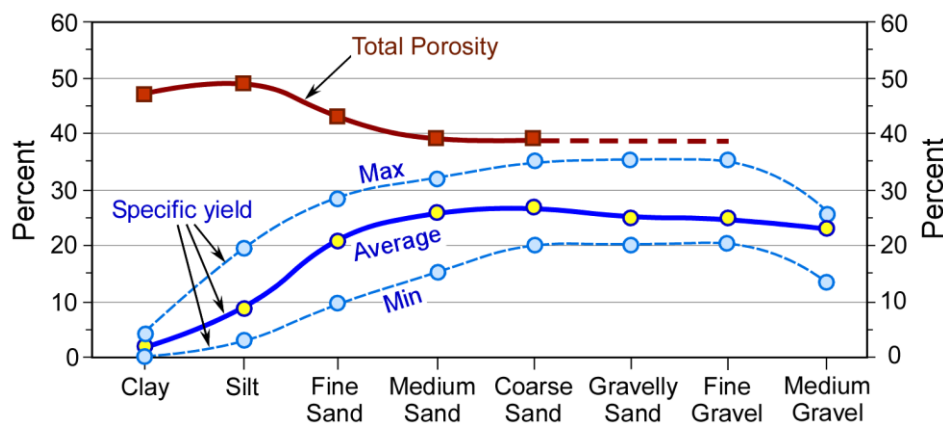
Figure 2.14 Total porosity vs. specific yield. Data from Wolff (1982) and Johnson (1967). USGS, in public domain.

The main challenge in using specific yield and effective porosity interchangeably is that values of effective (and total) porosity are often determined in the laboratory for small samples and must be extrapolated (upscaled) to real field conditions, i.e., to a much larger aquifer volume. One important distinction between the specific yield and the effective porosity concepts is that the specific yield relates to volume of water that can be freely extracted from an aquifer, while the effective porosity relates to groundwater flow through the interconnected pore space.

In any case, using total (instead of effective) porosity for calculations of extractable volumes of water would be completely erroneous, as pointed out by Meinzer (1923) in one of his classic publications:

The importance of water that a saturated rock will furnish, and hence its value as a source of water supply, depends on its specific yield – not on its porosity. Clayey or silty formations may contain vast amounts of water and yet be unproductive and worthless for water supply, whereas a compact but fractured rock may contain much less water and yet yield abundantly. To estimate the water supply obtainable from a given deposit for each foot that the water table is lowered, or to estimate the available supply represented by each foot of rise in the water table during a period of recharge, it is necessary to determine the specific yield. Estimates of recharge or of available supplies based on porosity, without regard to the water-retaining capacity of the material, may be utterly wrong."
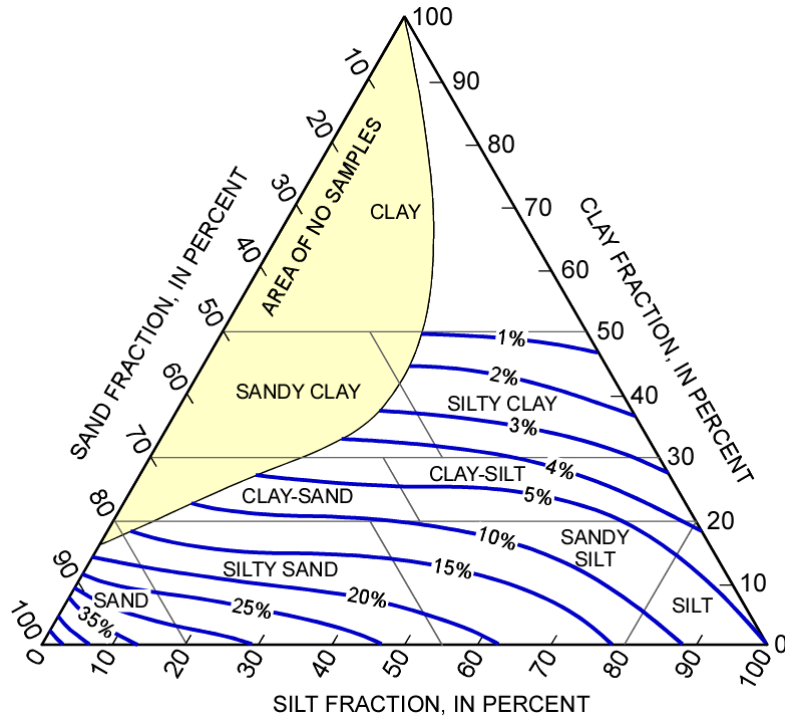
Figure 2.15 Soil classification triangle showing the relationship between particle size and specific yield. Lines of equal specific yield are at 1% and 5% intervals. Particle size of sand is 2 to 0.0625 mm, of silt it is 0.0625 to 0.004 mm, and of clay it is < 0.004 mm. This graph can also be used to find values of effective porosity as these two quantities are approximately the same. From Johnson, 1967. USGS, in public domain.

Storage of confined aquifers is entirely dependent on compression and expansion of both water and solids, or its elastic properties. Figure 2.16 shows the forces interacting in a confined aquifer: total load exerted on a unit area of the aquifer (σ_T), part of the total load borne by the confined water (ρ), and part borne by the structural skeleton (solids) of the aquifer (σ_e). If the total load exerted on the aquifer is constant, and if ρ is reduced because of pumping, the load borne by the skeleton of the aquifer will increase. This will result in a slight compaction (distortion) of the grains of material which means that they will encroach somewhat on pore space formerly occupied by water and water will be squeezed out. At the same time, the water will expand to the extent permitted by its elasticity. Conversely, if ρ increases, as in response to cessation of pumping, the hydraulic (piezometric) head builds up again, gradually approaching its original value, and the water itself undergoes slight contraction. With an increase in ρ there is an accompanying decrease in σ_e and the grains of material in the aquifer skeleton return to their former shape. This releases pore space that can now be re-occupied by water moving into the part of the formation that was previously influenced by the compression (Ferris et al., 1962).

Storage properties (storativity) of confined aquifers are defined by the *coefficient of storage*. Although firm limits cannot be established, the storage coefficients of confined aquifers may range from about 0.00001 to 0.001. In general, denser aquifer materials have smaller coefficient of storage. It is important to note that the value of coefficient of storage in confined aquifers may not be directly dependent on void content (porosity) of the aquifer material (USBR, 1977).

Specific storage (S_s) of confined aquifers is the volume of water released (or stored) by the unit volume of porous medium, per unit surface of the aquifer, due to unit change in the component of hydraulic head normal to that surface (detail explanation of the hydraulic head concept is given in next section.) The unit of specific storage is length^{-1} (e.g., m^{-1} or ft^{-1}) so that, when the specific storage is multiplied by aquifer thickness (b), it gives the coefficient of storage (S), which is a dimensionless number: $S = S_s b$. The specific storage is given as:

$$S_s = \rho_w g(\alpha + n\beta) \qquad (2.4)$$

where: ρ_w is the density of water; g is the acceleration of gravity; α is the compressibility of the aquifer skeleton; n is the total porosity, and β is the compressibility of water.
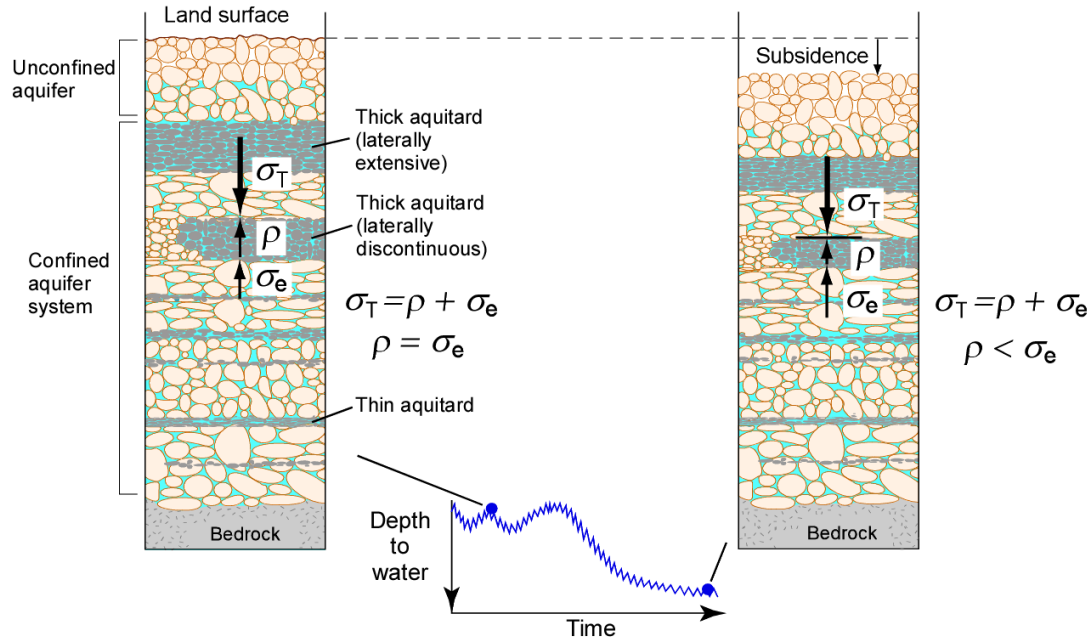
Figure 2.16 Left: In a confined aquifer system, the total weight of the overlying rock and water (σ_T) is balanced by the pore-fluid pressure (ρ) and the intergranular or effective stress (σ_e). Right: Groundwater withdrawal reduces fluid pressures (ρ). As the total stress (σ_T) remains nearly constant, a portion of the load is shifted from the confined fluid to the skeleton of the aquifer system, increasing the effective stress (σ_e) and causing some compression (reduction in porosity). Extended periods of lowered hydraulic head may result in irreversible compaction of the skeleton and land subsidence. Most of the land subsidence occurs because of the permanent compaction of the aquitards, which may be delayed due to their slow drainage. Modified from Galloway et al., 1999. USGS, in public domain..

All other things being equal, the radius of pumping well influence in a confined aquifer would be significantly larger than in an unconfined aquifer. This is because less water is withdrawn from the same aquifer volume in the case of confined aquifers due to the elastic nature of water release from the voids. In other words, to provide the same well yield (volume of water), a larger aquifer area would be affected in a confined aquifer than in an unconfined aquifer, assuming they initially have the same saturated thickness.

Storage capacity of a groundwater system may be irreversibly affected by extensive groundwater withdrawals. As shown in Figure 2.16, because of the hydraulic head decline in the aquifer system due to pumping, some of the support for the overlying material previously provided by the pressurized water filling the sediment pore space shifts to the granular skeleton of the aquifer system. This increases the intergranular pressure (load). Sand and gravel deposits are relatively incompressible, and the increased intergranular load has small effect on these aquifer materials. However, clay and silt layers comprising confining units and interbeds can be very compressible as water is squeezed from these layers in response to the hydraulic gradient caused by pumping. When long-term declines in the hydraulic head increase the intergranular load beyond the previous maximum load, the structure of clay and silt layers may undergo significant rearrangement, resulting in irreversible aquifer system compaction and land subsidence. The amount of compaction is a function of the thickness and vertical hydraulic conductivity of the clay

and silt layers, and the type and structure of the clays and silts. Because of the low hydraulic conductivity of clay and silt layers, the compaction of these layers can continue for months or years after water levels stabilize in the aquifer. In confined aquifer systems that contain significant clay and silt layers and are subject to large-scale groundwater withdrawals, the volume of water derived from irreversible compaction commonly can range from 10 to 30 percent of the total volume of water pumped. This represents a one-time mining of stored groundwater and a permanent reduction in the storage capacity of the aquifer system (Alley et al.,1999; Galloway et al.,1999).

The first recognized land subsidence in the United States from aquifer compaction as a response to groundwater withdrawals was in Santa Clara Valley (now known as Silicon Valley) in California. Some other well-known areas experiencing significant land subsidence due to groundwater mining include the basin-fill aquifers of south-central Arizona, Las Vegas Valley in Nevada, and the Houston-Galveston area of Texas.

Nothing, however, compares with the example of over-exploitation of confined aquifers and the related consequences illustrated in Figure 2.17. Mining groundwater for agriculture has enabled the San Joaquin Valley of California to become one of the world's most productive agricultural regions, while simultaneously contributing to one of the single largest alterations of the land surface attributed to humankind. In 1970, subsidence in excess of 1 foot had affected more than 5,200 square miles of irrigable land—one-half the entire San Joaquin Valley. The maximum subsidence, near Mendota, was more than 28 feet (9 meters). As discussed by Galloway et al. (1999), the economic impacts of land subsidence in the San Joaquin Valley are not well known. Damages directly related to subsidence have been identified, and some have been quantified. Other damages indirectly related to subsidence, such as flooding and long-term environmental effects, merit additional assessment. Some of the direct damages have included decreased storage in aquifers, partial or complete submergence of canals and associated bridges and pipe crossings, collapse of well casings, and disruption of collector drains and irrigation ditches. Costs associated with these damages have been conservatively estimated at 25 million US dollars. These estimates are not adjusted for changing valuation of the dollar, and do not fully account for the underreported costs associated with well rehabilitation and replacement. When the costs of lost property value due to condemnation, regarding irrigated land, and replacement of irrigation pipelines and wells in subsiding areas are included, the annual costs of subsidence in the San Joaquin Valley soar to $180 million per year in 1993 dollars (G. Bertoldi and S. Leake, USGS, written communication, March 30, 1993; from Galloway et al., 1999).
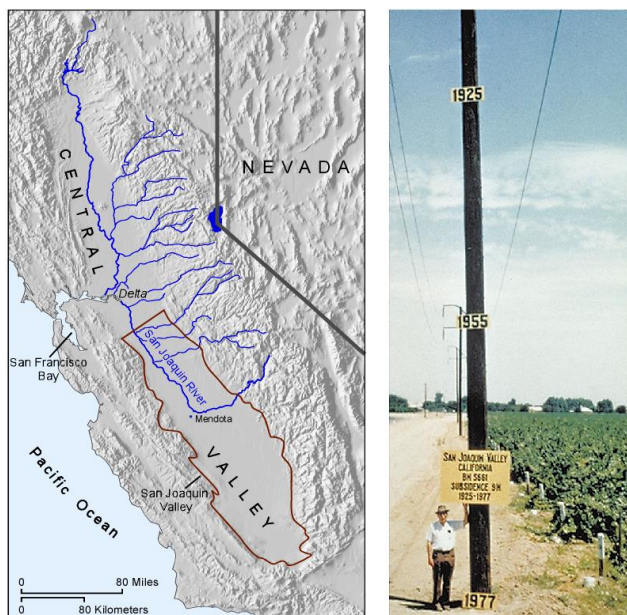
Figure 2.17 Approximate location of maximum subsidence in the United States identified by research efforts of Joseph Poland of the USGS (pictured). Signs on pole show approximate altitude of land surface in 1925, 1955, and 1977. The pole is near benchmark S661 in the San Joaquin Valley southwest of Mendota, California (the valey is outlined in the map on the left. Modified from Galloway et al., 1999. USGS, in public domain.

Lecture 3 Groundwater Flow, Part One

This lecture is based on the materials presented in Kresic, 2007 (*Hydrogeology and Groundwater Modeling, Second Edition*. Copyright CRC Taylor & Francis); Kresic, 2009 (*Groundwater Resources: Sustainability, Management, and Restoration.* Copyright McGraw Hill); Kresic and Mikszewski, 2013 (*Hydrogeological Conceptual Site Models: Data Analysis and Visualization*. Copyright CRC Taylor & Francis), and various publications by the authors of USGS.

Groundwater in the saturated zone is always in motion, in a three-dimensional space, because of the two key factors:

1. The effective porosity of rock is of such magnitude that it allows gravity groundwater flow; in other words, the rock is *permeable*. If the flow of groundwater due to gravity forces is negligible, the rock is not permeable, and the concepts of groundwater flow described further are not applicable.
2. There is *hydraulic gradient* in the three-dimensional direction; in other words, there is difference in the hydraulic head of groundwater between various points in that three-dimensional direction which causes groundwater to flow from the higher hydraulic head towards the lower hydraulic head.

A simple analogy would be flow of water through pipes or in open channels. The water will move if the hydraulic pressures at two ends of the pipe are different, or if the elevation of water surface at one end of the open channel is higher than the water surface elevation at the other end. If there is no such difference in "pressures" or elevations, the water will not move. This hydraulic pressure is called the *hydraulic head* in groundwater studies. However, term "fluid pressure" has specific meaning in hydrogeology and should not be equated with the hydraulic head.

3.1 Darcy's Law

French civil engineer Henry Darcy was first to quantitatively analyze, through a series of experiments, a downward flow of water through loose filter sands as part of design of water supply for the city of Dijon. In an appendix to his book, Les Fontaines Publiques de la Ville de Dijon published in 1856, he established that the rate of flow is given by the equation:

$$q = -\frac{K(h_2 - h_1)}{l} \qquad (3.1)$$

in which q is the volume of water crossing unit area in unit time, l is the thickness of the sand, h_2, and h_1 are the heights above a reference level of the water in manometers terminated above and below the sand, respectively, and K is a factor of proportionality. Note that equation (3.1) has dimension of length over time (L/T) and does not actually calculate the rate of flow (which has units L^3/T such as m^3/s or ft^3/d). Instead, it establishes an experimental, proportional relationship.

This experimental quantitative relationship, later shown to have real theoretical basis, became known as *Darcy's law*. In a dimensionally correct form, it states that the rate of fluid flow (Q) through a sand sample is

directly proportional to the cross-sectional area of flow (A) and the loss of the hydraulic head between two points of measurements, also called *hydraulic gradient* (Δh), and it is inversely proportional to the length of the sample (l) as shown in Figure 3.1:
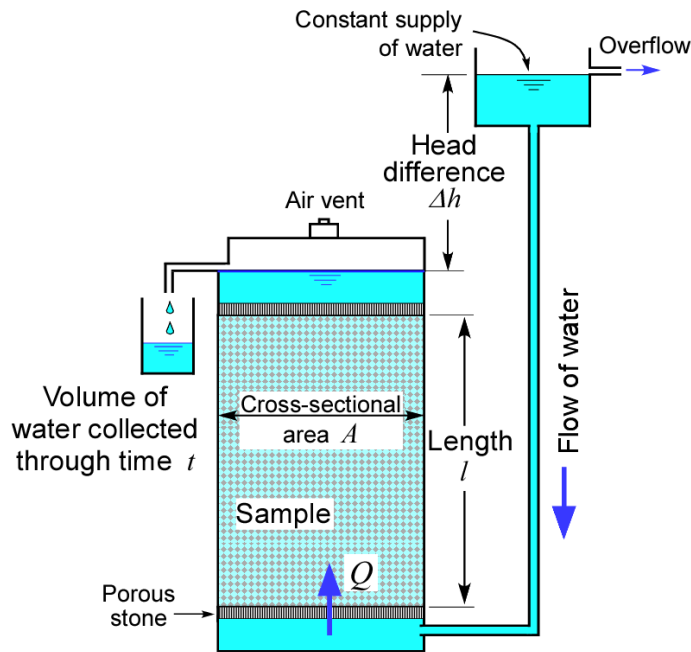
Figure 3.1 Schematic presentation of the constant head permeameter (similar to the one used by Henry Darcy) used to determine hydraulic conductivity of unconsolidated sediments. Modified from Kresic, 2007. Copyright CRC Taylor & Francis; permission is required for further use.

$$Q = KA\frac{\Delta h}{l} \qquad (3.2)$$

K is the proportionality constant of the law called *hydraulic conductivity* and has units of velocity (note, however, that K should not and cannot be equated to actual groundwater flow velocity – see Lecture 4, Section 4.2.) This constant is arguably the most important quantitative parameter characterizing the flow of groundwater.

It is not uncommon to find the minus sign in front of equation (3.2) in the literature with the following explanation: it indicates that the flow is in the direction of decrease in the hydraulic head (i.e., from the higher toward the lower hydraulic heads). However, although the explanation is correct, the minus sign should not be placed in front of equation (3.2) which is the solution of a differential form of Darcy's equation. The minus sign, which is correctly present in the differential equation, disappears during its integration and it is mathematically incorrect to show it as a part of equation (3.2).

The general hydraulic equation of the continuity of flow, which results from the principle of conservation of mass, is (for incompressible fluids):

$$Q = v_1 A_1 = v_2 A_2 = \text{ constant} \qquad (3.3)$$

which means that the volumetric flow rate (Q) through successive cross-sectional areas A_1 and A_2 in a stream of fluid is the same (there is no loss or gain of water). Average flow velocities at successive cross-sections 1 and 2 are v_1 and v_2 respectively. From equation (3.3), the velocity of flow can be generally expressed as:

$$v = \frac{Q}{A} \qquad (3.4)$$

Relating equations (3.2) and (3.4) gives another form of Darcy's equation where $\Delta h/l$ is the *hydraulic gradient*, i:

$$v = K\frac{\Delta h}{l} = K * i \qquad \left[\frac{m}{s} \text{ or } \frac{ft}{d}\right] \qquad (3.5)$$

Dimension of equation (3.5) is that of velocity but, as discussed further in Lecture 4 (Section 4.2), v is not true groundwater flow velocity. For this reason, v in Darcy's Law is sometimes called "specific discharge" or "Darcy's velocity" to avoid confusion, although this practice may sometimes be even more confusing to non-hydrogeologists and others dealing with groundwater without proper training.

3.2 Hydraulic Conductivity and Permeability

Another quantitative parameter used in studies of fluid flow though porous media is called *intrinsic permeability*, or simply *permeability*. It is defined as the ease with which a fluid can flow through a porous medium. In other words, permeability characterizes the ability of a porous medium to transmit a fluid (water, oil, gas, etc.). It is dependent only on the physical properties of the porous medium: grain size, grain shape and arrangement, or pore size and interconnections in general. On the other hand, the hydraulic conductivity is dependent on the properties of both the porous medium and the fluid. The relationship between the permeability (K_i) and the hydraulic conductivity (K) is expressed through the following formula:

$$K_i = K\frac{\mu}{\rho g} \qquad [m^2] \qquad (3.7)$$

where μ is the *absolute viscosity* of the fluid (also called *dynamic viscosity* or simply *viscosity*), ρ is the *density* of the fluid, and g is the *acceleration of gravity*. The viscosity and the density of the fluid are related through the property called *kinematic viscosity* (v):

$$v = \frac{\mu}{\rho} \qquad [m^2/s] \qquad (3.8)$$

Inserting the kinematic viscosity into equation (3.7) somewhat simplifies the calculation of the permeability since only one value (that of v) must be obtained from commonly available tables.

$$K_i = K\frac{v}{g} \qquad [m^2] \qquad (3.9)$$

Although it is better to express the permeability in the units of area (m^2 or cm^2) for reasons of consistency and easier use in other formulas, it is more commonly given in darcys (which is a tribute to Darcy by the oil industry and Wyckoff et al., who proposed the name for the unit in 1933):

$$1 \, darcy = 9.87 \times 10^{-9} \, cm^2 = 9.87 \times 10^{-13} m^2$$

When laboratory results of permeability measurements are reported in darcys (or meters squared), the following two equations (derived from equations 3.7 and 3.9) can be used to find the hydraulic conductivity:

$$K = K_i \frac{g}{v} \quad \text{or} \quad K = K_i \frac{\rho g}{\mu} \quad [\text{m/s}] \tag{3.10}$$

Kinematic viscosity of water at temperature of 20 °C is approximately 1×10^{-6} m^2/s, and gravity acceleration is often rounded to 10 m/s^2, which is the reason why the following approximate relation is used to convert permeability (given in m^2) to hydraulic conductivity (given in m/s):

$$K \ [\text{m/s}] \ = \ K_i \ [\text{m}^2] \times 10^7 \tag{3.11}$$

Since the effective porosity, as the main factor influencing the permeability of a porous medium, varies widely for both different and same rock types, the hydraulic conductivity has wide ranges as shown in Figure 3.2.
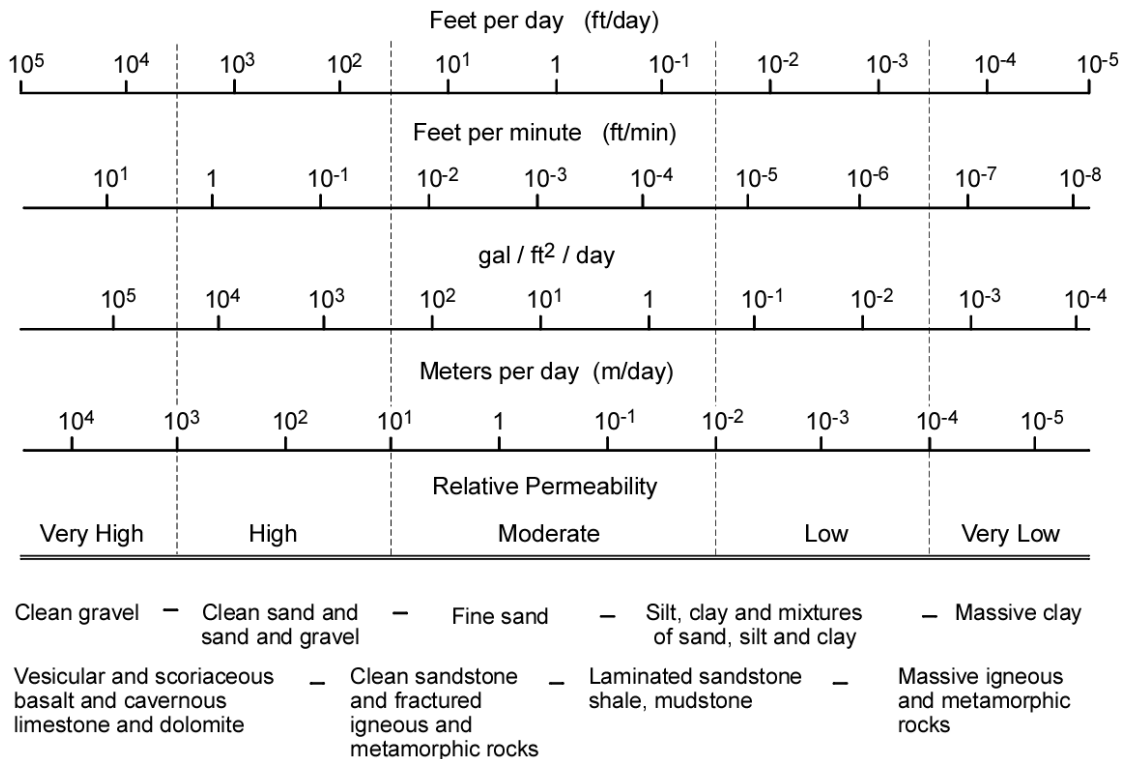
Figure 3.2 Range of hydraulic conductivity for different rock types. From USBR, 1977. In public domain.

Clear relationships exist between porosity and permeability, such that both generally decrease with depth in consolidated rock, or that fine-grained sediments (silt and clay) have lower permeability than coarse grained sediments (sand and gravel). However, an accurate quantitative prediction of permeability based on porosity data is rarely possible because of the heterogeneity of natural porous media. Very extensive field and laboratory measurements of this relationship have been routinely performed in the oil industry for decades, with plenty of available related literature. Two primary targets have been oil and gas reservoirs in carbonate and sandstone rocks worldwide. For example, Nelson and Kibler (2003) have compiled porosity and permeability measurements on cored samples from siliciclastic formations (sands, conglomerates, sandstones, siltstones, and shales) at 70 different

locations throughout the world (Figures 3.3 and 3.4 are examples from this source.) Three sands shown in Figure 3.3 have much higher porosity and smaller range of permeability than the sandstones example in Figure 3.4. At the same time, sands do not show any linear relationship between the two parameters. On the other hand, sandstones of all grain sizes clearly show a linear relationship.

As is the case with porosity, limestones have the widest range of hydraulic conductivity of all rocks. The following examples illustrate the variability of hydraulic conductivity of carbonate rocks. Chalk and some limestones may have high porosity, but since the pores are small (usually less than 10 micrometers, or μm), primary permeability is low and specific retention is high (Cook, 2003). For example, the mean interconnected porosity of the Lincolnshire Limestone in England is 15%, while the mean matrix hydraulic conductivity is only 10^{-9} m/s (Cook, 2003, after Greswell et al., 1998). The groundwater flow is largely restricted to the fractures. The aquifer hydraulic conductivity determined from pumping tests ranges between approximately 20-100 m/day, which is more than five orders of magnitude greater than the matrix hydraulic conductivity (Cook, 2003, after Bishop and Lloyd, 1990).
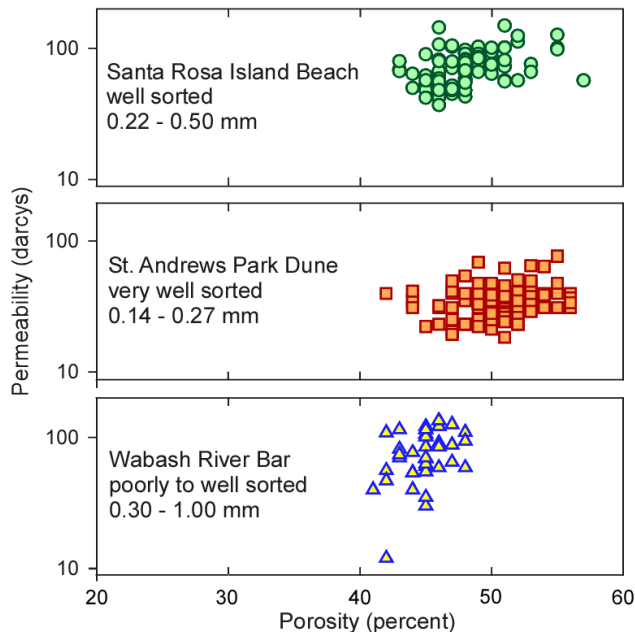
Figure 3.3 Porosity vs. permeability for three freshly deposited unconsolidated sand deposits (plotted by Nelson and Kibler, 2003; data from Pryor, 1973.) Permeabilities of the undisturbed samples were measured in a commercially available constant head–falling head permeameter adapted to the dimensions of the thin-wall aluminum sample tubes. Water permeabilities, in Darcy units, were measured at relatively low head pressures (50 cm of water) to prevent disturbance of the unconsolidated sand samples by elutriation and repacking. Porosity was measured by a modification of Ludwick's Volumeter and basing the calculations on the core volumes and grain volumes of the samples. USGS, in public domain.
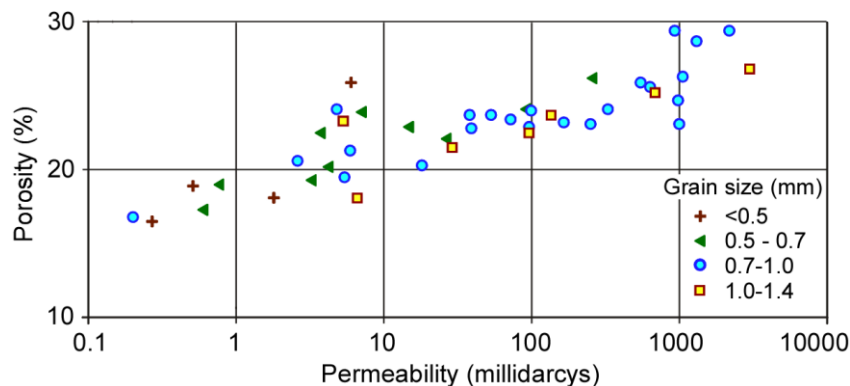
Figure 3.4 Porosity vs. permeability of Oligocene and Miocene sandstones at Yacheng Field, South China Sea Plotted by Nelson and Kibler, 2003; data from Bloch, 1991. USGS, in public domain.

The San Antonio segment of the Edwards aquifer in Texas, the United States, consists of Cretaceous limestones and dolomites that have undergone multiple periods of karstification. The average aquifer hydraulic conductivity, based on over 900 well pumping tests, is approximately 7 m/day, while the mean matrix hydraulic conductivity is approximately 10^{-3} m/day (Cook, 2003, after Halihan et al., 2000). Based on the results of 191 aquifer pumping tests, the median horizontal hydraulic conductivity of the Upper Floridan aquifer in Georgia, the United States, is 140.3 ft/d. Such high average value is, in part, the result of generally high effective matrix porosity of the Upper Floridan aquifer Tertiary carbonates, as illustrated with the data from west-central Florida (Figure 3.5).

Vesicular basalts can also have high hydraulic conductivity, but they are less permeable than limestone on average. Medium to coarse sand and gravel are rock types with the highest average hydraulic conductivities. Pure clays and fresh igneous rocks generally have the lowest permeability, although some field-scale bedded salt bodies were determined to have permeability of zero (Wolff, 1982). This is one of the reasons why salt domes were considered as potential depositories of high radioactivity nuclear wastes in various countries.
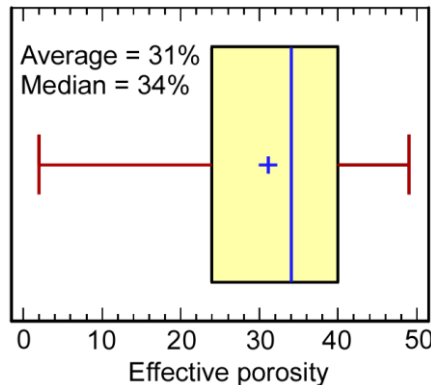
Figure 3.5 Box-and-Whisker plot of effective matrix porosity of the Upper Floridan carbonates in west-central Florida. The plot is based on analysis of 46 core samples from 10 different locations. Raw data from Knochenmus and Robinson, 1996. USGS, in public domain.
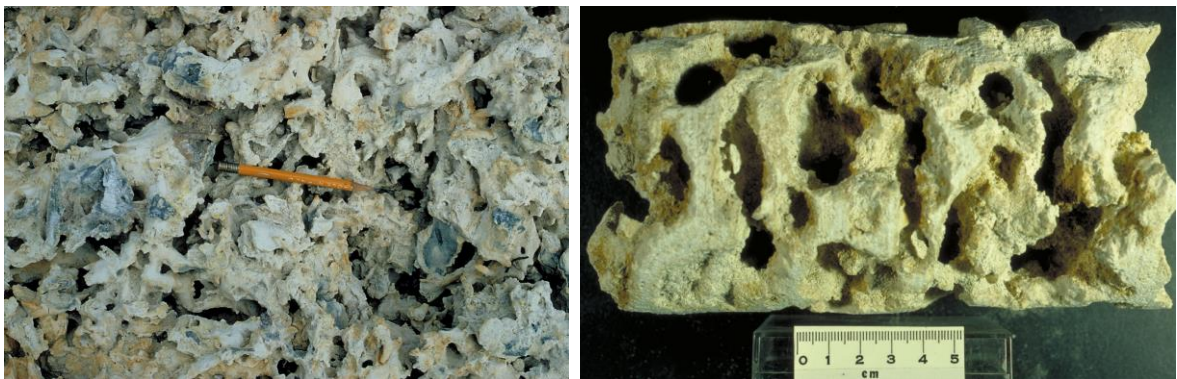
Figure 3.6 Young Florida limestones such as Miami oolite of the Biscayne aquifer shown here have very high primary matrix porosity which, together with the dissolution-enhanced secondary porosity makes them one of the most prolific aquifers in the world. Tested hydraulic conductivity can be as high as >1,000 ft/d. Photographs by George Sowers, printed with kind permission of Francis Sowers.

It has been shown that individually determined hydraulic conductivities from various locations within the same aquifer, or within the same geologic unit, approximately follow a logarithmic probability distribution as shown with examples in Figures 3.7 and 3.8. This observation is potentially useful when there is a need for an average value from multiple data. It is therefore advisable to use the geometric mean of individual measurements rather than the arithmetic mean.
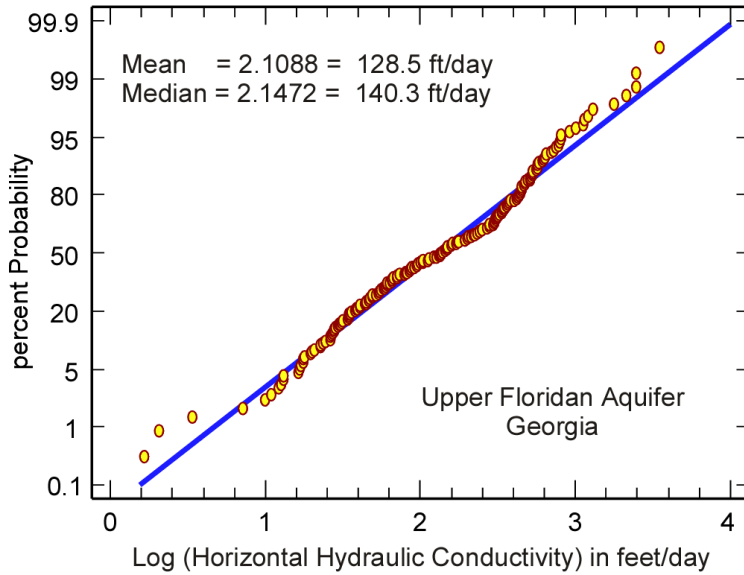
Figure 3.7 Distribution of horizontal hydraulic conductivity of the Upper Floridan aquifer in Georgia, the United States based on results of 191 aquifer pumping tests. Raw data from Clarke et al., 2004. USGS, in public domain.
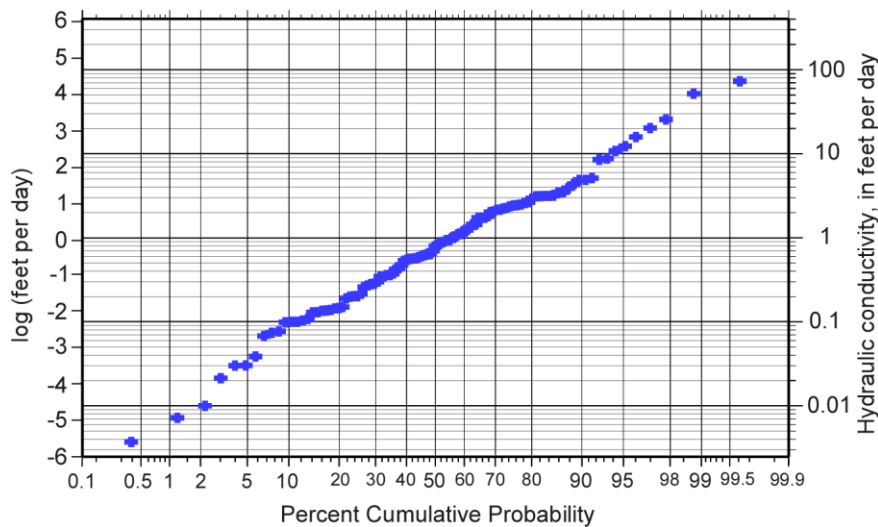
Figure 3.8 Distribution of hydraulic conductivity in the Piedmont regolith deposits, obtained from 105 slug tests at multiple sites in the greater Atlanta area and northern Georgia, the United States. The median value is 0.75 ft/d. Modified from Kresic, 2007. Copyright CRC Taylor & Francis; permission is required for further use.

3.3 Hydraulic Head and Hydraulic Gradient

The principle of the hydraulic head and the hydraulic gradient is illustrated in Figure 3.9. At the bottom of monitoring well #1, where the well screen is open to the saturated zone, the total energy (H) or the driving force for water at that point in the aquifer is:

$$H = z + h_p + \frac{v^2}{2g} \qquad (3.12)$$

where z is elevation above datum (datum is usually mean sea level, but it could be any reference level); h_p is pressure head due to pressure of fluid (groundwater) above that point; v is groundwater velocity; g is acceleration of gravity.
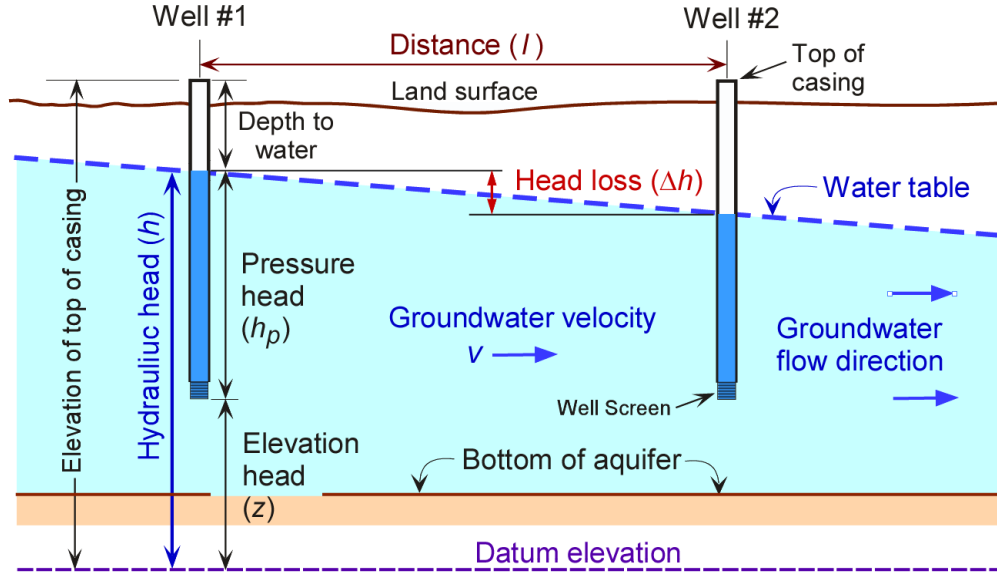
Figure 3.9 Schematic presentation of key elements for determining hydraulic head and hydraulic gradient in an unconfined aquifer. Modified from Kresic, 2007. Copyright CRC Taylor & Francis; permission is required for further use.

Since the groundwater velocity in most cases is very low, the third member on the right-hand side may be ignored for practical purposes and the equation (1.3) becomes:

$$H = h = z + h_p \qquad (3.13)$$

where h is the *hydraulic head*, sometimes called *piezometric head*. Pressure head represents pressure of fluid (p) of constant density (ρ) at that point in the aquifer:

$$h_p = \frac{p}{\rho g} \qquad (3.14)$$

In practice, the hydraulic head is determined in monitoring wells or piezometers by subtracting measured depth to water level from the surveyed elevation of the top of casing:

$$h = \text{elevation of top of casing} - \text{depth to water in the well} \qquad (3.15)$$

As the groundwater flows from well #1 to well #2 (Figure 3.9), it loses energy due to friction between groundwater particles and the porous media. This loss equates to decrease in the hydraulic head measured at the two wells:

$$\Delta h = h_1 - h_2 \qquad (3.16)$$

The *hydraulic gradient* (i) between the two wells is obtained when this decrease in the hydraulic head is divided by the distance (l) between the wells:

$$i = \frac{\Delta h}{l} \quad \text{[dimensionless]} \qquad (3.17)$$

It is important to emphasize that the groundwater flow takes place from a higher hydraulic head towards a lower hydraulic head, and not necessarily from a higher-pressure head to a lower-pressure head. One possible example illustrating this point is shown in Figure 3.10. In conclusion, one only must think in terms of differences in the hydraulic heads measured in the aquifer, not "worrying" about possible "oddities" such as an "unusual" geometric shape of the aquifer zone, the slope of the impermeable base, or the shape of confining layers. Some of these "oddities" are illustrated in Figure 3.11.

Except in case of some narrowly focused study of a very limited portion of the saturated (aquifer) zone, there is no such thing as strictly horizontal groundwater flow. Even in unconfined aquifers with a horizontal impermeable base, the flow of groundwater has a vertical component by default. This is illustrated in Figure 3.12 which shows groundwater flow from an area where aquifer recharge is dominant, towards an area where the groundwater discharges from the aquifer, such as to a surface water body or via a spring. In the recharge areas, the inflow of new water from percolating precipitation creates additional pressure head and displacement of the already stored water, which, in turn, displaces water in the discharge area. This displacement of water must be accommodated with both vertical and horizontal gradients. In many cases, especially in contaminant fate and transport studies, it is critically important to correctly characterize and quantify hydraulic gradients and groundwater flow in all three dimensions. For example, having three or more monitoring wells screened at same depths will do nothing in determining if there is a vertical flow component.
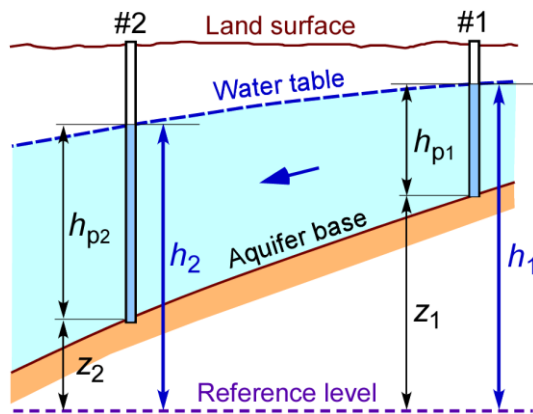
Figure 3.10 Groundwater flow is always from a higher hydraulic head towards a lower hydraulic head, not necessarily from a higher-pressure head towards a lower-pressure head. In this example, pressure head at well #2 is higher than at well #1, but the flow is from well #1 towards well #2 because $h_1 > h_2$. Modified from Kresic, 2007. Copyright CRC Taylor & Francis; permission is required for further use.
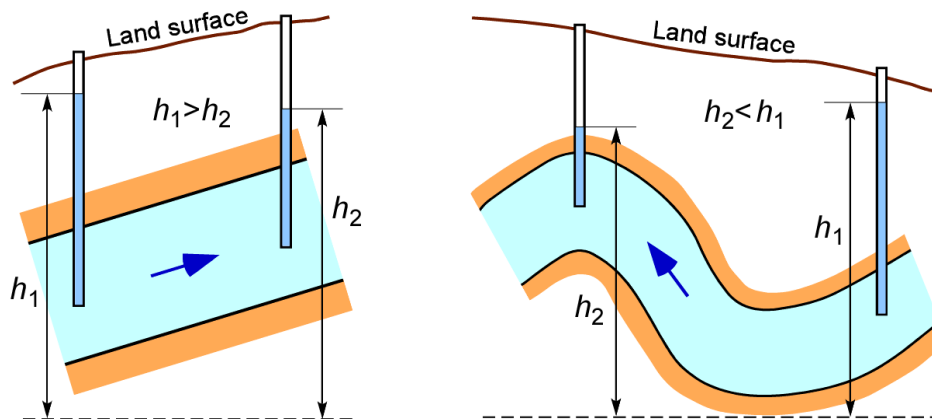
Figure 3.11 Some examples showing groundwater flow directions as they relate to slopes of water bearing layers (confined aquifers): the hydraulic gradient, and therefore the flow direction, can be in opposite direction of the aquifer slope. Modified from Kresic, 2007. Copyright CRC Taylor & Francis; permission is required for further use.
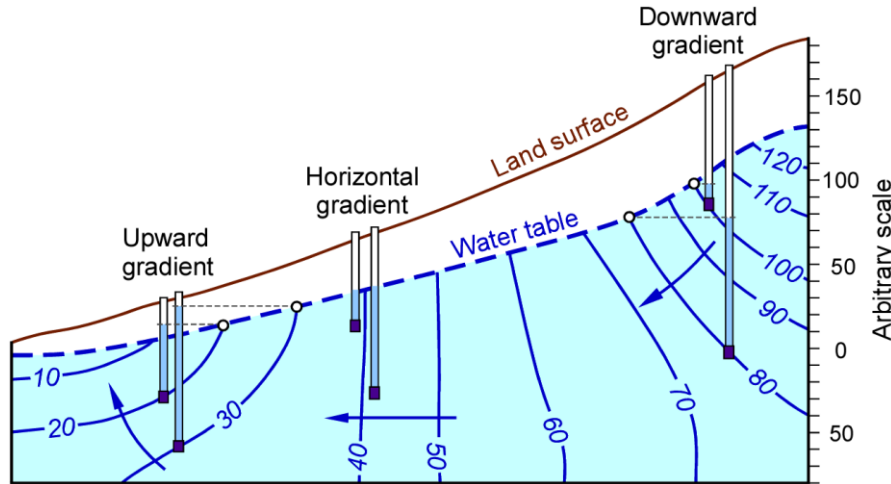
Figure 3.12 Movement of groundwater in an unconfined aquifer showing the importance of both vertical and horizontal hydraulic gradients. Modified from Winter, 1998. USGS, in public domain.

Confusion is sometimes present when using terms "pore water pressure", "hydraulic head", "pressure head", and "fluid pressure" without clearly understanding what any specific term is supposed to convey in a particular case. This sometimes happens in geotechnical engineering and soil mechanics fields where professionals commonly focus on the stability of various engineering structures (e.g., buildings, dams, levees) as affected by water present in the soil and rocks. This author has, unfortunately, witnessed multiple times how some geotechnical engineers equate "pore water pressure" with the hydraulic head, including readings from various instruments specifically designed to measure pore water pressure and not necessarily the elevation of water table or the piezometric head.

The water pressure within the soil voids, u, is termed neutral stress in soil mechanics. If the water is not moving, it can be computed from hydrostatics:

$$u = \gamma_w z_w \qquad (3.18)$$

where:

γ_w is the unit weight of water (62.4 lb/ft3, or 1 g/ml; in the SI system it is 9.81 kN/m³),
z_w is the vertical depth below water table to the location where the water table is computed.

If the water is moving, the water pressure can be computed from the pressure head (h_p) using reading from a piezometer (see Figure 3.9) by equation :

$$u = \gamma_w h_p \qquad (3.19)$$

The water pressure is uniform in all direction at one point but can change from one point to another because of the pressure head changes. Importantly, soil (rock) below water table is saturated and pressure head is greater than the atmospheric pressure, i.e., it is <u>positive</u>. At the water table it is <u>zero</u>, and above the water table including in the capillary fringe, it is <u>negative</u>, i.e., less than the atmospheric pressure (see Lecture 7.)

More discussion on various stresses that act on surfaces of an engineering structures resting on surface soil or built at some depth below ground surface including within saturated zone can be found in general textbooks on soil mechanics. An excellent one is *Introductory Soil Mechanics & Foundations: Geotechnical Engineering* by George Sowers; McMillan Publishing Co, New York, 1979.

3.4 Potentiometric Surface Maps

The potentiometric surface is the level to which groundwater would rise in piezometers or monitoring wells screened in the water-bearing formation, i.e., in the saturated zone being monitored. The potentiometric surface is equivalent to the water table in an unconfined aquifer. It is a hypothetical surface in case of confined aquifers as it represents the hydraulic heads which are, by definition, above the physical top of a confined aquifer (see Lecture 5.) In either case, maps of the potentiometric surface are created by plotting contour lines of the water level elevations recorded in individual piezometers (monitoring wells). They are one of the most important tools in hydrogeology, being essential in determining the hydraulic gradients, groundwater follow directions, flow velocity and rate, or serving as the basis for developing and calibrating groundwater flow models.

Measuring hydraulic heads and subsequently creating the piezometric surface maps are by no means straightforward tasks and require good planning by an experienced hydrogeologist. Ultimately, the number of piezometers and/or monitoring wells, their depths, screen lengths and frequency of water level recordings will be based on the final goal of the study.

When planning field measurements of the hydraulic head that will be used to create potentiometric surface maps, the following facts should always be taken into consideration:

1. Hydraulic head changes in response to aquifer recharge, both seasonally and, especially in unconfined aquifers, after each recharge episode (rainfall). Measurements in multiple wells should therefore be performed within the shortest time interval feasible (so–called *synoptic measurements*). To accurately assess seasonal influences on the hydraulic head fluctuations, at least one round of synoptic measurements should be performed per season.

2. Hydraulic head in confined aquifers changes in response to barometric pressure fluctuations; this is also true for unconfined aquifers but is much less pronounced in most cases. The only reasonable method to accurately determine the magnitude and importance of such changes is to measure the hydraulic head and the barometric pressure continuously using pressure transducers and data loggers. Note that the pressure transducers that are vented to the atmosphere automatically correct for the barometric pressure such that their data can be used directly.

3. Hydraulic head in coastal aquifers responds to harmonic tidal fluctuations. These changes can be accurately quantified only by performing continuous measurements.

4. Hydraulic head may change in response to some local hydraulic stress on the aquifer, such as operation of an extraction wells in vicinity.

Any of the above influences must be properly accounted for when interpreting the hydraulic head measurements. This is especially important when performing an aquifer pumping test and subsequently interpreting the data. The data should be corrected by subtracting that portion of the hydraulic head change attributable to each applicable external factor.

One common mistake by inexperienced hydrogeologists is to apply same approach of hydraulic head measurements and contouring of the potentiometric surface in different types of aquifers. For example, fractured rock and karst aquifers present great challenge even to more experienced professionals (see the next lecture.)

The following discussion is based mostly on the works of Kresic (1997, 2007), and Kresic and Mikszewski (2013.)

Manual contouring is frequently utilized in creating potentiometric surface maps as well as in general groundwater studies when representing other features of interest such as surfaces of hydrostratigraphic (geologic) layers or plumes of groundwater contaminants for example. It is utilized either as the only method or in conjunction with computer-based methods. A complete reliance on computer programs could, in some cases, lead to erroneous conclusions since they are not always able to interpret (recognize) features apparent to a hydrogeologist. This includes, for example, presence of geologic boundaries, heterogeneous porous media, influence of surface water bodies, or principles of groundwater flow. Thus, manual contouring or manual adjustment of computer-generated maps is an integral part of hydrogeologic studies.
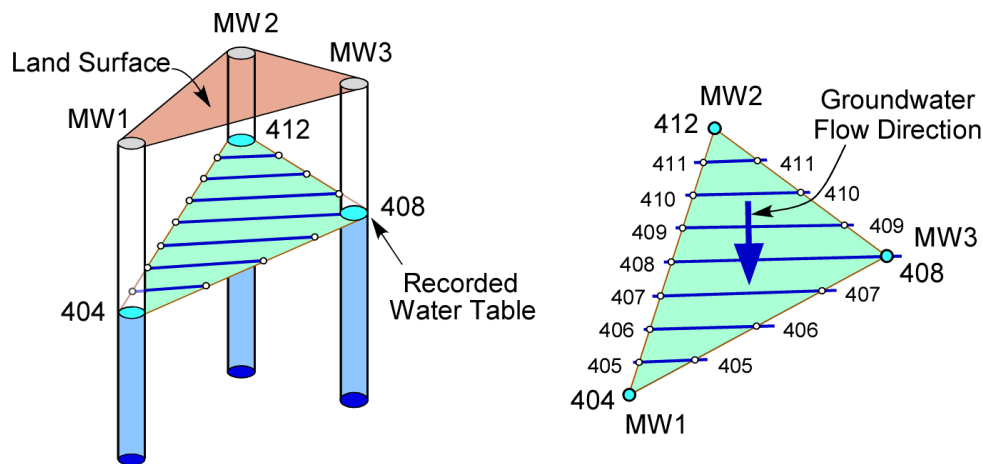
Figure 3.13 Left: Finding the position of the water table in three dimensions using data from three monitoring wells (numbers are water levels in meters or feet above sea level). Right: Construction of water table contour lines by triangulation with linear interpolation. Modified from Kresic and Mikszewski, 2013. Copyright CRC Taylor & Francis; permission is required for further use.

Manual contouring is often initially based on triangular linear interpolation (the "three-point problem") as illustrated in Figure 3.13, combined with the hydrogeologic experience of the interpreter. The first draft manual map is not necessarily an exact linear interpolation between data points. Rather, it is an interpretation of the hydrogeologic conditions with contours that roughly follow available numeric data. An important but often ignored fact when manually drawing contour maps is that most if not all parameters that are contoured, including the hydraulic head, do not change linearly from one location to another. A notable exception, seldom present, includes the hydraulic gradient in a homogeneous confined aquifer of uniform thickness from which there is no addition (recharge) or withdrawal (pumping) of groundwater at the scale of interest.

Even though the first computer-generated contour map may be somewhat inaccurate because relevant hydrogeological features such as rivers, faults, or exposed bedrock may not be characterized by the data set, it is always desirable to have the final contour map as a (digital) computer file. This will allow its use in other applications including for various quantitative analyses, groundwater modeling, and visualization purposes. For example, having XYZ files of the water table aquifer (unconfined aquifer), the potentiometric surface of a confined aquifer, and the top and bottom of any hydrostratigraphic layers, will significantly simplify preparation of a numeric groundwater model.

If the available computer program cannot produce a satisfactory contour map (for example, there is a complicated mixture of impermeable and flow boundaries of groundwater flow), and it cannot be forced to do so by the interpreter, the solution is to digitize a manually drawn map (or "draw" the contours manually in a computer program such as ArcMap). This, however, may be a lengthy process and it is better to acquire an appropriate software package for contouring. Quite a few computer programs today offer a wide range of contouring methods, allow the interpreter to adjust the generated contours, and can display contour maps in a variety of formats. Some of the most powerful and widely used commercial programs include Surfer (developed by Golden Software) and the Geostatistical Analyst extension (and to a lesser extent the Spatial Analyst extension) to ArcGIS by ESRI. There are also several versatile programs in the public domain, such as Visual Sample Plan (https://www.pnnl.gov/projects/visual-sample-plan), and SADA (The University of Tennessee, Knoxville; https://www.sadaproject.net/), which include both contouring and Geographic Information System—GIS capabilities. Graphical User Interface (GUI) software packages developed to support popular groundwater modeling programs such as Modflow can also be used to create contour maps from field data and export them to other applications. Good example of a commercial software is Groundwater Vistas by Environmental Simulations (https://www.groundwatermodels.com/.) Processing Modflow Version 8 by Simcore Software, an excellent groundwater modeling program, is now in public domain and can be downloaded for free at https://www.simcore.com/wp/archive/.

Contouring programs require that the individual data points be presented with two spatial coordinates and value of the parameter to be contoured (the hydraulic head in this case.) Common to all programs is division of the two-dimensional space of interest into equally spaced vertical and horizontal lines, i.e., the creation of a contouring grid. In Surfer, the user can either specify the grid spacing or let the program automatically determine it from the range of distances between individual data points. The two basic requirements common to all contouring methods, namely data organization and creation of the grid, are shown schematically in Figure 3.14. What separates different contouring methods is the mathematic equations (i.e., the model) used to calculate the parameter values (e.g., water table elevation or contaminant concentration) at locations where it was not directly measured. During this process, called spatial interpolation, the calculated values of the parameter are assigned to the grid either at intersections of the grid lines, or at the centers of the cells (squares) formed by the grid lines. This means that the basis for any contour map that will be eventually drawn by a program is a numeric matrix of equally spaced rows and columns called raster file. Contour lines, for any contour interval specified by the user, connect identical numeric values in the grid. Some programs, such as Surfer, include options for smoothing the initial contours to give them a more natural look. Selecting a finer contouring resolution (i.e., smaller cell size or grid spacing) will generally also result in smoother contours. More on different contouring methods is provided by Kresic, 2007 (*Hydrogeology and Groundwater Modeling, Second Edition*, CRC Taylor & Francis).

The most important prerequisite for successfully contouring potentiometric surfaces is a thorough knowledge of general groundwater flow principles. For example, a novice is often caught in drawing (or letting a computer program create without subsequently correcting it) various depressions in the potentiometric surface from which there is no escape of groundwater (see question mark in Figure 3.14-bottom). Unless there is a valid hydrogeologic explanation (e.g., presence of a pumping well, or downward flow into an underlying aquifer through a window in the intervening aquitard), these depressions are an inadequate interpretation or may be the result of erroneous data. Similarly, mysterious local mounds in the water table may represent perched groundwater, or something more "exotic" such as inflow of water from leaky sewers or water lines. This all means that almost inevitable local "irregularities" in the potentiometric surface should not blur interpretations of the expected overall tendency of the groundwater flow in any specific case.
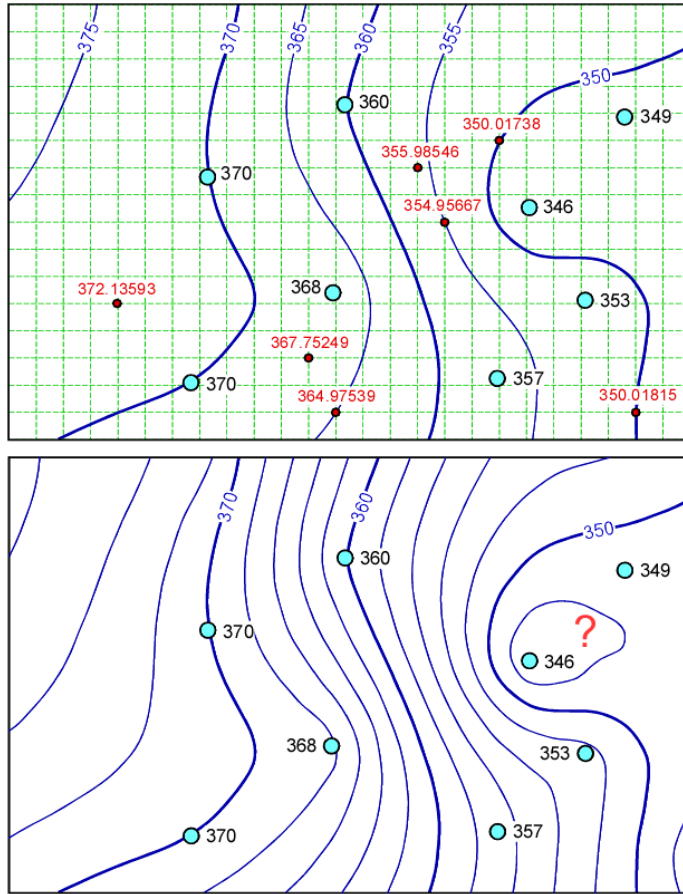
Figure 3.14 Portion of a contour map created using a computer program. *Top*: Eight discrete values measured in the field are shown with blue circles and black numbers with no decimal digits. The chosen mathematical model calculates interpolated values and assigns them to all grid nodes. Several computer-interpolated values (red numbers with five decimal digits) are shown with small red circles at intersections of dashed grid lines. Contour lines, with the contour interval of five, connect the same hydraulic head values in the grid. *Bottom*: same map with the contour interval of two. It is advisable to create several maps with different contour intervals as they may better reveal local variations in the hydraulic head (parameter) values. At the same time, this "finer" contouring can create potentially unreasonable presentations as shown with the question mark: contour 348 is closed indicating a sink (depression) in the water table. Unless there is some groundwater withdrawal at that location, or perhaps a window in an underlying aquitard that acts as a sink connecting the contoured aquifer and an aquifer below the aquitard, this contour should not be closed. From Kresic and Mikszewski, 2013. Copyright CRC Taylor & Francis; permission is required for further use.

Traditional use of the potentiometric surface contour maps is determination of the hydraulic gradients and groundwater flow directions. However, one should always remember that a contour map is a two-dimensional representation of a three-dimensional flow field and as such, it has limitations. If the area (aquifer) of interest is known to have significant vertical gradients, and enough field information is available, it is always recommended to create at least two contour maps: one for the shallow and one for the deeper aquifer depth. As with geologic and hydrogeologic maps in general, a contour map should be accompanied with several cross-sections showing locations and vertical points of the hydraulic head measurements with posted data. Probably the most incorrect and misleading case is when data from monitoring wells screened at different depths are lumped together and contoured as one "average" data package. A perfect example would be a fractured rock or karst aquifer with thick residuum (regolith) deposits and monitoring wells screened in the residuum and at various depths in the bedrock. If data from all the wells were lumped together and contoured as one dataset, it would be impossible to interpret where the groundwater is flowing for the following reasons:

- The residuum is primarily an intergranular porous medium in unconfined conditions (it has water table), and horizontal flow directions may be influenced by local (small) surface drainage features.

- The bedrock has discontinuous flow through fractures at different depths, which is often under pressure (confined conditions), and may be influenced by more regional features such as rivers or springs.

The flow in two distinct porous media (the residuum and the bedrock) may therefore be in two different general directions at a particular site, including vertical gradients from the residuum towards the underlying bedrock. Creating one "average" contour map for such a system would not make any hydrogeologic sense.

3.4.1 Influence of Hydraulic Boundaries

It has become standard practice in hydrogeology and groundwater modeling to describe the inflow and outflow of water from an aquifer with three general boundary conditions: 1) known flux, 2) head-dependent flux, and 3) known head, where "flux" refers to the groundwater flow rate and "head" refers to the hydraulic head.

One of the most important aspects of creating contour maps in alluvial aquifers is to determine the relationship between groundwater and surface water features. In hydraulic terms, the contact between an aquifer and a surface water body is an equipotential boundary. In case of lakes and wetlands, this contact can be approximated with the same hydraulic head. In case of flowing streams, the hydraulic head along the contact decreases in the downgradient direction (both surface water and groundwater flow downgradient). If enough measurements of a stream stage are available, it is relatively easy to draw the water table contours near the river and to finish them along the river-aquifer contact. However, often little, or no precise data is available on river stage, and, at the expense of precision, it must be estimated from a topographic map or from the monitoring well data by extrapolating the hydraulic gradients until they intersect the river.

For the purposes of creating contour maps of the potentiometric surface, either manually or with computer programs, it is important to remember the following simple rules regarding the influence of hydraulic boundaries:

- Contour lines must meet impermeable (no-flow) boundaries at right angles.

- Contour lines must parallel equipotential boundaries where the hydraulic head is constant along the boundary (e.g., a lake), or intersect the sloping boundary (e.g., a flowing river) at discrete points where the hydraulic head at the boundary (the river) has the same value as the corresponding equipotential contour line of groundwater.

Figure 3.15 shows some of the examples of surface water-groundwater interaction represented with the potentiometric surface contour lines in a basin filled with unconsolidated sediments. Such basins, common in the semi-arid western United States, may have permanent (perennial) or intermittent surface streams, and may be recharged by surface water runoff and underflow from the surrounding mountain fronts. They can also be connected with adjacent basins thus forming rather complex groundwater systems with various local and regional water inputs and water outputs. Availability of the hydraulic head data at various locations within the basin, and at various times, will determine the accuracy of the hydraulic head contours which therefore may or may not show existence or influence of various boundary conditions. Figure 3.15 indicates general inflow of groundwater from the east, and outflow to the west, and influence of two streams (A and B) entering the basin and losing water to the aquifer a short distance from the boundary. Potentiometric surface contour lines indicate the hydraulic connection between the aquifer and the river flowing through the basin, showing the river reaches that lose water to, or gain water from the aquifer.
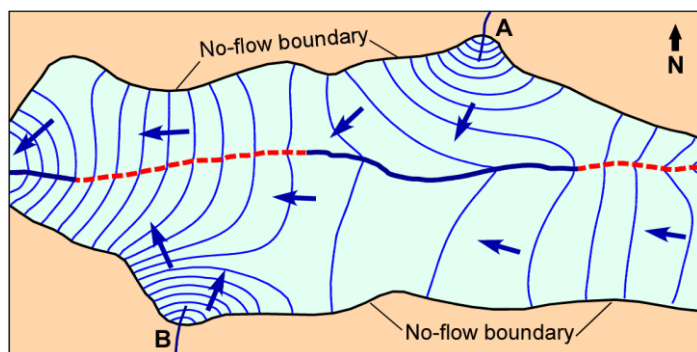
Figure 3.15 Potentiometric surface contour lines in a sedimentary basin, arrows indicate general directions of groundwater flow. The map shows influence of two surface streams (A and B) flowing into the basin from the surrounding bedrock areas and losing all water to the basin aquifer. The stream is hydraulically connected with the aquifer; blue line indicates gaining section of the stream; dashed red line indicates losing section of the stream. Modified from Kresic, 2009. Copyright McGraw Hill; permission is required for further use.

The most common mistake when creating potentiometric maps of unconfined aquifers is to let a computer program "ignore" presence of surface water features and accept the results as is. Figure 3.16 shows contours of a potentiometric surface created by three pumping wells located in the flood plain of a slow-moving perennial river. The wells are pumping from the unconfined alluvial aquifer. Figure 3.16-*Left* was created in Surfer using default linear kriging and ignoring the river. In comparison, the map in Figure 3.16-*Right* takes the river stage into account by utilizing a "breakline" option in Surfer. It is apparent that considering the river creates a much more logical map.
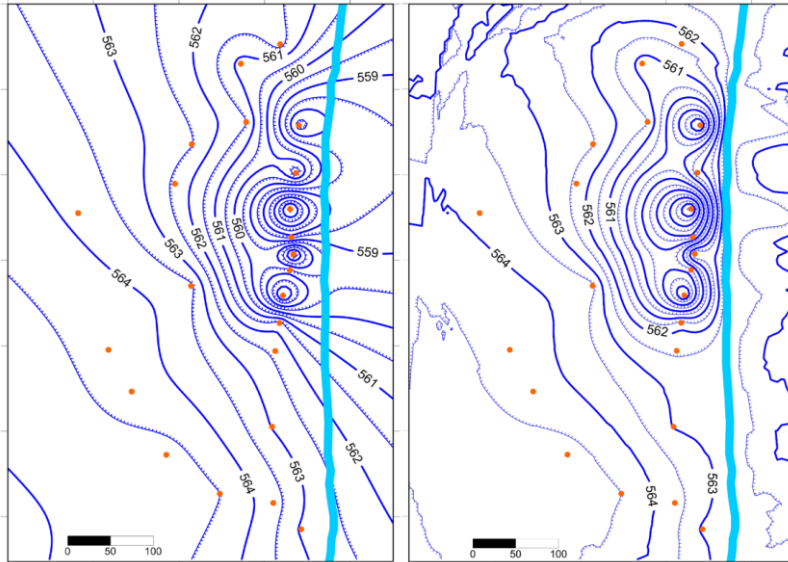
Figure 3.16 *Left*: Contour map of a water table influenced by three pumping wells near a river when the hydraulic connection between the aquifer and the river is not accounted for. Orange circles are locations of monitoring wells with field measurements. *Right*: The same map when the river elevation is accounted for by using breakline in Surfer. Note non-sensical contours created by the program in the areas without data points including on the other side of the river. These areas should be excluded from the final map. From Kresic and Mikszewski, 2013. Copyright CRC Taylor & Francis; permission is required for further use.

A breakline is a three-dimensional boundary file that defines a line with X, Y, and Z values at each vertex. When the gridding algorithm sees a breakline, it calculates the Z value of the nearest point along the breakline and uses that value in combination with nearby data points to calculate the grid node value. Surfer uses linear interpolation to determine the values between breakline vertices when gridding. Breaklines are not barriers to information flow, and the gridding algorithm can cross the breakline to use a point on the other side of the breakline. If a point lies on the breakline, the value of the breakline takes precedence over the point. Breakline applications include defining streamlines, ridges, and other breaks in the slope. Breaklines can be created in any text editor or directly within Surfer using the digitizer tool.
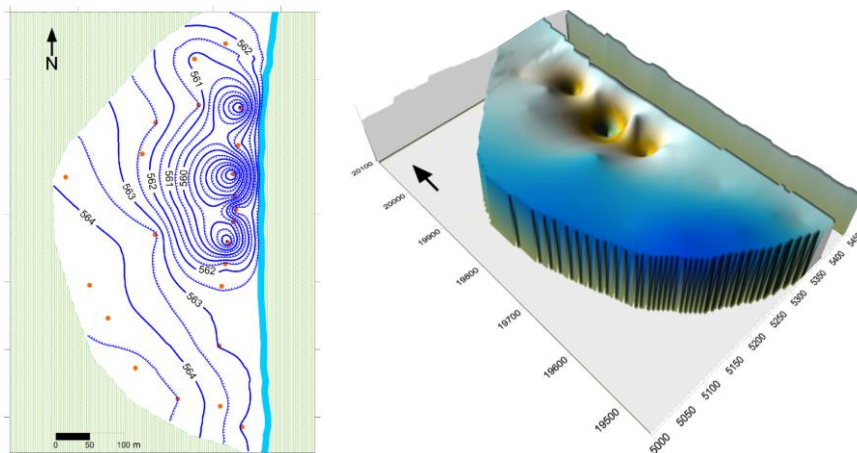
Figure 3.17 *Left*: Final contour map of the water table after post-processing of the results using grid blanking in Surfer (non-sensical contours in the area without data points are blanked, and not displayed— Surfer has effective option for creating a blanking breakline onscreen with a digitizer). *Right*: Surfer enables displaying the raster digital surface in 3D view that can be rotated, zoomed-in, and viewed from different angles for additional insight. From Kresic and Mikszewski, 2013. Copyright CRC Taylor & Francis; permission is required for further use.

47

They can be used for other purposes such as removing non-sensical contours in the areas without data. The program, by default, creates contours within the rectangle bounded by the minimum and maximum X and Y coordinates of available data. Any non-sensical areas should be removed from the final map. Surfer can do that automatically by using a "blanking breakline" feature defined by the user.

The contour map of the hydraulic head is one of two parts of a *flow net*: flow net in a homogeneous isotropic aquifer is a set of streamlines and equipotential lines, which are perpendicular to each other (see Figure 3.18). Streamline (or flow line) is an imaginary line representing the path of a groundwater particle as it flows through the aquifer. Two streamlines bound a flow segment of the flow field and never intersect, i.e., they are roughly parallel when observed in a relatively small portion of the aquifer. The main requirement of a flow net is that the flow rate between adjacent pairs of streamlines is the same (ΔQ in Figure 3.18), which enables calculations of flow rates in various portions of the aquifer, providing that the hydraulic conductivity and the aquifer thickness are known.
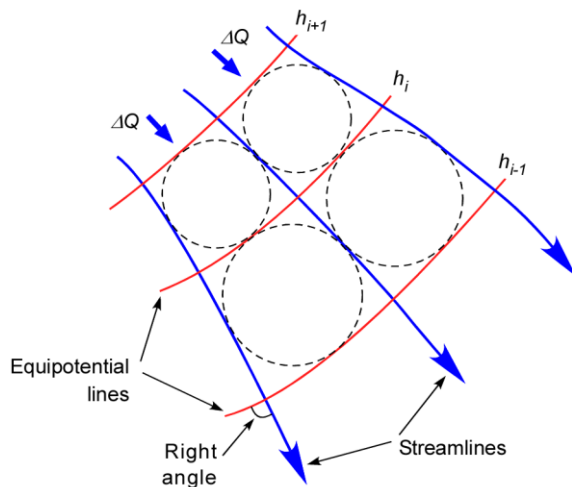
Figure 3.18. Flow net is a set of equipotential lines and streamlines which are perpendicular to each other in an isotropic porous media (aquifer). The equipotential line connects points with the same groundwater potential, i.e., hydraulic head—*h*. The streamline is an imaginary line representing the path of a groundwater particle as it flows through an aquifer. Flow rate between adjacent pairs of streamlines, ΔQ, is the same. Equipotential lines are more widely spaced where the aquifer is more transmissive. Modified from Kresic, 2009. Copyright McGraw Hill; permission is required for further use.

Equipotential line is a horizontal projection of the equipotential surface – everywhere at that surface the hydraulic head has a constant value. Two adjacent equipotential lines (surfaces) never intersect and can also be considered parallel within a small aquifer portion. These characteristics are the main reason why a flow net in a homogeneous, isotropic aquifer is sometimes called the net of small (curvilinear) squares. In general, the following simple rules apply for graphical flow net construction in heterogeneous, isotropic systems (Freeze and Cherry, 1979):

(1) Flow lines and equipotential must intersect at right angles throughout the system.

(2) Equipotential lines must meet impermeable boundaries at right angles.

(3) Equipotential lines must parallel constant-head boundaries.

(4) The tangent law must be satisfied at geologic boundaries (see next lecture and Figure 4.11).

(5) If the flow net is drawn such that squares are created in one portion of one formation, squares must exist throughout that formation and throughout all formations with the same hydraulic conductivity. Rectangles will be created in formations of different conductivity.

The last two rules make it extremely difficult to manually draw accurate quantitative flow nets in complex heterogeneous systems. If a system is anisotropic in addition, it would not be feasible to draw an adequate flow net manually in most cases. The ultimate tool for creating contour maps, tracking particles as they flow through the system, and calculating flow rates for any part of a groundwater system, is a numeric model, which can incorporate and test all known or suspected heterogeneities, boundaries, and anisotropy, in all three dimensions. Figures 3.19

and 3.20 show output from a model used to test influence of varying hydraulic conductivity and anisotropy on tracks of particles (denoted with small circles) released at certain locations in the aquifer.
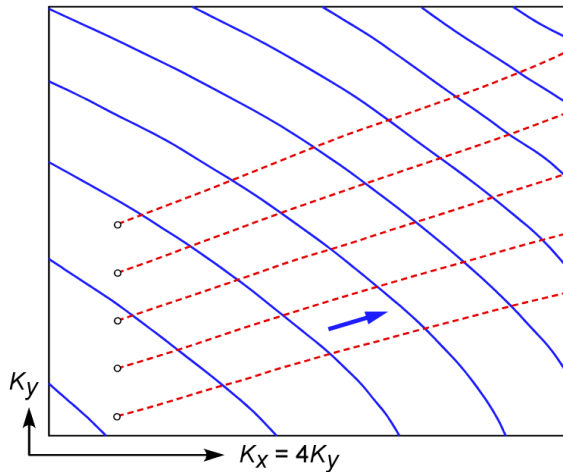
Figure 3.19 Influence of anisotropy on particle tracks (dashed lines). The hydraulic conductivity in X direction is 4 times higher than in Y direction. The aquifer is homogeneous and anisotropic. From Kresic, 2009. Copyright McGraw Hill; permission is required for further use.
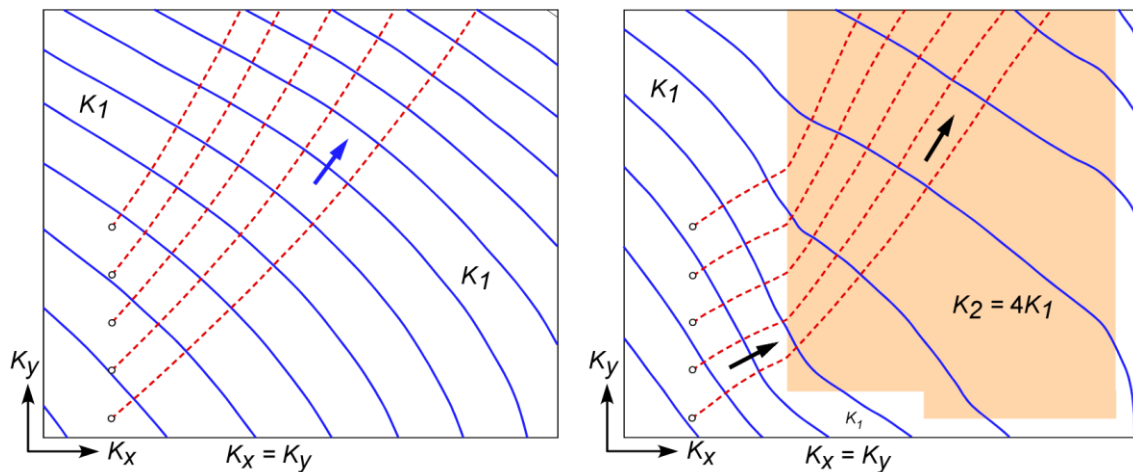
Figure 3.20: *Left*: Hydraulic head contour lines (in blue) and particle tracks (red-dashed) in an isotropic, homogeneous aquifer of uniform hydraulic conductivity (K_1). *Right*: Influence of a geologic boundary (heterogeneity) on contour lines and particle tracks. The shaded area has 4 times higher hydraulic conductivity than the rest of the flow field ($K_2=4K_1$). Aquifer is isotropic (the hydraulic conductivity is same in X and Y directions). Note wider spacing between the contours in the shaded area because of the higher K. From Kresic, 2009. Copyright McGraw Hill; permission is required for further use.

Hydrogeologic heterogeneity and anisotropy are discussed in detail in the next Lecture. In hydrogeology, these two terms refer to hydrogeologic (hydraulic) characteristics of porous media: effective porosity, specific yield, coefficient of storage, and hydraulic conductivity (permeability). If these characteristics are the same within the aquifer (aquitard) volume of interest, the porous media is <u>homogeneous</u>. If these characteristics do not have any preferred spatial orientation (i.e., they are the same in all directions), the porous media is <u>isotropic</u>.

Lecture 4 Groundwater Flow, Part Two

The flow of water in the subsurface porous media takes place for two main reasons: there is a hydraulic gradient, and the porous media is permeable. The velocity and direction of groundwater flow are directly influenced by the two key characteristics of the porous media—the hydraulic conductivity and the effective porosity, as well as their spatial distribution and orientation. These two characteristics depend on the fabric of porous media, which is a general term used to describe spatial and geometric relationship between all different elements of rocks (all types of rocks: unconsolidated sediments, consolidated sedimentary rocks, magmatic, and metamorphic rocks) that comprise aquifers and aquitards. The elements of rock fabric include grains of sedimentary rocks, and component crystals of magmatic and metamorphic rocks. Rock fabric also refers to various discontinuities in rocks, such as fissures, fractures, faults, fault zones, folds, and bedding planes (layering) for example. Without elaborating on the geologic portion of hydrogeology, it is appropriate to state that groundwater professionals lacking a thorough geologic knowledge (i.e., nongeologists) would likely have various difficulties in understanding the many important aspects of heterogeneity and anisotropy discussed further.

4.1 Anisotropy and Heterogeneity

The questions of anisotropy and heterogeneity in hydrogeology are arguably some of the most important ones every hydrogeologist will face throughout her or his career. At the same time, unfortunately, using so-called "rules of thumb" when selecting their quantitative measures to provide answers to many important problems seems to be prevalent in hydrogeologic practice. This, for example, includes accepting that the vertical hydraulic conductivity is ten times lower than the horizontal hydraulic conductivity without any site-specific evaluation or without even knowing where this rule of thumb came from to begin with. Some quantitative examples how using various rules of thumb in hydrogeology can lead to erroneous calculations and conclusions in decision-making process are provided in the Hydrogeology 101 Laboratory Manual, and some are provided in this Lecture (e.g., see Figure 4.15 and the accompanying text), and elsewhere in the textbook.

Common to these examples is that one should never accept previously published, peer-reviewed information at face value without independent, critical analysis. This includes publications by various government agencies. It is often desirable for a hydrogeologist to directly cite the United States Geological Survey (USGS) or the United States Environmental Agency (USEPA) as there will generally be less resistance from regulators in accepting the related concepts and conclusions. However, while these and other government agencies do produce many useful and accurate reports, they are not infallible. If the assumptions and results of some of their studies are wrong, it can lead to the rapid propagation of conceptual errors that can become entrenched in professional practice (Kresic and Mikszewski, 2013).

The widespread endorsement of scientific and engineering rules of thumb in a specific project setting, that are of unknown original context and with apparent conceptual and other problems, could be construed as an example of *groupthink*, where group pressures lead to a breakdown in independent thought and result in flawed decision-making (Irving Janis, 1971, 1972, 1982). Groupthink favors unanimity over accuracy and expert opinion, avoids criticism and controversy at all costs, and rationalizes bad decisions made in the past rather than exploring new solutions. To avoid groupthink, group members should remain as impartial as possible, and consult independent expert opinion from third parties removed from the impacts of the decision to be made (Kresic and Mikszewski, 2013.) In conclusion, this author strongly advises students of hydrogeology to familiarize themselves with various

writings on the groupthink theory and provides this quote from the 1971 landmark paper by Janis hoping it will spark interest.

The symptoms of groupthink arise when the members of decision-making groups become motivated to avoid being too harsh on their judgments of their leaders, or their colleagues' ideas. They adopt a soft line of criticism, even in their own thinking. At their meetings, all the members are amiable and seek complete concurrence on every important issue, with no bickering or conflict to spoil the cozy, "we-feeling" atmosphere.

The general concept of homogeneity and isotropy is shown schematically in Figure 4.1. In hydrogeology, these two terms refer to hydrogeologic (hydraulic) characteristics of porous media: effective porosity, specific yield, coefficient of storage, and hydraulic conductivity (permeability). If these characteristics are the same within the aquifer (aquitard) volume of interest, the porous media is <u>homogeneous</u>. If these characteristics do not have any preferred spatial orientation (i.e., they are same in all directions), the porous media is <u>isotropic</u>. Clean beach sand made of pure quartz grains of similar size is one example of a homogeneous isotropic rock (unconsolidated sediment). If, in addition to quartz grains, there are other mineral grains but all uniformly mixed, without groupings of any kind, the sediment is still homogeneous.

t limited scales (say, centimeter to decameter; or inch to ten yards), field measurements are hardly ever representative of large volumes of an aquifer or aquitard. In reality, aquifers and aquitards are more or less heterogeneous, and it is only a matter of convention, or agreement between various stakeholders, which portion of the subsurface under investigation may be considered homogeneous. At the same time, assuming homogeneity of an aquifer volume that seems appropriate for general water supply purposes may be completely inadequate for characterizing contaminant fate and transport at a particular site (Kresic, 2007).

The following discussion by Meinzer (1932, page 133) explains very eloquently the challenge of assessing homogeneity and isotropy of porous media:

The most serious difficulty…and one that up to the present time has not been effectively overcome is that of determining the true average permeability of the material that constitutes the water-bearing formation. Laboratory methods are available to determine accurately the permeability of the samples that are tested, but the difficulty lies in obtaining representative samples. Even apparently slight differences in texture may make great differences in permeability. A rather inconspicuous admixture of colloidal clay to an otherwise permeable sand may cut down greatly its capacity to conduct water. In a sand formation a few thin strata of coarse clean sand may conduct more water than all the rest of the formation. These permeable strata may be overlooked in the sampling, or if samples from them are taken it may be impossible to give them the proper weight in comparison with samples from other parts of the formation. Consolidated rocks are likely to contain joints and crevices which conduct much of the water and which therefore render laboratory methods inapplicable. On the other hand, unconsolidated samples can not easily be recovered and tested without disturbing the texture of the material and thus introducing errors of unknown but conceivably great amount. Moreover, samples taken at the outcrop of a formation may not be representative because of changes produced by weathering, and samples obtained from wells are generally nonvolumetric and greatly disturbed and may be either washed or mixed with clay of foreign origin. If the conditions of drilling can be controlled it may be possible to obtain an undisturbed or only moderately disturbed sample, especially if a core barrel is used, but such favorable conditions are rarely obtainable.

Term *Representative Elementary Volume*, or REV is often used to describe a volume that has all important characteristics of the aquifer (aquitard), including any heterogeneity and anisotropy, so that a quantitative analysis performed on the REV can be applied across the scale of interest ("Site"). However, this often does not mean the

same thing to different people, and it is highly problem specific. For example, academic researchers in the field of contaminant hydrogeology and groundwater remediation are usually occupied with testing new ideas on small laboratory samples of porous media, such as glass beads, clean sand, tight clay, or maybe a small plug from a limestone core. Extrapolating the results of such research to real field-scale problems always presents a major challenge. One approach is to assume that, although *heterogeneous* and *anisotropic* by default, the porous media at a particular *Site* can be approximated by some average characteristics reasonably accurately. This approach is in many cases the only one feasible, given the limitations of available funds and time for investigations. In any case, every REV is both scale-dependent and problem-specific and can vary even for the seemingly same porous media at the same site, depending on the final project goal.
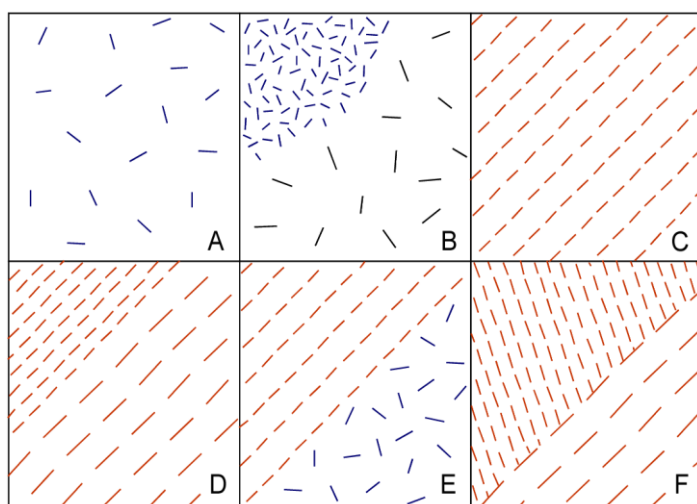
Figure 4.1 Schematic presentation of rock fabric that influences homogeneity and isotropy of porous media. A: homogeneous and isotropic; B: Overall heterogeneous and isotropic, with two different homogeneous and isotropic areas (volumes); C: homogeneous and anisotropic; D: overall heterogeneous and anisotropic, with two different areas that are each homogeneous and anisotropic; E: overall heterogeneous, with one area that is homogeneous and isotropic (blue hatching), and one area that is homogeneous and anisotropic; F: overall heterogeneous and anisotropic. Based on Dimitrijević, 1978. University of Belgrade. Acknowledgement is required for further use.
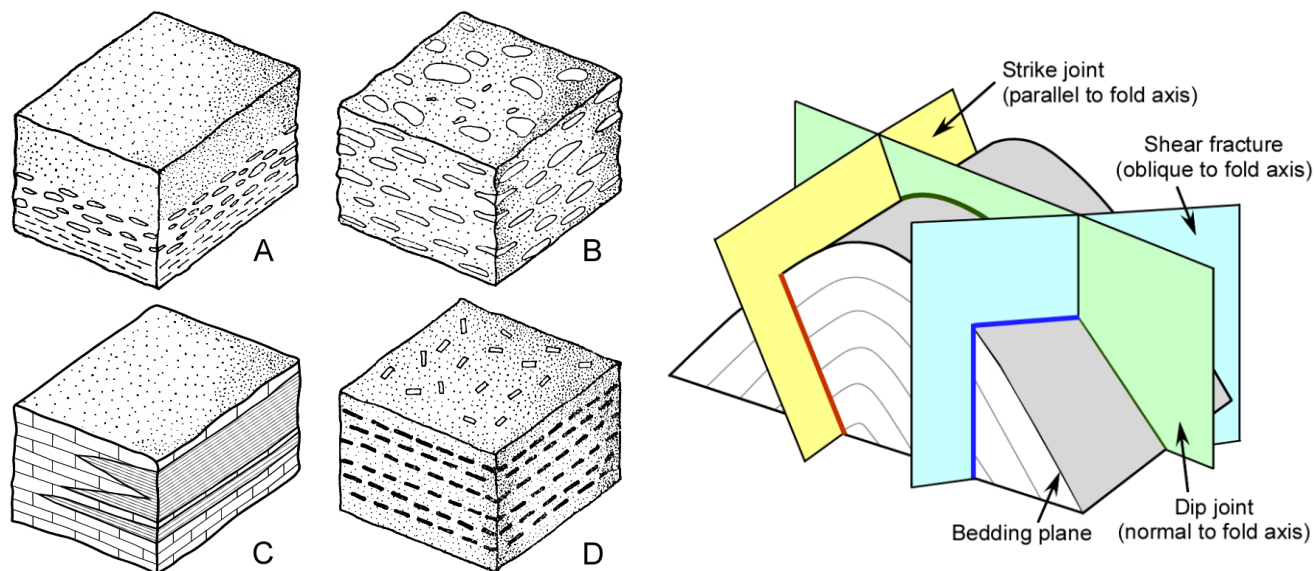
Figure 4.2 *Left*: Examples of lithologic discontinuities in rocks; A: gradation in unconsolidated sediments. B: "layering without layers". C: tongues in lithosomes. D: foliation in metamorphic rocks. Based on Dimitrijević, 1978; University of Belgrade. Acknowledgement is required for further use. *Right*: Bedding planes, fold-related joints, and fractures in general are mechanical discontinuities that can cause abrupt changes in groundwater flow directions.

Figure 4.2 and photographs in Figures 4.3 through 4.10 illustrate examples of geologic fabric of sediments and rocks in general, followed by some common expressions of anisotropy of the hydraulic conductivity. Care should be exercised when applying any of the equations and approaches to quantifying the anisotropy. This includes a thorough understanding of the fundamental differences that exist between unconsolidated sediments and well lithified fractured, folded, and faulted rocks, when it comes to the nature of groundwater flow in different types of porous media.
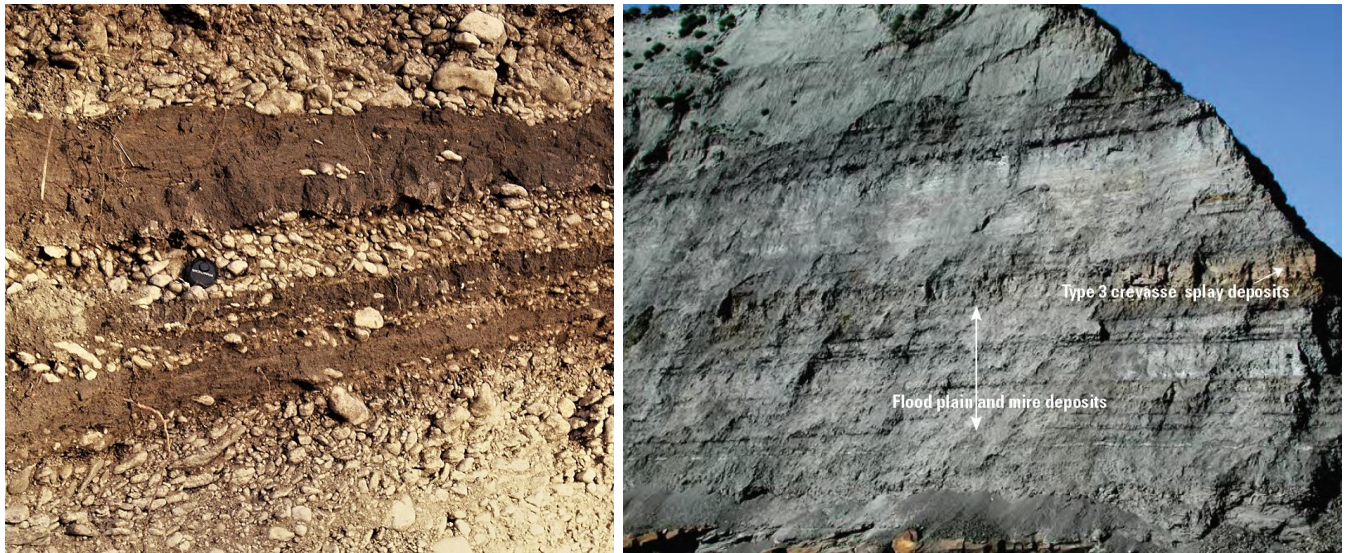
Figure 4 3 *Left*: Alluvial gravel and silt exposed on the bank of a stream near Fort Worth, Texas. *Right*: Interbedded sandstone, mudstone, and siltstone with minor coal and carbonaceous shale beds representing flood plain and coarsening-upward crevasse splay (Type 3 sandstones) deposits of the Prince Creek Formation. For scale, the crevasse splay deposits are 7 ft thick. Cretaceous Schrader Bluff and Prince Creek Formations in Colville River Bluffs, Alaska. From Flores et al., 2007. USGS, in public domain.

Figure 4.4 *Left*: alluvial fan deposits in a gravel pit in the Jordan River Valley, Jordan. Photo by Daniel J. Goode. USGS, in public domain. *Right*: Thick gravel deposits in San Isidro, Lima, Peru.

Figure 4.5 *Left*: Massive aeolian sandstone in Canyon de Chelly, Arizona with Anasazi cliff dwellings named White House Ruin. *Right*: Fractured cross-bedded aeolian Coconino Sandstone in Grand Canyon, Arizona.

Figure 4.6 *Left*: Horizontal alternating layers of limestone, claystone, and shale in the Boquillas Formation, Hot Springs area, Rio Grande valley, Big Bend National Park, Texas. Note extensive intra-bed and cross bed fracturing perpendicular to stratification. *Right*: dipping limestone layers with extensive fracturing perpendicular to stratification; Tara Mountain, Serbia.
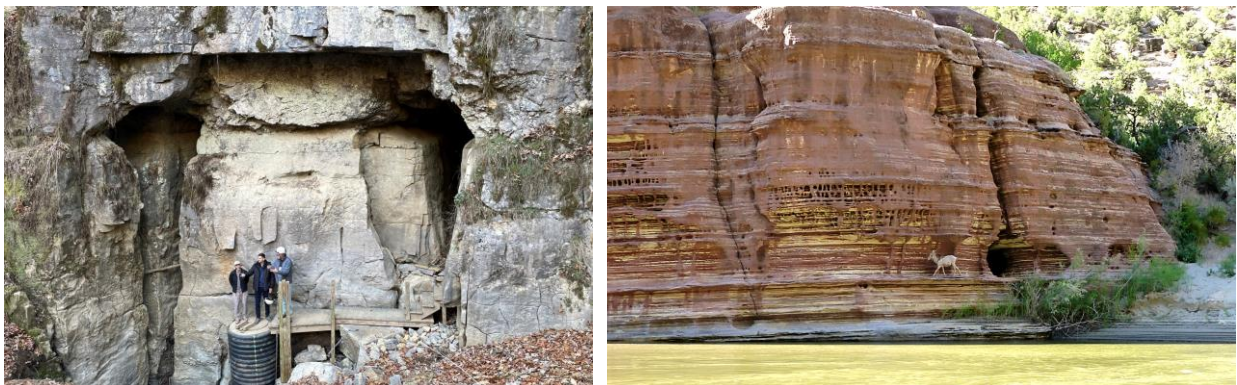
Figure 4.7 *Left*: Development of cave passages along vertical fractures intersecting near horizontal limestone layers at Water Sinks, Virginia. Photo courtesy of Katarina Kosič Ficco. *Right*: A single bighorn sheep walks along a narrow cliff ledge of Round Valley Limestone in Whirlpool Canyon on the Green River, Utah. Vertical fractures crossing nearly horizontal limestone beds are enlarged (karstified) by dissolution (photo credit NPS/Erin Cahill.)
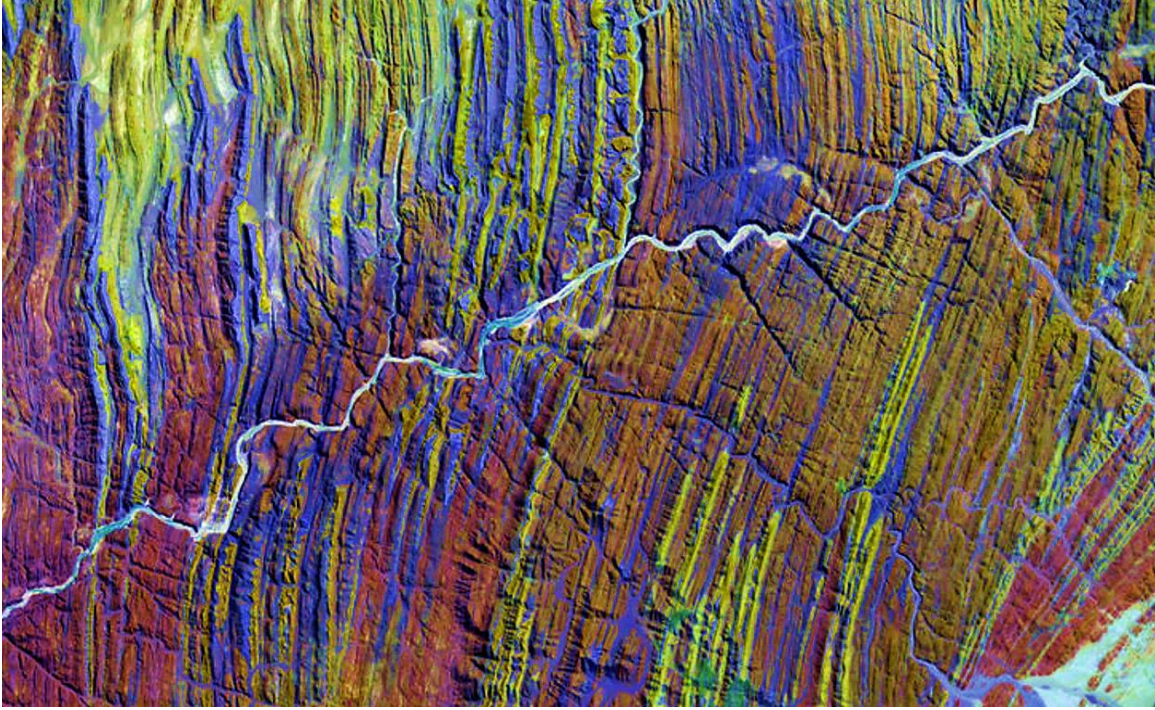
Figure 4.8 Landsat 7 false color satellite image of Namibia's Ugab River, seen here crossing folded, fractured, and faulted geological unit "Zerrissene Turbidite System" which is made up of low-grade metamorphosized Neoproterozoic sedimentary rocks. Image featured in USGS collection *Earth as Art 2*. Available at https://www.usgs.gov/media/images/ugab-river. USGS, in public domain.
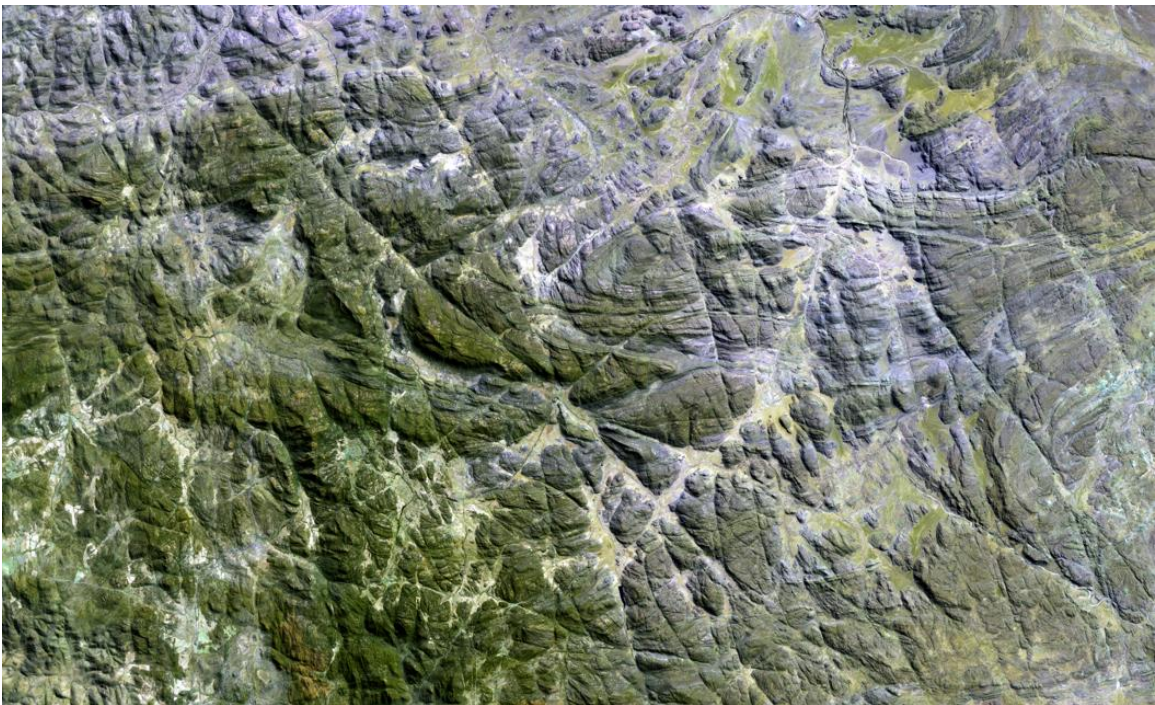
Figure 4.9 Landsat 7 false color satellite image of Namaqualand granite-gneiss complex in South Africa. Available at https://eros.usgs.gov/image-gallery/earth-as-art-1/namaqualand. USGS, in public domain.

Figure 4.10 Anisotropy impacting groundwater flow in metamorphic and magmatic rocks is for the most part due to fractures (joints). *Upper left*: Measuring fabric elements of fractured schistose greenstone at Bellevue Farm, Warrenton, Virginia; *Upper right*: slate in the Piedmont of Virginia; *Lower left*: gneiss in Atlanta, Georgia; *Lower right*: columnar joints in metamorphosed basalts of Piedmont, Virginia.

One important aspect of heterogeneity is that groundwater flow directions change at lithologic boundaries between unconsolidated or loosely consolidated sediments of notably different hydraulic conductivity such as the ones shown in Figures 4.3 and 4.4. An analogy would be refraction of light rays when they enter a medium with different density, e.g., from air to water. The refraction causes the incoming angle, or angle of incidence and the outgoing angle, or angle of refraction, to be different (angle of incidence is the angle between the orthogonal at the boundary and the incoming streamline; angle of refraction is the angle between the orthogonal at the boundary and the outgoing streamline). The only exception is when the streamline is perpendicular to the boundary— in which case, both angles are the same at 90°. The schematics shown in Figure 4.11 applies to both map and cross-sectional views as long as there is a clearly defined lithological boundary between the two porous media. Figure 4.12 shows a map view of a generic hydraulic conductivity field and the corresponding potentiometric surface contour lines simulated with a groundwater flow model. Lithologic contacts clearly influence the orientation and spacing between the contour lines.

Where there are well-defined bedding planes separating layers of lithified rocks, and there are fissures crossing such planes (see Figure 4.2-*Right* and photos in Figures 4.6 and 4.7), the above concept is not entirely applicable because of the roles these mechanical discontinuities (bedding planes and fissure/fracture planes) may play in changing groundwater flow directions.
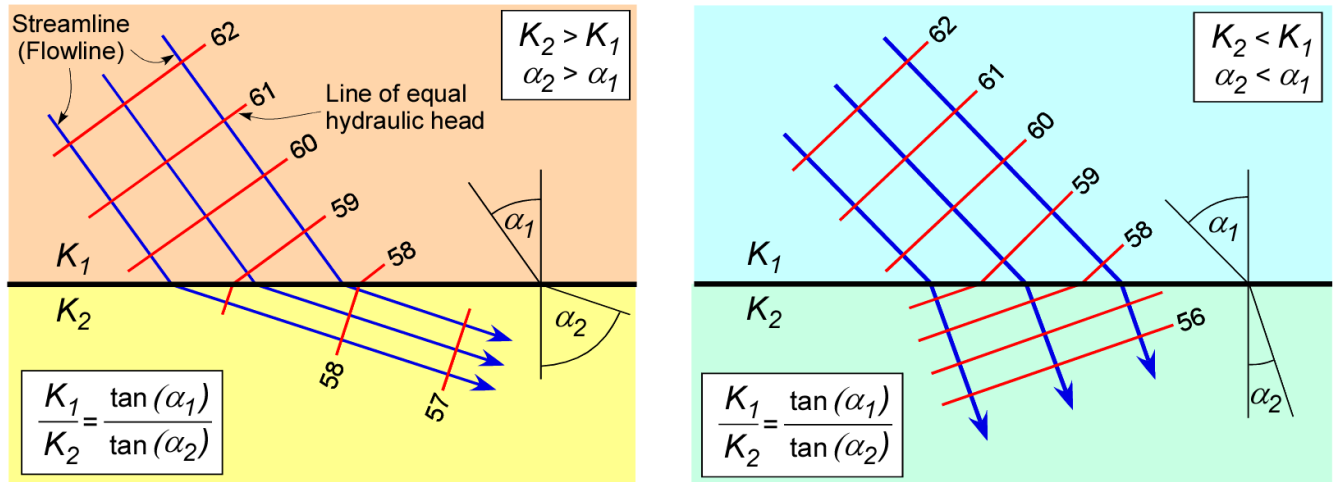
Figure 4.11 Refraction of groundwater flowlines (streamlines) at a boundary of higher hydraulic conductivity (left) and a boundary of lower hydraulic conductivity (right). Angle of incidence and angle of refraction are denoted with α_1 and α_2 respectively. Hydraulic conductivity is denoted with K.
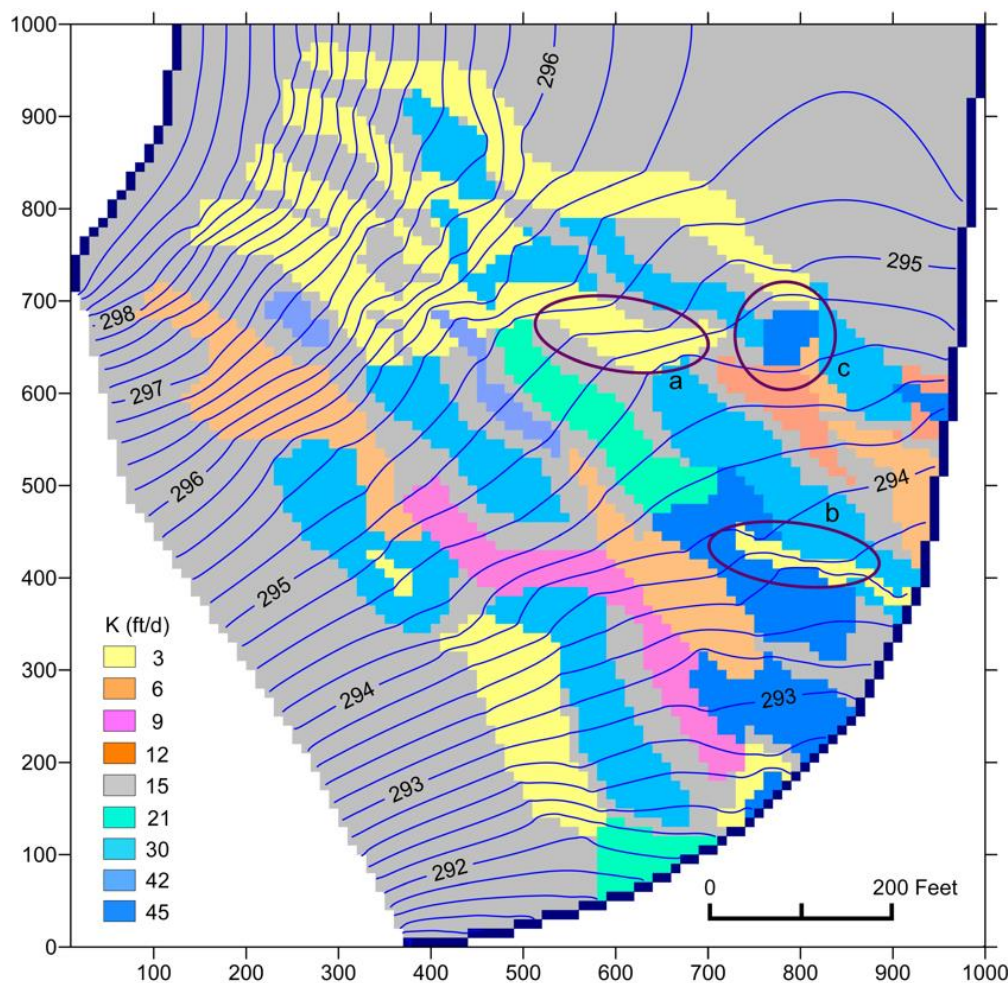
Figure 4.12 Groundwater flow field created in a numeric groundwater model through extensive variation of hydraulic conductivity, K (in feet per day). The confined aquifer thickness is uniform. Lower K creates steeper gradients (example areas **a** and **b**); higher K results in more widely spaced contours (area **c**). From Kresic and Mikszewski, 2013. Copyright CRC Taylor & Francis; permission is required for further use.

Contour lines of the potentiometric surface can change their orientation and spacing (i.e., the hydraulic gradient can change) not only because of the hydraulic conductivity changes or presence of anisotropy. The same can happen if the saturated aquifer thickness changes while the hydraulic conductivity remains the same (the porous medium is homogeneous). This relationship between the hydraulic conductivity (K) and the aquifer thickness (b) is described with the parameter called transmissivity:

$$T = b \times K \qquad (4.1)$$

It follows that an aquifer is more transmissive (more water can flow through it) when it has higher hydraulic conductivity and when it is thicker. The knowledge of this relationship helps in interpretation of the hydraulic head data and possible reasons for changes in the hydraulic gradient (see Figure 4.13).
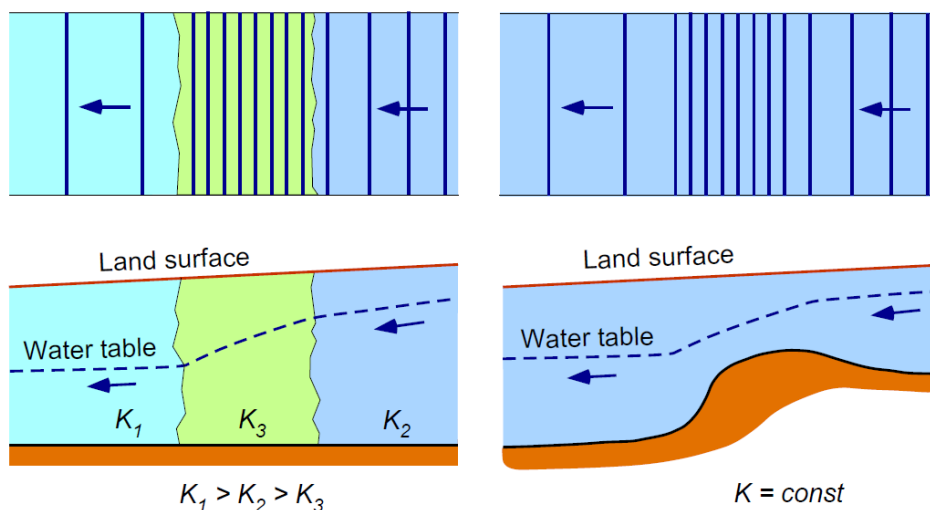
Figure 4.13 Maps (top) and cross sections (bottom) showing how changes in aquifer transmissivity affect potentiometric contours. In general, lower transmissivities are associated with steeper hydraulic gradients (more closely spaced contours), while higher transmissivities are associated with more widely spaced contours. Modified from Kresic, 2007. Copyright CRC Taylor & Francis; permission is required for further use.

It is sometimes expected or desired to find horizontal and vertical components of the hydraulic conductivity that may be anisotropic (it may be the highest in certain direction) or find components of such hydraulic conductivity that are parallel to the major axes of an orthogonal coordinate system where Y axis is commonly aligned with the geographical North (as most maps used in geology and hydrogeology are). This practice helps in simplifying various equations of groundwater flow or in setting up a numeric model with an orthogonal grid of rows and columns (MODFLOW, the most widely used numerical groundwater flow model worldwide, is an example). Unfortunately, the practice varies and often brings more confusion than not, including when indiscriminately referring to some "rules of thumb" while defying common sense at the same time.

Figures 4.14 through 4.18 show some examples of expressing the hydraulic conductivity with its various components in three-dimensional space (including discussion on a misleading and erroneous approach apparently applying a rule of thumb while ignoring field-based hydrogeologic evidence.) Various quantitative examples are provided in the Hydrogeology 101 Laboratory Manual.

$$K_h = K_d cos(\alpha)$$
$$K_v = K_d sin(\alpha)$$

$$K_{strike} = K_{dip} > K_n$$

Applicable to well solidified sedimentary rocks, *without* intrabed or crossbed fractures (joints)

$\alpha = 45°$ $K_h = K_v$ $\alpha < 45°$ $K_h > K_v$ $\alpha > 45°$ $K_v > K_h$
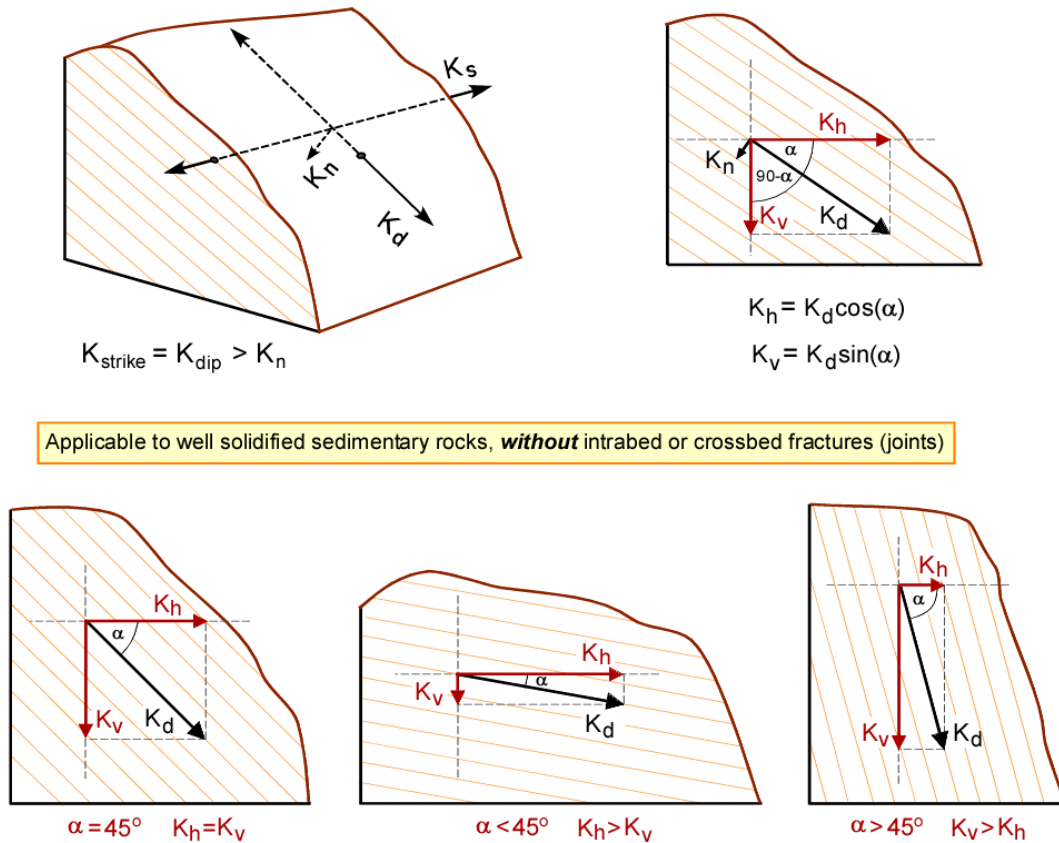
Figure 4.14 Principle of finding horizontal (K_h) and vertical (K_v) components of hydraulic conductivity in a layered, well-solidified and <u>non-fractured</u> sedimentary rock formation. *Top*: Along a bedding plane, the hydraulic conductivities along the strike (K_s) and the dip (K_d) are the same in all directions ($K_s=K_d$). The hydraulic conductivity component perpendicular/normal (K_n) to the bedding plane is significantly lower because of the mechanical discontinuity nature of bedding planes. *Bottom*: The relationship between K_h and K_v depends on the angle of dip (α): they have the same value when the dip is 45 degrees; K_v approaches K_n for sub-horizontal layers, and it approaches K_d for sub-vertical layers.

$$K_y = K_s \cos(\gamma)$$
$$K_x = K_h \cos(\beta)$$
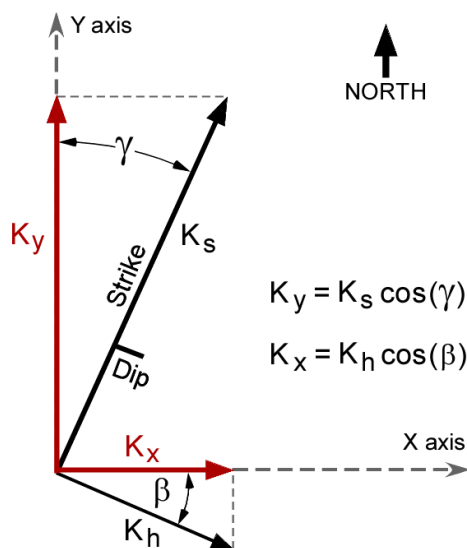
Figure 4.15 Finding two principal orthogonal components of the hydraulic conductivity (K_y and K_x) in a <u>non-fractured</u>, layered sedimentary rock, in a horizontal plane (e.g, a map view) of an orthogonal coordinate system where North is aligned with the Y axis. The components are determined from the hydraulic conductivity along the strike or dip of the bedding planes ($K_s=K_d$), and the horizontal hydraulic conductivity (K_h) determined as shown in Figure 4.14. Note that angles γ and β are the same by default.

59
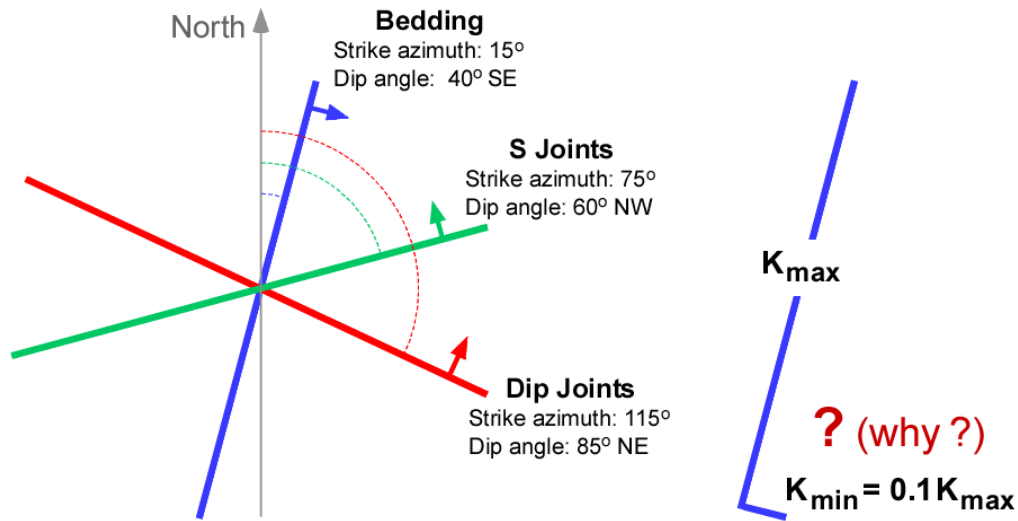
Figure 4.16 *Left*: Hypothetical statistical orientation of major structural elements like those commonly observed in sedimentary layers of the Blue Ridge, and the Valley and Ridge provinces of Virginia, Tennessee, and several other states in the eastern United States (see Figure 7.5 in Lecture 7). *Right*: Hypothetical Conceptual Site Model (CSM) by a non-hydrogeologist regarding two major axes of the hydraulic conductivity in a comparable setting. Such interpretation completely ignores the hydraulic role of different sets of joints and the dipping of bedding planes. The hypothetical non-hydrogeologist (who also may be the project manager) apparently insists that the hydraulic conductivity in the strike direction is the largest (K_{max}), and the hydraulic conductivity perpendicular to the strike is 10 times smaller (K_{min}), without any site-specific hydrogeologic testing to back that up. If this interpretation is not challenged by competent geologists and hydrogeologists and is adopted for creating a numerical model of groundwater flow for example, both the CSM and the groundwater flow model can be qualified as an unfortunate product of the so-called *groupthink* (see explanation of this term in the text).

Cave passages in soluble carbonate sediments provide an invaluable insight into the role geologic fabric plays in controlling groundwater flow directions. Such passages, developed by dissolution along initial discontinuities in the rock mass, are literary the evidence "written in stone". Hydrogeologists working in all fractured sedimentary rock environments, and not only in karst, are therefore advised to consult related speleological literature or, better yet (and for a start), visit a few easily and safely assessable caves because nothing can replace direct observations. This experience should, hopefully, change minds of those that still believe how knowledge of structural geology and hydrogeologic anisotropy is not necessary to make the "right" site-specific conclusions based on some convenient rules of thumb. Below is an illustrative excerpt from an excellent publication by Swezey et al. (2017) that illustrates the point (see also Figures 4.17 and 4.18). Incidentally, the setting is not too dissimilar to the hypothetical project site shown in Figure 4.16.

Collectively, the structural and stratigraphic setting of Burnsville Cove influences cave passage morphology. For example, many of the cave passages are tall and narrow, and follow joints. Other cave passages are relatively wide and have flat ceilings and (or) floors. Such passages typically form where the cave ceiling and (or) floor follows a bedding plane. Yet other cave passages have arched ceilings where the passages follow folds in the strata."…"In some instances, both bedding planes and joints exert strong controls on passage morphology, leading to a trapezoid passage profile with a narrow inverted V-shaped cavity at the top of the trapezoid shape.
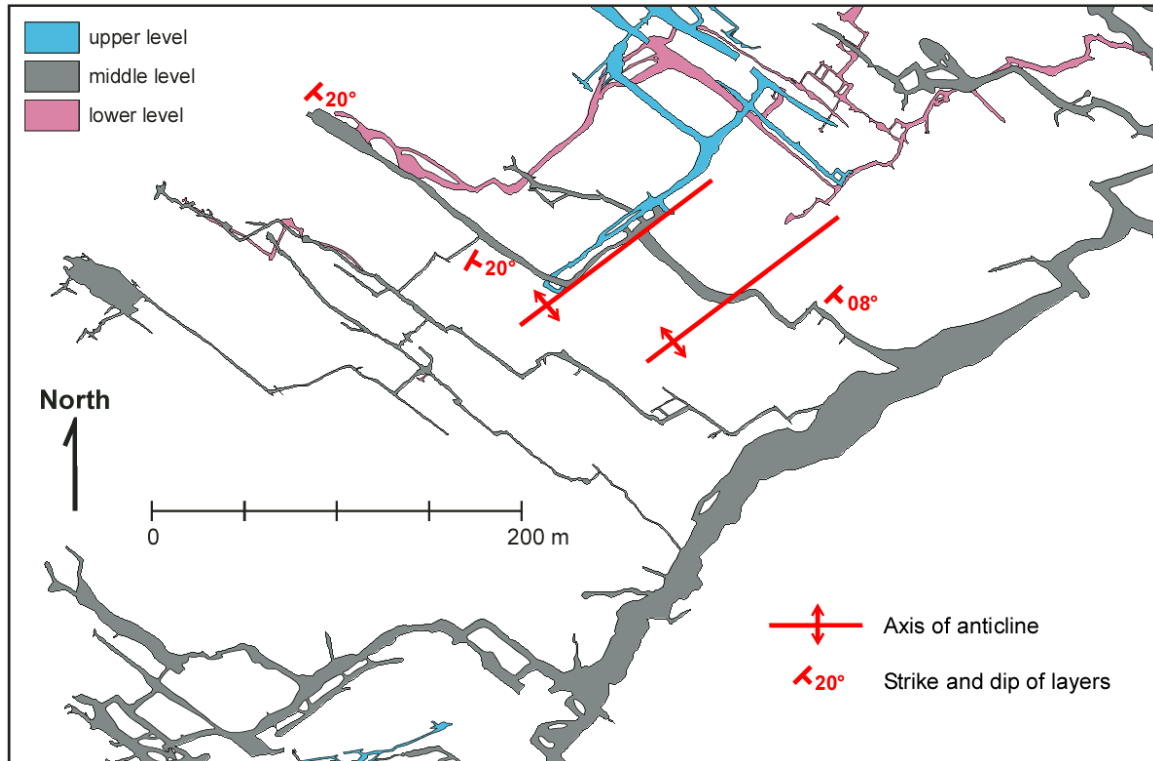
Figure 4.17 Section of map of Butler Cave – Sinking Creek Cave System, Bath County, Virginia showing mapped cave passages. Modified from Swezey et al., 2017, Geologic controls on cave development in Burnsville Cove, Bath and Highland Counties, Virginia. From the Blue Ridge to the Beach: Geological Field Excursions across Virginia. The Geological Society of America Field Guide 47; originally modified from White, 2015. Copyright The Geological Society of America; permission is required for further use.

Figure 4.18 Examples of fissure control on development of passages in caves of Highland and Bath Counties, Virginia. All photos courtesy of Phil Lucas.

Some (perhaps stubborn) practitioners may argue that, at their carbonate sediments site, there are no known caves and therefore there is no justification to apply knowledge from "elsewhere" as it would not be applicable. However, the fact that there are no known caves does not exclude the possibility that there are karstified interconnected features in the subsurface, however small (inaccessible) or large (cave passages yet to be discovered by dedicated cavers). The practitioners may go even further and argue how soluble sedimentary carbonate rocks are very different from "their own" fractured non-carbonate rocks such that there is no room for analogy. Nevertheless, it is a simple fact that groundwater flow in either case will be similarly influenced by various discontinuities in the rock mass some of which are shown on Figures 4.2-*Rigt* and 4.16-*Left*, regardless of their possible enhancement by dissolution or not (i.e., the rock type.)

Determining the hydrogeologic anisotropy of sediments and rocks should always be site-specific, must be based on hydrogeologic principles, and must include a thorough analysis of various geologic and structural elements that may contribute to it. The following discussion by Cohen, Faust, and Skipp (2009) and Figure 4.19 illustrate these points.

It has been hypothesized (e.g., Drew et al., 2004) that the most dominant fracture fabric features, which control groundwater flow in the Blue Ridge of Loudoun County, include (1) the pervasive northeast-striking, moderately to steeply dipping (generally to the southeast) metadiabase dikes that intrude the older metagranites, and (2) subparallel northeast-trending Paleozoic cleavage (schistosity). Northwest-trending foliation in the Mesoproterozoic basement rock, which was overprinted by dike intrusion and Paleozoic cleavage, is also observed in much of western Loudoun County.

In order to examine aquifer anisotropy in a more direct manner, automated water-level recording devices were deployed in numerous observation wells during aquifer tests conducted at seven sites in the Blue Ridge of Loudoun County. Data acquired during 22 tests where drawdown was observed at three or more observations wells were analyzed using the Papadopulous (1965) equation for nonsteady groundwater flow in an infinite anisotropic confined aquifer as implemented in the TENSOR2D (Maslia and Randolph, 1987) and AQTESOLV

*(beta version, Duffield, 2007) computer programs. The results shown for the analyses of 15 tests where the data reasonably fit an anisotropic solution are presented based on the AQTESOLV analysis in 4.18. The anisotropic aquifer analyses indicate that different tensor orientations are observed in different areas of 100 to 250 acre study sites and that observed anisotropy is <u>not always consistent with mapped geologic structural features</u> (*emphasis added*). Interpreted tensor orientations vary between N70E and N79W. Nine of the 15 orientations are between N5E and N38W (Cohen, Faust, and Skipp, 2009.)*
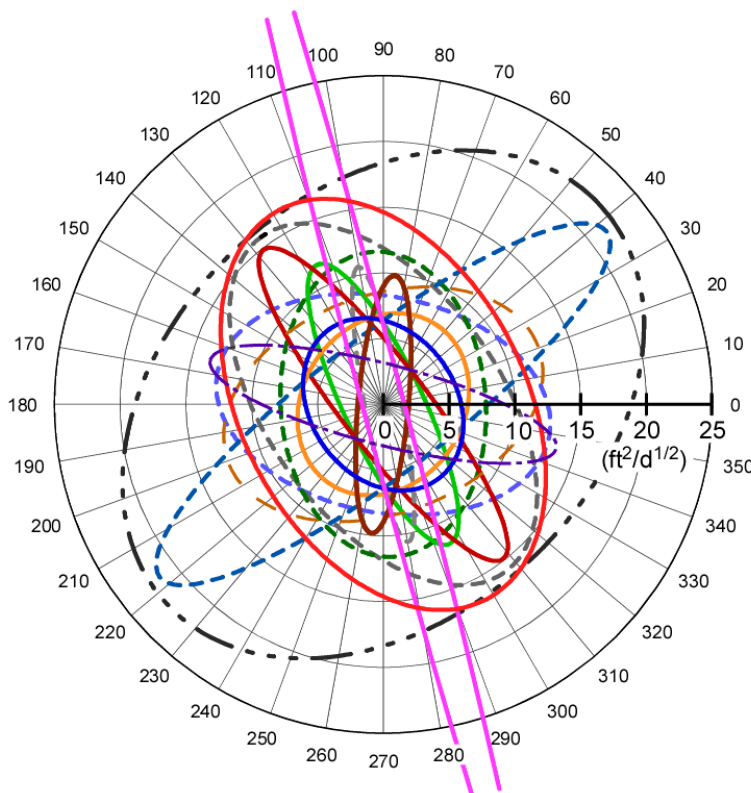
Figure 4.19 Anisotropic transmissivity tensor [(ft^2/d)$^{0.5}$] results for 15 aquifer tests at 7 sites in the Blue Ridge of Loudoun County, Virginia. Modified from Cohen, Faust, and Skipp, 2009. Copyright Geotrans, Inc. Permission is required for further use.

Sometimes it may not be feasible to estimate the principal directions of hydrogeologic anisotropy based on structural analysis of the rock fabric alone, and the only applicable method may be a tailored pumping test (see Figure 4. 19 and the accompanying explanation.) Photographs in Figure 20 illustrate this point, namely a structural "chaos" that is not uncommon in orogenic belts around the world. Hatcher (1995) provides the following illustrative discussion that further illustrates difficulty hydrogeologists often face in such environments.

In one practical application, Richard Nickelsen (1979) made a detailed study of a well-exposed series of deformed Pennsylvanian sandstone, coal, and shale layers at the Bear Valley strip mine in Pennsylvania. He was able to separate early jointing events from later faulting, cleavage formation, folding, later folding that produced new joint sets, and finally, more faulting, which also produced new joints."

Figure 4.20 *Left*: Large scale kink folds within the Triassic McCarthy Formation located near the Totschunda Fault in the Eastern Alaska Range (note person in the middle for scale). The formation is comprised of interbedded argillite (darker units) and micritic limestone (grey strata). Compressional deformation of the unit occurred during accretion of a volcanic-arc terrain onto the North American plate. Courtesy of Jeff Manuszak. *Right*: Intensely folded and faulted Mesozoic limestones in Durmitor National Park, Montenegro.

Faults are one of the key structural elements that can cause heterogeneity and anisotropy at various scales. They often form hydraulic boundaries for groundwater flow in both consolidated and unconsolidated rocks. They may have one of the following three roles: (1) preferential pathways for groundwater flow, (2) storage of groundwater due to increased porosity within the fault (fault zone), and (3) barriers to groundwater flow due to decrease in porosity within the fault. The following discussion by Meinzer (1923) illustrate these points:

Faults differ greatly in their lateral extent, in the depth to which they reach, and in the amount of displacement. Minute faults do not have much significance with respect to ground water except, as they may, like other fractures, serve as containers of water. But the large faults that can be traced over the surface for many miles, that extend down to great depths below the surface, and that have displacements of hundreds, or thousands of feet are very important in their influence on the occurrence and circulation of ground water. Not only do they affect the distribution and position of aquifers, but they may also act as subterranean dams, impounding the ground water, or as conduits that reach into the bowels of the earth and allow the escape to the surface of deep-seated waters, often in large quantities. In some places, instead of a single sharply defined fault, there is a fault zone in which there are numerous small parallel faults or masses of broken rock called fault breccia. Such fault zones may represent a large aggregate displacement and may afford good water passages.

63

The impounding effect of faults is caused by the following main mechanisms (Kresic, 2009):

- The displacement of alternating permeable and impermeable beds in such manner that the impermeable beds are made to abut against the permeable beds.
- Presence of clayey gouge along the fault plane produced by the rubbing and mashing during displacement of the rocks. (The impounding effect of faults is most common in unconsolidated formations that contain considerable clayey material.)
- Cementation of the pore space by precipitation of material, such as calcium carbonate, from the groundwater circulating through the fault zone.
- Rotation of elongated flat clasts parallel to the fault plane so that their new arrangement reduces permeability perpendicular to the fault.

Mozley et al. (1996) discuss reduction in hydraulic conductivity associated with high-angle normal faults that cut poorly consolidated sediments in the Albuquerque Basin, New Mexico. Such fault zones are commonly cemented by calcite, and their cemented thickness ranges from a few centimeters to several meters, as a function of the sediment grain size on either side of the fault. Cement is typically thickest where the host sediment is coarse grained and thinnest where it is fine grained. In addition, the fault zone is widest where it cuts coarser-grained sediments. Extensive discussion on deformation mechanisms and hydraulic properties of fault zones in unconsolidated sediments is given in Bense et al. (2003). Various aspects of fluid flow related to faults and fault zones are discussed in Haneberg et al. (1999).
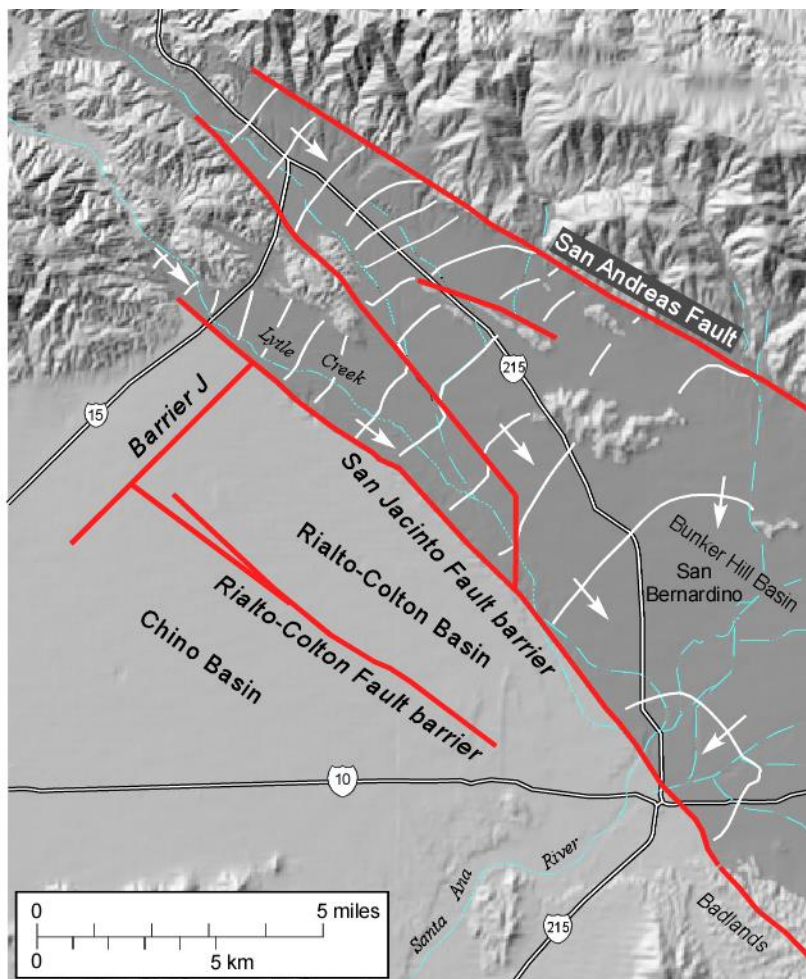
An example of major faults in unconsolidated alluvial-fill basins in southern California acting as impermeable barriers for groundwater flow is shown in Figure 4.20. The Rialto-Colton basin, which is heavily pumped for water supply, is almost surrounded by impermeable fault barriers, receives negligible recharge from precipitation, and very little lateral inflow in the far northwest from the percolating Lytle Creek waters. In contrast, the Bunker-Hill basin, which is also heavily pumped for water supply, receives most of its significant recharge from numerous losing surface streams, and runoff from the mountain front. As a result, the hydraulic heads in the Rialto-Colton basin (not shown on the figure) are hundreds of feet lower than in the Bunker-Hill basin.

Figure 4.20. Alluvial-fill basins in southern California. White lines are contours of hydraulic head; white arrows are general directions of groundwater flow; bold red lines are major faults. Modified from Danskin et al., 2006. USGS, in public domain.

As discussed by Hatcher (1995), joints frequently form adjacent to brittle faults. Movement along faults commonly produces a series of systematic fractures in which spacing decreases closer to the fault zone, and the number of sets of joints also increases. It is for this reason that fault zones in carbonate sediments and other rocks that do not have significant fine-grain fraction (sandstones are an example) do act as preferential flowpaths and can collect and transfer significant quantities of groundwater. Some of the largest springs in the United States and worldwide owe their existence to faults. For example, San Marcos and Comal Springs of Central Texas are the largest springs in the southwestern United States. The artesian springs emerge at the base of the Balcones Escarpment, a series of large-displacement faults that force the water of the karstic Edwards aquifer to discharge at the land surface (Figure 4.21). Another good example of fault-controlled springs are many springs in the classic Dinaric karst of former Yugoslavia, some of which are the largest in the world (see Lectures 6 and 8.)
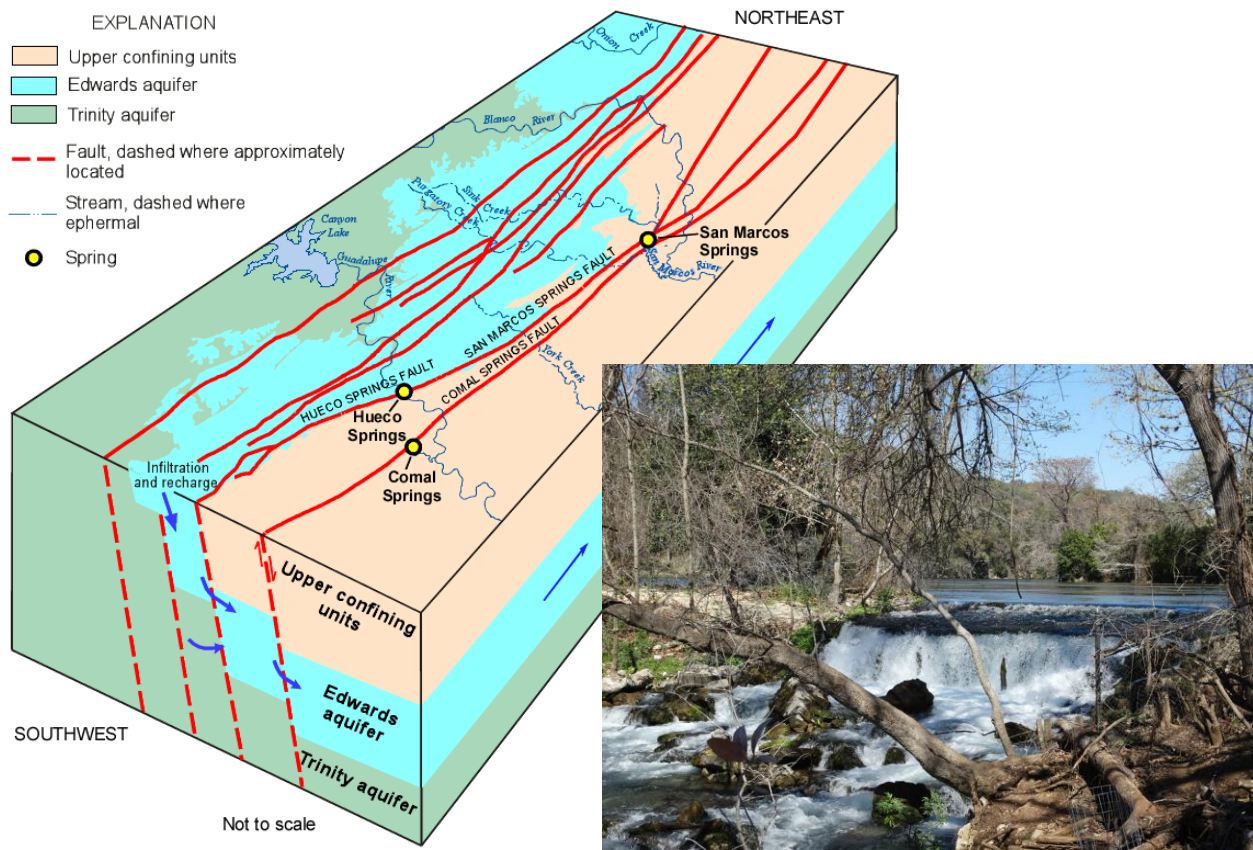
Figure 4.21 *Left*: Idealized block diagram of the Edwards aquifer in the vicinity of Comal, Hueco, and San Marcos Springs, south-central Texas. Modified from Musgrove and Crow, 2012. USGS, in public domain. *Right*: Figure 4.22 Main overflow from the basin of San Marcos Springs, Texas.

4.2 Groundwater Velocity and Flow Rate

The seepage velocity or Darcy's velocity, as defined by Darcy's law (see Lecture 3 and Equations 3.1 through 3.5), is the product of the hydraulic conductivity (K) and the hydraulic gradient (i)

$$v = K * i \qquad (4.1)$$

However, this is not the real velocity at which water particles move through the porous medium. Darcy's law, first derived experimentally, assumes that the groundwater flow (Q) occurs through the entire cross-sectional area (A) of a porous medium (sample) including both the voids and the grains—see Equation (b) in Figure 4.23. Since the flow takes place only through interconnected voids, the effective cross-sectional area of flow (A_{ef}) is the sum of the individual cross-sectional areas of voids—Equation (c). The total volume of flow is the sum of individual flows—Equation (d).

To preserve the principle of the continuity of flow (there is no gain or loss of water), a new equivalent velocity (v_L) that describes the flow through the effective cross-sectional area of voids is introduced—Equation (e). This velocity is called *linear velocity*. Since the effective cross-sectional area of flow is smaller than the total area, it follows that the linear velocity must be greater than Darcy's velocity: $v_L > v$. Equation (e) can be written as Equation (f) where the fraction at the right-hand side can then be multiplied by the width of aquifer (sample) segment of interest to obtain volumes—Equation (g).

The volume of effective (interconnected) voids that allows free gravity flow (V_{ef}), divided by the total volume of porous media (V), is the effective porosity (n_{ef}) and Equation (f) can be written as Equation (h). After inserting Equation (a) into Equation (h) and rearranging, the linear velocity is expressed with Equation 4.2.
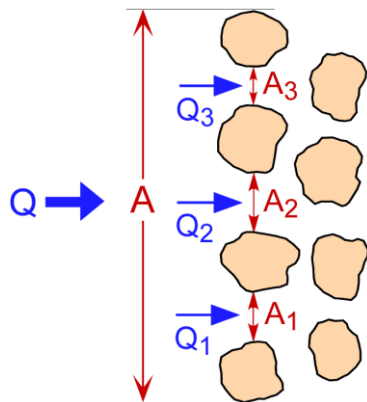
$$v = K * i \quad (a) \qquad v * A = v_L * A_{ef} \quad (e)$$
$$Q = v * A \quad (b) \qquad v = v_L * \frac{A_{ef}}{A} \quad (f)$$
$$A_{ef} = A_1 + A_2 + A_3 \quad (c) \qquad v = v_L * \frac{V_{ef}}{V} \quad (g)$$
$$Q = Q_1 + Q_2 + Q_3 \quad (d) \qquad v = v_L * n_{ef} \quad (h)$$

$$v_L = \frac{K * i}{n_{ef}} \quad (4.2)$$

Figure 4.23 *Left*: Schematic presentation of the volumetric flow rates and cross-sectional areas of flow. *Right*: Derivation of the equation of linear flow velocity.

The following example illustrates how two different choices of two basic hydrogeologic parameters reflecting heterogeneity can produce very different quantitative answers, even though both selections may seem reasonable. Consider the following scenario: point of contaminant release and a potential receptor are 2500 feet apart; the regional hydraulic gradient in the shallow aquifer, which consists of "fine sands", is estimated from available monitoring well data to be 0.002. How long would it take a dissolved contaminant particle to travel between the two points, if the contaminant does not degrade or adsorb to solid particles (i.e., it moves at the same velocity as water, it acts as a "conservative tracer")?

As shown in Figure 3.2, fine sand can have hydraulic conductivity anywhere between a little less than 1 foot per day and about 40 feet per day. Effective porosity (specific yield) of "sand" can vary anywhere between 20 and

45 percent (Figure 2.13). Assuming the lowest values from the two ranges, the linear velocity of a groundwater particle, using Equation (4.2), is:

$$v_L = \frac{K * i}{n_{ef}} = \frac{0.8\ ft/d * 0.002}{0.2} = 0.016\ ft/d$$

Based on this velocity, the time of groundwater (and dissolved contaminant) travel between the two points of interest would be 156250 days or about 428 years (2500 foot-distance is divided by the velocity of 0.016 ft/day). Using the highest values from the two ranges (40 ft/day and 45 percent), the time of travel would be about 14045 days or 38.5 years, which is a very significant difference, to say the least. This simple quantitative example shows inherent uncertainties in quantifying groundwater flow velocities, even when assuming that the porous medium is "homogeneous".

Two main forces act upon individual water particles that move through porous media: friction between the moving water particles and friction between the water particles and the solids surrounding the voids. This results in uneven velocities of individual water particles: some travel faster and some slower (Figure 4.24). This phenomenon is called *mechanical dispersion* and it is very important when quantifying transport of contaminants dissolved in groundwater (more on fate and transport of contaminants is presented in Lecture 13). Because of mechanical dispersion, the spreading of individual water (or dissolved contaminant) particles is in all three main directions with respect to the overall groundwater flow direction: longitudinal, transverse, and vertical. A very illustrative tool for demonstrating the effects varying hydraulic conductivity, porosity and hydraulic gradients have on velocity, flow directions and dispersion of fluid particles is available as a public domain computer program called *Particleflow* by Hsieh of the USGS (2001).
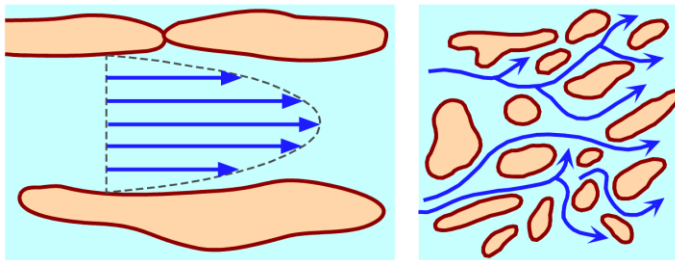
Figure 4.24 Schematic presentation of mechanical dispersion caused by varying velocity of water particles and tortuous paths between the porous medium grains. *Left*: Friction between water particles and grains results in slower velocities closer to the grains. From Franke et al., 1990. USGS, in public domain.

Calculation of groundwater flow rate (Q) in any aquifer setting, i.e., for both confined and unconfined aquifers of any cross-sectional area (A), and for the velocity vector in any direction (v), always starts with the basic equation of the continuity of groundwater flow:

$$Q = v * A \qquad (4.3)$$

This simple principle is illustrated in Figure 4.25 which shows groundwater flow in a single flow tube of an aquifer. There is no gain or loss of water in the flow tube between two cross-sectional areas (A_1 and A_2), which can be of different sizes. Three-dimensional surfaces of the same hydraulic head within the flow tube are called *equipotential surfaces*. Their horizontal projections, often shown on hydrogeologic maps of aquifers, are called *equipotential lines*.

Analytical equations describing groundwater flow in a truly three-dimensional setting, like the one shown in Figure 4.25, which would include all possible heterogeneities and anisotropies, are very complex and do not have closed solutions. It is for this reason that numeric models of groundwater flow are being increasingly utilized given the complex nature of most groundwater studies today. However, approximate analytical solutions based on various assumptions (simplifications) are still widely used since they often provide satisfactory results for simple field conditions.
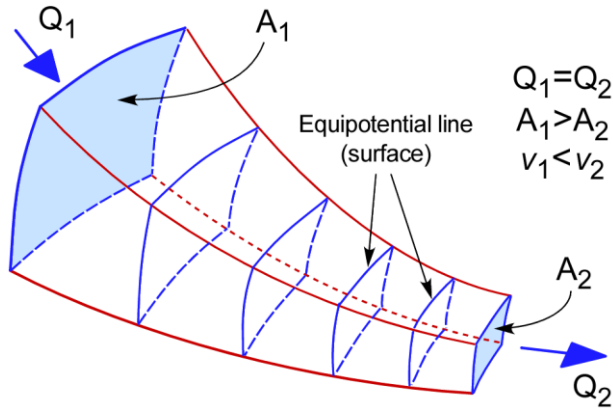
Figure 4.25 Groundwater flow tube in an aquifer showing principle of flow conservation—there is no gain or loss of water within the flow tube. Modified from Kresic, 2007. Copyright CRC Taylor & Francis; permission is required for further use.

4.2.1 Steady state Flow

Volumetric steady state flow rate (i.e., flow rate that does not change with time) in a homogeneous, isotropic, confined aquifer of constant thickness (b), which is resting on a horizontal base, can be calculated for any width of the aquifer (a) by directly applying Darcy's equation in its simplest form where the cross-sectional area of flow is $A = a * b$ (see Figure 4.26-*Left*):

$$Q = KA\frac{h_1 - h_2}{L} \qquad [m^3/s \text{ or } ft^3/\text{d}] \qquad (4.4)$$

Analytic solutions and quantitative examples of more complex situations where the aquifer thickness changes, the hydraulic conductivity is not uniform, or there are two sloping confined aquifers that merge into one, are presented in Kresic, 2007 (*Hydrogeology and Groundwater Modeling, Second Edition*. CRC Taylor & Francis).
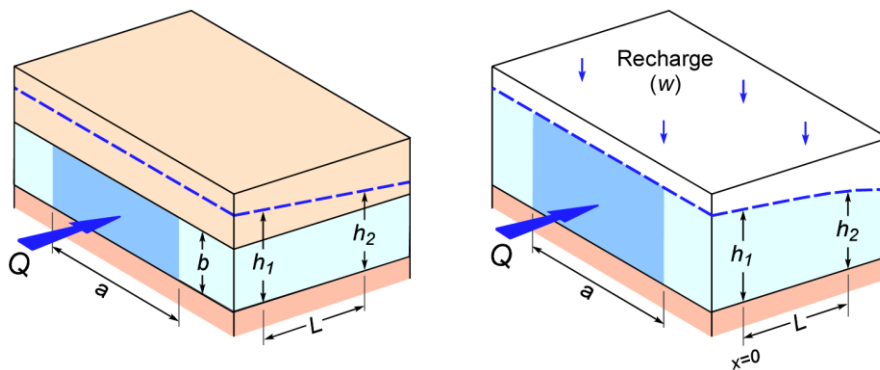
Figure 4.26 Elements for calculating confined (*Left*) and unconfined (*Right*) volumetric steady state flow rate using Equations (4.4) and (4.5) respectively.

Steady-state groundwater flow in an unconfined aquifer is in general somewhat more complex than in a confined aquifer for the following two reasons: 1) the aquifer is likely receiving water from aerial recharge or is losing water to evapotranspiration, and 2) the saturated thickness changes as the position of water table changes.

In the absence of any gain or loss of water (e.g., no recharge and no evapotranspiration), the steady state volumetric flow rate in a homogeneous, isotropic unconfined aquifer that is resting on a horizontal impermeable base is:

$$Q = a * K \frac{h_1^2 - h_2^2}{2L} \qquad (4.5)$$

In case of aquifer recharge (w), at the location where $x = 0$ and $h = h_1$ the flow is

$$Q = a * K \frac{h_1^2 - h_2^2}{2L} - w \frac{L}{2} \qquad (4.5a)$$

At any distance (x) from the coordinate beginning the flow is

$$Q = a * K \frac{h_1^2 - h_2^2}{2L} + w \left(x - \frac{L}{2} \right) \qquad (4.5b)$$

If the aquifer is losing water to evapotranspiration, term (w) becomes negative.

When two hydraulic heads along the flow path are known, the position of the hydraulic head at any distance (x) from the origin can be calculated using the following equation:

$$h_x = \sqrt{h_1^2 - (h_1^2 - h_2^2) \frac{x}{L}} \qquad (4.6)$$

Equations (4.5) and (4.6) assume that the groundwater flow in an unconfined aquifer is strictly horizontal, the velocity is constant along a vertical and proportional to saturated aquifer thickness, and the water table is "relatively flat." These assumptions are referred to as Dupuit's hypothesis after French scientist Jules Dupuit who formulated it in 1863, based on Darcy's law and laminar character of groundwater flow through unconsolidated porous media (Dupuit, 1863).

4.2.2 Radial Steady State Flow in Confined Aquifer (Thiem Equation)

Time-independent (steady state) groundwater flow toward a well in a fully confined (non-leaky) aquifer is described by the Thiem equation. It is attributed to German engineer G. Thiem who published it in 1906 in his doctoral dissertation on the results of experiments and mathematical study relating to his field method for determining aquifer parameters. Detail description of the Thiem equation application is given by Wenzell (1936). The equation is based on the following assumptions:

- The well fully penetrates the confined aquifer and receives water from the entire thickness of the aquifer.

- The well is pumping water from the aquifer at a constant rate.
- The flow toward the well is radial, horizontal, and laminar, i.e., the flow lines are parallel along each radial cross-section.
- The aquifer is homogeneous and isotropic and has uniform thickness and a horizontal base.
- After a certain period of pumping, the drawdown in the well does not increase anymore (it is stabilized), and the steady state flow conditions are established.

Explanation

Q Well pumping rate
r_w Well radius
h_w Hydraulic head in the well
h_r Hydraulic head at distance r
H Initial hydraulic head
b Thickness of the aquifer
R Radius of well influence
S_w Drawdown in the well
K Hydraulic conductivity
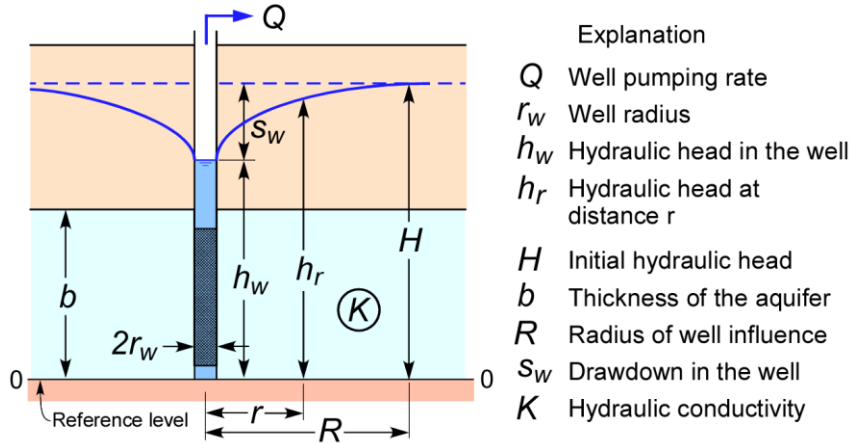
Figure 4.27 Elements for calculating groundwater flow rate toward a fully penetrating well in a confined aquifer using Thiem equation.

Although these conditions are seldom completely satisfied, there are several situations when a steady state approach to the well pumping test analysis may be justified for a preliminary assessment, such as when the drawdown relatively stabilizes ("quasi steady state conditions.") Figure 4.27 shows the elements for deriving the Thiem equation. As is the case with most other equations in hydrogeology, the flow rate (Q) is given as the product of the cross-sectional area of flow (A) and the flow velocity (v):

$$Q = A \cdot v \qquad (4.7)$$

The cross-sectional area of flow at distance r from the pumping well is the side of the cylinder with the radius r and the thickness b (which is the thickness of the confined aquifer):

$$A = 2\pi r b \qquad (4.8)$$

The velocity of flow at distance r is given as the product of the aquifer's hydraulic conductivity (K) and the hydraulic gradient which is an infinitesimally small drop in hydraulic head (dh) over an infinitesimally small distance (dr):

$$v = K \frac{dh}{dr} \qquad (4.9)$$

Inserting equations (4.9) and (4.8) into equation (4.7) and solving for boundary conditions at distances r_w and r from the well where the hydraulic heads are h_w and h_r respectively, gives the following solution for the hydraulic head (h_r) at any distance r from the well:

$$h_r = h_w + \frac{Q}{2\pi T} \ln \frac{r}{r_w} \qquad (4.10)$$

The following boundary conditions enable introduction of the *drawdown in the well* (s_w):

- At distance r_w (which is the well radius) the hydraulic head is h_w (head in the well),

- At distance R from the well (which is the radius of well influence) the hydraulic head is H (which is the undisturbed head, equal to the initial head before the pumping started).

$$H - h_w = s_w = \frac{Q}{2\pi T} \ln \frac{R}{r_w} \qquad (4.11)$$

The pumping rate of the well is:

$$Q = \frac{2\pi T s_w}{\ln \dfrac{R}{r_w}} \qquad (4.12)$$

Equation (4.11) can be rewritten to give the drawdown at any radial distance from the pumping well:

$$s_r = \frac{Q}{2\pi T} \ln \frac{R}{r} \qquad (4.13)$$

Noting all the constant terms in equation (2.21), the drawdown can be expressed as a function of distance only:

$$s_r = \frac{Q}{2\pi T} \ln R - \frac{Q}{2\pi T} \ln r \qquad (4.14)$$

or, when the constant terms are replaced with general numbers:

$$s_r = a - b \ln r \qquad (4.15)$$

Equation (4.15) means that the recorded data of drawdown versus radial distance from the pumping well would form a straight line when plotted on a semi-logarithmic graph paper. Figure 4.28 shows a graph drawdown vs. distance for two monitoring wells MW-1 and MW-2 located at distances r_1 and r_2 from the pumping well PW respectively. Note that the drawdown recorded in the pumping well does not fall on the straight line connecting the monitoring well data; it is below the straight lines indicating that there is an additional drawdown in the well because of the *well loss*. The well loss, which is inevitable at any well, is explained in detail in the Hydrogeology 101 Laboratory Manual. In short, it is a consequence of various factors such as disturbance of porous medium near the well during drilling, an improper (insufficient) well development, a poorly designed gravel pack and/or well screen, and possible turbulent flow through the well screen. Because of the well loss, at least two monitoring wells are needed to apply the Thiem equation for estimating aquifer properties using monitoring data. Using the pumping well drawdown and the drawdown in one monitoring well would give erroneous results.

The steady-state radius of well influence (R) is the intercept of the straight line connecting the monitoring well drawdowns with the zero drawdown. The aquifer transmissivity can be estimated by relating coordinates of any two points on the straight line:
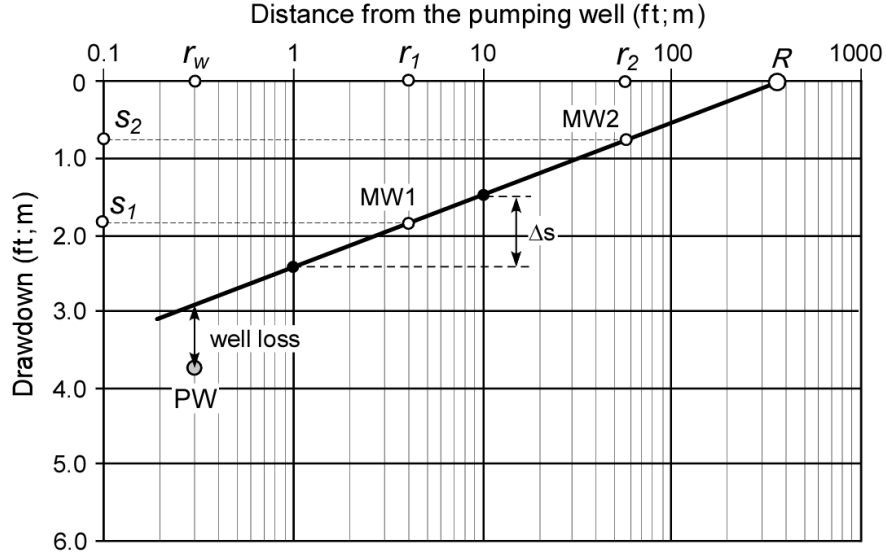
Figure 4.28 Graph drawdown versus distance for a pumping well with two monitoring wells. From Kresic, 2007. Copyright CRC Taylor & Francis; permission is required for further use.

$$s_1 = const - \frac{Q}{2\pi T} \ln\, r_1$$

$$s_2 = const - \frac{Q}{2\pi T} \ln\, r_2$$

$$s_1 - s_2 = \Delta s = \frac{Q}{2\pi T} \ln \frac{r_2}{r_1}$$

The transmissivity is then found from this difference in drawdown for the chosen points:

$$T = \frac{Q}{2\pi \Delta s} \ln \frac{r_2}{r_1} \qquad (4.16)$$

For practical purposes it is better to express the transmissivity in terms of the common logarithm or decadic logarithm (the logarithm to the base of 10 or log) since the corresponding graph is easier to use. Knowing that

$$\log x = 0.4343 \ln x$$

and replacing "pi" (π) with number 3.14, equation (4.16) becomes

$$T = \frac{0.366Q}{\Delta s} \log \frac{r_2}{r_1} \qquad (4.17)$$

If two points on the straight line are chosen to be one log cycle apart (i.e., the ratio of the distance coordinates r_2 and r_1 is 10), equation (4.17) reduces to the following simple form:

$$T = \frac{0.366Q}{\Delta s} \qquad (4.18)$$

This is the final equation for determining transmissivity of a confined aquifer using the Thiem method. The hydraulic conductivity of the aquifer porous media is found by dividing the transmissivity by the aquifer thickness. Note that aquifer storage cannot be found using the steady-state approach. Application of the Thiem equation to actual field data is provided in the Hydrogeology 101 Laboratory Manual.

4.2.3 Radial Steady State Flow in Unconfined Aquifer

Analysis of wells pumping from unconfined aquifers is more complex than that of confined aquifers since the top of the aquifer corresponds to the water table and its position changes due to pumping. In other words, the thickness of the aquifer (saturated zone) changes within the radius of the well influence: it is the smallest at the well perimeter (see Figure 4.29). If the aquifer impermeable base is horizontal, and the reference level is set at the base, the hydraulic head equals the water table, which simplifies the derivation of the flow equation.

Applying Dupuit's hypothesis allows the exact calculation of the flow rate, whereas finding the accurate position of the water table is more complicated and is based on various experimental (approximate) equations. Figure 4.29 illustrates the concept of Dupuit's hypothesis together with the real distribution of velocities around a pumping well. Dupuit's hypothesis states that:

- Equipotential lines are vertical.
- Velocity is constant along any given vertical (i.e., along approximated equipotential line).
- The velocity vector has only the horizontal component (i.e., the streamlines are horizontal and parallel).

However, the velocity vector has a vertical component, which increases closer to the well and the water table. The actual position of the water table is above the calculated one (Dupuit's parabola) and this difference at the well perimeter corresponds to the seepage face. At a certain distance from the well (denoted r^* in Figure 4.29) the difference between the actual and the calculated water table becomes very small and can be ignored for practical purposes.
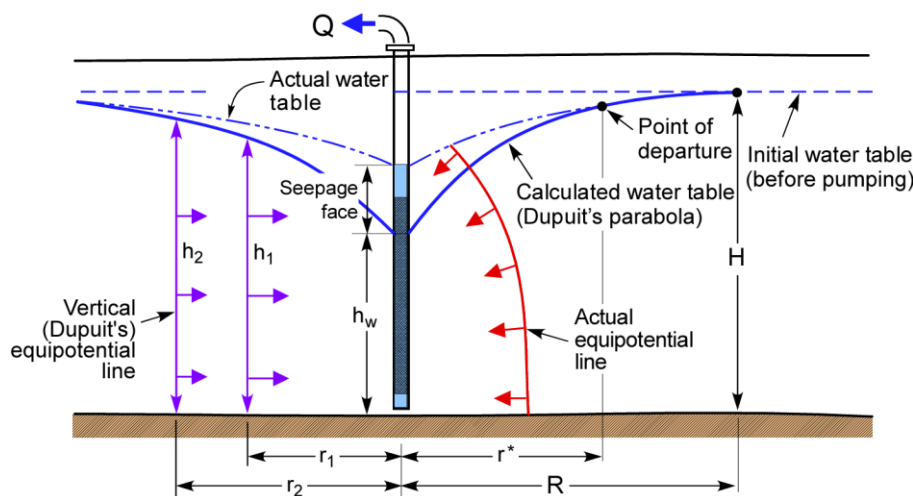
Figure 4.29 Schematic of radial groundwater flow towards a fully penetrating well pumping in an unconfined aquifer. Arrows show directions of groundwater flow. Modified from Kresic, 2007. Copyright CRC Taylor & Francis; permission is required for further use.

As always, the flow rate (Q) is given as the product of the cross-sectional area of flow (A) and the flow (seepage) velocity (v):

$$Q = A * v \qquad (4.19)$$

The cross-sectional area of flow at distance r from the pumping well is the side of the cylinder with radius r and thickness h (which is the thickness of the saturated zone at that distance):

$$A = 2r\pi h \qquad (4.20)$$

The velocity of flow at distance r is given as the product of the aquifer hydraulic conductivity (K) and the hydraulic gradient, which is an infinitesimally small drop in hydraulic head (dh) over an infinitesimally small distance (dr):

$$v = K\frac{dh}{dr} \qquad (4.21)$$

Inserting equations (4.20) and (4.21) into equation (4.19), and solving for boundary conditions

- At distance r_w (which is the well radius) the hydraulic head is h_w (head in the well).
- At distance r from the well the hydraulic head is h:

gives the following expression for the well pumping rate:

$$Q = \pi K \frac{(h^2 - h_w^2)}{\ln\dfrac{r}{r_w}} \qquad (4.22)$$

The well pumping rate for any other pair of known hydraulic heads and the corresponding distances from the well, such as the radius of well influence (R) and the well radius (r_w) is (see Figure 4.30)

$$Q = \pi K \frac{(H^2 - h_w^2)}{\ln\dfrac{R}{r_w}} \qquad (4.23)$$

If the heads (or drawdown) in two monitoring wells are known, the hydraulic conductivity can be found using the following equation:

$$K = \frac{Q \ln\dfrac{r_2}{r_1}}{\pi(h_2^2 - h_1^2)} \qquad (4.24)$$

The hydraulic conductivity and the radius of well influence can also be found graphoanalytically (see Figure 4.30), similarly to the confined aquifer case described earlier (after expressing natural logarithm as decadic logarithm)

$$K = \frac{0.733 \cdot Q}{\Delta(H^2 - h^2)} \log\frac{r_2}{r_1} \qquad (4.25)$$

If two points on the straight line are chosen to be one log cycle apart (i.e., the ratio of r_2 and r_1 is 10), equation (4.25) reduces to

$$K = \frac{0.733 \cdot Q}{\Delta(H^2 - h^2)} \qquad (4.26)$$
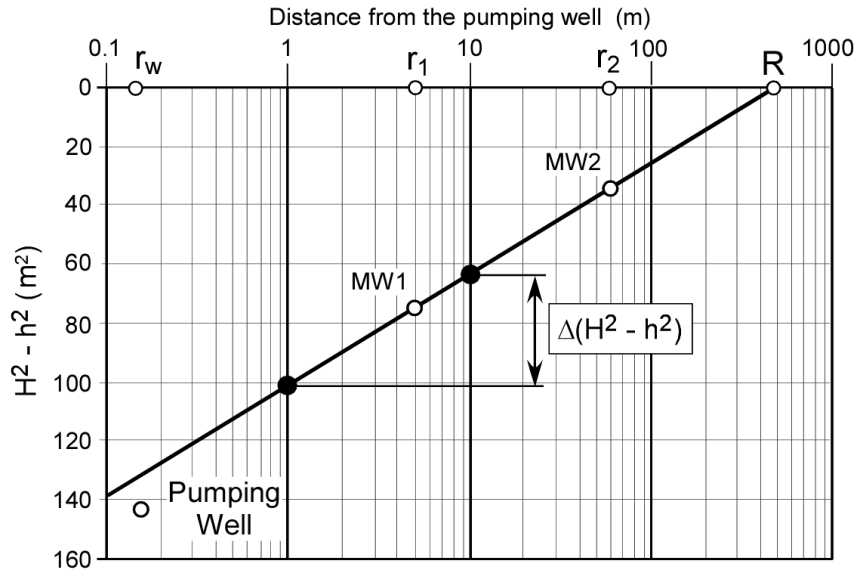
Figure 4.30 Semilogarithmic graph for determining hydraulic conductivity and radius of well influence using data from a pumping test in an unconfined aquifer. Modified from Kresic, 2007. Copyright CRC Taylor & Francis; permission is required for further use.

The radius of well influence is determined by the interception of the straight line drawn through the monitoring well points with the line of zero drawdown. Note that the straight line should be drawn only through the monitoring well points, since the actual drawdown recorded in the pumping well includes an additional drawdown component. This additional drawdown is a consequence of well losses, as well as presence of a seepage face along the well screen perimeter.

An equation, based on Dupuit's assumption, that describes the position of the water table (h) at distance (r) from the pumping well is

$$h = \left[h_w^2 + \frac{Q}{\pi K} \ln \frac{r}{r_w} \right]^{1/2} \qquad (4.27)$$

where h_w is the hydraulic head recorded in the well, and r_w is the well radius. This equation is also known as *Dupuit's parabola*.

The position of water table (h) at any distance (r) from the pumping well can be expressed in terms of other known heads and distances at which they are recorded. This is a more convenient method for calculating Dupuit's parabola since one does not need to know the hydraulic conductivity and the well pumping rate:

$$h = \sqrt{h_w^2 + (H^2 - h_w^2)\frac{ln\dfrac{r}{r_w}}{ln\dfrac{R}{r_w}}} \qquad (4.28)$$

where H is the initial hydraulic head (before pumping) and R is the radius of well influence.

The position of the actual water table is above the Dupuit's parabola, and several experimental (approximate) equations have been proposed for its calculation. One of the more common is the Babbitt-Caldwell equation (adapted from Kashef, 1987) which estimates the actual hydraulic head at the pumping well perimeter as:

$$h_0 = H - \frac{0.6}{H} \cdot \frac{H^2 - h_w^2}{ln\dfrac{R}{r_w}} \cdot ln\frac{R}{0.1H} \qquad (4.29)$$

The difference between the actual hydraulic head outside the pumping well (h_0) and the head measured in the pumping well (h_w) gives the length of the seepage face: $\Delta h = h_0 - h_w$ which includes the well loss.

4.2.4 Radial Transient Flow in Confined Aquifer (Theis Equation)

The following discussion is adopted from Kresic (2007). The Theis equation (Theis, 1935), which describes transient (non-equilibrium) groundwater flow toward a fully penetrating well in a confined aquifer, is the basis for most methods of transient pumping test analysis. Using the equation, aquifer transmissivity and storage can be determined from the drawdown measurements without requirement for drawdown stabilization. In addition, only one observation well is enough to estimate aquifer hydrogeologic parameters, as opposed to steady state calculations where at least two observation wells are needed.

The Theis equation gives drawdown (s) at any time after the beginning of pumping:

$$s = \frac{Q}{4\pi T}W(u) \qquad (4.30)$$

where Q is the pumping rate <u>kept constant</u> during the test, T is the transmissivity, and $W(u)$ is called *well function of u*, also known as the *Theis function*, or simply *well function*. Dimensionless parameter u is given as:

$$u = \frac{r^2 S}{4Tt} \qquad (4.31)$$

where r is the distance from the pumping well where the drawdown is recorded, S is the storage coefficient, and t is the time since the beginning of pumping. The well function of u is the exponential integral

$$W(u) = -E(-i) = -\int_u^\infty \frac{e^{-u}}{u} du \qquad (4.32)$$

which can also be expressed with the following series:

$$W(u) = -0.5772 - \ln u + u - \frac{u^2}{2 \cdot 2!} + \frac{u^3}{3 \cdot 3!} - \frac{u^4}{4 \cdot 4!} + \cdots \qquad (4.33)$$

or as

$$W(u) = \ln \frac{0.5615}{u} + \sum_{n=1}^{n=\infty} (-1)^{n+1} \frac{u^n}{n \cdot n!} \qquad (4.34)$$

Values of $W(u)$ for various values of the parameter u are given in Appendix A and can be readily found in groundwater literature. Also included is a theoretical graph for the Theis equation which can be used for curve matching of field observations as explained further and in the Hydrogeology 101 Laboratory Manual.

Theis derived his equation based on quite a few assumptions and it is very important to understand its limitations. If the aquifer tested and the test conditions significantly deviate from these assumptions (which, in fact, is very often the case in reality), other methods of analysis using appropriate analytical equations should be used. The equation (4.30) is valid for the following conditions (modified from Driscoll, 1986):

- The aquifer is homogeneous and isotropic.
- The aquifer is uniform in thickness and the pumping never affects its exterior boundary (the aquifer can be considered infinite in areal extent).
- The aquifer is confined, and it does not receive any recharge.
- Well discharge is derived entirely from aquifer storage.
- The water removed from storage is discharged instantaneously when the head is lowered.
- The pumping rate is constant.
- The radius of the well is infinitesimally small, i.e., the storage in the well can be ignored.
- The pumping well is fully penetrating: it receives water from the entire thickness of the aquifer, and it is 100 % efficient (there are no well losses).
- The initial potentiometric surface (before pumping) is horizontal.

The Theis equation can be used to determine aquifer transmissivity and storage if frequent measurements of drawdown versus time are performed in one or more observation wells. Equation (4.30) has no explicit solution and Theis introduced a graphical method, which gives T and S if other terms are known. Theoretical curve $W(u)$ versus $1/u$ is plotted on a graph paper with logarithmic scales as shown in Figure 4.31 (black lines graph). Field data of *drawdown (s)* versus *time (t)* for an observation well is plotted separately on a graph with the same scale (blue lines graph). This field data (blue circles) for the observation well is then superimposed on the theoretical curve (thick black line), also called *type curve*. It is essential that both graphs have identical logarithmic scales and cycles as shown in Figure 4.31. Keeping coordinate axes of the curves parallel, the field data is matched to the type curve.

Once a satisfactory match is found, a *match point* on the overlapping graphs is selected. The match point is defined by four coordinates, the values of which are read on two graphs: $W(u)$ and $1/u$ on the type curve graph (black lines graph), s and t on the field graph (blue lines graph.) The match point can be any point on the overlapping graphs, i.e., it does not have to be on the matching curve. Figure 4.31 shows two options for selecting a matching point: one chosen outside the matching curve to obtain convenient values of $W(u)$ and $1/u$: 1 and 100 respectively, and one on the matching curve which may seem more logical. However, both matching points should lead to the same values of T and S if the coordinates are read carefully. The transmissivity is calculated using a rearranged equation (4.30) and the match point coordinates s and $W(u)$:
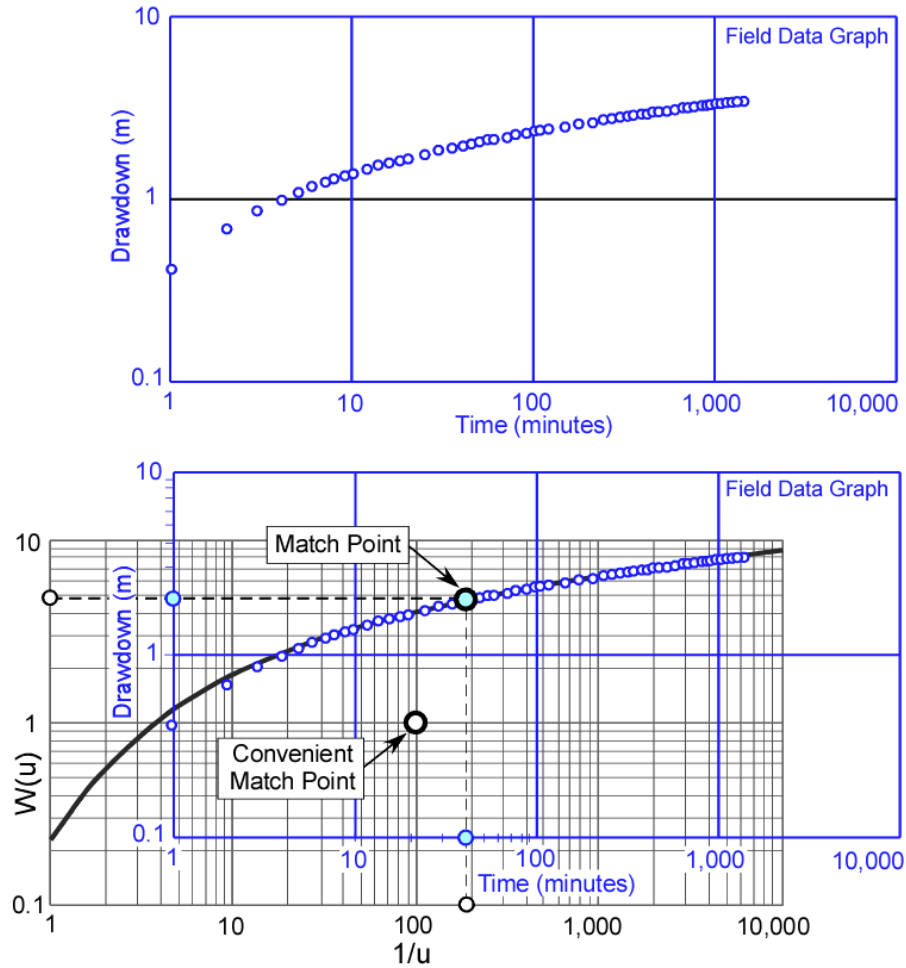
Figure 4.31 Graphoanalytical solution of the Theis equation for a pumping test data at a montoring well located 40.5 meters from the pumping test well. The fully penetrating well was pumping from a confined aquifer for 24 hours at a constant rate of 8 liters per second (0.008 m³/s). The black graph is the theoretical Theis curve. Copyright CRC Taylor & Francis; permission is required for further use.

The transmissivity is calculated using a rearranged equation (4.30) and the match point coordinates s and $W(u)$:

$$T = \frac{Q}{4\pi s} W(u) \qquad (4.35)$$

The storage coefficient is calculated using equation (2.60), the match point coordinates $1/u$ and t, and the transmissivity value already determined:

$$S = \frac{4Ttu}{r^2} \qquad (4.36)$$

For the example shown in Figure 4.31 the coordinates of the match point on the curve are:

$$W(u) = 4.75 \qquad\qquad 1/u = 180 \qquad\qquad u = 0.0055$$

$$s = 2.0\ m \qquad\qquad t = 39\ minutes = 2440\ seconds$$

The transmissivity is calculated using equation (4.35):

$$T = \frac{0.008 \ m^3/s}{4 \cdot \pi \cdot 2.0 \ m} \cdot 4.75 = 1.51 \times 10^{-3} \ m^2/s$$

The storage coefficient is calculated using equation (4.36):

$$S = \frac{4 \cdot 1.51 \times 10^{-3} \ m^2/s \cdot 2340 \ sec \cdot 0.0055}{(40.5 \ m)^2} = 4.7 \times 10^{-5}$$

The hydraulic conductivity (K) is calculated from the transmissivity (T) and the aquifer thickness (b=18m):

$$K = \frac{T}{b} = \frac{1.51 \times 10^{-3} \ m^2/s}{18 \ m} = 8.39 \times 10^{-5} \ m/s$$

General Note on Application of the Theis Equation

If the focused conceptual site model (CSM) developed prior to the test suggests that the aquifer should "behave" like a homogeneous confined aquifer, but the test field data cannot be matched to the theoretical Theis curve because of an "odd" shape, the reason may be that the CSM was not appropriate because one or more of the following (see also Figure 4.32):

- The aquifer is not confined.
- The aquifer is heterogeneous and/or anisotropic.
- There is a source of recharge/discharge such as leaky aquifer/aquitard conditions.
- The aquifer behaves as a dual porosity medium (fractured and karst aquifers).
- There is one or more hydraulic boundaries.

In such cases, a hydrogeologic assessment of the possible causes should be made and the pumping test should be analyzed with an appropriate method as illustrated with quantitative examples in Kresic, 2007 (*Hydrogeology and Groundwater Modeling, Second Edition*. CRC Taylor & Francis).
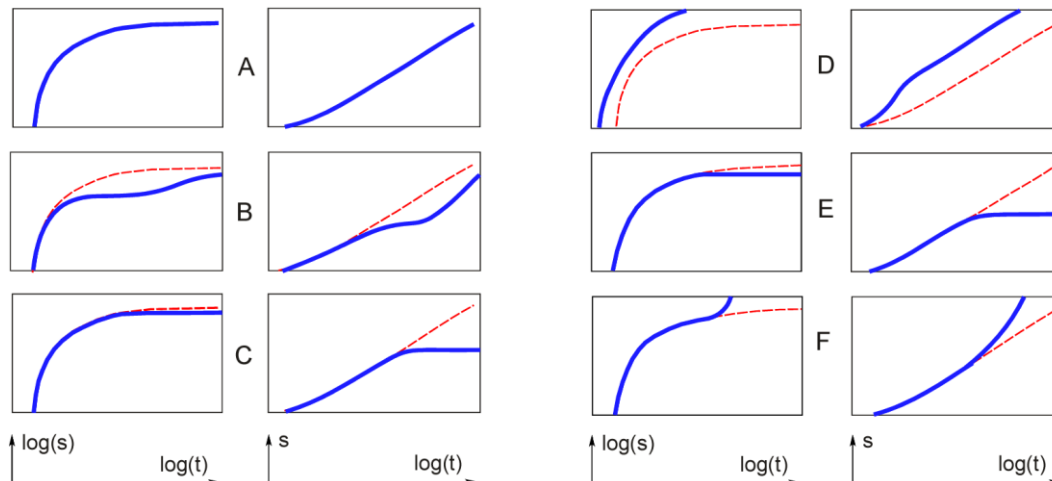
Figure 4.32 Log-log and semi-log curves of drawdown versus time for different types of aquifers and boundary conditions. Blue line—observed in the field, dashed red line—theoretical Theis curve. A: confined; B unconfined; C: leaky (or semi-confined); D: effect of partial penetration; E: effect of recharge boundary; F: effects of an impervious boundary. Modified from Griffioen and Kruseman, 2004. UNESCO, Paris, in public domain.

Lecture 5 Groundwater Flow, Part Three

5.1 Groundwater Flow in Fractured Rock and Karst Aquifers

This section is a compilation of the abbreviated materials from Kresic, 2007 (*Hydrogeology and Groundwater Modeling, Second Edition*. Copyright CRC Taylor & Francis); 2009 (Groundwater Resources: Sustainability, Management, and Restoration. Copyright by McGraw Hill); and 2013 (Water in Karst: Management, Vulnerability, and Restoration. Copyright McGraw Hill.

There is a wide array of possible approaches to calculate groundwater flow rates in fractured rock and karst aquifers. The simplest one is to assume that the porous media all behave similarly, at some representative scale, and then simply apply Darcy's equation. Although this *equivalent porous medium* (*EPM*) approach still seems to be the predominant in hydrogeologic practice, it is not always justified in anisotropic fractured rock or karst aquifers. Its inadequacy is emphasized when dealing with contaminant fate and transport analyses where all field scales are equally important, starting with contaminant diffusion into the rock matrix, and ending with predictions of most likely contaminant pathways in the subsurface. In the analytically most complicated, but at the same time the most realistic case, the groundwater flow rate is calculated by integrating the equations of flow through the rock matrix assuming it is laminar (Darcy's flow) with the hydraulic equations of flow through various sets of fractures, pipes, and channels. This integration, or interconnectivity between the four different flow components, can be deterministic, stochastic, or some combination of the two.

Deterministic connectivity is established by a direct translation of actual field measurements of the geometric fracture parameters such as dip and strike (orientation), aperture, and spacing between individual fractures (and bedding planes where applicable) in the same fracture set, and then doing the same for any other fracture set. Karst cavities are connected in the same way, by measuring the geometry of each individual cavity (cave). Finally, all the discontinuities (fractures and cavities) are connected based on the field measurements and mapping. As can be easily concluded, such deterministic approach includes many uncertainties and assumptions by default ("You have walked and measured this cave passage, but what if there are very similar ones somewhere in the vicinity you don't know anything about?").

Stochastic interconnectivity is established by randomly generating fractures or pipes using some statistical and/or probabilistic approach based on field measures of the geometric fracture (or pipe) parameters. An example of combining stochastic and deterministic approaches is when computer-generated (stochastic) fracture or pipe sets are intersected by a known major preferential flow path such as a fault or a cave. Except for relatively simple analytical calculations using homogeneous, isotropic, equivalent porous medium approach, most other quantitative methods for fractured rock and karst groundwater flow calculations include some type of modeling.
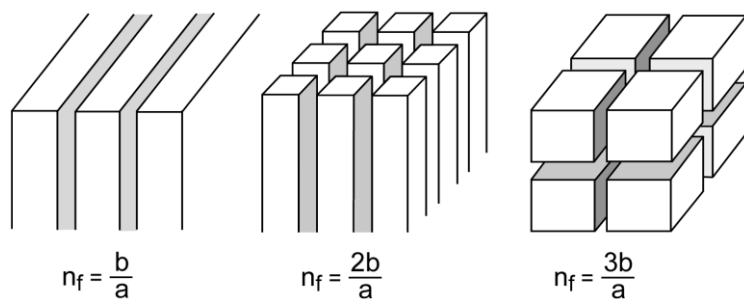
Figure 5.1 Fracture porosity (n_f) equations for the slides, matches, and cubes fracture models where a is the fracture spacing and b is the fracture aperture. Modified from Cohen and Mercer, 1993; Originally released by C.K. Smoley, CRC Press.

$$n_f = \frac{b}{a} \qquad n_f = \frac{2b}{a} \qquad n_f = \frac{3b}{a}$$
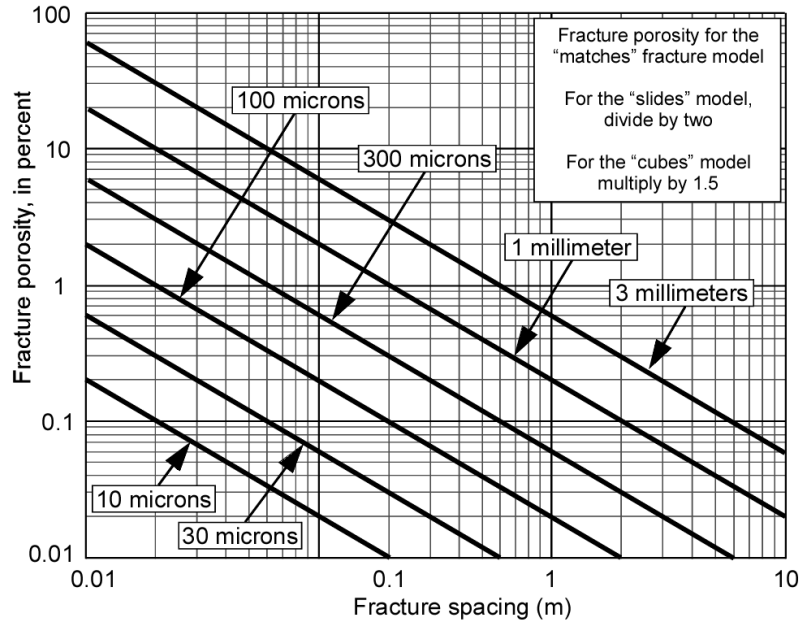
Figure 5.2 Fracture porosity is a function of fracture spacing and aperture. From Cohen and Mercer, 1993; Originally released by C.K. Smoley, CRC Press.

Figures 5.1 and 5.2 show determination of fracture porosity for three highly simplified geometric models of fracture sets. Porosity determined in this way can be used to approximate cross-sectional area (A) of flow in the aquifer that takes place through fractures and, together with some "equivalent" hydraulic conductivity (K) and the hydraulic gradient (i), calculate the "equivalent" groundwater flow rate using the well-known simple equation based on Darcy's Law: $Q = AKi$.
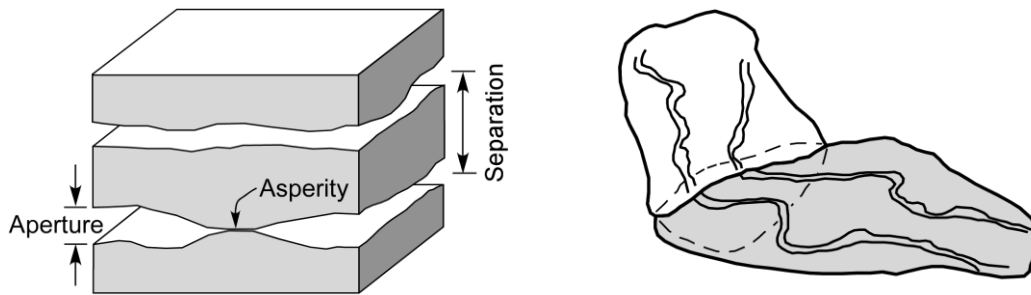
Figure 5.3 *Left*: Fracture aperture, asperity, and separation between two parallel fractures in the same fracture set. *Right*: Channeling in a fracture plane From Cacas, 1989. Doctoral dissertation, Ecole des Mines de Paris, Fontainebleau, France.

Fracture aperture (width) is parameter used most often in various single-fracture flow equations, while spacing between the fractures (separation) and fracture orientation is used when calculating flow through a set of fractures. However, these actual physical characteristics are not easily and meaningfully translated into equations attempting to describe flow at a realistic field scale:

1. As illustrated in Figure 5.3-*Left*, fracture aperture is not constant and there are voids and very narrow or contact areas called asperities. Various experimental studies have shown that the actual flow in a fracture is channeled through narrow, conduit-like tortuous paths (Figure 5.3-*Right*) and cannot be simply represented by the flow between two parallel plates separated by the "mean" aperture. In carbonate aquifers

81

this channeled flow may result in formation of karst conduits as the rock mass is being preferentially dissolved by the flowing groundwater.

2. Because of stress release, the aperture measure at outcrops or in accessible cave passages is not the same as an in-situ aperture. Aperture measured on drill cores and in borings is also not a true one – the drilling process commonly causes bedrock adjacent to fractures to break out thereby increasing the apparent widths of fracture openings as viewed on borehole-wall images (Williams et al., 2002).

3. Fractures have limited length and width, which can also vary between individual fractures in the same fracture set. Spacing between individual fractures in the same set can also vary. Since all these variations take place in the three-dimensional space, they cannot be directly observed, except through continuous coring and logging of multiple closely spaced boreholes, which is the main cost-limiting factor (see Figure 5.4.)

Fractures by default have limited extent in the 3D space of an aquifer, of which is little known. In order to simulate flow through a network of fractures, one has to decide on the spatial geometry of individual fractures and their interconnectivity within the entire aquifer volume of interest. This is done in many ways, including simulation with 2D fracture traces (orthogonal, or intersecting at an angle), 3D orthogonal disks, 3D disc clusters centered on seeds generated by a random process, or some 2D or 3D hierarchical model (Chilès, 1989a, 1989b; Chilès and Marsily, 1993; Long, 1983; Long et al., 1985). Whatever approach is selected, numeric models are arguably the only quantitative tool capable of solving groundwater flow through complex fracture networks.
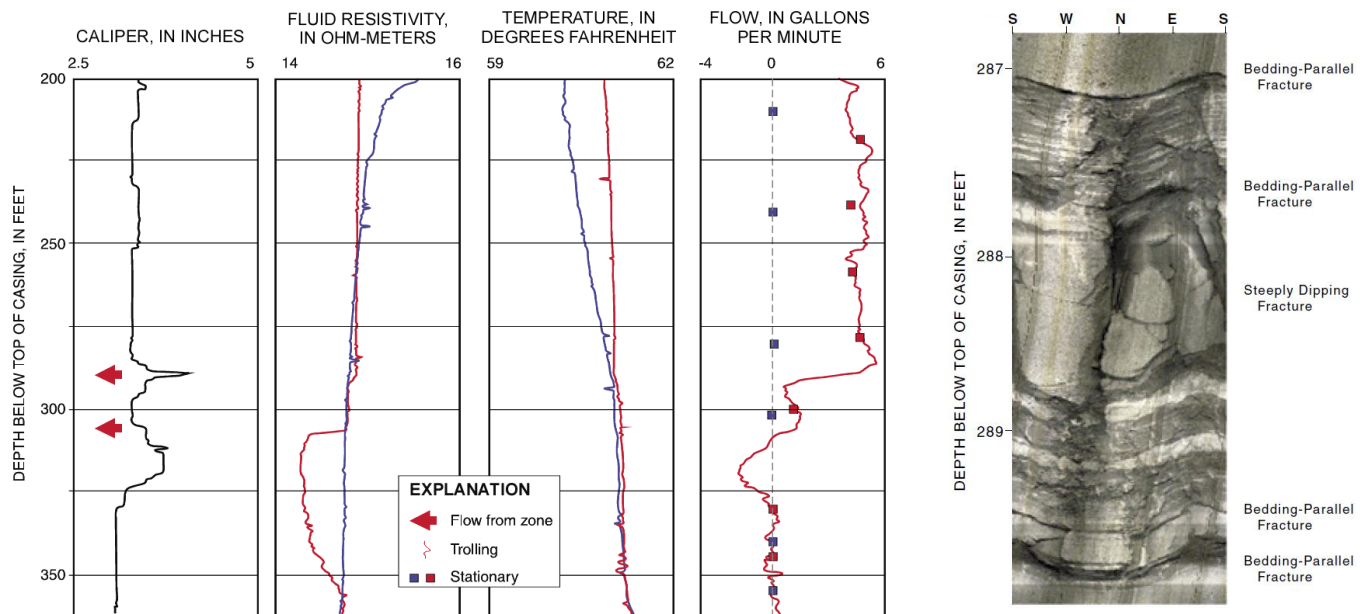
Figure 5.4 *Left*: Caliper, fluid-resistivity, temperature, and flowmeter logs of borehole RD-46B, Rocketdyne Santa Susana Field Laboratory, Ventura County, California (arrows indicate flow zones; blue indicates ambient conditions, red indicates pumped conditions; negative values indicate downflow, positive values indicate upflow). *Right*: Optical-televiewer image of the flow zone near 290 feet in borehole RD-46B showing intersection of a steeply dipping fracture and bedding-parallel fractures in mudstone and sandstone that provide majority of the flow. Rocketdyne Santa Susana Field laboratory, Ventura County, California. Modified from Williams et al., 2002. USGS, in public domain.

Evolution of analytical equations and various approaches in quantifying fracture flow is given by Whiterspoon (2000) and Faybishenko et al. (2000). In the simplest form, the hydraulic conductivity of a fracture with an aperture B (in Whiterspoon's notation $B = 2b$) and represented with two parallel plates is:

$$K = B^2 \frac{\rho g}{12\mu} \qquad (5.1)$$

where ρ is the fluid density, g is the acceleration of gravity, and μ is the fluid viscosity. The groundwater flow rate through a cross-sectional area $A = Ba$ (where B is the fracture aperture and a is the fracture width perpendicular to the flow direction) is:

$$Q = A * v = -a \left(\frac{\rho g}{12\mu}\right)\frac{dh}{dx} B^3 \qquad (5.2)$$

where dh/dx is the change in the hydraulic head (h) along the flow direction (x). In the definite form, this change is denoted with Δh and the minus sign disappears due to integration. The fracture flow approximation, called *Cubic law*, assumes that the representative aquifer volume acts as an equivalent porous medium (Darcian continuum). Whiterspoon gives another form of the cubic law:

$$\frac{Q}{\Delta h} = \frac{CB^3}{f} \qquad (5.3)$$

where C is a constant that depends on the geometry of the flow field and f is the roughness that accounts for deviations from ideal conditions, which assume smooth fracture walls and laminar flow. The roughness f is related to the Reynolds number (Re; indicator if the flow is turbulent or laminar), and the friction factor (Ψ) through the following equation:

$$f = \frac{\Psi Re}{96} \qquad (5.4)$$

The Reynolds number is given as:

$$Re = \frac{Dv\rho}{\mu} \qquad (5.5)$$

where D is the fracture hydraulic diameter assumed to be equal to 4 times the hydraulic radius (hydraulic radius is the ratio of the cross-sectional area of fluid flow through a fracture to the wetted perimeter of the fracture.)

For a relatively smooth fracture, where the ratio between fracture asperity and aperture is less than 0.1, the transition to turbulent flow is at Reynolds number of about Re=2400. As this ratio, which is the indicator of fracture roughness, increases, the Reynolds number for transition to turbulent flow decreases significantly. The friction factor (Ψ) is given by:

$$\Psi = \frac{D}{v^2/2g}\Delta h \qquad (5.6)$$

where v is the flow velocity. Equations of fluid flow in non-ideal fractures with influences of various geometric irregularities, and fracture network modeling approaches are discussed in detail by Bear et al. (1993), Zimmerman and Yeo (2000), and Faybishenko et al. (2000).

The examples in Figure 5.5 illustrate differences between calculations of representative groundwater velocity and flow rate through a confining low-permeable layer that behaves like a dual porosity medium where the flow takes place in both the rock matrix and the fractures. Figure 5.5(a) shows elements for calculation of vertical flow velocity and flow rate through a 4-meter-thick confining layer without fractures, having effective porosity of 3%. The linear velocity (v_L) is calculated using Darcy's law (Equation (4.2)

$$v_L = \frac{K_v * i}{n_{ef}} = \frac{K_v * (\frac{\Delta h}{L})}{n_{ef}} = \frac{5 \times 10^{-8} \text{cm/s} * \left(\frac{2 \text{ m}}{4 \text{ m}}\right)}{0.03} = 8.3 \times 10^{-7} \text{cm/s} = 26.3 \text{ } cm/yr$$

where K_v is the vertical hydraulic conductivity of the rock matrix, Δh is the difference in the hydraulic heads between the unconfined and confined aquifers (it is 2 m in this case), L is the thickness of the confining layer (4 m), and n_{ef} is the effective porosity (3 percent). The time of travel across the confining layer is 15.2 years, and it is found by dividing the thickness of the layer (travel distance; $L = 4m$) with the linear velocity ($v_L = 0.263 \text{ } m/yr$).
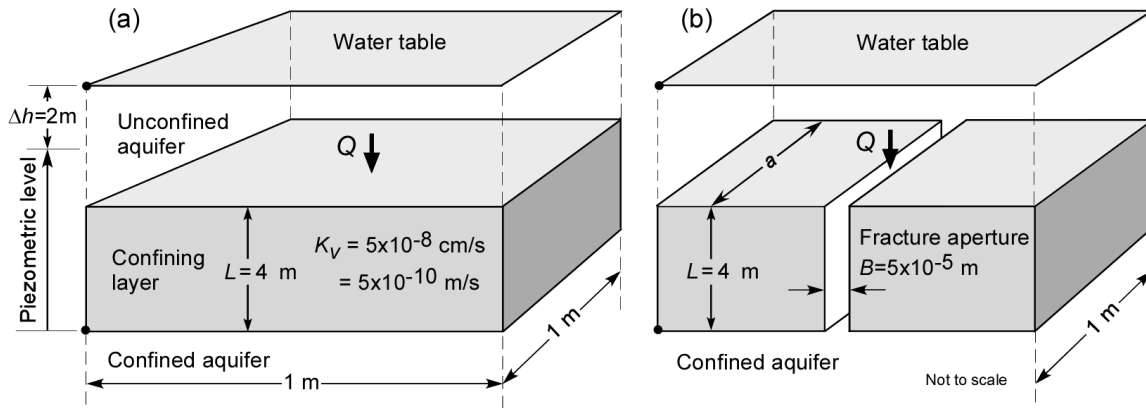
Figure 5.5 (a): Elements for calculating groundwater velocity and flow rate across an unfractured confining layer 4 m thick. Calculation based on Darcy's Law; explanation in text; (b): Elements for calculating groundwater velocity and flow rate through a single fracture with aperture B=5x10^{-5} m, crossing a confining layer 4 m thick; explanation in text. Concept based on Cherry et al., 2006.

The flow rate through the confining layer per unit area is found by multiplying the cross-sectional area of flow (A=1m^2 in this case) with the Darcy's velocity (not the linear velocity):

$$Q = v * A = K_v * \frac{\Delta h}{L} * A = 5 \times 10^{-10} \text{m/s} * \frac{2\text{m}}{4\text{m}} * 1\text{m}^2 = 5 \times 10^{-10} \text{ m}^3/\text{s} = 2.16 \times 10^{-5} \text{ m}^3/\text{day}$$

Figure 5.5(b) shows elements for calculating the flow velocity (v) through a single fracture of aperture $B = 5 \times 10^{-5}$m (50 microns) across a confining layer 4 m thick, using an equivalent hydraulic conductivity of the fracture (Equation 5.1):

$$v = K_f * i = B^2 \frac{\rho g}{12 \mu} * \frac{\Delta h}{L} = B^2 \frac{g}{12 v} * \frac{\Delta h}{L}$$

$$= (5 \times 10^{-5}\text{m})^2 * \frac{9.81 \text{ m/s}^2}{12 * 0.000001 \text{ m}^2/\text{s}} * \frac{2\text{m}}{4\text{m}} \quad = \quad 1.02 \times 10^{-3} \text{ m/s} \quad = \quad 88.3 \text{ m/day}$$

where K_f is the hydraulic conductivity of the fracture, v is the flow velocity through the fracture, μ is dynamic viscosity, ρ is water density, g is acceleration of gravity, and ν is kinematic viscosity. Note that dynamic viscosity and density are related through kinematic viscosity as follows: $\nu = \mu/\rho$. The kinematic viscosity of water at temperature of 20 °C is 1x10^{-6} m^2/s (McCutcheon et al., 1993), and the acceleration of gravity is rounded to 9.81 m/s^2.

The time of travel across the 4-meter-thick confining layer through a fracture is very short, less than one day, and it is calculated by dividing the distance of travel (L=4 m) with the flow velocity (v = 88.3 m/d). The equivalent hydraulic conductivity of the fracture is here calculated as 2.04 x 10^{-3} m/s, or seven orders of magnitude greater than the hydraulic conductivity of the rock matrix (5x10^{-10} m/s).

The flow rate through this single fracture, for a one-meter-long segment (a = 1m), is found by applying the so-called Cubic Law (Equation 5.2), i.e., by multiplying the flow velocity with the cross-sectional area of flow (A), where $A = a * B$ and $\rho/\mu = 1/\nu$

$$Q = A * v = a * B * B^2 \frac{\rho g}{12\mu} * \frac{\Delta h}{L} = aB^3 \frac{g}{12\nu} \times \frac{\Delta h}{L}$$

$$= 1 \text{ m} * (5 \times 10^{-5} m)^3 * \frac{9.81 \text{ m/s}^2}{12 * 0.000001 \text{ m}^2/\text{s}} * \frac{2m}{4m} \quad = \quad 4.4 \times 10^{-3} \text{ m}^3/\text{day}$$

Comparison of the results shows that both the flow velocity and the flow rate through a single fracture are incomparably higher than through the rock matrix. It is obvious that, in case of fractured rock aquifers, the actual water flux through them will mostly depend on the effective aperture (which considers presence of asperities and fill materials), the number, the three-dimensional extent, and the interconnectivity of all fractures present within a representative volume of the aquifer. However, in many cases it would be very difficult to accurately define the effective aperture and the geometry of the fractures (fracture systems) within a fractured rock aquifer, and various assumptions would have to be made.

Similarly to the effective porosity and the hydraulic conductivity, it is often challenging to define the hydraulic gradient for the area (volume) of a fractured rock aquifer of interest. There may be multiple fracture sets at various depths and of different dip, and they may have varying degrees of hydraulic connectivity including its complete absence. Installing piezometers (monitoring wells) at the same depth, or even at two different depths ("shallow" and "deep"), which is a rather common practice, may therefore not provide for an accurate interpretation of the representative hydraulic gradient if the wells are screened in different sets of fractures, or some of them are not intersecting fractures at all.

Figure 5.6 illustrates just some possible spatial relationships and hydraulic interactions between fractures and sets of fractures in bedrock aquifers. Differences in the hydraulic head between two fractures or fracture sets may produce vertical fluid flow in long boreholes. Water would enter the borehole at the fracture with the higher head and flow toward and into the fracture with the lower head. The vertical flow rate is limited by the fracture with the lower transmissivity. If the heads of the different transmissive zones are the same, no vertical flow will occur in the well or borehole. However, it is recognized that the borehole may facilitate vertical flow between fractures that

would not normally be present, so any interpretation of the hydraulic heads and possible vertical flows must be made with caution.

Presence of varying permeability intervals in a borehole (well) may be indicated by various methods of geophysical logging, and their actual flow contribution may be measured and calculated using borehole flow meters ("flowmeters"). Flowmeters can be utilized in various ways, with or without pumping of the well. During well pumping packers can be used to isolate portions of the open borehole for a more precise characterization.
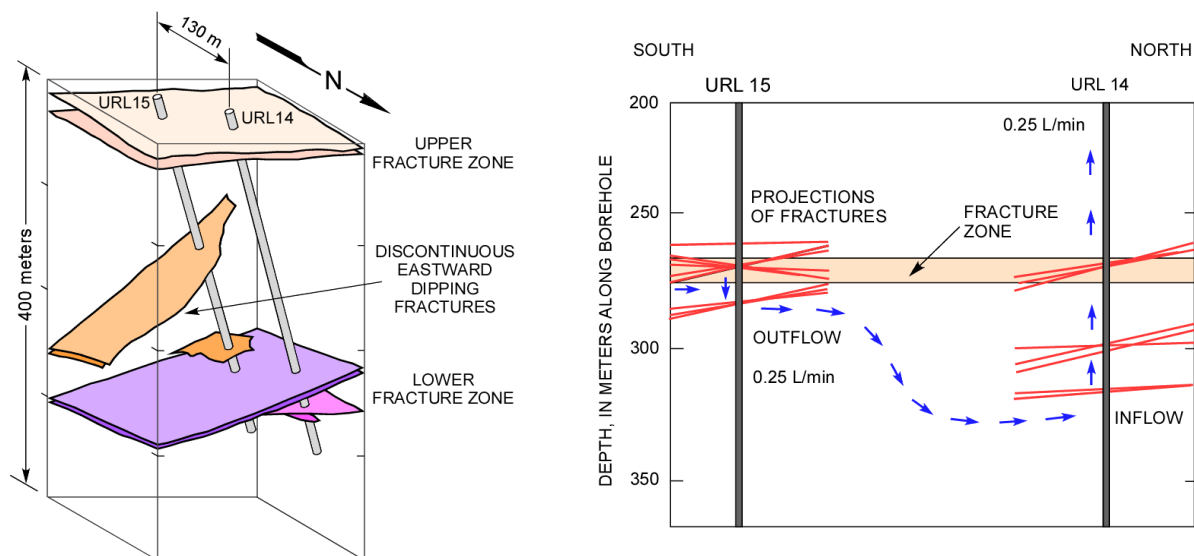
Figure 5.6 *Left*: Diagram showing orientation of fractures intersecting boreholes URL14 and URL15 determined from acoustic televiewer logs and projections of fractures between the two boreholes. *Right*: Diagram showing inferred hydraulic connection between boreholes URL14 and URL15 during crosshole pumping tests. Modified from Paillet, 1989. USGS, in public domain.

Simultaneous use of geophysical logging tools and flowmeters is likely the best available method for characterization of aquifer heterogeneity and subsequently the representative hydraulic heads and the hydraulic gradients (Paillet, 1994; Paillet and Reese, 2000; Molz et al., 1990). Integration of geophysical methods with conventional logging techniques can be used to define flow zones, lithology, and structure, as well as their relations within the aquifer (Figure 5.6-*Left*). Borehole flowmeters, whether vertical or horizontal, are used to both identify and quantify water producing zones in a well. Flow logging tests between boreholes ("crosshole" tests) can indicate the degree of connectivity of transmissive zones beyond individual borings (Figure 5.6-*Right*).

It became standard practice in hydrogeology to develop potentiometric surface contour maps for fractured bedrock aquifers as if they behave like unconsolidated sand and gravel aquifers, i.e., assuming a Darcian continuum where groundwater is flowing through the interconnected pore space (effective porosity) between solid grains: the so-called *equivalent porous media* approach or EPM. In contrast, a fractured bedrock aquifer is a *dual porosity medium* where groundwater flow in two distinct porous media, the fractures, and the surrounding rock matrix, is fundamentally different. Such EPM maps are often developed using data from all available wells (piezometers), possibly screened at similar depths in the bedrock, and contouring them together regardless of the information provided by the boring logs and geophysical logging (i.e., if the well screen intervals are monitoring the same set of hydraulically connected fractures or no fractures at all). Some practitioners may, using "best professional judgment", choose to exclude "strange" data from the contouring data set, such as significantly higher or lower individual data points that do not "behave" like the rest; or the wells that are screened entirely in the rock matrix

without any fractures. If enough monitoring wells are intersecting the predominant fracture network, the resulting map may be a reasonable approximation of the overall groundwater flow characteristics. One such map is shown in Figure 5.7: the contours are more widely spaced where there are more interconnected fractures, indicating a more transmissive portion of the aquifer, and the flow is always from the higher hydraulic heads towards the lower hydraulic heads including in the fractures. In addition, the question marks indicate where the contours are uncertain, either because of the absence of data points or because of questionable data. Maps like this one are routinely used to calculate hydraulic gradients and, subsequently, the linear groundwater flow velocity using equation 4.2. For example, the hydraulic gradient between contours 238 and 237 (which are given in feet above datum) is:
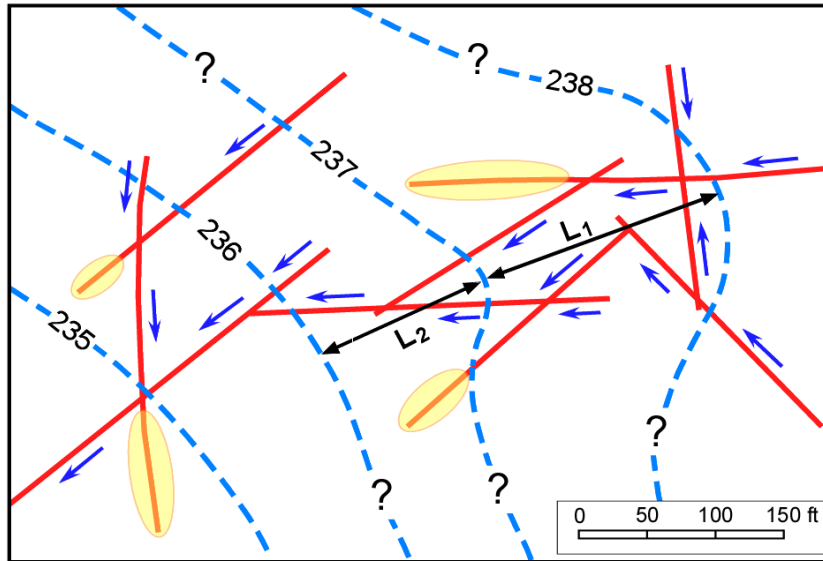
Figure 5.7 Hypothetical equipotential (piezometric) surface contour lines (blue dashed lines) with elevation in feet above datum, as commonly plotted in hydrogeologic practice, for a section of a fractured bedrock aquifer with hydraulically connected fractures (red lines) at approximately same depth below ground surface. The general groundwater flow is from the right to the left, with blue arrows showing flow direction inside the fractures. Yellow shaded areas represent "dead-end" fractures in which the flow is slow to stagnant. Explanation in text. Concept from Milojević, 1967. University of Belgrade; Acknowledgement required for further use.

$$i_1 = \frac{\Delta h_1}{L_1} = \frac{238ft - 237ft}{180ft} = 0.0056$$

and between contours 237 and 236 it is:

$$i_2 = \frac{\Delta h_2}{L_2} = \frac{237ft - 236ft}{130ft} = 0.0077$$

Again, this EPM approach should be applied with care since it does not differentiate between the flow, and therefore hydraulic gradients, in the fractures and in the matrix, nor it considers a degree of connectivity between these two porous media. Figure 5.8 illustrates this point and the complex nature of groundwater flow in a dual porosity medium. Especially challenging for interpretation of field-observed hydraulic heads at piezometers and monitoring wells is the presence of dipping fractures that connect (sub)horizontal fractures when there are vertical gradients in the aquifer, which is usually the case. For example, Figure 5.8 shows that, locally, the flow in a fracture may be in opposite directions because of the hydraulic influence of the intersection between two vertical fractures when there is downward hydraulic gradient in the aquifer. In addition, the local hydraulic gradients in the matrix can be at varying angles to the overall flow direction depending on the proximity of fractures which act as linear hydraulic sinks for the flow in rock matrix.
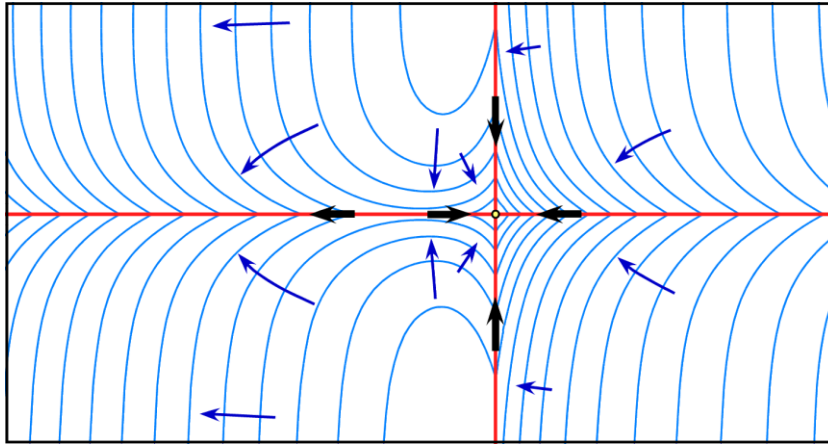
Figure 5.8 Portion, 30 feet across, of a proof-of-concept numeric model of a fractured rock aquifer with two sets of parallel fractures, perpendicular to each other (shown here is one intersection of two fractures from the two sets.) Fractures (red lines) are vertical parallel plates and are modeled explicitly, with aperture of 0.02 inches (0.5 cm) and equivalent hydraulic conductivity of 200 ft/d. The matrix has hydraulic conductivity of 0.01 ft/d. Blue contours are simulated hydraulic heads, blue arrows show flow direction in the matrix, black arrows show flow direction in the fractures. General regional flow direction is from right to left. There is a vertical hydraulic gradient between the regolith and the underlying bedrock aquifer, and this gradient propagates deeper into the bedrock. The flow in fractures in the center of the map is towards their intersection and downward because of this. The map view is solution for a horizontal aquifer section 30 feet below top of bedrock.

5.2. Groundwater Flow in Karst

Determining groundwater flow direction, hydraulic gradient, and flow rate in karst aquifers is the most challenging task in hydrogeology. This is because, in addition to the related challenges described for fractured rock aquifers, there is a third type of porosity in soluble carbonate rocks, namely dissolution-enhanced initial mechanical discontinuities (secondary porosity) which are formed by folding, fracturing, and faulting of the brittle sediments. These features are often called tertiary porosity or karst porosity, come in many different shapes, forms and sizes, and are interchangeably referred to as karst cavities, conduits, and channels, or preferential flowpaths in general.

Photographs in Figures 5.9 through 5.15 illustrate just some of the features that clearly differentiate karst from any other porous media. Most importantly, and unlike fracture networks in non-karstified rocks, the transmissive networks of karst conduits, channels and their various combinations can extend below topographic divides, creating extensive and usually unpredictable and surprising subsurface (hydrogeologic) drainage areas that give rise to numerous large springs around the world, including the largest.

Figure 5.9 Initial discontinuities such as fissures, fractures and bedding planes in carbonate rocks are enlarged by dissolution at the surface which continues deeper into the rock, creating various preferential flow paths within the aquifer such as interconnected voids, cavities, conduits, and channels. *Top left*: highly karstified Upper Silurian-Lower Devonian limestone in Highland County, Virginia. *Top right*: detail, 2m across, of limestone dissolution along fractures in the famous karst area of Ireland called Burren. *Lower left*: karstified limestone beds on the bank of Li River, Guangxi Province, China. *Lower right*: rudimentary sinkhole in Mesozoic limestone, 1m across, in Makarska, Croatia.
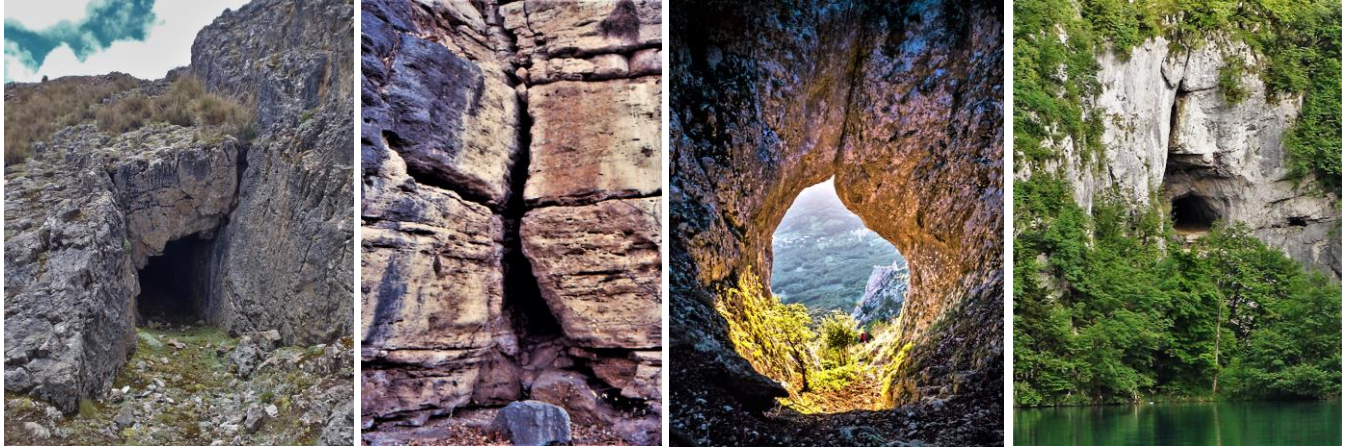
Figure 5.10 Former and current springs in karst are outlets of interconnected preferential flowpaths (networks of karst conduits and channels.) *Left*: Former spring in Shalipayco, Peruvian Andes. *Middle Left*: Spring at the outer ring of the Montezuma Lake, Arizona. *Middle Right*: Otlica Window, outlet of a former spring, Slovenia; photo courtesy of Matej Blatnik. *Right*: Former spring at Plitvice Lakes, Croatia.
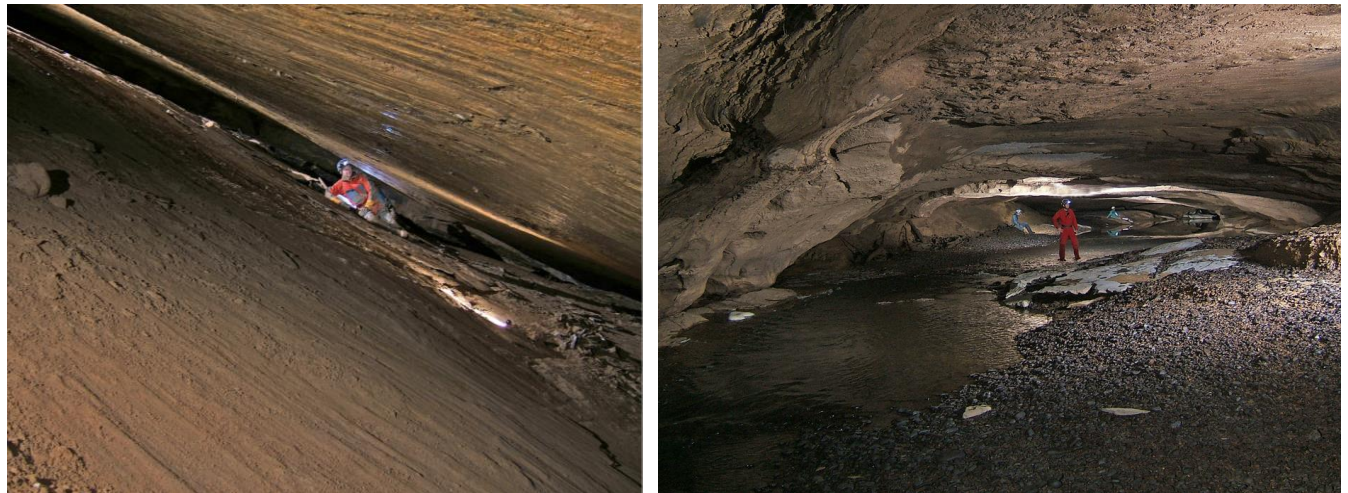
Figure 5.11 *Left*: Fault surfaces with slickensides in a Highland County, Virginia cave. *Right*: Low stream passage in Culverson Creek Cave system, West Virginia. Photographs courtesy of Phil Lucas.

Figure 5.12 Molnár János Cave in Budapest, Hungary with water temperature between 20 and 28 degrees Celsius. Budapest is the spa capital of Europe with numerous thermal springs issuing from the karst aquifer below the city. Photo courtesy of Radoslav Husák.

Figure 5.13 Screenshot of a diving video at Radium Springs, Georgia, the United States, October 31, 2015, taken by Guy Bryant with divers Kelly Jessop and Peter Buzzacott. Note high matrix porosity of the upper Eocene Ocala limestone enhanced by dissolution. Video available on YouTube (CDroHO56F-Y)

Figure 5.14 Radium Springs near Albany, Georgia, the United States is the largest spring in the state. It has an average flow rate of 70,000 gallons (265,000 liters) per minute. Entrance to submerged caves passages ("blue hole") is in the center right. The spring dries up during exceptional droughts, such as the one in 2012.
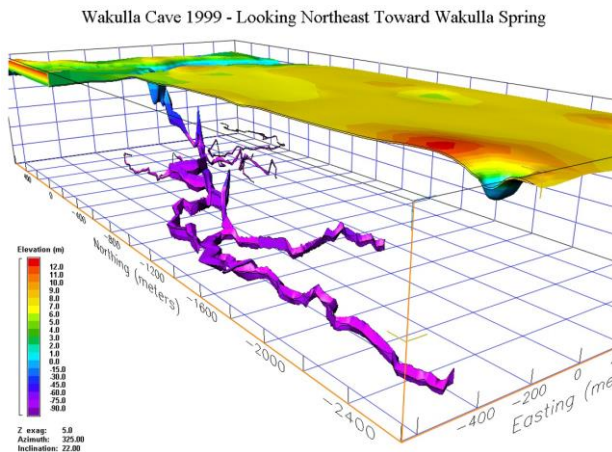
Figure 5.15 *Left*: View of the Wakulla Spring outlet from a cave diver's perspective. This first magnitude spring in Wakulla County, Florida is one of the largest and deepest freshwater springs in the world with miles of the explored submerged cave passages. It is a major tourist attraction. Several of the early *Tarzan* movies starring Johnny Weissmuller were filmed in the Wakulla Springs state park. Photo copyright David Rhea & Global Underwater Explorers 2006, printed with permission. *Right*: Computer-generated view of the submerged Wakulla Cave passages based on the cave diving surveys. The passages all converge toward the Wakulla Spring. Courtesy of Dr. Todd Kincaid.

5.2.1 Flow in Conduits

This section is based on the materials presented in Kresic, 2013, and Kresic and Stevanović, 2010. In many karst aquifers the most important portion of groundwater flow takes place in submerged interconnected solution cavities, commonly referred to as conduits, where the flow is under pressure most of the time. By definition, a conduit has one dimension, length, disproportionally larger than the other two. The most complicating and challenging factor when attempting to apply principles of pipe (conduit) hydraulics to real karst conduits is that their orientation and interconnectivity within the three-dimensional aquifer space is for the most part unknown and unpredictable. Notably, a network of accessible cave passages that has been mapped in the field often does not represent the conduit network where the actual flow is taking place most of the time. The accessible cave passages may have some visible flow along their floors and may become more active or even fully submerged during major recharge episodes, but the flow in the permanently saturated zone is taking place at lower horizons, usually inaccessible even to well-equipped, skillful cave divers.

Most importantly, the traditional hydraulics of pipes is based on the principle of flow continuity which assumes that there is no inflow or outflow of water through pipe walls. This is illustrated with Figure 5.16. The flow rate (Q) through an elementary flow tube is directly proportional to the cross-sectional area of the tube (a) and the flow velocity (v):

$$dQ = vda \qquad (5.7)$$

"Many" such elementary flow tubes can be combined into a realistic 3D portion of an aquifer through which the groundwater flow is taking place; if there is no loss or gain of water inside this (combined) realistic flow tube, however, the principle is the same:

$$Q = \int_A dQ = \int_A vda \qquad (5.8)$$

$$Q = \int_A dQ = \int_A vda \qquad (5.8)$$

$$Q = v_{av}A \qquad (5.9)$$

where A is the sum of all cross sections of the elementary flow tubes, and v_{av} is the average flow velocity within the realistic flow tube.
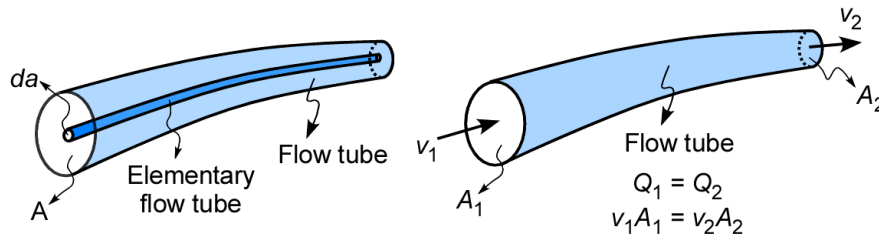
Figure 5.16 Flow tube in porous media; da = cross section of elementary flow tube; dQ = elementary flow rate; A, A_1, A_2 = cross sectional area of flow; Q_1 and Q_2 =flow rate; v_1 and v_2 = average flow velocity.

Two or more flow tubes can merge into one and the resulting flow rate is additive. Consequently, one flow tube can split into several where the sum of the new flows is equal to the initial flow. It should be noted that the term "tube" in aquifer hydraulics does not imply that the portion of the aquifer under consideration must look like (has shape of) a tube; what it means is that the flow lines (streamlines) of groundwater particles inside the tube remain inside, and there are no new particles entering the tube. In a karst aquifer, however, where there is an ongoing and significant exchange of water between the conduits (pipes) and the surrounding rock matrix including small fissures and fractures, the pipe flow hydraulics may not applicable.

Bernoulli Equation

Flow through a pipe of varying cross-sectional area is described by the Bernoulli equation for real viscous fluids as illustrated in Figure 5.17. Since there is no gain or loss of water in the pipe, the flow rate remains the same while other hydraulic elements change from one cross-section to another. The total energy line (E) of the flow decreases from the upgradient cross section towards the downgradient cross section of the same flow tube (pipe or conduit) due to energy losses. These losses or resistance to flow are the result of internal friction within the flowing fluid, friction between the fluid and the conduit walls, and the general flow turbulence including local losses caused by various conduit irregularities and wall roughness. Bernoulli equation is based on the principle of energy conservation where the energy losses represent an irreversible conversion of mechanical (flow) energy into heat energy. The following general equation is for the three flow cross sections, denoted as 1-1, 2-2 and 3-3 on Figure 5.17 (note that at the starting cross section 0-0 the flow velocity is zero):
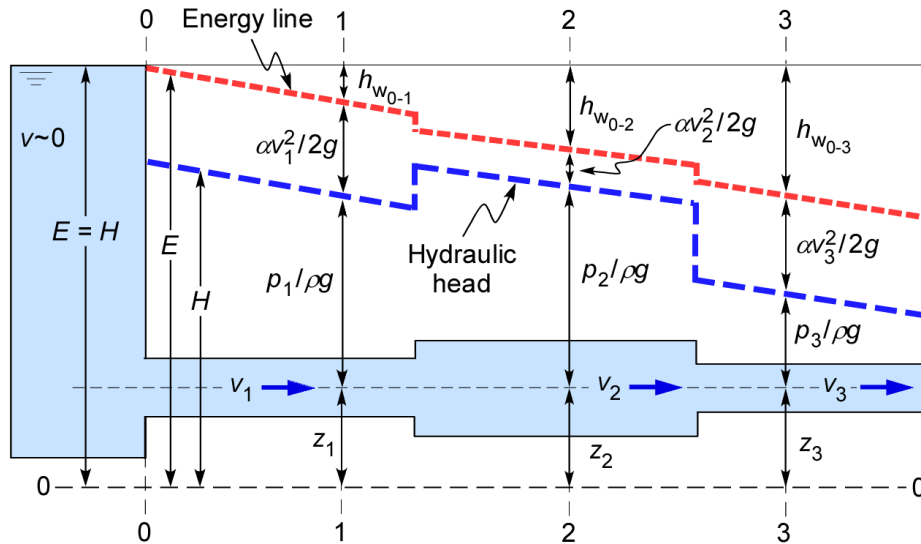
Figure 5.17 Illustration of the Bernoulli equation for flow of real viscous fluids through a pipe with the varying cross-sectional area. Energy line (E) at any given cross-section is the sum of the elevation head (z), the fluid pressure head ($p/\rho g$) and the velocity head ($\alpha v^2/2g$). The fluid pressure head and the elevation head give the hydraulic head–see Equation (5.10) Modified from Kresic, 2013. Copyright McGraw Hill; permission is required for further use.

$$E = z_1 + \frac{p_1}{\rho g} + \frac{\alpha v_1^2}{2g} + h_{w(0-1)} = z_2 + \frac{p_2}{\rho g} + \frac{\alpha v_2^2}{2g} + h_{w(0-2)} = z_3 + \frac{p_3}{\rho g} + \frac{\alpha v_3^2}{2g} + h_{w(0-3)} \quad (5.10)$$

where E is the energy of flow, z is the elevation head above the reference level, p is the fluid pressure, ρ is the fluid density, g is acceleration of gravity, v is average flow velocity, α is the Coriolis coefficient of velocity non-uniformity at a flow cross section (1.06< α <1.13), h_w is the total energy loss between two flow cross-sections.

Unlike the energy line (E), the hydraulic head line may go "up" and "down" along the same flow tube as the cross sectional area increases or decreases respectively. In other words, when the flow velocity decreases due to widening of the conduit, the hydraulic head increases because of the increased fluid pressure. The total energy line, which includes the velocity component ($\alpha v_2^2 / 2g$), can be directly measured only by the Pitot device whose installation is not feasible in most field conditions. Monitoring wells and piezometers, on the other hand, only record the hydraulic head, which does not include the flow velocity component. It is therefore conceivable that two piezometers in or near the same karst conduit may not provide useful information for the calculation of the real flow velocity and flow rate between them and may even falsely indicate the opposite flow direction. In fact, as discussed by Bögli (1980), water rising through a tube in an enlargement passage can flow backward over the main flow conduit and into another tube which begins at a narrow passage in the same main conduit.

There are various complicating factors when attempting to calculate flow through natural karst conduits using the pipe approach and Bernoulli equation:

1) Flow through the same conduit may be both under pressure and with free surface, and the conduit or part of it may eventually be completely drained of water as the permanently saturated zone is lowered.

2) Since conduit walls are irregular ("rough"), the related coefficient of roughness which contributes to energy losses must be estimated and inserted into the general flow equation.

3) Conduit cross section may vary significantly causing various local energy losses, particularly where it abruptly constricts or widens.

4) The flow may be both laminar and turbulent in the same conduit, depending on the flow velocity, cross-sectional area, and wall irregularities. The energy losses and the velocity distribution are quite different for these two flow regimes (see next section).

5) More than one conduit is usually "responsible" for transferring groundwater in the aquifer from one general area to another. The difficulties described earlier multiply when attempting to calculate groundwater flow rates through a network of conduits. While appropriate fluid mechanics solutions exist for pipe networks, the major challenge is accurately identifying and characterizing all the disparate branches in the field.

6) Portions of the conduit system, such as large chambers and vertical shafts may serve as storage reservoirs during and following periods of high recharge rather than simple flow-through conduits. Possible impacts of unknown reservoirs are unpredictable but can be assumed and tested with simple hydraulic equations.

Despite the limitations of the hydraulic calculations listed above, pipe and reservoir approaches to karst aquifer systems have been practiced considerably and with varying success. Wide availability of software packages for hydraulic calculations of pipes and reservoirs can make this and similar approaches quite appealing. However, similarly to all other flow calculations in karst, the number of assumptions and the required input parameters, most of which cannot be measured, quickly multiply with each additional pipe and reservoir such that the final solution is by default non-unique, and the model is over-parameterized. Nevertheless, the appeal of a play with assumed configurations of pipes (caves), and the possibility of eventually reaching the "just-right" solution, cannot be dismissed as illustrated with Figure 5.18.
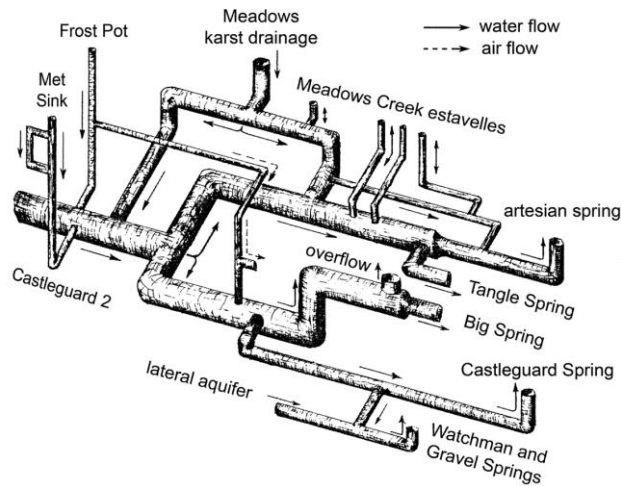
Figure 5.18 Pipe diagram of the Castleguard Valley karst aquifer, Alberta, based on dye tracing and cave observations. Smart, 1983. Hydrology of a glacierized alpine karst. Ph.D. thesis, McMaster University, Hamilton, Ontario, 343 p.

Laminar and Turbulent Flow

Flow in conduits is laminar when it takes place in parallel concentric layers (lamina) which do not mix. The maximum velocity is along the centerline of the conduit and decreases towards the walls where it becomes infinitesimally small, theoretically equal to zero. This is because the flow is along individual tubular fluid lamina between which there is viscous resistance to flow, with the highest resistance between the fluid and the conduit walls. At some critical velocity, the laminar flow will become turbulent with the formation of eddies and chaotic motion (mixing) of fluid particles in all three dimensions. In turbulent flow regime, however, there still is a thin layer of laminar flow next to the conduit walls, called boundary layer. Importantly, the turbulence increases the resistance to flow dramatically so that large increases in hydraulic head will be required to further increase the flowrate in the conduit.

Dynamic viscosity (μ) is the property of fluid which resists shear stress acting on it. Terms viscosity, absolute viscosity, and dynamic viscosity are used interchangeably, whereas kinematic viscosity (ν) is related to the dynamic viscosity as follows:

$$\nu = \frac{\mu}{\rho} \qquad (5.11)$$

where ρ is the fluid density.

Units of dynamic viscosity are Newton-second per meter squared (Ns/m^2), or kilogram per meter-second (kg/ms), or Pascal-second (Pas) with all three units being equal. The unit for kinematic viscosity (m^2/s) is impractically large so that another unit, centistoke (cSt), is more commonly used (1 cSt = 10^{-6} m^2/s). The unit for fluid density is kg/m^3.

In comparison to water for example, honey is much more viscous, and it moves much slower under the same hydraulic gradient because the resistance to flow (friction) between individual honey lamina is much higher than between the lamina of water. Water and gasoline are relatively low viscosity fluids which flow very easily. Motor oil and molasses are other examples of more viscous fluids which offer great resistance to flow. In the presence of suspended material, the viscosity of a liquid increases because its density is higher.

The Hagen-Poiseuille equation is commonly used in hydraulics to calculate the pressure loss (Δp) between two cross-sections of laminar flow of incompressible fluids in a circular tube:

$$\Delta p = \frac{128\mu L Q}{\pi d^4} \qquad (5.12a)$$

or

$$\Delta p = \frac{8\mu L Q}{\pi R^4} \qquad (5.12b)$$

where Q is the flow rate, μ is the dynamic (absolute) viscosity, L is the distance between the two cross-sections, d is the tube diameter, and R is the tube radius.

The pressure loss (Δp) and the hydraulic head loss (Δh) are related as follows

$$\Delta p = \rho g \Delta h \qquad (5.13)$$

where ρ is the fluid density and g is the acceleration of gravity.

The Hagen-Poiseuille equation can also be expressed with the hydraulic head loss (Δh) and the average flow velocity (denoted with capital V to distinguish it from kinematic viscosity, v):

$$\Delta h = \frac{32\mu L V}{\rho g d^2} \qquad (5.14)$$

$$V = \frac{\pi R^4}{8 L v} \Delta h \qquad (5.15)$$

In terms of the flow rate (Q), equation (5.12) can be written as

$$Q = \frac{\Delta p}{L} \frac{\pi d^4}{128\mu} = \frac{\Delta h}{L} \frac{\pi d^4 \rho g}{128\mu} \qquad (5.16)$$

The flow velocity at any radial distance r from the center of the tube is

$$V_r = \frac{1}{4\mu} \frac{\Delta p}{L} (R^2 - r^2) \qquad (5.17)$$

whereas the maximum flow velocity in the center of the tube is

$$V_{max} = \frac{1}{4\mu} \frac{\Delta p}{L} R^2 \qquad (5.18)$$

where R is the internal tube radius.

The maximum velocity of laminar flow in a circular tube is two times higher than the average flow velocity of the entire cross-sectional area of the tube (A) so that the flow rate can also be calculated as

$$Q = A \frac{V_{max}}{2} \qquad (5.19)$$

The Darcy-Weisbach equation can be used to calculate hydraulic head losses for both laminar and turbulent flows in a circular tube:

$$\Delta h = f\frac{L}{d}\frac{V^2}{2g} \qquad (5.20)$$

where f is the dimensionless experimental friction coefficient also known as the Darcy friction factor. As can be seen, the losses are proportional to the squared average velocity, whereas for laminar flow this relationship is linear.

From equation (5.20) the flow rate (Q) through a conduit can be calculated as

$$Q = A \times V = A \times \sqrt{\frac{\Delta h d 2g}{fL}} \qquad (5.21)$$

where A is the cross-sectional area perpendicular to flow.
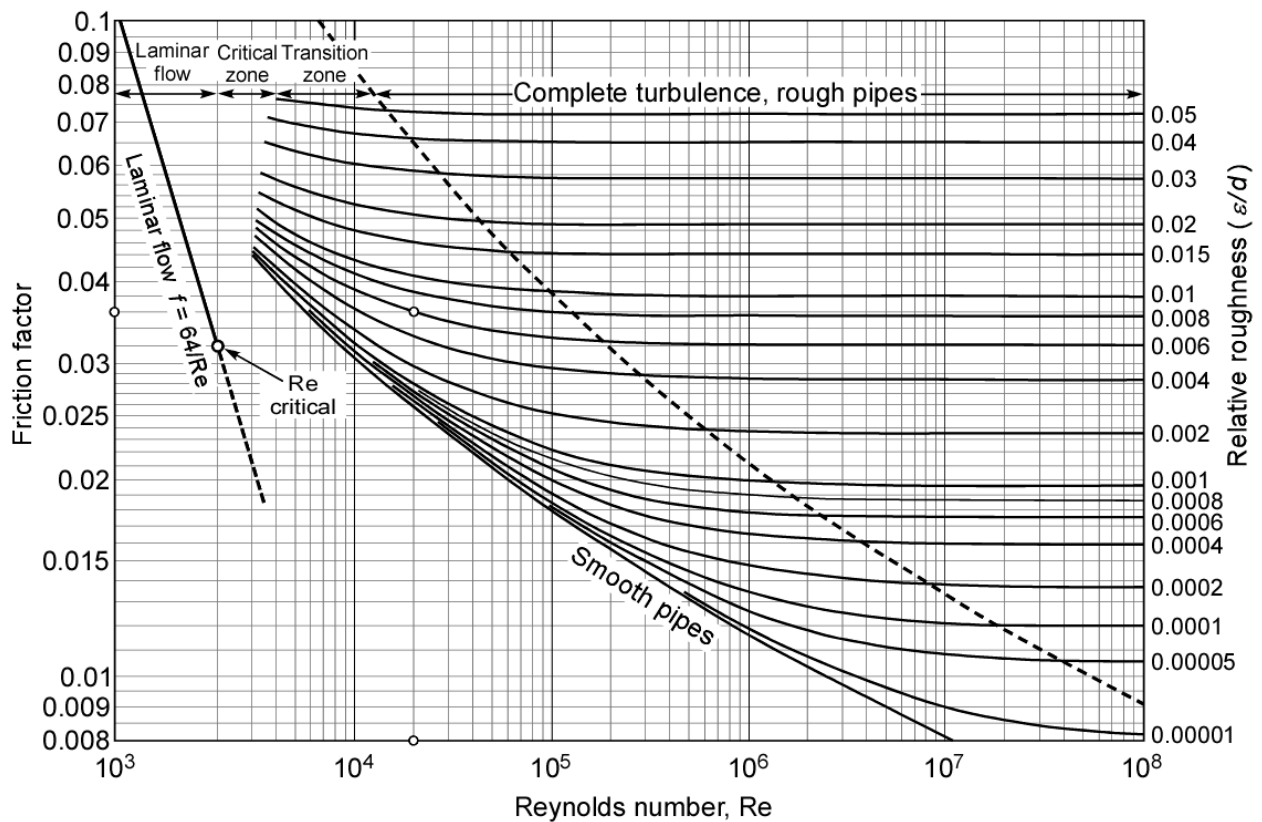
Figure 5.19 Moody Diagram for determining Darcy friction factor in pipes based on relative roughness of pipe walls and the Reynolds number. Modified from Moody, 1944.

The Darcy friction factor for common commercial pipes can be estimated from the experimental graph of Moody (1944) which relates the relative roughness of pipe walls and the Reynolds number (Figure 5.19). The relative roughness (ε/d) is the ratio of the absolute length of irregularities (ε) protruding from the pipe walls to the pipe internal diameter (d). For example, for a natural conduit 3 meters (300 cm) in diameter that has wall irregularities 1.8 cm long (which is not uncommon for scalloped walls), the relative roughness is 0.006. For the

Reynolds number of 20000 (bottom axis of the Moody Diagram) and the relative roughness line of 0.006 the friction factor is 0.036. In the complete turbulence zone, the friction factor is a function of the relative roughness only; it remains constant for the same relative roughness regardless of the Reynolds number. For purely laminar flow, where the Reynolds number (Re) is less than 2000, the friction factor is independent of the relative roughness:

$$f = \frac{64}{Re} \qquad (5.22)$$

The Darcy friction factor for turbulent flow (Reynolds number greater than approximately 4000) in rough conduits can also be calculated by numerically solving the Colebrook equation (Colebrook, 1939) where it is given implicitly (i.e., it is on both sides of the equation):

$$\frac{1}{\sqrt{f}} = -2 \, log_{10} \left(\frac{\frac{\varepsilon}{d}}{3.7} + \frac{2.51}{Re \, \sqrt{f}} \right) \qquad (5.23)$$

Another form of the Colebrook equation can be used to calculate the friction factor for flow with free surface such as in a pipe that is flowing partially full of fluid:

$$\frac{1}{\sqrt{f}} = -2 \, log_{10} \left(\frac{\varepsilon}{12R_h} + \frac{2.51}{Re \, \sqrt{f}} \right) \qquad (5.24)$$

where R_h is the hydraulic radius. For completely filled circular conduits, R_h = d/4 = (inside diameter)/4. For partially filled and conduits of other shapes the hydraulic radius is given as the ratio of the cross-sectional area of flow (A) to its wetted perimeter (P_w): $R_h = A / P_w$.

The Haaland equation (Haaland, 1983) can be used to directly calculate the Darcy friction factor for a fully flowing circular pipe. It approximates the implicit Colebrook equation with acceptable accuracy for practical purposes:

$$\frac{1}{\sqrt{f}} = -1.8 \, log_{10} \left[\left(\frac{\frac{\varepsilon}{d}}{3.7} \right)^{1.11} + \frac{6.9}{Re} \right] \qquad (5.25)$$

The Chézy equation is another widely used formula for calculating velocity in pipes (conduits) as well as in open channels (for which it was originally derived) using the hydraulic radius (R_h):

$$V = C * \sqrt{R_h J} \qquad (5.26)$$

where C is the Chézy coefficient and J is the loss of hydraulic head due to friction.

The Chézy coefficient, which is a function of wall roughness, and the Darcy friction factor (f) are related as follows:

$$C = \sqrt{\frac{8g}{f}} \qquad (5.27)$$

The Darcy friction factor and the empirical Manning's roughness coefficient (n) are related as

$$n = R_h^{1/6} \sqrt{\frac{f}{8g}} \qquad (5.28)$$

where the Manning's roughness coefficient has dimension of $m^{-1/3}s$. Note that all three friction factors, Darcy, Manning and Chézy, have been determined empirically by various researchers and their selection for any flow setting is subjective.

In the traditional hydraulics of pipes, it has been demonstrated with experiments and widely accepted that the critical Reynolds number at which the flow is not laminar any more is somewhere between 2000 (experiments of Moody) and 2300 (experiments performed by Osborne Reynolds; Reynolds, 1883, 1894). For smaller Reynolds numbers the influence of wall roughness will be dampened, and the flow will remain laminar; at higher Re numbers, the viscous force becomes smaller compared to the inertia force so that even small disturbances at the walls will be allowed to grow into turbulence. As can be seen from the Moody Diagram (Figure 5.19), the transition from laminar to turbulent flow is not abrupt and there is a relatively wide transition zone where various factors influence formation of turbulence. The conduit diameter (d), fluid kinematic viscosity (v), dynamic viscosity (μ), density (ρ), and flow velocity (V) all determine the Reynolds number:

$$Re = \frac{\rho V d}{\mu} = \frac{V d}{v} \qquad (5.29)$$
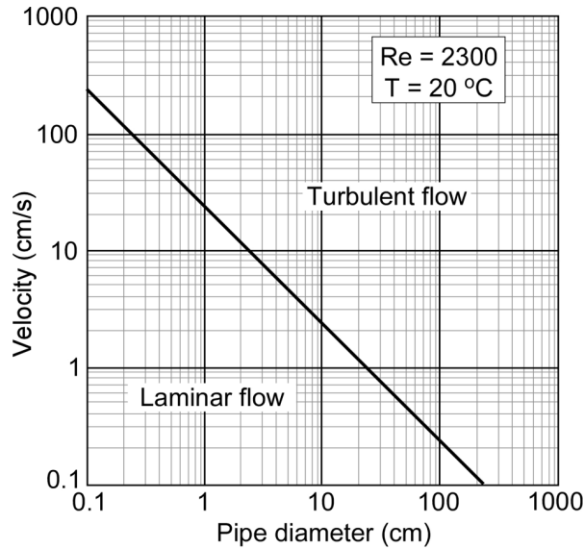
Figure 5.20 Graph of critical velocity separating laminar and turbulent flow regime for different pipe diameters and critical Reynolds number of 2300. The kinematic viscosity of water (v) at 20 ºC is approximately 1.01 x 10^{-6} m^2/s. The critical velocity is calculated as $V_{cr} = Re_{cr} \times v \times 1/d$. Modified from Vuković and Soro, 1985. University of Belgrade. Acknowledgement is required for further use.

In general, laminar flow occurs for low velocities, small diameters, low densities, and high viscosities, while turbulent flows occur for the opposite conditions: high velocities, large diameters, high densities, and low viscosities (Figure 5.20.) Extensive conduit wall irregularities also result in faster transition to turbulent flow (Figure 5.21). However, in the hydraulics of karst conduits there are many unknown factors related to the geometry

of submerged conduits as well as irregularities of conduit walls, so that any calculations described earlier are speculative and should be applied with care, advisably only at a hypothesis-testing (proof of concept) level.

Figure 5.21 Relict of an initial tubular conduit in Mammoth Cave, Kentucky, now rarely active and reshaped by downcutting towards lowered karstification base. Photo courtesy of Nenad Marić.

For example, for the same flow rate in a karst conduit the velocity may increase or decrease based on the conduit cross-sectional area and the flow may transition from laminar to turbulent and back. This includes a possibility that laminar flow in the center of the conduit has higher velocity than along some segments of the same conduit where the flow is completely turbulent. Turbulence also increases resistance to flow as a large part of the mechanical energy in the flow is spent on the formation of eddies which eventually dissipate their energy as heat. Consequently, much larger increases in the conduit entry pressure will be required to further increase the turbulent flowrate as compared to laminar flow.

Unfortunately, in various literatures on caves and karst there is a wide range of Reynolds numbers for which authors state that the flow is turbulent. This includes Re numbers as low as 10. None of such publications presents a basis for the reported Re numbers including experimental measurements of laminar and turbulent flow in actual karst conduits and their possible deviations from the well-established principles of classic hydraulics. Notwithstanding the fact that nothing is quite certain in karst, this author's advice is to avoid using unsubstantiated numbers and input parameters for hydraulic calculations in karst regardless of the authority which presented them.

5.2.2 Flow in Open Channels

Flow rate in karst channels which are not submerged (where the flow is with free surface – see Figure 5.22) can be calculated using the Chézy-Manning equation:

$$Q = A \frac{1}{n} R^{2/3} i_0^{1/2} \qquad (5.30)$$

where A is the cross-sectional area of flow, n is the Manning's roughness coefficient, R is the hydraulic radius, and i_0 is the slope of the channel bottom assumed to be equal to the hydraulic gradient (slope) of the free water surface (i.e., the flow is assumed to be uniform).

As indicated earlier, the hydraulic radius is calculated by dividing the cross-sectional area of flow with the wetted perimeter. For a trapezoidal channel shown in Figure 5.22-Left the cross-sectional area of flow (A) and the wetted perimeter (P_w) are:
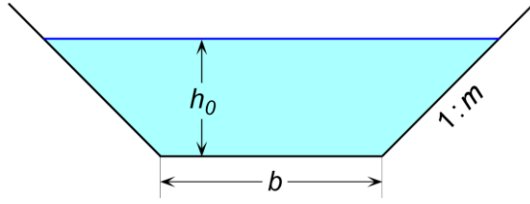
Figure 5.22 *Left*: General dimensions of a trapezoidal channel. *Right*: Cave passage in which open channel flow occurs after rains and persists in rainy season. In an earlier stage of cave development, the channel was fully submerged and with a high flow rate as evidenced by the well-developed scallops. Photo courtesy of Predrag Stošić Peca.

$$A = (b + mh_0)h_0 \qquad\qquad (5.31$$

$$P_w = b + 2h_0\sqrt{1 + m^2} \qquad\qquad (5.32)$$

which gives the following flow rate:

$$Q = (b + mh_0)h_0 \frac{1}{n}\left[\frac{(b + mh_0)h_0}{b + 2h_0\sqrt{1 + m^2}}\right]^{\frac{2}{3}} \times i_0^{\frac{1}{2}} \qquad (5.33)$$

For a rectangular channel, where $m = 0$, the flow rate is:

$$Q = bh_0 \frac{1}{n}\left[\frac{bh_0}{b + 2h_0}\right]^{2/3} \times i_0^{1/2} \qquad\qquad (5.34)$$

For wide channels, where the normal depth (h_0) is much smaller than the channel width, the wetted perimeter can be approximated by the channel width ($P_w \sim b$), and the hydraulic radius by the normal depth ($R \sim h_0$). In that case the flow is

$$Q = \frac{1}{n}bh_0{}^{5/3} \times i_0^{1/2} \qquad\qquad (5.35)$$

For channels with smooth surfaces, such as solid cement, the Manning's roughness coefficient ranges from 0.010 to 0.015 as finish gets rougher. For cemented rock it is between 0.017 and 0.030; for channel bottom lined with unconsolidated sediments it ranges between 0.022 and 0.030 depending on the sediment grain size; for rough channels with broken rocks or incised irregularly into rock it ranges from 0.035 to higher than 0.045.

In any case, calculating groundwater flow rate in open karst channels with various hydraulic equations is a very rough approximate at best given all the irregularities of almost all karst channels and assumptions that must be made. Photographs in Figures 5.23 and 5.24 illustrate this point.

Figure 5.23 Križna Jama Cave in Slovenia. Photo courtesy of Peter Gedei. More cave photos are available at https://petergedei.com/

Figure 5.24 *Left*: Hanke Channel section of the world-famous Škocjan Caves in Slovenia protected by UNESCO. Photo courtesy of Borut Lozej. *Right*: Rokina bezdana cave in Croatia. Photo courtesy of Dinko Stopić.

5.2.3 Groundwater Flow Velocity in Karst

Because of the widely varying hydraulic conductivity and effective porosity of karstified carbonates, as well as the presence of conduits and channels, the groundwater velocity in karst can vary over many orders of magnitude. One should therefore be very careful when making a (surprisingly common) statement such as "groundwater velocity in karst is very high". Although this may be true for the flow taking place in karst conduits, a disproportionally larger volume of any karst aquifer has relatively low groundwater velocities through small fissures and rock matrix. One common method for determining groundwater flow directions and apparent flow velocities in karst is dye tracing. However, most dye tracing tests in karst are designed to analyze possible connections between known (or suspect) locations of surface water sinking or focused recharge, and the locations of groundwater discharge such as springs (more on dye tracing tests is given in Lecture 13.) Since such connections commonly involve some type of preferential flow paths, the apparent velocities calculated from dye tracing tests are usually biased towards the high end.

Figure 5.25-*Left* shows the results of 43 tracing tests in karst regions of West Virginia, the United States. The median groundwater velocity is 716 meters per day, while 50% of the tests show values between 429 and 2655 m/d (25th and 75th percentile of the experimental distribution respectively). It is interesting that, based on 281 dye tracing tests, the most frequent velocity (14% of all cases) in the classic Dinaric karst of Bosnia and Herzegovina as reported by Milanović (1979) is quite similar: between 864 and 1728 m/d (Figure 5.25-*Right*). Twenty five percent of the results show groundwater velocity greater than 2655 m/day in West Virginia, and greater than 5184 m/day in Herzegovina. Neither the Bosnia and Herzegovina nor the West Virginia data show any obvious relationship between the apparent groundwater velocity and the hydraulic gradient between the locations of dye injection and downgradient locations of dye detection (Figure 5.26).
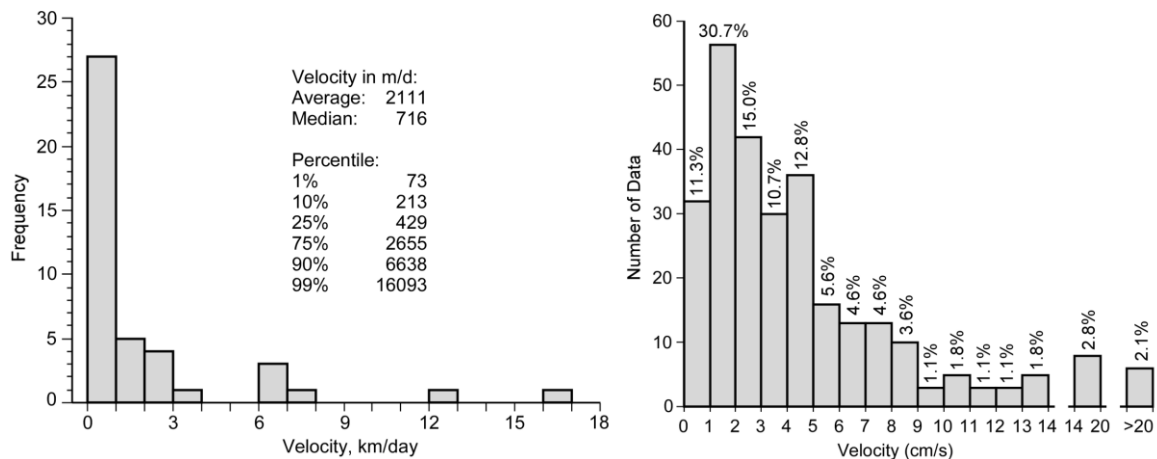
Figure 5.25 *Left*: Apparent groundwater flow velocities in the West Virginia karst based on 43 dye tracing tests. Data from Jones, 1977. Copyright Karst Water Institute; permission is required for further use. *Right*: Apparent groundwater flow velocities in the eastern Herzegovina karst based on 281 dye tracing tests. From Milanović, 1979, HE Trebišnjica, Institut za korištenje i zaštitu voda na kršu, Trebinje. Acknowledgment is required for further use.

Various approximate calculations of flow velocity have been made based on the geometry of scallops (Figures 5.27 and 5.28) sculptured on conduit walls by turbulent flow eddies (e.g., see Bögli, 1980; Palmer, 2007; Ford and Williams, 2007). Scallops are common in limestone and gypsum caves but much less so in dolomite as they require

homogeneous host rock with uniform mineral size. According to Palmer (2007), scallops are not formed if the water velocity is less than about 1 cm/s, because the turbulent eddies are not stable or uniform enough in such slow-moving water. At velocities greater than about 3 m/s the bedrock surfaces are usually abraded by sediment, which prevents scallops from forming. The same author provides a graph of flow velocity versus scallop length and advises its use for general estimates only. A quick estimate can also be made using the following relationship (Palmer, 2007):
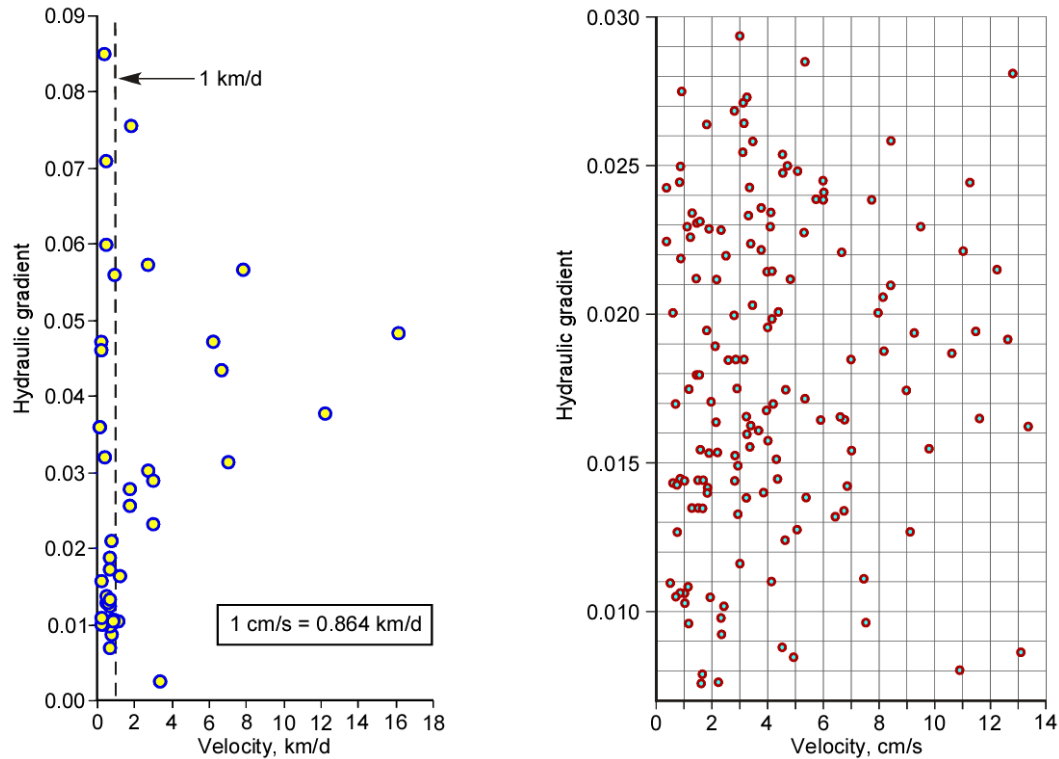
Figure 5.26 *Left*: Apparent groundwater flow velocity vs. hydraulic gradient for the 43 dye tracing tests in the West Virginia karst. Data from Jones, 1977. Copyright Karst Water Institute; permission is required for further use. *Right*: Apparent groundwater flow velocity vs. hydraulic gradient for the 281 dye tracing tests in the Bosnia and Herzegovina karst. From Milanović, 1979, HE Trebišnjica, Institut za korištenje i zaštitu voda na kršu, Trebinje. Acknowledgment is required for further use.

$$V(cm/s) = X/L \qquad (5.36)$$

where L is the mean scallop length in centimeters, and X is a number that depends on the temperature of the water that formed the scallops. $X=375$ at 0ºC, 275 at 10º, 210 at 20º, and 170 at 30º. For comparison, the calculated flow velocity for a canyon passage in White Lady Cave, Little Neath Valley, Unite Kingdom is 1.21 m/s and the flow rate is 9.14 m^3/s, for the cross sectional area of flow of 7.6 m^2 and scallop length of 4.1 cm (White, 1988).

Although the interconnected conduit (channel) porosity created by dissolution of carbonates provides for most of the flow in older carbonate rocks, it still occupies a significantly smaller overall volume of the aquifer compared to the matrix (primary) porosity. However, this general principle must be applied with great care at every karst site because the ratio between the total and effective porosities of any type (matrix, fracture, and solution) is scale dependent. Unfortunately, the concept of effective porosity is sometimes misinterpreted or misused in attempts to
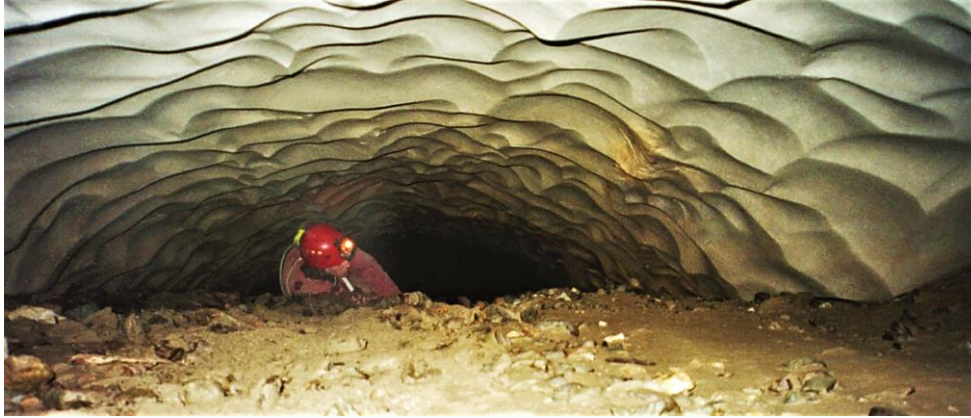
Figure 5.27 Giant scallops (facets) on the walls of an affluent syphon in Momačka Pećina cave, located in Džervinska Greda stripe karst, near Miroč Mountain, Eastern Serbia. Photo courtesy of Milorad Kličković.
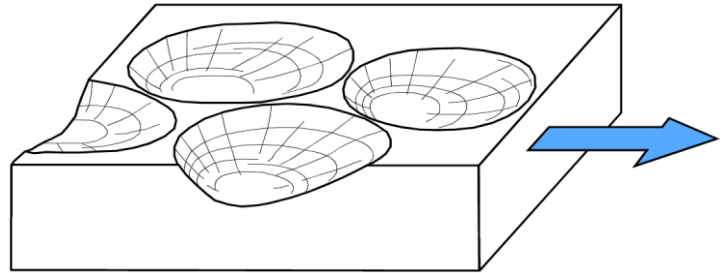
Figure 5.28 *Left*: Scalloped wall in a Bath County, Virginia cave. Photo courtesy of Phil Lukas. *Top*: Schematic of individual scallops and determination of flow direction based on their shape: the steeper slopes are on the upgradient side of flow. Note that individual scallops always overlap, and the entire wall surface is often covered as seen in the photograph.

quantify and numerically model groundwater flow in karst with inadequate tools. For example, analytical equations and numeric groundwater models based on Darcy's law are still often used to quantify groundwater velocity and flow in karst aquifers. This is justified by stating that the karst aquifer behaves as an equivalent porous medium (EPM) because all three porosity types are relatively uniformly distributed and interconnected at a particular scale (the Site) and therefore of equal importance for groundwater flow. It follows that the nature of groundwater flow through the overall karst aquifer volume is the same as, for example, through gravel deposits and can therefore be described with the simple Darcy's equation.

At the same time, practitioners applying this approach may in many cases be confronted with the fact that groundwater levels in some monitoring wells are rising and falling very quickly in response to recharge episodes, whereas this is not the case in other wells nearby. They also may acknowledge that the linear groundwater velocity (v_L) is very fast in certain portions of the aquifer as indicated by a dye tracing test. Note that the linear groundwater velocity in the EPM models is calculated as (see also Equation (4.2))

$$v_L = \frac{K * i}{n_{ef}} \qquad (5.37)$$

where K is the hydraulic conductivity of EPM, i is the hydraulic gradient, and n_{ef} is the effective porosity.

The problem arises when some karst practitioners simulate high groundwater velocities in the preferential flow paths by using a very small effective porosity in the Equation (5.37), or in numeric model cells representing these paths, smaller than in the surrounding cells that are supposed to simulate aquifer matrix without cavities. This, of course, does not make any hydrogeologic sense as illustrated in Figures 5.29 and 5.30: the "material" in box A (area, volume) cannot have the effective (or total) porosity smaller than in box B regardless of how convincing any related "expert" explanation or modeling justification may be. Needless to say, both the total and the effective porosity of a karst cavity (conduit) filled only with air or water is 100% such that Darcy's law does not apply.
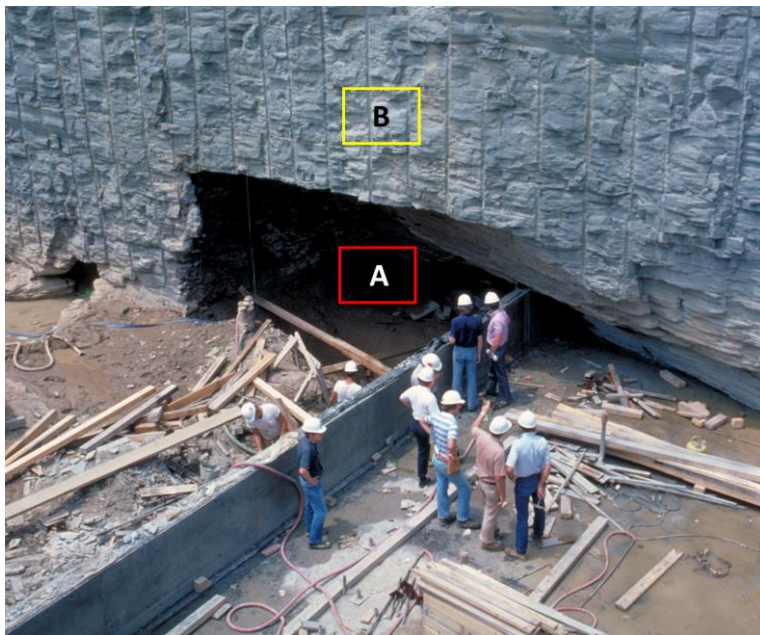
Figure 5.29 Cavity discovered below water table at a deep construction site (shown dewatered here) in Paleozoic limestone, Hartsville, Tennessee. Photo by George Sowers, printed with kind permission of Francis Sowers.
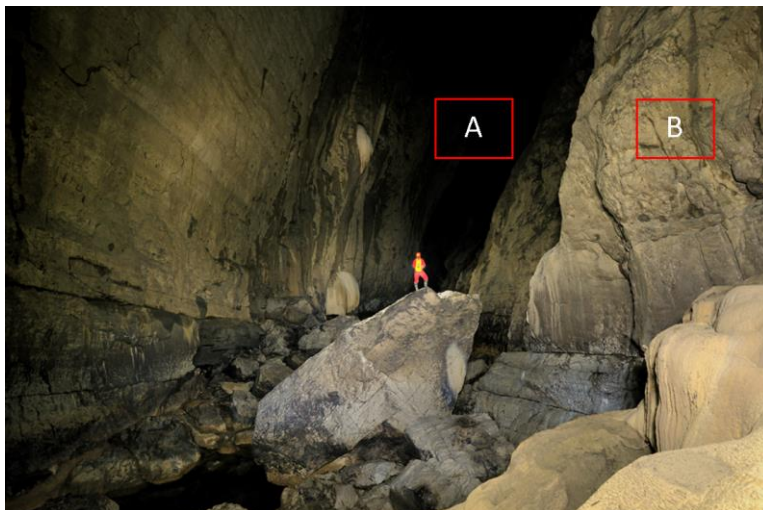
Figure 5.30 Part of the world-famous Škocjan Caves in Slovenia not accessible to tourists. Photo courtesy of Borut Lozej, Škocjan Caves Park.

5.2.4 Hydraulic Head and Hydraulic Gradient in Karst

As discussed in detail by Milanović (1979), Kresic (2013), and Kresic and Mikszewski (2013), groundwater level measurements in monitoring wells (piezometers) in karst must be designed, performed, and interpreted with great care. The most common conceptual error in karst hydrogeology is to draw maps of the potentiometric surface (water table, piezometric surface, and hydraulic head map are all interchangeably used terms) and use them to estimate groundwater flow directions and hydraulic gradients (see Figures 5.31 through 5.38). Preferential flow paths create local troughs (linear depressions) in the potentiometric surface that may be detected only if enough piezometers (monitoring wells) screened at right depths, and on either side of the conduit are available. This, however, is not the case at many sites because of the costs and difficulties associated with drilling in karst. In addition, the preferential flow path(s) of importance to the specific project may never be found because of the many uncertainties discussed earlier (see also Lecture 7 on karst aquifers.) In any case, extensive drilling in karst should be performed only after some preliminary investigations using non-invasive techniques such as geophysics, remote sensing, field mapping, or dye tracing are conducted to locate possible preferential flow paths (Kresic, 2013).

Figure 5.31 illustrates some key differences between a karst aquifer and an intergranular (unconsolidated sediments) aquifer, which both have the same general flow direction from the north to the south as shown on the map views. A triplet of wells, installed anywhere in the intergranular aquifer, would reasonably accurately determine the general groundwater flow direction based on the measured hydraulic head. In contrast, the same cannot be stated for the karst aquifer case where the three-well principle may give very different results depending on the position of individual wells relative to any preferential flow paths. Moreover, a group of closely spaced wells in karst may show a completely "random" distribution of the measured hydraulic head. One well may be completed in a homogeneous rock block, without any significant fractures and with low matrix porosity, and may even exhibit the so-called "glass effect" (no fluctuation of water table regardless of the precipitation-infiltration dynamics). On the other hand, a well ten or so feet away, screened near or within a preferential flowpath, may show the hydraulic head fluctuation of several meters or more as a response to wet and dry seasons and recharge episodes (Figure 5.32). In contrast, monitoring wells in young carbonates with high matrix porosity will often have much less pronounced water-level fluctuations (smaller amplitude) regardless of their location in the aquifer. This is because groundwater storage and flow rates are significant in both the rock matrix and the conduits.
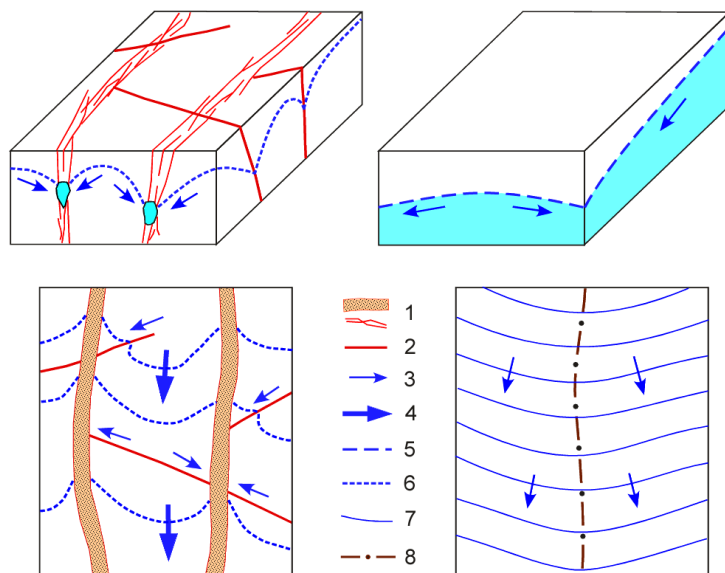
Figure 5.31 Schematic block diagram of groundwater flow in three-dimensions (top) and its map presentation (bottom) for a karst (*left*) and an intergranular, unconsolidated (*right*) aquifer. (1) Preferential flow path (e.g., fracture or fault zone or karst conduit/channel); (2) fracture/fault; (3) local flow direction; (4) general flow direction; (5) position of the water table in the intergranular aquifer); (6) position of the piezometric head in the karst aquifer; (7) water table contour line; (8) groundwater divide in the intergranular aquifer. Modified from Krešić, 1991. University of Belgrade. Acknowledgement is required for further use.
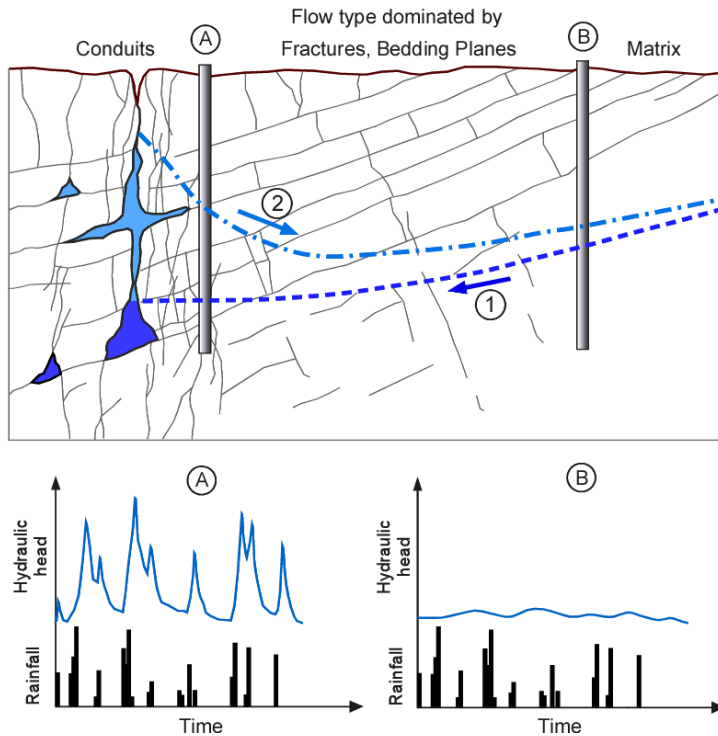
Figure 5.32 Response of the hydraulic head measured in monitoring wells to different types of flow in karst aquifers. A: Hydraulic head hydrograph reflecting rapid response of conduit flow to major recharge events and no significant storage in rock matrix. B: Delayed and dampened response of the low-storage matrix. 1: Flow direction during base flow conditions. 2: Flow direction at the peaks and following major recharge episodes. Flow additionally influenced by fractures may produce any combination of the two hydrographs. Modified from Kresic, 2007. Copyright CRC Taylor & Francis; permission is required for further use.

Regardless of the size of karst conduits, they are the main reason for the unique characteristics of karst aquifers, i.e., groundwater flow under pressure akin to pipe flow in conventional fluid mechanics. This pressure can be propagated fast and to great distances following major recharge episodes. The hydraulic head can sometimes rise tens of meters or more resulting in a complete flooding of all interconnected voids (channels, conduits) in the matter of hours (see Figure 5.33). This buildup of pressure in the hydraulic system is typical for karst aquifers developed in compacted older carbonates of Paleozoic and Mesozoic age having low matrix porosity of a few percent. The force created by high pressures can sometimes have a tremendous erosional and transport impacts (Figure 5.34).

Figure 5.33 Encounter with a summer storm in Bat River Cave, Minnesota Cave Preserve. *Upper left*: Cave passages were dry before the storm. *Upper right*: After sudden intense storm on August 18, 2007, a waterfall occurred where dry ceiling existed before (4:03 pm); *Lower Left*: The water begins to rise and becomes turbulent (4:17 pm); *Lower right*: Seconds after this photo was taken it was almost impossible to stand in the passage without getting swept away (4:59 pm). The cavers escaped by the ladder extending from the newly drilled vertical shaft to the cave. Photographs courtesy of John Ackerman.

One very important aspect of karstification is that the conduit/channel network continues to expand both laterally and vertically. Consequently, groundwater connections, i.e., flow directions, can often develop across topographic drainage divides when carbonate deposits are sufficiently thick and extensive. This is true for both local and regional scales of interest. The two most obvious results of this inconsistency between topographic and groundwater divides in karst terrains are sinking streams and large springs. In fact, karst aquifers give rise to the largest springs in the world (see Lectures 7 and 10) and are, generally, drained by only one or several springs due to a self-organized conduit network converging at the spring.

Dye tracing, the only direct method for determining drainage areas of karst springs and karst groundwater drainage areas in general, often results in unexpected connections (Figure 5.35). These connections vary in time depending on the season and major recharge events so that dye tracing tests must be repeated with different dyes

and for different hydrologic conditions to accurately determine groundwater flow directions and delineate surface and subsurface areas of interest. Assessing temporal variation of groundwater flow directions and hydraulic heads is a critical step at any site in karst for which a conceptual site model (CSM) is being developed. Quarterly water level measurements at monitoring wells, a common practice at contaminated groundwater sites in the United States, would not be sufficient in that regard as illustrated with the figures and photographs in this chapter.

Figure 5.34 Cavers looking up at wood logs brought in by the underground stream flood waters and left at a ledge near cave ceiling, Culverson Creek Cave System, West Virginia. Photo courtesy of Phil Lukas.
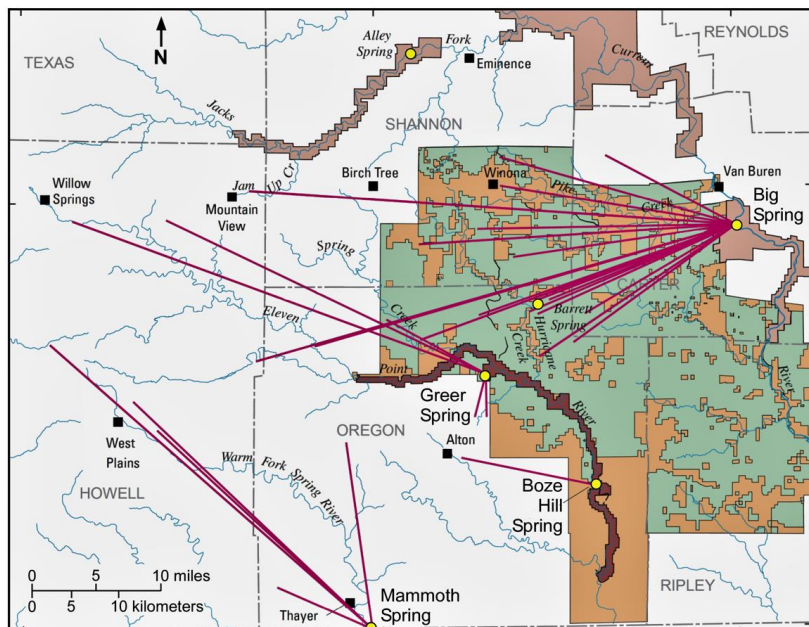
Figure 5.35 Results of dye-tracing investigations that successfully identified a hydrologic connection between a sinkhole or a losing stream reach and a major spring in south-central Missouri. Dye traces are in dark pink, different color polygons represent various land uses. Note how different dye traces cross different watersheds, sometimes intersect, and can be more than 30 miles long. Modified from Imes et al., 2007. USGS, in public domain.

One aspect of porosity in karst aquifers often receiving less attention is infill of cavities with unconsolidated sediments (see Figure 5.36). This transient type of porosity may change depending on the hydraulics of groundwater flow and recharge mechanisms such that the loose sediments may be flushed out of cavities, new sediments deposited, and everything in between. Filling of karst cavities may also be more consolidated and therefore more permanent. However, under certain circumstances such as due to constantly changing and high hydraulic pressures, even these deposits may break down and be washed out. This is of particular concern when designing and constructing dams and reservoirs in karst. Considering the presence and nature of intergranular porosity is also important for other aspects of karst aquifer management including quality of water supply and contaminant fate and transport.

In any case, using hydraulic head measurements at wells screened in the infill of cavities for any assessment of the flow characteristics in the aquifer should be done with great care so not to "compare apples and oranges."

Figure 5.36 "Serious Sediment Plug" in a Bath County, Virginia cave. Photo courtesy of Phil Lucas.

In conclusion, using only the hydraulic head information from monitoring wells (piezometers) for the purposes of assessing hydraulic gradients, groundwater flow directions, and overall flow characteristics in a karst aquifer using an EPM approach, would in some cases be insufficient and potentially may lead to erroneous conclusions. Interpretation of the hydraulic head measurements should always include a thorough understanding of various hydraulic factors such as flow through pipes and open channels, as well as "non-hydraulic" factors such as structural geology, limestone (carbonate) sedimentology, geologic history, and possible paleo-karstification (see Lecture 7). This assessment can be combined with dye tracing as needed (Figures 5.35 and 5.37; see also Lecture 15) to provide a better understanding of the subsurface flow conditions and possible existence and connections between any preferential flowpaths in karst.

One extreme but real-world example from the classic Herzegovina karst of a (initially) misinterpreted flow direction near a major karst spring is shown in Figure 5.38, re-emphasizing the need for a comprehensive interpretation of hydraulic head measurements in karst. By solely looking at the hydraulic head recorded at piezometers P4, P3, and P2, and ignoring P1, one could erroneously conclude that the groundwater flow is away from the spring, which is a hydrogeologic nonsense.

Figure 5.37 Dye tracing test with uranine in the karst system of Alta Cadena range near Malaga, Spain. Courtesy of Bartolome Andre Navarro, CEHIUMA.
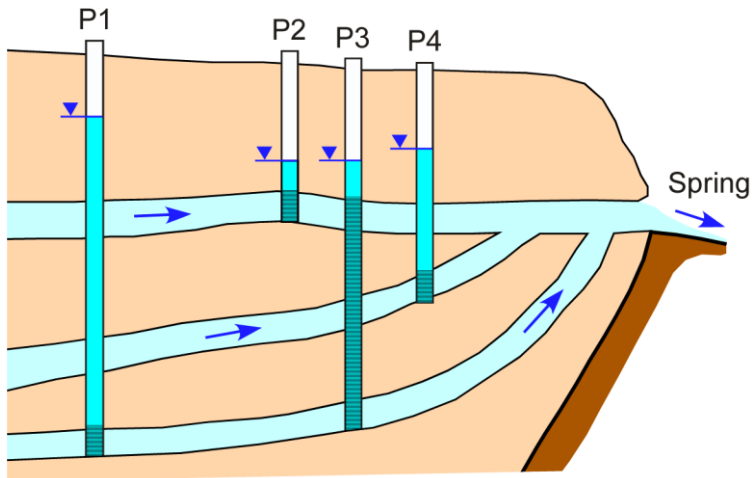
Figure 5.38 Example how closely spaced piezometers in clusters may register very different hydraulic heads depending on the depth and length of well screens. P1 is screened in the bottom conduit only and isolated from the rest of the formation by a grout seal. Similarly, P2 and P4 are screened only in the top and middle conduit respectively. P3 is screened in all three conduits. Modified from Kupusović, 1989. Published by Naš Krš, Sarajevo. Acknowledgment is required for further use.

Lecture 6 Aquifers and Aquitards, Part One

This lecture is based primarily on the materials presented in Kresic, 2007 (*Hydrogeology and Groundwater Modeling, Second Edition*. Copyright CRC Taylor & Francis); Kresic, 2009 (*Groundwater Resources: Sustainability, Management, and Restoration.* Copyright McGraw Hill); Kresic and Mikszewski, 2013 (*Hydrogeological Conceptual Site Models: Data Analysis and Visualization*. Copyright CRC Taylor & Francis), and various publications by the authors of USGS.

6.1 Definitions

Aquifer is defined as a geologic formation, or a group of hydraulically connected geologic formations which store and transmit significant quantities of potable groundwater. The word comes from two Latin words: *aqua* (water) and *affero* (to bring, to give). The two key terms, "significant" and "potable" in this definition are not easily quantifiable. The common understanding is that an aquifer should provide more than just several gallons or liters per minute to individual wells and that water should have less than 1000 milligrams of dissolved solids. For example, a well yielding 2 gal/min may be enough for an individual household. However, if this quantity is at the limit of what the geologic formation could provide via individual wells, such an "aquifer" is not considered as a source of significant public water supply. Another issue is groundwater quality. If the groundwater has naturally high total dissolved solids, say 5000 mg/l, it is traditionally disqualified from consideration as a significant source of potable water, regardless of the groundwater quantity. However, with an increasing water shortage worldwide and advancements in water-treatment technologies, such as reverse osmosis (RO), aquifers with brackish groundwater are increasingly interesting for development.

Word *aquitard* is derived from the Latin words: *aqua* (water) and *tardus* (slow) or *tardo* (to slow down, hinder, delay). An aquitard does store water and can transmit it, but at a much slower rate than an aquifer and so cannot provide significant quantities of potable groundwater to wells and springs. Determining the nature and the role of aquitards in hydrogeologic studies is very important in both water supply, and groundwater contamination/remediation projects. When the available information suggests there is a high probability for water and contaminants to move through the aquitard within a timeframe of generally less than one hundred years, such aquitard is called *leaky*. When the potential movement of groundwater and contaminants through the aquitard is estimated in hundreds or thousands of years, such aquitard is called *competent*.

Aquiclude, a related term, is generally much less used today in the United States but is still in relatively wide use elsewhere (Latin word *claudo* means to confine, close, make inaccessible). Aquiclude is equivalent to an aquitard of very low permeability, which, for all practical purposes, acts as an impermeable barrier to groundwater flow (note that there still is some groundwater stored in aquiclude, but it moves "very, very slowly"). A smaller number of professionals and some public agencies in the United States (such as the USGS, see Lohman et al., 1972) prefer to use term *confining bed* instead of aquitard and aquiclude. Accordingly, *semi-confining bed* would correspond to a leaky aquitard. USGS suggests additional qualifiers be specified to explain the nature of a confining layer (aquitard, aquiclude) of interest more closely, such as "slightly permeable" or "moderately permeable".

Figure 6.1 illustrates major aquifer types in terms of the character and position of the hydraulic head in the aquifer, relative to the upper aquifer boundary. The top of the saturated zone of an unconfined aquifer is called the *water table*. The hydraulic head at the water table equals the atmospheric pressure. The thickness of the saturated

zone and therefore the position of the water table may change in time due to varying recharge, but the hydraulic head at the water table is always equal to atmospheric pressure. Note that there may be a low permeable layer, such as clay, somewhere between the ground surface and the water table, but if there is an unsaturated (vadose) zone above the water table, the aquifer is unconfined. An impermeable or low-permeable bed of limited extent above the main water table may cause accumulation of groundwater and formation of a relatively thin saturated zone called *perched aquifer*. Groundwater in the perched aquifer may eventually flow over the edges of the impermeable bed due to recharge from the land surface and continue to flow downward to the main water table, or it may discharge through a spring or seep if the confining bed intersects the land surface.
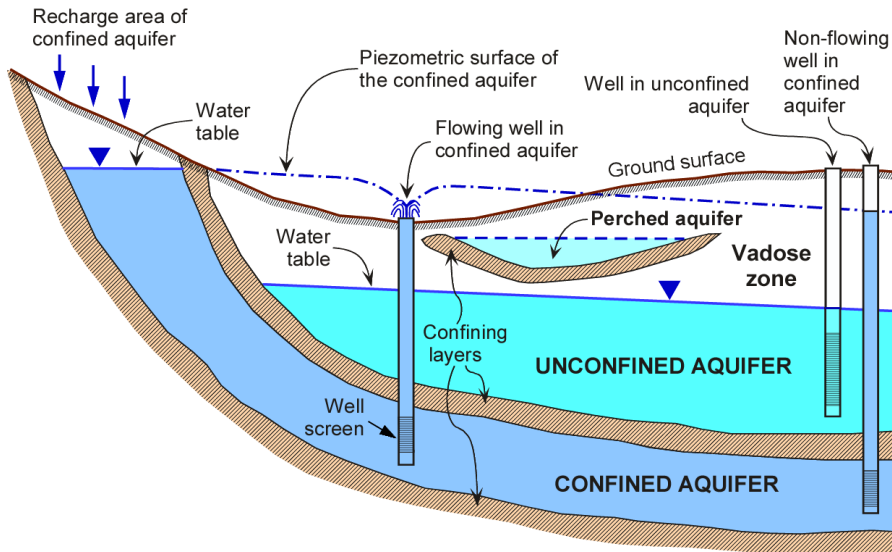
Figure 6.1 Schematic presentation of main aquifer types based on position of the hydraulic head. Modified from USBR, 1977. In public domain

A confined aquifer is bound above by an aquitard (confining layer), and its entire thickness is completely saturated with groundwater. The hydraulic head in the confined aquifer, also called *piezometric level* (or *piezometric surface*), is above this contact. The top of the confined aquifer is at the same time the bottom of the overlying confining bed. Groundwater in a confined aquifer is under pressure, such that static water level in a well screened only within the confined aquifer would stand at some distance above the top of the aquifer. If the water level in such a well rises above ground surface, the well is called a *flowing* or *artesian well* (see Figure 6.2) from French *puits artésien* or "wells of Artois", the French province where such wells were first drilled in 18th century.

Figure 6.2 Historic photograph of Clark Well No. 1, located on the north side of the Moxee Valley in North Yakima, Washington. The well was drilled to a depth of 940 feet into an artesian zone of the Ellensburg Formation and completed in 1897 at a cost of $2,000. The flow from the well was estimated at about 600 gallons per minute and was used to irrigate 250 acres in 1900. Photograph was taken by E.E. James in 1897 and was printed in 1901 in the U.S. Geological Survey Water-Supply and Irrigation Paper 55. In public domain.

The imaginary surface of the hydraulic head in the confined aquifer can be located based on measurements of the water level in wells screened in the confined aquifer. A water table of unconfined aquifers, on the other hand, is not an imaginary surface—it is the top of the aquifer and, at the same time, the top of the saturated zone below which all voids are filled with water. A *semiconfined aquifer* receives water from, or loses water to, the adjacent aquifer from which it is separated by a leaky aquitard.

Hydrogeologic structure is term used to define discharge and recharge zones of a groundwater (aquifer) system. Discharge and recharge are considered relative to both ground surface and subsurface. Four basic types shown in Figure 6.3 are:

(1) Open hydrogeologic structure. Recharge and discharge zones are fully defined (known). Recharge takes place over the entire areal extent of the system (aquifer) which is directly exposed to the land surface. Discharge of the system is either at the contact with the impermeable base (case 1a), or along a main erosional basis such as a large permanent river or coastal line (case 1b).

(2) Semi-open hydrogeologic structure. The discharge zone is fully defined, and the groundwater system is partially isolated from the land surface by low-permeable or impermeable cover. The recharge zones are mostly or partially known (cases 2a and 2b respectively).

(3) Semi-closed hydrogeologic structure. Recharge zones are known or partially known, whereas discharge zones are only partially known (case 3a) or unknown (case 3b).
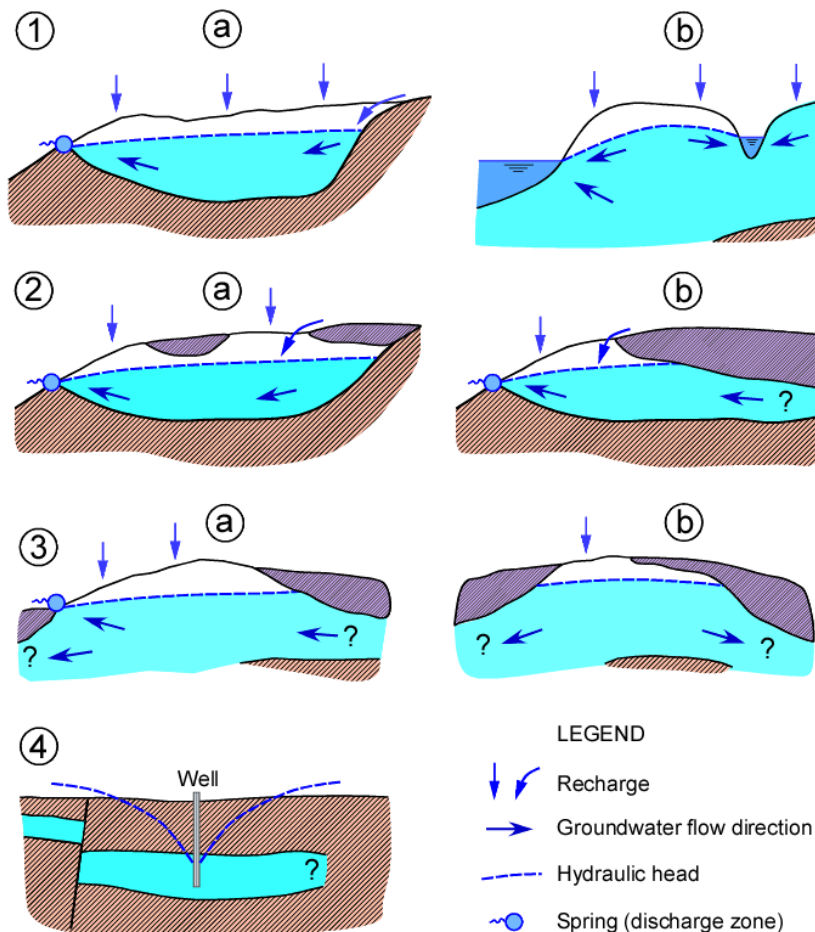
(4) Closed hydrogeologic structure. The aquifer is completely isolated by impermeable geologic units and does not receive recharge. In practice, such a system can only be discovered by drilling. The absence of any significant recharge (from the land surface or from adjacent aquifers) is manifested by large, continuingly increasing drawdowns during groundwater extraction (pumping.)

Figure 6.3 Types of hydrogeologic structures: (1) open; (2) semi-open; (3) semi-closed; (4) closed. Explanation in text. Modified from Kresic, 1991. Published by Naučna knjiga, Belgrade. Acknowledgement is required for further use.

LEGEND

Recharge

Groundwater flow direction

Hydraulic head

Spring (discharge zone)

In some cases, an aquifer may indeed be completely isolated from the "rest of the world". The presence of fresh water in it is testimony to a very different hydrogeologic past when the aquifer was receiving natural recharge from one or more sources such as precipitation, surface water bodies or adjacent aquifers. Various subsequent geologic processes, including faulting and folding, may have resulted in its complete isolation. Such aquifers are called *fossil aquifers* or *non-renewable aquifers*. In general, any aquifer that does not receive natural recharge, regardless of the hydrogeologic structure in which it is formed, is called non-renewable (see Figure 6.4.)

In summary, defining the geometric elements of an aquifer or a groundwater system is the first and most important step in the majority of hydrogeologic studies. It is finding the answers to the following questions regarding the groundwater:

1. Where is it coming from? (Contributing area).
2. Where is it entering the system? (Recharge area).
3. Where is it flowing? (Throughout the aquifer extent).
4. Where is it discharging from the system? (Discharge area).

Figure 6.4 On August 25, 2000, the Moderate-resolution Imaging Spectroradiometer (MODIS) acquired this image of the Acacus-Amsak region in Africa's Sahara Desert at the border between Algeria and Libya. The dendritic structures of ancient riverbeds are clearly visible. The area is underlined by a vast, deep (up to 250m below ground surface) non-renewable aquifer. Multidisciplinary studies (including paleoclimatology and paleobotany) suggest that this area was wet during the last glacial era, covered by forests, and populated by wild animals. On the area's rocks, archaeologists have found many rock paintings and engravings, faint traces of one of the most ancient civilizations of the world. Starting about 12,000 years ago, hunters rapidly learned domestication of buffalo and goat and developed one of the first systems of symbolic art. Extremely dry weather conditions began here about 5000 years ago, resulting in disappearance of surface streams and the civilization itself (NASA, 2007; image courtesy of Luca Pietranera, Telespazio, Rome, Italy). In public domain.

Figure 6.5 shows key spatial features of an aquifer system. *Recharge area* is the land surface through which the aquifer receives water via percolation of precipitation and surface runoff, or directly from surface water bodies such as streams and lakes. When part of a larger groundwater system, an aquifer may receive water from the adjacent aquifers, including through aquitards, but such contacts between the adjacent aquifers is usually not referred to as the recharge (or discharge) zones. Rather, they are referred to as the zones of lateral or vertical inflow (outflow) from the adjacent aquifers.

Discharge area is where the aquifer is losing water to the land surface, such as via direct discharge to surface water bodies (streams, lakes, wetlands, oceans) or discharge via springs. In an unconfined aquifer with a shallow water table, loss of water also happens via direct evaporation and plant root uptake, jointly referred to as evapotranspiration, which may be significant if riparian vegetation is abundant.

An area that gathers surface water runoff, which eventually ends up recharging the aquifer, is called *contributing area. Aquifer extent* is simply the envelope of its overall limits. It is very important to understand that aquifer geometry is always three-dimensional, and it should be presented as such, including with cross sections and two-dimensional maps for varying depths. Ideally, a three-dimensional computer model of the system geometry is generated as part of the hydrogeologic study and can also serve as the basis for subsequent development of a numeric groundwater flow model (see Lecture 12.)
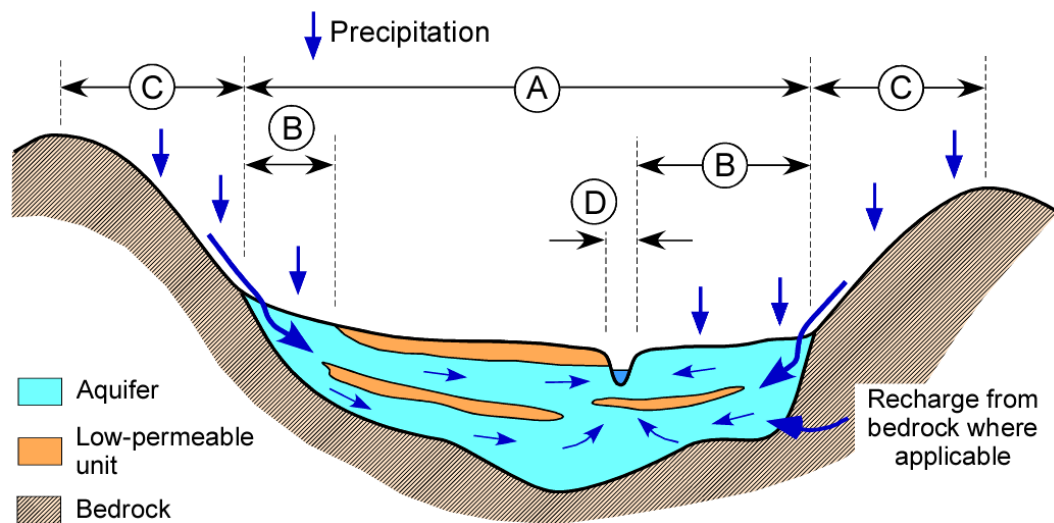
Figure 6.5 Key spatial elements of an aquifer. A: extent; B: recharge area; C: contributing area; D: discharge area. Modified from Kresic, 1991. Published by Naučna knjiga, Belgrade; acknowledgment is required for further use.

The most common classification of aquifers is based on the lithology of the porous media in which they are developed. Four main groups are: (1) unconsolidated sediments, (2) sedimentary rocks, (3) fractured rock (bedrock), and (4) karst aquifers. They are further subdivided based on specific depositional environments (for sediments) and their general geologic origin into various aquifer types that behave similarly in terms of groundwater flow and storage. Rocks and deposits with minimal permeability, that are not considered to be aquifers, consist of low-porosity intrusive igneous rocks, metamorphic rocks, shale, siltstone, evaporite deposits, silt, and clay.

An excellent overview of different types of aquifers and their main characteristics is The Ground Water Atlas of the United States (Miller, 1999). The Atlas provides a summary of the most important information available for each principal aquifer, or rock unit that will yield usable quantities of water to wells, throughout the 50 States,

Puerto Rico, and the U.S. Virgin Islands. The Atlas is an outgrowth of the Regional Aquifer-System Analysis (RASA) program of the USGS, a program that investigated 24 of the most important aquifers and aquifer systems in the United States and one in the Caribbean Islands. The objectives of the RASA program were to define the geologic and hydrologic frameworks of each aquifer system, to assess the geochemistry of the water in the system, to characterize the groundwater flow system, and to describe the effects of development on the flow system. Although the RASA studies did not cover the entire country, they compiled much of the data needed to make the assessments of groundwater resources presented in the Ground Water Atlas of the United States. The Atlas, however, describes the location, extent, and geologic and hydrologic characteristics of all the important aquifers in the United States, including those not studied by the RASA program. The Atlas is written so that it can be understood by readers who are not hydrogeologists and hydrologists. Simple language is used to explain the principles that control the presence, movement, and chemical quality of groundwater in different climatic, topographic, and geologic settings. The Atlas also provides an overview of groundwater conditions for consultants who need information about an individual aquifer. The entire Atlas is available on-line, and detailed printed sections with color maps can be ordered, at nominal cost, from the USGS. Excerpts from the Atlas are included in Lectures 6 and 7, together with other information on aquifer types and examples from around the world.

6.2 Aquifers in Unconsolidated Sediments

Aquifers developed in unconsolidated sediments, which are composed of various mixtures of grains of varying size and shape such as clay, silt, sand, and gravel, are called intergranular (or granular) aquifers. Depending on the predominance of certain grain fraction, such aquifers may be called sand or sand-and-gravel aquifers for example. It is also common to call a particular intergranular aquifer by the depositional process that created it. One such classification by the USGS groups unconsolidated sand and gravel aquifers into four broad categories: (1) stream-valley aquifers, located beneath channels, floodplains, and terraces in the valleys of major streams; (2) basin-fill aquifers, also referred to as valley-fill aquifers since they commonly occupy topographic valleys; (3) blanket sand and gravel aquifers; and (4) glacial-deposit aquifers. In many cases, more than just one process is responsible for creating unconsolidated deposits (for example, stratified glacial drift aquifer systems in stream valleys) and every attempt should be made to at least understand the most important depositional mechanisms. This because key characteristics of the intergranular porous media, such as anisotropy and heterogeneity, are a direct result of depositional processes. For example, an aquifer developed in thick aeolian sands (former sand dunes) should be very prolific, given enough historic or current natural recharge, because of the high storage capacity and effective porosity of the initial uniform (homogeneous) clean sands. On the other hand, alluvial deposits around a stream in a drainage area consisting of many different rock types may create very heterogeneous local flood plain aquifers.

6.2.1 Alluvial Aquifers

Alluvial aquifers usually consist of various proportions of gravel, sand, silt, and clay, deposited by surface streams as layers and lenses of varying thickness. When gravel and sand dominate, with finer fractions forming thin interbeds and lenses, the aquifer may be considered as one continuum providing water to a pumping well through its entire screen. It is therefore not uncommon to present alluvial aquifers using generalized cross-sections as shown in Figure 6.6.
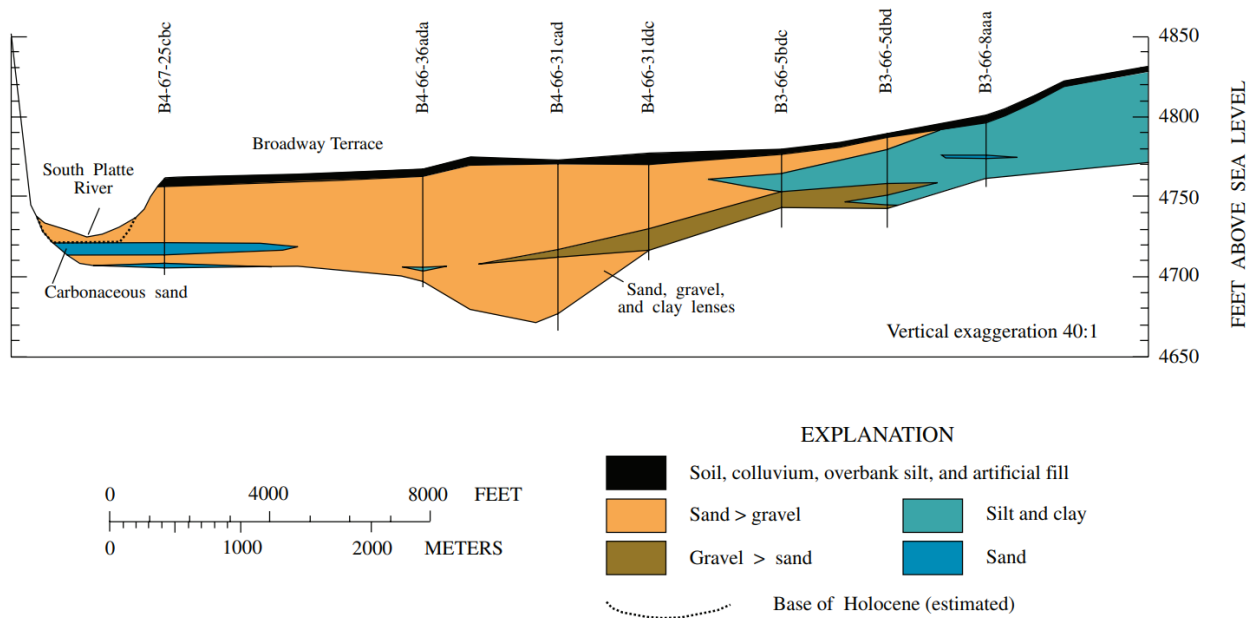
Figure 6.6 Simplified cross-section through alluvial fill of the South Platte River valley near Denver, Colorado. From Lindsey et al., 2005. USGS, in public domain.

Due to fluvial depositional mechanisms however, all alluvial aquifers show some degree of heterogeneity and sites where dissolved contaminants may move faster through layers of more permeable porous media, creating convoluted preferential pathways intersecting a well at discrete intervals. Detecting such pathways, although difficult, is often the key for successful groundwater remediation, whereas it may not be of much importance when quantifying groundwater flow rates for water supply. As a result, regulators often require fine-resolution (continuous) vertical profiling at hazardous waste sites to ensure that the screened interval of a monitoring well does not miss a lens of preferential contaminant transport (for example, using fine-resolution soil profiling tools, continuous coring, and collecting a groundwater sample every five or ten feet, or even with a finer resolution; see Lecture 14).

The areal extent and thickness of an alluvial aquifer depend on the size of the parent stream and the aquifer's location in the drainage area. Aquifers in flood plains of smaller streams and in higher upstream areas are of limited extent, rarely exceeding ten meters in thickness. On the other hand, alluvial aquifers developed in flood plains of major rivers are among the most prolific and widely used for water supply throughout the world. In addition to thick extensive deposits of sand and gravel, they are typically in direct hydraulic connection with the river, which provides for abundant aquifer recharge and well yield. Large well fields for public and industrial water supply are often designed to induce recharge from the river by creating increased hydraulic gradients from the river to the aquifer due to pumping. Collector wells are specially designed to maximize this induced recharge (Figures 6.7 and 6.8). The largest single collector well in the world constructed for the Board of Public Utilities in Kansas City, Kansas, has been pumped at rates of up to 2.4 m^3/s (55 mgd). New improved designs of these wells can result in individual lateral screens (see Figure 6.8) up to 250 ft (75 m) long and yields of several thousand gallons per minute or more. Examples include four municipal collector wells in Olathe, Kansas that each produce approximately 0.4 m^3/sec (6,300 gpm); a collector well for a municipality in Arizona that can produce up to 1.1 m^3/sec (17,400 gpm); and a municipal collector well in Boardman, Oregon that can produce 0.63 m^3/sec or 10,000 gpm (Stowe, 2009.)
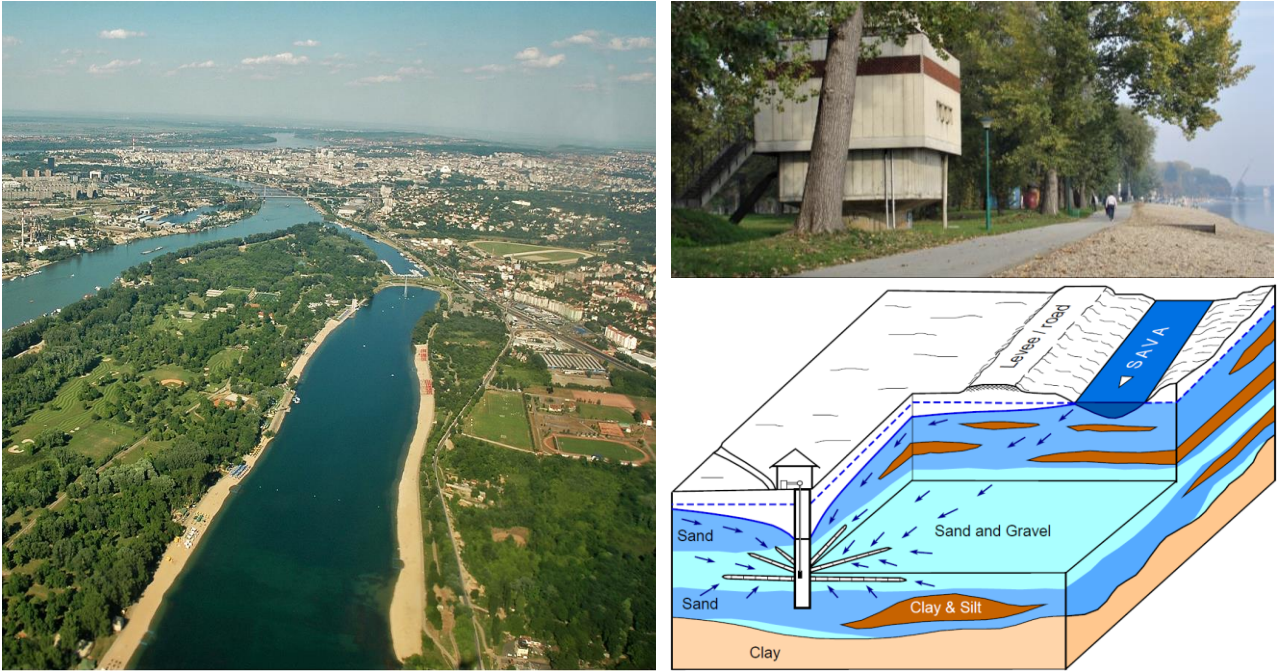
Figure 6.7 Over the course of six decades, the City of Belgrade Waterworks have installed the largest concentration of collector wells (originally referred to as Ranney wells) in the world, 99 of them. *Left*: Recharge basin (in the middle of the photo) built by damming a branch of River Sava on both ends. Sava (on the left) is a major tributary of River Danube (seen in far distance). The recharge basin, supplied by the filtered Sava water, enhances operation of tens of collector wells along its shores. Collector wells are also installed along both banks of Sava upstream for tens of miles. *Upper Right*: typical housing of a Belgrade Waterworks collector well. *Lower Right*: Schematic of a collector well in the Sava River alluvial aquifer. Modified from Milojević, 1967. Published by University of Belgrade; acknowledgment is required for further use.

The infiltration process filters river water as it percolates through riverbed sediments toward the aquifer (recharging it) and, ultimately, into the well screens, typically removing objectionable characteristics of the river water, such as turbidity and microorganisms. Because the recharge water from the river is usually infiltrated over a large area, infiltration rates are low, providing a high degree of filtration in most cases. This process of recharging aquifers and supporting well yields through a natural filtration process is generally referred to as riverbank filtration (RBF; Stowe, 2009.) However, RBF is often insufficient to completely remove various chemicals, viruses, and microorganisms that may be (and usually are) present in surface streams. For this reason, USEPA has specifically addressed quality and treatment of groundwater sources under direct influence of surface water (GWUDISW) with the federal Surface Water Treatment Rules that address disease-causing viruses and pathogens such as *Giardia lamblia* which are not found in "true" groundwater.

The induced infiltration to alluvial aquifers from surface water is not always desirable or permissible, as dewatering of small streams may occur during low-flow conditions that severely threatens the ecological health of the stream and/or affects downstream human consumptive uses. In some cases, alluvial water supply wells that have been operating for decades are now under increased regulatory scrutiny for inducing infiltration during low-flow conditions.
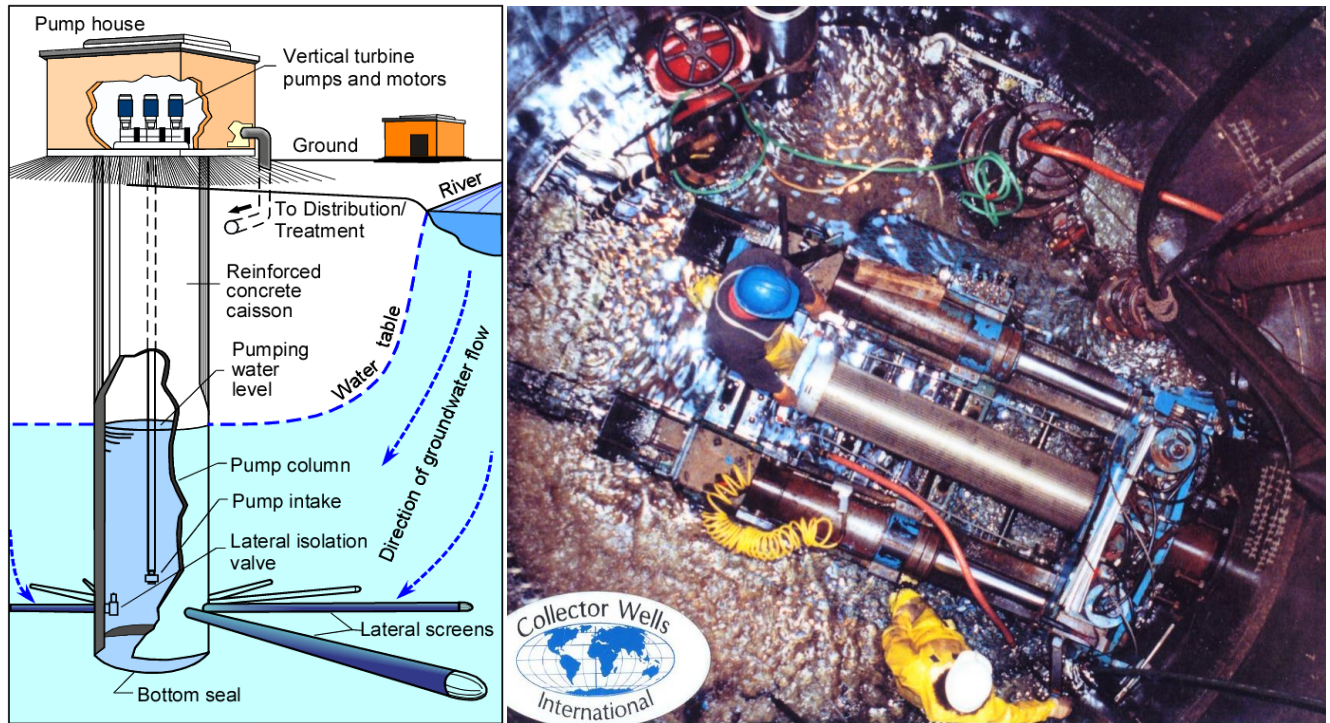
Figure 6.8 *Left*: Schematic of a typical radial collector well adjacent to riverbank. *Right*: Down view of installation of 12-inch diameter well screen in 13-foot diameter collector well. Courtesy of Collector Wells International, Inc., a Layne Christensen Company.
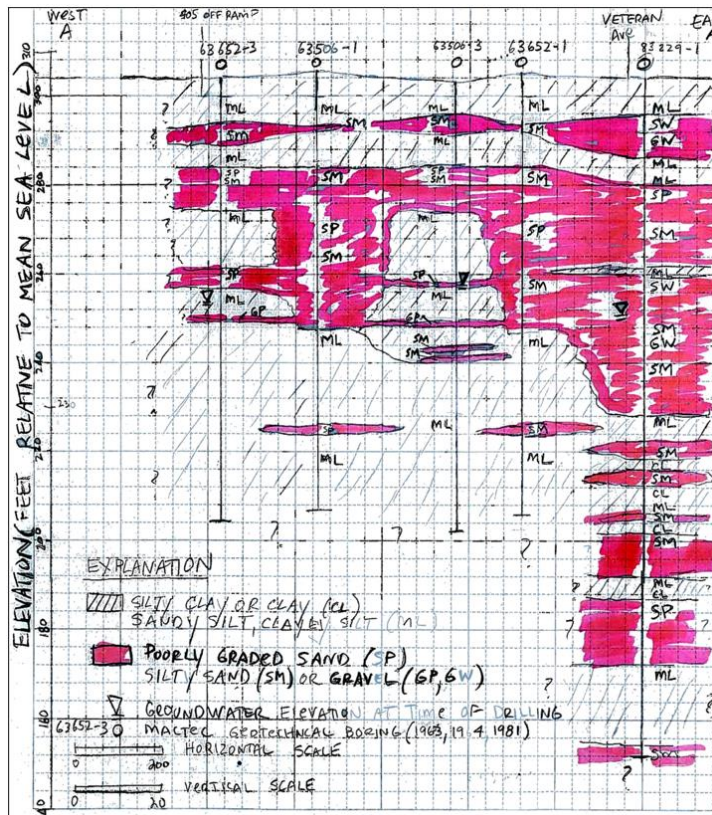
Notoriously difficult to characterize are aquifers developed in deposits left by meandering and braided streams, and in alluvial fans and deltas. Such deposits exhibit significant vertical and horizontal changes in sediment type and should therefore be represented by "anything" other than extensive and continuous layers of sand, gravel, or clay. This is illustrated in Figure 6.9 which shows a draft cross-section prepared as part of the subsurface characterization at a site in the Los Angeles basin. Figure 6.10 includes spectacular satellite images of four "complicated" fluvial depositional environments from around the world.

Figure 6.9 Very preliminary draft sketch of a cross-section based on geotechnical borings. Relatively more permeable alluvial sediments are colored in red. Courtesy of Tony Marino.
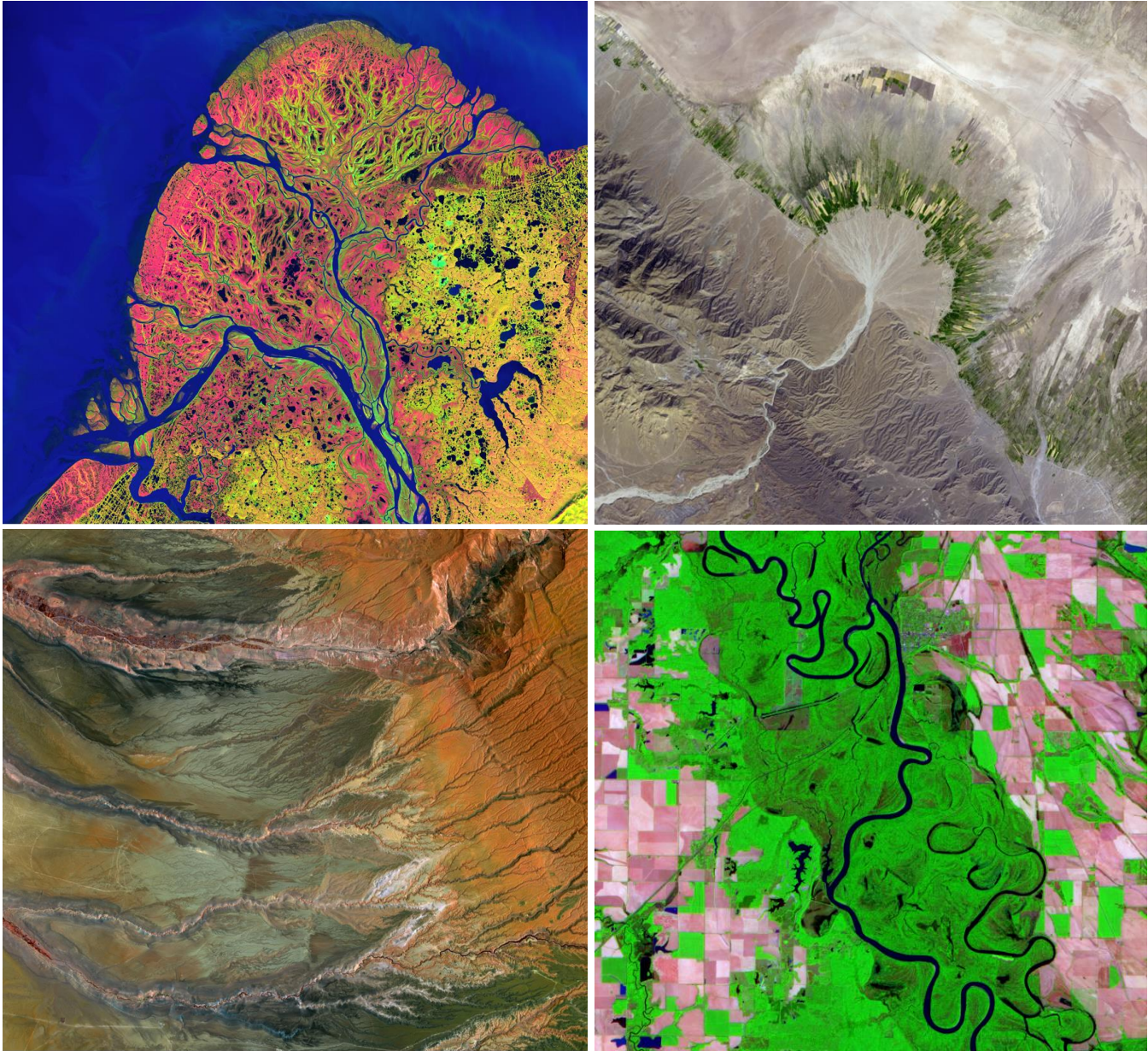
Figure 6.10 *Upper Left*: After beginning in northern British Columbia and flowing through Yukon in Canada, the Yukon River crosses Alaska, the United States, before emptying into the Bering Sea. Countless lakes, sloughs, and ponds are scattered throughout this scene of the Yukon Delta, one of the largest river deltas in the world. Landsat 7 falls color image available at https://eros.usgs.gov/image-gallery/earth-as-art-3. *Upper Right*: A broad belt of lush agricultural land in Fars province of Iran follows the curve of the alluvial fan and stretches out along a road that runs parallel to the ridgeline. The simulated natural color image was captured by the Advanced Spaceborne Thermal Emission and Reflection Radiometer (ASTER) on NASA's Terra satellite. NASA image created by Jesse Allen using data provided courtesy of NASA/GSFC/METI/ERSDAC/JAROS, and U.S./Japan ASTER Science Team; text by Rebecca Lindsey, https://earthobservatory.nasa.gov/. *Lower Left*: The jagged scars are extensive valleys carved by water flowing from the Andes Mountains in northern Chile. Landsat 8 false color image, https://eros.usgs.gov/image-gallery/earth-as-art-5. *Lower Right*: ASTER sensor on NASA's Terra satellite captured a false color image of the flood plain of White River in Arkansas. Image created by Jesse Allen, using data provided courtesy of NASA/GSFC/METI/ERSDAC/JAROS, and U.S./Japan ASTER Science Team; text by Holli Riebeek. In public domain.

6.2.2 Basin Fill Aquifers

Basin-fill aquifers consist of sand and gravel deposits that partly fill depressions which were formed by faulting or erosion or both (Figure 6.11.) Fine-grained deposits of silt and clay, where interbedded with sand and gravel, form confining units that retard the movement of groundwater, particularly in deeper portions. In basins that contain thick sequences of deposits, the sediments become increasingly more compacted and less permeable with depth. The basins are generally bounded by low-permeability igneous, metamorphic, or sedimentary rocks. The sediments that comprise the basin-fill aquifers mostly are alluvial deposits eroded by streams from the rocks in the mountains adjacent to the basins. They may locally include windblown sand, coarse-grained glacial outwash, and fluvial sediments deposited by streams that flow through the basins. Coarser sediment (boulders, gravel, and sand) is deposited near the basin margins and finer sediment (silt and clay) is deposited in the central parts of the basins. Some basins contain lakes or playas (dry lakes) at or near their centers. Windblown sand might be present as local beach or dune deposits along the shores of the lakes. Deposits from mountain glaciers locally form permeable beds where the deposits consist of outwash transported by glacial meltwater. Fluvial sands and gravel are common in and adjacent to the channels of through-flowing streams. Basins in arid regions might contain deposits of salt, anhydrite, gypsum, or borate produced by evaporation of mineralized water, in their central parts (Miller, 1999).
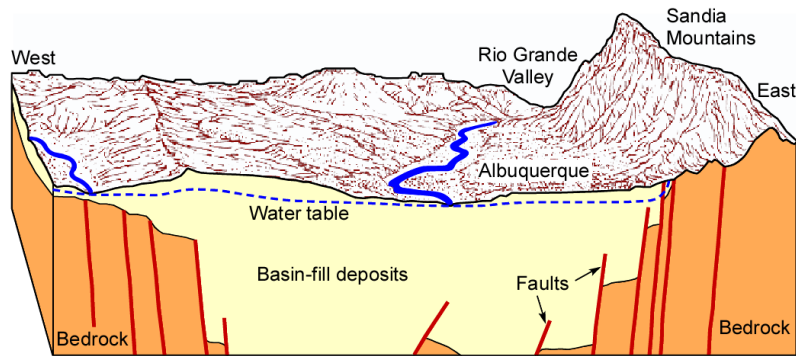
Figure 6.11 Schematic block-diagram of the basin-fill aquifer utilized for water supply of the city of Albuquerque, New Mexico. Modified from Robson and Banta, 1995. USGS, in public domain.

Recharge to basin-fill aquifers is primarily by infiltration of streamflow that originates as precipitation which falls on the mountainous areas that surround the basins (Figure 6.12.) This recharge, called mountain-front recharge, is mostly intermittent because the streamflow that enters the valleys is also mostly intermittent. As the streams exit their bedrock channels and flow across the surface of the alluvial fans, the streamflow infiltrates the permeable deposits on the fans and moves downward to the water table. In basins which are in arid climates, much of the infiltrating water is lost by evaporation or as transpiration by riparian vegetation (plants on or near stream banks).

Open basins contain through-flowing streams and commonly are hydraulically connected to adjacent basins. Some recharge might enter an open basin as surface flow and underflow (groundwater that moves in the same direction as streamflow) from an upgradient basin, and recharge occurs as streamflow infiltration from the through flowing stream. Before development, water discharges from basin-fill aquifers largely by evapotranspiration within the basin but also as surface flow and underflow into downstream basins. After development, most discharge is through withdrawals from wells. During early groundwater development stages in the western United States many wells in such basins were artesian and high yielding. Illustrative examples are the Los Angeles basin with many prolific aquifers at different depths, and San Bernardino Valley in California (Figures 6.13 and 6.14.) These days are long gone in basins with urban development or intensive irrigation for agriculture, but flowing wells are for now "doing just fine" in undeveloped basins such as the one shown in Figure 6.15.
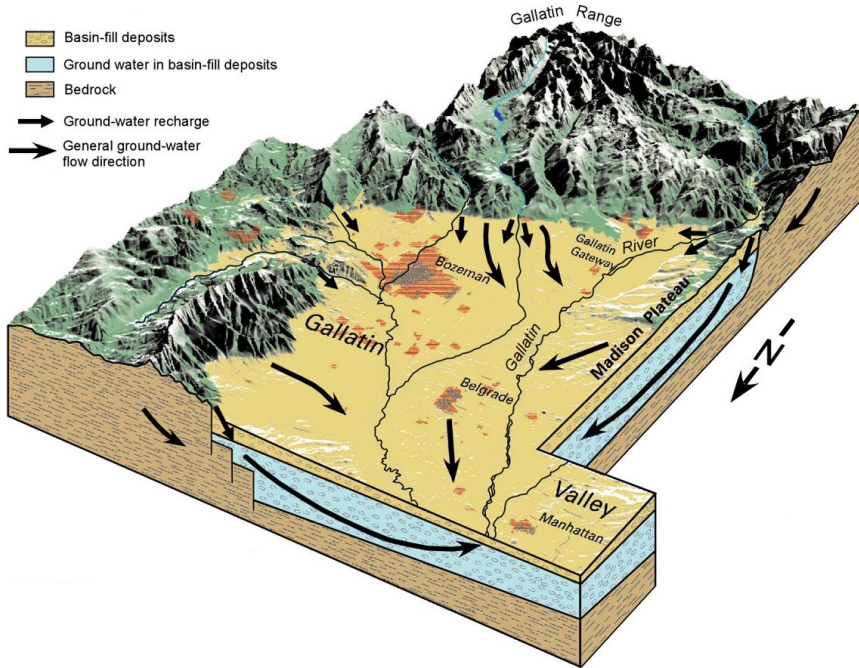
Figure 6.12 Perspective block diagram of the Gallatin Local Water Quality District, Montana, the United States. Modified from Taylor et al., 2001 and Kendy, 2001. USGS, in public domain.
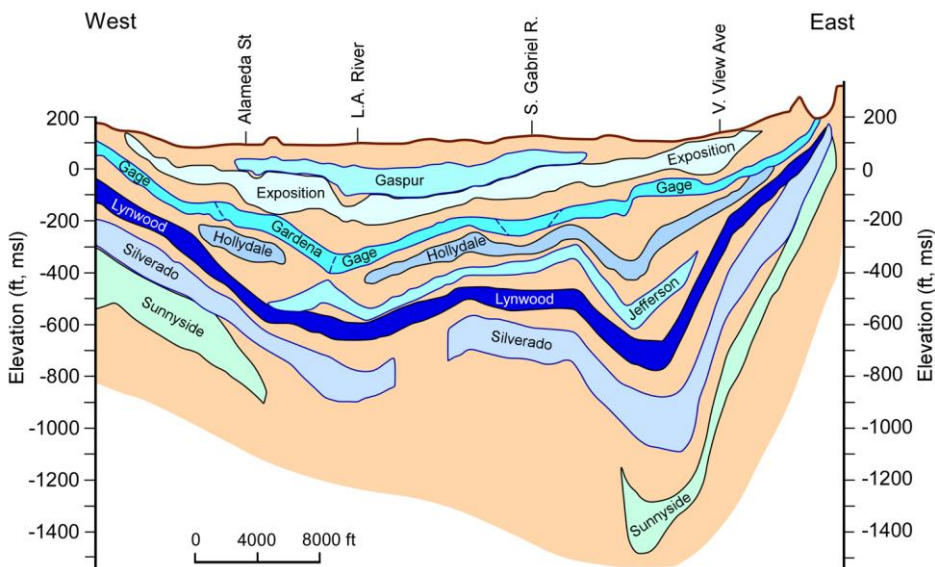
Figure 6.13 Generalized cross-section of Central Basin, Los Angeles, California, showing different aquifers in shades of blue; brown color indicates low-permeable aquitards in between. Modified from Santa Ana Watershed Project Authority, 2007; from Water Replenishment District of Southern California (WRD), 2004, modified from CADWR, 1962, Plate 4. In public domain.

Many basin-fill aquifers in southwestern alluvial basins, Great Basin (also known as Basin and Range physiographic province), basins in Southern California (Figure 6.16), and northern Rocky Mountain intermontane basins, are utilized for water supply and irrigation. Current groundwater extraction is usually from deeper, more protected portions of basins, although there are examples of unwanted effects of such extraction due to induced upconing (vertical upward migration) of highly mineralized saline groundwater. This water is residing at greater depths where there is no flushing by fresh meteoric water. Another negative effect of groundwater extraction from basin-fill aquifers in arid and semiarid climates is aquifer mining because of the lack of significant present-day natural aquifer recharge (Figure 6.17.)

Figure 6.14 *Left*: Flowing well on Antil Tract, San Bernardino Valley, San Bernardino County, California, 1905. Courtesy USGS Photographic Library, 2007. *Right*: Flowing well at Artesian Avenue in the San Bernardino Valley, in 1883. The valley surpassed every other valley in Southern California in the abundance of water. Artesian wells varied in depth from 60 to 410 feet, averaging 160 feet, and from two to eight inches in diameter. They were confined at that time to an area not exceeding four square miles in and around San Bernardino, but it was estimated that they were delivering 25 cubic feet of water per second, or over 16 million gallons per day, every day. Courtesy of City of San Bernardino, California. https://www.sbcity.org/about/history/streets_n_places/artesian_avenue.asp

Figure 6.15 Flowing artesian water well at the Bonham Ranch, southern Smoke Creek Desert, Nevada, 1994.
Photo courtesy of Terri Garside.
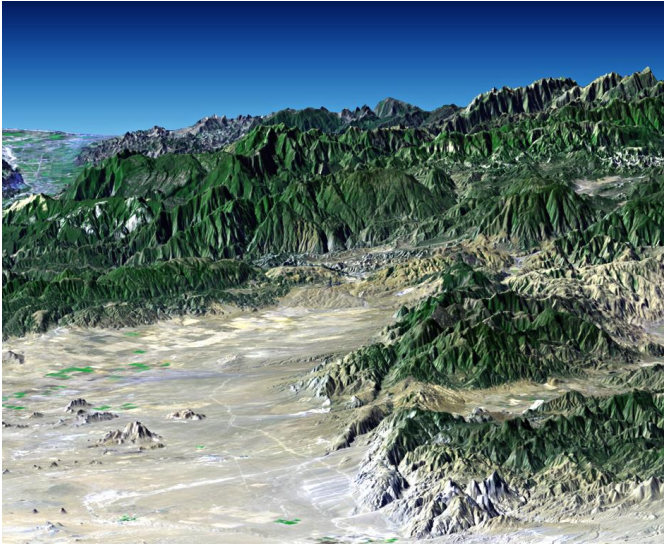
Figure 6.16 Image of Southern California, from the desert at Mojave to the ocean at Ventura (distant upper left); Tehachapi Mountains are in the right foreground. The elevation data used in this image was acquired by the Shuttle Radar Topography Mission (SRTM) aboard the Space Shuttle Endeavour and designed to collect three-dimensional measurements of the Earth's surface. The image is combination of the SRTM topography map and Landsat bands 1, 2 & 4. View width is 27 miles (43 kilometers), vertical exaggeration 3X. (Courtesy of NASA, 2022). In public domain.
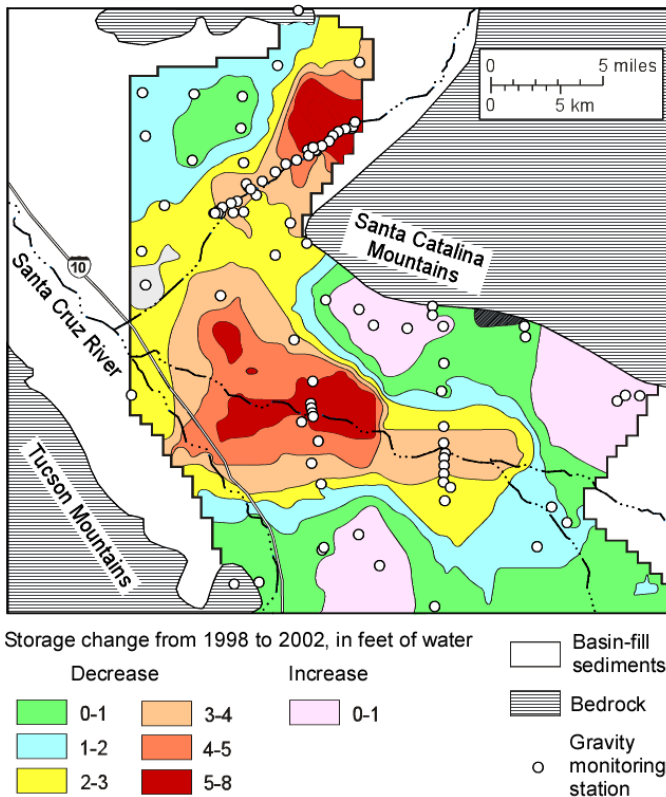
Figure 6.17 Example of groundwater storage change in part of the Tucson Basin, Arizona, the United States, determined by microgravity measurements. From Anderson and Woosley, 2005; source: Don Pool, USGS, written communication, 2003. USGS, in public domain.

As discussed by Kresic and Mikszewski (2013), in basins that contain thick sequences of deposits, the sediments become increasingly more compacted (consolidated), cemented, and less permeable with depth. Depending on the local ongoing sedimentary mechanisms, some basins may contain semi-consolidated sediments close to the land surface and may even exhibit some characteristics of fractured aquifers with well-defined fractures and fracture and fault zones. It is therefore important for a hydrogeologist developing a CSM not to rely solely on basin sediments description obtained from well drillers which are often re-circulated in various "official" reports by others. This is illustrated in Figure 6.18 which shows rock core samples collected from two different borings

completed in basin deposits previously generally described as "sand and gravel". It is experience of many professionals working in different hydrogeologic settings that well cuttings briefly described by water supply well drillers (often using rotary methods that break down consolidated or semi-consolidated material) are vastly different from the rock cores obtained during site-specific hydrogeologic characterizations. It is therefore puzzling that some professionals in the western United States still have hard time conceptualizing three-dimensional groundwater movement in the basins as something other than simple intergranular flow through "sand and gravel".

Figure 6.18 Rock core samples collected from a fault zone in aquifer developed in semi-consolidated Quaternary sediments near Phoenix Arizona (core diameter approximately 6 cm). Top left photo depicts conglomerate clasts vertically oriented along their long axis, likely a post depositional deformational feature. Top right photo illustrates potential groundwater circulation pathways through sediments partially cemented with calcium carbonate. Bottom photo depicts clear evidence of brittle deformation (faulting) with the observation of slikensides within the rock core. The cores are from borings completed in sediments routinely described as "sand and gravel" by water supply well drillers and in various published reports. Courtesy of Jeff Manuszak.

One important concept that often confounds the non-hydrogeologist is the impact of focused recharge on groundwater levels in portions of a basin that receive limited or no infiltration from directly overlying soils, such as sites with paved surfaces or very thick vadose zones (> 100 ft). For example, in semi-arid and arid groundwater basins in the American southwest, aerial recharge above a well is often negligible, yet over the course of the year, significant seasonal water level fluctuations may be seen in a well even in the absence of nearby groundwater pumping. The rise in potentiometric surface is often due to focused recharge via washes that become active during snowmelt events on the mountains surrounding a basin. This recharge creates pressure transients that propagate through the fractured portions of the aquifer faster than the theoretical rate of groundwater flow applicable to unconsolidated (loose) "sand and gravel". A well may experience a rapid rise in water level elevation in the spring when the wash is running despite being several miles away from the wash. In contrast, a linear transport of water over such distances, if interpreted as Darcian flow through intergranular porous media ("sand and gravel"), could take several or more years (Kresic and Mikszewski, 2013.)

6.2.3 Blanket Sand-and-Gravel Aquifers

Thick widespread sheet-like deposits that contain mostly sand and gravel form unconsolidated and semi-consolidated aquifers called blanket sand and gravel aquifers. They largely consist of alluvial deposits brought in from mountain ranges and deposited in lowlands. However, some of these aquifers, such as the High Plains aquifer in the United States (Ogallala aquifer), include large areas of windblown sand, whereas others, such as the surficial aquifer system of the southeastern U. S., contain some alluvial deposits but are largely comprised of beach and shallow marine sands (Miller, 1999). The High Plains aquifer extends over about 174,000 square miles in parts of eight states. The principal water-yielding geologic unit of the aquifer is the Ogallala Formation of Miocene age, a heterogeneous mixture of sand, gravel, silt, and clay that was deposited by a network of braided streams, which flowed eastward from the ancestral Rocky Mountains. Permeable dune sand is part of the aquifer in large areas of Nebraska and smaller areas in the other states. The Ogallala aquifer is principally unconfined and in direct hydraulic connection with the alluvial aquifers along the major rivers which flow over it.

The origin of water in the Ogallala aquifer is mainly from the last ice age, and the rate of present-day recharge is much lower. This has resulted in serious long-term water table decline in certain portions of the aquifer due to intensive groundwater extraction for water supply and irrigation (Figure 6.19.) Decreases in saturated thickness result in a decrease in well yields and an increase in pumping costs because the pumps must lift the water from greater depths – conditions occurring over much of the Ogallala aquifer. Despite this, the aquifer can still be described by the following quote: "The whole world depends on the Ogallala. Its pork ends up in Japanese and American supermarkets. Its beef goes everywhere…" (Opie, 2000, from McGuire et al., 2003).

Other major blanket sand and gravel aquifers in the United States include the Seymour aquifer of Texas which, like the High Plains aquifer, was deposited by braided, eastward flowing streams but has been dissected into separate pods by erosion; the Mississippi River Valley alluvial aquifer, which consists of sand and gravel deposited by the Mississippi River as it meandered over an extremely wide floodplain; and the Pecos River Basin alluvial aquifer, which is mostly stream-deposited sand and gravel, but locally contains dune sands (Miller, 1999).
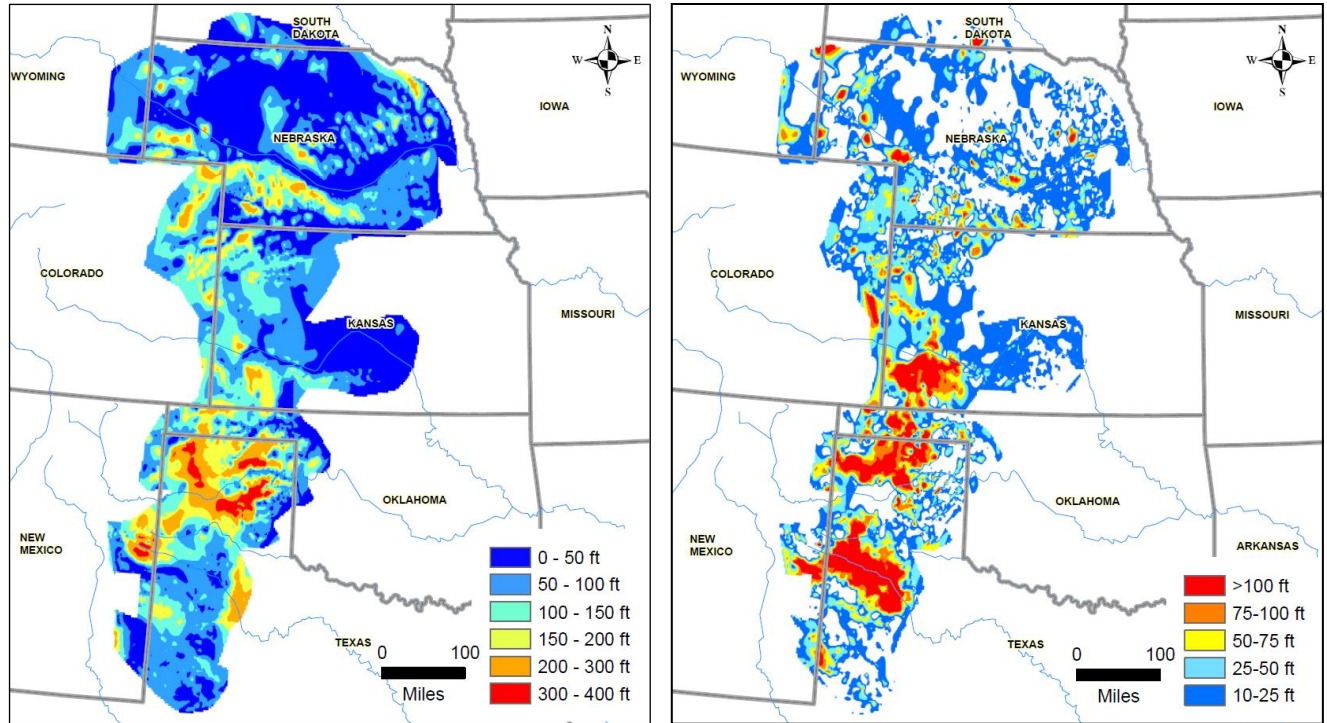
Figure 6.19 *Left*: Contour map of Ogallala Aquifer water table depth in feet below ground surface measured prior to groundwater development between the 1930s and 1980s (data from USGS, 2010). *Right*: Contour map of the drawdown in water table depth (feet) between pre-development and 2007 conditions. Both raster files created using raster math tools in ArcMap by ESRI, Inc. From Kresic and Mikszewski, 2013. Copyright CRC Francis & Taylor. Permission is required for further use.

6.2.4 Semiconsolidated Sand Aquifers

Sediments that primarily consist of semiconsolidated sand, silt, and clay, interbedded with some carbonate rocks, underlie the Coastal Plains that border the Atlantic Ocean and the Gulf of Mexico. The sediments extend from Long Island, New York, southwestward to the Rio Grande, and generally form a thick wedge of strata that dips and thickens seaward from a featheredge at its updip limit. Coastal Plain sediments are water-laid and were deposited during a series of transgressions and regressions of the sea. Depositional environments ranged from fluvial to deltaic to shallow marine, and the exact location of each environment depends upon the relative position of land masses, shorelines, and streams at a given point in geologic time. Complex interbedding and variations in lithology result from the constantly changing depositional environments. Some beds are thick and continuous for tens to hundreds of miles, whereas others are traceable only for short distances. Consequently, the position, shape, and number of the bodies of sand and gravel that form aquifers in these sediments vary greatly from place to place (Miller, 1999).

The semiconsolidated sand aquifers have been grouped into several major aquifer systems which interfinger with and grade into each other. The Northern Atlantic Coastal Plain aquifer system extends from North Carolina through Long Island, New York, and locally contains as many as 10 aquifers. Figures 6.20 and 6.21 show two generalized cross-sections of this system. The Mississippi Embayment aquifer system consists of six aquifers, five of which are equivalent to aquifers in the Texas coastal uplands aquifer system to the west. The coastal lowlands aquifer system extends from Rio Grande River in Texas across southern and central Louisiana, southern

Mississippi, southern Alabama, and the western part of the Florida panhandle. It contains five thick, extensive permeable zones, and has been used extensively for water supply throughout the region. Its heavy pumping in the Houston metropolitan area caused one of better-known cases of major land subsidence in the United States.
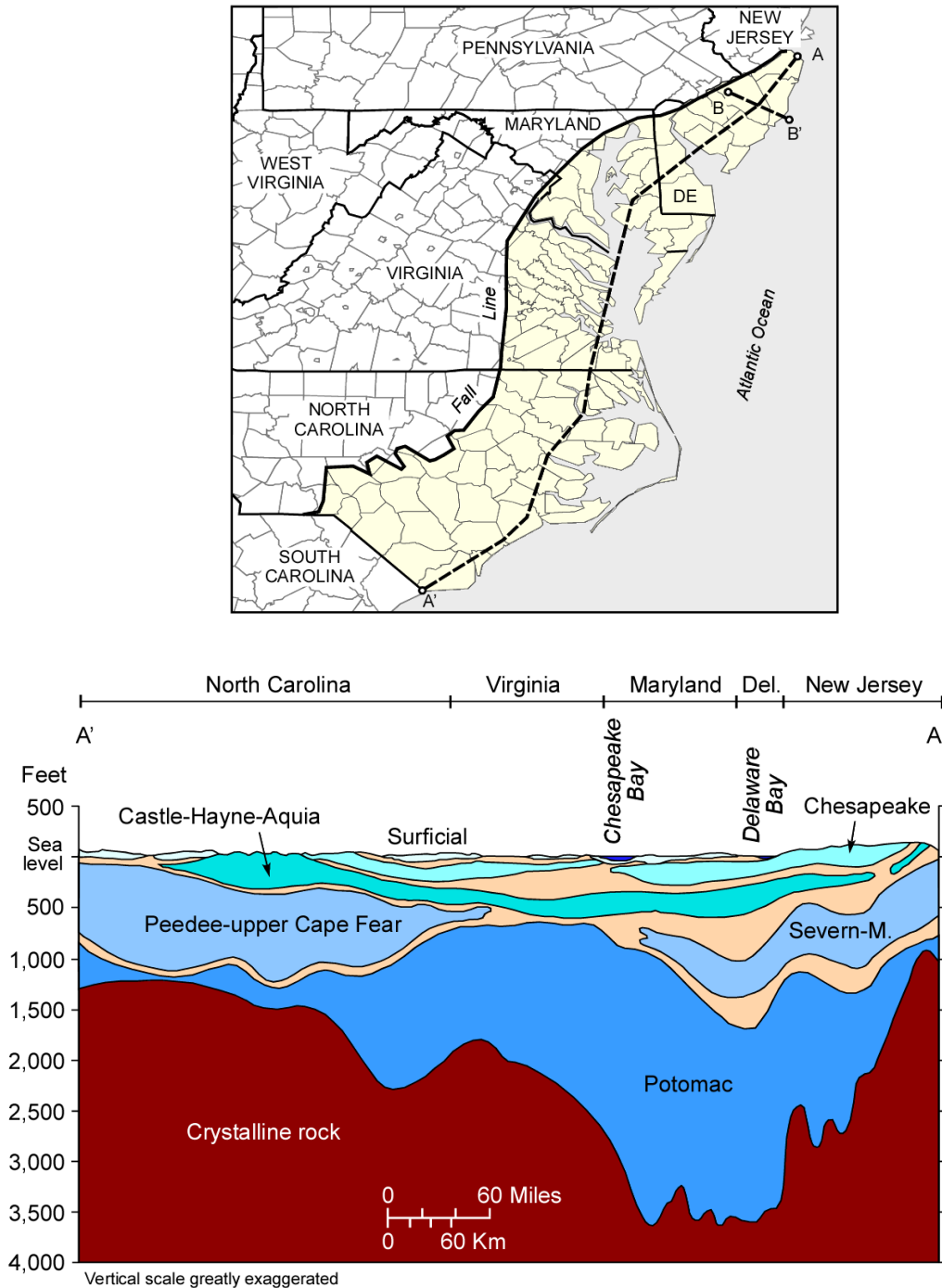
Figure 6.20 Hydrogeologic cross-section AA' showing principal aquifers (shades of blue) in the North Atlantic Coastal Plain aquifer system (Severn-M. is Severn-Magothy aquifer); the line of cross section is shown on the map at the top. Aquitards are shown in beige color. Modified from Trapp, 1992. USGS, in public domain.
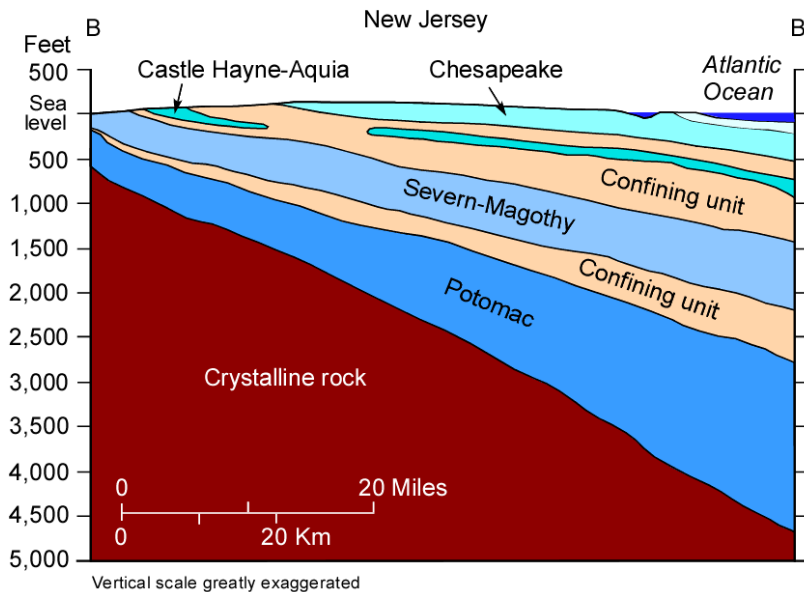
Figure 6.21 Hydrogeologic cross-section BB' showing principal aquifers in the North Atlantic Coastal Plain aquifer system. The line of cross section is shown in Figure 6.20. Modified from Trapp, 1992. USGS, in public domain.

The Southeastern Coastal Plain aquifer system consists of predominantly clastic sediments that crop out or are buried at shallow depths in large parts of Mississippi and Alabama, and in smaller areas of Georgia and South Carolina. Toward the coast, the aquifer system is covered either by shallower aquifers or confining units. Some of the aquifers and confining units of the Southeastern Coastal Plain aquifer system grade laterally into adjacent clastic aquifer systems in North Carolina, Tennessee, and Mississippi and adjacent States to the west; some also grade vertically and laterally southeastward into carbonate rocks of the Floridan aquifer system. Within each aquifer system, the numerous local aquifers have been grouped into regional aquifers that are separated by regional confining units consisting primarily of silt and clay, but locally are beds of shale or chalk. The rocks that comprise these aquifer systems are of Cretaceous and Tertiary age. In general, the older rocks crop out farthest inland, and successively younger rocks are exposed coastward (Miller, 1999).

Coastal plains aquifers have enabled continuing urban growth and development of the Atlantic and Gulf coasts for decades. However, they have been over-exploited in many locations, and are at a continuously increasing risk of saltwater encroachment in coastal areas with heavy pumping.

6.2.5 Glacial Deposit Aquifers

Glacial deposit aquifers are prime examples of heterogeneous aquifers of varying scale and interconnectivity. The distribution of the numerous sand and gravel beds that make up the glacial deposit aquifers and the clay and silt confining units that are interbedded with them is extremely complex. The glacial deposit aquifers either are localized in bedrock valleys or are in sheet-like deposits on outwash plains. The latter ones can be extensive, as in the coalescing gravel outwash plains of North America, the eastern Andes and the Himalayas-Pamir-Tienshan cordilleras, or quite narrow and sinuous, as in the glacial channels of the North German Plain and the Great Lakes in the United States (Morris et al., 2003).

Large areas of the north-central and northeastern United States are covered with sediments that were deposited during several advances and retreats of continental glaciers. The massive ice sheets planed off and incorporated soil and rock fragments during advances and redistributed these materials as ice-contact or meltwater deposits or both during retreats. Thick sequences of glacial materials were deposited in former river valleys cut into bedrock

whereas thinner sequences were deposited on the hills between the valleys. Figure 6.22 illustrates typical sediment types associated with river valley glacial deposits that are still being formed in glaciated terrains worldwide (Figure 6.23). Some of these deposits are formed at the ice-bedrock contact, and some fill cracks or crevasses in the ice. As the ice melts, outwash deposits of sand and gravel form deltas at the ice front or in glacial lakes and fluvial valley-train deposits downstream from the ice front.
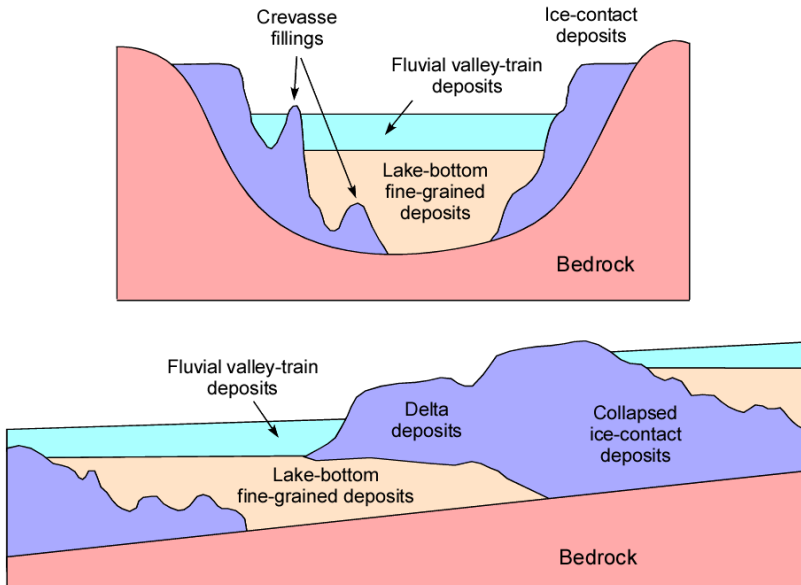
Figure 6.22 Coarse-grained glacial deposits are commonly found in bedrock valleys. Some of these deposits formed at the ice-bedrock contact, and some filled cracks or crevasses in the ice. As the ice melted, outwash deposits of sand and gravel formed deltas at the ice front or in glacial lakes and fluvial valley-train deposits downstream from the ice front. *Top*: Typical perpendicular cross-section. *Bottom*: Longitudinal cross-section. From Trapp and Horn, 1997, modified from Lyford, 1986. USGS, in public domain.

Figure 6.23 Glaciated terrain in Alaska with bedrock valleys filled with glacial deposits.
Photo courtesy of Jeff Manuszak.

The glacial ice and meltwater derived from the ice deposit several types of sediments, which are collectively called glacial drift. Till, which consists of dense unsorted and unstratified material that ranges in size from boulders to clay, is deposited directly by the ice (Figure 6.24). Outwash, which is mostly stratified sand and gravel (Figure 6.25), and glacial-lake deposits consisting mostly of clay, silt, and fine sand, are deposited by meltwater. Ice-contact deposits consisting of local bodies of sand and gravel are deposited at the face of the ice sheet or in cracks in the ice.

Figure 6.24 Glacial till of the Harbor Hill terminal moraine (Wisconsin interglacial period) exposed on Long Island Motor Parkway, 1/2 mile north of Creedmoor. Hempstead quadrangle. Queens County, New York. October 29, 1917. Courtesy USGS Photographic Library, 2007.

Figure 6.25 Stratified glacial sand and gravel, one mile north of Asticou, northeast of Lower Hadley Pond. Acadia National Park, Maine, Sep 14, 1907. USGS Photographic Library, 2007.

The glacial sand and gravel deposits form numerous local but highly productive aquifers. Yields of wells completed in aquifers formed by continental glaciers are as much as 3,000 gallons per minute (1,000 gpm equals 63 l/s) where the aquifers consist of thick sand and gravel. Locally, yields of 5,000 gallons per minute have been obtained from wells completed in glacial-deposit aquifers that are located adjacent to rivers and can obtain recharge from surface water (Figure 6.26). Aquifers that were formed by mountain glaciers yield as much as 3,500 gallons per minute in Idaho and Montana, and wells completed in mountain-glacier deposits in the Puget Sound, Washington area yield as much as 10,000 gallons per minute (Miller, 1999).

131

Figure 6.26 Development of a high yielding well in Michigan, completed in glacial sand and gravel.
Photo courtesy of Jim Brode.

Lecture 7 Aquifers and Aquitards, Part Two

This lecture is based primarily on the materials presented in Kresic, 2007 (*Hydrogeology and Groundwater Modeling, Second Edition*. Copyright CRC Taylor & Francis); Kresic, 2009 (*Groundwater Resources: Sustainability, Management, and Restoration.* Copyright McGraw Hill); Kresic, 2013 (Water in Karst: Management, Vulnerability, and Restoration. Copyright McGraw Hill); Kresic and Mikszewski, 2013 (*Hydrogeological Conceptual Site Models: Data Analysis and Visualization*. Copyright CRC Taylor & Francis); and various publications by the authors of USGS.

7.1 Sandstone Aquifers

Sandstone aquifers in the United States are more widespread than those in all other types of consolidated rocks. Although generally less permeable, and usually with a lower natural recharge rate than surficial unconsolidated sand and gravel aquifers, sandstone aquifers in large sedimentary basins are one of the most important sources of water supply both in the United States and worldwide. Loosely cemented sandstone retains significant primary (intergranular) porosity, whereas secondary fracture porosity may be more important for well-cemented and older sandstone. Regardless of the degree of fracturing, storage capacity of such deposits is high because of the thickness of major sandstone basins. Large sandstone aquifers that are exposed adjacent to domes and uplifts or that extend into large structural basins, or both are the Colorado Plateau aquifers (Figures 7.1), the Denver Basin aquifer system, Upper and Lower Cretaceous aquifers in North and South Dakota, Wyoming and Montana, the Wyoming Tertiary aquifers, the Mississippian aquifer of Michigan, and the New York sandstone aquifers (Miller, 1999).
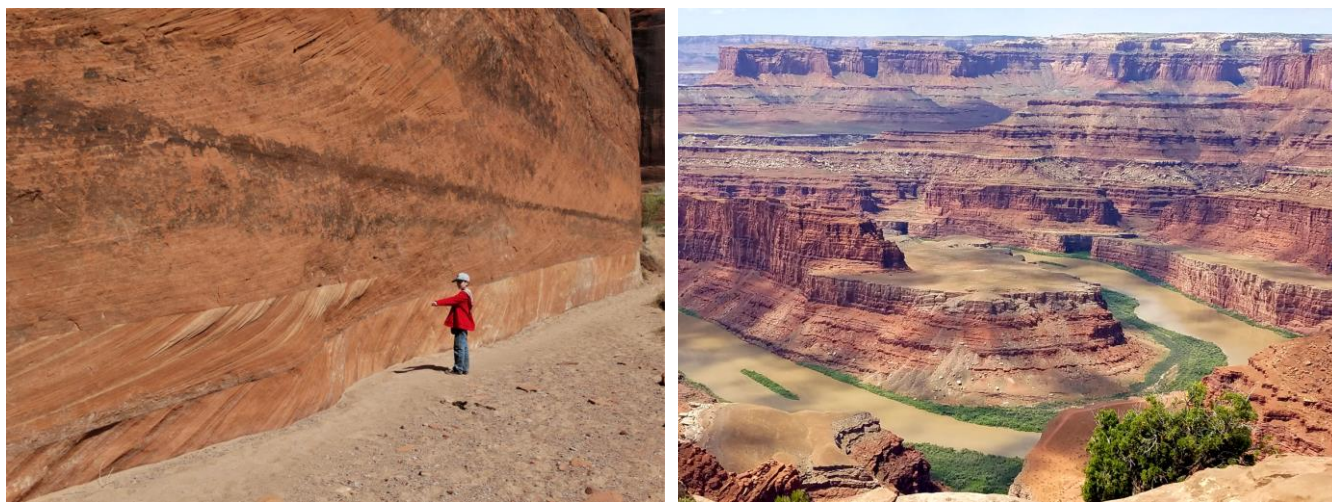
Figure 7.1 *Left*: Tangential cross stratification of the massive, unfractured, aeolian Lower Permian De Chelly Sandstone in Canyon de Chelly National Monument, located within the Navajo Reservation in the northeastern Arizona region of the Colorado Plateau. *Right*: Sedimentary sequence at Dead Horse Point State Park in Southern Utah, exposed in the Colorado River canyon. It is composed of mostly sandstones which form steep cliffs (Jurassic Kayenta formation is at the top), and mudstone, shale and siltstone which form ledges and slopes. Photo courtesy of USGS; in public domain.

The Cambrian-Ordovician aquifer system in the north-central United States is composed of large-scale, predominantly sandstone aquifers that extend over parts of seven States. The aquifer system consists of layered

rocks that are deeply buried where they dip into large structural basins. It is a classic confined, or artesian, system and contains three aquifers. In descending order, these are the St. Peter-Prairie du Chien-Jordan aquifer (sandstone with some dolomite), the Ironton-Galesville aquifer (sandstone), and the Mount Simon aquifer (sandstone). Confining units of poorly permeable sandstone and dolomite separate the aquifers. Low-permeability shale and dolomite compose the Maquoketa confining unit that overlies the uppermost aquifer and is considered to be part of the aquifer system. Wells that penetrate the Cambrian-Ordovician aquifer system commonly are open to all three aquifers, which are collectively called the sandstone aquifer in many reports. The rocks of the aquifer system are exposed in large areas of northern Wisconsin and eastern Minnesota. Regionally, groundwater in the system flows from these topographically high recharge areas eastward and southeastward toward the Michigan and Illinois Basins. Sub-regionally, groundwater flows toward major streams, such as the Mississippi and the Wisconsin Rivers, and toward major withdrawal centers, such as those at Chicago, Illinois, and Green Bay and Milwaukee, Wisconsin. One of the most dramatic effects of groundwater withdrawals known in the United States is shown in Figure 7.2. Withdrawals from the Cambrian-Ordovician aquifer system, primarily for industrial use in Milwaukee, Wisconsin, and Chicago, Illinois, caused declines in water levels of more than 375 feet in Milwaukee and more than 800 feet in Chicago from 1864 to 1980, with the pumping influence extending over 70 miles. Beginning in the early 1980s, withdrawals from the aquifer system decreased as some users, including the city of Chicago, switched to Lake Michigan as a source of supply. Water levels in the aquifer system began to rise in 1985 because of decreased withdrawals (Miller, 1999).
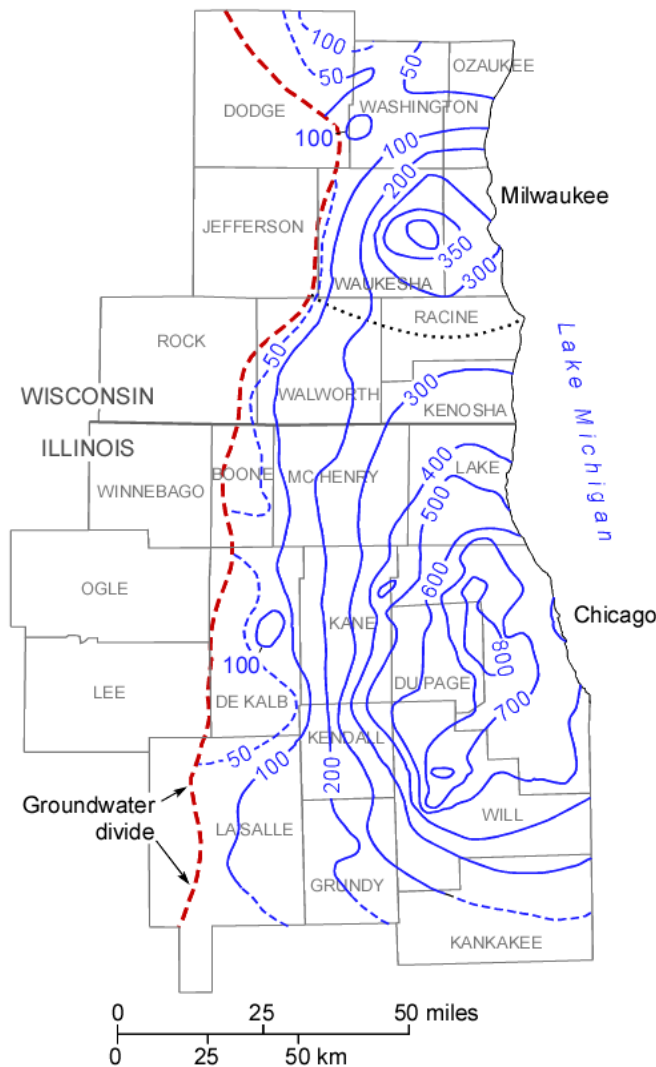
Figure 7.2. Decline of water levels in the Cambrian–Ordovician aquifer system from 1864 to 1980, as a result of large groundwater withdrawals centered at Chicago and Milwaukee. Drawdown contour lines are in feet; dashed where approximately located. Modified from Miller, 1999, and Young, 1992. USGS, in public domain.

The chemical quality of the water in large parts of the aquifer system is suitable for most uses. The water is not highly mineralized in areas where the aquifers crop out or are buried to shallow depths, but mineralization generally increases as the water moves downgradient toward the structural basins. The deeply buried parts of the aquifer system contain saline water.

Examples of continental-scale sandstone aquifers include the Guaraní aquifer system in South America, the Nubian Sandstone Aquifer System in Africa, and the Great Artesian Basin in Australia. The Guaraní Aquifer System (also called Botucatu aquifer) includes areas of Brazil, Uruguay, Paraguay, and Argentina. Water of very good quality is exploited for urban supply, industry, irrigation and for thermal, mineral and tourist purposes. This aquifer is one of the most important fresh groundwater reservoirs in the world, due to its vast extension (about 1,200,000 km^2), and volume (about 40,000 km^3). The aquifer storage volume could supply a total population of 5.5 billion people for 200 years at a rate of 100 liters per day per person (Puri et al., 2001). The gigantic aquifer is in the Paraná and Chaco-Paraná Basins of southern South America. It is developed in consolidated aeolian and fluvial sands (now sandstones) from the Triassic-Jurassic, usually covered by thick basalt flows (Serra Geral Formation) from the Cretaceous, which provide a high confinement degree. Its thickness ranges from a few meters to 800 m. The specific capacities of wells vary from 4 m^3/h per meter of drawdown to more than 30 m^3/h/m. (Rebouças and Mente, 2004).

The rocks of the Nubian Sandstone Aquifer System in northern Africa (NSAS; Figure 7.3), which is shared by Egypt, Libya, Sudan, and Chad, vary in thickness from zero in outcrop areas to more than 3,000 meters in the central part of the Kufra and Dakhla Basins, and range in age from Cambrian to Neogene. The main productive aquifers, separated by regional confining units, are (from land surface down) Miocene sandstone, Mesozoic (Nubian) sandstone, Upper Paleozoic-Mesozoic sandstone, and Lower Paleozoic (Cambrian-Ordovician) sandstone (Salem and Pallas, 2001). In some locations, the confined portions of the system provided water to high-yielding artesian wells such as the one shown in Figure 7.4. The groundwater of the Nubian Basin is generally of high quality. The total dissolved solids (TDS) range from 100 to 1,000 parts per million, with an increased salinity northward toward the Mediterranean Sea where the freshwater–saline water interface passes through the Qattara depression in Egypt. In Libya, the TDS of the deep Nubian aquifers ranges from 160 to 480 mg/l, and from 1,000 to 4,000 mg/l in the shallow aquifers (Khouri, 2004).

Figure 7.3. Nubian Sandstone Aquifer System (NSAS) in North Africa. Modified from Bakhbakhi, 2006. UNESCO, in public domain

The rocks of the Nubian Sandstone Aquifer System in northern Africa (NSAS; Figure 7.3), which is shared by Egypt, Libya, Sudan, and Chad, vary in thickness from zero in outcrop areas to more than 3,000 meters in the central part of the Kufra and Dakhla Basins, and range in age from Cambrian to Neogene. The main productive aquifers, separated by regional confining units, are (from land surface down) Miocene sandstone, Mesozoic (Nubian) sandstone, Upper Paleozoic-Mesozoic sandstone, and Lower Paleozoic (Cambrian-Ordovician) sandstone (Salem and Pallas, 2001). In some locations, the confined portions of the system provided water to high-yielding artesian wells such as the one shown in Figure 7.4. The groundwater of the Nubian Basin is generally of high quality. The total dissolved solids (TDS) range from 100 to 1,000 parts per million, with an increased salinity northward toward the Mediterranean Sea where the freshwater–saline water interface passes through the Qattara depression in Egypt. In Libya, the TDS of the deep Nubian aquifers ranges from 160 to 480 mg/l, and from 1,000 to 4,000 mg/l in the shallow aquifers (Khouri, 2004).

Because of the semi-arid to arid climate, the present-day natural recharge of the NSAS is negligible and countries in the region have formed a joint commission for assessment and management of this crucial, non-renewable source of water supply.

The Great Artesian Basin (GAB) in Australia covers more than 1.7 million square kilometers and is one of the largest groundwater basins in the world. It underlies parts of Queensland, New South Wales, South Australia, and the Northern Territory. The basin is up to 3,000 m thick and contains a multi-layered confined aquifer system, with the main aquifers occurring in Mesozoic sandstones interbedded with mudstone. The GAB contains a vast volume of groundwater (estimated at 64,900 million megaliters) and it is a vital resource for pastoral, agricultural and extractive industries as well as for many towns' water supplies, supporting at least $12.8 billion in economic activity annually (Frontier Economics 2016). The GAB also supports significant Indigenous cultural values and sustains a range of groundwater-dependent ecosystems (GDEs), including iconic mound springs across central Australia (Ransley et al., 2015; Geoscience Australia, 2022.)

Figure 7.4   Flowing well at Kharga Oasis, Egypt, 1961. Published in U.S. Geological Survey Water Supply Paper 1757-O. USGS, in public domain.

Groundwater in the GAB has been exploited from flowing wells since artesian water was discovered in 1878, allowing an important pastoral industry to be established. Wells are up to 2,000 m deep, but average about 500 m. Artesian flows from individual wells exceed 10 million liters per day (more than 100 L/s), but the majority have much smaller flows. The accumulated discharge of these wells (including water supply wells in about 70 towns, as

in most cases the artesian groundwater supply is the only source of water) is about 1,200 million L/day, compared to the maximum flow rate of about 2,000 million L/day from about 1,500 flowing artesian wells around 1918. Non flowing artesian wells, which number about 20,000, are generally shallow – several tens to hundreds of meters deep. It is estimated that these generally windmill operated pumped wells supply on average 0.01 million L/day per well and produce a total of about 300 million L/day. High initial flow rates and pressures of artesian wells have diminished because of the release of water from elastic storage in the groundwater reservoir. Exploitation of the aquifers has caused significant changes in the rate of natural aquifer discharge. Spring yields have declined because of well development in many parts of the Basin, and in some areas, springs have ceased to flow (Habermehl, 2006).

7.2 Fractured Bedrock Aquifers

This category includes aquifers developed in metamorphic and igneous crystalline rocks. Examples in the United States include the crystalline rocks of the Blue Ridge and Piedmont regions of the eastern United States (Figure 7.5), northern Minnesota, and northeastern Wisconsin. Metamorphic and igneous crystalline rocks underlie most of the Blue Ridge and Piedmont and range in composition from felsic to ultramafic and range in age from Middle Proterozoic for granitic rocks in the Blue Ridge to Triassic-Jurassic for the unmetamorphosed dikes and sills of mafic composition that intrude older Piedmont rocks. Rocks that crop out in the Piedmont underlie parts of the Atlantic Coastal Plain at depth (Daniel and Dahlen, 2002).
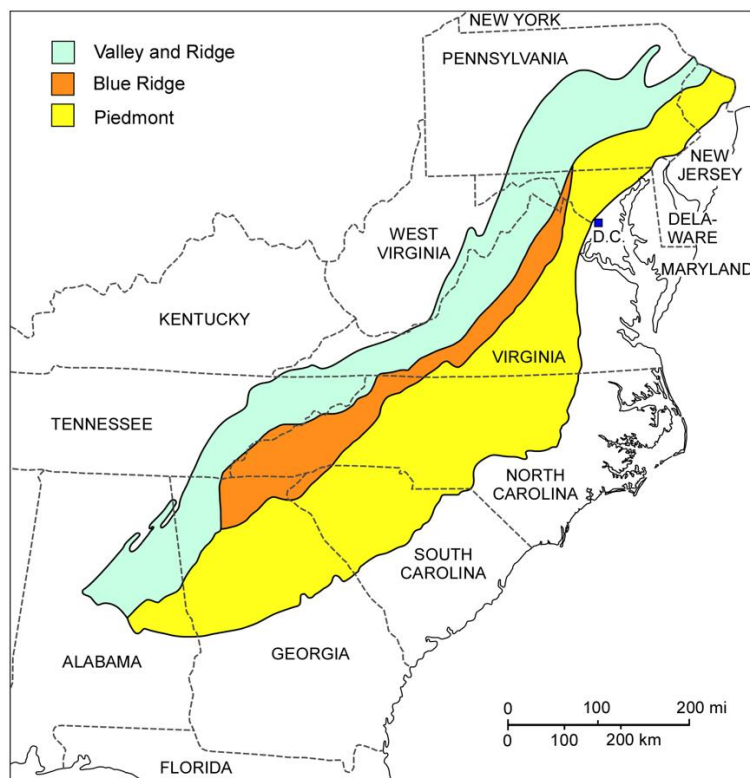
Figure 7.5 Crystalline metamorphic and magmatic rocks (fractured rock aquifer type) are predominant in the Piedmont and Blue Ridge provinces, whereas carbonate rocks and sandstone are predominant in the Valley and Ridge province where there are fully developed karst aquifers in limestone and dolomite. Modified from Daniel et al., 1997. USGS, in public domain.

One important aspect of fractured bedrock aquifers is that natural directions of groundwater flow can be related to surface topography. Just like surface water, groundwater flows from a higher hydraulic head toward a lower hydraulic head, i.e., from pronounced topographic highs (hills) to pronounced topographic lows (valleys) respectively. The concept is shown on Figure 7.6, which is very similar to an example from a guidance manual on

developing conceptual hydrogeological models for fractured rock aquifers in the Piedmont and Mountain Region of North Carolina, the United States (Figure 7.7). This manual of the North Carolina Department of Environment and Natural Resources explains, in detail, the importance of topography for determining groundwater recharge and discharge zones, and flow directions.

Figure 7.7 shows that the path of natural groundwater movement is relatively short and almost invariably restricted to the zone underlying the topographic slope extending from a topographic divide to an adjacent stream. Thus, the concept of a local slope-aquifer system applies. On the opposite sides of an inter-stream topographic divide are two similar slope-aquifer systems, as shown by (A) and (B). Two similar slope-aquifer systems occur on the opposite sides of a drainage basin (B) and (C). The region as a whole is a network of slope-aquifers where an individual aquifer represents a unit of the groundwater flow regime that is seemingly separated and free of impact from adjacent, similar units. Commonly, the slope-aquifer system includes smaller hill-and-dale configurations that are observed as topographic "spurs" (ridges branching from a main ridge or mountain crest). Similar undulations, although of lesser amplitude, may also occur in the underlying water table and form important natural groundwater flow-control features. The crests of the water table undulations represent natural groundwater divides within a slope-aquifer system and may limit the area of influence of wells or the extent of contaminant plumes located within their boundaries (LeGrand, 2007).
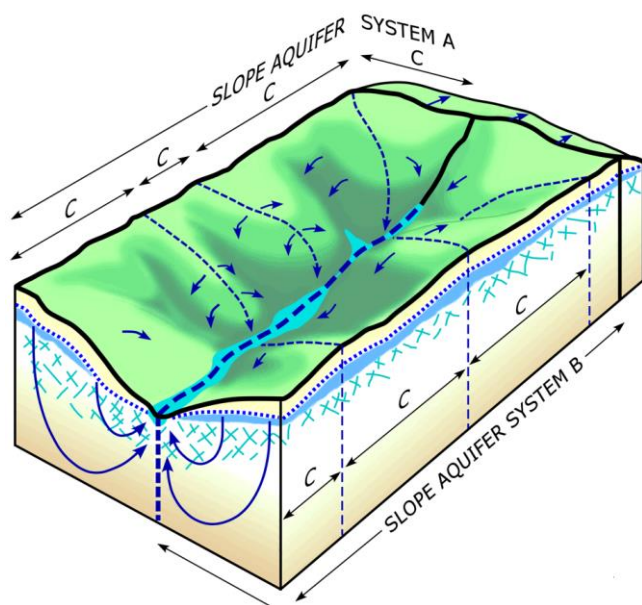
Figure 7.6 *Left*: Conceptual view of the North Carolina Blue Ridge and Piedmont groundwater flow system showing the unsaturated zone (lifted), the water table surface, the saturated zone, and directions of groundwater flow. Daniel and Dahlen, 2002; from Daniel, 1990. USGS, in public domain. *Right*: Rappahannock River incised into Piedmont metamorphic rocks near Warrenton, Virginia.

Because regolith has a much higher storage capacity than bedrock, the regolith can be thought of as a groundwater reservoir or "sponge" that feeds the underlying bedrock discontinuities. Joint concentrations, fractures enhanced by dissolution, and other discontinuities in bedrock, and combinations of these features, also can store a substantial quantity of water. The storage capacity of the regolith/bedrock system is mainly influenced by differences in the weathering characteristics of various rock types. Thin saprolite is developed on more resistant, quartz-rich rock types, whereas thick saprolite is developed on less resistant rock types rich in potassium feldspar. The biotite gneiss unit is particularly susceptible to deep weathering and typically has a thick saprolite cover. Mafic

rocks (such as amphibolite) typically are characterized by thin saprolite cover because of the general lack of potassium feldspar. In compositionally layered rocks, saprolite may develop between layers of more competent rock. This weathering profile is common where less chemically resistant rock (such as biotite gneiss) is interlayered with more chemically resistant rock such as amphibolites (Williams et al., 2005).
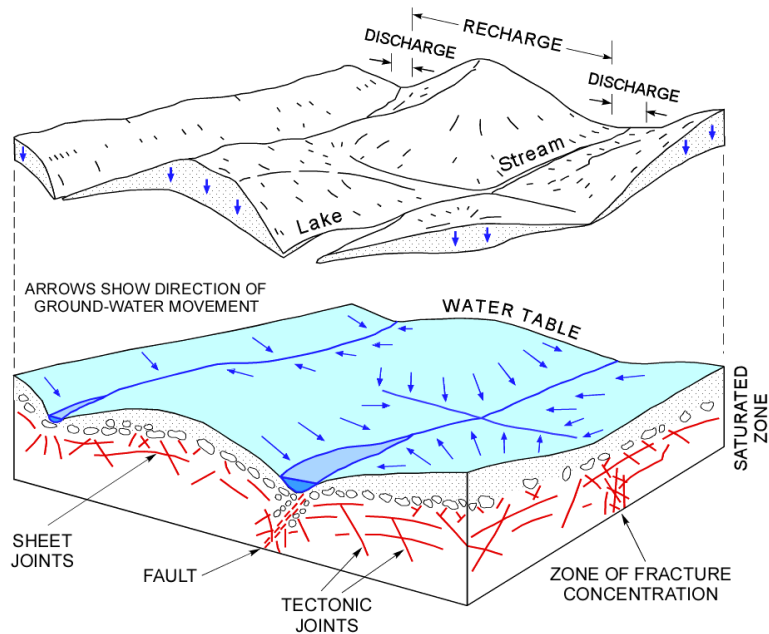
Figure 7.7 Conceptual view of double slope-aquifer systems and its compartments (C). All blue arrows indicate groundwater flow directions. Modified from LeGrand, 2007. North Carolina Department of Environment and Natural Resources; in public domain.
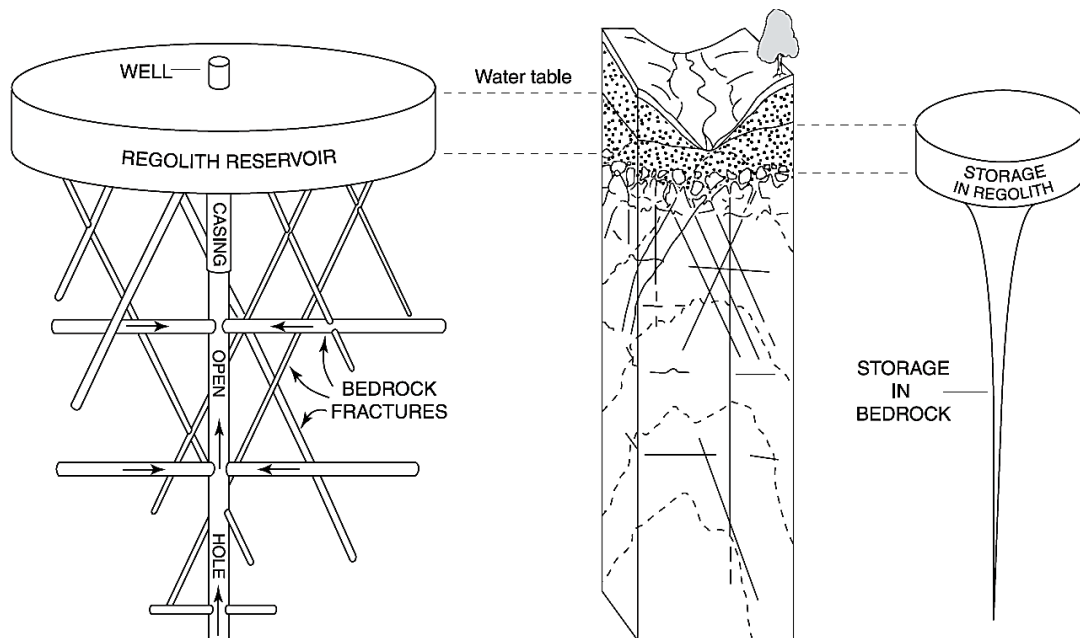
Figure 7.8 The reservoir-pipeline conceptual model of the Blue Ridge-Piedmont groundwater system and the relative volume of groundwater storage within the system. From Daniel and Dahlen, 2002. USGS, in public domain.

The bedrock, in which fractures typically decrease in number with increasing depth, can be generally considered as a zone of low permeability. In general, however, understanding the hydrogeology of crystalline rocks is complicated because of complex structure and porosity that is almost exclusively secondary. As a result, the hydraulic conductivity of fractured bedrock aquifers is extremely variable, and not easily defined for a particular geologic formation or even a particular rock type (Daniel and Dahlen, 2002). Consequently, the distinction between aquifers and confining units, which is the usual approach for describing the hydrogeologic framework of a CSM, is not applicable in fractured bedrock aquifers.
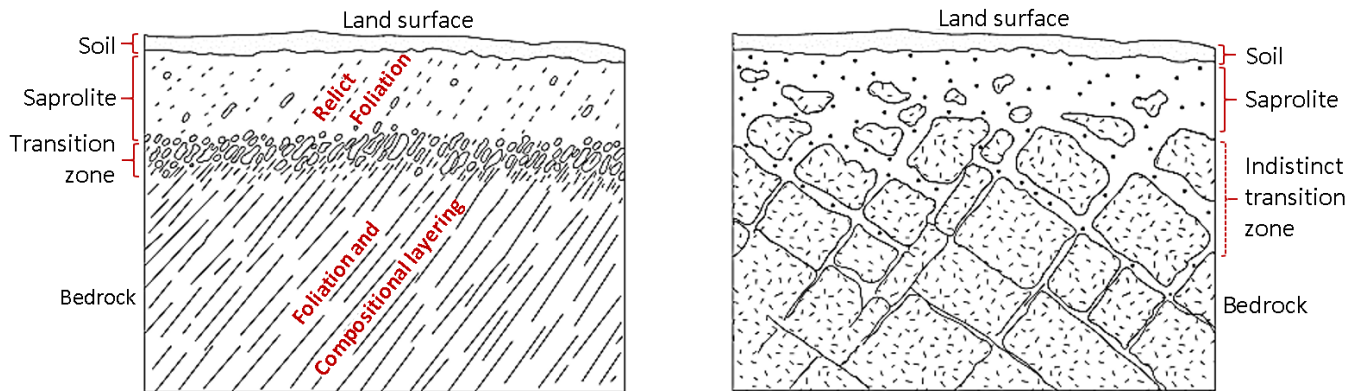
Figure 7.9 Conceptual variations of transition zone thickness and texture that develop on different parent rock types. *Left*: distinct transition zone on highly foliated schists, gneisses, and slates; *Right*: An indistinct transition zone on massive bedrock. From Daniel and Dahlen, 2002. USGS, in public domain.

Figure 7.10 Photograph taken during the excavation phase of a coal tar remediation project shows distinctive reddish-brown mottling in a weathered siltstone where oil seeps occur along shallow dipping (3-4 degrees) bedding plane fractures. Courtesy of Peter Thompson; photograph by Leo E. Arbaugh, Jr. of the U.S. Army Corps of Engineers.

When present, fractures typically occur in sets, which are often composed of two sets of nearly vertical fractures at approximately right angles to each other, and a third, nearly horizontal, set (Figure 7.6–*Left* and Figure 7.8). As discussed by LeGrand (2007), in gneiss and schist, the orientation of some joints and fractures tends to parallel the foliation and compositional layering, which are rarely horizontal. In massive rocks, particularly granite, nearly horizontal tension joints often occur in the upper one hundred feet of bedrock. Many non-horizontal fracture

patterns can be traced by observing their topographic expression on the ground or on topographic maps. Almost invariably, fractures that are not horizontal are represented by depressions in the topography or by an alignment of topographic features such as stream segments. LeGrand (1952) demonstrated that many fractures are enlarged by dissolution, especially in gneiss and schist containing silicates of calcium. Many of these enlarged fractures underlie draws or linear depressions in surface topography.

Because fractures in the bedrock decrease in size and abundance with depth, contamination of these aquifers is difficult to remediate, especially if the contaminants are heavier than water and have low solubility in water (dense non-aqueous phase liquids or DNAPLs). Contaminants that settle or move into deeper parts of fractured-rock aquifers tend to become trapped as fracture widths become narrower and groundwater velocities diminish (Daniel and Dahlen, 2002).

As mentioned earlier, prediction of the natural direction of groundwater flow in fractured rock aquifers can be related to surface topography. Groundwater moves continuously from uphill areas toward streams where it discharges as small springs and as bank channel seepage into streams. Small springs and seeps are also common in draws and other topographic depressions, especially near the base of valleys (Figure 7.11). Springs and seeps at higher elevations are commonly of the wet-weather type and may suggest poorly fractured rocks below (LeGrand, 2007).

Figure 7.11 Simple capture of a low yielding but permanent spring tapped for water supply of a farmhouse before the Civil War. Many similar springs are still used as sources of potable water in the Virginia's Piedmont physiographic province, although drilled wells are now the main form of private water supply in the region.

To emphasize again, Figure 7.7 illustrates that the perennial-stream drainage basin is a complete flow-system cell, similar to and yet generally separate from surrounding basins (LeGrand, 1958 and 2007). Described differently, hydraulic heads beneath upland areas decrease with depth, resulting in the overall downward movement of groundwater and providing the mechanism for recharge to the aquifer. For example, a well 75 feet deep is likely to have a higher water level than a well 300 feet deep at the same upland site. Hydraulic head beneath lowland areas increases with depth, indicating upward movement of groundwater. For example, a well 300 feet deep is likely to have a higher water level than a well 75 feet deep at the same lowland site. Although this concept has been verified in the field countless times, every so often a regulatory agency will insist that "site-specific" data including installation of expensive deep bedrock wells be collected to verify the same concept yet one more time.

Unfortunately, it still occasionally appears that the simple presence of fractures to some stakeholders means groundwater can flow "anywhere" regardless of the above-described conceptual model and general hydraulic principles of groundwater flow. Nevertheless, groundwater cannot move upgradient, i.e., against the higher hydraulic gradient ("uphill"), in any porous media including in bedrock fractures. Groundwater flow in fractures is always from higher hydraulic heads towards lower hydraulic heads and ultimately the discharge zones where fractures intersect ground surface (Figure 7.12).

Figure 7.12 Frozen discharge of groundwater along margins of a 9-ft wide dike (denoted by arrows) and fractures in gneiss at the north portal to tunnel at Marys Rock in the Blue Ridge Mountains, located at mile marker 32.2 on Skyline Drive in Virginia.

Well yields in igneous and metamorphic fractured rock aquifers are generally low compared to those of sedimentary rock terrains, so that use of groundwater as a supply has usually been restricted to domestic wells or small municipal and industrial supplies. However, in the Piedmont physiographic province of the United States, there is a growing interest in the use of bedrock groundwater for larger supplies, especially during emergencies like prolonged droughts. This is mainly because most favorable surface-water sites have already been developed, and because of increased concerns regarding the environmental impacts of reservoir construction, inter-basin transfer of water, and declining surface-water quality.

As discussed by Harned (1989) and Lindsay et al. (1991), although crystalline rocks in the Piedmont and Blue Ridge physiographic provinces are typically described as yielding only small quantities of groundwater to wells, this description is based upon large numbers of shallow wells drilled for domestic supplies requiring 2 to 10 gpm. Unfortunately, the reported yield to a well drilled for a domestic supply is rarely an indication of the full aquifer potential at that site. Thus, if many of these domestic wells were drilled deeper, it is probable that additional water-producing fractures within an aquifer would be intersected (see Figure 7.13). In addition, most homes and their wells are located on ridges, hilltops, or slopes which are the least favorable areas for obtaining large yields of groundwater.

Results of studies in several areas of the Piedmont physiographic province show that the aquifers can sometimes provide significant amounts of water to wells. Daniel and Sharpless (1983) identify more than 300 wells in an 8-county area of central North Carolina with yields at or above 50 gpm. Cressler et al., (1983) report that a significant number of wells in the Piedmont physiographic province in Georgia yielded more than 100 gpm and that some wells yielded nearly 500 gpm. They also identify 66 wells used primarily for industrial and municipal supplies, at

flow rates significantly above those of domestic consumption, that had been in use for periods of 12 to more than 30 years without declines in yield. Similarly, Cederstrom (1972) reports that well yields of 100 to 300 gal/min were common for bedrock wells in the Piedmont and Blue Ridge physiographic provinces from Maine to Virginia. Williams et al. (2005) provide detailed discussion of water-bearing characteristics of various crystalline rocks in the Lawrenceville, GA area where more than a dozen high-yielding wells are utilized for public and industrial water supply.
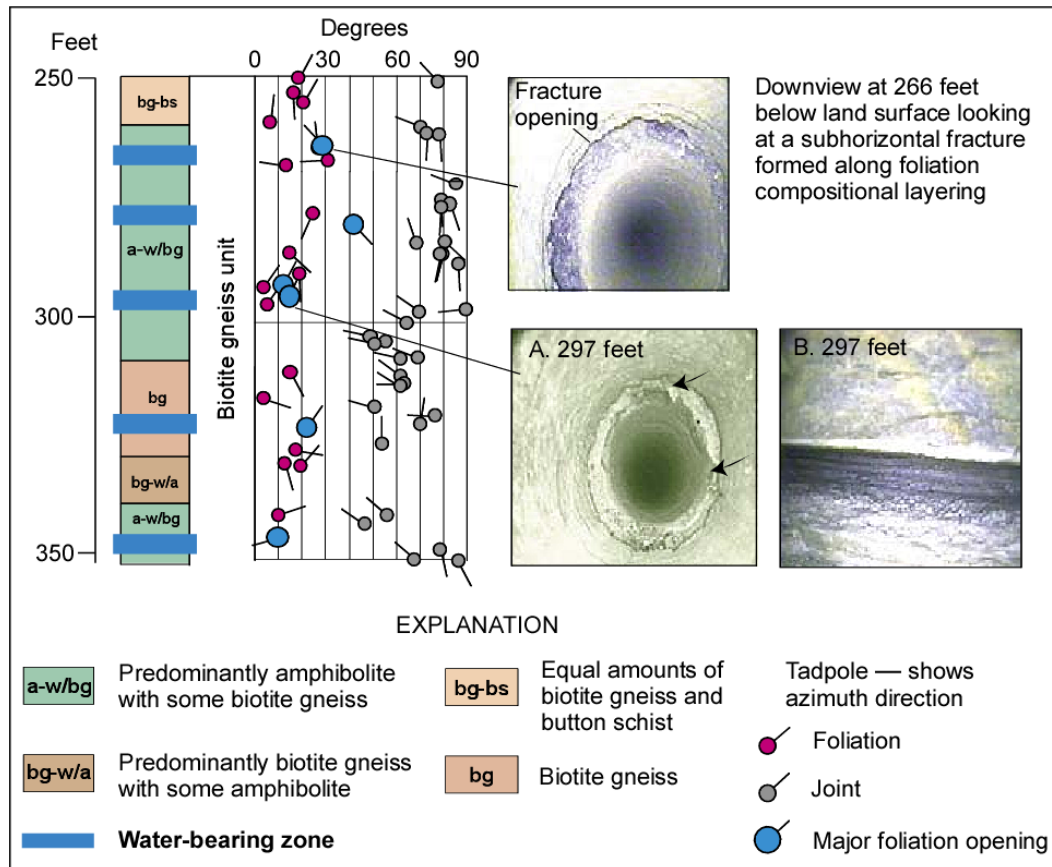
Figure 7.13 Subsurface lithologic characteristics, water-bearing zones, structural tadpole plot and borehole camera images for part of the geophysical log of well 14FF59 in Lawrenceville, GA. Images A and B show subhorizontal fracture at 297 feet below land surface formed parallel to compositional layering; high-angle joints (black arrows) terminate into the fracture from below; aperture is 3– 4 inches. Modified from Williams et al., 2005. USGS, public domain.

Cohen, Faust, and Skipp (2009) present a comprehensive hydrogeologic study of Loudoun County, which is located in northern Virginia approximately 30 miles west of Washington D.C. The County has been one of the fastest growing counties in the United States since the 1980s. In its western portion, the primary source of municipal, commercial, and individual domestic water supplies is groundwater pumped from thousands of wells drilled into the fractured metamorphic rock of the Blue Ridge Geologic Province. The County has created an extensive database of location, construction, and yield information for approximately 19,000 water wells, including 11,500 wells in the Blue Ridge Province of which 1,800 are hydrogeologic study test wells. Statistical analyses were performed using the database to evaluate differences in well yield characteristics as a function of rock type, proximity to

lineaments, proximity to streams, proximity to faults, and other factors. Using GIS methods, well data were attributed to specific rock units, and well distances were calculated to lineaments, streams, and faults. For illustration, well yield distribution curves for bedrock types in the Blue Ridge Province are shown in Figure 7.14 Overall, yield distributions in the metagranites are similar and tend to be higher than yield distributions associated with non-granitic rocks, the Catoctin metabasalt, and the Harpers phyllite/metasiltstone. Notably, the highest median well yield is from Swift Run Formation which consists of heterogeneous assemblage including pebbly to cobbly quartzite and feldspathic metaconglomerate, feldspathic quartzite, and metasandstone, locally crossbedded.

Approximately 5 to 10 percent of all the wells are reported to yield less than one gallon per minute (gpm) or 0.06 l/s, which is the minimum acceptable yield for domestic wells in Loudoun County. Less than 5% of the wells have very high yields (>50 gpm) desirable for community water-supply use. Given the cost of drilling, this emphasizes the need to use scientific methods (e.g., lineament analysis and surface geophysical surveys) to increase the probability of drilling high-yield wells for community water-supply development.
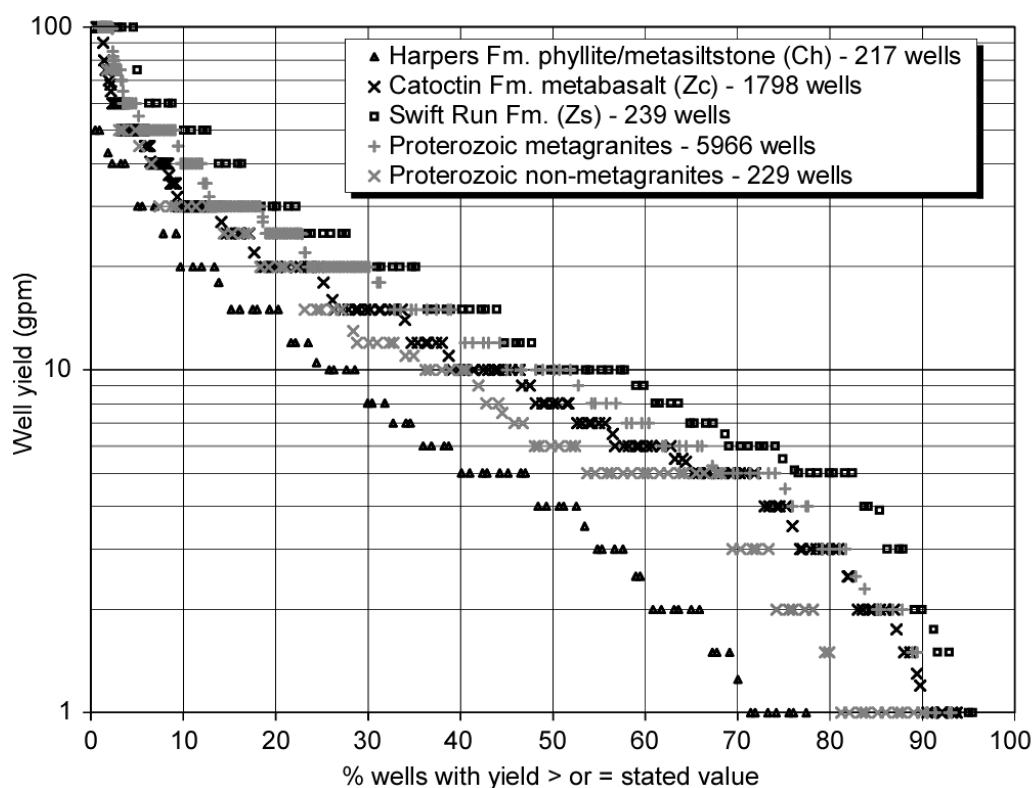
Figure 7.14 Well yield distributions in Loudon County, Virginia by rock type. From Cohen, Faust, and Skipp, 2009. Copyright Geotrans, Inc. Permission is required for further use.

Mean and median well depths in the Blue Ridge of Loudoun County have increased from approximately 300 to 500 feet between 1980 and 2007. Well drillers generally continue drilling to greater depths until a satisfactory yield is achieved at a particular location.

7.3 Karst Aquifers

As discussed by Kresic and Mikszewski (2013), developing a hydrogeologic conceptual site model (CSM) for a karst site is the most difficult task in hydrogeology. Countless examples of concepts that resulted in wasted or unplanned efforts and funds abound for just about every aspect of hydrogeologic practice in karst terrains. This includes construction of dams and reservoirs that cannot hold water because of the excessive leakage, flooded tunnels and other infrastructure (Figure 7.15), inadequate development of water supply sources, and unsuccessful groundwater remediation. In addition to the natural complexities of karst aquifers, there are two other main reasons for the ongoing difficulties in developing accurate CSMs for karst sites:

- Attempts to treat karst as an "equivalent porous medium" (EPM) and develop hydrogeologic concepts only applicable to intergranular aquifers (e.g., sand and gravel). This leads to quantitative analyses and numeric modeling of karst aquifers with inappropriate equations and models.

- Regulatory policies and politics that purposely or inadvertently result in misclassifying a site as non-karstic; typical examples include use of terms such as "carbonate aquifer" or "fractured rock aquifer" while ignoring clear evidence of karstification.

Figure 7.15 *Left*: Montejaque Dam in the Sierra de Grazalema, Spain, was abandoned before the Second World War because of large losses of water from the reservoir and at the dam site through numerous sinks and other karst features. This arc dam on the river Compobuche-Guadares, a tributary of the Guadiaro river, is 83.75 m high with an 84-m long crest. After heavy rains, the reservoir behind the dam fills with water only to lose it soon after rains stop. *Right*: Hydrotechnical tunnel in Dabarsko Polje, Herzegovina, flooded during construction. Photographs courtesy of Petar Milanović.

Unfortunately, both "unnatural" reasons listed above are still very common in the hydrogeologic practice despite significant advances in characterization, quantification, and management of karst hydrogeologic systems made over the last several decades worldwide. While there is no excuse for a working professional hydrogeologist to treat karst as an EPM or "fractured rock", some stakeholders may be less critical when it is government regulatory agencies engaging in this erroneous practice. It is suspected that regulators often take this stance because the very presence of karst may mean that a task at hand is infeasible (a related term is "technically impracticable," see Lecture 13 Groundwater Contamination and Remediation). In many parts of the world, however, the population living in karst environments understand and can appreciate this simple fact and is given enough credit by various government agencies when there is a common problem to solve. This, however, is not the case in some highly litigious societies such as the United States where there are examples of continuous, misguided, and expensive

efforts in trying to deal with groundwater contamination in karst without even acknowledging the nature of the problem.

It is not uncommon that at fractured bedrock sites a zone of concentrated groundwater flow and preferential flow of contaminants exists within the weathered transition zone between the overlying clayey saprolite and the competent unweathered rock (see Figure 7.9). In such cases, the saprolite and the underlying bedrock are less or not affected downgradient of the contaminant source zone. Unfortunately, although this concept is not at all applicable to karst, it has been applied indiscriminately at some contaminated sites in a misguided effort to "localize" the problem and justify various attempts of "active" groundwater remediation at any cost. Such approaches, aimed at pleasing certain stakeholders and/or avoiding hard decisions, have a high likelihood of failure in karst. This is simply because the karstification process creates preferential flowpaths deep into the underlying "bedrock" (such as limestone and dolomite). These preferential flowpaths can develop and interconnect at various depths, and can be vertical, horizontal and anything in between. They also share one comment element that may be the reason for all the controversy – their orientation and depths are often <u>unpredictable</u> (e.g, see Figure 7.16). This is true for karst aquifers worldwide: in Texas, Tennessee, Kentucky, Virginia, or Florida in the United States, in France, China, Ukraine, Turks and Caicos, in classic karst of The Dinarides (the area in The Balkans, Europe where the word karst comes from), and the student can extend the list to include all areas, large and small, that are underlain by carbonate and other soluble rocks.
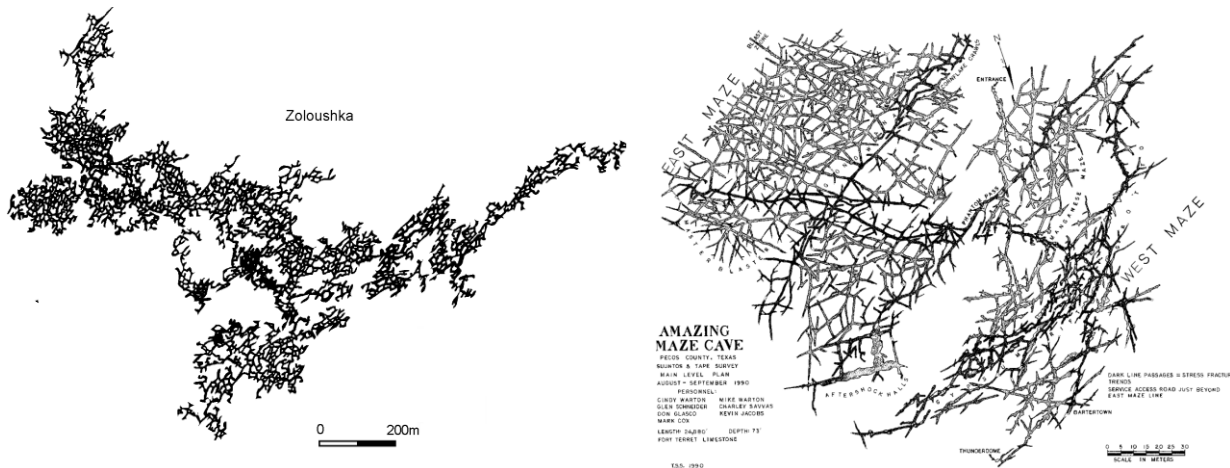
Figure 7.16 *Left*: The third longest gypsum cave in the world, Zoloushka (90.2 km) in Ukraine. Courtesy of the speleological club Chernivtsy (from Klimchouk, 2011; printed with permission.) *Right*: Amazing Maze Cave near Bakersfield in Pecos County, 30 miles east of Fort Stockton is the third longest in Texas with 4.7 miles of surveyed passages. Courtesy of Texas Speleological Society.

One likely reason for mischaracterizing karst aquifers are some widely cited definitions of karst terrains in general, such as this one in the 1960 edition of the American Geological Institute Dictionary of Geology:

"*In Karst, the limestone rocks are honeycombed by caverns and openings dissolved by groundwater. Most of the drainage is underground and the land is left dry and relatively barren. The landscape is dotted with sinkholes, interspersed with abrupt ridges and irregular protuberant rocks. Dry valleys are common, and valleys containing streams often end abruptly where the latter plunge into underground channels and caves, sometimes to reappear as large springs miles away. These features are so characteristic of the Karst district of the eastern Adriatic coast that the name karst has been applied to them elsewhere.*"

What is still hard to understand by some is that the terms karst and karst aquifer do not necessarily imply the presence of sinkholes at the land surface and caves that can be easily accessed by a passerby or a spelunker. In other words, in an aquifer developed in limestone, dolomite and other soluble rocks, there will always be conduits and voids of varying size and (unknown) spatial extent that even the most skillful caver cannot possibly access (Figure 7.17), or field investigation methods cannot discover even after spending significant funds (Figure 7.18). Consequently, the role of a karst hydrogeologist in developing CSMs is to cost-effectively use multiple investigative tools applicable to karst, narrow down the inevitable uncertainties, and reduce risks associated with management decisions.

Figure 7.17   Cavities of varying size discovered at a deep (seen dewatered here) construction site in Hartsville, Tennessee. Photographs by George Sowers; printed with kind permission of Francis Sowers.

Understanding that the groundwater engineering risks in karst can never be fully eliminated and conveying this to all interested parties is arguably the most important aspect of karst hydrogeology regardless of the specific project goal (Kresic and Mikszewski, 2013; Kresic, 2013.)

The density, size, and geometry of individual conduits in the karst aquifer network can vary by many orders of magnitude depending on site-specific characteristics such as: mineral composition, stratigraphy, tectonic fabric, recharge mechanisms, and position of the erosional base. One of the most common errors made by hydrogeologists not experienced in karst is to rely solely on investigative borings and monitoring wells when developing a CSM for a "limestone" ("carbonate") aquifer site. Declaring that the aquifer (site) is non-karstic based on three, five or even ten borings that did not encounter a large "void" is a typical example. Similarly, a non-karst hydrogeologist may conclude that the aquifer is not karstic because test wells cannot produce "large" yields that, somehow, are expected from a karst aquifer. Figure7.17 illustrates these points. One can easily imagine a boring advanced into the large cavity shown in the top photograph or the smaller cavity in the bottom photograph. In such case hardly any hydrogeologist would argue that the limestone is not karstified (an inexperienced driller not equipped for drilling in karst may even lose some of his/her equipment when this happens). One could also imagine another boring completed in solid rock adjacent to either cavity that could be used, by some, as "evidence" of non-karst.

Figure 7.18 shows that surprises can happen even after extensive and expensive investigations are performed by professionals who grew up surrounded by karst. Borings #1 and #4 at a future dam site encountered "single small voids" whereas borings #2 and #3 were completed in solid limestone. A grout curtain subsequently designed to deal with "limited" karstification failed to achieve results even after injecting disproportionally more grout than what was designed. A 20-m long exploration gallery was then excavated into the dam abutment and discovered a cave with a large hall up to 20 m high. The cave was surveyed in detail resulting in a complete re-design of the grout curtain. As can be seen, parts of the cave almost completely surround boring #3.
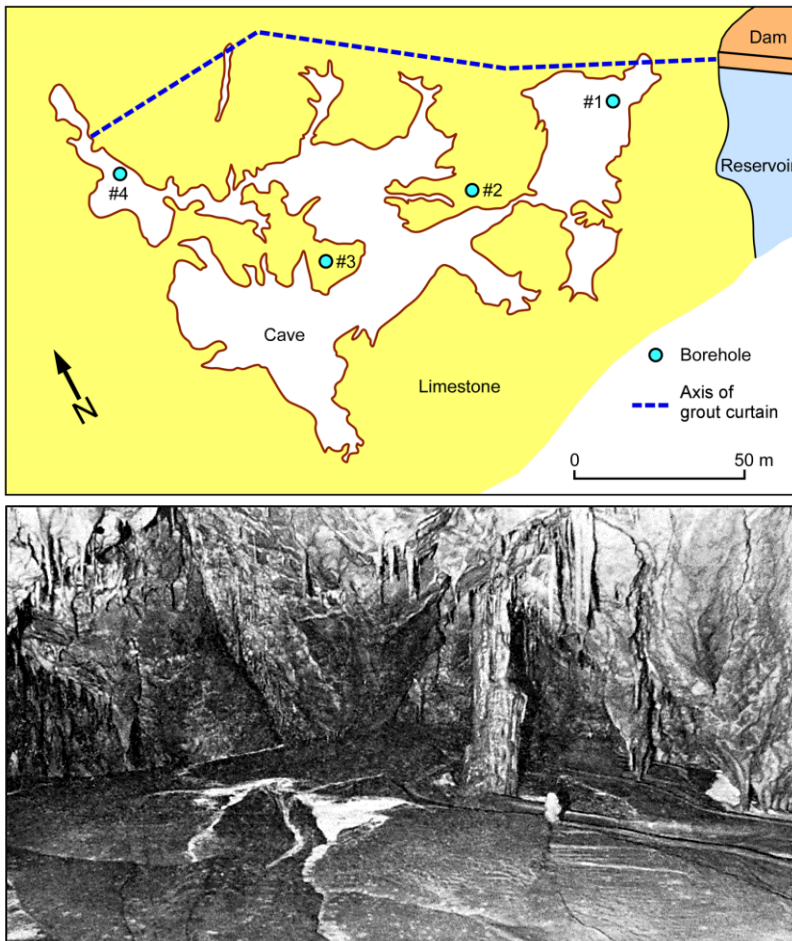
Figure 7. 18 *Top*: Cave in the left abutment of Sklope Dam, Croatia discovered with an exploration gallery which was excavated after extensive grouting failed to achieve backpressure. *Bottom*: The grout mass on the cave floor. Modified from Božičević, 1971; photo courtesy of Srećko Božičević.

In the past, the author has attended meetings of stakeholders evaluating the feasibility of groundwater remediation at several large federal facilities underlain by carbonate rocks in one of the southern United States. At one such meeting, a consultant working for a federal client brought and passed around a boring core sample similar to the one shown in Figure 7.19-*Top*. Based on that core sample, the consultant qualified the aquifer underlying the Site as non-karstic and therefore relatively easy to conceptualize. The groundwater at the Site was and still is contaminated with dissolved chlorinated solvents together with dense non-aqueous phase liquids (DNAPLs).

The regulatory agency overseeing the Site characterization and remediation efforts refused to use word karst for the underlying aquifer. Instead, the aquifer was referred to as consisting of "partially weathered rock" and (deeper) "competent bedrock". Over one hundred million US dollars have been spent at the Site on various investigation and remediation activities spanning more than 20 years. Incidentally, the results of quite a few field

investigation efforts including drilling and borehole geophysics revealed presence of highly transmissive zones deep in the "competent bedrock" where the tested hydraulic conductivity of discrete borehole intervals exceeded 1000 ft/day. In addition, great difficulties during drilling of some borings were reported including drop of drilling tools, loss of drilling fluid, and unstable/collapsing borehole walls. Finally, everyone involved in the project accepted the fact that the aquifer beneath the site is drained by a single large spring which, on average, discharges over 30 million gallons of water every day. Yet, the word karst was all but banned at the Site.

Figure 7.19 Two core samples from the same boring in Ordovician Lexington Limestone near Lexington, Kentucky. Core diameter is 4.5 cm (approximately 2 in.)

The regulatory agency overseeing the Site characterization and remediation efforts refused to use word karst for the underlying aquifer. Instead, the aquifer was referred to as consisting of "partially weathered rock" and (deeper) "competent bedrock". Over one hundred million US dollars have been spent at the Site on various investigation and remediation activities spanning more than 20 years. Incidentally, the results of quite a few field investigation efforts including drilling and borehole geophysics revealed presence of highly transmissive zones deep in the "competent bedrock" where the tested hydraulic conductivity of discrete borehole intervals exceeded 1000 ft/day. In addition, great difficulties during drilling of some borings were reported including drop of drilling tools, loss of drilling fluid, and unstable/collapsing borehole walls. Finally, everyone involved in the project accepted the fact that the aquifer beneath the site is drained by a single large spring which, on average, discharges over 30 million gallons of water every day. Yet, the word karst was all but banned at the Site.

In contrast, two drilling core samples shown in Figure 7.19 are both from one boring completed in carbonate sediments near Lexington, Kentucky, the state in which citizens and environmental regulators alike understand the meaning of word karst. Dozen or so borings completed in limestone at this site were continuously cored up to 150 feet depths but only a handful of solution features similar to the one shown in Figure 7.19-*Bottom* were found. Nevertheless, no one involved in the project had to be persuaded that the underlying aquifer is karstic because the Site was in limestone, in the state of Kentucky.

The situations shown in Figures 7.17 and 7.18 can happen at any depth within a karst aquifer including hundreds or thousands of feet below ground surface and below the water table. The depth to which karstification has progressed, the so-called base of karstification, is not uniform and varies from site to site. The degree of karstification and fracture density generally decrease with depth but can locally reach much greater depths. As the erosional basis for karst groundwater discharge is not necessarily at a static elevation and may be constantly lowered due to surface stream incision, sea level regression, or other factors, the depth of karstification and the depth to the water table would consequently increase in time as well. For example, in some areas of the Dinaric carbonate platform in Europe the depth to the water table exceeds 1000 meters (Figures 7.20 and 7.21) while cavities and

voids of varying size have been discovered with investigative drilling at depths of several thousand meters below sea level.

Even more impressive are examples of deep karstification on the Arabica Karst Massif, part of the Western Caucasus mountains bordering the Black Sea. The Krubera Cave (Figure 7.22) in the breakaway republic of Abhazia (formerly in Georgia) is the second deepest cave in the world: 2191 meters or 7188 feet as of May 2022 (the nearby Veryovkina Cave is the world's deepest at 2212 meters or 7257 feet). Krubera has a very steep profile and reveals an enormous thickness of the vadose zone.
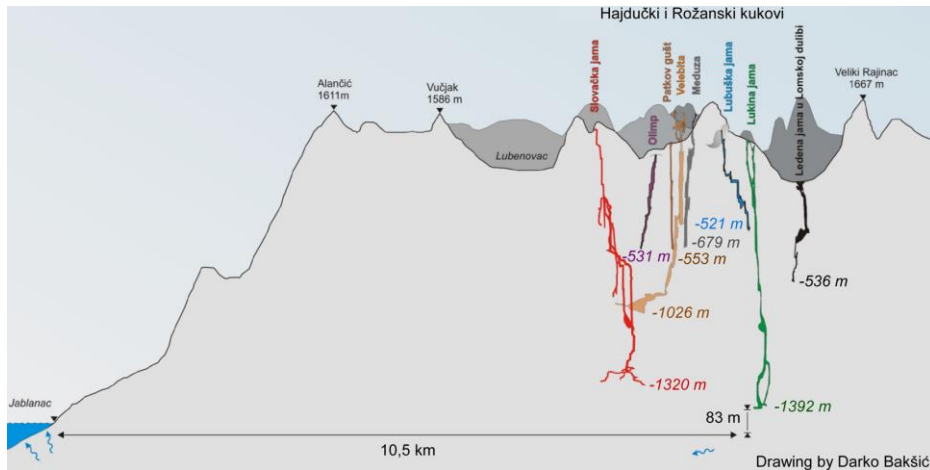
Figure 7.20 Cluster of deep jamas (pits) on the Velebit Mountain, Croatia. As of October 2020, the depth of Lukina Jama, the deepest Croatian pit, is 1431 meters (4695 feet) including 41 m of the submerged passages at the bottom. This part of the Dinaric karst is drained by numerous coastal and submarine springs in the Adriatic Sea such as Jablanac (shown schematically in the left). Courtesy of Croatian Speleological Server (2010; www.speleologija.hr.)

Figure 7.21 Two spectacular vertical pits on the Velebit Mountain, Croatia: Munižaba (*Left)* and Šlapice (*Right*). Photographs courtesy of Dinko Stopić, Karlovac Speleological Club, Karlovac, Croatia.

A.Klimchouk, Ukr.S.A. - UISK, 2006

Gelgeluk Valley S.head

Genrikhova Bezdna

Kujbushevskaja

-956m

Martel's

-1110m

Ortobalagan Valley

-1004m

Krubera

Berchil Ridge

0   100   200   300   400   500m

-2191m

-500m

Berchil'skaja

Berchil 2495m

-1785m

-2080m

Ortobalagan glacial through

Berchil'skaja

Arabiksaja System

Krubera
2256m

Kujbyshevskaja
2180m

-95

Genrikhova Bezdna
2110m

-120

-160

-340

-500

-440

-500

-640

-590

-700

-740

-1004

-1110

-1200

-1300

2000m

-1710

256 m above sea level

-2080

-2191
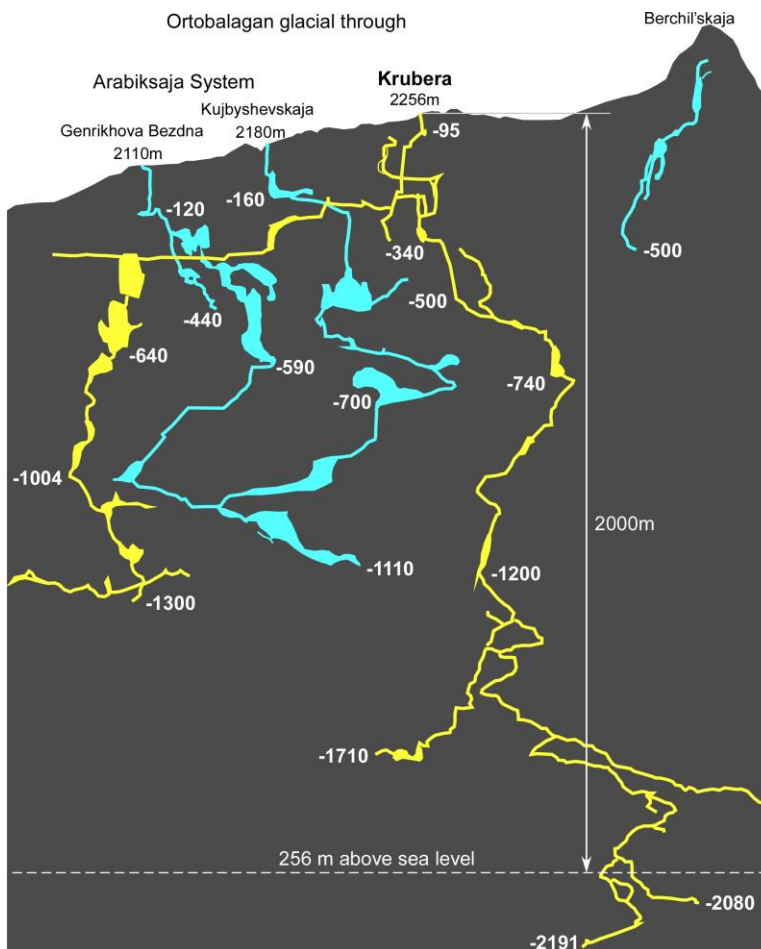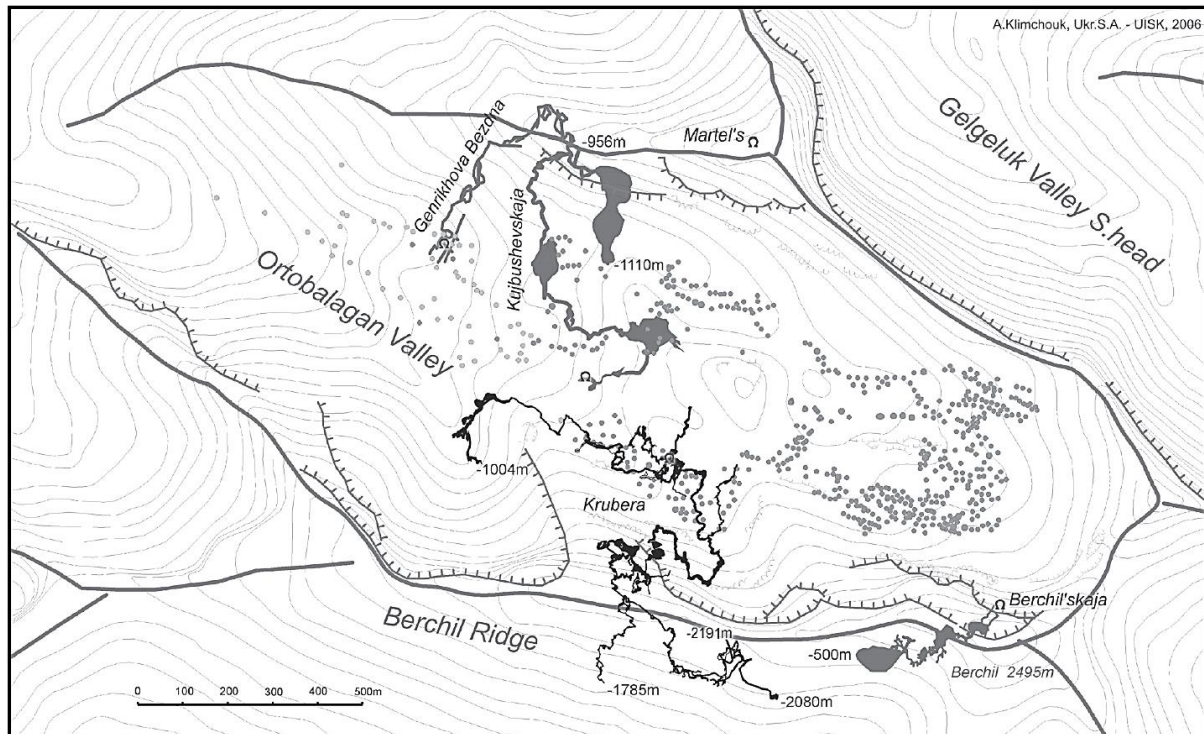
Figure 7.22 *Top*: Major caves in the Ortobalagan valley, Western Caucasus, breakaway republic of Abhazia (formerly in Georgia.) Dots indicate dolines. *Left*: Combined cave profile along the axis of the Ortobalagan valley. Krubera Cave is shown in yellow (bottom of the cave is 2191 meters below ground surface), other caves in blue. Simplified from Klimchouk, Samokhin, and Kasian, 2009. Printed with permission from the authors.

151

The lower boundary of the vadose zone (the top of the phreatic zone) is at an elevation of about 110 m above sea level (asl) at low flow, which suggests a low overall hydraulic gradient of 0.007 to 0.008 towards the Black Sea. Low-TDS groundwater is tapped by boreholes in the shore area at depths of 40m to 280m, 500m, 1750m, and 2250m below sea level, which suggests the existence of a very deep freshwater flow system. Submarine discharge along the Black Sea coast is reported at depths up to ~400 m below sea level (bsl). A large, closed submarine depression is revealed at the sea-floor next to the Arabika Massif, with its deepest point at ~400 m bsl. These facts point to the possibility that the main karst system in Arabika could have originated in response to the Messinian salinity crisis (5.96‑5.33 Ma) when the Black Sea (Eastern Paratethys) could have almost dried up, as did the adjacent Mediterranean where a dramatic sea-level drop is well established. Further development of the thick vadose zone and the super-deep caves has been caused by subsequent uplifts during the Pliocene-Pleistocene (Klimchouk et al., 2009.)

Similarly, along the coasts of Florida in the United States, Yucatan in Mexico, and the Caribbean islands there are numerous submarine springs and submerged cave passages testifying that the sea level in the past was also lower (Figure 7.23).

Figure 7.23 Cave divers in submerged passages of the Nohoch Nah Chich cave in the Yucatan Peninsula. The abundant speleothems were formed prior to the cave submergence. Photograph courtesy of David Rhea, Global Underwater Explorers.

To emphasize: defining depth of karstification at every project site is as uncertain as predicting spatial distribution of karst cavities or finding them. Nevertheless, it has been proposed that, similarly to the primary porosity, the degree of karstification generally decreases with depth and reaches the point below which solution openings (karst voids) are absent (e.g., see Ford and Williams, 2007, page 115; Milanovic, 2004, page 10). This base of karstification is an irregular surface due to various heterogeneities of the carbonate deposits including uneven fracturing of the rock mass. Karstification also deepens in time as the level of aquifer discharge is lowered. The levels (locations) of aquifer discharge, such as a major surface stream or a spring at the contact with non-soluble rocks, are lowered due to normal erosion of the land surface. In relatively thin carbonate deposits the karstification will eventually reach non-soluble rocks underlying the carbonates.

As suggested by Milanovic (2004), the karstification decreases exponentially with depth and at depths greater than 300 m the rock mass can be considered non-karstified for practical purposes. Locally, in tectonic zones, the karstification can extend deeper than 300 m but these zones do not represent a significant rock volume and are expressed in two dimensions. The largest volume of karst voids (storage) is developed within the zone of water table fluctuation. Karstification decreases below the lowest groundwater levels and the base of karstification, and the minimum water table level coincide (emphasis added). Generally, the slope of the base of karstification leads to the zone of aquifer discharge. The most active karst channels are directly above the base level. The existence of karst drains below this level is not excluded, but they are rare and of limited transport capacities (Milanovic, 2004).

However, while the above-proposed concept of karstification may be applicable to some situations, it does not explain numerous documented hydrogeological systems developed in thick carbonate sequences which extend well below locations of aquifer discharge and the minimum water table. In fact, the largest springs in the world, on all continents, are in karst and are of ascending type with deep confined conduits (deep below minimum water table) having extraordinary transport capacities often exceeding tens of m^3/s. Their drainage areas are measured in hundreds of square kilometers or more. Quite a few of these springs, also called *vauclusian* springs after Fontaine de Vaucluse, the source of river Sorgue in Provance, France have been explored by cave divers in recent years worldwide (see Lecture 10 on springs). The ascending character and the existence of a deep siphon at the Fontaine de Vaucluse were acknowledged by French explorers in the 19th century. In 1985, the vertical submerged conduit of the spring was explored to a depth of 315 m (950 feet) using a small submarine robot called MODEXA 350. The camera of the robot showed a sandy floor at this depth. The spring can produce more than 200 m^3/s after heavy rainfall (Showcaves, 2022) and has a sustained minimum discharge rate exceeding 10m^3/s or 230 million gallons per day (Kresic, 2013). Jovan Cvijić, the father of modern karst geomorphology and hydrogeology, understood this nature of groundwater flow in karst very well when developing his concepts early in the 20th century (Figure 7.24; Cvijić, 1918). It is therefore puzzling that some hydrogeologists, a century after, still believe how the base of karstification, and the minimum water table level coincide and therefore there is very little, if any, groundwater action below, for all practical purposes. More on springs in general including in karst is presented in Lecture 10.
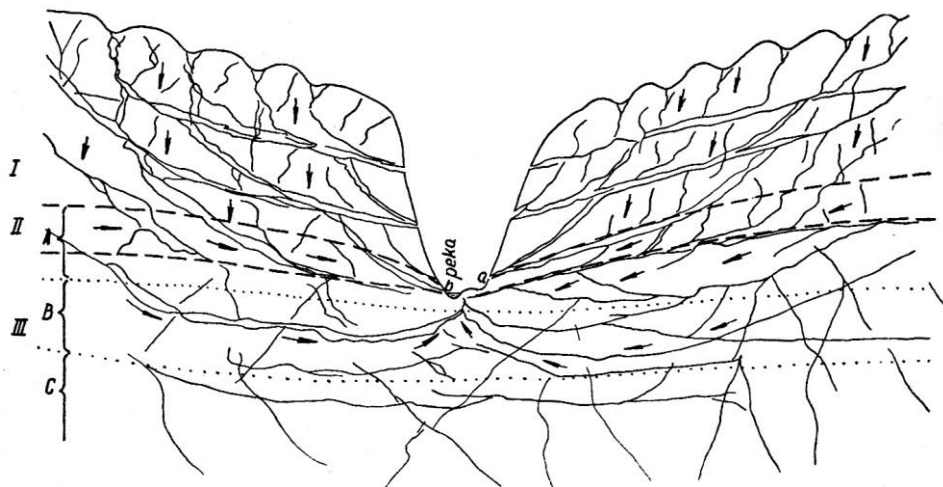
Figure 7.24 Schematic of groundwater circulation in karst proposed by Cvijić in 1918. (I) Unsaturated zone. (II) Transitional zone. (III) Permanently saturated zone. (A) Zone of intensive horizontal flow; the upper limit is maximum water table; the lower limit is a multi-year minimum water table. (B) Zone of siphonal flow. (C) Zone of slower siphonal flow and stagnant water. Arrows indicate direction of groundwater flow. "*peka*" denotes river; *a* is intermittent spring; *b* is permanent spring. From Milojević, 1967. University of Belgrade. Acknowledgment required for further use.

Paleokarst is term usually used to describe karst features (voids, cavities) at any depth explained by the burial of carbonate sediments below non-soluble rocks. The carbonates were karstified at earlier times when exposed at the surface or when in near-surface settings. These paleocavities may subsequently be filled with clastic deposits or may remain open. In some cases, the existence of karstification at great depths (several kilometers or so) can be explained by the fact that the same general area with carbonate rocks may have been subject to multiple periods of karstification depending on the geologic and tectonic history. In thick karst aquifers developed in active geologic environments it is often possible to find very permeable zones, together with large karst conduits, at greater and varying aquifer depths. These zones may indicate position of a paleo water table where karstification intensity was high.

In any case, open karst cavities at great depths may be preserved even where pressure increases to lithostatic values, due to the high rigidity of limestone and dolomite. Numerous such examples from around the world are provided by Andreychouk et al. (2009) including from North America where data reveals that Mesozoic and Paleozoic carbonate rocks may exhibit enhanced secondary porosity, up to 15-20 %, at depths up to 10 km. As concluded by the authors, available data unequivocally indicate that karst can develop throughout the entire section of the Earth's crust that is accessible by drilling. The distribution of karst voids at different depths is irregular. Relatively large cavities, with dimensions exceeding meters, occur in the top few kilometers. Smaller pores, vugs, and enlarged fractures prevail deeper. The authors note that this spatial heterogeneity can be exaggerated, at least partly, by the technical difficulties of identifying large cavities at great depths. Nevertheless, the available data from many regions of the world strongly suggest that the cavernosity of carbonate rocks within the 4 to 5 km depth interval is increased relative to that of the overlying units.

Andreychouk et al. (2009) also present an appealing explanation for the presence of very deep karstification commonly regarded to be the result of dissolution by descending (infiltrating) water and CO_2 in it. This traditional concept of karst formed by groundwater flowing downwards due to hydrostatic pressure or gravity in general is often referred to as *exogenic* karst. The authors argue that deep karstification can also be the result of dissolution by ascending fluxes of thermal liquid-vapor fluids, of endogenic and metamorphic origin. Listed below are key facts in support of this *endogenic* karst concept:

- Lithostatic zone (LSZ) comprises the lowest parts of the Earth's crust that have been studied (to a depth >12-15 km). The pressure in this zone is controlled by lithostatic load and by endogenic sources. A characteristic feature of the LSZ is the decreased density of rocks due to permanent natural hydro-fracturing. The data from very deep drilling suggest that hydro-fractured rocks are concentrated in certain horizons and zones along the migration pathways of the deep-seated fluids. The degree of porosity and fracturing in such zones is significantly higher than in the overlying meso-zone, and may reach the values characteristic of the shallow karst (hydrostatic zone). Due to hydro-fracturing, "traditional" aquitard and aquiclude rocks lose their confining properties in the lithostatic zone.

- Waters in the LSZ belong to sodium-bicarbonate type and have relatively low mineralization. They are enriched in specific deep-seated components, such as CO_2, He, F, and As, some of which have characteristic isotopic properties. Compared to their counterparts from near-surface settings, the fluids in the LSZ have anomalously high aggressiveness with respect to many sedimentary, metamorphic and igneous rocks. The predominantly ascending character of the fluxes of this water ensures removal of the dissolved matter from the lithostatic zone.

- The development of karst in the upper, exokarst zone is primarily governed by external factors, such as the infiltration and inflow of meteoric water, the expulsion of formation waters under the pressure of the overlying rocks, by topographic relief, and climate. In the lower, endokarst zone not only the carbonates

but also the silicate and aluminosilicate rocks, traditionally considered only weakly or very weakly soluble, can be subject to intense dissolution by fluxes of ascending deep-seated fluids. For example, one of the most abundant and stable, resistant forms of silica under crustal conditions, quartz, at T = 300 to 350°C and P = 200 to 250 MPa acquires an aqueous solubility similar to that of gypsum and anhydrite in typical near-surface conditions.

- The depth of penetration of infiltration waters into the Earth's crust is finite, so that below some given depth the infiltration concept is no longer applicable. In any case, this concept cannot be valid at depths where pressure is much higher than hydrostatic ("suprahydrostatic"), because these zones represent impermeable barriers for gravity-driven infiltration waters.
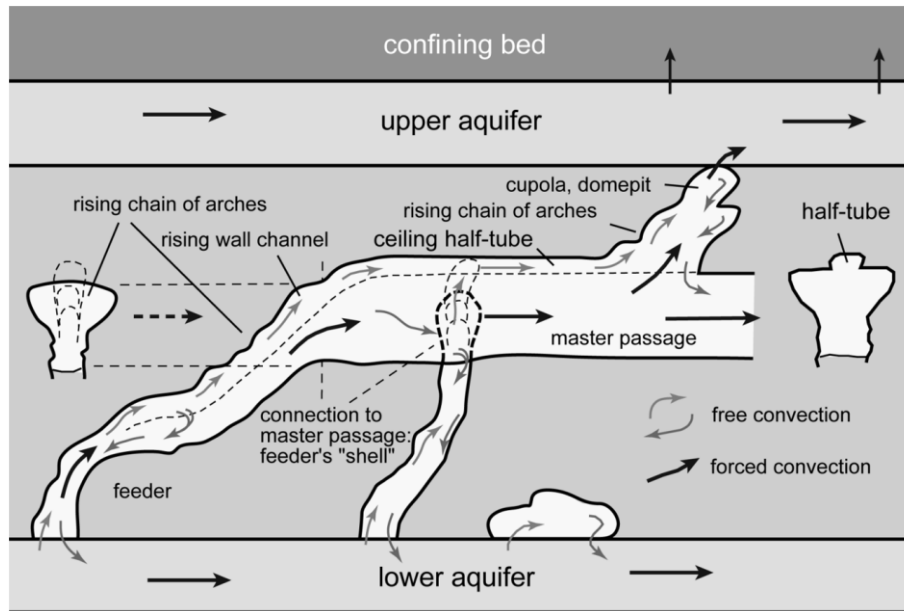
Figure 7.25 Morphologic suite of rising flow, diagnostic of hypogenic transverse origin of caves. Modified from Klimchouk, 2011; printed with permission from the author.

In a series of publications, Palmer (1991, 2007), Klimchouk (1992, 1994, 2011) and Klimchouk et al. (2000) established the concept of hypogenic (endogenic) karst, previously largely ignored by karst hydrogeologists trained in traditional karst settings. As mentioned earlier, the well-established concept, applicable to many open hydrogeologic structures, explains the karstification to be the result of carbonate rock dissolution by infiltrating (descending) waters enriched with soil and atmospheric CO_2, the so called exogenic or epigenic karst. In contrast, hypogenic karst is created by ascending waters that, in addition to CO_2, may carry upwards other acidic fluids such as sulfuric acid and dissolved H_2S the origin of which is deep (endogenic) such as due to metamorphism, magmatic and tectonic processes. Dissolution of carbonates by ascending groundwater is enhanced in semi-confined and confined hydrogeologic settings where cross-formational diffuse flow of the acidic fluids can take place over large areas and create karst cavities by slowly "eating away" the rock mass (Figure 7.25). This process can result in formation of very convoluted and extensive karst cavities along previously weakened portions of the rock (such as due to fracturing and faulting) as well as in relatively competent rock. Hypogenic karst does not have to be deep and exclusively the result of dissolution by endogenic fluids such as sulfuric acid. The sufficient triggers for its development are an ascending groundwater flow and some degree of the carbonate aquifer confinement with less permeable rocks. In many cases there will be an overlap between the ascending and descending flows (i.e., the hypogenic and exogenic karst respectively), especially at the locations of regional groundwater discharge.

In summary, the only relevant characteristics of an aquifer to be qualified as karstic is that a portion of groundwater flow in it is taking place through a network of interconnected channels, conduits, and various other voids created by dissolution of the rock. These voids can be the result of several physical and chemical processes involving descending (infiltrating) water, as well as ascending groundwater that may also carry acidic fluids such as dissolved H_2S, sulfuric acid, and CO_2 from greater depths. Regardless of the actual mechanism involved, the relative size and the number of interconnected karst voids are irrelevant; if they are present, at any scale, the aquifer is karstic. As explained earlier, what sets karst aquifers apart is their unique porosity, often referred to as triple porosity, which consists of the rock matrix porosity, the porosity of fractures, and the porosity of solution openings (enlarged fractures, karst channels, conduits, and all cavities in general).

Probably the only common characteristics karst aquifers share with other aquifer types on a regional scale is that the groundwater must move from the areas of aquifer recharge to the areas (points) of aquifer discharge due to the hydraulic gradient in between, the aquifer transmissivity, and the effective porosity. In karst, this flow can often take quite unexpected local turns defying the expectations of professionals not used to working in such a complex groundwater environment. In many karst aquifers it is not uncommon to have a couple of wells only few meters apart and screened at the same depth below ground surface, with one well influenced by a major conduit and being quite prolific, and the other one completed in solid rock matrix yielding very little water or essentially dry.

The three most important characteristics of regional groundwater flow in karst aquifers are: (1) natural groundwater divides in karst aquifers often do not coincide with surface water (topographic) divides as a result of losing, sinking, and dry streams; (2) groundwater velocities in conduits could be extremely high, on the order of hundreds of meters or more per day; and (3) aquifer discharge is often localized through large karst springs, which have subsurface drainage areas commonly larger than the topographic ones.

A large permanent karst spring usually represents the end point of an integrated karst water system, developed both at the land surface and in the subsurface. Such a system is sometimes referred to as *springshed*, the term commonly used in Florida.
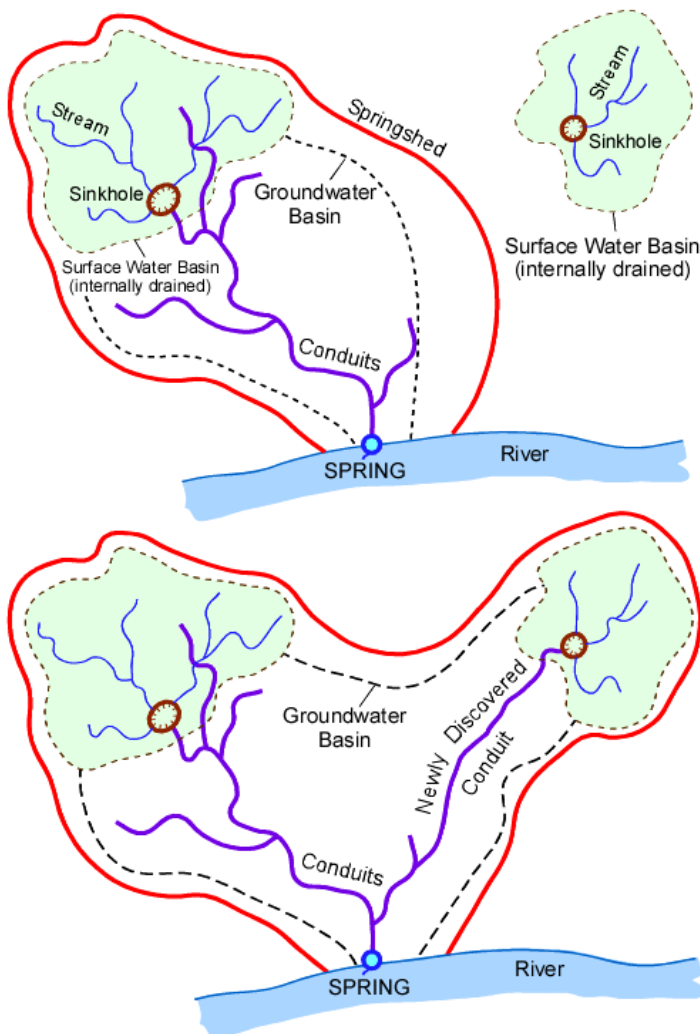
Figure 7.26 *Top*: Springshed boundary depicting surface water and groundwater basins. *Bottom*: Revised springshed boundary based on results of cave diving exploration and tracer tests that confirm presence of conduits connecting a nearby surface water basin to the springshed. Modified from Arthur et al., 2002. Florida Geological Survey; in public domain.

A good starting point for characterizing available groundwater in a karst aquifer is to determine its regional carbonate litostratigraphy and geologic setting. Several major karst types are closely associated with the thickness of carbonate sediments, their age, and the position of regional erosional basis for both the surface streams and the groundwater flow. Large epicontinental carbonate shelf platforms, at the scale of hundreds to thousands of kilometers, and thousands of meters thick, together with isolated carbonate platforms in open-ocean basins, have developed through the Paleozoic and Mesozoic eras, with the trend continuing into the Cenozoic era. At the same time, smaller (tens to hundreds of kilometers wide) carbonate platforms and build-ups associated with intracratonic basins have also developed (James and Mountjoy, 1983). Both types have been redistributed and reshaped during various phases of plate tectonics and can presently be found throughout the world, both adjacent to oceans and seas or deep inside the continents.

The utilization of karst aquifers developed in the Mesozoic platforms of Euro-Asia, originally using springs, has been documented since the beginnings of civilizations in the Old World (Mediterranean and Middle East) and Europe, and it is still irreplaceable in most European and Middle Eastern countries. In addition to modern well fields, public water supply is still largely based on the use of springs by small and large utilities alike (Kresic and Stevanovic, 2010.)
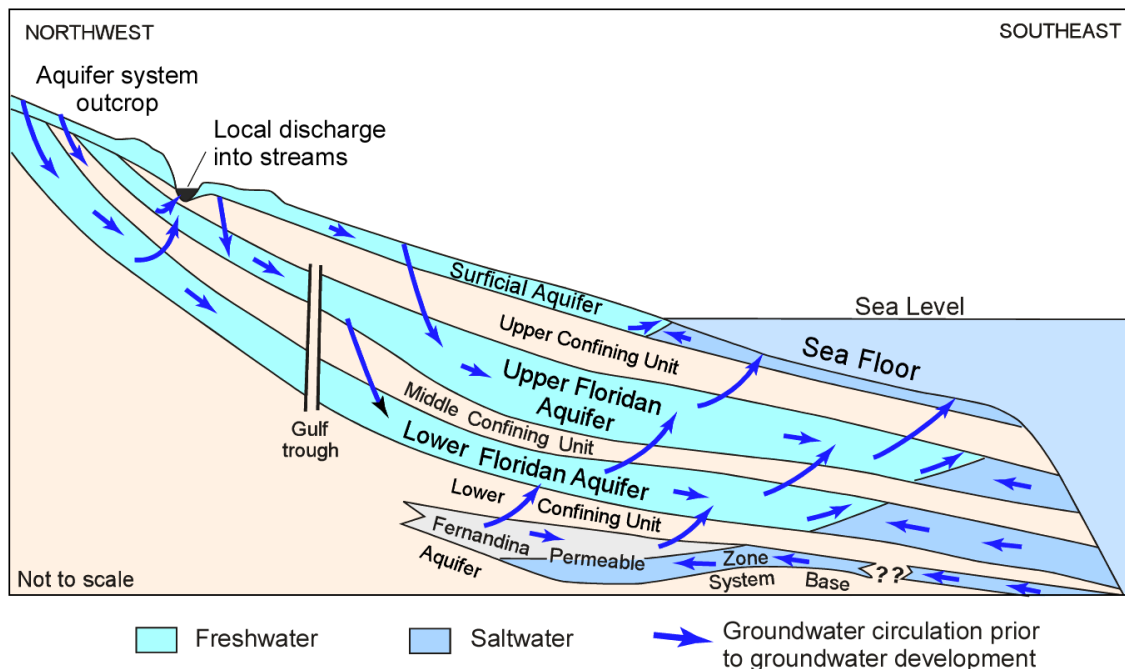
Figure 7.27 Schematic cross section of Floridan aquifer system from northwest to southeast Georgia. The Lower Floridan aquifer in this area includes a highly permeable unit called the Fernandina permeable zone. This zone is the source of a considerable volume of fresh to brackish water that leaks upward through the middle confining unit and ultimately reaches the Upper Floridan aquifer. From Barlow, 2003; modified from Krause and Randolph, 1989. USGS, in public domain.

Like the Euro-Asian Mesozoic platforms, the Floridan aquifer in the southeast United States (North and South Carolinas, Georgia, and Florida) is also developed on a thick epicontinetal platform but with gently sloping undisturbed carbonate layers mostly covered with less permeable clastic sediments (Figure 7.27). The aquifer consists primarily of limestone and dolomite of Paleocene to Miocene age. Regional flow directions are from the inland outcrops towards the Atlantic Ocean and the Gulf of Mexico, with submerged discharge zones along the continental shelf. Florida has over 20 well-documented large offshore springs and a number of undocumented ones.

These springs provided resources to prehistoric people and wildlife when the sea level was lower. Evidence for occupation of offshore sites has been discovered by researchers from the Florida State University Department of Anthropology, which have conducted surveys at and near some offshore springs and have recovered an abundance of chert tools (Scott et al., 2004). Although some of the offshore springs may be discharging brackish to saline water today, they almost certainly discharged fresh water during times of lower sea levels when prehistoric human occupation occurred at these sites. It is estimated that there are nearly 700 springs in Florida of which 33 are the first magnitude springs with an average discharge greater than 100 cubic feet per second (2.83 cubic meters per second). Florida has one of the largest concentrations of freshwater springs on Earth.

Karst of the large Caribbean islands, such as Cuba, Hispaniola, Puerto Rico, and Jamaica, is an example of relatively small carbonate platforms laying on a low permeable, usually magmatic base. Surface karst features are fully developed including sinkholes and cone-shaped hills ("mogote karst" in Puerto Rico and "cockpit karst" in Jamaica). Regional groundwater flow direction is from the upland-highland recharge areas towards the coastline, with the submerged discharge zones along the fresh water-saltwater interface.

When of considerable thickness, young carbonate sediments may constitute important aquifers for both local and centralized water supply worldwide. Examples include the Bahamas and numerous other islands in the Caribbean, the Yucatán peninsula of Mexico, much of British Honduras and Guatemala, Jamaica, Barbados, Bermuda, the Cebu limestone of the Philippines, the Jaffna limestone in Sri Lanka, low-lying coral islands of the Indian oceans such as the Maldives, and portions of Cambodia and Vietnam. The high infiltration capacity of young carbonate sediments in coastal areas and islands means that there are few streams or rivers, and groundwater may be the only available source of water supply. This source is often very vulnerable to salt (sea) water encroachment due to over-pumping of fresh groundwater.

This author's favorite little karst aquifers are on The Turks and Caicos Islands which form the southern extent of the Bahamas Archipelago. The islands and banks of the islands are geographically, geologically, and ecologically part of this single archipelago, with Pleistocene carbonates (often in the form of oolites and eolianites) providing the foundation for Holocene reefs and sediments (Logan and Sealey, 2013). The Caicos islands abound in karst relief forms such as spectacular blue holes and caves (Figure 7.28), and underwater caves many of which are yet to be explored.

Figure 7.28 *Left*: A blue hole on East Caicos. Courtesy of https://www.visittci.com/nature-and-history/geology-ecology-climate. *Right*: The open-gallery entrance to Indian Cave on Middle Caicos.

Most karst areas in the United States constitute portions of carbonate platforms now located away from the coast lines (Figure 7.29). Examples include Edwards Group limestone in Texas and karst of Kentucky, Tennessee, Missouri, and Indiana, all of which have very prolific aquifers.

EXPLANATION OF MAP UNITS

Humid climate region (>30 inches (in.) average annual precipitation)

Dry climate region (≤30 in. average annual precipitation)

Approximate maximum extent of Pleistocene ice

Humid Climate Karst

Carbonate rocks at or near the land surface

Carbonate rocks buried beneath <300 feet (ft) of insoluble sediments

Carbonate rocks buried beneath ≤50 ft of glacially derived insoluble sediments

Carbonate rocks buried beneath >50 ft of glacially derived insoluble sediments

Unconsolidated calcareous or carbonate rocks at or near the land surface

Unconsolidated calcareous or carbonate rocks buried beneath <300 ft of insoluble sediments

Evaporite rocks at or near the land surface

Evaporite rocks buried beneath ≤50 ft of glacially derived insoluble sediments

Evaporite rocks buried beneath >50 ft of glacially derived insoluble sediments

Quartz sandstone buried beneath ≤50 ft of glacially derived insoluble sediments

Quartz sandstone buried beneath >50 ft of glacially derived insoluble sediments

Dry Climate Karst

Carbonate rocks at or near the land surface

Carbonate rocks buried beneath ≤50 ft of glacially derived insoluble sediments

Carbonate rocks buried beneath >50 ft of glacially derived insoluble sediments

Unconsolidated calcareous or carbonate rocks at or near the land surface

Evaporite rocks at or near the land surface

Evaporite rocks buried beneath ≤50 ft of glacially derived insoluble sediments

Evaporite rocks buried beneath >50 ft of glacially derived insoluble sediments

Figure 7.29 Karst and potential karst areas in soluble rocks in the contiguous United States. From Weary and Doctor, 2014. Available at https://pubs.usgs.gov/of/2014/1156/ USGS, in public domain.

Figure 7.30 shows The Catfish Farm well near San Antonio, Texas which created a vertical column of water rising 10 m above the surface when first drilled. Regional groundwater flow in these aquifers is directed towards large karst springs located at the lowest contact between karst and non-karst, or towards the lowest permanent surface stream intersecting the carbonates. Groundwater discharge along such streams is commonly through large springs, often submerged due to present-day river damming.

Probably the best-known karst terrain in the United States is in the Mammoth Cave area of central Kentucky (Figure 7.31). Recharge water enters the aquifer through sinkholes, swallow holes, and sinking streams. Surface streams are scarce because most of the water is quickly routed underground through solution openings. In the subsurface, water moves through caverns and other types of large solution openings which riddle the Mississippian limestones that underlie the Mammoth Cave Plateau and the Pennyroyal Plain to the south and southwest of it. Many of these cavities form the large, extensive passages of Mammoth Cave, the world's longest and best studied cave system.

Figure 7.30 The highest capacity drilled well in the world, capable of sustained pumping of 40000 gallons per minute (2.5 m^3/sec), located on the Ron Pucek's Catfish Farm near San Antonio, Texas. Photo copyright by Gregg Eckhardt; printed with kind permission.
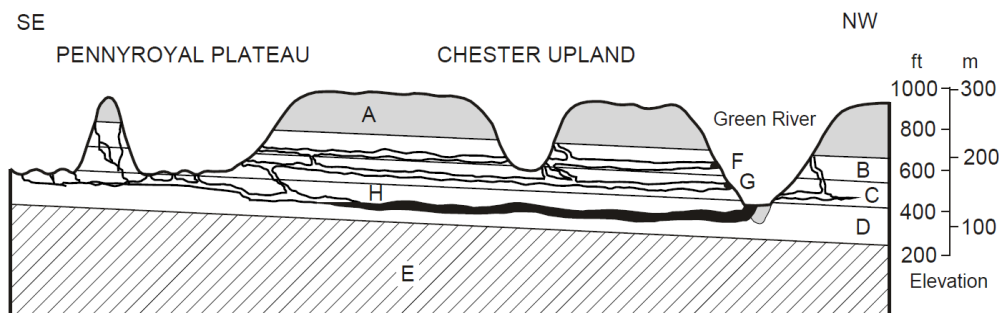
Figure 7.31 Generalized profile through Mammoth Cave. A = caprock of interbedded sandstone, shale, and limestone (Chesterian Series); B = Girkin Formation; C = Ste. Genevieve Limestone; D = St. Louis Limestone; E = impure limestone and detrital rocks; F = upper cave levels of late Tertiary age; G, H = typical levels of Quaternary age (partial flooding of the lowest level is due to late Pleistocene alleviation of the Green River). From Palmer, 1985. Kentucky Geological Survey, in public domain.

In Nevada and Utah in the United States carbonates and other sedimentary rocks are deposited on the continental shelf of the ancestral coast of North America between 570 million and 280 million years ago. The layers of ancient marine sediments have a cumulative thickness of as much as 40 thousand feet (over 12 thousand meters). All the sedimentary rocks in this sequence, where deformed and fractured, may transmit some groundwater flow, but the carbonate-rock layers, because of their brittleness and dissolution by flowing water, are the principal

aquifers (Dettinger, 1989). Due to tectonic forces (faulting and folding), these carbonate aquifers have complex shapes and are connected to aquifers of other rock types. Some of the blocks may be highly productive aquifers, whereas others may transmit only moderate quantities of water or impede flow altogether. Regional groundwater flow, through both the carbonate-rock aquifers and basin-fill aquifers is from the areas of recharge (rain and snow on the mountain ranges) towards the areas of discharge (springs, playas).

Figures 7.32 and 7.33 show the results of a regional groundwater flow study in southern Nevada. The total rate of flow in carbonate-rock aquifers is estimated to be about 77 thousand acre-feet per year (approximately 3 cubic meters per second; note that one acre-foot equals 1233 cubic meters). The main discharge is at several warm-water springs or through the basin-fill sedimentary aquifers that partly fill valleys, while the rest flows out of Nevada into adjacent states, mostly California (Dettinger, 1989). It is interesting that, due to very low recharge (Nevada and Utah are high-desert terrains) the entire flow in this vast area is less than the average flow of some individual first-magnitude springs in Florida.
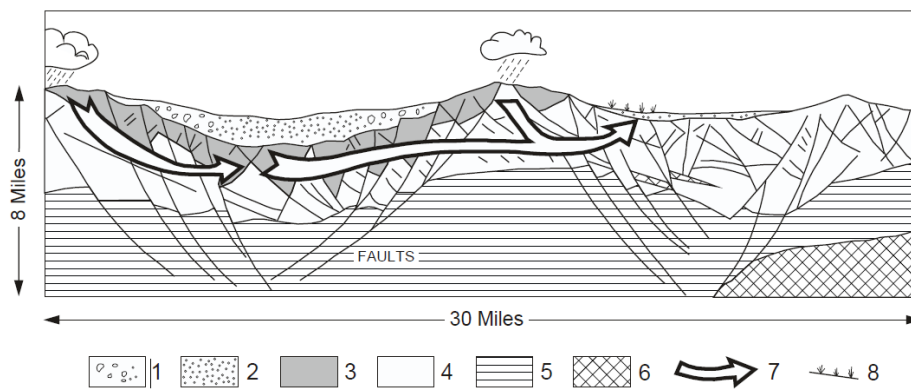
Figure 7.32 Schematic hydro-geologic section of southern Nevada (1) Basin-fill aquifers; (2) Clay and silt; (3) Volcanic rocks: aquifers as well as layers that impede flow; (4) Carbonate rock aquifers; (5) Non-non-carbonate sedimentary rocks impeding flow; (6) Crystalline basement (7) Groundwater flow path; (8) Playas, springs, and native vegetation. From Dettinger, 1989. USGS, in public domain.
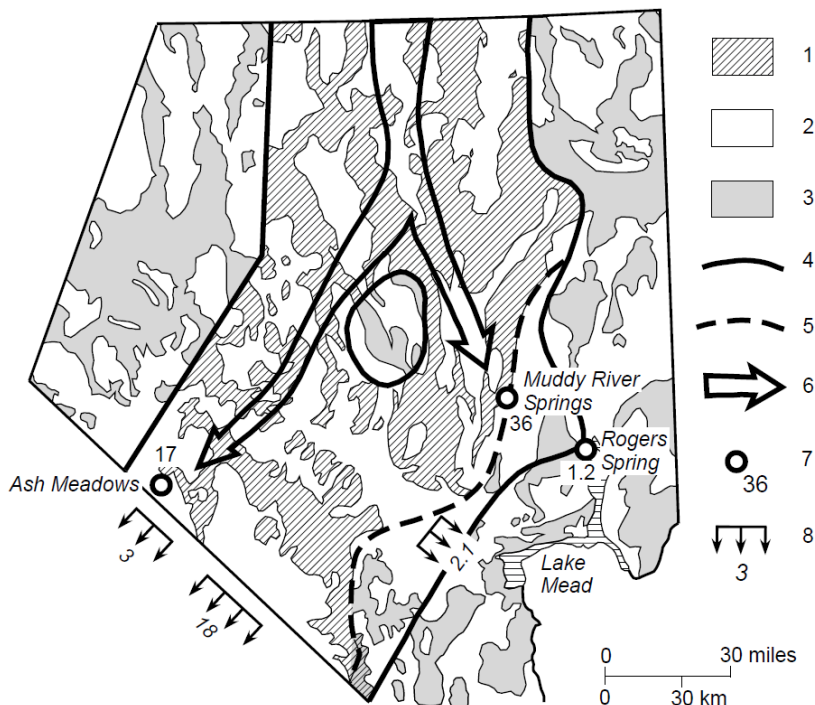
Figure 7.33 Components of regional groundwater budget within Central Corridor in southern Nevada. (1) Carbonate rock outcrops within Central Corridor; (2) Basin fill; (3) Areas underlain by thin or isolated carbonate rocks, or carbonate rocks that may contain poor-quality water; (4) Boundary of Central Corridor; (5) Western limit of rock sequences containing salt-bearing minerals and overlying carbonate rocks. Groundwater east of this line is generally poor quality; (6) General direction of regional groundwater flow; (7) Spring with the annual discharge in acre-feet per year; (8) Regional groundwater outflow to adjacent aquifers/states, in acre-feet per year. From Dettinger, 1989. USGS, in public domain.

161

In the United States, sandstone and carbonate rock deposits are often interbeded over large areas and form aquifers of a mixed type, called sandstone and carbonate-rock aquifers. This aquifer type is present mostly in the eastern half of the Nation, but also occurs in Texas and in Oklahoma, Arkansas, Montana, Wyoming, and South Dakota. The carbonate rocks generally yield more groundwater than do the sandstone rocks, owing to dissolution and larger open-pore space (Maupin and Barber, 2005).

Recent studies have found that karstified rocks and aquifer systems cover approximately 15% of the Earth's ice-free land. The greatest areas of karst outcrops are in the United States, China, Canada, and Russia. In the Mediterranean basin, groundwater is generally more abundant in karst than in other aquifers and has been extensively exploited. Karst groundwater is also widely used in the Middle East, China, North America, and northern and eastern Africa. It is estimated that karst aquifers currently supply approximately 10% of the global population with drinking water, and in some parts of the world they are the only water resource available (Stevanovic, 2018.)

7.3.2 Epikarst

The ill-defined term epikarst has been gaining popularity, bringing more confusion into various aspects of developing hydrogeological conceptual site models in karst. For many karst hydrogeologists involved in solving practical engineering problems throughout the world this term simply refers to the shallow, more weathered (more karstified) portion of the subsurface. Higher karstification is the result of a higher density of fractures at and near land surface (which is typical for any solidified rock), and an abundant supply of carbon dioxide from the atmosphere and the soil layer, where present (dissolution of CO_2 in water creates carbonic acid, the main agent of carbonate rock dissolution and karstification). Figure 7.34 illustrates one such highly weathered zone, equivalent to epikarst, with an abundance of unconsolidated residuum sediments and large infilled dissolutional features.

Figure 7.34 Highly weathered and karstified carbonates ("epikarst") in a road cut near Knoxville, Tennessee. Photo by George Sowers, printed with kind permission of Francis Sowers.

Detailed description of the epikarst concept is provided by Ford and Williams (2007), among others. Common to this and other descriptions is that epikarst contains a perched water zone sitting well above the main saturated zone of the karst aquifer. From this perched aquifer (epikarst), water percolates to the main, deeper aquifer primarily via isolated vertical drains (shafts) that usually form beneath sinkholes. Because of the contrast in permeability between the epikarst (permeability is higher in the shallower, more weathered rock) and the underlying competent rock, as well as the limited transfer capacity of the isolated drains (which are also narrowing down with depth), the epikarst is underdrained. The result of this is formation of a permanent or semi-permanent perched saturated zone in which most groundwater moves horizontally toward the vertical shafts (drains). Epikarst characteristics vary based on recharge pattern (climate of the site), the degree of weathering, and the presence of soil/residuum.

Unfortunately, the above-described hydrogeologic concept of epikarst is being applied indiscriminately, including at sites where there is clear evidence of its complete absence. In fact, many karst areas worldwide show absence rather than presence of perched aquifers sitting above some main, deeper, permanently saturated karst aquifer zone. Photographs in Figures 7.35 through 7.39, as well as Figures 7.20 through 7.22 illustrate the absence of epikarst water in terrains as geographically diverse as Slovenia, Dominican Republic, Mexico, Texas, Alabama, Croatia, and Abkhazia. It also would be erroneous, at any karst site, to assume that the transfer of infiltrating (percolating) water from the land surface to some deeper permanently saturated karst aquifer zone is happening only via vertical shafts below sinkholes, whatever their number and density may be.

Figure 7.35 Lipica Quarry, Slovenia, with no signs of perched epikarst water. Photo courtesy of Blaž Kogovšek.

Figure 7.36 Dry railroad cut in limestone, Dominican Republic, showing no signs of perched epikarst zone. Photographs by George Sowers, printed with kind permission of Francis Sowers.

Countless world-wide examples of dry shallow monitoring wells, tunnels, exploration galleries, and surveyed cave passages at various depths, as well as groundwater tracing tests show that the concept of epikarst as explained above does not hold water in many site-specific settings (Kresic, 2013). People in many parts of the world cannot drill or dig any shallow wells to obtain drinking water from karst terrains for any reasonable period because the subsurface is completely dry from the land surface down to the permanently saturated aquifer at depths of tens or hundreds of meters. All precipitation that falls over the karst terrain quickly finds its way deep into the subsurface through fractures and dissolution features without creation of any shallow perched water zone (aquifer).

The best locations to observe if a perched water zone in epikarst exists, and the groundwater in it is indeed flowing mainly horizontally/laterally, would be natural or artificial vertical walls that cut deep into the karst subsurface. Somewhere along these walls, one then should be able to see groundwater discharge relatively close to the land surface, and no such discharge further below, in the same carbonate formation. Ideal locations would be quarry, road, railroad, and other infrastructure vertical cuts (Figures 7.35 and 7.36), deeply cut canyons (Figure 7.37), or deep, large, vertical, and observable natural shafts such as pits and sinkholes (Figures 7.38 and 7.39). However, more often than not, trickles of water or waterfalls that appear on such walls may last for some time but will disappear after cessation of rainfall as quickly as they appeared. For example, Red Lake near Imotski, Croatia (Figure 7.39), one of the deepest sinkholes in the world and of significant perimeter, does not show any perched water seeping out of "epikarst" along the entire depth of its vertical walls.

Figure 7.37 Upstream entrance to the Santa Elena Canyon, Rio Grande River, Mexico, with dry vertical walls. Photo courtesy of Eric Leonard, NPS; in public domain.

Figure 7.38 *Left*: Neversink in northern Alabama is 162 feet deep. Ribbony waterfalls originate at the land surface after spring rains, but the pit walls are dry most of the time. After a few years of trying to preserve the pit in its pristine natural state, the Southeastern Cave Conservancy gathered funds from donations and bought the property outright in 1995. Photo courtesy of Geary Schindel. *Right*: Entrance to the Valdina Farm Sinkhole, intermittent sink of flood waters of the nearby Seco Creek, Texas. The vertical pit walls are dry most of the time, down to its bottom at 58 feet. Photo courtesy of Dave Bunnell.

The author has been engaged in discussions about the hydrogeologic significance of epikarst during which its advocates were, in support of their theory, citing examples from carbonate terrains in the United States. At the same time, they were qualifying some other karst terrains, such as the classic Dinaric karst, as an exception to the rule.

Figure 7.39 Red Lake near Imotski, Croatia, one of the deepest sinkholes in the world, is a window to the permanently saturated zone, i.e., the karst aquifer. The water table is marked by the level of the lake. Total depth of the sinkhole is 513 m, and depth of water in the sinkhole is about 250m during average low conditions. Photo courtesy of Branimir Jukić.

The main argument explaining the unique hydraulic role of epikarst in such discussions appears to be flat-layered and supposedly sparsely fractured carbonates. This rather unusual geologic condition, in otherwise brittle limestone and dolomite that are easily and extensively fractured and faulted, would presumably result in the horizontal groundwater flow toward sparse vertical drains below sinkholes. Another problem with the theory is the fact that carbonate layers, in addition to being fractured, are often not horizontal (flat) because of folding which has happened on all continents many times during geologic history, including in the Americas. For example, looking at photographs in Figure 7.40, it is hard to imagine that there would be any significant horizontal flow in the presumed epikarst zone, towards some sparse vertical shafts.

Several practical questions arise from the theoretical, academic concept of groundwater flow in epikarst:
- Can the presumed perched saturated zone in epikarst be utilized for water supply, even at a very local scale?
- Is this zone permanent, semi-permanent, or intermittent (and for how long)?
- If there is dissolved contamination detected in the perched saturated epikarst zone, can it be hydraulically contained by extraction wells or linear drains for example?
- Is it possible, as part of groundwater remediation efforts, to locate occasional vertical shafts (drains) in epikarst and focus the aquifer remediation efforts there? (Because the contaminated groundwater in the areas between these occasional drains moves laterally towards the drains and not vertically downward at any appreciable rate.)

Figure 7.40 Examples of folded carbonate sediments. *Left*: Peruvian Andes; photo courtesy of Mark Etienne. *Right*: Folded limestone on Durmitor Mountain, Montenegro; photo courtesy of Predrag Stošić Peca.

An illustrative example of a karst terrain provided by Palmer (2007) may help examine possible answers to these and other practical questions. Figure 7.41 shows the distribution of sinkholes over Blue Spring Cave, Indiana, the United States. The map includes only those sinkholes that appear on the 1:24000 topographic quadrangle. As noted by Palmer, the actual number of sinkholes is <u>several times greater</u> (emphasis added) than is shown on the topographic map. The main passable (non-submerged) passages in the cave are about 8-12 m in diameter. Limestone is exposed at the surface, beneath 2-5 m of soil, over the entire cave. The surface rock unit is mainly the prominently bedded St. Louis limestone. Most of the cave is in the underlying massive Salem Limestone.
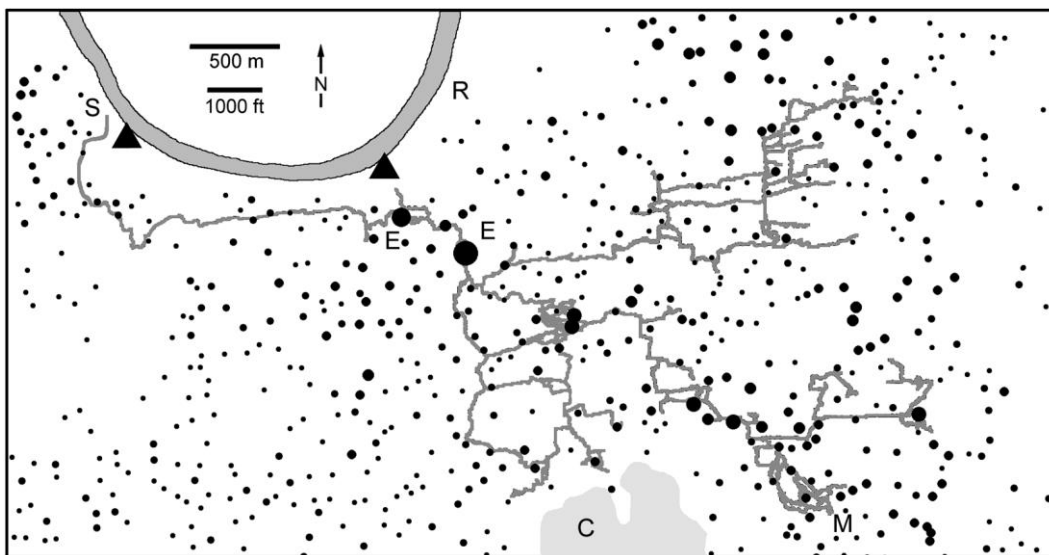
Figure 7.41 Sinkhole distribution over Blue Spring Cave, Indiana. Nearly all sinkholes are in the bedded St. Louis Limestone. The largest penetrate into the underlying prominently jointed Salem Limestone. Cave passages are shown in gray. E = main cave entrances; M = inflow of main cave stream; S = Blue Spring; R = east fork of White River; C = sandstone cap-rock over limestone. Black triangle symbol denotes abandoned spring alcove, largest black dot is sinkhole at least 25 m deep, smallest dot is sinkhole about 3 m deep; intermediate sinkhole depths are shown in proportion to their dot size. From Palmer, 2007; printed with permission from the author.

166

Hundreds of small sinkholes seem to have a random distribution in relation to the cave, but the deepest are located over the main stream passage. The stream in the main passage is an important agent in removing sediment and collapse debris from deep sinkholes. As suggested by Palmer, most of the infiltration in the region enters small sinkholes from where it is drained down by at least one sollutionally enlarged conduit. However, most small sinkholes have no apparent relation to the mapped cave passages, so that it is uncertain where all this water flows.

As suggested by Palmer, it is possible that many such sinkholes drain into small inaccessible passages and, in general, the sinkhole drainage converges into relatively few streams before it joins the traversable parts of the cave (Palmer, 2007).

By reading this brief discussion and by looking at the map in Figure 7.41, it appears that the answer to all previously posed practical questions regarding epikarst would have to be negative, including its very existence. Namely, the density of sinkholes would effectively invalidate the concept and any possibility that there is some significant, continuous, shallow, perched aquifer zone in the area where the flow of groundwater water is mainly horizontal, towards sparce vertical shafts.

Without engaging in additional academic discussions about representative scales of the epikarst hydraulic concept (Is the perched area 100 ft^2, one acre, one hectare, or more? Is the thickness of the saturated epikarst water zone 1ft, 6ft, 15ft, or more? Is the horizontal spacing between possible vertical drains/shafts 50ft, 113ft, 759ft, or more?), this author cautions novice hydrogeologists to carefully design field investigations and continuously monitor groundwater at their site, at various depths. This will enable them to make informed conclusions as to the presence of "perched water in epikarst" and its practical importance for their project. At the same time, it will help them avoid possibly becoming part of a groupthink, not capable of critical thinking.

7.4 Basaltic and Oher Volcanic Rock Aquifers

Volcanic rocks have a wide range of chemical, mineralogical, structural, and hydraulic properties. The variability of these properties is due largely to rock type and the way the rock was ejected and deposited. Pyroclastic rocks, such as tuff and ash deposits (Figure 7.42), might have been placed by flowing of a turbulent mixture of gas and pyroclastic material, or might form as windblown deposits of fine-grained ash. Where they are unaltered, pyroclastic deposits have porosity and permeability characteristics like those of poorly sorted sediments; where the rock fragments are very hot as they settle, however, the pyroclastic material might become welded and almost impermeable. Silicic lavas, such as rhyolite or dacite, tend to be extruded as thick, dense flows and have low permeability except where they are fractured.

Basaltic lavas tend to be fluid and form thin flows that have a considerable amount of primary pore space at the tops and bottoms of the flows. Numerous basalt flows commonly overlap and the flows commonly are separated by soil zones or alluvial material that form permeable zones. Basalts are the most productive aquifers of all volcanic rock types.

The permeability of basaltic rocks is highly variable and depends largely on the following factors: the cooling rate of the basaltic lava flow, the number and character of interflow zones, and the thickness of the flow. The cooling rate is most rapid when a basaltic lava flow enters water. The rapid cooling results in pillow basalt, in which ball-shaped masses of basalt form, with numerous interconnected open spaces at the tops and bottoms of the balls.

Figure 7.42 Field geologist with finger on a nonconformity between underlying volcanic tuff, and overlying debris flow deposits on the island of Santorini (Thera) in Greece. Photo courtesy of Jeff Manuszak.

In the United States, aquifers in basaltic and other volcanic rocks are widespread in Washington, Oregon, Idaho, and Hawaii, and extend over smaller areas in California, Nevada, Wyoming, and Texas. The Snake River Plain regional aquifer system in southern Idaho and southeastern Oregon is a large graben-like structure that is filled with basalt of Miocene and younger age. The basalt consists of many flows, the youngest of which was extruded about 2,000 years ago. The maximum thickness of the basalt, as estimated by using electrical resistivity surveys, is about 5,500 feet (Miller, 1999). The permeability of basaltic rocks is highly variable and depends largely on the following factors: the cooling rate of the basaltic lava flow, the number and character of interflow zones, and the thickness of the flow. The cooling rate is most rapid when a basaltic lava flow enters water. The rapid cooling results in pillow basalt, in which ball-shaped masses of basalt form, with numerous interconnected open spaces at the tops and bottoms of the balls. Large springs that discharge thousands of gallons per minute issue from pillow basalt along the walls of the Snake River Canyon, and elsewhere in the general area of Twin Falls, Idaho such as in Earl M. Hardy Box Canyon Springs Nature Preserve (Figures 7.43 and 7.44; see also Chapter 9 on springs).
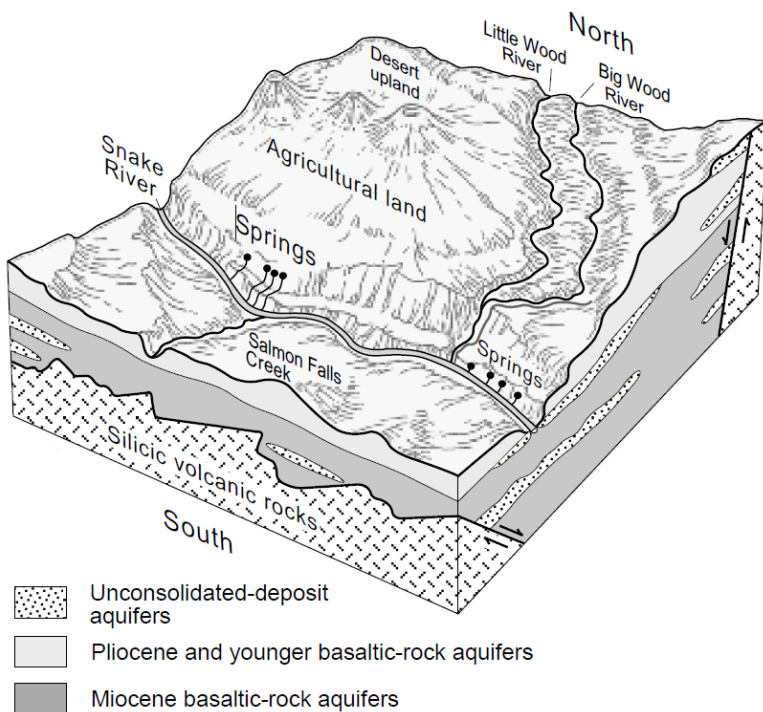
Figure 7.43 Basalt of Miocene and younger age fills the graben-like trough on which the Snake River Plain has formed. Low-permeability, silica-rich volcanic rocks bound the basalt, which is locally interbedded with unconsolidated deposits. From Miller, 1999. USGS, in public domain.

168

Figure 7.44 Box Canyon Spring near Twin Falls, Idaho. *Top*: the spring basin. *Bottom*: closeup of the flow generated by the spring several thousand feet downstream of the basin where it emerges.

In general, permeable but relatively thin rubbly or columnar lavas may act as preferential flow paths but have only limited storage (Figure 7.45). Overlying and underlying thick, porous but poorly permeable, volcanic ash may act as the storage medium for this dual system. The prolific aquifer systems of the Valle Central of Costa Rica and of Nicaragua and El Salvador are examples of such systems (Morris et al., 2003).

In glaciated terrains permeable gravels and sands of outwash plains may be found interbedded with multiple lava flows and volcanic ash deposits resulting in thick prolific, heterogeneous aquifer systems (Figure 7.46).

Figure 7.45 Columnar basalt near Terlingua, Big Bend area, southwest Texas, the United States.

Figure 7.46 Columnar basalt topping Yellowstone River canyon in Wyoming, the United States. Fluvioglacial gravels and volcanic ash are beneath the basalt.

As discussed by Whitehead (1994), Pliocene and younger basaltic rocks are mainly flows but, in many places in the Cascade Range, the rocks contain thick interbeds of basaltic ash, as well as sand and gravel beds deposited by streams and glaciers. Most of the Pliocene and younger basaltic rocks were extruded as lava flows from numerous vents and fissures concentrated along rift or major fault zones in the Snake River Plain. The lava flows spread for as much as about 50 miles from some vents and fissures. Overlapping shield volcanoes that formed around major vents extruded a complex of basaltic lava flows in some places. Thick soil, much of which is loess, covers the flows in many places. Where exposed at the land surface, the top of a flow typically is undulating and nearly barren of vegetation. The barrenness of such flows contrasts markedly with those covered by thick soil where agricultural development is intensive. The thickness of the individual flows is variable; the thickness of flows of Holocene and Pleistocene age averages about 25 feet, whereas that of Pliocene-age flows averages about 40 feet.

In some shield-volcano eruptions, basaltic lava pours out quietly from long fissures instead of central vents and floods the surrounding countryside with lava flow upon lava flow, forming broad plateaus. Lava plateaus of this type can be seen in Iceland, southeastern Washington, eastern Oregon, and southern Idaho. Along the Snake River in Idaho, and the Columbia River in Washington and Oregon, these lava flows are beautifully exposed and measure

more than a mile in total thickness. This geologic environment has in many ways acted hydrogeologicaly as karst because of the existence of sinking streams and the development of integrated networks of overlapping and intersecting lava flows that drain at some of the most spectacular large springs in the United States. Often present in lava flows are interconnected lava tubes at various depths below the water table which may act similarly to karst conduits thus feeding springs of variable discharge rate that react quickly to rainfall events. For this reason, some practitioners describe such an environment as pseudokarst (Figure 7.47).

Figure 7.47 Lava tube in Craters of the Moon National Monument, Idaho, the United States.

Silicic volcanic rocks in the United States are present chiefly in southwestern Idaho and southeastern Oregon where they consist of thick flows interspersed with unconsolidated deposits of volcanic ash and sand. Silicic volcanic rocks also are the host rock for much of the geothermal water in Idaho and Oregon. Big Springs in Fremont County, Idaho is the source of the South Fork of the Henrys Fork River. Designated as a National Natural Landmark in 1980, is the only first-magnitude spring in the United States that emanate from rhyolitic lava flows of the Madison Plateau.

Worldwide, extensive lava flows occur in west-central India, where the Deccan basalts occupy an area of more than 500 000 km^2. Other extensive volcanic terrains occur in Central America, Central Africa, while many islands are entirely or predominantly of volcanic origin, such as Hawaii, Iceland (Figure 7.48) and the Canaries. Some of the older, more massive lavas can be practically impermeable (such as the Deccan) as are the dykes, sills and plugs which intrude them (Morris et al., 2003).

Figure 7.48 Hraunfoss, large springs emerging from a lava flow in Iceland. The country's longest lava tube, Víðgelmir, can be found near the waterfall. This tube is 1,595 m (5,200 feet) long up, to 15.8 m (52 feet) high, and 16.5 m (54 feet) wide. Photo courtesy of William B. White.

7.5 Aquitards

This section is based on materials presented in Kresic (2007, 2009), and Kresic and Mikszewski (2013). Although aquitards play a very important role in groundwater systems, in many cases they are still evaluated qualitatively rather than quantitatively. Field and laboratory research studies have only recently started including the role of aquitards in the fate and transport of various contaminants in the subsurface. A similar effort has yet to materialize in the evaluation of the role of aquitards in the storage of groundwater available for water supply. Aquitards can release ("leak") significant volumes of water to adjacent aquifers which are being stressed by pumping; they can also transfer water from one aquifer to another, both under natural conditions and as a result of artificial groundwater withdrawal. Understanding various roles aquitards can play in a hydraulically stressed groundwater system is especially important when designing artificial aquifer recharge systems and predicting long-term exploitable reserves of groundwater.

One usually thinks of an aquitard, when continuous and thick, and when overlying a highly productive confined aquifer, as a perfect "protector" of the valuable groundwater resource. Various sedimentary, magmatic, and metamorphic rocks can act as aquitards depending on their mineral composition and effective porosity. Clay-rich rocks are always good candidates provided they are relatively extensive (Figure 7.49). However, some professionals would argue that every aquitard leaks, and it is only a matter of time when existing shallow groundwater contamination would enter the confined aquifer and threaten the source. Of course, it does not help anyone (i.e., interested stakeholders) if such professionals rely only on their "best professional judgment" and are much less specific in terms of the "reasonable amount of time" after which the contamination would break through the aquitard. If confronted with some field-based data, such as the thickness and the hydraulic conductivity of the aquitard porous material, they may have the "best" answer ready in hand: "But the measurements did not include flow through the fractures, and we all know that all rocks and sediments comprising an aquitard, including clay, do have some fractures, somewhere."

The truth is, as always, somewhere in between. There are protective *competent* thick aquitards, of high *integrity*, which would not allow migration of shallow contamination to the underlying aquifer for thousands of years or more. Good examples are regional aquitards stretching for hundreds of miles along and off the Atlantic coast of the eastern United States. They prevent downward vertical migration of seawater into the freshwater aquifers utilized for more than 150 years as main sources of water supply for millions of people. If viewed in terms of hundreds of thousands of years or more, this fact may not entirely contradict statements made by some that any aquitard will leak, given enough time. However, such statements, often made because of some underlying agenda such as a lawsuit, should be ignored by working hydrogeologists. Instead, when applicable to the CSM, full attention should be given to site-specific aquitard evaluations.

For example, Hendry and Wassenaar (2010) used high-resolution one-dimensional profiles of naturally occurring environmental tracers (^{3}H, δD, δ^{18}O, ^{14}C-DIC, ^{14}C-DOC, ^{36}Cl, ^{4}He, and major ions) and hydraulic data to study residence times, transport mechanisms, and sources of pore water and solutes in an aquitard system in Saskatchewan, Canada. The aquitard system consisted of 80m of plastic clay-rich Battleford till disconformably overlying 77m of Late Cretaceous plastic marine clay. Individual tracers independently revealed molecular diffusion as the dominant transport mechanism in the unoxidized nonfractured till and clay. This study showed that solute transport in clay-rich aquitards is typically slow with groundwater velocities less than 1 m per 1 thousand years, proving such aquitards are suitable for long-term isolation of most wastes.

Figure 7.49 *Left*: Example of a classic Bouma sequence deposited by a turbidity current within a submarine fan environment. The lighter bands are coarse grained deposits (now sandstone) that fine upward into darker silts and clays (now shale). This outcrop scale photograph also shows a small-scale fault as observed by the truncated bedding (see rock hammer to key into location). The photograph was taken from the Nutzotin Mountain sequence within Wrangell-St Elias National Park and Preserve. *Right*: Outcrop in eastern Alaska illustrating interbedded lithified submarine fine sands (light color) and clay (darker color). The sediments comprising the rock were deposited by successive turbidity flows which form repetitive graded sequences often capped by substantial clay layers. Individual stratigraphic horizons are laterally continuous over tens to hundreds of meters. The continuous layers like these can often form effective aquitards for circulating fluids. Photographs courtesy of Jeff Manuszak.

There also are *leaky* aquitards, of low integrity, which do not prevent such migration for more than several decades or so. Of course, if an aquitard is not continuous, or is only a few feet thick in places, all bets are off. In such cases, the site-specific conditions in the adjacent aquifers would play the key role in contaminant transport. These conditions, in a "worst" case, may include large regional drawdowns caused by pumping in the underlying confined aquifer, and the resulting steep hydraulic gradients between the two aquifers (the shallow and the confined) separated by a discontinuous aquitard (Figure 7.50).

Contamination with dense non-aqueous phase liquids (DNAPLs), which are denser than water, is especially difficult to assess or predict since they can move irrespective of the groundwater hydraulic gradients in an aquifer-aquitard-aquifer system. However, it is surprising how many investigations in contaminant hydrogeology fail to collect more (or any) field information on the aquitard, even though determining its role may be crucial for success of a groundwater remediation project.
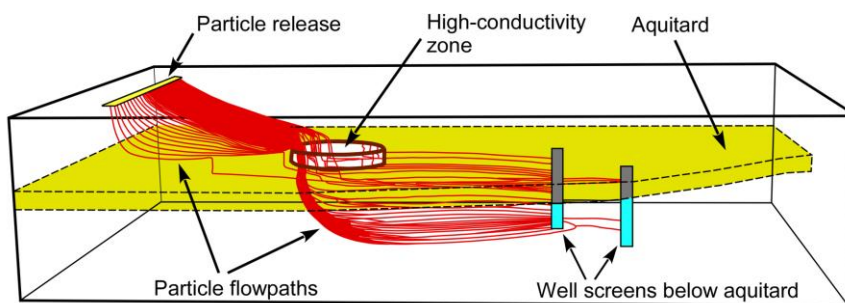
Figure 7.50 Results of a 3D particle tracking model showing the effects of pumping below the aquitard, and a high-conductivity zone (window) in the aquitard on flowpaths of particles released in the shallow aquifer above the aquitard. Modified from Chiang et al., 2002. Printed with permission from the author.

173

The only direct method for determining if actual flow through an aquitard is taking place is dye tracing, but it is of no practical use due to normally very long travel times through aquitards. Several indirect methods, which utilize hydraulic head measurements in the system and chemical and isotopic analyses of water residing in an aquitard, can be used to assess the rates of groundwater movement through it reasonably accurately. However, caution should be used when relying on hydraulic head data collected from monitoring wells that are not completed in the aquitard itself. A difference in the hydraulic heads measured in the overlying and underlying aquifers does not necessarily mean that groundwater is moving between them at any appreciable rate. The existence of the actual flow can be indirectly confirmed only by hydraulically stressing (pumping) one of the aquifers and confirming the obvious related hydraulic head change in the other two units (i.e., including the aquitard itself). When interpreting the hydraulic head changes (fluctuations) caused by pumping, all possible natural causes such as barometric pressure changes or tidal influences should be accounted for.

Figure 7.51 illustrates how possibly misleading conclusions can result from measuring the hydraulic heads at only one depth in the surficial aquifer (say, at MP-4A, where the head is 180.07 ft), and only one depth in the confined aquifer (MP-4F, the head is 61.77 ft). The vertical difference between these two hydraulic heads is 118.3 feet, which may lead one to believe that there must be a significant vertical flow downward through the aquitard caused by such a strong vertical hydraulic gradient (incidentally, the confined aquifer is being pumped for water supply). However, the head difference between the last two ports in the aquifer above the aquitard, at all multi-port wells, is absent for all practical purposes: it is within one hundredth of one foot, upwards or downwards. The flow gradient near the bottom of the upper aquifer is basically horizontal indicating absence of advective flow (free gravity flow) of groundwater from the unconfined aquifer into the underlying aquitard. The higher downward vertical gradients at shallow depths in the unconfined aquifer may be the result of recharge, possibly combined with the influence of some lateral pumping (boundary) in the unconfined aquifer.
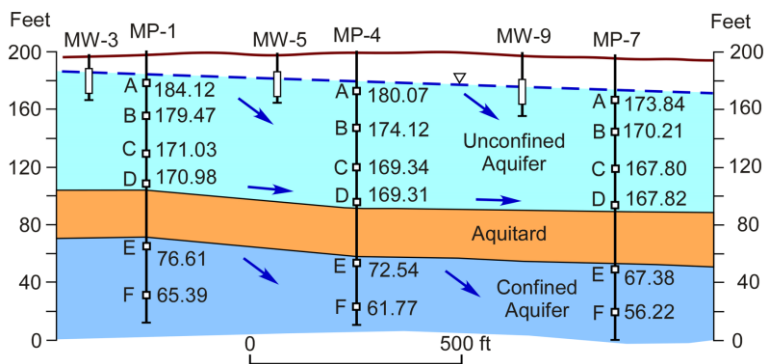
Figure 7.51 Measurements of the hydraulic head at multi-port monitoring wells screened above and below an aquitard. The confined aquifer is being pumped for water supply with an extraction well located approximately 4600 feet from MP-7. Modified from Kresic, 2007. Copyright CRC Taylor & Francis. Permission is required for further use.

When measurements of the hydraulic head are available at various depths within an aquitard, a more definitive conclusion as to the probable rates and velocities of groundwater flow through it can be made, including presence of possibly varying hydraulic head inside the aquitard caused by heterogeneities. Figure 7.52 shows recommended setup of monitoring wells for a long-term aquifer test designed to evaluate characteristics of a confined aquifer and possible interactions with the unconfined aquifer, as well as the integrity of the aquitard that separates them. Continuous measurements of the hydraulic head at different depths within the entire system can be made with cluster wells, with multi- port wells, or with their combination.
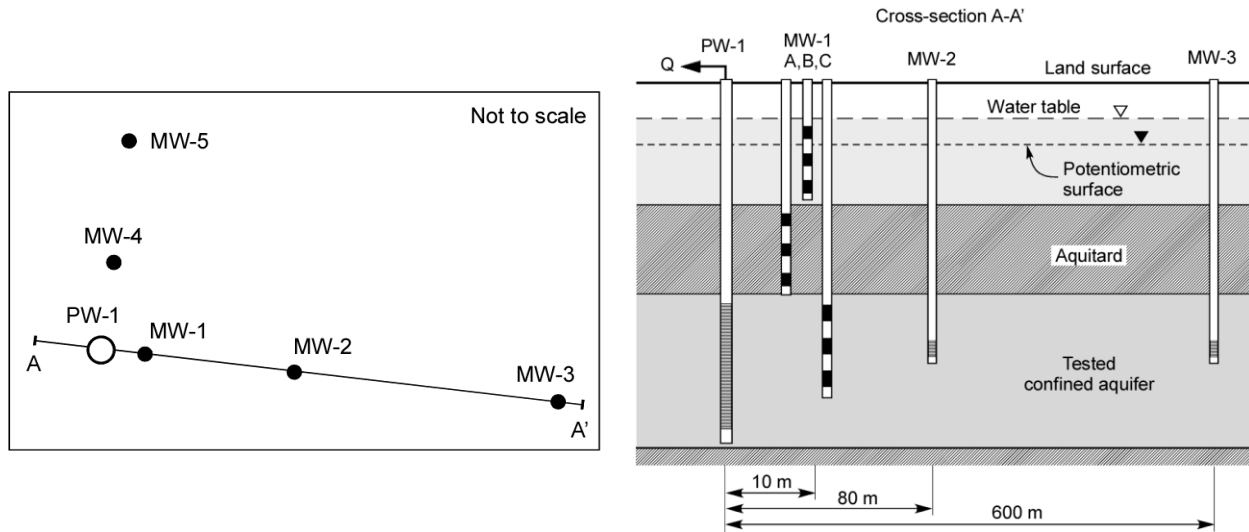
Figure 7.52 An example of a pumping test monitoring well network designed to determine characteristics and anisotropy of the tested confined aquifer, and nature of the aquitard including possible leakage from the aquitard and the unconfined aquifer into the underlying confined aquifer. PW-1: pumping well; MW-1 cluster of multiport wells; MW-2 and MW-3: single screen monitoring wells. *Left*: map view; *Right*: cross-section.

Juana-Diaz Formation in southern Puerto Rico is an example of a thick aquitard of marine origin that still contains highly mineralized water entrapped in the sediment during its original deposition. This formation overlies reef limestone, which contains groundwater with sharply different chemical characteristics (Figure 7.53). Most of the monitoring wells drilled in the Juana-Diaz Formation at the waste disposal site were initially dry or had negligible yields. Little water that did collect in the exposed horizon of a boring was likely through exudation of the trapped connate water with movement initiated by the pressure differences between the corresponding horizon of the formation and the drill-hole.
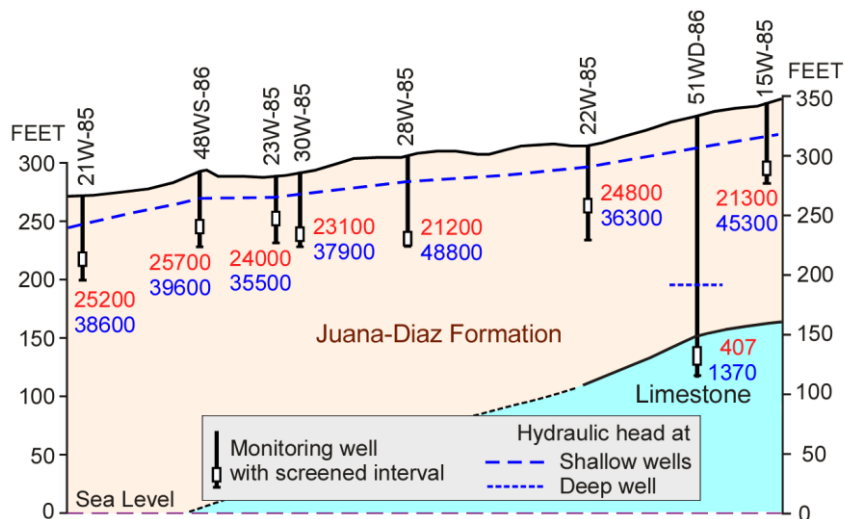
Figure 7.53 Chloride concentrations (top red number) and total dissolved solids (bottom blue number), in milligrams per liter, in groundwater at a waste disposal site in Puerto Rico, United States. Modified from Kresic, 1999. Law Engineering and Environmental Services. Permission is required for further use.

Age dating of this water using environmental isotopes of oxygen and carbon shows groundwater residence time in the Juana-Diaz Formation below the site is on the order of thousands of years. However, the most compelling evidence of the absence of any significant flow in the formation, due to possible present-day flushing with fresh water, is the chemical composition of groundwater: chloride concentrations across the site range from 18500 to

175

25700 mg/L, sulfate concentrations range from 1780 to 4010 mg/L, total dissolved solids range from 31100 to 45300 mg/L, and sodium concentrations range from 4160 to 8270 mg/L. For comparison, average concentrations of these species in seawater are 19000 mg/L for chloride, 2700 mg/L for sulfate, and 10500 mg/L for sodium (Hem, 1989). If the saline groundwater within the formation were moving downward due to free advective (gravity) flow, the concentrations of various constituents in the underlying limestone would have to be much higher, especially considering density differences between the saline water in the Juana-Diaz Formation and the fresh water in the limestone. On the other hand, downward migration of any dissolved constituents that may be entering the Juana-Diaz sediments from the land surface via percolating rainfall, would not be possible due to the same density differences: newly infiltrated low-mineralized water cannot flow through the denser saline water. In conclusion, based solely on the collected hydrochemical information, the Juana-Diaz Formation at the site is a *competent* aquitard that should prevent any migration of potential surficial contamination down to the underlying reef limestone. This includes any possible faults or fractures in the formation since those would also contain saline water.

Sometimes, depending on the contrast in hydraulic conductivity (permeability) between adjacent rocks, a hydrostratigraphic unit that otherwise would not necessarily be considered as one, may play the role of an aquitard. This is illustrated in Figure 7.54 where thinly bedded shaly sandstone is overlain by the massive Cliff House Sandstone in the Mesa Verde National Park, Colorado. Water percolating through the massive sandstone sometimes emerges in form of seeps along this contact.

Figure 7.54 Contact between thinly bedded shaly sandstone and the overlying massive Cliff House Sandstone in the Mesa Verde National Park, Colorado.

Lecture 8 Groundwater Recharge

This lecture is based on the materials presented in Kresic (2007), Kresic and Mikszewski (2009, 2013), and Kresic and Stevanovic (2010.) As discussed in Lecture 1, groundwater recharge terms are often used interchangeably, sometimes causing confusion. In general, *infiltration* refers to any water movement from the land surface into the subsurface. This water is called potential recharge indicating that only a portion of it may eventually reach water table (saturated zone). The term *actual recharge* should be used to avoid any possible confusion: it is the portion of infiltrated water that reaches the aquifer, and it is confirmed based on groundwater studies. The most obvious confirmation that actual groundwater recharge is taking place is a rise in the water table elevation (hydraulic head). However, the water table can also rise due to cessation of groundwater extraction (pumping) and this possibility should always be considered. *Effective infiltration* and *deep percolation* refer to water movement below the root zone and are often equated to the actual recharge. Evapotranspiration (ET; loss of water to the atmosphere) is sometimes called *negative recharge*. ET takes place both above surface (evaporation from various surfaces, transpiration by plants) and in the subsurface (evaporation from the shallow water table and from the vadose zone; water uptake by plant roots). It therefore should be clear what exactly is being evaluated for a particular project and how does it relate to any assessment of the actual groundwater recharge.

Understanding and quantifying recharge processes is the prerequisite for any analysis of the groundwater resources sustainability. Unfortunately, this task is too often reduced to simply estimating a percentage of total annual precipitation that becomes groundwater recharge and then using that percentage as the "average recharge" rate for various calculations or groundwater modeling at all spatial and time scales. However, groundwater recharge is variable at all scales, in both space and time. It is therefore by default that any estimate of recharge involves averaging various quantitative parameters that affect it including their extrapolation-interpolation in time and space. This also means that there will always be a degree of uncertainty associated with quantitative estimates of recharge, and that this uncertainty would also have to be analyzed and quantified. In other words, groundwater recharge is both a probabilistic and a deterministic process: when it rains (laws of probability), the infiltration of water into the subsurface and the eventual recharge of the water table will follow physical (deterministic) laws. At the same time, both sets of laws (equations) use parameters that are either measured directly or estimated in some (preferably quantitative) way but would still have to be extrapolated-interpolated in space and time. For this reason, the quantification of groundwater recharge is one of the most difficult tasks in hydrogeology.

An important initial step in recharge analysis is to consider the scale of the study area since the approach and methods of quantification are directly influenced by it. For example, it may be necessary to delineate and quantify local areas of variable recharge within several acres or tens of acres at an industrial site where groundwater contaminants were introduced into the subsurface. This scale of investigation would obviously not be feasible or needed for groundwater resources assessment at a river basin (watershed) scale. Notably, recharge rate has implications on the shape and transport characteristics of groundwater contaminant plumes. More or less direct recharge from land surface may result in a more or less diving plume respectively, even without significant vertical hydraulic gradients. Different recharge rates also result in different overall concentrations – higher recharge results in lower concentrations (assuming that the incoming water is not contaminated). Figure 8.1 illustrates this point.
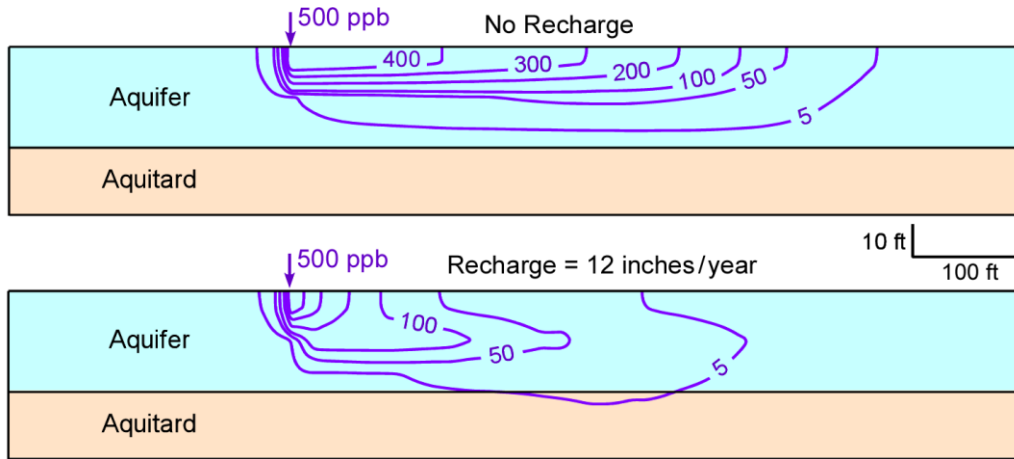
Figure 8.1 Influence of recharge rate on a model-simulated plume, three years after release of a contaminant, cross-sectional view. Constant contaminant concentration at the source, applied at the water table, is 500 ug/L (micrograms per liter, or parts per billion, or ppb). Contour lines are in ppb. Regional hydraulic gradient in the aquifer is from left to right and there is no assigned vertical hydraulic gradient. No retardation, degradation, or adsorption of the contaminant is simulated (see Lecture 13 for the explanation of these terms.) Modified from Kresic, 2007; Copyright CRC Taylor & Francis; permission is required for further use.

Rainwater that successfully infiltrates into the subsurface and percolates past the root zone may sometimes take tens, or even hundreds of years to traverse the vadose zone and reach the water table. The effects of recharge reduction are thus abstract, as groundwater users do not face immediate consequences. As a result, land use changes are often made without consideration of impacts to groundwater recharge.

Natural and anthropogenic climate changes also alter groundwater recharge patterns, the effects of which will be faced by future generations.

8.1 Factors Influencing Groundwater Recharge

8.1.1 Climate

Climate is defined as an aggregate of weather conditions, representing a general pattern of weather variations at a location or in a region. It includes average weather conditions, as well as the variability of elements and information on the occurrence of extreme events. The nature of both weather and climate is expressed in terms of basic elements, the most important of which are: (1) the temperature of the air, (2) the humidity of the air, (3) the type and amount of cloudiness, (4) the type and amount of precipitation, (5) the pressure exerted by the air, and (6) the speed and direction of the wind. These elements constitute the variables by which weather patterns and climatic types are characterized. They all also influence the water budget of an area primarily by affecting natural processes of aquifer recharge, and aquifer discharge via evapotranspiration (Lutgens et al., 2018.)

The main difference between weather and climate is the time scale at which these basic elements change. Weather is constantly changing, sometimes from hour to hour, and these changes create almost an infinite variety of weather conditions at any given time and place. In comparison, climate changes are more subtle and were, until relatively recently, considered important for time scales of hundreds of years or more, and usually only discussed in academic circles. A broader definition of climate is that it represents the long-term behavior of the interactive

climate system, which consists of the atmosphere, hydrosphere, lithosphere, biosphere, and criosphere or ice and snow that are accumulated on the earth's surface (Lutgens et al., 2018). At a minimum, and regardless of the project scale and scope, long-term precipitation data and air temperatures for the closest available climate gauging station should be analyzed as they relate to the site's groundwater. It is also generally recommended to include a rain gauge at hydrogeological study sites, as precipitation can vary greatly over small distances.

The simplest classifications of climate are based on annual precipitation. Strahler and Strahler (1978, p. 129, from Bedinger, 1987) refer to arid climates as having 0 to 250 mm/year (millimeters per year) precipitation, semiarid as having 250 to 500 mm/year precipitation, and subhumid as having 500 to 1,000 mm/year precipitation.

The soil-water balance of Thornthwaite (1948) provides a classification of climate by calculating the annual cycle of soil-moisture availability or deficiency, thus providing measures of soil moisture available for plant growth. Strahler and Strahler (1978) discuss the worldwide distribution of 13 climatic types based on the average annual variations of precipitation, potential evapotranspiration, and the consequent soil-moisture deficit or surplus. Soil-water balance models, which are very similar to the soil-moisture model for classifying worldwide climate, have been developed to estimate recharge. These models utilize more specific data, such as soil type and moisture-holding capacity, vegetation type and density, surface-runoff characteristics, and spatial and temporal variations in precipitation. Various soil-water balance models used in estimating recharge in arid and semiarid regions of the world are discussed by Bedinger (1987) who includes an annotated bibliography of 29 references. The estimated recharge rates have wide scatter, which is attributed to differences in applied methods, real differences in rates of infiltration to various depths and net recharge, and varying characteristics of soil types, vegetation, precipitation, geology, topography, and climatic regime.

8.1.1.1 Precipitation

An example illustrating interconnections between recharge from precipitation and water table fluctuations in a fractured rock aquifer is given by Cressler et al. (1983) and shown in Figure 8.2. In this example, the main period of groundwater recharge results from heavy rains in late winter, when evapotranspiration is low. It is reflected by a peak in the water table hydrograph appearing a few days after heavy rainfall in late March. The time after a storm that the peak appears in the water level is directly related to the vertical hydraulic conductivity of the material in the unsaturated zone and the depth to water table. The hydrograph also shows that little recharge took place during the growing season (April through September) even though the area received significant rainfall during these months. The declining water level indicates continuing groundwater discharge that is not equaled or exceeded by recharge until fall, when evapotranspiration is low.

While the above example represents a very useful form of analysis, it is important to remember that water level fluctuations in a well are not entirely caused by aerial recharge (i.e., recharge from infiltration of precipitation above the well). Local and regional recharge from up gradient areas will cause a water table rise across an aquifer independent of aerial recharge in some locations. It is often counterintuitive to the non-hydrogeologist when a paved area experiences a significant water table rise, for example. For groundwater remediation applications, areas are often paved to limit aerial recharge to support dewatering; however, recharge in other areas of the watershed must also be accounted for to predict the relative impact of the paving on water table fluctuations. Failure to do so may result in the compromise of a dewatering system from unacceptable water table rise.
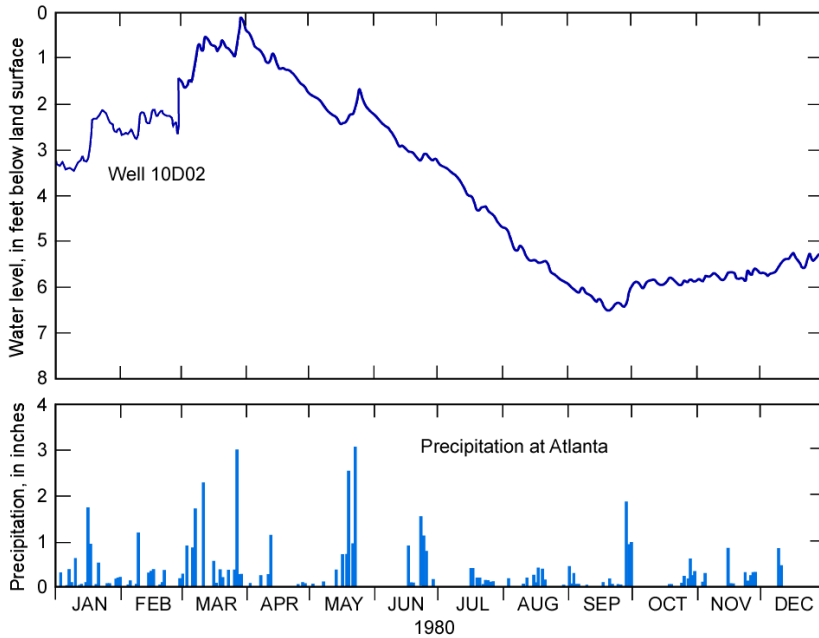
Figure 8.2 An example of response of well water level change to rainfall. From Cressler et al., 1983. USGS, in public domain.

The common limiting factor for many groundwater projects is a relatively short period of site-specific data on the hydraulic head (water table, potentiometric surface) fluctuations. Even when this record is longer than several years for example, it usually has only quarterly water level data thus not allowing for a more detailed analysis of aquifer recharge and its natural cycles. To determine where the site-specific data belong in terms of natural hydrologic and climatic cycles, it is very helpful to analyze long-term data from wells or springs in the same or similar hydrogeologic and climate settings that may be available from government agencies. Figure 8.3 shows daily discharge rate of Annie Spring in Oregon versus daily precipitation at Crater Lake gauging station for 28 years. The graphs illustrate the presence of both long-term and annual natural cycles and, in this case, certain delay in the spring's response to precipitation of about six months. The highest precipitation, mainly in the form of snowfall, is in November-December, whereas the discharge peaks in June following a complete snowmelt. The Annie Spring's hydrologic system behaves like a perfect clock, without any visible long-term trend unrelated to natural periodicity. However, in some other settings such a trend may be present indicating anthropogenic influences including accelerated climate change.

Based on a detailed study of a wide area in the mid-continent United States spanning six states, Dugan and Peckenpaugh (1985) concluded that both the magnitude and proportion of potential recharge from precipitation decline as the total precipitation declines (see Figure 8.4), although other factors, including climatic conditions, vegetation, and soil type also affect potential recharge. The limited scatter among the points in Figure 8.4 indicates a close relationship between precipitation and recharge. Furthermore, the relationship becomes approximately linear where mean annual precipitation exceeds 30 inches and recharge exceeds 3 inches. Presumably, when the precipitation and recharge are less than these values, disproportionably more infiltrating water is spent on filling the moisture deficit in dry soils. The extremely low recharge in the western part of the study area, particularly Colorado and New Mexico, appears to be closely related to the high potential evapotranspiration found in these regions.
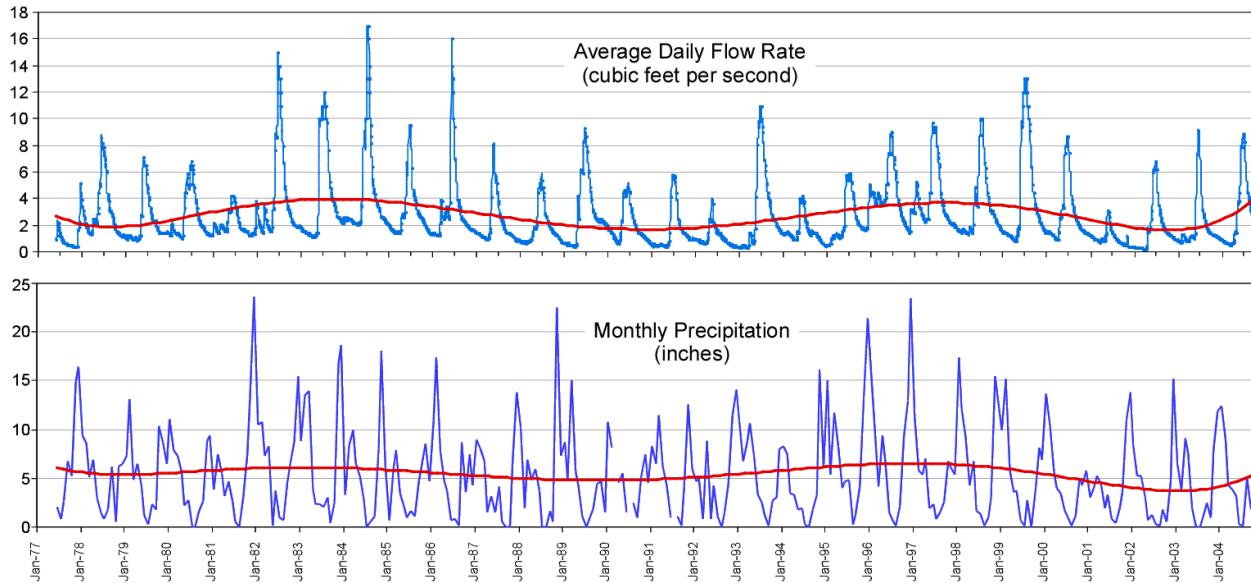
Figure 8.3 Top: Average daily discharge rate, in cubic feet per second (cfs), at the Crater Lake Spring, Oregon (data from USGS, 2008). Bottom: monthly precipitation, in inches, at Crater Lake, Oregon (data from Oregon Climate Service, 2008). The natural periodic cycle is presented with the 6th order polynomial (red) line. Modified from Kresic and Bonacci, 2010. Copyright Elsevier Inc., permission is required for further use,

Seasonal distribution of precipitation also shows a strong relationship to recharge. Areas of high cool-season precipitation tend to receive higher amounts of recharge. Where potential evapotranspiration is low and long winters prevail, particularly in the Nebraska and South Dakota parts of the study area, effectiveness of cool-season precipitation as a source of recharge increases. Overall, however, when cool-season precipitation is less than 5 inches, recharge is minimal. Dugan and Peckenpaugh (1985) conclude that generalized patterns of potential recharge are determined mainly by climatic conditions. Smaller variations within local areas, however, are related to differences in land cover, soil types and topography.
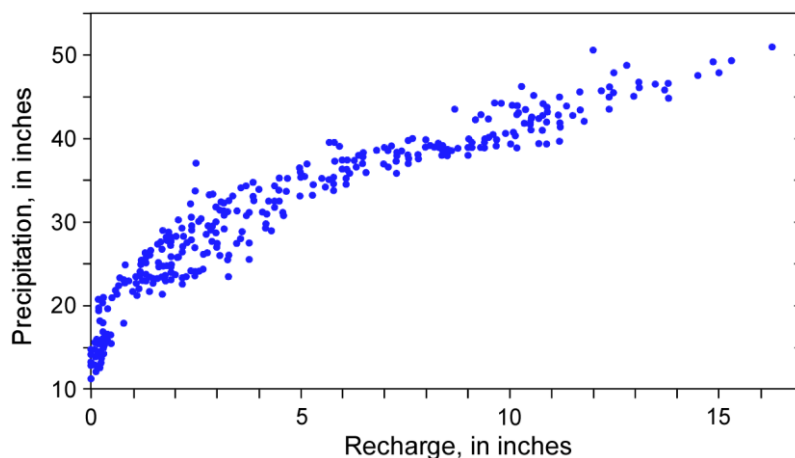
Figure 8.4 Computed mean annual recharge using soil-moisture program versus mean annual precipitation, by model grid element, mid-central United States. Modified from Dugan and Peckenpaugh, 1985. USGS, in public domain.

A large portion of groundwater recharge is derived from winter snowpack, which provides a slow, steady source of infiltration. Topographically higher elevations typically receive more precipitation, including snow, than valleys or basins. Coupled with low potential evapotranspiration (PET) they produce ideal recharge conditions. This fact is especially important in areas such as the Basin and Range province of the United States where the so-called

mountain block recharge (MBR) is critical component of a groundwater system water balance (Figure 8.5; Wilson & Guan, 2004). High-elevation recharge produces the confined aquifer conditions that millions of people rely on for potable water. Snowmelt recharge in mountain ranges occurs in a cyclical pattern, described as follows (Flint and Flint, 2006):

- During the daytime, snowmelt infiltrates thin surface soils and migrates down to the soil-bedrock interface.
- The soil-bedrock interface becomes saturated, and once the infiltration rate exceeds the bulk permeability of the bedrock matrix, moisture enters the bedrock fracture system.
- At night, snow at the ground surface refreezes while stored moisture in surface soils drains into the bedrock.

This wetting-drying cycle of snowmelt recharge minimizes surface water runoff and promotes infiltration. Rapid snowmelt produces surface runoff which also significantly contributes to basin groundwater recharge along the mountain front.
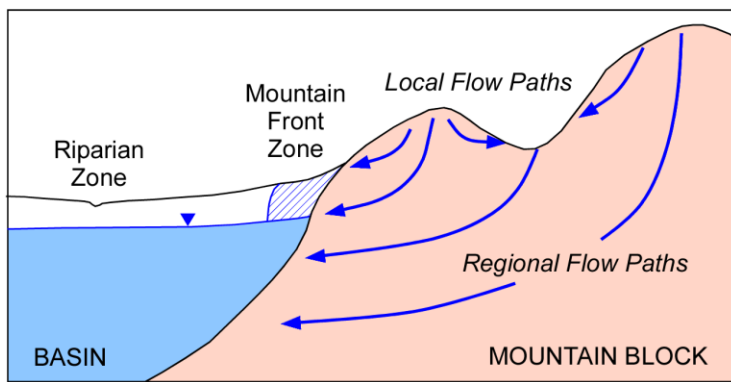
Figure 8.5 Schematic of mountain block contribution to recharge of a groundwater system. From Wilson and Guan, 2004; copyright American Geophysical Union; permission is required for further use.

Snowmelt can provide critical recharge for low-lying areas where potential evapotranspiration (PET) is high. The snowpack in such areas is usually smaller than that at higher elevations, but often snowmelt still provides the vast majority of recharge in a calendar year. Thanks to the presence of a major Department of Energy site, many studies have been conducted in Hanford, Washington, the United States to quantify recharge on the Columbia Plateau. Lysimeters were installed below numerous sites of differing vegetative cover, including sand dunes, grasslands, riparian areas, and agricultural fields. The results revealed that snowmelt plays an integral role in groundwater recharge on the Plateau. During winter months at Hanford, temperatures cool enough to lower PET rates. When temperatures rise above freezing, snowmelt occurs, resulting in infiltration. Rapid snowmelt may lead to ponding of water where slopes are insignificant, creating prolonged infiltration periods (Fayer and Walters, 1995). Years of limited snow cover produce much less recharge than years with extended durations of snow cover—a very important fact when considering the potential impact of climate change on snowpack and groundwater recharge.

Variations of precipitation and air temperature are also very important for recharge. In some years it may never rain (or snow) enough to cause any recharge in semi-arid climates with high PET. Even that portion of rainfall that infiltrates into the shallow subsurface may be evapotranspired back to the atmosphere before it percolates deeper than the critical depth of evapotranspiration. Higher air temperatures cause more evapotranspiration from the shallow subsurface and a higher soil moisture deficit (drier soil).

8.1.1.2 Evapotranspiration (ET)

Just like precipitation, evapotranspiration (ET) depends on general climatic conditions in the study area. Globally, approximately 65 percent of all precipitation falling on landmass returns to the atmosphere through ET, which can be defined as the rate of liquid water transformation to vapor from open water, bare soil, or vegetation with soil beneath (Shuttelwort, 1993). Transpiration is defined as the fraction of total ET which enters the atmosphere from the soil through the plants. The rate of ET, expressed in inches per day or millimeters per day, has traditionally been estimated using meteorological data from climate stations located at points within a region, and parameters describing transpiration by certain types of vegetation. By far most methods for estimating ET are developed for agricultural cropland and the purposes of irrigation with an abundant related literature available. The majority of such methods are based on a rather ambiguous concept of potential evapotranspiration (PET) introduced by Thornthwaite (1946, 1948) which is of little practical use for determining actual ET in most real field settings. PET is defined as the rate at which ET would occur from a large area completely and uniformly covered with growing vegetation which has access to an unlimited supply of soil water and without advection or heat-storage effects.

Potential evaporation, E_0, is the quantity of water evaporated per unit area, per unit time from an idealized, extensive free water surface under existing atmospheric conditions. This is a conceptual entity which measures the meteorological control on evaporation from an open water surface. E_0 is commonly estimated from direct measurements of evaporation with evaporation pans (Shuttelwort, 1993). Note that E_0 is also called potential evapotranspiration (PET) even though as defined it does not involve plant activity.

Reference crop evapotranspiration, E_c, is the rate of evaporation from an idealized grass crop with a fixed crop height of 0.12 m and albedo of 0.23, and a surface resistance of 69 sm^{-1} (Shuttelwort, 1993). This crop is represented by an extensive surface of short green grass cover of uniform height, actively growing, completely shading the ground, and not short of water. When estimating actual evapotranspiration from a vegetated surface it is common practice to first estimate E_c and multiply it by an additional complex factor called the crop coefficient, K_c.

There are many proposed and often rather complex empirical equations for estimating PET using various parameters such as air temperature, solar radiation, radiation exchange for free water surface, hours of sunshine, wind speed, vapor pressure deficit, relative humidity, and aerodynamic roughness (for example, see Singh, 1993; Shuttleworth, 1993; and Dingman, 1994). The main problem in applying empirical equations to a very complex physical process such as evapotranspiration is that in most cases such equations produce very different results for the same set of input parameters. As pointed out by Brown (2000), even in cases of the most widely used group of equations referred to as "modified Penman equations," the results may vary significantly (Penman proposed his equation in 1948 and it has been modified by various authors ever since).

The PET from an area can be estimated from the free water evaporation assuming that the supply of water to the plant is not limited. Actual evapotranspiration, ET_{act}, equals the potential value, PET, as limited by the available moisture (Thornthwaite, 1946). On a natural watershed with many vegetal species, it is reasonable to assume that ET_{act} rates do vary with soil moisture since shallow-rooted species will cease to transpire before deeper-rooted species (Linsley and Franzini, 1979). A moisture-accounting procedure can be established using the continuity equation:

$$P - R - G_0 - ET_{act} = \Delta M \qquad (8.1)$$

where P is precipitation, R is surface runoff, G_0 is subsurface outflow, and ΔM is the change in moisture storage. ET_{act} is estimated as:

$$ET_{act} = E_0 \frac{M_{act}}{M_{max}} \qquad (8.2)$$

where E_0 is potential evaporation, M_{act} is the computed soil moisture stage on any date and M_{max} is an assumed maximum soil moisture content (Kohler, 1958, from Linsley and Franzini, 1979).

In addition to available soil moisture, plant type is another important component of actual evapotranspiration, as certain species require more water than others. A Colorado State University study in eastern Colorado examined the water requirements of different crops in 12 agricultural areas (Broner and Schneekloth, 2007). On average, corn required 24.6 inches/season, sorghum required 20.5 inches/season, and winter wheat required 17.5 inches/season.

Allen et al. (1998) present detailed guidelines for computing crop water requirements together with representative values for various crops. Native vegetation to semi-arid and arid environments is more adept at surviving in low moisture soils and generates much lower ET_{act} values than introduced species. ET_{act} increases with increasing plant size and canopy densities. With regards to stage of development, actively growing plants will transpire at a much greater rate than dormant plants (Brown, 2000). Wind augments PET by actively transporting heat from the air to vegetation, and by facilitating the transfer of water vapor from vegetation to the atmosphere. Humidity and temperature together determine the vapor pressure deficit (VPD), a measure of the "drying power" of the atmosphere. The VPD quantifies the gradient in water vapor concentration between vegetation and the atmosphere. It increases with increasing temperature and decreasing humidity (Brown, 2000.)

The main problem with various PET and ET_{act} calculations is illustrated in Figure 8.6. Namely, the results of this "formal" analysis may imply that during summer months, in many climatic settings including temperate humid climates, there should be no net aquifer recharge from rain since ET exceeds the amount of available rainfall. This, of course, is not the case as the recharge occurs throughout calendar year, including the summer months, and its magnitude will also depend on other factors such as the soil type (land cover), topography, and geology. For example, clean uniform sand, gravel, or barre, karstified limestone will quickly infiltrate large percentage of rainfall during summer storms deeper into the subsurface, pass the root zone.
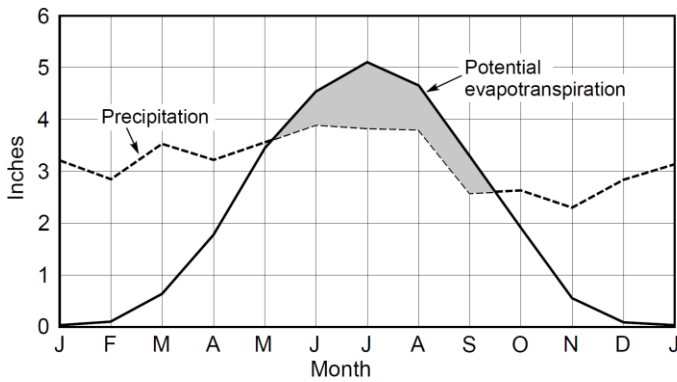
Figure 8.6 Monthly precipitation and adjusted potential evapotranspiration for Lewisburg, West Virginia calculated by the Thornthwaite (1948) method. From Jones, 1977. Copyright Karst Waters Institute. Permission is required for further use.

Based on statistical analysis of 254 drainage areas from around the world, Turc proposed the following simple method of estimating ET_{act} from precipitation and air temperature data (Gray, 1973):

$$ET_{act} = \frac{P}{\left[0.90+\left(\frac{P}{I_T}\right)^2\right]^{1/2}} \qquad (8.3)$$

where P is the annual precipitation (mm), I_T is the evaporative capacity of air $= 300+25T+0.05T^3$, T is the average annual air temperature (ºC).

For a shorter period of 10 days, ET_{act} is determined using a more complex equation which takes into account soil moisture and crop type:

$$ET_{act} = \frac{P+E_{10}+K}{\left[1+\left(\frac{P+E}{I_T}+\frac{K}{2I_T}\right)^2\right]^{1/2}} \qquad (8.4)$$

where E_{10} is the estimated evaporation from bare soil, not higher than 10 mm, during 10 days without precipitation, P is the actual precipitation during the 10-day period, and I_T is the evaporative capacity of air given as

$$I_T = \frac{(T+2)\sqrt{R_{si}}}{16} \qquad (8.5)$$

where T is the average air temperature in the 10-day period (°C), and R_{si} is the incoming solar energy (cal/cm²/day). K is the crop factor given as

$$K = 25\left(\frac{Mc}{G}\right)^{1/2} \qquad (8.6)$$

where M is the final growth of dry matter (kg/ha), c is the crop constant (1.33 for short grass), and G is the length of vegetative period (days).

Figure 8.7 shows regional PET patterns across the continental United States. The highest PET values are found in areas of high temperatures and low humidity, such as the deserts of southeastern California, southwestern Arizona, and southern Texas (Healy et al., 2007). Mountainous regions exhibit low PET values due to colder temperatures and the prevalence of moist air. It is interesting that southern Florida has remarkably high PET rates rivaling those in desert environments. This may be attributable to the dense vegetative cover of the sub-tropical Florida landscape, or the more seasonal trends in annual precipitation (i.e., more defined rainy and dry seasons.)

A very detailed study of evapotranspiration rates by vegetation in the spring-fed riparian areas of Death Valley, United States area was performed by the United States Geological Survey. The study was initiated to better quantify the amount of groundwater being discharged annually from these sensitive areas and to establish a basis for estimating water rights and assessing future changes in groundwater discharge in the park (Laczniak et al., 2006).
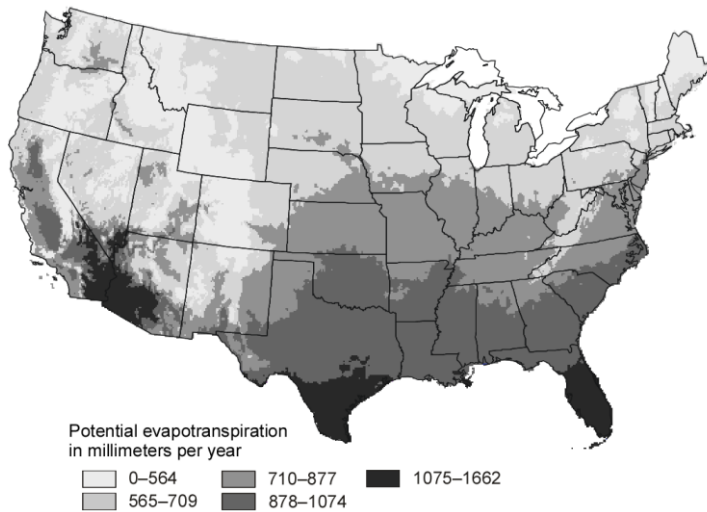
Figure 8.7 Potential evapotranspiration (PET) map of the continental United States. From Healy et al., 2007. USGS, in public domain

Evapotranspiration (ET) was estimated volumetrically as the product of ET-unit (general vegetation type) acreage and a representative ET rate. ET-unit acreage was determined from high-resolution multi-spectral imagery; and a representative ET rate was computed from data collected in the Grapevine Springs area using the Bowen-ratio solution to the energy budget, or from rates given in other ET studies in the Death Valley area. The groundwater component of ET was computed by removing the local precipitation component from the ET rate.
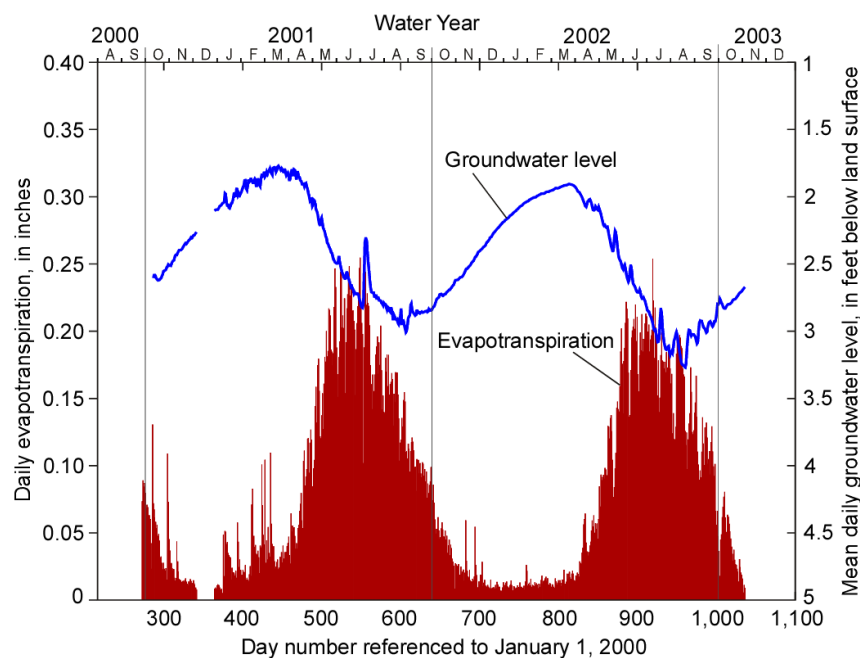
Figure 8.8 Daily evapotranspiration and mean daily groundwater level at Grapevine Springs ET site, September 28, 2000–November 3, 2002 (day numbers 272 and 1,038, respectively). From Laczniak et al., 2006. USGS, permission is required for further use.

The results of the study show that ET at the Grapevine Springs site generally begins increasing in late spring and peaks in the early through mid-summer period (June and July). During this peak period, daily ET ranged from about 0.18 to 0.25 inches (Figure 8.8), and monthly ET ranged from about 5.7 to 6.2 inches. ET totaled about 2.7 feet in water year 2001 and about 2.3 feet in water year 2002. The difference in precipitation between the two water years is nearly equivalent to the difference in annual ET. Annual trends in daily ET show an inverse relation with water levels—as ET begins increasing in April, water levels begin declining, and as ET begins decreasing in September, water levels begin rising. The slightly greater ET and higher water levels in water year 2001 compared with water year 2002 are assumed to be a response to greater precipitation. The groundwater component of ET at the Grapevine Springs ET site ranged from 2.1 to 2.3 feet, with the mean annual groundwater ET from high-density vegetation being 2.2 feet (Laczniak et al., 2006).

8.1.2 Geology and Topography

When soil cover is thin or absent, the lithologic and tectonic characteristics of the bedrock play dominant roles in aquifer recharge. Fractured bedrock surface and steep or vertical bedding greatly increase infiltration, while layers of sparsely fractured, low-permeable bedrock sloping at the same angle as the land surface may almost eliminate it (Figure 8.9.) Barre karst areas, where rock porosity is greatly increased by dissolution (Figure 8.10 *Left*), or dissected karst relief without surface streams (Figure 8.10 *Right*) generally have the highest infiltration capacity of all geologic media.

Figure 8.9 Influence of bedding dip and angle on infiltration (aquifer recharge). *Middle*: Steeply dipping beds enhance infiltration and aquifer recharge. *Right*: Layers of slate dipping at a similar angle as the hill slope greatly reduce infiltration.

Figure 8.10 *Left*: "Karren Jungle", intensively dissolved barre limestone on the Kačanik Mountain, Montenegro. Photo courtesy of Dobrisav Bajović Bajone. *Right*: Sinkholes in Monroe County, West Virginia. Photo courtesy of William Jones.

Steeper slopes, with the uniform vegetative cover and soil permeability, generally have more runoff and less infiltration. Depressions in land surface collect runoff and retain water longer thus enhancing infiltration. Topography also plays significant role on the general influence of various climate factors: In most regions of the world precipitation increases with elevation due to uplifting of the horizontally moving air masses when they encounter a topographic barrier. As the air masses move up and flow over the barrier, they cool down and precipitate an increasing amount of rain and snow. The downward movement of air on the lee side causes adiabatic warming which dissipates the clouds and creates a rain shadow (Figure 8.11.) Although this orographic effect exhibits many variations based on local characteristics (e.g., wind speeds, steepness, and height of the barrier), it commonly accounts for much of the spatial variation of precipitation and must be considered when estimating average precipitation over an area. If there are not enough gauging stations at different altitudes in the drainage area with a significant relief difference, simple contouring of precipitation would likely produce inaccurate estimates unless appropriate corrections were made.
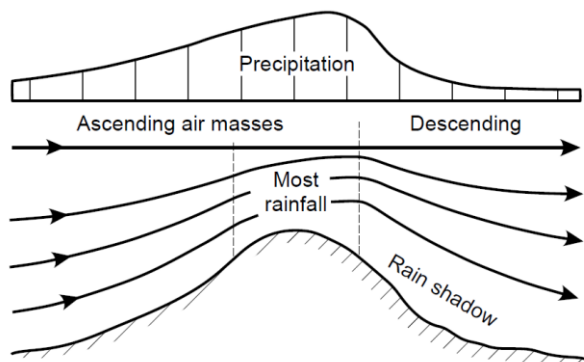
Figure 8.11 Influence of topography on precipitation, the so-called orographic effect. From Jevdjević, 1956. University of Belgrade. Acknowledgement required for further use.

187

As discussed by Dingman (1994), the orographic effect can carry over into many hydrologic relations. For example, average streamflows, dry season streamflows, and floods were all significantly related to elevation in central New England, USA.

8.1.3 Land Cover and Land Use

The quantity and quality of groundwater are profoundly affected by the historic and current land use and land cover at both regional and local scales. Understanding historic land use/land cover and comparing it with the current and projected land use/land cover is therefore of critical importance to the project at hand. Three main trends in land use and the associated human-induced changes in land cover have been taking place worldwide and disrupting natural hydrologic cycles:

(1) Conversion of forests into agricultural land.

(2) Rapid urbanization in undeveloped and developing countries converting all other land uses into urban land.

(3) Rapid decentralization of cities (i.e., suburbanization) and reforestation of former agricultural land, particularly in the United States and other developed countries.

Urban development and the creation of impervious surfaces beyond a city core inevitably result in increase of runoff and soil erosion. In turn, this reduces infiltration potential and groundwater recharge. Increased sediment load carried by surface streams often results in the formation of fine-sediment deposits along stream channels which reduces hydraulic connectivity and exchange between surface water and groundwater in river flood plains. Clear-cutting of forests also alters the hydrologic cycle and results in increased erosion and sediment loading to surface streams. Conversion of low-lying forests into agricultural land may increase groundwater recharge, especially if it is followed by irrigation (although it is important to remember that often such recharge is "irrigation return," and the origin of water may be the underlying aquifer in question; irrigation return may be a small fraction of the groundwater originally pumped). In contrast, cutting of forests in areas with steeper slopes will generally decrease groundwater recharge because of the increased runoff, except in cases of very permeable bedrock such as karstified limestone.

In general, urban development results in decreased infiltration rates and increased surface runoff because of the increasing area of various impervious surfaces (rooftops, asphalt, concrete). However, the infiltration rate varies significantly within an urban area based on actual land use. This is particularly important when evaluating fate and transport of contaminant plumes, including development of groundwater models for such diverse areas. For example, a contaminant plume may originate at an industrial facility with high percentage of impervious surfaces resulting in negligible infiltration, and then migrate towards a residential area where infiltration rates may be rather high because of the open space (yards) and watering of lawns. By eliminating infiltration as a driving force, paving and rooftops may play a positive role in preventing further downward migration of contaminants through the vadose zone. In undeveloped countries, where the booming of megacities and associated slums causes many societal and environmental problems, groundwater recharge rates may actually increase due to leaky water lines and unregulated sewage disposal, contaminating groundwater resources (particularly shallow and dug wells) and adding yet another problem to the list.

Agricultural activities have had direct and indirect effects on the rates and compositions of groundwater recharge and aquifer biogeochemistry. Direct effects include dissolution and transport of excess quantities of fertilizers and associated materials, and hydrologic alterations related to irrigation and drainage. Some indirect effects include changes in water–rock reactions in soils and aquifers caused by increased concentrations of dissolved oxidants, protons, and major ions. Agricultural activities have directly or indirectly affected the

concentrations of many inorganic chemicals in groundwater, such as NO_3^-, N_2, Cl, $SO4^{2-}$, H^+, P, C, K, Mg, Ca, Sr, Ba, Ra, and As, as well as a wide variety of pesticides and other organic compounds (Böhlke, 2002; see also Figure 8.12.)

Figure 8.12 *Left*: Wearing protective gear is part of handling toxic farm chemicals safely. Courtesy of Tim McCabe, National Resources Conservation Service (NRCS.) *Right*: Pesticide application on leaf lettuce in Yuma, Arizona. Courtesy of Jeff Vanuga, NRCS. In public domain.

For hazardous waste site investigation and remediation, the current and historical industrial/commercial land uses at a site comprise what is typically termed the "facility profile" of the conceptual site model (CSM). The nature of manufacturing processes and historical waste handling practices must be understood to identify potential contaminants and their disposal locations. Historical aerial photographs are often useful in identifying former burn pits, infiltration ponds, surface water discharge points, and lagoons/cesspools. In New England, which has long been a manufacturing center, legacy contamination at hazardous waste sites may date back to the 1700s. In many cases, these sites have been converted for different industrial uses over time, leading to a wide variety of potential contaminants that could be found in soil or groundwater. A classic example is the use of mill buildings dated from the 1700s-1800s for electronics or other manufacturing purposes in the 1950s through the 1970s. Metals contamination may be caused by the former use, while chlorinated solvents contamination may be caused by the latter. The presence of urban fill material at such sites from different eras, involving various workings and re-workings of the surface topography, may also complicate the CSM as contaminant origins may be unclear.

The impact of vegetative cover on recharge also depends on climatic variations. In drier and warmer years plants will uptake a higher percentage of the infiltrated water than during average years, and this will also vary for different plant species. What all this means is that the relationship between precipitation and actual groundwater recharge is not linear; simply adopting values of certain quantitative parameters measured during one or two years as representative of the long-term groundwater recharge would be erroneous. Figure 8.13 illustrates some of the above points. Recharge rates for a 30-year period were simulated for different vegetation covers based on extensive site-specific, multi-year field analyses of various soil properties, vegetation root density, root water uptake, and infiltration rates (Fayer and Walters, 1995.). The starting point for all three simulations was the same soil water content in 1957. The model-simulated recharge rates show two orders of magnitude difference in recharge for soil with bunchgrass, compared to one order of magnitude difference for non-vegetated soil. At the same time, there is much less overall variation in recharge for the vegetated than for the non-vegetated soil.
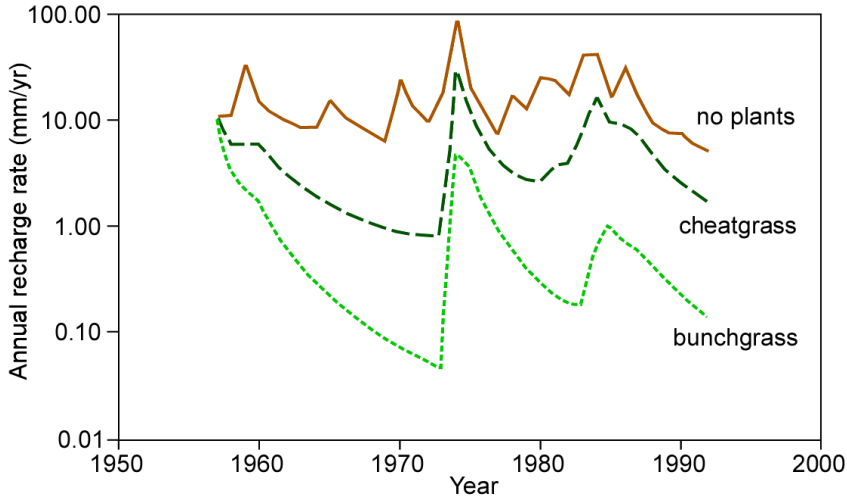
Figure 8.13 Simulated recharge rates for Ephrata sandy loam and three different vegetation covers, Hanford Site, Washington, the United States. Modified from Fayer and Walters 1995. Pacific Northwest National Laboratory, in public domain.

The bare soil surface can become encrusted with, or sealed by, the accumulation of fines or other arrangements of particles that prevent or retard the entry of water into the soil. As rainfall starts, the fines accumulated on bare soil may coagulate and strengthen the crust and/or enter the soil pores and seal them off. A soil may have excellent subsurface drainage characteristics but still have a low infiltration rate because of the retardant effect of surface crusting or sealing (King, 1992). This low-permeable crust is the main reason why bare soil has lower infiltration capacity than soil with vegetative cover. Consequently, bare soil is much more easily eroded by surface runoff. Presence of vegetation protects the soil surface from the impact of rainfall. Root systems of vegetation tend to enhance soil porosity and permeability. Organic matter greatly increases pore sizes and pore-size distribution (King, 1992).

The influence of different land cover on aquifer recharge is illustrated in Table 8.1. Urban areas and development generally decrease infiltration rates and increase surface runoff because of the increasing presence of various impervious surfaces (rooftops, asphalt, concrete). However, as illustrated in Table 8.1, infiltration rate varies significantly within an urban area based on actual land use. This is particularly important when evaluating fate and transport of contaminant plumes, including development of groundwater models for such diverse areas. For example, a contaminant plume may originate at an industrial facility with high percentage of impervious surfaces resulting in hardly any actual infiltration, and then migrate towards a residential area where infiltration rates may be rather high because of the open space (yards), various vegetative cover, and watering of lawns.

Table 8.1 Estimates of mean annual recharge based on mean annual precipitation, generalized surficial geology, and land-use and land-cover categories from the Willamette Lowland Regional Aquifer System Analysis. Modified from Lee and Risley, 2002. USGS, in public domain.

Land use and land cover	Area (mi^2)	Precipitation (in/year)	Recharge (in/year)	Recharge %
Undeveloped and nonbuilt-up	641	44.2	24.1	54.5
Residential	13	43.3	12.7	29.3
Built-up	35	45.0	13.3	29.6
Urban	99	43.7	8.1	18.5
All categories	788	44.2	21.4	48.4

8.2 Rainfall-Runoff Relationship

Most natural groundwater recharge is derived directly from rainfall and snowmelt that infiltrate into the subsurface and migrate to the water table. To quantify recharge from precipitation, it is important to understand rainfall-runoff relationships. Rainfall will infiltrate the subsurface until the rate of precipitation exceeds the infiltration capacity of the soil, at which point ponding and subsequent surface runoff will occur. Runoff either collects in discrete drainage channels or moves as overland sheet flow. The infiltration continues throughout the storm event, even as runoff is being produced. The infiltration rate after ponding begins to decrease and asymptotically approaches the saturated hydraulic conductivity of the soil media. Figure 8.14 illustrates a typical infiltration curve for a homogeneous uniform soil which shows a constant infiltration rate while it is higher than rainfall intensity, and the topsoil horizon is still not completely saturated (the horizontal portion of the curve.) Once the topsoil horizon is saturated, the ponding at the land surface occurs and the surface runoff starts. This start of surface runoff happens at the ponding time (t_p; the time since the start of rainfall.) The infiltration capacity then decreases with time and eventually reaches the saturated hydraulic conductivity of the soil (K_s). For example, the infiltration patterns for four different rainfall events for the same soil with the saturated hydraulic conductivity of 0.001 cm/s are shown in Figure 8.15. Notably, the precipitation rate that is less than the saturated hydraulic conductivity (dotted red line) will result in no ponding and a constant infiltration rate equal to the precipitation rate.
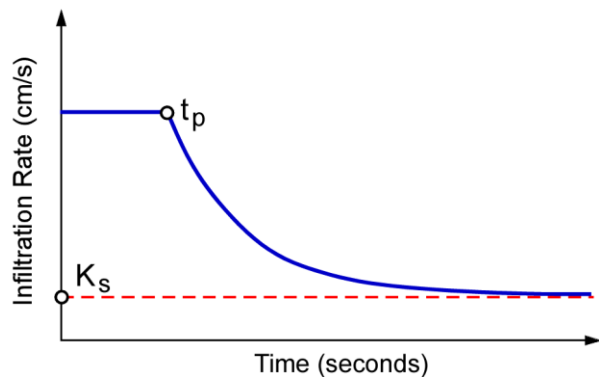
Figure 8.14 Infiltration curve for a homogeneous uniform soil with saturated hydraulic conductivity of K_s. The ponding time (t_p) is the time since the beginning of rainfall when the topsoil becomes fully saturated and the ponding at the land surface and surface runoff start. Modified from Kresic, 2007. Copyright CRC Francis & Taylor, permission is required for further use.

Key to the rainfall-runoff relationship is the soil type, the antecedent moisture condition, and the land cover. Soils that are well-drained generally have high effective porosities and high hydraulic conductivities (such as sands and gravels), whereas soils that are poorly drained (such as clays) have higher total porosities and lower hydraulic conductivities. These physical properties combine with the initial moisture content to determine the infiltration capacity of surficial soils. Wet, poorly drained soils (e.g., clayey soils) will readily produce runoff, while dry, well-drained soils (e.g., clean sands and gravels) will readily absorb rainfall. Land cover determines the fraction of precipitation available for infiltration. Impervious, paved surface prevent any water from entering the soil column, while bare to vegetated fields are conducive to infiltration.

Simple calculations of runoff and water retention volumes in a watershed are often performed using the U.S. Department of Agriculture Soil Conservation Service (SCS) Runoff Curve Number (CN) method, updated in Technical Release 55 (TR-55) of the U.S. Department of Agriculture (2009). TR-55 presents simplified procedures for estimating direct surface runoff and peak discharges in small watersheds. While it gives special emphasis to urban and urbanizing watersheds, the procedures apply to any small watershed in which certain limitations are met.

Hydrologic studies to determine runoff and peak discharge should ideally be based on long-term stationary streamflow records for the area. Such records are seldom available for small drainage areas. Even where they are

available, accurate statistical analysis of them is usually impossible because of the conversion of land to urban uses during the period of record. It therefore is necessary to estimate peak discharges with hydrologic models based on measurable watershed characteristics.
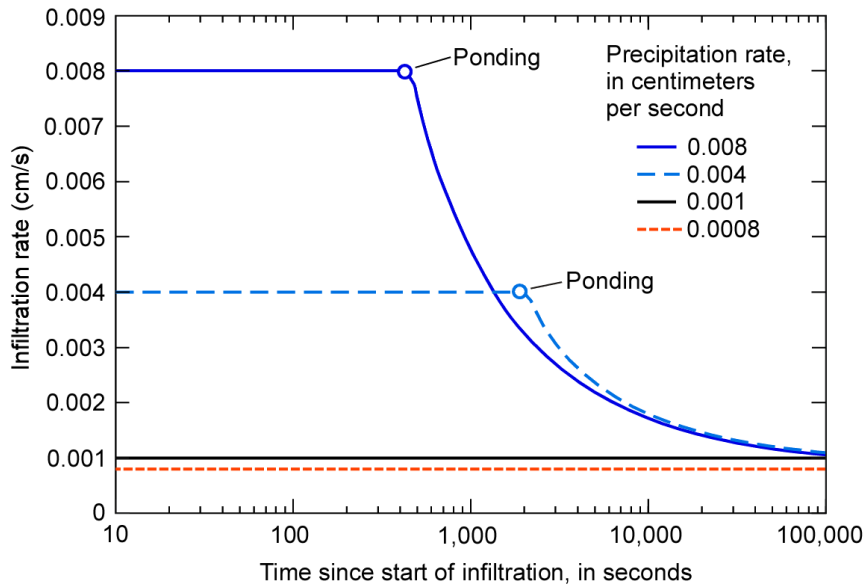
Figure 8.15 Infiltration in a one-dimensional soil column for four different rainfall intensities and a soil with saturated hydraulic conductivity of about 0.001 cm/s. Modified from Heally et al., 2007. USGS, in public domain.

In TR-55, runoff is determined primarily by amount of precipitation and by infiltration characteristics related to soil type, soil moisture, antecedent rainfall, cover type, impervious surfaces, and surface retention. Runoff travel time is determined primarily by slope, length of flow path, depth of flow, and roughness of flow surfaces. Peak discharges are based on the relationship of these parameters and on the total drainage area of the watershed, the location of the development, the effect of any flood control works or other natural or manmade storage, and the time distribution of rainfall during a given storm event.

While the SCS method enables calculation of runoff, it does not provide for exact estimation of infiltration, which is only one of the calculated overall water retention components. The calculated volume of water retained by the watershed includes terms for evapotranspiration and interception by vegetation. Knowledge of the vegetative conditions of the watershed in question will help determine the distribution of rainfall retention.

8.3 Methods for Estimating Groundwater Recharge

As discussed by Kresic and Mikszewski (2009), direct quantitative measurements of groundwater recharge flux reaching the water table and expressed as volume per time (e.g., ft^3/day or m^3/day) are either cost-prohibitive or not feasible. Installation, operation, and maintenance of lysimeters, which are the only devices capable of direct measurement of the recharge flux in vadose zone, is very expensive. Moreover, because of the inherent heterogeneity of soils, many lysimeters would be needed for any reliable estimate of recharge at a scale greater than the extent of one single lysimeter. In semi-arid and arid regions with deep water tables, installation of lysimeters is not feasible. Likely because of these simple facts every now and then a prominent hydrogeologist has to remind decision-makers that "Project designs and management strategies need to be flexible enough not to require radical change if initial predictions prove wrong, due to incorrect assumptions about recharge rates and

other hydrogeological factors." (Foster, 1988). Similarly, "Groundwater recharge estimation must be treated as an iterative process that allows progressive collection of aquifer-response data and resource evaluation. In addition, more than one technique needs to be used to verify results." (Sophocleous, 2004).

Indirect estimates of groundwater recharge have numerous limitations, particularly in arid environments. First and foremost, calculations are highly sensitive to changes in physical and empirical matric head-moisture curve fit parameters. This problem is exacerbated at low moisture contents in arid environments, where order of magnitude changes in flux result from small variations in physical measurements. These difficulties are especially problematic for the Darcian and numerical modeling methods, which rely on limited point measurements of pressure head, unsaturated hydraulic conductivity, and moisture content (these terms are explained in detail in Lecture 9.) The water table fluctuation method experiences similar problems in semi-arid settings due to the significant time lag between infiltration at the ground surface and a corresponding rise in the water table (Sophocleous, 2004).

Another major problem with indirect physical methods is their reliance on idealized, theoretical equations which do not accurately depict flow mechanisms in the vadose zone. It has been known for decades that infiltration occurs in form of an uneven front even in seemingly homogeneous soils. This can be explained by several different mechanisms that can form such preferential flow paths ("channeling"): wormholes, fractures, dendritic networks of enhanced moisture, and contact points of differing soil media (Nimmo, 2007). Water velocity through these "macropores" is often an order of magnitude greater than movement through the soil matrix. The macropores issue may further complicate measurement in semi-arid and arid environments, where normally dry fractures may only become activated after threshold rainfall events. In humid environments, higher moisture contents persist in surface soils and there is less sensitivity with regards to pressure head and unsaturated hydraulic conductivity. The water table fluctuation method is also more useful as immediate changes in water table elevation are visible after recharge events (Sophocleous, 2004). To summarize, indirect physical methods are better suited in humid climates where water managers can have a better handle on the water balance. Heterogeneity and hydraulic sensitivity dominate semi-arid and arid environments, where the influence of preferential flow through macropores further compromises accuracy of recharge estimates. When measured physical parameters fall in the dry range, recharge flux calculations are often in error by at least an order of magnitude (Sophocleous, 2004). Illustrative examples how to choose appropriate techniques for quantifying groundwater recharge are given by Scanlon et al. (2002).

8.3.1 Water Table Fluctuations

Rise in water table after rainfall events is the most accurate indicator of actual aquifer recharge. It can also be used to estimate the recharge rate which is assumed to be equal to the product of water table rise and specific yield (Figure 8.16):

$$R = S_y \Delta h \qquad (8.7)$$

where R is recharge (dimension of length, e.g., inches); S_y is specific yield (dimensionless); Δh is water table rise (dimension of length).
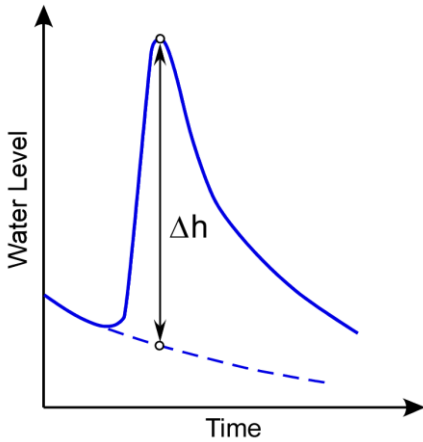
Because of its simplicity and general availability of water level measurements in most groundwater projects, the water-table fluctuation method may be the most widely used method for estimating recharge rates in humid regions (Healy and Cook, 2002). The main uncertainty in applying this approach is the value of specific yield which in many cases would have to be assumed.

Figure 8.16 Principle of water table fluctuation method. Copyright McGraw Hill, permission is required for further use.

An important factor to consider when applying the water table fluctuation method is water level measurement frequency. Delin and Falteisek (2007) point out that measurements made less frequently than about once per week may result in as much as a 48 percent underestimation of recharge based on an hourly measurement frequency (Figure 8.17).
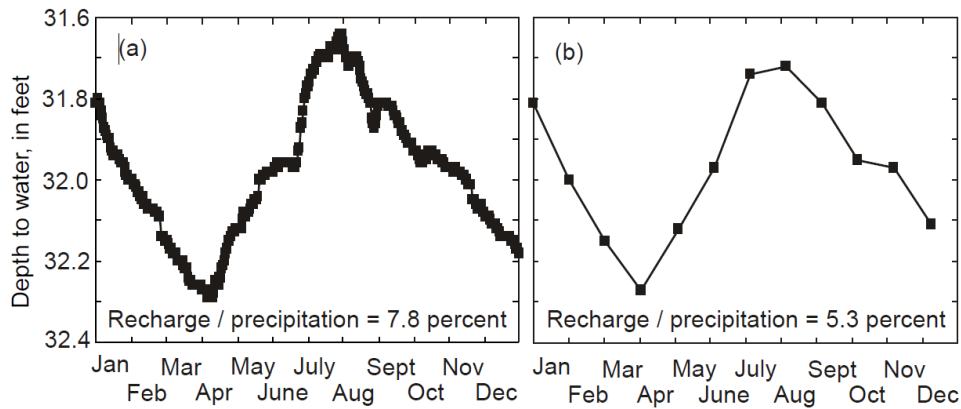
Figure 8.17 Hydrographs and recharge estimates for a well near Bemidji, Minnesota, the United States, for calendar year 2002 based on the water-table fluctuation method and a water-level measurement frequency of once every (a) day, (b) month. Modified from Delin and Falteisek, 2007. USGS, in public domain.

Zaidi et al. (2007) use the double water-table fluctuation method and an extensive network of observation wells to calculate water budget for a semi-arid crystalline rock aquifer in India. The monsoonal character of rainfall in the area allows division of the hydrologic year into two distinct dry and wet seasons and application of the following water budget equation twice a year:

$$R + RF + Q_{in} = E + PG + Q_{out} + S_y \Delta h \qquad (8.8)$$

where two parameters, natural recharge, R, and specific yield, S_y, are unknown. Water-table fluctuations, Δh, are measured, and other components of the water budget are independently estimated: RF is the irrigation return flow, Q_{in} and Q_{out} are horizontal inflows and outflows in the basin respectively, E is evaporation, and PG is groundwater extraction by pumping. The method is called the "double water-table fluctuation" because the equation is applied

194

two times (for wet and dry season) so that both unknowns (recharge and specific yield) can be solved. This eliminates inaccuracies associated with estimating specific yield at large field scales.

8.3.2. Stream Baseflow Separation

A surface stream hydrograph is the final quantitative expression of various processes that transform precipitation into stream flow. Separation of the surface stream hydrograph is a common technique of estimating the individual components that participate in the flow formation. Theoretically, they are divided into: flow formed by direct precipitation over the surface stream, surface (overland) runoff collected by the stream, near-surface flow of the newly infiltrated water (also called underflow), and groundwater inflow. However, it is practically impossible to accurately separate all these components of stream flow generated in a real physical drainage area. In practice, the problem of component separation is therefore reduced to an estimation of the *baseflow*, formed by groundwater, and *surface runoff*, which is the integration of all the other components. In natural long-term conditions, in the absence of artificial groundwater withdrawal, the rate of groundwater recharge in a drainage basin of a permanent gaining stream is equal to the rate of groundwater discharge. If all groundwater discharges into the surface stream drainage network, either directly or via springs, it follows that the stream baseflow equals the groundwater recharge in the drainage basin. This simple concept is illustrated in Figure 8.18.
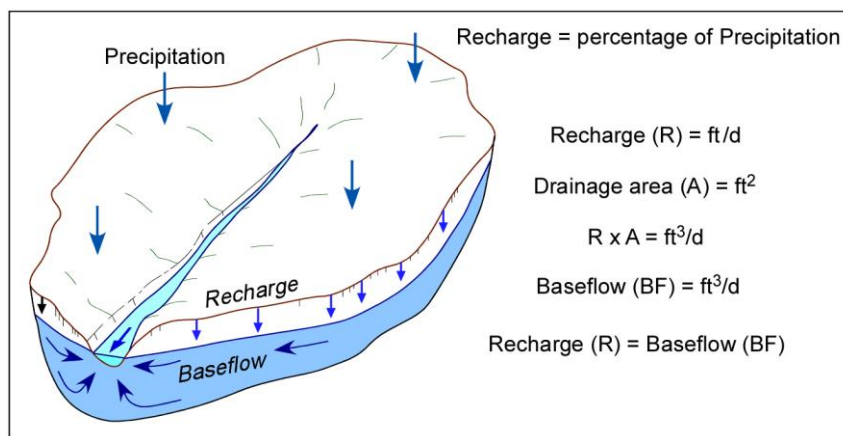
Figure 8.18 Estimation of aquifer recharge from surface stream baseflow. Modified from Kresic, 2007. Copyright CRC Francis & Taylor, permission is required for further use.

Although some professionals view the hydrograph separation methods as a "convenient fiction" because of their subjectivity and lack of rigorous theoretical basis, they do provide useful information in the absence of detailed (and expensive) data on many surface water runoff processes and drainage basin characteristics that contribute to stream flow generation. Importantly, as discussed by Raffensperger et al. (2017), baseflow analysis is a valuable strategy in understanding the dynamics of the groundwater system, groundwater discharge to streams, and the transport of chemicals to streams, and is critical to effective water policy and management. Population growth is associated with increasing demands on freshwater resources for industry, agriculture, and human consumption, and water shortages are not uncommon, even in humid regions. Ensuring safe concentrations of contaminants associated with wastewater effluent requires accurate estimation of baseflow discharge, and contaminants that enter stream systems via soil or groundwater storage may be most highly concentrated during baseflow.

In any case, various baseflow separation methods should be applied with care and regarded only as approximate estimates of the actual groundwater recharge. In addition, geologic and hydrogeologic characteristics of the basin

should be well understood before attempting to apply the method. The following examples illustrate some situations where baseflow alone should not be used to estimate groundwater recharge (Kresic, 2007):

1. Surface stream flows through a karst terrain where topographic divide and groundwater divide are not the same. The groundwater recharge based on baseflow may be grossly overestimated or underestimated depending on the circumstances.

2. The stream is not permanent, or some river segments are losing water (either always or seasonally); locations and timing of the flow measurements are not adequate to assess such conditions.

3. There is abundant riparian vegetation in the stream floodplain, which extracts a significant portion of groundwater via evapotranspiration.

4. There is discharge from deeper aquifers, which have remote recharge areas in other drainage basins.

5. A dam regulates the flow in the stream.

Figure 8.19 shows a simple hydrograph (flow rate or Q vs. time) generated by a rainfall (precipitation, P) event. The beginning of flow after a rainfall episode is marked with point A, and the time between the beginning of rainfall and the beginning of flow, called the starting time, with t_s. The time at which the hydrograph raises to its maximum (point C), is called the concentration time – t_c. The time from maximum discharge until the end of the hydrograph, when the discharge theoretically equals zero (point E), is the falling time – t_f. Together, the concentration time and the falling time are called the base time of the hydrograph – t_b. The time between the centroid of the precipitation episode (C_P) and the centroid of the hydrograph (C_H) is called the retardation time (t_r). The time interval for recording the amount of precipitation and the flow rate at the spring is Δt.

The shape of the hydrograph is defined by its base (AE), the rising limb (AB), the crest (BCD) and the falling limb (DE). The falling limb also corresponds to the recession period. B and C are inflexion points where the hydrograph curve changes its shape from convex to concave and vice versa. Point D is the end of direct runoff after the rain. It is also called the beginning of recession.
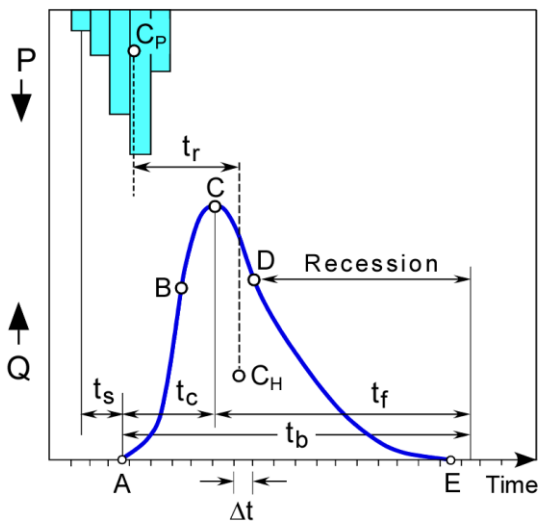
Figure 8.19 Components of a hydrograph (explanation in text). From Kresic 1997. Copyright CRC Lewis Publishers, permission is required for further use.

The shape of a discharge hydrograph depends upon the size and shape of the drainage area, as well as the precipitation intensity. When a rainfall episode lasts longer, and the intensity is lower, the hydrograph has a bigger time base and vice versa: intensive short storm events cause sharp hydrographs with small time bases. The area under the hydrograph is the volume of discharged water for the recording period.
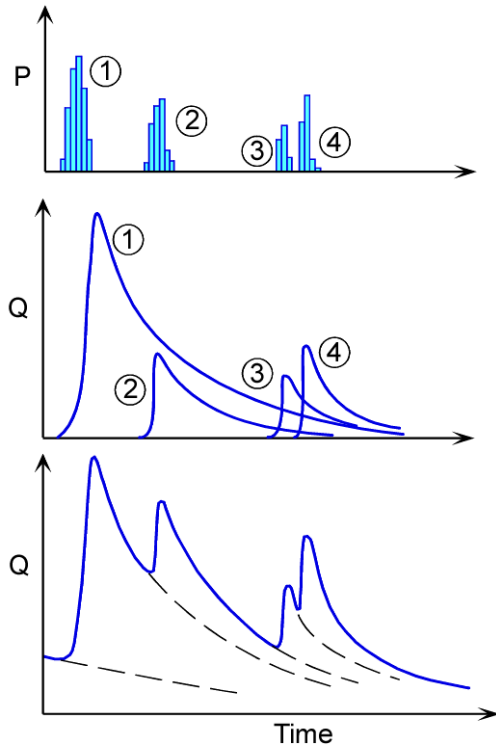
Figure 8.20 Complex hydrograph (bottom) formed by single hydrographs (middle) as the result of several precipitation (P) events (top). Modified from Jevdjević, 1956. University of Belgrade. Acknowledgment is required for further use.

The recorded hydrograph often has a more complex shape, which reflects the influence of antecedent precipitation. Actual hydrographs are formed by the superposition of single hydrographs corresponding to separate precipitation events (Figure 8.20).

The first method of hydrograph component separation shown in Figure 8.21 (line ABC) is commonly applied to surface streams with significant groundwater inflow. Assuming that point C represents the end of all surface runoff and the beginning of flow generated solely by groundwater discharge, the late near-straight line section of the hydrograph is extrapolated backwards until it intersects the ordinate of the maximum discharge (point B). Point A, representing the beginning of surface runoff after rainfall, and point B are then connected with the straight line. The area under the line ABC is the baseflow or the groundwater component of the surface stream flow.

Figure 8.21 Hydrograph formed by rainfall event showing two common methods of baseflow separation. From Kresic 1997. Copyright CRC Lewis Publishers, permission is required for further use.

197

The second graphical method of baseflow separation is used for surface streams in low permeable terrain without significant groundwater flow. It is conditional since point D (called the hydrograph falling time) is found by the following empirical formula (Linsley et al., 1975):

$$N = 0.8A^{0.2} \quad \text{(days)} \tag{8.9}$$

where A is the drainage area in square kilometers. In general, this method gives short falling times: for an area of 100 km^2 N is 2 days, and for 10000 km^2 N is 5 days. Thus, the method should be applied cautiously after analyzing enough single hydrographs and establishing an adequate area-time relationship.

As illustrated in Figure 8.23, graphical methods of baseflow separation may not be applicable at all in some cases. A stream with alluvial sediments having significant bank storage capacity may, during floods or high river stages, lose water to the subsurface so that no baseflow is occurring (Figure 8.22a). Or a stream may continuously receive baseflow from a regional aquifer which has a different primary recharge area than the shallow aquifer and maintains a higher head than the stream stage (Figure 8.22b). Although one could use the same approach and separate either of the two hydrographs, it would not be possible to make any conclusions as to the two groundwater components of the surface stream flow without additional field investigations.

One field method is chemical separation of the stream flow hydrograph using dissolved inorganic constituents or environmental tracers. It is often more accurate than simple graphical techniques because "pure" surface water runoff and "pure" groundwater (baseflow) component of a hydrograph virtually always have significantly different chemical signatures. An illustrative example is provided by Ladouche et al. (2001) and available for free download at https://core.ac.uk/download/pdf/12041614.pdf.
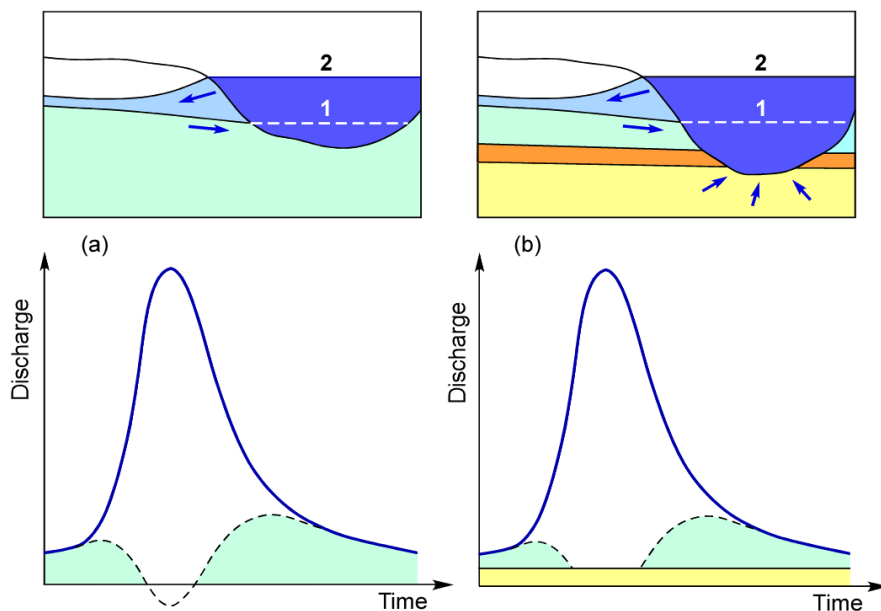
Figure 8.22 Stream hydrograph (bottom) showing flow components after major rise due to rainfall when: (a) the stream stage is higher than the water table; (b) the stream stage is higher than the water table in the shallow aquifer (light blue), but lower than the hydraulic head in the deeper aquifer (yellow) which is discharging into the stream incised through a low permeable layer (orange). 1: Stream stage before rainfall. 2: Stream stage during peak flow. Modified from Kresic and Mikszewski, 2009. From Kresic 1996. Copyright CRC Taylor & Francis, permission is required for further use.

A simple mixing model (e.g., Pinder and Jones, 1969) can be used to separate the streamflow components. This model is based on two mass conservations – one for water and one for the geochemical tracer. It allows separation of the relative contribution of the baseflow (groundwater component) and the surficial runoff generated by rainfall and entering the stream:

$$Q_{total} = Q_{baseflow} + Q_{runoff} \qquad (8.10)$$

$$Q_{total} \times C_{total} = Q_{baseflow} \times C_{baseflow} + Q_{runoff} \times C_{runoff} \qquad (8.11)$$

where Q is the flow rate and C is the concentration of the chemical tracer which, by default, should have a very different concentration in the rainfall vs. groundwater; silica, calcium, total dissolved solids (TDS), or specific conductance are good examples.

If C_{runoff} is much smaller than $C_{baseflow}$ (which is true for the concentrations of calcium and silica in rainwater compared to most aquifers), the input mass of Ca or Si is relatively small compared to their mass in the baseflow (in the pre-rainfall, "old" aquifer water):

$$Q_{runoff} \times C_{runoff} << Q_{baseflow} \times C_{baseflow} \qquad (8.12)$$

From equation (8.11) it follows, after excluding the (small) new input mass, that:

$$Q_{baseflow} = \frac{Q_{total} \times C_{total}}{C_{baseflow}} \qquad (8.13)$$

The new surface runoff component is

$$Q_{runoff} = Q_{total} - \frac{Q_{total} \cdot C_{total}}{C_{baseflow}} \qquad (8.14)$$
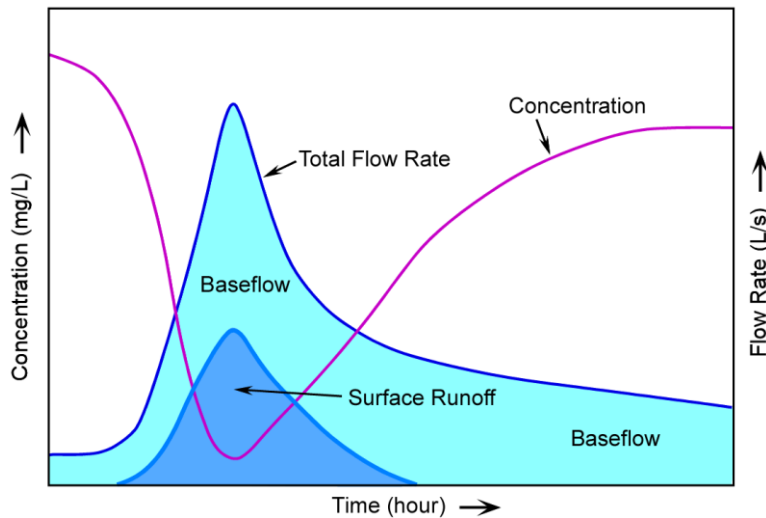
Figure 8.23   Chemical separation of the streamflow discharge hydrograph based on concentration of a geochemical tracer monitored before, during and after a rainfall event. The overall tracer concentration in the stream decreases soon after the inflow of new surface runoff water because its concentration in rainfall is small to negligible. After surface runoff peaks, the concentration increases again because of the dominant role of baseflow.

By applying equations (8.13) or (8.14) it is possible to estimate the streamflow hydrograph components formed by the inflow of rainwater (surface runoff) and groundwater (baseflow, or discharge of aquifer water to the stream) if the streamflow discharge measurements and a continuous chemical monitoring of the stream water and the groundwater adjacent to the stream are performed before, during, and after the rainfall event. This is illustrated in Figure 8.23.

Risser et al. (2005b) present a detailed application and comparison of two automated methods of hydrograph separation for estimating groundwater recharge based on data from 197 streamflow gaging stations in Pennsylvania. The two computer programs – PART and RORA (Rutledge, 1993, 1998, 2000) developed by the USGS are in public domain and available for free download from the USGS web site. The PART computer program uses a hydrograph separation technique to estimate baseflow from the streamflow record. The RORA computer program uses the recession-curve displacement technique of Rorabaugh (1964) to estimate groundwater recharge from each storm period. The RORA program is not a hydrograph-separation method; rather, recharge is determined from displacement of the streamflow-recession curve according to the theory of groundwater drainage.

The PART program computes baseflow from the streamflow hydrograph by first identifying days of negligible surface runoff and assigning baseflow equal to streamflow on those days; the program then interpolates between those days. PART locates periods of negligible surface runoff after a storm by identifying the days meeting a requirement of antecedent-recession length and rate of recession. It uses linear interpolation between the log values of baseflow to connect across periods that do not meet those tests. A detailed description of the algorithm used by PART is provided in Rutledge (1998, p. 33-38).

Rorabaugh's method utilized by RORA is a one-dimensional analytical model of groundwater discharge to a fully penetrating stream in an idealized, homogenous aquifer with uniform spatial recharge. Due to the simplifying assumptions inherent in the equations, Halford and Mayer (2000) caution that RORA may not provide reasonable estimates of recharge for some watersheds. In fact, in some extreme cases, RORA may estimate recharge rates that are higher than the precipitation rates. Rutledge (2000) suggests that estimates of mean-monthly recharge from RORA are probably less reliable than estimates for longer periods and recommends that results from RORA not be used at time scales smaller than seasonal (three months), because results differ most greatly from manual application of the recession-curve displacement method at small time scales. It should be noted that neither RORA nor PART computer programs can account for situations shown in Figure 8.22 or other possible complex relationships between surface streams and groundwater.

8.3.3 Environmental Tracers

As discussed by Trček and Zojer (2010), environmental isotopes and other natural tracers are irreplaceable in general groundwater studies as they may provide answers on contemporary and historic recharge at time scales varying from days to thousands of years. They are useful in finding answers about possible mixing of groundwater of different age and origin within a groundwater system, or sources of groundwater recharge. In addition, as discussed by Sophocleous (2004), tracer studies are often surprising and cast doubt on the utility of physical methods of recharge assessment. A classic example is an attempt to quantify recharge at grassland and irrigated sites above the High Plains (Ogallala) aquifer. Using Darcian methodology based on physical vadose zone measurements, the calculated flux below the root zone ranged from 0.1 to 0.25 mm/yr for a grassland site. Alternative analysis of chloride profiles led to estimates of 2.5 to 10 mm/yr at the same exact location. This discrepancy of one to two orders of magnitude shows that preferential flow in some cases may be a dominant recharge mechanism and illustrates the major need for more research in this area. This is even more emphasized in karst environments where preferential flow paths in both the residuum sediments and the underlying carbonates are the matter of fact.

Environmental tracers commonly used to estimate age of young groundwater (less than 50-70 years old) are chloride (Cl), ratio of tritium and helium-3 (^{3}H/^{3}He), and chlorofluorocarbons (CFCs). Because of various

uncertainties and assumptions that are associated with sampling, analysis, and interpretation of the environmental tracer data, groundwater ages estimated by use of the CFC and ^{3}H-^{3}He methods are regarded as apparent ages and must be carefully reviewed to ensure that they are geochemically consistent and hydrologically realistic (Rowe et al., 1999). Isotopes typically used for determination of older groundwater ages are carbon-14, oxygen-18 and deuterium, and chlorine-36, with many other isotopes increasingly studied for their applicability (Geyh, 2000).

Although reference is often made to dating of groundwater, the age applies to the date of introduction of the tracer substance, and not the water. Unless one recognizes and accounts for all the physical and chemical processes that affect the concentrations of an environmental tracer in the aquifer, the tracer-based age is not necessarily equal to the transit time of the water (Plummer and Busenberg, 2007).The concentrations of all dissolved substances are affected, to some extent, by transport processes. For some tracers, the concentrations can also be affected by chemical processes, such as degradation and sorption during transit. For this reason, the term "age" is usually qualified with the word "model" or "apparent", that is, "model age" or "apparent age". The emphasis on model or apparent ages is needed because simplifying assumptions regarding the transport processes are often made and chemical processes that may affect tracer concentrations are usually not accounted for (Plummer and Busenberg, 2007).

The best source for various studies on the application of environmental isotopes in surface water and groundwater studies are the proceedings of the international conferences organized by the International Atomic Energy Agency (IAEA), as well as the related monographs published by the Agency, many of which are available for free download at its web site (www.iaea.org).

Mass balance of a natural environmental tracer in the soil pore water may be used to measure infiltration where the sole source of the tracer is atmospheric precipitation and where runoff is known or negligible. The relationship for a steady state mass balance is (Bedinger, 1987):

$$R_q = (P - R_s) \cdot \frac{C_p}{C_z} \qquad (8.15)$$

where R_q (infiltration) is a function of P (precipitation), R_s (surface runoff), C_p (tracer concentration in precipitation) and C_z (tracer concentration in the soil moisture).

In the ideal model, the tracer content of soil water increases with depth by the loss of soil water to evapotranspiration and conservation of tracer. The tracer content of soil water attains a maximum at the maximum depth of evapotranspiration. The model postulates a constant content of tracer in the soil moisture from this point to the water table.

The mass balance equation (8.15) assumes that recharge occurs by piston flow. However, it has been shown that diffusion and dispersion are important components of tracer flux in the unsaturated zone. Johnston (1983, from Bedinger, 1987) proposed the following equation for mass balance where runoff is negligible:

$$P \cdot C_p = -D_s - \frac{\partial C}{\partial Z} + C_z \cdot R_q \qquad (8.16)$$

where D_s is the diffusion-dispersion coefficient and $\partial C / \partial C_z$ is the rate of change in soil-moisture concentration with depth. P, C_z, and R_q are as defined in equation (8.15).

Departures from the ideal model of tracer variation with depth are common and have been attributed to changes in land use, such as clearing of native vegetation, replacement of native vegetation by cropped agriculture, bypass mechanisms for infiltrating water through the soil profile, and changes in climate (Bedinger, 1987).

8.3.3.1 Chloride

Chloride (Cl) is a widely utilized environmental tracer since it is conservative and highly soluble. Knowledge of wet and dry deposition cycles of Cl on the ground surface can be used in conjunction with vadose zone samples to determine the recharge rate at a site. Chloride is continuously deposited on the land surface by precipitation and dry fallout. The high solubility of Cl enables its transport into the subsurface by infiltrating water. Because Cl is essentially nonvolatile and its uptake by plants is minimal, it is retained in the sediment when water is removed by evaporation and transpiration. An increase in Cl within the root zone of the shallow subsurface, therefore, is proportional to the amount of water lost by evapotranspiration (Allison and Hughes, 1978, from Coes and Pool, 2005). Izbicki (2002) cites high Cl concentrations near the base of the root zone as proof that groundwater recharge is not occurring at desert sites removed from intermittent washes or arroyos.

In areas where active infiltration is occurring, an increase in Cl in the shallow subsurface will generally be absent, and concentrations will be very low through the unsaturated zone. In areas where little to no active infiltration is occurring, an increase in Cl in the shallow subsurface will be present. After reaching maximum they will stay relatively constant down to the water table. However, there are published studies showing that Cl concentrations in arid areas with little infiltration may decrease below the peak concentration in the root zone due to varying factors such as paleoclimatic variations and non-piston flow (Coes and Pool, 2005).

If the Cl deposition rate on the land surface is known, the average travel time of Cl (t_{Cl}) to a depth in the unsaturated zone (z) can be calculated by (Coes and Pool, 2005):

$$t_{Cl} = \frac{\int_0^z Cl_{soil} \cdot dz}{Cl_{dep}} \qquad (8.17)$$

where Cl_{soil} is chloride mass in the sample interval (M/L^3) and Cl_{dep} is chloride deposition rate (M/L^2/t).

The above equation entails several assumptions: (1) flow in the unsaturated zone is downward-vertical and piston type; (2) bulk precipitation (precipitation plus dry fallout) is the only source of Cl and there are no mineral sources of Cl; and (3) the Cl deposition rate has stayed constant over time; and (4) there is no recycling of Cl within the unsaturated zone. Figure 8.24 shows examples of chloride and tritium concentrations in a thick unsaturated zone in the semi-arid climate of Arizona, the United States.
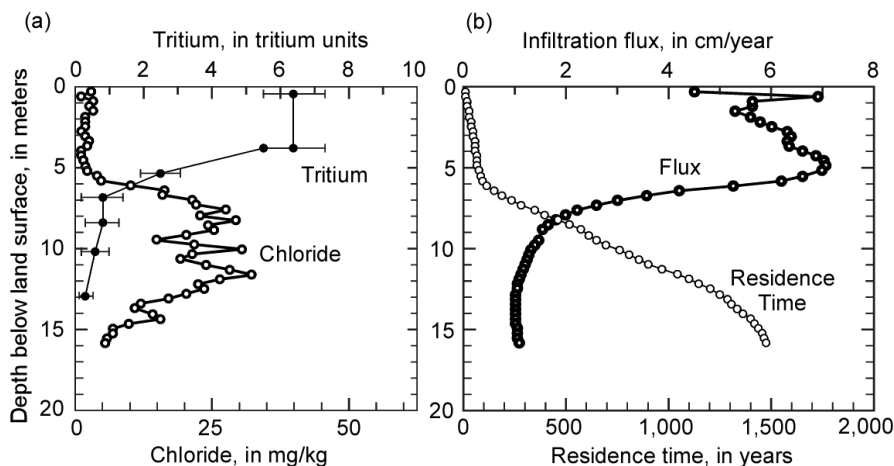
Figure 8.24 Determination of basin-floor infiltration at borehole BF1, Sierra Vista sub-watershed, Arizona, the United States. (a) Sediment-chloride and pore-water tritium data; tritium values include standard error of estimate bars, (b) residence time and infiltration flux, calculated from chloride data. From Coes and Pool, 2005. USGS, in public domain.

8.3.3.2 Tritium

Tritium (3H), a naturally occurring radioactive isotope of hydrogen with the half-life of 12.43 years, has been used extensively as a hydrologic tracer and dating tool. It is produced naturally in the upper atmosphere by bombardment of nitrogen with cosmic radiation and, although few measurements are available, it is estimated that the natural concentration of tritium in precipitation is between 5 and 20 TU (Kauffman and Libby, 1954). Large quantities of tritium were released to the atmosphere during thermonuclear weapons testing from 1952 until the late 1960s, with maximum releases occurring in the early 1960s. As a result, the amount of tritium in precipitation sharply increased during testing as tritium was introduced into the water cycle and decreased after testing ended. The atmospheric-testing peak therefore provides an absolute time marker from which to estimate groundwater age. However, because radioactive decay and hydrodynamic dispersion have greatly reduced maximum tritium concentrations in groundwater, identification of the 1960's atmospheric-testing peak has become increasingly difficult. The interpretation of ages from tritium data alone is further complicated by the fact that monitoring and extraction wells are commonly screened over intervals that represent a wide range of groundwater ages. Changes in the amount of tritium in precipitation through time, radioactive decay, hydrodynamic dispersion, and mixing water of different ages in the subsurface typically preclude the use of this isotope for quantitatively estimating groundwater residence times and recharge rates.

8.3.3.3 Tritium-Helium-3 (^{3}H-^{3}He)

The ^{3}H/^{3}He method was developed to remove the ambiguity associated with tritium-age estimation. Radioactive decay of tritium produces the noble gas helium-3 (^{3}He). Determination of the ^{3}H/^{3}He ratio, therefore, can be used to estimate the apparent date when a sample of water entered the aquifer as recharge. Because these substances virtually are inert in groundwater, unaffected by groundwater chemistry, and not derived from anthropogenic contamination, ^{3}H/^{3}He dating can be applied to a wide range of hydrologic investigations since the input function of ^{3}H does not have to be known (Kay et al., 2002; Geyh, 2000). Possible applications include site characterization, corroboration of the results of other age-dating methods, surface water-groundwater interaction studies, and calibration and interpretation of groundwater flow models (Aeschbach-Hertig et al., 1998; Sheets et al., 1998; Szabo et al, 1996.)

The activity of ^{3}H in the sample ($^3H_{spl}$) is given as (Geyh, 2000):

$$^3H_{spl} = \ ^3H_{init}e^{-\lambda \cdot t} \tag{8.18}$$

where $^3H_{init}$ is the activity of initial tritium, λ is the radioactive decay constant, and t is time since decaying started (absolute age). The growth of ^{3}He in a sample is given by

$$^3He_{spl} = \ ^3H_{init}(1 - e^{-\lambda \cdot t}) \tag{8.19}$$

Combining Equations (8.18) and (8.19), the unknown and variable initial ^{3}H activity ($^3H_{init}$) is eliminated, and the age of water (t) is obtained from

$$^3He_{spl} = \ ^3H_{spl}(e^{-\lambda \cdot t} - 1) \tag{8.20}$$

$$t = -\frac{\ln\left(1 + \dfrac{^3He_{spl}}{^3H_{spl}}\right)}{\lambda}$$

(8.21)

The ^{3}He concentration in the sample must be corrected for admixed ^{3}He from the Earth's crust and from the atmosphere.

The concentration of tritiogenic ^{3}He will increase as tritium decays; thus, older waters will have higher ^{3}He$_{trit}$ / ^{3}H ratios.

8.3.3.4 Chlorofluorocarbons and Sulfur Hexafluoride

Clorofluorocarbons (CFCs), together with tritium and an emerging environmental tracer sulfur hexafluoride (SF6), can be used to trace the flow of young water (water recharged within the past 50 years) and to determine the time elapsed since recharge. Information about the age of young groundwater can be used to define recent recharge rates, refine hydrologic models of groundwater systems, predict contamination potential, and estimate the time needed to flush contaminants from groundwater systems. CFCs also can be used to trace seepage from rivers into groundwater systems, provide diagnostic tools for detection and early warning of leakage from landfills and septic tanks, and to assess susceptibility of water-supply wells to contamination from near-surface sources (Plummer and Friedman, 1999).

Chlorofluorocarbons are stable, synthetic organic compounds that were developed in the early 1930s as safe alternatives to ammonia and sulfur dioxide in refrigeration and have been used in a wide range of industrial and refrigerant applications. Production of CFC-12 (dichlorodifluoromethane, CF2Cl2) began in 1931, followed by CFC-11 (trichlorofluoromethane, CFCl3) in 1936, and then by many other CFC compounds, most notably CFC-113 (trichlorotrifluoroethane, C2F3Cl3). CFC-11 and CFC-12 were used as coolants in air conditioning and refrigeration, blowing agents in foams, insulation, and packing materials, propellants in aerosol cans, and as solvents. CFC-113 has been used primarily by the electronics industry in semiconductor chip manufacturing, in vapor degreasing and cold immersion cleaning of microelectronic components, and in surface cleaning. Probably better known to the public as Freon^{TM}, CFCs are nontoxic, nonflammable, and non-carcinogenic, but they contribute to ozone depletion. Therefore in 1987, 37 nations signed an agreement to limit release of CFCs and to halve CFC emissions by 2000. Production of CFCs ceased in the United States as of January 1, 1996, under the Clean Air Act. Current estimates of the atmospheric lifetimes of CFC-11, CFC-12, and CFC-113 are about 45, 87, and 100 years, respectively.

Groundwater dating with CFC-11, CFC-12 and CFC-113 is possible because (1) their amounts in the atmosphere over the past 50 years have been reconstructed, (2) their solubilities in water are known, and (3) concentrations in air and young water are high enough that they can be measured. Age is determined from CFCs by relating their measured concentrations in groundwater back to known historical atmospheric concentrations and to calculated concentrations expected in water in equilibrium with air.

For best results, the apparent age should be determined using multiple dating techniques because each dating technique has limitations. CFC dating is best suited for groundwater in relatively rural environments without localized, non-atmospheric CFC contamination from septic systems, sewage effluent, landfills, or urban runoff. The dating method appears to work well in shallow, aerobic, sand aquifers that are low in particulate organic matter,

where results can be accurate within 2-3 years before the study date. Even where there are problems with CFC dating of groundwater, the presence of CFCs indicates that the water sample contains at least some post-1940s water, making CFCs useful as tracers of relatively recent recharge. Where CFC and ^{3}H/^{3}He ages agree, or where all three CFCs indicate similar ages, considerable confidence can be placed in the apparent age (Plummer and Friedman, 1999).

An example of groundwater dating with CFCs in agricultural areas on the Delmarva Peninsula of Maryland and Virginia, the United States is shown in Figure 8.25. The results indicate that water recharged since the early 1970s exceeds the U.S. Environmental Protection Agency drinking water Maximum Contaminant Level (MCL) for nitrate of 10 mg/L (as N), while water recharged prior to the early 1970s, before the heavy use of nitrogen fertilizers, does not exceed the MCL (Böhlke and Denver, 1995, from Plummer and Friedman, 1999).
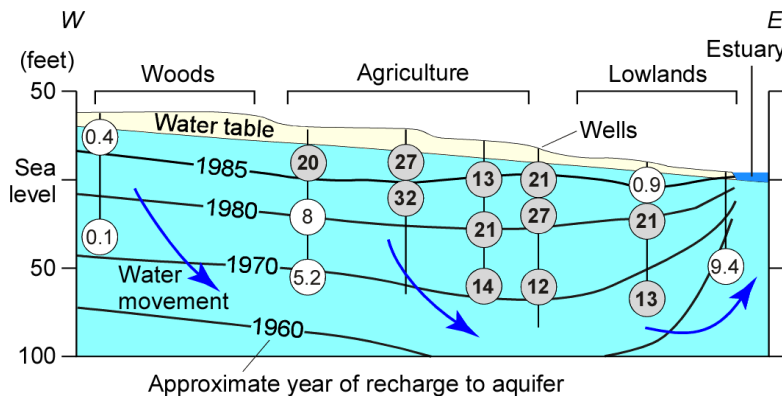
Figure 8.25 CFCs and nitrate concentrations were measured between June 1989 and January 1990 on a section of the Delmarva Peninsula, in the Fairmount watershed. Groundwater dating reveals a pattern of high nitrate concentrations moving slowly toward the estuary. Numbers within circles show nitrate concentrations, in milligrams per liter (mg/L, as N). Bold numbers indicate concentrations higher than 10 mg/L Modified from Plummer and Friedman, 1999. USGS, in public domain.

Nitrate concentrations in groundwater under woodlands were low, whereas groundwater recharged under agricultural fields had nitrate concentrations that exceeded the MCL. CFC concentrations indicate that groundwater now discharging to streams that drain agricultural areas of the Delmarva and then flow into the Chesapeake Bay or the Atlantic Ocean, was recharged in nearby fields in the 1960s and 1970s (Böhlke and Denver, 1995; Focazio et al., 1998). Thus, even if the application of nitrogen fertilizers to the fields stopped today, streams, rivers, and estuaries can be expected to receive increasing amounts of nitrate from groundwater discharge until the contaminated water is flushed through the system (Modica et al., 1998). Up to 30 years may be needed to flush the high-nitrate water present in the analyzed agricultural watersheds (Plummer and Friedman, 1999).

The use of sulfur hexafluoride (SF6) is a promising alternative to using CFCs in dating groundwater as atmospheric CFC concentrations continue to fall. Industrial production of SF6 began in 1953 with the introduction of gas-filled high-voltage electrical switches. SF6 is extremely stable and is accumulating rapidly in the atmosphere. The historical atmospheric mixing ratio of SF6 is being reconstructed from production records, archived air samples, and atmospheric measurements. The mixing ratio is also being retrieved from concentrations measured in seawater and in previously dated groundwater. A preliminary reconstruction has been made of northern-hemisphere SF6 mixing ratios (Figure 8.26). As atmospheric CFC concentrations fall, an even more sensitive dating tool will be the ratio of SF6 to, for example, CFC-12. Although SF6 is almost entirely of human origin, there is likely a natural, igneous source of SF6 that will complicate dating in some environments. USGS scientists have successfully used SF6 to date shallow groundwater on the Delmarva Peninsula, Maryland, and water from springs in the Blue Ridge Mountains of Virginia, the United States with SF6 (Plummer and Friedman, 1999).
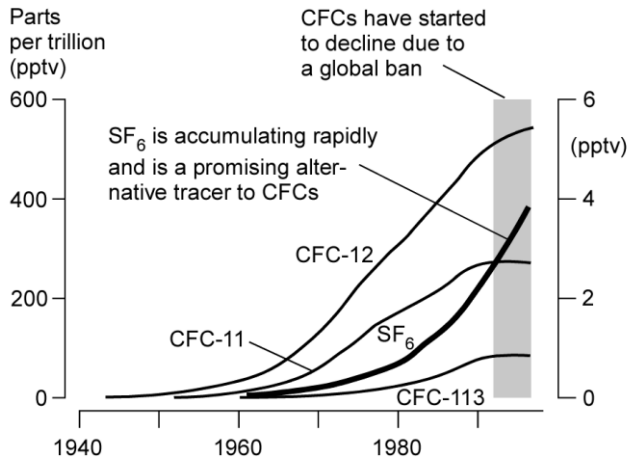
Figure 8.26 CFCs and sulfur hexafluoride (SF6) concentrations mixing ratios for air over North America during several decades. From Plummer and Friedman, 1999. USGS, in public domain.

8.3.4 Lysimeters

Lysimeters are vessels filled with soil that are placed below land surface and collect the percolating water. They usually extending deeper in the soil column to measure actual vertical infiltration from below the root intake zone. Measurements of this flux are therefore the closest to the actual recharge of unconfined aquifers with relatively shallow water table in unconsolidated sediments. The construction and design of lysimeters vary significantly depending on their purpose. Photographs in Figure 8.27 show one of the most elaborate and expensive lysimeter facilities today, designed to directly measure various quantitative and qualitative parameters of water migrating through the vadose zone. Lysimeter stations may be equipped with a variety of automated instruments including tensiometers which measure matric potential at different depths and instruments that measure actual flux (flow rate) of infiltrating water at different depths. Some stations may also include piezometers for recording water table fluctuations. Water quality parameters may also be measured and recorded automatically. More detail on lysimeter construction can be found in Pruitt and Lourence (1985).

Worldwide, the primary use of lysimeters was traditionally in agricultural studies, although more recently their utilization is increasing in general groundwater studies for water supply and contaminant fate and transport. Data collected from lysimeters is often used to calibrate empirical equations or numeric models for determining other water balance elements such as evapotranspiration.

Figure 8.27 *Left*: Array of lysimeters operated by Helmholtz Center Munich, Germany. *Right*: Below-ground view of one of the lysimeters. Photographs courtesy of Dr. Sascha Reth.

Lysimeters may have varying degrees of vegetation and contain disturbed or undisturbed soil. The clear advantage of lysimeters is that they enable direct measurement of the quantity of water descending past the root zone over a time period of interest. Net infiltration flux is easily calculated from these measurements, eliminating much uncertainty in surficial processes like evapotranspiration and runoff. Lysimeters also capture infiltration moving rapidly through preferential flow pathways like macropores and fractures. The main disadvantages of lysimeters are their expensive construction costs and difficult maintenance requirements. These costs generally limit the total depth of lysimeters to about ten feet, which inhibits direct correlation of net infiltration with actual groundwater recharge since low permeability clay layers may lie below the bottom of the lysimeter (Sophocleous, 2004). Additionally, lysimeters constructed with disturbed soils may have higher moisture contents, possibly skewing measurement results and overestimating recharge.

Major difficulty when extrapolating lysimeter data to a much wider aquifer recharge area is the inevitably high variability in soil and vegetative characteristics. Figure 8.28 illustrates this with the range of cumulative percolation rates at seven lysimeters all installed on a 100-square-foot plot located within a 2.8 square-mile watershed in Pennsylvania, the United States. Even at the 100 square feet scale, the coefficient of variation between monthly rates at individual lysimeters is greater than 20 percent for six months, with the June, July and August values of about 50, 100 and 60% respectively. Figure 8.29 shows mean monthly recharge rates for seven lysimeters during the 1994-2001 period of record. The mean annual recharge rate was 12.2 inches or 29 percent of precipitation. In comparison, this rate was 24 percent as calculated with the water table fluctuations method, 25 percent as calculated with the PART hydrograph baseflow separation method, and 29 percent using a daily water balance HELP3 model (Risser et al., 2005b).
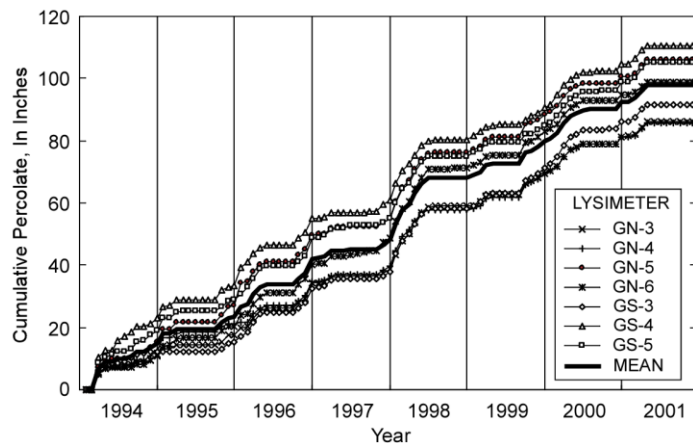
Figure 8.28 Range of cumulative percolation rates at seven lysimeters installed on a 100 square feet plot located within a 2.8 square-mile watershed in Pennsylvania, the United States. From Risser et al., 2005b. USGS, in public domain.
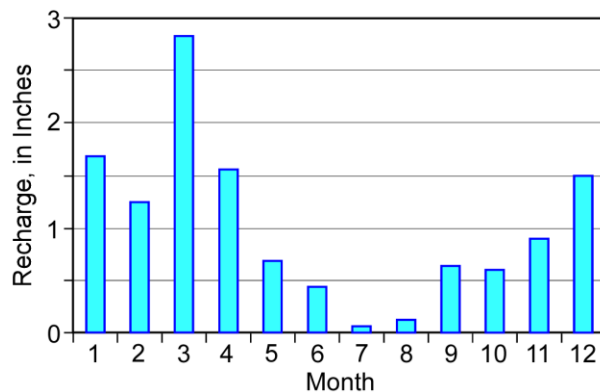
Figure 8.29 Mean monthly recharge rates for the seven closely spaced lysimeters during 1994-2001 period of record. Data from Risser et al., 2005b. USGS, in public domain.

Lecture 9 Flow in Unsaturated Zone

This lecture is based on the materials presented in Lappala et al. (1987), Kresic (2007), Kresic and Mikszewski (2009, 2013), van Genuchten et al., (1991), Šimůnek et al. (1999), Šimůnek et al. (2022), and USGS (2022b; available at https://wwwrcamnl.wr.usgs.gov/uzf/.)

The following discussion by Šimůnek et al. (1999) illustrates the importance of the unsaturated zone as an integral part of the hydrologic cycle:

The zone plays an inextricable role in many aspects of hydrology, including infiltration, soil moisture storage, evaporation, plant water uptake, groundwater recharge, runoff, and erosion. Initial studies of the unsaturated (vadose) zone focused primarily on water supply studies, inspired in part by attempts to optimally manage the root zone of agricultural soils for maximum crop production. Interest in the unsaturated zone has dramatically increased in recent years because of growing concern that the quality of the subsurface environment is being adversely affected by agricultural, industrial and municipal activities. Federal, state and local action and planning agencies, as well as the public in large, are now scrutinizing the intentional or accidental release of surface-applied and soil-incorporated chemicals in the environment. Fertilizers and pesticides applied to agricultural lands inevitably move below the soil root zone and may contaminate underlying groundwater reservoirs. Chemicals migrating from municipal and industrial disposal sites also represent environmental hazards. The same is true for radionuclides emanating from energy waste disposal facilities.…The past several decades have seen considerable progress in the conceptual understanding and mathematical description of water flow and solute transport processes in the unsaturated zone. A variety of analytical and numerical models are now available to predict water and/or solute transfer processes between the soil surface and groundwater table. The most popular models remain the Richards' equation for variably saturated flow, and the Fickian-based convection-dispersion equation for solute transport. Deterministic solutions of these classical equations have been used, and likely will continue to be used for (1) predicting water and solute movement in the vadose zone, (2) analyzing specific laboratory or field experiments involving unsaturated water flow and/or solute transport, and (3) extrapolating information from a limited number of field experiments to different soil, crop and climatic conditions, as well as to different soil and water management schemes.

The flow in unsaturated zone starts with the infiltration of water at the land surface. As discussed in Lecture 8, the initial soil water content and the saturated hydraulic conductivity of the soil media are the primary factors affecting the soil water infiltration process. The wetter the soil initially, the lower will be the initial infiltration rate (due to a smaller suction gradient), and the constant infiltration rate will be attained more quickly. In general, the higher the saturated hydraulic conductivity of the soil, the higher the infiltration rate. The infiltration rate decreases with increasing clay content in the soil and increases with increasing non-capillary porosity through which water can flow freely under the influence of gravity. Presence of certain clays such as montmorillonite, even in relatively small quantities, may dramatically reduce infiltration rate as they become wet and swell. Runoff conditions on soils of low permeability develop much sooner and more often than on uniform, coarse sands, and gravels, which have infiltration rates higher than most rainfall intensities.

The flow (water transmission) rates can vary at different horizons in the unsaturated soil profile. After saturation of the uppermost horizon, the infiltration rate is limited to the lowest transmission rate encountered by the infiltrating water as it travels downward through the soil profile. As water infiltrates through successive soil horizons and fills in the pore space, the available storage capacity of the soil will decrease. The storage capacity available in any horizon is a function of the porosity, horizon thickness, and the amount of moisture already present.

Total porosity and the size and arrangement of the pores have significant effect on the availability of storage. During the early stage of a rainfall event, the infiltration process will be largely affected by the continuity, size, and volume of the larger-than-capillary ("non-capillary") pores, because such pores provide relatively little resistance to the infiltrating water. If the infiltration rate is controlled by the transmission rate through a retardant layer of the soil profile, then the infiltration rate, as the rainfall progresses, will decrease as a function of the decreasing storage availability above the restrictive layer. The infiltration rate will then equal the transmission rate through this restrictive layer until another, more restrictive, layer is encountered by the water (King, 1992). The soil infiltration capacity decreases in time and eventually asymptotically reaches the value of overall saturated hydraulic conductivity (K_s) of the affected soil column as illustrated in Figure 8.14 (see Lecture 8).

The main hydraulic characteristic of the unsaturated zone is the negative fluid pressure head, which is lower than the atmospheric pressure. This negative pressure head is often called *matric potential*, and sometimes *suction*. The unsaturated soil will "suck" water or fluid from a porous cup of an instrument used to measure the pressure head above the water table. Conversely, sampling soil water requires application of enough pressure to overcome the soil matric potential: the water must be extracted by suction. The matric potential, caused by capillary and adhesive forces, is a function of water content and sediment texture: it is stronger in less saturated and finer soils. As the soil saturation increases, the pressure head becomes "less negative". At full saturation, at the water table, the pressure head is zero and equals the atmospheric pressure. Below the water table, the pressure head is positive and increases with depth. This is schematically illustrated in Figure 9.1 for a downward flux of infiltrating water.

Small negative pressure heads (less than about 100 kPa) can be measured with tensiometers, which couple the measuring fluid in a manometer, vacuum gage, or pressure transducer to water in the surrounding partially saturated soil through a porous membrane. The pressure status of water held under large negative pressures (greater than 100 kPa) may be measured using thermocouple psychrometers, which measure the relative humidity of the gas phase within the medium, and with heat dissipation probes or HDPs (Lappala et al., 1987; McMahon et al., 2003). The measuring instrumentation may be permanently installed in wells screened at different depths to measure soil moisture profile, or measurements may be performed on a temporary basis using direct push methods, such as cone penetrometers equipped with tension rings.
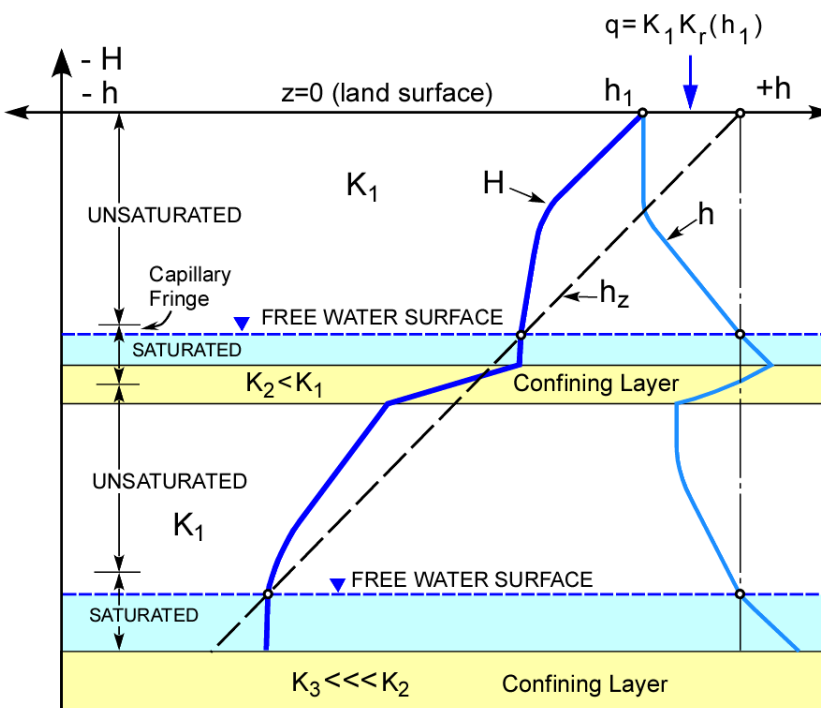
Figure 9.1 Relation among matric pressure (capillary), elevation, and total potentials for downward flux through layered media with a perched water table and a deep water table. H: total potential (unit of length or L); h: matric pressure potential (L); hz: elevation potential (L); K_1, K_2, K_3: saturated hydraulic conductivity of materials 1, 2, and 3 (LT^{-1}); $K_r(h_1)$: relative hydraulic conductivity of Layer 1 at h_1 (dimensionless); q: surface volume flux rate per unit area (LT^{-1}). From Lappala et al., 1987. USGS, in public domain.

Similarly to groundwater flow in the saturated zone, the flow of water in the unsaturated zone is governed by two main parameters – the change in the total potential (hydraulic head) along the flowpath, and the hydraulic conductivity. However, both parameters depend on the volumetric water content in the porous medium: they change in time and space as the soil becomes more or less saturated in response to water input and output (e.g., due to infiltration and evapotranspiration). The unsaturated hydraulic conductivity is always lower than the saturated hydraulic conductivity because of the presence of air in the voids, and it increases with the increasing saturation. Quantification of flow processes in the unsaturated zone is therefore more complex than in the saturated zone since it requires determination of two dynamic (time-dependent) parameters.

The water-retention characteristic of the soil describes the soil's ability to store and release water and is defined as the relationship between the soil water content and the matric potential. The water-retention characteristic is also known as *moisture characteristic curve*, which when plotted on a graph shows water content at various depths below ground surface versus matric potential (Figure 9.2-Left). Again, the matric potential is always negative above the water table since the suction pressure is lower than the atmospheric pressure. The matric potential is a function of both the water content and sediment texture: it is stronger in less saturated and finer soils. As the soil saturation increases, the matric potential becomes "less negative." At the water table, the matric potential is zero and equals the atmospheric pressure. Other terms that are synonymous with matric potential but may differ in sign or units are soil water suction, capillary potential, capillary pressure head, suction head, matric pressure head, tension, and pressure potential (Rawls et al., 1993).
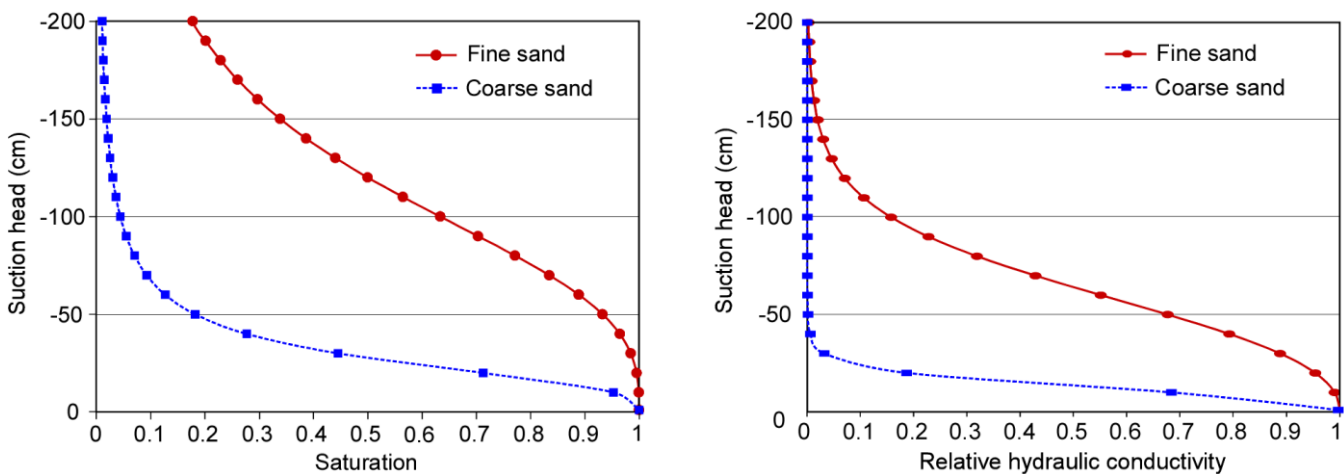
Figure 9.2 Left: Two characteristic moisture curves for fine and coarse sand. Right: Relative hydraulic conductivity for the same fine and coarse sand. Modified from Kresic and Mikszewski, 2009. Copyright McGraw Hill, permission is required for further use.

As the moisture content increases, suction pressure decreases causing a corresponding increase in hydraulic conductivity. As a result, soils with high antecedent moisture contents will support a greater long-term drainage rate than dry soils. At saturation (i.e., at and immediately above the water table in the capillary fringe), the hydraulic conductivity of the soil media is equal to the saturated hydraulic conductivity. Figure 9.2-Right shows unsaturated hydraulic conductivity as the function of matric potential for the same two soil types shown in Figure 9.2-Left.

9.1 Darcy's Law

Flow in the vadose zone can be best understood through interpretation of Darcy's Law for unsaturated flow in one dimension. The governing equation (known as the Darcy-Buckingham equation) is:

$$q = -K(\Psi)\frac{\partial H}{\partial z} = -K(\theta)\frac{\partial}{\partial z}(\Psi + z) \qquad (9.1)$$

where q is flow per unit width; $K(\Psi)$ is the unsaturated hydraulic conductivity given as function of the matric potential; θ is soil moisture content; H is the total water potential, z is the elevation potential; and Ψ is the matric potential or pressure head.

The matric and elevation potentials (heads) combine to form the total water potential (head). Pressure head is negative in the unsaturated zone (causing the "suction" effect), zero at the water table, and positive in the saturated zone. As in the saturated zone, water in the vadose zone moves from large to small water potentials (heads).

For deep vadose zones common to the American West, soil hydraulic properties can be used to simply calculate recharge flux using Darcy's law. The underlying assumption of the "Darcian method" is that moisture content becomes constant at some depth, such that there is no variation in matric potential or pressure head (h) with depth (z), and that all drainage is due to gravity alone (see Figure 9.3). Under these conditions, the deep drainage rate is approximately equal to the measured unsaturated hydraulic conductivity (Nimmo et al, 2002). The equations describing this relationship are:

$$q = -K(\Psi)\left[\frac{d\Psi}{dz} + 1\right]$$

$$\frac{d\Psi}{dz} \approx 0$$

$$q \approx -K(\Psi) \qquad\qquad (9.2)$$

Alternatively, knowledge of matric potential (pressure head) at different depths enables direct calculation of recharge flux from the above equation. Velocity of the recharge front can be calculated by dividing the flux by soil moisture content.
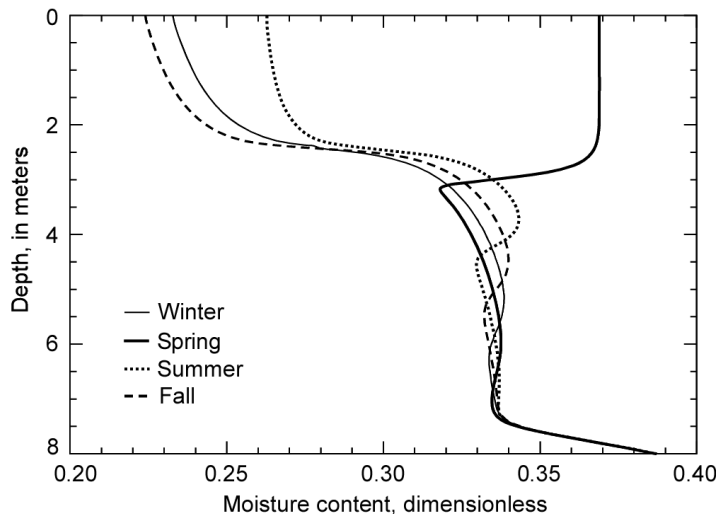
Figure 9.3 Hypothetical moisture-content profiles at four different times of the year. As depth increases, the variation in moisture content decreases. Four profiles merge at the top of capillary fringe and reach full saturation at the water table. From Healy et al., 2007. USGS, in public domain.

Darcy's law illustrates the complexity of unsaturated flow, as both hydraulic conductivity and pressure head are functions of the soil moisture content (θ). Another crucial factor influencing drainage rates is vadose zone lithology. Deep vadose zones often have a high degree of heterogeneity, created by distinct depositional periods. This limits the application of Equation (9.2). Layers of fine-grained clays and silts are common to deep basins of the American West. As a result, moisture percolating through the vadose zone often encounters low permeability strata, such as the calcified sediment layer shown in Figure 9.4. Presence of low-permeable intervals in the vadose zone greatly delays downward migration and may cause significant lateral spreading. Therefore, the time lag for groundwater recharge may be on the order of hundreds of years or more for deep vadose zones with fine-grained sediments. Furthermore, moisture is lost to lateral spreading and storage. Detailed lithologic characterization of the vadose zone is essential in quantification of groundwater recharge as well as in planning and designing artificial recharge systems. Knowledge of site-specific geology is also helpful in qualitatively understanding the time scale of vadose zone processes.
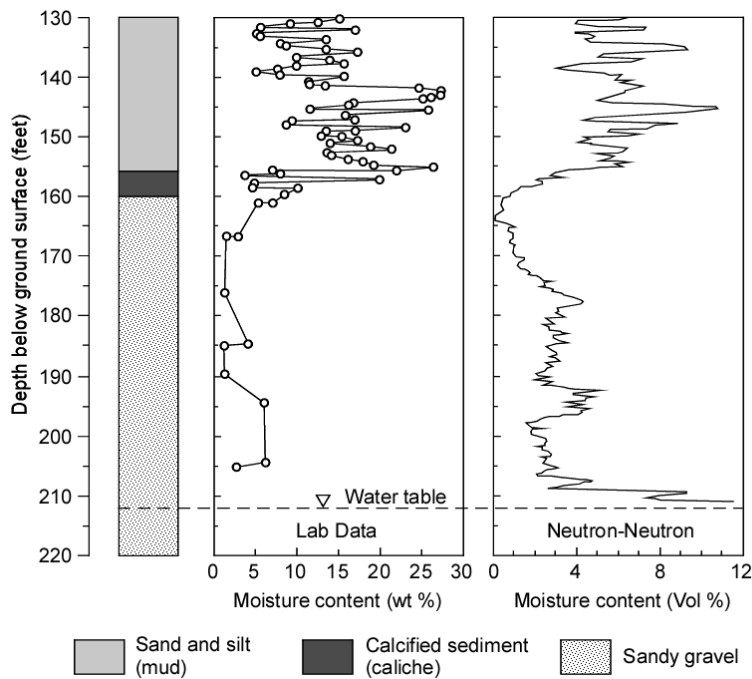
Figure 9.4 Lithology and moisture distribution as a function of depth within a borehole in a deep vadose zone. Modified from Serne et al., 2002. Pacific Northwest National Laboratory, in public domain.

9.2 Equations of Richards, Brooks and Corey, and van Genuchten

Water flow in variably saturated soils is traditionally described with the Richards equation (Richards, 1931) as follows (van Genuchten et al., 1991):

$$C \frac{\partial h}{\partial t} = \frac{\partial}{\partial z}\left(K \frac{\partial h}{\partial z} - K\right) \qquad (9.3)$$

where h is the soil water pressure head, or matric potential (with dimension L); t is time (T); z is soil depth (L); K is the hydraulic conductivity (LT^{-1}); C is the soil water capacity (L^{-1}) approximated by the slope ($d\theta/dh$) of the soil

water retention curve, $\theta(h)$, in which θ is the volumetric water content ($L^3 L^{-1}$). Equation (9.3) may also be expressed in terms of the water content if the soil profile is homogeneous and unsaturated ($h \leq 0$):

$$\frac{\partial \theta}{\partial t} = \frac{\partial}{\partial z}\left(D \frac{\partial \theta}{\partial z} - K\right) \qquad (9.4)$$

where D is the soil diffusivity ($L^2 T^{-1}$) defined as

$$D = K \frac{dh}{d\theta} \qquad (9.5)$$

The unsaturated soil hydraulic functions in the above equations are the soil water retention curve, $\theta(h)$, the hydraulic conductivity function, $K(h)$ or $K(\theta)$, and the soil water diffusivity function $D(\theta)$.

Several functions have been proposed to empirically describe the soil water retention curve. One of the most widely used is the equation of Brooks and Corey (van Genuchten et al., 1991; Šimůnek et al., 1999):

$$\theta = \begin{cases} \theta_r + (\theta_s - \theta_r) \cdot (\alpha h)^{-\lambda} & (h < -1/\alpha) \\ \theta_s & (h \geq -1/\alpha) \end{cases} \qquad (9.6)$$

where θ is the volumetric water content; θ_r, is the residual water content; θ_s is the saturated water content; α is an empirical parameter (L^{-1}) whose inverse ($1/\alpha$) is often referred to as the air entry value or bubbling pressure; α has negative value for unsaturated soils; λ is a pore-size distribution parameter affecting the slope of the retention function; h is the soil water pressure head, which has negative values for unsaturated soil. Equation 9.6 may be written in a dimensionless form as follows:

$$S_e = \begin{cases} (\alpha h)^{-\lambda} & (h < -1/\alpha) \\ 1 & (h \geq -1/\alpha) \end{cases} \qquad (9.7)$$

where S_e, is the effective degree of saturation, also called the reduced water content ($0 < S_e < 1$):

$$S_e = \frac{\theta - \theta_r}{\theta_s - \theta_r} \qquad (9.8)$$

The residual water content, θ_r in Equation (9.8) specifies the maximum amount of water in a soil that will not contribute to liquid flow because of blockage from the flow paths or strong adsorption onto the solid phase (Luckner et al., 1989, from van Genuchten et al., 1991). Formally, θ_r may be defined as the water content at which both $d\theta/dh$ and K go to zero when h becomes large. The residual water content is an extrapolated parameter and may not necessarily represent the smallest possible water content in a soil. This is especially true for arid regions where vapor phase transport may dry out soils to water contents well below θ_r. The saturated water content, θ_s, denotes the maximum volumetric water content of a soil. The saturated water content should not be equated to the porosity of soils; θ_s of field soils is generally about 5 to 10% smaller than the porosity because of entrapped or dissolved air (van Genuchten et al., 1991).

The Brooks and Corey equation has been shown to produce relatively accurate results for many coarse-textured soils characterized by relatively narrow pore-or particle-size distributions. Results have generally been less accurate for many fine-textured and undisturbed field soils because of the absence of a well-defined air-entry value for these soils. A continuously differentiable (smooth) equation proposed by van Genuchten (1980) significantly improves the description of soil water retention:

$$S_e = \frac{1}{[1+(\alpha h)^n]^m} \tag{9.9}$$

where α, n and m are empirical constants affecting the shape of the retention curve ($m=1-1/n$). By varying the three constants, it is possible to fit almost any measured field curve. It is this flexibility that made the van Genuchten equation arguably the most widely used in various computer models of unsaturated flow, and contaminant fate and transport. Combining Equations (9.8) and (9.9) gives the following form of the van Genuchten equation:

$$\theta(h) = \theta_r + \frac{\theta_s - \theta_r}{[1+(\alpha h)^n]^{\,1-1/n}} \tag{9.10}$$

One of the widely used models for predicting the unsaturated hydraulic conductivity from the soil retention profile is the model of Mualem (1976) which may be written in the following form (van Genuchten et al., 1991):

$$K(S_e) = K_s S_e \left[\frac{f(S_e)}{f(l)}\right]^2 \tag{9.11}$$

$$f(S_e) = \int_0^{S_e} \frac{1}{h(x)}\,dx \tag{9.12}$$

where S_e is given by Equation (9.8); K_s is the hydraulic conductivity at saturation; and l is an empirical pore-connectivity (tortuosity) parameter estimated by Mualem to be about 0.5 as an average for many soils.

Detailed solution of the Mualem's model by incorporating Equation (9.9) is given by van Genuchten et al. (1991). This solution, sometimes called van Genuchten-Mualem equation, has the following form:

$$K(S_e) = K_o S_e^l \left\{1 - \left[1 - S_e^{n/(n-1)}\right]^{1-1/n}\right\}^2 \tag{9.13}$$

in which K_o is the matching point at saturation. This parameter is often similar, but not necessarily equal, to the saturated hydraulic conductivity (K_s). Fitting the van Genuchten-Mualem equation to soil data gives good results in most cases (Figure 9.5). It is important to note that the curve-fitting parameters and those representing matching-point saturation and tortuosity tend to lose physical significance when fit to laboratory data. Hence, one must remember that these terms are best described as mathematical constants rather than physical properties of the soils in question.

Rosetta (Schaap et al., 2001) and RETC (van Genuchten et al., 1991) are two useful public-domain programs developed at the U.S. Salinity Laboratory for estimating unsaturated zone hydraulic parameters required by the Richards and van Genuchten equations. The programs provide models of varying complexity, starting with simple ones such as percentages of sand, silt, and clay in the soil, and ending with rather complex options where laboratory data are used to fit unknown hydraulic coefficients.
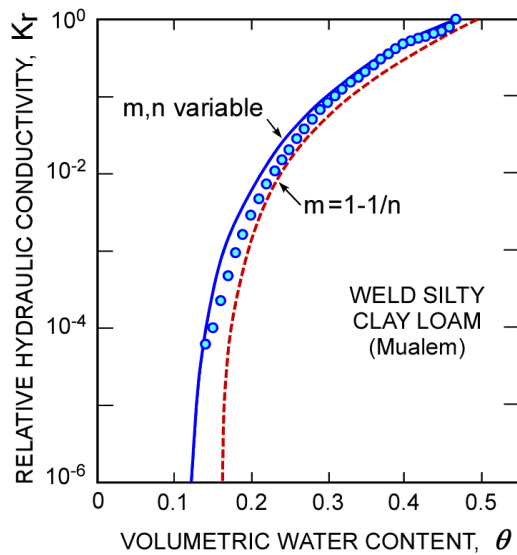
Figure 9.5 Observed and fitted relative conductivity curves for Weld silty clay loam; Mualem's model with *l*=0.5. From van Genuchten et al., 1991. U.S. EPA, in public domain.

Rosetta is Windows-based program for estimating unsaturated hydraulic properties from surrogate soil data such as soil texture data and bulk density. Models like this are often called pedotransfer functions (PTFs) because they translate basic soil data into hydraulic properties. Rosetta can be used to estimate the following properties:

1. Water retention parameters in the van Genuchten equation.
2. Saturated hydraulic conductivity
3. Unsaturated hydraulic conductivity parameters in the van Genuchten-Mualem equation

Rosetta offers five (PTFs) that allow the prediction of the hydraulic properties with limited or more extended sets of input data. This hierarchical approach is of a great practical use because permits optimal used of available input data. The five models use the following input data:

1. Soil textural classes.
2. Sand, silt, and clay percentages.
3. Sand, silt, and clay percentages and bulk density.
4. Sand, silt, and clay percentages, bulk density and a water retention point at pressure of 330 cm (33 kPa).
5. Sand, silt, and clay percentages, bulk density and water retention point at pressures of 330 cm and 15000cm (33 and 1500 kPa)

The first model is based on a lookup table that provides class average hydraulic parameters for each USDA soil textural class (see Figure 9.6 and Table 9.1). The other four models are based on neural network analysis and provide more accurate predictions when more input data variables are used. All estimated hydraulic parameters are accompanied by uncertainty estimates that allow an assessment of the reliability of Rosetta's predictions.

Table 9.1 gives class-average values of the seven unsaturated zone hydraulic parameters for the twelve USDA textural classes. For the θ_r, θ_s, α, n and K_s parameters, the values have been generated by computing the average values for each textural class. For K_o and l, the values were generated by inserting the class average values of θ_r, θ_s, α, n into Model C2 (explained in the Rosetta's help file). This means that K_o and l are based on predicted parameters and may not be very reliable. The values in parentheses give the one standard deviation uncertainties of the class average values.
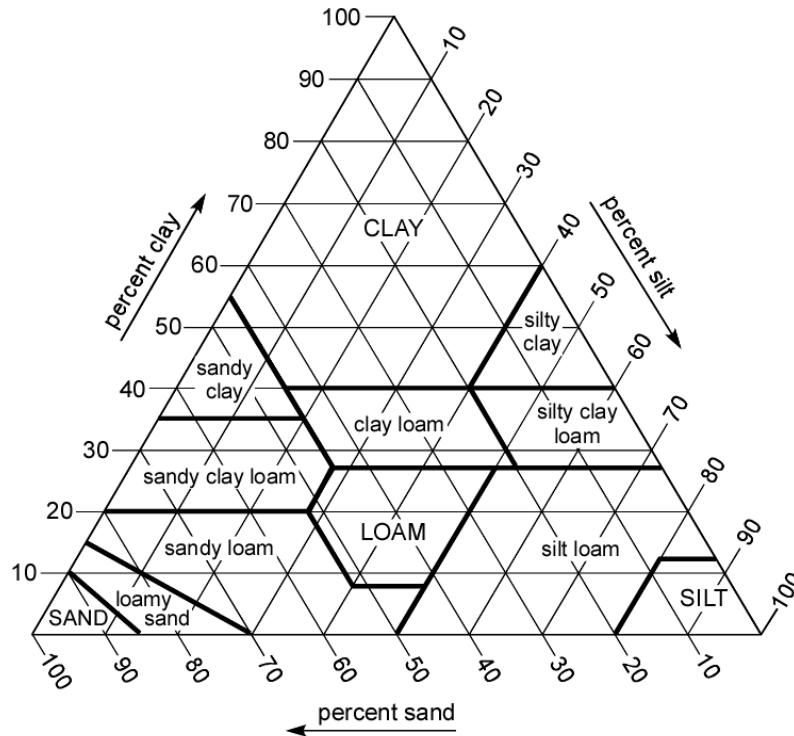
Figure 9.6 U.S. Department of Agriculture 12 basic textural classes of soils with the percentages of clay, silt, and clay. From USDA, 2017. U.S. Department of Agriculture, in public domain

Table 9.1 ROSETTA Class Average Hydraulic Parameters for twelve USDA textural soil classes. Available at https://cals.arizona.edu/research/rosetta/, in public domain.

Texture Class	N	θ_r cm³/cm³		θ_s cm³/cm³		log(α) log(1/cm)		log(n) log10		K_s log(cm/day)		K_o log(cm/day)		l	
Clay	84	0.098	(0.107)	0.459	(0.079)	-1.825	(0.68)	0.098	(0.07)	1.169	(0.92)	0.472	(0.26)	-1.561	(1.39)
Clay Loam	140	0.079	(0.076)	0.442	(0.079)	-1.801	(0.69)	0.151	(0.12)	0.913	(1.09)	0.699	(0.23)	-0.763	(0.90)
Loam	242	0.061	(0.073)	0.399	(0.098)	-1.954	(0.73)	0.168	(0.13)	1.081	(0.92)	0.568	(0.21)	-0.371	(0.84)
Loamy Sand	201	0.049	(0.042)	0.390	(0.070)	-1.459	(0.47)	0.242	(0.16)	2.022	(0.64)	1.386	(0.24)	-0.874	(0.59)
Sand	308	0.053	(0.029)	0.375	(0.055)	-1.453	(0.25)	0.502	(0.18)	2.808	(0.59)	1.389	(0.24)	-0.930	(0.49)
Sandy Clay	11	0.117	(0.114)	0.385	(0.046)	-1.476	(0.57)	0.082	(0.06)	1.055	(0.89)	0.637	(0.34)	-3.665	(1.80)
Sandy Clay Loam	87	0.063	(0.078)	0.384	(0.061)	-1.676	(0.71)	0.124	(0.12)	1.120	(0.85)	0.841	(0.24)	-1.280	(0.99)
Sandy Loam	476	0.039	(0.054)	0.387	(0.085)	-1.574	(0.56)	0.161	(0.11)	1.583	(0.66)	1.190	(0.21)	-0.861	(0.73)
Silt	6	0.050	(0.041)	0.489	(0.078)	-2.182	(0.30)	0.225	(0.13)	1.641	(0.27)	0.524	(0.32)	0.624	(1.57)
Silty Clay	28	0.111	(0.119)	0.481	(0.080)	-1.790	(0.64)	0.121	(0.10)	0.983	(0.57)	0.501	(0.27)	-1.287	(1.23)
Silty Clay Loam	172	0.090	(0.082)	0.482	(0.086)	-2.076	(0.59)	0.182	(0.13)	1.046	(0.76)	0.349	(0.26)	-0.156	(1.23)
Silty Loam	330	0.065	(0.073)	0.439	(0.093)	-2.296	(0.57)	0.221	(0.14)	1.261	(0.74)	0.243	(0.26)	0.365	(1.42)

The RETC computer program provides several options for describing or predicting the hydraulic properties of unsaturated soils. These properties define the soil water retention curve, $\theta(h)$, the hydraulic conductivity function, $K(h)$ or $K(\theta)$, and the soil water diffusivity function, $D(\theta)$. The soil water retention function is given by equation (9.10) which contains five independent parameters, i.e., the residual water content θ_r, the saturated water content θ_s, and the shape factors α, n and m. The predictive equations for K and D add two additional unknowns: the pore

connectivity parameter, l, and the saturated hydraulic conductivity, K_s. Hence, the unsaturated soil hydraulic functions contain up to seven potentially unknown parameters.

The restrictions $n \to \infty$ (i.e., the Brooks-Corey restriction), $m=l-l/n$ and $m=1-2/n$, will reduce the maximum number of independent parameters from 7 to 6. The RETC code may be used to fit any one, several, or all of the 6 or 7 unknown parameters simultaneously to observed data. RETC can be applied to four broad classes of problems (van Genuchten et al., 1991):

1. Direct calculation of the unsaturated soil hydraulic characteristics from the user-specified parameters: α, n, m, θ_r, θ_s, l, and K_s. Values for l and K_s are not needed when only the retention function is being calculated.

2. Fitting the unknown retention parameters (with or without restricted m, n values) to observed soil water retention data. The fitted retention parameters are subsequently used to predict the hydraulic conductivity and diffusivity functions by making use of the models of Mualem or Burdine.

3. Predicting $\theta(h)$ from observed K/D data. In some instances, experimental conductivity data may be available but no observed retention data. Such situations sometimes arise for certain coarse-textured or gravelly soils when tensiometers fail to operate correctly. RETC may then be used to fit the unknown hydraulic coefficients to observed conductivity data using one of the available predictive conductivity or diffusivity models.

4. Simultaneous fit of retention and K/D data. This option results in a simultaneous fit of the model parameters to observed water retention and hydraulic conductivity or diffusivity data.

Once the calculated unsaturated hydraulic conductivity and the related soil moisture profiles are fitted to the field data, or estimated based on general soil characteristics (e.g., grain size and density), the Richards' equation can be used to calculate water flux moving through the unsaturated zone and eventually reaching the water table, thus becoming aquifer recharge. The solution of the flow equation requires boundary and initial conditions, such as soil moisture profile (initial condition) and one or more of the following: prescribed head and flux boundaries, boundaries controlled by atmospheric conditions (e.g., infiltration and/or evapotranspiration), and free drainage boundary (e.g., drainage to the underlying groundwater flow system). In most practical cases, application of computer programs for the variably saturated flow is preferable compared to complex and lengthy analytical solutions. Two such programs in public domain and widely used for their versatility and robustness, and friendly graphical user interface, are VS2DRTI by the USGS, and HYDRUS-1D developed at the U.S. Salinity Laboratory of the U.S. Department of Agriculture.

RETC, Rosetta version 1.0, HYDRUS 1D version 3.01, and other useful public domain models can be downloaded from the Agricultural Research Service, U.S. Department of Agriculture website at https://www.ars.usda.gov/. The same site lists numerous references on flow, and solute fate and transport in unsaturated and variably saturated zones, many of which are available as downloadable pdf files. Rosetta version 1.2 can be downloaded from https://cals.arizona.edu/research/rosetta/rosetta.html.

VS2DRTI – a public domain graphical software package for simulating water flow, heat transport, and reactive solute transport in variably saturated porous media (vadose zone + saturated zone) can be downloaded from the USGS software site at www.usgs.gov/software/

Lecture 10 Groundwater Discharge. Coastal Groundwater. Springs

This lecture is based on the materials presented in publications by the USGS (Barlow, 2003; Galloway et al., 2003; Winter et al., 1998), and Kresic (2007, 2009), Kresic and Stevanovic (2010), and Kresic and Mikszewski (2013).

All groundwater that is not withdrawn artificially, such as for water supply, agricultural drainage and irrigation, or construction and mine dewatering for example, or is not lost to evapotranspiration, will eventually discharge into various surface water bodies, either directly or via springs. Surface water and groundwater are inseparable parts of the same hydrologic cycle and there is a continuous exchange of water between the two. However, they are often studied separately, even in cases of closely related problems. This division still holds firm with many professionals, but the artificial boundaries between the surface water and groundwater projects are quickly fading away since there is growing awareness that management and protection of surface water resources cannot be accomplished without the management and protection of groundwater resources, and vice versa.
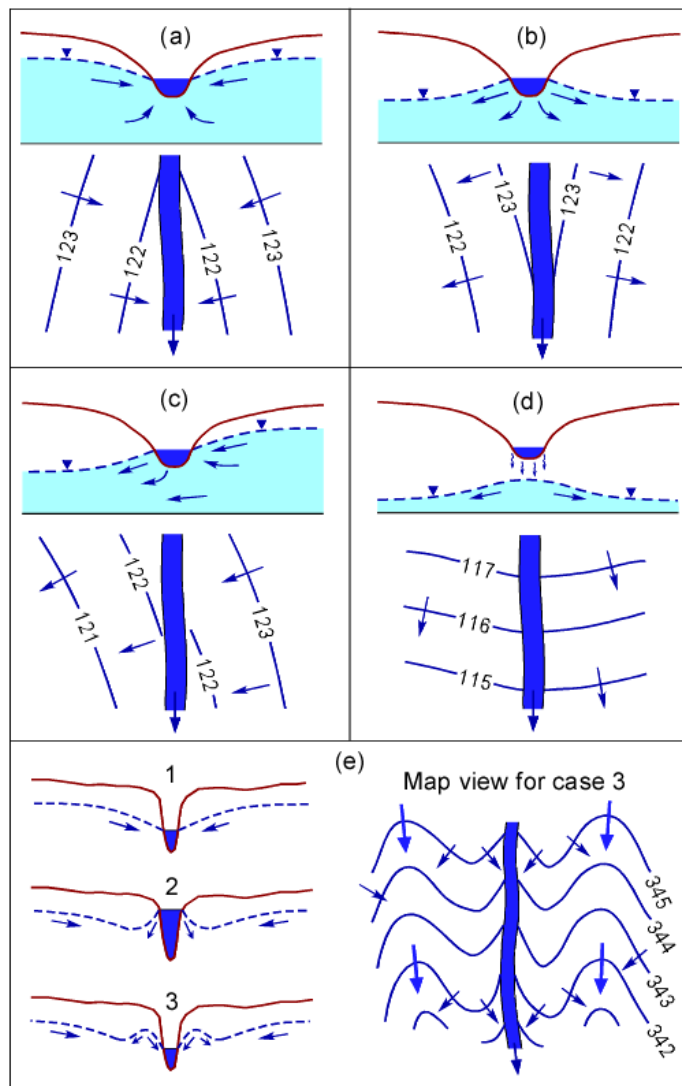
As emphasized in Lecture 1, most perennial surface streams and lakes would not have permanent flow without groundwater contribution called baseflow. At the same time, excessive withdrawal of groundwater may cause depletion or complete cessation of flow in a surface stream, or disappearance of lakes and wetlands. Changes in land use, such as urban development, may alter patterns of surface water runoff and reduce aquifer recharge and, by extension, natural groundwater discharge. Contamination of surface streams adjacent to large well fields used for water supply may, in some cases, threaten groundwater quality in the underlying aquifer because of the induced inflow of contaminated surface water. Conversely, discharge of contaminated groundwater into a surface water body may have negative impact on human health and the environment which depends on surface water.

Figure 10.1   Basic hydraulic relationships between groundwater and surface water shown in cross-sectional views (top), and map views showing hydraulic head contour lines. (a) Perennial gaining stream; (b) Perennial losing stream; (c) Perennial stream gaining water on one side and losing water on the other side; (d) Losing stream (also called ephemeral stream) disconnected from the underlying water table; (e) Contour lines reflecting recent rise (case #2) and then drop (case #3) in river stage. Modified from Kresic, 2007. Copyright CRC Taylor & Francis, permission is required for further use.

218

Figure 10.1 illustrates basic hydraulic relationships between surface streams and underlying aquifers. However, depending on local hydrogeologic and climatic conditions, and human impacts (e.g., operation of dams and locks), the same stream may be losing or gaining water in different sections, and this pattern may change seasonally. Major meandering streams with large flood plains that are seasonally flooded may have quite complicated surface water-groundwater relationships, especially if there are old inactive ("oxbow") or buried meanders. In addition, such streams are often regional bases for groundwater discharge from deeper confined aquifers, which further complicates the assessment of surface water-groundwater interactions (Figure 10.2).
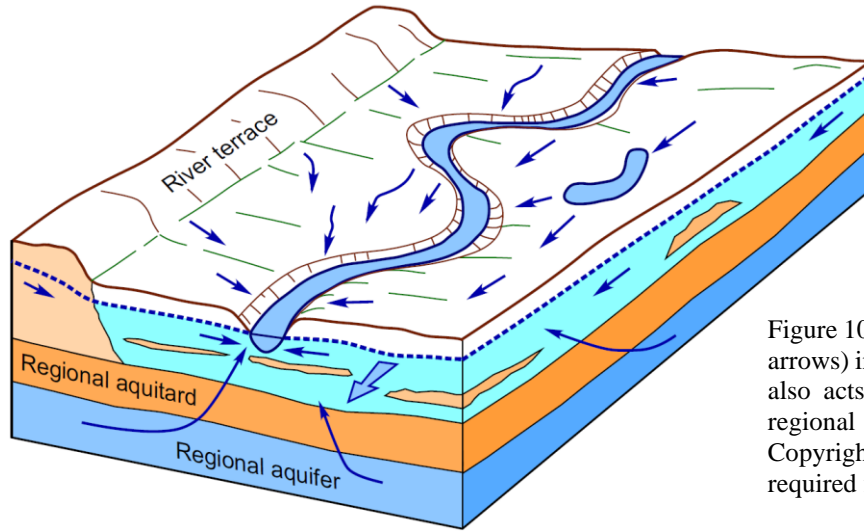
Figure 10.2 Groundwater flow directions (shown with arrows) in a flood plain of a meandering stream which also acts as a groundwater discharge zone for the regional aquifer. Modified from Kresic, 2007. Copyright CRC Taylor & Francis, permission is required for further use.

The simplest way to confirm if a stream segment is gaining water from groundwater discharge is also the most obvious: one must only observe stream banks and channel bottom for signs of discharge in form of springs, seepage springs, and/or bubbles of gas freed from the groundwater due to pressure drop (Figure 10.3).

Current hydraulic status of a stream segment (gaining or losing) can be determined using different methods, of which at least two should be combined for the verification of results. Detail description of various instruments and methodologies is given in Winter et al. (1998), Galloway et al. (2003), Sonestrom and Constantz (2003), and Greswell (2005).
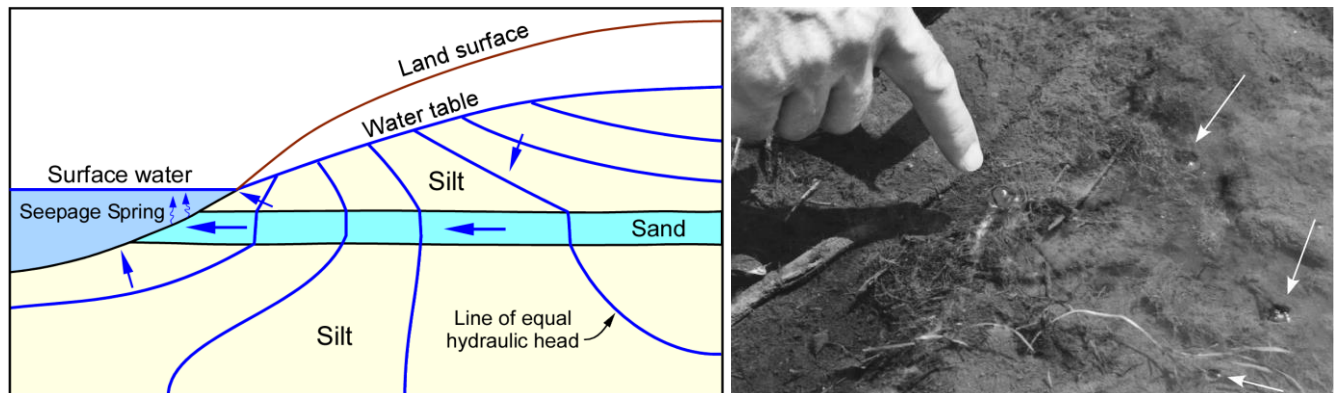
Figure 10.3 *Left*: Submerged seepage spring discharging into a gaining stream. Modified from Winter et al., 1998. USGS, in public domain. *Right*: Bubbles of gas freed from the discharging groundwater due to pressure drop; streambed of Honey Creek in Ann Arbor, Michigan.

The most widely used hydrogeologic approach, and arguably still the most accurate, is the traditional continuous recording of the hydraulic heads in piezometers placed perpendicular to the stream (or a surface water body of interest), including in the aquifer material below the stream channel. Piezometer differs from a monitoring well in that it has only its bottom open to the aquifer, as opposed to a well, which has a screen of certain length. Piezometer therefore accurately records the hydraulic head at the elevation of its bottom. Monitoring wells with longer screens may be used if in conjunction with 3D borehole flowmeters. An ideal placement of piezometers, on either side of the stream, is shown in Figure 10.4. Note that, if the line of piezometers is just on one side of the stream, it would not be possible to accurately state that the stream is truly gaining or losing water since the other side may behave differently (see Figure 10.1).
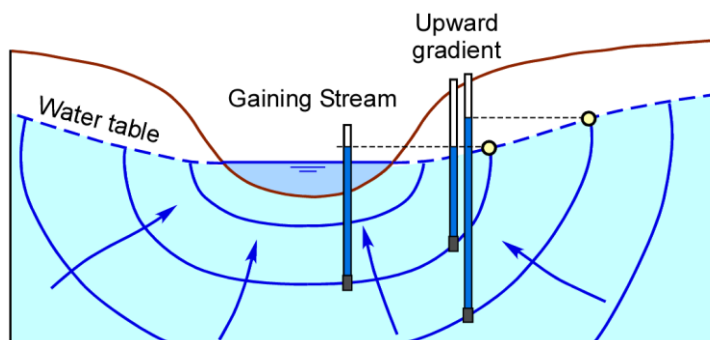
Figure 10.4 Placement of piezometers for determining the hydraulic role of a stream segment. In the case shown, the stream segment is gaining water, i.e., groundwater discharges into the stream. Modified from Kresic, 2007. Copyright CRC Taylor & Francis, permission is required for further use

Care should be taken to place piezometers both outside and inside the so-called *hyporheic zone* if such zone is present (Figure 10.5.) Hyporheic zone (*hypo* – Greek word for under or beneath, *rheos* – stream, *rheo* – to flow) has different definitions based on various scientific fields that have interest in it. For example, biologists and ecologists usually focus on the role of the hyporheic zone as a habitat and refuge for freshwater invertebrate fauna and as a location for salmonid egg development. Probably second in scale, the hydrology literature considers processes that control water flow within the hyporheic zone in terms of the exchange of water between the river channel and the adjacent hyporheic sediments. A smaller pool of literature exists within the hydrogeological, and geochemical fields, primarily describing the fate and transport of contaminants present in the discharging groundwater as they interact with the sediments and biota of the hyporheic zone. Some researchers use term *riparian zone* either interchangeably or in conjunction with hyporheic zone to emphasize presence and influence of organics-rich sediments and vegetation (Winter et al., 1998.)
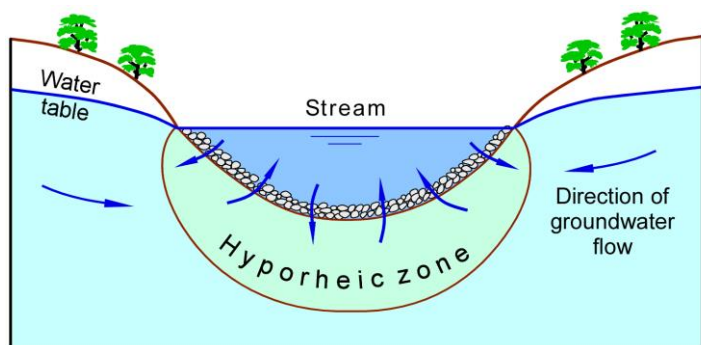
Figure 10.5 Schematic of a hyporheic zone. Modified from Winter et al., 1998. USGS, in public domain.

As illustrated in Figure 10.6, the rate of flow between the aquifer and the river will depend on the difference between the hydraulic head in the aquifer directly below the riverbed and the river stage (hydraulic head of the river), as well as on the hydraulic conductance of the river-aquifer interconnection. The hydraulic conductance is a lumped parameter that relates the river segment length (L), width (W), the riverbed sediment thickness (M), and the hydraulic conductivity of the riverbed sediment (K) as follows:

$$C = \frac{K \times L \times W}{M} \qquad (10.1)$$

The dimension of C is squared length per time, e.g., ft^2/d or m^2/s

The flow rate (Q, in ft^3/d or m^3/s) between the aquifer and the river for the given segment is:

$$Q = C \times \Delta h \qquad (10.2)$$

where Δh is the difference between the hydraulic head in the aquifer and that of the river (river stage).

For the same river segment, a lower conductance corresponds to more fines (e.g., silt) in the riverbed sediment and therefore a lower hydraulic conductivity, resulting in a lower flow rate between the aquifer and the river. Thicker riverbed sediments will have the same effect.
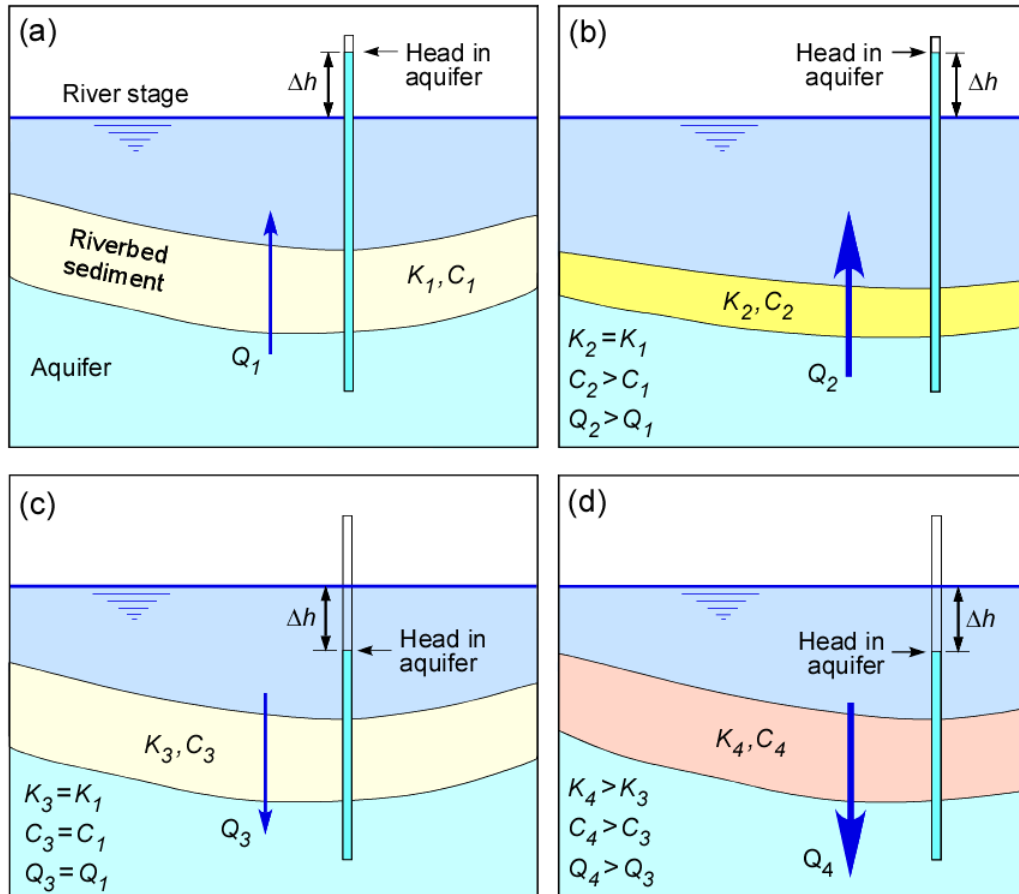
Figure 10.6 Schematic of water exchange between groundwater (aquifer) and river (surface water body). K is hydraulic conductivity of riverbed sediment, C is riverbed conductance, Q is flow rate between the aquifer and the river, Δh is hydraulic gradient between the aquifer and the river, same in all 4 cases but with different direction. (a) and (b) show gaining stream; (c) and (d) show losing stream. Lower hydraulic conductivity of the riverbed sediments, and their greater thickness result in lower conductance, and lower flow rate. Modified from Kresic, 2009. Copyright McGraw Hill, permission required for further use.

Temperature has long been recognized as an important water-quality parameter. Differences between temperatures in a stream and surrounding sediments can be analyzed to trace the movement of groundwater to and from streams, and to better understand the magnitudes and mechanisms of stream—groundwater exchanges. Although airborne and satellite thermal imaging for water resources studies is common (Figure 10.7), the

availability of robust handheld thermal imaging cameras allows hydrogeologists to cost effectively and rapidly image real-time variations in temperature at high resolution in the field at scales from a few centimeters to tens of meters (Figure 10.8). Using drones equipped with thermal cameras literary brings this technique to a whole new level. Thermal imaging can be used to rapidly identify, visualize, and quantify differences in water temperature that may indicate groundwater discharging to the surface (USGS, 2021). The information can be used to:

- localize groundwater discharge,
- help characterize local hydrogeologic conditions, and
- optimize sampling and monitoring locations.
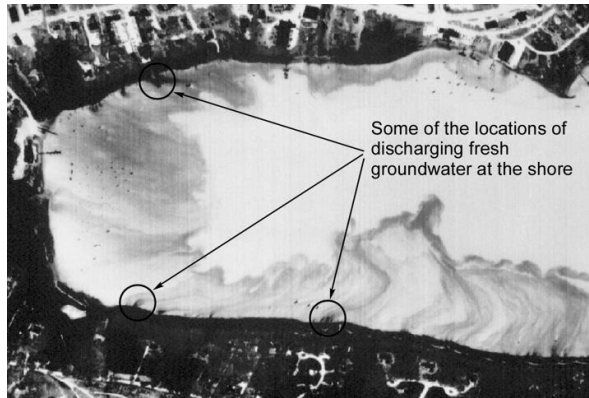
Figure 10.7 Aerial thermal infrared scan of Town Cove, Nauset Marsh, Cape Cod, Massachusetts. Discharging fresh ground water is visible as dark (relatively cold) streams flowing outward from shore over light-colored (warm) but higher density estuarine water. Data were collected at low tide at 9:00 p.m. eastern daylight time on August 7, 1994. From Barlow, 2003; photo by John Portnoy, Cape Cod National Seashore. USGS, in public domain.
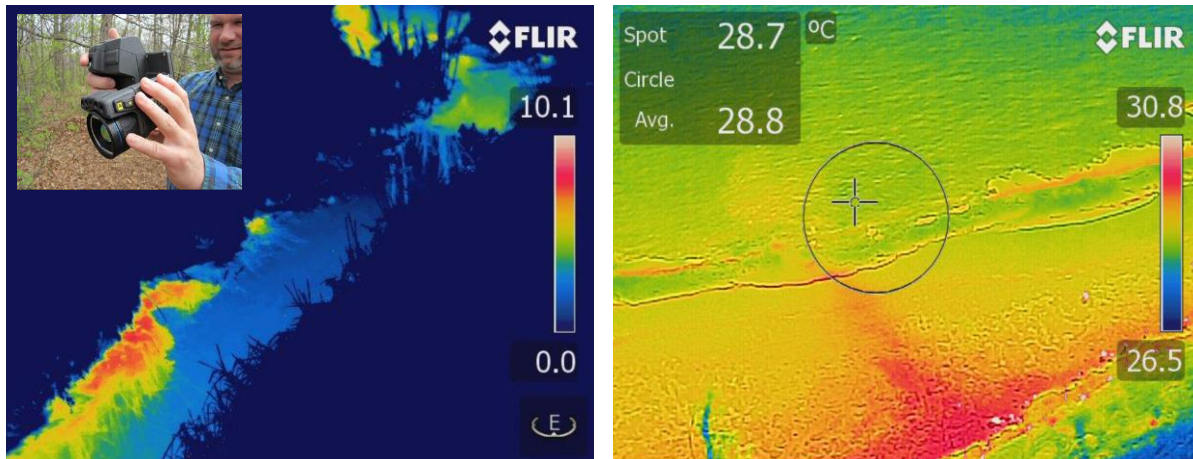
Figure 10.8 *Left*: Thermal image indicates water temperature, where warmer temperatures are represented as red and cooler temperatures as blue. The image presents an area where warmer groundwater (red) may be discharging into a cooler (blue) stream in late fall at Tidmarsh Farms, Massachusetts. The image spans an area about 6 meters across. Temperature is in degrees Celsius. Inset photo shows a high-resolution thermal image camera. (Credit: USGS/Martin Briggs.) *Right*: Thermal image indicates water temperature, where warmer temperatures are represented as red and cooler temperatures as blue. The image presents an area where warmer groundwater (red) may be discharging into a lagoon. Temperature is in degrees Celsius. Courtesy of USGS Utah Science Center and USGS Arizona Water Science Center. In public domain.

Measuring temperature of water, and temperature of streambed sediment at various depths including below the hyporheic zone in the aquifer, is a relatively inexpensive method for an immediate indication of the flow regime character. Typically, heat movement caused by temperature differences is traced by continuous monitoring of temperature pattern in the stream and streambed followed by interpretation using numerical models. For example, reaches of the channel in which sediment-temperature fluctuations are highly damped relative to in-stream

fluctuations indicate high rates of groundwater discharge to the stream (that is, groundwater discharge to a strongly gaining reach). Conversely, segments of the stream channel where fluctuations in streambed temperatures closely follow in-stream fluctuations indicate high rates of water loss through streambed sediments (that is, groundwater recharge from a losing reach). To quantify the rates, location, and timing of stream-flow gains and losses, an array of temperature sensors is deployed in the stream and adjacent sediments (Stonestrom and Constantz, 2003).

Figure 10.9 illustrates thermal and hydraulic responses to four possible streambed conditions. A and B show gaining and losing perennial streams that are connected to the local groundwater system. C and D show dry and flowing ephemeral streams that are separated from the local groundwater system by an intervening unsaturated zone (ephemeral streams lose water when flowing). The flowing stream has large diurnal variations in temperature which are generally dampened beneath the channel bottom. For a gaining stream (A) diurnal variation in the streambed is only slight because water is flowing up from depths where temperatures are constant on diurnal time scales. For a losing stream (B) the diurnal variations, although dampened, are obvious since the downward flow of water transports heat from the stream into the sediments. In either case, larger or smaller flow of water (advective heat transfer) causes larger or smaller contrasts. Consequently, enough temperature sensors should be placed at varying depths to cover all possible variations. In general, surface water temperature in the losing stream has greater diurnal variations than in the gaining stream since regional groundwater is not flowing into the stream.
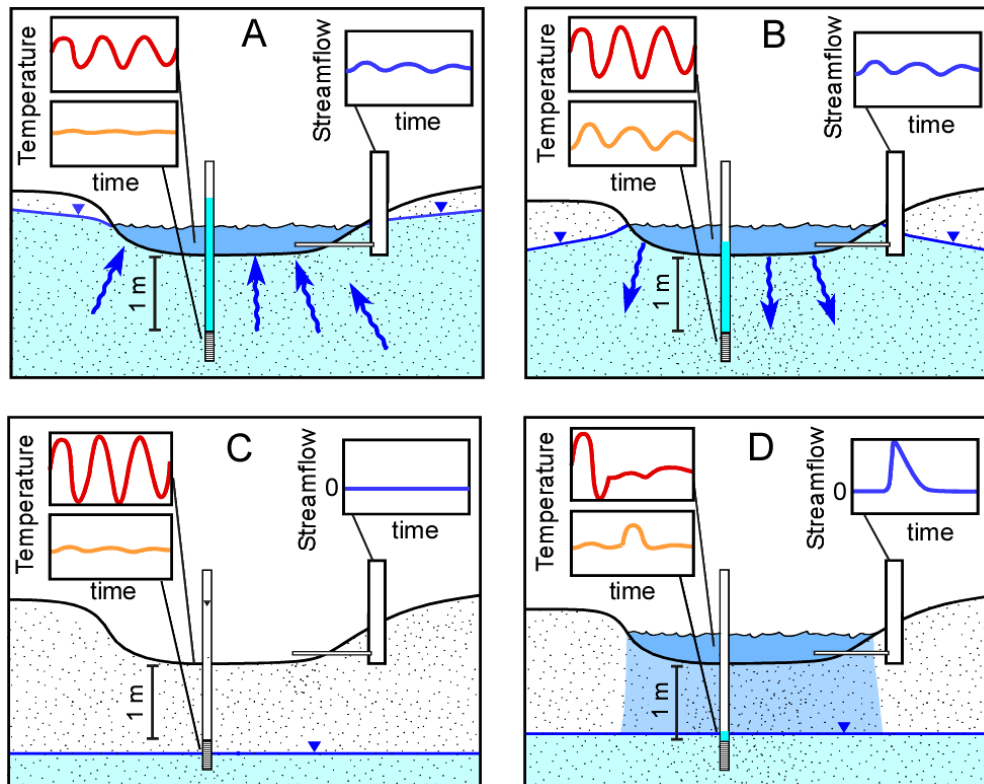
Figure 10.9 Four basic types of hydraulic and thermal responses in surface streams and streambed sediments. A: perennial stream, gaining reach. B: perennial stream, losing reach. C: ephemeral stream without flow. D: ephemeral stream with flow. Modified from Stonestrom and Constantz, 2003. USGS, in public domain.

Figure 10.10 is an example of a gaining perennial stream (corresponding to case A in Figure 10.9) where streambed temperatures at shallow depths are similar to the stream temperature, while at greater depths they are generally colder and slowly increase with time during the summer, reflecting the groundwater temperature with no effect from fluctuating surface temperatures (Conlon et al., 2003). Measured temperatures can be used for calibration of numeric models capable of simulating both the heat transfer and flow through porous media, such as VS2DH/T by USGS, which can then be used to estimate the flow exchanges between the surface stream and the underlying aquifer.
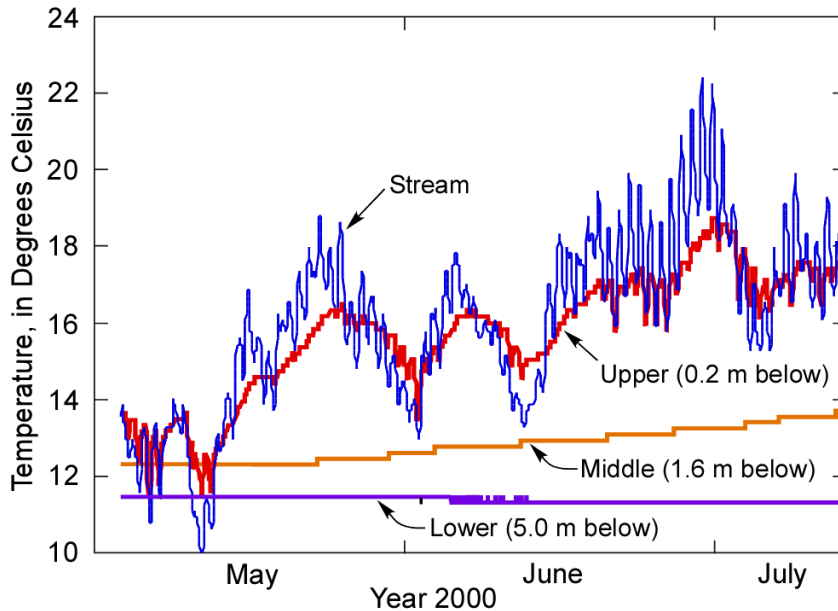
Figure 10.10 Temperatures at Zollner Creek, Central Willamette Basin, Oregon. Modified from Conlon et al., 2003. USGS, in public domain.

Flow measurements at successive stream segments is a common method of determining if the stream is losing or gaining water between the segments. However, because of the large variability of flow conditions in the same stream and the associated potential measurement errors, this method should be applied with great care in order to avoid false conclusions. For example, if only one set of measurements is made at a few locations, with several or more hours separating them, and the stream flow is under the influence of recent precipitation, the results would almost certainly be misleading since the flow wave is moving rapidly. It is therefore best if the flow measurement method is based on continuous recording of the stream stage (or flow) at successive stream segments for at least several days. In addition, the derived flow hydrographs provide information on the actual change of volume of water between the segments, which is the only real measure of gain or loss. Various methods for measurement and computation of stream flow are described by Rantz et al. (1982).

10.2 Coastal Groundwater

Fresh groundwater that does not discharge into surface streams, lakes and marshes, is not evaporated from the water table or transpired by plants and is not withdrawn artificially will eventually discharge into seas and oceans under either unconfined (shallow) or confined (deep) conditions. This direct discharge may be very significant in coastal areas with permeable surficial sediments and rocks where surface water drainage is minor or absent. For example, karst comprises 60 percent of the shoreline of the Mediterranean and is estimated to contribute 75% of its freshwater input, mostly via direct discharge to the sea (UNESCO, 2004; see photographs in Figure 10.11).

Knowledge concerning the submarine discharge of groundwater (SDG) has existed for many centuries. The Roman geographer Strabo, who lived from 63 B.C. to 21 A.D., mentioned a submarine fresh groundwater spring four kilometers from Latakia, what is today's Syria, near the Mediterranean island of Aradus. Water from this

spring was collected from a boat, utilizing a lead funnel and leather tube, and transported to the city as a source of fresh water. Other historical accounts tell of water vendors in Bahrain collecting potable water from offshore submarine springs for shipboard and land use, Etruscan citizens using coastal springs for "hot baths" (as described by Pausanius, ca. 2nd century A.D.) and submarine "springs bubbling fresh water as if from pipes" along the Black Sea (according to Pliny the Elder, ca. 1st century A.D.; from UNESCO, 2004). Until relatively recently, most studies of submarine springs were driven almost exclusively by potable water supply objectives. One of the arguments for continuing efforts in that respect is that even if the captured water is not entirely fresh it may be less expensive to desalinate than undiluted seawater. Another argument is that discharge of freshwater across the sea floor may be considered a waste, especially in arid regions. In such places, the detection of SGD may provide new sources of drinking and agricultural water (UNESCO, 2004).

Figure 10.11 Two submarine karst springs discharging at the Adriatic coastline in Croatia. *Left*: Vrulja Dubci near Brela, Makarska Riviera. *Right*: Vrulja Plantaža, Paklenica National Park (note a boat for scale). Photo courtesy of Dražen Perica.
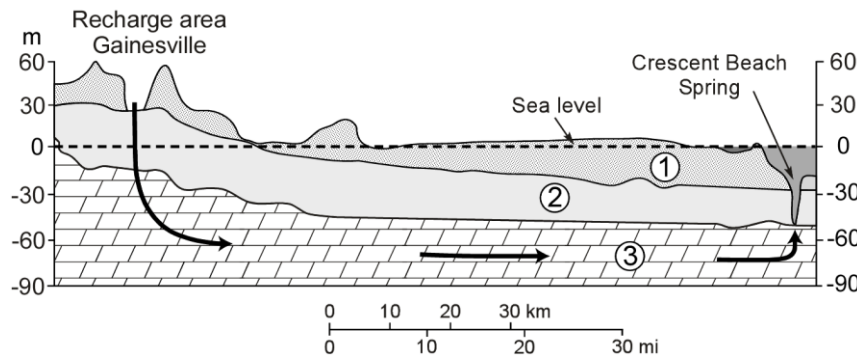
Figure 10.12 Idealized cross section of groundwater flow to Crescent Beach Spring, Florida. (1) Post-Miocene deposits (Green clay, sand and shell); (2) confining unit (Hawthorn Formation); (3) Upper Floridan aquifer (Eocene Ocala Limestone). The morphology of the spring vent and discharge characteristics were investigated in detail. Modified from Barlow, 2003. USGS, in public domain.

The groundwater flow towards the coast and its submarine discharge are driven by the hydraulic gradient between the inland recharge areas and the sea level (Figure 10.12). If the aquifer is confined and well protected by a thick aquitard, the groundwater flow may continue well beyond the coastline with the ultimate discharge taking place along distant submarine aquifer outcrop. As discussed by Barlow (2003), the generally low chloride concentrations in the Upper Floridan aquifer along the Georgia coast have been attributed to the thick confining unit that overlies the Upper Floridan aquifer in that area (see Figure 10.13). The confining unit has created relatively high groundwater heads that have kept the freshwater-saltwater interface offshore. In fact, freshwater flow has been observed to extend as far as 50 miles offshore of southeast Georgia (Johnston et al., 1982). However, along the coast in South Carolina and extending to Tybee Island, Georgia, high chloride concentrations in water from the

aquifer system are attributed to intrusion of offshore saltwater caused by large groundwater withdrawals from the Upper Floridan aquifer in the Savannah, Georgia, and the Hilton Head Island, South Carolina, areas. Saltwater most likely enters the aquifer system by lateral intrusion from offshore areas combined with some downward vertical leakage of seawater to the Upper Floridan aquifer where the overlying confining unit is thin or absent (Krause and Clarke, 2001).
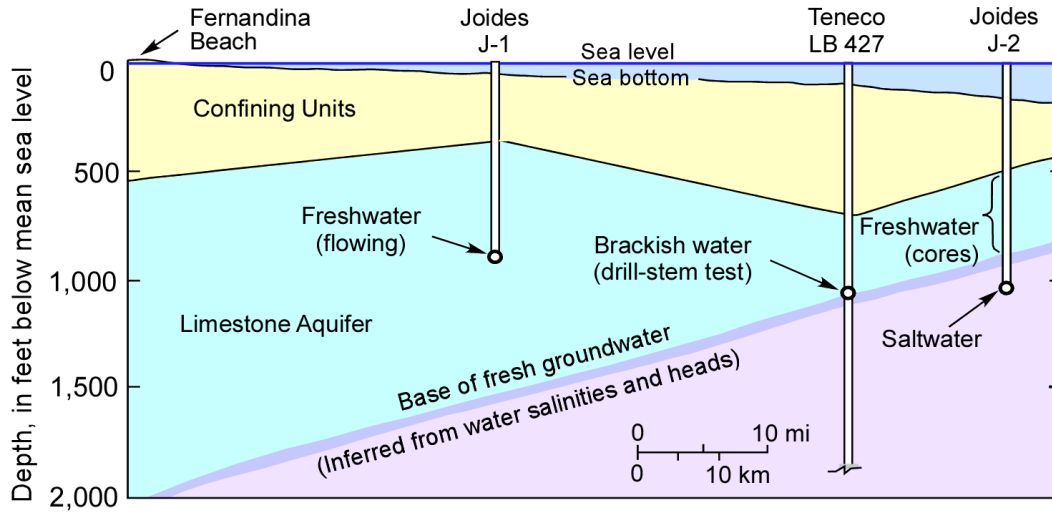
Figure 10.13 Inferred position of the freshwater-saltwater interface based on hydraulic testing and water analyses at offshore exploratory oil wells, Atlantic Ocean off the coast of Georgia and Florida. From Johnston et al., 1982. USGS, in public domain.
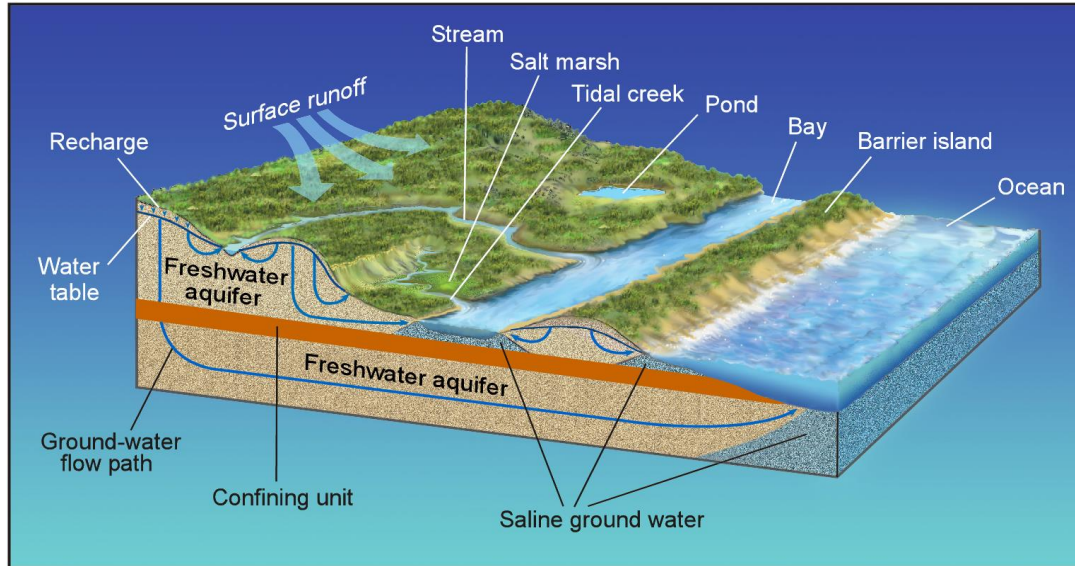
Figure 10.14 Shallow (unconfined) and deep (confined) submarine discharge of fresh groundwater showing flow paths in an idealized watershed along the Atlantic coast. Fresh groundwater is bounded by saline groundwater beneath the bay and ocean. Fresh groundwater discharges to coastal streams, ponds, salt marshes, and tidal creeks and directly to the bay and ocean. From Barlow, 2003. USGS, in public domain.

The submarine groundwater discharge is schematically illustrated in Figure 10.14. Depending primarily on the porous media characteristics, the interface between the freshwater and the saline water intruded naturally from the sea may be rather sharp or there may a wider transitional (mixing) zone in between. In any case, this interface has

a characteristic quantifiable shape because of the density difference between freshwater and saltwater. Lighter (less dense) fresh groundwater overlies more dense saltwater and the thickness of the freshwater above the interface with saltwater can be estimated based on the ratio of their respective densities. This relationship was first recognized by Ghyben and Herzberg, two European scientists who derived it independently in the late 1800s:

$$z = \frac{\rho_f}{\rho_s - \rho_f} h \qquad (10.3)$$

where z is the thickness of freshwater between the interface and the sea level; ρ_f is density of freshwater; ρ_s is density of saltwater; h is the thickness of freshwater between the seal level and water table (Figure 10.15).
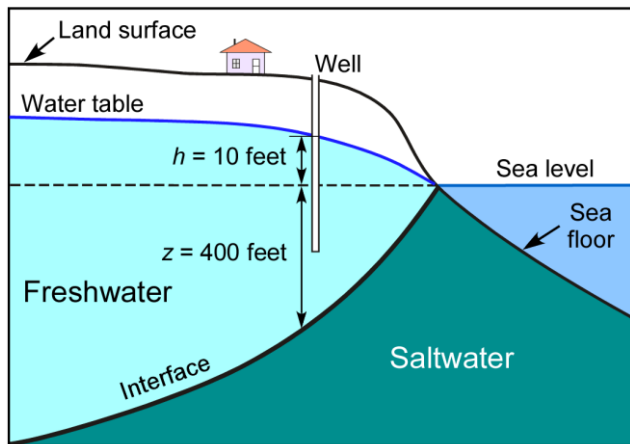
Figure 10.15 Illustration of the Ghyben-Herzberg hydrostatic relationship between freshwater and saltwater. Modified from Barlow, 2003. USGS, in public domain.

Freshwater has a density of about 1.000 grams per cubic centimeter (g/cm^3) at 20ºC, whereas that of seawater is about 1.025 g/cm^3. Although this difference is small, equation (10.3) indicates that it results in 40 ft of freshwater below sea level for every 1 ft of freshwater above sea level as illustrated with the example in Figure 10.15:

$$z = 40h \qquad (10.4)$$

Although in most applications this simple equation is sufficiently accurate, it does not describe the true nature of freshwater-saltwater interface since it assumes hydrostatic conditions (no movement of either water). In reality, fresh groundwater discharges into the saltwater body (sea, ocean) with a certain velocity and through a seepage surface of certain thickness, thus creating a transition zone in which two waters of different density mix by the processes of dispersion and molecular diffusion. Mixing by dispersion is caused by spatial variations (heterogeneities) in the geologic structure, the hydraulic properties of an aquifer, and by dynamic forces that operate over a range of time scales, including daily fluctuations in tide stages, seasonal and annual variations in groundwater recharge rates, and long-term changes in sea-level position. These dynamic forces cause the freshwater and saltwater zones to move seaward at times and landward at times. Because of the mixing of freshwater and saltwater within the transition zone, a circulation of saltwater is established in which some of the saltwater is entrained within the overlying freshwater and returned to the sea, which in turn causes additional saltwater to move landward toward the transition zone (Barlow, 2003).

By convention, freshwater is defined as water having total dissolved solids less than 1,000 mg/l and chloride concentration less than 250 mg/l. For common seawater, these values are 35,000 and 19,000 mg/l respectively. Everything in between would correspond to a mixing zone. The thickness of a mixing zone depends on local conditions in the aquifer but, in general, it is much smaller than the general vertical field scale of interest. In many

cases, quantitative analyses and groundwater modeling codes assume sharp interface between fresh water and saltwater.

Discharge of freshwater causes flow lines in the aquifer to deviate from horizontal as illustrated in Figure 10.16. Because Dupuit's hypothesis about vertical equipotential lines does not apply, the true vertical thickness of freshwater is somewhat greater than the one estimated using the Ghyben-Herzberg equation, as first recognized by Hubbert (1940). The slope of the interface (α) can be calculated using the following equation (Davis and DeWiest, 1991):

$$\sin\alpha = \frac{\partial z}{\partial s} = -\left[\frac{1}{K_f} \times \frac{\rho_f}{\rho_f - \rho_s} V_f - \frac{1}{K_s} \times \frac{\rho_f}{\rho_f - \rho_s} V_s\right] \qquad (10.5)$$

where s is the trace of the interface in a vertical plane; K_f and K_s are hydraulic conductivities for freshwater and saltwater respectively; V_f and V_s are velocities of freshwater and saltwater along the interface respectively. Equation (10.5) can be simplified if it is assumed that saltwater is stagnant compared to freshwater which flows over it, so that the second term in the brackets becomes zero.
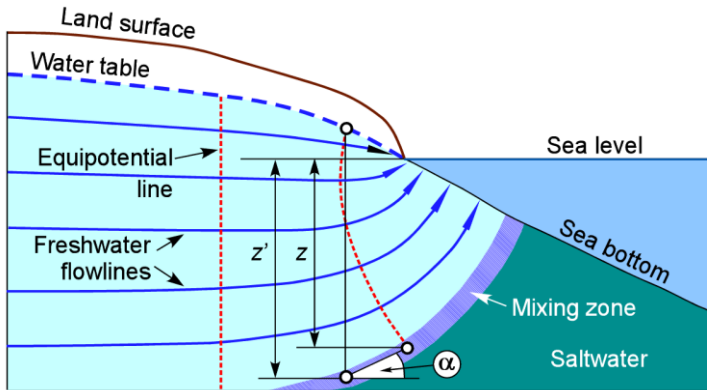
Figure 10.16   Hydrodynamic relationship between freshwater and saltwater in an unconfined coastal aquifer. α is angle of the interface slope. True depth to salt water (z') is greater than the one assumed based on the Ghyben-Herzberg relationship (z) because the equipotential lines are not strictly vertical. Modified from Kresic, 2007. Copyright CRC Taylor & Francis, permission is required for further use.

Understanding submarine groundwater discharge mechanisms, as well as the dynamic nature of the freshwater-saltwater interface, is particularly important for islands. People who live on small coral islands are heavily reliant on fresh groundwater as their dominant source of potable water. On such islands, groundwater is found as a thin veneer of freshwater, called a freshwater lens, floating over saltwater in the unconfined aquifer. A typical example is Tarawa atoll in the Pacific Ocean, which consists of coral sediments and limestone of unknown thickness, overlying a volcanic seamount. The freshwater lenses in the islands of Tarawa atoll are up to 30 m deep (Figure 10.17; Falkland, 1992, from Metai, 2002). Two major geological layers are found within this 30 m zone, a younger layer (Holocene age) consisting largely of unconsolidated coral sediments overlying an older layer (Pleistocene age) of coral limestone. Unconformity between these two layers is at depths generally between about 10 and 15 meters below mean sea level (Jacobson and Taylor, 1981, from Metai, 2002). This unconformity is very significant to the formation of freshwater lenses. The Pleistocene limestone below the unconformity has relatively high permeability which enhances the mixing of freshwater and seawater. Mixing is less likely to occur in the relatively less permeable upper Holocene sediments.
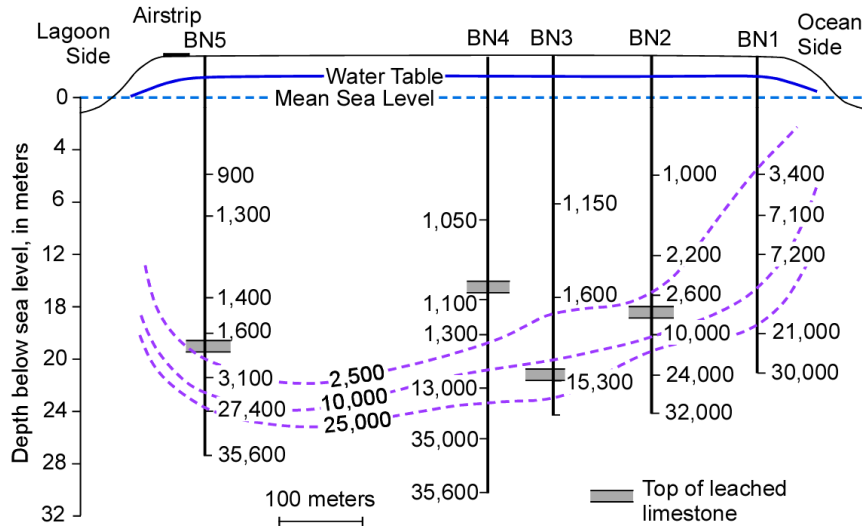
Figure 10.17 Depth of freshwater limits at selected cross-sectional area, Tarawa atoll in the Pacific Ocean. Numbers and contours are for concentration of total dissolved solids (TDS) in mg/L. Modified from Metai, 2002. Pacific Regional Consultation on Water in Small Island Countries.

Island aquifers are vulnerable to any change in the delicate water balance between recharge from rainfall, evapotranspiration from the water table, mixing with the surrounding saltwater, and discharge into the open sea (ocean) water. Uncontrolled groundwater withdrawal may cause saltwater intrusion and loss of freshwater and can have serious consequences for island people. Unfortunately, likely sea level rise caused by climate change would have similar impact on low-lying islands even if groundwater management practices were prudent.

10.2.1 Coastal Karst Aquifers

Similarly to unique hydraulic characteristics of fresh groundwater flow in karst aquifers, there are notable differences between freshwater-saltwater interactions in coastal karst aquifers compared to porous media aquifers where the principles illustrated in Figures 10.15 and 10.16 do apply. The presence of preferential flowpaths such as karst conduits, where Darcy's law is not applicable (see Lecture 5.2), greatly complicates things. As discussed by Kresic and Panday (2021), these interactions can be explicitly simulated with a physically based, novel dual-density groundwater flow, and fate and transport model MODFLOW-USG which is released by the United States Geological Survey and is in public domain (Panday et al., 2013; Kresic and Panday, 2018; Panday, 2020). This is illustrated with Figure 10.18 which shows comparison between two simulations of a conceptual coastal karst aquifer. The traditional Darcian porous media, non-conduit simulation (Figure 10.18-*Top*) shows a classic wedge interface between the fresh groundwater and seawater within the aquifer. The simulation with the conduit (Figure 10.18-*Bottom*) shows re-distribution of the groundwater salinity due to mixing of incoming fresh water in the conduit and the seawater in and around it. The conduit acts as a drain, disturbing the classic wedge shape with mixing of water from above and below it.

Model results for simulation of a recharge episode from the rain lasting 5 days are shown in Figure 10.19. During the rainfall event the mixing of freshwater and seawater creates a "diluted bubble"; this is followed by the intrusion of the sea water back landward after the end of the rainfall event. The complex dynamic relationship between the seawater and the incoming fresh water during the rain event is best illustrated with the constantly changing directions of velocity vectors in the system. For example, the mixing of freshwater and seawater starts at day one of the rainfall but is limited to a narrow zone around the conduit, and almost exclusively in the upward direction where the high freshwater head in the conduit can overcome the dense seawater head (Figure 10.19-*Left*

and Figure10.20). The strong upward gradient from the conduit results in discharge of this mixed ("brackish") water at the sea floor above – activation of a submarine spring. The redistribution of the hydraulic head in the system also causes instability in the conduit itself resulting in formation of several internal hydraulic divides.
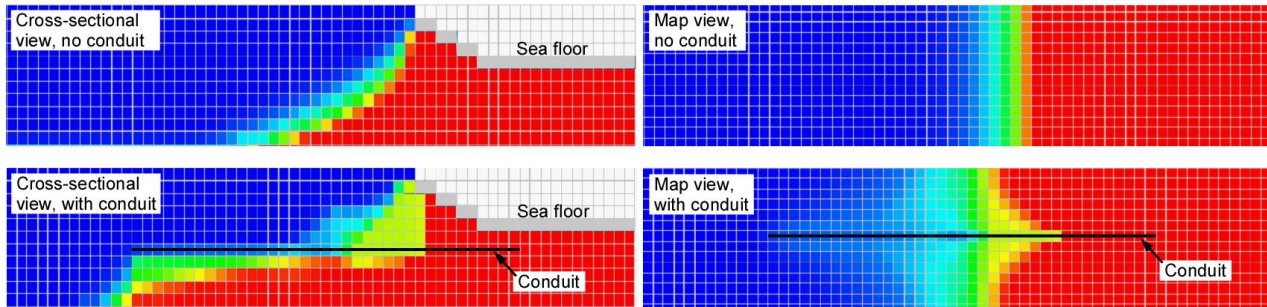
Figure 10.18 Results of the variable-density steady-state simulation of the freshwater-seawater interface without (top two figures) and with a conduit extending between onshore and offshore, below sea floor (bottom 2 figures). Blue color denotes fresh groundwater, red color denotes seawater within the aquifer, mixing zone is denoted with other colors. Modified from Kresic and Panday, 2021. Copyright Springer Nature Switzerland AG, permission required for further use.
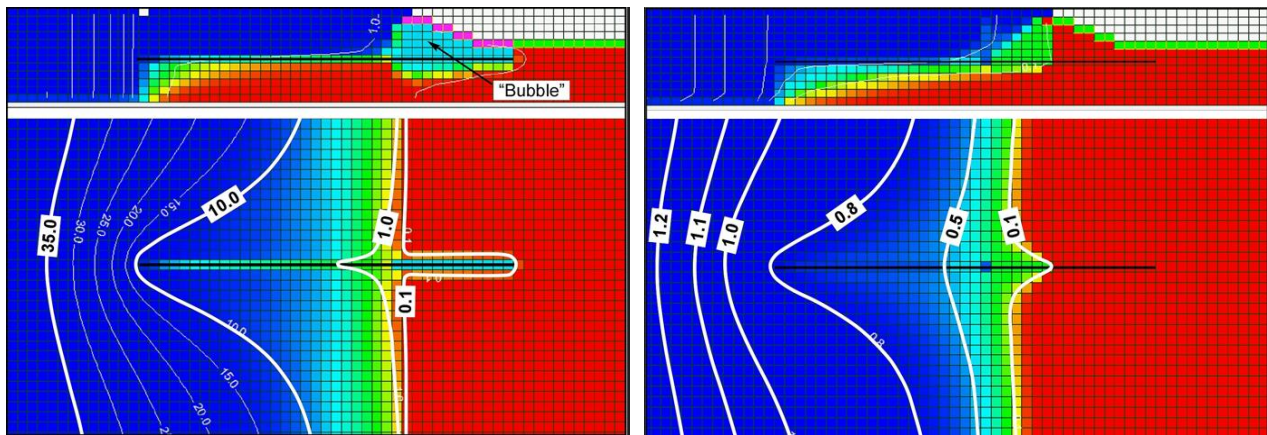
Figure 10.19 Results of the transient model for the end of a 5-day rainfall episode (left) and 100 days after (right) with a conduit. The map views show contours of the simulated hydraulic head, in feet above sea level, in model layer where the conduit (black line) is placed. Blue color denotes fresh groundwater, red color denotes seawater within the aquifer, mixing zone is denoted with other colors From Kresic and Panday, 2021. Copyright Springer Nature Switzerland AG, permission required for further use.
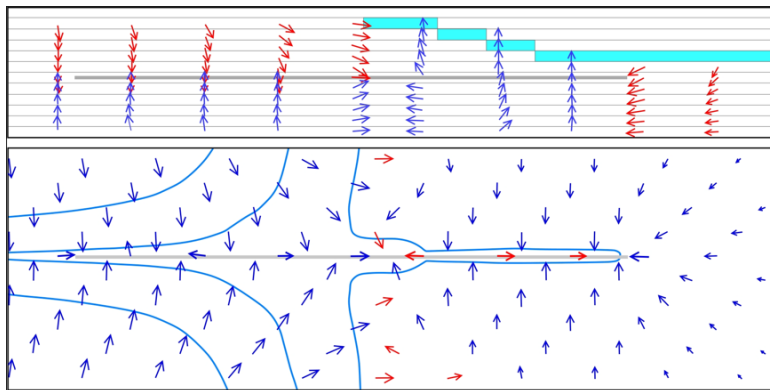
Figure 10.20 Calculated velocity vectors in the area around the conduit, in cross-sectional and map views, at the end of day 1 of the rainfall episode. Blue vectors have an upward direction, red vectors have a downward direction. From Kresic and Panday, 2021. Copyright Springer Nature Switzerland AG, permission required for further use.

10.2.1 Saltwater Intrusion

During the last several decades, groundwater use in coastal areas worldwide has dramatically increased due to rapid population growth. With this increase came the public recognition that groundwater supplies are vulnerable to overuse and contamination. Groundwater development depletes the amount of groundwater in storage and causes reductions in groundwater discharge to streams, wetlands, and coastal estuaries, and lowered water levels in ponds and lakes. Contamination of groundwater resources has resulted in degradation of some drinking water supplies and coastal waters. Although overuse and contamination of groundwater are common for all types of aquifers, the proximity of coastal aquifers to saltwater creates unique challenges with respect to groundwater sustainability. Two main concerns are saltwater intrusion into freshwater aquifers and changes in the amount and quality of fresh groundwater discharge to coastal saltwater ecosystems. Saltwater intrusion is the movement of saline sea water into freshwater aquifers caused primarily by groundwater pumping from coastal wells. Because saltwater has high concentrations of total dissolved solids and certain inorganic constituents, it is unfit for human consumption and many other uses. Saltwater intrusion reduces fresh groundwater storage and, in extreme cases, leads to the abandonment of supply wells when concentrations of dissolved ions exceed drinking-water standards (Barlow, 2003). The problem of saltwater intrusion was recognized as early as 1854 on Long Island, New York (Back and Freeze, 1983), thus predating many other types of drinking-water contamination issues in the news.

When natural conditions in a coastal aquifer are altered by groundwater withdrawal, the position and shape of the freshwater-saltwater interface, as well as the mixing zone thickness, may change in all three dimensions and result in saltwater intrusion (encroachment). The presence of leaky and discontinuous aquitards and pumping from different aquifers or different depths in the same aquifer, may create a rather complex spatial relationship between freshwater and saltwater. Figure 10.21 shows a simple case of saltwater intrusion caused by well pumpage from an unconfined homogeneous aquifer resting on an impermeable horizontal case. As the pumping rate and drawdown increase, the interface continues to move landward until it reaches the critical hydraulic condition. At this point the hydraulic head at the groundwater divide caused by pumping and the interface toe are positioned on the same vertical. Any further increase in the pumping rate or lowering of the hydraulic head will result in a rapid advance of the interface until new equilibrium is reached, with the interface toe landward of the well (Bear, 1979). In many cases this lateral intrusion of saltwater would result in complete abandonment of the well.
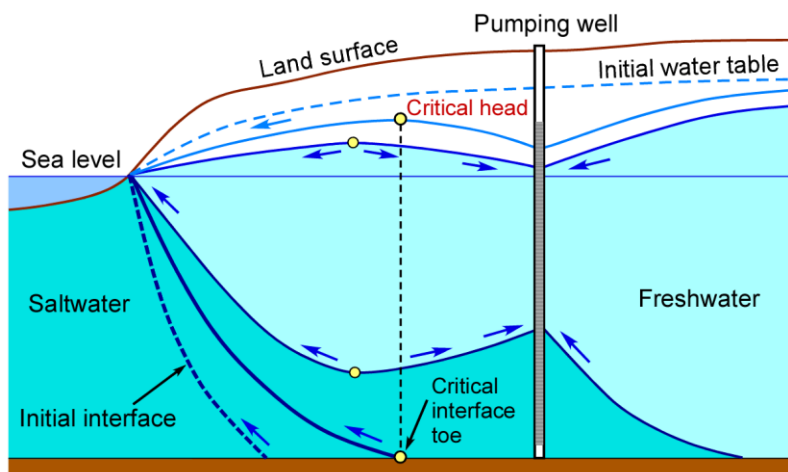
Figure 10.21 Changing freshwater-saltwater interface position resulting from a single well pumping in a coastal unconfined aquifer. Explanation in text. Modified from Strack, 1976, and Bear, 1979.

Well pumping above the saltwater-freshwater interface will cause up-coning of the denser saltwater, which is not necessarily always accompanied by a significant lateral landward movement of the interface. This up-coning

may reach the well and also result in cessation of pumping due to unacceptable concentrations of total dissolved solids and other constituents in the extracted water. However, unlike in the case of complete lateral saltwater encroachment, once the pumping stops and the hydraulic head of freshwater increases, the cone of dense saltwater dissipates relatively quickly driven by gravity.

Strack (1976), Bear (1979), Kashef (1987) and Bear et al. (1999) provide analytical solutions for calculating the positions and movement of the saltwater-freshwater interface for various cases of groundwater extraction including stratified aquifer-aquitard systems. Excellent public domain (free) computer programs for three-dimensional numeric modeling of density-dependent groundwater flow include Modflow-USG and Modflow 6, both released by the United States Geological Survey (available at https://www.gsienv.com/product/modflow-usg/ and https://www.usgs.gov/mission-areas/water-resources/software.)

Under natural, stable, and homogeneous conditions, hydraulic gradients of fresh groundwater in coastal aquifers are towards the sea, forming an interface between the discharging groundwater and seawater as illustrated in Figures 10.15 and 10.16. However, seawater intrusion is typically a complex three-dimensional phenomenon influenced by the heterogeneous nature of coastal sediments, the spatial variability of coastal aquifer geometry and the distribution of extraction wells. It is therefore not possible to apply simple analytical equations to solving real-world problems, such as prediction of the effects of sea-level rise on underlying fresh groundwater. The effective management of coastal groundwater systems requires an understanding of the specific seawater intrusion mechanisms leading to salinity changes, including landward movements of seawater, vertical freshwater-seawater interface rise, or "up-coning", and the transfer of seawater across aquitards of multi-aquifer systems (Simmons et al., 2007). Other processes, such as relic seawater mobilization, salt spray, atmospheric deposition, irrigation return flows and water-rock interactions may also contribute to coastal aquifer salinity behavior and need to be accounted for in water resource planning and operation studies (e.g., Werner and Gallagher, 2006; FAO, 1997). Variable density groundwater flow and solute transport modeling is arguably the only feasible tool for assessing the effects of the above listed processes.

As discussed by Simmons et al. (2007), when embarking on groundwater modeling in coastal areas, it is essential to realize that the textbook conception of fresh and saline groundwater distribution, which is classically conceived of as a freshwater lens overlying a wedge of saline groundwater, is seldom encountered in real field settings due to the dynamic nature of shorelines. The most conspicuous manifestations of transient effects are offshore occurrences of fresh groundwater and onshore occurrences of salt water. In many instances, these waters occur too far offshore to be explained by active sub-sea outflow of fresh water due to topographic drive. Moreover, lowest salinities often occur at substantial depths beneath the seafloor and are overlain by more saline pore waters, suggesting absence of discharge pathways. These waters therefore are considered paleo-groundwaters that were emplaced during glacial periods with low sea level. During subsequent periods of sea-level rise, salinization was apparently slow enough to allow relics of these fresh waters to be retained.

For proper predictive modeling of the effects of see-level rise on groundwater resources, it is very important to understand that in many flat coastal and delta areas, the coastline during the recent geologic past was further inland than it is today. As a result, vast quantities of saline water were retained in the subsurface after the sea level retreated. Such occurrences of saline groundwater are sometimes erroneously attributed to seawater intrusion, i.e., the inland movement of seawater due to aquifer over-exploitation. Effective water resource management requires proper understanding of the various forcing functions on groundwater salinity distribution on a geological timescale (Kooi and Groen, 2003). High salinities are maintained for centuries to millennia, or sometimes even longer, when the presence of low-permeability deposits prevents flushing by meteoric water (Groen et al., 2000). Rapid salinization due to convective sinking of seawater plumes occurs when the transgression is over a high-permeability

substrate, as illustrated in Figure 10.22. This process is responsible for the occurrence of saline groundwater up to depths of 400 m in the coastal area of the Netherlands (Post and Kooi, 2003).
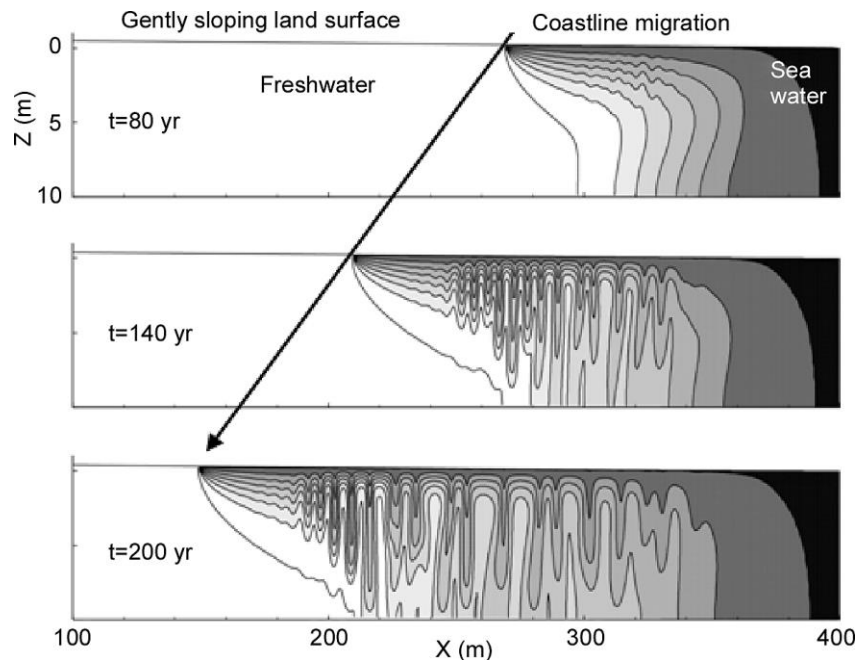
Figure 10.22 Variable density flow simulation showing salinization lags behind coastline migration during transgression on a gently sloping surface and development of offshore brackish groundwater. Highly unstable convective fingering is seen as dominant vertical salinization mechanism. After Kooi et al., 2000; copyright American Geophysical Union. Permission is required for further use.

The large spatial and time scales involved in modeling the effects of seawater intrusion pose special challenges. In particular, the high-resolution model grid required to capture convective flow features imposes a severe computational burden that limits the size of the model domain. Other complications include the lack of information on boundary conditions, insufficient data for proper parameterization, especially for the offshore domain, and unresolved numerical issues with variable-density codes. Resolving these issues represents a continuing challenge for groundwater professionals.

10.3 Springs

A spring is a location at the land surface where groundwater discharges from the aquifer, creating a visible flow. This discharge is caused by difference in the elevation of the hydraulic head in the aquifer and the elevation of the land surface where the discharge takes place. The opening through which groundwater discharges is called the spring's orifice. Springs issuing from consolidated rocks usually have a well-defined orifice (Figure 10.23-*Left*), as opposed to springs in unconsolidated sediments, although the latter ones may also have a clearly visible, (but usually small) orifice (Figure 10.23-*Right*). Sometimes, the orifice can be at the bottom of a spring pool and not readily visible, or it may be covered by sediments and rock debris.

When the flow cannot be immediately observed but the land surface is wet compared to the surrounding area, such discharge of groundwater is called a seep. A seepage spring is a general term used to indicate diffuse discharge of water, usually from unconsolidated sediments, such as sand and gravel, or from loose soil.

Figure 10.23 *Left*: Spring on Šar Mountain in North Macedonia, discharging from an opening in stratified marble. Photo courtesy of Zlatko Ilijovski. *Right*: Small spring ("gushet") issuing from residuum soil at a creek bank. The larger of the two orifices is about 2 in. (5 cm) in diameter.

A fracture (or fissure) spring refers to concentrated discharge of water from a bedding plane, joint, cleavage, fault, or other breaks in the consolidated rock (Figure 10.24). The term tubular spring (or cave spring) is sometimes used to describe flow from a relatively large opening (cave) in the rocks; such springs are characteristic of karst aquifers (see Lecture 7.3 and various photos in this Lecture). The largest springs in the world, including in the United States, belong to this category.
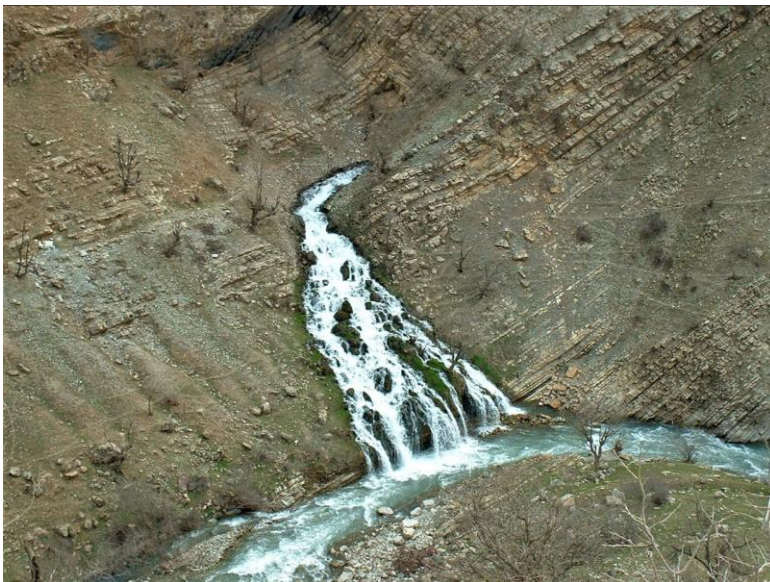
Secondary springs issue from locations located away from the primary spring discharge, which is covered by colluvium (rock fall fragments) or other natural debris and therefore not visible. When capturing such springs every attempt should be made to remove all the debris and locate the primary spring orifice(s), since the secondary discharge locations tend to migrate over time.

Figure 10.24 A typical descending gravity spring issuing from the Cretaceous Kometan Formation in northern Iraq. Photo courtesy of A. Holm.

As discussed by Meinzer (1927b), "The water seldom issues from a single opening and may issue from a great many openings, which may be close together or scattered over a considerable area. What is considered a single spring in one locality in another locality may be regarded as a group of springs, each of which has an individual

name. Some springs are designated in the singular and some in the plural, for example, Silver Spring and Thousand Springs. The idea that underlies this usage is that, if the water issues from a single opening or several openings close together, it forms a "spring," whereas if it issues from a number of openings that are farther apart, it forms "springs". However, local terminology is so variable in this respect that there is no consistent distinction between "a spring" and "springs," and often there is no uniformity in usage of terms even for the same group of openings."

Although all springs (except some associated with young volcanism and hydrothermal activity, where discharge is driven by gases and temperature gradients) ultimately discharge at the land surface because of the force of gravity, they are usually divided into two main groups based on the nature of the hydraulic head in the underlying aquifer at the point of discharge:

- Gravity springs emerge under unconfined conditions where water table intersects land surface and can be formed in any type of porous media.
- Artesian springs discharge under pressure due to confined conditions in the underlying aquifer. They are also called ascending or rising springs and usually drain fractured rock and karst aquifers where groundwater circulation in fractures and conduits (under pressure) reaches great depths, well below the ultimate point of discharge at the spring (Figure 10.25). In karst terrains they are sometimes called Vauclusian springs after spring Fontaine de Vaucluse in southern France.
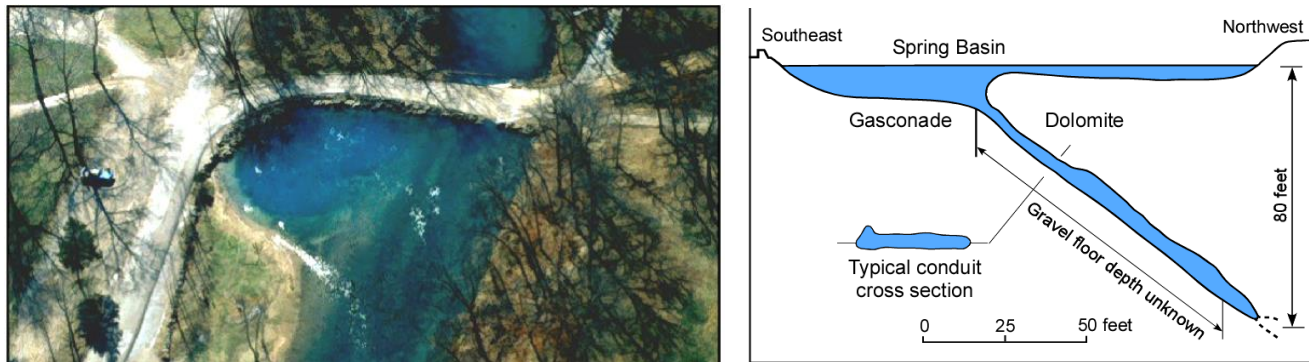
Figure 10.25 Longitudinal cross-section through first magnitude Bennet Spring in Dallas County, Missouri, United States, with average flow about 114 million gallons per day. Data supplied by D. Rimbach, M. Tatalovich, and M. Grussemeyer. Modified from Vineyard and Feder, 1982; photo courtesy of Missouri Department of Natural Resources. In public domain.

Contact springs issue at contacts between water-bearing, permeable rocks (permeable porous media in general) and less-permeable underlying rocks. When this contact slopes toward the spring, in the direction of groundwater flow, and the aquifer is above this impermeable contact, the spring is called a descending contact spring (Figure 10.26a). When the impermeable contact slopes away from the spring, in direction opposite of the groundwater flow, the spring is called an overflowing contact spring (Figure 10.26b).

Depression springs are formed in unconfined aquifers when the topography intersects the water table, usually due to surface stream incision (Figure10.27a). Possible contact between the aquifer and the underlying low-permeable formation is not the main reason for spring emergence (this contact may or may not be known).

When surface stream cuts through alternating layers of permeable and impermeable sediments (rocks), the original depression springs may be transformed into contact springs at various elevations above the stream channel (Figure10.27b). Such springs are often found along depositional and erosional river terraces.
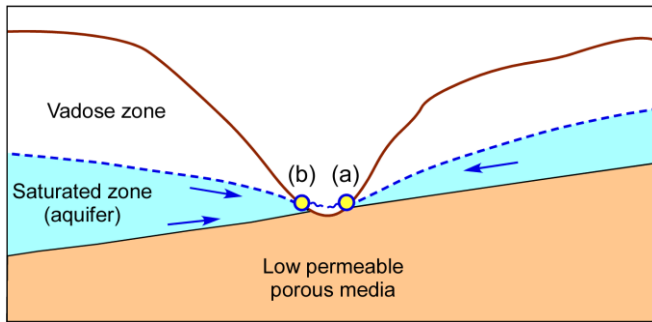
Figure 10.26 Contact gravity springs: (a) Descending; (b) Overflowing. Modified from Milojević, 1967. University of Belgrade; acknowledgment is required for further use.
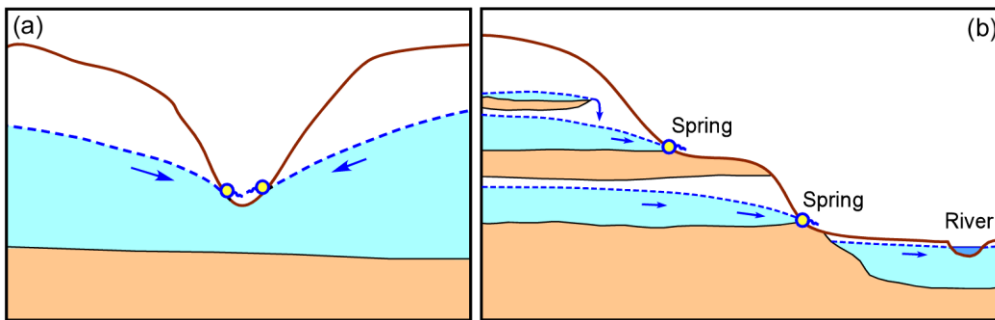
Figure 10.27 (a) Depression springs formed by active incision of a surface stream and located near the stream channel; (b) Previously depression springs, now contact gravity springs along river terraces. Modified from Milojević, 1967. University of Belgrade; acknowledgment is required for further use.

Depression springs draining local groups of interconnected fractures are common in fractured rock aquifers and are not necessarily located close (adjacent) to a surface stream—any erosional depression intersecting water-bearing fractures can cause emergence of a spring. Small depression springs in fractured rock aquifers have been used as sources of local water supply around the world throughout human history (Figure 10.28).

Geomorphology and geologic fabric (rock type and tectonic features, such as folds and faults) play the key role in the emergence of springs. When site-specific conditions are rather complicated, springs of formally different types, based on some classifications, may appear next to each other, causing confusion. For example, a lateral impermeable barrier in fractured rock, caused by faulting, may force groundwater from greater depth to ascend and discharge at the surface through the overlying alluvial sediments in the stream valley (Figure 10.29).

Figure 10.28 Simple capture of a small spring issuing from fractures in metamorphic rocks of the Piedmont physiographic province, the United States. Many other similar springs are still used as sources of both potable and non-potable water, although drilled wells are now the main form of water supply in the region.

236

This water may have elevated temperature due to the normal geothermal gradient in the Earth crust or because of a nearby magmatic source of heat; such springs are called thermal or "hot" springs. At the same time, groundwater of normal temperature may issue at a "cold" gravity spring located very close to the thermal spring, at the contact with less permeable alluvial fine-grained sediments, such as clays. Yet, a third spring may be present with its temperature somewhere in between, depending on the precipitation pattern, seasonal influences, and the mixing mechanism of groundwaters with different temperatures.
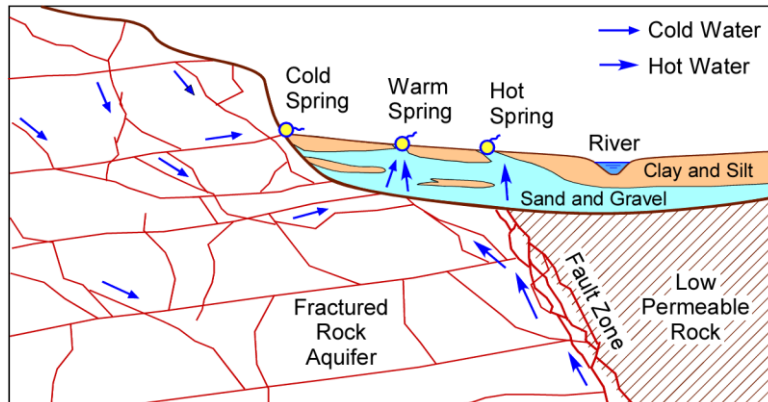
Figure 10.29   Three springs of different temperature in a barrier fault zone overlain by alluvium. Modified from Kresic, 2010. Copyright Elsevier; permission is required for further use.

Figure 10.30 shows some examples of barrier springs; the term generally refers to springs at any lateral contact between the aquifer and a low-permeable rock (sediment). Such contact can have many shapes, caused by depositional processes or tectonic movements which form a variety of faults and folds. When groundwater is forced to ascend from greater aquifer depths along the contact due to hydrostatic pressure, the spring is called ascending or artesian. Such springs commonly have stable water temperature that, if higher than the average air temperature at the location, makes them thermal springs.
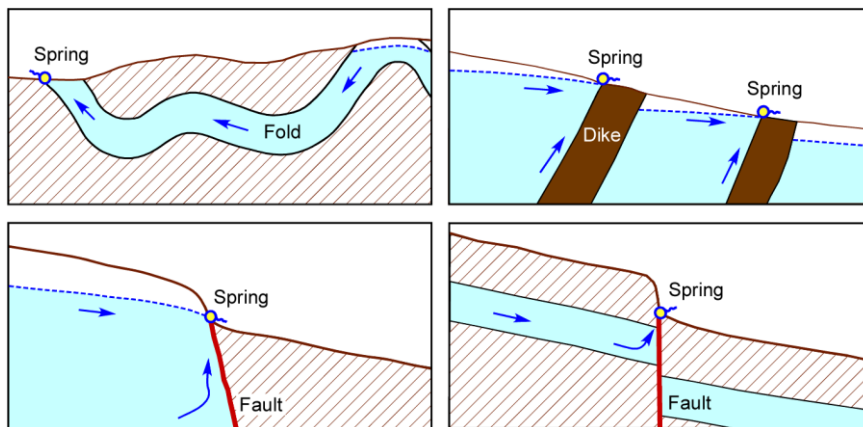
Figure 10.30   Several types of barrier springs issuing at lateral contacts between saturated permeable rocks (aquifers, in blue) and low-permeable rocks or barriers. Modified from Kresic, 2010. Copyright Elsevier; permission is required for further use.

Intermittent springs discharge only for a period of time, reflecting directly the aquifer recharge pattern. They can be found in consolidated and unconsolidated rocks of all types, but the most fascinating are intermittent springs discharging from karst aquifers. As explained in more detail in Lecture 8, karstified rocks can receive a large percentage of precipitation and quickly transmit this newly infiltrated water towards a previously dry spring. Figure 10.31 shows two such springs which are among the largest in the world. Both drain extensive karst aquifer of the Boka Kotorska Bay in Montenegro. The aquifer receives the highest annual precipitation in Europe of over 5,000

mm. Yet, these and many other springs along the coast of Montenegro are intermittent because the aquifer extends well below the Adriatic Sea level and the discharge of groundwater is at the sea floor most of the time.

Figure 10.31 *Top*: When flowing, spring Spila Risanska is used for water supply of the Montenegrin town Risan. Photo courtesy of Petar Milanović. It is usually dry in summer months when the rainfall is the lowest (top right; photo by Neven Kresic). *Bottom*: Intermittent karst spring Sopot, discharging over 200 m^3/s after heavy summer storm. Photo courtesy of Igor Jemcov. Photo of the spring cave when dry (lower right) by Neven Kresic.

Ebb-and-flow springs, or periodic springs, are usually found in limestone (karst) terrain. Their discharge occurs in relatively uniform time intervals (periods) and is explained by the existence of a siphon in the rock mass behind the spring (Figure 10.32). The siphon fills up and empties with regularity, regardless of the recharge (rainfall) pattern. A better-known example from the United States is Periodic Spring in the Bridger-Teton National Forest near Jackson, Wyoming. Situated at the base of limestone cliffs, the spring discharges about 285 gallons per second. Springwater gushes from an opening for several minutes, stops abruptly, then begins a new cycle a short time later. Intermittent water flows range anywhere from 4 to 25 minutes and the water is clear and cold (U.S. Forest Service Intermountain Region, 2008).
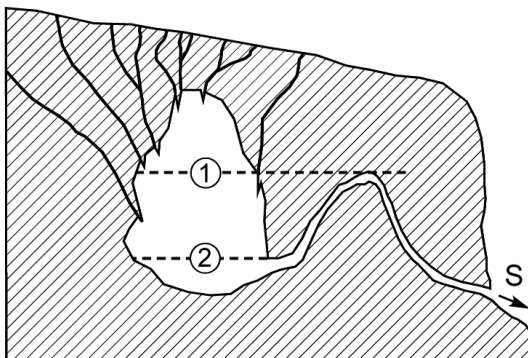
Figure 10.32 Schematic of an ebb-and-flow (periodic) spring. When water in the cavity reaches level 1, the siphon becomes active, and the spring (S) starts flowing. When the level drops to position 2, the spring stops flowing. From Radovanović, 1897. Published by Srpska književna zadruga, Belgrade. Acknowledgment is required for further use.

Estavelle has a dual function: it acts as a spring during high hydraulic heads in the aquifer and as a surface water sink during periods when the hydraulic head in the aquifer is lower than the body of surface water where the estavelle is located (Figure 10.33).
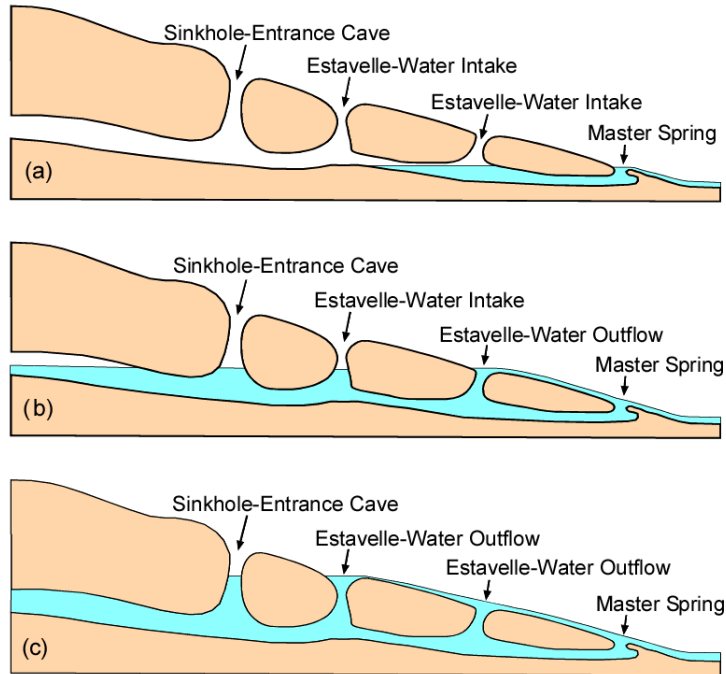
Figure 10.33 Hypothetical stream profile showing sequential reversal of flow in estavelles: (a) Low flow, only lower sections of karst drainage system flooded, estavelles are sinkholes (swallow holes); (b) medium flow, headward flooding of karst drainage system, lowest estavelle becomes spring (rising); and (c) high flow, storage capacity of karst drainage system exceeded, estavelles become springs, water backs up in headward caves. Modified from Vineyard and Feder, 1982. Missouri Department of Natural Resources, in public domain.

10.3.1 Classification of Springs

There have been various proposed classifications of springs, based on different characteristics explained in the previous sections, of which the most common are:

- Discharge rate and uniformity.
- Character of the hydraulic head creating the discharge (descending or gravity springs and ascending or artesian springs).
- Geologic and geomorphologic structure controlling the discharge (depression, contact, barrier, and submerged springs).
- Water quality and temperature.

Various attempts have been made to group springs of different hydraulic or geologic characteristics into new types based on some focused perspective. For example, a classification of springs based on the microhabitats and ecosystems they support is proposed by Springer and Stevens (2009). Another example is the classification of Florida springs proposed by Copeland in 2003 (*Florida Spring Classification System and Spring Glossary*.)

Meinzer's description of springs along Snake River in Idaho, the United States, is a textbook example of all key elements of spring characterization that can also serve as bases for spring classification (Meinzer, 1927b, Large springs in the United States, pages 42 to 50). The following short excerpts from the Meinzer's work illustrate these elements (underlined):

Spring size

Many large springs issue on the north side of Snake River between Milner and King Hill, Idaho, nearly all of them in the canyon below Shoshone Falls or in short tributary canyons (fig. 12). According to the measurements that have been made the total discharge of these springs was 3,885 second-feet in 1902, before any irrigation developments had been made on the north side, and averaged 5,085 second-feet in 1918, after the north-side irrigation project had been developed. The great volume of water discharged by these springs can perhaps be better appreciated by recalling that in 1916 the aggregate consumption of New York, Chicago, Philadelphia, Cleveland, Boston, and St. Louis, with more than 12 million inhabitants, averaged only 1,769 million gallons a day (2,737 second-feet), or only slightly more than one-half of the yield of these Snake River springs in 1918. In. fact, these springs yield enough water to supply all the cities in the United States of more than 100,000 inhabitants with 120 gallons a day for each inhabitant. As shown in Figure 12 and in the following table, there are 11 springs or groups of springs that yield more than 100 second-feet, of which 1 yields more than 1,000 second-feet, 3 yield between 500 and 1,000 second-feet, and 7 yield between 100 and 500 second-feet. (Note that second-feet corresponds to cubic feet per second or ft^3/s.)

Fluctuation in discharge

The flow of these springs is relatively constant, and in this respect they differ notably from most of the large limestone springs.

Role of geology

These springs issue chiefly from volcanic rocks or closely related deposits. The water-bearing volcanic rocks are largely basalt, but they also include jointed obsidian and rhyolite. A large part of the basin of Snake River above King Hill, Idaho, was inundated with basaltic lava during the Tertiary and Quaternary periods, and the lava rock is in many parts so broken or vesicular that it absorbs and transmits water very freely....At the Thousand Springs the water can be seen gushing from innumerable openings in the exposed edge of a scoriaceous zone below a more compact sheet of lava rock. At Sand, Box Canyon, and Blind Canyon Springs the water, according to Russell, comes from a stratum consisting largely of white sand which is overlain by a thick sheet of lava. At most of the springs there is so much talus that the true source of the water can not be observed, but it probably issues chiefly from the large openings in scoriaceous or shattered basalt where the basalt overlies more dense rocks. The fact that most of the springs are confined to rather definite localities and issue at points far above the river indicates that the flow of the ground water to the springs is governed by definite rock structure. The great body of groundwater is obviously held up in the very permeable water-bearing rocks by underlying impermeable formations. It may be that the underlying surface which holds up the water is a former land surface and that the principal subterranean streams which supply the springs follow down the valleys of this ancient surface....At most of the springs the water issues at considerable heights above river level.

Drainage area, recharge, source of water

The lava plain lying north and northeast of these large springs extends over a few thousands of square miles and receives the drainage of a few thousand square miles of bordering mountainous country. The great capacity of the broken lava rock to take in surface water is well established and is, moreover, shown by the fact that in the entire stretch of more than 250 miles from the head of Henrys Fork of Snake River to the mouth of Malade River no surface stream of any consequence enters Henrys Fork or the main river from the north. The greater part of this vast lava plain discharges no surface water into the Snake, and a number of rather large streams that drain the

mountain area to the north lose themselves on this lava plain. A part of the water that falls on the plain and adjoining mountains is lost by evaporation and transpiration, but a large part percolates into the lava rock and thence to the large springs.

<u>Water quality</u>

The water of these springs does not contain much mineral matter. It is generally very clear, although the water of some of the springs, such as the Blue Lakes, has a beautiful blue color and a slight opalescence due to minute particles in suspension. So far as is known, all the springs have about normal temperatures.

<u>Utilization and preservation</u>

On account of the notable height above the river at which most of these springs issue, together with the great volume of water which they discharge, they are capable of developing a great amount of water power. Large power plants have already been installed at Malade Springs and at Thousand and Sand Springs, and other large plants could be installed at other springs, especially at Clear Lakes, Box Canyon, and Bickel Springs....At the Crystal Springs the clear, cold water is utilized in a fish hatchery, where great quantities of trout are raised....The most spectacular feature of these springs is the cataracts which they form, or which they formed before they were harnessed to develop electric energy (pls. 9 and 10). Thousand Springs formerly gave rise to a strikingly beautiful waterfall 2,000 feet long and 195 feet high. Snowball Spring, which discharges 150 to 160 second-feet, is at the east end of the Thousand Sprigs and is included with them in Figure 12. Formerly its water dashed over the rough talus slope, forming a cataract of great beauty that suggested a snowbank. The Niagara Springs, which issue from the canyon wall 125 feet above the river level, also form a spectacular cataract." (See Figure 10.34.)

Meinzer's classification of springs based on average discharge expressed in the U.S. units is still widely used in the United States (Table 10.1). The same table also includes Meinzer's classification based on the metric system. However, the classification based solely on average spring discharge, without specifying other discharge parameters, is not very useful when evaluating the potential for spring utilization. For example, a spring may have a very high average discharge, but it may be dry or just trickling most of the year.
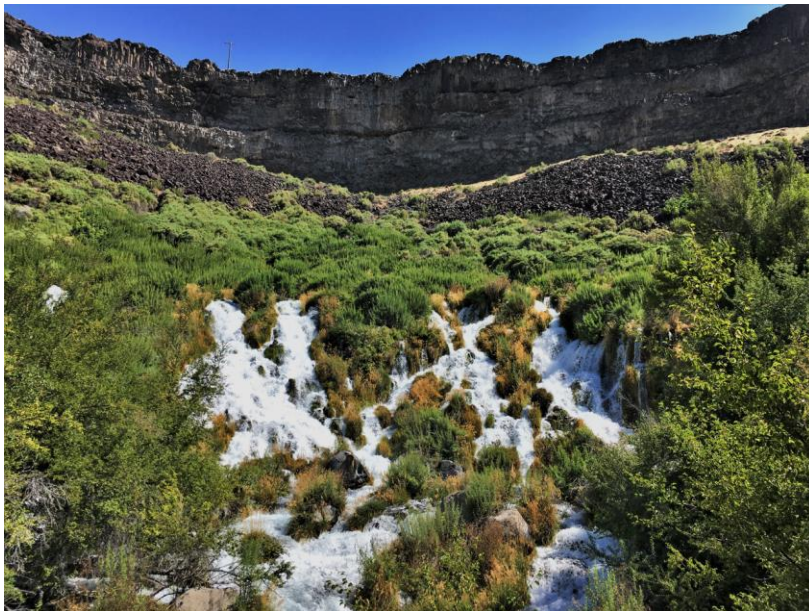
Figure 10.34 Niagara Springs, National Natural Landmark, and part of the world-famous Thousand Springs complex along the Snake River in Idaho, the United States. Note horizontal discontinuities on the cliff, marking different lava flows.

Table 10.1 Classification of Springs Based on Average Discharge Rate. Modified from Meinzer, 1923a.
USGS, in public domain.

Classification in the United States		Classification Based on The Metric System		
Magnitude	Discharge	Magnitude	Discharge in Metric Units	Discharge in English Units (approximate)
1	100 ft³/s or more	1	10 m³/s or more	353 ft³/s or more
2	10 to 100 ft³/s	2	1 to 10 m³/s	35 to 353 ft³/s
3	1 to 10 ft³/s	3	0.1 to 1 m³/s	3.5 to 35 ft³/s
4	100 gpm to 1 ft³/s	4	10 to 100 l/s	158 gpm to 3.5 ft³/s
5	10 to 100 gpm	5	1 to 10 l/s	16 to 158 gpm
6	1 to 10 gpm	6	0.1 to 1 l/s	1.6 to 16 gpm
7	1 pint/min to 1 gpm	7	10 to 100 cm³/s	1.25 pints per minute to 1.6 gpm
8	Less than 1 pint/min	8	Less than 10 cm³/s	less than 1.25 pints per minute

ft³/s is cubic feet per second; gpm is gallons per minute; m³/s is cubic meters per second; l/s is liters per second.

Practice in most countries is that the springs are evaluated based on the minimum discharge recorded over a long period, typically longer than several hydrologic years (hydrologic year is defined as spanning all wet and dry seasons within a full annual cycle). When evaluating availability of spring water, it is important to include a measure of spring discharge variability, which should also be based on periods of record longer than one hydrologic year. The simplest measure of variability is the ratio of the maximum and minimum discharge:

$$I_v = \frac{Q_{max}}{Q_{min}} \qquad (10.3)$$

Springs with the index of variability (I_v) greater than 10 are considered highly variable (e.g., see Figure 10.35), and those with $I_v < 2$ are sometime called *constant* or *steady springs*.

Meinzer proposed the following measure of variability expressed in percentage:

$$V = \frac{Q_{max}-Q_{min}}{Q_{av}} \times 100 (\%) \qquad (10.3)$$

where Q_{max}, Q_{min} and Q_{av} are maximum, minimum, and average discharge respectively. Based on this equation, a constant spring would have variability less than 25 percent, and a variable spring would have variability greater than 100 percent.

According to United States Geological Survey (USGS, 1995), most first-magnitude springs in the United States are in Florida, 27 of them, and they all are draining karstified limestone of the Floridan Aquifer. Missouri has 12 first-magnitude springs (Beckman and Ninchey, 1944), all of them discharging from the karst aquifers of the Ozark Mountains region. The only forts magnitude spring in Arkansas, Mammoth Spring (located in the Mammoth Spring State Park), also discharges from the Ozark limestones. Eleven first-magnitude spring in Idaho are concentrated in the Snake River valley and drain extensive Quaternary basalt lava flows with thin sedimentary units of the Snake River Plain; the twelfth first-magnitude spring in Idaho, Big Spring, emerges from rhyolitic lava flows of the Island Park caldera which is adjacent to Yellowstone National Park. The spring starts the flow of the Henrys Fork, tributary to Snake River. Metolius Springs in Deschutes National Forest, Oregon discharge as a group about 200 yards apart with an almost constant flow rate of 45,000 to 50,000 gallons per minute (100 to 110 ft³/s), just about enough to join the company of Nation's first magnitude springs (Peterson and Groh, 1972). Comal Springs and San Marcos Springs draining karstic Edwards Aquifer are the only first-magnitude spring in Texas, with the average flow rate

of about 332 and 152 ft^3/s respectively. Giant Springs in Montana, with the average flow rate of 156 million gallons per day (241 ft^3/s), concludes the list of first magnitude springs in the United States. It was discovered by the Lewis and Clark Expedition in 1805. This is also the site of the Roe River, once listed in the Guinness Book of World Records as the world's shortest river.

Figure 10.35 Aqua Spring has the largest flow rate and the largest variation of flow of all springs in the Bullpasture Gorge, Virginia, the United States. *Left*: Average flow conditions. *Right*: High flow rate after heavy rainfall carrying a heavy sediment load. The boils or mounds of water above the spring are more than ten feet high. Photographs courtesy of Phil Lukas.

Most Florida springs occur where the limestone of the Floridan Aquifer is exposed at the land surface. Springs drain large amounts of groundwater from the Floridan Aquifer. These springs contribute to the relatively constant temperature and steady flow rate of many of Florida's rivers. The sum of the average flow from Florida's 27 first-magnitude springs is estimated to be 9,400 ft^3/s (6,075 Mgal/d), or about 76 percent of the average flow of all the known springs in Florida. Several first-magnitude springs are nationally or even internationally known, such as Silver Springs, Rainbow Springs, Wakulla Springs (Figure 10.36; see also Figure 5.15 in Lecture 5), and Weeki Wachee Springs. About 70 springs are second-magnitude springs; these collectively discharge about 2,600 ft^3/s (1,680 Mgal/d) or about 21 percent of the total discharge from all known Florida springs.

Spring Creek Springs and Crystal River Springs are the two largest springs in Florida. Discharge measured from Spring Creek Springs (a group of eight known spring vents) in 1974 was about 2,000 ft^3/s (1,293 Mgald). The average discharge from Crystal River Springs is 878 ft^3/s (567 Mgal/d) from 30 individual spring vents. Both springs are located near the coast. The discharge of springs near the coast commonly is affected by tides.

Silver Springs in Marion County, Florida is the largest inland spring in the United States based on average discharge (note that the plural in the name indicates a group of closely spaced springs.) Measured combined discharge from this group of springs ranges from 517 to 1,290 ft^3/s (334 to 834 Mgal/d), and the average adjusted discharge is 700 ft^3/s (452 Mgal/d) based on records from 1946 to 2014 (Sutherland et al., 2017). The highest recorded discharge from any inland Florida spring is 1,910 ft^3/s (1,234 Mgal/d), measured at Wakulla Springs. This maximum discharge is about 50 percent greater than the maximum measured discharge from Silver Springs. Wakulla Springs also has the greatest range in discharge of all Florida springs, from 25 ft^3/s to 1,910 ft^3/s (16 to 1,234 Mgal/d); however, the average discharge (391 ft^3/s, 253 Mgal/d) is less than that of Silver Springs (700 ft^3/s, 452 Mgal/d).
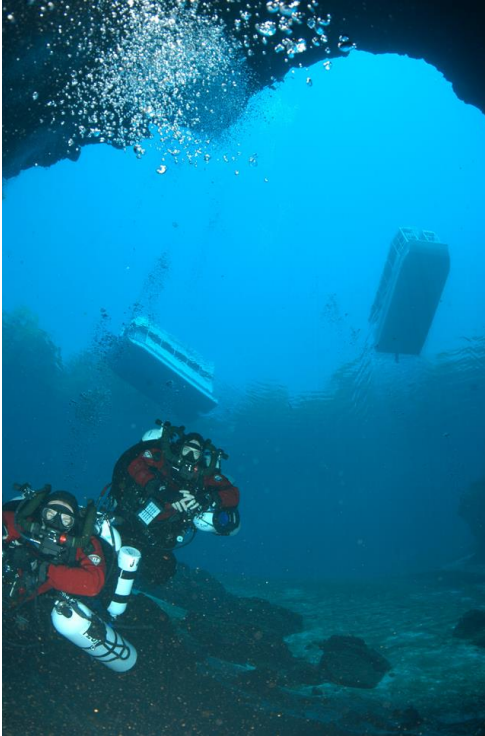
Figure 10.36 Wakulla Springs, 14 miles south of Tallahassee, Florida, the United States. It is one of 27 first magnitude springs in Florida and has the average flow of approximately 391 cubic feet per second, or 253 million gallons per day. According to the Edward Ball Wakulla Springs State Park website, Wakulla means "river of the crying bird" or "strange and mysterious waters." Archaeological evidence suggests that humans have occupied Wakulla Spring for nearly 15,000 years. The vent extends into a massive network of caverns and tunnels that have been extensively mapped by Woodville Karst Plain Project divers. At its discharge point, the spring vent is approximately 180 feet below land surface at the southern end of the spring pool. The relatively warm water discharge from Wakulla Spring provides a winter thermal refuge for the Florida manatee (Northwest Florida Water Management District, 2022) The spring was a backdrop for scenes of the 1941 movie *Tarzan's Secret Treasure* starring Johnny Weissmuller as Tarzan, with Maureen O'Sullivan as Jane and Johnny Sheffield as Boy. Photo copyright and courtesy of David Rhea and Global Underwater Explorers.

According to the analysis of the St. Johns Water Management District (Sutherland et al., 2017; SJRWMD, 2022; see Figure 10.37) Silver Springs system, which feeds the Silver River, has experienced a dramatic decline in flow of approximately 32 percent since the 1940s due to long-term rainfall deficit, flow suppression related to increases in submersed aquatic vegetation (SAV) downstream in Silver River, and, to a lesser degree, regional groundwater pumping.
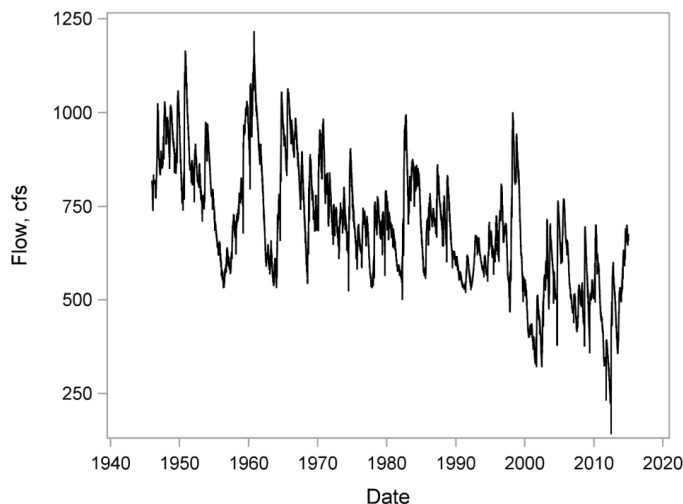
Figure 10.37 Flow hydrograph for the spatially adjusted period of record for the Silver River, USGS gaging station 02239501. From Sutherland et al., 2017. USGS, in public domain.

Worldwide, the classic Dinaric karst is unrivaled with most first-magnitude springs of which the largest one, the Trebišnjica Springs ($Q_{max} > 800$ m^3/s), is now submerged by a reservoir. The Buna River Spring near Mostar, Bosnia and Herzegovina is the largest spring issuing from a single cave, with the minimum and maximum flow rates exceeding 10 m^3/s and 400 m^3/s respectively (Figure 10.38).

In the Dinaric region of former Yugoslavia there are 230 springs with a minimal discharge of over 100 l/s, while about 100 springs have a minimal discharge of over 500 l/s. The World Karst Aquifer Maps (WOKAM) project confirms that the region has the densest concentration of large springs, with minimal discharge exceeding 2 m^3/s, in the world (Kresic and Stevanović, 2022.) Karst aquifers of Turkey and China host a dozen or so first-magnitude springs, whereas a few such springs are found in other well-known karst areas including France, The European Alps, The Middle East, Mexico, and Papua New Guinea (Milanović, 1979, 2004; Ford and Williams, 2007; Kresic and Stevanovic, 2010).
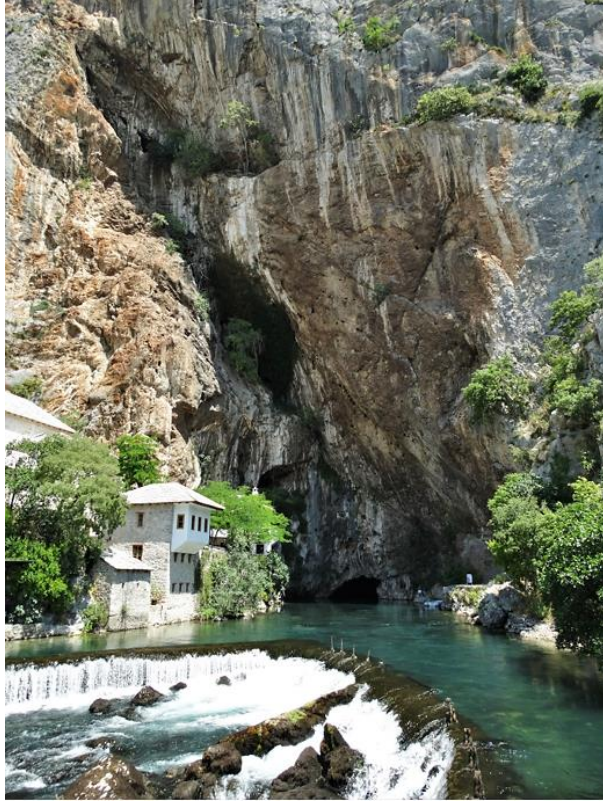
Figure 10.38 Spring of the Buna River near Mostar, Bosnia and Herzegovina emerges from a cave in Mesozoic limestone. It is one of the largest springs in the world, with the maximum discharge of approximately 400 m^3/s or 9 billion gallons a day. The measured long-term average discharge is 24 m^3/s (850 ft^3/s or 550 million gallons a day, Mgald). For comparison, the largest inland spring (group of springs) in the United States, Silver Springs in Florida, had the average discharge rate of 700 ft^3/s or 452 Mgald before the dramatic steady decline as explained in the text. The Buna River Spring is of Vauclusian type (ascending), with the bottom of the main syphon channel, explored by cave divers, at 73 m (240 feet) below the elevation of the vent in the cave.

10.3.2 Thermal and Mineral Springs

Thermal springs are divided into *warm springs* and *hot springs* depending on their temperature relative to the human body temperature of 98 degrees Fahrenheit or 37 degrees Celsius: hot springs have a higher and warm springs a lower temperature. A warm spring has temperature higher than the average annual air temperature at the location of discharge. Water temperature of both groups of thermal springs can fluctuate in time reflecting more or less surficial influence.

Geysers and fumaroles (also called solfataras) are generally found in regions of young volcanic activity. Surface water percolates downward through the rocks below the Earth's surface to high-temperature regions surrounding a magma reservoir, either active or recently solidified but still hot. There the water is heated, becomes less dense, and rises back to the surface along fissures and cracks. Sometimes, these features are called dying volcanoes, because they seem to represent the last stage of volcanic activity as the magma, at depth, cools and hardens.

Erupting geysers provide spectacular displays of underground energy suddenly unleashed, but their mechanisms are not completely understood. Large amounts of hot water are presumed to fill underground cavities. The water, on further heating, is violently ejected when a portion of it suddenly flashes into steam. A slight decrease in pressure or an increase in temperature causes some of the water to boil. The resulting steam forces overlying water up through the conduit and onto the ground. This loss of water further reduces pressure within the conduit system, and most of the remaining water suddenly converts to steam and erupts at the surface (Figure 10.39). This cycle can be repeated with remarkable regularity, as for example, at Old Faithful Geyser in Yellowstone National Park, which erupts on an average of about once every 65 minutes (USGS, 2009a, 2009b).

Figure 10.39 Yellowstone National Park in the United States is home to more than 10,000 hydrothermal features (hot springs being the most common), including more than 500 geysers, the largest concentration in the world.

Fumaroles, which emit mixtures of steam and other gases, are fed by conduits that pass through the water table before reaching the surface of the ground. Hydrogen sulfide (H2S), one of the typical gases issuing from fumaroles, readily oxidizes to sulfuric acid and native sulfur. This accounts for the intense chemical activity and brightly colored rocks in many thermal areas (USGS, 2009a).

Thermal springs are heated by the naturally occurring thermal energy within the Earth (geothermal energy). Measurements in boreholes indicate that temperature increases downward within the Earth's crust at an average rate of about 30ºC/km. Although most of the thermal energy is stored in rocks, water and steam contained in fractures and pore spaces of the rocks are the only naturally occurring media available for transferring this energy to the Earth's surface. In the United States, average groundwater temperatures from 5 to 15 m deep are 5–7ºC above the mean annual air temperature (Reed, 1983).

As discussed by Meinzer (1923a, 1927b, 1940), many of the thermal springs in the Western United States issue along faults, and most of them probably derive their heat from hot gases or liquids that rise from underlying bodies of intrusive rock and in volcanically active areas (Figure 10.40). In many cases, the host aquifers for thermal water are karstified carbonates covered by non-karstic rocks (Figure 10.41). Basin-fill sediment may act as a thermal blanket that traps heat in relatively shallow aquifers beneath large areas of some of the basins. Nice examples of springs produced by the rise of deep waters through fault openings are found along the edges of the mountain ranges of Nevada and western Utah. Many of these springs have large yields, some of them discharging several cubic feet a second. The abundance of these springs and the copious flow of some of them are even more impressive because of the aridity of the region in which they occur. The mountain ranges of this region consist largely of tilted fault

blocks, and in many places, there are recent fault scarps in the alluvial slopes at the foot of the mountains. The springs are situated along the general courses of the fault scarps and the yield of many of them is larger than would be expected from their topographic drainage areas. Some of the largest springs occur along narrow dry ranges that supply but little water and have relatively uniform flow throughout the year, whereas ordinary springs in the region fluctuate more with the season. Notably, quite a few thermal springs issue from pools that are believed to be associated with fractures and fault conduits. Similar settings are also found in other parts of the American West (Figure 10.42).

Figure 10.40 Hot Creek flows through the Long Valley Caldera in a volcanically active region of east-central California. This stretch of the creek, looking upstream to the southwest, has long been a popular recreation area because of the warm waters from its thermal springs. These springs, however, are unpredictable and can suddenly erupt with violence and at boiling temperature. Because of this danger, the U.S. Forest Service has had to close parts of the Hot Creek Geologic Site to visitors. USGS Photo courtesy of Chris Farrar. More details available at http://pubs.usgs.gov/fs/2007/3045

While in the Western United States thermal springs commonly occur along normal faults, in the Eastern United States they occur in regions of folded and thrust-faulted rocks. Figure 10.43 shows three possible models of fluid circulation in such areas according to Sorey et al., (1983a); other models are presented by Breckenridge and Hinckley (1978) and Hobba et al. (1979). Early descriptions of thermal springs in several provinces of the Appalachian Mountains primarily dealt with their therapeutic and recreational values (Moorman, 1867; Crook, 1899; Fitch, 1927). The springs occur in areas of steeply dipping folded rocks that are transected by nearly vertical east-west-trending fracture zones. Correlation of springs with topographic lows, or gaps, apparently results from the fact that easily eroded areas correspond to zones containing many fractures, which, in turn, provide the increased vertical permeability needed to establish a hydrothermal-convection system. Thermal springs always issue from either carbonate rocks or sandstones. Chemical analyses of the spring waters issuing from carbonate rocks exhibit consistently low concentrations of dissolved silica and high concentrations of magnesium and calcium, which indicate that the flow of warm water is restricted to the carbonate rocks. Analyses of waters from springs issuing from fractured sandstone show higher concentrations of dissolved silica and lower concentrations of magnesium and calcium, which indicates that flow is restricted to the sandstone beds (Sorey et al., 1983a).

Geochemical considerations suggest that reservoir temperatures are not substantially higher than the measured surface temperatures at most eastern thermal springs; observed temperatures range from 18 to 41°C. The occurrence of these springs in areas of average heat flow and relatively low temperature gradients (Costain et al., 1976; Perry et al., 1979) indicates that the depths of hydrothermal circulation are generally between 1 and 3 km.

Figure 10.41 *Left*: Boiling River discharging from a limestone cave at the bottom of the Yellowstone River Valley. This thermal spring is the largest in the United States, with water temperature of 140ºF (60ºC). The limestone is exposed by downcutting of the river through thousands of feet thick volcanic ash deposits and lava flows that buried the carbonate sediments. *Right*: One of the ascending Mammoth Springs discharging along a fault and draining a small portion of the limestone aquifer exposed at the Boiling River spring.

Figure 10.42 *Left*: Hot spring in Stanley, Idaho, the coldest town in the conterminous United States. *Right*: Ascending thermal spring in the channel of the Rio Grande River, Big Bend National Park, Texas. The spring is located adjacent to a cliff comprised of thinly bedded limestone (note limestone outcrop in the pool.) The higher hydraulic head in the little pool maintains clear water as opposed to often muddy water of the river.

Figure 10.44 shows The Homestead's spa pool fed by the historic Octagon Spring in Hot Springs, Bath County, Virginia. The spring's temperature is steady 98ºF (37ºC). Several other hot springs ranging between 90- and 108-degrees Fahrenheit comprise this group of the warmest thermal springs in Virginia. There are also cold karst springs on the grounds of the resort, one of the best known and oldest spas in the United States. A hiking trail through the forest above the resort leads to one of the largest, albeit hidden, sinkholes in The Appalachians.

Only several miles away are historic Warm Springs where the Men's Bath House was built in 1761 and has been in use ever since (Figure 10.45). This part of Virginia also has some of the best-kept secrets: swimming caves with thermal waters on private lands that can be visited only by select few.
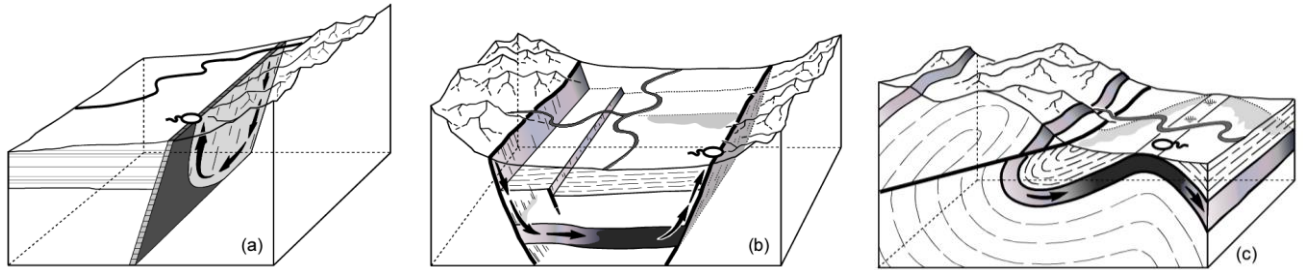
Figure 10.43 Conceptual models for types of hydrothermal-convection systems in which low-temperature geothermal-resource areas in category of isolated thermal springs and wells occur. (a) Fault plane; (b) Deep reservoir; (c) Margin of anticline. Arrows indicate direction of fluid circulation; dark shading shows location of reservoir containing low-temperature geothermal resources. From Sorey et al., 1983a. USGS, in public domain.

Figure 10.44 Homestead's spa pool in Hot Springs, Virginia, fed by the historic Octagon Spring (inset).

In the past, the use of hot springs and geothermal water in general in the United States was primarily for hot-water baths and pools. After 1920, however, the abundance of inexpensive natural gas for heating baths and pools caused a rapid decline in the use of natural hot water. In Europe, however, the spa tourism is still very popular with many world-famous spas. The spa capital of Europe is indisputably Budapest, the capital of Hungary (Figures 10.46 and 10.47). First started by the Romans, the tradition of using hot springs issuing from the underlying karst aquifer continued and was enhanced during the Ottoman rule in the 16th century. The golden age of Budapest spas and luxurious baths in exclusive hotels was under the Austro-Hungarian Empire in the 19th and early 20th centuries, in part thanks to drilling deep thermal wells in the city.

The term mineral spring (and mineral water) has a very different meaning in different countries and could be very loosely defined as a spring with water having one or more chemical characteristics different from normal potable water used for public supply. For example, water can have elevated content of free gaseous carbon dioxide (naturally carbonated water), high radon content ("radioactive" water, still consumed in some parts of the world as "medicinal" water of "miraculous" effects), high hydrogen sulfide content ("good for skin diseases" and "soft skin"), high dissolved magnesium, or simply have the total dissolved solids higher than 1000 mg/L. Some water bottlers, exploiting a worldwide boom in the use of bottled spring water, label water derived from a spring as

"mineral" even when it has no unusual chemical or physical characteristics. In the United States, public use and bottling of spring and mineral water is under control of the Food and Drug Administration and such water must conform to strict standards including source protection.

Figure 10.45 The Men's Bath House in Warm Springs, Bath County, Virginia is the oldest spa structure in the United States. It was built in 1761 and has been in use ever since. Nearby is the Women's Bath built in 1836. The name for the two baths was changed in the 20th century from "Warm Spring Pools" to "Jefferson Pools" before being returned to its original name in 2021. Famous bathers include Thomas Jefferson, who spent three weeks in 1819 bathing three times a day and described the waters in a letter to his daughter, Martha Jefferson Randolph, as being of "first merit". The spa is part of The Homestead, a resort hotel in nearby Hot Springs.

Figure 10.46 Széchenyi thermal spa and bath complex in Budapest, Hungary. With 1.7 million annual visitors, 15 indoor and 3 outdoor pools and almost 3,000 square meters of water surface, Széchenyi can feel more like an amusement park than a thermal bath. Photo courtesy of https://www.offbeatbudapest.com/budapest-city-guide/best-thermal-baths/

Figure 10.47 Gellért Baths is Budapest's second most popular bath, after Széchenyi. It is attached to Hotel Gellért, an art nouveau landmark from 1918. Photo courtesy of gellertfurdo.hu. https://www.gellertbath.hu

10.3.3 Photographs of Select Springs

The hope of the author is that the photographs that follow will help inspire future hydrogeologists to do what is in their power to help protect springs (and, by extension, all groundwater in general) for their current and future beneficial uses worldwide. It is at springs that groundwater finally emerges to become visible, often in spectacular ways, and always confirming how invaluable and irreplaceable groundwater is for supporting and sustaining life on Earth. To that extent, the Karst Commission of the International Association of Hydrogeologists (IAH; https://karst.iah.org/) in 2022 started a project called MIKAS (Most Important Karst Aquifer Springs) with the goal to select, label, and protect the most important karst springs worldwide.

The following excerpts from the anthological work by Gunnar Brune, titled *Major and Historical Springs of Texas* and published in 1975 by the Texas Water Development Board, are applicable to historical significance of springs around the world, and their subsequent demise, caused first by ignorance and unrestricted land use and then by the overwhelming pressure of population growth and inadequate regulations:

Springs were vital to the survival of Texas' earliest inhabitants, over 30,000 years ago. At an archeological site near Lewisville in Denton County, radiocarbon analysis has dated the remains of these early new-world men at 37,000+ years old, including crude sculptures, spears, and spear throwers (Newcomb, 1961). These early Americans always made their campgrounds near water, whether it was a spring, spring-fed stream, a river, or a lake. Bedrock mortars or rock mills were worn into the rock by the Indians as they ground stool, acorns, and other nuts, mesquite beans and grain. These mortars can still be seen at many Texas springs. It is also noteworthy that the Pueblo Indians of west Texas used spring water for irrigation of crops long before the arrival of the Europeans (Taylor, 1902; Hutson, 1898).

Because the springs were so vital to the life of both the Indians and the white man, it is not surprising that many battles were fought over their possession. In 1650 when Spanish explorers first visited Big Spring in Howard County, they found the Comanche and Pawnee Indians fighting for its possession. When a network of forts was strung across Texas, they were, in nearly all cases, located near springs in order to have a reliable supply of pure water. Later the covered-wagon and stagecoach routes came to rely heavily upon springs. For example, the "Camino Real" or King's Highway, completed by the Spanish colonists about 1697 from Natchitoches, Louisiana, to San Antonio and Mexico, passed 13 major Texas springs and many more minor ones. Most of the springs in West Texas are very small in comparison to those in central and east Texas, because of the very low rainfall and recharge. Nevertheless, they often meant the difference between life and death to the early pioneers.

Nearly all of the larger springs were used for water power by the early settlers. At least 61 were used in this way. Gritsmills, flour mills, sawmills, cotton gins, and later electric generating plants were powered by the flow of spring water.

In the late 1800's, many medicinal or health spas sprang up around the more mineralized springs. At least 25 springs, chiefly in east Texas, were believed to be beneficial in curing various ailments. Most of these waters are high in sulfate, chloride, iron, and manganese.

Many of the early settlements relied entirely on spring water. At least 200 towns were named for the springs at which they were located. About 40 still are shown on the official Texas State Highway Map, but many of the springs have dried up.

Throughout the long period during which various Indian tribes occupied Texas, spring flow remained unchanged except as affected by wet and dry climatic cycles. At the time of Columbus' epic voyages Texas abounded with springs which acted as natural spillways to release the excess storage of underground reservoirs. Early explorers described them as gushing forth in great volume and numbers. The very early accounts usually describe not springs but "fountains". This is an indication of the tremendous force with which these springs spouted forth before they were altered by modern man. As an example, less than 100 years ago Big Boiling Spring, one of the Salado Springs (Bell County) was still described as a fountain rising 5 feet high. Such natural fountains ceased to exist in Texas many years ago.

Probably the first effect upon ground-water tables and spring flow was the result of deforestation by the early white settlers. Deforested land was placed in cultivation or pasture. The deep open structure of the forest soils was altered as the organic matter was consumed and the soils became more impervious. Heavy grazing by introduced stock animals was probably especially harmful. Soon the soils were so compacted that they could take in only a small fraction of the recharge which they formerly conveyed to the underground reservoir.

This reduction of recharge affected larger areas as more and more land was placed in pasture. However, the effect upon water tables and spring flow was probably relatively small in comparison with later developments. In the middle 1800's deep wells began to be drilled. It was found that flowing wells could be brought in nearly everywhere. The "Lunatic Asylum" well in Austin, drilled to the basal Trinity Sands, threw water 40 feet high. Water from a well south of San Antonio reaching the Edwards Limestone rose 84 feet above the surface of the ground (Hill and Vaughn, 1898). Nothing could have had a more disastrous effect upon spring flows than the release of these tremendous artesian pressures through flowing wells. Most of these wells were allowed to flow continuously, wasting great quantities of water, until the piezometric heads were exhausted and the wells stopped flowing.

Although the effects of flowing wells upon spring flow were severe, there was more to come. When the wells ceased flowing, pumping began. Ground-water levels were systematically drawn down, as much as 700 feet in some areas. At first pumping for municipal and industrial use was primarily responsible. In recent years tremendous quantities of ground water have been withdrawn for irrigation, amounting to about 80 percent of the total ground water used in Texas. As a result, some streams which were formerly "gaining" streams, receiving additional water from streambed seeps and springs, are now "losing", and many streams have ceased flowing. Thousands of small springs have dried up, and the larger springs have generally suffered a decrease in flow.

Natural spring waters if taken at their source are considered to be ground water and no permit is required for their use. Once they issue forth and flow in watercourse, however, they become public surface waters. As such, a permit from the Texas Water Rights Commission is required for their use.

A spring is normally a spillway for an underground reservoir. This reservoir may be overlain by land belonging to a number of owners. If the landowners other than the spring owner choose to pump ground water heavily, lowering the water table and causing the spring to cease flowing, the spring owner has no recourse in the courts to prevent them.

An example is Comanche Springs at Fort Stockton (Pecos County). These artesian springs, issuing from a Comanchean limestone ground-water reservoir, formerly flowed as much as 66 ft³/s, and served the Comanche and other Indians for uncounted thousands of years. From 1875 on the springs were the basis for an irrigation district which supplied water to 6,200 acres of cropland. Heavy pumping of the aquifer lowered the water table so that the spring discharge began to fall off in May 1947 (U.S. Bureau of Reclamation, 1956). The irrigation district sought an injunction in 1954 to restrain pumping which interfered with the normal flow of Comanche Springs. The injunction was denied by the courts, and the springs ceased to flow in March 1961. (See Figures 2.11 and 2.12 in Lecture 2.)

Figure 10.48 Spring of river Cetina in Croatia is sometimes called "The Eye of the Earth". The submerged vertical channel explored by cave divers is over 150 m (490 feet) deep. Photo courtesy of Branimir Jukić.

Figure 10.49 Groundwater discharging from the Redwall-Muav aquifer, feeds Vaseys Paradise Spring that cascades into the Colorado River 31.7 miles below Lees Ferry. Grand Canyon National Park, Coconino County, Arizona, the United States. Photo courtesy of Abe Springer.

Figure 10.50 Aerial view of the Boka Spring and Waterfall near the village of Žaga in western Slovenia. The stream, also called Boka, is formed by the karst spring issuing from a vertical limestone cliff. It flows for about 100 feet over a rocky shelf before falling over the rocks as a spectacular 2-stage waterfall 450 feet high. Photo courtesy of Matej Blatnik.
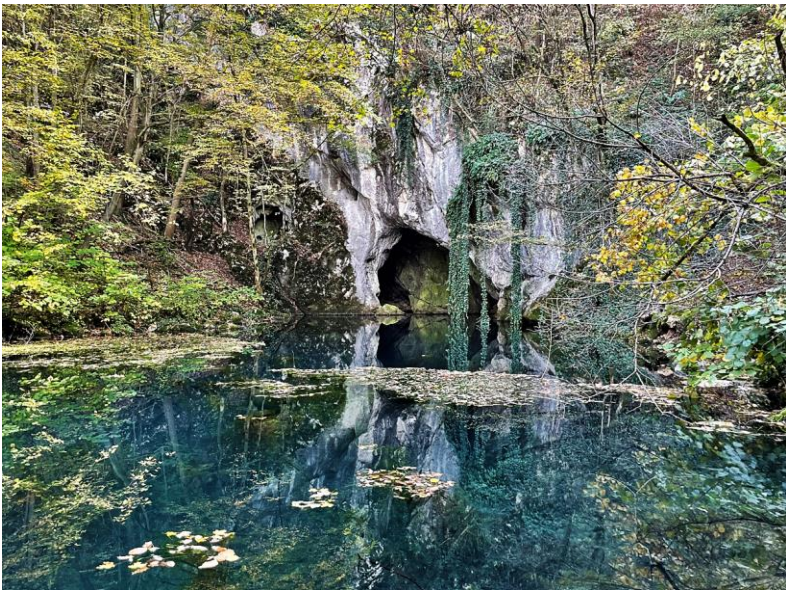
Figure 10.51 Krupaja Spring, Eastern Serbia.
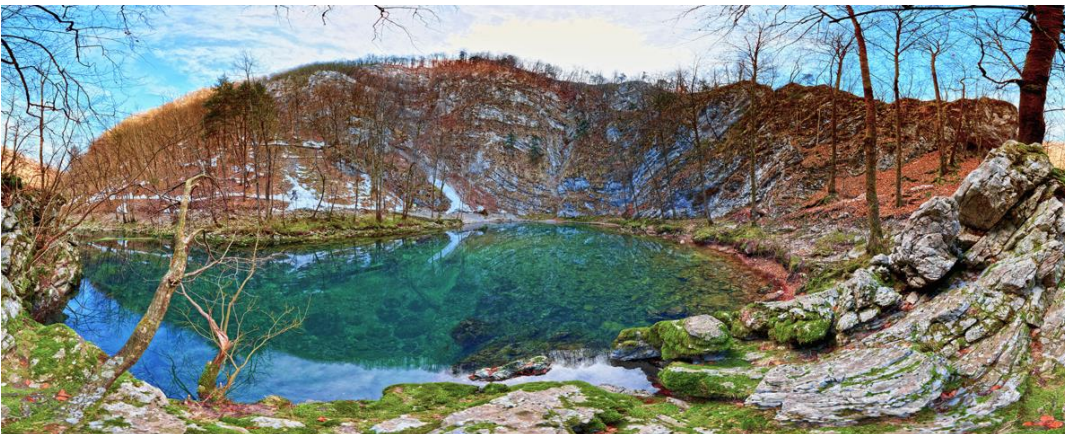
Figure 10.52 Wild Lake Spring near Idrija, Slovenia. Photo courtesy of Boštjan Burger.

Figure 10.53 *Left*: Spring of river Savica, Slovenia. *Right*: spring emerging from the monumental opening of the Stopića Cave in Serbia, more than 60 m (190 feet) high. Photographs courtesy of Zoran Stevanović.
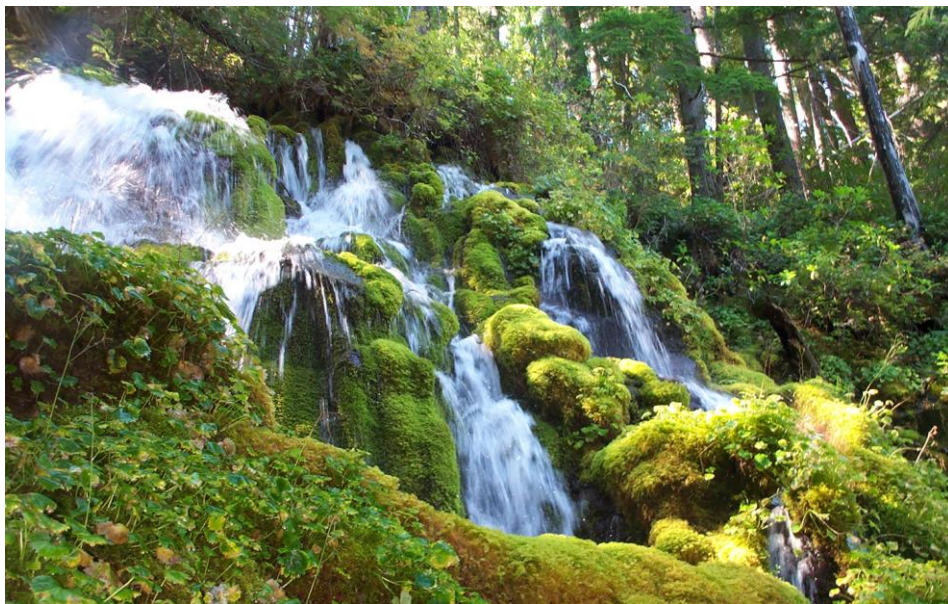
Figure 10.54 Roaring Springs on the south Fork of McKenzie River, in the Cascades Range of Oregon, the U.S. emerge from a 50-m long horizontal fracture from a single lava flow. Photo courtesy of Gordon Grant.

Figure 10.55 Photos of better-known springs in Florida, the United States. *Left*: Ginnie Spring near Santa Fe River, located within a privately-operated park and resort, called Ginnie Springs Outdoors (photo by H. Means.) *Right*: Jackson Blue Spring, about 5 miles east of Marianna. Aerial photo by T. Scott.
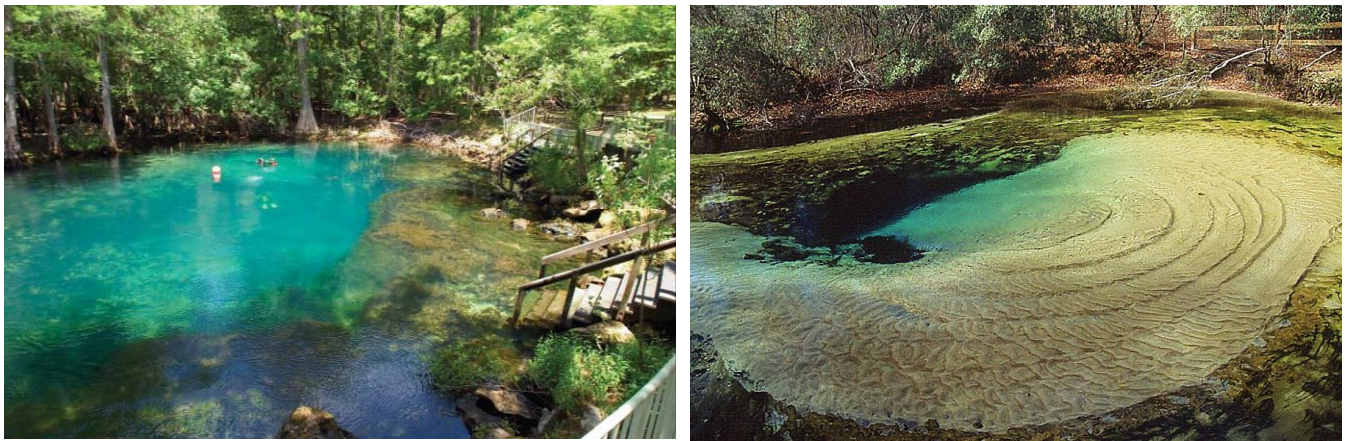
Figure 10.56 Photos of better-known springs in Florida, the United States. *Left*: Manatee Spring, approximately 7 miles west of Chiefland within Manatee Springs State Park (photo by T. Scott.) *Right*: Williford Spring, located on NFWMD land 23 miles southwest of the Cottondale exit on Interstate 10 (photo by R. Means.). Many more photos of Florida springs are available in Rosenau et al., 1977. Various information on Florida springs including programs for their protection can be found at https://floridadep.gov/springs/

Figure 15.57 Blue Spring state park in Orange City, Florida has been recognized as a manatee sanctuary. The spring flow maintains a consistent temperature of 72 degrees, providing a safe sanctuary for the West Indian Manatee seen in the photo. From November 15 to March 1, the spring and spring flow are closed to all water-related activities, including swimming, snorkeling, scuba diving, and boating, to provide a safe warm water sanctuary for manatees throughout the winter season. Courtesy of Florida DEP. https://floridadep.gov/springs/

Figure 10.58 Tirta Empul ("Holly Spring" in Balinese) on the island of Bali, Indonesia. The temple built around it in 962 AD by King Sri Warmadewa of the ancient Warmadewa dynasty of Bali (10th-14th centuries) is considered one of the five most holy temples in all of Bali by the Balinese Hindu community. The spring is the holiest water source in Bali, thought to have been blessed by The God Indra and able to purify those who bathe there. It is dedicated to Vishnu, the Hindu God of water. The spring emerges from massive tuff deposits. Photo courtesy of Vojislav Ilić.

Figure 10.59 Ras El Maa karst spring in Chefchaouen, northern Morocco. The spring is the main (and ancient) source of water supply for the population and provides water for numerous public and private fountains, gardens, and water mills. Photo courtesy of Prof. Dr. Andreo Navarro Bartolome, CEHIUMA.

Figure 10.60 *Left*: Blue Spring in Shannon County, Missouri, the United States called "Spring of the Summer Sky" by Native Americans, is 14 miles east of Eminence or 14 miles west of Ellington off State Route 106. It has the average flow rate about 85 million gallons per day. With the depth of 310 feet, it is the deepest spring in the country. Blue Spring is owned by the Missouri Department of Conservation and is completely surrounded by the National Park Service land. *Right*: Double Spring in Ozark County, Missouri has the average flow rate about 100 million gallons per day. It is on private property and has no public access without permission of the owner. Photos available at http://www.dnr.mo.gov/env/wrc/springsandcaves.htm

Figure 10.61 *Left*: Greer Spring, the second largest in the state of Missouri, the United States, has the average flow rate of 214 million gallons per day. It is located about 18 miles south of Winona off of Highway 19. The spring comes out of two sources from the ground. From under the mouth of a cave (shown here) and down a little further where it comes up as a "bubble" in the stream. It is managed by the U.S. Forest Service. Photo courtesy of Jimmy Sexton, River Hills Traveler; available at www.riverhillstraveler.com/greer-spring-one-missouris-beautiful-natural-treasures. *Right*: Big Spring, the largest spring in Missouri, is located four miles south of Van Buren at the end of State Route 103. The average flow rate is 276 million gallons per day. The spring area is managed by the National Park Service (see also Figure 5.36 in Lecture 5.) Photo available at http://www.dnr.mo.gov/env/wrc/springsandcaves.htm#Big

Figure 10.62 Barton Springs in Austin, Texas, the Unites States in the state park of the same name. In 2006, the USGS published a scientific investigations report that summarized water quality sampling performed at the springs. The water was contaminated by persistent low concentrations of atrazine, chloroform, and tetrachloroethane (organic solvent chemical). In 2008, the fight to preserve Barton Springs was the subject of *The Unforseen*, a documentary co-produced by the famous actor and movie director Robert Redford, who learned to swim there as a child. The movie uses the struggle over development in the Barton Creek watershed to illustrate the many clashes between private property rights and resource protection that are occurring across the country. Courtesy of Gregg Eckhardt. More information at https://www.edwardsaquifer.net/barton.html.)

Figure 10.63 Zulum Spring, Kurdistan province, Iraq. *"In Kurdistan no spring seemed devoid of some unusual feature. There truly must have been spirits within those mountains"* wrote Hamilton, the famous author of the "Road through Kurdistan" (book reprinted in 2004). Zulum, means Evil, probably due to the large cave from which water is emerging and then falling with noise over the 20m high waterfall. The spring is located directly at the border between Iran (recharge side) and Iraq (discharge side). The spring's discharge is in the range 0.35-6 m^3/s and provides potable water to nearby Iraqi towns Khurmal and Halabja. Text and photo courtesy of Zoran Stevanović.

Figure 10.64 Margoon Spring, Fars Province, Iran. The spring emerges from a sub-horizontal bedding plane of Asmari limestone formation. Springwater drops as waterfall 60m high, one of the most beautiful tourist attractions in the region. Text and photo courtesy of Zoran Stevanović.

Figure 10.65 The larger of Clay Springs in the South Snake Valley, Utah, the United States, issues from a deep unexplored pool. The spring is threatened by the proposed expansion of the Southern Nevada Water Authority water supply system (groundwater extraction by large-capacity wells) driven by the growth of Las Vegas and the ongoing exceptional drought in the Southwest. Photo courtesy of Gretchen Baker, www.ProtectSnakeValley.com.

Figure 10.66 *Left*: Black Tiger Spring in the city of Jinan, Shandong Province, China. With the maximum flow rate of about 1.4 million cubic feet per day, it is the second largest among the 72 named springs in Jinan (after the Baotu Spring). It emerges from a submerged limestone cave on a steep cliff as an artesian (ascending) spring. The water is funneled to flow out of the mouths of three ornamental stone-carved tiger heads into a square-shaped spring pool. During the Ming Dynasty (1368-1644), the Black Tiger Temple was located above the cave and the spring. *Right*: Baotu Spring is the largest artesian spring in Jinan. The spring pool is fed by three submerged vents with the maximum combined flow rate of about 1.6 cubic meters per second. The water jets from the spring are said to have been more than 20 meters high. Since the 1970s however, many of the Jinan springs have stopped flowing multiple times because of the aquifer overexploitation by wells. Photos courtesy of Qiang Wu.

Figure 10.67 San Pedro Springs in Sant Antonio, Texas, the United States. Like most Edwards Aquifer springs, Sand Pedro Springs are crystal clear with beautiful aquamarine color. Two pools shown are fed by the four largest of the San Pedro Springs. San Antonio was founded on the nearby banks in 1718, and the site was the social and recreational center of the young frontier town for many decades. In 1729, the lands around the springs were declared to be a public place by King Philip V of Spain, making it one of the oldest public parks in the United States. Today, due to heavy pumping demands on the Edwards Aquifer, the San Pedro Springs flow only during times of heavy rainfall. Courtesy of Gregg Eckhardt. Photo copyright by Gregg Eckhardt, printed with kind permission.

Figure 10.68 *Left*: Ricks Spring, located 15.7 miles up Logan Canyon Scenic Byway (Utah 89) in Wasatch-Cache National Forest, Utah, the United States. Historically, Ricks Spring was used as a mountain spring water source until visitors became ill after drinking from it. Ice jams on the Logan River in 1972 and dye traces led scientists to find that the water of Ricks Spring was actually coming directly from the Logan River through a fracture in the rock. Folded rocks gave way to fractures and it is evident one of these fractures allows the river water to seep through the rock and exit at Ricks Spring. Interpretive signs point out the folding and fracturing as well as denote who the spring was named after. Courtesy of U.S. Forest Service. *Right*: Spring Cueva del Gato in Andalusia, Southern Spain. The spring cave has about 4km long explored underground channel. Photo courtesy of Zoran Stevanović.

Figure 10.70 *Left*: Quasi spring called "aquifer's eye" in Gerbile, Somali Province, Ethiopia. Features like this can be single water source for humans and animals for tens of kilometers away. There is no visible outflow, but ascending water seepage from the underlying carbonate aquifer regularly refills the pond *Right*: Boohodle spring, Somaliland Province, Somalia. One of typical springs issuing from a platform type karst aquifer in arid environment. It is discharging a few liters per second but, as the only water source in the entire area, it is very important for local villagers and nomads. Photos courtesy of Zoran Stevanović.

Figure 10.71 Bekhal Spring in Rawanduz, Zagros Mountains, northern Iraq has the maximum discharge rate greater than 17 m³/s. Photo courtesy of Zoran Stevanović.
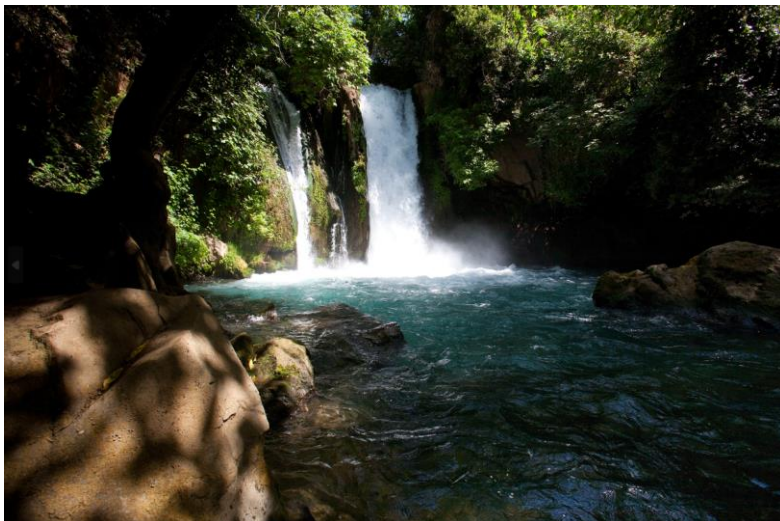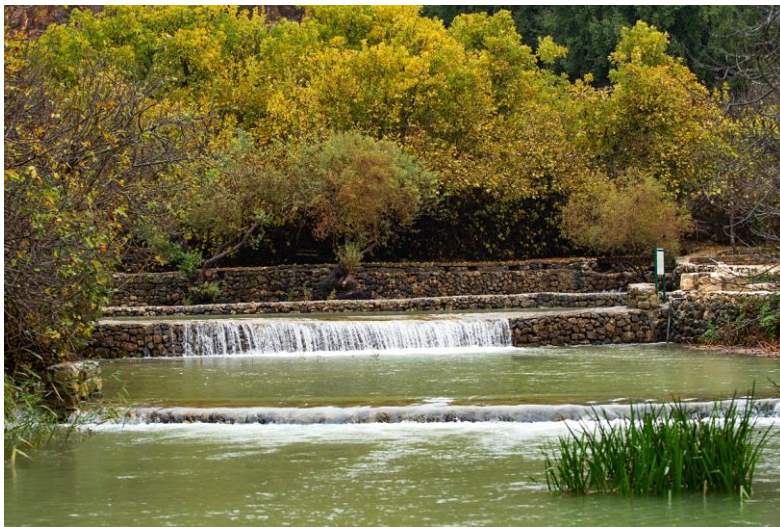
Figure 10.72 The spring of Banias (Hermon) (top photo) originates at the foot of Mount Hermon, whose summit is 2814 meters above sea level. This spring is one of the main water sources that feed the Upper Jordan River. Historic ruins of the ancient city of Panias, including the Temple of God Pan exist nearby. The spring feeds the Hermon Stream, which also receives water from several tributaries. The total flow in the river amounts to about 125 million cubic meters of fresh, high quality water per year. Hermon Stream flows powerfully in a steep canyon. The steep slope produces waterfalls (bottom photo). The water of the stream is used for irrigation, but only after it has flowed through thick vegetation that provides shelter for many types of animals.

Courtesy of Avi Burg. Photos taken by Doron Nissim, Israel Nature and Parks Authority.

Figure 10.73 The Taninim Springs are the final drainage of the Western Mountain Aquifer in the central Israel. The spring water is slightly salty, so it was not used for agriculture, but it sustains a diverse world of flora and fauna. The springs are called Taninin, crocodiles in Hebrew, as these reptiles were present in the nearby swamps until their extinction at the beginning of the 20th century. The stream fed by these springs, which is about 25 km long, also contains seasonal flood water, and this water was used as part of the water supply system for the ancient city of Caesarea, which was an important city in the Roman world. Sophisticated dams built down the stream, created a large reservoir from which the water flowed in aqueducts. The photo shows the dam's regulating device. During the Byzantine and Ottoman periods, the water was used to drive a chain of flour mills. Courtesy of Avi Burg. Photo taken by Doron Nissim, Israel Nature and Parks Authority.
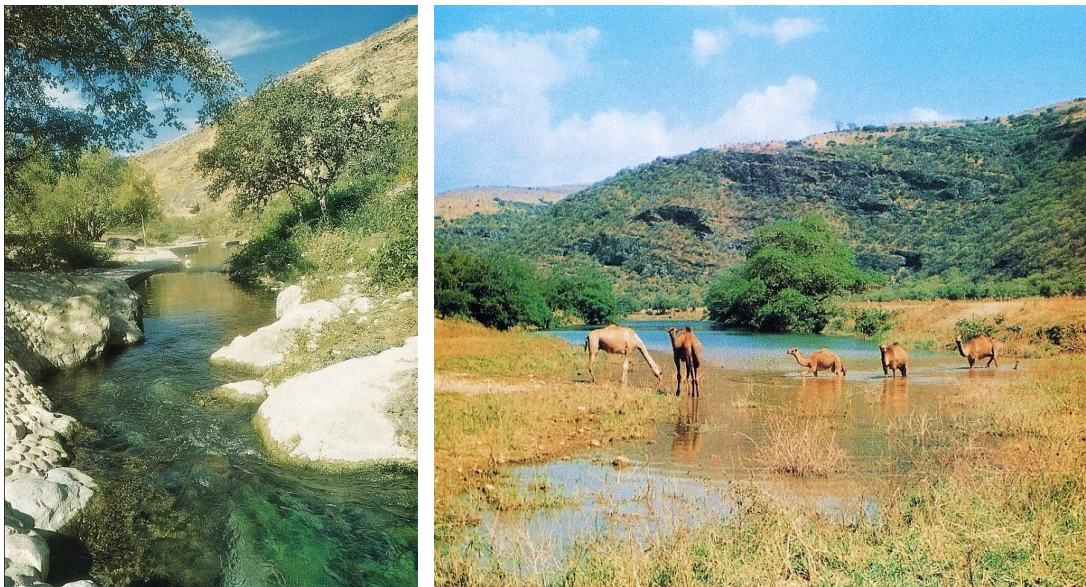
Figure 10.74 Razat cold spring (left), with an average flow of 180 L/s, and Darbat cold spring (right), with an average flow of 100 L/s, are the two largest cold springs in the Sultanate of Oman. They are protected by Diwan of the Royal Court (Chebaane et al., 1994).
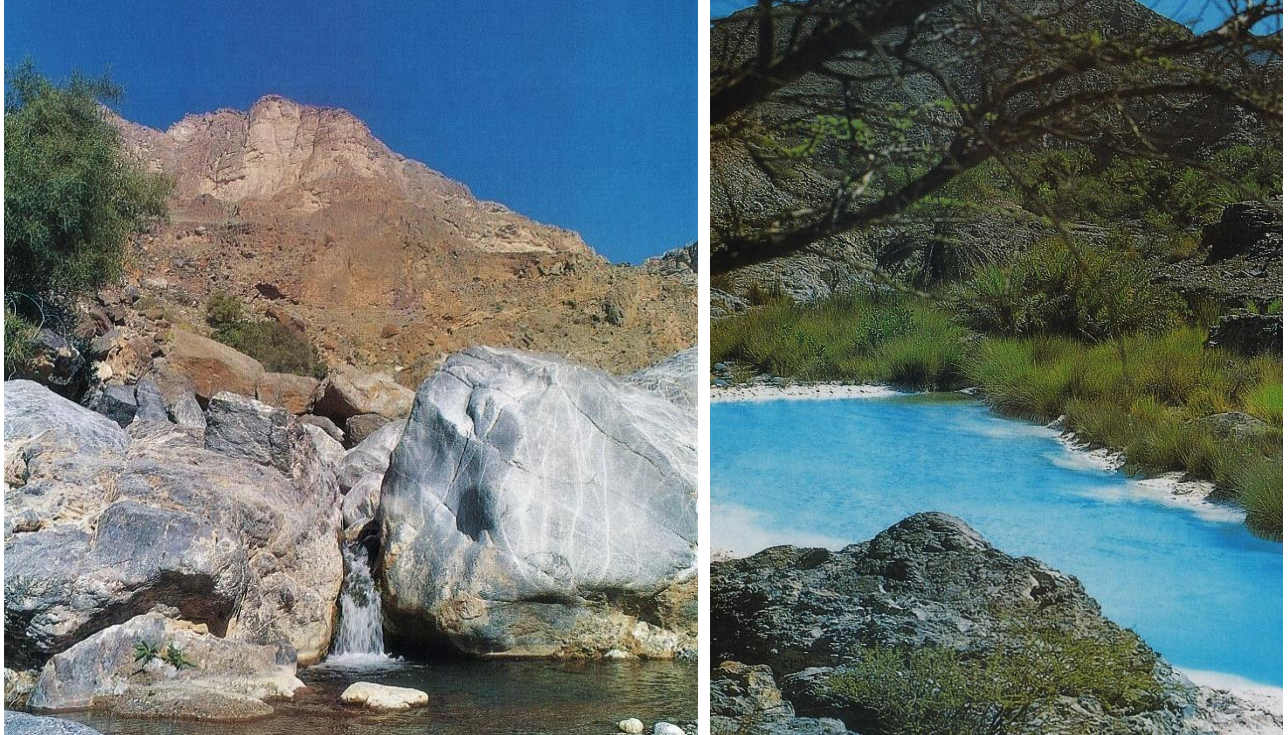
Figure 10.75 *Left*: Picturesque Al Ayla cold spring, with an average flow of 20 L/s, is in the heights of the Wilayat Al Awabi mountain in NE Oman. *Right*: The blue color of this spring pool in Oman is the result of mixing of the alkaline spring with wadi water that has bicarbonate. The calcite from the precipitate initially gives water a milky appearance. Once the calcite precipitate is deposited on the bottom of the pool as a white coating it reflects the color of the blue water (Chebaane et al., 1994).

Figure 10.76 *Left*: Water of the Sahanoot Spring in Oman is diverted by the irrigation canal. *Right*: Jabal Akhdhar farms are supplied irrigation water by the springs from the Oman's Dakhliyah mountains (Chebaane et al., 1994).

Figure 10.77 The Spring (source) of the Mlava river (Vrelo Mlave), the largest karst spring in the Serbian Carpathians with a maximum discharge of 20 cubic meters per second. Photo courtesy of Branislav Petrović.

Figure 10.78 *Majerov izvor* (Mayer's Spring) is the most important source of the Gacka river in Croatia. It is a typical Vauclusian karst spring. Photo courtesy of Dražen Perica.

Lecture 11 Groundwater Chemistry

This lecture is based primarily on the materials presented in Mathess (1982), Hem (1989), Davis and DeWiest (1991), Aiken (2002), Appelo and Postma (2005), Kresic (2007 and 2009), and Dragišić and Živanović (2014).

Groundwater is a complex solution which, in natural conditions, commonly contains tens of chemical constituents including ions, molecules, gases, colloids, and suspended particles. Depending on the host environment (type of porous media and its recharge), it can also contain natural organic substances and microorganisms. Importantly, because of the various anthropogenic influences, it can (and usually does) contain synthetic (artificially produced) organic substances, and excess amounts of inorganic constituents such as metals which, although also naturally occurring, may have significantly elevated concentrations indicating likely anthropogenic impacts. Good examples are "forever chemicals" (PFAS or Per-and Polyfluoroalkyl Substances, a group of infamous manufactured chemicals), and arsenic respectively.

The diverse chemical composition of groundwater is a result of interactions between water, lithosphere (rocks of all types), atmosphere, and biosphere including all human activities. The water cycle depicted on Figure 1.1 in Lecture 1 illustrates the unbreakable connection between atmospheric water, surface water, and groundwater. Again, the presence of "forever chemicals" in all three water compartments illustrates this point: PFAS may have entered the atmosphere via technological processes of their manufacturing at the "Primary Source" (manufacturing plant), traveled in the atmosphere attached to atmospheric water, were deposited on the ground surface via atmospheric precipitation such as rainfall, entered the subsurface via infiltrating water, reached groundwater, traveled via groundwater, and finally discharged into a surface water body. The surface water body (such as a river) may have flooded and therefore acted as a "Secondary Source" of PFAS: the flood water infiltrated into the subsurface, reached the groundwater, and the vicious cycle continued to present day. PFAS may have been discharged directly into the river at the location of Primary Source, perhaps years ago, have entered the cycle, and are continuing to impact human health and the environment.

Water is the most effective natural solvent of environmental substances thanks to its unique, and to some extent still mysterious, characteristics. As it flows through porous media, it dissolves minerals constituting the host rocks and attains chemical composition ("footprint") reflecting the host's geochemistry. This is the key reason why understanding and interpreting groundwater chemistry, sometimes referred to as "hydrochemistry", is one of the most important aspects of hydrogeologic practice.
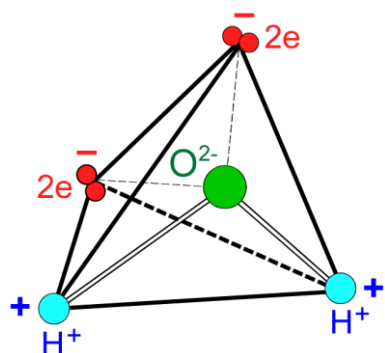
Pure water is a colorless transparent liquid without taste or scent. Water molecule has an asymmetric distribution of the hydrogen nuclei with respect to the oxygen nucleus and the two pairs of unshared electrons as illustrated in Figure 11.1. The water molecule has a shape of a distorted tetrahedron, with the oxygen atom located at its center. Two positively charged hydrogen atoms are connected to the oxygen atom with covalent bonds. Together with two

Figure 11.1 Molecule of water is a distorted tetrahedron, with the oxygen nucleus in its center.

pairs of unshared electrons (negatively charged) that belong to oxygen, they form a strong dipole which is the main reason why water is the most powerful solvent.

The covalent bonds between the hydrogen atoms and the oxygen atom form an angle of 104.5 degrees, while this angle in the molecule of ice is 109 degrees resulting in a regular tetrahedron, which is one of the reasons for the firm (solid) structure of ice.

Two corners of the tetrahedron with the hydrogen atoms are strongly positive because of the lack of electrons (hydrogen nuclei share electrons with the oxygen nucleus), while two corners with the unshared electron pairs that belong to the oxygen atom are strongly negative. Water molecules are connected between themselves with strong hydrogen bonds: hydrogen atom (proton) of one water molecule is bonded to the negatively charged side of another water molecule. This hydrogen bonding is one reason for the unique behavior of water. For example, breaking hydrogen bonds to boil and evaporate water takes considerable energy – water has higher specific heat than any common substance (1 cal/g per 1 degree Celsius, or 4.186 joule/gram °C).

The polarity of molecules, in general, is quantitatively expressed with the dipole moment, which is product of the electric charge and the distance between the electric centers. Dipole moment for water is 6.17×10^{-30} Cm (kulon-meters), which is higher than for any other substance and explains why water can dissolve more solids and liquids and in greater concentrations than any other liquid. Figure 11.2 illustrates schematically the process of dissolution of ionized substances, such as sodium chloride, by water. Salt ions are easily and quickly separated by shells of dipole water molecules, which explains their high solubilities in water. Organic substances with polarized molecules, such as methanol, are also highly soluble in water: hydrogen bonds between water and methanol molecules can readily replace the very similar hydrogen bonds between different methanol molecules and different water molecules. Methanol is therefore said to be *miscible* in water (its solubility in water is infinite for practical purposes). On the other hand, many non-polar organic molecules, such as benzene and carbon tetrachloride for example, have very low water solubility.
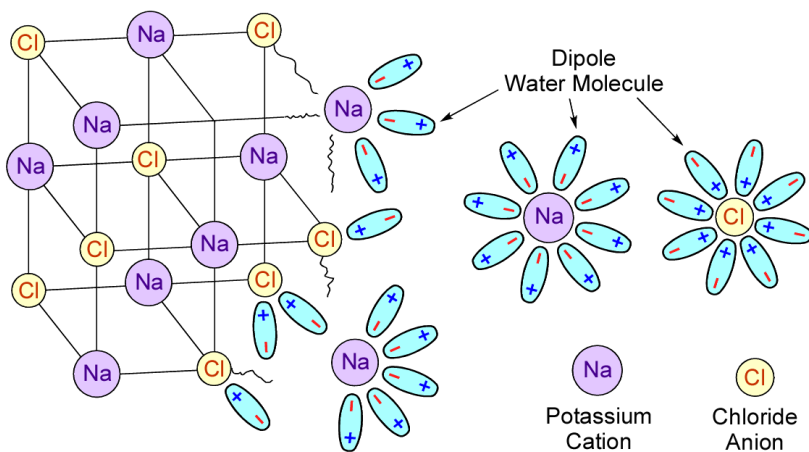
Figure 11.2 Schematic presentation of sodium chloride dissolution by water. Electrostatic forces holding together the crystal ionic lattice of halite are broken by strongly polar water molecules. Sodium cation (positively charged) and chloride anion (negatively charged) are finally separated in the solution by shells of dipole water molecules From Dimitrijević, 1988. University of Belgrade; acknowledgement required for further use.

In addition to the common water molecule with mass 18 (common oxygen-16 plus two common hydrogen-1: $^{16}O + ^{1}H + ^{1}H$), there are water molecules with masses of 19 through 24 because of the existence of natural and artificial isotopes of oxygen and hydrogen. Three natural and stable isotopes of oxygen are ^{16}O, ^{17}O, and ^{18}O (with ^{16}O constituting 99.76%). The unstable isotopes (^{14}O, ^{15}O, and ^{19}O) have very short half-lives (77, 118, and 30 seconds respectively) and therefore no importance in natural waters (Matthess, 1982). Proportion of deuterium (^{2}H or D), the stable natural isotope of hydrogen, is 0.000149 (compared to 99.9844% of common ^{1}H), while the

proportion of the radioactive isotope tritium (^{3}H or T) is 1.3×10^{-18}. All isotopes of oxygen and hydrogen combine to form 18 water molecules and 12 ion species. In this mixture, the proportion of heavy water (^{1}H^{2}H^{16}O and ^{2}H^{2}H^{16}O) is very low, about 0.03%.

Complete chemical analyses of groundwater (those looking for "all" possible naturally occurring constituents) would generally show more than 50 elements at levels detectable in commercial laboratories, and more at scientific laboratories capable of detecting very low concentrations. Constituents that are commonly present at concentrations greater than 1 milligram per liter (mg/L) in most geologic settings are sometimes called primary, major, or macro constituents of groundwater. Such components are analyzed by default because they most obviously reflect the type of rocks present in the subsurface and are therefore used to compare general genetic types of groundwater. Some of the elements commonly present in groundwater at concentrations between 0.01 and 10 mg/L are significant for understanding its genesis and are also often analyzed by default. They are sometimes referred to as either secondary or minor constituents. Metallic elements that are usually found at concentrations less than 0.1 mg/L and less than 0.001 mg/L, are sometimes called secondary (minor) constituents and trace constituents, respectively. However, the significant concentrations and the relative importance of different groundwater constituents are site and regulations specific, and these do vary in different parts of the world, and in time. A good example is arsenic, considered for a long time to be a "minor" or "trace" constituent. However, as more and more analyses of groundwater used or considered for water supply became available both in the United States and worldwide, arsenic emerged as the major groundwater constituent simply because of the new regulatory drinking water standard of 0.01 mg/L (10 ppb).

About 35 or so important natural inorganic groundwater constituents, recognizing the relativity of word "important", can be divided into the following two practical analytical groups:

1. *Primary constituents* analyzed routinely

- Cations: Ca^{2+}, Mg^{2+}, Na^+, K^+, Fe^{2+} (and other iron forms)
- Anions: HCO_3^-, CO_3^{2-}, Cl^-, SO_4^{2-}, NO_3^- (and other nitrogen forms)
- Silica as SiO_2 (present mostly in uncharged form)

2. *Secondary constituents* analyzed as needed

- Elements/Anions: boron (B), bromine/bromide (Br), fluorine/fluoride (F), iodine/iodide (I), and phosphorus/phosphate (P)
- Metals, and non-metallic elements: aluminum (Al), antimony (Sb), arsenic (As), barium (Ba), beryllium (Be), cadmium (Cd), cesium (Cs), chromium (Cr), copper (Cu), lead (Pb), lithium (Li), manganese (Mn), mercury (Hg), nickel (Ni), rubidium (Rb), selenium (Se), silver (Ag), strontium (Sr), zinc (Zn)
- Radioactive elements: radium (Rd), uranium (U), alpha particles, beta particles
- Organic matter (total and dissolved organic carbon—TOC, DOC)
- Dissolved oxygen (and/or reduction-oxidation potential, Eh)

Almost all primary and secondary inorganic constituents listed above are included in the list of primary or secondary drinking water standards by the United States Environmental Protection Agency (see Lecture 12). Most of them, when in excess of a certain concentration, are considered contaminants, and such groundwater is not suitable for human consumption. Notably, groundwater contamination may be the result of both naturally occurring inorganic substances, and those introduced by human activities.

11.1 Primary Groundwater Constituents

Typically, the primary constituents dissolved in fresh groundwater make up more than 90% of total dissolved solids in a sample. The following elements and ionic species, in particular, have been widely used to describe the chemical type and origin of groundwater: cations of calcium (Ca^{2+}), magnesium (Mg^{2+}), sodium (Na^+) and potassium (K^+), and anions of hydrocarbonate (HCO_3^-) and carbonate (CO_3^{2-}), chloride (Cl^-), and sulfate (SO_4^{2-}). The reason why they are the most prevalent in natural groundwaters is that the most important soluble minerals and salts occurring in relatively large quantities in rocks are calcium carbonate ($CaCO_3$), magnesium carbonate ($MgCO_3$), their combination ($CaCO_3 \times MgCO_3$), sodium chloride ($NaCl$), potassium chloride (KCl), calcium sulfate ($CaSO_4$), and hydrous calcium sulfate ($CaSO_4 \times 2H_2O$). The five elements (Ca, Mg, Na, K, Cl) are abundant in various sedimentary, magmatic, and metamorphic rocks and are constantly released to the environment by weathering and dissolution.

Although aluminum and iron and are the second and the third most abundant metallic elements in the Earth's crust, respectively, they rarely occur in natural groundwater in concentrations exceeding 1 mg/L (Hem, 1989). Naturally occurring forms of aluminum are especially stable under near-neutral pH, and aluminum is not considered to be a major dissolved phase constituent. The exceptions are waters with very low pH such as acidic mine drainage. The chemical behavior of iron and its solubility in water are rather complex and depend strongly on the redox potential and pH. The forms of iron present are also strongly affected by microbial activity. Various ferrous complexes are formed by many organic molecules, and some of the complexes may be significantly more resistant to oxidation than free ferrous ions and also insoluble in groundwater. The presence of various forms of iron in groundwater is also important when evaluating the degradation of organic contaminants or deterioration of well screens by iron bacteria. For all these reasons, iron is considered one of the primary groundwater constituents and it is commonly analyzed, even though its dissolved ionic forms are found in most groundwaters in smaller concentrations compared to the major ions.

Unlike aluminum and iron, silicon, being the second only to oxygen in the Earth's crust, is found in appreciable quantities in most groundwaters, usually between 1 and 30 mg/L when expressed as silica. The relative abundance of silica in natural water is due to its many different chemical forms found in minerals and rocks. This fact is contrary to the common belief that silica is not soluble in water and is therefore not present in groundwater. The most abundant forms of silica dissolved in water are thought not to form ions, although the complicated groundwater chemistry of silica is still not well understood (Hem, 1989; Mathess, 1982).

11.1.1 Calcium

Calcium is the most abundant of the alkaline-earth metals and is a major constituent of many common rock minerals and solutes in natural waters. Calcium has only one oxidation state, Ca^{2+}. It is an essential element for plant and animal life forms. Its presence in aqueous systems is due mainly to the more soluble solids containing calcium and is governed to great extent by the equilibria between the solute and gaseous phases of the carbon dioxide species. Calcium also participates in cation-exchange equilibria at surfaces of aluminosilicates (clays) and other minerals (Hem, 1989). Although calcium is an essential constituent of many igneous rock minerals, especially of the chain silicates pyroxene and amphibole, and the feldspars, its concentration in the groundwater in magmatic terrains is generally low. This is mainly because of the slow rate of decomposition of most igneous-rock minerals.

Calcium at low concentrations also occurs in groundwater that has been in contact with metamorphic rocks, which contain silicate minerals with calcium. Groundwater in silicate terrain often contains less than 100 mg Ca^{2+}/L, although this concentration may be elevated due to presence of soil/regolith sediments where the content of CO_2 in the ground air is consistently 10-100 times that of the atmosphere (Matthess, 1982). CO_2 forms carbonic acid in reaction with water and the acid accelerates dissolution of some calcium-bearing minerals.

Proportionally much higher concentrations of calcium are found in groundwaters in carbonate sedimentary rocks such as *limestone*, composed of calcite and aragonite (both have the formula of $CaCO_3$), *dolomite*, composed of calcite and mineral dolomite $CaMg(CO_3)_2$, calcium sulfates *anhydrite* ($CaSO_4$) and *gypsum* ($CaSO_4 \times 2H_2O$), and, more rarely, sedimentary rock *fluorite* composed of calcium fluoride (CaF_2). Calcium is also a component of some types of zeolites and montmorillonite (Hem, 1989). In sandstone and other intergranular rocks, calcium carbonate is commonly present in the form of cement between rock grains and may be dissolved by the flowing groundwater. The following equations express the general reactions between calcium carbonate and the CO_2–water system:

$$CO_2 + H_2O = H_2CO_3 = H^+ + HCO_3^- \qquad (11.1)$$

$$HCO_3^- = H^+ + CO_3^{2-} \qquad (11.2)$$

$$CaCO_3 + H^+ = Ca^{2+} + HCO_3^- \qquad (11.3)$$
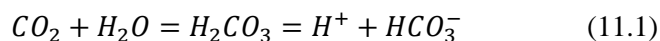
The predominant influence of equilibria between the solute and gaseous phases of CO_2 on the calcite dissolution and precipitation processes greatly depends on pH and water temperature. Calculations determining if a particular solution is in thermodynamic equilibrium with calcite must therefore include pH (ionic activity of H^+), water temperature, concentration of free dissolved CO_2, and ionic activities of Ca^{2+} and HCO_3^- in the solution. Hem (1989) and Matthess (1982) provide a detail discussion of calcite solubility including use of various reaction constants, nomograms and ionic strength graphs. When groundwater undersaturated with respect to calcite flows through a porous medium rich with soluble calcite, the dissolution process commonly creates secondary porosity (voids) in the rock. Karst terrains are a typical example for this reaction. In time, the groundwater may become supersaturated with respect to calcite but may still keep it in solution (dissolved) due to various geochemical interactions and conditions that influence the carbonate equilibria. When the subsurface conditions abruptly change, calcium carbonate may precipitate at this geochemical barrier; typical examples are speleothems in caves, travertine (calc-sinter) deposits at springs, cementation of faults, or incrustation of well screens. The presence of sodium and potassium salts generally increases the solubility of calcium carbonate.

Concentrations of calcium in normal potable groundwater generally range between 10 and 100 mg/L, with some limestone and gypsum groundwaters exceeding this amount. The most commonly noticed effect of calcium in groundwater is *hardness*, or its reaction with soap demonstrated by the inability of soap to either cleanse or lather. Ions of magnesium, iron, manganese copper, barium, and zinc also cause a similar difficulty. Hardness is defined as the soap neutralizing power of these ions (Davis and DeWiest, 1991). Since all the ions except magnesium and calcium usually occur in low concentrations, hardness is attributed to the sum of effects of only calcium and magnesium dissolved in groundwater (the effect of alkaline-earth metals). It is calculated on the basis of calcium alone, as the concentration of equivalent calcium carbonate expressed in milligrams per liter. If the hardness exceeds the alkalinity (bicarbonate + carbonate in milligrams per liter of $CaCO_3$ or other equivalent units), the excess is termed "noncarbonated hardness" and may be reported as such. In some European countries, hardness values are reported in *degrees of hardness*, all in terms of calcium carbonate. One French degree is equivalent to

10 mg/L, one German degree to 17.8 mg/L, and one English or Clark degree to 14.3 mg/L (Hem, 1989). In the U.S., it is now generally accepted that the "ideal" drinking water should not contain more than 80 mg/L of hardness.

11.1.2 Magnesium

Magnesium is a common alkaline-earth element essential in plant and animal nutrition and has only one oxidation state of significance in water chemistry, Mg^{2+}. Although magnesium and calcium behave similarly in water solutions to some extent (such as when creating water hardness), the geochemical characteristics of magnesium are quite different because its ions are smaller than calcium ions (Hem, 1989). In magmatic rocks magnesium is typically a major constituent of the dark-colored ferromagnesian minerals such as olivine, pyroxenes, amphiboles, and dark-colored micas. In metamorphic rocks magnesium is a common constituent of minerals chlorite and serpentinite.

Sedimentary rocks containing magnesium carbonate (*magnesite*), $MgCO_3$, and the double calcium-magnesium carbonate *dolomite* ($CaCO_3 \times MgCO_3$) are, similarly to calcite, soluble under the influence of CO_2 gas dissolved in groundwater. Although the solubility of $MgCO_3$ in pure water is greater than that of calcium carbonate, its actual solubility in the field conditions is much harder to determine because of the presence of various other hydrated magnesium carbonate forms such as nesquehonite, landsfordite and basic hydromagnesite. Dolomite and magnesium hydroxide (brucite) in sediments are poorly soluble, while the solubility of magnesium chloride and sulfate is distinctly higher (Mattes, 1982). The magnesium ion, Mg^{2+}, will normally be the predominant form of magnesium in solution, while the complex $MgOH^+$ will not be significant below about pH 10 (Hem, 1989). Magnesium occurs in significant amounts in most limestones and especially in dolomites. The dissolution of these rocks brings magnesium into groundwater, but the chemical reaction is not readily reversible. Magnesium concentration tends to increase along the flowpath as the precipitate formed may be nearly pure calcite. Mature groundwaters in carbonate sedimentary terrains therefore often have a high Mg:Ca ratio since the conditions for direct precipitation of dolomite from solution are not commonly found in normal groundwater (Hem, 1989).

Despite the higher solubility of most of its compounds, the magnesium content in potable (low-mineralized) groundwater is generally below that of calcium, most probably because of the lower general abundance of magnesium. Occasional exceptions occur in magnesium-rich aquifers, such as olivine-basalts, serpentines and dolomite rocks (Matthess, 1982).

11.1.3 Sodium and Potassium

Potassium is slightly less common than sodium in igneous rocks but more abundant in all the sedimentary rocks. However, in the ocean water, although notable, the concentration of potassium is far less than that of sodium. In most freshwater aquifers, if the sodium concentration substantially exceeds 10 mg/L, the potassium concentration is commonly half or a tenth that of sodium (Hem, 1989). In some dilute natural waters in which the sum of sodium and potassium is less than 10 mg/L, the potassium concentration may be equal or even exceeding that of sodium. These facts point out the very different behavior of the two alkali metals in natural systems. Sodium tends to remain in solution rather persistently once liberated from silicate-mineral structures. There are no important precipitation reactions that can maintain low sodium concentrations in water. Sodium may be retained by adsorption on mineral surfaces, especially by clays, which have high cation-exchange capacity. However, the interactions between surface sites and sodium (monovalent ion) are much weaker than the interactions with divalent ions such as calcium. Cation exchange processes therefore tend to extract divalent ions from the solution and to replace them

with monovalent ions (such as sodium). Potassium feldspars orthoclase and microcline ($KAlSi_3O_8$) are less soluble than feldspars with sodium and are less soluble than the sodium plagioclase albite ($NaAlSi_3O_8$). The soluble salts of sodium, such as halite, are readily dissolved and removed from sediments after environmental changes, such as sediment leaching by freshwater after sea level regression. Although potassium salts are also highly soluble and potassium is generally as abundant as sodium in rocks, it seldom occurs in concentrations equal to sodium in natural waters. However, reactions involving water chemistry of potassium are still not well understood so that quantifications of the different behavior of sodium and potassium are difficult. In addition, potassium has remained one of the more difficult ions to analyze accurately, which is the main reason why sodium and potassium are usually lumped together within the cation group of major groundwater constituents when reporting analytical results.
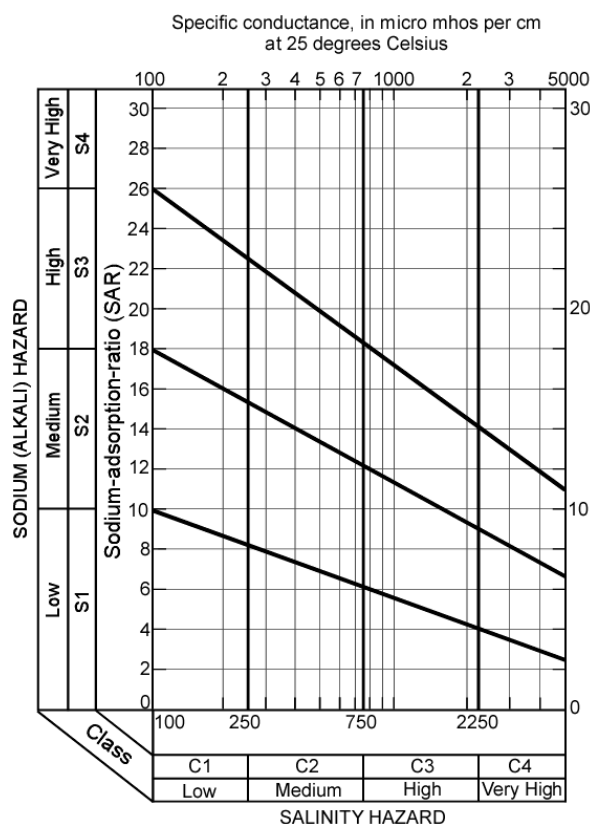
Although there are indications that biological factors may play an important role in controlling the availability of potassium for solution in groundwater, the following two generalizations are still used to explain the difference between the concentrations of sodium and potassium in most natural groundwaters: (1) the potassium concentrations are low because of the high degree of stability of potassium-bearing alumino-silicate minerals, and (2) potassium from solution is incorporated strongly into some clay-mineral structures, such as in spaces between crystal layers of ilite and, unlike sodium, cannot be removed by further ion-exchange reactions (Hem, 1989).

Figure 11.4 Diagram for use in interpreting analyses of irrigation water. From Hem, 1989. USGS, in public domain.

Excessive sodium content in groundwater used for irrigation may damage soil structure as sodium replaces calcium and magnesium adsorbed on the soil clays and colloids. Two principal effects of this replacement are a reduction in soil permeability and a hardening of the soil. The U.S. Salinity Laboratory Staff (1954) defined the *sodium-adsorption ratio* (SAR) of water as:

$$SAR = \frac{Na^+}{\left[0.5 \times \left(Ca^{2+} + Mg^{2+}\right)\right]^{1/2}} \qquad 11.4$$

where ion concentrations are expressed in milliequivalents per liter.

The SAR predicts reasonably well the degree to which irrigation water tends to enter into cation-exchange reactions in soil (Hem, 1989). Values of SAR are therefore included in chemical analyses of irrigation water and

water that might be considered for that use. The value is empirical and of otherwise limited geochemical significance. Figure 11.4 shows a diagram commonly used to assess suitability of water for irrigation. The graph relates SAR to the specific conductance ("salinity"; see Section 11.6) of water and divides water into various hazard classes. Detail discussion on these classes, as they relate to crop tolerance for salinity and soil types, is given by the U.S. Salinity Laboratory Staff (1954).

11.1.4 Iron

Iron is one of the most abundant elements in magmatic rocks, particularly as part of dark-colored minerals such as pyroxenes, amphiboles, biotite, magnetite, and, especially, the olivine, which is a solid solution whose end members are forsterite (Mg_2SiO_4) and fayalite (Fe_2SiO_4). For the most part, iron in these minerals is in ferrous (Fe^{2+}) oxidation state. Ferric iron (Fe^{3+}) is present in magnetite, Fe_3O_4 (Hem, 1989). When these minerals are exposed to water, the iron that is dissolved generally precipitates in the vicinity as sedimentary species. In reducing conditions, when sulfur is available, the precipitate is in form of ferrous polysulfides, or siderite ($FeCO_3$) when sulfur is less abundant. In oxidizing conditions, the precipitate (sediment) will be ferric oxides or oxyhydroxides such as hematite, Fe_2O_3, or goethite, $FeO(OH)$. Ferric hydroxide, $Fe(OH)_3$, is freshly precipitated material with poorly developed crystal structure, commonly referred to as *gel*. Availability of iron for aqueous solution is strongly affected by pH and redox (Eh) conditions, where catalytic action of microorganisms plays the key role in oxidation to ferric (Fe^{3+}) iron under aerobic conditions, or the reduction to divalent, ferrous iron (Fe^{2+}) under anaerobic conditions.
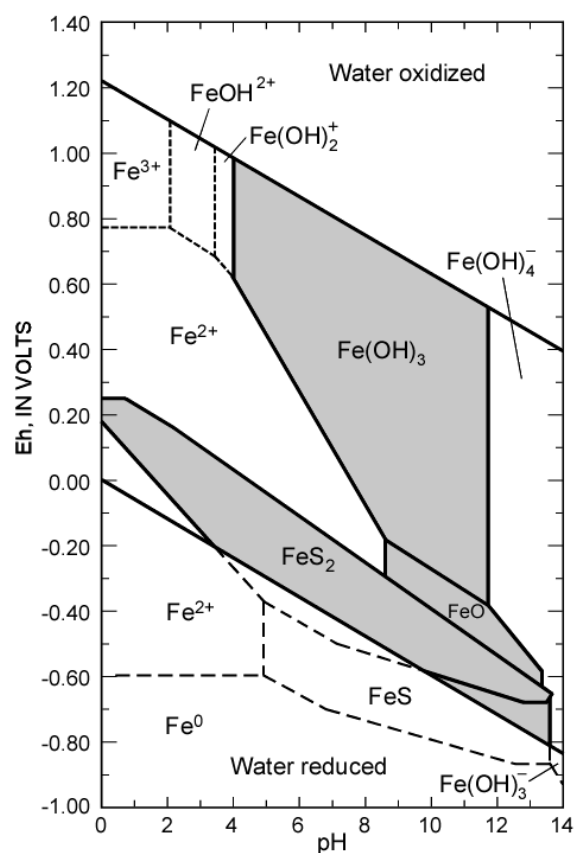
Figure 11.5 shows how small changes in pH, and Reduction-Oxidation Potential or Redox (Eh; see Section 11.7) affect the stability of various iron compounds. For example, when pyrite, FeS_2, is exposed to oxygenated water or ferric hydroxide, $Fe(OH)_3$, is in contact with reducing substances, iron will tend to go into solution. The most common form of iron in solution is the ferrous ion Fe^{2+}. The ferrous iron concentrations in reducing conditions are commonly between 1 and 10 mg/L. Groundwater with pH between 6 and 8 can be sufficiently reducing to retain as much as 50 mg/L of ferrous iron at equilibrium, when bicarbonate activity does not exceed 61 mg/L. This type of water is clear when first extracted from a well, but it may soon become cloudy and then brown from precipitating ferric hydroxide.

Figure 11.5 Fields of stability for solid (shaded areas) and dissolved forms of iron as a function of pH and Eh at 25°C and 1 atmosphere pressure. Activity of sulfur species is 96 mg/L as SO_4^{2-}, carbon dioxide 61 mg/L as HCO_3^-, and dissolved iron 65 μg/L. From Hem, 1989. USGS, in public domain.

Because of the unstable nature of ferrous iron in a sample, it should be preserved to prevent precipitation of original dissolved iron due to oxidation. An increase in dissolved ferrous iron may indicate presence of organic substances, including pollution by human activities. Ferric iron can occur in acid solutions as Fe^{3+}, $FeOH^{2+}$, and $Fe(OH)_2^+$, and in polymeric hydroxide forms. Ferric iron can form various inorganic solution complexes with many anions beside OH^-, such as with chloride, fluoride, sulfate, and phosphate (Hem, 1989.)

11.1.5 Bicarbonate and Carbonate

Bicarbonate or hydrocarbonate (HCO_3^-), and carbonate (CO_3^{2-}) ions in groundwater are mostly derived from the atmospheric and soil CO_2, and dissolution of carbonate rocks such as calcium carbonate. Interestingly, the bi-prefix comes from the observation that baking soda produces twice as much carbonate (CO_3) per sodium as washing soda; both were widely used before their chemical formulas were known. Thus, HCO_3^- became bicarbonate, even though it only has one carbonate, and CO_3^{2-} became carbonate.

Term *alkalinity* is often used as a synonym for the measure of bicarbonate and carbonate contents in groundwater. Note that this usage of the word alkalinity is contrary to the common chemical usage in which only water with a pH of more than 7.0 is considered to be alkaline (Davis and DeWiest, 1991).

Groundwater generally contains more than 10 mg/L but less than 800 mg/L bicarbonate, usually between 50 mg/L and 400 mg/L (Davis and DeWiest, 1991; Matthess, 1982). Concentrations above 1000 mg/L can occur in water of low alkaline earth content, especially at high CO_2 concentrations caused by endogenetic or diagenetic processes such as in fault zones and regional metamorphic zones. When there is oversaturation with respect to partial pressure of atmospheric CO_2, precipitation of calcium carbonate (travertine, calc-sinter) will occur at the contact with atmosphere. The usual concentration of free dissolved (aggressive) CO_2 in groundwater, i.e., CO_2 not already bound to bicarbonate-carbonate, is 10-20 mg/L (Matthess, 1982). Under equilibrium conditions, the pH value of water indicates the fractions of different carbonate species (Figure 4.12.). Bicarbonate ions are predominant between pH of 6 and 8.5. Bicarbonate dissociation into carbonate starts at pH of about 8.35, and carbonate dominates in highly alkaline waters. If pH is less than 5, the solution contains only free CO_2.
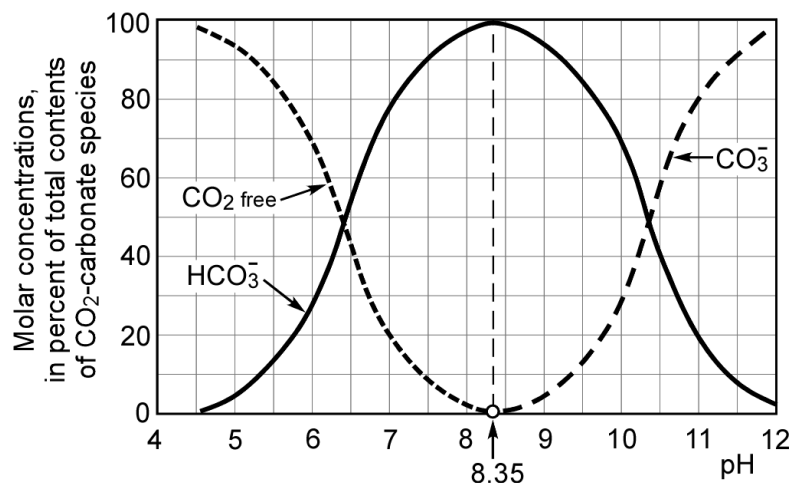
Figure 11.6 Relationship between free CO_2, bicarbonate and carbonate species for various values of pH. (Ovchinikov, 1955, from Milojević, 1967. Acknowledgement required for further use.

11.1.6 Chloride

Chlorine is the most abundant element in the group of halogens, which includes fluorine, bromine, and iodine. More than three-fourths of the total amount of chlorine present in the Earth's outer crust, atmosphere and hydrosphere is in form of the ion chloride (Cl^-) dissolved in the ocean water. Average concentration of chloride in the ocean water is about 19,000 mg/L, by far the highest of all other constituents (the next highest is sodium, 10,500 mg/L, followed by sulfate, 2,700 mg/L, magnesium, 1,350 mg/L, and calcium, 410 mg/L; Hem, 1989). Based on the average contents of chloride in rocks, only a small part of its content in the ocean water is due to rock weathering. The bulk of it originates from degassing of the Earth's crust by volcanic emanations, which early in Earth's history gave rise to the chlorine in the primeval atmosphere and oceans (Matthess, 1982). Chlorine is volatile, dissolves readily in water and is not stable in the atmosphere. Because of its strong and rapid oxidizing effect, chlorine has long been used as a disinfectant in purification of water supplies.

Chloride is present in the various rock types in concentrations lower than any of the other primary constituents of groundwater. Sedimentary rocks, particularly the evaporates, are considerably more important sources of chloride than magmatic rocks. In general, chloride in groundwater comes from four different sources: (1) chloride from ancient seawater entrapped in sediments, (2) solution of halite and related minerals in evaporates, (3) concentration by evaporation, of chloride contributed by rain or snow, and (4) dry fallout from the atmosphere, particularly in arid regions (Davis and DeWiest, 1991). Chloride also enters the hydrologic cycle from liquid and solid waste materials, fertilizers, and highway salt.

Concentration of Cl^- in normal potable groundwater is less than 30 mg/L, with higher values commonly indicating the admixture of mineralized waters or anthropogenic pollution (Matthess, 1982). Once dissolved in groundwater, chloride remains in solution and its behavior is often referred to as "conservative": chloride ions do not significantly enter into oxidation or reduction reactions, form no important solute complexes with other ions unless the chloride concentrations is extremely high, do not form salts of low solubility, are not significantly adsorbed on mineral surfaces, and play few vital biochemical roles (Hem, 1989). For all these reasons, chloride has been often used as a conservative tracer. In fact, Kaufman and Orlob (1956, from Hem, 1989) concluded that chloride ions move with the water through most soils tested with less retardation or loss than any of the other tracers tested, including tritium.

11.1.7 Sulfate

Sulfate (SO_4^{2-}) ion is an oxidized form of sulfur, produced primarily when sulfide minerals undergo weathering in contact with aerated water. Hydrogen ions are also produced in this oxidation process in considerable quantity (Hem, 1989). Sulfur is widely distributed in reduced form in both magmatic and sedimentary rocks as metallic sulfides. Pyrite, in particular, constitutes a major source of both sulfate and ferrous iron in groundwater. Its oxidation is also promoted by humans through combustion of fossil fuels and smelting of ores containing pyrite. Sulfate occurs in some magmatic-rock minerals of the feldspathoid group, but the most extensive and important occurrences are in evaporate sediments, most of which are soluble in water (Hem, 1989).

Soluble calcium sulfate as gypsum, or as anhydrite, makes up a considerable part of many evaporate-rock sequences. Strontium sulfate is less soluble than calcium sulfate, and barium sulfate is almost insoluble, but these two salts are relatively rare. Soluble sodium sulfate is formed in some closed-basin lakes (Hem, 1989). It is believed that most sulfates are presently being recycled from the atmosphere and from the solution of sulfate minerals in the sedimentary rocks, although in the history of the hydrosphere most sulfates probably originated from the oxidation

of sulfides from magmatic rocks and gasses (Davis and DeWiest, 1991). All atmospheric precipitation contains sulfate, which is one of the major dissolved constituents of rain and snow. This sulfate is derived from the oxidation of sulfur dioxide and hydrogen sulfide gasses, and from dust particles containing sulfate minerals.

Anthropogenic sulfur emissions, such as burning of fossil fuels and ore smelting, are a major factor in producing rain of low pH (acid rain) that has had many undesirable ecologic effects in northern Europe and parts of North America. In some areas, however, nitrogen oxides are equal or more important contributors to acid rain. One of the most prolific natural sources of hydrogen sulfide is from the bacterial reduction of organic material in tidal mud flats. Sulfate-reducing bacteria (sulfur bacteria) are active in groundwater where they derive energy from the oxidation of organic compounds and in the process obtain oxygen from the sulfate anions (Matthess, 1982). The resulting reduction of sulfate ions produces hydrogen sulfide as a by-product, most of which will remain in the subsurface as gas. If iron is present in the water under moderately reducing conditions, iron sulfide may be precipitated, thus removing both iron and sulfide from the water (Matthess, 1982). The rotten-egg odor of hydrogen sulfide can be detected by most people in waters that have only a few tenths of a milligram per liter H_2S.

Groundwater associated with oil deposits, in areas of magmatic activity, and in deep reducing aquifers may attain high concentrations of hydrogen sulfide in excess of 100 mg/L. The sulfate content of normal groundwater in magmatic rocks and intergranular sedimentary rocks is usually less than 30 mg/L. In gypsum and anhydrite deposits SO_4^{2-} concentration may reach the saturation point of gypsum, corresponding to about 1360 mg/L. Very low or even zero sulfate concentrations are typical for groundwaters in which bacterial reduction has been taking place (Matthess, 1982).

11.1.8 Nitrate (Nitrogen Forms)

Nitrogen occurs in groundwater as uncharged gas ammonia (NH_3) which is the most reduced inorganic form, nitrite and nitrate anions (NO_2^- and NO_3^- respectively), in cationic form as ammonium (NH_4^+), and at intermediate oxidation states as a part of organic solutes. Some other forms such as cyanide (CN^-) may occur in groundwater affected by waste disposal (Rees et al., 1995; Hem, 1989). Three gaseous forms of nitrogen may exist in groundwater: elemental nitrogen (oxidation state of zero), nitrous oxide (N_2O; slightly oxidized, +1), and nitric oxide (NO; +2). All three, when dissolved in groundwater, remain uncharged gasses (Rees et al., 1995).

Ammonium cations are strongly adsorbed on mineral surfaces. Nitrate is readily transported by groundwater and stable over a considerable range of conditions. The nitrite and organic species are unstable in aerated water and easily oxidized. They are generally considered indicators of pollution by sewage or organic waste. The presence of nitrate or ammonium might be indicative of such pollution as well, but generally the pollution would have occurred at a site or time substantially removed from the sampling point. Ammonium and cyanide ions form soluble complexes with some metal ions, and certain types of industrial waste effluents may contain such species (Hem, 1989).

Extensive application of nitrogen fertilizers has caused an increase in nitrate concentrations over wide agricultural areas in many countries. Nitrogen oxides, present in atmosphere to considerable extent due to combustion of fossil fuels, undergo various chemical alterations that produce H^+ and finally leave the nitrogen as nitrate. These processes can lower the pH of rain in the same way sulfur oxides do. Because of the many ways human activities influence various forms of nitrogen in the environment, and the public health concerns associated with the elevated concentrations of nitrite and nitrate in potable groundwater, there is a large number of scientific

investigations of the sources of nitrogen, nitrogen cycle and related groundwater impacts (e.g., Keeney, 1990; Rees et al., 1995; Mueller et al., 1995).

Sources of various forms of nitrogen in groundwater are primarily derived from the biologic activity of plants and microorganisms in the environment, from animal waste, and from many anthropogenic activities including agriculture, sewage disposal, and utilization of fossil fuels. Non-industrially impacted rain may have a total nitrogen concentration of about 6 mg/L, and rainfall of 10 in/yr. would yield a nitrogen load to the soil column of about 13 pounds per acre per year in such case. Significant evaporation of such rainwater could result in high concentrations of nitrogen in the infiltration water (Rees et al., 1995). Geologic sources of nitrogen are much less significant. Lithologic units that typically have high nitrate concentrations include shales and Pleistocene-age loess that were deposited during periods favoring plant growth (Rees et al., 1995).

Nitrogen can undergo numerous reactions that can lead to storage in the subsurface, or conversion to gaseous forms that can remain in the soil for periods of minutes to many years. The main reactions include: (1) immobilization/mineralization, (2) nitrification, (3) denitrification, and (4) plant uptake and recycling (Keeney, 1990).

Immobilization is the biological assimilation of inorganic forms of nitrogen by plants and microorganisms to form organic compounds such as amino acids, sugars, proteins, and nucleic acids.

Mineralization is the inverse of immobilization. It is the formation of ammonia and ammonium ions during microbial digestion of organic nitrogen.

Nitrification is the microbial oxidation of ammonia/ammonium ion first to nitrite, then ultimately to nitrate. Nitrification is a key reaction leading to the movement of nitrogen from the land surface to the water table because it converts the relatively immobile ammonium form (reduced nitrogen) and organic nitrogen forms to a much more mobile nitrate form. Chemosynthetic autotrophic soil bacteria of the family *Nitrobacteriaceae* are believed to be principally responsible for the nitrification process. Ammonium oxidizers, including the genera *Nitrosomonas*, *Nitrosospira*, *Nitrosolobus*, and *Nitrosvibrio*, oxidize ammonium to nitrite. The nitrite oxidizing bacteria, which oxidize nitrite to nitrate, include the genus *Nitrobacter*. Nitrification can also be carried out by heterotrophic bacteria and fungi (Rees et al., 1995). The nitrogen used by plants is largely in the oxidized form.

Denitrification is the biological process that utilizes nitrate to oxidize (respire) organic matter into energy usable by microorganisms. This process converts the nitrate to more reduced forms, ultimately yielding nitrogen gas that can diffuse into the atmosphere. Uptake of nitrogen by plants also removes nitrogen from the soil column and converts it to chemicals needed to sustain the plants. Because the plants eventually die, the nitrogen incorporated into the plant tissues ultimately is released back to the environment, thus completing the cycle (Rees et al., 1995).

Concentrations of various nitrogen species in groundwater are determined and reported in different ways in published analyses. Most studies and laboratories engaged in analyses of groundwater contamination report ammonia, amino and organic nitrogen, and nitrite either separately or as a combined figure in terms of equivalent concentration of elemental nitrogen. Studies interested in general (inorganic) groundwater chemistry usually require reporting of nitrate ion (NO_3^-) only, since nitrite (NO_2^-) is rarely present in concentrations large enough to influence ionic balance to a noticeable degree (Hem, 1989). Nitrate concentrations in most unpolluted natural groundwaters in the U.S. are usually less than 2 mg/L (Mueller et al., 1995). Examples of much higher values include groundwaters often associated with arid climates and leaching of nitrate-bearing deposits in caves, caliche, and playas (Matthess, 1982). Shallow aquifers underlying areas impacted by anthropogenic activities, especially

the application of fertilizers, may have nitrate concentrations of several hundred mg/L or more. Nitrite concentrations in natural unpolluted groundwaters are usually in trace amounts, i.e., much less than 1 mg/L. Higher concentrations often indicate contamination by anthropogenic sources or animal waste.

11.1.9 Silica

The term "silica", meaning the oxide of silicon (SiO_2), is widely used in referring to silicon in natural water, but it should be understood that the actual form is uncharged hydrated monomolecular silicic acid, H_4SiO_4 or $Si(OH)_4$, which is for the most part a true solution (Hem, 1989; Matthess, 1982). The bulk of silica occurring in groundwater comes from the weathering of silicate minerals. Amorphous silica also contributes to total dissolved silica, while crystalline silica, particularly quartz, is almost insoluble in water. In natural non-thermal groundwaters, silica is usually found in concentrations between 1 and 30 mg/L, and such waters are mostly undersaturated with respect to amorphous silica (Matthess, 1982). The solubility of silica is not affected by pH in the 0-9 range. However, high temperatures and/or pH>9 may result in very high concentrations and supersaturation of groundwater with respect to silica. For example, Feth et al. (1961) report pH of 11.6 and more than 3400 mg/L of dissolved SiO_2 in water of Aqua de Ney, a cold spring near the town of Mount Shasta in California (Hem, 1989).

11.2 Secondary Groundwater Constituents

Secondary constituents of importance for most natural groundwaters of drinking water quality include metals, fluoride, and organic matter. The term heavy metals (or trace metals) is applied to the group of metals and semi-metals (metalloids) that have been associated with contamination and potential toxicity or ecotoxicity; it usually refers to common metals such as copper, lead, or zinc. Some define a heavy metal as a metal with an atomic mass greater than that of sodium, whereas others define it as a metal with a density above 3.5 to 6 g/cm3. The term is also applied to semimetals (elements such as arsenic, which have the physical appearance and properties of a metal but behave chemically like a nonmetal) presumably because of the hidden assumption that "heaviness" and "toxicity" are in some way identical. Despite the fact that the term heavy metal has no sound terminological or scientific basis, it has been widely used in scientific environmental literature (van der Perk, 2006). Heavy metals commonly found in natural fresh groundwater include zinc, copper, lead, cadmium, mercury, chromium, nickel, and arsenic.

Metals occur naturally as part of many primary and secondary minerals in all types of rocks. In natural waters, they are present mainly at low concentrations (usually much less than 0.1 mg/L), and as cations, although some semimetals such as arsenic may occur as oxyanions (e.g., arsenate, AsO_4^{3-}). Their generally low concentrations in groundwater are due to the high affinity to adsorption and precipitation in soils and aquifer porous media. The maximum natural concentrations of metals are usually associated with ore deposits and oxidized, low-pH water. Many solids control the fixation (immobilization) of metals including clay minerals, organic matter, iron, manganese, and aluminum oxides and hydroxides for adsorption, and poorly soluble sulfide, carbonate, and phosphate minerals for precipitation (Bourg and Loch, 1995; from van der Perk, 2006). The pH of groundwater is the most important factor controlling the fate and transport of metals in the subsurface. In general, decreasing pH results in higher mobility of heavy metals and vice versa. More on general characteristics, hydrochemistry, and mobility of metals in the subsurface can be found in Bourg and Loch (1995), Appelo and Postma (2005), and van der Perk (2006).

Arsenic has emerged as one of the most widespread natural contaminants in groundwater in various regions of the world. Since it can occur both naturally and as a result of anthropogenic contamination, arsenic is covered in more detail later as a naturally occurring groundwater contaminant.

In addition to inorganic (mineral) substances, groundwater always contains natural organic substances, and almost always some living microorganisms (mainly bacteria), even at depths of up to 3.5 km in some locations (Krumholz, 2000). Organic matter in surface and groundwater is a diverse mixture of organic compounds ranging from macromolecules to low-molecular-weight compounds such as simple organic acids and short-chained hydrocarbons. In groundwater, there are three main natural sources of organic matter: organic matter deposits such as buried peat, kerogen, and coal; soil and sediment organic matter; and organic matter present in waters infiltrating into the subsurface from rivers, lakes, and marine systems (Aiken, 2002). Various components of naturally occurring hydrocarbons (oil and gas) and their breakdown products formed by microbial activity are a significant part of groundwater chemical composition in many areas throughout the world. A very large number of artificial organic chemicals have become part of groundwater reality over the last several decades because, if analyzed using appropriate analytical methods, they are often detected.

Organic matter in groundwater plays an important role in controlling geochemical processes by acting as proton and electron donors-acceptors and pH buffers, by affecting the transport and degradation of pollutants and by participating in mineral dissolution and precipitation reactions. Dissolved and particulate organic matter may also influence the availability of nutrients and serve as a carbon substrate for microbially mediated reactions. Numerous studies have recognized the importance of natural organic matter in the mobilization of hydrophobic ("water-hating") organic species, heavy metals, and radionuclides. Many contaminants that are commonly regarded as virtually immobile in aqueous systems can interact with dissolved organic carbon (DOC) or colloidal organic matter, resulting in migration of hydrophobic chemicals far beyond the distances predicted by the structure and activity relationships (Aiken, 2002).

Several significant, although poorly understood, mechanisms can be responsible for the transport or retention of organic molecules in the subsurface. Once in the system, organic compounds, whether of anthropogenic or natural origin, can be truly dissolved, or associated with immobile or mobile particles. Mobile particles include DOC, DOC-iron complexes, and colloids. Positively charged organic solutes are readily removed from the dissolved phase by cation exchange, which can be a significant sorption mechanism. Organic solutes that may exist as cations in natural waters include amino acids and polypeptides. Hydrophilic neutral (e.g., carbohydrates and alcohols) and low-molecular weight anionic organic compounds such as organic acids are retained the least by aquifer solids. Hydrophobic synthetic organic compounds interact strongly with the organic matter associated with the solid phase of porous media. These interactions are controlled, in part, by the nature of the organic coatings on solid particles, especially with respect to its polarity and aromatic carbon content. Interactions of hydrophobic organic compounds with stationary particles can result in strong binding and slow release rates of these compounds (Aiken, 2002).

11.3 Gasses in Groundwater

Gasses in groundwater can be of atmospheric, biogenic, and radioactive origin, as well as due to degassing of Earth's mantle (Dragišić and Živanović, 2014.) They can be dissolved in groundwater, and in free form, as bubbles. With a decrease in pressure, dissolved gasses can transfer to free gasses, such as at locations of groundwater discharge at the land surface, at springs and seeps, or to surface water bodies (see Figure 10.3 in Lecture 10).

Dissolution of gasses in groundwater is temperature dependent – it increases with lower temperatures and decreases with higher temperatures.

Most common atmospheric gasses in groundwater are nitrogen, oxygen, carbon dioxide, and methane. Radioactive gas radon, and noble gasses helium and argon, which are present in the atmosphere in small amounts, are primarily of the radiogenic origin—they are formed by radioactive decay of their parent elements naturally occurring in the rocks, uranium and thorium, and radioactive isotope of potassium, ^{40}K (parent of argon), respectively.

Typical gasses formed by biochemical processes in the presence of microorganisms and in reducing conditions (low oxygen content) are hydrogen sulfide, carbon dioxide, hydrogen, nitrogen, and hydrocarbon gasses such as the predominant methane, and to much lesser degree ethene, propane and butane.

Metamorphic gasses, formed due to high pressure and temperature in the Earth's crust, are mostly carbon dioxide, hydrogen sulfide, and methane.

Gasses in groundwater that originate from magmatic (volcanic) activities are sometimes called *juvenile* gasses. They include carbon dioxide, carbon monoxide, sulfur dioxide, hydrogen sulfide, nitrogen, chlorine, hydrogen, and argon.

Gasses of radioactive origin, formed by radioactive decay of the uranium and thorium chains, include helium, argon, radon, thoron (isotope of radon), and actinon, the last three being radioactive.

Nitrogen (N_2) is the most prevalent gas in groundwater, usually of atmospheric origin, particularly in shallow water bearing zones. There, its amount is proportional to the partial pressure of the gas. Less commonly, nitrogen is the product of volcanism and biochemical processes such as decomposition of organic matter in oil deposits.

Oxygen (O_2) is primarily of atmospheric origin. Its presence in groundwater is of great practical biological and chemical significance. In porous media and groundwater, it is consumed on the oxidation of organic substances, iron, and sulfides, typically in the presence of microorganisms.

Hydrogen (H_2) is the result of water dissociation, decomposition of organic substances, and hydrolysis of sulfates of metals such as iron, copper, aluminum, and others, in the zones of oxidation of sulfide minerals. It is also present in deep groundwater horizons with reducing conditions, as well as in the areas of modern volcanism.

Methane (CH4) is a colorless and flammable hydrocarbon gas belonging to the group of saturated aliphatic hydrocarbons. It is produced in anaerobic conditions by degradation of organic substances in the presence of methanogenic bacteria. The sources of methane are coal, oil, and gas deposits, and wetland (swamp) environments.

Hydrogen sulfide (H_2S) appears in areas of volcanic activity together with other gasses. It is also associated with certain types of mineral and thermal groundwaters. In deep water-bearing horizons and structures it is formed by anaerobic degradation of organic compounds with high content of sulfur in the presence of sulfate-reducing bacteria. In dissolved phase, hydrogen sulfide is present in groundwater as anion of hydrosulfide (HS^-), and sulfide (S^{2-}).

11.4 Chemical Zonation of Groundwater

Groundwater, with naturally elevated concentrations of total dissolved solids,(TDS) exceeding 1000 mg/L, can be found in deeper portions of sedimentary basins of all scales. Higher TDS concentrations are the result of longer residence times of groundwater and slow rates or complete absence of present-day recharge with freshwater.

More mineralized groundwater can sometimes also be found at shallow depths in unconfined aquifers, particularly in arid regions, where evaporation from the water table results in increased concentration of dissolved minerals. Finally, shallow groundwater may have naturally elevated TDS concentrations because of mixing with brackish groundwater migrating from deeper aquifers.

When TDS concentrations in groundwater exceed 50,000 mg/L, it is called brine. Brines are generally associated with geologic formations of marine origin rich in evaporates such as anhydrite, gypsum, or halite (jointly often referred to as salts). The origin of groundwater contained in such formations may be trapped sea water that was never flushed by fresh groundwater and became more mineralized in time. Various geologic processes including tectonics may also allow fresh groundwater to circulate into buried evaporates and dissolve them thus becoming brine. Brine groundwater can naturally migrate upward via faults or other geologic features and contaminate shallow freshwater aquifers and surface water bodies.

With the exploding demand for reliable water supply worldwide, followed by advances in technology and a decrease in desalination costs, brackish groundwater has become increasingly targeted for large-scale development. Another reason for the growing interest in brackish groundwater is the fact that the overpumping of many fresh groundwater aquifers allows them to become contaminated by brackish groundwater.

The city of El Paso, Texas, the United States, is a prime example illustrating the vertical upward migration of more mineralized groundwater residing in deeper portion of a deep basin aquifer due to extensive pumping of the shallow freshwater zone aquifer (Figure 11.7; see also figure 10.21 in Lecture 10.), as well as a large-scale development of brackish water for water supply (see Lecture 14).
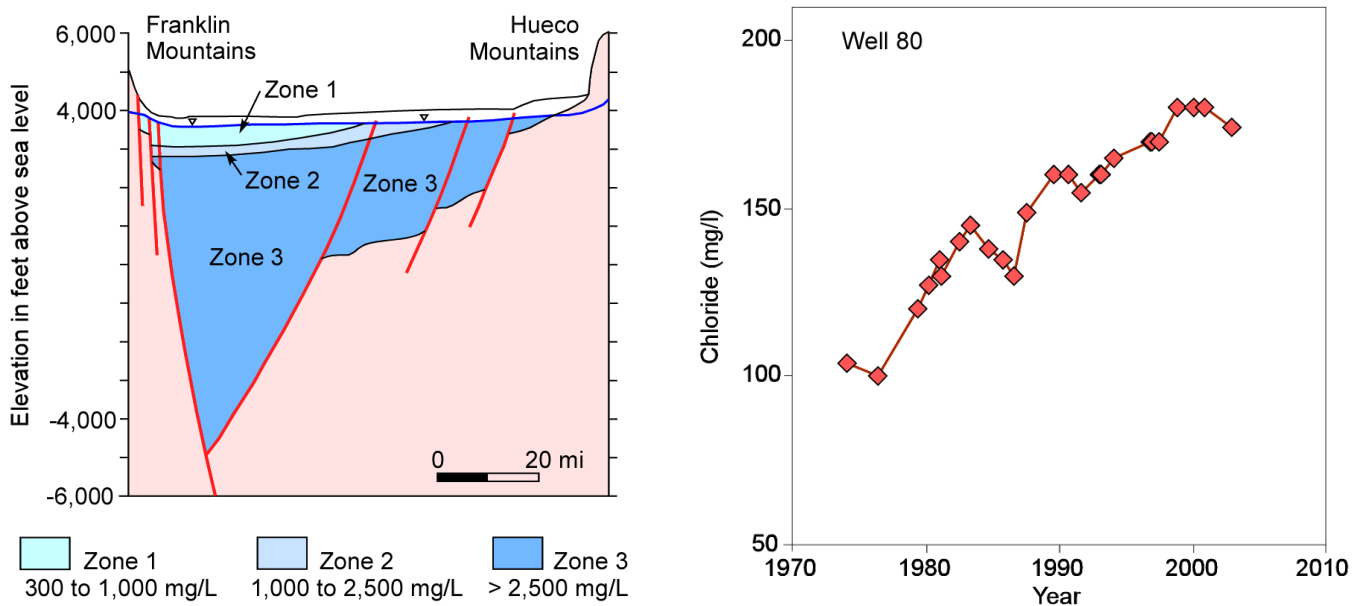
Figure 11.7 *Left*: Cross-section of the Hueco Bolson, Ela Paso area, Texas, showing three zones of total dissolved solids (TDS) concentrations in the deep basin aquifer. *Right*: Rising chloride concentration at one of El Paso Water Utility wells caused by overpumping of the shallow freshwater zone and up coning of brackish water from the deeper zones. Modified from Hutchinson, 2004. EPWU, in public domain.
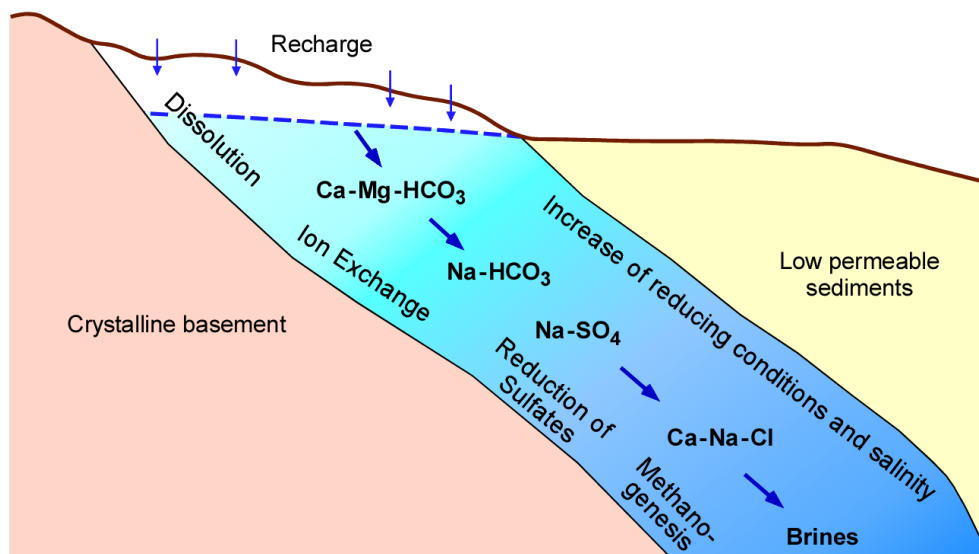
Figure 11.8 Chemical zonation of groundwater. Modified from Dragišić and Živanović, 2014; and Rivet et al., 2006.

Chemical zonation of groundwater with depth is best observed in deep artesian basins, large, thick sedimentary platforms, and continental shields. This is illustrated in Figure 11.8. Water infiltrating from the ground surface dissolves minerals in the soil on its way to the water table. This process is enhanced by the presence of week carbonic acid which is formed by the interaction between dissolved CO_2 in the soil and water. The result of this initial dissolution of minerals is the enrichment with soluble hydrocarbonates (anions) of calcium, magnesium, and sodium. Predominant cations are calcium and magnesium. As the groundwater flows deeper, various sorption and ion exchange processes take place resulting in the replacement of hydrocarbonates with sulfates, and deeper with chlorides. The change in the content of cations is less pronounced than that of anions, but the sodium generally increases with depth. Calcium increases again at greater depths, and the transformation of chemical composition of groundwater may eventually end with the formation of brines. However, as mentioned earlier, the origin of brines is not always well defined.

Other components also show common changes with depth: concentrations of iron, manganese, silica, and barium generally decrease, and concentrations of bromide, potassium, and radium increase (Dragišić and Živanović, 2014.)

11.5 Solubility. Water Chemistry Units

As emphasized earlier, water is the most effective *solvent* of environmental substances in all three forms – solid, liquid and gaseous. Substances subject to dissolution by water (or any other liquid) are called *solutes*. True solutes are in the state of separated molecules and ions, which all have very small dimensions (commonly between 10^{-6} and 10^{-8} cm), thus making water solution transparent to light. Colloidal solutions have solid particles and groups of molecules that are larger than ions and molecules of the solvent. When colloidal particles are present in large enough quantities, they give water an opalescent appearance by scattering light. Although there is no one-agreed-to definition of what exactly colloidal sizes are, a common range cited is between 10^{-6} and 10^{-4} cm (Matthess, 1982).

Amount of a solute in water is expressed in terms of its concentration, usually in milligrams per liter (mg/L or parts per million – ppm) and micrograms per liter (parts per billion – ppb). It is sometimes difficult to distinguish between certain true solutes and colloidal solutions that may carry particles of the same source substance. Filtering and/or precipitating colloidal particles before determining true dissolved concentration of a solute may be necessary

in some cases. This especially because drinking water standards for most substances are based on dissolved concentrations. Laboratory analytical procedures are commonly designed to determine total concentrations of a substance and do not necessarily provide indication of all the individual species (chemical forms) of that substance that may be present in the water sample. If needed, however, such speciation can be requested. For example, determination of individual chromium species, rather than the total chromium concentration, may be important in groundwater contamination studies since hexavalent chromium or Cr(VI) is more toxic and has different mobility than trivalent chromium, Cr(III), in groundwater.

Another common way to express concentration of a substance in solution is using *moles per liter*. A mole of a substance is its atomic or molecular weight in grams. A solution having a concentration of one mole per liter is a *molar* solution; thus, the *molarity* of a solution is its concentration in a weight per volume unit. The SI unit for molarity is mole per cubic meter (mol/m^3), which is the same as millimole per liter (mmol/L). A *molal* solution is one that contains one mole of solute per 1000 grams of solvent. For dilute solutions up to about 0.01 molar, these two units (molar and molal) are equal, within ordinary experimental error (Hem, 1989). Concentrations in milligrams per liter are readily converted to millimoles per liter by dividing them by the atomic or formula weight of the constituent. For example, to convert 1.8 mg/L of aluminum to millimoles, this concentration must be divided by the atomic weight of aluminum:

$$\text{millimoles/L} = \frac{\text{concentration of aluminum, in mg/L}}{\text{atomic weight of aluminum}} = \frac{1.8}{26.98} = 0.07 \text{ millimoles/L}$$

Table 11.1 shows the conversion factors based on the atomic and formula weights for common constituents dissolved in water. Concentrations in millimoles per liter are used in mass-law calculations, which describe various chemical processes including dissolution of substances in water and chemical reactions between different species in solution.

Ionic charge of a substance can be taken into account to compare different ions present in the solution, i.e., to determine their chemical equivalence. *Equivalent weight* of an ion is obtained when the formula weight of that ion is divided by its charge (valence). When the concentration value in milligrams per liter of a species is divided by this equivalent weight, the results is an equivalent concentration called *milligram-equivalents per liter*, or *milliequivalents*, or "*meq*" when abbreviated. For example, to find milliequivalents of 1.8 mg/L of aluminum, which has valence (charge) of 3, the first step is to find its equivalent weight:

$$\text{equivalent weight} = \frac{\text{atomic weight of aluminum}}{\text{valence of aluminum ion}} = \frac{26.98}{3} = 8.99$$

The second step is to divide the aluminum concentration, in milligrams per liter, by the equivalent weight:

$$\text{milliequivalents per liter} = \frac{\text{concentration of aluminum}}{\text{equivalent weight}} = \frac{1.8}{8.99} = 0.20 \text{ meq}$$

Table 11.1 shows concentration conversion factors from milligrams per liter to milliequivalents per liter for common ions present in natural water solutions.

Table 11.1 Conversion factors: milligrams per liter × F1 = milliequivalents per liter; milligrams per liter × F2 = millimoles per liter; based on 1975 atomic weights, referred to carbon-12. Modified from Hem, 1989, USGS.

Element/Species	F1	F2	Element/Species	F1	F2
Aluminum (Al^{3+})	0.11119	0.03715	Magnesium (Mg^{2+})	0.08229	0.04114
Ammonium (NH_4^+)	0.05544	0.05544	Manganese (Mn^{2+})	0.03640	0.01820
Antimony (Sb)	–	0.00821	Mercury (Hg)	–	0.00499
Arsenic (As)	–	0.01334	Molybdenum (Mo)	–	0.01042
Barium (Ba^{2+})	0.01456	0.00728	Nickel (Ni)	–	0.01704
Beryllium (Be^{2+})	0.22192	0.11096	Nitrate (NO_3^-)	0.01613	0.01613
Bicarbonate (HCO_3^-)	0.01639	0.01639	Nitrite (NO_2^-)	0.02174	0.02174
Boron (B)	–	0.09250	Phosphate (PO_4^{3-})	0.03159	0.01053
Bromide (Br^-)	0.01252	0.01252	Phosphate (HPO_4^{2-})	0.02084	0.01042
Cadmium (Cd^{2+})	0.01779	0.00890	Phosphate ($H_2PO_4^-$)	0.01031	0.01031
Calcium (Ca^{2+})	0.04990	0.02495	Potassium (K^+)	0.02558	0.02558
Carbonate (CO_3^{2-})	0.03333	0.01666	Rubidium (Rb^+)	0.01170	0.01170
Cesium (Cs^+)	0.00752	0.00752	Selenium (Se)	–	0.01266
Chloride (Cl^-)	0.02821	0.02821	Silica (SiO_2)	–	0.01664
Chromium (Cr)	–	0.01923	Silver (Ag^+)	0.00927	0.00927
Cobalt (Co^{2+})	0.03394	0.01697	Sodium (Na^+)	0.04350	0.04350
Copper (Cu^{2+})	0.03147	0.01574	Strontium (Sr^{2+})	0.02283	0.01141
Fluoride (F^-)	0.05264	0.05264	Sulfate (SO_4^{2-})	0.02082	0.01041
Hydrogen (H^+)	0.99216	0.99216	Sulfide (S^{2-})	0.06238	0.03119
Hydroxide (OH^-)	0.05880	0.05880	Thorium (Th)	–	0.00431
Iodide (I^-)	0.00788	0.00788	Titanium (Ti)	–	0.02088
Iron (Fe^{2+})	0.03581	0.01791	Uranium (U)	–	0.00420
Iron (Fe^{3+})	0.05372	0.01791	Vanadium (V)	–	0.01963
Lead (Pb^{2+})	0.00965	0.00483	Zinc (Zn^{2+})	0.03059	0.01530
Lithium (Li^+)	0.14407	0.14407			

In an analysis expressed in milliequivalents per liter, unit concentrations of all ions are chemically equivalent. This means that if all ions have been correctly determined, the total milliequivalents per liter of cations is equal to the total milliequivalents per liter of anions. When this is not the case, in addition to possible analytical and computational errors, it may be that some of the ionic species usually considered minor and therefore not analyzed, are present in higher concentrations.

Laboratory analyses do not always provide information on the exact form and charge of ionic species detected, which is one disadvantage of using milliequivalents. In addition, an equivalent weight cannot be computed for species whose charge is zero but may be present in significant concentrations, as is often the case with silica.

Table 11.2 Chemical analysis of a water sample expressed in four ways. Modified from Hem, 1989, USGS.

Constituent	mg/L or ppm	meq/L or epm	percent of meq/L	mM/L
Calcium (Ca)	37	1.85	6.1	0.925
Magnesium (Mg)	24	1.97	6.5	0.985
Sodium (Na) & Potassium (K)	611	26.58	87.4	26.58
Bicarbonate (HCO₃)	429	7.03	23.1	7.03
Sulfate (SO₄)	1010	21.03	69.2	10.52
Chloride (Cl)	82	2.31	7.6	2.31
Fluoride (F)	0.6	0.03	0.1	0.03
Nitrate (NO₃)	0.0	0.00	0.0	0.000
Boron (B)	0.2	–	–	0.019
Silica (SiO₂)	7.9	–	–	0.131
Iron (Fe)	0.17	–	–	0.003
Calculated dissolved solids	1980	60.80	200	48.535
Hardness as CaCO₃, Total	191			1.91
Sp. Con. (micromhos at 25°C)	2880			
pH	7.3			

Table 11.2 shows a single water analysis for major dissolved constituents expressed in milligrams per liter, milliequivalents per liter, percentage of total cation and anion equivalents, and millimoles per liter. It is assumed that the dissolved bicarbonate would be converted to carbonate in the dry residue, with loss of an equivalent amount of carbon dioxide and water (Hem, 1989). This and additional conversion factors for the computations in Table 11.2 are given in Table 11.3.

Table 11.3 Conversion factors for quality of water data. Modified from Hem, 1989.

To convert	To	Multiply by
Ca^{2+}	$CaCO_3$	2.497
$CaCl_2$	$CaCO_3$	0.9018
HCO_3^-	$CaCO_3$	0.8202
*HCO_3^-	CO_3^{2-}	0.4917
Mg^{2+}	$CaCO_3$	4.116
Na_2CO_3	$CaCO_3$	0.9442
NO_3^-	N	0.2259
N	NO_3^-	4.4266

The *water solubility* of a given substance is the maximum amount of that substance water can dissolve and maintain in solution that is in equilibrium with the solid or liquid source of the substance. Solubilities of various inorganic and organic substances are extremely variable, from those that are infinite (e.g., for liquid substances *miscible* with water such as methanol) to those that are quite low, such as for Non-Aqueous Phase Liquids (LNAPLs) which are *immiscible* with water. Terms *hydrophilic* (water-loving) and *hydrophobic* (water-hating) are sometimes used in reference to water-solubility and water-insolubility respectively.

* In the reaction $2HCO_3^- = CO_3^{2-} + H_2O + CO_2$

The water solubility of a substance is controlled by quite a few factors, including water temperature, pressure, concentrations of hydrogen (H^+) and hydroxyl (OH^-) ions, i.e., pH of water, redox potential (Eh), and relative concentrations of other substances in the solution. The relationships between these variables in actual field conditions are complex and constantly changing, so that exact solubilities of various substances of interest cannot be determined. However, principles of analytic laboratory chemistry combined with some general assumptions and geochemical modeling, can be used to establish reasonable limits of natural solubilities of common substances. Various general texts in chemistry list aqueous solubilities for inorganic and organic compounds, which can be used for initial analyses (see Lide, 2005).

The *solubility product*, which is a concept of physical chemistry, is an equilibrium constant for the solution of a compound that dissociates into ions. For a saturated solution of a compound, the product of the molar concentrations of the ions is a constant at any fixed temperature. For example, the chemical equation representing the dissolution of gypsum is:

$$CaSO_4 + 2H_2O = Ca^{2+} + SO_4^{2-} + 2H_2O \qquad (11.5)$$
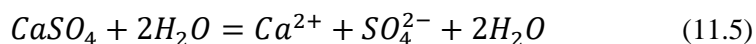
and the corresponding solubility product (K_{sp}) expression is (with water having activity of 1):

$$[Ca^{2+}] \times [SO_4^{2-}] = K_{sp} \qquad (11.6)$$

For pure water, i.e., an ideal solution conditions, the solubility product for gypsum is $10^{-4.6}$ at temperature of 25°C. The solubility of gypsum in moles per liter is equal to the activity of calcium and sulfate ions since 1 mole of gypsum dissolves in pure water to give 1 mole of each in solution. Thus, the saturation solubility of gypsum in pure water at 25°C is:

$$\text{solubility} = [Ca^{2+}] \times [SO_4^{2-}] = \sqrt{10^{-4.6}} = 10^{-2.3} \text{ mol/liter}$$

However, the dissolution of gypsum is not this simple, as sulfate ion would always react with some hydrogen ion (or with some water molecules) to form some HSO_4^- ions, and this activity will be highly dependent on pH and other variables.

Published values of individual solubility products often disagree with each other because of experimental difficulties. In addition, applying mineral solubility products for pure water (ideal solution) when estimating solubility in the field conditions would be erroneous since, to be precise in saturation calculations, it is necessary to know the chemical form (single ions, complex ions, or neutral molecules) and activity of all ionic species in a given solution, including possible chemical reactions between various ions. Therefore, simple geochemical solubility calculations based on published solubility products are only rough approximations. Additional complicating factor is that the so-called *activity* of an ionic species is not constant and changes with concentration of both the individual ion considered and the other ions present in the solution. In other words, for dilute solutions, it is often assumed that the activity of an ion equals its mole fraction (concentration) in the solution, but this assumption may lead to significant errors for more concentrated solutions. In either case, it would be more correct to determine the actual ionic activities of ions for which the solubility calculations are made, as these activities are influenced by all the constituents in the solution.

The solubility product, and therefore solubility, generally increase with temperature, but not in all cases. For substances that exhibit phase changes at certain temperature, such as inversion of gypsum to anhydrite, the

solubility product decreases after the inversion temperature (e.g., 60°C for the gypsum-anhydrite inversion). The solubility of solid inorganic substances is independent of pressure in common groundwater systems. Figure 11.9 shows dependence of solubility on temperature for some common solid inorganic substances. The solubility product also increases with the rising concentration of the solution. This effect is especially noticeable in highly concentrated mineralized water and NaCl brines, in which the concentration can reach very high values (Matthess, 1982).

When an ionic substance (AB), such as halite (HCl; A=H, B=Cl), dissociates in an ideal solution to form positively and negatively charged ions, the following relationship is true at equilibrium:

$$K = \frac{[A^+] \cdot [B^-]}{[AB]} \qquad (11.7)$$

where AB is the solid substance, A^+ is the cation part in dissolved phase, B^- is the anion part in the dissolved phase, and K is the general constant of the reaction. At saturation, this general constant is exactly equal to the solubility product, K_{sp}, and the solution is in equilibrium between the solid and dissolved phases of the substance (no additional dissolution or precipitation of the substance from solution should occur). When $K < K_{sp}$, the solution is *undersaturated* with respect to AB and can dissolve (hold) more of it. When $K > K_{sp}$, the solution is *supersaturated,* and precipitation of AB should occur.
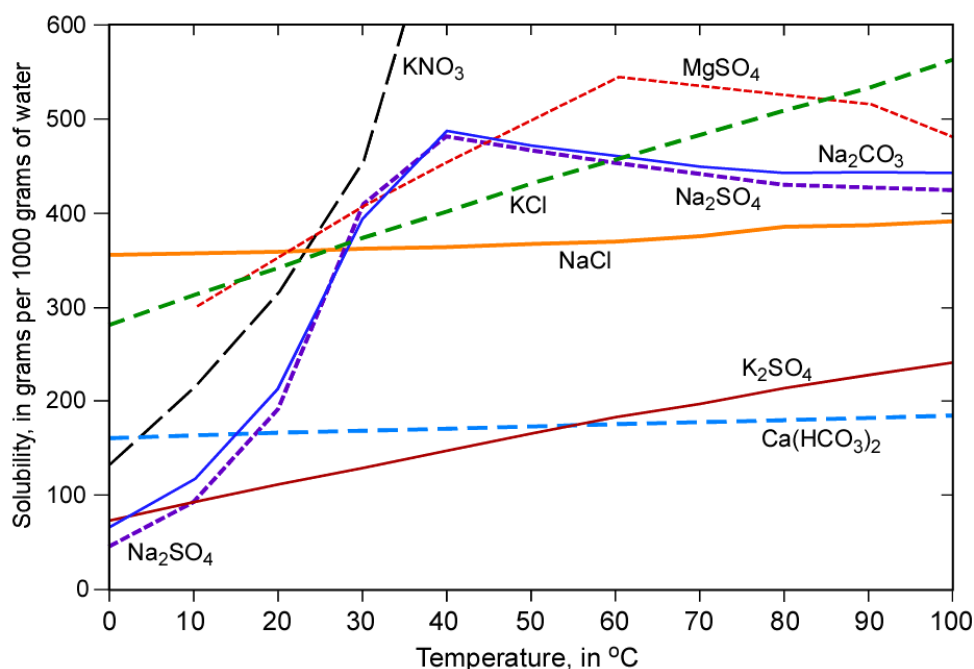
Figure 11.9 Solubilities of some solid inorganic substances in water at different temperatures. Data from Matthess, 1982; modified from Kresic, 2007. Copyright CRC Taylor & Francis; permission required for further use.

As can be seen from the previous discussions about natural groundwater systems, many of the simple analytical laboratory and theoretical considerations cannot fully describe all the complexities of site-specific geochemical conditions that influence chemical characteristics of groundwater. Arguably, the use of geochemical models is the only satisfactory approach to a more comprehensive understanding of various chemical reactions simultaneously taking place in a groundwater system, including evolution of groundwater chemistry along a flowpath. The most

widely used geochemical model for natural and contaminated waters is PHREEQC developed at the USGS (https://www.usgs.gov/software/phreeqc-version-3).

Speciation modeling available in PHREEQC uses a chemical analysis of a water to calculate the distribution of aqueous species based on an ion-association aqueous model. The most important results of speciation calculations are saturation indices for minerals, which indicate whether a mineral should dissolve or precipitate. Speciation modeling is useful in situations where the possibility of mineral dissolution or precipitation needs to be known, as in water treatment, aquifer storage and recovery, artificial recharge, and well injection. Inverse modeling capability of PHREEQC can be used to deduce geochemical reactions and mixing in local and regional aquifer systems, and in aquifer storage and recovery studies. It calculates geochemical reactions that account for the change in chemical composition of water along a flowpath. For inverse modeling, at least two chemical analyses of water are needed at different points along the flow path, as well as a set of minerals and gases that are potentially reactive. Mole transfers of phases are calculated that account for the change in water composition along the flowpath. The numerical method applied accounts for uncertainties in analytical data. Appelo and Postma (2005) provide detail tutorial on the applications of PHREEQC for simulating numerous geochemical reactions of many different inorganic and organic solutes in both natural and contaminated groundwaters.

11.5.1 Solubility of Organic Substances

Organic liquids and solids are generally much less soluble in water when compared to inorganic salts, bases, and acids. However, there are organic liquids, such as some alcohols and solvent stabilizers (1,4-dioxane for example), that are highly soluble or even completely miscible with water due to their polar nature and hydrogen bonds. As a rule, the most soluble organic species are those with polar molecular structure or those containing oxygen or nitrogen in a simple, short molecular structure. Examples include alcohols or carboxylic acids, which form hydrogen bonds with water molecules and fit easily into the structure of water. Without hydrogen bonding, the solubility of organic substances diminishes, since forcing a nonpolar organic molecule into the tetrahedral structure of water requires considerable energy. The importance of hydrogen bonding decreases with increasing molecule length and size. The larger the organic molecule is, the larger the space that is required in the water structure and the less soluble the compound is. For example, smaller alcohol molecules such as methanol and ethanol are infinitely soluble, whereas octanol is only slightly soluble. This effect is also clear when examining the solubility of aromatic compounds such as benzene, toluene, naphthalene, and biphenyl. The solubility is inversely proportional to the molecular mass or size of the molecules: it is the highest for benzene, which has the smallest molecular mass (78.0 g/mol) of the four, and the lowest for biphenyl, which has the largest molecular mass (154.0 g/mol). The respective reported aqueous solubilities of benzene and biphenyl are 1780 and 7.48 g/m^3, respectively (Domenico and Schwartz, 1990).

Organic liquids that are hydrophobic (immiscible) because of their nonpolar nature will always dissolve in water to some extent, even though the bulk of their volume may remain in a separate ("free") liquid phase for considerable periods of time. Such liquids are called non-aqueous phase liquids or NAPLs. Free NAPL phase may be distributed in different ways in the subsurface, such as relatively extensive contiguous volumes of the liquid called *NAPL pools*, or small globules and ganglia partially or completely surrounded by water (such globules and ganglia are often called *residual phase*).

Dissolution of different NAPL phases in actual field conditions will depend on various factors such as effective and total porosities of the porous media, groundwater flow rates, surface contact area between the NAPL and groundwater (i.e., geometry of different NAPL phases), and fate and transport characteristics including adsorption

and diffusion (see Lecture 12). Assuming that a NAPL would dissolve in the flowing groundwater, following some published solubility value for pure water would therefore be erroneous.

An important consideration when estimating site-specific solubilities of organic contaminants in the subsurface is that they are often commingled (there are more than one in a mixture), which decreases their individual aqueous solubilities. The exception is the presence of cosolvents, such as alcohols, which would act to increase solubilities of some NAPLs.

Effective aqueous solubility (S_i^e) of an individual liquid compound i, in mg/L, is given as follows:

$$S_i^e = X_i S_i \qquad (11.8)$$

where X_i = mole fraction of the individual compound, and S_i = pure-phase solubility of liquid phase of the individual compound. This relationship is based on Raoult's law initially developed for gaseous compounds (see next section).

Laboratory analyses suggest that Equation (11.8) is a reasonable approximation for mixtures of sparingly soluble hydrophobic organic liquids that are structurally similar and that effective solubilities calculated for complex mixtures (e.g., gasoline and other petroleum products) are unlikely to be in error by more than a factor of 2 (Cohen and Mercer, 1993.)

The true dissolution of NAPLs in the subsurface is often referred to as rate limited because of various limiting factors, all of which act to decrease pure-water solubility. Even when assuming that some of these factors can be estimated accurately at a certain site, it is almost impossible to reasonably accurately determine the distribution of free-phase and residual NAPLs in the porous media including their actual geometric shapes needed to determine contact areas with water. When comparing two NAPL bodies with the same volume of product (free phase), all other factors being equal, the time needed for a complete dissolution will be longer for a NAPL body with the smaller contact area. For example, a NAPL pool resting on an impermeable layer is exposed to groundwater flow only at the top, while irregular, suspended, and disconnected NAPL bodies have proportionally much greater contact areas and are more quickly dissolved (depleted). More on fate and transport of contaminants including true dissolution of NAPLs in flowing groundwater is given in Lecture 12.

11.5.2 Solubility and Volatilization of Gasses

Two types of gasses must be considered when estimating gaseous solubility in water: those that do not chemically react with water, such as hydrogen, oxygen, nitrogen and helium for example, and those that do react with water, such as hydrogen sulfide (H_2S), hydrogen chloride (HCl) or carbon dioxide (CO_2). In the latter case, a fraction of the gas would not follow *Henry's Law*, which states that the amount of the dissolved gas in water is directly proportional to its pressure above the interface with water. However, because the reactive gasses are transformed in water usually in small amounts (e.g., CO_2 transforms to carbonic acid to the extent of about 1%), the deviation from Henry's Law is not large. Henry's Law can be expanded to state that the dissolved concentration of a gas is also inversely proportional to its temperature: at a constant pressure, the solubility of gasses increases with the decreasing temperature and vice versa. At the water boiling temperature, all gasses escape the solution. When there is more than one gas in the mixture (as is the case with air), Henry's Law applies to the partial pressure of each individual gas. Henry's Law relationship is expressed as:

$$C_g = \frac{P_g}{K_H} \qquad\qquad (11.9)$$

where C_g is the concentration of the gas in water (solution), in moles per volume (m^3 or liter); P_g is the (partial) pressure of the gas in the gaseous phase above the interface with water (the unit is in atmospheres, atm, or Pascals, Pa); K_H is Henry's law constant, or simply Henry's constant, in atm/(mol/dm^3), or Pa/(mol/m^3).

Published values of Henry's constant for gasses, both common inorganic and various organic, vary greatly and should be used with caution when attempting to calculate gas concentrations in groundwater. A rather extensive compilation of Henry's constant values for inorganic and organic substances is given by Sander (1999).

In general, reactive gasses have much higher water solubilities than the non-reactive gasses (see Table 11.4.). Note that most reactive gasses, such as H_2 and H_2S, cannot persist in the atmosphere because their partial pressure is close to zero.

Table 11.4 Solubility of common gasses, at three different temperatures, when in equilibrium with the atmosphere (mixture of gasses), and with the pure gas. From Alekin, 1953 and 1962; Milojević, 1967; Matthess, 1982.

Gas	In equilibrium with pure gas			In equilibrium with atmosphere		
	20ºC	10ºC	0ºC	20ºC	10ºC	0ºC
O2	43.39	53.70	69.48	9.6	11.9	15.4
N2	19.01	23.12	29.42	15.1	18.3	23.4
CO2	1689	2319	3347	0.5	0.7	1
H2S	3929	5112	7027	N/A	N/A	N/A

Volatilization refers to mass transfer from liquid and solid to the gaseous phase. Chemical properties affecting volatilization include vapor pressure, Henry's constant, and aqueous solubility. Other factors influencing volatilization rate are concentration of contaminant in soil, soil moisture content, soil air movement, sorptive and diffusive characteristics of the soil, soil temperature, and bulk properties of the soil such as organic-carbon content, porosity, density, and clay content (Lyman et al., 1982; from Cohen and Mercer, 1993).

The tendency of a dissolved organic chemical to volatilize from the aqueous solution increases with an increase in Henry's Law constant. The same is true for the free liquid phase of a chemical that has a high Henry's constant. Henry's constant has been determined for many organic liquids and is readily available in reference books (see Table 12.1 in Lecture 12); however, the published values vary from source to source and should be used with caution. Organic chemicals with a high Henry's constant are called volatile and include a very important group of common organic groundwater contaminants such as aromatic and halogenated hydrocarbons (e.g., benzene and trichloroethylene).

Transport of these chemicals in the subsurface may occur in both the dissolved and gaseous phases and may involve multiple exchanges between the two phases as the site-specific conditions change in time and space. According to Henry's Law, a decrease in vapor (gas) pressure above the solution would cause volatilization (escape) of the dissolved gas into the gaseous phase above the interface. This phenomenon has been widely exploited in remediation of groundwater contaminated with volatile organic compounds through use of various

techniques that increase pressure gradients between the dissolved and gaseous phases. For example, application of vacuum in the unsaturated zone above water table would volatilize an aromatic organic compound from both the dissolved phase and the free phase (if present), which is the principle of a remediation technology called soil vapor extraction. This technology is commonly used to remediate soil and groundwater contaminated with NAPLs.

Raoult's Law has been used to quantify the volatilization of individual constituents from a mixture of NAPLs. This law relates the ideal vapor pressure and relative concentration of a chemical in solution to its vapor pressure over the NAPL solution (Cohen and Mercer, 1993):

$$P_A = X_A \cdot P_A^o \qquad (11.9)$$

where P_A is the vapor pressure of chemical A over the NAPL solution, X_A is the mole fraction of chemical A in the NAPL solution, P_A^o is the vapor pressure of the pure chemical A.

In natural systems, dissolution, and volatilization of gasses from groundwater are rather slow processes. In cases where there are significant natural changes in pressure and temperature within the porous media along the groundwater flow path, dissolution and volatilization of gasses may be fast or even abrupt. A good example is escape of carbon dioxide or hydrogen sulfide into the atmosphere at mineral springs fed by deeply circulating groundwater. Groundwater at great depths is exposed to high subsurface pressures, which may result in a high content of dissolved gasses if there is a source (e.g., a magmatic or a metamorphic process). When such water discharges at the land surface, the gasses escape because of the pressure difference, creating bubbles or odor (e.g., smell of rotten eggs in case of H_2S). Deep artesian wells often show the same mechanism.

11.6 Total Dissolved Solids (TDS). Specific Conductance. Salinity

The total concentration of dissolved material in groundwater is called *total dissolved solids* (TDS). It is commonly determined by weighing the dry residue after heating the water sample usually to 103°C or 180°C (the higher temperature is used to eliminate more of the crystallization water). TDS can also be calculated if the concentrations of major ions are known. However, for some water types, a rather extensive list of analytes may be needed to accurately obtain the total. During evaporation, approximately one half of the hydrogen carbonate ions are precipitated as carbonates and the other half escapes as water and carbon dioxide. This loss is taken into account by adding half of the HCO⁻3 content to the evaporation (dry) residue. Some other losses, such as precipitation of sulfate as gypsum and partial volatilization of acids, nitrogen, boron, and organic substances, may contribute to a discrepancy between the calculated and the measured TDS.

Solids and liquids that dissolve in water can be divided into electrolytes and nonelectrolytes. Electrolytes, such as salts, bases, and acids, dissociate into ionic forms (positively and negatively charged ions) and conduct electrical current. Nonelectrolytes, such as sugar, alcohols, and many organic substances, occur in aqueous solution as uncharged molecules and do not conduct electrical current. The ability of 1 cm³ of water to conduct electrical current is called *specific conductance* (or sometimes simply *conductance*, although the units are different). Conductance is the reciprocal of resistance and is measured in units called *Siemen* (International System) or *mho* (1 Siemen equals 1 mho; the name mho is derived from the unit for resistance—*ohm*, by spelling it in reverse).

Specific conductance is expressed as *Siemen/cm* or *mho/cm*. Since the *mho* is usually too large for most groundwater types, the specific conductance is reported in *micromhos/cm* or *microSiemens/cm* (μS/cm), with instrument readings adjusted to 25°C, so that variations in conductance are only a function of the concentration and

type of dissolved constituents present. Measurements of specific conductance can be made rapidly in the field with a portable instrument, which provides for a convenient method to quickly estimate TDS and compare general types of water quality.

For a preliminary (rough) estimate of TDS, in milligrams per liter, in fresh potable water, the specific conductance in micromhos/cm can be multiplied by 0.7. Pure water has a conductance of 0.055 micromhos at 25°C, laboratory distilled water between 0.5 and 5 micromhos, rainwater usually between 5 and 30 micromhos, potable groundwater ranges from 30 to 2000 micromhos, sea water from 45,000 to 55,000 micromhos, and oil field brines have commonly more than 100,000 micromhos (Davis and DeWiest, 1991).

As discussed by Hem (1989), the proportionality constant, A, in the linear relationship between the total dissolved solids (TDS) and the specific conductance (SC), is between 0.54 and 0.96 for nearly the full range to be expected in natural groundwaters, with 0.55 to 0.75 being the most common:

$$TDS\ (mg/L)\ =\ A \times SC\ (\mu mhos/cm) \qquad (11.10)$$

Importantly, natural waters are not simple solutions as they contain a variety of both ionic and undissociated species which do not conduct electrical current readily. The conductance determination therefore cannot be expected to be simply related to ion concentrations or to dissolved solids (Hem, 1989.) Still, the Equation (11.10) is useful for site-specific evaluations if a satisfactory set of relationships between specific conductance and ion concentrations can be developed from a few years of intensive sampling. Conductivity probes for field applications are widely available and affordable and may produce accuracy of ± 2% or better.

Figure 11.10 illustrates a reasonably well-defined relationship for the range of observed values of TDS and SC in composite samples of water from the Gila River at Bylas, Arizona. The whole set of data fits a straight-line regression closely (the coefficient of regression is 0.98), with the value for A in Equation (11.10) of 0.59.
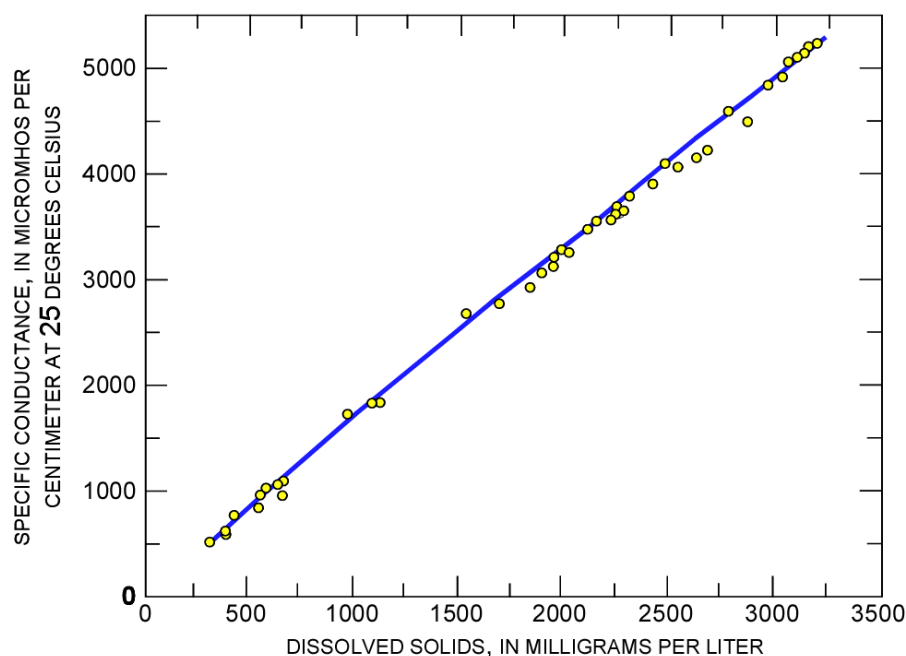
Figure 11.10 Dissolved solids and specific conductance of composites of daily samples, Gila River at Bylas, Arizona, October 1,1943 to September 30, 1944. From Hem, 1989. USGS, in public domain.

Depending on the nature od salts (ions) dissolved in groundwater and their concentrations, the relationship between TDS and EC varies and may be non-linear, especially for very high concentrations of salts where the slope decreases slightly. This is because the property called ionic mobility decreases by increasing concentration owing to interferences and interactions among the ions (Hem, 1989).

The response to of the conductance value to temperature change is somewhat different for different salts and different concentrations, but for most low mineralized waters an increase of 1°C increases conductance by about 2 percent over the range of temperature usually applicable to laboratory conditions.

Term *salinity* is often used for total dissolved salts (ionic species) in groundwater, in the context of water quality for agricultural uses and/or human and livestock consumption. Various salinity classifications based on certain salts and their ratios have been proposed (see Matthess, 1982). One problem with the term salinity is that a salty taste may be already noticeable at somewhat higher concentrations of NaCl (e.g., 300-400 mg/L), even though the overall concentration of all dissolved salts may not "qualify" a particular groundwater to be called "saline". In practice, it is common to call water with less than 1000 milligrams per liter (1 g/L) dissolves solids *potable* or *fresh*, and water with more than 10,000 mg/L *saline*.

11.7 Hydrogen-Ion Activity (pH)

Hydrogen-ion activity, or pH, is probably the best-known chemical characteristics of water. It also the one that either directly affects or is closely related to most geochemical and biochemical reactions in groundwater. Whenever possible, pH should be measured directly in the field since groundwater, once outside its natural environment (aquifer), quickly undergoes several changes which directly impact pH, the most important being temperature and the CO_2-carbonate system. Incorrect values of pH may be a substantial source of error in geochemical equilibrium and solubility calculations.

By convention, the content of hydrogen ion in water is now expressed in terms of its activity "pH" rather than its concentration in milligrams or millimoles per liter. Although hydrogen ion (H^+) is being continuously formed by dissociation of water, its concentration in natural waters that are not strongly acidic is very low. For example, at pH 7 (neutral conditions), there are only 1×10^{-7} moles of hydrogen ion in one liter of water, compared to 10^{-4} moles per liter and up for major constituents in groundwater. Dissociation of water into H^+ and OH^- (hydroxyl) ions is a reversible reaction and this equilibrium for a dilute solution is expressed with the following equation:

$$K_w = \frac{[H^+] \cdot [OH^-]}{[H_2O]} \qquad (11.11)$$

where K_w is the constant equal to the product of activities of H^+ and OH^- when the activity of the pure liquid water is assumed to be 1 at 25°C by convention.

This ion-activity product of H^+ and OH^- at 25°C is $10^{-14.000}$ in exponential terms. This can be expressed in terms of the negative logarithm as $-\log(K_w) = 14.00$. In other words, when omitting the negative sign by convention, the logarithmic product of the H^+ and OH^- activities is 14. By definition, when the number of hydrogen ions equals the number of hydroxyl ions, the solution is neutral, and the hydrogen ion activity is pH=7 (note that log[7] times log[7] is log[14]). Theoretically, when there are no hydrogen ions, pH=14 and the solution is purely alkaline (base); when there are no hydroxyl ions, the solution is a pure acid with pH=1. Accordingly, when the activity (concentration) of hydrogen ions decreases, the activity of hydroxyl ions must increase because the product of the

two activities is always the same, i.e., 14. For example, when pH=5 (slightly acidic solution), pOH=9. In terms of actual concentrations of the two ions, this would translate into H^+ concentration of 10^{-5}, or 1 mole of H^+ in 100,000 m^3 of water (which is equal to 1 millimole in 100,000 liters); the concentration of OH^- would be 10^{-9} or 1 mole in 1,000,000,000 m^3 of water.

The reaction of dissolved carbon dioxide with water is one of the most important in establishing pH in natural water systems. This reaction is represented by the following three steps (Hem, 1989):

$$CO_2(g) + H_2O(l) = H_2CO_3(aq) \qquad (11.12)$$

$$H_2CO_3(aq) = H^+ + HCO_3^- \qquad (11.13)$$

$$HCO_3^- = H^+ + CO_3^{2-} \qquad (11.14)$$
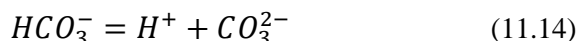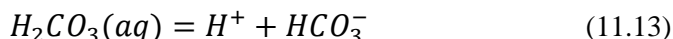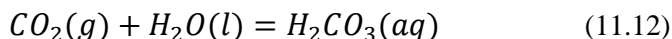
where g, l, and aq denote gaseous, liquid and aqueous phases, respectively. The second and third steps produce hydrogen ions which influence the acidity of solution. Other common reactions that create hydrogen ions involve dissociation of acidic solutes such as:

$$H_2PO_4^- = HPO_4^{2-} + H^+ \qquad (11.15)$$

$$H_2S(aq) = HS^- + H^+ \qquad (11.16)$$

$$HSO_4^- = SO_4^{2-} + H^+ \qquad (11.17)$$
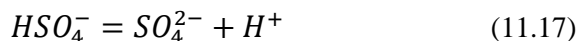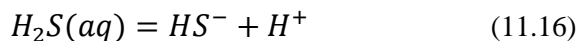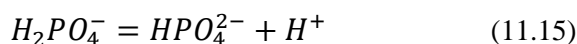
Many of the reactions between water and solid species consume H^+ resulting in creation of OH^- and alkaline conditions. One of the most common is hydrolysis of solid calcium carbonate (calcite):

$$CaCO_3 + H_2O = Ca^{2+} + HCO_3^- + OH^- \qquad (11.18)$$

Note that equation (11.18) explains why lime dust (calcium carbonate) is often added to acidic soils in agricultural applications to stimulate growth of crops that do not tolerate such soils. The reaction described by equation (11.18) is accelerated when dissolved CO_2 creates carbonic acid in reaction with water (equation 11.12) which then also attacks calcite.

The pH of water has a profound effect on the mobility and solubility of many substances. Only a few ions such as sodium, potassium, nitrate, and chloride remain in solution through the entire range of pH found in normal groundwater. Most metallic elements are soluble as cations in acid groundwater but will precipitate as hydroxides or basic salts with an increase in pH. For example, all but traces of ferric ions will be absent above a pH of 3, and ferrous ions diminish rapidly as the pH increases above 6 (Davis and DeWiest, 1991).

11.8 Reduction-Oxidation Potential (Eh)

Reduction and oxidation can be broadly defined as gain of electrons and loss of electrons, respectively. For a particular chemical reaction, an *oxidizing agent* is any material that gains electrons, and a *reducing agent* is any material that loses electrons. The reduction process is illustrated with the following expression (Hem, 1989):

$$Fe^{3+} + e^- = Fe^{2+} \qquad\qquad (11.19)$$

where ferric iron (Fe^{3+}) is reduced to the ferrous state by gaining one electron. The symbol "e^-" represents the electron, or unit negative charge. This expression is a "half-reaction" for the iron reduction-oxidation couple; for the reduction to take place there must be a source of electrons, i.e., another element has to be simultaneously oxidized (lose electrons). Together with the hydrogen ion activity (pH), reduction and oxidation reactions play key role in solubility of various ionic substances. Microorganisms are involved in many of the reduction-oxidation reactions and this relationship is especially important when studying fate and transport of contaminants subject to biodegradation.

The electric potential of a natural electrolytic solution with respect to the standard hydrogen half-cell measuring instrument is expressed (usually) in millivolts or mV. This measured potential is known as *reduction-oxidation potential* or *redox* and is denoted with Eh ("h" stands for hydrogen). Observed Eh range for groundwater is between +700 and -400 mV. Positive sign indicates that the system is oxidizing, and negative that the system is reducing. The magnitude of the value is a measure of the oxidizing or reducing tendency of the system. Eh, just like pH, should be measured directly in the field. Concentration of certain elements is a good indicator of the range of possible Eh values. For example, notable presence of H_2S (>0.1 mg/L) always causes negative Eh. If oxygen is present in concentrations greater than 1 mg/L, Eh is commonly between 300 and 450 mV. Generally, an increase in content of salts decreases Eh of the solution.

The redox state is determined by the presence or absence of free oxygen in groundwater. Newly percolated (recharge) water often supplies oxygen to groundwater in the range from 6 to 12 mg/l. At the water table oxygen is also dissolved directly from the soil air and can be carried into deeper groundwater levels by diffusion and flow dispersion. The depth of the oxidizing zone in an aquifer varies greatly based on local hydrogeologic and geochemical conditions. Oxidation processes are faster in warm and humid climates than in cold and arid climates. Oxygen can be consumed in a number of different geochemical reactions, the most direct being oxidation of iron and manganese compounds. Microbial activity also consumes oxygen and may rapidly create reducing environment in a saturated zone with an excess in dissolved organic carbon (which is a nutrient for microbes) such as in cases of groundwater contamination with organic liquids. Determining redox potential in an aquifer is particularly important in contaminant fate and transport and remediation studies. For example, oxidizing (*aerobic*) conditions favor biodegradation of petroleum hydrocarbons such as gasoline, while reducing (*anaerobic*) conditions favor biodegradation of chlorinated compounds such as tetrachloroethene (PCE). Another example of the importance of redox conditions in an aquifer is the state of metal ions, such as iron and chromium. In slightly acidic to alkaline environments, Fe(III) precipitates as a highly adsorptive solid phase (ferric hydroxide), whereas Fe(II) is very soluble and does not retain other metals. The reduction of Fe(III) to Fe(II), therefore, releases not only Fe^{2+} to the water, but also any contaminants that were adsorbed to the ferric hydroxide surfaces. Hexavalent Cr(VI) is a toxic, relatively mobile ion whereas trivalent Cr(III) is inert, relatively insoluble, and strongly adsorbs to solid surfaces (Johnson et al., 1989).

Based on oxygen demand of the various bacterial species, an oxygen content between 0.7 and 0.01 mg O_2/liter at 8°C water temperature has been commonly defined as threshold oxygen concentration for the boundary between oxidizing and reducing conditions. However, field observations suggest that reducing conditions may appear at considerably higher oxygen contents (Matthess, 1982). Bacteria present in groundwater catalyze most redox reactions. This catalytic capability is produced by the activity of enzymes that normally occur within the bacteria. Enzymes, which are protein substances formed by living organisms, have the power to increase the rate of redox reactions by decreasing the activation energies of the reactions. They accomplish this by strongly interacting with

complex molecules representing molecular structures halfway between the reactant and the product (Pauling and Pauling, 1975, from Freeze and Cherry, 1979).

Bacteria and their enzymes are involved in redox processes to acquire energy for synthesis of new cells and maintenance of old cells. If the redox reactions that require bacterial catalysis are not occurring at significant rates, a lack of one or more of the essential nutrients for bacterial growth is likely the cause. There are various types of nutrients, some of which are required for incorporation into the cellular mass of the bacteria. Carbon, nitrogen, sulfur, and phosphorous compounds and many metals are in this category. Other nutrients are substances that function as electron donors or energy sources, such as water, ammonia, glucose, and hydrogen sulfide (H_2S). Substances that function as electron acceptors in redox reactions are oxygen, nitrate, and sulfate (Freeze and Cherry, 1979). The key principle of bioremediation of contaminated groundwater is stimulation of bacterial activity that produces certain redox reactions. This stimulation is accomplished by delivering nutrients and/or electron acceptors into the saturated zone targeted for remediation.

The redox potential generally decreases with rising temperature and pH, and this decrease results in an increasing reducing power of the aqueous system. Reducing systems, in addition to the absence or very much reduced oxygen content, have noticeable content of iron and manganese, occurrence of hydrogen sulfide, nitrite and methane, absence of nitrate, and often a reduction or absence of sulfate (Matthess, 1982).

Stability diagrams, which relate pH and Eh to chemical forms of a substance, are often used to draw conclusions about its occurrence and chemical behavior in a particular system. An example for the various forms of iron is given in Figure 11.5. Another example of a stability diagram developed for a water sample collected from a hypothetical monitoring well to evaluate possible attenuation mechanisms of dissolved cobalt reaching the well is shown in Figure 11.11 Based on the analysis, the dissolved cobalt is likely immobilized by co-precipitation with iron oxyhydroxides (goethite) that precipitate under oxidizing conditions.
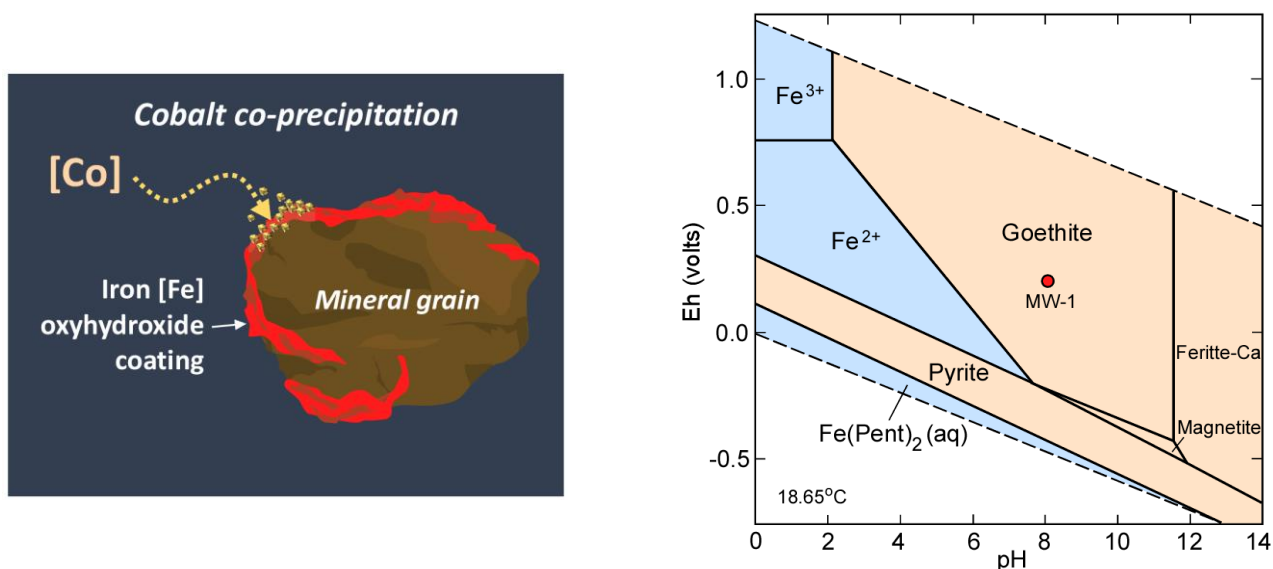
Figure 11.11 Geochemical model illustration of likely immobilization of dissolved cobalt by co-precipitation with iron. *Left*: Schematic of the process. *Right*: Eh-pH diagram for the water sample collected at a hypothetical monitoring well MW-1. The sample falls in the field of solid goethite the presence of which was confirmed in the sediments at the site. The stability diagram was created by Act2 module of Geochemist's Workbench software package based on constituents' analyses of the water sample. Courtesy of Ali Akbari and Hariprasad Parthasarathy, Geosyntec Consultants.

11.9 Alkalinity

The alkalinity of a solution may be defined as the capacity for solutes it contains to react with and neutralize acid. An example illustrating the practical meaning of this definition in earth-related sciences is the ability of some soils rich with calcium carbonate to neutralize acid rains. This is often referred to as the soil buffering capacity. In almost all natural waters, the alkalinity is produced by the dissolved carbon dioxide species, bicarbonate and carbonate. In other words, except for waters having high pH (greater than about 9.50) and some others that have unusual chemical compositions, the alkalinity of groundwater can be assigned entirely to dissolved bicarbonate and carbonate without serious error (Hem, 1989). The most common practice is to report alkalinity in terms of an equivalent amount of calcium carbonate. Table 11.3 provides factors for converting common calcium and carbonate ionic species into equivalent calcium-carbonate.

11.10 Visualization of Groundwater Analyses

A common practice in hydrogeology when interpreting the results of chemical analyses is to present the concentrations of major ionic species graphically. Piper diagrams (Piper, 1944) are convenient for plotting the results of multiple analyses on the same graph, which may reveal grouping of certain samples and indicate their common or different origin. Circle diagrams are often used on hydrogeologic maps as a convenient way to quickly compare chemical composition of samples collected at various locations. Different ions can be shown in different colors, while the size of the circle may be used to represent the total dissolved solids in the sample. Both methods are illustrated in Figure 11.12 for two groundwater samples with notably different chemical composition of major ions.

As a rule of thumb, the primary constituents make up more than 90% of total dissolved solids in a groundwater sample. Because of this, six ionic species in particular have been widely used to graphically present major chemical types of groundwater: <u>cations</u> of calcium, magnesium, and (expressed together) sodium + potassium; and <u>anions</u> of chloride, sulfate, and (expressed together) hydrocarbonate + carbonate. In an analysis expressed in milliequivalents per liter, unit concentrations of all ions are chemically equivalent. This means that if all ions have been correctly determined, the total milliequivalents per liter of the three major cations (Ca, Mg, and Na+K) is equal to the total milliequivalents per liter of the three major anions (Cl, SO_4, and HCO_3+CO_3). When this is not the case, in addition to possible analytical and computational errors, it may be that some of the ionic species usually considered minor and therefore not analyzed, are present in higher concentrations. For example, nitrate anion (NO_3) in agricultural and otherwise contaminated areas is present in considerable amount, often more than 10 mg/L.

The graphs in Figure 11.12 are plotted using percentages of milliequivalents per liter for each ion within its respective group. Results of the chemical analyses for samples #1 and #2 expressed in additional units are given in the tables. Concentrations expressed in milligrams per liter can be converted into milliequvalents per liter using conversion factors listed in Table 11.1.

There are quite a few other graphical methods for representing the results of groundwater chemical analyses (e.g., see Alekin, 1962, and Hem, 1989). One of the more often used is the Stiff diagram, which gives an irregular polygonal shape that can help in recognizing possible patterns in multiple analyses (Figure 11.13).

The reason why the six ionic species used to plot Piper and Circle diagrams shown in Figures 11.12 and 11.13 are the most prevalent in natural groundwaters is that the most important soluble salts occurring in relatively large quantities in rocks are calcium carbonate ($CaCO_3$), magnesium carbonate ($MgCO_3$), their combination ($CaCO_3 \times MgCO_3$), sodium chloride (NaCl), calcium sulfate ($CaSO_4$), and hydrous calcium sulfate ($CaSO_4 \times 2H_2O$).
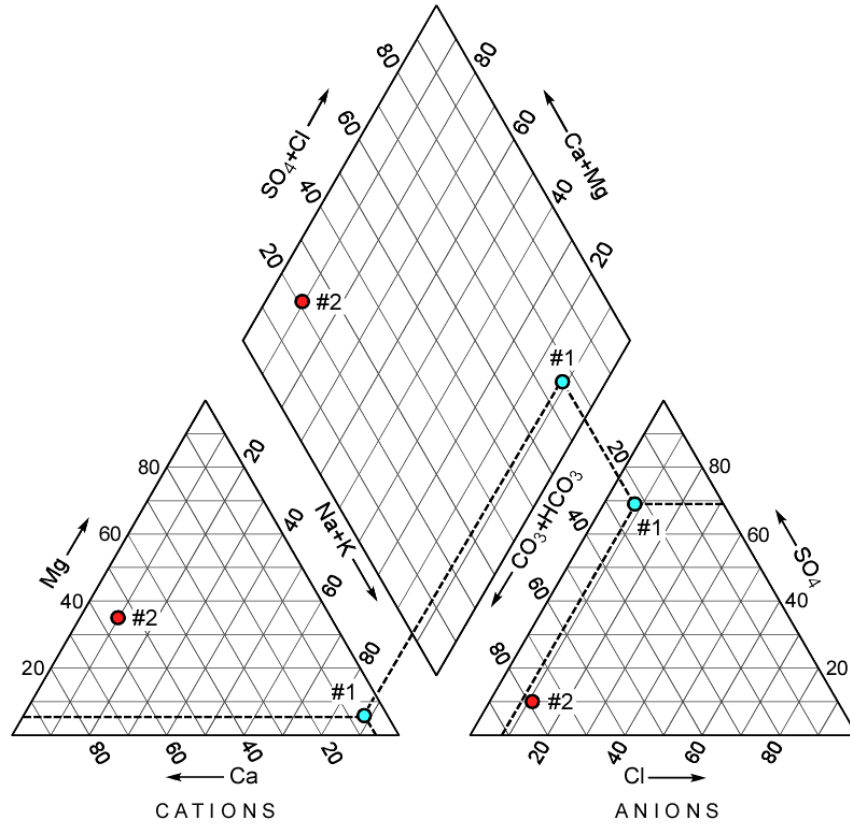
ANALYSIS #1				ANALYSIS #2			
IONS	mg/L	meq/L	% meq/L	IONS	mg/L	meq/L	% meq/L
Calcium (Ca)	37	1.85	6.1	Calcium (Ca)	144	7.19	55.5
Magnesium (Mg)	24	1.97	6.5	Magnesium (Mg)	55	4.52	34.9
Sodium (N } Potassium (K) }	611	26.58	87.4	Sodium (N } Potassium (K) }	29	1.24	9.6
Bicarbonate (HCO$_3$)	429	7.03	23.1	Bicarbonate (HCO$_3$)	622	10.19	78.8
Sulfate (SO$_4$)	1010	21.03	69.2	Sulfate (SO$_4$)	60	1.25	9.7
Chloride (Cl)	82	2.31	7.6	Chloride (Cl)	53	1.49	11.5
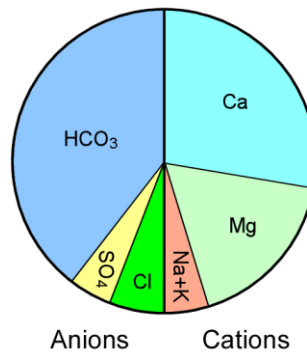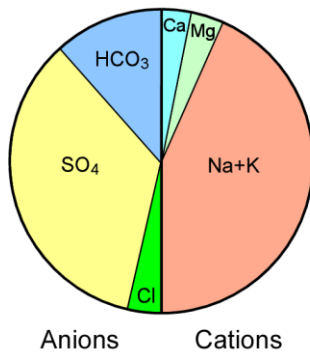
Figure 11.12 Piper and Circle diagrams for two groundwater samples. Modified from Kresic, 2007. Copyright CRC Taylor & Francis; permission required for further use.
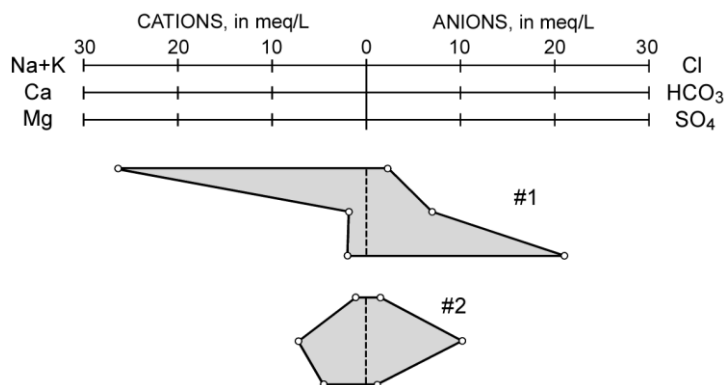
Figure 11.13 Stiff diagrams for water analyses shown in Figure 11.12. Copyright CRC Taylor & Francis; permission required for further use.

Although aluminum is the third most abundant element in the Earth's crust, because of its chemical properties it rarely occurs in solution in natural water in concentrations greater than a few tenths or hundredths of a milligram per liter (Hem, 1989). The exceptions are waters with very low pH such as acidic mine drainage. Iron, the second most abundant metal in the Earth's crust, is also found in relatively small concentrations in groundwater, rarely exceeding 1 mg/L. The chemical behavior of iron and its solubility in water depend strongly on the redox potential and pH as discussed earlier (e.g., see Figure 11.5). The forms of iron present in groundwater are also strongly affected by microbial activity. Various ferrous complexes are formed by many organic molecules, and some of the complexes may be significantly more resistant to oxidation than free ferrous ions. For all these reasons, iron is considered one of the primary groundwater constituents, even though its dissolved ionic forms are in most groundwaters found in smaller concentrations compared to the major ions.

Contrary to the examples of aluminum and iron, element silicon, being the second only to oxygen in the Earth's crust, is found in appreciable quantities in most groundwaters, usually between 1 and 30 mg/L when expressed as silica. Relative abundance of silica in natural water is due to its many different chemical forms found in minerals and rocks. This fact goes contrary to the common belief that silica is not soluble in water and is therefore not present in groundwater. Most abundant forms of silica dissolved in water are thought not to form ions, although the complicated groundwater chemistry of silica is still not well understood. Consequently, when it is important to present the silica content in a groundwater sample graphically, a bar graph based on milliequivalents or millimoles per liter is often used (Figure 11.14).
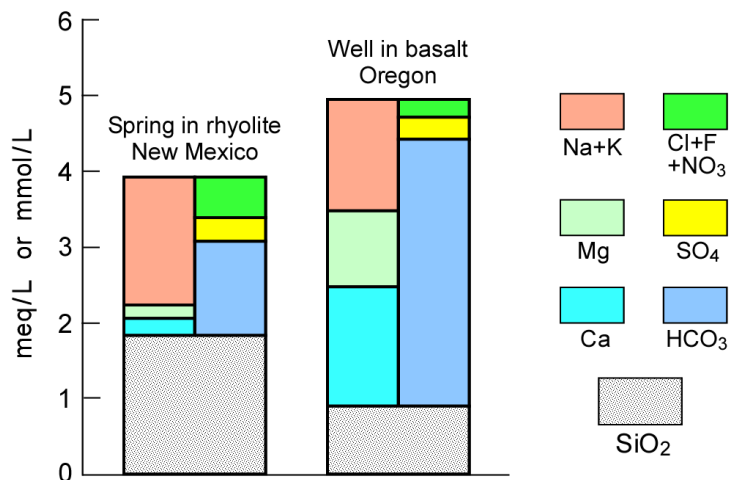
Figure 11.14 Graphs of major groundwater constituents including silica for two samples obtained from igneous rocks. Modified from Hem, 1989. USGS, in public domain.

Box-and-Whisker plots (or simply "box" plots) are useful for comparing statistical parameters of samples known to be collected from different aquifers. For example, Figures 11.15 and 11.16 show results of chemical analyses of groundwater from three different aquifers in coastal North Carolina, the United States. The most obvious from the Piper diagram presentation is that the surficial aquifer samples have a wide scatter, ranging from calcium bicarbonate to sodium chloride types. The source of the calcium and bicarbonate is most likely carbonate shell material in sediments of the surficial aquifer; however, the lower concentrations of these analytes compared with those in the Castle Hayne and Peedee aquifers (Figure 11.16) are probably a result of less abundance of carbonate material in the surficial aquifer and the leaching and removal of these chemical constituents by infiltrating precipitation from the surficial deposits. The lowest pH values for recent groundwater samples were measured in the surficial aquifer and indicate the leaching and removal of carbonate minerals (Harden et al., 2003). The pH of groundwater in the surficial aquifer was slightly acidic and ranged from 4.8 to 7.5 pH units, with a median value of about 6.9 (Figure 11.16). The median dissolved-solids concentration (residue at 180°C) in the surficial aquifer was about 110 mg/L, almost three times less than in the Castle-Hayne aquifer, which is the deepest among the three. The highest dissolved-solids concentration of 870 mg/L was detected in a surficial aquifer well at Bald Head Island. This well also has the highest chloride concentration. Groundwater at Bald Head Island is known to be salty and is treated by reverse osmosis for supply purposes (Harden et al., 2003).
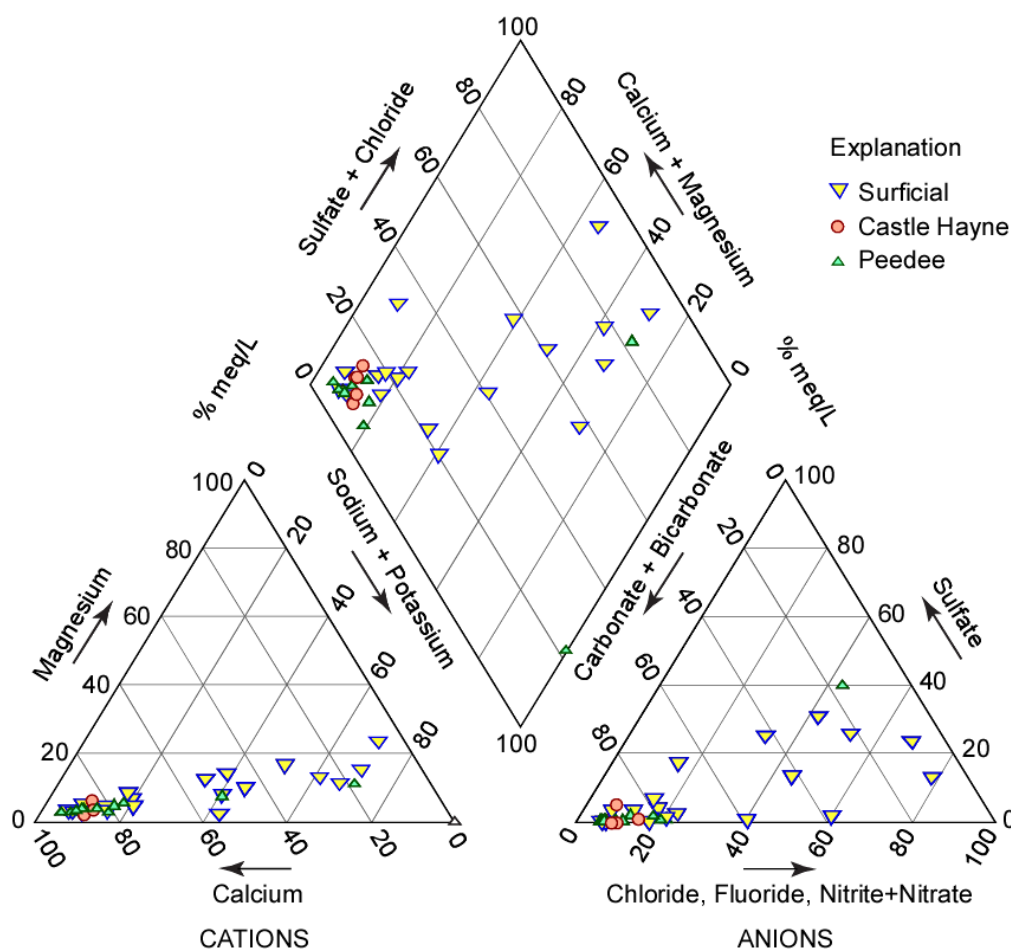
Figure 11.15 Piper diagram showing July–August 2000 groundwater quality in Brunswick County, NC. Modified from Harden et al., 2003. USGS, in public domain.
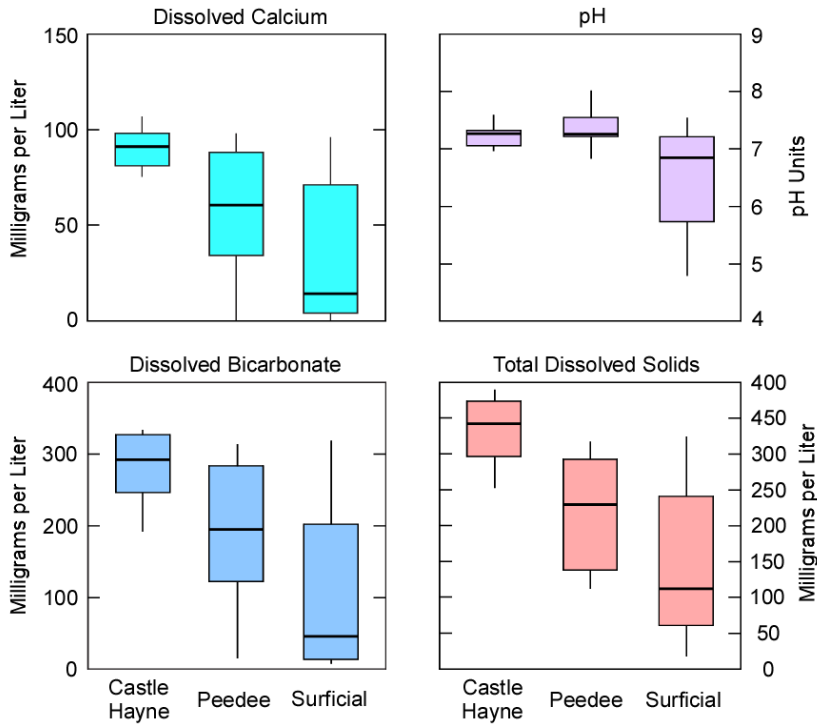
Figure 11.16 Concentrations of selected chemical constituents in groundwater samples collected during July–August 2000, Brunswick County, NC. Bottom and top of the box are 25th and 75th percentiles, respectively. Bold line inside the box is median value. Vertical lines outside the box extend to 10th and 90th percentiles. Modified from Harden et al., 2003. USGS, in public domain.

Lecture 12 Groundwater Contamination

This lecture is based on the materials presented in Kresic (2007, 2009, 2013), Kresic and Mikszewski (2013), and in various publications by the United States Environmental Protection Agency (U.S. EPA) and other related federal and state programs. Many of the publications can be accessed from the links provided at the U.S. EPA web sites

> https://www.epa.gov/ground-water-and-drinking-water
> https://www.epa.gov/superfund/how-superfund-addresses-groundwater-contamination
> https://clu-in.org/contaminantfocus
> https://www.epa.gov/remedytech/remediation-technologies-cleaning-contaminated-sites

Any water that contains disease-causing or toxic substances is defined as contaminated (U.S. EPA, 2000a). This definition does not differentiate between possible sources of contamination or types of contaminants—any substance of natural or synthetic origin that is toxic to humans or can cause disease is defined as a groundwater (water) contaminant. In the broadest sense, all sources of groundwater contamination and contaminants themselves can be grouped into two major categories: naturally occurring and synthetic (artificial; anthropogenic). Some natural contaminants, such as arsenic and uranium, may have significant local or regional impacts on groundwater supplies. However, anthropogenic sources and synthetic chemical substances have much greater negative effects on the quality of groundwater resources.

Almost every human activity has the potential to impact groundwater directly or indirectly to a certain extent. Figure 12.1 illustrates some of the land-use activities that can result in groundwater contamination. An exponential advancement of analytical laboratory techniques in the last several decades has demonstrated that many synthetic organic chemicals are widely distributed in the environment, including in groundwater, and that a considerable number of them can now be found in human tissue and organs of people living across the globe.
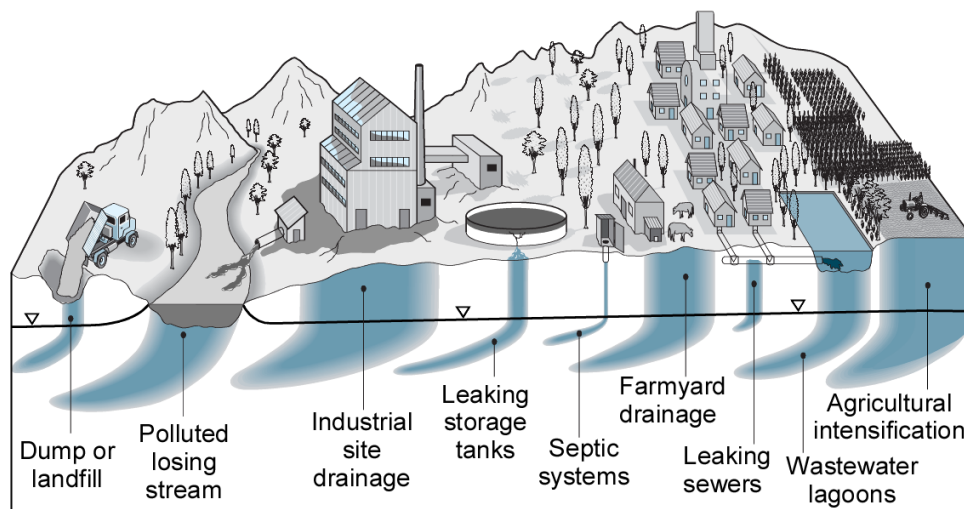
Figure 12.1 Land use activities commonly generating a groundwater threat. From Foster et al., 2002-2005. The World Bank, acknowledge required for further use.

Strongly related to the ever-increasing public awareness of environmental pollution is a very rapid growth in consumption of bottled drinking water, also across the globe. Many consumers are ready to pay a premium for brands marketed as "pure spring water" or "water coming from deep pristine aquifers", so that major multinational corporations are frantically looking for groundwater resources that can be marketed as such. In general, there is still a lot of truth in the following statement, very much appreciated by many groundwater professionals: groundwater in general is much less vulnerable to contamination than surface water (karst aquifers being an exception), it is of better quality, and thus requires less investment in water supply development. It is however also true that, in general, it takes longer, and it is more difficult to restore a groundwater (re)source once it becomes contaminated.

In developed industrialized countries, regulatory agencies are mostly concerned with groundwater contamination caused by organic synthetic chemicals. For example, in 1993 the U.S. EPA reported that rapid growth of the chemical industry in the United States in the second half of the 20th century resulted in common industrial and commercial use of at least 63,000 synthetic organic chemicals, with 500 to 1,000 being added each year. Health effects brought about by long-term, low-level exposure to many of these chemicals are not yet, or may never be fully assessed.

In less developed countries, contamination of water supplies by organic chemicals is of minor or of no concern compared to health problems related to poor sanitary conditions and diseases caused by pathogenic organisms (bacteria, parasites, and viruses). The primary health-related goal in such countries is disinfection of drinking water and development of safe water supplies. Even a simple sanitary design of water wells such as the one shown in Figure 12.2 can dramatically improve the health and lives of population dependent on groundwater.

Figure 12.2 Villagers in Northern Ghana collect water at a new sanitary well equipped with hand-pump.
Photo courtesy of Jenny VanCalcar.

Groundwater contamination is most common in highly developed areas, agricultural areas, and industrial complexes. Frequently, groundwater contamination is discovered long after it has occurred. One reason for this is the slow movement of groundwater through groundwater systems, sometimes as little as fractions of a foot (meter) per day. This often results in a delay in the detection of groundwater contamination. In some cases, contaminants introduced into the subsurface decades ago are only now being discovered at locations of groundwater use. This also means that the environmental management practices of today will have effects on groundwater quality well into the future (U.S. EPA, 2000a).

12.1 Regulatory Background

In 1970, the *United States Environmental Protection Agency* (U.S. EPA) was established as an independent agency. A major factor in its establishment was an implicit understanding of the need for Federal enforcement authority. The drinking water, air pollution control, and solid waste programs were moved from the Public Health Service to U.S. EPA. Water pollution control moved from the Department of Interior to U.S. EPA. A 1972 study detected 36 chemicals in treated water taken from treatment plants that drew water from the Mississippi River in Louisiana. Cancer was found to be present at higher rates in the population using the public water supply in New Orleans than in the population using private wells. These surveys raised concerns and prompted U.S. EPA to conduct a national survey to detail the quality of drinking water. The survey showed that drinking water was widely contaminated on a national scale, particularly with synthetic organic chemicals. Contamination was especially alarming in large cities. This survey raised concerns about drinking water in the public health community and in the general public. Increased concern and awareness of contamination of drinking water supplies prompted Congress to enact the Safe Drinking Water Act (SDWA) in 1974. The purpose of SDWA was to establish national enforceable standards for drinking water quality and to guarantee that water suppliers monitor water to ensure that it meets national standards (U.S. EPA, 2022a).

The SDWA, Title XIV of the Public Health Service Act, is still the key federal law for protecting public water supplies from harmful contaminants. It was substantially amended in 1986, 1996, and 2018, and is administered by the U.S. EPA through programs that establish standards and treatment requirements for public water supplies, finance drinking water infrastructure projects, promote water system compliance, and control the underground injection of fluids to protect underground sources of drinking water. The 1974 law established the current federal-state arrangement in which states may be delegated primary implementation and enforcement authority for the drinking water program. The state-administered Public Water Supply Supervision (PWSS) Program remains the basic program for regulating the nation's public water systems. Forty-nine states have assumed this authority (Humphreys and Tiemann, 2021.)

Federal drinking water regulations apply to the approximately 144,653 privately and publicly owned water systems that provide piped water for human consumption to at least 15 service connections or that regularly serve at least 25 people. These water systems vary greatly in size and type, ranging from large municipal systems to systems operated by homeowner associations, schools, and campgrounds. Nearly 49,600 of the regulated public water systems are community water systems (CWSs), which serve the same residences year-round. These water systems provide water to more than 312 million people. All federal regulations apply to these systems. Most community water systems (81%) are relatively small, serving 3,300 or fewer individuals.

As of 2021, U.S. EPA reports that, of 144,653 public water systems, 130,029 rely on groundwater and 14,563 rely on surface water. Among 49,591 community water systems, 37,953 rely on groundwater and 11,613 rely on

surface water. The remaining systems did not identify whether their source was groundwater or surface water (Humphreys, 2021.)

National Interim Drinking Water Regulations (renamed to *National Primary Drinking Water Regulations* in the 1986 SDWA amendments) established either the maximum concentration of pollutants allowed in drinking water, or the minimum treatment required for water that is delivered to customers. *Maximum Contaminant Level Goal* (*MCLG*) is the maximum level of a contaminant in drinking water at which no known or anticipated adverse health effects would occur. A *Maximum Contaminant Level* (*MCL*) is an enforceable requirement. It is the maximum permissible level of a contaminant in water that can be delivered to any user of a public water system. An MCL is set as close to an MCLG as possible, taking into account the costs and benefits and feasible technologies. For some contaminants, there is not a reliable method that is economically and technologically feasible to measure the contaminant, particularly at low concentrations. In these cases, U.S. EPA establishes a *treatment technique* (*TT*). A treatment technique is an enforceable procedure or level of technological performance that public water systems must follow to ensure control of a contaminant. The hazardous waste (RCRA) and Superfund programs also use MCLs to define acceptable cleanup levels for contaminated water.

The 1986 SDWA amendments were prescriptive and required U.S. EPA to issue drinking water regulations for 83 specified contaminants by 1989. Further, U.S. EPA was required to regulate an additional 25 contaminants (to be specified by U.S. EPA) every three years and to designate the best available treatment technology for each contaminant regulated.

The 1986 Amendments also initiated the groundwater protection program, including the *Wellhead Protection Program*. The law specified that certain program activities, such as delineation, contaminant source inventory, and source management, be incorporated into *State Wellhead Protection Programs,* which are approved by U.S. EPA prior to implementation. In addition, the *Sole Source Aquifer Demonstration Program* was added to the existing sole source aquifer provision. This program provides funding to identify and provide the special protections needed for sole source aquifers.

Increased monitoring requirements and monitoring for organic chemicals at a greater number of water systems led to increased detection of chemicals and the identification of potential problems from the widespread presence of organic chemicals. In addition, increased monitoring detected previously unidentified microbial problems. The increased detection of previously unknown water system contaminant problems created a need for water system operators and States to develop risk communication skills to inform the public of impacts of contaminants on their health. Increased knowledge of *Giardia* improved methods for detecting the pathogen, and continuing outbreaks of the disease prompted tightened requirements for surface water treatment. This included lowered turbidity standards, disinfectant contact time (CT) calculations and strict criteria to avoid filtration.

Along with increased treatment requirements for surface water systems, some groundwater supplies were recognized as providing water of essentially surface water quality. These sources are recharged by surface water to the extent that pathogens, such as *Giardia* cysts, can contaminate the water. These sources are known as *Ground Water Under the Direct Influence* (of surface water) or *GWUDI*. Identification of GWUDI sources and regulation as surface water systems was required. *Public notification* requirements increased the communication between water systems and consumers, further increasing awareness of contamination of drinking water. Public notification requirements were strictly prescribed and included broadcast and printed notices depending on the severity of the contamination problem. More stringent *coliform monitoring* requirements in the 1986 Amendments increased the frequency of coliform detection. Increased requirements for follow-up monitoring after initial detection revealed

even more problems. This led to greater awareness of the inadequacy of some sources of water, even after treatment (U.S. EPA, 2022d).

Among the key provisions, the 1996 SDWA Amendments authorized a *Drinking Water State Revolving Loan Fund* (DWSRF) program to help public water systems finance projects needed to comply with SDWA rules. The amendments also established a process for selecting contaminants for regulation based on health risk and occurrence, gave U.S. EPA some added flexibility to consider costs and benefits in setting most new standards, and established schedules for regulating certain contaminants (such as *Cryptosporidium*, arsenic, and radon). The law added several provisions aimed at building the capacity of water systems (especially small systems) to comply with SDWA regulations, and it imposed many new requirements on the states including programs for source water assessment, operator certification and training, and compliance capacity development. The amendments also required that community water suppliers provide customers with annual *consumer confidence reports* that provide information on contaminants found in the local drinking water (Tiemann, M., 2005).

Two programs established by U.S. EPA in the 1980's have had the largest impact on the rapid development of hydrogeology and many scientific and engineering disciplines related to groundwater remediation. *Comprehensive Environmental Response, Compensation, and Liability Act* (*CERCLA* or *Superfund*), provides for the cleanup of inactive and abandoned waste sites including impacted groundwater. *Resource Conservation and Recovery Act* (*RCRA*) regulates hazardous waste generation, storage, transportation, treatment, and disposal, including remediation of contaminated groundwater at active industrial and other facilities (U.S. EPA, 1986; 1994).

12.2 Common Groundwater Contaminants and Their Sources

Groundwater contamination can occur as relatively well-defined, localized plumes emanating from specific *point sources* such as leaking underground storage tanks (LUSTs), spills, landfills, waste lagoons, and industrial facilities. *Nonpoint sources* of contamination refer to pollution discharged over a wide land area, not from one specific location. They include forms of diffuse pollution caused by sediment, nutrients, and organic and toxic substances originating from land use activities such as agriculture or urban development. Rainwater, snowmelt, or irrigation water can wash off these substances together with soil particles and carry them with surface runoff to surface streams. A portion of this contaminant load dissolved in water can also infiltrate into the subsurface and eventually contaminate groundwater.

Results of the first nationwide study of potential contaminant sources conducted by the U.S. EPA and state environmental protection agencies is shown in Figure 12.3. Each state was requested to indicate the 10 top sources that potentially threaten their groundwater resources. States added sources as was necessary based on state-specific concerns. When selecting sources, states considered numerous factors, including

- The number of each type of contaminant source in the state.
- The location relative to groundwater sources used for drinking water purposes.
- The size of the population at risk from contaminated drinking water.
- The risk posed to human health and/or the environment from releases.
- Hydrogeologic sensitivity (the ease with which contaminants enter and travel through soil and reach aquifers).
- The findings of the state's groundwater assessments and/or related studies.

For each of the 10 top sources, states identified the specific contaminants that may impact groundwater quality. As seen in Figure 12.3, the sources most frequently cited by states as a potential threat to groundwater quality are

LUSTs. Septic systems, landfills, industrial facilities, and fertilizer applications are the next most frequently cited sources of concern. If similar sources are combined, five broad categories emerge as the most important potential sources of groundwater contamination: (1) fuel storage practices, (2) waste disposal practices, (3) agricultural practices, (4) industrial practices, and (5) mining operations.

Fuel Storage Practices

Fuel storage practices include the storage of petroleum products in underground and aboveground storage tanks. Underground storage tank (UST) is any system having 10 percent of the total tank volume below ground. Although tanks exist in all populated areas, they are generally most concentrated in the more heavily developed urban and suburban areas of a state. Storage tanks are primarily used to hold petroleum products such as gasoline, diesel fuel, and fuel oil. Leakages can be a significant source of groundwater contamination. The primary causes of tank leakages are faulty installation or corrosion of tanks and pipelines. Petroleum products are complex mixtures of hundreds of different compounds. Over 200 gasoline compounds can be separated in the mixture. Compounds characterized by higher water solubility are frequently detected in groundwater. Four compounds, in particular, are associated with petroleum contamination: **b**enzene, **t**oluene, **e**thylbenzene, and **x**ylenes, commonly named together as **BTEX**. Petroleum-related chemicals threaten the use of groundwater for human consumption because some, such as benzene, are known to cause cancer even at very low concentrations.
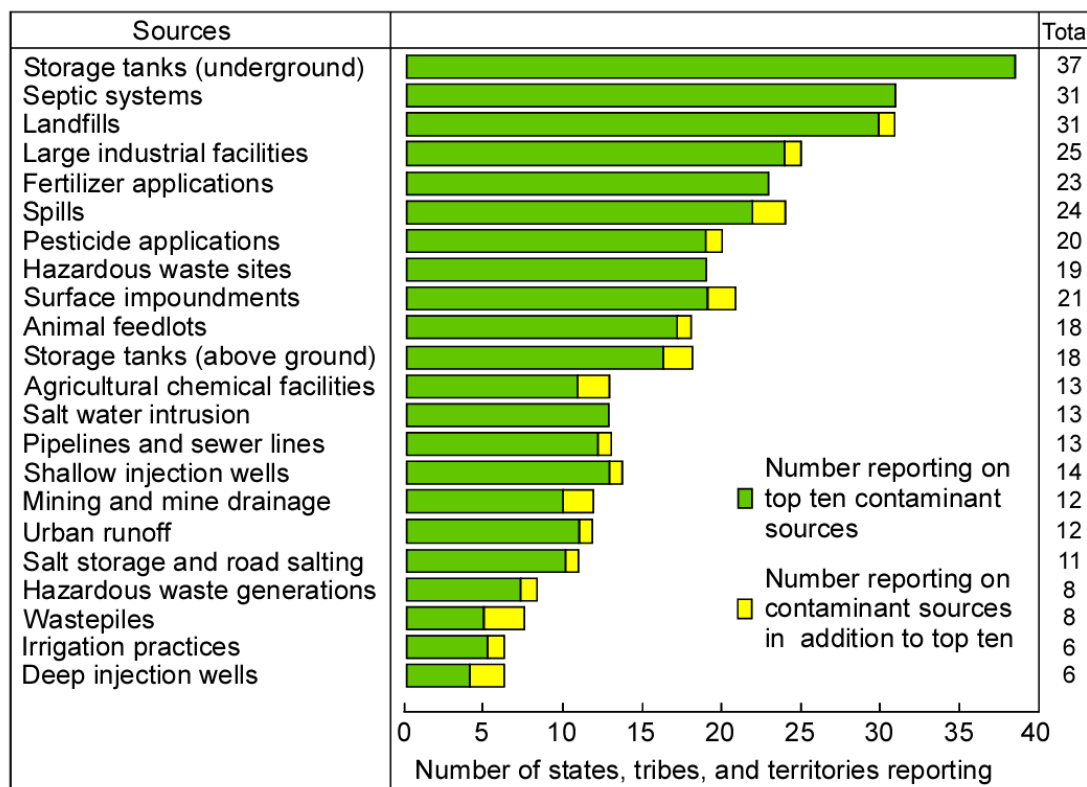
Figure 12.3 Major sources of groundwater contamination in the United States. From U.S. EPA, 2000a. In public domain

Waste Disposal Practices

Waste disposal practices include septic systems, landfills, surface impoundments, deep and shallow injection wells, dry wells, sumps, wastepiles, mining waste tailings, land application, and illegal disposal. Any practice that involves the handling and disposal of waste has the potential to impact the environment if protective measures are not taken. Contaminants most likely to impact groundwater include metals, volatile organic compounds (VOCs), semivolatile organic compounds (SVOCs), nitrates, radionuclides, and pathogens. As reported by the U.S. EPA (2000a), the state survey indicates that in many instances present-day groundwater contamination is the result of historic practices at waste disposal sites.

Leaking sewer lines in urban areas and industrial complexes can cause groundwater contamination with a variety of contaminants. Together with the leaky water supply lines, these also contribute to rising water tables under many large urban centers.

Land application is a general term for spreading of sewage (domestic and animal) and water-treatment plant sludge over tracts of land. This practice, still controversial, when improperly executed can cause widespread groundwater contamination in hydrogeologically sensitive areas. The problem with all sewage disposal practices is the presence of various pharmaceuticals, hormones and personal care products (PPCPs) that are being continuously released to the environment including groundwater. During 1999 to 2000, the United States Geological Survey (USGS) implemented first-ever national reconnaissance of "emerging pollutants" in surface waters and groundwaters in 36 states. The objective of the study was to establish baseline occurrence data including for some commonly used PPCPs. Samples were collected from 142 streams, 55 wells, and seven wastewater-treatment effluents. The findings, published in March 15, 2002, issue of Environmental Science and Technology, show a widespread of PPCPs in surface water and groundwater. Since then, USGS scientists analyzed presence of pharmaceuticals and hormones in samples from 1,100 wells pumping from drinking-water aquifers, confirming their presence in both public-supply and domestic supply wells (Bexfield et al., 2019.)

According to the U.S. EPA (2000a), discharges to surface impoundments such as pits, ponds, lagoons, and leach fields are generally underregulated. They usually consist of relatively shallow excavations that range in area from a few square feet to many acres and are or were used in agricultural, mining, municipal, and industrial operations for the treatment, retention, and disposal of both hazardous and nonhazardous wastes. As a consequence, they have the potential to leach metals, VOCs, and SVOCs to groundwater. For example, in Colorado, wells located downgradient from tailings ponds or cyanide heaps associated with mining operations often exhibit high concentrations of metals; in Arizona, surface impoundments and leach fields are identified as significant sources of VOCs.

Agricultural Practices

Agricultural practices that have the potential to contaminate groundwater include animal feedlots, fertilizer and pesticide applications, irrigation practices, agricultural chemical facilities, and drainage wells. Groundwater contamination can be a result of routine applications, spillage, or misuse of pesticides and fertilizers during handling and storage, manure storage and spreading, improper storage of chemicals, and irrigation return drains serving as a direct conduit to groundwater. Fields with overapplied and misapplied fertilizers and pesticides can introduce nitrogen, pesticides, cadmium, chloride, mercury, and selenium into the groundwater. Fertilizers and pesticides are applied both in rural agricultural areas on crops and orchards and in urban-suburban settings on lawns and golf courses.

Livestock is an integral component of many states' economies. As a consequence, concentrated animal feeding operations (CAFOs), where animals are kept and raised in confined areas, occur in many states. CAFOs congregate animals, feed, manure and urine, dead animals, and production operations on a small land area. Such operations can pose a number of risks to water quality and public health, mainly because of the amount of animal manure and wastewater they generate. Animal feedlots often have impoundments from which wastes may infiltrate into groundwater. Livestock waste is a source of nitrate, bacteria, TDS, and sulfates.

Shallow unconfined aquifers in many states have become contaminated from the application of fertilizer. Crop fertilization is the most important agricultural practice contributing nitrate to the environment. Nitrate is considered by many to be the most widespread groundwater contaminant. To help combat the problems associated with the overuse of fertilizers, the U.S. Department of Agriculture's Natural Resources Conservation Service assists crop producers in developing nutrient management plans.

Pesticide use and application practices are of great concern for groundwater quality worldwide. The primary route of pesticide transport to groundwater is by leaching through the vadose zone or by spills and direct infiltration through drainage controls. Pesticide infiltration is generally greatest when rainfall is intense and occurs shortly after the pesticide is applied. Within sensitive areas, groundwater monitoring has shown fairly widespread detections of pesticides, specifically the pesticide atrazine.

Industrial Practices

Raw materials and waste handling in industrial processes can pose a threat to groundwater quality. Industrial facilities, hazardous waste generators, and manufacturing and repair shops, all present the potential for releases. Storage of raw materials at the facility is a problem if the materials are stored improperly and leaks or spills occur. Examples include chemical drums that are carelessly stacked or damaged, and dry materials that are exposed to rainfall. Material transport and transfer operations, including accidental spills and leaks at these facilities can also be a cause for concern. The most common industrial contaminants are metals, VOCs, SVOCs, and petroleum compounds. VOCs are associated with a variety of activities that use them as degreasing agents.

Mining Operations

Mining can result in a variety of water contamination problems caused by pumping of mine waters to the surface, by leaching of the spoil material in tailing ponds, by waters naturally discharging through the mine, and by milling and spoil wastes, among others (Figure 12.4). Literally thousands of miles of streams and numerous aquifers have been contaminated by highly corrosive mineralized waters originating in the coal mines and dumps of Appalachia. In many western states, mill wastes and leachates from metal sulfide operations have seriously affected both surface water and groundwater (U.S. EPA, 1990).
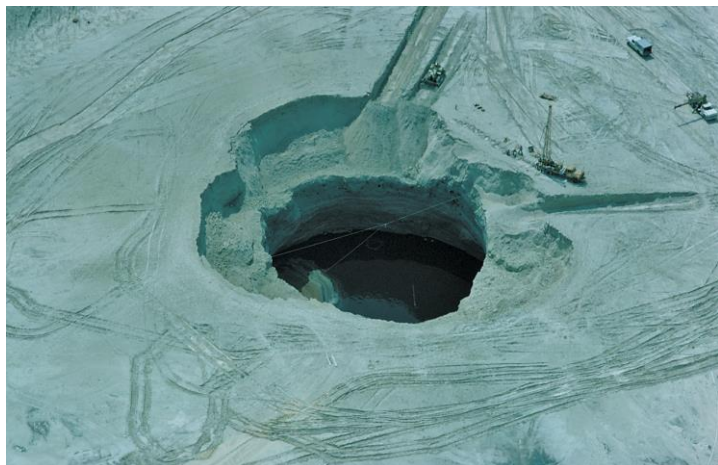
Figure 12.4 A gaping sinkhole formed abruptly on June 27, 1994, within a 400-acre, 220-ft high gypsum stack at a phosphate mine in south-central Florida. Note trucks and the drilling rig for scale. Photo by late Professor George Sowers, printed with kind permission of Francis Sowers.

Potential impacts of various contaminant sources on large public water supply wells are of most concern due to often extensive capture zones of these high-yielding wells. The screened or open intervals of such wells are commonly from tens to hundreds of feet in length; therefore, the pumped water is generally a mixture of waters of different ages that enter the well at different depths and are associated with different potential sources of contamination (Eberts et al., 2005). For example, Figures 12.5 and 12.6 illustrate a case where water entering the well may be coming from two distinct areas: (1) water from the urban area may contain contaminants from point sources, such as chlorinated solvents from dry-cleaners and machine shops, and will enter the top portion of the well screens; (2) water that has traveled from the more distant agricultural area, where recharge water may contain contaminants such as agricultural pesticides and fertilizers, will enter the middle and bottom portions of the well.
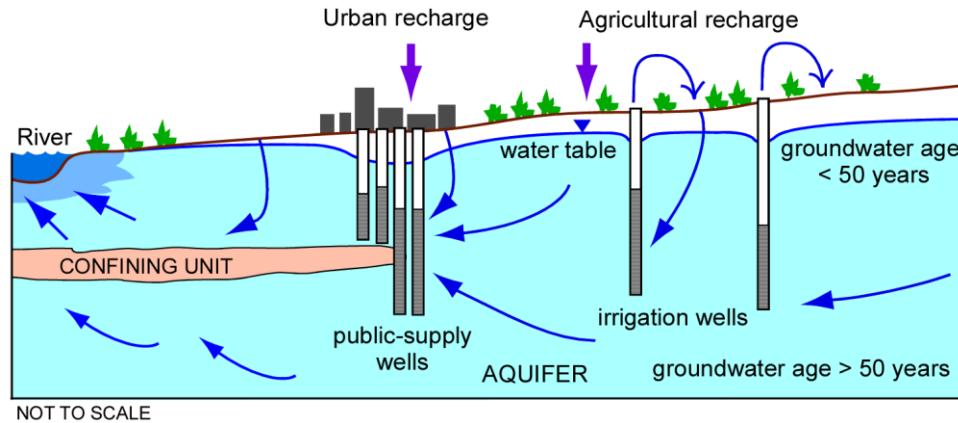
Figure 12.5 An aquifer system and public water system in an urban setting. The water entering the well screens of the public supply wells is of different ages and from different areas because of their long screen intervals, which commonly make public supply wells vulnerable to contamination from multiple sources. In this example, sources of contaminants may include those associated with urban and agricultural land use activities. Aquifer materials may also serve as sources of natural contaminants such as arsenic. Modified from Eberts et al., 2005. USGS, in public domain.
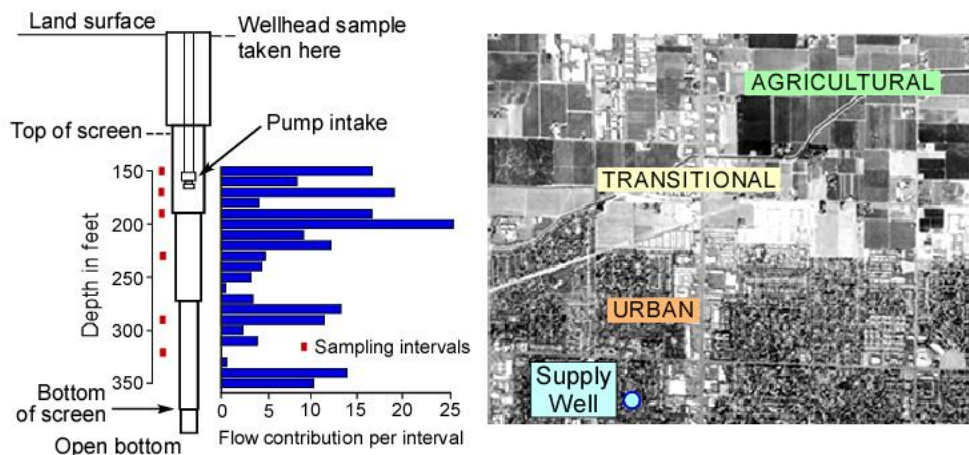
Figure 12.6 Inflow at different depths within a public supply well. The aerial photo shows an approximately 63-square-mile area near the well. Water entering the well screen is associated with different potential sources of contaminants because of the different land-use activities in the areas contributing recharge to various intervals along the well screen, as well as the different aquifer materials through which water flows between the recharge areas and the well. The amount of contamination that might be contributed by any given interval is related to the volume of water that flows into the well along the interval and the concentration of any associated contaminants. Modified from Eberts et al., 2005. USGS, in public domain.

In some cases, the same type of contaminant may originate from very different sources, both point and non-point, impact the aquifer, and cause real headache even to seasoned environmental attorneys used to various improbable cases. *Nitrogen* in different forms is the best example of such a contaminant as discussed by Seiler of the USGS (1996): potential sources of the nitrogen in groundwater flow systems in Nevada include domestic sewage, animal wastes, fertilizers, natural sources, and munitions constituents. Partially based on a detail study of sources of nitrogen in groundwater underlying valleys in Washoe County, Nevada, Seiler provides a very informative general overview of nitrogen occurrence in groundwater.

Twelve common groups of contaminants that have impacted groundwater at over 1,000 Superfund sites in the United States are shown in Figure 12.7. As can be seen, halogenated volatile organic compounds (VOCs), metals and metalloids, and BTEX are each found at more than 50% of the Superfund sites. Brief description of different groups of groundwater contaminants is provided further.
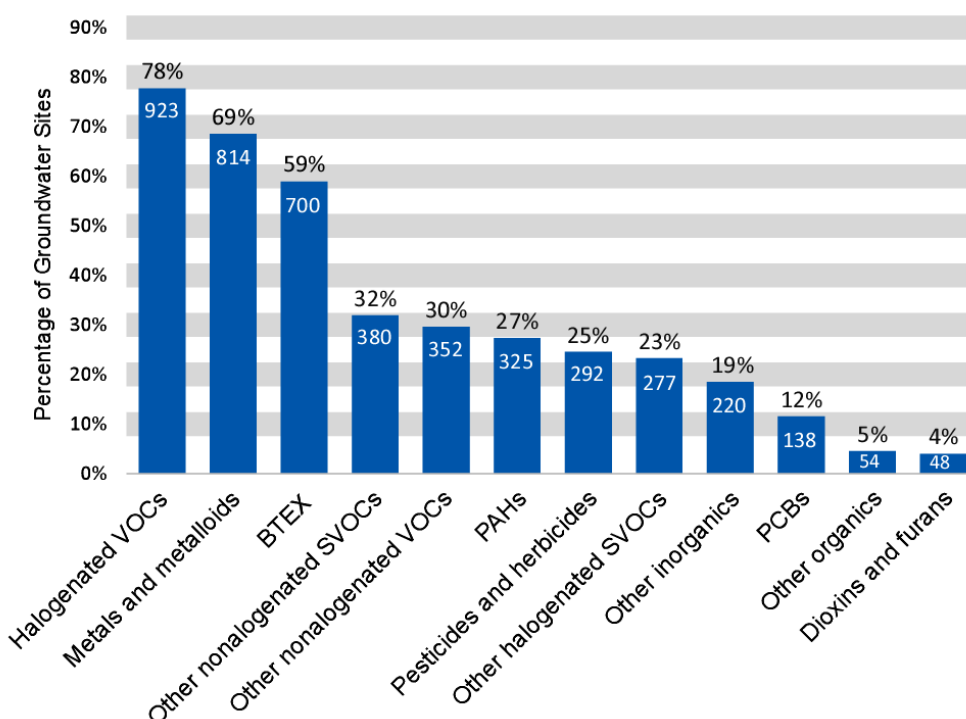
Figure 12.7 Detailed contaminants of concern (COCs) in groundwater at Superfund sites, for years 1981-2017; number of groundwater sites with identified COCs and a remedy is 1,187. From U.S. EPA, 2020. In public domain.

12.3 Synthetic Organic Contaminants (SOCs)

Concern about SOCs in the drinking water supplies of some cities was a significant cause of the passage of the 1974 Safe Drinking Water Act (SDWA), even though data were scarce. In 1981, the U.S. EPA conducted the Ground Water Supply Survey to determine the occurrence of volatile organic chemicals (VOCs) in public drinking water supplies using groundwater. The survey showed detectable levels of these chemicals in 28.7 percent of public water systems serving more than 10,000 people and in 16.5 percent of smaller systems. Other U.S. EPA and state

surveys also revealed VOCs in public water supplies. The U.S. EPA has used these surveys to support regulation of numerous organic chemicals, many of which are carcinogenic (Tiemann, 1996).

SOCs are synthetic (anthropogenic) compounds that are used for a variety of industrial and agricultural purposes and include organic pesticides. SOCs can be divided into two groups: VOCs and nonvolatile (semivolatile) compounds.

Disinfection of drinking water is one of the major public health advances of the twentieth century. Disinfection is a major factor in reducing the typhoid and cholera epidemics that were common in American and European cities in the nineteenth century and the beginning of the twentieth century. While disinfectants are effective in controlling many microorganisms, certain disinfectants (notably chlorine) react with natural organic and inorganic matter in source water and distribution systems to form *disinfection by-products* (*DBPs*), which are almost all organic chemicals (chromate and bromate are notable exceptions). A large portion of the U.S. population is potentially exposed to DBPs through its drinking water. More than 240 million people in the United States are served by public water systems that apply a disinfectant to water to protect against microbial contaminants. Results from toxicology studies have shown several DBPs (e.g., bromodichloromethane, bromoform, chloroform, dichloroacetic acid, and bromate) to be carcinogenic in laboratory animals. Other DBPs (e.g., chlorite, bromodichloromethane, and certain haloacetic acids) have also been shown to cause adverse reproductive or developmental effects in laboratory animals. Epidemiological and toxicological studies involving DBPs have provided indications that these substances may have a variety of adverse effects across the spectrum of reproductive and developmental toxicity: early term miscarriage, still birth, low birth weight, premature babies, and congenital birth defects (U.S. EPA, 2003b). DBPs are of special concern when studying the potential for artificial aquifer recharge using treated wastewater.

VOCs and SVOCs

VOCs are synthetic chemicals used for a variety of industrial and manufacturing purposes. Among the most common VOCs are degreasers and solvents such as benzene, toluene, and trichloroethene (TCE); insulators and conductors such as polychlorinated biphenyls (PCBs); dry-cleaning agents such as tetrachloroethylene (PCE); and gasoline compounds (BTEX). VOCs have the potential to cause chromosome aberrations, cancer, nervous system disorders, and liver and kidney damage.

VOCs were detected in many aquifers across the United States in a study conducted by the USGS (Zogorski et al., 2006). The complexity of explaining VOC contamination in aquifers was confirmed in this assessment through statistical models for 10 frequently detected compounds. Factors describing the source, transport, and fate of VOCs were all important in explaining the national occurrence of these VOCs. For example, the occurrence of PCE was statistically associated with the percentage of urban land use and density of septic systems near sampled wells (source factors), depth to top of well screen (transport factor), and presence of dissolved oxygen (fate factor). As concluded by the USGS, this national-scale statistical analyses provided important insights about the factors that are strongly associated with the detection of specific VOCs. The widespread occurrence of VOCs indicates the ubiquitous nature of VOC sources and the vulnerability of many of the country's aquifers to low-level VOC contamination. The findings for VOCs indicate that other compounds with widespread sources and similar behavior and fate properties may also be occurring (Zogorski et al., 2006).

SVOCs are operationally defined as solvent-extractable organic compounds that can be determined by gas chromatography/mass spectrometry (GC/MS). They include polycyclic aromatic hydrocarbons (PAHs), azaarenes, nitrogenated compounds, phenols, phthalates, ketones, and quinones. Many of these SVOCs have been designated as priority pollutants by the U.S. EPA because of their toxicity and association with industrial activities and

processes. They are referenced in the Clean Water Act of 1977. SVOCs that are priority pollutants include phthalates used in plastics, phenols used as disinfectants and in manufacturing chemicals, and PAHs. PAHs and azaarenes contain fused carbon rings that form during the incomplete combustion of organic matter, including wood and fossil fuels (such as gasoline, oil, and coal). Azaarenes are distinguished from PAHs by having a nitrogen atom substituted for a carbon in the fused ring structure. Azaarenes tend to occur in association with PAHs in affected soils and streambed sediment samples because fossil fuel combustion is the primary source of both PAHs and azaarenes. However, additional sources of PAHs include natural or anthropogenic introduction of uncombusted coal and oil and industrial use of PAHs in the dye and plastic industries (Nowell and Capel, 2003; from Lopes and Furlong, 2001).

Most SVOCs are moderately to strongly hydrophobic (i.e., they have fairly low water solubility and fairly high octanol-water partition coefficients). Consequently, they tend to sorb to soil and sediment and partition to organic matter in water.

Pesticides

If treatment is not used to protect plants, insects and fungus can destroy crops. Unfortunately, so far, the only proven efficient method for plant protection on a large scale is through the application of chemicals. Plant extracts have been used as pesticides since Roman times, nicotine since the seventeenth century and synthetic pesticides since the 1930s (Paul Muller discovered the insecticide properties of DDT in 1939). Today, new active compounds are registered in different countries every year and usually must be handled with care because of their toxic properties (see Figure 8.12 in Lecture 8).

The word pesticide refers to any chemical that kills pests and includes insecticides, fungicides, and nematocides; it also generally includes herbicides. Extensive use of pesticides is not confined to rural agricultural areas only. They are commonly used in both urban and suburban settings on lawns, parks, and golf courses.

Pesticides used in the 1950s and 1960s, such as DDT and dieldrin, were generally characterized by low aqueous solubility, strong sorption by soil components, and broad-spectrum toxic effects. These pesticide properties are now known to accumulate in the environment and cause adverse impacts on aquatic ecosystems via persistence and biomagnifications.

In 1992, the U.S. EPA issued the Pesticides in Ground Water Database (1971–1991), which showed that nearly 10,000 of 68,824 tested wells contained pesticides at levels that exceeded drinking water standards or health advisory levels. Almost all the data were from drinking water wells. The U.S. EPA has placed restrictions on 54 pesticides found in groundwater, 28 of which are no longer registered for use in the United States but may still be present in soils and groundwater due to this widespread historic use (Tiemann, 1996).

In 2006, the USGS published the results of a nationwide study conducted during 1992 to 2002. One or more pesticides or their degradation products were detected in water more than 90 percent of the time during the year in streams draining watersheds with agricultural, urban, and mixed land uses. In addition, some organochlorine pesticides that have not been used in the United States for years were detected along with their degradation products and by-products in most samples of whole fish or bed sediment from streams sampled in these land use settings. Pesticides in groundwater were detected in more than 50 percent of wells sampled to assess shallow groundwater in agricultural and urban areas.

In a European survey on the occurrence of organic pollutants in groundwater, Loos et al. (2010) found atrazine, a weed killer widely used to protect corn crops, to be the most frequently detected pesticide (herbicide) in

groundwater across Europe. The same pattern could be seen in more recent literature from European countries (Hertzman, 2017). Atrazine has been banned for use in the European Union since 2004. In contrast, the U.S. EPA has concluded that the risks from atrazine for approximately 10,000 community drinking water systems using surface water are low and did not ban this pesticide, which continues to be the most widely used pesticide in the United States. Incidentally, as stated by the agency, 40,000 community drinking water systems using groundwater were not included in the related study, and private wells used for water supply were not mentioned in the agency's decision to allow continuous use of atrazine (U.S. EPA, 2003). In 2018, U.S. EPA reapproved atrazine for continuing use.

As reported by Britt E. Erickson in the September 21, 2020 issue of Chemical and Engineering News "EPA's decision to reapprove atrazine continues an unlawful pattern by the Trump administration of approving toxic pesticides without rigorously analyzing or accounting for their harmful effects," Sylvia Wu, a senior attorney at the Center for Food Safety, says in a statement." and "The agency's decision "provides much needed regulatory certainty for farmers during a time when few things are certain," Gary Marshall, CEO of the Missouri Corn Growers Association, says in a statement released by the EPA."

12.4 Non-Aqueous Phase Liquids (NAPLs)

Nonaqueous-phase liquids (NAPLs) are hydrocarbons that exist as a separate, immiscible phase when in contact with water and/or air. Differences in the physical and chemical properties of water and NAPL result in the formation of a physical interface between the liquids, which prevents the two fluids from mixing. NAPLs are typically classified as either light nonaqueous phase liquids (LNAPLs), which have densities less than that of water, or dense nonaqueous phase liquids (DNAPLs), which have densities greater than that of water (Table 5.1). It is very important to make the distinction between the actual NAPL liquid in free phase, and the chemical of the same name dissolved in water. For example, most common organic contaminants such as PCE, TCE, and benzene can enter the subsurface as both free-phase NAPL and dissolved in percolating water. However, the fate and transport of free-phase NAPL and the same chemical dissolved in groundwater are quite different.

The most common groundwater contamination problems related to LNAPLs result from the release of petroleum products. Leaky USTs at gas stations and other facilities are arguably the most widespread point-sources of groundwater contamination in developed countries (e.g., see Figure 12.3). Gasoline products are typically multicomponent organic mixtures composed of chemicals with varying degrees of water solubility. Some gasoline additives such as MTBE (which is not in use anymore in the U.S.) and alcohols such as ethanol are highly soluble. Other components (e.g., BTEX) are slightly soluble. Many components (e.g., n-dodecane and n-heptane) have relatively low water solubility under ideal conditions (Newell et al., 1995). At the end of the refining process, finished gasoline commonly contains more than 150 separate compounds; however, some blends may contain as many as 1000 compounds (Mehlman, 1990; Harper and Liccione, 1995). In addition to BTEX, which on average make about 16 percent of a typical gasoline blend, three minor components of gasoline, naphthalene, vinyl benzene (styrene), and 1,2,4-trimethylbenzene (124-TMB), are commonly detected in contaminated groundwater (Lawrence, 2006). Individual BTEX compounds are also widely used as solvents and in manufacturing (Swoboda-Colberg, 1995).

When a mixture of pure LNAPLs (e.g., fuel) is released to the subsurface, the components of the fuel may remain in the original free phase, dissolve into and migrate with any water present in the vadose zone, absorb to solid material in the soil, or volatilize into soil gas. Therefore, a three-phase system consisting of water, product, and air is created within the vadose zone. Infiltrating water dissolves the components within the LNAPL (e.g.,

benzene, toluene, xylene, and others) and carries them to the water table. These dissolved constituents then form a contaminant plume emanating from the area of the residual product, where LNAPL phase is immobile (trapped by the porous media). If enough product is spilled, free LNAPL will flow downward to the water table and form a pool floating on it, being lighter (less dense) than water (see Figure 12.8).

Many of the components commonly found in LNAPLs are volatile and can partition into the soil air and be transported by molecular diffusion in all directions within the vadose zone and away from the area of the residual mass. These vapors may partition back into the water phase and spread contamination over a wider area. They can also diffuse across the land surface boundary into the atmosphere (Palmer and Johnson, 1989).

Fluctuations of the water table, combined with the downgradient migration of the three contaminant phases (product pool, phase dissolved in groundwater, and vapor phase), may create a complex horizontal and vertical distribution (redistribution) of the contaminant in the subsurface, especially if the porous media is heterogeneous (presence of clay lenses and layers).
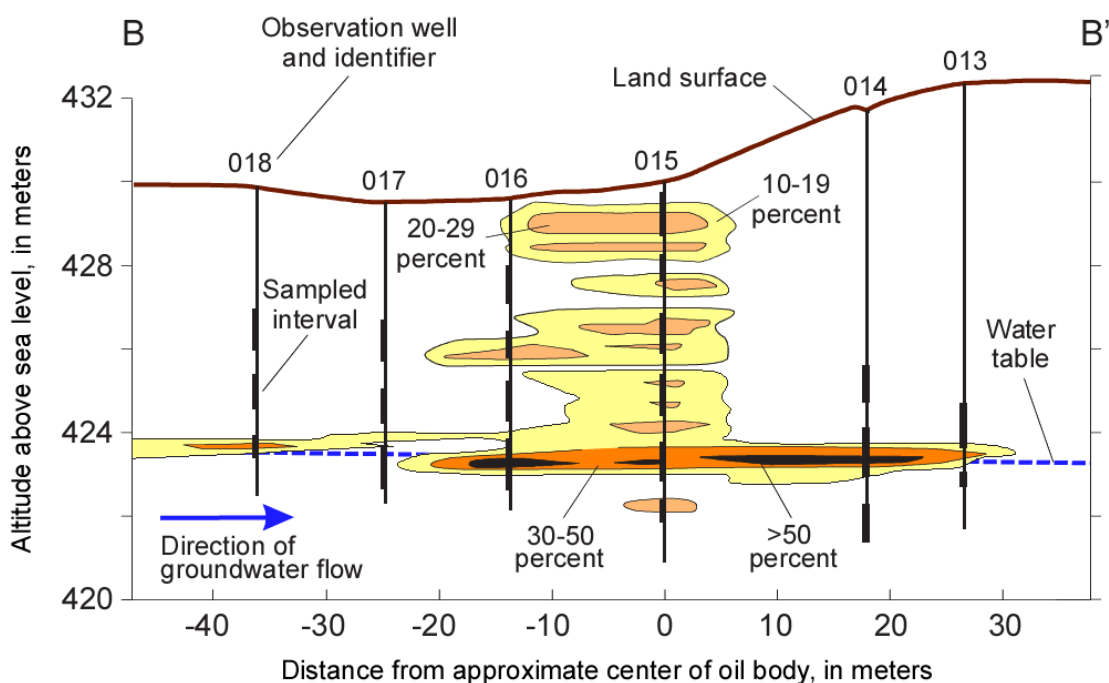
Figure 12.8 Oil saturation distribution in the North Oil Pool. On August 20, 1979, approximately 16 kilometers northwest of Bemidji, Minnesota, the land surface and shallow subsurface were contaminated when a crude-oil pipeline burst, spilling about 1,700,000 L (liters) (about 10,700 barrels) of crude oil onto a glacial outwash deposit. Oil movement was affected by sediment properties, and their variability, which has resulted in a complex distribution of oil in the subsurface at the North Oil Pool. Geostatistical analysis and multiphase-flow simulations have been used to explain how spatial variability affects the oil distribution (Dillard et al., 1997). As of 1996, the leading edge of the oil floating on the water table at the North oil pool had moved about 40 m downgradient of the spill site. Modified from Delin et al., 1998. USGS, in public domain.

Accumulations of LNAPL at or near the water table are susceptible to "smearing" from changes in water table elevation such as those that occur due to seasonal changes in recharge and discharge, or tidal influence in coastal environments. Mobile LNAPL floating on the water table will move vertically as the groundwater elevation fluctuates. As the water table rises or falls, LNAPL will be retained in the soil pores, leaving behind a residual

LNAPL "smear zone." If smearing occurs during a decline in groundwater elevations, residual LNAPL may be trapped below the water table when groundwater elevations rise. A similar situation may develop during product recovery efforts. LNAPL will flow toward a recovery well or trench in response to the gradient induced by water table depression. LNAPL residual will be retained below the water table as the water table elevation returns to pre-pumping conditions (Newell et al., 1995).

The major types of DNAPLs are halogenated solvents, coal tar, creosote-based wood-treating oils, PCBs, and pesticides. As a result of widespread production, transportation, utilization, and disposal practices, particularly since 1940s, there are numerous DNAPL contamination sites in North America and Europe. The potential for serious long-term contamination of groundwater by some DNAPL chemicals at many sites is high due to their toxicity, limited solubility (but much higher than drinking water limits), and significant migration potential in soil gas, in groundwater, and/or as a separate phase. DNAPL chemicals, especially chlorinated solvents, are among the most prevalent groundwater contaminants identified in groundwater supplies and at waste disposal sites (Cohen and Mercer, 1993).

Halogenated solvents, particularly chlorinated hydrocarbons, and brominated and fluorinated hydrocarbons, to a much lesser extent, are DNAPL chemicals encountered at numerous contaminated sites. These halocarbons are produced by replacing one or more hydrogen atoms with chlorine (or another halogen) in petrochemical precursors such as methane, ethane, ethene, propane, and benzene. Many bromocarbons and fluorocarbons are manufactured by reacting chlorinate hydrocarbon intermediates (such as chloroform or carbon tetrachloride) with bromine and fluorine compounds, respectively. DNAPL halocarbons at ambient environmental conditions include chlorination products of methane (methylene chloride, chloroform, and carbon tetrachloride), ethane (1,1-dichloroethane, 1,2-dichloroethane, 1,1,1-trichloroethane, and 1,1,2,2-tetrachloroethane), ethene (1,1-dichloroethene, 1,2-dichloroethene isomers, TCE, and tetrachloroethene), propane (1,2-dichloropropane and 1,3-dichloropropene isomers), and benzene (chlorobenzene, l,2-dichlorobenzene, and l,4-dichlorobenzene); fluorination products of methane and ethane such as 1,1,2-trichlorofluormethane (Freon-11) and 1,1,2-trichlorotrifluorethane (Freon-113); and bromination products of methane (bromochloromethane, dibromochloromethane, dibromodifluoromethane, and bromoform), ethane (bromoethane and 1,1,2,2-tetrabromoethane), ethene (ethylene dibromide), and propane (l,2-dibromo-3-chloropropane).

Coal tar and creosote are complex chemical mixture DNAPLs derived from the destructive distillation of coal in coke ovens and retorts. Historically, coal tar has been produced by coal tar distillation plants and as a by-product of manufactured gas plant and steel industry coking operations. Creosote blends are used to treat wood alone or diluted with coal tar, petroleum, or, to a very limited extent, pentachlorophenol. In addition to wood preservation, coal tar is used for road, roofing, and water-proofing solutions. Considerable use of coal tar is also made for fuels (Cohen and Mercer, 1993).

The compositions of creosote and coal tar are quite similar, although coal tar generally includes a light oil component (<5 percent of the total) consisting of monocyclic aromatic compounds such as BTEX. Consistent with the composition of creosote and coal tar, PAHs (in addition to BTEX compounds) are common contaminants detected in groundwater at wood-treating sites (Rosenfeld and Plumb, 1991; Cohen and Mercer, 1993).

PCBs are extremely stable, nonflammable, dense, and viscous liquids that are formed by substituting chlorine atoms for hydrogen atoms on a biphenyl (double benzene ring) molecule. PCBs, which are not produced any more in the United States and now have a very restricted regulated use, were historically used in oil-filled switches, electromagnets, voltage regulators, heat transfer media, fire retardants, hydraulic fluids, lubricants, plasticizers, carbonless copy paper, dedusting agents, and other products. PCBs were frequently mixed with carrier fluids prior

to use. Due to their widespread historic use and persistence, PCBs are often detected in the environment at very low concentrations. The potential for DNAPL migration is greatest at sites where PCBs were produced, utilized in manufacturing processes, stored, reprocessed, and/or disposed of in quantity (Cohen and Mercer, 1993).

DNAPLs can have great mobility in the subsurface because of their relatively low solubility, high density, and low viscosity. Hydrophobic DNAPLs do not readily mix with water (they are immiscible) and tend to remain as separate phases (i.e., nonaqueous). The relatively high density of these liquids provides a driving force that can carry product deep into aquifers. DNAPL infiltrating from the land surface because of a spill or leak may encounter two general conditions: (1) in the presence of moisture (water) within the vadose zone; DNAPL exhibits viscous fingering during infiltration (when a high-density, low-viscosity fluid (DNAPL) displaces a lower-density, higher-viscosity fluid (water), the flow is unstable, resulting in the occurrence of viscous fingering); and (2) if the vadose zone is dry, viscous fingering is generally not observed (Palmer and Johnson, 1989).
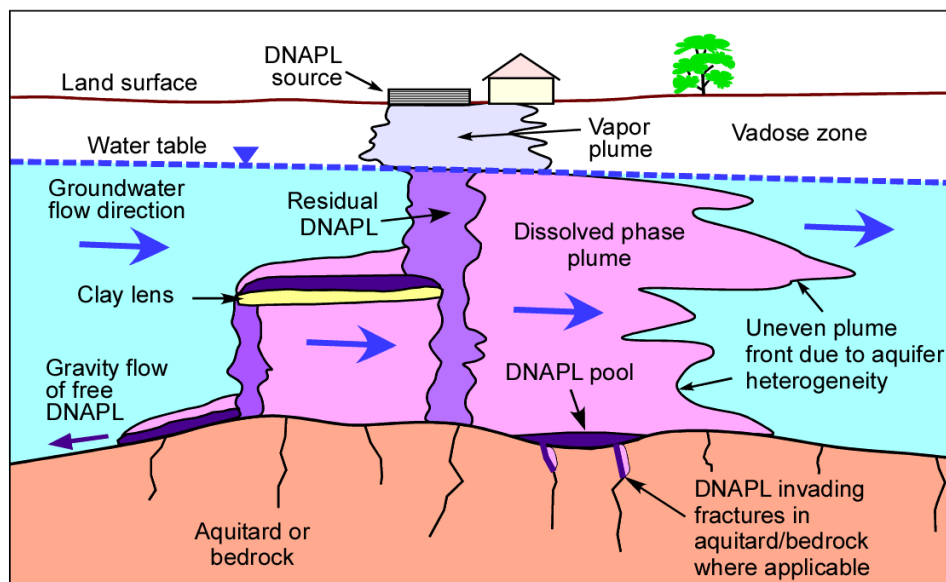
Figure 12.9 Schematic of possible migration pathways of free phase DNAPL and dissolved contaminant plumes in the subsurface. Modified from Kresic, 2007. Copyright CRC Taylor & Francis; permission required for further use.

When a spill of DNAPL is small, it will flow through the vadose zone until it reaches residual saturation, i.e., until all the mobile DNAPL is trapped in the porous media. This residual DNAPL may still cause formation of a dissolved plume in the underlying saturated zone (aquifer) by partitioning into the vapor phase; these dense vapors may sink to the capillary fringe where they are eventually dissolved in water and transported downgradient. Infiltrating water can also dissolve the residual DNAPL and transport it down to the water table.

Once DNAPL enters the saturated zone, its further migration will depend on the amount (mass) of product and the aquifer heterogeneity, such as the presence of low permeable lenses and layers of clay. Figure 12.9 shows examples of free phase (mobile) DNAPL accumulation over low-permeable layers. This free-phase (pooled) DNAPL serves as a continuing source of dissolved-phase contamination, which is carried downgradient by the flow of groundwater. As it migrates, the DNAPL may leave a residual phase in the porous media of the saturated (aquifer) zone along its path. This residual phase also serves as a source of dissolved-phase contamination. Being denser than water, free-phase DNAPL moves because of gravity, not because of the hydraulic gradients normally present in natural aquifers. Consequently, DNAPL encountering a low permeable layer may flow along its slope, in a different (including opposite) direction from the dissolved plume, as shown in Figure 12.9. This free-phase DNAPL would also create its own dissolved-phase plume. Migration of DNAPL in the unsaturated and saturated zones may create a rather complex pattern of multiple secondary sources of free and residual-phase DNAPL, and

multiple dissolved plumes at various depths within the aquifer. This pattern may not be definable based on the hydraulics of groundwater flow alone and, in any case, presents a great challenge when attempting to restore an aquifer to its beneficial use: "Once in the subsurface, it is difficult or impossible to recover all of the trapped residual" (U.S. EPA, 1992).

Two invaluable technical resources for the general study and characterization of DNAPLs in the subsurface are books by Cohen and Mercer (1993) and Pankow and Cherry (1996).

12.5 Metals and Metalloids

Because of their abundance at contaminated sites and potential toxicity to living organisms, the metals and metalloids of concern are aluminum, antimony, arsenic, barium, beryllium, cadmium, chromium, cobalt, copper, lead, manganese, mercury, molybdenum, nickel, selenium, silver, strontium, thallium, vanadium, and zinc. Phillips and Williams (1965) consider all of these elements to be metals, with the exception of arsenic and selenium, which are nonmetals. Webster's New World Dictionary (1970) defines a metal as an element that acts as a cation in chemical reactions, forms a base with the hydroxyl radical, and can replace the hydrogen of an acid to form a salt. Unlike the other elements listed, antimony, arsenic, molybdenum, selenium, and vanadium generally occur as oxyanions in waters and soils, and not as cations. These elements are sometimes described as metalloids (Langmuir et al., 2004).

While some metals are essential as nutrients, all metals can be toxic at some level including minute amounts. Impairments result when metals are biologically available at toxic concentrations affecting the survival, reproduction, and behavior of living organisms.

As emphasized by Langmuir et al. (2004), for reasons that may be unrelated to human activity, many surface waters and groundwaters contain natural concentrations of metals that exceed the U.S. EPA drinking water standards (Runnells et al., 1992). Soils can also contain naturally elevated levels of metals (McBride, 1994; Salminen and Tarvainen, 1997). When a regulatory decision is made to restore affected groundwaters or soils to a presumed earlier state, it is obviously unrealistic to assign cleanup goals that are below preexistent metal levels. It is therefore critically important to attempt to distinguish between metal amounts that were naturally present, and amounts added because of human activities.

Two concepts are important when assessing possible contamination with metals. The first is that of geochemical baseline (Salminen and Tarvainen, 1997; Salminen and Gregorauskiene, 2000), which may also be described as ambient concentration. This is the regional metal concentration in a medium, a concentration that has not been further increased by a local source of contamination. Baseline values may have been elevated by regional contamination. For example, arsenic concentrations in soils exceed 9 parts per million (ppm) in a 100-kilometer-wide, 1,000-kilometer-long belt that extends southwest from New York state across Pennsylvania, Ohio, and Kentucky (Gustavsson et al., 2001). There is evidence that these high arsenic values are chiefly derived from the burning of coal (Smith, 2003). An assessment of arsenic contamination of soils by a local source in this area would need to account for the high regional baseline values (Langmuir et al., 2004).

The second concept is that of background, which is the concentration of a metal in a medium as it existed before being affected by human activity. Background concentrations are a function of regional geology and local soil and sediment conditions. The metal background in soils also depends on the depth of the sampling (i.e., location within the soil profile) and whether the analysis is of the total soil or of a specific size fraction (Salminen and Tarvainen, 1997). Metal concentrations are generally higher in the fine-grained fraction of soils than in the coarse fraction

(sand fractions and medium/coarse silt fraction). It is important to note that baseline and background metal concentrations are not single values, but a distribution of values that can range over orders of magnitude over distances of a few centimeters in porous media and meters in surface waters (Gustavsson et al., 2001). It is also important to recognize that background metal concentrations can exceed environmental quality criteria at some sites (Langmuir et al., 2004).

Arguably the most defensible way to distinguish background or baseline concentrations and more elevated metal values in the groundwaters of a given area is to use statistical analysis. Cumulative probability plots can be drawn onto which all of the concentration data for a metal are plotted (Levinson et al., 1987; Fleischhauer and Korte, 1990). Such plots may allow the classification of samples into a background or baseline group and one or more contamination groups, with an estimate of the median and standard deviation for each group. Such a plot for Cd in groundwaters of Front Range of Colorado is shown in Figure 12.10 (Langmuir and Klusman, 1997).
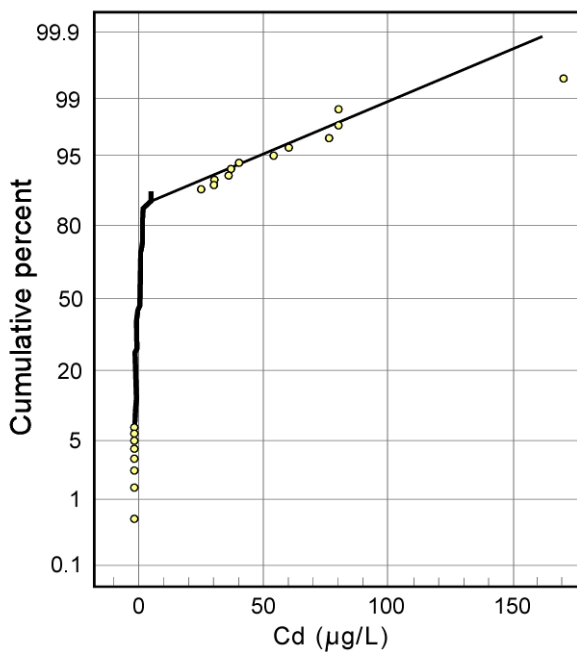
The mobility i.e., dissolution, sorption-desorption, and immobilization of metals is strongly dependent on pH and Eh conditions in the aquifer. If these conditions are changed from the natural equilibrium, for whatever reason, some metals that are naturally occurring in the aquifer porous media may dissolve into the groundwater or otherwise become mobile resulting in their elevated concentrations.

Figure 12.10 Cumulative percent plot of cadmium concentrations in Colorado Front Range ground waters. Cd concentrations in the 10^1–10^2 µg/L range are anomalously elevated. Concentrations below 10 µg/L are presumably background values. The linear trend of higher values can be derived from the data. Modified from Langmuir et al., 2004. U.S.EPA, in public domain.
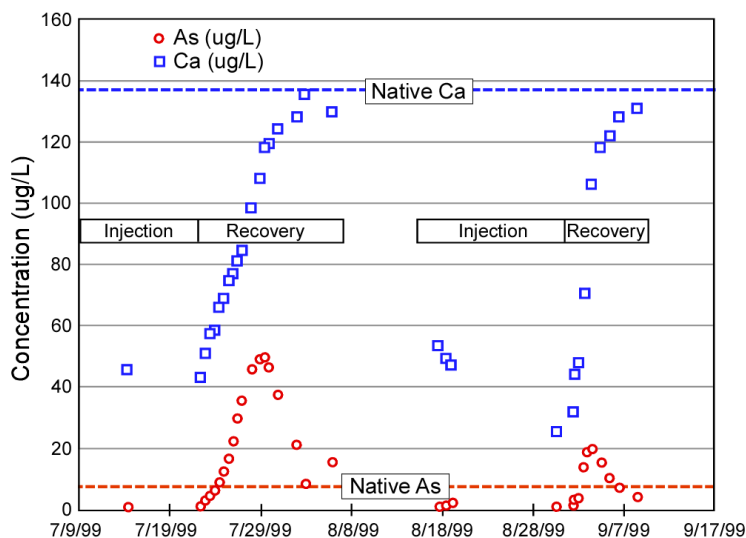
Figure 12.11 Punta Gorda, Florida ASR cycle tests: As and Ca distributions in pumped water. Modified from Arthur et al., 2002. Florida Geological Survey, in public domain.

284

When elevated concentrations of metals are associated with a contaminated site, it sometimes may be necessary to perform the so-called "alternative source evaluation" or ASE to evaluate if the source of metals is from the manufacturing and other above-ground practices at the site, or the metals are naturally occurring in the porous media underlying the site and may have been mobilized due to changed geochemical conditions.

For example, combined results from aquifer storage and recovery (ASR) cycle tests in Florida show that arsenic is mobilized from the aquifer system matrix into the injected waters, with peak concentrations exceeding 100 μg/L during some cycles. In the injected water and native aquifer water the concentration of As is less than 10 μg/L (see Figure 12.11).

Preliminary results indicate that these mobilization reactions take place on the order of days, perhaps hours. The main reason for the mobilization of arsenic from the minerals (e.g., pyrite) in the aquifer limestones is a much higher content of dissolved oxygen (DO) in the source (i.e., surface) waters for ASR than native groundwater. Once these waters are introduced into a reduced aquifer, selective leaching and/or mineral dissolution may release As and other metals into the injected water (Arthur et al., 2002).

Arsenic

Arsenic is widely distributed throughout the earth's crust, especially in minerals and ores that contain copper or lead. Natural arsenic in groundwater is largely the result of dissolved minerals from weathered rocks and soils. Principal ores of arsenic are sulfides (As_2S_3, As_4S_4, and FeAsS), which are almost invariably found with other metal sulfides. The hydrogen form of arsenic is arsine, a poisonous gas. Arsenic also forms oxide compounds.

Arsenic release from iron oxide appears to be the most common cause of widespread arsenic concentrations exceeding 10 μg/L in groundwater. This can occur in response to different geochemical conditions, including release of arsenic to groundwater through the reaction of iron oxide with either natural or anthropogenic (i.e., petroleum products) organic carbon. Iron oxide also can release arsenic to alkaline groundwater, such as that found in some felsic volcanic rocks and alkaline aquifers of the western United States. Sulfide minerals in rocks may act both as a source and as a sink for arsenic, depending on local geochemistry. In oxic (aerobic, oxygenated) water, dissolution of sulfide minerals, most notably pyrite and arsenopyrite, contributes arsenic to groundwater and surface water in many parts of the United States. Other common sulfide minerals, such as galena, sphalerite, marcasite, and chalcopyrite, can contain 1 percent or more arsenic as an impurity.

Dissolved arsenic in groundwater exists primarily as oxy anions with formal oxidation states of III and V. Either arsenate [As(V)] or arsenite [As(III)] can be the dominant inorganic form in groundwater. Arsenate generally is the dominant form in oxic waters with dissolved oxygen >1 mg/L. Arsenite dominates in reducing conditions, such as sulfidic (dissolved oxygen <1 mg/L with sulfide present) and methanic (methane present) waters. Aqueous and solid-water reactions, some of which are bacterially mediated, can oxidize or reduce aqueous arsenic. Both anions are capable of adsorbing to various subsurface materials, such as ferric oxides and clay particles. Ferric oxides are particularly important to arsenate fate and transport, as ferric oxides are abundant in the subsurface and arsenate strongly adsorbs to these surfaces in acidic to neutral waters. An increase in the pH to an alkaline condition may cause both arsenite and arsenate to desorb, and they are usually mobile in an alkaline environment (Dowdle et al., 1996; Harrington et al., 1998; Welch et al., 2000; U.S. EPA, 2022a). The toxicity and mobility of arsenic vary with its valency state and chemical form. As(III) is generally more toxic to humans and four to 10 times more soluble in water than As(V) (U.S. EPA, 1997).

Figure 12.12 Arsenic keratoses on the palms of a patient who ingested arsenic from a contaminated well over a prolonged period. Photo courtesy of Dr. Joseph Graziano.

The disease symptoms caused by chronic arsenic ingestion, arsenicosis, develop when arsenic-contaminated water is consumed for several years. Various physiological effects of arsenic exposure are described at the Agency for Toxic Substances and Disease Registry at https://www.atsdr.cdc.gov

Symptoms of poisoning may develop only after more than 10 years of exposure to arsenic, while it may take 20 years of exposure for some cancers to develop. Long-term ingestion of arsenic in water can first lead to problems with kidney and liver function, and then to damage of the internal organs including lungs, kidney, liver, and bladder. Arsenic can disrupt the peripheral vascular system leading to gangrene in the legs, known in some areas as black foot disease. This was one of the first reported symptoms of chronic arsenic poisoning observed in China (province of Taiwan) in the first half of twentieth century. A correlation between hypertension and arsenic in drinking water has also been established (Petrusevski et al., 2007).

Industrial products containing arsenic include lead-acid batteries, light-emitting diodes, paints, dyes, metals, pharmaceuticals, pesticides, herbicides, soaps, and semiconductors. Anthropogenic sources of arsenic in the environment include mining and smelting operations, agricultural applications, and disposal of wastes that contain arsenic (U.S. EPA, 2022a). Arsenic is a contaminant of concern at many remediation sites. Because arsenic readily changes valence states and reacts to form species with varying toxicity and mobility, effective treatment of arsenic can be challenging.

Chromium

Elemental chromium (Cr) is a transition group metal found naturally in rocks, soil, and living organisms. It occurs in combination with other elements as chromium salts, some of which are soluble in water. The pure metallic form does not occur naturally. Chromium can exist in several chemical forms with oxidation numbers ranging from –2 to +6. However, in the environment, it commonly exists in only two stable oxidation states, Cr(VI) and Cr(III), which have greatly contrasted toxicity and transport characteristics. Chromium speciation in the environment, particularly in groundwater, is affected primarily by Eh (oxidizing or reducing conditions) and pH (acidic or alkaline conditions). In general, hexavalent chromium, Cr(VI), predominates under oxidizing conditions, and trivalent chromium, Cr(III), predominates under more reducing conditions. It should be noted that the term hexavalent chromium is somewhat of a misnomer. This is because Cr(VI) is not present in the environment as a free cation (whereas several species of Cr(III) exist in the environment as cations). In fact, as all Cr(VI) species are oxides, they act like a divalent anion rather than a hexavalent cation (Kimbrough et al., 1999, from Stanin, 2005).

Chromium contamination of soil and groundwater is a significant problem worldwide. The extent of this problem is due primarily to its use in numerous industrial processes (i.e., metal plating and alloying, leather tanning,

wood treatment, chemical manufacturing), but also its natural presence in rocks enriched in chromium. Chromite ore ($FeCr_2O_4$) is the most important commercial ore associated with ultramafic and serpentine rocks. Chromium is also associated with other ore bodies (e.g., uranium and phosphorites) and may be found in tailings and other beneficiation wastes from mining operations where acid mine drainage can make the chromium available to the environment (U.S. EPA, 2022b). Compared to the results of contamination of soil and groundwater by industrial and mining practices, the naturally occurring concentrations of chromium in soil and groundwater are low, commonly less than 10 µg/L (Hem, 1989). However, rather high concentrations of naturally occurring hexavalent chromium, in the range between 100 and 200 µg/L, have been observed in uncontaminated groundwater in Paradise Valley north of Phoenix, Arizona (Robertson, 1975). Thus, both anthropogenic and natural sources of chromium can lead to locally elevated levels in soils and groundwaters.

The two different forms of chromium are quite different in their properties: charge, physiochemical characteristics, mobility in the environment, chemical and biochemical behavior, bioavailability, and toxicity. Most notably, Cr(III) is a trace element essential for the proper functioning of living organisms, whereas Cr(VI) exerts toxic effects on biological systems. In addition, the more toxic Cr(VI) compounds are generally more soluble, mobile, and bioavailable in the environment compared to Cr(III) compounds. Therefore, it is important to distinguish between the two forms of chromium rather than discussing this element as "total chromium".

Solubility can significantly limit the concentration of Cr(III) in groundwater at a pH above 4. The low solubility of the Cr(III) solid phases, Cr_2O_3 and $Cr(OH)_3$ (Hem, 1977), is likely the major reason why Cr(III) generally makes up a small percentage of the total chromium concentration in natural or contaminated groundwaters. Cr(III) tends to be essentially immobile in most groundwaters because of its low solubility (Calder, 1988). On the other hand, there are no significant solubility constraints on the concentrations of Cr(VI) in groundwater. The chromate, CrO_4^{2-} and dichromate, $Cr_2O_7^{2-}$ ions are water soluble at all pH. However, chromate can exist as a salt of a variety of divalent cations, such as Ba^{2+}, Sr^{2+}, Pb^{2+}, Zn^{2+}, and Cu^{2+}, and these salts have a wide range of solubilities. The rates of precipitation/dissolution reactions between chromate, dichromate anions, and these cations vary greatly and are pH dependent. An understanding of the dissolution reactions is particularly important for assessing the environmental effects of chromium because Cr(VI) often enters the environment by dissolution of chromate salts (Rai et al., 1987, from Stanin, 2005).

Cr(VI) can be transported considerable distances in groundwater due in part to its high solubility. For example, Hem (1989) cites an incident of shallow groundwater contamination by hexavalent chromium released from an industrial waste disposal pit in Long Island, New York, where Cr(VI) persisted in concentrations as high as 14 mg/L more than 3000 feet away from the original source, for more than 20 years after the release (Perlmutter et al., 1963). If, however, the transported Cr(VI) enters an area with relatively low Eh, it can be reduced readily to Cr(III) in the presence of organic matter, especially where pH is low. Cr(VI) can also be reduced by Fe(II) and dissolved sulfides (Stanin, 2005). Cr(III) generally is transported only short distances by groundwater because of its low solubility. If, however, the redox conditions along the transport pathway change from reducing to oxidizing, Cr(III) can be transformed to the more soluble Cr(VI). Under natural conditions, Cr(III) has been found to be oxidized to Cr(VI) by manganese (Bartlett and James, 1979).

12.6 Microbiological Contaminants

Microbiological contaminants are microorganisms potentially harmful to humans or animals. Jointly called pathogens, they include parasites, bacteria, and viruses. Pathogens are by far the most widely spread water contaminants. According to World Health Organization, some 829,000 people are estimated to die each year from

diarrhea as a result of unsafe drinking-water, sanitation and hand hygiene. Globally, at least 2 billion people use a drinking water source contaminated with feces, while about 368 million people obtain their water from unprotected wells and springs. Where proper sanitation facilities are lacking, waterborne diseases can spread rapidly (WHO, 2022).

Although surface water is the primary recipient and host of pathogen contamination, shallow groundwater is also greatly affected in many regions with poor or nonexistent sanitation. However, some pathogens, such as parasites *Giardia* and *Cryptosporidium*, are naturally present in surface water bodies and are not necessarily associated with poor sanitation practices. For this reason, the U.S. EPA has instituted specific water-treatment requirements for public supply systems using "groundwater under direct influence" (GWUI) of surface water.

The increased efforts to reclaim and reuse wastewaters and gray waters pose additional public health concerns. These concerns are heightened by the fact that the indicators of the "sanitary quality" of waters, i.e., the total- and fecal-coliform bacteria, are unreliable indicators of the presence of a number of key pathogenic agents including enteric viruses and cyst-forming protozoans. Wastewater reclamation does not have a specific meaning in terms of the degree of treatment for different reclamation projects. Some reuses of wastewater are allowed with very little additional treatment beyond the conventional sewage treatment, of addressing enteric viruses and cyst-forming protozoans.

Cryptosporidium (see photograph in Figure 12.13), which cannot be seen without a very powerful microscope, is a microscopic parasite that causes the diarrheal disease cryptosporidiosis. Both the parasite and the diarrheal disease are commonly known as "crypto." The infectious dose for crypto is less than 10 organisms and, presumably, one organism can initiate an infection. As late as 1976, it was not known to cause disease in humans. In 1993, 403,000 people in Milwaukee, Wisconsin, became ill with diarrhea after drinking water contaminated with the parasite, resulting in the largest waterborne disease outbreak ever documented in the United States (Tiemann, 1996). Crypto is still a leading cause of waterborne disease among humans in the United States (CDC, 2022). It is commonly found in lakes and rivers and drinking water and recreational water is the most common way to spread the parasite. Crypto is protected by an outer shell that allows it to survive outside the body for long periods of time and makes it very resistant to chlorine disinfection.
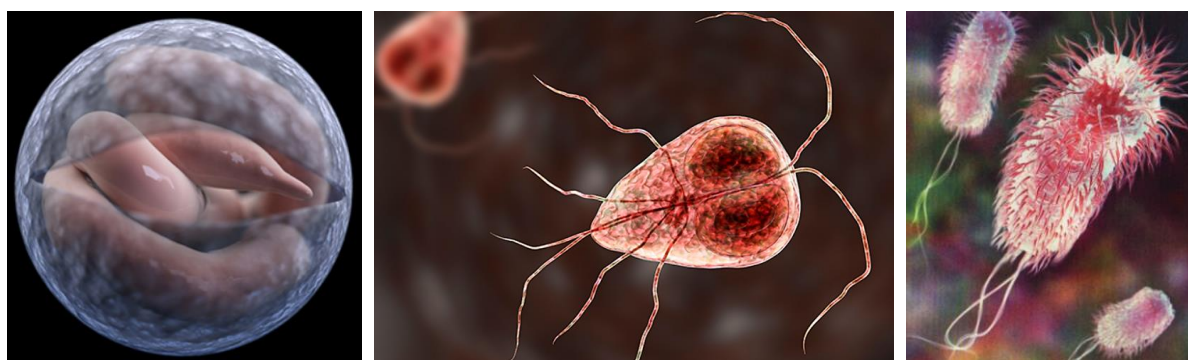
Figure 12.13 Parasites Cryptosporidium (left) and Giardia (center). Courtesy of Center for Disease Control (https://www.cdc.gov/parasites/). Right: Bacteria Escherichia coli or E. coli. Courtesy of USGS, in public domain.

Giardia (see photograph in Figure 12.13) was only recognized as a human pathogen capable of causing waterborne disease outbreaks in the late 1970s. It is found on surfaces or in soil, food, or water that has been contaminated with feces from infected people or animals. The parasite spreads easily including from person to

person and through contaminated water, food, surfaces, or objects. The most common way people get sick is by swallowing contaminated drinking water or recreational water (for example, lakes, rivers, or pools).

Giardia's occurrence in relatively pristine water as well as wastewater treatment plant effluent called into question water system definitions of "pristine" water sources. This parasite, now recognized as one of the most common causes of waterborne disease in humans in the United States, is found in every region of the U.S. and throughout the world. In 1995, outbreaks in Alaska and New York were caused by *Giardia*. The outbreak of giardiasis in Alaska affected 10 people and was associated with untreated surface water. The outbreak in New York affected an estimated 1,449 people and was associated with surface water that was both chlorinated and filtered. The symptoms of giardiasis include diarrhea, bloating, excessive gas, and malaise.

Viruses are among the smallest of the disease-causing microorganisms found in the aquatic environment. More than 120 different types of potentially harmful enteric viruses are excreted in human feces and are widely distributed in type and number in domestic sewage, agricultural wastes, and septic drainage systems (Gerba, 1988; from Banks and Batiggelli, 2002). Many of these viruses are stable in natural waters and have long survival times with half-lives ranging from weeks to months. Because they may cause disease even when just a few virus particles are ingested, low levels of environmental contamination may affect water consumers.

Outbreaks of waterborne disease attributed to enteric viruses are poorly documented, even though viruses are commonplace in natural waters contaminated with human feces. Illnesses in humans caused by waterborne viruses range from severe infections such as myocarditis, hepatitis, diabetes, and paralysis to relatively mild conditions such as self-limiting gastroenteritis. Currently, enteric viruses are included in the National Primary Drinking Water Standards issued by the U.S. EPA, while several other groups are on the contaminant candidate list (CCL). Studies of possible groundwater contamination with viruses are still very rare, but because of their presence on the CCL, and the new groundwater rule promulgated by U.S. EPA in 2006, the interest of the scientific community has increased.

In a nationwide study by the USGS, microbiological data were collected from 1,205 wells in 22 study units of the National Water-Quality Assessment (NAWQA) program during 1993 to 2004. The samples of untreated groundwater were analyzed primarily for concentrations of total-coliform bacteria, fecal-coliform bacteria, and *E. coli*, and for the presence of coliphage viruses (Embrey and Runkle, 2006). Nearly 30 percent of the analyzed wells tested positive for coliform bacteria. With at least one well in each study unit or principal aquifer testing positive, fecal-indicator bacteria were geographically widespread.

Generally, coliform bacteria were detected more frequently and in higher concentrations in wells completed in sandstone or shale, and in sedimentary, carbonate, and crystalline rocks than for wells in unconsolidated materials, in semiconsolidated sand, or in volcanic rocks. More than 50 percent of sampled wells completed in carbonate rocks (limestone and dolomite) or in crystalline rocks (schist and granite) tested positive for coliform bacteria. The Floridan, Piedmont and Blue Ridge, Ordovician, and Valley and Ridge aquifers, all of which had high detection rates or concentrations of coliform bacteria, are composed of these fractured and porous rocks. The lowest rates of detections (less than 5 percent) were for wells in the Basin and Range and Snake River aquifers. Materials in these aquifers are primarily unconsolidated sand, gravel, and clay, or basalt with interbeds of sand, gravel, or clay.

Escherichia coli or *E. coli* (photograph in Figure 12.13) is a type of fecal coliform bacteria that is commonly found in the intestines of warm-blooded organisms. Most *E.coli* strains are harmless, but some can cause serious food poisoning. *E. coli* in groundwater is a strong indicator of sewage or animal waste contamination.

12.7 Emerging Contaminants

As defined by the U.S. EPA (2022c), the drinking water Contaminant Candidate List (CCL) is a list of contaminants that are currently not subject to any proposed or promulgated national primary drinking water regulations but are known or anticipated to occur in public water systems. Contaminants listed on the CCL may require future regulation under the Safe Drinking Water Act (SDWA). Publishing the CCL does not impose any requirements on public water systems. If U.S. EPA decides to regulate a contaminant on the list in the future (as part of the regulatory determination process), the Agency will start a separate rulemaking process with opportunity for public comment. On July 19, 2021, U.S. EPA published the Draft Fifth CCL which includes 66 chemicals, three chemical groups (per- and polyfluoroalkyl substances (PFAS), cyanotoxins, and disinfection byproducts (DBPs)), and 12 microbes. These 66 candidates were selected from a universe of chemicals used in commerce, pesticides, biological toxins, disinfection byproducts, and waterborne pathogens (https://www.epa.gov/ccl/draft-ccl-5-chemicals).

The main difficulty with the entire process of drinking water regulation is that humanity now lives in a chemical universe created by our diverse activities. Literally hundreds of thousands of synthetic chemicals are being widely used in manufacturing and for various other purposes, with more than 1000 new ones introduced each year. In comparison, the U.S. EPA's CCL 5 list has 66 candidates under evaluation. It is simply not feasible, and it would certainly be cost prohibitive for any society, to engage in regulation of thousands of chemicals that may be present in water supplies at some minute concentrations, but of which is little known regarding their effects on human health and the environment at such low concentrations. Instead, it is likely that the entire field of water resources management will be forced to take a holistic approach where drinking water regulations will be an integral part of much broader environmental regulations, including those of the carbon cycle. Simple examples are the questions of water treatment and the cost of it, including the required energy: Is it better to "completely" treat the drinking water or the wastewater, no matter what, and how many chemical substances constitute the "complete" list? How do we estimate the true cost and benefits of our decisions with respect to the society and the environment?

Thanks to the widespread use of the Internet, the public around the globe is becoming increasingly informed about various environmental concerns almost instantaneously. Traditional media is following this trend by also publishing on the Internet. The result is an ever-increasing transparency when it comes to discussing the effects of environmental degradation on drinking water resources. The following quotes from an article published in the *Las Vegas Sun* illustrate this point and the role of media (October 20, 2006. *Chemicals cause changes in fish and raise concerns for humans*, by Launce Rake):

> *There's something wrong with the fish. It's been confounding scientists for years: Male fish are developing female sexual characteristics in Lake Mead and other freshwater sources around the country. On Thursday, the U.S. Geological Survey released a four-page summary of more than a decade of studies linking wastewater chemicals to those changes. But a scientist who has studied the issue for years complains that the report understates the danger of those toxins at Lake Mead and elsewhere. The researcher had aired his concerns seven months ago—shortly after he was fired by the USGS.*

> *The federal agency says the researcher was fired for failing to publish his data. The researcher says the federal agency wouldn't allow him to publish. Both sides, however, agree on the basic issue: In Lake Mead and in other freshwater sites, scientists have found traces of pharmaceuticals, pesticides, chemicals used in plastic manufacturing, artificial fragrances and other substances linked to changes in fish and animals. Thursday's report noted that the primary source for the chemicals in Lake Mead was the Las Vegas Wash, a man-made river made up almost entirely of treated wastewater from cities in the Las Vegas Valley.*

Gross said the problem is acute in Lake Mead and in other freshwater sites. One element left out of the Thursday report is evidence of sperm failure in fish, he said. "On a national scale we see alterations in fish," said the scientist, who continues to research hormone-disrupting chemicals in Florida and other states. "Endocrine (a hormone) disruption is widespread across the United States and is widespread in Lake Mead." Gross said his conclusions, shared by other researchers, are not popular: "The (Southern Nevada)Water Authority doesn't want to hear it. My agency doesn't want to hear it. The Department of Interior does not want to deal with it. They want to make the argument that there is nothing to worry about, but common sense just suggests it is not that simple."

Studies documenting sexual abnormalities in fish in the Potomac River—source of drinking water for millions in the Washington, D.C., area—raised similar concerns in September. Water officials there said the studies showed no evidence that drinking water was unsafe, but the studies did not answer the question on potential impacts to human health.

Notably, the new CCL 5 list published by the U.S. EPA in 2021 does not include any of the pharmaceutical and personal care products commonly referred to as PPCPs. This is a diverse group of chemicals comprising all human and veterinary drugs (available by prescription or over the counter, including the new genre of "biologics"), diagnostic agents (e.g., X-ray contrast media), "nutraceuticals" (bioactive food supplements such as huperzine A), and other consumer chemicals, such as fragrances (e.g., musks) and sunscreen agents (e.g., methylbenzylidene camphor); also included are "excipients," the so-called "inert" ingredients used in PPCP manufacturing and formulation (Daughton, 2007). Nanomaterials are an emerging subgroup of microcostituents considered by many as the next industrial wonder. They are already present in cosmetics, sunscreens, wrinkle-free clothing, and food products. Because of their small size, nanomaterials pose a challenge in terms of detection and treatment. Also because of their size they can enter all human organs including the brain, but very little is known of their fate and transport in the environment.

Only a subset of PPCPs, such as synthetic steroids, is known to be direct-acting endocrine disruptors. However, little is known about the individual and combined effects of long-term exposure to most PPCPs and their degradation products at very low concentrations. Some pharmaceuticals are not completely metabolized after consumption by humans or animals and are excreted in their original form, while others are transformed into different compounds (conjugates). Almost 20 percent of prescription drugs are flushed down the toilet unused, according to some estimates (Jeyanayagam, 2008). Domestic sewage is a major source of PPCPs, and concentrated animal feeding operations (CAFOs) are a major source of antibiotics and possibly steroids (Daughton, 2007).

Releases of PPCPs to the environment are likely to continue as the human population increases and ages; the pharmaceutical industry formulates new prescription and nonprescription drugs and promotes their use, and more wastewater is generated, which enters the hydrologic cycle and may impact groundwater resources (Masters et al., 2004).

In comparison, the U.S. EPA showed a relatively quick recent action in case of the "forever chemicals" (collectively referred to as PFAS) which became a household name over the last couple of years or so because of an increased coverage of the mainstream media (including likely effects of a Hollywood movie "Dark Waters" released in 2019.), and because of the scrutiny by the state and federal legislators pressured by their voters. The following explanation about the future "destiny" of the forever chemicals is provided by Heather Paul of Environmental Standards:

Beginning in 2023, public water systems will be required to monitor for 29 per- and polyfluoroalkyl substances (PFAS) and lithium in drinking water. The requirement is part of the fifth Unregulated Contaminant Monitoring Rule (UCMR5), which was published by the U.S. EPA on December 27, 2021. UCMR5 is just the latest revision to the UCMR, which allows the U.S. EPA to gather data about emerging drinking water contaminants. As part

of the Safe Drinking Water Act (SDWA), the U.S. EPA proposes a new list of up to 30 contaminants for monitoring every 5 years. The 5-year span covered by UCMR5 allows for planning in 2022, sample collection and analysis from 2023-2025, and data reporting in 2026. The U.S. EPA undergoes a multi-tiered process for selecting which contaminants will be monitored under each revision to UCMR. It starts by identifying contaminants expected to occur in drinking water systems nationally, which are not subject to regulation under the SDWA, and which have approved and validated drinking water analytical methods. The U.S. EPA also considers the degree of public concern, any critical health endpoints, and cost effectiveness of the applicable analytical methods, among other factors (Heather Paul, 2022. Revisions to the Unregulated Contaminant Monitoring Rule (UCMR). The Standard, September 2022, volume 39, Environmental Standards, www.envstd.com).

An "interim" destiny of PFAS can be inferred from the following statement by the U.S. EPA: "On August 26, 2022, EPA issued a proposal to designate two of the most widely used PFAS as hazardous substances under CERCLA, or Superfund. This rulemaking would increase transparency around releases of these harmful chemicals and help to hold polluters accountable for cleaning up their contamination." (https://www.epa.gov/pfas)

Lecture 13 Contaminant Fate and Transport. Groundwater Remediation

13.1 Contaminant Fate and Transport (F&T)

This lecture includes abbreviated and revised versions of the materials presented in Kresic (2007, 2009, 2013), Kresic and Mikszewski (2013), and U.S. EPA (2020).

Contaminants in the vadose and saturated zones are subject to various fate and transport processes, which govern their mobility and longevity (Figure 13.1). Contaminants can enter the subsurface dissolved in the infiltrating water or as immiscible liquids (NAPLs), which, in time, will also dissolve into the ambient vadose zone water and groundwater. Depending on the characteristics of the contaminant and the geochemical environment, the velocity of contaminant migration may be retarded with respect to groundwater velocity. This retardation (slowing down) of the contaminant can happen because it may sorb onto the soil (rock) particles and/or the organic matter present in the porous media, or because it may diffuse into the pore space of the solids and dead-end pores between the solids. The contaminant may also enter into various biogeochemical reactions with the native groundwater and solids, which can change its character and mobility. Irreversible precipitations from the solution (i.e., immobilization) or a complete degradation (mineralization of the organic contaminant) can permanently remove the contaminant from the flowing groundwater.

Unfortunately, predicting contaminant concentrations at some distance from the source and after a certain time of travel is often very difficult because of the various contaminant fate and transport (F&T) mechanisms, many (if not all) of which cannot be quantified exactly. It is, therefore, not uncommon for two or more parties ("stakeholders") to arrive at very different answers as to the expected (predicted) contaminant concentrations, using presumably the same conceptual site model. This fact is especially important when considering that most legal, engineering, and management decisions about contaminated groundwater are based on predicted contaminant concentrations, in both time and space. Some of the related questions include the following:

- When and how much contaminant were introduced into the subsurface?
- Who is responsible for groundwater contamination (whose plume is it)?
- How long would it take for the contaminant to reach point A?
- What will be the contaminant concentration when it reaches point A?
- Will this remedial technology reach the groundwater cleanup goal expressed as acceptable contaminant concentration at points A, B, C?
- How long will this remedial technology have to be implemented before cleanup goals are achieved?
- What will be the cost of implementing this remedial technology?
- What will be the life-cycle cost of this remedial alternative?
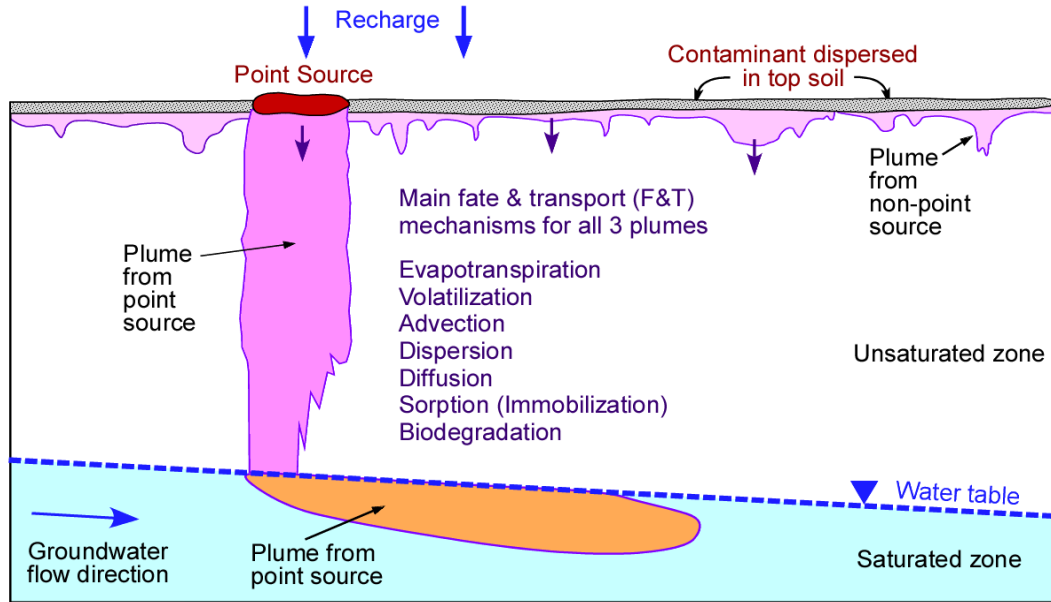
Figure 13.1 Migration of dissolved contaminants ("plumes") in vadose and saturated zones, and main fate and transport (F&T) mechanism affecting it.

In too many cases there are no unique quantitative answers to these and similar questions. This is probably the main reason why attorneys and courts are inevitable and often the most important players in resolving groundwater management and restoration issues, at least in the United States. Another possible explanation is that water resources and environmental regulations in the United States, as well as the societal framework, may not be conducive to a more holistic approach to management of water (groundwater) resources. In any case, selection of "representative" quantitative parameters used in calculations of contaminant fate and transport is not a straightforward process; it always leaves enough room for criticism by those willing to practice it. One obvious answer to this problem is to collect as much site-specific (field) information as possible.
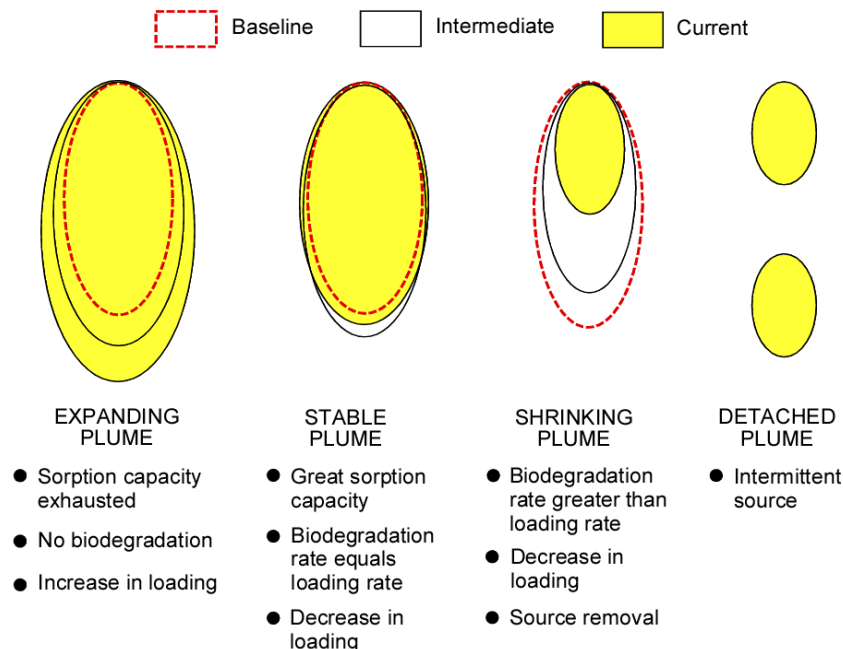
Figure 13.2 Influence of various fate and transport (F&T) processes on plume development; while most F&T processes may be present in any given case, the bullets list only those with possibly greatest net effect. Modified from U.S. EPA, 1977. In public domain.

294

After it has been subject to a variety of complex and rapid interactions in the source zone, the dissolved, mobile contaminant phase flowing away from the source is usually characterized by slower reactions and the flow system may be described as in (quasi)equilibrium for practical purposes.

Although this assumption helps to greatly simplify F&T calculations, it is not entirely correct because whenever the front of a moving contaminant plume encounters uncontaminated groundwater, the system enters into nonequilibrium conditions. Figure13.2 illustrates four main types of contaminant plumes with respect to various possible F&T processes influencing their development. Each plume type, expanding, stable, shrinking, and detached, is to a varying degree subject to all the F&T processes discussed further (the exception are constituents that do not biodegrade or volatilize, such as metals.)

13.1.1 Advection

Advection is transport of a contaminant dissolved in groundwater due to the flow of the groundwater itself. It refers to the average linear flow velocity of the bulk of contaminant, i.e., to the center of mass of the moving contaminant. As explained in the next section, some dissolved contaminant particles, just like some water particles, will move faster than the others, resulting in the longitudinal, transverse, and vertical spreading of the dissolved contaminant mass. This spreading, or contaminant dispersion, results in mixing of the contaminant with the native groundwater. However, the bulk of the dissolved contaminant will move with the average linear groundwater velocity (v_L), which is given as follows (see also Lecture 4.2 and Figure 4.23):

$$v_L = \frac{K \times i}{n_{ef}} \qquad (13.1)$$

where K = hydraulic conductivity, which has units of length per time (m/d; ft/d); i = hydraulic gradient (dimensionless); n_{ef} = effective porosity of the porous aquifer material (dimensionless)

All other things in a porous medium being equal (hydraulic gradient and hydraulic conductivity), a change in effective porosity will change the linear groundwater velocity through that medium (e.g., higher effective porosity will decrease the groundwater velocity). However, if effective porosity changes, this means that the porous material also changes, which then means that the hydraulic conductivity changes as well. Therefore, it is very important to understand that one cannot assume a change in effective porosity without considering the related change of the hydraulic conductivity. Because the hydraulic conductivity can change a couple of orders of magnitude for the seemingly same material, it is a much more "sensitive" parameter (i.e., it has a greater impact on the calculated velocity) than the effective porosity, which can only change within a limited range. However, changing the effective porosity by a factor of 2 will simply double or cut in half the time of travel. Finally, using the same effective porosity of, say 25 percent for "all" porous media at a site (e.g., silt, gravel, and clay), would be completely erroneous, regardless of the intended level of effort (e.g., "back-of-the-envelope" calculation).

The advection term of contaminant F&T, which translates to contaminant residence time between the source zone and the location of interest such as a receptor, is particularly important when considering contaminants that degrade. The longer groundwater resident times would result in a more significant decrease in the contaminant concentration, since more time will be available for its degradation before it reaches the receptor.

13.1.2 Dispersion

Dispersion is three-dimensional spreading of fluid particles as they flow through porous media. For a dissolved contaminant it is best described as a process of mixing between the impacted groundwater (plume) and clean groundwater being displaced by it. Dispersion always takes place, and the main result of this mixing is a decrease in concentration of the dissolved contaminant. Dispersion is specific to a porous medium and is considered independent of the flowing fluid. Following is one of the most illustrative discussions on dispersion and its use in hydrogeologic calculations, by Franke et al. (1990) of the USGS.

At the microscopic (pore) scale, velocity varies from a maximum along the centerline of each pore to zero along the pore walls, as shown in Figure 13.3a; both the centerline velocity and the velocity distribution differ in pores of different size. In addition, flow direction changes as the fluid moves through the tortuous paths of the interconnecting pore structure, as shown in Figure 13.3b. At a larger (macroscopic) scale, local heterogeneity in the aquifer causes both the magnitude and direction of velocity to vary as the flow concentrates along zones of greater permeability or diverges around pockets of lesser permeability. In this discussion, the term "macroscopic heterogeneity" is used to suggest variations in features large enough to be readily discernible in surface exposures or test wells, but too small to map (or to represent in a mathematical model) at the scale at which we are working. For example, in a typical problem involving transport away from a landfill or waste lagoon, macroscopic heterogeneities might range from the size of a baseball to the size of a building.
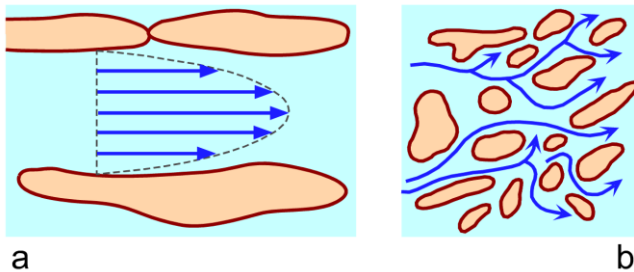
Figure 13.3 (a) Approximate fluid velocity distribution in a single pore. (b) Tortuous paths of fluid movement in an unconsolidated porous medium. From Franke et al., 1990. USGS, in public domain.

The pore-scale or microscopic velocity variations contribute only slightly to this overall dispersion; macroscopic variations contribute more significantly, whereas "mappable" variations generally have the largest effect.

If it were possible to generate a model or a computation that could account for all of the variations in velocity in natural aquifers, dispersive transport would not have to be considered (except for molecular diffusion); sufficiently detailed calculations of advective transport theoretically could duplicate the irregular tracer advance observed in the field. In practice, however, such calculations are impossible. Field data at the macroscopic scale never are available in sufficient detail, information at the "mappable" scale rarely is complete, and descriptions of microscopic scale variations are impossible except in a statistical sense. Even if complete data were available, however, an unreasonable computational effort would be required to define completely the natural velocity variations in an aquifer.

Although the phenomenon of dispersion has a physical explanation that is relatively easy to understand, the process itself cannot be feasibly measured in the field. There are not widely accepted or routinely applied methods of quantifying field-scale dispersion, and there are still very few credible large-scale field experiments that can help in better understanding dispersion in heterogeneous porous media. It has been argued that defining the actual field

distribution of hydraulic conductivity and its anisotropy to a satisfactory level of detail would eliminate the need for quantifying yet another uncertain parameter such as dispersion. However, it is apparent that in many cases it would also not be feasible to determine distribution of the hydraulic conductivity and effective porosity (and therefore the velocity field) with very fine resolution, particularly in cases of large travel distances. It is for this reason that the dispersion is explicitly included, through surrogate parameters, in common equations of contaminant fate and transport, in an attempt to somehow account for deviations from the average linear (advective) flow velocity.

In a narrower sense, scientists and engineers define dispersion as the sum of two processes: *mechanical dispersion* and *diffusion*. Defined in this way, dispersion is often called *hydrodynamic dispersion* (D_x) and, for the main direction of groundwater flow (in X direction), it is given as:

$$D_x = \alpha_x v_x + D_e \qquad (13.2)$$

where α_x is longitudinal dispersivity, in dimension of length (meters or feet); v_x is linear groundwater velocity (ft/d; m/d); D_e is coefficient of effective diffusion (cm^2/s), described in next section.

Mixing due to mechanical dispersion occurs along the main direction of groundwater flow (this is called *longitudinal dispersion*), as well as perpendicular to the main flow direction (*transverse dispersion*). There is also a third main direction of mixing called *vertical dispersion*. Dispersion causes some solute particles to advance faster that the bulk of contamination, thus creating a hallo ("cloud") of low concentrations around the main portion of the plume. For the purposes of quantifying the effects of three-dimensional dispersion along the main direction of groundwater flow, the following equations relating linear groundwater velocity (*v*) and parameter called *dispersivity* (α) are used in practice:

$$D_L = \alpha_L \times v_x \qquad D_T = \alpha_T \times v_x \qquad D_V = \alpha_V \times v_x \qquad (13.3)$$

Where D_L, D_T, and D_V are longitudinal, transverse and vertical (mechanical) *dispersion* respectively, and α_L, α_T, and α_V are longitudinal, transverse and vertical dispersivity respectively. Dispersivity has unit of length. There is a general practice to use transverse dispersivity 10 times smaller than the longitudinal dispersivity, and the vertical dispersivity one to two orders of magnitude smaller than the longitudinal dispersivity.

Most researchers and practitioners, as well as government agencies such as U.S. EPA (e.g., see Wiedemeier et al., 1998, and Aziz et al., 2000), have concluded that the dispersion is dependent on the length of solute flow being observed: the greater the plume length, the larger the value of longitudinal dispersivity. There are still discussions regarding the nature of this relationship (e.g., is it linear or non-linear, is there a practical limit after which the dispersion stabilizes and does not increase with the increasing plume length) but there is a general agreement that dispersion depends on both the scale and the time of flow.

Figure 13.4 is an example of an experimental dispersivity graph cited and utilized widely, and indiscriminately (note the wide scatter of data and the data reliability indication). A rule of thumb, suggested by the U.S. EPA, is that the longitudinal dispersivity could be initially estimated from the plume length as being 10 times smaller (Wiedemeier et al., 1998; Aziz et al., 2000). This means that, for example, if the plume length is 300 feet, the initial estimate of the longitudinal dispersivity is about 30 feet. There are also other suggested empirical relationships relating the plume length and the longitudinal dispersivity such as that of Xu and Eckstein (1995; see Figure 13.4). Recognizing the limitations of the available and reliable field-scale data on dispersivity, the Agency also suggests

that the final values of dispersivities used in F&T calculations should be based on calibration to the site-specific (field) concentration data. The main reason why very few (if any) projects for practical groundwater remediation purposes consider field determinations of dispersivity, is that it would require many monitoring wells and application of large-scale tracer tests. Such studies are expensive by default and are usually not feasible due to generally slow movement of tracers in intergranular porous media over long distances.

Unfortunately, dispersion remains one of the more uncertain and unquantifiable fate and transport processes, posing a significant challenge to both the practitioners and the legal community (courts), in trying to find the most appropriate ways of incorporating it into predictive fate and transport models.
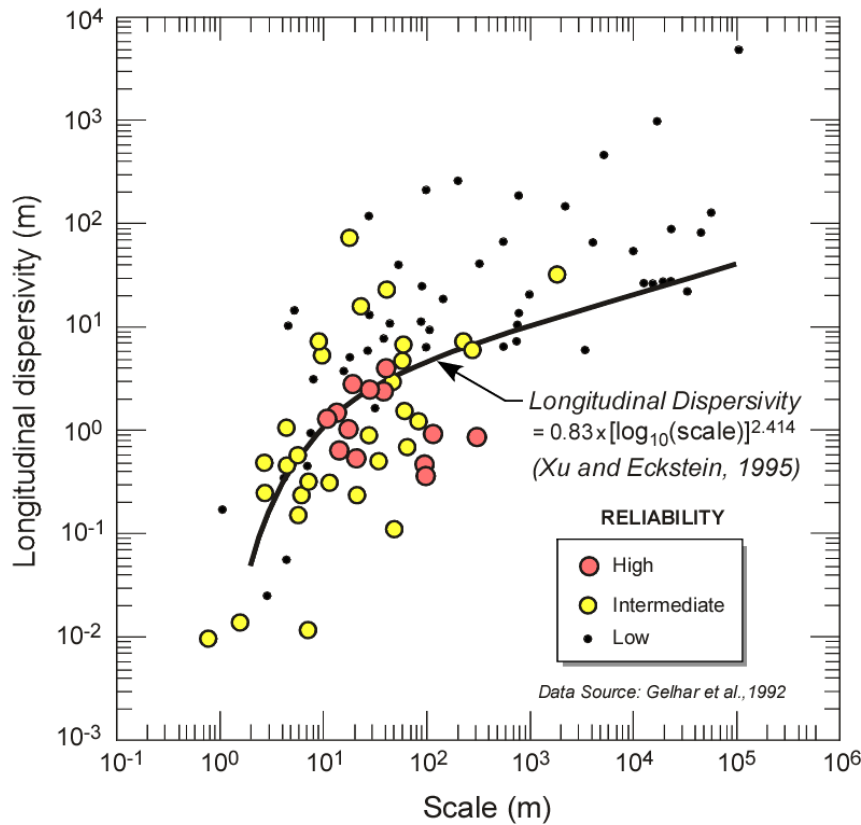
Figure 13.4 Longitudinal dispersivity versus scale data reported by Gelhar et al. (1992). Size and color of circle represent general reliability of dispersivity estimates. High reliability data are accurate within a factor of about 2 or 3. Graph modified from Aziz et al., 2000. U.S. EPA, in public domain.

Selecting a "representative" value of longitudinal dispersivity and then applying it to predictive models of contaminant fate and transport is a rather subjective process. Modeling should, therefore, include a thorough sensitivity analysis of this parameter, with the understanding that "*more emphasis should be placed on field study and the accurate determination of hydraulic conductivity variations and other non-homogeneities and less on incorporating somewhat arbitrary dispersion coefficients into complex mathematical models*" (Molz et al., 1983).

13.1.3 Diffusion

When the groundwater velocity becomes very low, due to small pore sizes and very convoluted pore-scale pathways, diffusion may become an important fate and transport process. Porosity that does not readily allow advective groundwater flow (flow under the influence of gravity) but does allow movement of the contaminant due to diffusion, is sometimes called diffusive porosity. Dual-porosity medium has one type of porosity that allows preferable advective transport through it; it also has another type of porosity where free gravity flow is significantly smaller than the flow taking place through the higher effective (advective) porosity. Examples of dual-porosity media include fractured rock, where advective flow takes place preferably through fractures, while the advective flow rate through the rest of the rock mass, or rock matrix, is comparably lower, is much lower, or absent for

practical purposes. This gradation depends on the nature of matrix porosity; in some rocks such as sandstones and young limestones, matrix porosity may be high and it may allow a significant rate of advective flow, often as high as or higher than through the fractures. In most hard rocks however, matrix porosity is usually low, often less than 5 percent, and it does not provide for significant advective flow. Other examples of dual-porosity media include fractured clay and residuum sediments. In some cases, various discontinuities and fractures in such media may serve as pathways for advective contaminant transport, while the bulk of the sediments may have a high overall matrix porosity and low effective porosity where advective transport is slow. Flow of solutes with high concentration through the fractures may result in the solute diffusion into the surrounding matrix.

Diffusion is defined as movement of a contaminant from higher concentration toward lower concentration solely due to concentration gradients; it does not involve "bulk," free-gravity movement of water particles (as in case of advection and dispersion). The contaminant will move as long as there is a concentration gradient, including when these gradient reverses, such as when fractures are flushed out by clean groundwater and the contaminant starts to move from the invaded rock matrix back into the fractures (the so-called back-diffusion).

The rate of diffusion for different chemicals (solutes) in water depends on the concentration gradient and the coefficient of diffusion, which is solute specific (different solutes have different coefficients of diffusion). The diffusion coefficients for electrolytes, such as major ions in groundwater (Ca^{2+}, Mg^{2+}, Na^+, K^+, HCO_3^-, Cl^-, and SO_4^{2-}) range between 1×10^{-9} and 2×10^{-9} m^2/s at 25∘C (Robinson and Stokes, 1965; from Freeze and Cherry, 1979). Coefficient of diffusion is temperature dependent and decreases with the decreasing temperature (e.g., at 5°C these coefficients are about 50 percent smaller than at 25°C). Table 13.1 lists aqueous diffusion coefficients for some common organic contaminants.

Table 13.1 Aqueous diffusion coefficients (D_0) for some common organic chemicals
From Cohen and Mercer, 1993; and Pankow and Cherry, 1996.

Chemical	Water diffusion coefficient (cm²/s)	Chemical	Water diffusion coefficient (cm²/s)
Benzene	1.0 E-5	1,1-Dichloroethene	9.5 E-6
Ethylbenzene	8.3 E-6	trans-1,1-Dichloroethene	9.5 E-6
Toluene	9.0 E-6	Dichloromethane	9.1 E-6
Xylenes	8.4 E-6	Methylene chloride	1.1 E-6
Carbon tetrachloride	7.1 E-6	Nitrobenzene	7.6 E-6
Carbon disulfide	1.1 E-5	Trichloroethene (TCE)	1.0 E-5
Chlorobenzene	7.9 E-6	Tetrachloroethylene (PCE)	1.0 E-6
Chloroform	9.1 E-6	1,1,1-Trichloroethane	9.4 E-6

In porous aquifer materials, the apparent diffusion coefficients are smaller than in free water. This is because solute molecules (or ions) have to travel longer paths due to solid particles in the soil, which act as obstacles. These convoluted paths of travel are described with term *tortuosity*. The apparent effective diffusion coefficient is therefore used to calculate rate of solute diffusion in the subsurface, rather than the aqueous phase diffusion coefficient. The effective diffusion coefficient (D_e) can be determined by using the known (experimentally determined) tortuosity of the porous media (rock) in question, or by multiplying the *aqueous diffusion coefficient*

(D_0) with an empirical coefficient, called *apparent tortuosity factor* (τ), which can range between zero and 1. This empirical coefficient is related to the aqueous (D_0) and effective (D_e) diffusions, and the rock matrix porosity (θ_m) through the following expression (Parker et al., from Pankow and Cherry, 1996):

$$\frac{D_e}{D_0} = \tau \cong \theta_m^p \qquad (13.4)$$

where the exponent *p* varies between 1.3 to 5.4 depending on the type of porous geologic medium. Low porosity values result in small τ values and low D_e values.

Laboratory studies of non-adsorbing solutes show that apparent tortuosity usually has values between 0.5 and 0.01. For example, for generic clay τ is estimated at 0.33, for shale/sandstone it is 0.10, and for granite it is quite small: 0.06 (Parker et al., from Pankow and Cherry, 1996).

Concentration profile of a non-sorbing solute in subsurface, moving only due to diffusion and in one direction (*x*) from the high-concentration layer into the zero-concentration layer, can be analytically calculated for various times (*t*) based on Fick's Second Law using Crank's equation (Freeze and Cherry, 1979):

$$C_i(x, t) = C_0 \; erfc \times \left(\frac{x}{2} \times \sqrt{D_e t} \right) \qquad (13.5)$$

where C_0 is the initial concentration on the high-concentration side of the contact between two layers, and *erfc* is complimentary error function.

13.1.4 Sorption and Immobilization

Sorption is the general term that describes immobilization of the contaminant particles by the porous media, regardless of the actual mechanism. It may be the result of various more specific processes caused by geochemical interactions between the solids and the dissolved contaminant. Cation exchange would be one example of sorption where the contaminant is immobilized by the mineral (usually clay) surfaces. This immobilization may not be permanent, and the contaminant may be released back into the water solution by the reverse process when geochemical conditions in the aquifer change (e.g., change of pH or inflow of another chemical species with the greater affinity for cation exchange with the mineral surfaces).

Sorption results in distribution of a solute between the solution (groundwater where it is dissolved) and the solid phase (where it is held by the solids of the aquifer). This distribution is called *partitioning* and it is quantitatively described with the term *distribution coefficient* (or adsorption coefficient, or partition coefficient), and denoted with K_d. Importantly, K_d is a generic term devoid of any particular mechanism. It is used to describe the general partitioning of aqueous phase constituents to a solid phase due to sorption.

Because of sorption, the contaminant movement in groundwater is slowed down relative to the average groundwater velocity. This effect of sorption is called *retardation*, and the affinity of different solutes(chemicals dissolved in groundwater) to be retarded is quantified with a parameter called *retardation factor*, denoted with R. The overall effect of sorption is decrease in dissolved contaminant concentration.

When a contaminant is associated with the solid phase, it is not immediately apparent if it was <u>ad</u>sorbed on to the surface of a solid, <u>ab</u>sorbed into the structure of a solid, precipitated as a 3-dimensional molecular structure on the surface of the solid, or partitioned into the organic matter (Sposito, 2016).

Adsorption is a term often used to describe a process of contaminant particles (molecules) "sticking" to aquifer materials simply because of the affinity for each other. For example, many hydrophobic organic contaminants are adsorbed onto particles of organic carbon present in the aquifer and can be desorbed if conditions change. Adsorption is commonly used interchangeably with sorption, a more generic term, which often causes confusion. *Absorption*, a rather vague term, usually refers to contaminant incorporation "deep" into the solid particle structure, and it has chemical connotation. The term, however, is seldom used since its net effect would be equal to a permanent removal from the flow system (unless, of course, enough investigation data is available to confirm that is the case.)

Dissolution and precipitation are more likely to be the key processes where chemical nonequilibium exists, such as at a point source, an area where high contaminant concentrations exist, or where steep pH or redox gradients exist. Adsorption and desorption will likely be the key processes controlling contaminant migration in areas where chemical equilibrium exists, such as in areas far from the point source.

The distribution coefficient, K_d, is defined as the ratio of the contaminant concentration associated with the solid (C_s) to the contaminant concentration in the surrounding aqueous solution (C_w) when the system is at equilibrium:

$$K_d = \frac{C_s}{C_w} \qquad (13.6)$$

Retardation due to sorption, R, is defined as:

$$R = \frac{v_w}{v_c} \qquad (13.7)$$

where v_w is linear velocity of groundwater through a control volume; v_c is velocity of contaminant through a control volume. If the contaminant is sorbed (retarded), the retardation coefficient, R, will be greater than 1. It is usually calculated using the following equation

$$R = 1 + \frac{\rho_b \times K_d}{n} \qquad (13.8)$$

where ρ_b is bulk density of aquifer porous media (mass/length^3); K_d is distribution coefficient (length^3/mass); n is porosity of the media at saturation (dimensionless). This equation can also be written as

$$R = 1 + \left(\frac{1-n}{n}\right) \rho_s \times K_d \qquad (13.9)$$

where ρ_s is the particle density of porous media (mass/length^3), which is often assumed to be 2.65 g/cm^3 for most mineral soils (in the absence of actual site-specific information).

The sorption retardation term does not equal unity when the solute interacts with the soil; almost always the retardation term is greater than 1 due to solute sorption to soils, except in the cases of ideal chemical tracers such as chloride or tritium. Rarely, the retardation factor is less than 1, and such circumstances are thought to be caused by anion exclusion (USEPA, 1999a, 1999b).

The relationship between the concentration of chemical sorbed onto solid surfaces (C_s) and the concentration remaining in aqueous solution (C_w) at equilibrium is referred to as the sorption isotherm because laboratory

experiments for determining distribution coefficient values are performed at constant temperature. Sorption isotherms generally exhibit one of three characteristic shapes, depending on the sorption mechanism. These isotherms are referred to as the Langmuir isotherm, the Freundlich isotherm, and the linear isotherm, which is a special case of the Freundlich isotherm (Figure 13.5). The Langmuir isotherm model describes sorption in solute transport systems in which the sorbed concentration increases linearly with increasing solute concentration at low concentrations and approaches a constant value at high concentrations (experimental line flattens out). The sorbed concentration approaches a constant value because there are a limited number of sites on the aquifer matrix available for contaminant sorption. The Langmuir equation is described mathematically as follows (Devinny et al., 1990; from Wiedemeier et al., 1998):

$$C_s = \frac{KC_w b}{1 + KC_w} \qquad\qquad (13.10)$$

where C_s is sorbed contaminant concentration (mass contaminant/mass soil); K is equilibrium constant for the sorption reaction (µg/g); C_w is dissolved contaminant concentration (µg/mL); b is maximum sorptive capacity of the solid surface.
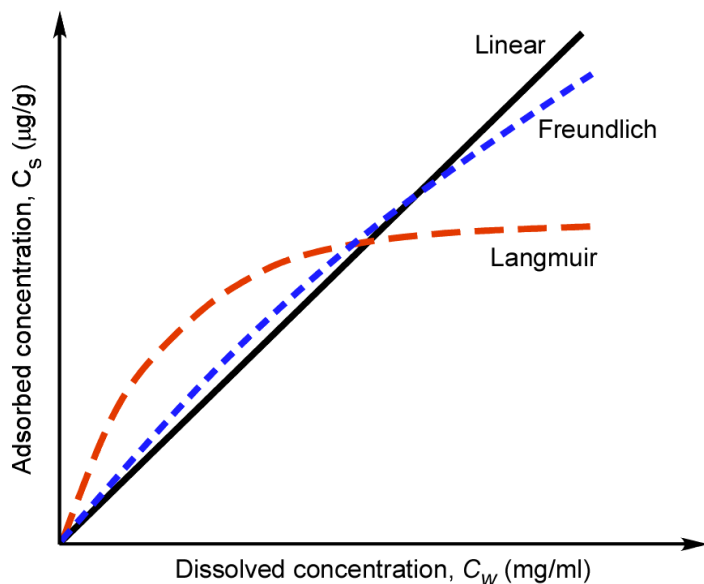
Figure 13.6 Sorption isotherms Modified from Kresic, 2009. Copyright McGraw Hill; permission required for further use.

The Langmuir isotherm model is appropriate for highly specific sorption mechanisms where there are a limited number of sorption sites. This model predicts a rapid increase in the amount of sorbed contaminant as contaminant concentrations increase in a previously pristine area. As sorption sites become filled, the amount of sorbed contaminant reaches a maximum level equal to the number of sorption sites, b.

The Freundlich isotherm is a modification of the Langmuir isotherm model in cases when the number of sorption sites is large (assumed infinite) relative to the number of contaminant molecules. This is generally a valid assumption for dilute solutions (e.g., downgradient from a petroleum hydrocarbon spill in the dissolved BTEX plume) where the number of unoccupied sorption sites is large relative to contaminant concentrations. The Freundlich isotherm is expressed mathematically as (Devinny et al., 1990, modified from Wiedemeier et al., 1998):

$$C_s = K_d C_w^n \qquad (13.11)$$

where K_d is distribution coefficient; C_s is sorbed contaminant concentration (mass contaminant/mass soil, mg/g); C_w is dissolved concentration (mass contaminant/volume solution, (mg/ml); n is chemical-specific coefficient. The value of n in this equation is a chemical-specific quantity that is determined experimentally. Values of n typically range from 0.7 to 1.1 but may be as low as 0.3 and as high as 1.7 (Lyman et al., 1992).

The simplest expression of equilibrium sorption is the linear sorption isotherm, a special form of the Freundlich isotherm that occurs when the value of n is 1. The linear isotherm is valid for a dissolved species that is present at a concentration less than one half of its solubility (Lyman et al., 1992). For example, this is a valid assumption for BTEX compounds partitioning from fuel mixtures into groundwater. Dissolved BTEX concentrations resulting from this type of partitioning are significantly less than the pure compound's solubility in pure water.

The linear sorption isotherm is expressed as follows (Jury et al., 1991; from Wiedemeier et al., 1998):

$$C_s = K_d C_w \qquad (13.12)$$

where the notification is the same as in Eq. (13.11). Distribution coefficient K_d is the slope of the linear isotherm plotted using experimental laboratory data.

Adsorption of dissolved contaminants is very dependent on pH. Because adsorption of anions is coupled with a release of OH^- ions, anion adsorption is greatest at low pH and decreases with increasing pH. Adsorption of cations is coupled with a release of H^+ ions, such that cation adsorption is greatest at high pH and decreases with deceasing pH (see Figure 13.7). It should be noted that some contaminants may be present as dissolved cations or anions depending on geochemical conditions (U.S. EPA, 1999a).
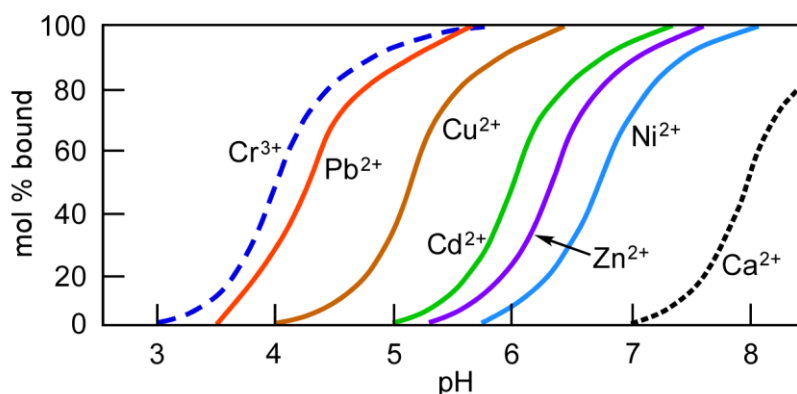
Figure 13.7 Example of adsorption of various metal cations and oxyanions, each at 5×10^{-7} M, by ferrihydrite (sum of Fe[III] is 10^{-3} M). There are 2×10^{-4} M of reactive sites on the oxyhydroxide. The dashed curves are calculated. After Stumm, 1992; from Langmuir et al, 2004. U/.S. EPA, in public domain.

Importantly, as discussed by Langmuir et al. (2004) "The application of single partition coefficient values for individual metals should be limited to regional and national scale studies where accuracy is not required, and bounding or representative values are adequate. Metal partition coefficients can vary by several orders of magnitude over short distances (meters or less) in porous media because of changes not only in pH, but also in metal complex formation, metal adsorption competition, the solid/solution ratio, the relative abundances, the surface areas, and the surface charge densities of the different metal-sorbing phases."

Similarly, as discussed by the U.S. EPA (1999a), soil and geochemists knowledgeable of sorption processes in natural environments have long known that generic or default K_d values can result in significant error when used

to predict the absolute impacts of contaminant migration or site-remediation options. Therefore, for site-specific calculations, K_d values measured at site-specific conditions are essential. The general methods used to measure K_d values include the laboratory batch method, *in-situ* batch method, laboratory flow-through (or column) method, field modeling method, and K_{oc} method for organic solutes (see next section). The advantages, disadvantages, and, perhaps more importantly, the underlying assumptions of each method are summarized in a two-volume reference text (U.S. EPA, 1999a,b), which also includes a conceptual overview of geochemical modeling calculations and computer codes as they pertain to evaluating K_d values and modeling of adsorption processes.

13.1.4.1 Sorption of Organic Solutes

Organic solutes tend to preferably adsorb onto organic carbon present in the aquifer porous media. This organic carbon in the soil is of various forms – as discrete solids, as films on individual soil grains, or as stringers of organic material in soil grains. Distribution coefficient (K_d) can be calculated for different organic solutes based on fraction soil organic carbon contents (f_{oc}) and partition coefficient with respect to the soil organic carbon (K_{oc}), using the following equation:

$$K_d = f_{oc} \cdot K_{oc} \qquad (13.13)$$

For various reasons (including time needed and the expense) practitioners often forgo site-specific determination of K_d and will instead calculate K_d using published K_{oc} values. However, as discussed by Gurr (2008; from Kresic, 2009), regulatory agencies, researchers, and practitioners alike are far from united around standard K_{oc} values for nonpolar organics, even for well-studied contaminants. It is easy to find multiple K_{oc} values for a single contaminant that vary by orders of magnitude. And when one considers that these values are often reported as log K_{oc}, small variations in the reported log value can translate into decades when the retardation factor is used to determine contaminant migration time periods.

For example, on the U.S. EPA's website *Environmental Modeling Community of Practice, On-line Tools for Site Assessment Calculation* (https://www3.epa.gov/ceampubl/learn2model/part-two/onsite/retard.html) there are a few "databases" offered for selection of certain F&T parameters needed to calculate the coefficient of retardation R using Equation (13.8). Based on the database selection made, K_{oc} value for TCE can vary anywhere between 94 L/kg and 166 L/kg (R=2.3). If all other parameters in Equation (13.8) are equal, this translates to the calculated R value of 1.7 and 2.3 respectively.

For PCE, this range is even wider: 79 L/kg (R=1.6) to 661 L/kg (R=6.3). Presumably, all the available values are endorsed by the U.S. EPA since there is no guidance which one is "more accurate" than another.

The range in measured K_{oc} values is understandable since sorption to natural organic matter is an inherently complicated process. In addition to inevitable laboratory errors and use of non-standard laboratory procedures, the differences in the measured K_{oc} values can be explained by natural organic carbon chemistry which can vary substantially from one soil to the next. Nonpolar organics can also sorb to organic carbon still dissolved in the aqueous phase, and to colloids suspended in the water. If these factors are not accounted for in the experimental method, the measured K_{oc} value may be skewed (Schwarzenbach, 2003).

While measuring K_{oc} values can be difficult and error-prone, the simplicity of calculating partitioning from K_{oc} is attractive and easy to understand, and thus is not likely to soon be replaced with another method. Given such diversity in quality and result, attempting to systematically choose reliable values from either published databases

or calculated values is a much more responsible approach than choosing a number at random from published sources (Gurr, 2008, from Kresic, 2009).

The octanol-water partition coefficient (K_{oc}) is a much easier value to measure experimentally compared to K_{oc}. The simple process of allowing a chemical to reach equilibrium concentrations in a mixture of pure octanol and pure water was developed by the pharmaceutical industry to estimate the lipophilicity of pharmaceuticals. Environmental chemists have adopted this value to estimate hydrophobicity of organic contaminants (Schwarzenbach et al., 2003). And since hydrophobicity is also an important element in soil/water partitioning, many investigators have searched for a mathematical relationship between K_{ow} and K_{oc}. To date, however, no investigator has proven that there is an exact relationship between the two. Based on a thorough analysis, Gurr (2008; from Kresic, 2009) concludes that the primary value of various proposed experimental relationships between K_{ow} and K_{oc} is for estimating parameters for emerging contaminants that are not well known. Regulators and chemical manufacturers, especially, can use these relationships to evaluate environmental risk. When familiar and well-studied contaminants are considered, it appears that there is no basis for using K_{ow}–based calculated values in the sorption analyses.

13.1.5 Biodegradation

Soils and porous media in groundwater systems contain a large variety of microorganisms, ranging from simple prokaryotic bacteria and cyanobacteria to more complex eukaryotic algae, fungi, and protozoa. Over the past decades, numerous laboratory and field studies have shown that microorganisms indigenous to the subsurface environment can degrade a variety of organic compounds, including components of gasoline, kerosene, diesel, jet fuel, chlorinated ethenes, chlorinated ethanes, the chlorobenzenes, and many other compounds (Wiedemeier et al., 1998). To obtain energy for growth and activity, under aerobic conditions (in the presence of molecular oxygen) many bacteria couple the oxidation of organic compounds (food) to the reduction of oxygen in the surrounding porous media. In the absence of oxygen (anaerobic conditions), microorganisms may use compounds other than oxygen as electron acceptors.

As discussed by Wiedemeier et al. (1998), biodegradation of organic compounds in groundwater occurs via three mechanisms: 1. Use of the organic compound as the primary growth substrate; 2. Use of the organic compound as an electron acceptor; 3. Cometabolism.

The first two biodegradation mechanisms involve the microbial transfer of electrons from electron donors (primary growth substrate) to electron acceptors. This process can occur under aerobic or anaerobic conditions. Electron donors include natural organic material, fuel hydrocarbons, chlorobenzenes, and the less oxidized chlorinated ethenes and ethanes. Electron acceptors are elements or compounds that occur in relatively oxidized states. The most common naturally occurring electron acceptors in groundwater include dissolved oxygen, nitrate, manganese (IV), iron (III), sulfate, and carbon dioxide. In addition, the more oxidized chlorinated solvents such as PCE, TCE, DCE, TCA, DCA, and polychlorinated benzenes can act as electron acceptors under favorable conditions. Under aerobic conditions, dissolved oxygen is used as the terminal electron acceptor during aerobic respiration. Under anaerobic conditions, the electron acceptors listed above are used during denitrification, manganese (IV) reduction, iron (III) reduction, sulfate reduction, methanogenesis, or reductive dechlorination. Chapelle (1993) and Atlas (1984) discuss terminal electron-accepting processes in detail. The third biodegradation mechanism is cometabolism. During cometabolism the compound being degraded does not benefit the organism. Instead, degradation is brought about by a fortuitous reaction wherein an enzyme produced during an unrelated reaction degrades the organic compound (Wiedemeier et al., 1998).

Fuel hydrocarbons are rapidly biodegraded when they are utilized as the primary electron donor for microbial metabolism under aerobic conditions. Biodegradation of fuel hydrocarbons occurs naturally when sufficient oxygen (or other electron acceptors) and nutrients are available in the groundwater. The rate of natural biodegradation is generally limited by the lack of oxygen or other electron acceptors rather than by the lack of nutrients such as nitrogen or phosphorus. The rate of natural aerobic biodegradation in unsaturated soil and shallow aquifers is largely dependent on the rate at which oxygen enters the contaminated media. Biodegradation of fuel hydrocarbons is discussed in detail by ASTM (1998), and Wiedemeier et al. (1999).

Bouwer et al. (1981) were the first to show that halogenated aliphatic hydrocarbons (such as chlorinated solvents PCE and TCE) could be biologically transformed under anaerobic conditions in the subsurface environment. Since that time, numerous investigators have shown that chlorinated compounds can degrade via reductive dechlorination under anaerobic conditions.

Anaerobically, biodegradation of chlorinated solvents most often proceeds through a process called reductive dechlorination. Highly chlorinated compounds such as PCE, TCE, or TCA are more oxidized and thus are less susceptible to oxidation. Therefore, they are more likely to undergo reductive reactions than oxidative reactions. The reductive dechlorination of PCE to TCE, and then TCE to DCE, and finally DCE to vinyl chloride (VC) is one of such reactions during which the halogenated hydrocarbon is used as an electron acceptor, not as a source of carbon, and a halogen atom is removed and replaced with a hydrogen atom. Each step requires a lower redox potential than the previous one. PCE degradation occurs in a wide range of reducing conditions, whereas VC is reduced to ethene only under sulfate-reducing and methanogenic conditions. During each of these transformations, the parent compound (R-Cl) releases one chloride ion and gains one hydrogen. Two electrons are transferred during the process, which may provide a source of energy for the microorganism. This reductive anaerobic reduction of chlorinated solvents is expressed with the following general equation:

$$R - Cl + H^+ + 2e \rightarrow R - H + Cl^- \qquad (13.14)$$

where R–Cl is chlorinated solvent structure.

Because chlorinated compounds are used as electron acceptors during reductive dechlorination, there must be an appropriate source of carbon for microbial growth for reductive dehalogenation to occur. Potential carbon sources can include low-molecular-weight organic compounds (lactate, acetate, methanol, and glucose), fuel hydrocarbons, by-products of fuel degradation (e.g., volatile fatty acids), or naturally occurring organic matter (Wiedemeier et al., 1998). Bioremediation technologies often involve injection of carbon sources ("food"), which stimulate the native microorganisms and accelerate biodegradation.

Reductive dechlorination processes result in the formation of intermediates that are more reduced than the parent compound. These intermediates are usually more susceptible to oxidative bacterial metabolism than to further reductive anaerobic processes. For example, because of the relatively low oxidation state of VC, this compound more commonly undergoes aerobic biodegradation as a primary substrate than reductive dechlorination. For this reason, there may be accumulation of VC or DCE as a result of reductive dechlorination in some cases, as these cannot be further degraded in the absence of oxygen and specific microorganisms capable of a complete dechlorination.

Bioaugmentation, which is a remedial technology of adding exogenous bacteria (i.e., bacteria not native to the contaminated aquifer), helps in preventing accumulation of the reductive dechlorination intermediates such as VC.

Vinyl chloride (VC) is more toxic and more mobile in groundwater than the parent compounds and its accumulation is an undesired result of biodegradation.

Table 13.1 Trends in Contaminant, Electron Acceptor, Metabolic By-product and Total Alkalinity concentrations during biodegradation. From Wiedemeier et al., 1998. U.S. EPA, in public domain.

Analyte	Terminal electron accepting process	Trend in analyte concentration during biodegradation
Fuel Hydrocarbons	Aerobic respiration, denitrification, manganese (IV) reduction, iron (III) reduction, methanogenesis	Decreases
Highly Chlorinated Solvents and Daughter Products	Reductive dechlorination	Parent compound concentration decreases, daughter products increase initially and then may decrease
Lightly Chlorinated Solvents	Aerobic respiration, denitrification, manganese (IV) reduction, iron (III) reduction (direct oxidation)	Compund concentration decreases
Dissolved Oxygen	Aerobic respiration	Decreases
Nitrate	Denitrification	Decreases
Manganese (II)	Manganese (IV) reduction	Increases
Iron (II)	Iron (III) reduction	Increases
Sulfate	Sulfate Reduction	Decreases
Methane	Methanogenesis	Increases
Chloride	Reductive Dechlorination or Direct Oxidation of Chlorinated Compound	Increases
Oxidation-Reduction Potential	Aerobic Respiration, Denitrification, Manganese (IV) Reduction, Iron (III) Reduction, Methanogenesis	Decreases
Alkalinity	Aerobic Respiration, Denitrification, Iron (III) Reduction, and Sulfate Reduction	Increases

As discussed by Wiedemeier et al. (1998), biodegradation causes measurable changes in groundwater chemistry. Table 13.1 summarizes these trends. During aerobic respiration, oxygen is reduced to water, and dissolved oxygen concentrations decrease. In anaerobic systems where nitrate is the electron acceptor, the nitrate is reduced to NO_2^-, N_2O, NO, NH_4^+, or N_2 via denitrification or dissimilatory nitrate reduction, and nitrate concentrations decrease.

In anaerobic systems where iron (III) is the electron acceptor, it is reduced to iron (II) via iron (III) reduction, and iron (II) concentrations increase. In anaerobic systems where sulfate is the electron acceptor, it is reduced to H_2S via sulfate reduction, and sulfate concentrations decrease. During aerobic respiration, denitrification, iron (III)

reduction, and sulfate reduction, total alkalinity will increase. In anaerobic systems where CO_2 is used as an electron acceptor, it is reduced by methanogenic bacteria during methanogenesis, and CH_4 is produced. In anaerobic systems where contaminants are being used as electron acceptors, they are reduced to less chlorinated daughter products; in such a system, parent compound concentrations will decrease, and daughter product concentrations will increase at first and then decrease as the daughter product is used as an electron acceptor or is oxidized. As each subsequent electron acceptor is utilized, the groundwater becomes more reducing and the redox potential of the water decreases.

Lawrence (2006) provides a detailed literature review and discussion on various degradation mechanisms of VOCs commonly found in groundwater.

Figures 13.8 and 13.9 illustrate the impact of various fate and transport (F&T) processes discussed in the preceding sections, including biodegradation, on contaminant concentrations as it travels downgradient from the source zone. In the most general sense, processes that do not involve microorganisms are called *abiotic*. These include sorption, dispersion, diffusion, dilution and volatilization for example. There is, however, some confusion as to the "correct" meaning of the term *abiotic*, since many chemical reactions in the subsurface are facilitated by microorganism, including very important inorganic redox reactions. Some redox-controlled reactions chemically transform contaminants, both inorganic and organic, and may completely remove them from the flow system. An example is precipitation of an insoluble mineral compound, which most people would not define as "degradation or destruction". However, the net fate and transport effect of this (bio)chemical transformation of the contaminant may be the same as complete destruction. The following discussion by U.S. EPA (1999c) probably best describes the Agency's concerns as to the fate and transport of inorganic contaminants, which are generally thought not to be biodegradable:

MNA (monitored natural attenuation) may, under certain conditions (e.g., through sorption or oxidation-reduction reactions), effectively reduce the dissolved concentrations and/or toxic forms of inorganic contaminants in groundwater and soil. Both metals and non-metals (including radionuclides) may be attenuated by sorption reactions such as precipitation, adsorption on the surfaces of soil minerals, absorption into the matrix of soil minerals, or partitioning into organic matter. Oxidation-reduction (redox) reactions can transform the valence states of some inorganic contaminants to less soluble and thus less mobile forms (e.g., hexavalent uranium to tetravalent uranium) and/or to less toxic forms (e.g., hexavalent chromium to trivalent chromium). Sorption and redox reactions are the dominant mechanisms responsible for the reduction of mobility, toxicity, or bioavailability of inorganic contaminants. It is necessary to know what specific mechanism (type of sorption or redox reaction) is responsible for the attenuation of inorganics so that the stability of the mechanism can be evaluated. For example, precipitation reactions and absorption into a soil's solid structure (e.g., cesium into specific clay minerals) are generally stable, whereas surface adsorption (e.g., uranium on iron-oxide minerals) and organic partitioning (complexation reactions) are more reversible. Complexation of metals or radionuclides with carrier (chelating) agents (e.g., trivalent chromium with EDTA) may increase their concentrations in water and thus enhance their mobility. Changes in a contaminant's concentration, pH, redox potential, and chemical speciation may reduce a contaminant's stability at a site and release it into the environment. Determining the existence, and demonstrating the irreversibility, of these mechanisms is important to show that a MNA remedy is sufficiently protective.

Inorganic contaminants persist in the subsurface because, except for radioactive decay, they are not degraded by the other natural attenuation processes. Often, however, they may exist in forms that have low mobility, toxicity, or bioavailability such that they pose a relatively low level of risk. Therefore, natural attenuation of inorganic contaminants is most applicable to sites where immobilization or radioactive decay is demonstrated to be in effect and the process/mechanism is irreversible.

In groundwater contamination and remediation studies term *biotic* is now almost exclusively applied to biochemical reactions which "degrade" (transform) or completely "destroy" organic chemical compounds due to microbial activity and involvement of enzymes. Hydrolysis is one example of a direct chemical reaction between water and some organic compounds that frequently results in formation of alcohols and alkenes (Johnson et al., 1989). Although hydrolysis may sometimes be indirectly facilitated by microorganisms, it is generally considered an *abiotic* reaction because it does not involve enzymes, which can be produced only by microorganisms. For practical (simplification) purposes, term *biotic* is therefore used as a synonym to *biodegradation*.
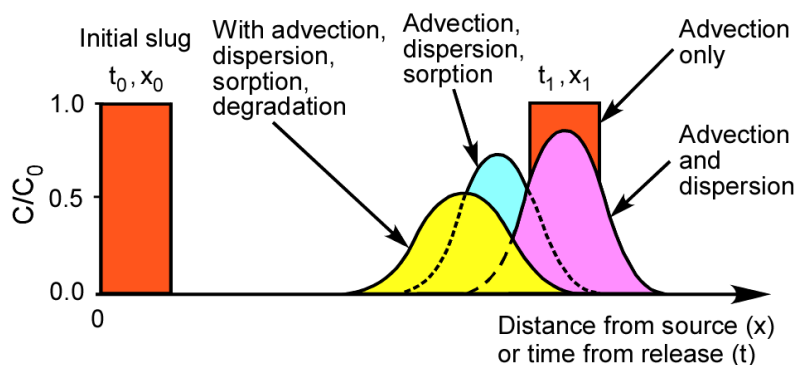
Figure 13.8 Changes in concentration of a contaminant slug from an instantaneous, one-time release, as it travels away from the source; the graph is applicable to both the time and the distance scales. C_0 is the initial concentration; C/C_0 is the relative concentration. Modified from Wiedemeier et al., 1998. U.S. EPA, in public domain.
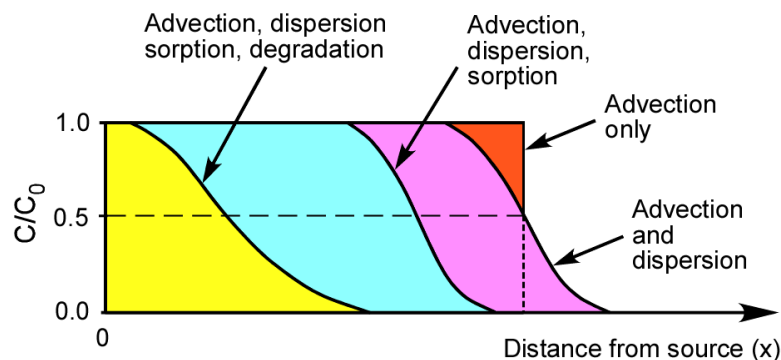
Figure 13.9 Changes in concentration of a contaminant from a continuous source with constant strength as it travels away from the source in direction of groundwater flow. C_0 is the initial concentration; C/C_0 is the relative concentration. Modified from Wiedemeier et al., 1998. U.S. EPA, in public domain.

Degradation Rate

Many chemicals will undergo zero or first order degradation in the dissolved, solid and/or gaseous phase. A first order degradation is described by the following equation:

$$C = C_0 e^{-kt} \qquad (13.15)$$

where:

C is the concentration at time t; C_0 is the initial concentration at time t = 0; *k* is the first order degradation rate constant (units = time^{-1}); *t* is the time.

First order degradation can also be stated in terms of a chemical's half-life. The half-life is the time it takes for half of the contaminant to degrade:

$$\frac{C}{C_0} = 0.5 = e^{-kt} \qquad (13.16)$$

$$t_{1/2} = \frac{ln\,2}{k} = \frac{0.693}{k} \qquad\qquad (13.17)$$

As can be seen, the contaminant half-life and the first-order degradation constant can both be used in quantitative analyses, but consistently, so that there is no confusion. For example, a 2-year half-life is equivalent to a first-order rate constant of 0.35 per year. Practitioners, and analytical equations, consistently use the first-order degradation constant in the same units of time as all other time-dependent parameters.

Some chemicals undergo zero-order degradation, which is described by the following equation:

$$C = C_0 - k_0 t \qquad\qquad (13.18)$$

where k_0 is the zero-order rate constant (units = mass/volume-time). Zero order kinetics does not typically occur for most common organic compounds found in groundwater.

The key parameter in all calculations involving contaminant degradation and its "half-life", is the degradation constant k. Unfortunately, is also one of the most difficult to accurately determine in the field, and it may change in time as geochemical conditions at the site change. It is also the least likely parameter to be accepted by regulatory agencies in case all other *abiotic* parameters, such as advection, recharge (very important when considering effects of potential dilution), sorption, and dispersion, are *not reasonably accurately established* for the particular site. In case of sequential decay reactions, such as those involving chlorinated solvents, degradation constants are certain to vary for different daughter products and may not even be applicable for some of them. In other words, some daughter products may be less biodegradable or not biodegradable at all in certain conditions.

U.S. EPA published a very informative work on different methods commonly used to determine the degradation rate constant *k*, including discussions on associated uncertainties and applicability of individual methods (Newell et al., 2002). The key point is that constant k may mean different things to different people and in different context. It is therefore very important to make a clear distinction between the general *attenuation constant*, and the *(bio)degradation constant*. Although either constant can be used to quantitatively describe a general decrease in contaminant concentration in time (a first-order decay process), the degradation constant should be used only if the associated biological process is confirmed, and its rate quantified.

The more general (apparent) attenuation constant includes both abiotic and biotic processes, without making distinction between them. It is relatively easily determined from the measured contaminant concentrations at monitoring wells, at multiple times, by establishing a quantitative relationship between the concentration decrease and the time. This is illustrated in Figure 13.10. However, it would be completely erroneous to include, in a mathematical equation of contaminant fate and transport, this general constant and any (or all) of the processes that may have caused the concentration decrease. By doing this, one would account for the same process twice (e.g., sorption included as a separate parameter, and also through the apparent attenuation parameter), therefore overestimating the actual natural attenuation.
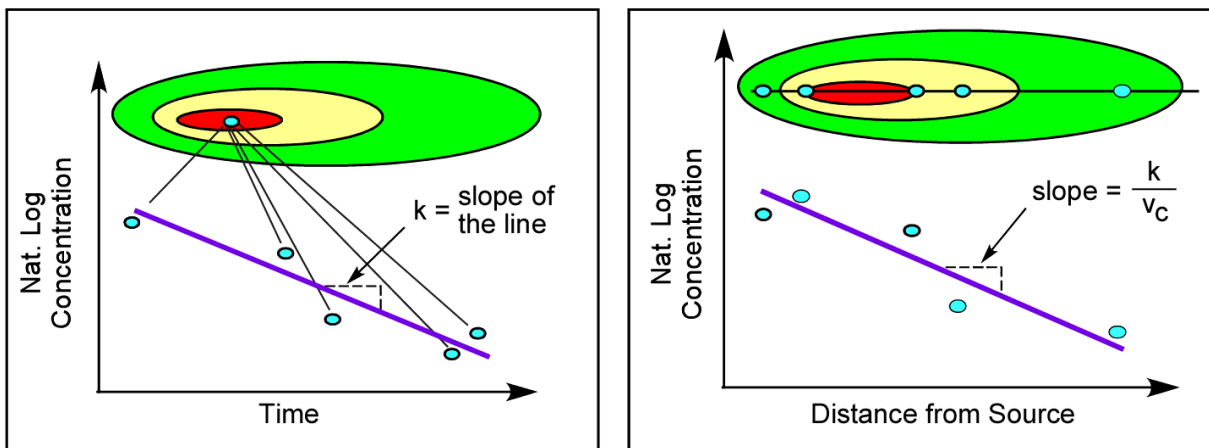
Figure 13.10 Determining rate constant from the monitoring well concentration data. *Left*: Concentration vs. time rate constant for individual wells. *Right*: Concentration vs. distance for a line of wells along groundwater flow direction; v_c is contaminant velocity, equal to linear groundwater velocity divided by the retardation factor. Modified from Newell et al., 2002. U.S. EPA, in public domain.

The (bio)degradation rate constant applies to both space and time, but only to one degradation mechanism. Quantification of this parameter is arguably the most critical part of contaminant fate and transport studies and remediation projects that consider biodegradation, in any form, as a potentially viable alternative. It can be performed in the laboratory, using controlled, time-consuming microcosm studies with soil and groundwater samples from the site. It can also be estimated during F&T model calibration of all other abiotic fate and transport parameters. Whatever the case may be, selecting a literature value should be the last option, and only for the "screening" purposes. Since every site will have a very specific degradation rate for any contaminant, and this rate may change in time, the author deliberately did not include any table of "literature values" of degradation rate constants. This is, again, simply because every organic chemical may or may not degrade at any particular site. Every effort should be made to avoid using literature values because it may result in very misleading results, whatever any stakeholders were hoping for.

13.1.6 Analytical Equation of Contaminant Fate and Transport

The general equation of contaminant fate and transport (F&) in one dimension, i.e., along the horizontal (X) axis, known as advection-dispersion equation, is as follows

$$\frac{\partial C}{\partial t} = \frac{D_x}{R}\frac{\partial^2 C}{\partial x^2} - \frac{v_x}{R}\frac{\partial C}{\partial x} \pm Q_S \qquad (13.19)$$

where

C is dissolved contaminant concentration (kg/m³, or mg/L);
t is time (day);
D_x is hydrodynamic dispersion in x direction (m²/day);
R is retardation coefficient (dimensionless);
X is distance from the source along X axis (m);
v_x is linear groundwater velocity in X direction (m/day);

Q_s is general term for source or sink of contaminant, such as due to biodegradation (kg/m³/dan). This term can also be expressed using the first-rate degradation constant, λ (1/day) which gives:

$$\frac{\partial C}{\partial t} = \frac{D_x}{R}\frac{\partial^2 C}{\partial x^2} - \frac{v_x}{R}\frac{\partial C}{\partial x} - \lambda C \qquad (13.20)$$

Equations (13.19) and (13.20) do not have an explicit solution and various approximate solutions, based on simplifying assumptions, have been proposed by different authors. One of the more widely used and simple analytical equations for an instantaneous point source, which takes into account hydrodynamic dispersion in all three Cartesian directions, X, Y and Z, and calculates the concentration at the *x,y,z* coordinate, is the Baestle equation, formulated by Domenico and Schwartz (1990) as:

$$C(x,y,z,t) = \left[\frac{C_0 V_0}{8(\pi t)^{3/2}(D_x D_y D_z)^{1/2}}\right] exp\left[-\frac{X-v_c t}{4D_x t} - \frac{Y^2}{4D_y t} - \frac{Z^2}{4D_z t} - \lambda t\right] \qquad (13.21)$$

where:

X, Y, Z are distances in the x,y,z directions from the center of the gravity of the contaminant mass;

t   is time;

C_0 is the initial concentration of the contaminant at the source;

V_0 is the initial volume of the released contaminant, such that $C_0 V_0$ equals the mass of contaminant which has entered the saturated zone;

D_x, D_y, D_z are coefficients of hydrodynamic dispersion in all three main directions, *x,y* and *z*;

v_c is the velocity of contaminant in one dimension, equal or lower than that of water; it is lower when the contaminant is retarded due to sorption for example);

λ is the degradation constant.

The maximum contaminant concentration caused by a point source spill occurs at the center of the spreading plume, where *y=z=0*, and *x=v_c t* :

$$C_{max} = \frac{C_0 V_0 e^{-\lambda t}}{8(\pi t)^{3/2}(D_x D_y D_z)^{1/2}} \qquad (13.22)$$

Probably the most widely used and similar analytical equation is referred to as *Domenico equation* first introduced in 1987 (Domenico, 1987) and based on an approach previously published by Domenico and Robins (1985). The key advantage of the Domenico and Robbins (1985) approach is that it provides a closed form solution of Equation (13.19) without involving numerical integration procedures. Due to this computational advantage, the Domenico solution has been widely used in several public domain analytical programs, including the U.S. EPA Excel-based programs BIOCHLOR and BIOSCREEN (Newell et al. 1996; Aziz et al. 2000).

Although the Domenico equation has been extensively used in the industry, its approximate nature continues to be a subject of scientific debate. For example, West and Kueper (2004) compared the BIOCHLOR model against a more rigorous analytical solution and concluded that the Domenico equation can produce errors up to 50%. Guyonnet and Neville (2004) compared the Domenico equation against the Sagar (1982) solution and presented the results in a nondimensional form. They concluded that for groundwater flow regimes dominated by advection

and mechanical dispersion, discrepancies between the two solutions can be considered negligible along the plume centerline. However, these errors may increase significantly outside the plume centerline.

Based on a rigorous mathematical analysis, Srinivasan et al. (2007) conclude that the approximate Domenico equation can be expected to produce reasonable estimates for advection-dominated problems; however, it can introduce significant errors for longitudinal dispersion-dominated problems. The key assumption used to derive the Domenico equation is the time reinterpretation step, where the time t in the transverse dispersion terms is replaced with x/v. This substitution process is valid only when the longitudinal dispersivity is zero. For all nonzero longitudinal dispersivity values, the solution will have a finite error. The spatial distribution of this error is highly sensitive to the value of α_x and the position of the advective front (vt); it is relatively less sensitive to other transport parameters. The authors conclude that the error in the Domenico solution will be low when solving transport problems that have low longitudinal dispersivity values, high advection velocities, and large simulation times.

After their analysis of the approximate Domenico solution, West et al. (2007) conclude that its accuracy is highly variable and dependent on the selection of input parameters. For solute transport in a medium-grained sand aquifer, the Domenico (1987) solution underpredicts solute concentrations along the centerline of the plume by as much as 80% depending on the case of interest. Increasing the dispersivity, time, or dimensionality of the system leads to increased error. Because more accurate exact analytical solutions exist, the authors suggest that the Domenico (1987) solution, and its predecessor and successor approximate solutions, need not be employed as the basis for screening tools at contaminated sites (West et al., 2007).

Karanovic et al. (2007) of S.S. Papadopoulos & Associates present an enhanced version of BIOSCREEN that supplements the Domenico (1987) solution with an exact analytical solution for the contaminant concentration. The exact solution is derived for the same conceptual model as Domenico (1987) but without invoking approximations in its evaluation that introduce errors of unknown magnitude in the analysis. BIOSCREEN-AT provides a simple and direct way to calculate an exact solution to the transport equation and, if desired, to assess the significance of the errors introduced by the Domenico (1987) solution for site-specific applications. The program is available for free download at https://www.sspa.com/software/bioscreen. Figure 13.11 shows screenshots of the modified example problem provided by the BIOSCREEN-AT author M. Karanovic. The values and sensitivity of all key F&T processes can be quickly calculated and evaluated via user-friendly interface. The program can simulate F&T of any contaminant, inorganic or organic, dissolved in groundwater. It includes an option to simulate instantaneous biodegradation of hydrocarbons using analytical data of groundwater chemistry.

Importantly, BIOSCREEN-AT and similar analytical programs should be used for screening purposes only as they assume steady state (time-independent) conditions, completely homogeneous and isotropic (uniform) porous media, and do not account for any aquifer recharge or groundwater withdrawal. Numeric models are irreplaceable for the simulation of most natural groundwater systems where all parameters of groundwater flow and contaminant F&T parameters do change in time and in all three dimensions.

BIOSCREEN-AT Natural Attenuation Decision Support System
S.S. Papadopulos & Associates, Inc.   Version 1.45   *M.Karanovic (Jul 2007)*

Data Input Instructions:
115 → 1. Enter value directly....or
↑ or   2. Calculate by filling in grey
0.02   cells below. (To restore
          formulas, hit button below).
Variable* → Data used directly in model.
20 → Value calculated by model.
          (Don't enter any data).

1. HYDROGEOLOGY
Seepage Velocity*	Vs	335.225	(ft/yr)
or		↑ or	
Hydraulic Conductivity	K	8.1E-03	(cm/sec)
Hydraulic Gradient	i	0.01	(ft/ft)
Porosity	n	0.25	(-)

2. DISPERSION
Longitudinal Dispersivity*	alpha x	35.049	(ft)
Transverse Dispersivity*	alpha y	3.505	(ft)
Vertical Dispersivity*	alpha z	0.289	(ft)
or		↑ or	
Estimated Plume Length	Lp	2500	(ft)

3. ADSORPTION
Retardation Factor*	R	1.2	(-)
or		↑ or	
Soil Bulk Density	rho	1.7	(kg/l)
Partition Coefficient	Koc	38	(L/kg)
FractionOrganicCarbon	foc	8.0E-4	(-)

4. BIODEGRADATION
1st Order Decay Coeff*	lambda	8.7E-1	(per yr)
or		↑ or	
Solute Half-Life	t-half	0.80	(year)

or Instantaneous Reaction Model
Delta Oxygen*	DO	5.78	(mg/L)
Delta Nitrate*	NO3	17	(mg/L)
Observed Ferrous Iron*	Fe2+	11.3	(mg/L)
Delta Sulfate*	SO4	100	(mg/L)
Observed Methane*	CH4	0.414	(mg/L)

5. GENERAL
Modeled Area Length*	2500	(ft)
Modeled Area Width*	500	(ft)
Simulation Time*	5.00	(yr)

6. SOURCE DATA
Source Thickness   10   (ft)

Source
Width (ft)	Conc.(mg/L)
100	9

☐ Exponentialy Decaying Conc.

View of Plume Looking Down
Observed Centerline Concentrations at Monitoring Wells
If No Data Leave Blank or Enter "0"

7. FIELD DATA FOR COMPARISON
Concentration (mg/L)	9.0		2.476		1.134		.348		.016	
Dist. from Source (ft)	0	250	500	750	1000	1250	1500	1750	2000	2250	2500

8. CHOOSE TYPE OF OUTPUT TO SEE:

RUN — View Centerline
RUN — View Plume
View BIOSCREEN

Recalculate This Sheet
Paste Example Dataset
Paste Dataset from BIOSCREEN
Restore Formulas for Vs,

DISSOLVED HYDROCARBON CONCENTRATIONS IN PLUME (mg/L at Z=0)

Distance from Source (ft)
	0	250	500	750	1000	1250	1500	1750	2000	2250	2500
No Degradation	9.000	4.550	2.621	1.801	1.309	0.872	0.448	0.153	0.031	0.004	0.000
1st Order Decay	9.000	2.460	0.723	0.250	0.094	0.036	0.012	0.003	0.001	0.000	0.000
Field Data from Site	9.000		2.476		1.134		0.348		0.016		

# of TimeSteps   20   Displayed Time=5 years   Return to Input   View Plume Output

Figure 13.11 Screenshots of the BIOSCREEN-AT input page (top) and the resulting graph of contaminant concentration vs. distance from the source after 5 years of travel time (bottom).

13.2 Groundwater Remediation

13.2.1 Introduction

The Ground Water Task Force (GWTF), established in the fall of 2002 as part of the U.S. EPA's *One Cleanup Program* to improve the planning and quality of groundwater remediation programs dealing with brownfields, federal facilities, leaking underground storage tanks, and RCRA Corrective Action and Superfund sites, provides the following discussion on the importance of groundwater resources and their vulnerability (GWTF, 2007):

Ground water use typically refers to the current use(s) and functions of groundwater as well as future reasonably expected use(s). Groundwater use can generally be divided into drinking water, ecological, agricultural, industrial/commercial uses or functions, and recreational. Drinking water use includes both public supply and individual (household or domestic) water systems. Ecological use commonly refers to groundwater functions, such as providing base flow to surface water to support habitat; groundwater (most notably in karst settings) may also serve as an ecologic habitat in and of itself. Agricultural use generally refers to crop irrigation and live-stock watering. Industrial/commercial use refers to in any industrial process, such as for cooling water in manufacturing, or commercial uses, such as car wash facilities. Recreational use generally pertains to impacts on surface water caused by groundwater; however, groundwater in karst settings can be used for recreational purposes, such as cave diving. All of these uses and functions are considered "beneficial uses" of groundwater. Furthermore, within a range of reasonably expected uses and functions, the maximum (or highest) beneficial groundwater use refers to the use or function that warrants the most stringent groundwater cleanup levels.

Groundwater value is typically considered in three ways: for its current uses; for its future or reasonably expected uses; and for its intrinsic value. Current use value depends to a large part on need. Groundwater is more valuable where it is the only source of water, where it is less costly than treating and distributing surface water, or where it supports ecological habitat. Current use value can also consider the "costs" associated with impacts from contaminated groundwater on surrounding media (e.g., underlying drinking water aquifers, overlying air— particularly indoor air, and adjacent surface water). Future or reasonably expected values refer to the value people place on groundwater they expect to use in the future; the value will depend on the particular expected use or uses (e.g., drinking water, industrial). Society places an intrinsic value on groundwater, which is distinct from economic value. Intrinsic value refers to the value people place on just knowing clean groundwater exists and will be available for future generations, irrespective of current or expected uses. While the value of groundwater is often difficult to quantify, it will certainly increase as the expense of treating surface water increases, and as existing surface water and groundwater supplies reach capacity with continuing development.

Groundwater vulnerability refers to the relative ease with which a contaminant introduced into the environment can negatively impact groundwater quality and/or quantity. Vulnerability depends to a large extent upon local conditions including, for example, hydrogeology, contaminant properties, size or volume of a release, and location of the source of contamination. Shallow groundwater is generally more vulnerable than deep groundwater. Private (domestic) water supplies can be particularly vulnerable because (1) they are generally shallower than public water supplies, (2) regulatory agencies generally require little or no monitoring or testing for these wells, and (3) homeowners may be unaware of contamination unless there is a taste or odor problem.

The general debate on the definition and objectives of groundwater remediation (restoration) is an ongoing one. Its nature is often, and somewhat misleadingly, simplified to emphasize the diverging interests of groundwater "polluters" and "protectors" of groundwater, with the public caught somewhere in between. There are many different opinions at various regulatory levels (local, state, and federal) as to the objectives and goals of groundwater restoration. The following excerpts are from a memorandum written by a regulator in the United States, referencing the above U.S. EPA discussion paper (Pierce, 2004):

I think there is general agreement that it would be very difficult to set a national policy covering the many diverse issues raised in this discussion paper and by the commenters. There is abundant literature and discussion developed by the scientific community and commercial development interests that ground water has value; and its use, protection, and cleanup need to be addressed to varying degrees. Ground water Use, Value, and Vulnerability (UVV) has been, and most likely will remain, a state and local government issue because it is intrinsically bound to land use (e.g. zoning) and development. These have been traditionally viewed as being under the authority of state and local governments. Dealing with UVV issues is a site-specific process that depends on a large number of local factors, both scientific and political.

The role of USEPA should be largely one of educator to the regulators, the regulated community, and the public. This education would be more technical than policy oriented. EPA could also act as discussion facilitator and, if asked, mediator on UVV issues affecting a site and, as far as possible, allow state and local regulators to continue to make decisions regarding setting cleanup goals protective of existing and potential drinking water supplies. These decisions would involve input from EPA and other Federal interests as well as from an active public participation program. Informed decisions by local regulators are the most effective way to address UVV issues.

Addressing these issues needs to be a dynamic interactive process and not just guidance documents and policy statements. There are certainly plenty of those. A comprehensive national UVV guidance would be hard to formulate and would be ignored by many. Any national policy should be general in nature recognizing that each State has its own UVV issues most of which require unique solutions.

The main recommendation to the U.S. EPA by this Georgia state regulator is to set an overall tone of good environmental stewardship and adopt a national policy statement regarding groundwater goals for the Agency. This statement should reflect the view that: 1) no aquifer will be degraded, and 2) any degraded aquifer ultimately needs to be restored to its natural condition.

The above view is far from being a lonely one, and many stakeholders determined to protect human health and the environment have commended this and similar views. However, what makes achieving restoration of some already contaminated aquifers to their natural condition difficult are the nature of contamination, and the nature of certain complex hydrogeologic environments. Unfortunately, the nature of contamination can only to a limited extent be controlled or mitigated at a local "land use and development" level, whereas hydrogeologic conditions cannot be controlled at all. In some cases, in order to restore contaminated aquifers to their natural condition, the local socio-economic structure, as well as the laws of the entire society, would have to be radically changed. Even then, it may take tens or hundreds of years for aquifers to return to their natural condition, if the definition of natural conditions means the absence of any anthropogenic substances in groundwater.

Two examples of non-point source groundwater contamination that require both the highest-level (federal) regulatory actions, and the local land-use changes in order to protect human health and the environment are the use of pesticides such as atrazine, and the presence of naturally occurring contaminants such as arsenic.

In its "Public Statement for Atrazine", the U.S. Agency for Toxic Substances and Disease Registry (ATSDR) states the following (https://wwwn.cdc.gov/TSP/PHS/PHS.aspx?phsid=336&toxid=59):

Atrazine, one of the most widely used herbicides in the United States, is intentionally applied to crops, especially corn, sugarcane, pineapples, and sorghum. Therefore, people who live near areas where these crops are grown, especially farm workers and herbicide applicators who apply atrazine, may be exposed to atrazine because it is used in agriculture. You may be exposed to atrazine if you are nearby when crops are treated with atrazine, if you are involved in the application of atrazine to crops, or if you are near other places where it is applied. Most of the time, atrazine is not found in high concentrations in the air, but may be found in higher concentrations in the air near disposal facilities or near areas where it is being applied to crops. You may also be exposed to atrazine by digging in dirt that has atrazine in it. Your children may be exposed to atrazine by playing in dirt that contains atrazine. You and your children may also be exposed to atrazine if you drink water from wells that are contaminated with the herbicide.

As mentioned earlier in Lecture 12, U.S. EPA did not even consider private wells used for drinking water supply when allowing the continuing use of this pesticide (U.S. EPA, 2003). Incidentally, according to Centers for Disease Control and Prevention, over 15 million households in the United States use private wells for drinking water supply (https://www.cdc.gov/healthywater/drinking/private/wells/index.html)

In their 2006 article titled "European Union bans atrazine, while the United States negotiates continued use", authors Jennifer Beth Sass and Aaron Colangelo write:

Atrazine is a common agricultural herbicide with endocrine disruptor activity. There is evidence that it interferes with reproduction and development, and may cause cancer. Although the U.S. Environmental Protection Agency (EPA) approved its continued use in October 2003, that same month the European Union (EU) announced a ban of atrazine because of ubiquitous and unpreventable water contamination. The authors reviewed regulatory procedures and government documents, and report efforts by the manufacturer of atrazine, Syngenta, to influence the U.S. atrazine assessment, by submitting flawed scientific data as evidence of no harm, and by meeting repeatedly and privately with EPA to negotiate the government's regulatory approach. Many of the details of these negotiations continue to be withheld from the public, despite EPA regulations and federal open-government laws that require such decisions to be made in the open. (Int J Occup Environ Health. 2006 Jul-Sep;12(3):260-7. doi: 10.1179/oeh.2006.12.3.260.)

Interestingly, in September 2020 the U.S. EPA announced a ban on atrazine use in Hawaii and in the U.S. territories of Puerto Rico, Guam, American Samoa, the U.S. Virgin Islands and the North Mariana Islands, while the use of atrazine in the rest of the United States will continue. Some reflections on this decision by the Agency are provided on the web site of Center for Biological Diversity (https://biologicaldiversity.org/). They include the following quotes:

Research has linked atrazine to birth defects and cancer in people, and even miniscule doses can chemically castrate frogs.

It has been banned or is being phased out in more than 35 countries but is the second-most commonly used herbicide in the United States.

The EPA's agreement with conservation groups to assess atrazine's harm to endangered species came after an earlier "preliminary risk assessment" found that the amount of the pesticide released into the environment in the United States is likely to be harming most species of protected plants and animals, including mammals, birds, amphibians and reptiles.

A similar thought-provoking topic discussed by Kresic and Mikszewski (2013) is the absence of any current regulatory policy related to arsenic (As) in private drinking water supplies in eastern New England. Arsenic occurs naturally in metasedimentary bedrock units in the regions that are extensively tapped by private water supply wells. In 2003, it was estimated that over 100,000 people across eastern New England were using private water supplies with arsenic concentrations above the Federal Maximum Contaminant Level (MCL) of 10 µg/L (Ayotte et al, 2003). This represents a widespread exposure to a chemical universally acknowledged as poisonous.

In contrast to the policies of allowing atrazine and arsenic exposure, environmental regulations require the expenditure of millions and hundreds of millions of dollars to remediate Superfund and state-led contaminated sites where the exposure often constitutes a very low risk (e.g., one in a million excess lifetime cancer risk), or is hypothetical in nature (e.g., potential future consumption of groundwater). For example, at the Visalia Pole Yard Superfund site over $30 million were spent to remediate groundwater contamination that was not posing an actual risk (a more detailed discussion is provided further in this Lecture). This is a classic example of policy that permits self-inflicted risk while disproportionately targeting externally inflicted risk, ignoring the relative costs and benefits of the overall outcome. One potential declaration of this ideology is presented below (modified from Kresic and Mikszewski, 2013):

> *When protecting human health and the environment, it is not our place to address risk related to naturally occurring contamination, societal or individual lifestyle choices, but we will act aggressively to remedy any minimal level of risk caused by a third-party agent.*

In other words, when point-source groundwater contamination is caused by known potentially responsible parties (PRPs) whose pockets are much deeper than those of individual households, the approaches to groundwater remediation would in many cases depend on the prevailing interpretation of the existing regulations at the local, state, and federal levels, and much less on the cost-benefit and risk analyses. As illustrated earlier, Georgia and quite a few other states in the United States have adopted a zero-tolerance for groundwater degradation by large polluters such as various industries and military installations. These PRPs are consequently required to restore their portions of contaminated aquifers to pristine natural conditions, often regardless of the underlying hydrogeologic characteristics, the risks, and the associated costs.

It has been estimated that there are more than 20,000 mega-sites in the European countries, requiring extensive remediation (cleanup) of contaminated soils and groundwater, with the projected costs of tens to hundreds of billions US dollars (Rügner and Bittens, 2006). At most of these sites, the cleanup efforts have not started yet as the regulatory agencies and various stakeholders are trying to develop restoration approaches that would balance risks to human health and the environment with socio-economic realities. One reason for this strategy is that many of the mega-sites, legacy of the cold war and past industrial growth, are also owned by the governments, and the remediation costs would have to be paid by all citizens. In addition to the complex mega-sites, there are many tens of thousands of other sites with similar problems. For example, it is estimated that 14,000 sites in the small country of Denmark alone are contaminated from various chemical spills (Danish EPA, 1999) where typical contaminants include chlorinated solvents, gasoline/fuels, coal tar and creosote (Gudbjerg, 2003). A more recent factor in developing pragmatic and realistic groundwater restoration strategies in the European countries is the complex question of carbon footprint, energy consumption, climate change, and the ongoing economic crisis.

In contrast to the European practice, because of the Superfund program (officially called Comprehensive Environmental Response, Compensation, and Liability Act (CERCLA) of 1980) and similar state-led initiatives, groundwater remediation has become a lucrative field in the United States with innumerable consultants and technology vendors offering solutions for a wide variety of contaminants and geologic settings. The cleanup of

hazardous waste sites with groundwater contamination is a major element of professional hydrogeology in the United States. It is likely that every professional hydrogeologist will work on a groundwater remediation project at some point in his or her career. As discussed by Kresic and Mikszewski (2013), to the general public, invoking the term Superfund conjures up images of burning rivers, rusted 55-gallon drums leaking fluorescent fluids on the ground, contaminated wells, and mutated aquatic life. While in many instances these stereotyped attributes (mutations aside) are in fact accurate, often the perception of contamination is just as important as the actual data defining the nature and extent of contamination, and the risks associated with any existing or potential exposures to the contamination.

Similarly, the perception of environmental clean-up is often more important than rigorous quantification of the costs and true environmental, social, and economic benefits of complicated remediation projects. For example, there are many installed pump-and-treat groundwater remediation systems in the United States that have very significant energy requirements, with the associated costs rising steadily. There are also examples where such systems are extracting hundreds of millions of gallons of water annually, with only few tens of pounds or less of the actual groundwater contaminant. In addition, these large quantities of water, after treatment, are usually being discharged to surface streams or sewers without being used or returned to the aquifer. It is therefore likely that, even in the United States, the sustainability of certain groundwater remediation efforts will be increasingly questioned by various stakeholders, and not just by those that are paying the bill.

As discussed by Winpenny (2003), water supply is usually a local responsibility, and its costs are seldom fully covered. Most water utilities in both developed and developing countries rely heavily on subsidies and are far from being able to create their own capital. Since there is little political will to raise tariffs, and governments are either unwilling or unable to provide financing, utilities are trapped in a vicious spiral of under-spending on essential maintenance, resistance to fee increase, and inability to cope with groundwater contamination. In litigious societies such as the United States, this situation is fertile ground for the legal profession (attorneys). In societies that are more pragmatic or not so rich, governments and water-sector agencies play key roles in the various disputes that arise from groundwater contamination. They also help both groundwater users and alleged polluters by creating a more flexible regulatory environment that emphasizes risk- and economy-based, sustainable approaches to the allocation of resources for surface water and groundwater restoration and management.

One possible roadmap to a more efficient and less confrontational approach to groundwater restoration is the establishment of a groundwater remediation trading system, similarly to the widely discussed carbon emissions trading. For example, large companies and parts of the government with seemingly deep pockets (such as Departments of Defense and Energy), responsible for groundwater contamination at multiple sites, would be able to trade their existing and future remediation costs based on priorities developed by risk and cost-benefit analyses. This, of course, would include providing secure drinking water supplies to the affected groundwater users thus eliminating risks to human health.

At the same time, some endemic groundwater contamination problems caused by small businesses unable to pay the full cost of groundwater cleanup, such as dry-cleaner shops, would be covered by common funds (this has already been practiced by some states in the United States). Such funds would also be used to support prevention of future groundwater contamination, including active protection of vulnerable groundwater recharge areas.

What this all may mean in an ideal world, is that hundreds of millions of dollars would not be spent annually on a handful of sites where groundwater restoration to natural conditions may not be feasible within a reasonable timeframe or may be too costly for the given benefits. Rather, the funds and the resources would be spent at other sites where the cost-benefit ratio would be much more favorable. Common funds could also be used to fully protect

valuable uncontaminated sources. Although this approach may seem farfetched given the complex regulatory and litigation framework in the United States, it may work elsewhere to the benefit of both the society and the environment.

13.2.2 Remediation Technologies

In general, and regardless of the underlying hydrogeology which may or may not limit their applicability, remediation technologies fall into one of the following categories (modified from U.S.EPA, 2010 and 2020; Kresic, 2013; Kresic and Mikszewski, 2013 and 2023):

- Source Treatment Remedies – In-situ or ex-situ treatment of soil, sediment, sludge, and/or non-aqueous phase liquids (NAPLs) at or near the point of contaminant disposal. Example in-situ technologies include soil vapor extraction (SVE), in-situ thermal treatment, bioremediation, in-situ chemical oxidation, and flushing. Technologies are often combined; for example, in-situ thermal treatment typically requires installation of SVE and multi-phase extraction systems in addition to heating elements. Ex-situ remediation primarily consists of soil excavation with subsequent treatment, incineration and/or disposal.

- Source Containment Remedies – In-situ containment of contaminated soil, sediment, sludge or NAPL. Example technologies include landfill caps, vertical barrier walls, and solidification/stabilization.

- Groundwater (Dissolved Plume) Treatment Remedies – In-situ treatment of contaminants primarily existing in the dissolved aqueous phase at high concentrations within or downgradient of the source area. Example technologies include air sparging, permeable reactive barriers (PRBs), bioremediation, in-situ chemical oxidation, and in-situ chemical reduction.

- Pump and Treat – Extraction and ex-situ treatment of contaminated groundwater to prevent further plume migration. Note that pump and treat was originally conceived to be an effective means of groundwater treatment; however, years of operational data demonstrate that it is better described as a plume containment remedy, with an ancillary benefit of enhanced groundwater flushing which results in a minor reduction in overall clean-up time.

- Monitored Natural Attenuation (MNA) – The reliance on natural attenuation factors, such as biodegradation, dissolution, dilution, sorption, and volatilization, to achieve remedial objectives within a reasonable time frame compared to that of other remedial technologies. MNA involves a detailed, controlled, and comprehensive monitoring system, and is often paired with source and/or dissolved contaminant plume treatment or containment to expedite site clean-up.

Detail technical overviews of groundwater remediation technologies and extensive literature for free download are available at the following websites:

https://clu-in.org/remediation (U.S. EPA site featuring remediation technology selection tools)
https://frtr.gov/matrix (Federal Remediation Technologies Roundtable site with Technology Screening Matrix)
https://itrcweb.org/home (Interstate Technology and Regulatory Council; search "groundwater remediation")

Kresic and Mikszewski (2013, 2023) point out that trends in groundwater remediation technology usage over time can be measured through public Record of Decision (ROD) documents produced by the U.S. EPA for each Superfund site. As explained in U.S. EPA, 1999d, ROD:

"...describes the technical parameters of the remedy, specifying the methods selected to protect human health and the environment including treatment, engineering, and institutional control components, as well as cleanup levels."

As a result, RODs and other CERCLA decision documents (ROD amendments and Explanations of Significant Differences (ESDs)) provide informative snapshots in time of the remediation marketplace, illustrating changes in the preferred remedial approaches and individual technologies. Figure 13.12 presents the number of Superfund technology selections over time and includes the most recent data published by U.S EPA (2020). Several interesting trends highlighted by Figure 13.12 are summarized below:
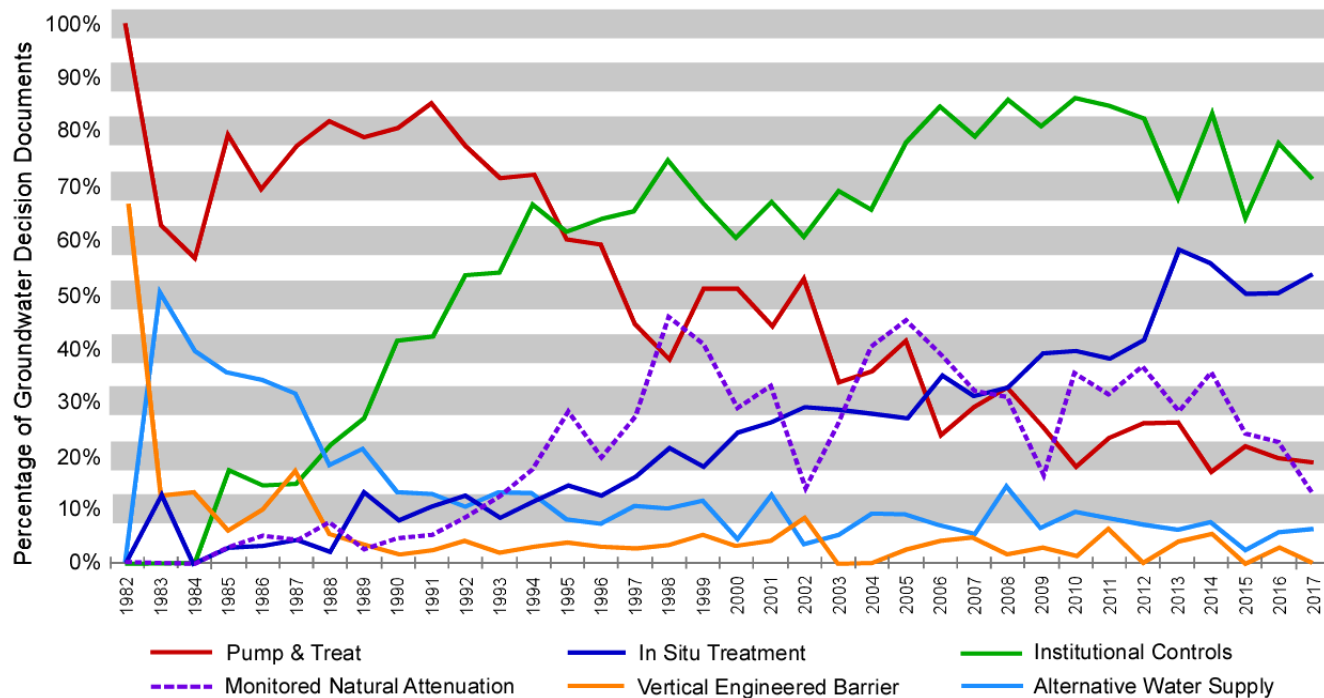
Figure 13.12 Selection Trends for Decision Documents (total of 2,541) with Groundwater Remedies (FY 1982-2017). Decision documents may be included in more than one category. Modified from U.S. EPA, 2020. In public domain.

- The use of pump and treat increased in the late 1980s and was the dominant remedial approach throughout the 1990s. Note that the early 1990s also represented the timeframe with the greatest number of RODs published, peaking at 197 in 1991 (U.S. EPA, 2010). The number of annual pump and treat selections decreased dramatically since its peak. This decline reflects an increased understanding of the technology's limited efficacy in terms of mass removal and clean-up time reduction, while a relative stabilization at approximately 20% selections since 2010 reflects the on-going need for the technology as a containment measure to prevent further migration of contaminant plumes.

- The annual number of in-situ remedies has increased steadily and became dominant since the late 2000s, not counting the institutional controls.

- The in-situ groundwater treatment and MNA were selected more often than pump and treat since the mid-2000s. Note that the reduced number of MNA selections between 2001 and 2003 was at least partially triggered by the 1998 and 1999 publishing of U.S. EPA documents regarding the proper use of MNA

(Wiedemeier et al., 1998; U.S. EPA, 1999c). The rebound in 2004-2005 was achieved after consultants and regulators alike adjusted to the new MNA framework and figured out how to best incorporate the technology.

In addition to the general increase in knowledge and understanding of physical, chemical, and biological processes, the increased selection of in-situ groundwater treatment and MNA was driven by the following factors:

1. In-situ groundwater treatment with technologies such as in-situ chemical oxidation can remove significantly more contaminant mass than conventional pump and treat systems.

2. Clean-up timeframes using MNA are often not remarkably different from those with pump and treat systems or those where source and/or groundwater treatment have reached a point of diminishing returns.

3. MNA is often perceived by potentially responsible party (PRP) groups as a significantly less costly alternative than active remediation. Note that this is not always the case as MNA requires extensive monitoring over long periods of time.

4. PRP groups with experience operating pump and treat systems for years and years with no end in sight became more receptive to innovative technologies with higher capital costs to avoid perpetual operation of the existing or installation of additional pump and treat systems.

The recent remedial approaches selected in Superfund decision documents, as measured by the years 2006 through 2017, are indicative of a balanced approach where technologies can be selected or combined as appropriate to meet site-specific objectives (see Figure 13.13). This represents significant progress from the early 1990s, when pump and treat was seemingly a "default" option.
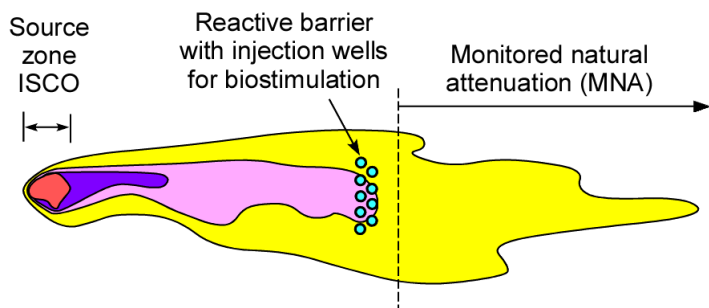
Figure 13.13 Groundwater (dissolved plume) remedial alternatives consisting of three in-situ technologies ISCO stands for In-situ Chemical Oxidation. Modified from Kresic, 2009. Copyright McGraw Hill, permission required for further use.

Preferences regarding individual in-situ technologies have also changed significantly over the lifetime of Superfund, as demonstrated by Figures 13.14 and 13.15 for source control remedies, and groundwater (dissolved plume) treatment remedies, respectively. Figure 13.14 demonstrates that Soil Vapor Extraction (SVE) remains the preferred in-situ source control option, but that its use has decreased significantly since peaking in 1991. Aside from the reduced number of RODs, this decline was likely caused by an increased understanding of the limitations of ambient-temperature SVE, most notably the difficulty in treating contaminants with low volatility and those that reside deep below the water table, such as dense non-aqueous phase liquids (DNAPLs). SVE also has difficulty removing contaminants within low-permeability strata.
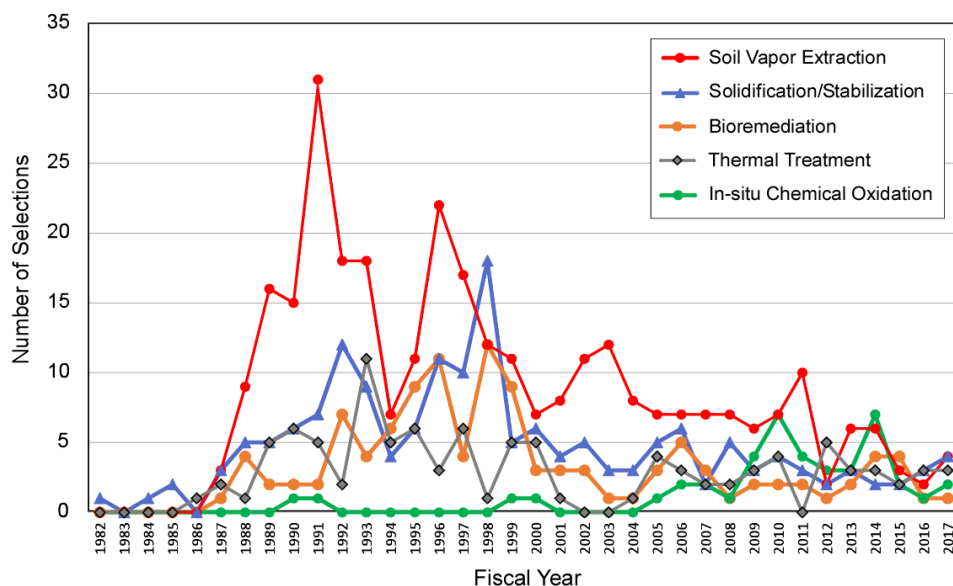
Figure 13.14 Original graph illustrating number of source control remedy selections by fiscal year at Superfund sites. Data from U.S. EPA, 2020 (Appendix B).

The annual number of bioremediation, thermal treatment, in-situ chemical oxidation, and solidification/stabilization selections has remained relatively constant since the mid-2000s; however, these technologies now comprise an increased percentage of in-situ source control remedies. Over the course of the 2000s, thermal treatment has emerged as a more prevalent technology, rivaling the number of ambient temperature SVE selections. It is important to know that thermal treatment almost always requires an SVE system, and the technology is therefore best thought of as "thermally-enhanced SVE." Therefore, even if the use of thermal treatment increases significantly in the coming years, the in-situ source control marketplace can still be classified as SVE-centric.
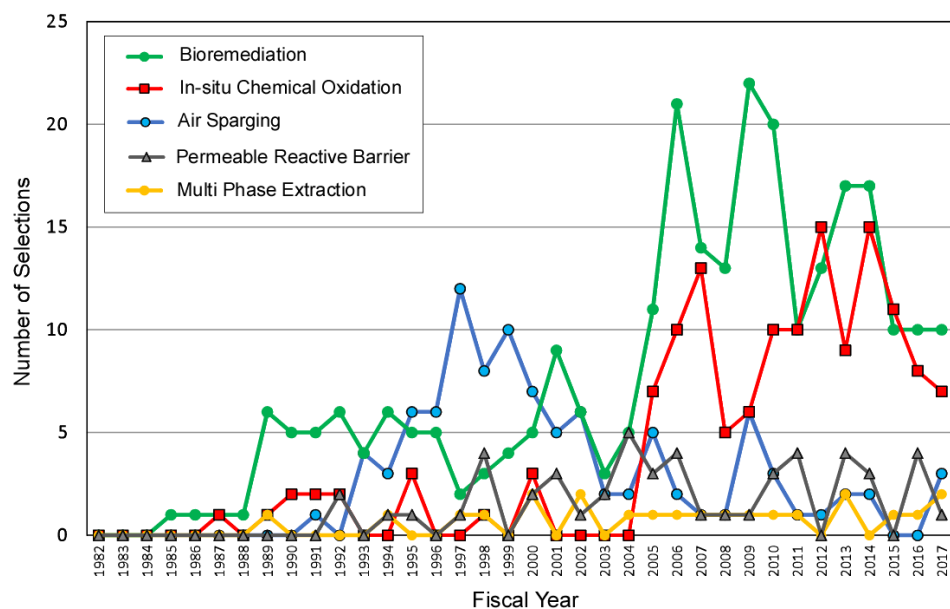
Figure 13.15 Original graph illustrating number of groundwater (dissolved plume) remedy selections by fiscal year at Superfund sites. Data from U.S. EPA, 2020 (Appendix B).

Figure 13.15 demonstrates that the absolute number and distribution of technology selections for in-situ groundwater treatment have changed significantly over time. Like SVE for source control, air sparging was the dominant groundwater technology during the 1990s. However, unlike SVE, air sparging appears to be somewhat

obsolete, as its frequency of selection was greatly surpassed by both bioremediation and chemical treatment (most notably in-situ chemical oxidation) in the 2000s. The limitations of air sparging are very similar to those of SVE; in fact, air sparging typically requires an SVE system to remove volatilized contaminants from the vadose zone. In-situ chemical oxidation and bioremediation remain dominant technologies since the mid-2000s.

Despite the continually evolving technological and political landscape, one thing that has remained constant in Superfund is the objective of restoring contaminant groundwater to its beneficial use. This beneficial use is often considered drinking water, as measured by Maximum Contaminant Levels (MCLs), to ensure that a pristine groundwater resource is available to future generations.

13.2.2.1 Pump and Treat

Pump and treat (P&T) is the most common method for remediating groundwater contaminated with dissolved chemicals, including industrial solvents, metals, and hydrocarbons such as fuel oil. Groundwater is extracted, typically by vertical wells but also other means such as horizontal interceptor trenches and drains and conveyed to an above-ground treatment system that removes the contaminants (Figure 13.16).

P&T is a long-term remedy which can last for decades, and for some sites is expected to last for hundreds of years (i.e., indefinitely). For this reason, there is increasing emphasis on avoiding the installation of P&T systems wherever possible and limiting the construction of new systems to sites where hydraulic containment is necessary to prevent human and/or ecological receptors from being exposed to contaminants at concentrations that present an unacceptable risk. For example, a site where a contaminant plume is threatening to impact off-site residential wells would benefit from a P&T syst em that intercepts the plume prior to reaching the wells.

Figure Left: Outdoor treatment facilities. From EPA-542-F-21-021. In public domain. *Right*: Control room for a P&T system with five extraction wells; treatment tank is on the left.

The most commonly stated objectives of a P&T system during first couple of decades of groundwater remediation in the United States were to provide hydraulic containment of contaminated groundwater to prevent further migration, and to expedite restoration of groundwater quality to applicable regulatory criteria such as MCLs. However, years of operational experience have proven that using P&T to achieve the latter objective, groundwater quality restoration, is usually infeasible within a reasonable amount of time (e.g., <30 years). Tailing and rebound effects can result in concentrations persisting above clean-up criteria for decades. Tailing is the progressively

slower rate of contaminant concentration decline during pump and treat operation (Figure 13.17), while rebound is the relatively rapid increase in concentration after pumping cessation (U.S. EPA, 1996d).

Some of the physical and chemical processes that result in the impracticability of using P&T as a pure remediation measure are (modified from Cohen et al, 1994): (1) Contaminant desorption and NAPL dissolution; (2) Precipitate dissolution; (3) Groundwater velocity variation, preferential pathways, and "dead-end pores" – all caused by heterogeneity; and (4) Matrix diffusion. Matrix diffusion involves contaminant diffusion into and back-diffusion out of low permeability media such as clay and bedrock and is a subject that has received considerable attention in academia and more recently by regulatory agencies.
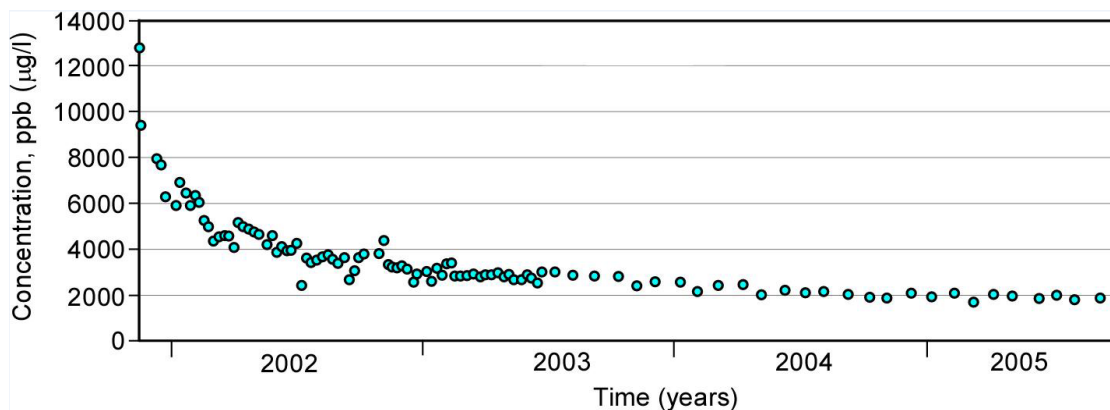
Figure 13.17 Time-series plot of 1,4-dioxane concentrations at new vertical extraction well in one of the longest and oldest groundwater plume of the contaminant in the United States. Courtesy of Farsad Fotouhi.

To emphasize, P&T's optimal usage is as a plume containment, or management of migration (MOM), remedy. Two important terms with respect to plume containment are the P&T's capture zone and radius of influence (ROI). These two terms are not synonymous, and often there is significant confusion on this issue. The capture zone for a pumping well is the three-dimensional volume of the porous media within which groundwater will flow to the pumping well for extraction and subsequent treatment. The ROI of a pumping well is the furthest horizontal distance away from the well where pumping causes a discernable aquifer response (e.g., a measurable drawdown). The concept of a capture zone versus the radius of well influence is illustrated on Figure 13.18. While MW-3 is within the radius of influence of pumping well PW (i.e., there is measurable lowering of the hydraulic head), it is not within PW's capture zone, and it would be erroneous to conclude that contaminated groundwater at MW-3 would be extracted by the pump and treat system. In other words, ROI is the zone in which the hydraulic head is lowered because of the well operation, but the groundwater flow direction is not reversed from the pre-pumping direction.

Consequently, the well capture zone can be verified only if there are enough monitoring wells (piezometers) that show the actual gradient reversal in all three dimensions. It is also very important to understand that the drawdown in the well, i.e., the pumping water level in the extraction well, cannot be used to demonstrate the capture zone if an inadequate number and locations of monitoring wells (piezometers) are selected. This is illustrated in Figure 13.18 where data from the monitoring well MW-3 and the pumping well PW would not be sufficient to demonstrate that MW-3 is within the capture zone, even though the water elevation in MW-3 is higher than in PW. In addition, if the water elevation in PW is not available and corrected for the well loss, three downgradient monitoring wells would be needed to delineate the PW capture zone.

If a contaminant plume is hydraulically contained, contaminants moving with the groundwater will not spread beyond the capture zone. Failed capture, illustrated schematically on Figure 13.19, can allow the plume to grow, which may cause harm to receptors and may increase the ultimate cost or duration of the groundwater remedy (USEPA, 2008). For this reason, regulatory agencies place special emphasis on the performance of P&T systems for hydraulic containment of contaminant plumes and require that such systems be regularly monitored and periodically evaluated for their efficiency, and to confirm continuing containment.
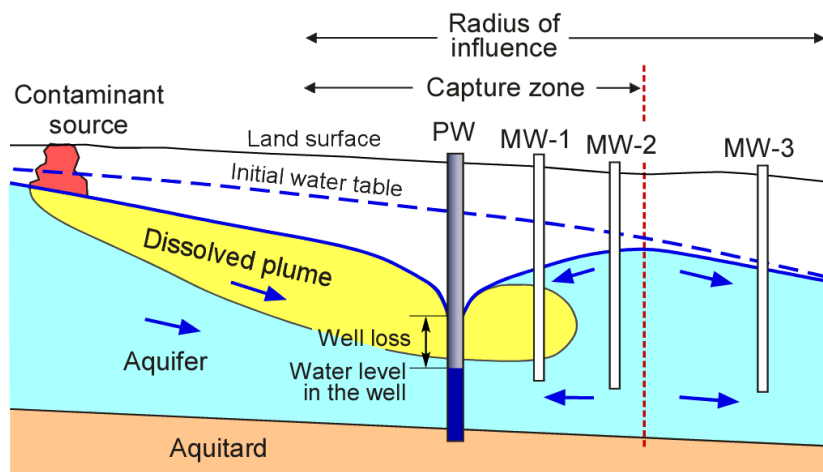
Figure 13.18 Conceptual cross-section illustrating the difference between the capture zone and the radius of influence of the pumping well (PW). Note the effect of well loss on the water level in the pumping well. Modified from Kresic, 2009. Copyright McGraw Hill, permission required for further use.
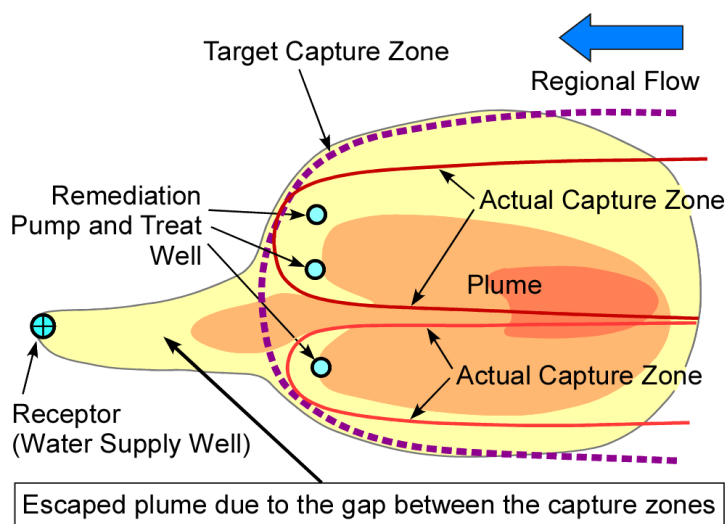
Figure 13.19 Failed capture of contaminant plume. Modified from U.S. EPA, 2008. In public domain.

13.2.2.2 Soil Vapor Extraction (SVE) and Air Sparging

SVE is the process of removing and treating volatile and some semi-volatile organic compounds from the unsaturated zone. By applying a vacuum through a system of wells, contaminants are pulled to the surface as vapor or gas. Often, in addition to vacuum extraction wells, air injection wells are installed to increase the air flow and improve the removal rate of the contaminant. An added benefit of introducing air into the soil is that it can stimulate bioremediation of some contaminants. Used alone, SVE cannot remove contaminants in the saturated zone. It is

therefore often combined with groundwater extraction, which lowers the water table and increases the thickness of the unsaturated soil from which more residual NAPL and sorbed volatile organic compounds (VOCs) can be stripped (volatilized).

Air sparging has primarily been used to remove VOCs from the saturated subsurface through stripping but can be effective in removing volatile and nonvolatile contaminants through other, primarily biological, processes enhanced during its implementation. Oxygen added to the contaminated groundwater and vadose-zone soils also can enhance biodegradation of contaminants below and above the water table. The injection of ozone into the aquifer is referred to as ozone sparging and is a form of chemical treatment.

The basic air sparging system strips VOCs by injecting air into the saturated zone to promote contaminant partitioning from the liquid to the vapor phase. Off-gas is then captured through an SVE system (Figure 13.20), with vapor-phase treatment prior to its recirculation or discharge into the air (USACE, 2008). Steam can be injected in conjunction with, or instead of, air to incorporate a thermal treatment element to traditional air sparging technology.

Air sparging is generally considered a mature technology. It is relatively easy to implement and well known to regulatory agencies, and the equipment necessary for it is generally inexpensive and easily obtained. Therefore, air sparging has been one of the most practiced engineered technologies for in situ groundwater remediation. Critical aspects governing its effectiveness include the presence and distribution of preferential airflow pathways, the degree of groundwater mixing, and potential precipitation and clogging of the soil formation by inorganic compounds.
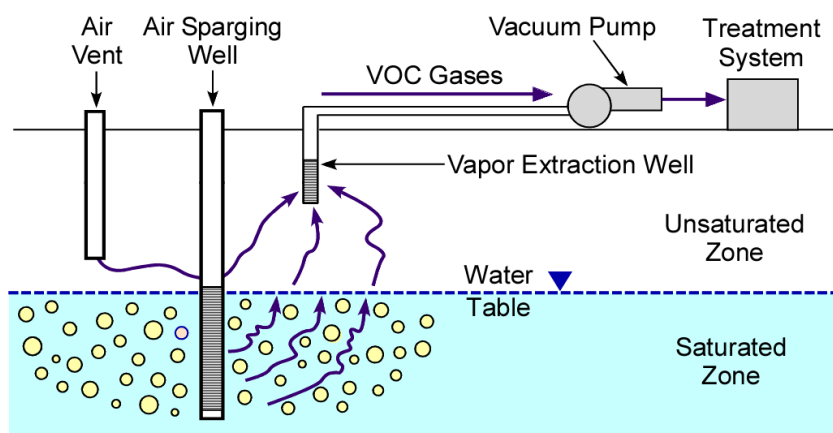
Figure 13.20 Illustration of a combined air sparging and SVE system. Modified from U.S. EPA 1996a. In public domain.

13.2.2.3 Multi-Phase Extraction

Multi-Phase Extraction (MPE) simultaneously extracts both groundwater and other liquids such as NAPLs and/or vapors (USACE, 1999). In the case of vapors, the water table is lowered in order to dewater the saturated zone so that the SVE process can be applied to the newly exposed soil. This allows the volatile compounds sorbed on the previously saturated soil to be stripped by the induced vapor flow and extracted. In addition, soluble VOCs present in the extracted groundwater are also removed (U.S. EPA, 1997b).

MPE systems can be implemented to target all phases of contamination associated with a typical NAPL spill site. These systems remove residual vadose zone soil contamination residing in soil gas, dissolved in soil pore-space moisture, and adsorbed to soil particles. MPE also effectively removes dissolved and free-phase LNAPL and DNAPL contamination in groundwater (U.S. EPA, 1997a). Examples of MPE wells are shown in Figure 13.21.
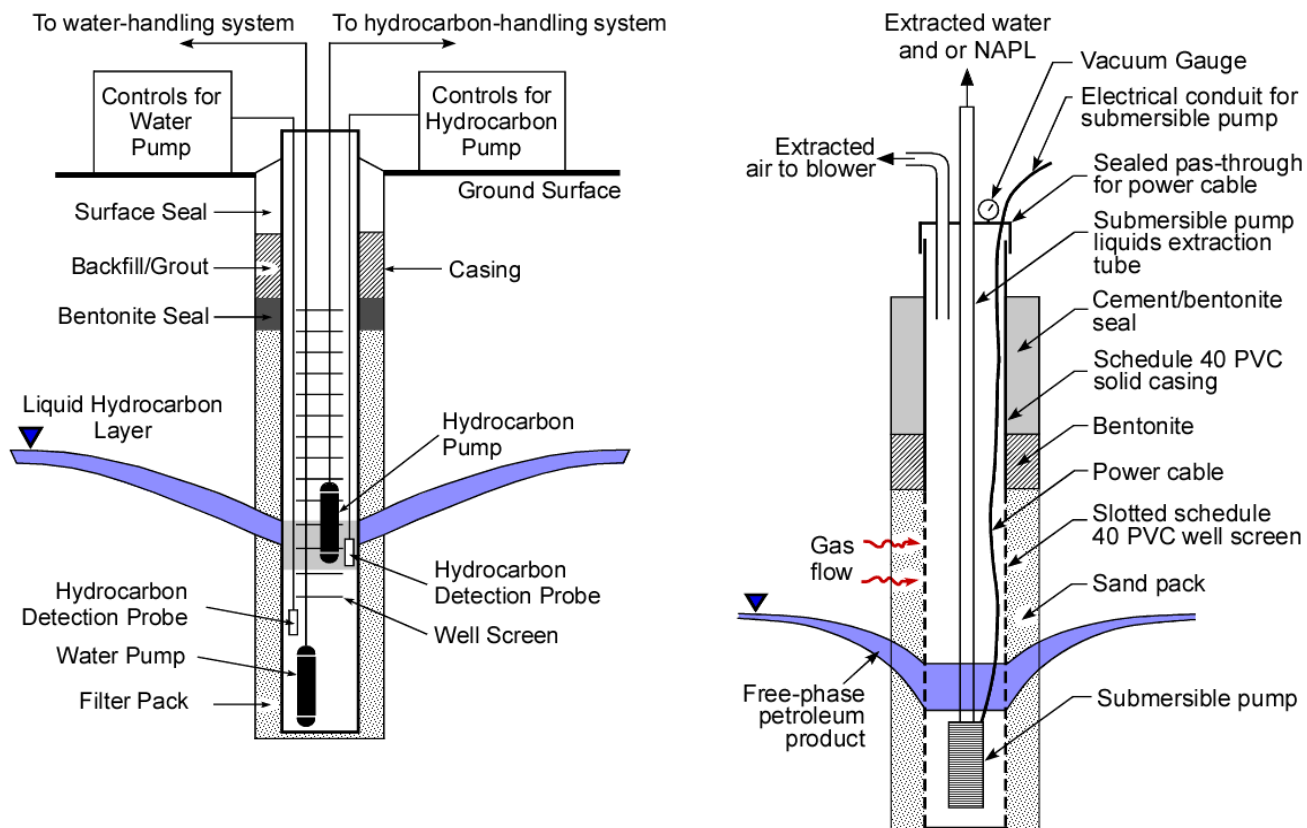
Figure 13.21 *Left*: Conventional LNAPL recovery using dual pump system. Modified from BATTELLE, 1997. *Right*: Typical dual-phase extraction (DPE) system. Modified from USACE, 1999. In public domain.

13.2.2.4 In Situ Chemical Oxidation (ISCO)

ISCO is the introduction of a chemical oxidant into the subsurface for transforming groundwater or soil contaminants to nonhazardous or less toxic compounds that are more stable, less mobile, or inert. The resulting reduction/oxidation (redox) reactions involve the transfer of electrons from one chemical to another. Specifically, one reactant is oxidized (loses electrons) and one is reduced (gains electrons). There are several different forms of oxidants that have been used for ISCO; however, the following five are the most common: (1) potassium or sodium permanganate (Figures 13.22 and 13.23); (2) Fenton's catalyzed hydrogen peroxide; (3) hydrogen peroxide; (4) ozone; and (5) sodium persulfate. Each oxidant has advantages and limitations, and while applicable to soil contamination and some source zone contamination, they have been applied primarily toward remediating dissolved plumes (U.S. EPA, 2006).

As discussed by Huling and Pivetz (2006), the persistence of the oxidant in the subsurface is important, since this affects the contact time for advective and diffusive transport and ultimately the delivery of oxidant to targeted zones in the subsurface. For example, permanganate persists for long periods of time, and diffusion into low-

permeability materials and greater transport distances through porous media are possible. Hydrogen peroxide has been reported to persist in soil and aquifer material for minutes to hours, and the diffusive and advective transport distances will be relatively limited. Radical intermediates formed using hydrogen peroxide, persulfate, and ozone, which are largely responsible for various contaminant transformations, react very quickly and persist for very short periods of time (<1 second).

Some oxidants are stronger than others, and it is common to calculate a relative strength for all oxidants using chlorine as a reference. However, all commonly used oxidants have enough oxidative power to remediate most organic contaminants. The standard potentials are a useful general reference of the strength of an oxidant, but these values do not indicate how these will perform under field conditions. Four major factors play a role in determining whether an oxidant will react with a certain contaminant in the field: (1) kinetics, (2) thermodynamics, (3) stoichiometry, and (4) delivery of oxidants. On a microscale, kinetics or reaction rates are, perhaps, most important. In fact, reactions that would be considered thermodynamically favorable based on the standard potential values may be impractical under field conditions. The rates of oxidation reactions are dependent on many variables that must be considered simultaneously, including temperature, pH, concentration of the reactants, catalysts, reaction by-products, and system impurities such as natural organic matter (NOM) and oxidant scavengers (ITRC, 2005).

One undesired effect of ISCO is mobilization of naturally present metals in the porous media and this possibility must be evaluated before implementing the remedy.

Figure 13.22 Direct permanganate mixing with contaminated regolith soil over fractured metamorphic rock near Atlanta, GA. Photo courtesy of Rick Marotte, Law Engineering and Environmental Services, Inc.
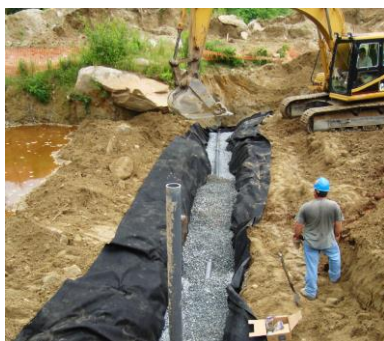
Figure 13.23 *Left*: Installation of a horizontal injection well in a gravel-filled trench design to inject 4% sodium-permanganate solution into a source zone in southern New England. *Right*: ISCO treatment area. The trailer contains a pump to inject the permanganate under pressure. Courtesy of Woodard & Curran, Inc.

13.2.2.5 In Situ Thermal Treatment

In situ thermal heating methods were first developed by the petroleum industry for enhanced oil recovery. These methods were adapted to the treatment of soil and groundwater. Initial variations included hot water injection, steam injection, hot air injection, and electric resistive heating (ERH). Thermal conductive heating was developed in the late 1980s and early 1990s. Currently, steam injection (or steam-enhanced extraction, SEE), ERH, and thermal conductive heating are used for remediation of soil and groundwater in source zones contaminated with chlorinated solvents. These in situ thermal treatment technologies have also been used for treating other volatile and semi-volatile organic contaminants (SVOCs), such as PCBs, PAHs, pesticides, and various fuels, oils, and lubricants that are less amenable to other treatment methods. For example, hot water injection has been used to enhance the recovery of low-volatility and low-solubility oils. RF heating, a variety of ERH that uses radiofrequency energy, has been applied to remediation of various contaminants in the unsaturated zone, but its applicability in the saturated zone has been limited (U.S. EPA, 2004; USACE, 2006).

All thermal technologies are used to lower the viscosity of NAPL and increase the vapor pressure and solubility of VOCs or SVOCs, thus enhancing their removal. Vapor extraction is an integral part of these remediation systems to ensure the removal and treatment of mobilized contaminants. Liquid extraction is also used during steam injection, and sometimes with other thermal technologies when groundwater flow rates are high and/or when the contaminant being recovered is semi-volatile (U.S. EPA, 2006).

To reiterate, vaporization is the main mechanism used in these technologies to enhance the recovery of VOCs. Vapor pressures of organic compounds increase exponentially with temperature, causing significant redistribution to the vapor phase as the subsurface is heated. When an NAPL is present, the combined vapor pressure of the NAPL and water determine the boiling temperature, and co-boiling of the two liquids occurs at temperatures less than the boiling point of water. For example, an azeotropic mixture of PCE and water will boil at 88°C, more than 30°C less than the 121°C boiling point for pure PCE and significantly less than the boiling point of water (U.S. EPA, 2004).

Lower energy ERH (Figure 13.24) can enhance biotic or abiotic contaminant destruction. It delivers an electrical current between metal rods-electrodes installed underground and co-located with SVE wells. The heat generated as movement of the current meets resistance from soil converts groundwater and water in soil into steam, vaporizing contaminants. A low-energy ERH approach raises the subsurface temperatures to approximately 30 to 60°C to enhance the rate of biotic and abiotic contaminant dechlorination, respectively.

Figure 13.24 ERH system for remediation of contaminated soil and groundwater. Note that the surface was paved to prevent cooling effects of aerial recharge. From EPA-542-F-21-016; in public domain.

13.2.2.6 Bioremediation

Bioremediation is a technology that uses microorganisms to treat contaminants through natural biodegradation mechanisms (intrinsic bioremediation) or by enhancing natural biodegradation mechanisms through the addition of microbes, nutrients, electron donors, and/or electron acceptors (biostimulation). This technology, performed *in situ* (below ground, in place) is capable of degrading organic compounds to non-toxic materials such as carbon dioxide (CO_2), methane, and water through aerobic or anaerobic processes (U.S. EPA, 2001). It includes adding or stimulating the growth of microorganisms, which metabolize contaminants or create conditions under which contaminants will chemically convert to non-hazardous or less toxic compounds or compounds that are more stable, less mobile, and/or inert.

Bioaugmentation is the addition of microbes to the subsurface where organisms able to degrade specific contaminants are deficient. Microbes may be "seeded" from populations already present at a site and grown in aboveground reactors or from specially cultivated strains of bacteria having known capabilities to degrade specific contaminants (U.S. EPA, 2000).

The most commonly used methods to deliver liquid substrates for bioremediation are via installed injection wells or direct-push well points, or by direct injection through temporary direct-push probes (Figure 13.25). Direct-push methods are commonly used for shallow groundwater applications in unconsolidated formations at depths less than approximately 50 ft. This technique is constrained by soil characteristics such as grain size or degree of cementation (i.e., gravel and cobbles, or caliche inhibits use of direct-push technology).

Figure 13.25 Biostimulation, or injection of vegetable oil underground to improve conditions for bioremediation. From EPA-542-F-21-004; in public domain.

Direct injection through direct-push probes (e.g., Geoprobe®) does not leave well points in place and is only practical for long-lasting substrates such as HRC®, vegetable oil emulsions, or whey slurries. These substrates release carbon over periods of 6 months to several years and typically require injection on 7.5 to 15-ft centers to treat the target zone (Parsons, 2004). Permanent wells are typically used for continuous or multiple injections or recirculation of soluble substrate. Use of permanent injection wells is also necessary where direct-push technology is impractical, such as greater treatment depths and difficult lithology. Existing monitoring or extraction wells from previous investigation or remediation activities may also be used where applicable.

13.2.2.7 Permeable Reactive Barriers

The concept of a PRB is relatively simple. Reactive material is placed in the subsurface where a plume of contaminated groundwater must flow through it, typically under its natural gradient (creating a passive treatment system), and treated water comes out the other side (Figure 13.26). The PRB is not a barrier to the flow of groundwater, but it is a barrier to the contaminant. When properly designed and implemented, PRBs are capable of remediating a number of contaminants to regulatory concentration goals (U.S. EPA, 1998b). PRBs can be installed in various configurations, using trenches or by injecting reactive materials into the subsurface via boreholes. If the injected materials serve to enhance biodegradation of the contaminant(s), such barriers are called biobarriers.

The PRB treatment zone may contain metal-based catalysts for degrading volatile organics, chelators for immobilizing metals, nutrients and oxygen for microorganisms to enhance biodegradation, or other agents. Degradation reactions break down the contaminants in the groundwater into benign by-products. A precipitation wall reacts with the contaminants to form insoluble products that remain in the wall as the water passes. A sorption wall adsorbs or chelates contaminants to the wall surface (U.S. EPA, 1998b). In general, contaminant treatment in PRB may occur through physical, chemical, or biological processes (ITRC, 2011).

Granular iron has been the most widely used reactive media in full-scale PRBs (Figure 13.27). The prevalent use of granular iron, or zero-valent iron (ZVI), stems mainly from its documented ability to abiotically degrade a variety of contaminant types, the most common of which are the chlorinated solvent compounds such as perchloroethylene (PCE) and trichloroethylene (TCE). The abiotic process involves corrosion (oxidation) of ZVI and reduction of dissolved chlorinated hydrocarbons. The process induces highly reducing conditions that cause substitution of chlorine atoms by hydrogen in the structure of chlorinated hydrocarbons.

In the past decade or so, alternative PRB designs using non-iron-based reactive materials to treat additional contaminants have gained popularity. For example, reactive materials such as compost, zeolites, activated carbon, apatite, and limestone have been used to control pH, metals, and radionuclides, whereas materials designed to stimulate secondary processes (e.g., adding carbon substrate and nutrients to enhance microbial activity) have been used in temporary (non-permanent) barriers created by injection boreholes (see earlier Figure 13.25).
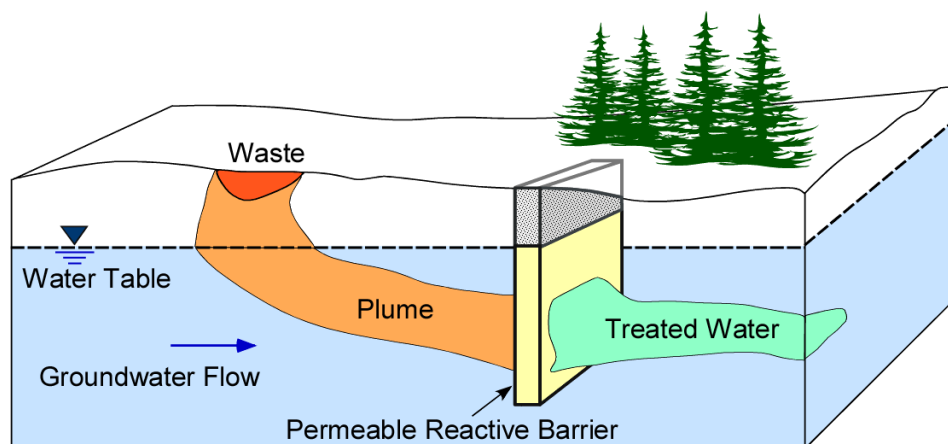
Figure 13.26 Example of a plume being treated by a permeable reactive barrier (PRB). Modified from U.S. EPA, 1998b. In public domain.

Figure 13.27 *Left*: Installation of ZVI PRB at a U.S. Coast Guard facility using a one-pass trencher. *Right*: Coarse-grained ZVI being placed in a trenched PRB. Courtesy of ITRC, 2011. Copyright ITRC; acknowledgement required for further use.

13.2.2.8 Monitored Natural Attenuation (MNA)

MNA, sometimes referred to as passive bioremediation, is defined as use of natural F&T processes, such as contaminant dilution, volatilization, degradation, adsorption, diffusion, dispersion, immobilization, and chemical reactions with subsurface materials to reach site-specific remediation goals (Wiedemeier et al., 1998; U.S. EPA, 1999a; Chapelle et al., 2007). In the engineering practice, the effectiveness of MNA is evaluated on a site-by-site basis by considering three lines of evidence: (1) historical monitoring data showing decreasing concentrations and/or contaminant mass over time, (2) geochemical data showing that site conditions favor contaminant transformation or immobilization, or (3) site-specific laboratory studies documenting ongoing biodegradation processes.

A major difficulty in confirming and measuring natural attenuation lies in its complexity and in the fact that most of the dominant and critical attenuation mechanisms cannot be determined directly. For example, in current practice, there is no direct field measure that biodegradation is occurring. Instead, laboratory microcosm studies using groundwater and soil samples from the site, and/or samples of indicators that measure conditions suitable for biodegradation and breakdown products are collected at the site to provide evidence that biodegradation is occurring. Therefore, multiple parameters are needed, plus an understanding of their relationships to accurately assess MNA. The stakeholder or decision makers determine the amount of evidence needed in order to make a defensible decision. The question then arises, how much evidence is enough?

It has been emphasized by regulatory agencies and practitioners alike that MNA is not a "do-nothing" approach because it involves (ITRC, 1999)

- Characterizing the F&T of the contaminants to evaluate the nature and extent of the natural attenuation processes.
- Ensuring that these processes reduce the mass, toxicity, and/or mobility of subsurface contamination in a way that reduces risk to human health and the environment to acceptable regulatory levels.
- Evaluating the factors that will affect the long-term performance of natural attenuation.
- Monitoring of the natural processes to ensure their continued effectiveness.

MNA has been the favorite first option for consideration at most (if not all) groundwater contamination sites for decades now. Although it has been approved as the sole remedy at a relatively few complex sites, it is always very attractive as a supplemental remedy for three main reasons: it is noninvasive, does not require use of energy and working equipment, and has a much lower implementation cost compared to various engineered groundwater remediation systems. However, installation of monitoring wells, which is a necessary part of any MNA remedy, may involve a significant initial cost.

One of the potentially most attractive aspects of MNA to general public is that it is "noninvasive": unlike many elaborate engineered site cleanup facilities, it is "quietly" working below ground so that the land surface aboveground may continue to be used. In its effort to educate the public on the benefits of natural attenuation and bioremediation in general and to alleviate concerns that MNA is not a "do-nothing" groundwater remedial alternative, U.S. EPA has published various pamphlets (e.g., U.S. EPA, 1996b). Importantly, the Agency generally expects that MNA will only be appropriate for sites that have a low potential for contaminant migration (U.S. EPA, 1999c).

13.2.2.9 Impermeable Barriers

Impermeable barriers, sometimes referred to as vertical engineered barriers (VEB) are built below ground to control the flow of groundwater. VEBs may be used to divert the direction of contaminated groundwater flow to keep it from reaching drinking water wells, wetlands, or streams. They also may be used to contain and isolate contaminated soil and groundwater to keep them from mixing with clean groundwater. VEBs differ from permeable reactive barriers in that they do not clean up contaminated groundwater (U.S. EPA, 2020). Common types of VEBs include slurry walls and sheet pile walls (Figure 13.28).
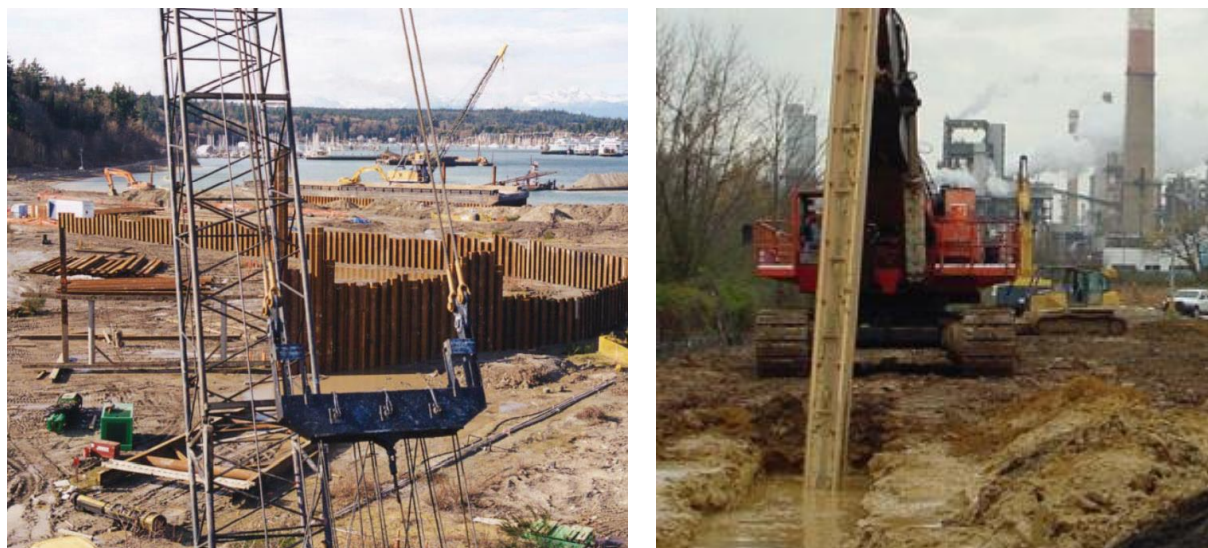
Figure 13.28 *Left*: Installation of sheet piling. *Right*: Construction of a slurry wall. From EPA-542-F-21-026. In public domain.

Slurry walls are considered baseline barrier technology. "It is the expert consensus" that, if properly designed and constructed, slurry walls can successfully contain waste at contaminated sites (Rumer and Mitchell, 1996). Slurry walls have been used for pollution control since 1970, and the technology is accepted and regarded as an

effective method of isolating hazardous waste and preventing the migration of pollutants (Pearlman, 1999). Barriers installed with the slurry trenching technology consist of a vertical trench excavated along the targeted section of the site, filled with bentonite slurry to support the trench and subsequently backfilled with a mixture of low-permeability material. Such walls are usually keyed into an underlying aquitard (a low-permeability soil or rock formation), or a few feet below the groundwater elevation when the objective is to contain LNAPL.

Deep soil mixing technology was developed in Japan and consists of in situ mixing of soil and a slurry. The specially designed equipment typically consists of large-diameter counter-rotating augers mixing in situ soils with additives. A water-bentonite or cement slurry is injected into the soil as the augers are advanced, resulting in a column of thoroughly mixed soil. This technology is also referred to as solidification and stabilization (see next section). A continuous barrier is created by overlapping columns. Deep soil mixed barriers can achieve permeabilities of $10-7$ cm/s. Because potentially contaminated materials are not excavated, the advantages of using deep soil mixing technology include reduction of health-and-safety risks and elimination of costs associated with handling and disposal of contaminated soils (USEPA, 1998a).

Sheet-pile cutoff walls are constructed by driving vertical strips of steel, precast concrete, aluminum, or wood into the soil, forming a subsurface barrier wall. The sheets are assembled before installation and driven or vibrated into the ground, a few feet at a time, to the desired depth. Sheet-pile walls traditionally have consisted of steel sheeting with some type of interlock joint. Plastic has been substituted for steel in a number of applications. Sheet-pile walls have long been used for a wide variety of civil engineering applications, but their use in environmental situations has been limited. Sheet-pile wall installation is limited to shallow depths and unconsolidated materials. Although steel sheet-pile walls are strong and steel will not hydrofracture, the interlocking joints present a leakage problem. The ability of steel sheet piling to meet a typical $10-7$ cm/s design performance standard depends on the type of material used to seal the interlocking joints.

Grout barriers ("walls" or "curtains") have been used extensively for civil engineering projects (e.g., see USACE, 1984), but less frequently at hazardous waste sites. These are usually more expensive than other techniques, and the barriers have higher permeability. However, grout walls can have greater depths than any other type of subsurface barriers and can extend through bedrock. Construction of grouted barriers involves injection of a grout into the subsurface. Pressure grouting and jet grouting are both forms of injection grouting, in which a particulate or chemical grout mixture is injected into the pore spaces of the soil or rock. Particulate grouts include slurries of bentonite, cement, or both and water. Chemical grouts generally contain a chemical base, a catalyst, and water or another solvent. Common chemical grouts include sodium silicate, acrylate, and urethane. Particulate grouts have higher viscosities than chemical grouts and are therefore better suited for larger pore spaces, whereas chemical grouts are better suited for smaller pore spaces (USEPA, 1998a; USACE, 1995).

13.2.2.10 Other Technologies

Solidification and Stabilization (S/S) refer to a group of remediation methods that prevent or slow the release of contaminants to groundwater. These methods usually do not destroy the contaminants. Instead, they keep them from leaching above regulatory levels into the surrounding porous media. Solidification and stabilization are often used together. Solidification involves mixing the impacted soil and sediments, including in the saturated zone, with a binding agent, which is a substance that makes unconsolidated sediments bind together. Common binding agents include cement, asphalt, fly ash, and clay. Like solidification, stabilization involves mixing impacted soil and sediments with binding agents. However, the binding agents also cause a chemical reaction with contaminants to make them less likely to be released into the surrounding porous media. For example, when soil contaminated with

metals is mixed with water and lime — a white powder produced from limestone — a reaction changes the metals into a form that will not dissolve in groundwater (U.S. EPA, 2020).

Flushing involves flooding a zone of contamination with an appropriate solution to remove the contaminant from the soil. Water or liquid solution is injected or infiltrated into the area of contamination. The contaminants are mobilized by solubilization, formation of emulsions, or a chemical reaction with the flushing solutions. After passing through the contamination zone, the contaminant-bearing fluid is collected and brought to the surface for disposal, recirculation, or on-site treatment and reinjection. Flushing solutions may be water, acidic aqueous solutions, basic solutions, chelating or complexing agents, reducing agents, cosolvents, or surfactants (U.S. EPA, 2006).

Institutional Controls (ICs) are defined by U.S. EPA as "non-engineered instruments, such as administrative and legal controls, that help to minimize the potential for human exposure to contamination and/or protect the integrity of a response action. ICs typically are designed to work by limiting land and/or resource use or by providing information that helps modify or guide human behavior at a site. ICs are a subset of Land Use Controls (LUCs). LUCs include engineering and physical barriers, such as fences and security guards, as well as ICs. Some common examples of ICs include zoning restrictions, building or excavation permits, well drilling prohibitions, easements, and covenants (U.S. EPA, 2020.)

Technical Impracticability (TI) waiver may be included in a RD (remedial decision) document when determined that groundwater restoration is technically impracticable from an engineering perspective. As stated by the Agency "While U.S. EPA is committed to restoring groundwater at Superfund sites, there are circumstances that may warrant waiving the requirement for groundwater restoration." U.S. EPA (2020)

TI waivers generally will be applicable only for ARARs (applicable or relevant and appropriate requirements) that are used to establish cleanup performance standards or levels, such as chemical-specific MCLs (maximum contaminant levels) or State ground-water quality criteria. (U.S. EPA, 1993).

One hundred and five (105) decision documents from FYs 1988 through 2017 specify TI waivers for groundwater (U.S. EPA, 2020.) These 105 documents are for 96 sites (note that sites may issue multiple TI waivers to address different plumes or areas of the site.)

Vapor Intrusion Mitigation. Vapor intrusion is the movement of chemical vapors from contaminated soil, groundwater or sewer lines into nearby buildings. Vapors enter buildings primarily through openings, such as cracks and seams in the foundation or basement walls, gaps around utility lines, and sump pits. They can also enter homes from sewer lines due to chemicals disposed of in drains. Once inside the home or workplace, inhaled chemical vapors may pose health risks for occupants. In some cases, buildup of vapors, such as those from methane or gasoline, may cause explosive conditions. Vapor intrusion mitigation removes or decreases the amount of vapor that enters a home. The long-term response to vapor intrusion into buildings is to remove or reduce the underground contamination that is the source of vapors – usually contaminated groundwater, subsurface soil or sewer lines.

Vapor intrusion mitigation methods are available for both existing buildings and those planned for construction near the contaminated area. Chemical vapor entry into buildings can be mitigated by (U.S. EPA, 2022e):

- Sealing openings: Filling cracks in the floor slab and gaps around pipes and utility lines in basement walls or pouring concrete over unfinished dirt floors.
- Installing vapor barriers: Placing sheets of geomembrane or strong plastic beneath a building to prevent vapor entry. Vapor barriers are best installed during building construction but can be installed in existing buildings that have crawl spaces.

- Passive venting: Installing a venting layer beneath a building, usually with a vapor barrier. Wind or the buildup of vapors moves the vapors through the venting layer toward the sides of the building where they vent to outside air. A venting layer can be installed before building construction or underneath existing buildings.
- Sub-slab depressurization: Connecting a blower (an electric fan) to a suction pit underneath the building foundation, which vents vapors from below the foundation to outside air.
- Building over-pressurization: Adjusting the building's heating, ventilation, and air-conditioning (HVAC) system to make the pressure indoors greater than the sub-foundation pressure.

13.2.3 Sustainable Groundwater Remediation

As discussed by Kresic and Mikszewski (2013), the Visalia Pole Yard remediation project is often hailed by U.S. EPA as an exemplary success story, a fact that has likely contributed to the rapid growth of in-situ thermal technology in the 2000s. For example, in a publication prepared for the U.S. EPA, Ryan (2010) states:

"The Visalia Pole Yard Superfund site attained all soil and groundwater remediation goals, becoming one of the best examples to date of a site with massive quantities of DNAPL in the saturated zone that has achieved and sustained drinking water standards following a source-mass depletion remedy."

To remediate groundwater contaminated by creosote and pentachlorophenol to applicable standards, the following activities were conducted over a thirty-one-year period:

- Groundwater pump and treat with discharge to publicly owned treatment works (1975-1985).
- Construction and operation of an on-site groundwater treatment system to continue operating the pump and treat system (1985-1997).
- Steam-enhanced extraction (1997-2000).
- Installation and operation of an enhanced biodegradation system with continued pump and treat operation (2000-2004).
- Excavation of shallow soils from 0-10 feet below ground surface (2006). (U.S. EPA, 2009c).

The final close out report for the site listed the total remedial cost between 1996 and 2006 as approximately $30 million (over two-thirds of which was the thermal remediation). Costs for the first twenty years of pump and treat operation and treatment building construction <u>were not provided</u>, nor was the total energy consumed by the thermal remediation (USEPA, 2009c). Without digging deeper, it may appear that the end result of clean groundwater justifies this significant expenditure, and that the remediation was necessary to protect human health and the environment and to restore beneficial use of the property and its underlying groundwater. Unfortunately, as detailed in the ROD (USEPA, 1994) and the final site close out report (U.S. EPA, 2009c), this was not the case.

First of all, no private or public drinking water was contaminated by the Visalia Pole Yard site. The following text is taken directly from the ROD (U.S. EPA, 1994):

"The primary contribution to risk for each of these populations (on- and off-site occupational workers and off-site residents) *is the estimated hypothetical future ingestion of groundwater from the intermediate aquifer. On-site wells are used for groundwater monitoring and treatment extraction purposes only. <u>Thus, groundwater exposures evaluated in this risk assessment are hypothetical</u>* (emphasis added)*"*

Kresic and Mikszewski (2013) acknowledge that contamination of potential future drinking water resources has long been justification for requiring remediation to MCLs, and the above quotation is only provided to illustrate that there were no actual exposures associated with the site that exceeded risk thresholds at the time of the ROD. In fact, the general public was not particularly interested in the clean-up in the first place, as evidenced by the "Community Relations Activities" section of the site close out report (U.S. EPA, 2009c – emphasis added):

> *"Community involvement activities included the development of a Community Relations Plan (CRP), prior to initiation of the RI/FS activities. The CRP included development of a community profile and a list of key local contacts. <u>The community profile indicated the surrounding area was mainly businesses that had little interest in the site cleanup activities</u>. Copies of the Draft ROD were made available at the local public library, DTSC and USEPA Region IX Record Center. Notification of the issuance of the Draft ROD was made. A Public Notice was also placed in the local newspaper. A Public Meeting was held in Visalia, California on October 13, 1993, to provide information on the proposed cleanup. <u>There were no members of the public in attendance at the meeting.</u>"*

More disturbing is that the five-year review specifically stated that "there are no specific redevelopment plans currently planned for the site." Site redevelopment opportunities were actually <u>severely limited</u> by a "Covenant to Restrict Use of Property, Environmental Restriction," which was required as part of the ROD. The following text related to this covenant is taken from U.S. EPA, 2009c:

> *"As remedial action objectives are based on industrial cleanup standards, prohibited Site Uses include: residences, human hospitals, schools, and day care centers for children. Prohibited Activities include: soil disturbance greater than ten feet below grade, <u>and the installation of water wells for any purpose</u>* (emphasis added)."

When considering all of the above information, it is unclear who or what exactly benefited from the remediation, other than the site environmental consultant and thermal remediation vendor. The community was unaffected by the site and did not participate actively in site redevelopment plans (of which there were none), and future use of the groundwater that was remediated to site-specific standards (because of a hypothetical future exposure risk) is strictly prohibited by law. Additionally, the contaminated groundwater did not discharge to a surface water feature or result in any known adverse ecological impact. It therefore seems that $30 million+ was spent simply to prove the point that remediation of DNAPL sites to some standard is feasible. It is still perplexing however that the site closure report strictly prohibits any future use of groundwater underlying the site including installation of any wells (Kresic and Mikszewski, 2013). In other words, no one will ever be able to find out if the groundwater at the site is suitable as a drinking water source and if many tens of millions of dollars were spent reasonably in that respect.

The frequency with which sites such as the Visalia Pole Yard are aggressively remediated with unclear benefits leads to the question posed by many over the past forty years, "Are Superfund clean-ups really worth the cost?" Two working papers produced by the Massachusetts Institute of Technology (MIT) Department of Economics seek to answer the above question, evaluating the benefits of Superfund from an economic (Greenstone and Gallagher, 2008) and public health (Currie et al, 2011) perspective.

Greenstone and Gallagher (2008) assess the economic benefits of Superfund by comparing housing market outcomes in the areas surrounding the first 400 sites selected for Superfund clean-up to the areas surrounding the 290 sites that narrowly missed qualifying for the program. The results of the study indicate that Superfund clean-ups lead to changes in local residential property values that are statistically indistinguishable from zero. This is also true for property rental rates, housing supply, total population, and the types of individuals living near the sites.

This conclusion indicates that economic benefits of Superfund likely fall short of the high costs of the program. Potential explanations for and implications of this phenomenon are provided in the paper, as quoted below:

"In our view, the most likely explanations are that the people that choose to live near these sites do not value the clean-ups or that consumers have little reason to believe that the clean-ups substantially reduce health risks. In either case, the results mean that local residents' gain in welfare from Superfund clean-ups falls well short of the costs. Unless there are substantial benefits that are not captured in local housing markets, less ambitious clean-ups like the erection of fences, posting of warning signs around the sites, and simple containment of toxics might be a more efficient use of resources."

The Currie et al (2011) study clearly demonstrates the need to eliminate actual (not hypothetical) contaminant exposures related to hazardous waste sites. However, how to most efficiently eliminate existing and prevent future exposures across the country is beyond the realm of Superfund as we know it.

<u>Sustainable groundwater remediation</u> is an emerging field that has been specifically developed to counteract the irrational mind-set of the Visalia Pole Yard clean-up and other similar projects. The concept was originally introduced by the US Sustainable Remediation Forum (SURF) in a 2008 white paper (SURF, 2009), and has since rapidly spread throughout the United States and European Union (EU). In its Summer 2011 issue, the journal *Remediation* published the first guidance documents on the subject, which together present a framework for sustainable remediation, detail necessary steps in completing environmental footprint analysis and life-cycle assessments, and identify metrics for incorporating sustainable practices in remediation projects (see Simon, 2011 for an overview). Unfortunately, more than a decade later, the concept has gained exactly zero ground among various regulators in the United States which continue to insist on a pyrrhic struggle to remediate groundwater to MCLs regardless of the associated costs, socio-economic benefits, and risks. In many cases this struggle includes complex hydrogeologic environments where the restoration of groundwater to MCLs may take hundreds of years and/or may be technically impracticable to begin with.

The above discussion brings up another concept, highly contested and yet to be clearly defined by the regulatory agencies: <u>reasonable timeframe for groundwater remediation</u>. The position of U.S. EPA is that a reasonable timeframe for restoring groundwater to beneficial uses depends on the particular circumstances of the site and the restoration method employed. A comparison of restoration alternatives from the most aggressive to passive will provide information concerning the approximate range of time periods needed to attain groundwater cleanup levels. An excessively long restoration timeframe, even with the most aggressive restoration methods, may indicate that groundwater restoration is technically impracticable from an engineering perspective (U.S. EPA, 1996). Notably, however, the various U.S. EPA Regions have differing views on the use of technical Impracticability (TI) Waivers, including definition of "reasonable". For example, as of 2023, Region 4 (Alabama, Florida, Georgia, Kentucky, Mississippi, North Carolina, South Carolina, Tennessee and 6 Tribes) has issued only one such waiver since the U.S. EPA published the guidance on TI waivers in 1993.

It should be noted that a "reasonable time frame" is sometimes generically applied to be 100 years, based on the order-of-magnitude number provided by U.S. EPA (1993). However, there is no accepted definition of "reasonable" as applied to groundwater restoration because it is dependent on the applicable technologies and site-specific conditions such as hydrogeology. This leads to confusing and contradictory interpretations of what "reasonable" really means. In some instances, stakeholders have interpreted timescales on the order of 600 years to be "reasonable," whereas others have viewed timescales greater than 30 years to be technically impracticable (Deeb et al, 2011). Consequently, in case of the former interpretation, a remedial measure estimated to reduce the cleanup time to 300 years may be considered reasonable and practicable versus a 600-year cleanup time estimated

under baseline conditions. It is not clear how a clean-up time of 300 years is reasonable in any way, shape, or form. Consider for example that 300 years ago the year was 1723 and the United States of America did not even exist.

There are also definitive technical reasons why choosing between remedies with clean-up timeframes in the hundreds of years is fundamentally wrong. Economically, most of the net present value of any remedial alternative will be captured in the first thirty years of costs indicating that long-term remedial cost differences 100 or more years in the future are irrelevant. The accuracy of numerical modeling at these timescales is also questionable, as quoted below from a U.S. EPA-issued ROD (U.S. EPA, 1999e):

"The longer the time frame simulated, the greater the uncertainty associated with the modeling result. While the time to reach remedial objectives at all points in the Joint Site groundwater will likely be on the order of 100 years, simulations greater than the order of 50 years into the future are generally not reliable or useful. EPA has used simulations of 10-25 years for comparing remedial alternatives, even though the remedial action is not complete in that time frame under any of the alternatives. This provides a measure of each alternative's relative performance and progress at 25 years toward meeting the remedial objectives."

This U.S. EPA statement directly contradicts other ROD decision documents where modeling is used to justify selection of one remedial approach over another when both alternatives have estimated clean-up times greater than 100 years. Inconsistent regulatory guidance regarding technical standards of practice and, more fundamentally, inconsistent interpretation of what constitutes a "reasonable" timeframe will continue to hinder sustainable remediation approaches until social and economic factors are considered in the clean-up process and incorporated into regulations.

Sustainable remediation is defined as a remedy or combination of remedies whose net benefit on human health and the environment is maximized through the judicious use of limited resources (SURF, 2009). This is achieved by balancing economic growth, protection of the environment, and social responsibility to improve the quality of life for current and future generations (U.S. EPA, 2011d). Thus, the "triple bottom line" of sustainable remediation is measured by environmental, social, and economic factors (Butler et al, 2011). A diagram illustrating interconnections within the triple bottom line is presented in Figure 13.29.
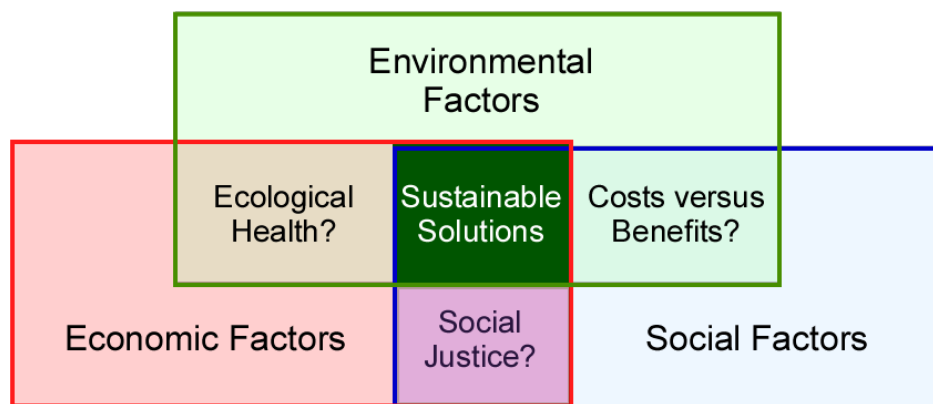
Figure 13.29 Sustainable remediation's triple bottom line. Modified original figure from Kresic and Mikszewski, 2013. Based on concept from U.S. EPA, 2011d. Sustainable remediation attempts to achieve the optimal balance between social, environmental, and economic factors.

The Sustainable Remediation Framework, defined by Holland et al (2011), is characterized by the following key elements:

- Process-based implementation that includes several decision points necessary to achieve the final outcome. This is an alternative to the more rigid and traditional goal-based implementation where all focus in placed on meeting a specific regulatory requirement (e.g., MCLs).

- Future-use planning that manages the entire site clean-up process with the preferred end-use or future use in mind. This includes a transition strategy that efficiently moves the project from the remediation stage to the long-term use stage after achieving remedial objectives.

- A tiered sustainability evaluation that maximizes the positive sustainability impacts of the project, as measured through metrics such as such as carbon dioxide emissions, groundwater or energy use, local laborers trained, local suppliers utilized, or native species reintroduced to site habitat (see Butler et al, 2011 for additional metrics).

- Development of a sustainable conceptual site model (CSM) that incorporates sustainable elements, as shown in Figure 13.30. The sustainable CSM can be used to answer complex questions regarding the beneficial use of groundwater at the site, the feasibility of reaching site closure, and how achieving remedial goals will change site risk; and

- Implementation of sustainable remedial measures, including but not limited to:

  - Using in-situ technologies that mimic natural processes and/or result in contaminant mineralization rather than phase transfer. For example, bioremediation, which can result in complete contaminant destruction in-situ, is preferable to thermal remediation where phase change is often required to extract contaminants from the subsurface and to potentially dispose of remediation waste off site.

  - Minimizing or eliminating emissions and natural resource (e.g., energy, water) consumption; this includes minimizing transportation requirements wherever possible.

  - Using renewable energy to power remedial operations.

  - Recycling or reusing soil or demolition materials.

  - Training and employing local workers.

  - Conducting collaborative community events before, during, and after remedy selection and implementation.

In the United States, there has been significant recent interest in "green remediation," a practice defined and encouraged by the U.S. EPA. Green remediation considers all environmental effects of cleanup actions and incorporates options to minimize the environmental footprints of these actions (USEPA, 2011e). Thus, green remediation shares several core elements with sustainable remediation, such as the minimization of energy use and emissions during remediation. However, as discussed by Kresic and Mikszewski (2013), there are critical fundamental differences between the two concepts that are often easy to disguise because of the way that the terms "green" and "sustainable" are often interchanged. For example, the following are key U.S. EPA perspectives on green remediation, quoted directly from U.S. EPA, 2011d:

- *Greener cleanups are not an alternative approach to setting cleanup levels and selecting remedies.*
- *Cleaning up sites for reuse supports sustainable development.*
- *Reducing the environmental footprint of a cleanup does not justify changing the end point.*

CONCEPTUAL SITE MODEL

Traditional Elements

➤Contaminant Source & Release Mechanism

➤Impacted Media

➤Migration Pathways

➤Receptors & Exposure Routes

➤Current & Future Land Use

➤Resource Input & Output

➤Net Environmental Benefit

➤Stakeholder Economic & Social Well-Being

➤High-Level Land-Use Planning

Sustainable Elements
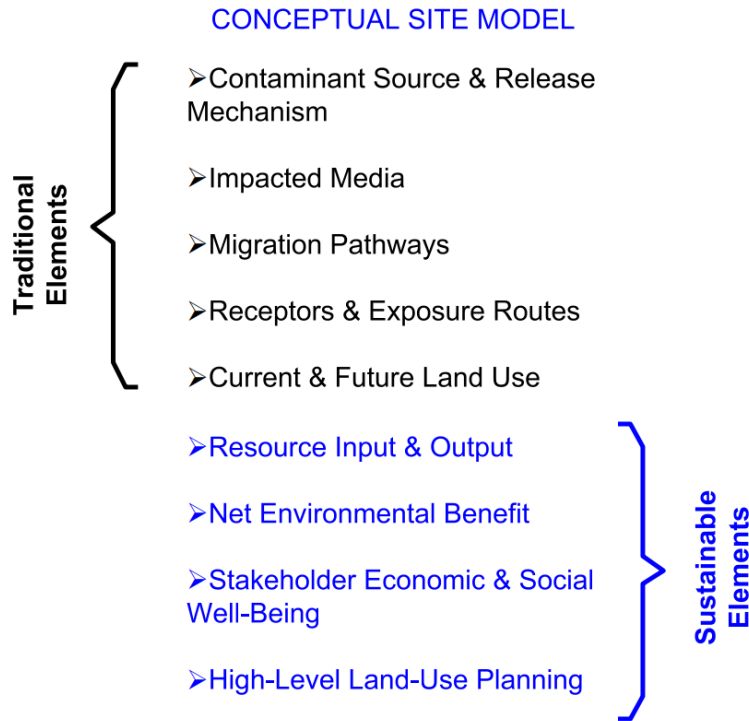
Figure 13.30 Expansion of the traditional conceptual site model to include sustainability factors, as proposed by Holland et al (2011). From Kresic and Mikszewski, 2013. Copyright CRC Taylor & Francis; permission required for further use.

Simply put, green remediation does not incorporate sustainability considerations in selecting the remedial approach or the preferred end-use. Green remediation is strictly process related, while sustainable remediation incorporates social and economic factors to address broader land management issues (USEPA, 2011d). This is unfortunate, as the greatest opportunity to realize sustainable outcomes are in the early stages of remedial implementation while setting the remedial specification and strategy (NICOLE, 2010).

With these fundamental limitations, the potential exists for green remediation to become a good example of what has been termed "LEED brain" in reference to miss-use of the Leadership in Energy and Environmental Design (LEED) building-certification program. LEED brain is a term originally coined by Schendler and Udall (2005) to reflect the absurdity of LEED certifying fundamentally non-sustainable projects because of the inclusion of expensive green features such as rooftop fuel cells and "benches made of salvaged eucalyptus wood" (Owen, 2009).

Owen, (2009) presents an excellent example of LEED brain in his analysis of the Philip Merrill Environmental Center of the Chesapeake Bay Foundation (CBF), which was opened in 2001 and became the first building to be certified as LEED platinum. The CBF facility has innumerable green technologies such as geothermal wells, composting toilets, rainwater-collection systems, and showers for bicyclists. However, the facility was constructed at a remote location along the Chesapeake Bay and is inaccessible to mass transit. The previous CBF headquarters was in downtown Annapolis, MD, and the relocation "turned all of the foundation's eighty employees into automobile commuters" (Owen, 2009). Furthermore, the CBF is an hour-long drive from Baltimore or Washington, DC, which is where most visitors will be coming from by car. This penny-wise, pound-foolish approach to sustainability will not result in a net environmental benefit and fosters the dangerous misconception that sustainability (as measured by the quantity of green gadgets) is very expensive. An alternative (and much less expensive) building in a downtown location accessible to mass transit would have been a much more sustainable

solution for the CBF, regardless of the number of composting toilets used in the construction (Kresic and Mikszewski, 2013).

A transition towards sustainable remediation practices is critical in ensuring the long-term viability of environmental protection programs in the United States and around the World. On-going budget and debt crises will continue to threaten financial resources dedicated to environmental clean-ups, and the remediation industry must do more with less in order to survive. One great danger is political embrace of the Forget About the Aquifer approach, in which all attempts at groundwater restoration will be abandoned in favor of cheaper water supply alternatives (Ronen et al, 2011). The shortcomings of remedial technologies and current clean-up ideologies highlighted in this lecture are not meant to discourage further clean-ups or disparage the idea that pristine environmental resources have intrinsic value. Quite on the contrary, the hope is to galvanize support for holistic and technically sound approaches that can achieve better remedial outcomes while also freeing-up financial resources for assessment and proper management of as many contaminated sites as possible (Kresic and Mikszewski, 2013).

The conceptual diagram in Figure 13.31 illustrates this hope. When published in the book by Kresic and Mikszewski ten years ago, it had optimistically projected the last two phases of the "remediation evolution" the years of which are now grayed out. The updated diagram reflects the continuing hope of the author that sustainable groundwater remediation will eventually become the new norm.
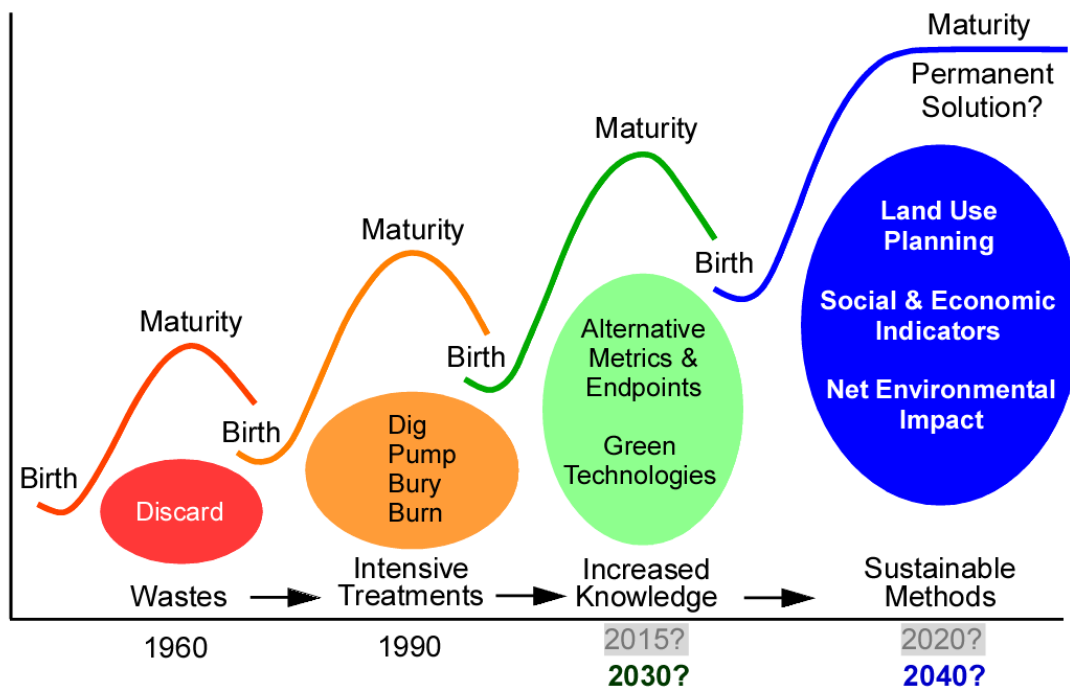
Figure 13.31 Conceptual diagram illustrating the evolution of societal thinking about waste and environmental clean-ups, adapted from a figure originally presented in SURF, 2009. This version has been expanded by Kresic and Mikszewski in 2013 from the original to include the future phases we may be entering in not-so-distant future (Increased Knowledge and Sustainable Methods).

Lecture 14 Field Investigations, Part One

This lecture is based on the materials presented by USGS (Keys, 1990; Lapham et al., 1997; Taylor and Alley, 2001), U.S. EPA (Aller et al., 1991; U.S. EPA, 1986, 1993a, 1995a, 2018), Nielsen (2006), Kresic (2013), and Kresic and Mikszewski (2013), as well as the documents available for download at the U.S. EPA web page titled *Publications on Characterization and Monitoring Technologies for Cleaning Up Contaminated Sites*: https://www.epa.gov/remedytech/publications-characterization-and-monitoring-technologies-cleaning-contaminated-sites

14.1 Health and Safety

It is standard practice in the environmental industry that all field work must have a Site Health and Safety Plan (HASP) which describes the potential hazards of the work site, along with controls and procedures selected to minimize those hazards. Implementation of the HASP requires appropriate training of the field work personnel and management's (e.g., Project Manager, Department Manager, Company Management) commitment to provide such training, adequate resources for field work, self-assessment, and employee involvement. In the United States, Occupational Safety and Health Administration (OSHA; www.osha.gov) requires that employees and their supervisors identify workplace hazards and be trained in the specific hazards and control measures associated with their assigned tasks. Although not explicitly required by OSHA, the written HASP is a valuable tool in providing the field personnel training, and a resource for addressing each identified hazard (OSU, 2023). As discussed by Nielsen et al. (2006), a good HASP must address a wide range of topics, including some that may seem to be unrelated to health and safety. The following sections should be included in the plan:

- Safety staff organization and responsibility of key personnel.
- Safety and health hazard assessment for site operations.
- Personnel protective equipment requirements.
- Methods to assess personal and environmental exposure.
- Standard operating safety procedures, work practices, and engineering controls.
- Site control measures.
- Required hygiene and decontamination procedures.
- Emergency equipment and medical emergency procedures.
- Emergency response plan and contingency procedures.
- Logs, reports, and record keeping.

A model HASP for environmental investigations can be found in Maslansky and Maslansky (1997); procedures for evaluating HASPs can be found in U.S. EPA (1989); health and safety planning for remedial investigations is covered in U.S. EPA (1985); and detailed discussion of various aspects of HASPs is provided by Maslansky and Maslansky (2006).

Potential hazards of field investigations are many and are beyond the scope of this textbook. Photographs in Figure 14.1 serve to illustrate couple of situations where protective clothing, eye wear, gloves, and respirators are used to minimize exposure to chemicals in groundwater that pose specific toxicity or safety concerns.
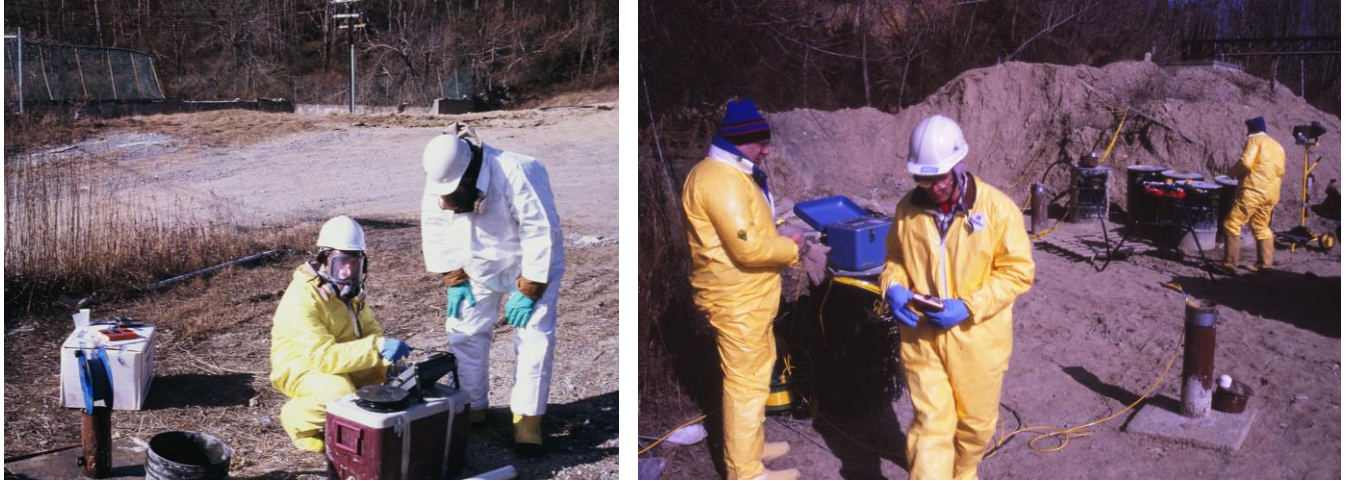
Figure 14.1 Use of personal protective equipment (PPE) during sampling of groundwater impacted by volatile organic compounds (left), and setup for an aquifer pumping test (right) by hydrogeologist Roger Pennifill and his crew of Ebasco Environmental, Inc. at Mattiace Petrochemical Superfund site, Glen Cove, New York.

14.2 Surface Geophysical Investigations

Geophysical techniques can be used to plan and supplement the subsurface investigative boring program. For example, surface geophysical surveys may be used to verify and modify the initial conceptual model prior to drilling boreholes. Based upon the results of the geophysical surveys, boreholes can be effectively located to obtain necessary hydrogeologic information. Information obtained from initial boreholes can be used to evaluate the geophysical data and resolve any ambiguities associated with the preliminary interpretation of the geophysical survey results. The use of surface to borehole geophysical methods may allow better resolution of geophysical and borehole data and may help delineate the subsurface geology between boreholes. When continuous lithologic logging and sampling are not performed, borehole geophysical methods should be used to correlate unsampled with sampled core sections (Cal/EPA, 1995).

The greatest benefits of geophysical methods come from using them early in the site characterization process since they are typically nondestructive, less risky, cover more area spatially and volumetrically, and require less time and cost than using investigative borings and monitoring wells. However, great skill is required in interpreting the data generated by these methods, and their indirect nature creates uncertainties that can only be resolved by use of multiple methods and direct observation. Consequently, preliminary site characterization by geophysical methods will usually be followed by direct observation through the boring/coring, logging, and installation of monitoring wells (U.S. EPA, 1993b).

Geophysical techniques can be used for various purposes in hydrogeologic studies including:

- Geologic characterization, including assessing types and thicknesses of strata and the topography of the bedrock surface below unconsolidated material, and mapping of fractures, cavities, and paleochannels.
- Aquifer characterization, including depth to water table, water quality, hydraulic conductivity, and fractures.
- Contaminant plume identification, both vertical and horizontal distribution including monitoring changes over time.
- Locating buried wastes and other anthropogenic features through identification of buried metal drums, subsurface trenches, and other features (e.g., cables, pipelines).

Surface geophysical methods usually involve wave generators and sensors at or near the ground surface. They include electrical, electromagnetic, magnetic, seismic, acoustic, gravimetric, ground penetrating radar, and thermal methods. Useful publications and descriptions of various surface and borehole geophysical methods are provided at the USGS website https://water.usgs.gov/ogw/bgas/methods.html. Figures 14.2 through 14.6 show some examples of surface geophysical methods typically used in hydrogeologic studies.

Figure 14.2 *Left*: Electromagnetic survey (EM) with terrain conductivity meter (antenna). Photo courtesy of Jeff Manuszak. *Right*: Shallow seismic reflection survey using light ATV mounted Accelerated Weight Drop in rugged terrain. Photo courtesy of Finn B. Michelsen.
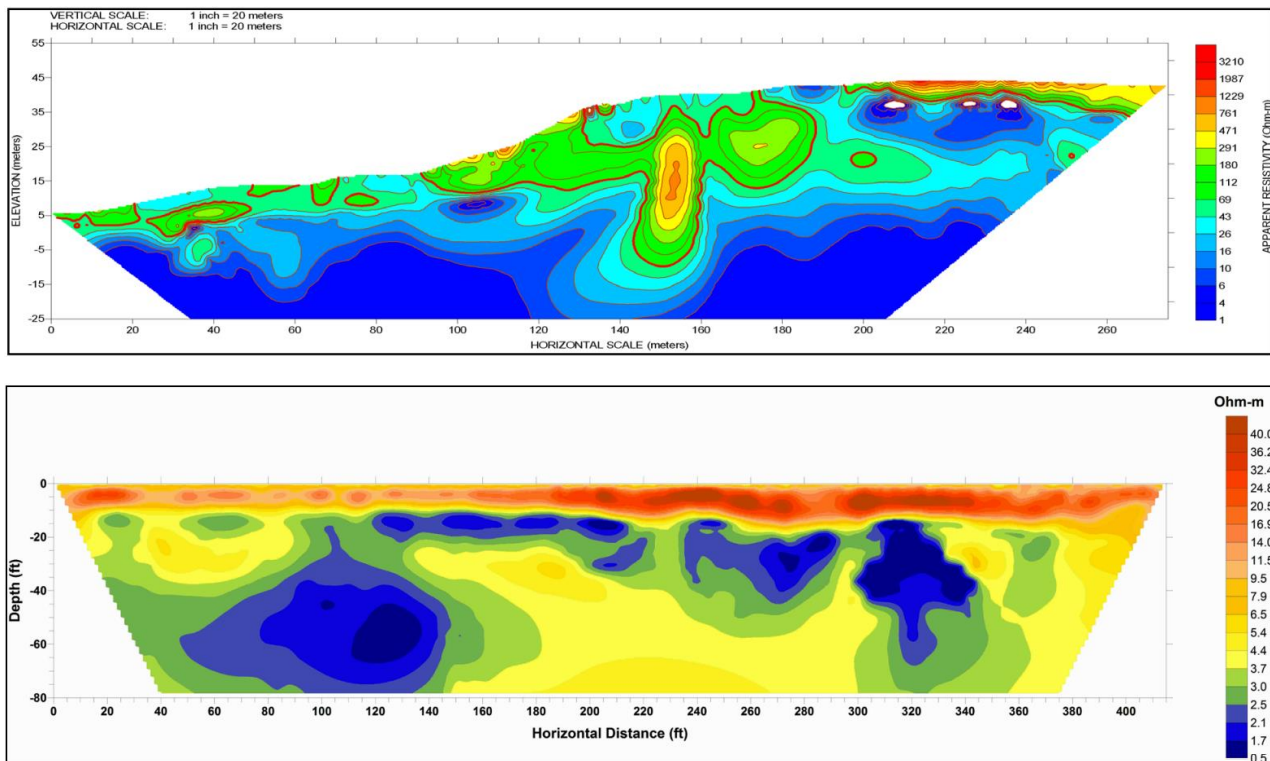
Figure 14.3 *Top*: 2D resistivity inversion section profile for delineation of altered soil zones and depth to competent zones along a 200-meter slope. Zones indicating severely weathered and unstable soil and rock are indicated by the zones with higher resistivity. The section shows large arcuate features near the slope edge. *Bottom*: 2D resistivity inversion section profile for delineation of cavities and active "solution zones" (blue color) in mature, complex karst limestone formation (southeastern USA). Courtesy of Finn B. Michelsen.

Figure 14.4 *Left*: Surveying with Geometrics Ohm mapper capacitively coupled resistivity meter. *Middle*: Scintrex CG-3M microgravity meter. *Right*: Borehole video inspection setup. Photos courtesy of Timothy Bechtel.

Figure 14.5 (A) Cross section showing geologic description of test-hole cuttings superimposed on inverse-modeling results for direct current (DC) resistivity profile #4. (B) geologic description of test-hole cuttings superimposed on conceptual model based on geologic description and inverse-modeling results for DC resistivity along profile #4, Franklin and Webster Counties, south-central Nebraska. Modified from Teeple et al., 2009. USGS, in public domain.

Figure 14.6 The grid of 2D resistivity profile lines is used to build a 3-dimensional data model. Depth-slices represent the extraction of the variation of horizontal resistivity in the x,y plane at depths of 13 feet (left) and 20 feet (right) below ground surface and were used to map extent of Ocala Limestone and solution zones/cavities on a project in Florida, the U.S. Blue shades (low resistivity) indicate possible cavities, whereas orange colors (high resistivity) indicate clayey sediments/residuum over limestone. Courtesy of Finn B. Michelsen.

It cannot be overemphasized that, when geophysical methods are applied individually and, worse yet, without a field confirmation from borings, their results may be misleading. For example, see Figure 14.5 where "resistive shale" and "sand and gravel" have similar resistivity. Another example are some geophysical properties of different karst features that appear together in the subsurface and can mask each other so that any interpretation is ambiguous at best: air-filled cavities and clay-filled cavities have opposite resistivity signature so that a mixture of open and filled cavities cancels each other out.

Geophysics is recommended not as a replacement for borings or other direct testing of the subsurface features, but as a reconnaissance tool to identify areas that might require additional borings, and areas where fewer borings may be necessary thereby optimizing the number and location of borings, and minimizing the overall investigation cost. The most common reconnaissance geophysical techniques are electrical methods based on rock resistivity and conductivity, electromagnetics (EM), spontaneous Potential (SP), and seismics. Using these methods data can be collected relatively rapidly over large areas. In contrast, microgravity surveys are labor-intensive and typically cost two to three times what an electrical, EM, SP, or seismic survey would cost for similar data coverage. Therefore, microgravity surveys are rarely used for reconnaissance. Instead, they are a cost-effective way of providing detailed mapping.

14.3 Borehole Logging and Cross-Sections

A borehole log is the written record of drilling, sampling and, if installed, well construction activities for a given borehole prepared by hydrogeologist or engineer or by the driller. These reports are prepared on site as the borehole is advanced and often are the sole record of significant events that occurred during field work (Ruda and Farrar, 2006).

Identification of the lithology (sometimes referred to as "hydrostratigraphy" in case of hydrogeologic investigations) underlying the site is the first crucial step in developing a hydrogeological conceptual site model (CSM). It includes visual logging of the lithologic samples extracted from the borings. Boring may be accompanied by geophysical logging which is recommended. Representative core samples may also be sent to laboratory for additional characterization including geochemistry, mineralogy, and paleontology, as well as various geotechnical and hydrogeological testing. This includes testing of both disturbed and undisturbed lithologic samples ("core"). When the soil (rocks) and/or groundwater at the site are impacted or are suspected to be impacted by contaminants, the collected lithologic and/or groundwater samples are analyzed for certain parameters on site and may be sent to the laboratory for further analyses.

As emphasized by Kresic and Mikszewski (2013), boring logs and cross-sections derived from them are critical elements of hydrogeological investigations that can be used to present a wide variety of data. Boring logs represent point measurements of the subsurface, while cross-sections interpolate these point measurements into a continuous two-dimensional profile. This is similar to the interpolation of point measurements of hydraulic head into a continuous potentiometric surface. Boring logs and cross-sections can also be used to present:

- Measurements of the potentiometric surface (groundwater elevation at monitoring wells)
- Field screening results from photoionization detectors (PIDs) and other instruments
- Soil and groundwater laboratory analytical results (i.e., hydraulic conductivity, contaminant concentrations)
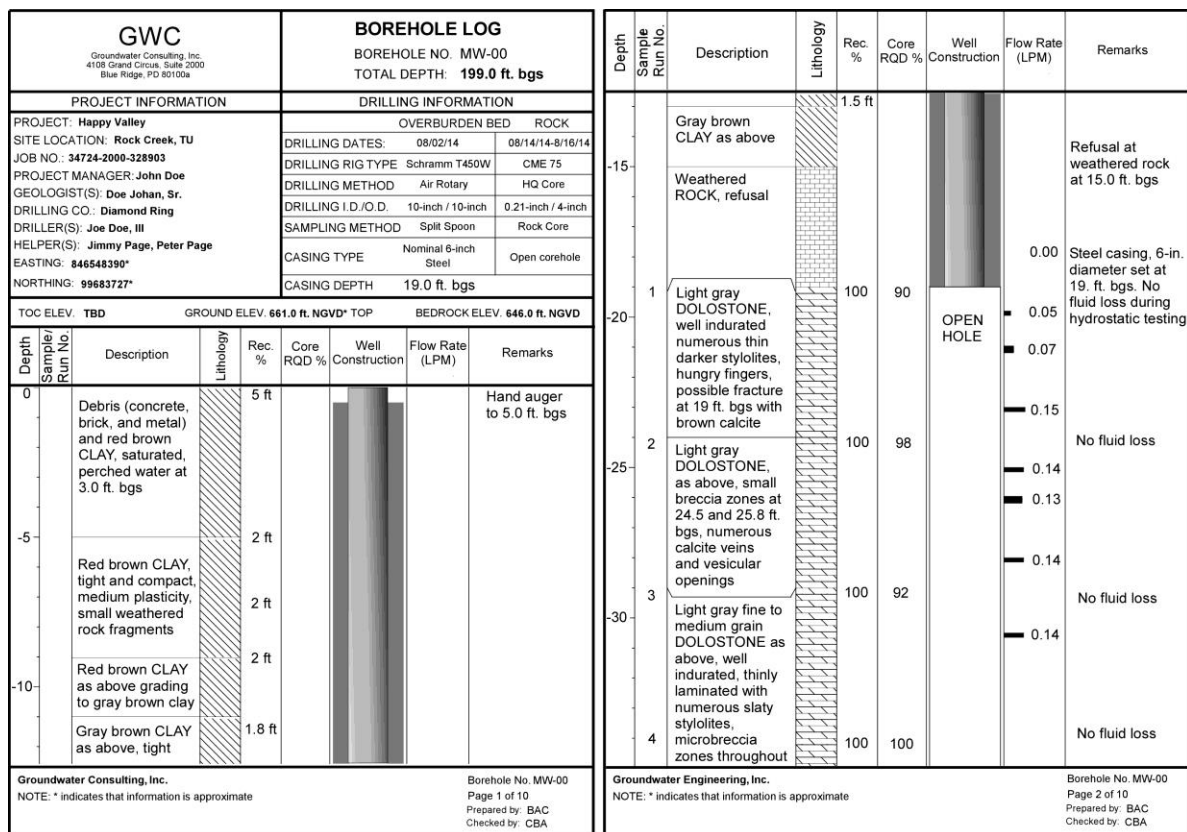
Figure 14.7 Example boring log for a bedrock well drilled using air rotary method, and sampling with split-spoon in the unconsolidated sediments, and rock coring in the bedrock. Modified from Kresic and Mikszewski, 2013. Copyright CRC Taylor & Francis; permission required for further use.

Figure 14.7 is a typical boring log used in a hydrogeological site investigation. It presents a classification of the soil or rock at each depth interval, along with a corresponding graphic. Well construction information, in this case an open-hole bedrock well, is also provided. Note that different soil (unconsolidated sediments) classification methodologies are used in professional practice, with common examples being the United Soil Classification System (USCS; see Table 14.1), the United States Department of Agriculture Classification System, and the Burmeister Classification System. For consolidated ("solid") rocks, the boring log commonly includes descriptions of any fractures, voids (cavities), and discontinuities in general including their number and orientation, any infillings, rock quality designation (RQD), percent core recovery, and other notable characteristics (e.g., see Ruda and Farrar, 2006).

Table 14.1 United Soil Classification System (USCS)

MAJOR SOIL GROUPS		GROUP SYMBOLS	COMMON NAMES
Coarse-grained Soils; more than half material is larger than No. 200 sieve size			
Gravels more than half of coarse fraction is larger than No.4 sieve size (equivalent to 1/4 in. for visual classification)	Clean gravels little or no fines	GW	Well-graded gravels, gravel-sand mixtures, little or no fines
		GP	Poorly graded gravels, gravel-sand mixtures, little or no fines
	Gravels with appreciable amount of fines	GM	Silty gravels, gravel-sand-silt mixtures
		GC	Clayey gravels, gravel-sand-silt mixtures
Sands more than half of coarse fraction is smaller than No.4 sieve size (equivalent to 1/4 in. for visual classification)	Clean sands little or no fines	SW	Well-graded sands, gravelly sands, little or no fines
		SP	Poorly graded sands, gravelly sands, little or no fines
	Sands with appreciable amount of fines	SM	Silty sands, sand-silt mixtures
		SC	Clayey sands, sand-silt mixtures
Fine-grained Soils; more than half material is smaller than No. 200 sieve size			
Silts and Clays Liquid limit is less than 50		ML	Inorganic silts and very fine sands, rock flour, silty or clayey fine sands or clayey silts with slight plasticity
		CL	Inorganic clays of low to medium plasticity, gravelly clays, sandy clays, silty clays, lean clays
		OL	Organic silts and organic silty clays of low plasticity
Silts and Clays Liquid limit is greater than 50		MH	Inorganic silts, micaceous or diatomaceous fine sandy or silty soils, elastic silts
		CH	Inorganic clays of high plasticity, fat clays
		OH	Organic clays and silts of medium to high plasticity
Highly Organic Soils		Pt	Peat and other highly organic soils

In general, one should use a consistent classification system for each boring log at a site and include more information than is provided simply by the USCS nomenclature. For example, solely classifying a soil as "SM: Silty Sand" under the USCS system does not convey any information about the following characteristics:

- The estimated fraction of silt (i.e., 20-50%)
- The gradation of the sand
- The presence of trace amounts of gravel or clay
- The color, moisture content, density, and angularity of the soil
- The presence of odors or other indicators of contamination.

Therefore, it is advisable to use a more robust classification system that incorporates the above parameters. With knowledge of the above parameters, it is very easy to determine the corresponding USCS classification, and commonly the USCS term can be added to the comprehensive soil description at the end in parenthesis (Kresic and Mikszewski, 2013).

After consolidating soil boring logs, the hydrogeologist can interpret the data to create informative cross-sections that become key elements of the CSM. Cross-section development is an art form that requires a detailed understanding of both site-specific data and the regional geological and depositional environment. Knowledge and experience in geology, most notably surficial processes, are paramount. Because professional judgment and interpretation are used to create cross-sections, two different hydrogeologists may create significantly different cross-sections using the same boring log data. This phenomenon is demonstrated by Figure 14.8, which is a cross-section created in AutoCAD, a program commonly used to create digital cross-sections. The connected, colored polygons represent the original interpretation of stratigraphy; however, red-line mark-ups indicate alternative, equally plausible interpretations. The question regarding which interpretation is correct depends upon which version is more representative of the geological processes applicable to the site (Kresic and Mikszewski, 2013).
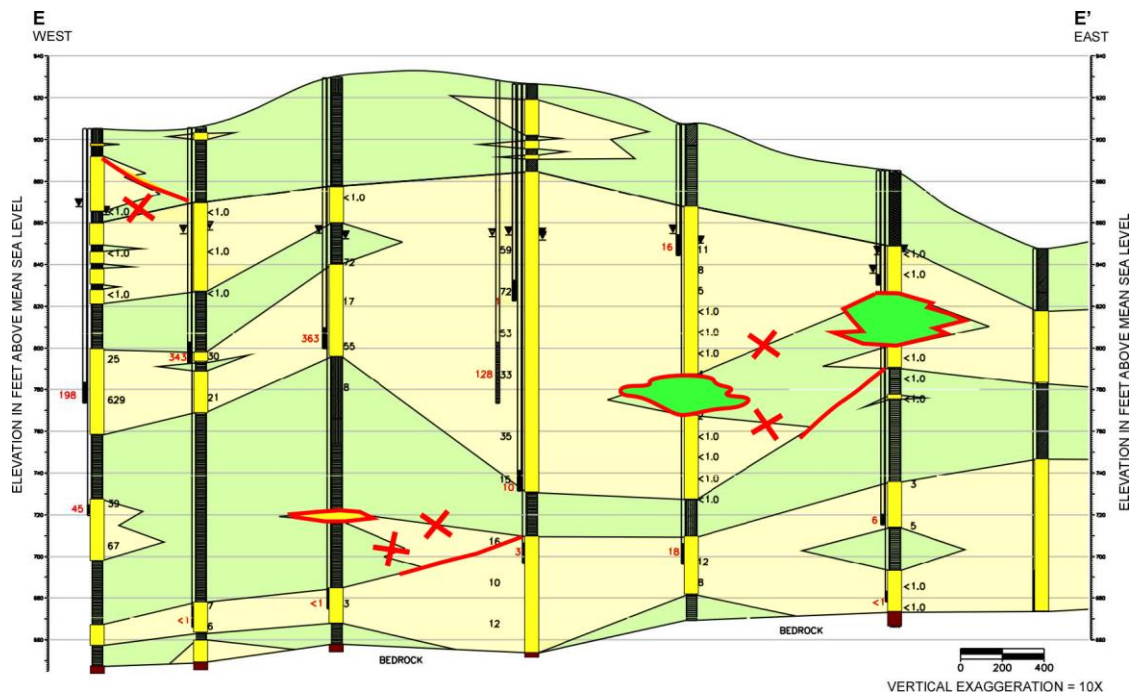
Figure 14.8 Geologic cross section created in AutoCad in large "tablecloth" format (note small lettering). Alternative interpretations are marked in red. Cross section courtesy of Farsad Fotouhi.

14.4 Borehole Drilling and Core Sampling Methods

Various drilling methods may be used to drill boreholes, collect samples, and install environmental monitoring wells under various subsurface conditions. However, U.S. EPA and state agencies prefer methods that case the hole during drilling to minimize possible cross-contamination between different lithologic (hydrostratigraphic) units and depths (U.S. EPA, 2018). In that regard, the two most widely used methods are hollow-stem augers (HSA) in shallow unconsolidated sediments, and sonic methods using an override system in both unconsolidated sediments and solid rocks. Other drilling methods may be used where specific subsurface, or project criteria dictate, particularly in hard rocks and at greater depths.

It is important to emphasize that any groundwater sampling method can cause cross-contamination that affects groundwater sample quality and/or long-term water quality in at least three ways (U.S. EPA (2005):

- Causing contaminant drag-down;
- Creating hydraulic conduits; and
- Biasing samples from improperly decontaminated equipment.

In evaluating the potential for cross-contamination and developing a sampling plan, the site geology, the types of contaminants present, and the sampling methods and equipment used should be examined. For example, drilling a hole through an aquitard creates a potential conduit for contaminant migration. If DNAPLs are perched on top of the aquitard and precautions are not taken, they may migrate down the borehole and contaminate a previously uncontaminated aquifer. In short, the potential for cross-contamination should be considered when advancing any type of groundwater sampling tool or monitoring well into the subsurface because it can result in sample bias, incorrect decisions, or the spread of contaminants (U.S. EPA, 2005).

In cases where cross-contamination is likely or possible, it will be necessary to case off sections of the borehole prior to advancing the borehole to the desired depth to avoid possible vertical migration of contaminants between stratigraphic units or across natural confining layers. Drilling fluids used for the installation of one casing should generally not be re-used for the installation of another casing, particularly where contamination is suspected or present. In general, however, drilling fluids (including air) should be used only when minimal impact to the surrounding formation and groundwater can be ensured. In any case, drilling fluids, drilling fluid additives, or lubricants that impact the analysis of hazardous constituents in groundwater samples should not be used (CA/EPA, 1995).

14.4.1 Hollow-Stem Auger

The hollow-stem, continuous-flight auger is the most frequently employed tool for drilling borings and installing monitoring wells in unconsolidated materials. Augers are likened to giant screws, and continuous flighting refers to a design in which the flights ("threads") of the auger extend the entire length of the auger core or stem. Individual auger sections, typically 5-feet in length, are also called "flights." When drilling, a cutting head or bit, generally with carbide teeth, is attached to the first auger flight, and as the auger is rotated downward, additional auger flights are attached, one at a time, to the upper end of the previous auger flight. As the augers are advanced downward, the cuttings move upward along the continuous flighting.

The hollow-stem or core of the auger allows drill rods and samplers to be inserted through the center of the augers (Figure 14.9). Soil sampling is typically performed with split-spoon, barrel, and thin-wall (Shelby tube)

samplers. **Split-spoons** are tubes constructed of high strength alloy steel with a tongue and groove arrangements running the length of the tube, allowing it to be split in half (Figure 14.4). The two halves are held together by a threaded drive head assembly at the top, and a hardened shoe at the bottom, with a beveled cutting tip. The sampler is driven by a 140-pound weight dropped through a 30-inch interval (ASTM Standard D3550/D3550M), and the number of blows required to drive the sampler provides an indication of the compaction/density of the formation being sampled. **Barrel samplers** are similar to split-spoons, except they cannot be taken apart. A core extruder might be required to remove the core from the barrel. They are less commonly used than split-spoons. Both types of samplers provide disturbed samples not suitable for typical geotechnical and hydrogeological laboratory tests.

Collection of samples with **thin-wall** or **Shelby tube** samplers is similar to split-spoon sampling, except that the tube is pushed into the soil using the weight of the drill rig, rather than driven. The tube is attached to a nonrotating sampling rod, or a wireline assembly that allows the auger to rotate while the tube remains stationary as undisturbed material enters the tube, and the auger flights advance. The undisturbed samples can be used in the laboratory to determine various properties of the soil (sediment) including hydraulic conductivity. One disadvantage of thin-wall samplers is that gravel or cobbles can disturb sample collection or damage walls of the sampler.

Figure 14.9 *Left*: Driving (hammering) split-spoon sampler through hollow-stem auger. *Right*: soil samples are exposed after retrieving and splitting the sampler. Bottom right photo shows collection of hydrocarbon-contaminated soil sample for laboratory analysis. Top right photo courtesy of Dawit Yifru.

14.4.2 Direct-Push Logging

Direct push technology (DPT), also known as "direct drive," "drive point," or "push technology", refers to an extensive family of tools used for performing subsurface investigations by driving, pushing, and/or vibrating small-diameter hollow steel rods into the ground. It uses hollow drive rods either driven percussively or by large forces from a rig weighted or anchored to the ground. Percussive rigs are used for general soil and groundwater investigations and the push only rigs are generally used for cone penetrometer testing (CPT). DPT does not bring cuttings to the surface but instead compresses them into the borehole walls. Small rigs (Figure 14.10), small crews required, and reduced investigation-derived waste (IDW) make DPT operations an economical investigation tool. Although significant depths have been explored with DPT, investigations are generally limited to 100 ft (and more practically 50 ft) in unconsolidated materials (U.S. EPA, 2005, 2018; ITRC, 2006a).

Figure 14.10 DPT rigs are small, maneuverable, and easily adaptable to various drilling conditions including in closed spaces. Left photo courtesy of Jeff Manuszak, right photo courtesy of Nick McMillan.

DPT rods can also be equipped with probes that provide continuous in-situ measurements of subsurface properties (e.g., geotechnical characteristics and contaminant distribution). The most common equipment is a conductivity probe that measures the bulk conductivity (or resistivity) of the adjacent soil as it is advanced. The differences in conductivity can be related to changes in stratigraphy. Although actual soil logs are important to correlate probe readings with actual site conditions, in general, finer-grained sediments (silts and clays) are more conductive than coarser sediments (sands, gravels). Conductivity probes are also affected by soil water content and ionic strength so they can be used to locate contaminant plumes that have a different salt content than naturally occurring water/soils.

DPT and CPT are frequently used in initial site characterization for stratigraphic logging of soft soils, and to help in siting of monitoring wells including their screen intervals. Continuous measurement of soil properties minimizes the possibility of overlooking thin strata that could influence soil behavior (see Figure 14.11). For this reason, the technology is often referred to as "high resolution site characterization". It includes hydraulically pushing a cone-shaped instrument into the soil and measuring its resistance to penetration. Use of a four-channel piezocone allows estimation of hydraulic properties of the soil by measuring pore pressure changes in response to the stresses created by the CPT. Porous probe permeameters can be used in a falling-head or constant-head mode,

as a relatively simple and inexpensive method for determining hydraulic conductivity in the vicinity of the probe. One additional advantage of CPT is that no contaminated fluids are produced during measurements of hydraulic properties.

The combined results of the CPT and piezocone tests can help identify potential preferential contaminant transport pathways in the subsurface. These pathways are especially useful for targeting groundwater sampling locations. Using point-in-time DPT sampling to identify which of these pathways are contaminated can further define optimum intervals for monitoring well screens (U.S. EPA, 2005).
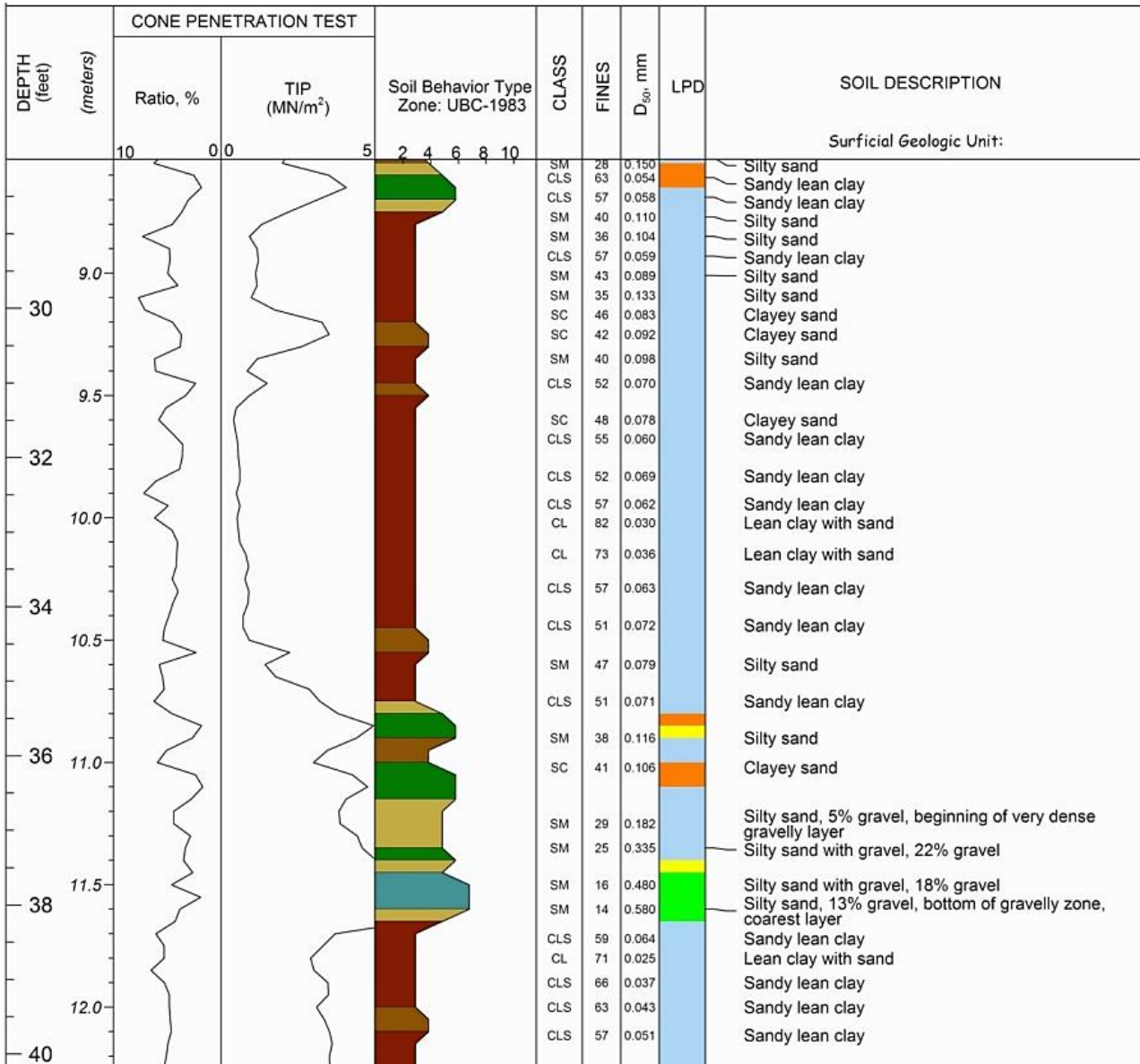
Figure 14.11 CPT log of a boring SNC007c showing tip resistance, friction ratio, UBC soil behavior type, and liquefaction potential display. From Bennett et al., 2011. USGS, in public domain.

14.4.3 Sonic (Rotosonic) Methods

These methods generally alternately advance concentric hollow drill stems using rotation in conjunction with axial vibration of the drill stem. After each stage of drill stem advancement, the inner string is removed with a core of drill cuttings (core barrel) while the outer "override" string remains to hold the borehole open. It is an advanced form of drilling which employs the use of high-frequency, resonant energy generated inside the sonic head to advance a core barrel or casing into subsurface formations. During drilling, the resonant energy is transferred down the drill string to the bit face at various sonic frequencies. Simultaneously rotating the drill string evenly distributes the energy and impact at the bit face. The resonant energy is generated inside the sonic head by two counter-rotating weights. A pneumatic isolation system inside the sonic head prevents the resonant energy from transmitting to the drill rig and preferentially directs the energy down the drill string. The soil or rock core can be removed nearly intact from the inner casing for examination of the stratigraphy prior to sampling or disposal.

While there are several ways to drill using rotosonic method (depending upon site-specific conditions and project objectives), the most common means involves advancing a core barrel, which is overridden by a larger diameter drill string that cases the open bore hole and prevents collapse (Figure 14.12).

Figure 14.12 The sonic drilling procedure. **Step 1** (**left**): The core barrel is advanced using sonic frequencies. When necessary this step can be performed using no fluids, air, or mud. **Step 2** (**middle**): After the core barrel is in place, casing is sonically advanced over the core barrel, protecting the bore hole's integrity in loose unconsolidated ground, i.e., preventing collapse. **Step 3** (**right**): The core barrel is retrieved, producing a relatively undisturbed sample with near 100% core recovery. Steps 1 through 3 are repeated to depth. Courtesy of Fred Hafner, Boart Longyear™

Sonic drilling provides a continuous, relatively undisturbed core sample from both unconsolidated and consolidated (hard) rocks (Figures 14.13 and 14.14). During typical core barrel sampling, the core barrel is advanced 3.05 m (10 ft) using sonic frequencies. Continuous cores have been obtained at depths as great as 700 feet (215 m). Samples can also be extruded into plastic sleeves, minimizing the loss of volatile organic compounds.

The flexibility of advancing a temporary outer casing as the borehole is drilled minimizes the risk of cross contamination. More information on sonic drilling and sampling can be found at https://www.boartlongyear.com/insite/sonic-drilling-works/

Figure 14.13 Retrieving rock sample from core barrel advanced with a sonic drill rig. Courtesy of *Royal Eijkelkamp* (www.royaleijkelkamp.com).

Figure 14.14 *Left*: Examining and sampling a 10-foot sonic core of silty sand retrieved in plastic sleeve. Courtesy of Nick McMillan. *Right:* Sonic cores of clay (yellow to brown color) and white "sand". In this case, "sand" is weakly cemented Ocala limestone which lost its cohesion due to sonic drilling and can therefore be easily mischaracterized (see also Figure 5.13 in Lecture 5).

14.4.4 Rotary Methods

Rotary methods consist of a drill pipe or drill stem coupled to a drilling bit that rotates and cuts through the soils. The cuttings produced from the rotation of the drilling bit are transported to the surface by drilling fluids which generally consist of water, drilling mud, or air. The fluids are forced down through the drill pipe, and out through the bottom of the drilling bit. The cuttings are then lifted to the surface between the borehole wall and the drill pipe (or within a concentric drill stem in reverse rotary). Except in the case of air rotary, the drilling fluid provides a hydrostatic pressure that reduces or prevents borehole collapse. When considering this method, it is important to evaluate the potential for contamination when fluids and/or air are introduced into the borehole. Due to the introduction of the various circulating fluids, the use of rotary methods requires that the potential for contamination by these fluids be evaluated. Water and mud rotary methods present the possibility of trace contamination of halogenated compounds when municipal water supplies are used as a potable water source. Air rotary drilling can introduce contamination by lubricants or entrained material in the air stream. Unless contaminated formations are cased off, the circulation of drilling fluids presents a danger of cross contamination between formations. In any of the rotary methods, care must be exercised in the selection and use of compounds to prevent galling of drill stem threads (U.S. EPA, 2018).

Dual-rotary methods are advantageous for installing wells (both monitoring wells and water-supply wells) in difficult conditions such as unconsolidated deposits with cobbles and boulders, and in unstable consolidated rock

such as karst formations. They are also successful where prevention of cross-contamination between aquifers (water-bearing zones) is critical. Dual-rotary drilling rig utilizes a lower rotary drive which advances casing with a (usually) carbide studded ring welded to the casing bottom. This drive operates completely independently from the top drive which simultaneously handles a drill string equipped with a down-the-hole hammer, drag bit or rolling cone rock bit to drill inside or ahead through the casing. When the casing is advanced ahead of the bit or air hammer, cross contamination and borehole stability problems are minimized. Once the casing is in place, rock coring or well installation can be accomplished in a controlled environment.

Diamond core drilling with rotary methods is a common technique for extracting core samples. It is ideal for semi-consolidated/cemented rock to hard rock environments. Rock coring is generally accomplished with a diamond tip rock core barrel attached to a drill rig. The coring recovers a cylindrical rock core by rotating and advancing the hollow core barrel. There is a wide selection of drill bits and core barrels to choose from based on rock types and core sizes (https://earthengineering.com/geotechnical-investigations/rock-coring; see also Figure 14.15).

Figure 14.15 Students of hydrogeology attending session on rock coring technologies, Texas Hydro-Geo Workshop, Boerne, TX, 2015.

Wireline coring allows rapid placement and withdrawal of the core barrel within the drill rods therefore the rods do not need to be removed to recover each individual core sample. The overshot recovery tool, attached to the winch by a steel cable, is lowered down the center of the rods. When it reaches the back of the core barrel it latches on to it and disengages it from the drill rods. The winch then pulls the complete barrel and its core sample to the surface (Figure 14.16). The only time the drill rods are removed is on completion of the borehole or if the core bit needs replacing (https://earthengineering.com/geotechnical-investigations/rock-coring/).

Figure 14.16 Core sample of compact limestone taken by wire line technique. Courtesy of Zoran Stevanović.

The rock samples provide significant information about the engineering nature of the rock formation. Some important properties obtained from the rock coring are the type of rock, Rock Quality Designation (RQD), percent recovery and hardness/soundness of the rock. This information is used in a wide array of engineering applications including hydrogeologic characterization.

The easiest way to characterize the amount of material recovered during rock coring is to calculate "core recovery" as the amount (i.e., length) of material divided by the total length of the core run (presented as a percentage). Rock Quality Designation (RQD) (ASTM D6032) is a modified core recovery percentage in which the lengths of all sound rock core pieces over 100 mm in length are summed and divided by the length of the core run. Pieces of core that are not hard and sound should not be included in the EQD evaluation even if they are at least 100 mm in length. The purpose of the soundness requirement is to downgrade rock quality where the rock has been altered and/or weakened by weathering. For the RQD evaluation, lengths must be measured along the centerline of the core. Core breaks caused by the drilling process should be fitted together and counted as a single piece of sound rock core. Drilling breaks are usually evidenced by rough fresh surfaces. However, for naturally fractured and stratified rocks it may be difficult to identify core breaks caused by drilling (see Figure 14.17). In this case, the RQD should be estimated conservatively.

Figure 14.17 Dolomitic rock core from deep exploration boring at a site in Peruvian Andes. *Left*: Upper, highly weathered portion of bedrock with a clay-filled cavity. *Right*: Broken-up core in highly fractured and karstified (vuggy) section of bedrock at ~600 meters (1,970 feet) below ground surface.

14.5 Geophysical Logging

The most important objective of borehole geophysics is to obtain more information from a boring/well than can be obtained from drilling, sampling, and testing. Drilling any kind of a test borehole or well is an expensive procedure. The test borehole or well provides access to the ground-water system at one point; therefore, each test hole or well provides a valuable opportunity to obtain vertical profiles or records of many kinds of data. The cost-benefit ratio for recording geophysical logs usually is quite favorable. That is why all oil wells drilled anywhere in the world are logged. Although the unit costs for drilling most water wells are less than those for drilling oil wells and the value of the product usually is less, the cost of logging usually also is less.

Stratigraphic correlation is a common use of geophysical logs; logs also permit lateral extrapolation of quantitative data from test or core holes. Using logs, a measured value at a point in a water well can be extrapolated in three dimensions, thereby increasing its value greatly. Many techniques used in surface geophysics are similar to techniques in borehole geophysics, and the two are considered together when a comprehensive groundwater investigation is planned. Most surface geophysical surveys cannot be uniquely interpreted; geophysical logs, such as acoustic-velocity and resistivity logs, can provide detailed profiles of data that are useful in interpreting surface surveys, such as seismic and resistivity surveys.

Geophysical logging cannot replace sampling completely, because some sample data are needed for each study area to aid in log analysis. A log analyst cannot evaluate a suite of logs properly without some information about the local geology. Logs do not have a unique response; for example, gamma-log anomalies from shale are indistinguishable from anomalies from granite. No absolute rules for log interpretation exist. To maximize results from logs, at least one core hole should be drilled in each depositional basin or unique aquifer system. If coring the entire interval of interest is too expensive, intervals for coring and laboratory analysis can be selected on the basis of geophysical logs obtained from a nearby hole. Laboratory analysis of core is essential either for direct calibration of logs or for checking calibration done by other means. Because of the effect of chemical composition of the rock matrix, calibration of logs made in one rock type may not be valid in other rock types.

Subtle changes in the rock matrix can produce large changes in log response. Gross errors can be made by just "matching the wiggles." Even within one depositional basin, the response of one type of log may shift, because of lateral facies changes (U.S. EPA, 1993b; Keys, 1990.)

The characteristics of the borehole to be logged may place constraints on the type of borehole logging method that can be used—the primary consideration when identifying borehole logging methods of potential value for a specific situation. These characteristics include:

- Whether a casing is present. Electric methods, for example, require uncased holes.
- If cased, the type of casing. Borehole radar, for example, can be used with a polyvinyl chloride (PVC) casing, but not with a steel casing.
- Borehole diameter must be large enough for the instrument of interest. Some logs (e.g., dielectric and nuclear magnetic resonance logs) require borehole diameters that are considerably larger than are typically drilled for monitoring wells at contaminated sites (i.e., larger than 2 or 4 in. diameter.)
- Whether borehole fluid (e.g., groundwater or drilling fluid) is present. Electric logs, sonic logs, and any fluid characterization log require borehole fluid.
- The radius of measurement of specific methods can range from near the borehole surface (spontaneous potential and SP resistance logs) to more than 100 meters for borehole radar in highly resistive rock.
- Many logging methods require calibration or corrections for such factors as temperature, borehole diameter, and fluid resistivity.

The most commonly used borehole logging methods in hydrogeologic and contaminated site investigations involve spontaneous potential (SP), single-point resistance, fluid conductivity, natural gamma, neutron, sonic, caliper, temperature, and flowmeters. The nuclear logging methods are especially versatile because they can be used in cased monitoring wells. Geophysical logging is performed readily in various access and field conditions (Figure 14.8).

A bewildering number of specific borehole logging methods are available, and papers describing new methods or innovative adaptation of older methods appear every year. Schlumberger (1974) lists almost four dozen, and

Keys (1990) lists more than two dozen that have potential applications in groundwater investigations. Equally confusing to the uninitiated is the fact that the same logging technique may be called by several different names. For example, the terms gamma-gamma and density are commonly used for the same log, and acoustic waveform logs also are called variable density, three-dimensional (or 3D) velocity, and full waveform sonic logs. The summary tables and detailed descriptions of major logging methods are provided in very informative publications by USGS (Keys, 1990) and U.S. EPA (1993b) and are briefly described below. Examples of geophysical logs are shown in Figures 14.19 through 14.22.

Electrical and Electromagnetic Logging Methods. Electrical logging measures the flow of electric current in and adjacent to a boring, using the same principles as various surface methods: electromagnetic induction; magnetotellurics, and microwave sensing. Spontaneous potential logs, one of the most commonly used electrical logs, simply records the changes in current flow that result from changes in lithology. Single-point resistance and normal, focused, and lateral resistivity logs all measure resistivity using the same principles as surface resistivity measurements. These logs require conductive drilling mud or groundwater with high salinities to work well and, consequently, are not well suited for near-surface investigations in freshwater aquifers. Normal resistivity logs, however, are widely used to measure variations in water quality. Induction logs are also unaffected by the presence of plastic (e.g., PVC) well casings, making them particularly useful for locating electrically conductive contaminant plumes in existing wells.

Nuclear Logging Methods. Nuclear logging includes all methods that either detect the presence of unstable isotopes or create such isotopes in the vicinity of a borehole. Each type is potentially useful in hydrogeologic studies of the vadose and/or saturated zones because none require conductive media, as do most electrical logging methods. Most of these nuclear logs also allow quantitative interpretation of bulk density, porosity, salinity, and unsaturated moisture content. Natural gamma, gamma-gamma, and neutron logs are the most common nuclear methods used in groundwater studies.

Figure 14.18 Geophysical borehole logging setup. Photo courtesy of Dawit Yifru.

Acoustic and Seismic Logging Methods. Acoustic logging tools incorporate the signal source and the receiver on the same probe and are used in single boreholes. They are especially valuable for characterizing secondary porosity and fractures. Borehole seismic methods can use various surface-borehole or borehole-borehole source and geophone/hydrophone configurations. They are used primarily for stratigraphic, fracture, and geotechnical characterization.

Lithologic and Hydrogeologic Characterization Logs. <u>Caliper logs</u> have numerous variants but all are intended to measure borehole diameter. They provide essential data for interpreting other types of logs that are affected by variations in borehole diameter and generate some data on lithology and secondary porosity. Fluid temperature can be measured as a gradient (also called thermal resistivity), or changes measured over time at one or more points can be tracked (as when injected water of a different temperature is used as a tracer). <u>Fluid flow measurements</u> can locate zones of high permeability (fractures and solution porosity) and areas of leakage in artesian wells. The development of thermal and electromagnetic borehole flowmeters that can sense water movement either vertically or horizontally (or both) at very low velocities has greatly enhanced the ability to characterize variations in hydraulic conductivity in boreholes (see Lecture 15). <u>Borehole television cameras</u> have the advantage of allowing visual inspection of a borehole for such things as fracture detection and monitoring well integrity. <u>Borehole magnetometers</u> operate on the same principles as surface magnetometers. Magnetometer probes can be especially useful when drilling is required in areas where the presence of buried ferrous metal wastes is suspected. In such situations, lowering the probe to the bottom of the hole approximately every 5 feet may provide advanced warning of the presence of buried drums that are outside the detection limit of surface instruments.
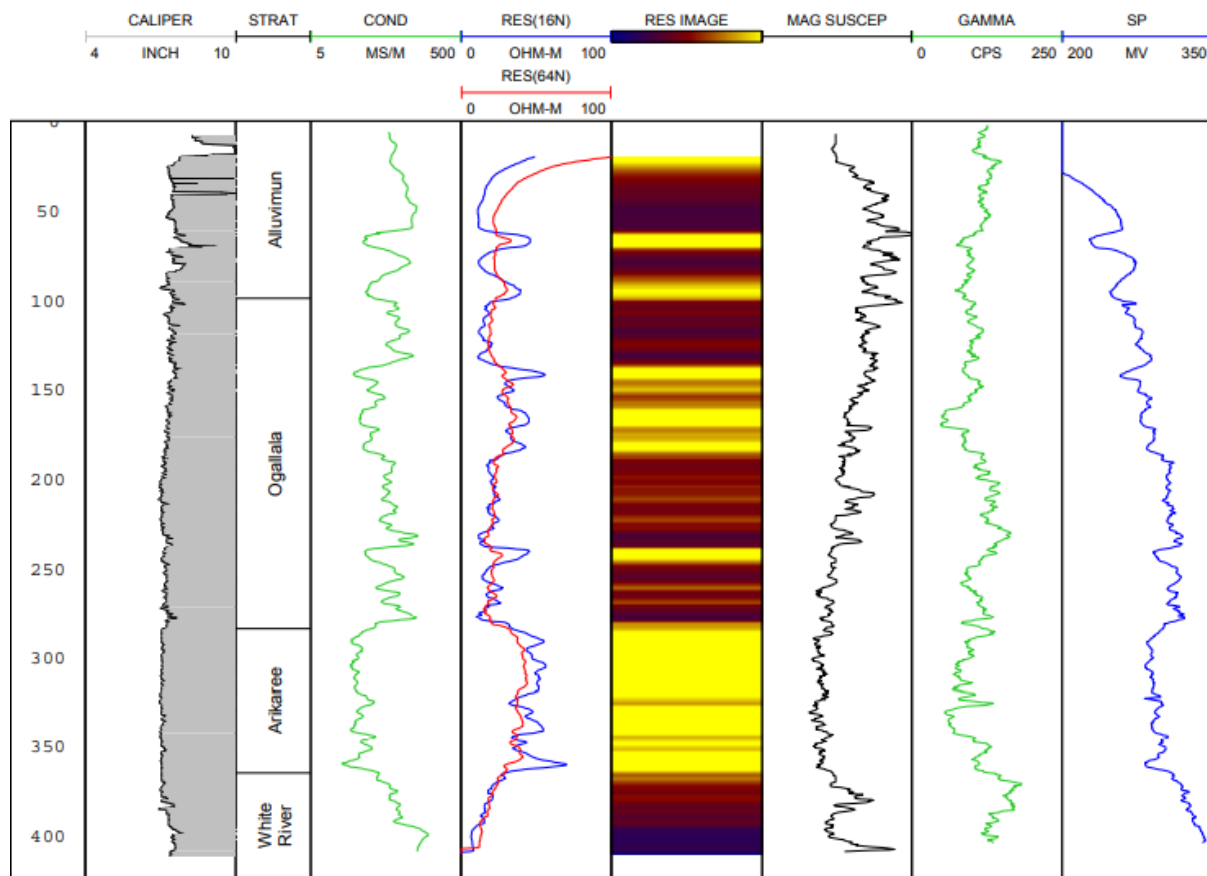
Figure 14.19. Composite of stratigraphic and geophysical logs for test hole 72B. CALIPER (caliper, in inches); STRAT (stratigraphic units); COND-MS/M (conductivity, in millisiemens per meter); RES (16N)-OHM-M (short-normal resistivity, in ohm-meters); RES (64N)-OHM-M (long-normal resistivity, in ohm-meters); RES IMAGE (color-scale representation of the short-normal resistivity, darker colors are less resistive, whereas lighter colors are more resistive); MAG SUSCEP (magnetic susceptibility shown on a relative scale with increasing susceptibility to the right); GAMMA-CPS (gamma, in counts per second); and SP-MV (spontaneous-potential, in millivolts). From Anderson et al., 2009. USGS, in public domain.

Figure 14.19 shows a composite geophysical log for test hole 72B in the High Plains (Ogallala) aquifer, Central Platte River basin, Nebraska. The lower part of the Ogallala Formation between 185 and 285 ft below land surface (BLS) appears to be finer grained than the upper part with a few coarser grained beds; it is characterized by generally lower resistivity/higher conductivity, higher gamma activity, and lower neutron counts. The middle part of the Ogallala between 140 and 185 ft BLS is coarser grained and identified by higher resistivity/lower conductivity, lower gamma activity, and higher neutron counts. The upper part of the Ogallala is fine grained and characterized by generally lower resistivity/higher conductivity, and higher gamma and lower neutron counts, except for sporadic coarse-grained zones that exhibit higher resistivity/lower conductivity and lower gamma activity. The contact between the Ogallala Formation and the overlying alluvium is identified by a marked increase in electrical resistivity and a corresponding decrease in conductivity, along with lower gamma counts. The Ogallala-alluvium contact is penetrated in the various test holes at depths ranging from 58 to 101 ft BLS (Anderson et al., 2009).

| GAMMA CONDUCTIVITY | TEMPERATURE SPECIFIC CONDUCTANCE | MECHANICAL and ACOUSTIC CALIPERS | ACOUSTIC TELEVIEWER | OPTICAL TELEVIEWER |
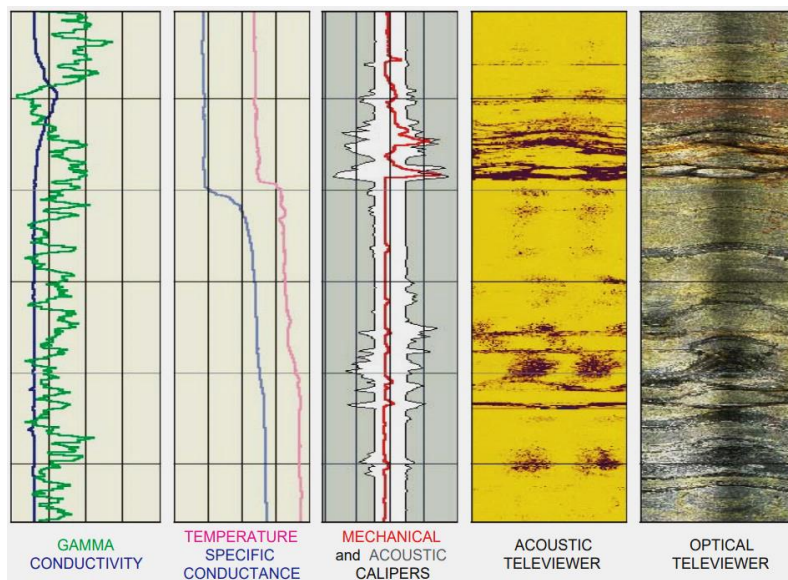
Optical- and acoustic-televiewer (OTV and ATV) imaging, usually performed in tandem, have become a norm in characterization of fractured rock and karst aquifers. Examples are shown in Figures 14.20 and 14.21. The use of electrical resistance cross-hole tomography to determine the presence and 3D orientation of fractures in the subsurface is illustrated in Figure 14.22.

Figure 14.20 Geophysical logs from a section of borehole MW109R, University of Connecticut landfill study area, Storrs, Connecticut. From Johnson et al., 2002. USGS, in public domain.
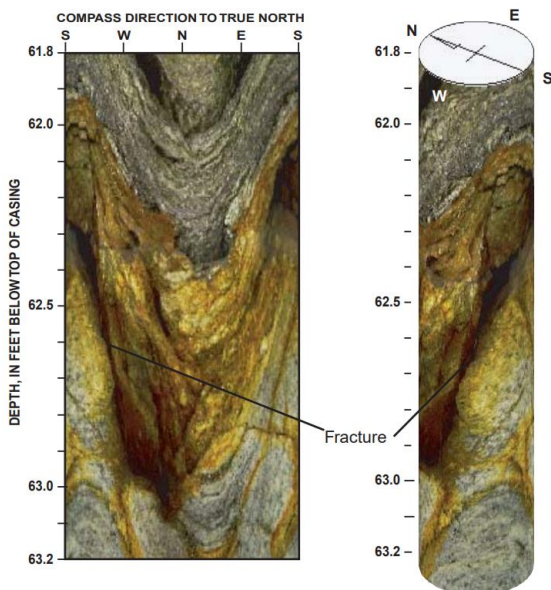
Figure 14.21 Optical televiewer (OTV) log of a section of borehole MW109R, as an "unrolled" 360-degree scan of the borehole wall, and "rolled" into a virtual core (right). From Johnson et al., 2002. USGS, in public domain.
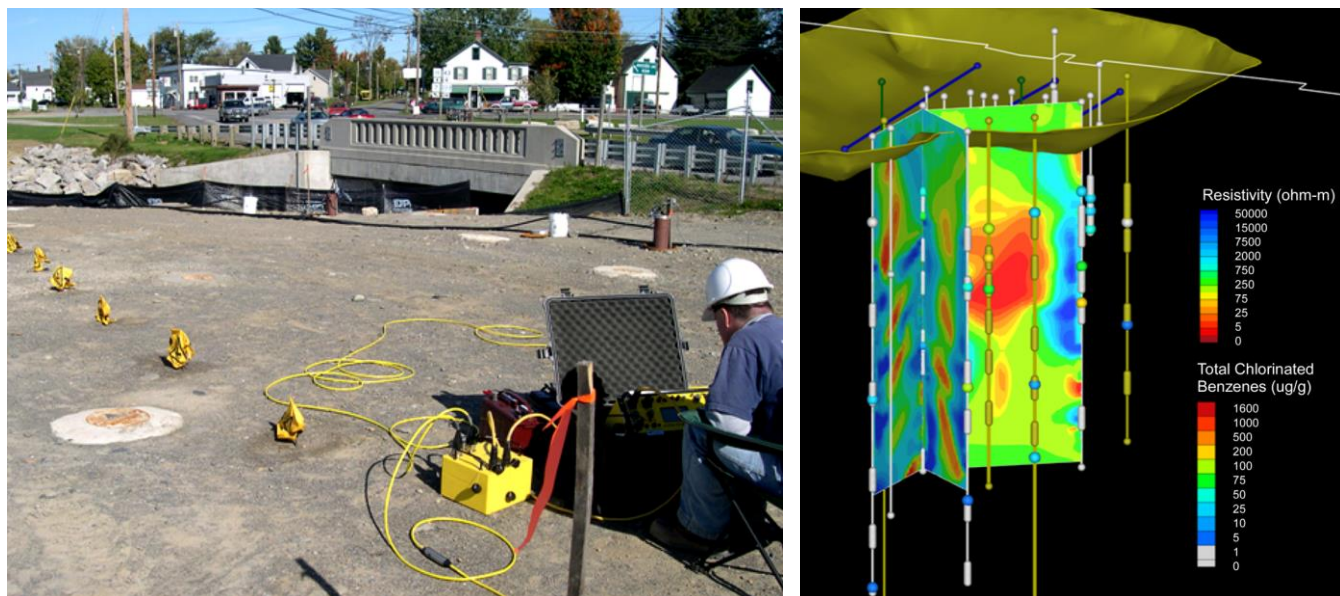
Figure 14.22 *Left*: Setup for determining presence and 3D orientation of fractures using electrical resistivity tomography between boreholes. *Right*: Electrical resistivity tomography results shown in panels between boreholes; concentration of contaminants of concern are for discrete sampling points shown as spheres. Courtesy of Peter Thompson, Scott Calkin, and Rod Rustad.

14.6 Monitoring Wells

Monitoring wells are arguably the most important component of almost any hydrogeologic field investigations program. They provide direct access to the saturated zones in aquifers and aquitards (different hydrostratigraphic units) and can be used for a variety of purposes including measurements of hydraulic heads (and therefore determination of groundwater flow directions), vertical gradients and interactions between hydrostratigraphic units, (including migration of contaminants when present), groundwater sampling, and aquifer testing.

Boring, logging, and installing monitoring wells in select borings at representative locations and depths is also the most expensive part of hydrogeologic field investigations. Consequently, in case of groundwater contamination and remediation projects, tension often exists between regulators and potentially responsible parties (PRPs) as to the "right" (sufficient) number of monitoring wells and the groundwater monitoring program in general. The following points from an often cited, early regulatory guidance document by U.E. EPA (1986), help illustrate this (see also Figure 14.23).

At a site with groundwater contamination, horizontal and vertical placement of wells (and screen lengths) should reflect all the waste management practices and hydrogeologic factors including hydrostratigraphic units that may serve as potential pathways for contaminant migration.

Generally, the lengths of screens should reflect the vertical extent of the potential contaminant pathway at the desired sampling location. However, shorter well screens (not fully penetrating the depth of the water-bearing unit) should be employed in thick units where dilution effects may impair potential contaminant detection.

The downgradient wells must be designed and installed to immediately detect releases of hazardous waste constituents to the uppermost aquifer. The upgradient wells must be located and constructed to provide representative samples of groundwater in the same portion of the aquifer(s) monitored by the downgradient wells to permit a comparison of groundwater quality.
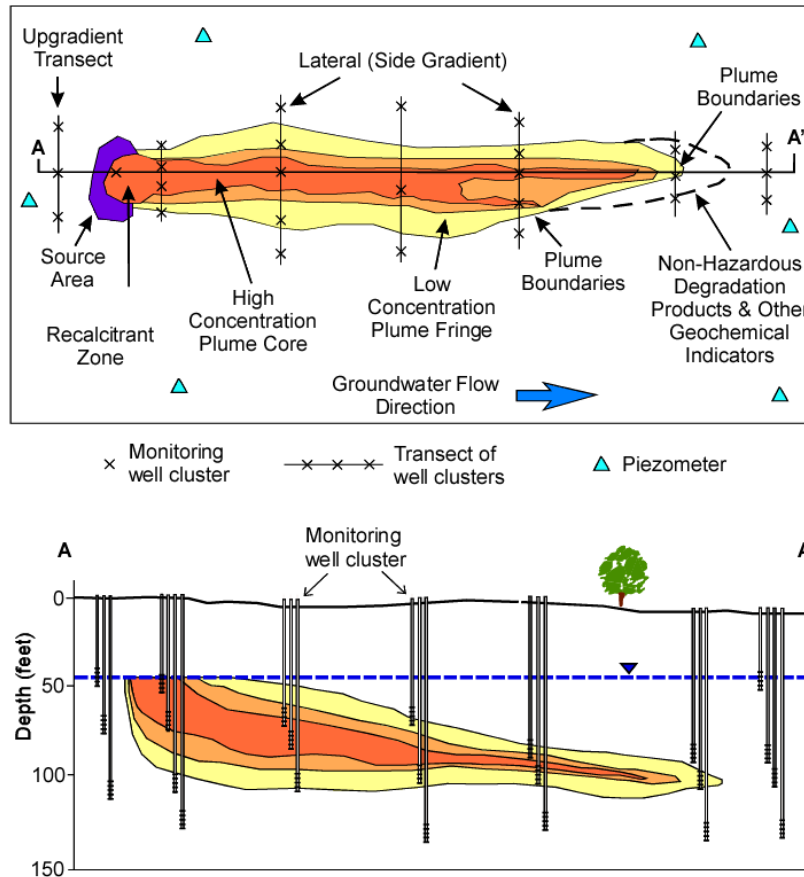
Figure 14.23 Example of a monitoring well network at a groundwater contamination site. From Ford et al., 2007. U.S. EPA, in public domain.

By regulation, the owner/operator must install a minimum one background well. However, a facility that uses only one well for sampling background water quality may not be able to account for spatial variability. It is, in fact, a very <u>unusual</u> (emphasis added) circumstance in which only one background well will fully characterize background water quality. In most cases the owner/operator should install multiple background monitoring wells. This includes enough monitoring wells to allow for depth-discrete comparison of water quality.

Screening the entire thickness of the uppermost aquifer will not allow the owner/operator to obtain depth-discrete water quality data. Instead, the owner/operator should use shorter well screens in order to do so.

There are geologic and hydrogeologic situations for which determination of the hydraulically upgradient location is often difficult. Examples of such cases where further characterization may be necessary is when waste management units are:

- Above groundwater mounds;
- Located above aquifers in which groundwater flow directions change seasonally;
- Containing significant amounts of NAPLs;
- Located in areas where nearby surface water can influence groundwater levels (e.g., river floodplains);
- Located near intermittently or continuously used production wells; and
- Located in karst areas or faulted areas where fault zones may modify flow.
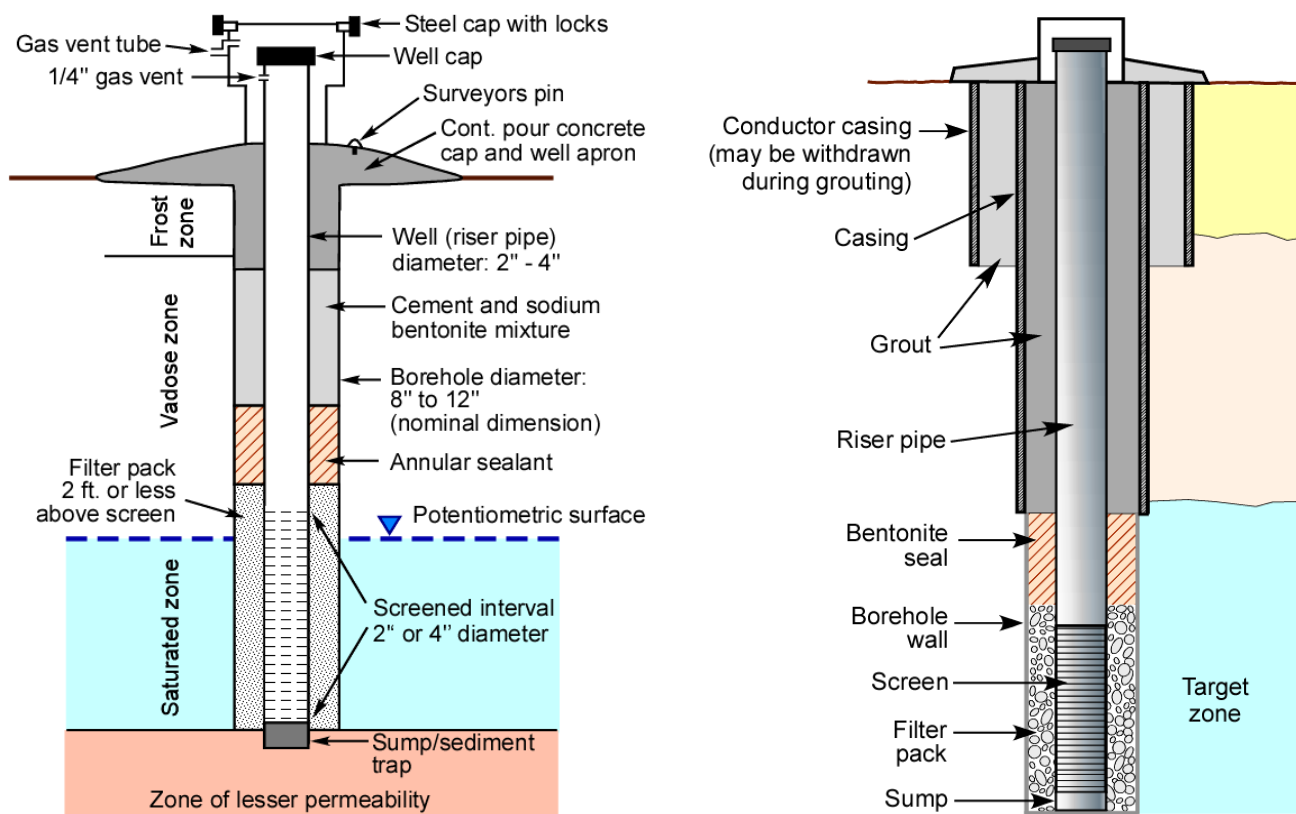
Figure 14.24 *Left*: Typical design of a standard monitoring well. Modified from U.S. EPA, 1986.
Right: Double-cased monitoring well.

Typical design of a **standard monitoring well** is shown in Figure 14.24 together with a **double-cased monitoring well**. Standard wells are usually shallow and do not have to extend to some less permeable formation as shown in Figure 14.24. In other words, they can "hang" in the aquifer and not be fully-penetrating. In fact, most regulatory agencies require that the monitoring well screens are not longer than 10 feet, with 5-foot screens being preferable. If the targeted aquifer is thick and there is need to delineate vertical extension of the contamination, multiple wells with short screens at varying depths will have to be installed (see Figure 14.23).

Double-cased or sometimes triple-cased monitoring wells are constructed when there is reason to believe that interconnection of two aquifers by well construction may cause cross-contamination or when flowing sands make it impossible to install a monitoring well using conventional methods. They are also typically installed for monitoring bedrock aquifers which are overlain by shallow aquifers and/or saturated zone in the residuum (regolith), regardless of any cross-contamination concerns.

As specified by Aller et al. (1997), and Cal/EPA (1995), a pilot borehole should be bored through the overburden and/or the contaminated zone into the clay confining layer or bedrock. An outer casing (sometimes called surface or pilot casings) should then be placed into the borehole and sealed with grout. The borehole and outer casing should extend into tight clay a minimum of two feet and into competent bedrock a minimum of 1 foot. The total depths into the clay or bedrock will vary, depending on the plasticity of the clay and the extent of weathering and\or fracturing of the bedrock. The final depths should be approved by a senior field geologist. The size of the outer casing should be of sufficient inside diameter to contain the inner casing, and the 2-inch minimum

annular space. In addition, the borehole should be of sufficient size to contain the outer casing and the 2-inch minimum outer annular space, if applicable.

As discussed earlier in Section 14.4.4, dual-rotary methods are particularly suitable for installing both monitoring and water supply wells, including double-cased wells in difficult conditions such as unconsolidated deposits with cobbles and boulders, and in unstable consolidated rocks such as karst formations (see Figure 14.25). They also are successful where prevention of cross-contamination between aquifers (water-bearing zones) is critical.

Depending on the site-specific conditions, the following drilling methods may be suitable for the installation of environmental monitoring wells (see also Section 14.4): hollow stem auger (HAS), sonic (rotosonic), air rotary (which can be supplemented with down-the-hole (DTH) percussion hammers driven by the air stream to rapidly penetrate bedrock materials), and cable tool. In all cases, the preferred methods are those that case the hole during drilling.

Figure 14.25 Rotary drill bit on a dual rotary drill rig used to install a monitoring well in a karst aquifer in New York state, U.S. Courtesy of Mark Bauer.

When drilling in deeper consolidated deposits, air rotary drilling (Figure 14.26) is frequently the preferred method because no drilling fluids are employed. However, oil from air compressors may contaminate the borehole, and special filters are required to minimize this effect. In some cases, drillers may use foams to help lift cuttings to the surface and increase the speed of drilling.

Mud rotary is an undesirable drilling method because contamination can be introduced into the borehole from the constituents in the drilling mud, cross contamination can occur along the borehole column, and it is difficult to remove the drilling mud from the borehole after drilling and during well development. The drilling mud can also carry contaminants from a contaminated zone to an uncontaminated zone thereby cross contaminating the borehole. If a rotary method is selected, only potable water with sodium bentonite, polyanionic cellulose (PAC), partially hydrolyzed polyacrylamide (PHPA) or other advanced wetting agents should be used.

All materials used should have adequate documentation as to manufacturer's recommendations and product constituents. QA/QC samples of drilling muds and potable water should be sampled at a point of discharge from the circulation system to assure that pumps and piping systems are not contributing cross contamination (U.S. EPA, 2018).

Clustered monitoring wells consist of individual monitoring wells situated close together, but not in the same borehole. Their purpose is similar to nested monitoring wells, i.e., to monitor groundwater conditions at various depths and/or water-bearing zones (aquifers).

Figure 14.26. Air rotary drilling during a monitoring well installation at a coal ash landfill in Eastern United States. Courtesy of Ted Wilson.

Nested monitoring wells consist of two or more casing strings within the same borehole. Normally, the screen interval of each casing string is designed to obtain water from different depths, aquifers, or water-bearing zones. There are quite a few design variations of nested wells, including types of casing strings, means of isolating screen intervals, types of screens or sampling ports, and methods of sample retrieval. Collectively, various designs of nested monitoring wells are referred to as "**multi-level monitoring wells**" (Figures 14.27 and 14.28). Water-level measurements and groundwater sampling can be performed with permanently installed (dedicated) devices/pumps or done periodically with portable equipment.

As emphasized by California Department of Water Resources (1991), a nested monitoring well can be difficult to construct because of multiple casings within the same borehole. Care is required during construction to ensure water-bearing zones for each casing string are hydraulically isolated from one another and the annular seals are effective. Some regulatory agencies may prohibit the use of nested monitoring wells for certain contamination or investigations. Typically, this is due to uncertainties about whether water-bearing strata can be isolated, and whether the annular seals in a nested well are always effective. Poorly constructed multi-level monitoring wells can provide preferential pathway for the movement of poor-quality groundwater or groundwater contaminants from one water-bearing unit to another which is another reason why some regulatory agencies prohibit their use for certain groundwater contamination investigations out of concern for water quality and data quality requirements.

Figure 14.27 Examples of commercially available multi-level monitoring systems. *Left photo*: FLUTe, Flexible Liner Underground Technologies (https://www.flut.com/). *Two right photos*: single-casing Multilevel Groundwater Monitoring System CMT by Solinst (https://www.solinst.com/products/multilevel-systems-and-remediation/). All photos courtesy of Peter Thompson.
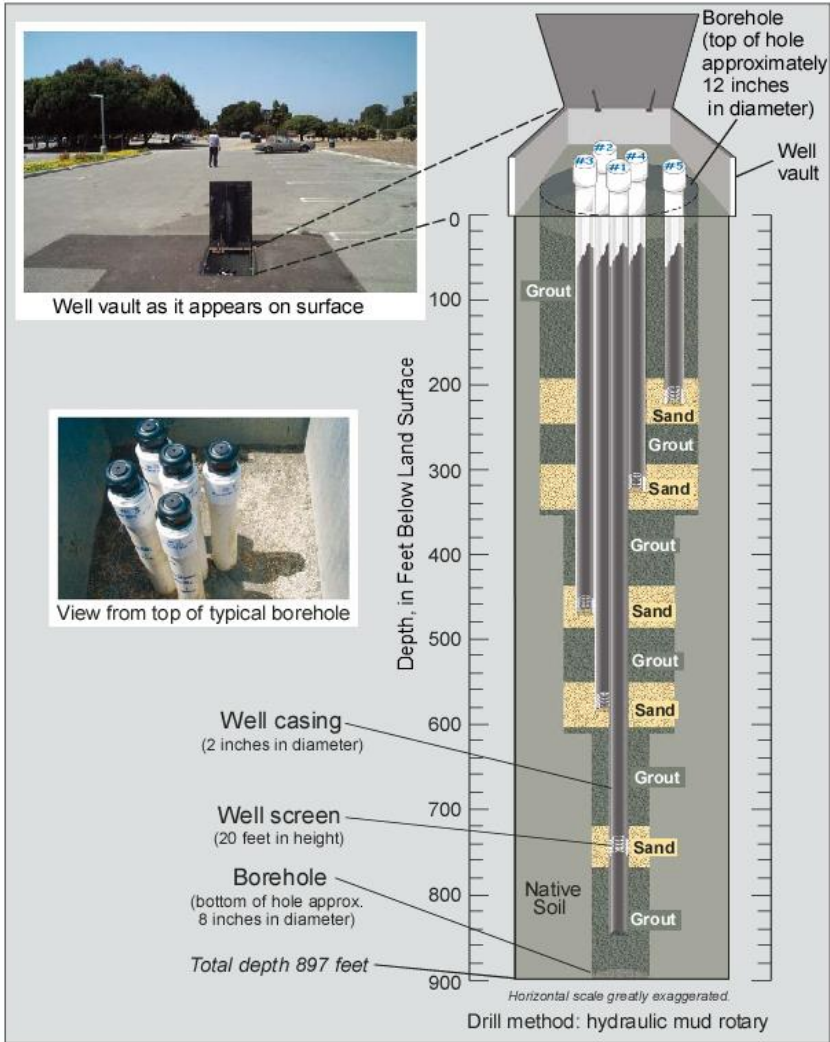
Figure 14.28 Components of typical USGS multiple well monitoring site. From Reichards, et al., 2003. USGS, in public domain.

Figure 14.29 Typical completion of a monitoring well showing riser pipe, concrete surface pad, and bumper guards for surface protection. Hollow stem auger drill rig is in the background. Photo courtesy of Dawit Yifru.

14.6.1 Filter Pack and Well Screen Design

Selection of a monitoring well screen and filter pack is one of the key components of well design. Their combined role is to prevent inflow of fines from the formation into the well and to provide for proper well development and future sampling of groundwater. Some professional, however, defer a more detail analysis to a "default" selection, sometimes justifying such approach as "conservative" and therefore acceptable to an overseeing regulatory agency. Namely, the selection of 0.010" screen slots with a 20-40 sand filter pack, or 0.005" screen slots with 100 sand filter pack for very fine formations is often made regardless of the actual characteristics of the screened interval, including in cases of uniform, medium-size sands for example. While this approach may be acceptable, it limits any potential changes in the future utilization and role of the monitoring well. For example, the well, especially if it is a 4-inch well, may be used to extract groundwater or inject fluids as part of the groundwater remedy system. Many monitoring wells are also used to conduct slug tests or pumping tests for estimating the hydraulic conductivity (K) of the porous media (see Lecture 15). If the well screen and filter pack hydraulically do not match the adjacent porous media, this essential parameter for developing a quantitative hydrogeological CSM and evaluating groundwater remedial alternatives (if the groundwater is contaminated) will almost certainly be mischaracterized.

Table 14.2 provides size specifications for the general selection of filter (i.e., sand) packs for fine formation materials. ASTM standard D5092, Design and Installation of Ground Water Monitoring Wells in Aquifers, may be consulted for further guidance on specifications for sand appropriate for these applications.

It should be noted that the selection of screen type and openings, and filter pack for water supply wells is a much more elaborate process. Screens of such wells are much longer and may include multiple intervals because the main goal is to maximize the well pumping rates (see Lecture 16).

Table 14.2 Recommended primary filter (sand) pack size for common screen slot sizes (Lapham et al., 1997; modified from ASTM, 1992, p. 128)

Size of screen opening, in millimeters (inches)	Slot number	Filter (sand) pack mesh size designations
0.125 (0.005)	5	100
0.25 (0.010)	10	20 to 40
0.50 (0.020)	20	10 to 20
0.75 (0.030)	30	10 to 20
1.0 (0.040)	40	8 to 12
1.5 (0.060)	60	6 to 9
2.0 (0.080)	80	4 to 8

14.6.2 Well Development

The main purpose of developing new monitoring wells is to remove the residual materials remaining in the wells after installation has been completed, and to try to re-establish the natural hydraulic flow conditions of the formations which may have been disturbed by well construction, around the immediate vicinity of each well. Any contamination or formation damage from well drilling and any fines from the natural formation must be removed

to provide a particulate-free discharge. A variety of techniques are available to remove such contamination and develop a well. To be effective, all these techniques require reversals or surges in flow to avoid bridging by particles, which is common when flow is continuous in one direction.

As recommended by U.S. EPA (2005, 2018), a newly completed monitoring well should not be developed for at least 24-48 hours after the surface pad and outer protective casing are installed. This will allow sufficient time for the well materials to cure before development procedures are initiated. The well should be developed until the column of water in the well is free of visible sediment, and the pH, temperature, turbidity, and specific conductivity have stabilized. In most cases the above requirements can be satisfied; however, in some cases the pH, temperature, and specific conductivity may stabilize but the water remains turbid. In this case the well may still contain well construction materials, such as drilling mud in the form of a mud cake and/or formation soils that have not been washed out of the borehole. Excessive or thick drilling mud cannot be flushed out of a borehole with one or two well volumes of flushing. Continuous flushing over a period of several days may be necessary to complete the well development. If the well is pumped to dryness or near dryness, the water table should be allowed to sufficiently recover (to the static water level) before the next development period is initiated.

Caution should be taken when using high rate pumps and/or large volume air compressors during well development because excessive high rate pumping and high air pressures can damage or destroy the well screen and filter pack. The onsite geologist should make the decision as to the development completion of each well. All field decisions should be documented in the field logbook.

The following development procedures, listed in approximate increasing order of the energy applied to the formation materials, are generally used to develop wells (U.S. EPA, 2018): (1) Bailing; (2) Pumping/over-pumping/backwashing; (3) Surging; (4) Backwashing ("rawhiding"); (5) Jetting; and (6) Compressed air (with appropriate filtering): airlift pumping and air surging

These development procedures can be used, individually or in combination, to achieve the most effective well development. In most cases, over-pumping and surging will adequately develop the well without imparting undue forces on the formation or well materials. Because of the danger of introducing contaminants with the airstream, the possibility of entraining air in the aquifer, and the violent forces imparted to the formation, air surging is the least desired method of development and should only be used where there is a specific need for the procedure.

Air-lift pumping is permissible where an eductor pipe is used and several well volumes of water are removed from the well by other pumping means after air-lift pumping. Additional time before the first sampling event should be allowed when using air development methods, particularly airlift. The selected development method(s) should be approved by a senior field geologist before any well installation activities are initiated.

Wells can require a considerable length of time to equilibrate with the aquifer after construction and development. The length of time between development and the first sampling event should be as long as possible with times from 1 to 14 days recommended. The possibility of the first sampling event's results being non-representative should always be considered (U.S. EPA, 2018).

14.6.3 Direct-Push Wells

These monitoring wells are installed by Direct-Push technology (DPT) to permit short-term or long-term monitoring of groundwater and are usually two inches in diameter or less and constructed of PVC and/or stainless steel. They are easier to install, replace, and cheaper than standard monitoring wells. Since DPT wells are installed for periods of several months to several years, the annulus of the boring around the well casing is usually sealed to prevent possible downward migration of contaminants from the shallow saturated zone into the aquifer (U.S. EPA, 2005).

Surface protection is required to prevent tampering with the well. A slotted or screened section permits groundwater to flow into the well under ambient hydrostatic pressure. Groundwater may be collected from monitoring wells using bailers, various pumps, or passive sampling devices.

Point-in-time water-level measurements and sampling tools are typically used during site characterization to identify groundwater flow directions and plume boundaries or hot spots. They cannot be used for long-term monitoring or trend analysis since the boreholes need to be decommissioned upon completion of sampling. In contrast, temporary and permanent monitoring wells are typically used to provide trend analysis of contaminant groundwater concentrations over an extended period of time.
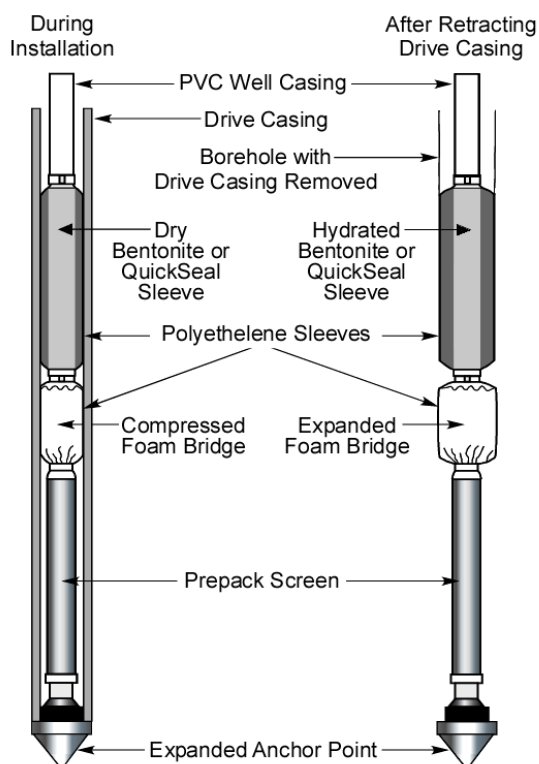
The primary regulatory issue concerning direct push wells is that most states require a minimum annular space for a monitoring well that cannot be met by the Direct Push installation technique. However, publications by U.S. EPA (2005) and ITRC (2006a) discuss detail design of such wells including use of pre-pack filters, sealing off (grouting) the wells in undesired sections of the porous media investigated, and well development, which all are key aspects of installing regular monitoring wells. Summaries of case studies related to the performance of Direct Push wells for long-term monitoring are also presented and indicate that DPT wells perform satisfactorily in this capacity.

An example of a DPT monitoring well is shown in Figure 14.30, and Table 14.3 lists advantages and disadvantages of wells installed using Direct Push technology.

Figure 14.30   Example of protected-screen Direct Push well installation. Modified from ITRC, 2006a. Copyright ITRC; acknowledgement required for further use.

Table 14.3. Advantages and limitations of Direct-Push wells. Modified from ITRC, 2006a. Copyright ITRC; acknowledgement required for further use.

Advantages	Limitations
Minimal waste "cuttings"	Not applicable when cobbles or consolidated materials are present
Fewer well development wastes	Not accepted for long-term monitoring in most states
Rapid installation and site characterization	Debate remains regarding aquifer testing capabilities
Less worker exposure to contaminants	Well diameter limitations
Representative chemistry and field parameter measurements	Cross-contamination of aquifers
Minimal environmental disturbance	Potential for higher turbidity in wells with no filter pack

14.7 Piezometers

Piezometers, as opposed to monitoring wells, only measure the hydraulic head at one discrete point in the water-bearing zone (or aquitard if needed) and are not used to collect water samples. Ideal (theoretical) piezometer is open to the formation only at its very tip where water can enter and then rise in the riser pipe to the elevation of the hydraulic head in the formation next to the tip (Figure 14.31). Piezometers therefore have less strict regulatory requirements and are easier and cheaper to install because their effective diameter can be less than one inch and there is no need for screens, filter packs, and hydraulic development. However, confusion exists in the practice since "piezometers" are often constructed in the same manner as monitoring wells, including sometimes 10-foot-long screens and filter packs. The only apparent difference in such cases is in their nomenclature, i.e., it is understood (assumed) that they will not be used to collect water samples or monitor groundwater quality.

One practical reason for installing piezometers with the same technologies and design applicable to monitoring wells (i.e., drilling method, casing, grouting, sealing off any overlying water-bearing zones) is the requirement to prevent any crossflow between different units along the piezometer boring and riser pipe.
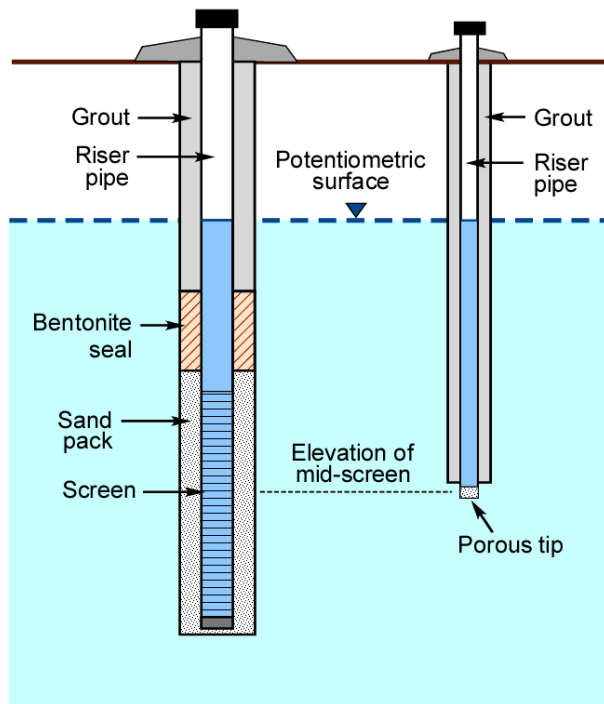
Figure 14.31 Comparison of a monitoring well (left) and a piezometer (right) installed at the same location to measure the hydraulic head in the water-bearing zone. By convention, it is understood that the hydraulic head measured at the monitoring well corresponds to the elevation of the mid-screen.

Vibrating wire piezometers (VWP) have been routinely used in civil and geotechnical engineering to measure positive or negative (such as in unsaturated conditions) pore water pressure in soil, rock, and concrete including following applications (www.encardio.com):

- Construction control, stability investigation and monitoring of earth dams, embankments, foundations, shallow underground works, and surface excavations.
- Uplift and pore pressure gradients in foundations, embankments, abutments, and fills.
- The hydrological investigations, groundwater elevation studies, and water supply operations.
- Waste and environmental applications.
- Soil improvement and stability, and slope stability.

VWP (Figure 14.32) is an electromagnetic type of piezometer that records the pore water pressure at a certain elevation by measuring frequency of vibration of a tension wire in the sensor. This frequency changes when the pore water pressure in the surrounding porous media at the installation elevation of the sensor (piezometer) changes. The changes are recorded by the instrument including conversion to the pore water pressure in applicable engineering units. VWPs are fitted with a data logger for continuing readings thus eliminating the need for manual labor. Together with easy and affordable installation, this is the main reason for the popularity of VWPs among civil and geotechnical engineers. However, they are seldom used in hydrogeologic and environmental investigations because of the following reasons:

- There is no possibility to independently (manually) check the readings, collect groundwater samples, or measure any physical or chemical water parameter in-situ because of the absence of physical access to groundwater.
- They cannot be replaced if malfunctioning.
- They cannot be recalibrated (adjusted) if there is evidence of an inadequate initial setup (calibration). This because there is no possibility to establish the real baseline reference such as the hydraulic head in the adjacent porous media. Before deployment, the sensors are calibrated above ground against known pressure, typically in barrels of water.

If necessary to install and utilize VWPs in a groundwater-related project, it is strongly recommended that classic piezometers and/or short-screen monitoring wells be installed next to VWPs at several key locations to manually verify and check their readings on an ongoing basis.

One practical advice to both novice and experienced hydrogeologists that are engaged in a geotechnical or civil engineering project, such as an earth dam, is that everyone involved must agree as to the difference between pore water pressure and the hydraulic head (see Lecture 3 and Figure 3.10 for example). In other words, the hydrogeologist must be sure that the network of VWPs is reporting the hydraulic head separately from any other parameter (such as the pore water pressure), and that any conversions and equations needed to translate from the electronic/frequency signals recorded by the VPW sensor to the hydraulic head value are correct.
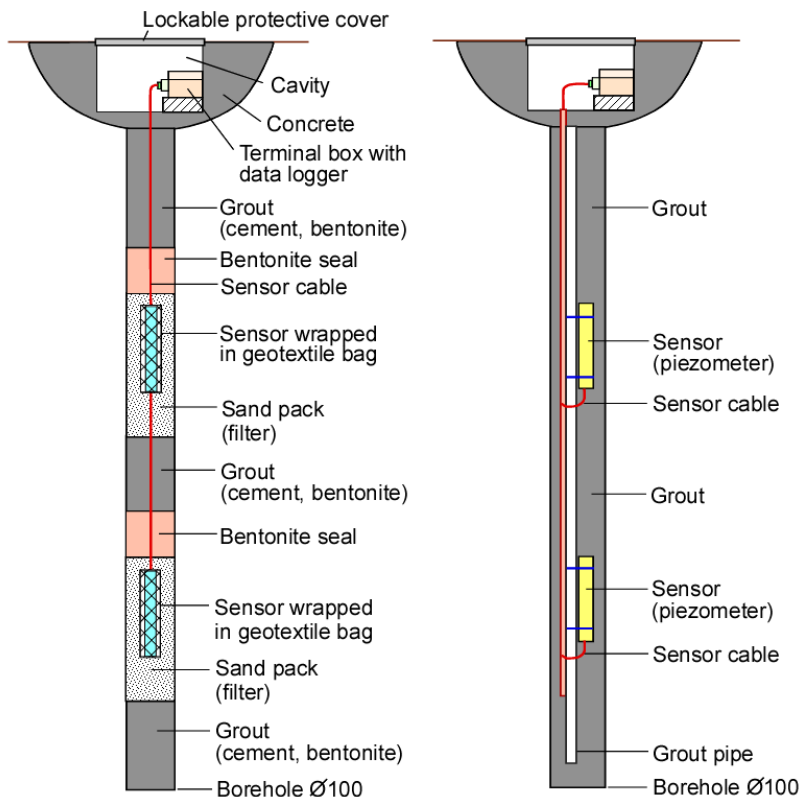
Figure 14.32 *Left*: Installation of multiple VWPs in a borehole using traditional method, which involves placement of sand pockets surrounding the sensors, and bentonite seals and grout columns to separate VWPs at different levels. *Right*: Installation with fully grouted method. Modified from www.encardio.com

Lecture 15 Field Investigations, Part Two

15.1 Groundwater Monitoring and Sampling

Regular and systematic monitoring of groundwater resources is the most important prerequisite for their effective management. Unfortunately, according to a worldwide inventory of groundwater monitoring compiled by the International Groundwater Resources Assessment Centre (IGRAC), in many countries systematic monitoring of groundwater quantity or quality, even at a regional scale, is minimal or nonexistent (Jousma and Roelofsen, 2004). This lack of monitoring may result in undiscovered degradation of water resources due to either overexploitation or contamination, leading to the following scenarios:

- Declining groundwater levels and depletion of groundwater reserves
- Reductions in stream/spring baseflows or flows to sensitive ecosystems such as wetlands
- Reduced access to groundwater for drinking water supply and irrigation
- Use restrictions due to deterioration of groundwater quality
- Increased costs for pumping and treatment
- Subsidence and foundation damage

As explained in an excellent publication by USGS (Taylor and Alley, 2001), groundwater systems are dynamic and adjust continually to short-term and long-term changes in climate, groundwater withdrawal, and land use. Water-level measurements from monitoring wells are the principal source of information about the hydrologic stresses acting on aquifers and how these stresses affect groundwater recharge, storage, and discharge. Long-term, systematic measurements of water levels provide essential data needed to evaluate changes in the resource over time, to develop groundwater models and forecast trends, and to design, implement, and monitor the effectiveness of groundwater management and protection programs. Illustrative examples of using long-term, publicly available groundwater monitoring data to assess historic trends and implications of the ongoing groundwater drought of historic proportions in California are provided in the Guest Lecture by Alex Mikszewski.

The frequency of water level measurements is among the most important components of a water level monitoring program. Although often influenced by economic considerations, the frequency of measurements should be determined to the extent possible regarding the anticipated variability of water level fluctuations in the monitoring wells and the data resolution or amount of detail needed to fully characterize the hydrologic behavior of the aquifer. Typically, collection of water level data over one or more decades is required to compile a hydrologic record that encompasses the potential range of water level fluctuations in an observation well and to track trends with time.

Figure 15.1 Monitoring well equipped with automatic water-level sensing and recording instruments programmed to make measurements at 15-minute intervals. The well is part of a SCADA system and has autonomous solar energy source. Courtesy of Nick McMillan.

Water level monitoring may involve "continuous" or periodic measurements. Continuous monitoring involves the installation of automatic water-level sensing and recording instruments that are programmed to make measurements in monitoring wells at a specified frequency (Figure 15.1). Such programs are increasingly utilizing remote data transmission and storage including algorithms to analyze data time-series and detect trends/unusual events (Figure 15.2). Many large water utilities and groundwater remediation sites are implementing this approach using technology commonly referred to as SCADA (or Supervisory Control And Data Acquisition). It is a computer-based facility used to provide a centralized operation of services, such as well pumpage, water treatment, and water distribution. With SCADA, various sites in the water supply (or groundwater remediation) system can be monitored and controlled from a central operations facility. SCADA consists of three main parts: (1) sensors for continuous monitoring and programmable logic controllers (PLCs) at remote sites, (2) communications system, and (3) control center.

Continuous monitoring provides the highest level of resolution of water level fluctuations. Hydrographs constructed from frequent water level measurements collected with continuous monitoring equipment can be used to accurately identify the effects of various stresses on the aquifer system and to provide the most accurate estimates of maximum and minimum water level fluctuations in aquifers.
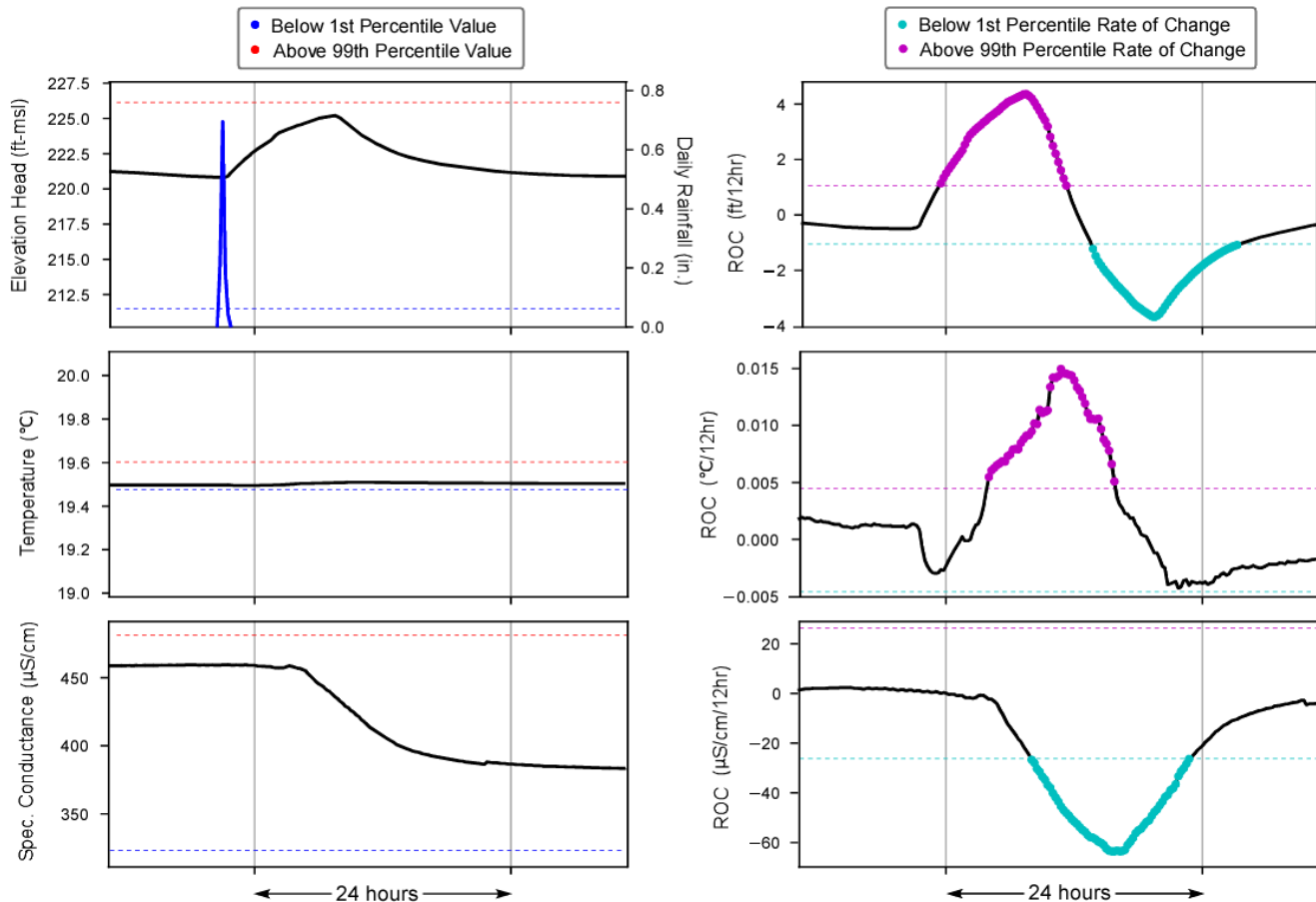
Figure 15.2 Example of graphs generated by a SCADA system for a monitoring well at a site in Eastern United States. The data on water level, temperature, and specific conductance are recorded every 15 minutes. Raw data are shown on the left hydrographs, and the rates of change for the three parameters automatically calculated by the system are on the right hydrographs. The confidence intervals are automatically updated every week.

Periodic groundwater-level measurements are those made at scheduled intervals (weeks, months, or years) and are generally used for water-table or potentiometric surface mapping and to reduce the costs of long-term monitoring. Periodic measurements are made by manually using electronic-sensor probes, chalked metal tapes, or acoustic sounding devices (Figure 15.3). Potential drawbacks to periodic monitoring are that hydraulic responses to short-term stresses may occur between measurements and may be missed, extreme water-level fluctuations cannot be determined with certainty, and apparent trends in water levels potentially are biased by the choice of measurement frequency.

Synoptic water level measurements are a special type of periodic measurement in which water levels in wells are measured within a relatively short period and under same hydrologic conditions. Synoptic water level measurements provide a "snapshot" of hydraulic heads in an aquifer. Synoptic measurements commonly are taken when data are needed for mapping the altitude of the water table or potentiometric surface, determining hydraulic gradients, or defining the physical boundaries of an aquifer.

Figure 15.3 Examples of manual water-level measurements in monitoring wells. *Left*: Student of hydrogeology learns how to take measurement with an acoustic sounding probe. Courtesy of Zoran Stevanović. *Right*: Taking measurement at a 385-m deep monitoring well in Peruvian Andes with an electronic sensor probe.

An example of the effects of different measurement frequencies is provided by water-level hydrographs for an observation well in Massachusetts completed in bedrock to a depth of 740 feet. A daily water-level hydrograph for the Massachusetts well and hydrographs that would have been obtained for the same well if measurements had been made only monthly or quarterly are shown in Figure 15.4-*Left*. Comparing the effects of different measurement frequencies on the hydrographs illustrates several features. First, monthly water-level measurements for this well generally are adequate to discern overall seasonal patterns in water levels and long-term trends but miss some short-term effects from pumping or recharge. Second, unless quarterly measurements correspond with regular patterns of seasonal variability of water levels, it can be difficult or impossible to discern anything beyond simple long-term water-level trends. Figure 15.4-*Right*, which overlays the daily and quarterly hydrographs from Figure 15.4-*Left*, illustrates how less frequent water-level measurements lead to lower estimates of the range of fluctuations in water levels in an observation well.
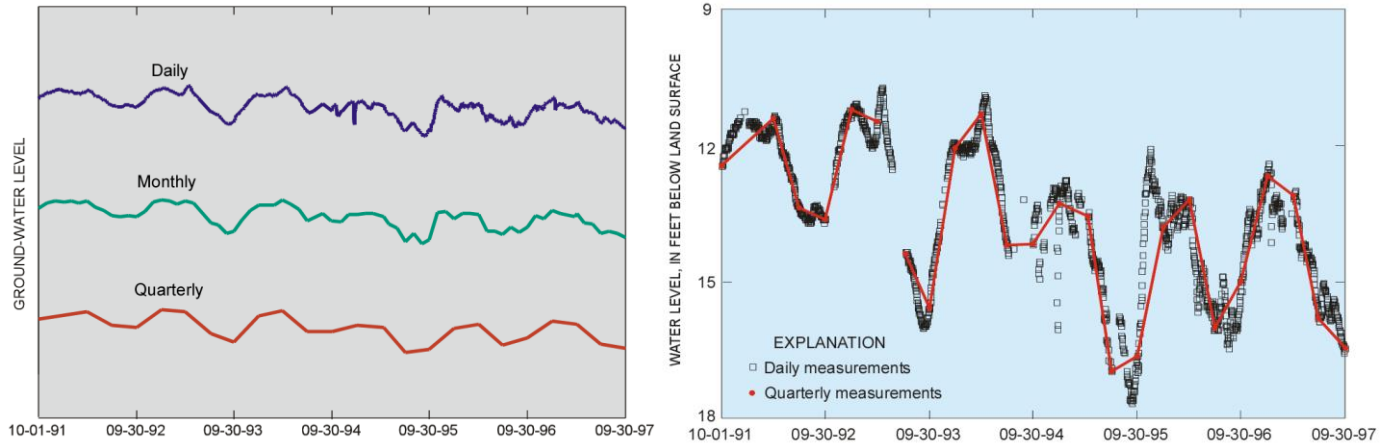
Figure 15.4 *Left*: Water-level hydrographs for well PDW 23 in western Massachusetts, based on daily, monthly, and quarterly measurements, plotted to same scale but vertically offset. *Right*: Overlaid daily and quarterly hydrographs for well PDW 23. Modified from Taylor and Alley, 2001. USGS, in public domain.

In some cases, sampling frequency becomes the most critical parameter for the success of a monitoring program. Notwithstanding the limitations associated with the high frequency (e.g., daily), continuous or real-time monitoring, such as relatively high cost and feasibility of implementation, a site-specific situation may deem any other sampling interval entirely inadequate. For example, Figure 15.5 shows discharge measured at 10- or 15-minute intervals at the Wilson Spring in Central Basin karst region of Tennessee, the United States (Williams and Farmer, 2003). Nonisokinetic dip-sampling methods were used to periodically (mostly during baseflow conditions) collect samples of volatile organic compounds (VOCs) from the spring. During selected storms, automatic samplers were used to collect samples, which were analyzed using a portable gas chromatograph (GC). Quality-control samples included trip blanks, equipment blanks, replicates, and field-matrix spike samples. Significant changes in water quality and discharge were detected with rapid changes observed during storms. Specific conductance ranged from 81 to 663 µS/cm, and chloroform concentrations ranged from 0.073 to about 34 mg/L. The greatest change was observed during the first storm during fall 2000, when chloroform concentrations increased from about 0.5 to about 34 mg/L.
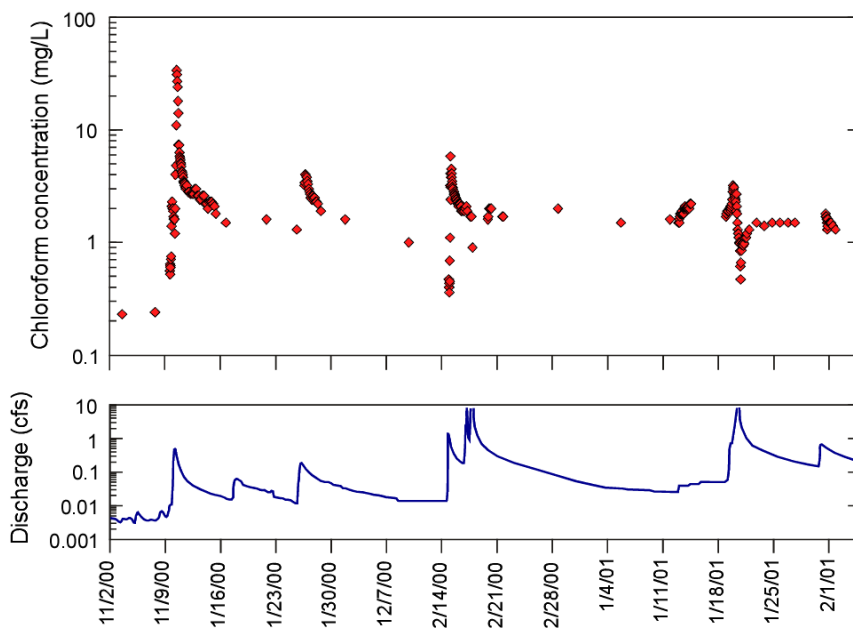
Figure 15.5 Results of high-frequency measurements at Wilson Spring in Central Karst region of Tennessee. Modified from Williams and Farmer, 2003. USGS, in public domain.

414

From these results, it is apparent that a sampling interval of 1 week or 1 month would not provide any meaningful information as to the actual volumes of water discharging from the aquifer, response of the aquifer to precipitation events, and the actual range of concentrations (fluctuation) of a possible contaminant. It is precisely for this reason why the U.S. EPA, in its Ground Water Rule (see Appendix B), emphasized vulnerability to contamination of aquifers with potentially high groundwater velocities, such as karst, fractured rock, and gravel aquifers. U.S. EPA (1992) specifically points out the following groundwater monitoring challenges in karst:

> In aquifers dominated by conduit flow, subsurface conduits are the primary pathways that contaminant releases follow. Identifying and intercepting these conduits with wells is an extremely formidable task. Identifying contaminant transport pathways requires detailed site characterization beyond what is usually performed at most sites. In addition, the wide fluctuations in the water table that are characteristic of aquifers dominated by conduit flow make identification and satisfactory monitoring of the uppermost aquifer particularly difficult.

> In certain circumstances, the Regional Administrator may request that a strategy of monitoring seeps, springs, and cave streams be applied to supplement monitoring well systems in all aquifers dominated by conduits that drain to springs and that discharge on land or along the shores of streams, rivers, lakes, or seas. In terranes where conduit flow predominates, springs and cave streams (if they have been shown by tracer studies to drain from the facility being evaluated) are the easiest and most reliable sites at which to monitor groundwater quality (Quinlan, 1989; Quinlan, 1990).

> Springs, seeps, and directly accessible cave springs may need to be tested by tracing not only during moderate flow, but also during flood flow and base flow, to prove their usefulness for monitoring. During flood conditions, water levels in streams, rivers, and lakes may rise, and some of this water may move temporarily through conduits that are dry during low-flow conditions and discharge into adjacent ground-water basins. There are certain characteristics of water movement in a karst aquifer dominated by conduit flow that should be recognized if a monitoring strategy is to be effective. One characteristic is distributary flow. During periods of high stage, water (and contaminants if they are present) from the headwaters or mid-reaches of a groundwater basin may flow to all springs in its distributary system. Distributary flow is most pronounced in areas of aggradation of river valleys (e.g., Mammoth Cave, Kentucky) where many alternate conduits at and below base level are available (deep sediment fill covering the bedrock floor of the valley).

> The placement of wells in karst terranes with subsurface conduits is rarely effective. Installing a suite of wells to intercept cave streams that have been shown by tracing to flow from the facility is a good strategy, but cave streams can be *practically impossible* (emphasis added) to locate.

> A second alternative for selecting monitoring well locations in aquifers with conduit flow is to place wells along fractures or fracture trace intersections. Tracer studies should be used to verify a hydraulic connection with the ground water beneath a facility under base-flow and flood-flow conditions. Although some cave passages coincide with various types of fracture traces and lineaments, not all fractures and fracture-related features are directly connected with cave passages. Many cave streams are developed along bedding planes and are thus unaffected by vertical fractures. This fact lessens the probability that a well drilled on a fracture trace or lineament, or at the intersection of such linear features, will intercept a cave stream.

The USGS works in collaboration with partners to monitor groundwater levels using the framework of the National Groundwater Monitoring Network (NGWMN). This collaborative groundwater network of Federal, State, and local agency data providers aims to build and refine a national network of wells that meet specific criteria related to quality, accessibility, density, and frequency of measurement criteria. More ca be found at https://www.usgs.gov/programs/groundwater-and-streamflow-information-program/groundwater-monitoring

15.1.1 Groundwater Sampling

The goal of groundwater sampling is to collect samples that are representative of in-situ groundwater conditions and to minimize changes in groundwater chemistry during sample collection and handling. Experience has shown that groundwater sample collection and handling procedures can be a source of variability in water-quality concentrations due to differences in sampling personnel, sampling procedures, and equipment (U.S. EPA, 1995a).

Whenever possible, several key chemical and physical parameters of water should be determined in the field (Figure 15.6) before sending sample to the laboratory because the sample will not be representative of the true field conditions once it is collected and handled. This is usually done with sensors/probes for pH, temperature, turbidity, electrical conductance (conductivity), and oxidation-reduction potential (ORP and redox are common acronyms).

Figure 15.6 Monitoring spring water quality. Field equipment includes probes for measuring electrical conductivity, pH, water temperature, redox potential (ORP), and turbidity. Note a flow measurement device in the front. Courtesy of Zoran Stevanović.

A publication by U.S. EPA Region 4 (2017) describes general and specific procedures, methods, and considerations to be used and observed when collecting groundwater samples for field screening or laboratory analysis. The procedures contained in this document are to be used by field personnel when collecting and handling groundwater samples in the field. As specified by the Agency, if is determined that any of the procedures described are either inappropriate, inadequate, or impractical and that another procedure should be used to obtain a groundwater sample, the variant procedure will be documented in the field logbook, along with a description of the circumstances requiring its use.

Chain-of-Custody and Records Management. A chain-of-custody procedure should be designed to allow the reconstruction of how and under what circumstances a sample was collected, including any problems encountered. It is intended to prevent misidentification of the samples, to prevent tampering with the samples during shipping and storage, to allow easy identification of any tampering, and to allow for the easy tracking of possession.

To prevent sample misidentification, the field staff should affix a label to each sample container. Sample labels should be sufficiently durable to remain legible even when wet. Sample labels should contain, at a minimum, the following information: ·

- Sample identification number;
- Name and signature of collector;
- Date and time of collection;
- Place of collection; and
- Parameters requested (if space permits).

Both field and laboratory Quality Control (QC) samples should be prepared during the sampling event. It is recommended that the following samples be analyzed with each batch of samples (a batch may not exceed 20 samples):

- One field duplicate; ·
- One equipment rinsate (required only when non-disposable equipment is being used); ·
- One matrix spike (when appropriate for the method); and ·
- One duplicate sample (either a matrix duplicate or a matrix spike duplicate).
- Trip blank when samples are being analyzed for volatile organic analytes. A trip blank should be submitted with samples each day that samples are collected.

Sampling Procedures. Several different groundwater sampling procedures can be used, which vary primarily through the criteria used to determine when a sample is representative of groundwater conditions. No single method or procedure is universally applicable to all types of groundwater sampling programs; therefore, consideration should be given to a variety of factors when determining which method is best suited to site-specific conditions. These site-specific conditions include sampling objectives, equipment availability, site location, and physical constraints. In addition, procedures for sample holding times, sample preserving procedures, and sample shipping methods to analytical laboratories should be specified for each contaminant to be analyzed. For example, samples for the analysis of VOCs should be put on ice and shipped overnight to the laboratory.

Purging is the process of removing stagnant water from a well, immediately prior to sampling, causing its replacement by groundwater from the adjacent formation that is representative of aquifer conditions. Sampling is the process of obtaining, containerizing, and preserving (when required) a groundwater sample after the purging process is complete. There are several approaches to well purging and sampling that may be appropriate in various circumstances or for various combinations of available equipment. They are briefly summarized in Table 15.1.

In order to determine when a well has been adequately purged, field investigators should monitor, at a minimum, the pH, specific conductance and turbidity of the groundwater removed, and the volume of water removed during purging. An adequate purge is achieved when the pH and specific conductance of the groundwater have stabilized, and the turbidity has either stabilized or is below 10 Nephelometric Turbidity Units (NTUs); the pH should remain constant within 0.1 Standard Unit (SU) and specific conductance should not vary more than 5 percent (U.S. EPA, 2017).

Bailers (Figure 15.7) are among the simplest of groundwater sampling devices. A bailer is a rigid tube that fills with water when lowered into the well; when raised back out of the well, it is sealed on one or both ends, typically by a ball and seat mechanism. Bailers that seal only at the bottom are called single check valve bailers, bailers that seal at both ends are called double check valve bailers or point-source bailers. Bailers are relatively inexpensive to purchase or fabricate, easy to clean, portable, simple to operate, and require no external power source. Disadvantages of bailers are that their use can be time consuming and labor intensive and that the transfer of water to a sample container may significantly alter the chemistry of groundwater samples due to degassing, volatilization, or aeration (oxidation).

Table 15.1 Purge and Sample Strategies with Equipment Considerations. From U.S. EPA, 2017

Purging Strategy	Purge Eqpt	Purge Eqpt	Comments
Multi-Volume Purge		Bailer	Advantages: Consistent results can be achieved with minimal skill level required. Common, simple equipment can be used. Disadvantages: Can result in large volumes of purge water. Can take extended periods of time with large diameter wells or long water columns.
In this traditional method, 3-5 well volumes of water are removed from the top of the well column while verifying the stability of water quality parameters. Following the well purge, the well is sampled from the top of the water column.	Bailer	Bailer	Bailers are rarely used for purging due to effort required, the difficulty of lowering turbidity adequately, and the possibility of aerating the upper water column.
	Electric Submersible Pump	Bailer	Common multiple-volume setup when depth to water exceeds 25 feet. Abbreviated pump decontamination proceedure can be used between wells.
	Electric Submersible Pump	Electric Submersible Pump	Requires full pump decontamination and new tubing at each well. In most cases the pump would be deployed to the screened interval instead to perform Low-Flow sampling.
	Peristaltic Pump	Peristaltic Pump	Common multiple-volume setup when depth to water is less than 25 feet. Special sampling techniques are required for the collection of SVOCs and VOCs.
Low-Flow Methods			Advantages: Lower volume of purged water. May be faster, especially with longer water columns. Disadvantages: Requires greater skill for consistent results. Higher tubing costs than multi-volume method
The pump or tubing is placed within the screened interval and the well is purged to stable water quality parameters while maintaining stable drawdown of the water level.	Electric Submersible Pump	Electric Submersible Pump	Commonly used when depth to water exceeds 25 feet. Pump is cleaned to sample equipment standards prior to sampling each well and new or dedicated tubing used for each well. Concerns have been raised concerning VOC loss from agitation in the turbine section or from sample heating.
	Peristaltic Pump	Peristaltic Pump	Commonly used where depth to water is less than 25 feet. Special sampling techniques required for the collection of SVOCs and VOCs. Concerns have been raised concerning VOC loss from vacuum created in sample tubing.
	Bladder Pump	Bladder Pump	Least danger of VOC loss as entire sample trai8n is under positive pressure and little sample heating occurs. Difficult to remove large volumes of water in reasonable time. Mild surging effect may keep turbidity elevated in sensitive wells.
Minimum-Purge, No-Purge Methods			Advantages: Very little or no waste water. Well suited to repeat sampling events. Likely faster with lower costs. Disadvantages: Not directly equivalent to other methods. Vertical stratification or vertical flow conditions in the screened interval can result in deceptive or non-intuitive anaytical results.
Predicated on the assumption that aquiifer flow through the well maintains the water in the screened interval in a state equivalent to that in the aquifer. This assumption should be proven or the data quakified. Sampling is conducted with little or no purge, or by equilibrating a sampler in screened interval	Pumps, various	Pumps, various	In the minimum-purge method, the internal volume of sample tubing and pump is calculated. One volume of the pump and tubing is purged to flush the equipment and the well is then sampled.
	na	Passive Diffusion Bags	In most common form, a sealed water-filled polyethylene bag is allowed to equilibrate in the water column. Suitable primarily for VOCs. Generally require 2 week minimumin-situ residence time.
	na	Hydrasleeves	Collect a fixed volume of water from specific interval. Requires duplicate samplers or redeployment for larger volumes. Sorption issues may bias results.
	na	Snap sampler	Deploys a sample container in the sampling intervcal where it is allowed to equilibrate (commonly for two weeks) before being sealed in-situ by the sampler mechanism and retrieved. Limited to specific containers.

Bladder pumps (also referred to as gas squeeze pumps) are submersible mechanisms consisting of a flexible membrane (bladder) enclosed in a rigid (usually stainless steel) housing. The internal bladder can be compressed and expanded under the influence of gas (air or nitrogen). Bladder volumes (e.g., volume per cycle) and sampler geometry can be modified to increase the sampling abilities of the pump. Automated control systems are available to control gas flow rates and pressurization cycles. Bladder pumps prevent contact between the gas and water sample and can be fabricated entirely of fluorocarbon resin and stainless steel. Pohlmann and Hess (1988) determined that bladder pumps can be suitable for collecting ground-water samples for almost any given organic or inorganic constituent. Disadvantages of bladder pumps include the large gas volumes required (especially at depth), and potential bladder rupture.

Figure 15.7 Purging a monitoring well with a bailer before collecting sample for laboratory analysis.

Low-Flow (Minimal Drawdown) is a method of preparing a well for sampling which, unlike traditional purging methods, does not require the removal of large volumes of water from the well (Figure 15.8). The term "low-flow" refers to the velocity at which groundwater moves through the pore spaces of the formation adjacent to the screen during pumping. It does not necessarily reflect the flow rate of the water discharged by the pump at the ground surface. The focus of low-flow purging and sampling is on collecting high-quality samples by minimizing the impact of pumping on well hydraulics and aquifer chemistry. Because the flow rate used for purging is, in many cases, the same as or only slightly higher than the flow rate used for sampling, the process is a continuum and is referred to as "low-flow purging and sampling" (U.S. EPA, 2005).

Figure 15.8 *Left*: Low-flow sampling equipment. Courtesy of *In-Situ* (https://in-situ.com/us/low-flow-sampling). *Right*: Low-flow sampling at a site in Pennsylvania, U.S. Photo courtesy of Jeff Manuszak.

Although minimizing the disturbance of sampling on the aquifer is important for all types of groundwater sampling devices, it can be particularly important for DPT point-in-time samplers and exposed screen wells because installation of a filter pack generally is not feasible with these tools. Low-flow purging and sampling generally are appropriate for collecting groundwater samples in a wide variety of situations. It can be used to sample all categories of aqueous phase contaminants and naturally occurring analytes, including VOCs, SVOCs, trace metals and other inorganics, pesticides, PCBs, radionuclides, and microbiological constituents and often is particularly appropriate for situations where colloidal transport is an issue (i.e., radionuclides, metals, and hydrophobic compounds). However, low-flow methods generally are not applicable to the collection of NAPLs because they do not respond to the effects of pumping in the same manner as groundwater.

Sampling of Direct Push wells can be performed with bailers, check-valve pumps, peristaltic pumps, or narrow-diameter bladder pumps. Several small-diameter bladder pumps (down to ½- inch in diameter) are commercially available. Because exposed-screen monitoring wells do not have an annular seal, caution is required for sampling contaminants if the well is pushed through NAPL or significant soil contamination.

Special porous sampling cones can be used with conventional cone-penetration equipment, which allow collection of soil gas or groundwater samples from a desired depth by lowering specially designed vials down the casing to the cone. One-time samples are helpful for characterizing the extent of contaminant plumes, but are not suitable for ongoing monitoring (U.S. EPA, 2005).

There are a number of probes that can be attached to DPT rigs to detect contaminants in the subsurface without retrieving groundwater samples. These include induced fluorescence systems and volatilization and removal systems. Two widely available systems used with CPT rigs are the Site Characterization Analysis Penetrometer System, or SCAPS, and the Rapid Optical Screening Tool, or ROST™. Both use a CPT-deployed laser-induced fluorescence (LIF) probe to qualitatively identify the types and relative concentrations of petroleum hydrocarbons present. This is accomplished by transmitting ultraviolet (UV) light from a nitrogen laser through a sapphire window into the soil. The UV light causes polynuclear aromatic hydrocarbon (PAH) components to fluoresce, and the varying intensity of the fluorescence is indicative of the amounts of the PAHs present. The spectrum of the fluorescence describes the distribution of PAHs present in the hydrocarbon (or often contaminant mass), which can be used for rough fingerprinting of the type of hydrocarbon (U.S. EPA, 2005).

Passive samplers acquire a sample from a discrete location or interval in a well, without the active transport associated with a pump or purge technique. In wells, all these passive methods rely on the well water being in equilibrium with the formation water. Some of the diffusion-based samplers are limited to certain suites of analytes. The passive samplers can be classified into three categories (ITRC, 2006):

1. Devices that recover a grab sample. Samples are an instantaneous representation of conditions at the sampling point at the moment of sample collection.
2. Devices that rely on diffusion of the analytes to reach equilibrium between the sampler and the well water. Samples are time-weighted toward conditions at the sampling point during the latter portion of the deployment period. The degree of weighting depends on analyte and device-specific diffusion rates. Typically, conditions during only the last few days of sampler deployment are represented.
3. Devices that rely on diffusion and sorption to accumulate analytes in the sampler. Samples are a time-integrated representation of conditions at the sampling point over the entire deployment period. The accumulated mass and duration of deployment are used to calculate analyte concentrations in the sampled medium.

15.2 Stream and Spring Flow Measurements

The following three general methods can be applied to flow measurements in surface streams and in subsurface karst channels: (1) weirs and flumes, (2) area-velocity, and (3) dye tracers. These and other more specialized techniques such as Acoustic Doppler Current Profiler (ADCP; see Figure 15.9) are described in detail in a series of technical publications by the USGS available for free download at: http://pubs.usgs.gov/twri/. The National Groundwater and Streamflow Information Program by USGS offers general information on the topic at
https://www.usgs.gov/programs/groundwater-and-streamflow-information-program

Particularly useful is a joint publication by several US government agencies entitled Water Measurement Manual (Bureau of Reclamation, 2001), available online or for free download at
https://usbr.gov/tsc/techreferences/hydraulics_lab/pubs/wmm/wmm.html

As discussed by NNPSMP (2008), the flow variables and the frequency with which they are measured depend on the project objectives and data analysis plans. For example, single measures of instantaneous spring or stream discharge are highly unlikely to satisfy any of the common objectives of water management because they represent only a snapshot in time. If conducted as part of a synoptic survey within a study watershed, however, such data might be useful in comparing the hydrologic behavior of subwatersheds, characterizing the relative magnitudes of sediment (or contaminant) loads or flows from subwatersheds, or calibrating a hydrologic model for the study watershed.

Figure 15.9 Doppler radar hydrometry of a river in karst. Following the rope extended between two river sides doppler collects and calculates information on riverbed depth and water velocity. Such hydrometry is essential method to estimate hidden water losses or inflows along the river. Courtesy of Zoran Stevanović.

Streams and springs without permanent gages and sufficient data record present special challenge when determining characteristic flows needed for various calculations. Long-term minimum baseflow is of particular importance for various applications such as determining maximum allowable loading rates of a groundwater contaminant that are still protective of in-stream water quality standards. In the United States, this flow is typically referred to as 7Q10, or 7-day, consecutive low flow with a 10-year return frequency (i.e., the lowest streamflow for seven consecutive days that would be expected to occur once in 10 years).

Flow measurement at successive stream segments is a common method of determining if the stream is losing or gaining water between the segments. However, because of the variability of flow conditions in the same stream and the associated potential measurement errors, this method should be applied with great care in order to avoid false conclusions. For example, if only one set of measurements is made at a few locations, with several or more hours separating them, and the streamflow is under the influence of recent precipitation, the results would almost certainly be misleading since the flow wave is moving rapidly. It is therefore best if the flow measurements are performed after a long period without precipitation and the applied method is based on a continuous recording of the stream stage at successive stream segments. Flow hydrographs derived in this way provide information on the actual change of volume of water between the segments, which is the only real measure of gain or loss.

15.2.1 Weirs

Weir is a structure that water flows through or over that has a known relationship between stage and flow. If a weir can be used, discharge measurement can be as simple as observing the stage of water just upstream of the it and consulting a table or using a simple equation to calculate discharge.

Weirs are commonly named by the shape of their blade overflow opening shape for sharp-crested weirs (Figure 15.10) or the flow control section shape for broad-crested weirs. Thus, weirs are classified as rectangular, trapezoidal, or triangular. In the case of sharp weirs, the triangular weir is also called a V-notch weir, and one popular kind of trapezoidal weir is the Cipolletti weir (Figure 15.10). In the case of rectangular or Cipolletti weirs, the bottom edge of the notch in the thin plate is the crest, and the side edges (which are vertical or flare up and outward) are the sides or ends. The point of the triangle is the crest of a V-notch weir. The lowest elevation of the overflow opening of the sharp-crested weirs is the head measurement zero reference elevation (Bureau of Reclamation, 2001).
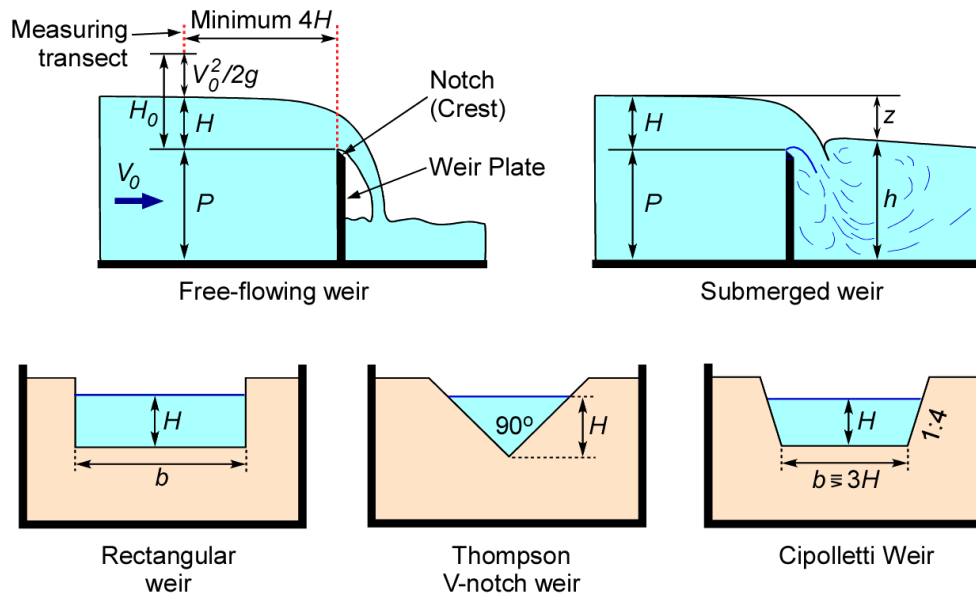
Figure 15.10 Sharp-crested weirs for small stream and spring flow measurements. Explanation in text.

The water surface drops noticeably as flow approaches the crest. This continuing drop of water surface or drawdown results from the acceleration of the water as it approaches the weir. The drop in water surface between the upgradient measuring station and the notch is equal to the change of velocity head, or $V^2/2g$, between the two (Figure 15.10). Velocity of approach is equal to the discharge divided by the flow section area at the head measuring station. Downstream water rising above the weir crest elevation produces a submerged weir condition (Figure 15.10 – top right). When the downstream water surface is near or above the crest elevation of a sharp-crested weir, accuracy of measurement should not be expected. The use of a submerged weir as a flow measurement device is not good practice and should only be done as a temporary procedure.

In practice, weirs can range from small wood or metal plates temporarily mounted across small ditches or streams to more permanent installations involving concrete walls and other structures (Figure 15.11). Note that erecting any obstruction in a stream will create a pool upstream and care must be taken to avoid creating the potential for flooding during high flows. In some cases, a permit may be required. A weir discharge measurement

consists of measuring depth or head, H, relative to the crest at the proper upstream location in the weir pool and then using a table or equation for the specific kind and size of weir to determine discharge. Commonly, a staff gage, having a graduated scale with the zero placed at the same elevation as the weir crest, measures head. Putting staff gages in stilling wells dampens wave disturbances when reading head.

Figure 15.11 *Left*: Rectangular weir measuring outflow from a spring in Winchester, Virginia formerly utilized for public water supply. *Middle*: Sharp-crested 120 degrees V-notch weir. *Right*: Prefabricated H flume. Two right photographs courtesy of Don Meals, Tetra Tech, Inc., from NNPSMP, 2008; in public domain.

When the weir is not submerged, the general flow equation for a rectangular sharp-crested weir is

$$Q = mb\sqrt{2g}\ H_0^{3/2} \qquad (15.1)$$

where m is the overflow coefficient, b is the width of the weir (overflow), g is the acceleration of gravity, and H_0 is the total energy of the overflow that includes the overflow height, H, and the velocity component.

The overflow coefficient takes values $0.40 < m < 0.48$, with $m = 0.42$ used most often in practice. As the velocity of the overflow is usually not measured, this equation is replaced by a more practical one

$$Q = m_0 b\sqrt{2g}\ H^{3/2} \qquad (15.2)$$

where the overflow coefficient, m_0, is calculated by the empirical formula of Bazen:

$$m_0 = \left(0.405 + \frac{0.0027}{H}\right) \times \left[1 + 0.55\left(\frac{H}{H+P}\right)^2\right] \qquad (15.3)$$

Triangular V-notch sharp-crested weir with the 90-degree angle (Figure 15.10), also known as Thompson weir, is often used for precise measurements of low flow rates such as in small streams and laboratories. The flow rate is calculated as

$$Q = 0.32\sqrt{2g}\ H^{5/2} \qquad (15.4)$$

$$Q = 1.4H^{5/2} \qquad (15.5)$$

In Equation (15.5) the height of the overflow (*H*) is given in meters, and the flow rate (*Q*) is obtained in m³/s.

For the widely used Cipolletti weir the flow rate is calculated as

$$Q = 0.42b\sqrt{2g} \ H^{3/2} \qquad\qquad (15.6)$$

$$Q = 1.86bH^{3/2} \qquad\qquad (15.7)$$

In Equation (15.7), the height of the overflow (H) is given in meters, and the flow rate (Q) is obtained in m^3/s.

When the downgradient elevation of the water surface is higher than the elevation of the rectangular weir crest, that is, for the condition that h > P (see Figure 15.10), the weir is submerged. The general conditions for a weir to be submerged is z/P<0.7, in which case the flow rate is a function of both the upgradient and the downgradient head: $Q = f(H,h)$. The flow rate can be calculated using

$$Q = \sigma_s m_0 b\sqrt{2g} \ H^{3/2} \qquad\qquad (15.8)$$

where σ_S is the coefficient of submergence calculated using the empirical formula of Bazen:

$$\sigma_S = 1.05\left(1 + 0.2\frac{H-z}{P}\right) \times \sqrt[3]{\frac{z}{H}} \qquad\qquad (15.9)$$

and the overflow coefficient, m_0, is calculated using equation (15.3).

Cipolletti and rectangular weirs are often used for measuring discharge rate of large karst springs which can have wide range of flows, from tens of L/s to many m^3/s.

Flumes are specially shaped open channel flow sections that restrict the channel area, resulting in increased velocity and a change in water level as water flows through a flume. The discharge through a flume is determined by measuring the stage in the flume at a specific point, depending on the type of flume. In general, flumes are used to measure discharge where weirs are not feasible. Flumes are well suited to measurement of flows containing sediment because the increased velocity through the flume tends to make it self-cleaning. Commonly used flumes include the Parshall, Palmer-Bowlus, and H flumes (see Figure 15.11). Flumes come in a wide range of sizes denoting the maximum depth of flow they can accommodate and can be purchased as prefabricated units or built on-site. Most devices have exacting specifications for installation that may present construction challenges. More information on weirs and flumes is provided in Bureau of Reclamation (2001).

15.2.2 Velocity-Area Method

The velocity of moving water varies both across a stream channel and from the water surface to the bottom of the stream because of friction and irregularities in cross section and alignment. Friction caused by the rough channel surfaces slows the water near the bottom and sides of a channel so that the fastest water is usually near the center of the channel and near the surface. On a river bend, the water on the outside of the bend moves faster than the water on the inside of the bend, as it has to cover more distance in the same time. It is therefore necessary to perform a number of velocity measurements across the stream channel and at different depths. Figure 15.12 is a schematic of the velocity-area method applicable to any surface or subsurface stream channel. The discharge in each subsection is computed by multiplying the subsection area by the measured average velocity that, in this case, is the average of two velocities measured at 0.2 and 0.8 subsection depths. The total discharge is then computed by summing the discharge of each subsection. To apply the method, a straight reach, reasonably free of large rocks or

obstructions, with a relatively flat streambed, away from the influence of abrupt changes in channel width should be selected.

Determining the cross-sectional area of a flowing stream usually involves measuring water depths at a series of points across the stream and multiplying by the width of the stream within each segment represented by the depth measurement. The segment areas are then summed to determine the entire cross-sectional area. Commonly, the stream width is divided into 20 to 25 segments using tape or string to mark the center of each segment on a cable stretched across the stream perpendicular to the flow. Streams less than 10 ft (3 m) wide may not allow as many segments. Typically, the stream is divided into enough segments so that each one has no more than 10 percent of the total streamflow. Segment width is generally measured using a cable, steel tape, or similar piece of equipment. Segment depth is measured using a wading rod, if conditions permit, or by suspending a sounding weight from a calibrated cable and reel system off a bridge, cableway, or boat or through a hole drilled in ice.

To deal with the variability in stream velocity within any cross-sectional area segment, studies by USGS support several general rules of thumb:

- Maximum velocity occurs at 5% to 25% of the depth, this percentage increases with increasing stream depth.
- Mean velocity in a vertical profile is approximated by the velocity at 0.6 depth.
- Mean velocity in a vertical profile is more accurately represented by the mean of the velocities at 0.2 and 0.8 depth.
- The mean velocity in a vertical profile is 80% to 95% of the surface velocity, the average of several hundred observations being 85%.

In some shallow streams, it may be possible to measure flow velocity at only one depth.
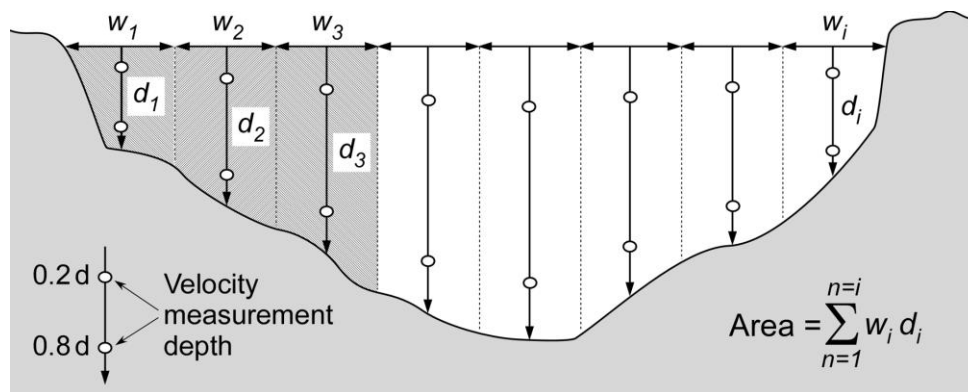
Figure 15.12 Schematic of the velocity-area method of streamflow measurements. Stream is divided into segments and discharge rate in each segment is calculated by multiplying the segment area with the flow velocity in that segment. The flow velocity is measured at two depths equaling 0.2 and 0.8 of the total depth of a segment. The total stream discharge is obtained by summing the segment discharges.

The most common current meter used by the USGS for measuring streamflow velocity is the Price AA current meter that has a wheel of six metal cups that revolve around a vertical axis (Figure 15.13). An electronic signal is transmitted by the meter on each revolution allowing the revolutions to be counted and timed. Because the rate at which the cups revolve is directly related to the velocity of the water, the timed revolutions are used to determine the water velocity. The Price AA meter is designed to be attached to a wading rod for measuring in shallow waters

or to be mounted just above a weight suspended from a cable and reel system for measuring in fast or deep water. In shallow water, the Price-Pigmy current meter can be used (Figure 15.13). It is a two-fifths scale version of the Price AA meter and is designed to be attached to a wading rod. A third mechanical current meter, also a variation in the Price AA current meter, is used for measuring water velocity beneath ice. Its dimensions allow it to fit easily through a small hole in the ice, and it has a polymer rotor wheel that hinders the adherence of ice and slush.

Figure 15.13 Measurement of underground flow with Price-Pigmy meter and wading rod. (Photograph courtesy of William Jones, Karst Waters Institute.) Inset: Price AA current meter on a round wading rod.

There is a strong relationship between river stage and discharge and, as a result, a continuous record of stream discharge can be determined from the continuous record of stage. The development of an accurate stage–discharge relation requires numerous discharge measurements at all ranges of stage and streamflow (Figure 15.14). In addition, these relations must be continually checked against ongoing discharge measurements because stream channels are constantly changing. Changes in stream channels are often caused by erosion or deposition of streambed materials, seasonal vegetation growth, debris, or ice. Reliable stream gaging therefore involves obtaining a continuous record of stage, making periodic discharge measurements, establishing, and maintaining a relationship between the stage and discharge, and applying the stage–discharge relation to the stage record to obtain a continuous record of discharge that is critical for water resources management.
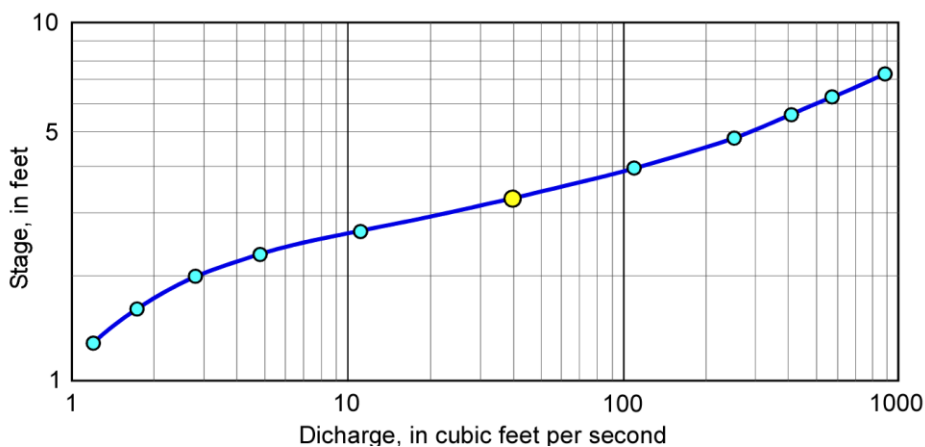
Figure 15.14 Example of a typical stage–discharge relation; here, for the large yellow dot, the discharge of the stream is 40 cubic feet per second (ft^3/s) when the stage is 3.30 feet (ft). The smaller blue dots on the curve represent concurrent measurements of stage and discharge. Modified from USGS, 2005. In public domain.

Most USGS stream gages measure stage and consist of a structure in which instruments used to measure, store, and transmit the stream–stage information are housed. Stage, sometimes called gage height, can be measured using a variety of methods. One common approach is with a stilling well in the riverbank (Figure 15.15) or attached to a bridge pier. Water from the river enters and leaves the stilling well through underwater pipes allowing the water surface in the stilling well to be at the same elevation as the water surface in the river. The stage is then measured inside the stilling well using a float or a pressure, optic, or acoustic sensor. The measured stage value is stored in an electronic data recorder on a regular interval, usually every 15 minutes.
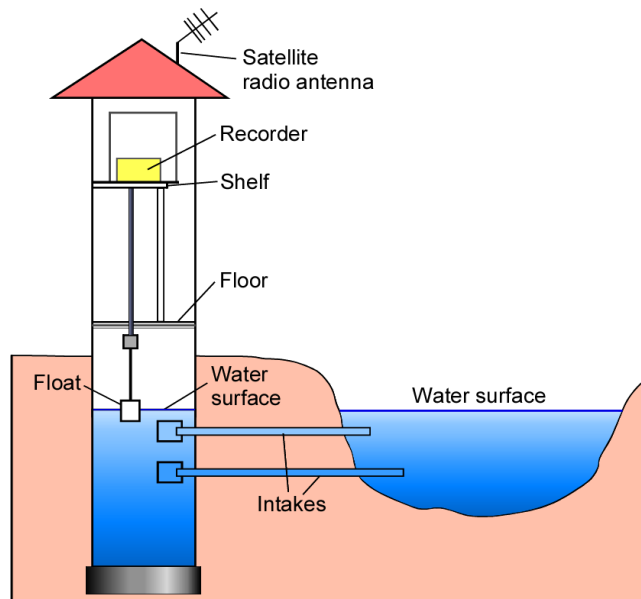
Figure 15.15 Diagram of a typical USGS stream gage with stilling well. Modified from USGS, 2005. In public domain.

Most of the stage and streamflow information produced by the USGS is available in near real time through the National Water Information System (NWIS) Web site (http://waterdata.usgs.gov/nwis/). In addition to real-time stream gage data, the NWIS Web site also provides access to daily discharges and annual maximum discharges for the period of record for all active and discontinued stream gages operated by the USGS. This includes monitoring wells and springs throughout the United States.

15.2.3 Slope-Area Method

The slope-area method consists of using the slope of the water surface in a uniform reach of channel and the average cross-sectional area of that reach to give a rate of discharge. The discharge may be computed from the Manning formula:

$$Q = \frac{1.486}{n} AR_h^{2/3} S^{1/2} \qquad (15.10)$$

Q is discharge (ft^3/s); A is mean area of the channel cross section (ft^2); R_h is mean hydraulic radius of the channel (ft); S is energy slope of the flow; and n is a roughness factor depending on the character of the channel lining.

A straight reach of the channel should be chosen at least 200 ft and preferably 1000 ft in length. If the reach is free of rapids, abrupt falls, or sudden contractions or expansions, then the water surface slope is the same as the energy slope. The slope, S, may be determined by dividing the difference in the water surface elevations at the two

ends of the reach by the length of the reach. A gage point, carefully referenced to a common datum level, should be placed on each bank of the channel and in the center of the reach, in stilling wells if possible.

The hydraulic radius, Rh, is defined as the area of the cross section divided by its wetted perimeter. Where the channel is of regular cross section, and the depths at the ends of the course are equal, and the area and the wetted perimeter will be constant throughout the course. In irregular channels, the area and the wetted perimeter at several cross sections will be required, and a mean value will be used in computing the hydraulic radius. A static pressure tube can be used to measure depth of flow.

The roughness factor, n, depends on the character of the channel. It may vary from 0.010, where conditions approaching the ideal are maintained to 0.060, where the channel is strewn with stones and debris or is about one-third full of vegetation. Because the proper selection of the roughness for many streams is difficult and is, at best, an estimate, the discharge determined by the slope-area method is only approximate. Care must be taken to determine the slope and areas simultaneously if the water levels are changing. Section 5.2.2 in Lecture 5 provides other flow equations, including friction factors that can be used with this method.

15.3 Aquifer Testing

Aquifer testing in the field includes methods of recording changes of the hydraulic head in response to either natural or artificial stresses on the aquifer. These stresses may be as "simple" as the natural aquifer recharge by newly infiltrated water after a rainfall event, or as complex as a long-term pumping test for development of a major well field for water supply. In any case, the aquifer field tests are designed to collect sufficient information, on both the stresses and the hydraulic head changes, needed to establish a quantitative relationship between the two. In turn, this quantitative relationship, expressed by one or more analytical equations, enables an estimation of the aquifer hydrogeologic parameters such as transmissivity (hydraulic conductivity), storage properties, and leakance from adjacent aquitards where applicable. It is important to understand that none of these parameters can be measured directly (like water temperature for example). Rather, their quantification is just an estimate, accuracy of which depends on both the field method applied and the interpretation of the collected information by a professional. In other words, interpretation of field test results is not unique and in most cases requires a solid hydrogeologic experience.

For many hydrogeologists the term "aquifer field test" implies pumping of a test well and recording of the related hydraulic head change (*well drawdown*) in the pumped well and one or more observation wells/piezometers in its vicinity. The collected information on the time-dependent well pumping rates and the drawdown in observation wells is then analyzed to obtain estimates of the aquifer transmissivity and aquifer storage properties such as specific yield for unconfined aquifers and coefficient of storage for confined aquifers (see Lecture 4). This so-called aquifer (or well) *pumping test* is still the main and default type of field testing in water supply hydrogeology. When designed properly, the test can also provide information on the test well efficiency and specific capacity, which are very important factors for optimum groundwater extraction. Note that some professionals incorrectly use term "pump test" instead of pumping test; pump test should be what the term implies – a test of a well pump.

Pumping tests are much less frequent in contaminant hydrogeology primarily because of the two main concerns: 1) disposal issues related to large quantities of contaminated water extracted during the test, and 2) possible alteration of contaminated groundwater (plume) flow directions. Consequently, various forms of slug tests are still considered default for contaminated aquifers because the contaminated groundwater is not extracted to the surface. When a detail evaluation or implementation of groundwater remediation alternatives includes a pump and treat system, it would often be required that an aquifer pumping test is performed to collect information necessary

for the remedial design. This because slug tests characterize a limited volume of the aquifer porous media in the immediate vicinity of the test well, as opposed to the pumping tests which evaluate response of a significantly larger aquifer volume.

Borehole flowmeters, hydrophysical testing, and packer tests, often in conjunction with pumping tests, are often utilized in the field to provide detail information on the aquifer heterogeneity and anisotropy, particularly in fractured rock and karst aquifers.

Several simple field tests, that only require recording of precipitation rates and continuous monitoring of the hydraulic head fluctuations in the aquifer and at a hydraulic boundary such as a surface water stream, may be very useful when estimating hydrogeologic parameters. For example, changes in the surface stream levels and their impact on the hydraulic head in the adjacent aquifer can be used to estimate aquifer parameters such as hydraulic diffusivity and transmissivity, as well as the aquifer recharge rate (Kresic, 2007). When two monitoring wells, located along the same known flow path, show response to major recharge events, a similar methodology can be applied to estimate aquifer hydraulic diffusivity and transmissivity between the two wells.

15.3.1 Slug Tests

Slug tests are performed in exploratory boreholes and small-diameter monitoring wells to find an approximate hydraulic conductivity of the porous media in the immediate vicinity of the well. Despite this limitation, and the fact that most methods in use cannot determine aquifer storage properties, slug test are widely applied in groundwater studies because of the following advantages:

- The cost is incomparably smaller than the cost of an average pumping test (not including the cost of a pumping well itself);
- The time needed for its preparation and the duration of the test are short;
- There is no need for observation wells;
- In case of contaminated aquifers, there are no issues associated with groundwater extraction and disposal.
- The test can be performed in exploratory boreholes that are only temporarily equipped with a screen;
- The results are not influenced by short-term or long-term changes such as variations of barometric pressure, or interference from nearby pumping wells.

Since the hydraulic conductivity calculated from a slug test is an estimate for a very small part of the aquifer around the borehole, it is recommended to test as many boreholes in the area of interest as possible to assess spatial distribution of the hydraulic conductivity.

In general, a slug test consists of quickly displacing a volume of water in the borehole (well) by adding or removing a "slug" (usually a solid cylinder of known volume; see Figure 15.16-*Left*) and then recording the change in the head at the well. Since the displaced volume of water is relatively small, the head displacement is also small and the recovery is fast. For this reason, it is necessary to quickly take as many measurements of the head in the well as possible in order to have enough data for the analysis. This is most accurately done with the help of a pressure transducer and a digital data logger, which can be programmed to take recordings every second, or with even smaller intervals during the initial portion of the test. Relatively quick recovery has been the main limitation of slug tests in highly permeable aquifers. However, research has led to development of methodologies for slug test analysis in such cases (Butler et al., 2003). Slug tests with packers can be used to determine vertical distribution of the hydraulic conductivity around a test well (Zermansky and McElwee, 2005).
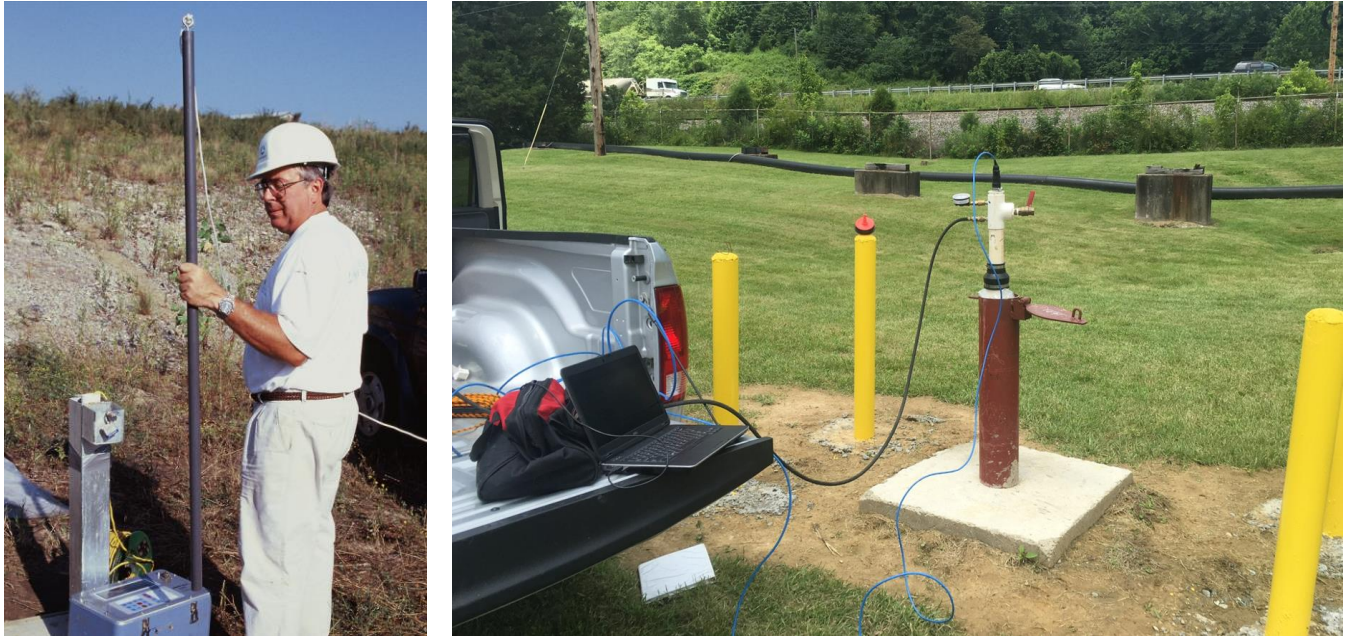
Figure 15.16 *Left*: Hydrogeologist Bob Seymour of Law Engineering and Environmental Services holds a solid cylinder ("slug") soon to be inserted into a monitoring well as part of slug testing at the Atlantic Steel brownfields site in Atlanta, Georgia. *Right*: Setup for an air-pressurized slug test. Photo courtesy of Dawit Yifru.

Modification of air-pressurized slug tests offers an efficient means of estimating the transmissivity (T) and storativity (S) of both low and highly permeable aquifers. Air-pressurized slug tests (Figure 15.16-*Right*) are conducted by pressurizing the air in the casing above the column of water in a well, monitoring the declining water level and then releasing the air pressure and monitoring the rising water level. If the applied air pressure is maintained until a new equilibrium water level is achieved and then the air pressure in the well is released instantaneously, the slug test solution of Cooper et al. (1967) can be used to estimate T and S from the rising water level data. (Shapiro and Green, 1995; Green and Shapiro, 1995, 1998). The total time to conduct the test can be reduced if the pressurized part of the test is terminated prior to achieving the new equilibrium water level (Figure 15.17).
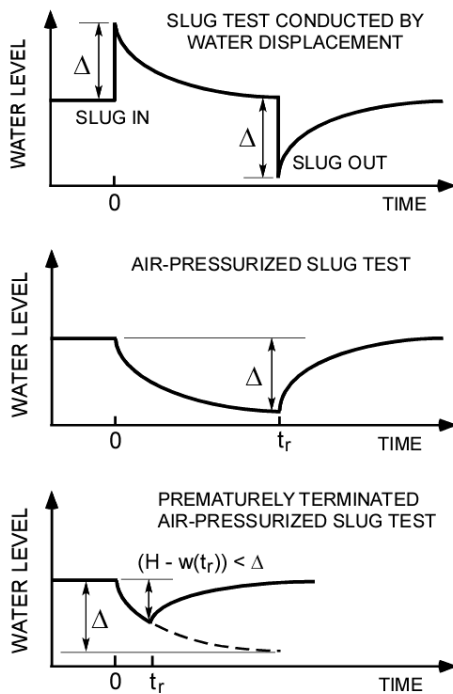
Figure 15.17 Schematic illustrating time-varying water level during (a) slug test conducted by water displacement, (b) air-pressurized slug test, and (c) prematurely terminated air-pressurized slug test, where Δ is the maximum change in water level due to water displacement or an applied air pressure, t_r is the time at which the pressurized part of the air-pressurized slug test is terminated, H is the initial water level at time $t = 0$, and $W(t_r)$ is the water level at time $t = t_r$. From Shapiro and Green, 1995. USGS, in public domain.

430

This is referred to as a prematurely terminated air-pressurized slug test. A public domain computer program called AIRSLUG for the analysis of air-pressurized slug test is described by Green and Shapiro (1995, 1998).

Three of the more commonly used methods of slug test analysis are Cooper et al. (1967) for confined aquifers, Hvorslev (1951) for confined aquifers, and Bouwer and Rice for unconfined and confined aquifers (1976). There are several commercially available computer programs that include various methods of slug test analysis such as AQTESOLV by HydroSOLVE and AquiferWin32 by Environmental Simulations Inc. The USGS series of ten Microsoft Excel-based programs for aquifer test analyses including three slug test methods: Bouwer and Rice, Green and Shapiro, and van der Kamp (Halford and Kuniansky, 2002).

Bouwer and Rice Method

The widely utilized Bouwer and Rice slug test can be used to determine the hydraulic conductivity in fully or partially penetrating and partially screened, perforated, or otherwise open wells (Bouwer and Rice, 1976; Bouwer, 1989). Although initially developed for unconfined aquifers, the test has been successfully used for confined aquifers given that the top of the screened section is below the overlying confining layer (Bouwer, 1989).

When water is instantaneously added to the well, the head is displaced upwards and then starts to fall as water enters the aquifer (the hydraulic gradient is from the higher head in the well toward a lower head in the surrounding porous medium). This type of slug test is called the *falling head test* (see Figure 15.18-*Left*). Water does not have to be added to the well in order to displace the head. A more common practice is to instantaneously lower into the well a heavy water-tight cylinder on a rod, which produces the same effect of head displacement. When water is quickly extracted from the well, (equivalent to instantaneously pulling the cylinder out), the head is displaced downwards and then starts to rise as water from the surrounding porous medium (aquifer) enters the well. This is called the *rising head test* (Figure 15.18-*Right*. Common practice in the field is to first perform the falling head test ("slug-in"), wait for the head stabilization, and then perform the rising head test by pulling the cylinder out ("slug-out"). If performed correctly, the falling head and the rising head test results should give similar values of the hydraulic conductivity.
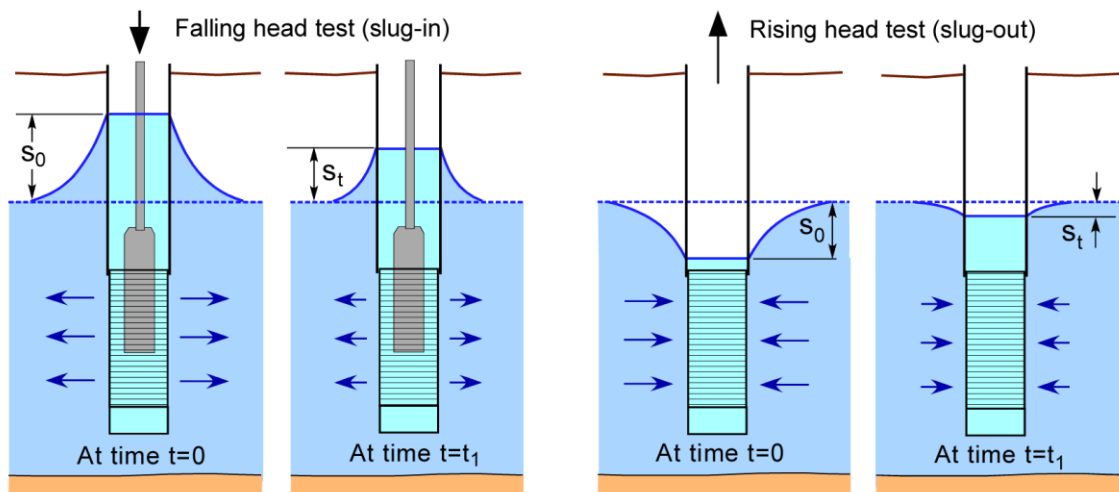
Figure 15.18 Schematic of falling head slug test (*left*), and rising head slug test (*right*). Sudden displacement from the initial water table is denoted with s_0. Modified from Kresic, 2007. Copyright CRC Taylor & Francis; permission is required for further use.

The elements needed for determining the hydraulic conductivity from the slug test data are shown in Figure 15.19. For reasons of consistency, the displacement of water level in the well is here denoted with s (equivalent to drawdown) rather than y as in the original work. The rate of water flow into the well, when the head in the well is lower than the initial water table in the surrounding aquifer, is given by the Thiem equation:

$$Q = 2\pi K L_e \frac{s}{\ln \dfrac{R_e}{r_w}} \qquad (15.11)$$

where:

Q is the flow rate

K is the hydraulic conductivity

L_e is the length of screened (perforated, open) section of the well

s is the vertical difference (displacement) between water level inside the well and water level outside the well (it is assumed
that water table in the aquifer does not change for duration of the test)

R_e is the effective radial distance over which s is dissipated

r_w is the radial distance of undisturbed portion of aquifer from centerline, *i.e.*, the radial distance from the center of the well to the undisturbed hydraulic conductivity of the aquifer.
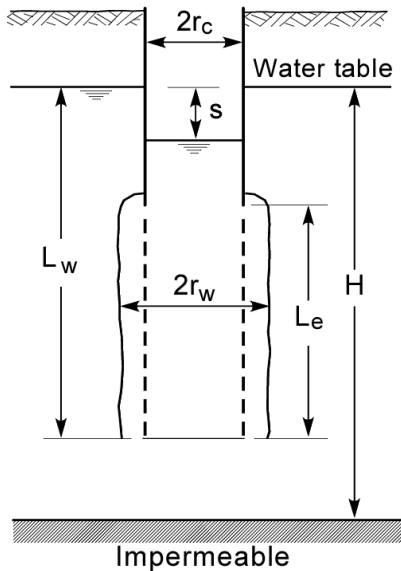
Values of R_e were determined experimentally by the authors and expressed in terms of the dimensionless ratio $\ln(R_e/r_w)$ which is calculated with the aid of the curves shown in Figure 15.20. The value of r_w is the radius of the screen plus the thickness of the gravel pack plus the thickness of the developed zone. In practice, the thickness of the developed zone is usually ignored since it is very difficult to define accurately.

Figure 15.19 Geometry and symbols for the Bouwer and Rice slug test in an unconfined aquifer with gravel pack and/or developed zone around well screen. Bouwer, H., 1989: The Bouwer and Rice slug test. *Ground Water*, 27(3), p. 304-309. Reprinted by permission of Ground Water Publishing Company. Copyright 1989. All rights reserved.

The rate of water level rise in the well is:

$$\frac{ds}{dt} = -\frac{Q}{\pi r_c^2} \qquad (15.12)$$

where r_c is the radius of the casing or other section of the well where the rise of water level is measured.

If the water rises in the screened portion of the well and there is a sand (gravel) pack around the screen, r_c should be adjusted to account for the total free-water surface area in the well and the gravel pack:

$$r_c^* = [(1-n) \cdot r_c^2 + nr_w^2]^{1/2} \qquad (15.13)$$

where n is effective porosity of the gravel pack.

Solving equation (15.12) for Q, equating the resulting expression to equation (15.11), then integrating, and solving for K gives the Bouwer-Rice equation (Bouwer, 1989):

$$K = \frac{r_c^2 \ln \dfrac{R_e}{r_w}}{2L_e} \cdot \frac{1}{t} \cdot \ln \frac{s_0}{s_t} \qquad (15.14)$$

where s_0 is displacement at time zero; s_t is displacement at time t.
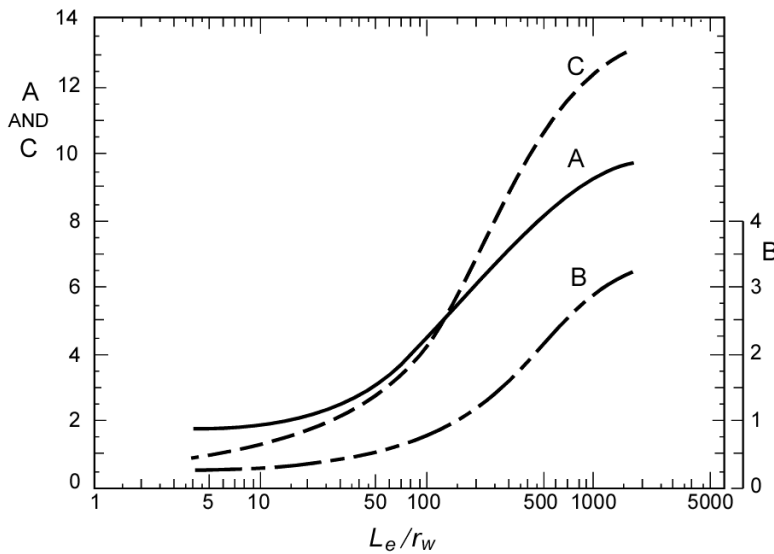
Figure 15.20 Dimensionless parameters A, B, and C as a function of L_e/r_w for calculation of $\ln(R_e/r_w)$ in the Bouwer and Rice slug test. Bouwer, H., 1989: The Bouwer and Rice slug test. *Ground Water*, 27(3), p. 304-309. Reprinted by permission of Ground Water Publishing Company. Copyright 1989. All rights reserved.

When the well is partially penetrating ($L_w<H$), the dimensionless ratio $\ln(R_e/r_w)$ is:

$$\ln \frac{R_e}{r_w} = \left[\frac{1.1}{\ln(L_w/r_w)} + \frac{A + B \cdot \ln[(H - L_w)/r_w]}{L_e/r_w} \right]^{-1} \qquad (15.15)$$

For fully penetrating wells this ratio is:

$$\ln \frac{R_e}{r_w} = \left[\frac{1.1}{\ln(L_w/r_w)} + \frac{C}{L_e/r_w} \right]^{-1} \qquad (15.16)$$

where A, B, and C are dimensionless numbers plotted in Figure 15.20 as a function of L_e/r_w.

The Hydraulic Conductivity. Since time (t) and displacement (s) are the only variables in logarithmic equation (15.14), the plot of t versus s on a semi-log paper must show a straight line. However, because the drawdown of the water table in the aquifer becomes more significant during the later part of the test, the basic assumption of equation (15.14) does not hold any more and data points start to deviate from the straight line. The slope of the best-fitting straight line through field data is found as:

$$\frac{\ln(s_1 / s_2)}{(t_2 - t_1)}$$

and then inserted into equation (15.14) with other known/calculated values to determine the hydraulic conductivity. s_1, t_1 and s_2, t_2 are the coordinates of any two points on the straight line. If the first point is chosen for time zero, the slope is then given as in equation (15.14):

$$\frac{\ln(s_0 / s_t)}{t - t_0} = \frac{1}{t} \cdot \ln \frac{s_0}{s_t}$$

Field data may often show the so-called *double straight-line effect* (Figure 15.21). The first straight line portion is explained by a highly permeable zone around the well (gravel/sand pack or developed zone), which quickly sends water into the well immediately after the water level in the well has been lowered (Bouwer, 1989). The second straight line is more indicative of the flow from the undisturbed aquifer into the well and its slope should be used in equation (15.14).
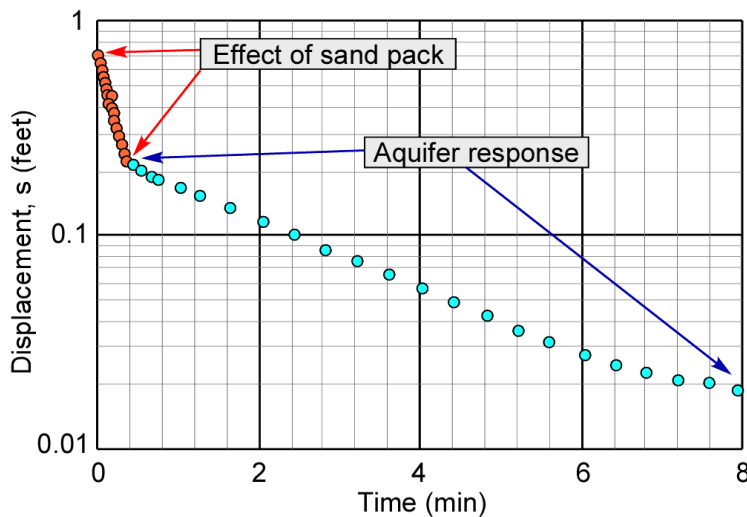
Figure 15.21 Example graph time vs. head displacement (*s*) for a falling head slug test.

One common mistake made by non-hydrogeologists (and improperly trained hydrogeologists) when interpreting slug test data (or any other aquifer test data) is accepting the so-called automatic fit solutions by a computer program. For example, AQTESOLV (http://www.aqtesolv.com), an excellent program for aquifer test analysis widely used around the world, automatically fits the observed data to a select theoretical model by default. This fit is based on simple statistics and has nothing to do with the real field conditions and the underlying reasons for a specific test response. The program, however, does provide for a versatile manual fit including "tweaking" of various parameters in the equations applicable to the selected model.

Although in some cases an automatic fit may be all that is needed (it makes perfect hydrogeologic sense), it will often be necessary to perform a manual fit and apply the hydrogeologic knowledge of the interpreter ("best professional judgment"). Figure 15.22 shows some real-world examples of improper interpretations of slug test data based on automatic fit, without any critical thinking by the interpreters. Most importantly, even a manual fit may not be applicable at all if the underlying field conditions are mischaracterized or not understood to begin with. A perfect example is a monitoring well screened across different lithologies (e.g., clay and sand, jointly denoted as "alluvium"): the result of however fitted solution in such case would be ambiguous at best. Is the obtained value of

hydraulic conductivity applicable to the sand portion or is it a lumped value? How should the elements needed for the calculation (see Figure 15.19) be adjusted/apportioned between the units (clay and sand)? Is the selected theoretical model (equation) even applicable in this case?
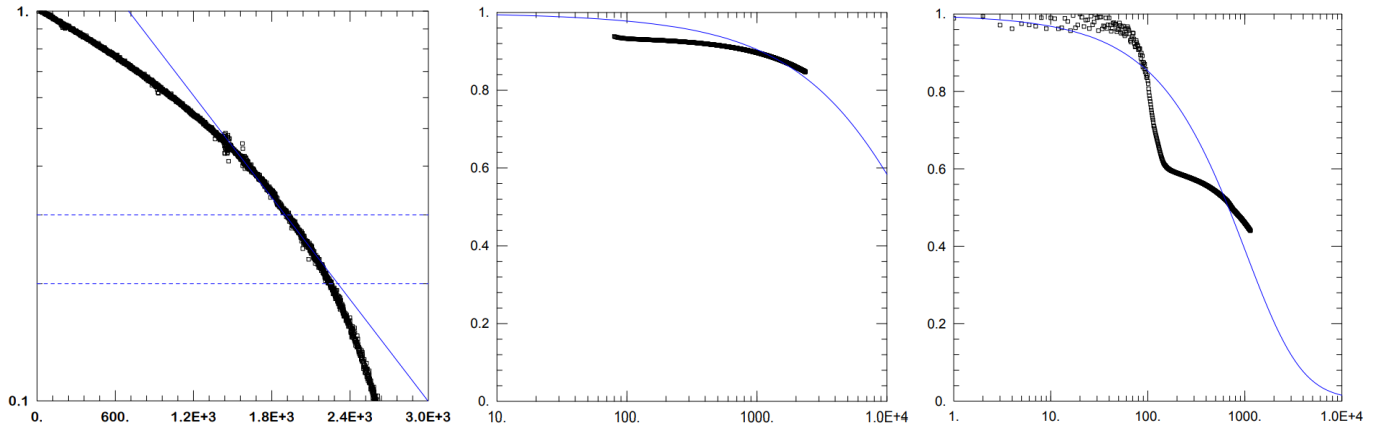
Figure 15.22 Some examples of matching curves (thin blue lines), generated automatically by a program from slug test data. All times (horizontal scale) are in seconds. None of these curves is correct.

15.3.2 Borehole Tests

Flowmeters can be used to measure borehole flow under ambient and pumped conditions. Measurements made under ambient conditions can help to delineate transmissive fractures and other permeable zones and to indicate the direction of vertical hydraulic gradients; they are also useful in interpreting fluid-conductivity logs and borehole water quality data. Measurements made under pumped conditions can be used to develop hydraulic conductivity profiles of aquifers (Williams and Lane, 1998). Differences in hydraulic head between two transmissive geologic units or preferential flow paths may produce vertical fluid flow in a borehole. Water enters the borehole at the unit with the higher head and flows toward and out of the unit with the lower head. The vertical flow rate is limited by the geologic unit or zone with the lower transmissivity. If the heads of the different transmissive zones are the same, no vertical flow will occur in the well or borehole. However, it is recognized that the borehole may facilitate vertical flow between aquifers and fractures that would not normally be present, so any interpretation of vertical flows must be made with caution (USGS, 2004a).

Single borehole flowmeter logging can be used to (1) Measure the rate of vertical flow; (2) Identify the direction of vertical flow; (3) Establish relative hydraulic gradients; and (4) Identify transmissive zones or geologic units open to borehole that are the source(s) of water or that could act as conduits for cross-flow in an open hole. Simultaneous use of geophysical logging tools and flowmeters is the best available method for in situ characterization of fractured rock and karst aquifers (Paillet, 2000, 2001; Paillet and Reese, 2000). An example is shown in Figure 15.23.

In cross-hole flowmeter profiling, a flowmeter is placed in one borehole while fluid is pumped out of or into another borehole at a constant rate. Cross-hole flowmeter profiling is used to identify cross-hole connections and provide data that can be used to solve for (1) Transmissivity; (2) Hydraulic head; and (3) Storage coefficient of the geologic unit or more permeable zones between the boreholes.
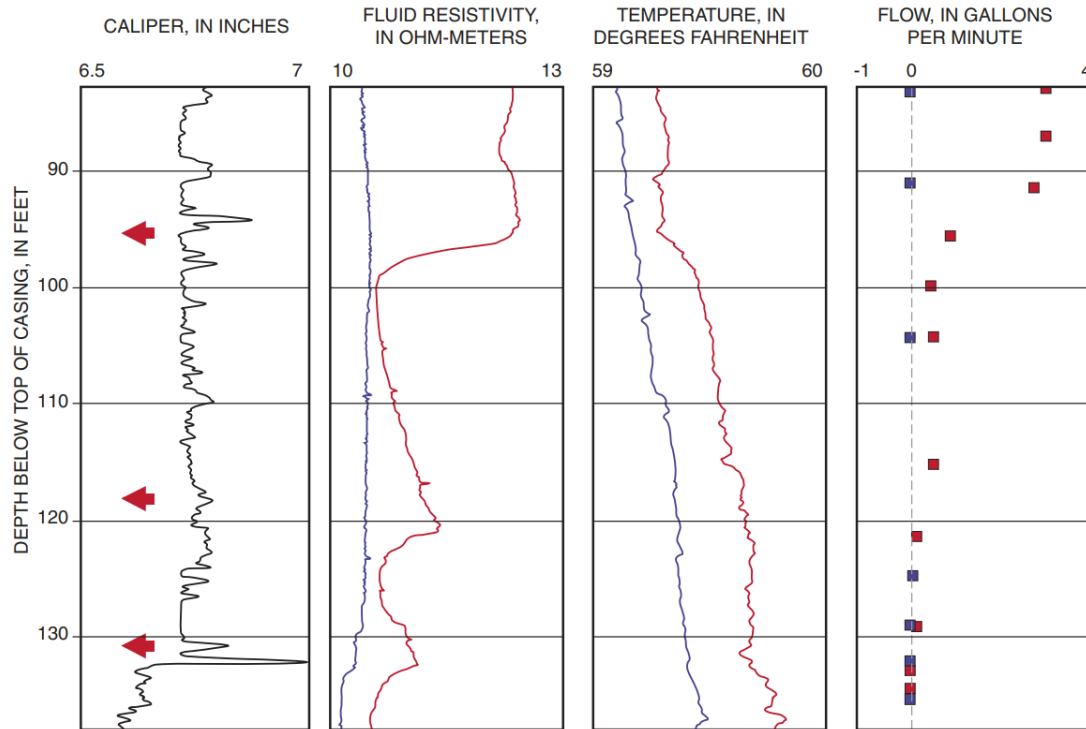
Figure 15.23 Caliper, fluid-resistivity, temperature, and flowmeter logs of borehole RD-46A, Rocketdyne Santa Susana Field Laboratory, Ventura County, California (red arrows indicate flow from zones to the borehole); blue indicates ambient conditions, red indicates pumped conditions; negative values indicate downflow, positive values indicate upflow). From Williams et al., 2002. USGS, in public domain.

The nature of the aquifer heterogeneities can affect the flowmeter measurements, which are particularly sensitive to flowmeter positioning relative to the preferential flow zone. Steeply inclined fractures may produce results that are difficult to interpret because of nonhorizontal flow across the borehole. The acoustic Doppler velocimeter is the only tool of the three point-measurement methods capable of measuring three-dimensional flow (Wilson et al., 2001).

Heat-pulse flowmeter (HPFM) measurements are made with the tool at a stationary position in the borehole. A heat grid in the tool is activated to heat a packet of water in the borehole. If there is flow in the borehole, the heated packet of water will move with the flow toward the upper or lower sensor in the tool. The difference in temperature between the sensors is monitored. The equipment measures the time from when the heat grid was first activated to the moment when the greatest temperature change is detected by one of the sensors. This information is then used to calculate a rate of flow and direction of flow at that particular location and time. An HPFM with a fully fitted diverter can usually measure flow of 0.01 to 1.5 gallons per minute. Figure 15.24 shows results of a heat-flowmeter characterization.

The electromagnetic flowmeter (EMFM) measurements can be made while trolling (moving) to generate a continuous flow profile over a depth range or while stationary in order to measure flow at a specific location in the borehole. Under trolling conditions, the movement of a flowmeter tool induces a measured flow in the direction opposite the direction of trolling. Measurements of ambient or stressed flow within the borehole are superimposed on the induced flow rates. An EMFM with a fully fitted diverter can generally measure flow from 0.05 to 10 gallons per minute.
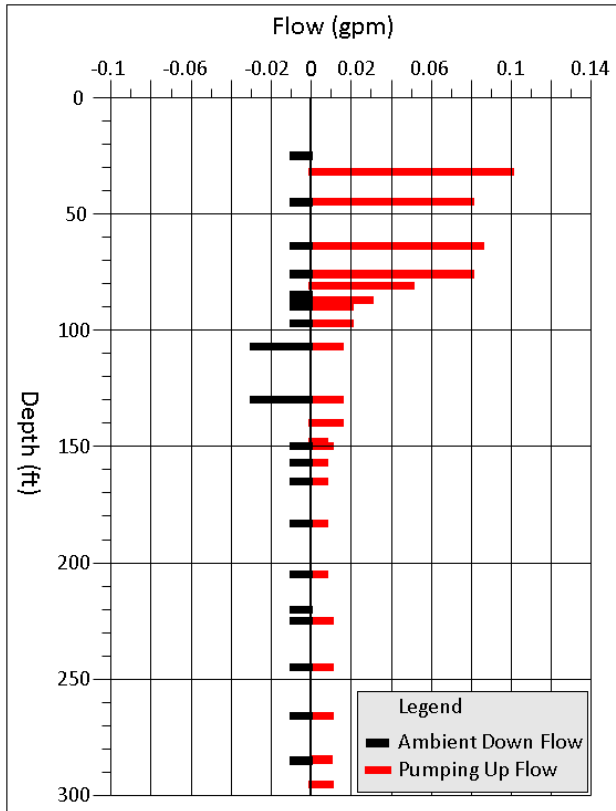
Figure 15.24 *Left*: Graph of ambient vs. pumping flow rates at discrete intervals in an open bedrock borehole. *Right*: Heat Pulse Flow Meter for characterization of fracture-specific groundwater flows in open bedrock boreholes under ambient and pumping conditions (shallow pump intake ~ 20 ft pumping at +0.1 gpm). *Right*: Graph of ambient vs. pumping flow rates at discrete intervals in an open bedrock borehole. Courtesy of Peter Thompson and Scott Culkin.

Spinner flowmeter (spinner) uses an impeller that revolves in response to fluid flow. As fluid moves through the impeller blades, rotating them, the number of impeller revolutions per second is automatically recorded and used to calculate the velocity of the fluid. Spinner measurements can be made while trolling to generate a continuous flow profile over a certain depth or while stationary in order to measure flow at a specific location in the borehole. Spinners can make measurements over a wide range of flow rates, although the tool often has poor resolution at very low flow rates. The minimum velocity that can be measured by a typical spinner flowmeter is about 5 feet per minute, limiting its use to higher flow conditions.

Hydrophysical Logging involves replacing the borehole fluid with deionized water, followed by a series of temperature and fluid-electrical-conductivity (FEC) logs that profile the borehole to determine where formation water is entering and leaving. A time series of FEC logs can identify the locations and rates of inflow and outflow. Hydrophysical logging can identify vertical flow as well as horizontal flow; it surveys a length of the borehole, rather than providing point measurements. This attribute makes hydrophysical logging a valuable method for obtaining profiles of flow characteristics in uncased wells or in wells with long screens (Figure 15.25).

The theory of hydrophysical logging is based on the law of mass balance and the linear relation between FEC and dissolved mass. By recording the changes in the electrical conductivity in the fluid column with depth, the locations of the water-producing zones can be determined, and the volumetric rate of inflow can be calculated.
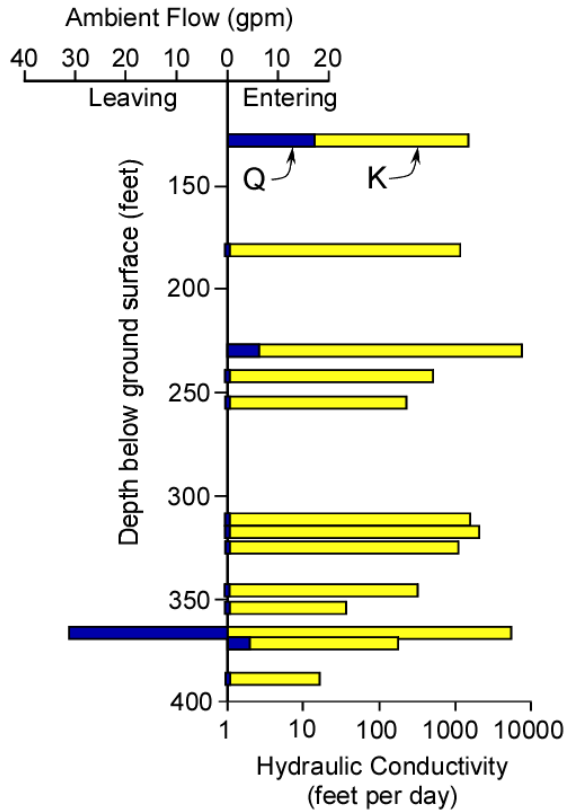
Figure 15.25 Results of hydrophysical logging in a deep boring in a carbonate aquifer. K, hydraulic conductivity; Q, ambient flow. Modified from Kresic, 2007; data courtesy of Army Environmental Center. Copyright CRC Taylor & Francis; permission is required for further use.

The computer code developed for analysis of horizontal-flow rates through each zone is based largely on borehole-dilution theory in which a mixing model is used to infer horizontal groundwater-flow velocity through a borehole. Although the theory for such analysis is well established, its application to hydrophysical logging experiments is innovative. Special considerations apply when using the theory in the fractured-rock environment; nonetheless, the theory provides promising results in such applications. A brief explanation of borehole dilution as applied to hydrophysical logging is provided by Williams et al. (2002).

The Hydraulic Profiling Tool (HPT) developed by Geoprobe® is a logging tool that measures the pressure required to inject a set flow of water into the soil as the probe is advanced into the subsurface. This injection pressure log is an excellent indicator of formation permeability. In addition to measurement of injection pressure, the HPT can also be used to measure hydrostatic pressure under the zero-flow condition. This allows the development of an absolute piezometric pressure profile for the log and prediction of the position of the water table. The piezometric profile can be used to calculate the corrected HPT pressure. This data along with the flow rate can then be used to calculate an estimate of hydraulic conductivity (K) in the saturated formation. The injection pressure along with electrical conductivity (EC) can be used to estimate groundwater specific conductance where the formation allows (https://geoprobe.com/direct-image/hpt-hydraulic-profiling-tool).

Figure 15.26 shows graphs of parameters measured directly in the borehole during the tool advancement, as well as the absolute piezometric pressure and estimated hydraulic conductivity graphs which are parameters typically calculated after the log is complete.
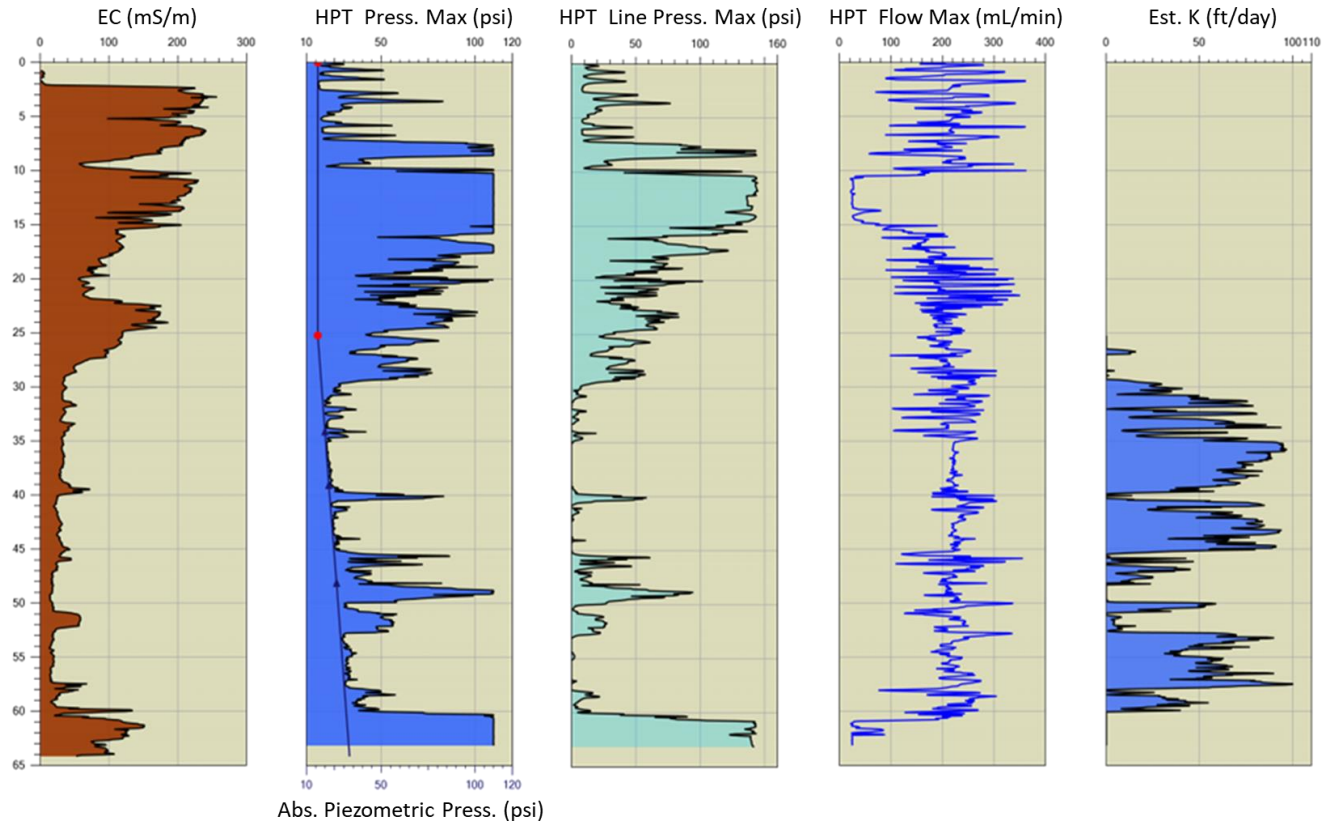
Figure 15.26 An HPT log which includes (from left to right) an EC (electrical conductivity), HPT Injection Pressure (top axis) with Absolute Piezometric Pressure (bottom axis), HPT Line Pressure, HPT Flow Rate and Estimated Hydraulic Conductivity (K). Comparison of EC and HPT pressure graphs shows there is generally finer grained/lower permeable soils in the upper portion of this log and coarser grained soils with higher permeability in the lower portion of the log. Courtesy of Geoprobe® (https://geoprobe.com/direct-image/hpt-hydraulic-profiling-tool).

15.3.3 Aquifer (Well) Pumping Tests

Aquifer pumping tests (often referred to as well pumping tests because they also can provide information on production well loss and efficiency) are among the most costly and labor-intensive field tests in hydrogeology (see Figures 15.27 through 15.37). It is therefore crucial to approach their planning and execution by following well-established and accepted practices and guidelines. There is an abundant published literature on the topic and numerous recommendations and guidance documents by the USGS (Ferris et al., 1962; Bental, 1963a,b; Stallman, 1971), the U.S. EPA (Osborne, 1993), the United States Army Corps of Engineers (USACE, 1999a), the United States Bureau of Reclamation (USBR, 1977), and the ASTM (1999). Other excellent reference books include Groundwater and Wells by Driscoll (1989), which covers all aspects of well design, drilling, and testing; Analysis and Evaluation of Pumping Test Data by Kruseman et al. (1991); and Aquifer Testing: Design and Analysis of Pumping and Slug Tests by Dawson and Istok (1992). Website dedicated to AQTESOLV, computer program for aquifer test analyses, has an excellent online manual on aquifer tests which can be downloaded as well (http://www.aqtesolv.com/).

An aquifer pumping test consists of the following main phases: (1) Definition of test objectives; (2) Development of a focused conceptual site model (CSM); (3) Test design; (4) Data collection (recording); and (5)

Data analysis. The question of defining the test objectives could simply be rephrased to "what exactly do you want to learn about the aquifer?" Is the test being conducted as part of a water budget study where the concern is defining transmissivity and storativity? Or is the test part of a water supply study where the concern is specific capacity and safe well yield? Is the test part of a groundwater contaminant transport study where the ultimate question is the velocity and direction of the groundwater (contaminant) flow? Is there any concern between the possible interconnection of two or more separated aquifers, such as a near-surface water table aquifer and a deeper artesian aquifer separated by an aquitard? A careful definition of the test objectives is therefore essential to ensure a successful test (USACE, 1999a).

Although aquifer pumping tests are performed to also provide data for development of a more detailed quantitative CSM, at the same time it is very important that already available hydrogeologic information be fully utilized in the test design. Ideally, this focused CSM includes locations (or their estimates) of any hydraulic boundaries that may impact drawdown measured in the pumped well and the monitoring wells. Hydraulic boundaries are contacts with less permeable formations (aquitards) in both the vertical and the horizontal directions, and all natural and artificial surface water features near the test site including more exotic ones such as leaky sewers. In karst aquifers, it is equally important not to oversee possible existence of subsurface equipotential boundaries such as flowing karst conduits and channels. Possible well interference due to other wells pumping in the vicinity should also be examined.

Preliminary estimates of the aquifer thickness and hydraulic conductivity including its anisotropy, as well as of the underlying and/or overlying aquitards (where applicable), are useful in predicting possible pumping rates for the test, radius of influence, and drawdown at the test well and various distances from it (i.e., at the existing or possible future monitoring wells). These estimates and other available information on the site hydrostratigraphy integrated within the CSM are then used in the next phase—the test design.

In contaminant hydrogeology, every attempt should be made to delineate the horizontal and vertical extent of groundwater contamination prior to any aquifer field test. This delineation should be followed by an analysis of possible impact of the proposed test on contaminated groundwater flow directions in all three dimensions.

Design of an aquifer pumping test includes the following key elements: (1) Design of the test well; (2) Design of monitoring wells (observation wells, piezometers); (3) Drawdown measurements; (4) Pumping design and analyses of well loss and efficiancy; (5) Duration of the test; and (6) Water discharge control, measurements, and disposal.

Design of Test Well

Whenever possible, the design of a test well should allow its easy conversion into a permanent extraction well in case the test results are favorable. Three main well design elements include well diameter, well screen and well pump. More detail on these and other design elements such as selection of gravel pack, grouting, and well development methods can be found in Lecture 16, and in Driscoll (1986) and Roscoe Moss Company (1990). In general, the well diameter should allow for 10 to 20 percent more pumping capacity than the maximum expected from the aquifer, and the pump should not be placed within the well screen but above or below it, in the cased portion of the well. This is to avoid rapid damage to the screen due to potential turbulent flow, clogging or sanding.

Ideally, the pumping well screen should span the entire saturated thickness of the aquifer: the so-called fully penetrating well. However, due to budgetary and other constraints (e.g., thick aquifer, presence of contamination at different depths) this is often not feasible or desirable. If the aquifer is being developed for water supply, and if certain aquifer portions are less permeable (e.g., there are thin layers or lenses of clay), the screen design may

include perforated intervals separated by solid casing. In such cases, it would be difficult to estimate the overall aquifer transmissivity if the screens of monitoring wells are not designed in the same way. When single monitoring well screens are placed within different aquifer intervals, it would be equally difficult to estimate the transmissivity of discrete aquifer intervals without knowing their relative contribution to the overall pumping rate of the test well. Utilization of borehole flowmeters in such (and all other) cases provides invaluable information needed for the data analysis and interpretation of aquifer characteristics in general (see Section 15.3.2).

Design of Monitoring Network (Monitoring Wells, Piezometers)

This component of the aquifer test design includes selection of the locations, screen depths and the number of monitoring wells. It is always advisable to use existing wells for monitoring whenever possible, even when they appear not to be suitable for various "traditional" reasons such as: 1) the well is not completed in the same aquifer zone as the pumping well, 2) it is too far from the pumping well (inappropriately located), or 3) the well logs and well completion documents are not available or reliable. In any of these or similar cases the cost of equipping the existing well(s) with transducers and collecting data on the hydraulic head changes during the test would be minimal compared to the overall cost of the test. In general, having more data on aquifer response (or absence of response), even when it is not easily explainable, is always better than not having such a "headache". Finally, project budgets will usually provide a practical constraint for the number of new observation wells, so well locations must be optim ized to fit the test objectives, and compromises often must be made (USACE, 1999a).

Figure 15.27 Hydrogeologist Andy Clark of Law Engineering and Environmental Services setting up a system for continuous monitoring of multiple monitoring wells at the startup of a pump-and-treat groundwater remediation at a site in New England. Cables from pressure transducers at the wells converge on the central datalogger. The site is paved, and many wells are flush mounted, which is necessary at operational industrial facilities with traffic.

The existing wells identified as potential observation wells should be field tested to verify that they are suitable for monitoring the aquifer response. The perforations of well screens of abandoned wells tend to become restricted by the buildup of iron compounds, carbonate compounds, sulfate compounds or bacterial growth because of not pumping the well. Consequently, the response test is one of the most important pre-pumping examinations to be made if such wells are to be used for observation (Osborne, 1993; Stallman, 1971). The reaction of all wells to changing water levels should be tested by injecting or removing a known volume of water into each well and measuring the subsequent change of water level. Any wells which appear to have poor response should be either redeveloped, replaced, or dropped from consideration in favor of another available well selected (Osborne, 1993).

Many of the "rules of thumb" proposed in the past hydrogeologic practice regarding "appropriate" locations and screen depths of the observation wells are quickly losing importance because of the rapidly increasing utilization of numeric groundwater models in the analysis of aquifer test results. Carefully designed numeric model, based on the quantitative conceptual site model (CSM), is the best available tool for verification of any analytical method (i.e., "curve-matching" method) used to interpret the test results. When applying the numeric modeling approach, virtually all collected data, including from wells that may seem "too far" from the pumping well, or with screen locations offset from the center of the screen of the pumping well, become equally important in verifying assumptions inherent in any conceptual site model.

Monitoring well system for an aquifer pumping test should ideally include the following:

- Wells with isolated multiple screen intervals or cluster wells used to assess possible vertical gradients caused by pumping. The "rule of thumb" for individual wells with one screen interval is to place their screen at approximately the same elevation in the aquifer as the center of the pumping well screen.

- Wells placed at different radial angles from the pumping well to enable determination of possible aquifer anisotropy. Wells located along the same general direction, even when on the opposite sides of the pumping well, cannot be used for this purpose.

- Wells placed at different distances from the pumping well, covering at least two log cycles (5, 80, and 350 feet for example) to allow application of the distance-drawdown analytical method, which is useful for determining the radius of well influence and its expansion in time.

It is possible to estimate aquifer transmissivity using drawdown measurements directly from the pumping well when data from the monitoring wells are not available. This procedure is often referred to as the "well specific capacity method". However, because of the well loss in the pumping well, and the assumptions that must be made regarding storativity, such estimates are only approximate.

The depth at which a monitoring well is installed depends on the aquifer type and its homogeneity. In an isotropic and homogeneous aquifer, the monitoring well should be installed at a depth that is half the length of the well screen. For aquifers consisting of sandy deposits with intercalations of less pervious layers, it is recommended to install a cluster of monitoring wells. If the aquifer is overlain by a partly saturated leaky aquitard, monitoring wells should also be installed in the shallow aquifer above the aquitard to check whether the water table is affected when the underlying aquifer is pumped (Griffioen and Kruseman, 2004).

Design of Drawdown Measurements

Design of drawdown measurements should provide for collection of as many accurate measurements of the water level in the test and monitoring wells as possible. Pre-pumping water levels should be measured at least 24 hours before start of the test pumping phase to detect any regional ("background") trends and perform data adjustments as needed later during the data analysis phase. In addition to recording water levels in all the wells, every effort should be made to record barometric pressure for the same reason of possible data adjustment: piezometric pressure of confined and semi-confined aquifers fluctuates in response to changes in barometric pressure. Finally, if not feasible to record directly, provision should be made to secure data on precipitation and water levels at nearby hydraulic boundaries, such as streams and lakes/reservoirs, which may be routinely collected by local, state, or federal agencies.

Before the era of automated data loggers and pressure transducers, various textbooks and manuals included recommendations as to the frequency of water level measurements during aquifer pumping tests. This was, to a

large extent, influenced by the limited feasibility and high labor costs of manual recording at multiple well sites during a relatively short period of time. Data loggers and transducers eliminate these limitations since water levels are measured continuously and can be recorded at any time interval specified by the user. Manual recordings in such case are made only sporadically to make sure the equipment is working properly. Whatever method of data measurements is selected, the main idea behind defining certain time intervals between data collection ("economizing") is the fact that drawdown increases more rapidly at the beginning of the test then later into the test. Similarly, it would not make much sense to measure water level at a distant monitoring well every minute or so at the beginning of the test when the drawdown may be measurable only after several hours or even days.

As most methods of aquifer test analyses include plotting time vs. drawdown data on a semi-log or log-log scale, the time interval between measurements should follow the logarithmic rule as well. Data loggers can be programmed to record drawdown on the logarithmic scale thus reducing the volume of stored information. In case of manual measurements, this means that the staff taking measurements can stop and catch some breath while running between various monitoring locations. The frequency of water levels measurements during the recovery phase (after the pump is shut off) should follow the same schedule as for the pumping phase until about 90-95% of the drawdown is recovered.

To emphasize, a continuous recording with data loggers and pressure transducers is much more reliable and precise than manual measurements and provides invaluable information that otherwise may remain undetected when collecting data manually. This is especially important when drawdown is small such as in highly transmissive aquifers or at more distant wells.

Pumping Design

It is usually desirable to pump at the maximum practical rate to stress the aquifer as much as possible for the duration of the test. This translates into more drawdown at the pumping well and the observation wells, and therefore more data available for the final analysis. The maximum rate will be limited by the efficiency of the well construction and the specific capacity of the well and should not cause dewatering below the pump intake during the duration of the test (USACE, 1999a).

The maximum pumping rate is usually determined based on a three-step pumping test (well specific capacity test) during which the well is pumped with three or more successively higher rates, each of which is kept constant for up to 8 hours (Figure 15.28). The results of such test are used to determine the well efficiency and, consequently, the acceptability of an inevitable well loss.
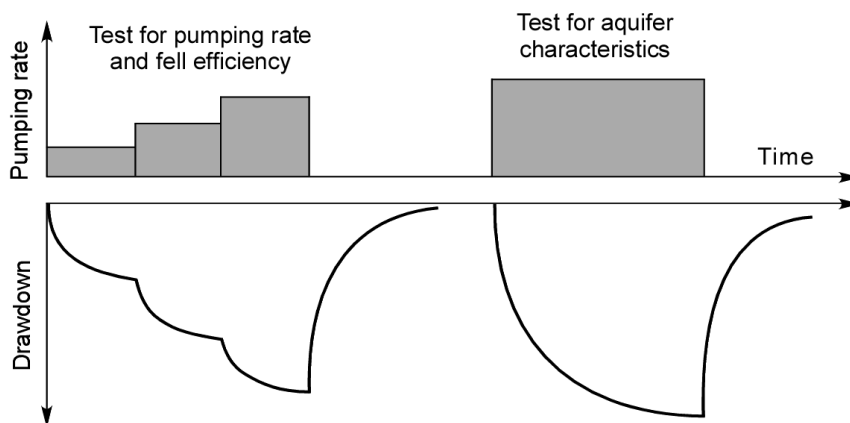
Figure 15.28 Pumping rate hydrographs and drawdown curves for a pumping test designed to determine well and aquifer characteristics. From Kresic, 2009. Copyright McGraw Hill; permission is required for further use.

Well Loss

Well loss is the difference between the actual measured drawdown in the pumping well and the theoretical drawdown due to groundwater flow through the aquifer porous media. This theoretical drawdown is also called the formation loss. Equations of theoretical drawdown should be applicable to the actual aquifer (formation) conditions, such as confined, unconfined, leaky, with delayed gravity response, quasi steady state, or transient. Well loss is the result of various factors, such as an inevitable disturbance of the porous medium near the well during drilling, an improper well development (e.g., drilling fluid is left in the formation and mud cake along the borehole is not removed), a poorly designed gravel pack or well screen, and turbulent flow through the gravel pack and the well screen. Well loss is always present in pumping wells, and its evaluation is an important part in deciding if the well performance is satisfactory or not. All wells will experience a decrease in well efficiency sooner or later, as indicated by an increased well loss. Three-step pumping test is the only reliable means of quantifying the well loss, and it should be performed not only after well completion but also periodically during well exploitation to evaluate the well performance and needs for possible well rehabilitation.

The total measured drawdown (s_w) at a well is combination of the linear losses and turbulent losses:

$$s_w = AQ + BQ^2 \qquad (15.17)$$

where A is the coefficient of the linear losses, B is the coefficient of turbulent losses, and Q is the pumping rate.

The turbulent losses are usually assumed to be quadratic, but other powers may be used to describe it. The linear losses (A) include both the formation loss (A_0) and the linear loss (A_1) in the near-screen zone:

$$A = A_0 + A_1 \qquad (15.18)$$

For practical purposes A_1 can usually be ignored. The formation loss or the theoretical drawdown in the well (s_0) is determined by using the appropriate equation for the specific flow condition. For example, in case of a quasi-steady state flow in a confined aquifer, the equation is:

$$s_0 = \frac{Q}{2\pi T} \ln \frac{R}{r_w} \qquad (15.19)$$

where s_0 is drawdown due to groundwater flow through the aquifer porous media (theoretical drawdown); T is the transmissivity, R is the radius of well influence; r_w is the well radius. The coefficient of linear formation loss (A_0) can be calculated as

$$A_0 = \frac{1}{2\pi T} \ln \frac{R}{r_w} \qquad (15.20)$$

A_0 can also be determined graphically if two or more monitoring well data are available, as shown in Figure 15.29-*Left*. The same graph shows that the s/Q ratio for the pumping well increases with the increasing pumping rate, whereas for the monitoring wells this ratio remains constant for all three steps.

The coefficients of the total linear loss (A) and the quadratic loss (B) can be determined from graph pumping rate (Q) versus drawdown-pumping rate ratio (s/Q), as shown in Figure 15.29-*Right*. The graph is a straight line of the following form:

$$\frac{s_w}{Q} = A + BQ \qquad (15.21)$$

where *A* is the intercept and *B* is the slope of the best-fit straight line drawn through the experimental data from the three pumping steps. After substituting values of *A* and *B* determined from the graph into Equation (15.17), it is possible to calculate the total (i.e., expected to be actually recorded) drawdown in the pumping well for any pumping rate. A graph similar to that in Figure 15.30 can be used to plot the calculated drawdown expected to be actually measured in the well, versus the theoretical formation drawdown (which does not include well loss).
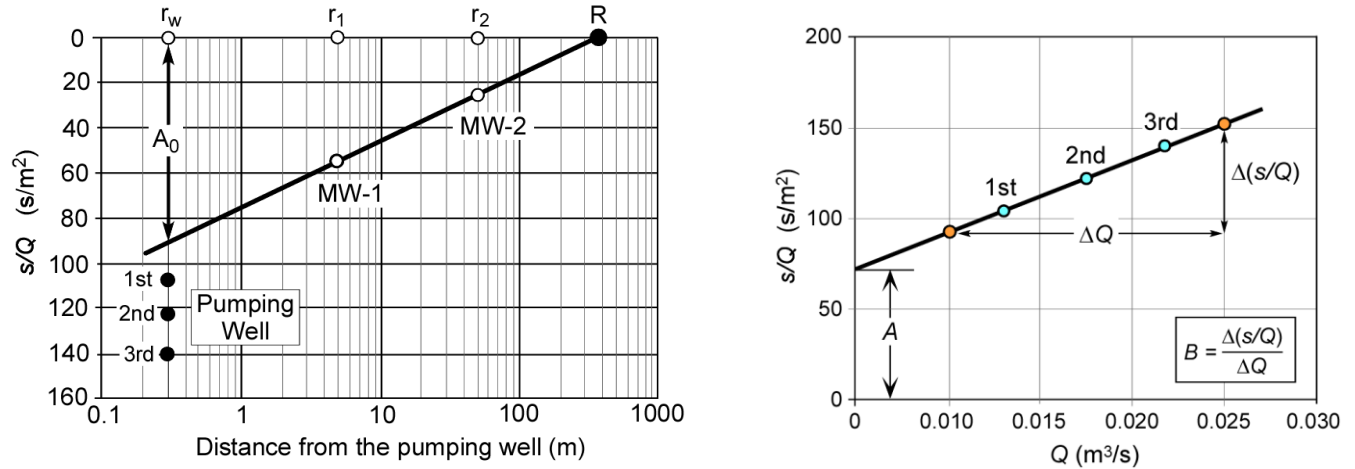
Figure 15.29 *Left*: Graph distance versus s/Q for three-step pumping test in quasi-steady-state conditions, showing data for pumping well and two monitoring wells. *Right*: Graph pumping rate (Q) versus drawdown-pumping rate ratio (s/Q) for a three-step well pumping test. From Kresic, 2009. Copyright McGraw Hill; permission required for further use.
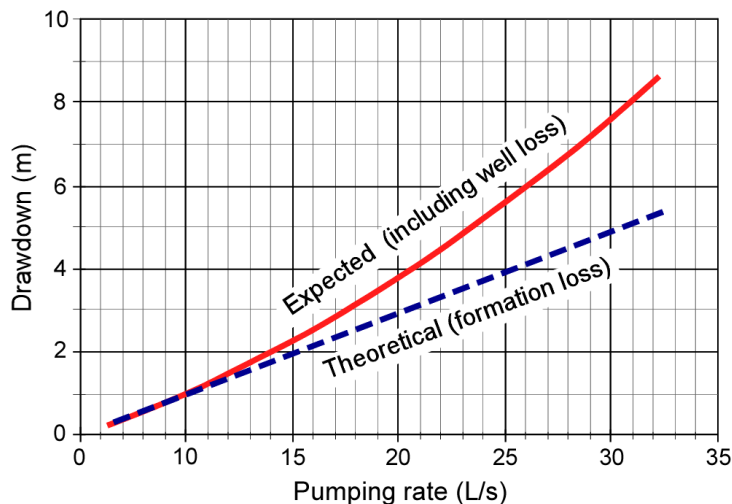
Figure 15.30 Pumping rate versus formation loss (theoretical drawdown) calculated with Equation (15.19) and the expected drawdown in the well calculated with Equation (15.17). From Kresic, 2009. Copyright McGraw Hill; permission required for further use.

The coefficient of turbulent (quadratic) well loss, *B*, smaller than 2500 to 3000 s²/m⁵ is usually considered acceptable. Larger coefficients may indicate potential problems with the well such as inadequate well design and/or development, clogging of the well screen or other deterioration of the well. Theoretically, *B* is not time dependent and should remain the same for different pumping rates. A common exception is pumping from karst and fractured

rock aquifers where turbulent well loss may increase with an increasing pumping rate. In such cases, the points on the graph Q vs. s/Q would form a parabola rather than a straight line.

In case of transient conditions in a confined aquifer, the coefficient of formation loss (A_0) is easily found by applying the Theis equation:

$$A_0 = \frac{1}{2\pi T} W(u) \qquad (15.22)$$

Parameter u for the well is given as:

$$u = \frac{r_w^2 \cdot S}{4Tt} \qquad (15.23)$$

where r_w is the well radius; S is the storage coefficient; T is the aquifer transmissivity; t is the time since the pumping started (see also Section 4.2.4 in Lecture 4). As shown by Cooper and Jacob, for small values of parameter u ($u<0.05$), i.e., sufficiently long pumping time, the well function $W(u)$ is:

$$W(u) = \frac{2.25Tt}{r_w^2 S} \qquad (15.24)$$

and the formation loss (A_0), which is equal to theoretical drawdown at the well, (s) can be written as:

$$s = \frac{Q}{2\pi T} \cdot \ln \sqrt{\frac{2.25Tt}{r_w^2 S}} \qquad (15.24)$$

Similarly to steady-state conditions, the coefficients of linear and turbulent well losses are found from a graph Q versus s/Q, as shown in Figure 15.29. However, because the radius of well influence in transient conditions increases with time, the drawdown recorded at the end of each step may have to be corrected if not sufficiently stabilized. Figure 15.31 shows the components of drawdown recorded at the end of each step and the error made if the three drawdowns (s_1, s_2, and s_3) were used to draw a graph Q versus s/Q without corrections. Kresic (2007) provides detailed explanation of this correction procedure.
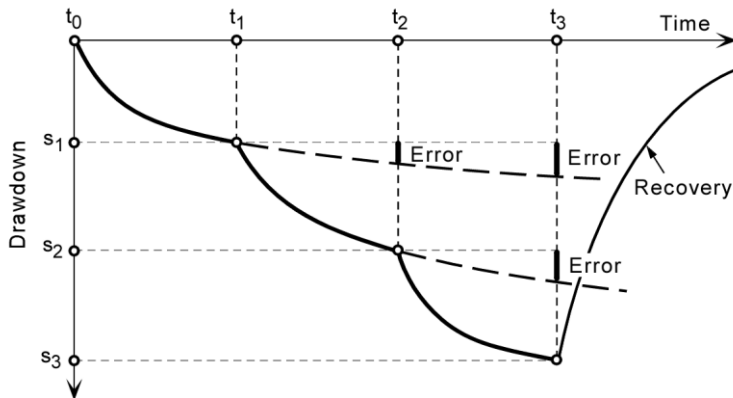
Figure 15.31 Components of drawdown recorded at the end of each step showing errors made if drawdowns s_1, s_2, and s_3 were used directly to draw graph Q versus s/Q. From Kresic, 2009. Copyright McGraw Hill; permission required for further use.

If the well loss is unacceptable, it will be necessary to redevelop the well prior to the aquifer test because of its inability to produce pumping rates needed to adequately stress the aquifer. Although pumping an inefficient well may not affect analysis of the test data collected at the monitoring wells (where there are no well losses), the overall utility of the test for any design purposes may be questionable.

Well Efficiency

Well efficiency is the ratio between the theoretical drawdown and the actual drawdown measured in the well. It is expressed in percent:

$$\text{Well Efficiency} = \frac{\text{Theoretical Drawdown}(s_0)}{\text{Measured Drawdown}(s_w)} \times 100\% \qquad (15.25)$$

As explained earlier, the theoretical drawdown is determined by applying an appropriate equation of groundwater flow towards a well (theoretical drawdown equals the formation loss). It can also be found graphically as explained earlier. In general, the difference between the theoretical drawdown and the measured drawdown increases with increasing pumping rate as shown in Figure 15.30. Consequently, well efficiency decreases with an increasing pumping rate. Determining well efficiency and well loss is highly recommended because it provides valuable information about the well performance and can be used to make an informed decision regarding the well pumping rate, maintenance, and rehabilitation. A well efficiency of 70% or more is usually considered acceptable. If a newly developed well has less than 65% efficiency, it should not be approved without a thorough analysis of the possible underlying reasons. This may include well re-development followed by new performance testing.

Well efficiency has always been a major concern in the water well industry, but in the past this concern has focused primarily on pumping equipment. Pump efficiencies can be easily calculated, and most pump manufacturers make this information available to their customers. Efficiencies of different pumps may vary by only a few percentage points. Well efficiency, on the other hand, can vary greatly even between wells completed in very similar hydrogeologic conditions and close to one another. However, the determination of well efficiency is still largely ignored because it is difficult to quantify different factors that contribute to it. Many variables affect well efficiency including the drilling procedure, screen design, filter pack size and well development methods.

Pumping Rate and Drawdown Recovery Analysis

All widely used methods of aquifer test analysis assume constant pumping rate for the duration of pumping. It is therefore very important to provide for a reliable energy source, and an adequate pump with enough power to maintain a constant pumping rate for the estimated maximum drawdown. In addition to the potentially large variation in discharge associated with the operation of pump motor or engine, the discharge rate is also related to the drop in water level near the pumping well during the aquifer test. As the pumping lift increases, the rate of discharge at a given level of power (such as engine rpm) will decrease. It will therefore be necessary to monitor and adjust the engine power during the test and keep the pumping rate constant. The pump should not be operated at its maximum rate. As a general rule, the pumping unit, including the engine, should be designed so that the maximum pumping rate is higher than the estimated long term sustainable yield of the aquifer (Osborne, 1993).

The pumping rate can vary for various reasons, intentional (such as during a step test) or unintentional, which is more common. A frequent problem during pumping tests in newly constructed wells is an improper (insufficient) well development, which results in erratic surges and drops of the pumping rate. Another example is a constant decrease of the pumping rate due to lowering of the hydraulic head in the well and the consequent decrease of the pump capacity. In both cases, an attempt to sporadically adjust the pumping rate may sometimes further aggravate the problem. Figure 15.33 shows the hydrograph of a pumping test initially designed to have the pumping rate of 8 liters per second and duration of 8 hours. Due to various problems, the pumping rate (recorded every 30 minutes) varied between 7.8 and 6.6 L/s. Practice shows that when the pumping rate varies less than 10 to 15 % during the test, the recovery data can be used for the transmissivity determination after necessary adjustments. In our case this variation is 15%, just "enough" to consider the result acceptable provided the adjustment are made as described further.

Recording and analyzing drawdown recovery is a mandatory part of every aquifer pumping test. Pumping at a test well lowers the potentiometric surface around the well and creates the *drawdown*. After pumping stops, there is an inflow of water from the aquifer into the previously created *cone of depression* in the potentiometric surface. This inflow causes a rise in the depleted hydraulic head, i.e., the drawdown *recovery* (see Figure 15.33). One of the advantages of the recovery analysis is that it can be used to calculate aquifer parameters with reasonable accuracy when the pumping rate was not kept constant during the test.

The actual varying pumping rate is replaced with an equivalent constant pumping rate which is used in calculations. The new pumping rate is <u>not</u> the average of all the recorded rates. Rather, it is the last pumping rate of a significant duration, 6.6 L/s in our case (see Figure 15.33). This last recorded pumping rate has the most influence on the future development of the cone of depression (drawdown) around the pumping well.

Figure 15.32 Installation of a submersible pump for an aquifer pumping test. Photo courtesy of Adrian Ezeagy.

Introduction of the new pumping rate requires an adjustment to the hydrograph time base so that the aquifer water balance does not change. In other words, the volume of water actually withdrawn must equal the volume of water that would have been withdrawn with the new adjusted pumping rate. The duration of pumping with the adjusted pumping rate, i.e., the new time base of the hydrograph (t^*), is found using the following general formula:

$$t^* = \frac{Q_1 \cdot t_1 + Q_2 \cdot (t_2 - t_1) + ... + Q_n \cdot (t_n - t_{n-1})}{Q_n} \qquad (15.26)$$

where:

t_1, t_2, t_{n-1}, t_n	are the times of the pumping rate change,
Q_1, Q_2, Q_{n-1}, Q_n	are the recorded pumping rates,
Q_n	is the last recorded pumping rate.

In this case the new time base of the hydrograph (t^*) is 8.75 hours (see Figure 15.33).

As can be seen, the new time base is longer than the time of actual pumping. The adjusted time at the beginning of pumping is set 8.75 hours backwards from the time at which the actual pumping stopped. Note that the point in time at which the actual pumping stopped remains the same, i.e., it is "fixed". The new time-zero (t_0), which is to the left of the beginning of the actual pumping, is now the reference point for the recovery analysis (see Figure 15.33).

When the pumping rate varies during the test, the drawdown data <u>should not</u> be used for the transmissivity calculation using the approaches described in Lecture 4. However, the residual drawdown recorded at the well during recovery can be used since it is assumed that the aquifer supplies water to the well at a constant rate (i.e.,

the imaginary recharge well injects water to the aquifer at a constant rate). Again, this constant rate equals the last recorded actual pumping rate of a significant duration (6.6 L/s in our case).
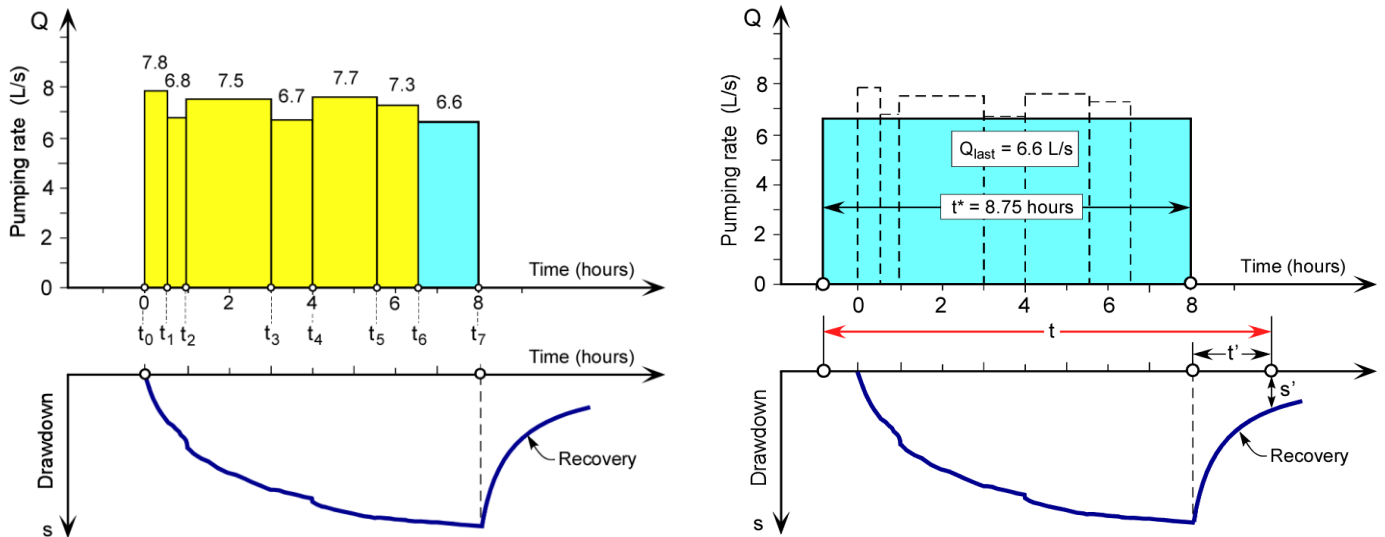
Figure 15.33 *Left*: Hydrograph of a varying pumping rate and the corresponding drawdown-recovery curve for an aquifer pumping test. *Right*: New adjusted hydrograph with the constant pumping rate of 6.6 L/s and the new time base of 8.75 hours. Note that the new beginning of the test is shifted to the left of the original startup time. Modified from Kresic, 2007. Copyright CRC Taylor & Francis; permission is required for further use.

Assuming that Theis equation is applicable (Equation (4.30) in Lecture 4), the aquifer transmissivity is found using a semi-log graph residual drawdown (s') versus t/t' ratio and choosing two points on the straight line over one log cycle ($\Delta s'$) as shown in Figure 15.34. Note that the t/t' ratio plotted on the graph should use the adjusted time since the beginning of test as shown with red arrows in Figure 15.33. This time is longer than the original time since the test startup. The time since the pumping stopped (t') remains the same and does not require correction. The transmissivity is then calculated using equation (15.27) where Q_{last} is the last recorded pumping rate of significant duration during the test, and $\Delta s'$ is the difference of residual drawdown between two points on the straight line one log cycle apart :
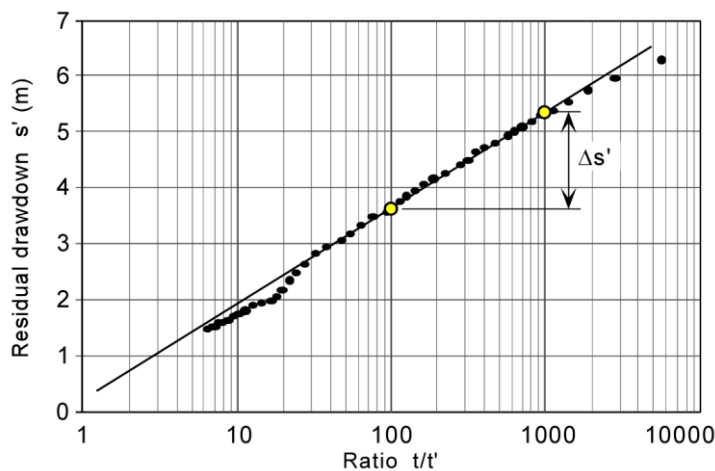
$$T = \frac{0.183 Q_{last}}{\Delta s'} \qquad (15.27)$$

Figure 15.34 Semi-log graph residual drawdown versus t/t′ ratio for determining aquifer transmissivity. From Kresic, 2007. Copyright CRC Taylor & Francis; permission is required for further use.

449

The drawdown recovery method of aquifer test analysis is based on the following principles and assumptions. The inflow of water from the aquifer during the recovery can be simulated with an imaginary well injecting water into the aquifer. This well has the same pumping rate as the real test well, only with the negative sign. Accordingly, the entire aquifer test can be simulated as a superposition of flows at two wells. This principle is illustrated in Figure 15.35. At the time when actual pumping stops, the imaginary well starts adding water to the aquifer and the real well continues extracting it at the same rate. Regarding the aquifer water balance, the effect of the two wells is the same as in case of the one real well. The resulting drawdown at any time after the actual pumping stops is the algebraic sum of the drawdown from the extraction well (that continues to operate) and the buildup (negative drawdown) from the introduced imaginary injection well:
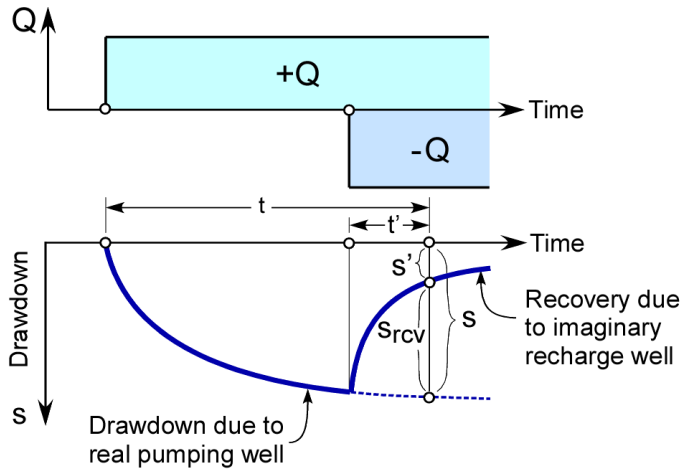
Figure 15.35 The principle of superposition of flows used to simulate the drawdown recovery during a well pumping test. Modified from Kresic, 2007. Copyright CRC Taylor & Francis; permission is required for further use.

$$s' = s + s_{rcv} \qquad (15.28)$$

where s' is the resulting drawdown measured at the well (*residual drawdown*), s is the drawdown from the extraction well, and s_{rcv} is the *recovery* (negative drawdown) from the recharge well. When these drawdown components are expressed with the Theis equation, it follows that:

$$s' = \frac{+Q}{4\pi T} \cdot W(u) + \frac{-Q}{4\pi T} \cdot W(u_{rcv}) \qquad (15.29)$$

The parameter u for the extraction well is:

$$u = \frac{r^2 S}{4Tt} \qquad (15.30)$$

where r is the radial distance from the pumping well where the drawdown is recorded; S is the storage coefficient; T is the transmissivity; t is the time since the actual pumping started.

The parameter u_{rcv} for the recharge (imaginary) well is:

$$u_{rcv} = \frac{r^2 S}{4Tt'} \qquad (15.31)$$

where t' is the time since the actual pumping stopped. When parameter u is less than 0.05, the Theis equation can be simplified as suggested by Jacob and Cooper and equation (15.29) becomes:

$$s' = \frac{Q}{4\pi T}\left(\ln\frac{2.25Tt}{r^2 S} - \ln\frac{2.25Tt'}{r^2 S}\right) \tag{15.32}$$

or

$$s' = \frac{Q}{4\pi T}\cdot\ln\frac{t}{t'} \tag{15.33}$$

Knowing that $\ln(x)=2.3\log(x)$, equation (15.33) can be written as:

$$s' = \frac{0.183Q}{T}\cdot\log\frac{t}{t'} \tag{15.34}$$

As seen from equation (15.34), the t/t' ratio vs. residual drawdown data recorded during the recovery would form a straight line on a semi log graph paper. This is the case, for the most part, for the data shown in Figure 15.34.

The difference between the residual drawdowns for any two points on the straight line is:

$$\Delta s' = \frac{0.183Q}{T}\cdot\log\frac{(t/t')_2}{(t/t')_1} \tag{15.35}$$

When the two points are chosen over one log cycle, the aquifer transmissivity is (same as Equation (13.27)):

$$T = \frac{0.183Q_{last}}{\Delta s'} \tag{15.36}$$

Duration of The Test

Practical constraints usually limit the time available for the test, and at a maximum it is useless to run the test beyond the point at which a (quasi) steady-state condition is reached (i.e., additional drawdown is insignificant), or the point at which the pumping well intake screen begins to dewater. However, if delayed gravity response, dual porosity, or karst nature of the aquifer is suspected, then terminating the test soon after first apparent stabilization of the drawdown is reached may be erroneous.

A typical time-drawdown curve in response to groundwater withdrawal from a well completed in a karst or fractured rock aquifer is shown in Figure 15.36-*Left*. Given enough pumping time and presence of all porosity types, the time-drawdown curve would show three distinct segments. The first portion of the curve, with a uniform slope, indicates a quick response from a well-connected network of secondary porosity, which may include large dissolutional openings and/or fractures. Drainage of this type of porosity, in the early stages of the test, is characterized by storage properties generally similar to that of confined aquifers. Unconfined intergranular aquifers often exhibit similar early response to pumping, due to sudden change in hydraulic pressure, with the storage coefficient significantly less than 1 percent (1×10^{-3} or less).

The flattening of the curve (curve portion 2) indicates that the initial source of water in large solutional openings (channels, conduits, cavities in general) and/or fractures is being supplemented by water coming from another set of porosity. This additional inflow of water starts when the fluid pressure in the conduits and/or large fractures decreases enough, resulting in the hydraulic gradients from the smaller fractures and fissures towards the larger fractures and/or karst conduits. This is a transitional portion of the curve. As the sources of water from different sets of secondary porosity features, possibly including water from the primary (matrix) porosity attain similar level of influence, the drawdown curve exhibits another relatively uniform slope (curve portion 3). Such rock formation

is often referred to as a dual-porosity formation because of the distinct hydraulic characteristics of different types of porosity present (Barenblatt et al., 1960).

Again, a similar response often happens in unconfined intergranular aquifers when additional water, due to gravity drainage, starts reaching the lowered water table. This is called delayed gravity response to pumping (see Figure 15.36-*Right*) and was first analyzed by Boulton (1954a,b). Neuman (1972, 1974, 1975) and Moench (1996) have since provided expanded solutions for unconfined aquifers with delayed gravity response that are still widely used today. If the test shown in Figure 15.36-*Right* was terminated after, for example, 480 minutes (8 hours), the true nature of the aquifer would not have been recognized.
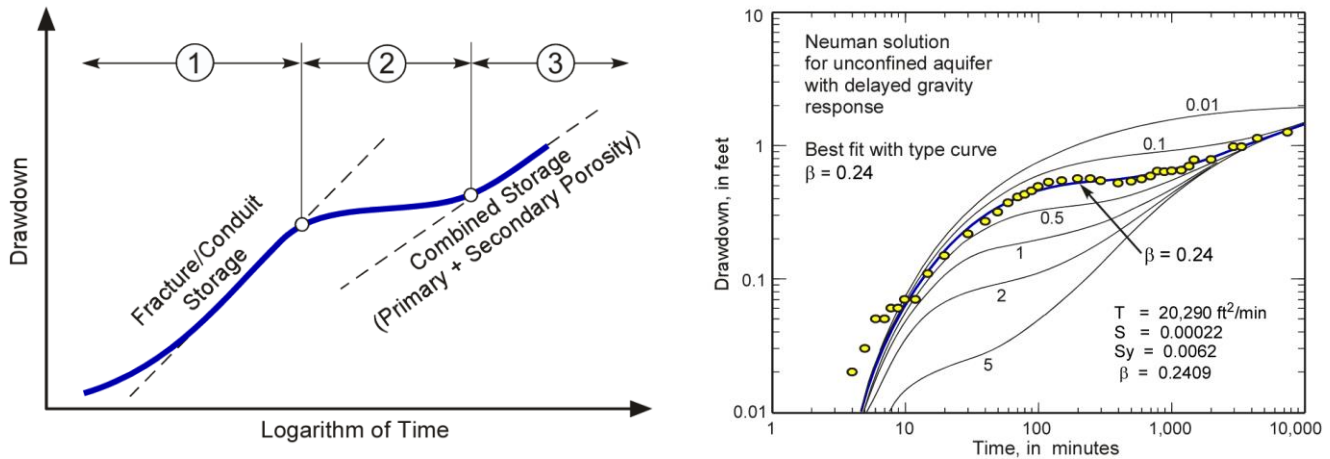
Figure 15.36 *Left*: Theoretical response of the time-drawdown curve caused by effects of specific porosity of karst aquifers. (1) Drawdown due to the initial drainage of secondary porosity (fractures and solution cavities/conduits). (2) Transitional drawdown. (3) Drawdown due to stabilized drainage of all porosity types, including matrix porosity. *Right*: example of curve fitting to experimental time vs. drawdown data using Neuman solution (type curves) for unconfined aquifer with delayed gravity response. From Kresic, 2007a; drawdown vs. time data from Green et al., 1999. Copyright Taylor & Francis; permission is required for further use.

Duration of aquifer pumping tests varies widely depending on the objectives and the aquifer characteristics. For example, in contaminated aquifers pumping test may last less than 6 hours in some cases in order to minimize the volume of extracted water. When developing an aquifer for public water supply, some regulators require that the test lasts longer than 72 hours. Ideally, a pumping test for large capacity wells used for major water supply purposes should have two phases as shown in Figure 15.28. In the first phase, a three-step test is conducted to determine the well efficiency and specific capacity. After a full recovery of the hydraulic head, the second phase should stress the aquifer with the highest feasible pumping rate (determined from phase one) for 24-72 hours or longer.

Water discharge control, measurements, and disposal

Frequent and accurate control and means of adjustment of the pumping rate during the test are essential for keeping it as nearly constant as possible. Common methods of measuring well discharge include the use of an orifice plate and manometer, an inline flow meter, an inline calibrated pitot tube, a calibrated weir or flume, or, for low discharge rates, observing the length of time taken for the discharging water to fill a container of known volume (e.g., 5 gallon bucket; 55 gallon drum).

Discharging water immediately adjacent to the pumping well can cause problems with the aquifer test, especially in tests of permeable unconfined alluvial aquifers or karst aquifers. The water becomes a source of

recharge, which will affect the results of the test. It is essential that the volumes of produced water, the storage needs, the disposal alternatives, and the treatment needs be assessed early in the planning process.

The produced water from the test well must be transported away from all observation wells so it cannot return to the aquifer during the test. This may necessitate the laying of a temporary pipeline (sprinkler irrigation line is often used) to convey the discharge water a sufficient distance from the test site. In some cases, it may be necessary to have on-site storage, such as steel storage tanks or lined ponds. This is especially critical when testing contaminated zones where water treatment capacity is not available. In many cases it may be necessary to obtain permits for on-site storage and final disposal of the contaminated fluids. Final disposal could involve treatment and reinjection into the source aquifer or appropriate treatment and discharge (Osborne, 1993).

Figure 15.37 Large capacity deep production well in Arizona being tested with the maximum feasible pumping rate. Tests like this produce large quantities of water which must be managed for extended period of time, including preventing the water to circle back to the aquifer and bias the test results. Photos courtesy of Chris Legg.

15.4 Dye Tracing

Groundwater tracing is a well-developed hydrogeologic field investigation method that has been applied with varying success primarily in aquifers with high groundwater flow velocities such as karst, highly fractured bedrock, and glacial outwash sand and gravel for example. It is of much less use in most other porous media because of the generally low groundwater flow velocities and the associated (prohibitively for most projects) long times of dye monitoring and detections at typical distances of interest. The following references in public domain, available for free download, are particularly useful for familiarizing with dye tracing: Davis et al. (1985), and Mull et al. (1988) both prepared for U.S. EPA; Wilson et al. (1986) and Taylor and Green (2008), both from USGS; Quinlan (1989); and Shook et al. (2004; a comprehensive publication entitled "Tracers and Tracer Testing: Design, Implementation, and Interpretation Methods" including a thorough mathematical background).

Dye tracing may help in answering a variety of questions including:

- Existence of underground connections between the points of interest, such as a sink or an industrial site with groundwater contamination and a spring or water supply well.
- Time of tracer travel and therefore groundwater flow velocity between the points of interest.
- Delineation of the hydrogeologic (subsurface) drainage area of a spring or a stream.
- Delineation of the capture zone of a water supply well (wellhead protection zone).
- Assessment of contaminant fate and transport parameters required for a groundwater model.
- Assessment of groundwater flow rates in a conduit or network of conduits.

Dye tracing can be quantitative and qualitative. The quantitative tracing includes continuous or frequent collection of tracer concentration data and flow rates at the locations of tracer discharge. This data is used to plot tracer breakthrough curves and determine mass recovery (balance) of the tracer (Figure 15.38). The qualitative dye tracing is performed with the simple goal of finding if there is a subsurface connection between the points of interest. It often precedes a quantitative test to help its planning including selection of sites for more frequent (or continuous) sampling thus minimizing cost. The main problem with performing only a qualitative test is a possibility that an old dye residing in the subsurface and not detected during background sampling may remobilize under new hydrologic conditions, interfere with the newly injected dye, and significantly bias the test interpretation. A carefully designed and executed quantitative dye-tracing test should help eliminate this concern. I
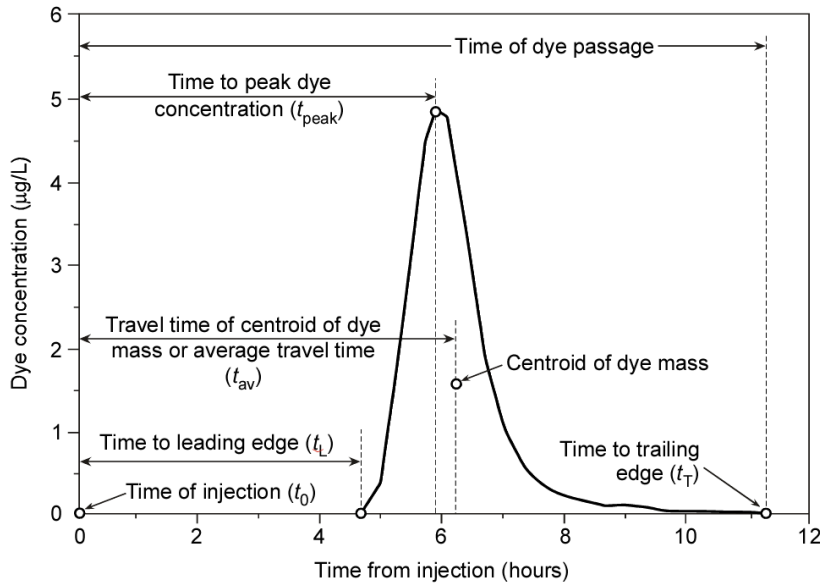
Figure 15.38 Characteristics of a simple dye breakthrough curve. Modified from Mull et al., 1988. U.S. EPA, in public domain.

15.4.1 Common Tracers

As suggested by U.S. EPA (1992), it is important to consult an individual who is experienced in groundwater tracing, and to obtain approval from the appropriate regulatory authorities before any tracer study is initiated. A tracer should have a number of properties to be considered useful and acceptable, including the following:

- Its potential chemical and physical behavior in groundwater should be understood;
- It should travel with the same velocity as the water and not interact with solid material;
- It should be nontoxic for most uses;
- It should be inexpensive;
- It should be easily detected with widely available and simple technology;
- It should be present in concentrations well above background concentrations of the same constituent in the natural system that is being studied; and
- It should not modify the hydraulic conductivity or other properties of the medium being studied.

The most widely used dyes in field studies are Fluorescein, Rhodamine B, Rhodamine WT, and Pontacyl Pink partially because they are easily visible in very dilute solutions. Rhodamine B and Rhodamine WT have been cleared as nontoxic by the U.S. Food and Drug Administration. Rhodamine and Pontacyl Pink are also quite stable with respect to fading by sunlight and to changes caused by waterborne chemicals. They do not tend to deposit on flow surfaces or sediments. These dyes are usually available in highly concentrated liquid or powder form, and

solutions are easily prepared (Figure 15.39). Pontacyl Pink dye comes as a 100% pure powder. It compares favorably with rhodamine WT as a water tracer and can be analyzed on most fluorometers using the same lamps and filters as for rhodamine WT (Bureau of Reclamation, 2001).

Either salt or dye may be conveniently used in tracer studies with equal potential accuracy. The only difference is that different detection equipment is needed. Dyes have an added advantage in that they can be detected visually, allowing simpler measurements of less accuracy that may be sufficient for some needs. Salt tracers are sensed and quantified by measuring evaporated dry weight, chemical titration, or by measuring electrical conductivity. Dye concentrations are measured by fluorimetry or color comparison standards. Sometimes, visual observation of a dye cloud is used, but considerable loss of accuracy occurs. Importantly, the detection limit for fluorescent dyes is lower than for nonfluorescent dyes, therefore, in general, less fluorescent dye is required for tracer tests (Quinlan, 1987).

Sodium chloride (NaCl) is the preferred salt used in the tracer injection solution. Finely ground salt should be purchased for ease in mixing the solution (Figure 15.40). Enough salt must be added to significantly increase the electrical conductivity of the water so that concentrations can be measured accurately. The required amount of salt can be estimated by analyzing the water for its background concentration, estimating the amount of flow to be measured, and using chemical handbook data from conductivity-salinity tables.

Figure 15.39 Left: Injection of Rhodamine WT into a water-level observation well. Photo courtesy of Charles J. Taylor, USGS. *Right*: Dilution of sodium fluoresceine prepared for dye tracing experiment in karst. Dilution of powdered tracer is with water, but use of NaOH and/or alcohol may accelerate the process. Courtesy of Zoran Stevanović.

Figure 15.40 Dye tracing experiment with salt (NaCl) at one of the swallow holes in a karst aquifer of western Serbia. The water truck is used to dissolve large quantities of the tracer and chase it down the swallow hole. Courtesy of Zoran Stevanović.

15.4.2 Tracer Injection and Sampling

In practice, tracer injection is best accomplished at locations that provide rapid, direct transport of the tracer into preferential flowpaths, thus minimizing its loss through photochemical decay, sorption, or other field conditions. This injection can be in form of a slug (instantaneous), or it can be continuous over several or more hours if the test is, in part, designed to estimate subsurface flow rates. Open-throated swallets in sinkholes and the swallow holes of sinking streams are ideal sites (Figure 15.41). In the absence of naturally occurring runoff (inflow), dyes can be injected into a stream of potable water discharged from a tanker truck or large carboy. In general, 300 to 500 gallons of water are a minimum quantity needed for dye injection, and quantities of 1000 gallons or more are preferable. Approximately one-half of the water is used to initiate flow into the swallet prior to dye injection. This is done to test the swallet's drainage capacity, to initiate flow, and to flush the flow path to minimize losses to sorption. The remainder of the water is discharged after the dye is injected as a "chaser." Under most conditions, this technique does not substantially change the naturally occurring flow conditions or alter hydraulic heads in the aquifer (Taylor and Greene, 2008).

Traditional manual sample collection for laboratory analyses is performed much less frequently today due to high labor costs associated with long stays in the field. Instead, automated samplers and probes with data loggers are used whenever possible because they can be installed in a variety of conditions and exclude possibility for cross-contamination of samples that is always a concern when samples are collected manually.

Figure 15.41 Injection of eosine OJ dye into a swallow hole in the Hughes Spring area. Photograph by Jaysson Funkhouser, USGS. From Galloway, 2004. USGS, in public domain.

When sampling fluorescent dyes with so-called passive samplers, usually packets of granular activated charcoal deployed in monitoring wells or other locations of interest (e.g., springs, surface streams) over days or weeks, several issues are of particular concern. It is believed that activated charcoal will ensure dye recovery because the supposed much lower dye concentrations found in water samples may not be detected, or sampling frequencies may not have been adequate. The ability of activated charcoal to continue sorbing and concentrating fluorescent dye provides a sound means for determining fluorescent dye occurrence when water samples are ambiguous. However, at best, activated charcoal will result in a qualitative tracing test only. More importantly, there is considerably more opportunity for sample contamination from handling. Still more serious is the demonstrated problem of false positives and false negatives associated with activated charcoal packets (Smart and Karunaratne, 2001; Smart and Simpson, 2001)

Despite the above concerns, the use of passive granular activated carbon detectors is popular for a variety of reasons as explained by Taylor and Greene (2008). The principal advantage of charcoal detectors is their economy and relative ease of use for groundwater reconnaissance studies, for simultaneous monitoring of many potential dye resurgence sites, and for mapping of conduit-flow paths or karst basin boundaries in areas where these are primarily or completely unknown. The detectors are relatively easy to conceal, thus minimizing the potential for disturbance and vandalism; and they are inexpensive.

Regardless of the selected sample collection method, it is of utmost importance that the following recommendations be followed.

- Duplicate samples should be collected for quality control.
- For the analytical laboratory control, several samples should be collected at remote sites where detection of dye is highly unlikely, such as city tap water.
- All samples should have chain of custody.
- Different people should inject dye, different should collect samples, and different should analyze them in the laboratory. Ideally, these three groups should not be in physical contact for the duration of the test to avoid any possibility, however remote, of cross contaminating the samples.
- A selected number of samples should be analyzed with a different method. For example, if water samples are analyzed with a field fluorometer, a number of samples should also be analyzed in the laboratory using a scanning spectrofluorophotometer.

15.4.3 Interpretation of Results

A well-developed hydrogeologic conceptual site model (CSM) for the project should serve as the basis for planning the dye-tracing test. A number of CSM elements will help decide where to inject the dye, where to take samples, which type of dye(s) to use, how much dye to inject, and when to start monitoring at selected sampling locations and how often. Important CSM elements include known or suspect locations of surface water sinking, likely preferential flow paths, hydrologic characteristics of the season, flow rates of surface streams and springs, anticipated predominant type of flow at the locations of dye injection (conduit, diffuse/matrix), estimated flow velocities in the subsurface, any groundwater withdrawals in the general area of the dye test, and other project-specific factors that may influence transport of dye between the location(s) of injection and sampling. Whenever feasible, sampling should also include selected water supply and/or monitoring wells in the test area.

Below is an example of a qualitative dye-tracing test that may have benefited from developing a CSM and using it to plan the test, thus leaving less room for possible erroneous conclusions. Apparently, the only goal of the test was to confirm if there is a connection between a known sink and a spring used for water supply. Notably, no flow measurements of any kind were performed during the entire test and the field visits only included sampling of the spring. The test was generally performed as follows:

- Place a passive dye sampler consisting of a bag of granular activated charcoal into the spring pool.
- Dump an arbitrary amount of a dye into the sink located several miles away from the spring (incidentally, the stream sinking into the sink is intermittent).
- Visit the spring once a week for 4 weeks after introducing the dye into the sink and replace the charcoal bags; analyze the charcoal samples in the laboratory for any presence of dye.
- Discontinue the sampling after 4 weeks since no dye was detected in the charcoal samples.
- Based on the absence of dye in the samples, conclude that there is no connection between the sink and the spring.

In addition to the most obvious concern regarding the above example, namely that the dye may have arrived at the spring during the fifth week after the injection, a number of other possibilities illustrate how a previously developed CSM would have helped in avoiding the following ambiguities and the possibly erroneous final conclusion:

- The sinking stream may have dried up at any time following the introduction of dye resulting in a considerable slowdown of the tracer movement.

- The flow rate of the sinking stream and/or the spring may have been too high for the mass of dye used resulting in dye dilution to nondetectable concentrations.
- The dye was inadequate for the characteristics of the spring, that is, it may have degraded below the detection limit under the sun light in the exposed spring pool due to high photochemical decay.
- Although apparently not of importance to the issue at hand (looking at possible connection between the sink and one particular spring), the dye may have discharged at unmonitored locations.
- The sink and the spring may be connected during different hydrologic conditions (seasons).

In contrast to the above example, an ill-conceived qualitative test can also result in a false positive result and conclusion that the connection between a sink and a spring exists, when in fact it does not. One common problem is that activated carbon enhances background concentrations of fluorescent dyes and other similarly appearing compounds. Available information shows that dye concentration by activated carbon may be as high as 1000 times the concentration in water (Käss, 1998).

Prior to any tracing efforts, background water samples need to be collected and analyzed for the tracer of interest. If the values obtained are low enough (e.g., few tenths of 1 µg/L), then the chosen tracer may be used. If not, then a different tracer should be chosen. Low background concentrations in samples will then need to be averaged and subtracted from every sample of recovered tracer from subsequent tracing efforts. For example, sodium fluorescein is used to color automobile antifreeze which is ubiquitous in the environment. If an improper background concentration of a tracer was conducted, or not conducted at all, such tracer study would be a waste of effort, possibly leading to false positive results "all over the place".

Breakthrough curves generated from tracer tests of preferential flow paths are typically positively skewed and may be quite simple, with one single sharp peak (Figure 15.38), or quite complex with several peaks, plateaus, and irregular oscillations. Multiple reasons may exist for complex curves and there is no simple book of recipes that can be used to select the right interpretation. Figures 15.42 and 15.43 show the results of several dye tracing tests and their possible interpretations.
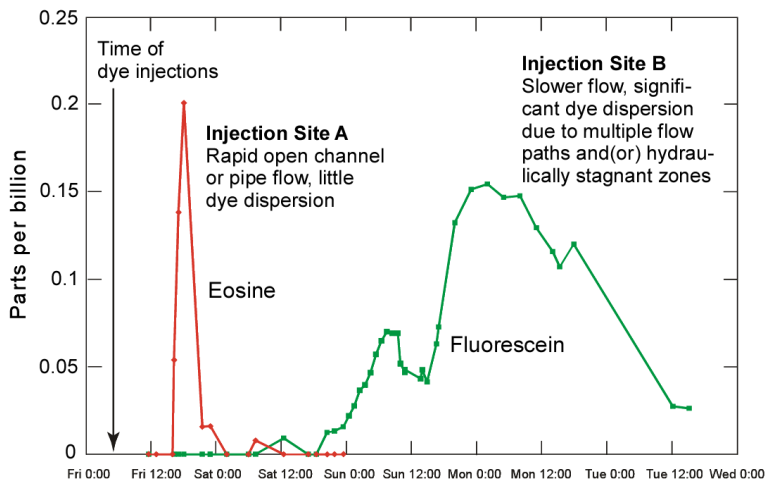
Figure 15.42 Example of dye-breakthrough curves for two dye-tracing tests conducted in the Edwards aquifer, Texas, showing a quick-flow response with little or no dispersion (Injection site A, left), and a slow-flow response showing the effects of dye dispersion (Injection site B, right). Courtesy of Geary Schindel, Edwards Aquifer Authority; from Taylor and Green, 2008. USGS, in public domain.

The accuracy of calculations of mean tracer residence time, flow velocities, and other hydraulic properties from breakthrough curves data is entirely dependent on tracer mass recovery. Few tests result in 100% recovery of dye, but as the percentage of mass recovery decreases, the margin of error in the calculated hydraulic parameters increases and confidence in the values obtained declines. Both the breakthrough curves and the tracer recovery may be affected by the internal aquifer structure. It therefore is important to assess tracer mass recovery as a starting point in the analysis of quantitative dye-tracing tests. The quality of the tracer experiment may be quantified in

terms of the relationship between the mass of dye tracer injected (M_{in}) during the experiment and the total mass of dye tracer recovered (M_r). A test accuracy index proposed by Sukhodolov et al. (1997) is calculated as

$$A_I = M_{in} - M_r / M_{in} \tag{15.37}$$

This index provides a semiquantitative assessment of the quality of the test. A value $A_I = 0$ indicates a perfect tracing experiment with no loss of tracer dye mass. A positive A_I value indicates that more tracer dye mass was

injected than was recovered—a common result, whereas a negative value indicates more dye mass was recovered than was injected—an impossibility unless residual tracer dye is present in the aquifer, errors are made in determining the dye concentration in test samples, or initial calculations of the injected dye mass are in error (Taylor and Greene, 2008).
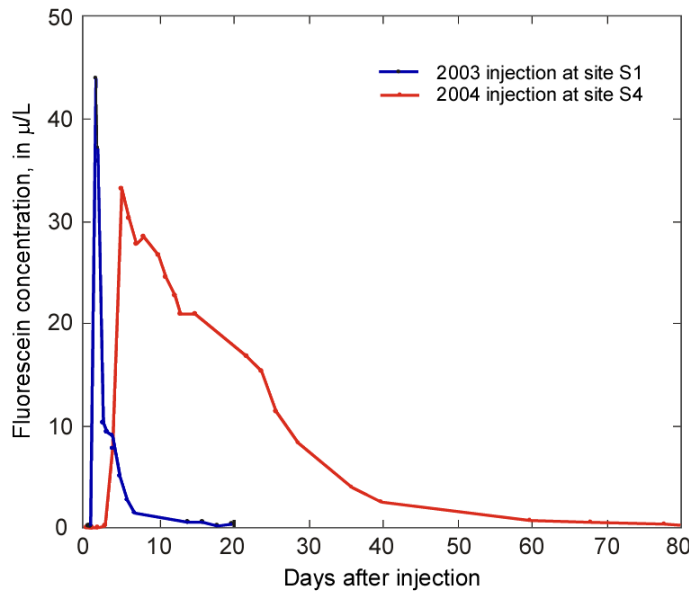
Figure 15.43 Comparison of fluorescein dye breakthrough curves for well NON for 2003 and 2004 injections in Spring Creek, South Dakota. The length of time that a solute would remain in the capture zone of well NON is almost an order of magnitude greater when streamflow recharge is receding (2004) than when streamflow recharge in Spring Creek is near the loss threshold rate (2003). Differences in recharge rates could substantially influence the transport of a potential contaminant introduced into the Spring Creek loss zone. The direction of a conduit flow path in the Spring Creek area was to the northeast with groundwater velocities that ranged from 770 to 6,500 feet per day. From Putnam and Long, 2007. USGS, in public domain.

In the previous equation, the value for M_r, the total mass of tracer dye recovered is given by the equation:

$$M_r = \int_0^\infty C(t)Q(t)dt \tag{15.38}$$

This equation assumes that the total dye mass is recovered at a single spring site. If dye has resurged at multiple spring outlets, these calculations are repeated for each site and the results are summed to obtain M_r.

If the tracer is conservative (not subject to decay or sorptive losses) and all of the water from the injection point is accounted for, the mass of dye recovered should be equal to the mass injected. None of the fluorescent tracers is completely conservative, but tracer tests with travel times of less than a few days should balance reasonably well if all of the resurgences have been monitored. A significant loss of the tracer from the system suggests that additional resurgences are present or some of the tracer has moved into storage areas along the flow route. Less conservative tracers usually produce a longer travel time estimate due to retardation caused by sorption and desorption along the flow route (Jones, 2012).

Storage of the tracer in the conduit system may be very complex. Storage may just represent very low velocity flow through one section of a branching conduit, called inline storage. A test done under conditions of diminishing flow may leave some of the dye abandoned in upper-level pockets to be remobilized when the flow increases at a later date. Some dye may become stored offline in lateral areas along the route such as small voids or in pores in the sediments. Inline storage tends to create dye pulses that correlate with flushing due to storm events. Dye from offline storage tends to drain slowly during groundwater recessions (Jones, 2012).

Lecture 16 Groundwater in Water Supply

16.1 Introduction

The first masterpieces in water supply engineering were inspired by groundwater and springs. The City of David (Jerusalem) was built on a limestone hill in which groundwater created karstic caves. The Gihon Spring, the only source of water for the city, is mentioned many times in the Bible. It made the founding of the City of David possible and sustained its existence for thousands of years. The Hebrew name of the spring is derived from the verb meaning "to gush forth," reflecting the flow of the spring, which is not steady, but intermittent, its frequency varying with the seasons of the year and annual precipitation. Its intermittent nature and the location outside city walls resulted in the construction of several waterworks to secure a reliable water supply. The entrance to the Warren's Shaft System, located within the ancient city's walls, was discovered by C. Warren in 1867 and named after him. The system is comprised of a 41-meter long irregularly shaped underground passage with a shaft at its end leading to the Gihon Spring (Figure 16.1). Although most scholars agreed that the Warren's Shaft System was man-made, a hydrogeological study conducted at the beginning of the 1980s suggested that the shaft and most of the tunnel were natural karst features in the rock adapted and combined by the builders of the system to make subterranean passage from the city to the spring possible (Frumkin and Shimron, 2006).

Figure 16.1 Waterworks at Gihon Spring in Jerusalem. *Left*: Spring cave; in the center of the image is a carved passageway that leads to the area of Warren's Shaft and Hezekiah's Tunnel. *Middle*: View of the interior of Hezekiah's Tunnel; water from the spring is still flowing through the tunnel which can be visited. *Right*: Man-made and natural entrances to the tunnels above the first century Pool of Siloam, with the large stairway leading into the pool. Photos courtesy of http://www.bibleistrue.com/qna/pqna21.htm.

During the reign of Hezekiah (739-687 BC), the Hezekiah's Tunnel (also known as the Siloam Tunnel) was dug underneath the City of David in Jerusalem apparently in preparation for an impending siege by the Assyrians. Hydraulic plaster was applied throughout the tunnel to seal voids of dissolution and tectonic origin. The 553 m long curving tunnel is one of the few intact, 8th century BC biblical structures that the public can still visit today. According to the Siloam inscription, it was excavated by two teams, one starting at each end of the tunnel and then meeting in the middle. It has been proposed that the tunnel, at least partially, followed natural underground features through which some water already flowed between the Gihon Spring and the Siloam Pool; the Siloam Inscription mentions that "there was a "zdh" in the rock", which could be interpreted as a fracture, or a karst feature, or both (Geva, 2023). Frumkin and Shimron (2006) suggest that the digging of the tunnel was accomplished by directing

the two teams from above using sounds generated by hammering on the solid rock through which the hewers were digging (arguably the first application of engineering geophysics in karst.)

The tunnel was cut into the rock in a 533 m-long, "S"-shaped course. In a straight line, the distance from the Gihon Spring to the Siloam Pool is only 325 m. The average width of the tunnel is about 60 cm; it is about 2 m high or less along most of its course (Figure 16.1) but reaches 3–4 m in some sections at the beginning and the end. The tunnel was finely carved out, with chisel marks visible. The downward slope from beginning to end is very gentle, approximately 2 m altogether, with an average gradient of 0.4% (Geva, 2023.)

The project is mentioned in the Bible (II Kings 20:20): "...and how he made a pool, and a conduit, and brought water into the city…" and again in II Chronicles 32:30: "This same Hezekiah also stopped the upper watercourse of Gihon and brought it straight down to the west side of the city of David."

Figure 16.2 *Top*: Jadro karst spring (average discharge is 10 m^3/s) was first captured by the Romans for water supply of the palace built in third century AC by Roman emperor Diocletian for his summer residence on the Adriatic coast. The palace, the largest ever built in the Roman empire, is in the Croatian port city of Split which still uses the spring for its water supply. Courtesy of Branimir Jukić. *Middle*: The aqueduct that brought water to the palace (photograph courtesy of Ivo Eterović). *Right*: Reconstruction of Diocletian's palace in Split by architect Ernest Hébrard. (From E. Hébrard and J. Zeiller, *Spalato, le Palais de Dioclétien*, Paris, 1912.)

Using aquifers and springs for water supply was perfected by the Romans who preferred spring water to any other. In virtually all Mediterranean countries that were part of the Roman Empire there are remains of Roman aqueducts originating at karst springs (Figure 16.2). The Aqua Appia was the first Roman aqueduct built, one of the eleven supplying drinking water to the city of Rome. It was constructed in 312 BC by Appius Claudius Caecus. The city of Rome still relies on karst springs for its water supply.

The Roman custom of building fountains at the endpoint of aqueducts that brought groundwater to Rome was revived in the 15th century, in the Renaissance. The Trevi Fountain shown in Figure 16.3 is the largest Baroque fountain in the city and one of the most famous fountains in the world, fabled for its water clarity. The site as a source of fresh, clean drinking water originally dates to 19 BC. It was the end point of the Acqua Virgo aqueduct, completed by Marcus Agrippa, during the reign of the emperor Augustus. Its source is from the 13-km-distant karst spring Salone, about 3 km from the Via Praenestina. According to a legend, thirsty Roman soldiers asked a young girl for water. She directed them to the spring that later supplied the aqueduct. The source was named the Aqua Virgo after her. Along its more-than-20 km length, the aqueduct dropped only 4 m to reach Rome in the center of the Campus Martius. At its height, the aqueduct could supply more than 100,000 cubic meters of water every day. After deteriorating with the fall of the Roman Empire, Aqua Virgo was repaired by Pope Adrian I in the 8th century. Following a complete restoration and extensive remodeling from its source to its terminus points from the Pincio to the Quirinale and within Campo Marzio, in 1453, Pope Nicholas V consecrated it Acqua Vergine (https://romanhistory.org/structures/aqua-virgo).

Figure 16.3 The Baroque Trevi Fountain in Rome designed by Nicola Salvi and finished in 1762. The fountain's facade and reef were constructed using travertine stone, a layered calcium carbonate formed by springs and quarried near Tivoli, 22 miles east of Rome. Travertine was also used to build the Colosseum. The statues are made of Carrara Marble. Water for the fountain is brought via Aqueduct Vergine, the revived ancient underground aqueduct Acqua Virgo, from the 13-km-distant karst spring Salone. Photo courtesy of Zoran Stevanović.

Springs were the first logical choice for both domestic and public water supply sources worldwide. In those European countries where karst aquifers and springs abound they are still widely used and preferred because of much lower water treatment costs and lower levels, or absence of endemic anthropogenic contamination compared to surface water. The same is true for groundwater in general. According to European Environment Agency (EEU), groundwater supplies 65% of drinking water and 25% of water for agricultural irrigation in the 27 European Union Member States (EEA, 2023). Good examples of European reliance on groundwater for public water supply are Denmark (100% from groundwater), Austria (99%), Switzerland (83%), Portugal (80%), Italy (80%), and Germany (72%), to name a few.

In Austria, most of the large cities like Vienna, Salzburg, Graz, Linz, and Innsbruck are supplied by karst aquifers and springs. Vienna is the classical example of a metropolis with 2 million inhabitants that enjoy high quality fresh water from karstic springs. These springs are located at the foot of four major karst massifs in the eastern part of the Northern Calcareous Alps. The biggest spring of the Eastern Alps, the Kläffer Spring (Figure 16.4) is the most important spring captured for Vienna, where water supply from karst springs dates to the 19th century. A 120-km long pipeline, originally called Kaiser Franz Josefs Water Main, was completed in 1873 and captured major springs in the Rax and Schneeberg area South of Vienna. The growing demand for water led to the construction of the 200-km long Second Vienna Water Main finished in 1910, that developed the Kläffer Spring and other smaller ones in the Hochschwab area Southwest of Vienna. A very detail description of the Vienna water supply facts including hydrogeology, water quality, spring capture engineering, and groundwater protection is provided by Plan, Kuschnig, and Stadler (2010).
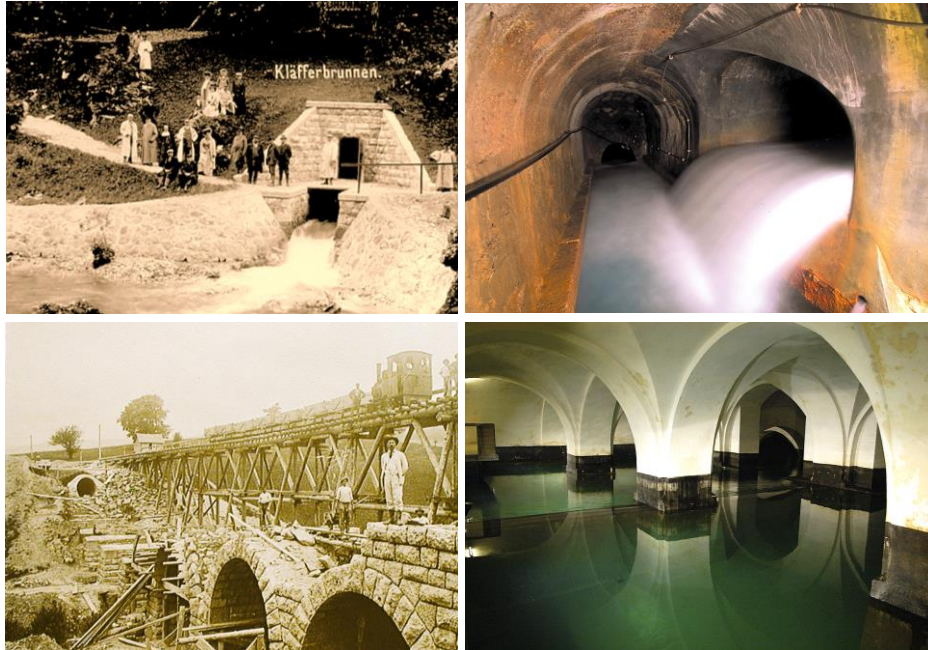
Figure 16.4 *Top left*: Historic picture of the entrance no. 11 and overflow of the Kläffer Spring (around 1910). *Top right*: Partially flooded overflow gallery of the Kläffer Spring underground capture. *Lower left*: Construction of an aqueduct of the Second Vienna Water Main. *Lower right*: One of the city waterworks' storage reservoirs at Vienna Rosenhügel with a volume of 120,500 m^3. Photos courtesy of Lukas Plan, Gerhard Kuschnig, and Hermann Stadler.

The largest cities on the Adriatic coast of Croatia obtain their water supply from karst springs—Rijeka, Split, and Dubrovnik (Figure 16.5); the same is true for the Adriatic coast of Montenegro—Kotor, Budva, Herceg Novi, and Bar. Four capital cities of the Western Balkans receive drinking water from the karstic aquifers and springs: Sarajevo (Bosnia & Herzegovina) Podgorica (Montenegro), Skopje (North Macedonia), and Tirana (Albania). And the list goes on.

Figure 16.5 *Left*: Great Fountain of Onofria at the entrance to Old City, Dubrovnik, Croatia. It was designed and built by the Italian architect Onofria della Cave in 1440. Water for the fountain, which includes the water storage reservoir, was conveyed from a group of springs by a 12-km-long system of canals and aqueducts. Dubrovnik is dotted with beautiful fountains for public drinking water supply with spring water (photos on the right).

The history of groundwater development in the United States is very similar to many other countries, and it reflects patterns of socioeconomic development. Groundwater as a resource is less understood than surface water, as it is "hidden" and inaccessible for direct observation. The first phase of groundwater development is generally characterized by unrestricted land use, growth of agriculture, and use of shallow aquifers, which allow human settlement of large areas including semiarid regions with scarce surface water resources (Figure 16.6-*Left*). The general result of uncontrolled early groundwater development is the lowering of the water table and widespread shallow groundwater contamination (Figures 16.6 and 16.7). The next phase reflects advances in well drilling technology (Figure 16.8), and irrigation and energy availability, which enable development of deeper aquifers on a large regional scale, more intensive agriculture (Figure 16.9), and faster population growth. Finally, as large-scale groundwater development brings more obvious consequences such as land subsidence, depletion of aquifer storage, and diminished flows of springs and surface streams, the challenge for science and engineering has changed from supporting the development of groundwater resources to understanding its sustainability and impact on the environment including ecological needs (Anderson and Woosley, 2005).

Figure 16.6 *Left*: A migrant family poses for a portrait during the Dust Bowl; dug well with a pulley is on the right. Photo courtesy of the Natural Resources Conservation Service; in public domain. *Right*: Dug well at historic Drayton Hall Plantation near Charleston, South Carolina, not in use for decades.

Figure 16.7 *Left*: Drilled well with pumping windmill, Big Bend, Texas; *Middle*: Driven well with a hand pump at a historic farmhouse on Eastern Shore, Maryland. *Right*: Dug well in Colonial Williamsburg, Virginia. Wells like these are not used for drinking water supply anymore because of widespread shallow groundwater contamination.

Figure 16.8 On the Edwards Aquifer website, Gregg Eckhardt provides the following description of the photograph:

San Antonio began to rely on artesian wells for its water supply several years after the first large wells were drilled in 1891. These are two of San Antonio's first municipal water supply wells, drilled at Market Street for George Brackenridge, who owned the water system and had a contract to supply the city. The photo shows the tremendous amount of pressure that Aquifer water was under at that time. If we estimate the two men in the photo to be around 5 1/2 feet tall, then the column of water shooting up from the well is around 25 feet high! The effect of releasing all this pressure through wells was that springflows began to decline immediately and significantly. By 1896 there were approximately 40 wells in the San Antonio area. By around 1900 San Antonio Springs had been reduced to just a trickle in most years.

This photograph appeared in R. T. Hill & T. W. Vaughan's 1896 report on the geology and underground waters of the Edwards Plateau. Hill and Vaughan were the first geologists to recognize that wells such as these had impacted springflows. They were the first people to accurately describe the Edwards and how it works.

Although they never used the word 'aquifer', they referred to the Edwards as an artesian groundwater system, accurately described the catchment and transmission of water in the Aquifer, and recognized its large extent from Brackettville to Austin.

http://www.edwardsaquifer.net/intro.html

Figure 16.9 Photographs taken on a commercial flight from Washington, D.C. to Los Angeles. Center-pivot irrigation systems are common sight west of Mississippi including in the arid basins of the Basin-and-Range physiographic province where any agriculture would not be possible without use of groundwater (see also Figure 1.10 in Lecture 1).

The competition for water has always been intense and long before long before ecological water needs were considered. For example, surface waters of the Colorado River Basin managed by a series of reservoirs are overallocated for water supply and irrigation uses. An analysis of in-stream water needs showed that flows in the Rio Grande, the Upper Colorado, and the Lower Colorado water-resource regions are insufficient to meet current needs for wildlife and fish habitat, much less allow for any additional off-stream use (Guldin, 1989).

The competition for and overallocation of surface water resources are not limited to the American West. For example, the population growth and the ongoing droughts in the American Southeast are fueling the disputes over surface water rights between Georgia, Alabama, and Florida. As in many other countries, the surface waters of the United States are largely developed, with little opportunity available to increase storage along main rivers because few suitable sites remain for dams, and there is general concern about the environmental effects of impoundments. The surface waters of the nation also receive and assimilate, to a large degree, significant quantities of point- and nonpoint-source contaminants (Anderson and Woosley, 2005).

Rivers are an important component of the natural environment as well as the economic infrastructure. They are crucial water supplies for municipal, industrial, and agricultural uses and are sources for recreation, power generation, and transportation of goods. The history of water policy in the United States is dominated by the construction of structures such as dams, canals, dikes, and reservoirs (Gleick, 2000). As pointed out by Anderson and Woosley (2005), many of the 77,000 dams in the United States were constructed largely without considering the environmental consequences. The dams on the Columbia River, for example, were constructed without the full understanding of the long-term consequences to fish populations.

Sustainable groundwater development has become a focal point of the integrated water resources management in many countries, including where use of surface water resources had an undisputable priority. Following are some of the reasons for this trend in regions where both surface water and groundwater resources are available:

- Groundwater development requires lower capital investment and simpler distribution systems, since it can be executed in phases and closer to end users.
- Surface water intakes and storage (reservoirs) are more vulnerable to seasonal fluctuations in recharge, as well as periods of drought; they are also more vulnerable to the projected impacts of climate change.
- Evaporative loss from surface water reservoirs is large, especially in semiarid and arid regions, whereas such loss from groundwater systems (storage) is mostly negligible or nonexistent.
- The environmental impacts of surface water reservoirs are incomparably less acceptable to the general public than just a generation ago.
- The general quality of surface water bodies and their sediments has been impacted by point- and nonpoint sources of contamination to a much greater extent and for longer periods of time, requiring more expensive drinking water treatment and use of a variety of chemicals.
- Surface water supplies are more vulnerable to accidental or intentional contamination.
- The ability of surface water systems to balance between daily and seasonal periods of peak demand and periods of low demand is limited. In contrast, water wells can simply be turned off and on, and their pumping rates can be adjusted as needed.

Proper groundwater development can completely avoid some of the above-listed problems inherent to surface water supplies; it can also alleviate most of them as part of the integrated management of both surface water and groundwater as discussed later in this Lecture.

Story of the American Windmill

Dorothy Ainsworth writes in her article titled "Water Pumping Windmills", published in the November/December, 2004 issue #90 of the Backwoods Home Magazine:

In the late 1880s and early 1900s, windmills were sprinkled all over the American landscape. They were indispensable to the late-comer settlers who were forced to move farther west to the sun-parched remote plains, after all the more desirable spots near rivers and streams had been taken. In the Great Plains and the vast territory known as the Great American Desert, water was more precious than gold. The American multi-bladed windmill bears little resemblance to its European counterpart. Unlike the Dutch "scoop" mills that could move 16,000 gallons an hour but only lift it 16 feet, the new Yankee design could lift water from hundreds of feet below the surface. It was invented in Connecticut in 1854 by a young mechanic named Daniel Halladay. Its wheel, made from wooden "sails," could be transported in sections and assembled on location.

He ingeniously designed the wheel to automatically turn its face into the wind by wind-pressure on the vertical tail behind it. If it got to spinning too fast, a weighted mechanism came into play that turned the wheel partially out of the wind to slow it down.

Halladay sold thousands of his machines, and before long there were 300 competing manufacturers producing similar wooden-bladed beauties. Then in 1886, Thomas Perry designed the more aerodynamic steel-bladed windmill, with curved blades (to catch more wind) and that design is still used today.

More on the American windmill facts, design, and how it changed the way of life can be found at https://www.backwoodshome.com/water-pumping-windmills/

Figure 16.10 Scene from the Big Bend National Park, Texas.

16.2 Price and Value of Groundwater

The concept of water as an economic good emerged during preparatory meetings for the Earth Summit of 1992 in Rio de Janeiro. It was brought forward and discussed extensively during the Dublin conference on Water and the Environment (ICWE, 1992), and became one of the four Dublin Principles, listed below:

Principle No. 1—*Freshwater is a finite and vulnerable resource, essential to sustain life, development, and the environment*. Since water sustains life, effective management of water resources demands a holistic approach, linking social and economic development with protection of natural ecosystems. Effective management links land and water uses across the whole of a catchment (drainage) area or groundwater aquifer.

Principle No. 2—*Water development and management should be based on a participatory approach, involving users, planners, and policymakers at all levels*. The participatory approach involves raising awareness of the importance of water among policymakers and the general public. It means that decisions are taken at the lowest appropriate level, with full public consultation and involvement of users in the planning and implementation of water projects.

Principle No. 3—*Women play a central part in the provision, management, and safeguarding of water*. This pivotal role of women as providers and users of water and guardians of the living environment has seldom been reflected in institutional arrangements for the development and management of water resources. Acceptance and implementation of this principle requires positive policies to address women's specific needs and to equip and empower women to participate at all levels in water resources programs, including decision making and implementation, in ways defined by them.

Principle No. 4—*Water has an economic value in all its competing uses and should be recognized as an economic good*. Within this principle, it is vital to recognize first the basic right of all human beings to have access to clean water and sanitation at an affordable price. Past failure to recognize the economic value of water has led to wasteful and environmentally damaging uses of the resource. Managing water as an economic good is an important way of achieving efficient and equitable use and of encouraging conservation and protection of water resources.

The following excerpts from an article published in China Daily on April 4, 2014 (titled "Price full cost of water") illustrate some of the points above. It is also quite uncharacteristic for its harsh criticism of the officials in China:

The three-tiered water pricing reform that Beijing is set to introduce is a badly-needed first step to deal with the looming water shortage the city faces.

To quench its growing thirst, however, the city must quickly raise water prices to cover at least the cost of water supply.

The two plans that the Beijing Water Authority released on Wednesday to solicit public opinion on progressively raising water prices all suggest a rise of about 1 yuan (16 US cents) for the first-tier water price that applies to 85 to 90 percent of households in the city.

This would mean a 25-percent rise in the water bills of most local families, which undoubtedly represents an effort to encourage water conservancy. But it hardly amounts to an adequate response to the Chinese capital's challenge of avoiding a looming crisis in water supply.

As one of the most thirsty cities in the world, Beijing's water resources are less than 300 cubic meters per capita, only one-eighth of the national rate and one-thirtieth of the world average.

Worse, the rapid growth of its population and economy, as well as disruptive climate change, have only increasingly widened the gap between Beijing's water usage and the available local water resources.

By adding no more than 20 yuan per month to the water bills of 90 percent of local families, it is doubtful if the two plans that the Beijing municipal government has come up with will really help build much momentum in water conservation practices.

On one hand, prices for water will remain relatively cheap. Most residential consumers in Beijing will pay 5 yuan (81 US cents) per cubic meter of water, compared with a global average of $2 per cubic meter.

On the other hand, the hiked prices would still not cover the total cost of water resources, supply and treatment. It is shocking to know that in such a thirsty city as Beijing, local residents are subsidized by about 2 yuan per cubic meter for their use of water.

As pointed out by van der Zaag and Savenije (2006), the interpretation of the concept "water as an economic good" has continued to cause confusion and heated debate between various interpreters of its "true" meaning. Two main schools of thought can be distinguished. The first school, the pure market proponents, maintains that water should be priced through the market. Its economic value would arise spontaneously from the actions of willing buyers and willing sellers. This would ensure that water is allocated to uses that are valued highest. The second school interprets "water as an economic good" to mean the process of integrated decision making on the allocation of scarce resources, which does not necessarily involve financial transactions (e.g., McNeill, 1998). The latter school corresponds with the view of Green (2000) who postulates that economics is about "the application of reason to choice." In other words, making choices about the allocation and use of water resources on the basis of an integrated analysis of all the advantages and disadvantages (costs and benefits in a broad sense) of alternative options.

Proponents of pure market principles also argue that rationalized global use of water is not possible when prices are subsidized and seriously distorted. In general, the agricultural sector is characterized by high subsidies worldwide, which includes below-market cost for irrigation water delivered through government-run irrigation projects, which are often highly inefficient. In some countries, governments subsidize the cost of energy needed to operate irrigation equipment, such as in India where installation of wells and well pumps in rural areas has been continuously promoted, including providing free energy to the farmers. Domestic and industrial water users commonly pay more than 100 times as much per unit of water as agricultural users (Cosgrove and Rijsberman, 2003).

Van der Zaag and Savenije (2006) argue that water is a "special economic good" because of its unique characteristics and that contradiction exists between the first and the fourth Dublin principle, if the latter is interpreted in a narrow market sense. Water is a good that is essential, non-substitutable, and too bulky to be easily traded over large distances. The consequence is that water is used when and where it is available. Except for a handful of cases (such as with bottled water), and unlike for most other goods, water characteristics make it unattractive for large-scale trading. As a result, water markets can only function on a local scale and must consider that the water flows downstream in case of surface water, of from upgradient to downgradient in case of groundwater. It can be argued, however, that it is rarely clear to all the existing and potential stakeholders which principles should be applied and which principles are fair or not fair when looking at the water market and economy. In the United States, this ambiguity is a fertile ground for litigation, especially when it comes to senior and junior water rights, as illustrated with the following excerpt from a news article (Barker, 2007):

Water experts, state officials and the businesspeople and farmers at the heart of Idaho's most heated water dispute are entering their third week of testimony in a case that could dictate how the state uses one of its most precious resources in the future.

At stake is whether the state shuts off the pumps that bring water to thousands of acres of farmland, factories and towns across central and eastern Idaho. Or will fish farmers, Clear Springs Foods and Blue Lakes Trout Farm, which have lost millions of dollars due to dropping flows from the springs on which they depend, face permanent losses?

The debate turns on legal principles that have been teased out in disputes among surface water users for nearly a century. But Schroeder and the Supreme Court may plow new ground on how the law treats disputes between people who pump their water from the ground and those who get their water from springs and rivers.

The justices will have to weigh two competing sections of constitutional water law: prior appropriation—first come, first served; and the imperative to use water for its full economic development.

The primary case in surface water law upheld the constitution's prior appropriation doctrine, but the U.S. Supreme Court also ruled in favor of full economic development in 1912. In that case, Henry Schoedde was watering his crops and running a mining operation by using water wheels with buckets to take the water out of the Snake River and lift it into his canals. He sued the Twin Falls Canal Co. because its Milner Dam threatened to lower the river to a point where his water wheels wouldn't turn. The U.S. Supreme Court ruled Schoedde did not own the current in the river and could not stop others from diverting water to protect it.

Schroeder, Tuthill and the Idaho Supreme Court will have to decide whether fish farmers, who use artesian springs that flow from an aquifer that was later tapped by thousands of groundwater pumpers, are like Schoedde and his water wheels.

Figure 16.11 The largest trout fisheries in the world are near Twin Falls, Idaho, along the Snake River section with the famous *Thousands Springs*. This fishery is supplied water from the Niagara Springs shown in Figure 10.34 in Lecture 10. Photo courtesy of Clear Springs Foods Inc.

The dispute was eventually resolved after the two parties agreed to a mitigation plan developed by the groundwater irrigators ("Groundwater Districts"), as illustrated by the following "dry" legal language from the final-final order signed on March 18, 2012, by the Interim Director of IDWR Gary Spackman:

On July 8, 2005, the Director entered a final order finding that pumping by junior ground water users causes material injury to certain water rights held by Clear Springs. The order was subject to an administrative hearing, judicial review, and an appeal to the Idaho Supreme Court, which upheld the Director's decision. Clear Springs Food, Inc. v. Spackman, 150 Idaho 790,252 P.3d 71 (2011).

On March 5, 2012, the Director of the Department of Water Resources ("Director" or "Department") received a Stipulated Mitigation Plan and Request for Order ("Mitigation Plan") filed jointly by counsel for Clear Springs Foods, Inc. ("Clear Springs") and the Ground Water Districts ("GWD"). The Mitigation Plan was filed pursuant to Rule 43.03.o of the Department's Rules for Conjunctive Management of Surface and Ground Water Resources ("CM Rules"). IDAPA 37.03.11 et seq.

Having reviewed the Mitigation Plan, the CM Rules, and the proceedings herein, the Director approves the Mitigation Plan. CM Rule 43.03. ORDER Based upon and consistent with the foregoing, IT IS HEREBY ORDERED as follows: The Mitigation Plan entered into between Clear Springs and the GWDs is APPROVED.

The price of water, in a narrow sense, is defined as the price water users are paying for the volume of water delivered per unit of time (e.g., cubic meters or gallons per month). This definition applies mostly to customers receiving water from third parties, such as homeowners or businesses supplied by public water utilities, or farmers paying for off farm water delivered by centralized irrigation systems. In many cases, which in general cover most freshwater withdrawals worldwide, the users are self-providers. Some examples include individual farmers and rural homeowners using water wells, large agricultural complexes (corporations), and industrial facilities diverting

water from surface streams or using their own water wells, or power plants withdrawing water from surface water reservoirs. In most, if not all cases, neither of the two large groups of water users—customers and self-providers—pays the full ("real") price of water, which should theoretically equate to the real value of water and include all of the following:

1. Capital cost of building water withdrawal and distribution systems.

2. Cost of operating and maintaining the system ("operations and maintenance" or O&M cost) including water treatment, water source and infrastructure maintenance, staff, and administrative costs.

3. Capital for future major investments for augmenting the existing or finding new sources of water, and expanding the distribution system.

4. Source protection cost reflecting its intrinsic value (water quality, reliability)

5. External societal cost

6. Environmental cost

7. Sustainability cost

In a market, the price of a commodity (good) is determined where the supply and demand curves intersect (Figure 16.12). In this depiction of an economic market, P* is the price that would clear the market. In other words, the quantity demand would equal the quantity supplied at that price. The market clearing quantity is depicted with Q*. To the left of Q*, the values of water (embedded in the demand curve) are all higher than the costs (depicted on the supply curve), and value also exceeds P* to the left of Q*. For quantities beyond Q*, however, value is less than cost, and application of the resource for this market is not efficient beyond that level (Raucher et al., 2005).

In markets where there are many suppliers and consumers, price is often viewed as a good estimate of the marginal value of the good to both consumers and producers. It is thus considered economically efficient to allow the market process (i.e., prices determined in competitive market) to dictate the allocation of resources (Raucher et al., 2005). However, as discussed earlier, water is a special economic good, with unique characteristics that preclude open competition for virtually all uses (bottled water market being an exception). For example, there is not a single urban center where a household can choose between, say, three water utilities each providing its services through its own infrastructure.
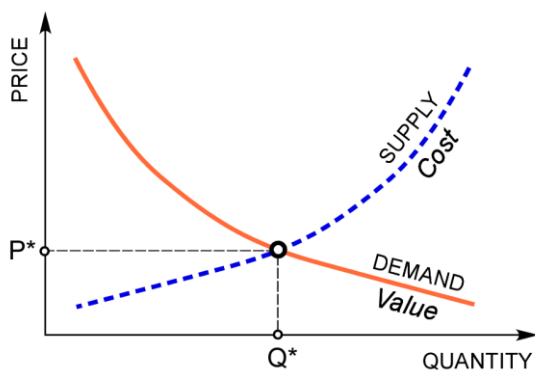
The value of water has different components, and they often mean different things to different people, and indeed societies. Market principles applicable to, say television sets, do not fully function in the water arena. As a result, all water users today, i.e., water utilities, agriculture, industry, are subsidized either directly or indirectly.

Figure 16.12 Supply and demand: price relative to value and cost (from Raucher et al., 2005; copyright 2005 American Water Works Association Research Foundation; permission is required for further use).

Direct subsidies should be easily identifiable and may include factors such as reduced energy cost for certain users (such as electricity and fuel required to operate irrigation systems), and reduced O&M costs for a public water supplier subsidized by the "public," including by those that are not necessarily directly served by the same system (e.g., through reduced or waived taxes). International financial institutions have been very active in analyzing various subsidies in the water sector and are increasingly conditioning their lending to the developing world governments and utilities on the adaptation of market principles in water pricing.

Results of an analysis of prices charged to residential customers by more than 200 water utilities in the United States are presented in Kresic, 2009. For this analysis, the utilities were grouped based on the predominant source of water extracted by the utility itself (>50 percent; purchased water was not considered) into groundwater-based and surface water-based. Of the 10 largest utilities surveyed, only one (Miami) is groundwater-based. However, regardless of the size, the groundwater-based utilities on average charge less to their customers than the surface water-based utilities: 23 percent less for the monthly usage of 1000 ft^3 and 22 percent less for the monthly usage of 3000 ft^3, based on the median price. This may be the result of lower water treatment costs and more favorable (closer) locations of groundwater extraction relative to the user base, although detailed related analysis was not conducted.

Economies of scale in water supply, particularly in the areas of source development and treatment, make it difficult for smaller water utilities to perform as well as larger water utilities. Declining unit costs of production indicate scale economies; as the volume of water produced (that is, withdrawn and treated) increases, the cost per gallon or cubic foot decreases. At lower unit costs, production is less costly in the aggregate and more efficient at the margin. Importantly, the economies of scale in water production are associated with the volume of water produced (not simply the number of service connections). Even smaller systems that are fortunate enough to have one or two large-volume customers will enjoy some economies of scale. Two utilities can have a comparable level of investment per customer and cost-of-service for the same number of residential customers, but if one also serves a large industrial firm and economies of scale are achieved, everyone in that community will enjoy lower water bills (USEPA and NARUC, 1999).

The intrinsic value of a water source is not necessarily always reflected in the price of water charged to customers, although certain aspects of it are easily quantifiable such as cost of water treatment. For example, treating water for water supply from a major river flowing through various urban and industrial areas is much more expensive than a simple preventive microbiological treatment (distribution system disinfection) of water extracted from a well-protected confined aquifer. Groundwater of high quality can also be blended with surface water thus reducing treatment cost. In that respect, groundwater used for water supply in general has higher intrinsic value than surface water. Several examples include:

- Utilization of groundwater in alluvial basins of large European rivers where utilities routinely extract groundwater from the alluvial aquifers and take advantage of riverbank filtration, rather than using river water directly.
- Accidental toxic spills and floods can take surface water supply out of service sometimes in the matter of days or even hours, whereas this is much less likely to happen with a groundwater-based water supply.
- In emergencies, including "unexpected" droughts, surface water-based utilities are often forced to look at groundwater as a last resort.
- In case of large urban centers, and when hydrologic and hydrogeologic characteristics are favorable, water utilities that develop both surface water and groundwater supplies are in a much better position to manage marginal cost of water and set stable, more realistic prices.
- Supplemental groundwater during periods of peak demand, such as dry and hot summer months, can eliminate needs for large surface water storage reservoirs and treatment plants, which become unused capacity during most of the year.
- Artificially storing water in the subsurface (aquifer storage) has two key advantages over surface reservoirs: virtually no evaporation loss and no surface land and habitat losses due to impoundment.
- In irrigation, groundwater can be applied to the fields in the immediate area where it is withdrawn from the aquifer, which eliminates needs for extensive network of canals and reservoirs where conveyance and evaporation losses are significant by default.

Prices paid for irrigation water are of considerable policy interest due to their importance as a cost of production and their impact on water demand. Increasingly, adjusting the water "price" in agriculture is viewed as a mechanism

to improve the economic efficiency of water use. However, as discussed earlier, water price adjustments to achieve socially desired outcomes can be difficult because prices paid for water by agricultural users are rarely set in the marketplace and generally do not reflect water scarcity. In the United States, individual states generally administer water resources and grant (not auction) rights of use to individuals without charge, except for minor administrative fees. As a result, expenditures for irrigation water usually reflect waters access and delivery costs alone—thus, costs to irrigators usually do not reflect the full social cost of water use. By contrast, those without an existing state-allocated water right—whether an irrigator, municipality, industry, or environmental group—that purchase annual water allocations or permanent water rights from existing users pay prices that more closely reflect the scarcity value of the resource (Gollehon and Quinby, 2006).

More difficult, and often not feasible, is to quantify that portion of the water cost attributable to external factors. This may include societal cost such as cost of health and wealth improvements of the population (Figure 16.13), or the cost of political stability/instability when favoring a certain group of users (e.g., urban versus agricultural users, or upgradient versus downgradient users). In some cases, a particular groundwater use can bring together various groups that otherwise may have diverging views of sustainability, or social and environmental justice (Figure 16.14). Figure 16.15 illustrates the value of water when considering the environmental cost which is not easily quantifiable.

Figure 16.13 San Solomon Springs, also known as Balmorhea Springs, is a popular state park in West Texas. The largest springs discharge inside the pool, with a steady rate of 15 million gallons per day. Information panels like the one on the left educate the visitors on the springs' features and their importance for the environment.

Figure 16.14 The spectacular Fountains of Bellagio, a free attraction at the Bellagio resort, located on the Las Vegas Strip in Las Vegas, Nevada. They entertain millions of Las Vegas Strip visitors per year and contribute significantly to the overall economy of the city. The Fountains were designed by WET Design and feature a musical fountain show performed in an 8.5-acre (3.4 ha) man-made lake in front of the resort. The show uses 1,214 water nozzles and 4,792 lights. The fountains shoot as high as 460 feet. Water for the fountain comes from the resort's private wells. Courtesy of www.feelingvegas.com

Figure 16.15 The Texas blind salamander is an endangered species, listed on March 11, 1967. It is aquatic salamander that is found only within one population living in Edwards Aquifer caves around San Marcos springs in Central Texas. It is troglobitic, or cave dwelling, which has resulted in it being eyeless. The Edwards Aquifer Habitat Conservation Plan (EAHCP) is a comprehensive, regional plan that defines how to protect threatened and endangered species that live in the Edwards Aquifer and the Comal and San Marcos springs. In 2013, the U.S. Fish and Wildlife Service (USFWS) issued an Incidental Take Permit to the Edwards Aquifer Authority, City of San Marcos, City of New Braunfels, Texas State University, and the City of San Antonio acting by and through the San Antonio Water System (collectively known as the EAHCP Permittees) to protect the Covered Species, including the Texas blind salamander, from activities such as groundwater pumping and disturbance from habitat restoration. EAHCP conservation measures help increase the likelihood of the threatened and endangered species survival during a catastrophic event, such as extreme drought (https://www.edwardsaquifer.org/habitat-conservation-plan/).

16.3 Groundwater Sustainability

The term "sustainable development" was popularized by the World Commission on Environment and Development in its 1987 report titled Our Common Future. The report, published as a book, is also known as the Brundtland Report, after the Chair of the Commission and former Prime Minister of Norway, Gro Harlem Brundtland. The aim of the World Commission was to find practical ways of addressing the environmental and developmental problems of the world. In particular, it had three general objectives:

- To re-examine the critical environmental and developmental issues and to formulate realistic proposals for dealing with them.
- To propose new forms of international cooperation on these issues that will influence policies and events in the direction of needed changes
- To raise the level of understanding and commitment to action of individuals, voluntary organizations, businesses, institutes, and governments

Our Common Future was written after 3 years of public hearings and over 500 written submissions. Commissioners from 21 countries analyzed this material, with the final report submitted to and accepted by the United Nations General Assembly in 1987. In various publications, debates, interpretations, and reinterpretations over the course of years, the findings of the commission and the final document (resolution) of the United Nations General Assembly were in many cases stripped down to the following widely cited single sentence which states that development is sustainable when: "meeting the needs of the present without compromising the ability of future generations to meet their own needs." Since this sentence seems to focus only on "human generations", it has been criticized by some as too narrow and failing to address the natural environment. However, the commission and the assembly did address the human and natural environments as a whole and in a holistic manner, which can be seen from the key related statements of the official UN resolution 42/187.

Thirty-five years after this UN Resolution, it seems little has changed in the practice of most governments and their "agencies" at various levels. They are either unable or unwilling to fully address and then act to start solving the many problems of unsustainable development. This is partly because of the political price they are afraid to pay, anticipating that many of the required urgent measures may be unpopular with the general public. At the same time the "public," to which politicians and bureaucrats often give little credit, is navigating between sensationalist

headlines and various contradicting scientific and technical reports while trying to formulate their own opinion. Educating the public (which by default consists of many "stakeholders" and many opinions) about various choices including tough ones is therefore the first but also the crucial step on the path of achieving sustainable development.

Groundwater is a perfect example of many misunderstandings, by both the public and the bureaucrats (politicians), of the meaning of sustainability. This may be because groundwater is mysterious by definition: as soon as we can see it, it is not groundwater anymore. It is troubling, however, when water professionals including those working for government agencies announce certain groundwater policies and qualify them as being "sustainable," even though there was no public debate or involvement of independent groundwater professionals.

The following example illustrates this point. It is a paraphrased paper of a "water specialist" working for a government agency in one of the Midwestern states in the United States. The article appeared in 2007, in the official journal of a nonprofit organization ostensibly working to educate the public about groundwater. The specialist was explaining how his state is fortunate to have precious groundwater resources that were used very successfully to better lives of its farmers through crop irrigation. The specialist also stated that in some parts of the state the aquifer water would last at least another 250 years and in some 25 years. And because it is readily available, it should be used to better the lives of farmers and whole communities even more by enabling additional irrigation of more corn fields. Those vast old and new corn fields would be used for production of ethanol in many plants that are being built and many more that would be built, all resulting in great benefits for the state rural communities, the state itself, the country, and indeed the whole world. More corn and more ethanol used for production of car fuel mean less burning of oil, less production of carbon, and it slows down global warming. What could be better? The specialist only forgot to speculate what would happen to those parts of his state where the aquifer runs dry after 25 years.

The multiple aspects of groundwater sustainability are addressed in the Alicante Declaration, which since its initiation has gained wide recognition among groundwater professionals worldwide. The declaration is the action agenda that resulted from the debates held in Alicante, Spain, on January 23rd to 27th, 2006, during the International Symposium on Groundwater Sustainability (ISGWAS). This call for action for responsible use, management, and governance of groundwater is reproduced below in its entirety.

Water is essential for life. Groundwater—that part of all water resources that lie underneath land surface—constitutes more than ninety five percent of the global, unfrozen freshwater reserves. Given its vast reserves and broad geographical distribution, its general good quality, and its resilience to seasonal fluctuations and contamination, groundwater holds the promise to ensure current and future world communities an affordable and safe water supply. Groundwater is predominantly a renewable resource which, when managed properly, ensures a long-term supply that can help meet the increasing demands and mitigate the impacts of anticipated climate change. Generally, groundwater development requires a smaller capital investment than surface water development and can be implemented in a shorter timeframe.

Groundwater has provided great benefits for many societies in recent decades through its direct use as a drinking water source, for irrigated agriculture and industrial development and, indirectly, through ecosystem and streamflow maintenance. The development of groundwater often provides an affordable and rapid way to alleviate poverty and ensure food security. Further, by understanding the complementary nature of ground and surface waters, thoroughly integrated water-resources management strategies can serve to foster their efficient use and enhance the longevity of supply.

Instances of poorly managed groundwater development and the inadvertent impact of inadequate land-use practices have produced adverse effects such as water-quality degradation, impairment of aquatic ecosystems, lowered groundwater levels and, consequently, land subsidence and the drying of wetlands. As it is less costly and more effective to protect groundwater resources from degradation than to restore them, improved water management will diminish such problems and save money. To make groundwater's promise a reality requires the responsible use, management, and governance of

groundwater. In particular, actions need to be taken by water users, who sustain their well-being through groundwater abstraction; decision makers, both elected and non-elected; civil society groups and associations; and scientists who must advocate for the use of sound science in support of better management. To this end, the undersigned recommend the following actions:

- *Develop more comprehensive water-management, land-use and energy-development strategies that fully recognize groundwater's important role in the hydrologic cycle*. This requires better characterization of groundwater basins, their interconnection with surface water and ecosystems, and a better understanding of the response of the entire hydrologic system to natural and human-induced stresses. More attention should be given to non-renewable and saline groundwater resources when such waters are the only resource available for use.
- *Develop comprehensive understanding of groundwater rights, regulations, policy and uses*. Such information, including social forces and incentives that drive present-day water management practices, will help in the formulation of policies and incentives to stimulate socially- and environmentally-sound groundwater management practices. This is particularly relevant in those situations where aquifers cross cultural, political or national boundaries.
- *Make the maintenance and restoration of hydrologic balance a long-term goal of regional water management strategies*. This requires that water managers identify options to: minimize net losses of water from the hydrologic system; encourage effective and efficient water use, and ensure the fair allocation of water for human use as well as ecological needs, taking into account long-term sustainability. Hydrological, ecological, economic and socioeconomic assessments should be an integral part of any water-management strategy.
- *Improve scientific, engineering and applied technological expertise in developing countries*. This requires encouraging science-based decision-making as well as "north-south" and "south-south" cooperation. Further, it is important that funds be allocated for programs that encourage the design and mass-dissemination of affordable and low-energy consuming water harnessing devices for household and irrigation.
- *Establish ongoing coordinated surface water and groundwater monitoring programs*. This requires that data collection become an integral part of water-management strategies so that such strategies can be adapted to address changing socio-economic, environmental, and climatic conditions. The corresponding data sets should be available to all the stakeholders in a transparent and easy way.
- *Develop local institutions to improve sustainable groundwater management*. This requires that higher-level authorities become receptive to the needs of local groups and encourage the development and support of strong institutional networks with water users and civic society.
- *Ensure that citizens recognize groundwater's essential role in their community and the importance of its responsible use*. This requires that science and applied technology serve to enhance education and outreach programs in order to broaden citizen understanding of the entire hydrologic system and its global importance to current and future generations.

One commonly held but inaccurate belief, when estimating groundwater availability and developing sustainable water supply strategies, is that groundwater use can be sustained if the amount of water removed is equal to recharge—often referred to as "safe yield." However, there is no volume of groundwater use that can be truly free of any adverse consequence, especially when time is considered. The "safe yield" concept is therefore a myth because any water that is used must come from somewhere. It falsely assumes that there will be no effects on other elements of the overall water budget. Bredehoeft (2002) provides illustrative discussions about the safe yield concept and the related "water budget myth." To examine the "safe yield myth" more carefully, an analogy is made comparing an aquifer and a reservoir behind a dam on a river (Figure 16.16). If withdrawals from a reservoir equal inflow, the river below the dam will be dry because there will be no outfall from the reservoir. The same principle can be applied to a groundwater reservoir (aquifer). If pumping (withdrawal) equals inflows (recharge), the outflows (subsurface flow or discharge to springs, streams, or wetlands) from the aquifer will decrease and may eventually reach zero, resulting in some adverse consequence at some point in time. The direct hydrologic effects

will be equal to the volume of water removed from the natural system, but those effects may require decades to centuries to be manifest. Because aquifer recharge and groundwater withdrawals can vary substantially over time, these changing rates can be critical information for developing groundwater management strategies (Anderson and Woosley, 2005).
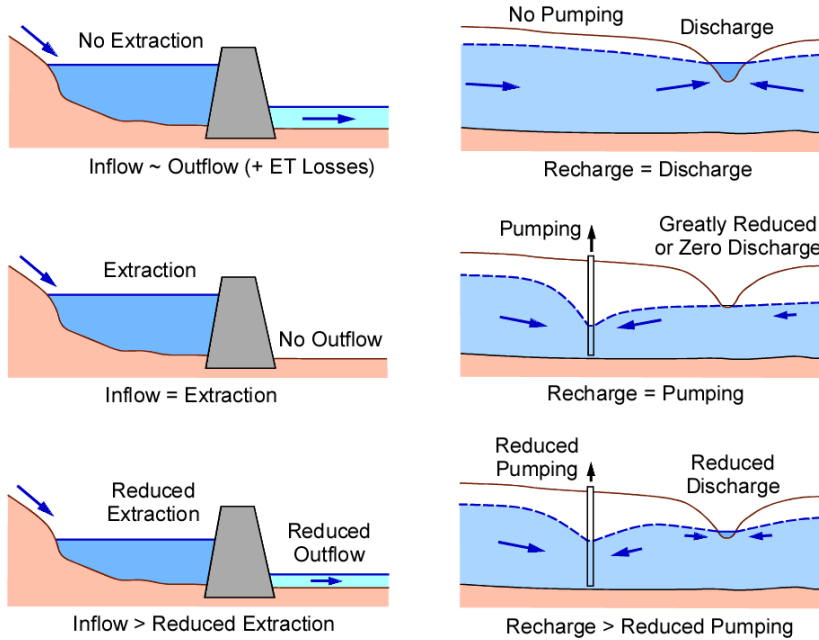

Figure 16.16 Comparison of water balance of a surface water reservoir (left) and an aquifer (right). Groundwater yield that is considered sustainable can be achieved only by accepting some consequences of groundwater withdrawal (pumping). Safe yield is referred by some as pumping equal to recharge, but as shown, can result in reduced or no discharge to surface stream or spring, and unacceptable consequences. Modified from Kresic, 2009. Copyright McGraw-Hill; permission is required for further use.
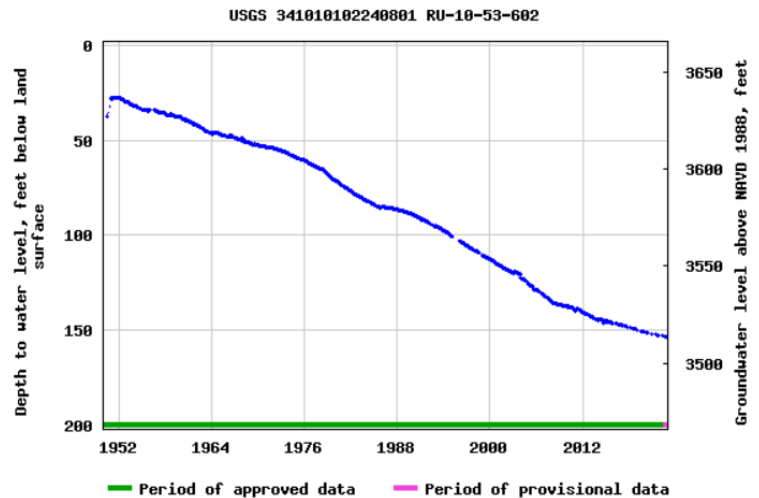

Figure 16.17 Examples of water storage depletion caused by withdrawal greater than recharge. *Left*: Depletion of surface water reservoir storage illustrated by the photograph of the July 2004 drought conditions of Lake Powell on the Colorado River, southern Utah (courtesy of USBR; http://www.usbr.gov/lc/region/g5000/photolab; in public domain). *Right*: Depletion of groundwater storage illustrated by the graph of water level measured in a USGS observation well for the period of record (last date shown is January 16, 2023). The well is in Lamb County, Texas and monitors the Ogallala Formation local aquifer. The real-time data is available at https://nwis.waterdata.usgs.gov/.

With an increased demand for water and pressures on groundwater resources, the decades-long debate among water professionals about what constitutes "safe" withdrawal of groundwater has now changed into a debate about

"sustainable use" of groundwater. The difference is not only semantic, and confusion has occasionally resulted. For example, there are attempts to distinguish between "safe yield" and "sustainable pumping" where the latter is defined as the pumping rate that can be sustained indefinitely without mining or dewatering the aquifer. Devlin and Sophocleous (2005), and Alley and Leake (2004) provide a detailed discussion of these and other related concepts.

What appears most difficult to understand is that the groundwater system is a dynamic one—any change in one portion of the system will ultimately affect its other parts as well. Even more important is the fact that most groundwater systems are dynamically connected with surface water. As groundwater moves from the recharge area toward the discharge area (e.g., a river), it constantly flows through the saturated zone, i.e., the groundwater storage (reservoir). If another discharge area (such as a well for water supply) is created, less water will flow toward the old discharge area (river). This fact seems to be paradoxically ignored by those who argue that groundwater withdrawals may actually increase aquifer recharge by inducing inflow from recharge boundaries (such as surface water bodies) and therefore result in "sustainable" pumping rates. Although such groundwater management strategy may be "safe" or "sustainable" for the intended use, another question is whether it has any consequences for the sustainable use of the surface water system, which is now losing water to rather than gaining it from the groundwater system.

Another argument for sustainable pumping is based on managing groundwater storage. This management strategy adjusts withdrawal (pumping) rates to take advantage of natural recharge cycles. For example, during periods of high demand, some water may be withdrawn from the storage by greatly increasing pumping rates and lowering the hydraulic heads. During periods of low demand and high natural recharge, this depleted storage would then be replenished. However, the same question of the sustainability of this approach remains. Any portion of the natural recharge that does not contribute to the natural (nonanthropogenic) discharge will have some consequences for the water users and water uses which rely on it. Depending on the volumes and rates of the denied groundwater discharge, the affected users may or may not be able to adapt to the new reality.

In most situations, groundwater extraction and management in general will need to keep a balance between the costs and benefits of management activities and interventions. It should consider the susceptibility to degradation of the hydrogeologic system involved and the legitimate interests of water users, including ecosystems and those dependent on downstream baseflow. Figure 16.20 illustrates a common evolution of groundwater resources development and the associated stages based on the impacts of the hydraulic stress (groundwater extraction) on the system.

The condition of excessive and unsustainable extraction (3A—Unstable Development) is included in Figure 16.18. For this case, the total abstraction rate (and usually the number of production wells) will eventually fall markedly as a result of near irreversible degradation of the aquifer system itself (Tuinhoff et al., 2002-2005a).

Groundwater management should have a clearly stated objective. This is true for any level of management, starting with a local water agency or water purveyor and ending at the national (federal) level. The management objective should include the establishment of threshold values for readily measured quantities such as groundwater levels, groundwater quality, land surface subsidence, and changes in streamflow and surface water quality where they impact or are impacted by groundwater pumping. When a threshold level is reached, the rules and regulations require that groundwater extraction be adjusted or stopped to prevent exceeding that threshold.
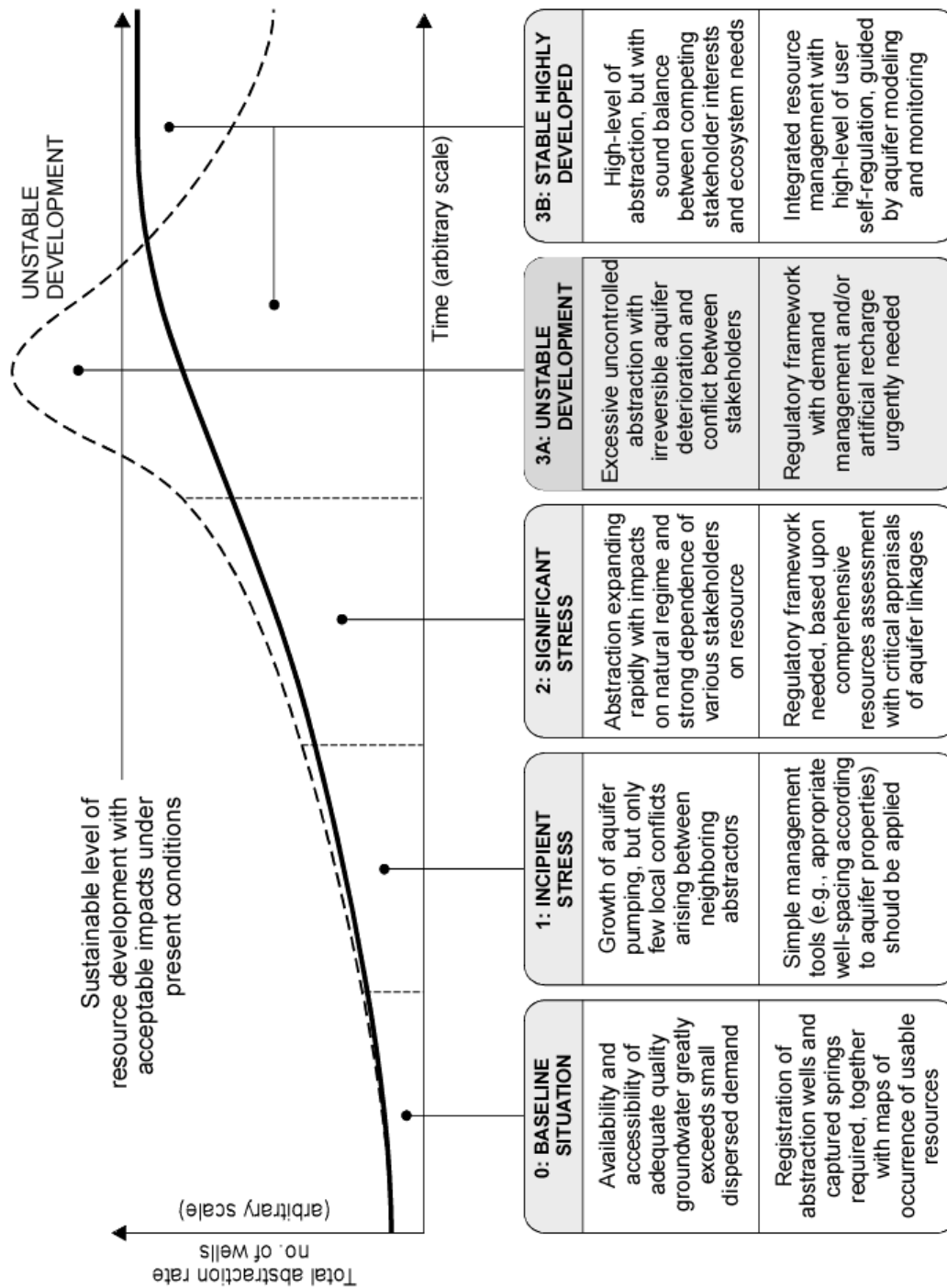
Figure 16.18 Stages of groundwater resource development in a major aquifer and their corresponding management needs. From Tuinhof et al., 2002-2005a

Lall, Josset, and Russo provide an illustrative discussion entitled "Groundwater Use, Monitoring, and Regulation: A Tale of Two States" in their 2020 paper *Snapshot of the World's Groundwater Challenges:*

During the 1987–1991 drought, reservoirs were depleted, groundwater pumping and farmer investment in water conservation increased, and California set up water banks and trading. During the 2015 drought, the governor of California mandated a 25% reduction in water use, except for agriculture, although it accounts for 80% of total water use. The lack of monitoring of agricultural well pumping meant the regulation would

not have been enforceable. Consequently, significant increases in groundwater depletion were reported. California introduced the Sustainable Groundwater Management Act that requires governments and water agencies to halt overdraft by the 2040s. Proposed reforms include data collection, modeling, and their Web access. Currently, groundwater use and quality data reporting and recording lag behind other US states. In 2016, fewer than 50% of the irrigation districts reported their water use as required. Kansas manages depletion in the High Plains aquifer by requiring measurement and reporting pump withdrawals. Kansas's Local Enhanced Management Area program introduced irrigator-driven regulatory proposals with governmental oversight in 2012. Between 2013 and 2017, water use was reduced by 31%, effectively stabilizing groundwater levels while maintaining farmers' profit. This showcases the effectiveness of combining data collection, stakeholder engagement, and regulation.

16.3.1 Non-Renewable Groundwater Resources

As discussed by Foster et al. (2002–2005a), groundwater resources are hardly ever strictly nonrenewable. However, in certain cases the period needed for replenishment (100s to 1000s of years) is very long in relation to the normal period of human activity in general and water resources planning in particular. For this reason, it is valid in such cases to talk of the utilization of nonrenewable groundwater or aquifer mining. Two general groups of groundwater systems fall into the category of nonrenewable:

1. Unconfined aquifers in areas where contemporary recharge is very infrequent and of small volume and the resource is essentially limited to static groundwater storage reserves (an example is the Ogallala Aquifer in Texas).
2. Confined portions of large aquifer systems, where groundwater development intercepts or induces little active recharge and the hydraulic head falls continuously with groundwater extraction (examples are the Nubian Sandstone Aquifer System of Africa, and the Great Artesian Basin in Australia).

Both groups involve the extraction of groundwater that originated as recharge in the distant past, including during more humid climatic regimes. The volumes of such groundwater stored in some aquifers are enormous. For example, total recoverable volume of freshwater in the Nubian Sandstone Aquifer System of Africa (see Figure 7.3 in Lecture 7) is estimated at about 15,000 km^3 (Bakhbakhi, 2006). For comparison, combined volume of water stored in the Great Lakes of the North America is 22,684 km^3. The term groundwater sustainability in the case of nonrenewable systems has an entirely social rather than physical (engineering, scientific) context. It implies that full consideration must be given not only to the immediate benefits, but also to the negative socioeconomic impacts of development and to the "what comes after" question—and thus to time horizons longer than 100 years (Foster et al., 2002–2005a). Figures 16.19 and 16.20 illustrate these points.

The expected benefits and predicted impacts of groundwater mining over a specified time-frame should be specified. Appropriate exit strategies need to be identified, developed, and implemented by the time that the groundwater system is seriously depleted. This scenario must include balanced socioeconomic choices on the use of stored groundwater reserves and on the transition to a less water-dependent economy. A key consideration in defining the exit strategy will be identification of the replacement water resource, such as desalination of seawater or brackish groundwater, and treated wastewater, including aquifer recharge with these replacements (Foster et al., 2002–2005a).
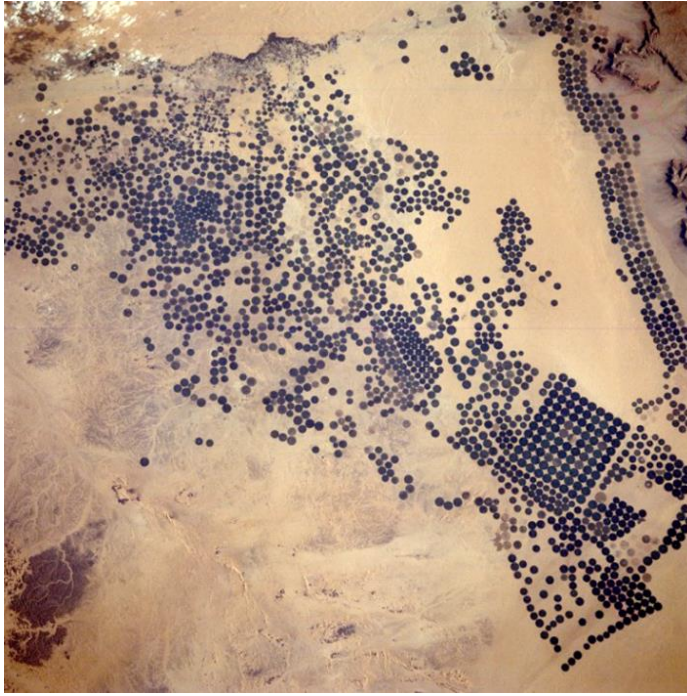
Figure 16.19 This photograph taken in 1990 by a Space Shuttle mission shows a location southwest of Riyadh in the Jabal Tuwayq area of Saudi Arabia. The following excerpts are from the NASA' description of the photograph: "The circular features that dot the desert landscape in this near-vertical photograph are created by pivoting sprinklers, a method of irrigation whereby water from a central well is spread by a sprinkler pivoting around that well. The diameter of these circular fields can vary from several hundred feet (tens of meters) to over a mile (2 kilometers)....The water is being extracted from subsurface reserves that infiltrated deep aquifers during geological periods when the climate was much wetter than at present.... complexes such as the one imaged extract deep fossil water reserves to achieve food crop production self-sufficiency in this desert environment. The significance of the Saudi expanded irrigated agriculture is that the depletion of this finite water resource is a short-term solution to a long-term need that will still exist when the water has been extracted."

(https://eol.jsc.nasa.gov/SearchPhotos/photo.pl?mission=STS032&roll=96&frame=32; in public domain.)

Figure 16.20 For the construction of Great Man-Made River project in Libya, prestressed concrete cylinder pipes 4 meters in diameter and 7.5 meters long, weighing up to 80 tons, were brought to the excavation sites using a fleet of some 128 specially designed transporters. Each pipe was buried in a trench approximately seven meters deep, excavation of which required the removal of some 100,000 cubic meters of material each working day. Excavation was carried out by large hydraulic excavators fitted with 7.6 m^3 buckets. *Left* photo courtesy of Jaap Berk, The Netherlands; in public domain. *Right* photo courtesy of https://alk3r.wordpress.com/2017/07/04/the-great-man-made-river-of-libya/.

The largest-ever groundwater project, anywhere in the world, is the so-called "The Great Man-Made River" in Libya. Generally, five main phases of the project are planned - three of them have been fully completed, the fourth is under construction, and the fifth should be completed by 2025. The total estimated cost is 27 billion U.S. dollars. With the completion of Phase III in 2009, GMR currently delivers 3.8 million m^3 of groundwater daily, transported via buried large diameter reinforced concrete pipes (Figure 16.20) for 4,071 km (2,530 mi) to the coastal cities and irrigation fields in the north. The system has 1,116 extraction wells (excluding inactive wells) up to 500 meters deep, and several reservoirs with the total capacity of 54.9 million m^3. The total capacity of the system with all phases built would be some 6.5 million cubic meters (230 million cubic feet) of water per day. In addition to self-sufficiency in food production and the safety of water supply for the industry and population, the main incentive

for initiating the project in 1983 was the cost of water to be delivered by it: 35 cents versus $3.75 per cubic meter of desalinized water (http://www.boinc.sk/clanky/libyas-great-man-made-river; Great Man-Made River Authority at https://gmra.com.ly/index.php/en).

16.4 Production Wells

Probably the first thought that comes to mind for many people when discussing groundwater development and use, in general, is a water well. For non-hydrogeologists and those who are not in related water supply professions, a well usually means a nondescript hole in the ground that somehow produces water; this may include an image of a fenced well house or a picturesque image of a dug well with a rotating wooden wheel and a bucket in the countryside. In any case, a relatively small number of people fully understand the complexity, importance, and cost of a properly constructed well used for public water supply. The same is true in many developed countries where modern drilling technologies have been routinely used for a long time to construct wells for both the public and the domestic supply; the end users usually leave this "well business" to well drillers and do not care to learn much about their own hole in the ground. However, hydrogeologists and groundwater professionals think of wells in many different contexts, and some of them spend lifetimes trying to better understand and design them (Kresic, 2009).

Siting and designing wells for public supply or large irrigation projects is very complex and should result from thorough considerations of multiple design elements. In most cases, selecting the final well location(s) and well design is not a straightforward task but rather a compromise made after considering various factors such as

- Capital cost.
- Vicinity to future users.
- Existing groundwater users and groundwater permits.
- Hydrogeologic characteristics and depth to different water-bearing zones (aquifers).
- Required flow rate of the water supply system and expected yield of individual wells.
- Well drawdown and radius of well (wellfield) influence.
- Interference between wells in the wellfield.
- Water treatment requirements.
- Energy cost for pumping and water treatment, and general operations and maintenance (O&M) costs.
- Aquifer vulnerability and risks associated with the existing or potential sources of contamination.
- Interactions with other parts of the groundwater system, and with surface water.
- Options for artificial aquifer recharge, including storage and recovery.
- Societal (political) requirements.
- Existence or possibility of an open water market.

The above factors are not all inclusive and are not listed in order of importance; sometimes just one or two are all that is needed for proceeding with the final design. However, as the development and use of groundwater resources is becoming increasingly regulated in the United States and in many other countries, it is likely that most of these factors will have to be addressed as part of a well-permitting process. Even in cases where permitting requirements are absent, it is prudent to consider most of the listed factors since they ultimately define the long-term sustainability of any new well or wellfield (Kresic, 2009).

Water wells have been used for centuries for domestic and public water supply throughout the world. Their depth, diameter, and construction methods vary widely and there is no such thing as a "one size fits all" approach

to well design. Answers to just about any question regarding well design can be found in the classic 1000-page book Groundwater and Wells by Driscoll (1986, published by Johnson Filtration Systems; third edition is now available from Johnson Screens, a brand of Aqseptence Group). Another exhaustive reference books on well design is Water Well Technology by Campbell and Lehr (1973) and Handbook of Ground Water Development by Roscoe Moss Company (1990). Various public-domain publications by U.S. government agencies provide useful information on the design and installation of water supply and monitoring wells (e.g., USEPA, 1975, 1991; U.S. Bureau of Reclamation (USBR), 1977; Aller et al., 1989, 1991; Lapham et al., 1997). Detail recommendations including regulations for designing production wells ("water wells") are provided by the California Department of Water Resources (June 1991; *California Well Standards*, Bulletin 74-90). This publication focuses on well protection such as selection of well location with respect to source of contamination and contaminants, and methods of sealing well casing to prevent contamination of shallow wells and cross-contamination between different water bearing units (aquifers).

Well design, installation, and well construction materials should conform to applicable standards. In the United States, the most widely used water well standard is the ANSI/AWWA A100 standard, but the authority to regulate products for use in, or contact with, drinking water rests with individual states, which may have their own standard requirements. Local agencies may choose to impose requirements more stringent than those required by the state (American Water Works Association, AWWA, 1998).

The design elements of vertical water wells include the following: (1) drilling method, (2) depth, (3) drilling and well casing diameter, (4) well screen, (5) filter (gravel, sand) pack, (6) well development, (7) well testing, and (8) selection and installation of the permanent pump. Whenever possible, a well design should be based on information obtained by a pilot boring drilled prior to the main well bore. Geophysical logging and coring (sample collection) of the pilot boring provide the following information: depth to and thickness of the water-bearing intervals in the aquifer, grain size, and permeability of the water bearing intervals, and physical and chemical characteristics of the porous media and groundwater. Unknown geology and hydrogeology of the formation(s) to be drilled may result in the selection of an improper drilling technology, sometimes leading to a complete abandonment of the drilling location due to various unforeseen difficulties such as flowing sands, collapse of boring walls, or loss of drilling equipment in karst cavities. If pilot boring is not feasible, some design parameters must be estimated, on the conservative side, and may significantly reduce well efficiency (e.g., selecting smaller screen openings or finer filter ack grain size to prevent entrance of fines).

Deep public supply wells, or thick stratification of permeable and low-permeable porous media, may require drilling with several diameters, and the installation of several casings of progressively smaller diameter, called telescoping casing. This is done to provide stable and plumb boreholes in deep wells and to bridge difficult or undesirable intervals (e.g., flowing sands, highly fractured and unstable walls prone to caving, and thick sequences of swelling clay). The cost of drilling increases progressively with the drilling diameter, and it is important to balance this cost with other design requirements, some of which may be desirable but not always necessary. For perspective, a public supply, high capacity well that is several thousand feet deep (say, 1000 m) may easily cost well over US $1 million. Such wells are drilled with powerful rigs, may use special drill bits, and have large diameter casings as shown in Figures 16.21 through 16.23.

Figure 16.21 *Left*: Combined roller cone bit in two stages for drilling deep, large-diameter production wells. Photo courtesy of Adrian Ezeagy. *Right*: Drilling rigs in operation in northern Iraq (Kurdistan Province). The combined rotary and down-the-hole hammer (DTH) techniques are applied to drill formations of unconsolidated topsoil and clay, and underlying limestone. Groundwater depth in this arid region is regularly below 50 meters, but a karst aquifer could be highly productive resulting at certain points with well yields exceeding 50 L/s. Courtesy of Zoran Stevanović.

Figure 16.22 This powerful rotary drill rig encountered an artesian water-bearing horizon at depth exceeding 400m (1,300 ft), Peru. Photo Courtesy of Dave Evans.

Figure 16.23 Large-diameter casing being installed in a deep production well in Arizona. Photo courtesy of Adrian Ezeagy.

Table 16.1 Common types of wells. Modified from Joint Departments of the Army and Air Force, 1987; in public domain.

Type	Diameter	Maximum Depth (ft)	Lining or Casing	Suitability	Disadvanatges	Method of Construction
Dug	3 to 20 feet	40	Wood, masonry, concrete, metal	Water near surface. May be constructed with hand tools	Large number of manhours required for construction. Hazard to diggers.	Excavation from within well
Driven	2 to 4 inches	50	Pipe	Simple using hand tools	Formation must be soft and boulder free.	Hammering a pipe into the ground
Jetted	3 or 4 inches	200	Pipe	Small diameter wells on sand	Only possible in loose sand formations.	High pressure water pumped through drill pipe
Bored	up to 36 inches	50	Pipe	Useful in clay formations	Difficult on loose sand and cobbles.	Rotating earth auger bucket
Collector	15 feet	130	Reinforced concrete caison	Used adjacent to surface recharge source such as river, lake or ocean	Limited number of Installation Contractors.	Caisson is sunk into aquifer. Preformed radial pipes (screens) are jacked horozontaly through ports near bottom
Drilled	Up to 60 inches	Up to 4000 depending on method	Pipe	Suitable for variety of formations and depths	Requires experienced Contractor and specialized tools (drill rigs).	a. Hydraulic rotary b. Cable tool percussion c. Reverse circulation rotary d. Dual rotary e. Hydraulic rotary-percussion f. Air rotary g. Rotosonic

Special attention should be given to the selection of drilling methods for wells that penetrate zones containing poor-quality water or contaminants that could move through the borehole during drilling and well construction materials and significantly degrade groundwater quality in other units before sealing material can be installed. Dual rotary and cable tool methods are good at preventing cross-contamination: casing is advanced as the drilling bit advances which bridges and isolates difficult or contaminated intervals. In dual rotary drilling, the casing can also be advanced ahead of the drill bit, minimizing loss of circulation and eliminating borehole stability problems associated with artesian conditions or karst formations. The Rotosonic method has the advantage of advancing the casing as the drilling progresses, but there is a limitation which caps the maximum well diameter at 12 inches (the usual maximum depths are less than 500-600 feet). Common well types, their drilling methods, and several key characteristics are listed in table 16.1.

Well Diameter and Casing

The diameter of a well has a significant effect on the well's construction cost. The diameter need not be uniform from top to bottom. Construction may be initiated with a large-diameter casing, which is usually called conductor casing, and drilling conditions may make it desirable to reduce the casing size and the boring diameter at a certain depth. In any case, the final well diameter must be large enough to accommodate the pump and the diameter of the screen (intake portion of the well where the water from the formation enters thew well). The factors that control diameter are (1) yield of the well; (2) riser pipe and screen diameter; (3) size of the pump; and (4) construction

method. The pump size, which is related to yield, usually dominates. The riser pipe may have the same diameter as the screen, or it may be larger in which case the screen and the casing are connected with a diameter reducer. In either case, the riser pipe diameter must satisfy two requirements: (1) the riser pipe (casing) diameter must be large enough to accommodate the pump of required capacity and to provide for easy maintenance access, and (2) the diameter of the casing must be sufficient to assure that the uphole velocity is less than 5 ft/s (1.5 m/s) to avoid an excessive pipe loss (Driscoll, 1986). Approximate well diameters for various yields are shown in Table 16.2.

The well casing diameter (which is different than the boring diameter) affects well yield but not to a major degree. Doubling the diameter of the well will produce only about 10-15 percent more water. Table 16.3 gives the theoretical change in yield that results from changing one well diameter to a new well diameter. For example, if a 12-inch well is enlarged to a 36-inch well, the yield will be increased by 19 percent. This relationship is valid for unconfined aquifers. For confined aquifers, the yield increase resulting from diameter doubling is generally less than 10 percent (Joint Departments of the Army and Air Force, 1987).

Table 16.2 Recommended well diameters for various pumping rates. Data from Driscoll, 1986.

Anticipated Well Yield		Optimum Casing Size		Smallest Casing Size	
gpm	L/s	in	mm	in	mm
less than 100	less than 5	6 ID	152 ID	5 ID	127 ID
75 to 175	5 to 10	8 ID	203 ID	6 ID	152 ID
150 to 350	10 to 20	10 ID	254 ID	8 ID	203 ID
300 to 700	20 to 45	12 ID	305 ID	10 ID	254 ID
500 to 1,000	30 to 60	14 OD	356 OD	12 ID	305 ID
800 to 1,800	50 to 110	16 OD	406 OD	14 OD	356 OD
1,200 to 3,000	75 to 190	20 OD	508 OD	16 OD	406 OD
2,000 to 3,800	125 to 240	24 OD	610 OD	20 OD	508 OD
3,000 to 6,000	190 to 380	30 OD	762 OD	24 OD	610 OD

Table 16.3 Change in yield percentage for variation of well diameter.
From Joint Departments of the Army and Air Force, 1987; in public domain.

Diameter (in.)	New Diamater (in.)						
	6	12	18	24	30	36	48
6	100	110	117	122	127	131	137
12	90	100	106	111	116	119	125
18	84	93	100	104	108	112	117
24	79	88	95	100	104	107	112
30	76	85	91	96	100	103	108
36	73	82	88	92	96	100	105
48	69	77	82	87	91	94	100

All permanent well casings must be continuous and watertight from top to bottom, except for the screen section, and must be grouted (i.e., they cannot be left loose). Grouting prevents possible short-circuiting of groundwater along the boring walls and between various aquifer intervals or aquifers, and contamination from the land surface.

In the United States, most states require that the upper casing be grouted a minimum depth from the land surface, usually 50 ft.

Casing material must be compatible with the groundwater chemistry to prevent corrosion or other failures. The selection of materials for well casing is critical in locations where there is likelihood of its exposure to significant concentrations of contaminants comprising low-molecular-weight petroleum products or organic solvents and their vapors. Casing materials such as polyethylene, polybutylene, polyvinyl chloride (PVC), and elastomers, such as used in jointing gaskets and packing glands, may be subject to permeation by lower-molecular-weight organic solvents or petroleum products (AWWA, 1998). If the well casing extends through such a contaminated area or an area subject to contamination, the well casing material should be selected accordingly to avoid health risks. Casing has to be strong and thick enough to provide for structural stability during its installation, well development, and use. This is especially important in deep wells where high formation pressures may cause casing to collapse if undersized (under designed). In general, selecting an inferior casing material will initially reduce the capital cost but may result in irreparable damage to the casing and premature loss of a well. ANSI/AWWA A100 standard provides specifications for casing materials and diameters, and calculations of minimum acceptable casing strengths.

Well Screen

The size of well-screen openings depends on the grain size distribution of the natural porous media. The size of screen openings is also dependent on the required filter pack characteristics (grain size and uniformity). The percentage of openings, the screen diameter, and the screen length should all be selected simultaneously to satisfy the following criteria: (1) maximize well yield, (2) maximize well efficiency by minimizing hydraulic loss at the screen, and (3) provide for structural strength of the screen, i.e., prevent its collapse due to formation pressure. The following equation can be used to determine the optimum relationship between different screen parameters (AWWA, 1998):

$$L = \frac{Q}{A_e V_e (7.48)} \qquad (16.1)$$

where L is the length of screen (ft); Q is the well yield (gallons per minute); A_e is the effective aperture area per foot of screen, in square feet. The effective aperture area should be taken as one-half of the total aperture area (ft^2/ft); V_e is the designed entrance velocity (ft/min).

As a rule of thumb, the screen entrance velocity should be equal to or less than 0.1 ft/s (0.03 m/s), since it has been shown that higher velocities cause turbulent well loss, may accelerate various screen problems such as corrosion and incrustation, and can transport sand particles (Walton, 1962; Driscoll, 1986). A lower entrance velocity is recommended for water of significant incrusting potential (USEPA, 1975). ANSI/AWWA standard for the upper limit of entrance velocity is 1.5 ft/s (0.46 m/s); the users of the standard are cautioned to thoroughly examine the issue of well-screen entrance velocity and site-specific (aquifer) conditions before the final selection. In naturally developed wells, screen apertures should be sized according to the following criteria (AWWA, 1998)

1. Where the uniformity coefficient of the formation is greater than 6, the screen aperture openings should retain from 30 to 40 percent of the aquifer sample.
2. Where the uniformity coefficient of the formation is less than 6, the screen aperture openings should retain from 40 to 50 percent of the aquifer sample.

3. If the water in the formation is corrosive or the accuracy of the aquifer sample is in doubt, a size selected should retain 10 percent more than in items 1 and 2.

4. Where fine sand overlies coarse sand, use the fine-sand aperture size for top 2 ft (0.61 m) of the underlying coarse sand. The coarse-sand aperture size should not be larger than twice the fine-sand aperture size.

For wells with filter pack, the screen-aperture openings should be sized to retain between 85 and 100 percent of filter pack material. There are many different types of screens and screen opening configurations offered worldwide by a variety of vendors (Figure 16.24). Some types may have advantages in certain conditions, and the final selection should be made after careful considerations of site-specific design requirements. Continuous slot screens provide maximum open area and access to the formation so that well development procedures are enhanced and through-screen head loss is reduced.

Figure 16.24 Common types of screens for high-capacity production wells. *Left*: Slotted casing, photo courtesy of Adrian Ezeagy. *Middle*: Shutter type screen, photo courtesy of Adrian Ezeagy. *Right*: Continuous slot wire-wound stainless-steel screen (often referred to as Johnson screen) welded to the riser pipe and being lowered into a newly drilled well.

Production well screen should be as long as possible and placed within a thick aquifer interval with the highest hydraulic conductivity. However, when the aquifer is stratified with less permeable interbeds, it is preferable to use multiple screen intervals separated by solid casing, including screens with varying slot size selected to match porous media in different water-bearing (production) intervals. This will prevent the continuous entrance of fines from the undesired intervals. It is recommended to select screen intervals such that the water level in the well during pumping always stays above the top of the screen. At the same time, the pump intake should not be placed within the screen interval but within the solid casing (also called a riser pipe or pump-housing pipe) above or below the screen. This prevents hydraulic stresses on the screen when the pump is turned on and off and problems associated with screen dewatering, which can accelerate screen corrosion and scaling (incrustation).

Filter Pack

Filter pack (also referred to as gravel pack or sand pack) is now routinely placed around well screens in wells completed in both uniform and heterogeneous (nonuniform) formations for the following reasons: (1) to stabilize the formation; (2) to minimize flow of fines and sand through the screen; (3) to enable larger screen openings, which can increase well efficiency and minimize rate of screen incrustation; and (4) to establish transitional velocity and pressure fields between the formation and the well screen, which also minimizes the incrustation rate. The placement of a filter pack makes the zone around the well screen more permeable and increases the effective

hydraulic diameter of the well. The filter pack allows the removal of finer formation material during well development, and it retains most of the aquifer's fine material during the well exploitation.

Well filter pack material should consist of nonreactive, smooth, rounded, spherical, granular material of highly uniform size and known composition which should not degrade after placement. Quartz sand usually satisfies these conditions. Filter pack material should be placed in the well boring by use of a tremie pipe (small-diameter pipe) or equivalent. Simply pouring the filter pack from the top of the annulus may and usually does result in creation of bridges and voids in the pack and should be avoided. The filter pack material is funneled through the tremie around the screen to prevent bridging. This method also reduces the tendency for selective sorting of the filter pack by grain size as it falls through the water down the annulus. The annulus is backfilled slowly from the bottom up to a distance above the top that is equivalent to about 20 percent of the screen length or 2 ft above the top of the screen, whichever is greater (ASTM, 1992). Sometimes, a secondary, finer grain-size filter pack (usually 2 feet or so in length) is installed above the main pack to prevent seepage of the casing sealant down to the screened interval (Lapham et al., 1997).

An alternative to completing the well with an externally introduced filter pack is to allow the collapse of the native materials around the well screen and casing. This method is applicable only if the native unconsolidated materials in the screened interval will collapse around the well to form a filter pack and result in a well that yields sediment-free water in samples collected after the well is developed. The installation of a filter pack can be difficult or impossible when installing a well in karst or highly fractured consolidated materials because of the size and configuration of void spaces at the borehole (ASTM, 1992, p. 127). A filter pack might not be necessary or desirable to use under these conditions. In some cases, the installation of a filter pack could plug water-bearing fractures.

Well screen and filter pack should never be installed within aquifer portions where clays are intimately associated with the productive fine-grained sand. It is not possible to design a sufficiently fine-grained filter pack that will prevent the intrusion of silts and clays (fines) in such cases. Consequently, every time the well is agitated by the pump, the fines are mobilized and become part or all of the turbidity that compromises the water quality. There currently is no design or development procedures that can fully overcome this problem.

It is generally considered that the minimum thickness of filter pack material that can be constructed effectively is 2 inches. Two inches is a desirable thickness in situations where there is adequate control to ensure good filter pack distribution. If there are doubts about the distribution, then the filter pack must be thickened to assure that there is adequate filtration and borehole support (U.S. EPA, 2018).

The following procedure should be used to determine the grain size of the filter pack (U.S. EPA (2018): The data from the sieve analysis are plotted on a grain-size distribution graph, and a grain-size distribution curve is generated. From this grain-size distribution curve, the uniformity coefficient (Cu) of the aquifer material is determined. The Cu is the ratio of the 60 percent finer material (d60) to the 10 percent finer material (d10):

$$Cu = d60 / d10 \qquad (16.1)$$

The Cu ratio is a way of grading or rating the uniformity of grain size. For example, a Cu of unity means that the individual grain sizes of the material are nearly all the same, while a Cu with a large number indicates a large range of particle sizes. As a general rule, a Cu of 2.5 or less should be used in designing the filter pack and well screen. Before designing the filter pack and well screen, the following factors should be considered:

1. The well screen slot openings should retain 90 percent of the filter pack material.

2. The filter pack material should be of the size that minimizes head losses through the pack and prevents excessive sediment (sand, silt, clay) movement into the well.
3. A filter material of varying grain sizes is not acceptable because the smaller particles fill the spaces between the larger particles thereby reducing the void spaces and increasing resistance to flow. Therefore, filter material of the same grain size and well-rounded is preferred (U.S. EPA, 2018):

The filter pack design is based on the gradation of the finest aquifer materials being analyzed. Steps to design a filter pack in aquifers are:
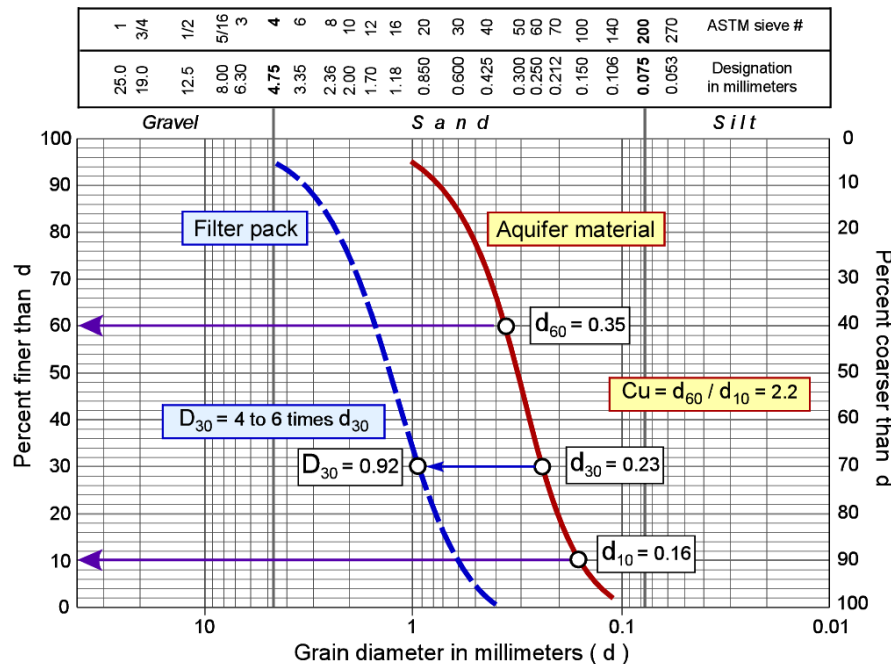

Figure 16.25 Example of a formation grain size distribution curve used to design well filter pack.

1. Construct a grain-size distribution curve, on a grain-size distribution graph, from the sieve analysis of the aquifer materials (Figure 16.25). The filter pack design (as stated above) is based on the gradation of the finest aquifer materials.
2. Multiply the d30 size from the grain-size distribution graph by a factor of four to nine (Pack-Aquifer ratio). A factor of four is used if the formation is fine-grained and uniform (Cu is less than 3), six if it is coarse-grained and non-uniform, and up to nine if it is highly non-uniform and contains silt. Head losses through filter packs increase as the Pack-Aquifer (P-A) ratios decrease. In order to design a fairly stable filter pack with a minimum head loss, the d30 size should be multiplied by a factor of four.
3. Plot the point from step 2 on the d30 abscissa of a grain-size distribution graph and draw a smooth curve with a uniformity coefficient of approximately 2.5.
4. A curve for the permissible limits of the filter pack is drawn plus or minus 8 per cent of the desired curve with the Cu of 2.5.
5. Select the slot openings for the well screen that will retain 90 per cent or more of the filter pack material.

Uniform gravel packs are generally preferred because well screens can be manufactured with varying sizes of openings to match the formation materials, and there is less possibility for separation during filter pack placement. Figure 16.26 illustrates the crucial role filter pack and well screen play in design and successful operation of a production well.
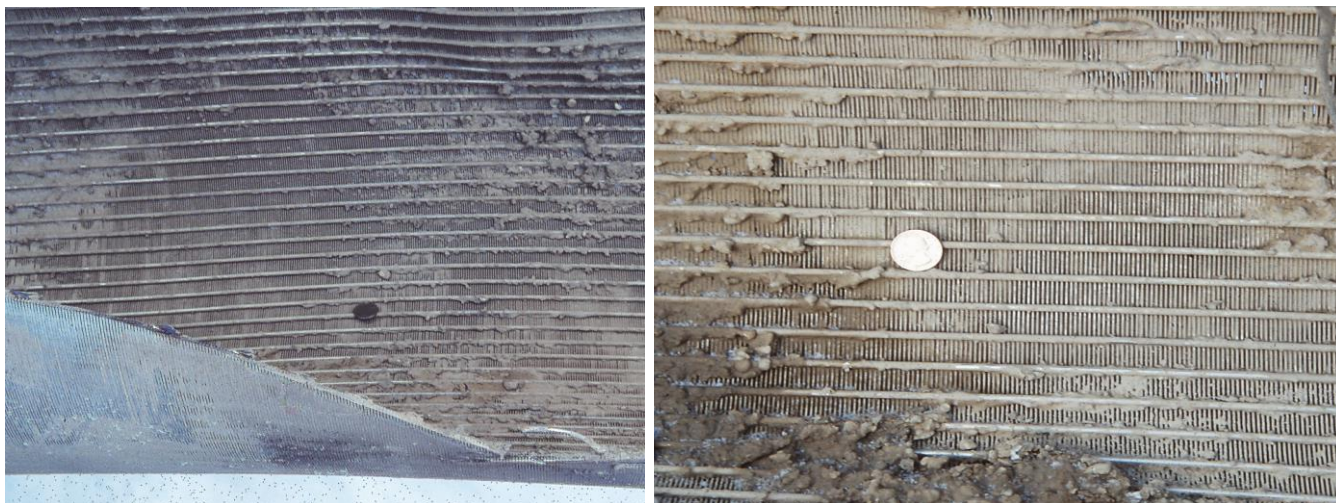
491

Figure 16.26 This screen was extracted from a failed production well located next to a large river in upstate New York. Because of an improper filter pack (too coarse) and screen design (openings too small), the screen became quickly completely clogged with fine silt that was interspersed with coarse glacio-fluvial sediments. The well was subsequently over-drilled and equipped with a proper screen and filter pack to prevent this from happening again. *Left*: Section of the screen cut to examine the interior. *Right*: Blowup of the clogged screen with a coin (US quarter) for scale.

Well Development

Proper well development will improve almost any well regardless of its type and size, whereas without development an otherwise excellent well may never be satisfactory. As discussed by USEPA (1975) and Driscoll (1986), in any well drilling technology the permeability around the borehole is reduced. Compaction, clay smearing, and driving fines into the wall of the borehole occur in the cable tool drilling method. Drilling fluid invasion into the aquifer and formation of a mud cake on the borehole walls are caused by direct rotary method. Silty and dirty water often clog the aquifer in the reverse rotary drilling method. In consolidated formations, compaction may occur in some poorly cemented rocks, where cuttings, fines, and mud are forced into fractures, bedding planes, and other openings, and a mud cake forms on the wall of the borehole.

Proper well development breaks down the compacted borehole wall, liquefies jelled mud, and draws it and other fines that have penetrated the formation (aquifer) into the well, from which they are removed by bailing or pumping. Well development also removes smaller grains initially present in the formation and creates a more permeable and stable zone adjacent to the well screen. Development of new wells is based on the mechanical action of water or air and should involve backwashing, i.e., movement of water in both directions through the well-screen openings. Chemicals should be used in well development only exceptionally, in small quantities, and with prior approval of both the well owner and the regulatory agency where applicable.

There are various methods of well development, and their selection depends primarily on the applied drilling technology and the formation characteristics. However, availability of the equipment and driller's preference in many cases play unjustifiably more important roles. It is often impossible to anticipate how a well will respond to certain types of development and how long it will take to achieve adequate development. Since a lump-sum basis for well development may result in unsatisfactory work, it is better to provide for development on a unit price per hour basis and continue until the following conditions have been met (AWWA, 1998):

1. Sand content should average not more than 5 mg/L for a complete pumping cycle of 2-hour duration when pumping at the design discharge capacity.

2. No less than 10 measurements should be taken at equal intervals to permit plotting of sand content as a function of time and production rate and to determine the average sand content for each cycle.

3. There should be no significant increase in specific capacity during at least 24 hours of development.

General methods of production well development are the same as for monitoring wells (see Lecture 14, Section 14.6.2). Photographs in Figures 16.28 and 16.29 illustrate some of the methods.

Figure 16.27 Well development methods. *Left*: Compressed air, photo courtesy of Dave Evans. *Right*: Wire brush, photo courtesy of Mark Bauer.

Figure 16.28 Well development methods. *Left*: Airlift, photo courtesy of Dr. Gerald Seaburn. *Right*: Bailer, photo courtesy of Mark Bauer.

Well Pump

The well pump raises water from the well and delivers it to the desirable height (elevation) such as a storage tank which can be under pressure ("pressure tank") to provide for uninterrupted further delivery to end users. The pump refers to both the pump itself and an electric motor, which together make up the pumping unit. There are many types and sizes of well pumps for water supply systems. Some are designed to transfer water from the well to the storage system as mentioned. Others also force water through the rest of the system. The design capacity of

the pump should exceed the system requirements. However, the capacity of the pump should not exceed the capacity of the well. If the peak system demand exceeds the maximum rate of well yield, the pump must be sized within the well capacity and the peak demand reached through added storage. Usually a large-size pressure tank can perform this function. Pump manufacturers publish charts giving the pump discharge capacity for their pumps at various operating pressures. The total dynamic head (TDH) of the pump must be calculated from the physical arrangement of the system and is represented by the following equation:

$$TDH = H_S + H_D + H_F + V^2/2g \qquad (16.1)$$

where H_S is suction lift or vertical distance from the waterline at drawdown under full capacity, to the pump centerline; H_D is discharge head or vertical distance from the pump centerline to the pressure level of the discharge pipe system; H_F is friction head or loss of head on pipe lines and fittings; $V^2/2g$ is velocity head or head necessary to maintain flow.
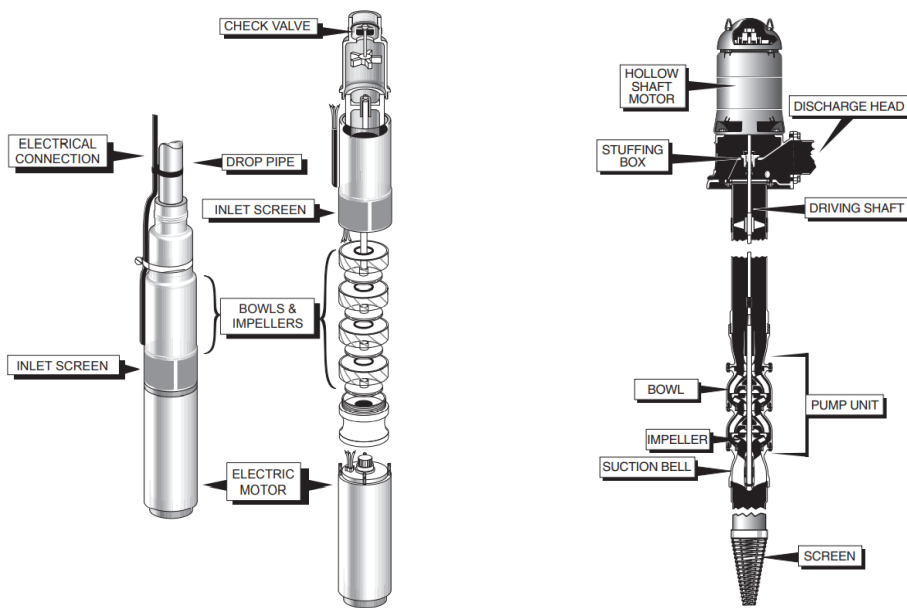

Figure 16.30 Two common types of vertical pumps for production wells. *Left*: Submersible turbine. Both the motor and the pump intake/hydraulic unit are submerged below the water level in the well. *Right*: Lineshaft turbine. The pump intake and hydraulic components are submerged, whereas the motor is located above ground, with easy access. From ATTAC, 2014.

Figure 16.31 Submersible well pumps come in many different sizes and capacity, from gallons per minute to tens of gallons per minute (shown on the photos), and as powerful as hundreds of gallons per minute or more, with the lift of hundreds of feet or more.

Well Completion

Well completion includes disinfection of the entire casing and the screen, installation of the permanent well pump, and construction of the well housing (wellhead) with all its sanitary requirements. Figure 16.30-*Left* shows the main design elements of a well completed in a shallow, unconfined aquifer. Figure 16.30-*Right* shows an example of well completion in deeper and in fractured bedrock aquifer where the productive interval is stable, open borehole, without a screen.

Probably the only design element of the entire well that cannot be guaranteed by any well driller, hydrogeologist, or engineer is the well yield and its long-term sustainability. It is not uncommon that, for various reasons, a well that costs several hundred thousand dollars to complete disappoints all stakeholders by producing less than its designed capacity. However, many such surprises can be avoided by following well-established hydrogeologic principles of aquifer evaluation and testing, and, of course, well design principles as explained.
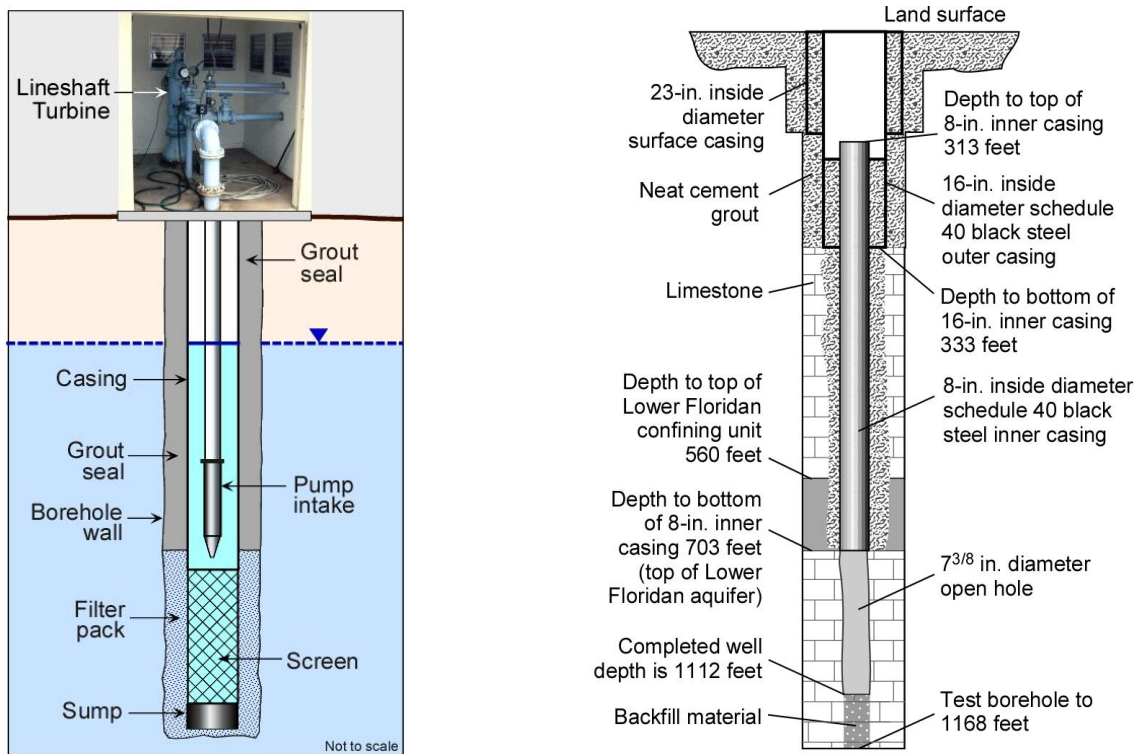

Figure 16.30-*Left* Schematic of a typical vertical well completed in unconfined aquifer. *Right*: Well-construction diagram for well HAAF 11 (36Q392) completed in the Lower Floridan aquifer, Hunter Army Airfield, Chatham County, Georgia. Modified from Clarke et al., 2010; USGS, in public domain.

16.5 Spring Development

As discussed earlier, springs were a preferred source of water supply for millennia. However, they continue to be under an ever-increasing pressure due to various anthropogenic influences that threaten their quality and quantity. Many of the springs that used to be reliable sources of the public drinking water supply are not in use anymore. The same is true for many small springs that were used for drinking water supply of individual households

and farms. The following excerpts from the publications addressing use of springs in Pennsylvania and Virginia, the United States, illustrate these points.

Roadside springs are a popular source of drinking water utilized regularly by more than 10% of the Pennsylvania population. Consumers of roadside springs most often point to perceived natural pureness and good taste as the main reasons for collecting spring water. However, research conducted by Penn State Extension from 2013 to 2015, on several dozen roadside springs found that nearly all fail health-based drinking water standards, many contain E. coli bacteria, and some even contain pathogenic Giardia and Cryptosporidium. Variation in E. coli and parasites shows that a single negative test result does not ensure those organisms are absent year-round.

These results suggest that untreated roadside springs are largely unsuitable as a drinking water source. Anyone considering the use of a roadside spring for drinking water or other household purposes (plants, aquariums, livestock, etc.) should have the water tested through a state accredited laboratory to ensure its safety. At a minimum, water should be tested for coliform bacteria, which can be done for a small amount of money at many labs around the state.

Testing for Giardia and Cryptosporidium in water is not affordable or practical for private citizens but results from this study suggest that these parasites may occur at any roadside spring containing coliform bacteria. Cryptosporidium and Giardia may be killed by boiling water for several minutes or using special water treatment filters. It may be easier to transport safe water to seasonal residences rather than treating roadside spring water.

In addition to bacteria problems, most roadside springs had slightly soft and acidic water, a combination that produces corrosive water that is aggressive toward metals and other materials. Given the corrosive nature of this water, it is important that roadside spring water be stored in containers approved for water storage even for non-drinking use. Water should also not be stored in containers for more than six months (PennState Extension article "Roadside Springs", August 2022, available at: https://extension.psu.edu/roadside-springs).

Of the 116 spring sources used by Virginia waterworks, the majority are located west of the Blue Ridge, where the geology is karst with heavily fractured and channeled limestones and dolomites. The Virginia Department of Health (VDH) regulates the use of springs as a public or community water source. According to the VDH, springs may be used for a public or community water source only if it is impossible to develop an acceptable well or other source of water. Before a spring is approved for a public or community water system, an extensive sanitary survey must be performed. Private homeowners developing a spring as a private water source are not required to carry out a sanitary survey, however, it is recommended that the private homeowner use the following procedure in performing their own sanitary survey.

Springs developed by private homeowners as their drinking water source are not regulated by the VDH. However, just because water from a spring looks clear and clean does not mean that it is safe to drink. Many disease-causing microorganisms, such as giardia or cryptosporidium, have no odor, color, or taste. Because of the possibility of contamination by surface water, springs are not recommended by the VDH for use as a drinking water source unless they are treated with an appropriate water treatment system.

In order to develop or upgrade an existing spring as a potentially safe, reliable drinking water source, there are two conditions. First, the flow must be sufficient to supply a household's daily needs throughout the year. Second, the spring must be adequately protected from possible contaminant sources. To properly develop a spring, the following components are necessary:

Figure 16.31 Roadside spring in disrepair on VA Route 211, about 1.5 miles before entrance to Skyline Drive National Park, Virginia.

1. A collection system to channel the flow to the spring box or storage system.

2. A reinforced-concrete spring box with an overflow pipe.

3. A cover that will keep surface water and other contaminants out of the spring box.

4. Easy access to clean and empty the spring box.

*5. A connection to a backup supply if the flow rate ceases to provide an adequate water supply. (*Virginia Water Resources Research Center, 1999. A homeowner's guide to the development, maintenance, and protection of springs as a drinking water source. Virginia Polytechnic Institute and State University, Blacksburg, Virginia, 83 p.)

There are three basic types of spring capture: (1) with minimal or no artificial intervention when the spring is used "as is," (2) with some form of engineering intervention aimed at securing the source for reliable use and protecting it from surface contamination, and (3) with engineering aimed at artificially increasing the spring discharge rate. Figure 7.11 in Lecture 7 illustrates the first type. This form of spring capture is not recommended for drinking water supply since the spring can be easily accessed by animals and contaminated by surface runoff.

A very detail discussion on the general principles of spring capture including engineering design illustrated with case studies is provided by Stevanović (2009; Chapter 9 in *Groundwater Hydrology of Springs: Engineering, Theory, Management, and Sustainability*, a book edited by Kresic and Stevanović).

Development of Small Springs

Most importantly, when used for potable water supply, a spring should be completely enclosed, protected from contamination, and equipped with fixtures for easy access, cleanup, and water distribution. One such design showing a typical capture of a contact gravity spring with a watertight basin ("spring box") constructed in place with reinforced concrete is illustrated in Figure 16.32. The basin should be vented to the surface and have easy access for maintenance. Three pipes equipped with valves should allow for (1) water overflow, (2) complete basin drainage for the cleanout and maintenance, and (3) transfer of water to supply or storage. All pipes should have screens on either end to prevent intrusion by vermin (bugs, small animals) and debris. If the water is of such quality that disinfection is the only treatment required, a chlorination tank or UV equipment may be housed in the maintenance room adjacent to the basin.
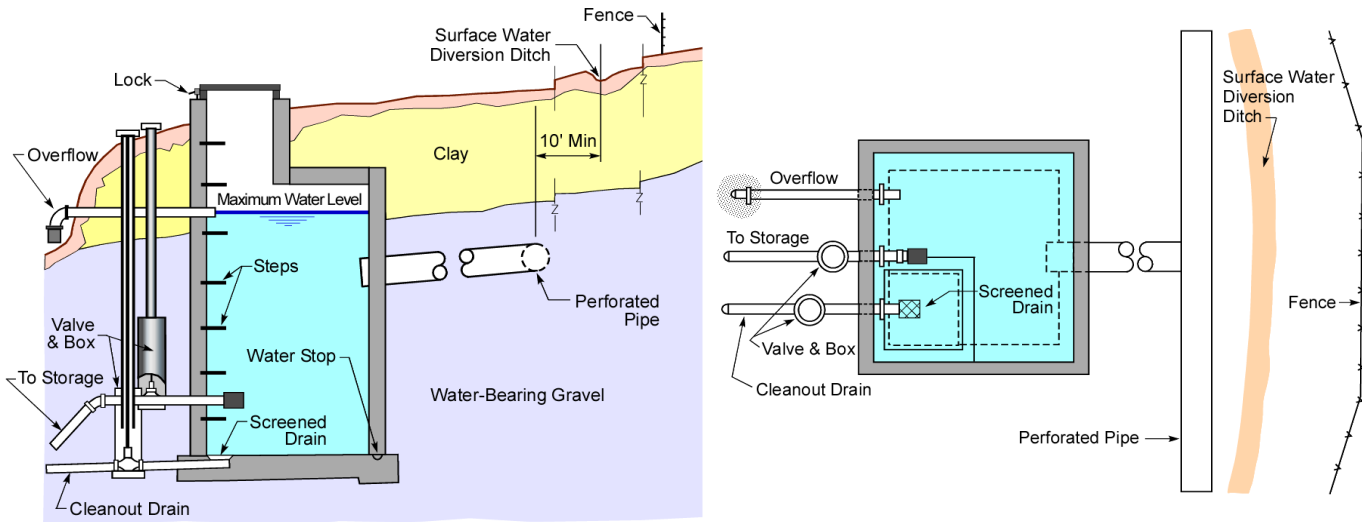
Figure 16.32 Typical capture of a gravity spring using spring box. *Left*: Cross-sectional view. *Right*: Plan view. Modified from U.S EPA, 1991; in public domain.

Sanitary protection of the spring at the surface is achieved by fencing, placement of an impermeable clay fill, and surface drainage ditches located uphill from the spring to intercept surface water runoff and carry it away from the source. Depending on site-specific conditions, the basic configuration of the spring capture shown in Figure 16.32 may include additional features such as drainage pipes (or galleries in case of fractured rock aquifers) extending into the saturated zone behind the spring box for intercepting more flow.

Spring capture should be built at the location of primary discharge of water from the subsurface since secondary springs may move in time. If the discharge is from colluvium and other types of rock debris, there is a high probability that the spring is secondary and located away from the primary discharge location, which may not be visible. In such cases, every attempt should be made to clear the rock debris and locate the primary spring.
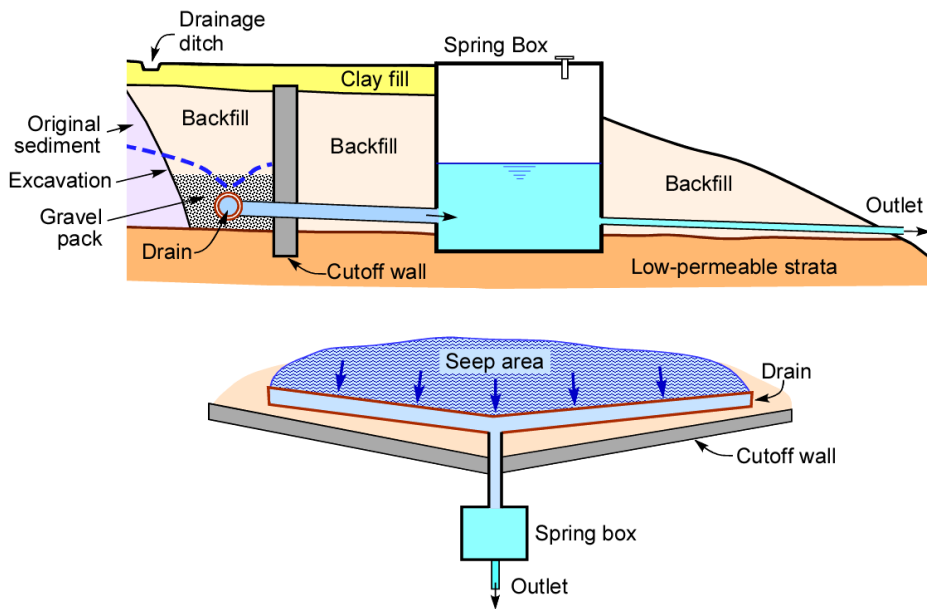

Figure 16.33 Capture of a seepage spring. *Top*: Cross-sectional view. *Bottom*; Plan view. Modified from Jennings, 1996; North Carolina Cooperative Extension Service; in public domain.

Springs are often contaminated with bacteria during construction or maintenance. All new and repaired spring capture systems should be disinfected using shock chlorination. If bacterial contamination occurs on a regular basis because of surface sources above the spring, continuous disinfection using chlorination, or some other method may be necessary. Shock chlorination requires concentration of at least 200 ppm chlorine (Jennings, 1996).

Capture of seepage springs, which occur where groundwater seeps from the soil over larger areas, is illustrated in Figure 16.33. The development process for seepage springs consists of intercepting flowing groundwater over a wide area underground and channeling it to a collection point. The basic steps are the following (modified from Jennings, 1996):

- Dig test holes in the general area of the seep including uphill from the seep to find where the impervious layer below the water-bearing layer is. Water flows on top of this layer in more permeable porous media (typically sand or gravel) toward the surface seep.
- Dig a 2-ft-wide (or wider as applicable) trench across the slope to a depth of at least 6 in. below the water-bearing layer and extending 4 to 6 ft beyond the overall length of the seep area on each side. Install a 4-in. collector tile (perforated drainage pipe) and surround the tile with gravel ("gravel pack").
- Connect the collector tile to a 4-inch line leading to the spring box. The spring box inlet must be below the elevation of the collector tile.

Seepage springs, usually when occurring as a group, can sometimes be utilized for public supply if their combined yield is adequate and the capture structure is properly engineered. An example of such capture is shown in Figure 16.34. The first step was to locate the primary discharge zone by partially excavating sediments in the narrow thin alluvial valley extending downgradient from the seeps. The observed groundwater discharge of 8 L/s was from three constant seeps (all at the same level) along a linear drainage zone 5 m long.
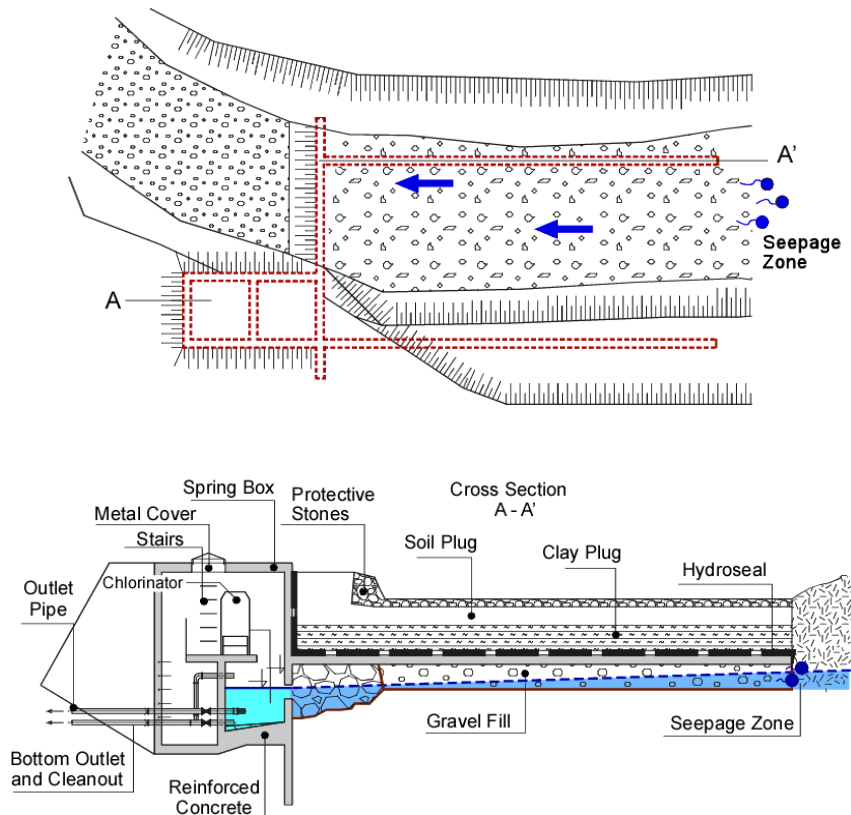

Figure 16.34 Capture design of a group of three seepage springs in an alluvial valley. *Top*: Map view of the excavation with the outline of the engineered structure (red dashed lines). *Bottom*: Cross-section of the spring capture. Courtesy of WIGA, Belgrade; design by Gaon, 1975; Copyright Hidroprojekt, Belgrade; permission is required for further use.

After removing large rock fragments and boulders, two parallel cutoff walls were built from reinforced concrete. After the walls were completed, alluvial material was washed, leveled, and covered by an impermeable clay plug. After compaction of the clay, a soil layer was placed on top and partially covered by rock fragments to prevent erosion. The channeled water, now fully captured and closed, was directed into a storage reservoir, also built from reinforced concrete. Next to the storage reservoir is a maintenance room, housing the control valves and an automated chlorinator. The entire structure is covered by soil except for a concrete plate with a top entrance. Approximately 5–6 L/s of water from the spring capture is diverted by gravity through a 700 m long pipeline (diameter 100 mm) to a pumping chamber at the village. From the chamber, water is pumped to two reservoirs above the village. Each reservoir can store 125 m^3 of water and supplies the distribution network (Gaon, 1975, from Stevanović, 2009).

Photographs in Figures 16.35 through 16.39 illustrate various types of small spring capture. Variations on the spring-box and seepage-springs capture designs and other useful information on using small springs for water supply can be found in USAID, 1982; Jennings, 1996; Skinner and Shaw, 1999; Virginia Water Resources Research Center, 1999; and Clemens et al., 2007.

Figure 16.35 *Left*: Karst spring Suvi Do (Žagubica, Carphatian karst of eastern Serbia). *Right*: Stapari karst spring captured by local villagers for their use (Dinaric karst of western Serbia). Photos courtesy of Zoran Stevanović.

Figure 16.36 *Left*: Abandoned capture of a spring historically used for water supply of a pre-civil war farmhouse in Rixeyville, Virginia. Two right photographs show capture of a fracture spring utilized for watering cattle on a farm near Saltville, Virginia.

Figure 16.37 *Left*: Capture of Hammam Sharqi Spring in the Sultanate of Oman. Part of water (seen here) from this hot spring (41°C) is used for irrigation. Photo courtesy of Dr. Mohamed Chebaane and Ministry of Water Resources, Sultanate of Oman. *Right*: Ancient spring intake Taalex Laasqoray Xudun, still actively used by local population; Sool Plateau-Sanaag, Puntland Province, Somalia. Courtesy of Zoran Stevanović.

Figure 16.38 *Left*: Spring house built on top of an ascending spring at a historic plantation in Bath County, Virginia. The house also served as a food storage because of the cool air maintained by the spring water. *Right*: Spring-box type capture of the Lakomica spring issuing at the contact between fractured limestone and underlying low-permeable diabase. Fence around the spring area prevents access to the capture. The spring supplies drinking water to a town in western Serbia.

Figure 16.39 Historic spring fountains abound in Belgrade., Serbia's capitol. *Left*: "Rebel Fountain", a seepage spring capture from the 18th century. It got its name from the original spring frequented by rebels against Ottoman rule in the Balkans. *Right*: Historic Topčider Fountain, another seepage spring capture, with a long cutoff (retaining) wall. Courtesy of Vojislav Ilić.

Development of Large Springs for Public Water Supply

The majority of springs used for public water supply of more than several hundred users are karst springs, which in general have the highest average flow rate among different types of springs. Large permanent karst springs usually discharge at topographically low contacts with low-permeable formations, and along surface streams which act as regional erosional bases of karst aquifers. In addition, the largest springs are almost always of ascending type (see Lecture 10). However, because of the diversity of karst formations, the complexity of karst processes, and the role of geology and tectonics in directing groundwater flow in karst, karst springs can be of any type: ascending, descending, cold, thermal, with uniform discharge, or with discharge varying between 0 and >200 m^3/s. For these reasons and depending on the spring yield and the number of users, the capture of such springs can be of a spring box–type (Figure 16.40), or with a pump pumping from the natural or engineered spring basin (Figure 16.41), or as complex and extensive as underground galleries or dams built to capture flow of large first-magnitude springs (see Figures 16.2 and 16.4).

Figure 16.40 Photograph of the outflow from the spring box of Hughes Spring near Zack, Arkansas. Hughes Spring supplies water for the city of Marshall, Arkansas, and the surrounding area. The mean annual discharge for Hughes Spring was 2.9 and 5.2 cubic feet per second for water years 2001 and 2002, respectively. Tritium data for Hughes Spring indicate that the discharge water is a mixture of recent recharge and sub-modern water (recharged prior to 1952). Photograph by Joel Galloway, USGS, from Galloway, 2004; in public domain.
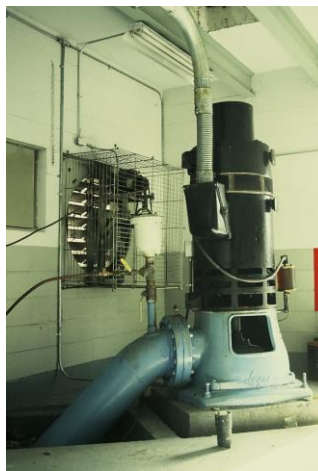

Figure 16.41 *Left*: Abandoned capture of a spring historically used for public water supply of Winchester, Virginia. *Right:* Pump house at a large spring utilized for public water supply of a township in one of the central U.S. states. The spring is one of the most productive in the state, supplying about 5 million gallons of water per day for domestic and municipal use.

Small spring box-type capture would usually not be advised for large karst springs because of (commonly) variable flow rates and maximum flows that may result in flooding and damaging of the capture structure. In such cases, the capture would have to be more elaborate and properly sized such that the term "spring box" would

probably not be adequate even though the main principle of the spring capture is the same. Various alternatives come to mind, such as (simply) "spring capture" or "capture structure" and similar. One example of a more elaborate capture of a large karst spring for public water supply with the minimum of 150 L/s (5 cubic feet per second) is shown in Figures 16.40 and 16.41.

The spring issues from several discharge points and has stable yield throughout the year (coefficient of uniformity is 1.5) with a measured minimum of 220 L/s. Given the proximity of discharge locations at the spring, it was concluded that the most convenient solution was to capture them all together and put them under one common roof. The spring capture has the following elements (Gaon, 1987):

- The main intake room covers the surface area where all the ascending springs discharge.
- The reinforced concrete walls are founded in unweathered limestone.
- The concrete ceiling is 1 m above the maximum water level inside the intake.
- The vents provide additional fresh air inside.
- The intake is filled with gravel and coarse sand materials.
- Water is channeled toward the clean water collection chamber with 100 m^3 capacity.
- From the chamber, water is diverted through a 500 mm pipe toward the pump room, where the chlorination takes place.
- Disinfection by chlorine is the only water treatment.
- Two centrifugal pumps lift the water to a 1400 m^3 reservoir above the city.
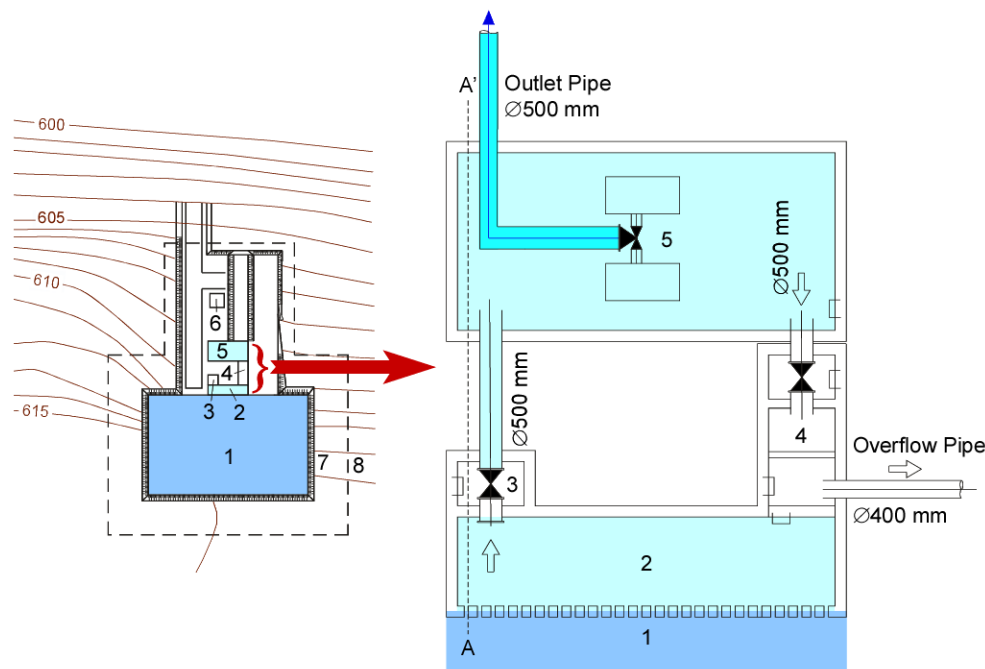

Figure 16.40 Plan view of the capture of a karst spring used for water supply of Sjenica, Western Serbia. (1) Main intake room covered by concrete roof above all ascending springs and filled with gravel. (2) Clean water collection chamber. (3) Access box for operating the valve. (4) Access room for overflow pipe. (5) Pump room with two centrifugal pumps. (6) O&M room. (7) Concrete walls. (8) Fence. Design by Gaon, 1987. Copyright Hidroprojekt, Belgrade; permission required for further use.
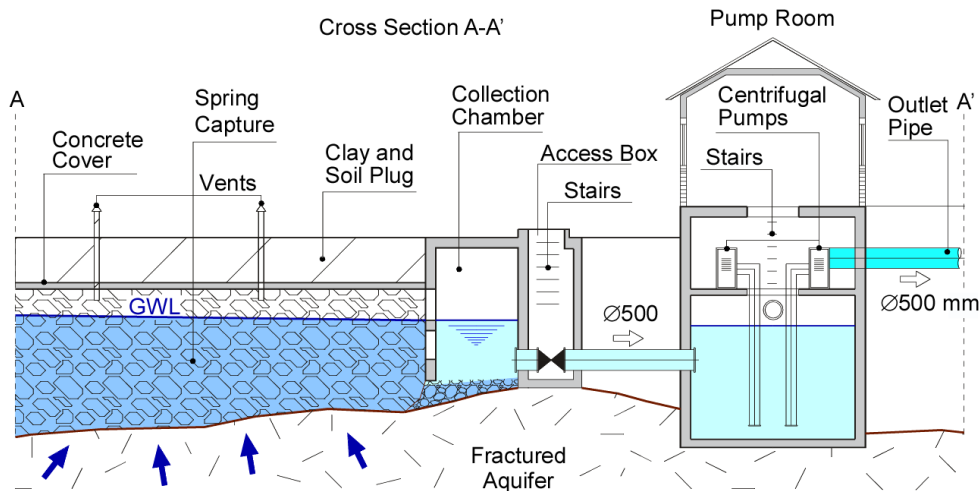
Figure 16. 41 Cross section A-A' of the Sjenica karst spring capture. Design by Gaon, 1987. Copyright Hidroprojekt, Belgrade; permission is required for further use.

The rate of natural discharge has often been a limiting factor when considering the use of a particular spring for public water supply. If the spring is capable of discharging large quantities of water during periods of nonpeak demand such as in spring or late fall when natural aquifer recharge is the highest, it may be possible to take advantage of this volume of "surplus" water. Namely, the sprung discharge may be regulated by overpumping during periods of peak demand (e.g., summer-early fall) followed by the replenishment of the depleted storage with the "surplus" water during periods of high natural recharge and low demand. The main prerequisite for this approach to work is that the aquifer has adequate storage capacity below the spring elevation. Management of the Lez Spring in France is a good example.

As explained by Fleury et al. (2008), groundwater is withdrawn from the spring by powerful pumps from three wells placed at the end of the main drain of this ascending spring, 400 m upstream from the main pool and well below the overflow level (Figure 16.42). The average pumping rate for the 1997–2005 period was 1.1 m^3/s. When pumping begins to withdraw the reserves, the water levels in the drain and in the spring pool drop to the level of the pool overflow and the spring dries up. Pumping then causes a drawdown within the drain that can reach several tens of meters at the end of the low-water period. These reserves are recharged naturally during the autumn and winter.

The hydraulic water level in the drain rises above that of the pool, and the spring begins to flow again. During the active pumping, when the Lez River flow is lower than the pumped flow, part of the pumped flow is channeled to the river. This return flow, set by the Declaration of Public Utility of June 5, 1981, is 160 L/s.

A recharge-discharge model was developed to help manage the Lez Spring groundwater withdrawals (Fleury et al., 2008). The model consists of three simulated reservoirs, all recharged by estimated effective precipitation: (1) saturated reservoir, (2) slow-flow infiltration zone reservoir, and (3) rapid infiltration zone reservoir. Effective infiltration is calculated based on the analysis of time series and the definition of transfer functions using TEMPO software by BRGM. Two modules are added to the saturated zone reservoir: a pumped volume and the returned flow. The model is used for estimating the volume of water (effective precipitation) needed to recharge the aquifer and it can accurately simulate the discharge at the spring and the water level in the drain.
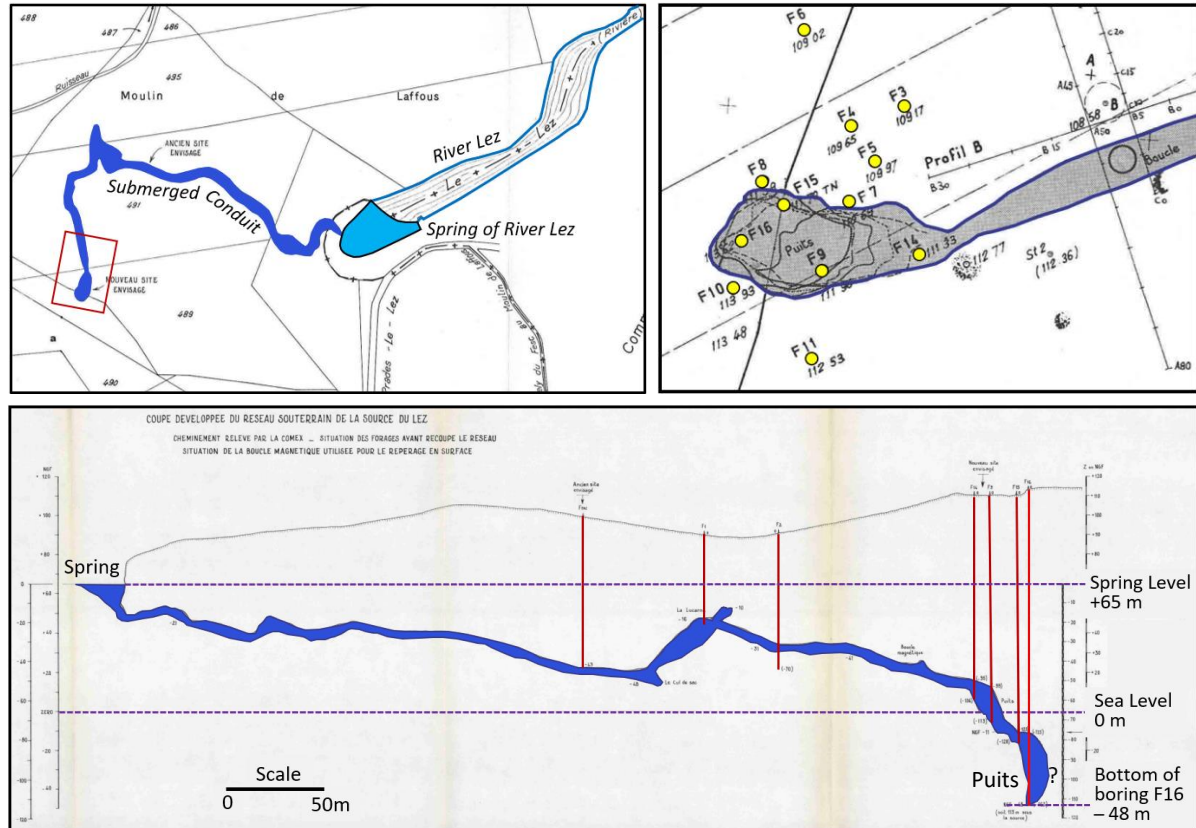
Figure 16.42 Spring of the Lez River (Source le Lez) captured for the water supply of Montpellier, France. *Top Left*: Map of the spring zone showing location of the submerged conduit (cave) which discharges into the spring basin. The red box is outline of the enlarged map shown in *Top Right*: yellow circles are investigative borings in and around the deepest portion of the cave (named "Puits" which means "Wells") where three large-diameter extraction wells are installed. In May 1979, Comex divers reached a point ~100 meters below elevation of the spring pool. *Bottom*: Cross-section of the conduit explored by cave diving and other investigative methods including geophysics and drilling. The deepest point is 113 meters below the spring pool elevation, in the Puits section, based on boring F16. Modified from BRGM, 1979 (original drawings are in public domain).

Figure 16.43 *Left*: Replacement of a high-capacity submersible pump in one of the extraction wells at the Spring of River Lez (Source du Lez) utilized for water supply of Montpellier, France. Photo courtesy of Jean Michel Valéry. *Right*: Old pumping installation at the spring. Photo courtesy of Arnaud Vestier, Service des Eaux, city of Montpellier.

16.6 Artificial Groundwater Recharge

Two terms have gained popularity in describing the concept of artificial aquifer recharge: (1) managed aquifer recharge (MAR) as a more general description for a variety of engineering solutions and (2) aquifer storage and recovery (ASR), which describes injection and extraction of potable water with dual-purpose wells. Artificial aquifer recharge should not be confused with induced aquifer recharge, which is a response of the surface water system to groundwater withdrawal as illustrated with Figure 16.16 and the accompanying discussion. Sometimes the induced recharge is referred to as indirect artificial aquifer recharge. Many groundwater supply systems in alluvial aquifers near large streams are intentionally designed to induce aquifer recharge for two main reasons: (1) increased capacity and (2) filtration of the river water en route to the supply well, which improves water quality.

The following discussion by Meinzer (1932) shows that early considerations and implementations of artificial aquifer recharge in the United States were made as early as at the beginning of the twentieth century:

Artificial recharge can be accomplished in some places by draining surface water into wells, spreading it over tracts underlain by permeable material, temporarily storing it in leaky reservoirs from which it may percolate to the water table, or storing it in relatively tight reservoirs from which it is released as fast as it can seep into the stream bed below the reservoir. Artificial recharge by some of these methods has been practiced in the United States and other countries. It was suggested by Hilgard in 1902 for southern California, where it has since received considerable investigation and has been adopted as a conservation measure. Drainage into wells has been practiced in many parts of the United States, chiefly to reclaim swampy land or to dispose of sewage and other wastes. The drainage of sewage or other wastes into wells can not be approved because it may produce dangerous pollution of water supplies. Drainage of surface water into wells to increase the ground-water supply for rice irrigation in Arkansas is now under consideration. Water spreading has been practiced to a considerable extent in southern California partly to decrease the effects of flood but largely to increase the supply of ground water. Storage in ordinary reservoirs and subsequent release has frequently been considered and the unavoidable leakage of some reservoirs has been used to increase the ground-water supply. Artificial recharge by damming stream channels in the permeable lava rocks of the Hawaiian Islands has been considered. In ground-water investigations that involve the question of safe yield attention should as a matter of course be given to the possibilities of artificial recharge.

The following statement, made 20 years ago, illustrates why artificial aquifer recharge has an ever-increasing importance in integrated water resources management. The California Department of Water Resources (DWR) in its 2003 update on water supplies in the state and various related issues, stated that:

The extent to which climate will change and the impact of that change are both unknown. A reduced snowpack, coupled with increased seasonal rainfall and earlier snowmelt may require a change in the operating procedures for existing dams and conveyance facilities. Furthermore, these changes may require more active development of successful conjunctive management programs in which the aquifers are more effectively used as storage facilities. Water managers might want to evaluate their systems to better understand the existing snowpack-surface water-groundwater relationship, and identify opportunities that may exist to optimize groundwater and other storage capability under a new hydrologic regime that may result from climate change. If more water was stored in aquifers or in new or re-tooled surface storage, the additional water could be used to meet water demands when the surface water supply was not adequate because of reduced snowmelt. (DWR, 2003).

The advantages of storing water underground as opposed to surface water reservoirs are often made clear during long periods of drought. For example, since the 1987–1992 droughts in California, there has been an expansion in groundwater recharge and storage capacity in the state. This trend will arguably now accelerate because of the ongoing drought in California (see Guest Lecture by Alex Mikszewski) and the over allocation of the Colorado River water on which California, Nevada, and Arizona are heavily dependent.

The important factors that must be considered for any type of artificial aquifer recharge are as follows (ASCE, 2001; U.S. EPA, 2004a; Kresic, 2009):

- Regulatory requirements.
- The availability of an adequate source of recharge water of suitable chemical and physical quality.
- Geochemical compatibility between recharge water and the existing groundwater (e.g., possible carbonate precipitation, iron hydroxide formation, mobilization of trace elements).
- The hydrogeologic properties of the porous media (soil and aquifer) must facilitate desirable infiltration rates and allow direct aquifer recharge. For example, existence of extensive low permeable clays in the unsaturated (vadose) zone may exclude a potential recharge site from future consideration.
- The water-bearing deposits must be able to store the recharged water in a reasonable amount of time, and allow its lateral movement toward extraction locations at acceptable rates. In other words, the specific yield (storage) and the hydraulic conductivity of the aquifer porous media must be adequate.
- Presence of fine-grained sediments may have an advantage of improving the quality of recharged water due to their high filtration and sorption capacities. Other geochemical reactions in the vadose zone below recharge facilities may also influence water quality.
- Engineering solution should be designed to facilitate efficient recharge when there is an available surplus of water, and efficient recovery when the water is most needed.
- The proposed solution must be cost-efficient, environmentally sound, and competitive to other water resource development options.

Aquifers that can store large quantities of water and do not transmit them away quickly are best suited for artificial recharge. For example, karst aquifers may accept large quantities of recharged water but in some cases tend to transmit them very quickly away from the recharge area. This may still be beneficial for the overall balance of the system and the availability of groundwater downgradient from the immediate recharge sites, as illustrated with examples from the Edwards Aquifer in Texas (discussed later in this Lecture). Alluvial aquifers are usually the most suited to storage because of the generally shallow water table and vicinity to source water (surface stream). Sandstone aquifers are in many cases very good candidates due to their high storage capacity and moderate hydraulic conductivity.

Three common methods of artificial aquifer recharge are (1) spreading water over the land surface; (2) delivering it to the unsaturated zone below the land surface via recharge trenches and vadose zone injection wells; and (3) injecting water directly into the aquifer via injection wells. A variety of engineering solutions and combinations of these three methods have been used to accomplish a simple goal—deliver more water to the aquifer (see Figures 16.44 and 16.45).

Table 16.4 provides a comparison of major engineering factors that should be considered when installing a groundwater recharge system, including the availability and cost of land for recharge basins (Fox, 1999). If such costs are excessive, the ability to implement injection wells adjacent to the reclaimed water source tends to decrease the cost of conveyance systems for injection wells. Surface spreading basins require the lowest degree of pretreatment while direct injection systems require water quality comparable to drinking water if potable aquifers

are affected. Low-technology treatment options for surface spreading basins include primary and secondary wastewater treatment with the possible use of lagoons and natural systems. RO is commonly used for direct injection systems to prevent clogging; however, some aquifer storage and recovery (ASR) systems have been operating successfully without membrane treatment when water was stored for irrigation. The cost of direct injection systems can be greatly reduced from the numbers presented in Table 16.4 if the aquifer is shallow and non-potable (USEPA, 2004a).
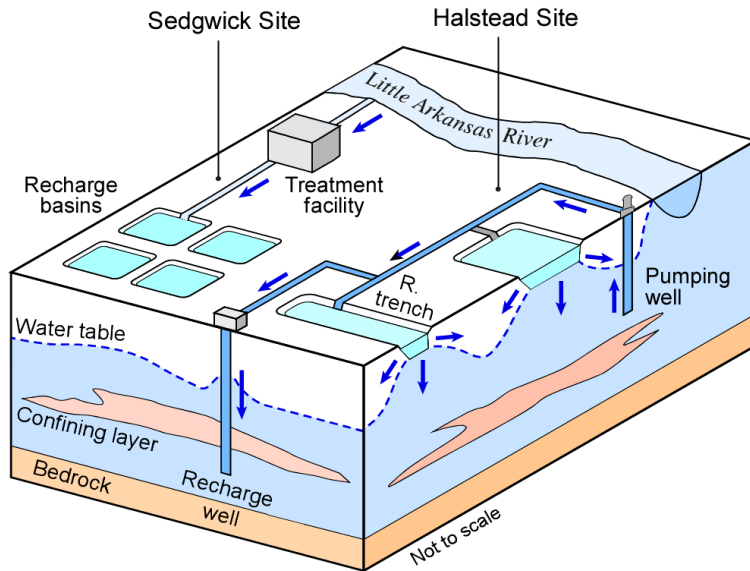

Figure 16.44 At the Halstead recharge demonstration site, the aquifer is artificially recharged by water pumped from a diversion well immediately adjacent to the Little Arkansas River at Wichita, Kansas, the United States. The diverted water is piped about 3 mi to the recharge site and recharged to the aquifer through direct-well injection, surface-spreading basins, and a recharge trench. At the Sedgwick recharge demonstration site water comes from a surface water intake in the Little Arkansas River. The surface water is treated with powdered activated carbon and polymers to remove organic contaminants and sediments. The treated water is then piped about 3 mi to the Sedgwick site and recharged through surface-spreading basins. Modified from Galloway et al., 2003. USGS, in public domain.

Table 16.4 Comparison of major engineering factors for Engineered Groundwater Recharge. From U.S. EPA, 2004a. In public domain

	Recharge Basins	Vadose Zone Injection Wells	Direct Injection Wells
Aquifer type	Unconfined	Unconfined	Unconfined or confined
Pretreatment requirements	Low technology	Removal of solids	High technology
Estimated major capital costs	Land and distribution system	$25,000-75,000 per well	$500,000-1,500,000 per well
Capacity	100-20,000 m^3/hectare-day	1,000-3,000 m^3/d per well	2,000-6,000 m^3/d per well
Maintenance requirements	Drying and scraping	Drying and disinfection	Disinfection and flow reversal
Estimated life cycle	>100 years	5-20 years	25-50 years
Soil aquifer treatment	Vadose and saturated zones	Vadose and saturated zones	Saturated zone

Artificial recharge by spreading is the most common technique of artificial aquifer recharge (Figures 16.45 and 16.46). Recharge is accomplished by spreading water over the ground surface or by conveying the raw water to infiltration basins and ditches. The operational efficiency of the spreading depends on the following factors (modified from Pereira et al., 2002):

- Presence of sufficiently pervious layers between the ground surface and the water table (aquifer).
- Enough thickness and storage capacity of the unsaturated layers above the water table.
- Appropriate transmissivity of the aquifer horizons.
- Surface water without excessive particulate matter (low turbidity) to avoid clogging.

The quantity of water that can enter the aquifer from spreading grounds depends on three basic factors: (1) The infiltration rate at which the water enters the subsurface; (2) The percolation rate, i.e., the rate at which water can move downward through the unsaturated zone until it reaches the water table (saturated zone); and (3) The capacity for horizontal movement of water in the aquifer, which depends on the hydraulic conductivity and thickness of the saturated zone.

Figure 16.45 Rio Hondo Coastal Spreading Grounds in Montebello Forebay. From Anders and Schroeder, 2003. USGS, in public domain.

The infiltration rate tends to reduce over time due to the clogging of soil pores by sediments carried in the raw water, growth of algae, colloidal swelling, soil dispersion, and microbial activity. A spreading basin is constructed with a flat bottom that is covered evenly by shallow water. This requires the availability of large surfaces of land for meaningful size recharge works. Several basins may be arranged in line so that excess water runs between the basins (Figure 16.45). Retaining basins may be used for settlement of suspended sediments before water enters the spreading basins. The settling of sediments may also be assisted with the addition of coagulation agents. In addition

to clogging, another major disadvantage of shallow infiltration basins is evaporation loss. Proper operations and regular maintenance of infiltration basins are therefore very important for the overall efficiency of spreading grounds and infiltration basins. More detail about the spreading basins design and various related issues is provided in Kresic, 2009.

Figure 16.46 Tonopah Recharge Site, Central Arizona Project. Inset: Delivery of recharge water to one of the basins Photographs courtesy of Philip Fortnam, Central Arizona Project.

Recharge (retention) dams are widely applied artificial recharge structures, the purpose of which is to delay the runoff of water in surface streams and provide the time needed for recharge into the local aquifer. The structures usually consist of low dams, including earth walls and gabions built to be toppled by floods. For example, several such dams have been built in the Edwards Aquifer recharge zone (Figure 16.46).

Figure 16.46 *Left*: Edwards Aquifer recharge dam on Seco Creek, Texas. *Middle*: During the flood events like the one shown on the left, part of the flood water is diverted towards the Valdina sink via artificial channel incised into the Edwards Limestone. Photographs courtesy of Edwards Aquifer Authority. *Right*: Valdina Sink when dry. Photo copyright Gregg Eckhardt. Printed with kind permission. See also www.edwardsaquifer.net/intro.html; and Figure 7.38 in Lecture 7.

Vadose zone injection wells for groundwater recharge with reclaimed water were developed in the 1990s and have been used in several different locations in the Phoenix, AZ, metropolitan area. Typical vadose zone injection wells are 6 ft (2 m) in diameter and 100 to 150 ft (30 to 46 m) deep. They are backfilled with porous media and a riser pipe is used to allow for water to enter at the bottom of the injection well to prevent air entrainment. An advantage of vadose zone injection wells is the significant cost savings as compared to direct injection wells. The infiltration rates per well are often similar to direct injection wells. A significant disadvantage is that they cannot be backwashed and a severely clogged well can be permanently destroyed. Therefore, reliable pretreatment is considered essential to maintaining the performance of a vadose zone injection well. Because of the considerable cost savings associated with vadose zone injection wells as compared to direct injection wells, a life cycle of 5 years for a vadose injection well can still make the vadose zone injection well the economical choice. Since vadose zone injection wells allow for percolation of water through the vadose zone and flow in the saturated zone, one would expect water quality improvements commonly associated with soil aquifer treatment to be possible (USEPA, 2004; Bouwer, 2002).

Saturated-zone injection wells can be used to recharge any type of aquifer, at any depth, thus eliminating problems associated with low permeable surficial soils and low-permeable layers in general. Direct injection requires water of higher quality than for surface spreading because of the absence of vadose zone and/or shallow soil matrix treatment afforded by surface spreading and the need to maintain the hydraulic capacity of the injection wells, which are prone to physical, biological, and chemical clogging. Treatment processes beyond secondary treatment that are used prior to injection include disinfection, filtration, air stripping, ion exchange, granular activated carbon, and Reverse Osmosis (RO) or other membrane separation processes. By using these processes or various subsets in appropriate combinations, it is possible to satisfy all present water quality requirements for water injection, including with reclaimed water. However, even when such high-quality water is used for recharge, trouble-free operations cannot be guaranteed for longer periods of well operation due to various geochemical and

mechanical processes, which tend to clog well screens and reduce permeability of the well gravel pack and adjacent aquifer material. A common practice is to inject water via dual-purpose wells, which are used to occasionally pump water back from the aquifer thus removing screen-clogging materials ("backwashing"). (U.S. EPA, 2004a.)

In many cases, the wells used for injection and recovery are classified by the USEPA as Class V injection wells. Some states require that the injected water must meet drinking water standards prior to injection into a Class V well. For both surface spreading and direct injection, locating the extraction wells as great a distance as possible from the recharge site increases the flow path length and residence time in the underground, as well as the mixing of the recharged water with the natural groundwater. Treatment of organic parameters does occur in the groundwater system with time, especially in aerobic or anoxic conditions (Gordon et al., 2002; Toze and Hanna, 2002).

In the United States, water used for well injection is usually treated to meet drinking water quality standards for two reasons. One is to minimize clogging of the well-aquifer interface, and the other is to protect the quality of the water in the aquifer, especially when it is pumped by other wells in the aquifer for potable uses. Direct injection into the saturated zone does not have the benefits of fine-textured unsaturated soils which often improve the quality of the recharged water in the case of recharge basins and vadose zone infiltration systems. Thus, whereas secondary sewage effluent can in many cases be used in surface infiltration systems for soil-aquifer treatment and eventual potable reuse, effluent for direct well injection must at least receive tertiary treatment (sand filtration and chlorination). This treatment removes remaining suspended solids and some microorganisms like giardia (protozoa), and cryptosporidium and parasites, like helminth eggs, by filtration. Bacteria and viruses are removed by chlorination, ultraviolet irradiation, or other disinfection (Bouwer, 2002).

Where groundwater is not used for drinking, water of lower quality can be injected into the aquifer. For example, in Australia, stormwater runoff and treated municipal wastewater effluent are injected into brackish aquifers to produce water for irrigation by pumping from the same wells. Clogging is alleviated by a combination of low-cost water treatment and well redevelopment, and groundwater quality is protected for its declared beneficial uses (Dillon and Pavelic 1996; Dillon et al., 1997). Turbidity of source water is often the main quality problem for all recharge facilities. In infiltration basins and trenches, fine suspended solids tend to clog contact surfaces and must be regularly removed after infiltration basins and trenches are drained (infiltration drains with this problem cannot be efficiently rehabilitated). For this reason, large recharge facilities often include separate settling basins.

One of the major concerns with any aquifer recharge project, using any type of recharge water, is the presence of bacteria and viruses. For example, enterovirus, giardia cysts, and cryptosporidium oocysts are often more than 10 percent of time tested positive in some treated and disinfected reclaimed water (USEPA, 2004). The survival or retention of pathogenic microorganisms in the subsurface depends on several factors including climate, soil composition, antagonism by soil microflora, flow rate, and type of microorganism. At low temperatures (below 4◦C or 39◦F) some microorganisms can survive for months or years. The die-off rate is approximately doubled with each 10◦C (18◦F) rise in temperature between 5◦C and 30◦C (41◦F and 86◦F) (Gerba and Goyal, 1985). Rainfall may mobilize bacteria and viruses that had been filtered or adsorbed, and thus, enhance their transport (USEPA, 2004).

Large-scale artificial recharge projects are currently being implemented or considered by major water utilities and government agencies throughout the United States and the world. Although still challenging in many ways, the benefits they offer for sustainable management of water resources clearly make these projects the trend of the future. More detailed information on artificial aquifer recharge can be found in National Research Council (1994), Pyne (1995), ASCE (2001), Bouwer (2002), Gale et al. (2002), IAH (2002), Gale (2005), Dillon and Molloy (2006),

and UNESCO (2006). The International Association of Hydrogeologists (IAH) maintains a MAR-dedicated page on its Web site (https://iah.org/), including various useful links to related information.

El Paso Water (EPWater) Groundwater Management and Aquifer Recharge Case Study

El Paso developed the first aquifer recharge facility in Texas in 1985. For decades, El Paso has been treating wastewater to drinking water standards and using it to recharge the Hueco Bolson aquifer. The Fred Hervey Reclamation Plant injects up to 3 million gallons per day.

Historically, the utility primarily used deep injection wells to put water directly into the Hueco Bolson aquifer. EPWater conducted research with the American Waterworks Research Foundation and concluded that excavated infiltration ponds were a more economical method for recharging the Hueco in terms of both construction and recurring operations and maintenance costs. The utility completed a feasibility study, which was approved by the U.S. Bureau of Reclamation in 2019 to expand use of aquifer recharge, using a combination of reclaimed water, treated river water and stormwater. Since that time, EPWater has constructed four infiltration ponds and reduced its dependency on injection wells (Figure 16.47).

During irrigation season, EPWater holds water rights that help meet peak summer water use. When the utility does not need its full allotment of river water, there is an opportunity to use a portion of that water to replenish the aquifer to support long-range drought resilience and groundwater sustainability.

El Paso is home to the world's largest inland desalination plant (Figure 16.47). The area aquifer have vast brackish groundwater resources that were previously unusable. The Kay Bailey Hutchison (KBH) Desalination Plant filters out the salts and creates a new supply of water.

A joint project of El Paso Water and Fort Bliss, El Paso's desalination plant can produce up to 27.5 million gallons of fresh water daily. To meet future water needs, EPWater plans to expand the plant in coming years to as much as 42 MGD. The wells from which water is pumped for desalination are strategically placed to slow or prevent brackish water intrusion toward freshwater wells. The concentrate is pumped to a surface injection facility and disposed via deep well injection into geological formations 22 miles northeast of the plant site (El Paso Water; https://www.epwater.org/).

Figure 16.47 *Left*: El Paso, Texas is home of the world's largest inland desalination plant. *Right*: One of the four infiltration basins for artificial aquifer recharge. Courtesy of El Paso Water https://www.epwater.org/

Groundwater Drought in California: A Case Study in Figures
Guest Lecture by Alex Mikszewski

Drought is a condition of relative water scarcity, for which no universal definition exists. A period of below-average precipitation may be termed *meteorological drought*, and a period of below-average runoff may be termed *hydrological drought* (CADWR, 2020). A lack of soil moisture may be referred to as *agricultural drought*, and while the term may not be widely used at present moment, a *groundwater drought* refers to a period of below-average groundwater levels. The USGS notes that common to all types of droughts is the persistence of "drier-than-normal conditions that result in *water-related problems*" (USGS, 2016). With respect to groundwater, these problems include but are not limited to:

- Water supply wells going dry, necessitating replacement or pursuit of alternative sources;
- Land subsidence;
- Increased abstraction rates reducing stream baseflow;
- Salt-water intrusion into aquifers;
- Increased pumping energy and costs; and
- Mining of aquifers devoid of recharge.

It has been extensively documented that California (Figure 1), the second largest state in the continental USA and by far the largest in terms of gross domestic product (GDP), is vulnerable to drought (CADWR, 2020). This is due to the large part agriculture, and specifically irrigated agriculture, contributes to the California economy. In 2021 the gross receipts of California farms totaled more than 51 billion USA dollars ($B), making California the largest agricultural state and accounting for approximately 12% of all USA farm receipts (USDA, 2022). When considering processing and retail levels, the total annual value of California agriculture may exceed $100B and the sector supports an estimated 1.2 million jobs (Johnson and Cody, 2015; CDFA, 2021). This abundance is produced despite a statewide average precipitation of only approximately 22 inches per year (CADWR, 2020). For comparison, the second largest agricultural state of Iowa receives a statewide average precipitation of approximately 35 inches per year (IDALS, 2021). California overcomes this water deficit through extraordinary transfers of water between basins and extensive pumping of groundwater. Groundwater typically accounts for approximately 40% of California's water supply, but this fraction increases during times of drought as surface water sources dwindle (CADWR, 2020).

The United States Geological Survey (USGS) estimated that in 2010 California used 25.8 million acre-feet (MAF) of water for irrigated agriculture, constituting approximately 61% of all statewide water withdrawals (USGS, 2014; Johnson and Cody, 2015). An acre-foot is the volume equivalent to a foot of water applied across an acre of land, or approximately 436 hundred cubic feet (Ccf), or 325,851 US gallons. For the same year (2010), the California Department of Water Resources (CADWR) estimated a higher irrigated agriculture usage of approximately 33 MAF (CADWR, 2014). Regardless of which number is used, the water used for irrigated agriculture in California is likely higher than the *total* water use of any other state in the USA, with approximately half of all irrigated acres supplied by groundwater (USDA, 2013; USGS, 2014). Like the total irrigation volume, estimates of the total irrigated acreage vary, with two examples being approximately 7.9 million acres (USDA, 2013) and 9.6 million acres (CADWR, 2022a). Of interest is that an assumed total annual irrigation volume of 25.8 MAF and a total irrigated acreage of 7.9 million acres translates to approximately 39 inches of water, or more than the statewide average annual precipitation of Iowa.

Figure 1 Map of California available at all welcome centers. Courtesy of
https://www.visitcalifornia.com/in/feature/california-welcome-centers

The precariousness of California agriculture has been exposed by a historic megadrought that began in 2000 and has gripped the Southwest United States with dryness unprecedented in modern times. This megadrought has seen major Colorado River reservoirs Lake Mead and Lake Powell drop to their lowest ever levels in 2021 and is likely being amplified by anthropogenic climate change (ACC) (Williams et al., 2022). The effects of drought led to passage of California's landmark Sustainable Groundwater Management Act (SGMA) of 2014, which requires local water agencies to develop and implement groundwater sustainability plans to "*avoid undesirable results and mitigate overdraft within 20 years*" (CDWR, 2022b). The so-called undesirable results are generally aligned with the six consequences of groundwater drought listed at the beginning of this Lecture. The SGMA has led to an unprecedented amount of groundwater monitoring data in the public domain, which is explored herein. These data show that groundwater exploitation in California has *increased* rapidly since passage of the SGMA, with deleterious consequences.

The growth of California agriculture and its water footprint throughout the 20th century, and the scale of the current megadrought and its effects on groundwater resources, are explored in the following series of annotated figures. All graphs, tables, and maps were produced using publicly available data that the reader can obtain for independent analysis. Sustainable management of groundwater in California is indeed a challenge with unavoidable trade-offs between agricultural revenue and jobs, food security, maintaining flow in wild and scenic rivers, land subsidence, and the energy required for groundwater pumping. Whether undesirable results of groundwater extraction can be avoided depends largely on how long the current megadrought persists, as the entire agricultural system in California was built during the anomalously wet conditions of the 20th century. A hydrologic correction appears to be in process, which will likely be amplified by ACC. It is unlikely for undesirable results to be avoided entirely; instead, the question is how they can be minimized.
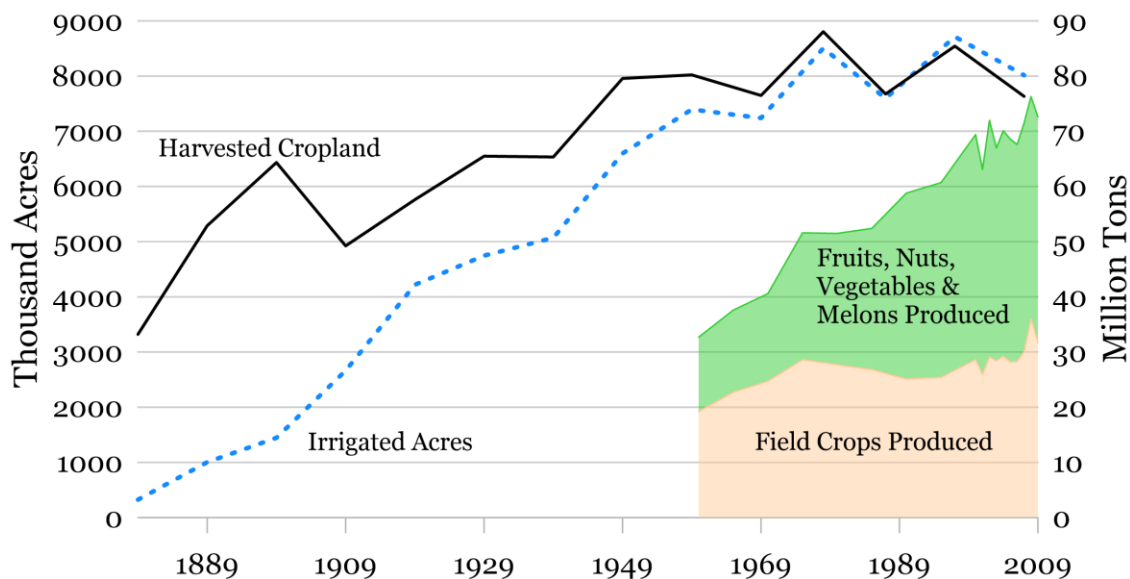

Figure 2 Irrigated agriculture in California increased dramatically during the 20th century, with nearly all harvested cropland (approximately 8 million acres) now being irrigated. Irrigated acres (dashed blue line) may exceed harvested cropland acres (solid black line) due to irrigated pasture. In the second half of the 20th century, production of high-value crops such as fruits, nuts, vegetables, and melons increased dramatically, eventually overtaking field crops in terms of million tons of output. The higher value of these crops means there is higher cost of fallowing fields and letting plants die. Data obtained from Olmstead and Rhode (2017) and Johnson and Cody (2015).
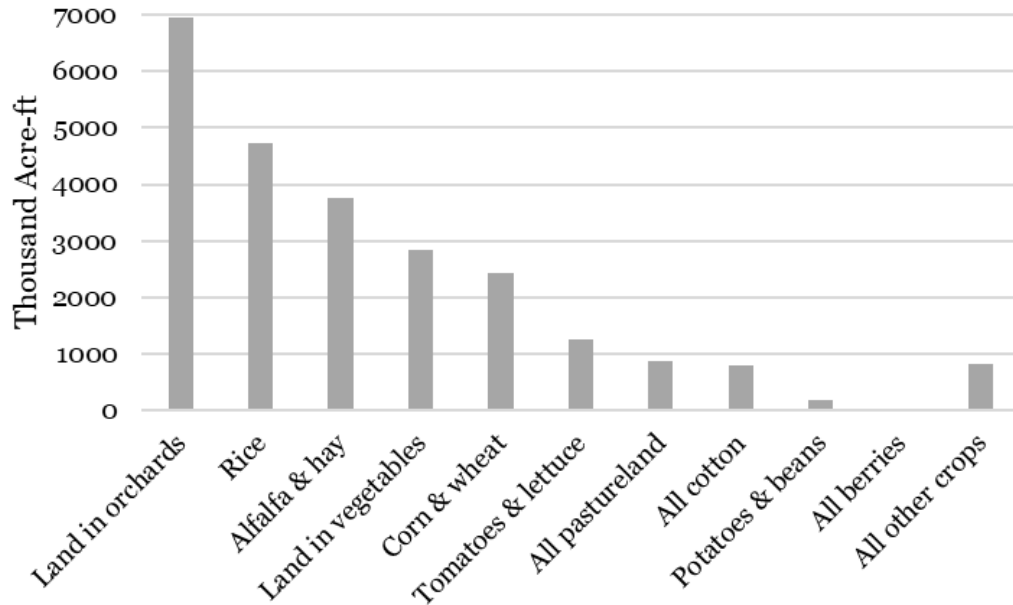
Figure 3 Estimate of total irrigation water applied to crops in California in 2013, based on Table 4 from Johnson and Cody (2015), with underlying data from USDA (2013). Most irrigation water, nearly 7 MAF, was dedicated to land in orchards, which includes almonds and pistachios.

Table 1 Total value of production and harvested acres for four crop categories in California in 2020 from CDFA (2021). Average water requirements for each category in acre-feet per acre harvested are estimated from Tables 4 and 5 of Johnson and Cody (2015). Between 2004 and 2020, the almond and pistachio harvest in California grew from a combined total of approximately 700 thousand acres, to over 2 million acres. Over the same timeframe, the hay harvest dropped from approximately 1.6 million acres to 825 thousand acres. This transition to higher value crops is logical considering the low price of water generally paid by farmers receiving surface water allocations from the Central Valley Project. However, during the on-going megadrought, allocations have not been met, meaning farmers must install wells or turn to the private water market, where costs up to $2,000 per acre-foot have been reported (Henry, 2022). For comparison, residential customers in Los Angeles in 2022 pay on average $7.77 per Ccf for basic indoor use, or $3,390 per acre-foot (LADWP, 2022). The agricultural production value ($) per acre-foot applied metric is a basic but useful indicator of the value of water in California.

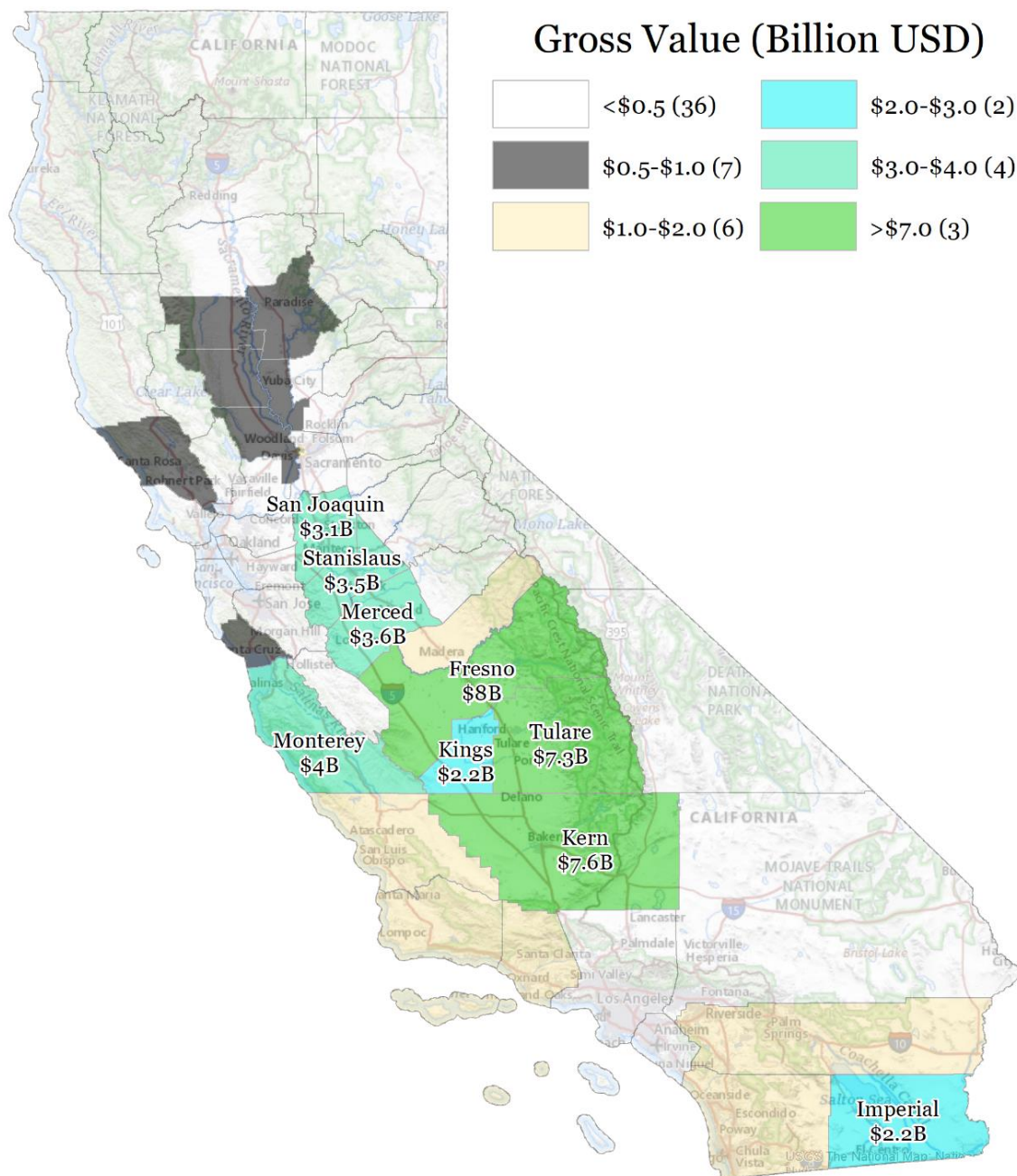|	Total Value ($1,000)	Harvested Acres (1,000)	Average Acre-Feet Applied per Acre	$/Acre-Foot Applied
Almonds & Pistachios	$8,493,680	1,622	3.5	$1,496
Lettuce	$2,275,284	199	2.5	$4,571
Hay	$680,310	825	3.8	$217
Wheat	$44,548	100	2.1	$212

Figure 4 Gross value of agricultural production in 2020 by county, totaling approximately $61.4B. The counties with the largest value of production are in the southern Central Valley (San Joaquin River and Tulare Lake hydrologic regions). The leading two commodities for Fresno County are almonds and pistachios, which are also the second and third leading commodities in Kern County. County-level data from CDFA (2021).
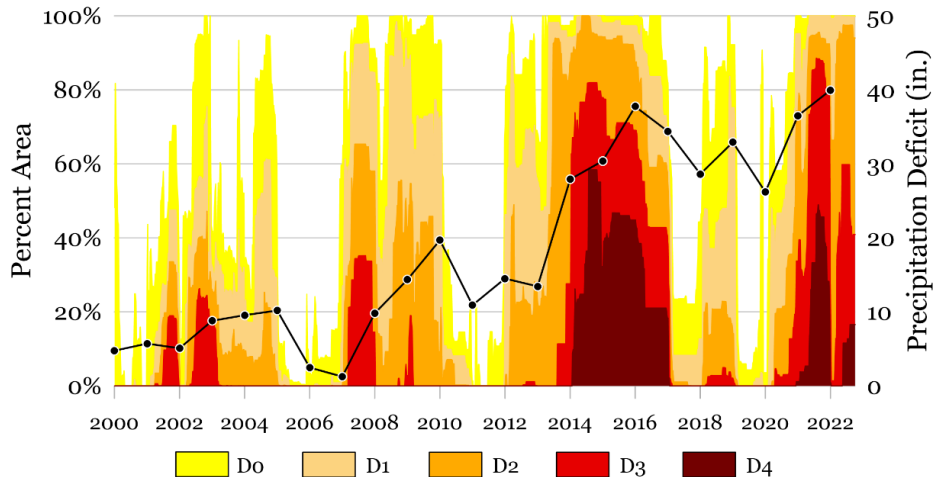
Figure 5 Percent of California in the five different acute drought categories established by the US Drought Monitor during the ongoing megadrought beginning in 2000. D0 is abnormally dry, D1 is moderate drought, D2 is severe drought, D3 is extreme drought, and D4 is exceptional drought. In 2022 nearly all of California is in a severe drought condition at a minimum. The cumulative statewide annual precipitation deficit is also presented in inches (black line, right axis), relative to the 1901-2000 annual mean, with data from NOAA (2022). Since 2000, there is an approximate 40-inch deficit in precipitation, which translates to reduced soil moisture and groundwater recharge. This in part explains the rapid return deterioration of drought conditions after the brief hiatus in 2019. Drought category data obtained from NDMC (2022). The US Drought Monitor is jointly produced by the National Drought Mitigation Center at the University of Nebraska-Lincoln, the United States Department of Agriculture, and the National Oceanic and Atmospheric Administration.
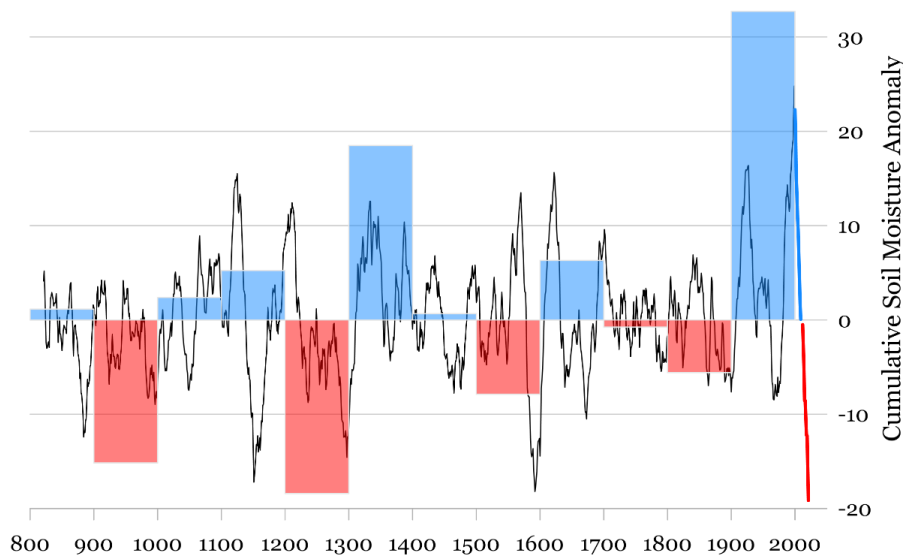

Figure 6 Rolling 22-year cumulative soil moisture anomaly (line) and cumulative soil moisture anomaly by century (bar) since 800 for the Southwest USA, using raw data from Williams et al. (2021) available at https://doi.org/10.25921/8pt9-hz08. The soil moisture anomaly represents the interannual standard deviation above or below the 800-2021 mean, with historic estimates from tree-ring reconstructions. The line graph illustrates the main finding of Williams et al. (2021), namely that the 22-year period between 2000-2021 (red line) was likely the driest 22-year period since 800, with a cumulative 22-year anomaly nearing -20 standard deviations. Two other significant findings made clear by the chart are that: 1) the 22-year period from 1978-1999 (immediately preceding the megadrought onset) had the highest 22-year soil moisture anomaly since 800 at over 20 standard deviations, and 2) the 20th century (1900-2000) had by far the highest cumulative soil moisture anomaly of any century since 800 (over 30 standard deviations). Thus, the growth of irrigated agriculture in California (Figure 2) corresponded with the wettest century on record, and the explosive growth of high-value crops in the south-Central Valley corresponded with the wettest 22-year period on record. While Williams et al. (2021) finds that the current megadrought is very likely exacerbated by ACC, in many respects it also represents a regression to the mean after the unprecedented high soil moisture in the 20th century.
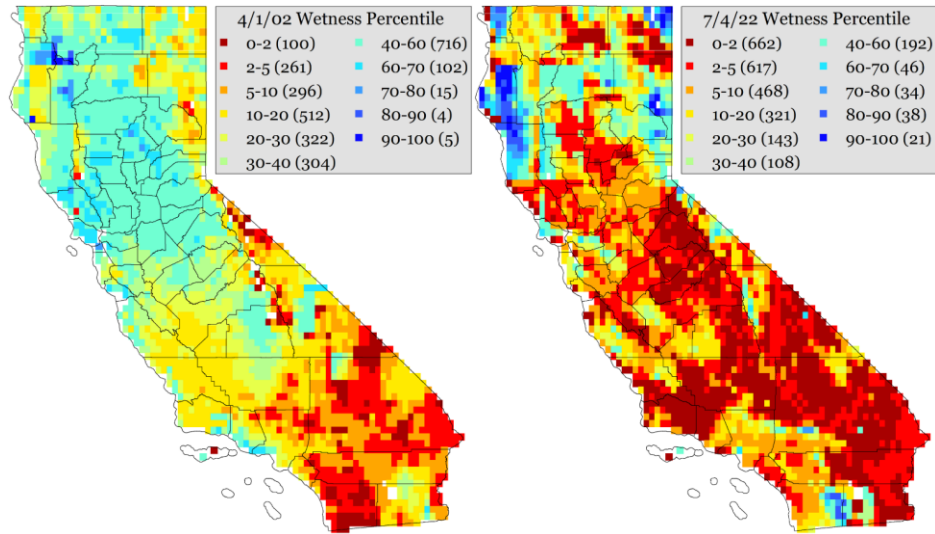
Figure 7 Shallow groundwater drought indicator maps for California generated from NASA's Gravity Recovery and Climate Experiment (GRACE) satellites for April 1, 2002 (the first available dataset) and July 4, 2022. The GRACE satellites detect minor changes in the Earth's gravity field due to changes in water storage on and beneath the land surface. The drought indication is expressed as a wetness percentile relative to the period 1948-2012, with water storage anomalies pre-2002 estimated with models based on long-term meteorological data. The numbers in parenthesis represent the number of grid cells within the designated wetness percentile. For example, on April 1, 2002, 361 out of 2,637 cells (13.7%) were below the 5th percentile relative to the 1948-2012 period. By July 4, 2022, more than 20 years into the megadrought, this fraction below the 5th percentile had increased to 48%. Data obtained from NASA (2022).
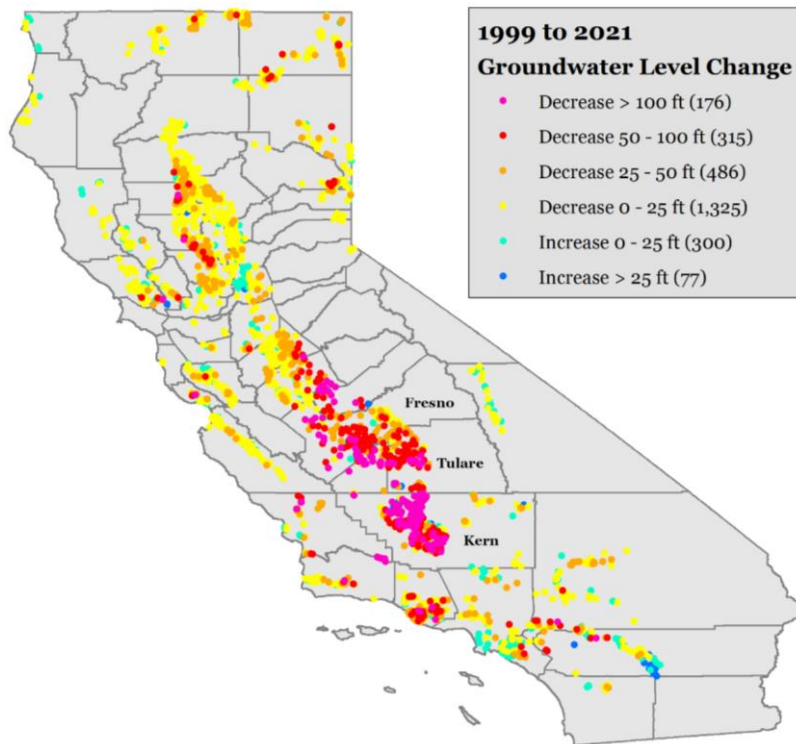

Figure 8 Groundwater level change for 2,679 wells in California, calculated as the average 1999 value (before megadrought onset) compared to the average 2021 value in the California Department of Water Resources (CADWR) Periodic Groundwater Level Measurements database (https://data.cnra.ca.gov/periodic-groundwater-level-measurements)

The numbers in parenthesis represent the number of wells within the designated groundwater level change category. For example, 491 out of the 2,679 wells (18.3%) experienced a level decrease of more than 50 feet. Wells with levels that decreased above 100 ft are clustered in the southern Central Valley, in the San Joaquin River and Tulare Lake hydrologic regions. This includes Fresno, Tulare, and Kern Counties, which are the three counties with the highest gross values of agricultural production (Figure 4).
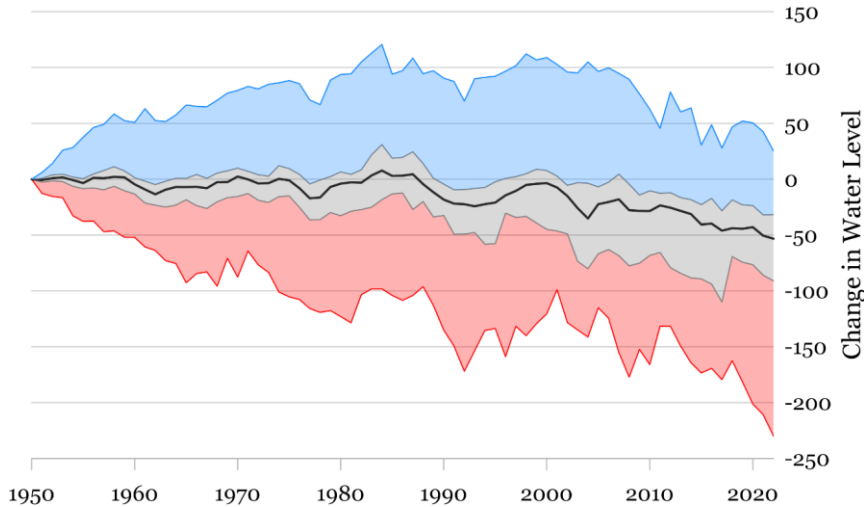
Figure 9 Cumulative groundwater level changes in feet for 73 wells with available data in 1950 in the San Joaquin Valley basin, from the CADWR Groundwater Sustainability Plan (GSP) dataset: https://data.cnra.ca.gov/dataset/gspmd (CADWR, 2022d). The black line is the median change for the group of wells, which was relatively stable until 2000 when the megadrought began, and the median change dropped to -50 feet relative to the 1950 value.

The gray shaded region corresponds to the interquartile range (25-75th percentile) level changes, while the blue shaded region corresponds to the 5th-25th percentile level changes, and the red shaded region corresponds to the 75-95th percentile level changes. More than 75 percent of the wells have experienced a decrease in water level above 25 feet. Beyond the possibility of wells going dry or having reduced productivity, such significant decreases in water level translate to increased pumping costs. For reference, Tulare County Cooperative Extension Publication IG6-96 provides the simple calculation that the energy required to lift one acre-foot of water one foot in elevation is 1.46 kilowatt-hours (kWh) at a typical operating system efficiency of 70% (UC Cooperative Extension, 1996). If 100 acres of land covered by almond and pistachio crops requires on average 350 acre-feet per year of irrigation (Table 1), the incremental energy required to lift groundwater 50 feet (the median change since 1950) is approximately 25,550 kWh per year. At a blended electricity rate of $0.20/kWh this translates to a cost of approximately $5,110 per year, which is negligible compared to the potential revenues that can be generated from this land.

Table 2: Number of statewide dry well reports and new well completion reports (irrigation and domestic) in California for the five water years (WYs) from 2017-2021, from CADWR (2022e). The two counties with the most irrigation wells installed over this timeframe were Tulare (969 wells) and Fresno (677 wells), with the two counties accounting for a combined 325 dry well reports (25% of the total over the 5 WYs).

	Dry Well Reports	Domestic Wells	Irrigation Wells	Total Wells
WY 2017	123	2,817	1,422	4,239
WY 2018	72	2,245	1,033	3,278
WY 2019	51	2,824	1,354	4,178
WY 2020	84	3,046	1,322	4,368
WY 2021	953	3,467	1,626	5,093
5-WY Totals	**1,283**	**14,399**	**6,757**	**21,156**
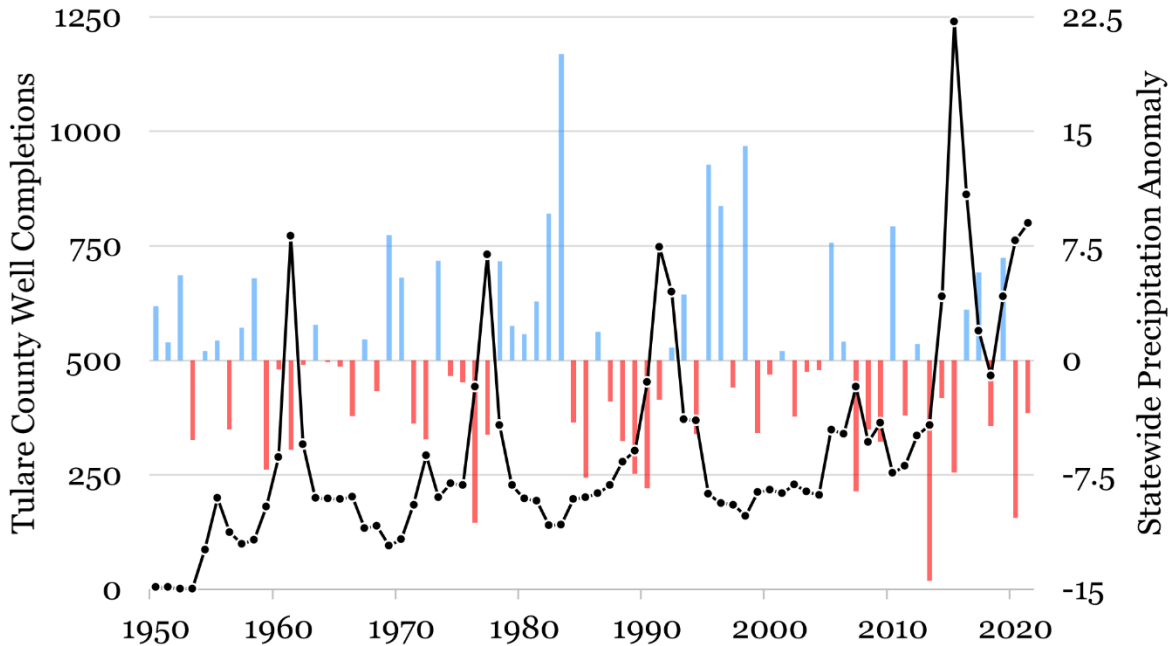
Figure 10 Annual number of reported well completions (irrigation and domestic) in Tulare County since 1950, plotted against the statewide average annual precipitation anomaly, in inches greater or less than the statewide average of 22.4 inches per year. The chart shows a clear pattern of increased well installations after multiple years of below-average precipitation, indicating increased reliance on groundwater during droughts. Data obtained from the CADWR Well Completion Report dataset, available at: https://data.cnra.ca.gov/dataset/well-completion-reports (CADWR, 2022f). Precipitation data from NOAA (2022).
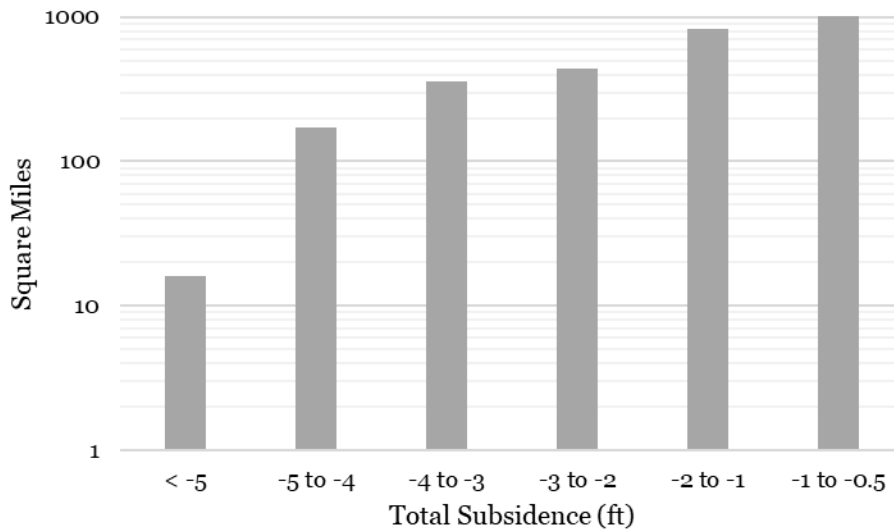
Figure 10 Land area subsidence in feet in the Tulare Lake and San Joaquin River hydrologic regions and between January 2015 and October 2021, from CADWR (2022e). These two regions accounted for approximately 97% of all land area with subsidence in California, with all subsidence greater than 4 ft in magnitude occurring in the Tulare Lake region.

References and Select Readings

Aeschbach-Hertig, W., Schlosser, P., Stute, M., Simpson, H.J., Ludin, A., and Clark, J.F., 1998. A ^{3}H/^{3}He study of groundwater flow in a fractured bedrock aquifer. *Ground Water*, v. 36, no. 4, pp. 661–670.

Aiken, G.R, 2002. Organic matter in ground water. In: Aiken, G.R. and E.L. Kuniansky (eds.), U.S. Geological Survey Open-File Report 02-89, pp. 21-23.

Alekin, O.A., 1953. Osnovi gidrohemii (Principles of hydrochemistry, in Russian). Gidrometeoizdat, Leningrad.

Alekin, O.A., 1962. Grundlages der wasserchemie. Eine einführung in die chemie natürlicher wasser. VEB Deutsch. Verl., Leipzig, 260 p. (originally published in Russian in 1953).

Allen, R.G, Pereira, L.S., Raes, D., and Smith, M., 1998. Crop evapotranspiration—Guidelines for computing crop water requirements. Food and Agriculture Organization (FAO) of the United Nations, Irrigation and Drainage Paper 56, Rome, Italy, 41 p.

Aller, L., Bennett, T.W., Hackett, G., Petty, R.J., Lehr, J.H., Sedoris, H., Nielson, D.M., and Denne, J.E., 1989. Handbook of Suggested Practices for the Design and Installation of Ground-Water Monitoring Wells; U.S. Environmental Protection Agency, EPA/600/4-89/034, 398 p.

Aller, L., Bennett, T.W., Hackett, G., Petty, R.J., Lehr, J.H., Sedoris, H., Nielson, D.M., and Denne, J.E., 1991. Handbook of Suggested Practices for the Design and Installation of Ground-Water Monitoring Wells; U.S. Environmental Protection Agency, EPA160014-891034, 221 p.

Alley, W.M., and Leake, S.A., 2004. The journey from safe yield to sustainability. *Ground Water*, vol. 42, no. 1, pp. 12–16.

Alley, W.M., Reilly, T.E., and O. L. Franke, 1999. Sustainability of ground-water resources. U.S. Geological Survey Circular 1186. Denver, Colorado, 79 p.

Allison, G.B., and Hughes, M.W., 1978. The use of environmental chloride and tritium to estimate total recharge to an unconfined aquifer. Australian Journal of Soil Resources, v. 16, pp. 181−195.

ASCE (American Society of Civil Engineers), 2001. Standard Guidelines for Artificial Recharge of Groundwater. ASCE Standard No. 34-01, 120 p.

Anders, R., and Schroeder, R.A., 2003. Use of water-quality indicators and environmental tracers to determine the fate and transport of recycled water in Los Angeles County, California. U.S. Geological Survey Water-Resources Investigations Report, 03–4279, Sacramento, CA, 104 p.

Anderson, M.T., and L.H. Woosley, Jr., 2005. Water availability for the Western United States—Key scientific challenges. U.S. Geological Survey Circular 1261, Reston, Virginia, 85 p.

Anderson, J.A., Morin, R.H., Cannia, J.C., and Williams, J.H., 2009. Geophysical log analysis of selected test holes and wells in the High Plains aquifer, Central Platte River basin, Nebraska: U.S. Geological Survey Scientific Investigations Report 2009–5033, 16 p.

Andreychouk V., Dublyansky Y., Yezhov Y., and Lysenin G., 2009. Karst in Earth's Crust: distribution and the main types. University of Silesia and Ukrainian Institute of Speleology and Karstology, Sosnowiec—Simferopol, 72 p.

Appelo, C.A.J., and Postma, D., 2005. Geochemistry, groundwater and pollution, 2nd edition. A.A. Balkema Publishers, Leiden, The Netherlands, 649 p.

Arthur, D.A., Dabous, A.A., and J.B Cowart, 2002. Mobilization of arsenic and other trace elements during aquifer storage and recovery, southwest Florida. In: Aiken, G.R. and E.V. Kuniansky (eds.), U.S. Geological Survey Artificial Recharge Workshop Proceedings, April 2-4, 2002, Sacramento, California, U.S. Geological Survey Open-File Report 02-89

References and Select Readings

Arthur, D.A., Upchurch, S., Skiles, W., Kincaid, T., Davis, H., and McGurk, B., 2004. Panel II. Delineation of springshed boundaries. Workshop to develop blue prints for the management and protection of Florida's springs, May 8-9, 2002, Ocala, Florida. Florida Geological Survey Special Publication No. 51.

ASTM (American Society for Testing and Materials), 1998. Standard Guide for Remediation of Ground Water by Natural Attenuation at Petroleum Release Sites. E 1943-98, West Conshohocken, PA.

ASTM, 1999. ASTM standards on determining subsurface hydraulic properties and ground water modeling, Second Edition. West Conshohocken, Pennsylvania, 320 p.

Atlas, R.M., 1984. Microbiology—fundamentals and applications. Macmillan, New York, 880 p.

ATTAC (Alaska Training/Technical Assistance Center), 2014.Introduction to Small Water Systems: A Course for Level I Operators. University of Alaska SE (UAS) Sitka Campus, Sitka, AK

AWWA (American Water Works Association), 1998. AWWA standard for water wells; American National Standard. ANSI/AWWA A100-97, AWWA, Denver, CO.

Ayotte, J.D., Montgomery, D. L., Flanagan, S.M., and Robinson, K.W., 2003. Arsenic in Groundwater in Eastern New England: Occurrence, Controls, and Human Health Implications. *Environmental Science & Technology*: Vol. 37, No. 10, 2075-2083.

Aziz, C.E., Newell, C.J., Gonzales, J.R., Haas, P., Clement, T.P., and Sun, Y., 2000. BIOCHLOR: Natural attenuation decision support system v. 1.0; User's manual. EPA/600/R-00/008. U.S. Environmental Protection Agency, Cincinnati, Ohio.

Back, W., and R.A. Freeze (eds.), 1983. Chemical hydrogeology. Benchmark Papers in Geology, 73, Hutchinson Ross Publication Company, Stroudsburg, PA, 416 p.

Baedecker, M.J. and I.M. Cozzarelli. 1992. The determination and fate of unstable constituents in contaminated groundwater. In: Lesage, S., and R. Jackson (eds), Ground water contamination and analysis at hazardous waste sites. New York: Marcel Dekker, Inc., pp. 425-461.

Bakhbakhi, M., 2006. Nubian sandstone aquifer. In: Foster, S. and D.P. Loucks (Eds.), 2006. Non-renewable groundwater resources; A guidebook on socially-sustainable management for water-policy makers. IHP-VI, Series on Groundwater No. 10, UNESCO, Paris, p. 75-81.

Banks, W.S.L., and Battigelli, D.A., 2002. Occurrence and distribution of microbiological contamination and enteric viruses in shallow ground water in Baltimore and Harford Counties, Maryland. U.S. Geological Survey Water-Resources Investigations Report 01-4216, Baltimore, MD, 39 p.

Barcelona, M.J, Wehrmann, H.A., Schock, M.R., Sievers, M.E., and J.R. Karny, 1989. Sampling Frequency for Ground-Water Quality Monitoring. Water Survey Division, Illinois Department of Energy and Natural Resources, Champaign, Illinois. EPA 600-4-89-032, Pre-issue Copy

Barcelona, M.J., H.A. Wehrmann, J.F. Keely, and W.A. Pettyjohn, 1990. Contamination of Ground Water: Prevention, Assessment, Restoration. Pollution Technology Review No. 184, Noyes Data Corporation, Park Ridge, NJ, 213 p.

Barenblatt, G.E., Zheltov, I.P, and Kochina, I.N., 1960. Basic concepts in the theory of seepage of homogeneous liquids in fissured rocks. *Journal of Applied Mathematics and Mechanics*, v. 24, pp. 1286-1303.

Barker, R., 2007. Water hearing will affect users statewide. Idaho Statesman (December 10).

Barlow, P.M., 2003. Ground water in freshwater-saltwater environments of the Atlantic coast. U.S. Geological Survey Circular 1262, Reston, Virginia, 113 p.

Bartlett, R.J. and James, B., 1979. Behavior of chromium in soils: III. Oxidation, *J. Environ. Qual.,* v. 8, p. 31–35.

Bathurst, R.G.C., 1975. Carbonate sediments and their diagenesis. Second Enlarged Edition. Developments in Sedimentology 12, Elsevier, Amsterdam, 658 p.

BATTELLE, 1997. Engineering evaluation and cost analysis for bioslurper initiative (A005). Prepared for U.S. Air Force Center for Environmental Excellence, Brooks AFB, Texas. BATTELLE, Columbus, OH, 87 p.

Bear, J., 1979. Hydraulics of groundwater. McGraw Hill Series in Water Resources and Environmental Engineering, McGraw Hill, New York, 567 p.

Bear, J., Tsang, C.F., and G. deMarsily (eds.), 1993. Flow and contaminant transport in fractured rock. Academic Press, San Diego, 548 p.

Bear, J., Cheng, A.H.-D., Sorek, S., Ouazar, D., and I. Herrera (eds.), 1999. Seawater intrusion in coastal aquifers—Concepts, methods and practices. Kluwer Academic Publishers, Dordrecht, The Netherlands, 625 p.

Beckman, H.C., and N.S. Ninchey, 1944. The Large Springs of Missouri. Vol. XXIX, Second Series. Missouri Geological Survey and Water Resources, Rolla, Missouri, 141 p.

Bedinger, M.S., 1987. Summary of infiltration rates in arid and semiarid regions of the world, with an annotated bibliography. U.S. Geological Survey Open-File Report 87-43, Denver, Colorado, 48 p.

Bennett, M.J., Noce, T.E., and Lienkaemper, J. J., 2011. Cone penetration tests and soil borings at the Mason Road site in Green Valley, Solano County, California; U.S. Geological Survey Open-File Report 2011- 1281, 52 p. and 3 data tables, available at http://pubs.usgs.gov/of/2011/1281/.

Bense, V.F., Van den Berg, E.H., and R.T. Van Balen, 2003. Deformation mechanisms and hydraulic properties of fault zones in unconsolidated sediments; the Roer Valley Rift System, The Netherlands. *Hydrogeology Journal*, v. 11, p. 319-332.

Bentall, R., compiler, 1963a. Shortcuts and special problems in aquifer tests. *U.S. Geological Survey Water-Supply Paper* 1545-C.

Bentall, R., compiler, 1963b. Methods of determining permeability, transmissibility, and drawdown. *U.S. Geological Survey Water-Supply Paper* 1536-I.

Bexfield, L.M., Toccalino, P.L., Belitz, K., Foreman, W.T., and Furlong, E.T., 2019. Hormones and pharmaceuticals in groundwater used as a source of drinking water across the United States. *Environmental Science and Technology*, DOI: 10.1021/acs.est.8b05592.

Bloch, S., 1991. Empirical prediction of porosity and permeability in sandstones. *American Association of Petroleum Geologists Bulletin*, v. 75, n. 7, pp. 1145-1160.

Boulton, N.S., 1954a. The drawdown of the water table under nonsteady conditions near a pumped well in an unconfined formation. *Inst. Civil Engineers Proc*. (London), pt.3, p. 564-579.

Boulton, N.S., 1954b. Unsteady radial flow to a pumped well allowing for delayed yield from storage. *Internat. Assoc. Sci. Hydrology Pub*. 37, p. 472-477.

Boulton, N.S., 1963. Analysis of data from non-equilibrium pumping tests allowing for delayed yield from storage. *Inst. Civil Engineers Proc*. (London), Vol. 26, pp. 469-482.

Boulton, N.S., 1970. Analysis of data from pumping tests in unconfined anisotropic aquifers. *Journal of Hydrology*, 10, pp. 369

Boulton, N.S., 1973. The influence of delayed drainage on data from pumping tests in unconfined aquifers: *Journal of Hydrology*, v. 19, no. 2, pp. 157-169.

Boulton, N.S., and J.M.A. Pontin, 1971. An extended theory of delayed yield from storage applied to pumping tests in unconfined anisotropic aquifers. *Journal of Hydrology*, 19, p. 157-169.

Bourg, A.C.M., and Loch, J.P.G., 1995. Mobilization of heavy metals as affected by pH and redox conditions. In: Salomons, W., and Stigliani, W.M. (eds.), Chapter 4, Biogeodynamics of pollutants in soils and sediments; Risk assessment of delayed and non-linear responses, Springer, Berlin, pp. 815-822.

Bouwer, H., 1989. The Bouwer and Rice slug test. *Ground Water*, v. 27, no.3, pp. 304-309.

Bouwer, H., 2002. Artificial recharge of groundwater: Hydrogeology and engineering. Hydrogeology Journal, vol. 10, pp. 121–142.

Bouwer, H., and R.C. Rice, 1976. A slug test method for determining hydraulic conductivity of unconfined aquifers with completely or partially penetrating wells. *Water Resources Research*, v. 12, no. 3, pp. 423-428.

Bouwer, E.J., Rittman, B.E., and McCarty, P.L., 1981. Anaerobic degradation of halogenated 1- and 2-carbon organic compounds. *Environmental Science & Technology*, vol. 15, no. 5, pp. 596–599.

Božičević, S., 1971. Primjena speleologije pri injektiranjima u krsu (Application of speleology in grouting of karst terranes; in Croatian). 1st Yugoslav Symposium on Hydrogeology and Engineering Geology, Herceg Novi.

Bögli, A., 1980. Karst hydrology and physical speleology. Springer-Verlag, New York, 284 p.

Böhlke, J-K, 2002. Groundwater recharge and agricultural contamination. *Hydrogeology Journal,* v. 10, no. 1, p. 153–179.

Böhlke, J.K., and Denver, J.M., 1995. Combined use of groundwater dating, chemical, and isotopic analyses to resolve the history and fate of nitrate contamination in two agricultural watersheds, Atlantic coastal plain, Maryland. *Water Resources Research*, v. 31, p. 2319-2339.

Breckenridge, R.M., and Hinckley, B.S., 1978. Thermal springs of Wyoming: Geological Survey of Wyoming Bulletin 60, 104 p.

Bredehoeft, J.D. 1997. Safe Yield and the Water Budget Myth. *Ground Water*, Vol. 35, No. 6, pp. 929.

Broner, I. and Schneekloth, J., 2007. Seasonal water needs and opportunities for limited irrigation for Colorado Crops. Colorado State University Extension, accessed on-line August 2007. http://www.ext.colostate.edu/Pubs/crops/04718.html

Brooks, R. H., and A. T. Corey, 1964. Hydraulic properties of porous media. *Hydrology Paper* No. 3, Colorado State Univ., Fort Collins, Colorado, 27 p.

Brown, P., 2000. Basis of evaporation and evapotranspiration. Turf Irrigation Management Series: I, the University of Arizona College of Agriculture, Tucson, Arizona, 4 p.

Brune, G., 1975. Major and Historical Springs of Texas, Texas Water Development Board Report 189, Austin.

Bureau of Reclamation, 2001. Water Measurement Manual. A Water Resources Technical Publication. Water Resources Research Laboratory, U.S. Department of Interior, Washington, D.C., various paging.

Butler, J.J., Jr., Garnett, E.J. and J.M. Healey, 2003. Analysis of slug tests in formations of high hydraulic conductivity. *Ground Water*, v. 41, no. 5, p. 620-630.

Butler, P.B., Larsen-Hallock, L., Lewis, R., Glenn, C. and Armstead, R., 2011. Metrics for Integrating Sustainability Evaluations into Remediation Projects. *Remediation Journal*, 21:81–87. doi: 10.1002/rem.20290

Cacas, M.C., 1989. Développment d'un modèle tridimensionel stochastique discret por la simulation de l'écoulement et des transports de masse et de chaleur en milieu fracturé. Ph.D. thesis, Ecole des Mines de Paris, Fontainebleau, France.

CADWR (California Department of Water Resources), 2022a. Agricultural Water Use Efficiency. Available at: https://water.ca.gov/Programs/Water-Use-And-Efficiency/Agricultural-Water-Use-Efficiency

CADWR (California Department of Water Resources), 2022b. Sustainable Groundwater Management Act (SGMA). Available at: https://water.ca.gov/programs/groundwater-management/sgma-groundwater-management

CADWR (California Department of Water Resources), 2022c. Periodic Groundwater Level Measurements. Available at: https://data.cnra.ca.gov/dataset/periodic-groundwater-level-measurements

CADWR (California Department of Water Resources), 2022d. GSP Monitoring Data. Available at: https://data.cnra.ca.gov/dataset/gspmd

CADWR (California Department of Water Resources), 2022e. Groundwater Conditions Report Water Year 2021. https://water.ca.gov/-/media/DWR-Website/Web-Pages/Programs/Groundwater-Management/Data-and-Tools/Files/Statewide-Reports/Groundwater-Conditions-Report-Fall-2021.pdf

CADWR (California Department of Water Resources), 2022f. Well Completion Reports. Available at: https://data.cnra.ca.gov/dataset/well-completion-reports

CADWR (California Department of Water Resources), 2020. California's Most Significant Droughts: Comparing Historical and Recent Conditions. Available at: https://water.ca.gov/water-basics/drought

CADWR (California Department of Water Resources), 2014. The Strategic Plan, California Water Today, Volume 1, Chapter 3 (California Water Balance by Water Year Data Table (MAF)), pp. 3-35.

CADWR (California Department of Water Resources), 2003. California's groundwater. Bulletin 118, Update 2003. State of California, The Resources Agency, Department of Water Resources, 246 p.

CADWR (California Department of Water Resources), 1991. California Well Standards. Water wells, Monitoring wells, Cathodic protection wells. Bulletin 74-90 (Supplement to Bulletin 74-81), Sacramento, CA, 82 p.

CADRW (California Department of Water Resources), 1961. Bulletin 104 Planned Utilization of the Ground Water Basins of Coastal Plain of Los Angeles County. Appendix A, Ground Water Geology.

Cal/EPA (The California Environmental Protection Agency), 1995. Drilling, Coring, Sampling and Logging at Hazardous Substance Release Sites: Guidance Manual for Ground Water Investigations, 27 p.

Campbell, M.D., and Lehr, J.H., 1973. Water Well Technology. McGraw-Hill, New York, 681 p.

CDC (Center for Disease Control), 2022. https://www.cdc.gov/parasites/

CDFA (California Department of Food & Agriculture), 2021. California Agricultural Statistics Review 2020-2021. Available at: https://www.cdfa.ca.gov/Statistics/PDFs/2021_Ag_Stats_Review.pdf

Cederstrom, D.J., 1972. Evaluation of yields of wells in consolidated rocks, Virginia to Maine: U.S. Geological Survey Water-Supply Paper 2021, 38 p.

Chapelle, F.H., 1993. Ground-Water Microbiology and Geochemistry. John Wiley & Sons, New York, 424 p.

Chebaane, M., Zaabi, A.A., Hamdy, A.A., Busafi, A.A., 1994. Springs of the Sultanate of Oman. Ministry of Water Resources, Sultanate of Oman, 37 p.

Chilès, J.P., 1989a. Three-dimensional geometric modeling of a fracture network. In: Geostatistical Sensitivity, and Uncertainty Methods for Ground-Water Flow and Radionuclide Transport Modeling, B.E. Buxton (ed.), Battelle Press, Columbus, Ohio, p. 361-385.

Chilès, J.P., 1989b. Modélisation géostatistique de réseaux de fractures. In: Geostatistics, M. Armstrong (ed.), Kluwer Academic Publ., Dordrecht, Netherlands, Vol.1, p.57-76.

Chilès, J.P. and G. de Marsily, 1993. Stochastic models of fracture systems and their use in flow and transport modeling. In: Flow and Contaminant Transport in Fractured Rock. J. Bear, C.F. Tsang and G. de Marsily, (eds.), Academic Press, San Diego, p. 169-236.

Choquette, P.W. and Pray, L.C., 1970. Geologic Nomenclature and Classification of Porosity in Sedimentary Carbonates. *American Association of Petroleum Geologists Bulletin*, 54, 207-250.

Clarke, J.S. et al., 2004. Hydraulic properties of the Floridan Aquifer System and equivalent clastic units in coastal Georgia and adjacent parts of South Carolina and Florida. Georgia Geologic Survey Information Circular 109, Atlanta, Georgia, 50 p.

Clemens, S.S., Swistock, B.R., and William E. Sharpe, W.E., 2007. Spring Development and Protection, Water Facts #4. The Pennsylvania State University, School of Forest Resources, College of Agricultural Sciences, Cooperative Extension, 6 p.

References and Select Readings

Clinton, T., 2007. Reclaimed Water Aquifer Storage and Recovery; Potential Changes in Water Quality. Water Reuse Foundation, Alexandria, VA, 146 p.

Coes, A.L., and Pool, D.R., 2005. Ephemeral-stream channel and basin-floor infiltration and recharge in the Sierra Vista subwatershed of the upper San Pedro basin, Southeastern Arizona. U.S. Geological Survey Open-File Report 2005–1023, Reston, Virginia, 67 p.

Cohen, R.M., and J.W. Mercer, 1993. DNAPL site evaluation. C.K. Smoley-CRC Press, Boca Raton, Florida.

Cohen, R. M., Vincent, A.H, Mercer, J.W., Faust, C.R., and Spalding, C.P., 1994. Methods for Monitoring Pump-and-Treat Performance. EPA Contract No. 68-C8-0058. Office of Research and Development, EPA/6OO/R-94/123, Ada, OK, 114 p.

Cohen, R.M., Faust, C.R., and D.C. Skipp, 2009. Case Study: Evaluating Groundwater Supplies in Fractured Metamorphic Rock of the Blue Ridge Province in Northern Virginia. In: Kresic, N., Groundwater Resources: Sustainability, Management, and Restoration. McGraw Hill, New York, p. 177-184

Colebrook, C.F., 1939. Turbulent flow in pipes, with particular reference to the transition region between smooth and rough pipe laws. *Journal of the Institution of Civil Engineers*, London, vol. 11, p. 133-156.

Cook, P.G., 2003. A guide to regional groundwater flow in fractured aquifers. CSIRO Land and Water, Seaview Press, Henley Beach, South Australia, 108 p.

Cooper, H.H., Jr., 1963. Type curves for nonsteady radial flow in an infinite leaky artesian aquifer. In: Bentall, R., Compiler: Shortcuts and special problems in aquifer tests. *U.S. Geological Survey Water-Supply Paper* 1545-C, p. C48-C55.

Cooper, H.H., Bredehoeft, J.D. and S.S. Papadopulos, 1967. Response of a finite-diameter well to an instantaneous charge of water, *Water Resources Research*, v. 3, no. 1, pp. 263-269.

Copeland, R., 2003. Florida Spring Classification System and Spring Glossary. Florida Geological Survey, Tallahassee, Florida, 17 p.

Cosgrove, W.J., and Rijsberman, F.R., 2000. World Water Vision: Making Water Everybody's Business. World Water Council, Earthscan Publications Ltd., London, 108 p.

Costain, J.K., Keller, G.V., and Crewdson, R.A., 1976. Geological and geophysical study of the origin of the warm springs in Bath County, Virginia. Blacksburg, Virginia Polytechnic Institute and State University Report for U.S. Department of Energy under Contract E-(40-1)-4920.

Cressler, C.W., Thurmond, C.J., and Hester, W.G., 1983. Ground water in the greater Atlanta region, Georgia: Georgia Department of Natural Resources, UoS. Environmental Protection Agency, and The Georgia Geologic Survey, in cooperation with U.S. Geological Survey, Information Circular 63, 143 p.

Crook, J.K., 1899. The mineral waters of the United States and their therapeutic uses. Lea Brothers & Co., New York, 588 p.

Cunningham, K.J., Kluesner, J.W., Westcott, R.L., Robinson, Edward, Walker, Cameron, and Khan, S.A., 2018, Sequence stratigraphy, seismic stratigraphy, and seismic structures of the lower intermediate confining unit and most of the Floridan aquifer system, Broward County, Florida (ver. 1.1, January 2018): U.S. Geological Survey Scientific Investigations Report 2017–5109, 71 p., 21 pls., https://doi.org/10.3133/sir20175109

Currie, J., Greenstone, M., and Moretti, E., 2011. Superfund Cleanups and Infant Health. Massachusetts Institute of Technology Department of Economics Working Paper Series. Working Paper 11-02.

Cuyk, S.V., Siegrist, R., Logan, A., Massen, S., Fischer, E., and Figueroa, L., 1999. Purification of wastewater in soil treatment systems as affected by infiltrative surface character and unsaturated soil depth. In: WEFTEC99, Conference Proceedings of Water Environment Federation.

Cvijić, J., 1918. Hydrographie souterraine et évolution morphologique du karst. Recueil des Travaux de l'Institut de Géographie alpine, Grenoble, t. VI, fasc. 4, p. 1-56

Darcy, H., 1856. Les fontaines publiques de la ville de Dijon; Exposition et application des principes a suivre et des formulas a employer dans les questions de distribution d'eau; Appendice, Note D. Victor Dalmont, editeur, Libraire des Corps Imperiaux des Ports et Chausses et des Mines, Paris.

Daniel, C.C., III, 1985. Statistical analysis of water-well records from the Piedmont and Blue Ridge of North Carolina: Implications for well-site selection and well design (abs.), Geological Society of America Abstracts with Programs, v. 17, no. 2, p. 86-87.

Daniel, C.C., III, 1987. Statistical analysis relating well yield to construction practices and siting of wells in the Piedmont and Blue Ridge provinces of North Carolina: U.S. Geological Survey Water-Resources Investigations Report 86-4132, 54 p.

Daniel, C.C. III, 1990. Evaluation of site-selection criteria, well design, monitoring techniques, and cost analysis for a ground-water supply in Piedmont crystalline rocks, North Carolina. U.S. Geological Survey Water-supply Paper; 2341-B, 35 p.

Daniel, C.C., III, and Sharpless, N.B., 1983, Ground-water supply potential and procedures for well-site selection Upper Cape Fear River Basin, Cape Fear River Basin Study 1981-83: North Carolina Department of Natural Resources and Community Development and U.S. Water Resources Council in cooperation with U.S. Geological Survey, 73 p.

Daniel, C.C. III, Douglas G. Smith, D.G., and Jo L. Eimers, J.L., 1997. Hydrogeology and simulation of ground-water flow in the thick regolith-fractured crystalline rock aquifer system of Indian Creek Basin, North Carolina. Chapter C, Ground-Water Resources of The Piedmont-Blue Ridge Provinces of North Carolina. U.S. Geological Survey Water-Supply Paper 2341, pp. C1-C137

Daniel, C.C. III, and Dahlen, P.R., 2002. Preliminary Hydrogeologic Assessment and Study Plan for a Regional Ground-Water Resource Investigation of the Blue Ridge and Piedmont Provinces of North Carolina, U.S. Geological Survey Water Resources Investigations Report 02-4105, Raleigh, N.C., 60 p.

Danish EPA, 1999. Natur og Miljøpolitisk Redegørelse 1999. Miljø- og Energiministeriet. (Nature and Environment Policy Statement 1999, in Danish). Environment and Energy, Copenhagen, Denmark. Available at http://www.mem.dk/publikationer/nmpr99/

Danskin, W.R., McPherson, K.R., and L.R. Woolfenden, 2006. Hydrology, description of computer models, and evaluation of selected water-management alternatives in the San Bernardino area, California. U.S. Geological Survey Open-File Report 2005-1278, Reston, VA, 178 p.

Davis, S.N., and R.J.M. DeWiest, 1991. Hydrogeology. Krieger Publishing Company, Malabar, Florida, 463 p.

Davis, S.N., D.J. Campbell, H.W. Bentley, and T.J. Flynn. 1985. Groundwater Tracers National Water Well Association, Worthington, Ohio, 200 p.

Dawson, K., and J. Istok, 1992. *Aquifer testing; design and analysis*. Lewis Publishers, Boca Raton, FL, 280 p.

Davis, S.N., and R.J.M. DeWiest, 1991. Hydrogeology. Krieger Publishing Company, Malabar, Florida, 463 p.

Deeb, R., Hawley, E., Kell, L., and O'Laskey, R., 2011. Assessing Alternative Endpoints for Groundwater Remediation at Contaminated Sites. ESTCP Project ER-200832, 232 p.

Delin, G.N., Essaid, H.I., Cozzarelli, I.M., Lahvis, M.H., and B.A. Bekins, 1998. Ground Water Contamination by Crude Oil near Bemidji, Minnesota. USGS Fact Sheet 084-98, 4 p.

Delin, G.N., and J.D. Falteisek, 2007. Ground-water recharge in Minnesota. U.S. Geological Survey Fact Sheet 2007-3002, 6 p.

Dettinger, M.D., 1989. Distribution of carbonate-rock aquifers in southern Nevada and the potential for their development, summary of findings, 1985-88. Program for the Study and Testing of Carbonate-Rock Aquifers in Eastern and Southern Nevada, Summary Report No. 1, Carson City, Nevada, 37 p.

References and Select Readings

Derek, F.C., and Paul Williams, P., 2007. Karst Hydrogeology and Geomorphology. Revised Edition. John Wiley & Sons Ltd, Chichester, England, 576 p.

Detay, M., 1997. Water Wells; Implementation, Maintenance and Restoration. John Wiley & Sons, Chichester, England, 379 p.

DEUS (Department of Energy, Utilities and Sustainability)., 2004. Integrated water cycle management guidelines for NSW local water utilities. New South Wales Government, 81 p.

Dieter, C.A., Maupin, M.A., Caldwell, R.R., Harris, M.A., Ivahnenko, T.I., Lovelace, J.K., Barber, N.L., and Linsey, K.S., 2018. Estimated use of water in the United States in 2015: U.S. Geological Survey Circular 1441, 65 p., https://doi.org/10.3133/cir1441. [Supersedes USGS Open-File Report 2017–1131.]

Dillard, L.A., Essaid, H.I., and Herkelrath, W.N., 1997, Multiphase flow modeling of a crude-oil spill site with a bimodal permeability distribution. *Water Resources Research*, v. 33, p. 1617-1632.

Dillon P., and Pavelic, P., 1996. Guidelines on the quality of stormwater and treated wastewater for injection into aquifers for storage and reuse. Research Report No 109, Urban Water Research Association of Australia, Water Services Association of Australia, Melbourne.

Dillon, P., et al., 1997. Aquifer storage and recovery of stormwater runoff. Water Journal of the Australian Water Association, vol. 24, no. 4, pp. 7–11.

Dillon, P., and Molloy, R., 2006. Developing Aquifer Storage and Recovery (ASR) opportunities in Melbourne; Technical guidance for ASR. CSIRO Land and Water Science Report 4/06, 24 p.

Dimitrijević, M.D., 1977. Geološko kartiranje (in Serbian; Geological Mapping). ICS, Beograd, 486 p.

Dimitrijević, N.S., 1988. Hidrohemija (in Serbian; Hydrochemistry,). Univerzitet u Beogradu (University of Belgrade), Beograd (Belgrade), 313 p.

Dingman, S.L., 1994. Physical hydrology. Macmillan Publishing Company, New York, 575 p.

Domenico, P.A. 1987. An analytical model for multidimensional transport of a decaying contaminant species. *Journal of Hydrology*, v. 91, no. 1–2, pp.49–58.

Domenico, P.A., and Robbins, G.A., 1985. A new method of contaminant plume analysis. *Ground Water*, vol. 23, no. 4, pp. 476–485.

Domenico, P.A., and F.W. Schwartz, 1990. Physical and chemical hydrogeology. John Wiley & Sons, New York, 824 p.

Dowdle, P.R., A.M. Laverman, and R.S. Oremland. 1996. Bacterial dissimilatory reduction of arsenic (V) to arsenic (III) in anoxic sediments. *Applied Environmental Microbiology* 62, no. 5: 1664-1669.

Dragišić, V., and Živanović, V., 2014. Opšta hidrogeologija (in Serbian; General Hydrogeology). Univerzitet u Beogradu (University of Belgrade), Rudarsko-geoloski Fakultet (School of Mining and Geology), Beograd (Belgrade), 487 p.

Drew, L.J., Southworth, S., Sutphin, D.M., Rubis, G.A., Schuenemeyer, J.H., and W.C. Burton, 2004. Validation of the relation between structural patterns in fractured bedrock and structural information interpreted from 2D-variogram maps of water-well yields in Loudoun County, Virginia. *Natural Resources Research*, 13(4):255-264.

Driscoll, F.G. 1986. Ground Water and Wells, 2nd edition. Johnson Division, St. Paul, Minnesota, 1089 p.

Dugan, J.T., and Peckenpaugh, J.M., 1985. Effects of climate, vegetation, and soils on consumptive water use and ground-water recharge to the central Midwest regional aquifer system, mid-continent United States. U.S. Geological Survey Water-Resources Investigations Report 85-4236, Lincoln, Nebraska, 78 p.

Dupuit, J., 1863. Études théoriques et pratiques sur le mouvement des eaux dans les canaux découverts et à travers les terrains perméables. Paris, Dunod, Editeur, Quai des Augustins, nº 49.

EC (European Commission), 2008. Groundwater protection in Europe. Luxembourg: Office for Official Publications of the European Communities, 35 p.

EC (European Commission), 2023. Water Framework Directive. https://environment.ec.europa.eu/topics/water/water-framework-directive_en#contact

EEA (European Environment Agency), 2023. Europe's groundwater — a key resource under pressure. Briefing. https://www.eea.europa.eu/publications/europes-groundwater

EEA (European Environment Agency), 2018-2020. Water use in Europe — Quantity and quality face big challenges. https://www.eea.europa.eu/signals/signals-2018-content-list/articles/water-use-in-europe-2014/

Ellis, D.V. 1987. Well Logging for Earth Scientists. Elsevier, New York, 532 p.

Embrey, S.S., and Runkle, D.L., 2006. Microbial quality of the Nation's ground-water resources, 1993–2004. U.S. Geological Survey Scientific-Investigations Report 2006-5290, Reston, VA, 34 p.

European Environment Agency, 2018-2020. Water use in Europe — Quantity and quality face big challenges. https://www.eea.europa.eu/signals/signals-2018-content-list/articles/water-use-in-europe-2014/ Accessed February 4, 2021.

Eurostat Data Browser, 2021. Annual fresh water abstraction by source and sector. https://ec.europa.eu/eurostat/databrowser/view/ Accessed February 20, 2021

FAO, 1997. Seawater intrusion in coastal aquifers: Guidelines for study, monitoring and control. Water Reports 11, Food and Agriculture Organization of the United Nations, Rome, 152p.

Falkland, A.C., 1992. Review of Tarawa freshwater lenses. Hydrology and Water Resources Branch, ACT Electricity and Water, Prepared for AIDAB.

Faybishenko, B., Witherspoon, P.A., and S.M. Benson (eds.), Dynamics of Fluids in Fractured Rock, Geophysical Monograph 122, American Geophysical Union, Washington, D.C., 400 p.

Fayer, M.J., and Walters, T.B., 1995. Estimating recharge rates at the Hanford Site. Pacific Northwest National Laboratory, Richland, Washington, various paging.

Ferris, J.G., Knowles, D.B., Brown, R.H., and R.W. Stallman, 1962. Theory of aquifer tests. U.S. Geological Survey Water Supply Paper 1536-E, Washington, D.C., 173 p.

Feth, J.H., Rogers, S.M., and C.E. Roberson, 1961. Aqua de Ney, California, a spring of unique chemical character. *Geochimica et Cosmochimica Acta*, v. 22, p. 75-86.

Fitch, W.E., 1927. Mineral waters of the United States and American spas. Lea & Febiger, New York, 799 p.

Fleischhauer, H.L., and N. Korte, 1990. Formulation of cleanup standards for trace elements with probability plots. *Environ. Manage*. 14(1):95-105

Flint, A.L., and Flint, L.E., 2006. Modeling soil moisture processes and recharge under a melting snowpack. Proceedings, TOUGH Symposium May 15–17, 2006, Lawrence Berkeley National Laboratory, Berkeley, California.

Flores, R.M., Myers, M.D., Houseknecht, D.W., Stricker, G.D., Brizzolara, D.W., Ryherd, T.J., and Takahashi, K.I., 2007, Stratigraphy and facies of Cretaceous Schrader Bluff and Prince Creek Formations in Colville River Bluffs, North Slope, Alaska: U.S. Geological Survey Professional Paper 1748, 52 p.

Focazio, M.J., Plummer, L.N., Bohlke, J.K., Busenberg, Eurybiades, Bachman, L.J., and Powers, D.S., 1998. Preliminary estimates of residence times and apparent ages of ground water in the Chesapeake Bay watershed and water-quality data from a survey of springs. U.S. Geological Survey Water-Resources Investigations Report 97-4225, 75 p.

Ford, D., and Williams, P., 2007. Karst hydrogeology and geomorphology. John Wiley and Sons Ltd, The Atrium, Chichester, West Sussex, England, 562 p.

References and Select Readings

Ford, R.G., Wilkin, R.T., and Puls, R.W., editors, 2007. Monitored natural attenuation of inorganic contaminants in ground water. Volume1–Technical basis for assessment. EPA/600/R-07/139, the U.S. Environmental Protection Agency, National Risk Management Research Laboratory, Ada, OK, 78 p.

Foster, S.S.D., 1988. Quantification of ground-water recharge in arid regions – a practical view for resource development and management. In: Simmers, I. (ed.), Estimation of natural ground-water recharge: NATO ASI Series C, Reidel Publishing Co., v. 222, pp. 323-338.

Foster, S., Nanni, M., Kemper, K., Garduño, H., and Tuinhof, A., 2002–2005a. Utilization of non-renewable groundwater; a socially-sustainable approach to resource management. Sustainable Groundwater Management: Concepts and Tools, Briefing Note Series Note 11, GW MATE (Groundwater Management Advisory Team), The World Bank, Washington, DC, 6 p.

Foster, S., Garduño, H., Kemper, K., Tuinhof, A., Nanni, M., and Dumars, C., 2002–2005b. Groundwater quality protection defining strategy and setting priorities. Briefing Note Series Note 8, GW MATE (Groundwater Management Advisory Team), The World Bank, Washington, DC, 6 p.

Foster, S., and Loucks, D.P., editors, 2006. Non-renewable groundwater resources; A guidebook on socially-sustainable management for water-policy makers. IHP-VI, Series on Groundwater No. 10, UNESCO, Paris, 103 p.

Franke, O.L., Reilly, T.E., Buxton, H.T., and D.L. Simmons, 1990. Study guide for a beginning course in ground-water hydrology; Part 1, course participants. U.S. Geological Survey Open-File Report 90-183, Reston, Virginia, 184 p.

Freeze, R.A., and Cherry, J.A., 1979. Groundwater. Prentice-Hall, Englewood Cliffs, NJ, 604 pp.

Folk, R.L., 1959. Practical petrographic classification of limestones. *Am. Assoc. Petroleum Geologists Bull.*, v. 43, no. 1, pp. 1-38.

Folk, R.L., 1980. Petrology of sedimentary rocks. Hemphill Publishing Company, Austin, TX, 182 p.

Foster, S., Nanni, M., Kemper, K., Garduño, H., and Tuinhof, A., 2002–2005a. Utilization of non-renewable groundwater; a socially-sustainable approach to resource management. Sustainable Groundwater Management: Concepts and Tools, Briefing Note Series Note 11, GW MATE (Groundwater Management Advisory Team), the World Bank, Washington, DC, 6 p.

Foster, S., Garduño, H., Kemper, K., Tuinhof, A., Nanni, M., and Dumars, C., 2002–2005b. Groundwater quality protection defining strategy and setting priorities. Briefing Note Series Note 8, GW MATE (Groundwater Management Advisory Team), the World Bank, Washington, DC, 6 p.

Foster, S., and Loucks, D.P., editors, 2006. Non-renewable groundwater resources; A guidebook on socially-sustainable management for water-policy makers. IHP-VI, Series on Groundwater No. 10, UNESCO, Paris, 103 p.

Frumkin, A., and Shimron, A., 2006. Tunnel engineering in the Iron Age: Geoarchaeology of the Siloam Tunnel, Jerusalem. *Journal of Archaeological Science* 33 (2): 227–237.

Gale, I., 2005. Strategies for Managed Aquifer Recharge (MAR) in semi-arid areas. UNESCO, Paris, 30 p.

Gale, I.N., Williams, A.T., Gaus, I., and Jones, H.K., 2002. ASR-UK: Elucidating the hydrogeological issues associated with Aquifer Storage and Recovery in the UK. British Geological Survey Report No. CR/02/156/N, UK Water Industry Research Limited, London, 45 p.

Galloway, J.M., 2004. Hydrogeologic characteristics of four public drinking-water supply springs in northern Arkansas. U.S. Geological Survey Water-Resources Investigations Report 03-4307, Little Rock, AR, 68 p.

Galloway, D.L., Alley, W.M., Barlow, P.M., Reilly, T.E., and Tucci, P., 2003. Evolving issues and practices in managing ground-water resources: case studies on the role of science. U.S. Geological Survey Circular 1247, Reston, VA, 73 p.

Galloway, D., Jones, D.R., and S.E. Ingebritsen, 1999. Land subsidence in the United States. U.S. Geological Survey Circular 1182, Reston, Virginia, 177 p.

Gaon, M., 1975. Design of spring capture and Mihajlovac's waterworks (in Serbian). Hidrosanitas, WIGA Co., Belgrade, Serbia (unpublished).

Gaon, M., 1987. Sjenica water supply project. Design and report [in Serbian]. Hidrosanitas, WIGA Co., Belgrade, Serbia (unpublished).

Gelhar, L. W., and Axness, C.L., 1983. Three-dimensional stochastic analysis of macrodispersion in aquifers. *Water Resources Research*, v. 19, no. 1, pp. 161-180.

Gelhar, L.W., Welty, C. and Rehfeldt, K.R., 1992. A critical review of data on field-scale dispersion in aquifers. *Water Resources Research*, v. 28, no. 7, pp. 1955-1974.

Geoscience Australia, 2022. Great Artesian Basin. https://www.ga.gov.au/scientific-topics/water/groundwater/gab Accessed April 15, 2022

Gerba, C.P., 1999. Virus survival and transport in groundwater. *Journal of Industrial Microbiology and Biotechnology*, vol. 22, no. 4, pp. 247–251.

Gerba, C.P., and Goyal, S.M., 1985. Pathogen removal from wastewater during groundwater recharge. In: Artificial Recharge of Groundwater. Asano, T., editor. Butterworth Publishers, Boston, MA, pp. 283–317

Geva, H., 2023. Jerusalem Archaeological Sites: Biblical Water Systems. Jewish Virtual Library. https://www.jewishvirtuallibrary.org/biblical-water-systems-in-jerusalem#author

Geyh, M., 2000. Groundwater, saturated and unsaturated zone. In: Mook, W.G. (ed.), Environmental isotopes in the hydrological cycle; principles and applications. IHP-V, Technical Documents in Hydrology, No. 39, Vol. IV, UNESCO, Paris, 196 p.

Ghilarov, A., 1998. Lamarck and the prehistory of ecology. *International Microbiology*, v. 1, p. 161-164.

Giles, R.V., Evett, J.B., and L. Chiu, 1994. Fluid Mechanics and Hydraulics (Third Edition). Schaum's Outline Series, McGraw Hill, New York, 378 p.

Gleick, P.H., 1994. Water, war, and peace in the Middle East. Environment, vol. 36, no. 3, p. 6.

Gleick, P.H., 1996. Basic water requirements for human activities: Meeting basic needs. Water International, vol. 21, no. 2, pp. 83–92.

Gleick, P.H., 2006. Water Conflict Chronology. Pacific Institute for Studies in Development, Environment, and Security, Oakland, CA. Available at: www.worldwater.org/ conflictchronology.pdf.

Green, C., 2000. If only life were that simple; optimism and pessimism in economics. *Physics and Chemistry of the Earth, Part B: Hydrology, Oceans, and Atmosphere*, vol. 25, Issue 3, pp. 205–212.

Gollehon, N., and Quinby, W., 2006. Irrigation resources and water costs. In: Agricultural Resources and Environmental Indicators. Wiebe, K., and N. Gollehon, editors. United States Department of Agriculture, Economic Research Service, Economic Information Bulletin 16, pp. 24-32. www.ers.usda.gov

Gordon, C., Wall, K., Toze, S., and O'Hara, G., 2002. Influence of conditions on the survival of enteric viruses and indicator organisms in groundwater. In: Management of Aquifer Recharge for Sustainability. Dillon, P.J., editor. A.A. Balkema Publishers, Lisse, the Netherlands, pp. 133–138.

Granger, R. J., Gray, D. M., 1989. Evaporation from natural nonsaturated surfaces, *J. Hydrol.*, 111, 21–29

Gray, D.M., 1973. Handbook on the Principles of Hydrology. Water Information Center Incorporated, Minnesota, 591 p.

Greene, E.A. and A.M. Shapiro, 1995. Methods of conducting air-pressurized slug tests and computation of type curves for estimating transmissivity and storativity: *U.S. Geological Survey Open-File Report* 95–424.

Greene, E.A. and A.M. Shapiro, 1998. AIRSLUG: A FORTRAN program for the computation of type curves to estimate transmissivity and storativity of prematurely terminated air-pressurized slug tests. *Ground Water*. v. 36, no. 2, p. 373–376.

Greene, E.A., Shapiro, A.M. and Carter, J.M., 1999. Hydrogeologic characterization of the Minnelusa and Madison Aquifers near Spearfish, South Dakota. U.S. Geological Survey Water-Resources Investigations Report 98-4156, Rapid City, South Dakota, 64 p.

Greenstone, M., and Gallagher, J., 2008. Does Hazardous Waste Matter? Evidence from the Housing Market and the Superfund Program. Massachusetts Institute of Technology, Department of Economics Working Paper Series. Working Paper 05-27.

Greswell R., *et al.*, 1998. The micro-scale hydrogeological properties of the Lincolnshire Limestone, UK. *Quarterly J. Eng. Geol.*, 31, pp.181–197

Griffioen, J. and G.P. Kruseman, 2004. Determining hydrodynamic and contaminant transfer parameters of groundwater flow. In: Kovalevsky, V.S., Kruseman, G.P. and K. R. Rushton (eds.), 2004. Groundwater studies: An international guide for hydrogeological investigations. IHP-VI, Series on Groundwater No. 3, UNESCO, Paris, France, pp. 217-238

Groen, J., Velstra, J. and Meesters, A.G.C.A., 2000. Salinization processes in paleowaters in coastal sediments of Suriname: evidence from ^{37}Cl analysis and diffusion modelling, *Journal of Hydrology*, v. 234, pp. 1-20.

Gudbjerg, J., 2003. Remediation by steam injection. Ph.D. Thesis, Environment & Resources DTU, Technical University of Denmark, 137 p.

Guldin, R.W. 1989. An analysis of the water situation in the United States: 1989–2040. Gen. Tech. Rep. RM–177. Fort Collins, CO: U.S. Department of Agriculture, Forest Service, Rocky Mountain Forest Experiment Station. 178 p.

Gurr, C., 2008. Recommended Koc values for nonpolar organic contaminants in groundwater. Groundwater Modeling and Geostatistics Knowledge Team White Paper, Malcolm Pirnie, Inc., Arlington, VA, 12 p.

Gustavsson, N., B. Bolviken, D.B. Smith, and R.C. Severson, 2001. Geochemical landscapes of the conterminous United States—New map presentations for 22 elements. U.S. Geological Survey Professional Paper 1648. http://geology.cr.usgs.gov/pub/ppapers/p1648/

GWTF (Ground Water Task Force), 2007. Recommendations from the EPA Ground Water Task Force; Attachment B: Ground water use, value, and vulnerability as factors in setting cleanup goals. EPA 500-R-07-001, Office of Solid Waste and Emergency Response, pp. B1-B14.

Haaland, S.E., 1983. Simple and explicit formulas for the friction factor in turbulent flow. *Journal of Fluids Engineering* (ASME), 103(5), pp. 89–90.

Habermehl, M.A., 2006. The Great Artesian Basin, Australia. In: Foster, S. and D.P. Loucks (Eds.), 2006. Non-renewable groundwater resources; A guidebook on socially-sustainable management for water-policy makers. IHP-VI, Series on Groundwater No. 10, UNESCO, Paris, pp. 82-88.

Halford, K.J., and Mayer, G.C., 2000. Problems associated with estimating ground-water discharge and recharge from stream-discharge records. *Ground Water*, v. 38, no. 3, pp. 331-342.

Halford, K.J. and E.L. Kuniansky, 2002. Documentation of spreadsheets for the analysis of aquifer-test and slug-test data. *U.S. Geological Survey Open-File Report* 02-197, Carson City, Nevada, 51 p.

Halihan T., Mace R.E. and J. M. Sharp Jr., 2000. Flow in the San Antonio segment of the Edwards aquifer: matrix, fractures, or conduits? In: Wicks C.M. and Sasowsky I.D. (ed.) Groundwater Flow and Contaminant Transport in Carbonate Aquifers. AA Balkema, pp. 129–146.

Hamilton, M., and Boeing, J., 2017. Re-Conceptualizing the Edwards Aquifer Authority Recharge Program: Staff Recommendations to Optimize and Protect the Edwards Aquifer. Edwards Aquifer Authority, San Antonio, TX

Haneberg, W., Mozley, P., Moore, J., and Goodwin, L. (Eds.), 1999. Faults and subsurface fluid flow in the shallow crust. American Geophysical Union Monograph, v. 113, pp. 51-68.

Harden, S.L., Fine, J.M., and Spruill, T.B., 2003. Hydrogeology and ground-water quality of Brunswick County, North Carolina. U.S. Geological Survey Water-Resources Investigations Report 03-4051, Raleigh, NC, 92 p.

Harrington, J.M., Fendorf, S.B., and R.F. Rosenzweig, 1998. Biotic generation of arsenic(III) in metal(loid)-contaminated sediments. *Environmental Science and Technology*, v. 32, no. 16, p. 2425-2430.

Harned, D.A. 1989. The hydrogeologic framework and a reconnaissance of ground-water quality in the Piedmont Province of North Carolina, with a design for future study. U.S. Geological Survey Water-Resources Investigations Report 88-4130, 55 p.

Hatcher, R.D. Jr., 1995. Structural Geology; Principles, Concepts, and Problems. Second Edition. Prentice Hall, Englewood Cliffs, New Jersey, 525 p.

HDR Engineering, Inc, and Paul Price Associates, Inc, 1991. Regional Water Supply Planning Study Phase III-Recharge Enhancement-Nueces River Basin. Nueces River Authority, Edwards Underground Water District, TX.

Healy, R.W., 1990. Simulation of solute transport in variably saturated porous media with supplemental information on modifications to the U.S. Geological Survey's Computer Program VS2D, U.S. Geological Survey Water Resources Investigations Report 90-4025, 125 p.

Healy, R.W., Winter, T.C., LaBaugh, J.W., and Franke, O.L., 2007. Water budgets: Foundations for effective water-resources and environmental management: U.S. Geological Survey Circular 1308, 90 p.

Heath, R.C., 1984. Ground-water regions of the United States: U.S. Geological Survey Water-Supply Paper 2242,

Hem, J.D., 1989. Study and interpretation of the chemical characteristics of natural water. Third Edition. U.S. Geological Survey Water-Supply Paper 2254. Washington, D.C., 263 p.

Henry, L., 2022. "Third year of drought pushes price of water to $2,000 an acre foot." SJV Water. Available at: https://sjvwater.org/third-year-of-drought-pushes-price-of-water-to-2000-an-acre-foot/

Hertzman, H., 2017. Atrazine in European groundwater. The distribution of Atrazine and its relation to the geological setting. Master's Degree Thesis in Theoretical Geoekology 15 ECTS. Dept. of Ecology and Environmental Science (EMG), Umeå University, Umeå, Sweden, 16 p.

Hilgard, E.W., 1906. Soils. Macmillan Co., New York, 206 p.

Hill, R.T., and T.W. Vaughn, 1898. Geology of the Edwards Plateau and Rio Grande Plain adjacent to Austin and San Antonio, Texas, with Reference to the Occurrence of Underground Waters. Eighteenth Annual Report of the United States Geological Survey, 1896-97, Part II.-Papers Chiefly of a Theoretic Nature, pp. 193-321; pl. xxi.-lxiv. Washington, Government Printing Office.

Hobba, W.A. Jr., Fisher, D.W., Pearson. F.J. Jr., and Chemerys, J.C., 1979. Hydrology and geochemistry of thermal springs of the Appalachians. U.S. Geological Survey Professional Paper 1044-E, p. E1-E36.

Hoekstra, A.Y., 2006. The global dimension of water governance: Nine reasons for global arrangements in order to cope with local water problems. Value of Water Research Report Series No. 20. UNESCO-IHE Institute for Water Education, Delft, the Netherlands, 33 p.

Hoekstra, A.Y., and Hung, P.Q., 2002. Virtual water trade. A quantification of virtual water flows between nations in relation to international crop trade. Value of Water Research Report Series No. 11. IHE Delft, Delft, the Netherlands, 66 p.

Holland, K. S., Lewis, R. E., Tipton, K., Karnis, S., Dona, C., Petrovskis, E., Bull, L. P., Taege, D. and Hook, C., 2011. Framework for Integrating Sustainability into Remediation Projects. *Remediation Journal*, 21:7–38. doi: 10.1002/rem.20288

Hsieh, P.A., 2001. TopoDrive and ParticleFlow—Two Computer Models for Simulation and Visualization of Ground-Water Flow and Transport of Fluid Particles in Two Dimensions: U.S. Geological Survey Open-File Report 01-286, 30 p.

Hubbert, M.K., 1940. The theory of ground-water motion. *Journal of Geology*, vol. 48, no. 8, pp. 785-944.

Hudgeons, G., 2013. Three-Dimensional Visualizations. In: Kresic, N., and Mikszewski, A., Hydrogeological Conceptual Site Models; Data Analysis and Visualizations. CRC Press, Taylor & Francis Group, Boca Raton, FL, London, New York, pp. 347-365.

Huling, S.G., and Pivetz, B.E., 2006. In-situ chemical oxidation. Engineering Issue, EPA/600/R-06/072, U.S. Environmental Protection Agency, Office of Research and Development, National Risk Management Research Laboratory, Cincinnati, OH, 58 p.

Humphreys, E.H., and Tiemann, M., 2021. Safe Drinking Water Act (SDWA): A Summary of the Act and Its Major Requirements. Congressional Research Service, https://crsreports.congress.gov RL31243

Hutchinson, W.R., 2004. Hueco Bolson groundwater conditions and management in the El Paso area. EPWU Hydrogeology Report 04-01.

Hutson, S.S., N.L. Barber, J.F. Kenny, K.S. Linsey, D.S. Lumia, and M.A. Maupin, 2004. Estimated Use of Water in the United States in 2000. U.S. Geological Survey Circular 1268, Reston, VA, 46 p.

ICWE (International Conference on Water and the Environment), 1992. The Dublin Statement and report of the conference. In: International Conference on Water and the Environment: Development Issues for the 21st Century, January26–31, 1992, Dublin, Ireland. See also http://www.un-documents.net/h2o-dub.htm

Imbrigiotta, T.E., J. Gibs, T.V. Fusillo, G.R. Kish, and J.J. Hochreiter, 1988. Field Evaluation of Seven Sampling Devices for Purgeable Organic Compounds. In A.G. Collins and A.J. Johnson, eds., Ground-Water Contamination: Field Methods. ASTM STP 963, ASTM, Philadelphia, pp. 258-273.

Imes, J.L., Plummer, L.N., Kleeschulte, M.J., and Schumacher, J.G., 2007. Recharge area, base-flow and quick-flow discharge rates and ages, and general water quality of Big Spring in Carter County, Missouri, 2000–04: U.S. Geological Survey Scientific Investigations Report 2007–5049, 80 p.

IAH (International Association of Hydrogeologists), 2002. Managing aquifer recharge. Commission on Management of Aquifer Recharge. IAH-MAR, 12 p.

IMFA (Israel Ministry of Foreign Affairs), 2003. Jerusalem–Water Systems of Biblical Times. Available at: http://www.mfa.gov.il/mfa/early%20history%20-%20archaeology/

ITRC (Interstate Technology & Regulatory Council), 2005. Technical and Regulatory Guidance for In Situ Chemical Oxidation of Contaminated Soil and Groundwater, 2nd ed. In Situ Chemical Oxidation Team, Interstate Technology & Regulatory Council, Washington, DC. 71 p. + appendices.

ITRC, 2006. Technology Overview of Passive Sampler Technologies. DSP-4. Washington, D.C.: Interstate Technology & Regulatory Council, Authoring Team. www.itrcweb.org.

ITRC, 2006a. The Use of Direct Push Well Technology for Long-term Environmental Monitoring in Groundwater Investigations. Technical and Regulatory Guidance. 71 p.

ITRC, 2010. A Decision Framework for Applying Monitored Natural Attenuation Processes to Metals and Radionuclides in Groundwater. Attenuation Processes for Metals and Radionuclides Team, APMR-1. Washington, DC.

ITRC, 2011. Permeable Reactive Barrier: Technology Update. SDMS DOCID#1142231, Permeable Reactive Barrier Work Group. Washington, D.C., 179 p. + Appendices

Izbicki, J.A., 2002. Geologic and hydrologic controls on the movement of water through a thick, heterogenous unsaturated zone underlying an intermittent stream in the Western Mojave Desert, Southern California. *Water Resources Research* Vol. 38, No. 3, doi: 10.1029/2000WR000197.

Jacobson G. and F.J. Taylor, 1981. Hydrogeology of Tarawa atoll, Kiribati. Bureau of Mineral Resources Record No. 1981/31, Australian Government.

James, N.P. and Mountjoy, E.W., 1983. Shelf-slope break in fossil carbonate platforms: an overview. In: Stanley D.J. and G.T. Moore (Eds.), The shelfbreak: critical interface on continental margins. SEPM Spec. Pub. No. 33, p. 189-206.

Janis, I.L., 1971. Groupthink. Psychology Today, **5**(6): 43–44, 46, 74–76

Janis, I.L., 1972. Victims of Groupthink: a Psychological Study of Foreign-Policy Decisions and Fiascoes. Houghton Mifflin, Boston.

Janis, I.L., 1982. Groupthink: Psychological Studies of Policy Decisions and Fiascoes. Houghton Mifflin, Boston.

Jennings, G.D., 1996. Protecting water supply springs. North Carolina Cooperative Extension Service, Publication no. AG 473-15.

Jevdjević, V., 1956. Hidrologija I deo (Hydrology; Part 1, in Serbo-Croatian). Hidrotehnicki institute Jaroslav Cerni, Posebna izdanja, Knjiga 4, Beograd, 404 p.

Johnson, A.I., 1967. Specific yield – compilation of specific yields for various materials. U.S. Geological Survey Water-Supply Paper 1662-D, 74 p.

Johnson, T.L., 1983. A comparison of well nests versus single-well completions; Ground Water Monitoring Review, vol. 3, no. 1, pp. 76-78.

Johnson, R., and B.A. Cody, 2015. California Agricultural Production and Irrigated Water Use. Congressional Research Service Report R44093. www.crs.gov

Johnson, R.L., Palmer, C.D., and W. Fish, 1989. Subsurface chemical processes. In: U.S. EPA, Transport and fate of contaminants in the subsurface, seminar publication. EPA/625/4-89/019, p. 41-56.

Johnson, C.D, Haeni, F.P., Lane, J.W. Jr., and White, E.A., 2002. Borehole-Geophysical Investigation of the University of Connecticut Landfill, Storrs, Connecticut Water-Resources Investigations Report 01-4033. Water-Resources Investigations Report 01-4033, 42 p.

Johnson, C.D., Mondazzi, R.A., and Joesten, P.K., 2011, Borehole geophysical investigation of a Formerly Used Defense Site, Machiasport, Maine, 2003–2006: U.S. Geological Survey Scientific Investigations Report 2009–5120, 333 p., at http://pubs.usgs.gov/sir/2009/5120/

Johnston, C.D., 1983. Estimation of groundwater recharge from the distribution of chloride in deeply weathered profiles from south-west Western Australia, in Papers of the International Conference on Groundwater and Man, v. 1, Investigation and assessment of groundwater resources, Sydney, 1983: Canberra, Australian Water Resources Council, Conference Series 8, pp. 143-152.

Johnston, R.H., Bush, P.W., Krause, R.E., Miller, J.A., and C.L. Sprinkleet, 1982. Summary of hydrologic testing in tertiary limestone aquifer, Tenneco offshore exploratory well--Atlantic OCS, lease-block 427 (Jacksonville NH 17-5). U.S. Geological Survey Water-Supply Paper 2180, Washington, D.C., 15 p.

Joint Departments of the Army and Air Force USA, 1987. Technical Manual TM 5813-1/AFM 88-10, Volume 1, Water Supply, Sources and General Considerations. Washington, DC.

Jones, W.K., 1977. Karst hydrology atlas of West Virginia. Special Publication 4, Karst Waters Institute, Charles Town, WV, 111 p.

Jones, W. K., 1984. Analysis and interpretation of data from tracer tests in karst areas. Nat Speleolog Soc Bull, 46: 41–47.

Jones, W. K., 2012. Water tracing in karst aquifers. In: White, B.W., and Culver, D.C. (eds.), Encyclopedia of Caves. Academic Press, Chennai, pp. 886–896.

Jones, J.R., Springer, A.E., Tobin, B.W., Zappitello, S.J., and Jones, N.A., 2017. Characterization and hydraulic behaviour of the complex karst of the Kaibab Plateau and Grand Canyon National Park, USA. In: Parise, M.,

References and Select Readings

Gabrovsek, F., Kaufmann, G., and Ravbar, N., Advances in Karst Research: Theory, Fieldwork and Applications. Geological Society, London, Special Publications, 466, https://doi.org/10.1144/SP466.5

Jousma, G., and Roelofsen, F.J., 2004. World-wide inventory on groundwater monitoring. IGRAC, Report no. GP 2004-1. International Groundwater Resources Assessment Centre, Utrecht, the Netherlands.

Kashef, A.A.I., 1987. Groundwater Engineering. McGraw Hill, Singapore, 512 p.

Kauffman, W.J., and Orlob, G.T., 1956. Measuring ground water movement with radioactive and chemical tracers. *American Water Works Association Journal*, v. 48, pp. 559-572.

Käss, W., 1998. Tracing technique in geohydrology. Balkema, Rotterdam, The Netherlands, 581p.

Kay, R.T., Bayless, E.R., and Solak, R.A., 2002. Use of isotopes to identify sources of ground water, estimate ground-water-flow rates, and assess aquifer vulnerability in the Calumet Region of Northwestern Indiana and Northeastern Illinois. U.S. Geological Survey Water-Resources Investigation Report 02-4213, Indianapolis, Indiana, 60 p.

Keeney, D., 1990. Sources of nitrate to ground water. *Critical Reviews in Environmental Control*, v. 16, pp. 257-304.

Kendy, E., 2001. Magnitude, extent, and potential sources of nitrate in ground water in the Gallatin Local Water Quality District, southwestern Montana, 1997–98. U.S. Geological Survey Water-Resources Investigations Report 01-4037.

Keys, W.S., 1990. Borehole Geophysics Applied to Ground-Water Investigations. Techniques of Water-Resources Investigations of the United States Geological Survey, Book 2, Chapter E2, 150 p.

Khouri, J., 2004. Groundwater resources and their use in Africa. In: Zektser, I.S. and L.G. Everett (eds.), Groundwater resources of the world and their use, IHP-VI, Series on Groundwater No. 6, UNESCO, Paris, France, p. 209-237.

Kimbrough, D.E., et al., 1999. A critical assessment of chromium in the environment. Critical Reviews in *Environmental Science and Technology,* v. 29, p. 1–46.

King, R.B., 1992. Overview and bibliography of methods for evaluating the surface-water-infiltration component of the rainfall-runoff process. U.S. Geological Survey Water-Resources Investigations Report 92-4095, Urbana, Illinois, 169 p.

Klimchouk, A.B., 1992. Large gypsum caves in the Western Ukraine and their genesis. *Cave Science* 19 (1), 3-11.

Klimchouk, A.B., 1994. Speleogenesis under confined conditions, with recharge from adjacent formations. Publ. Serv. Geol. Luxembourg, vol. XXVII: Comptes Rendus du Coll. Intern. de Karstologie a Luxembourg, pp. 85-95.

Klimchouk, A., 2011. Hypogene Speleogenesis: Hydrogeological and Morphogenetic Perspective. Second Edition. Special Paper No. 1, National Cave and Karst Research Institute Carlsbad, NM, 106 p.

Klimchouk, A.B., Ford, D., Palmer, A. and Dreybrodt, W. (Eds.), 2000. Speleogenesis: Evolution of Karst Aquifers. National Speleological Society, Huntsville, AL, 527 p.

Klimchouk, A.B., Samokhin, G.V., and Y.M. Kasian, 2009. The Deepest Cave in the World in the Arabika Massif (Western Caucasus) and its Hydrogeological and Paleogeographic Significance. Proceedings of the 15th International Congress of Speleology, *Speleogenesis*, pp. 898-905.

Klohe, C.A., and R.T. Kay, 2007. Hydrogeology of the Piney Point-Nanjemoy, Aquia, and Upper Patapsco Aquifers, Naval Air Station Patuxent River and Webster Outlying Field, St. Marys County, Maryland, 2000–06. U.S. Geological Survey Scientific Investigations Report 2006–5266, 26 p.

Knochenmus, L.A., and J.L. Robinson, 1996. Descriptions of anisotropy and heterogeneity and their effect on ground-water flow and areas of contribution to public supply wells in a karst carbonate aquifer system. U.S. Geological Survey Water-Supply Paper 2475, Washington, D.C., 47 p.

Kohler, M.A., 1958. Meteorological aspects of evaporation. Int. Assn. Sci. Hydr. Trans., General Assembly, Toronto, vol. III, pp. 423-436.

Kooi, H., and Groen, J., 2003. Geological processes and the management of groundwater resources in coastal areas. *Netherlands Journal of Geosciences*, v. 82, pp. 31-40.

Kooi, H., Groen, J., and Leijnse, A., 2000. Modes of seawater intrusion during transgressions. *Water Resources Research*, v. 36, no. 12, pp. 3581–3589.

Krause, R.E., and Randolph, R.B., 1989. Hydrology of the Floridan aquifer system in southeast Georgia and adjacent parts of Florida and South Carolina. U.S. Geological Survey Professional Paper 1403–D, 65 p.

Krause, R.E, and Clarke, J.S., 2001, Coastal ground water atbrisk—Saltwater contamination at Brunswick, Georgia, and Hilton Head Island, South Carolina: U.S. Geological SurveybWater-Resources Investigations Report 01–4107, 1 sheet.

Krešić, N., 1988. Karst i pećine Jugoslavije (in Serbo-Croatian; Karst and caves of Yugoslavia). Naučna knjiga, Belgrade, 149 p.

Krešić, N., 1991. Kvantitativna hidrogeologija karsta sa elementima zaštite podzemnih voda (Quantitative karst hydrology with elements of groundwater protection, in Serbo-Croatian). Naučna knjiga, Beograd, 196 p.

Kresic, N., 1997. Quantitative Solutions in Hydrogeology and Groundwater Modeling. CRC/Lewis Publishers, Boca Raton, FL, New York, 461 p.

Kresic, N., 1998. Hydrologic and hydrogeologic study; Costa Serena Project, Loiza, Puerto Rico. Law Environmental-Caribe, Santurce, Puerto Rico.

Kresic, N., 1999. Relevance of ASTM Standard D5717-95 to hydrogeologic conditions at PROTECO landfill facility, Peñuelas, Puerto Rico. LAW Engineering and Environmental Services, Kennesaw, Georgia.

Kresic, N., 2007. Hydrogeology and Groundwater Modeling. Second Edition. CRC Press, Taylor & Francis Group, Boca Raton, FL, London, New York, 807 p.

Kresic, N., 2007a. Hydraulic Methods. In: Goldscheider, N., and D.Drew (eds.), Methods in Karst Hydrogeology. International Contributions to Hydrogeology 26, International Association of Hydrogeologists, Taylor & Francis, London, pp. 65-92.

Kresic, N., 2009. Groundwater Resources. Sustainability, Management, and Restoration. McGraw Hill, New York, 852 p.

Kresic, N., 2010. Chapter 2, Types and Classification of Springs. In: Kresic, N., and Stevanovic, Z., eds., Groundwater Hydrology of Springs; Engineering, Theory, Management, and Sustainability. Elsevier, Butterworth-Heinemann, Amsterdam, pp. 31-85

Kresic, N., 2013. Water in Karst: Management, Vulnerability, and Restoration. McGraw Hill, New York, 708 p.

Kresic, N., and Mikszewski, A., 2009. Chapter 3 Groundwater Recharge. In: Kresic, N., 2009, Groundwater Resources. Sustainability, Management, and Restoration. McGraw Hill, New York, pp. 235-293

Kresic, N., and Bonacci, O., 2010. Spring Discharge Hydrograph. In: Kresic, N., and Stevanovic, Z., eds., Groundwater Hydrology of Springs; Engineering, Theory, Management, and Sustainability. Elsevier, Butterworth-Heinemann, Amsterdam, pp. 129-163

Kresic, N., and Mikszewski, A., 2013. Hydrogeological Conceptual Site Models; Data Analysis and Visualizations. CRC Press, Taylor & Francis Group, Boca Raton, FL, London, New York, 584 p.

Kresic, N., and Mikszewski, A., 2023. Sustainable Groundwater Remediation. Professional Education Workshop, (in preparation)

Kresic, N., and Stevanovic, Z. (eds.), 2010. Groundwater Hydrology of Springs; Engineering, Theory, Management, and Sustainability. Elsevier, Butterworth-Heinemann, Amsterdam, 592 p.

Kresic, N., and Panday, S., 2018. Numerical groundwater modelling in karst. In: Parise, M., Gabrovsek, F., Kaufman, G., and Ravbar, N. (eds), 2018. Advances in Karst Research: Theory, Fieldwork and Applications. Geological Society, London, *Special Publications 466*, p. 39-330

Kresic, N., and Panday, S., 2021. Modeling of groundwater flow and transport in coastal karst aquifers. *Hydrogeology Journal*, 29(1), p. 249-258

Kresic, N., and Stevanović, Z., 2021. The Lands of Karst, A Visual Story. Blue Ridge Press, Warrenton, VA, 380 p.

Krumholz, L.R., 2000. Microbial communities in the deep subsurface. *Hydrogeology Journal*, v. 8, no.1, pp. 4-10

Kruseman, G.P., de Ridder, N.A., and J.M. Verweij, 1991. *Analysis and Evaluation of Pumping Test Data* (completely revised 2nd edition). International Institute for Land Reclamation and Improvement (ILRI) Publication 47, Wageningen, The Netherlands, 377 p.

Kupusović, T., 1989. Measurements of piezometric pressures along deep boreholes in karst area and their assessment. Naš Krš, Vol. XV, No. 26-27, p. 21-30

Laczniak, R.J., Smith J.L., and DeMeo, G.A., 2006. Annual ground-water discharge by evapotranspiration from areas of spring-fed riparian vegetation along the eastern margin of Death Valley, 2002–02. U.S. Geological Survey Scientific Investigations Report 2006-5145, 36 p. Available at URL: http://pubs.water.usgs.gov/sir2006-5145.

Ladouche, B., Probst, A., Viville, D., Idir, S., Baqué, D., Loubet, M., Probst, J.-L., and Bariac, T., 2001. Hydrograph separation using isotopic, chemical and hydrological approaches (Strengbach catchment, France). Journal of Hydrology, vol. 242 (n° 3-4). pp. 255-274.

Lall, U., Josset, L., and Russo, T., 2020. Snapshot of the World's Groundwater Challenges. *Annual Review of Environment and Resources*, Volume 45, pp. 171-194.

Langmuir, D., 1997. Aqueous environmental chemistry. Prentice-Hall, Upper Saddle River, NJ, 600 p.

Langmuir, D., and R.L. Klusman, 1997. Natural background concentrations of metals that exceed drinking water standards: Defining background and the effect of sample filtration. Abstract, Geol. Soc. Am. Annual Meetings. Oct. 20-23. Salt Lake City UT, p. A-435.

Langmuir, D., Chrostowski, P., Vigneault, B., and R. Chaney, 2004. Issue Paper on the Ecological Effects of Metals. Environmental Protection Agency, Risk Assessment Forum, Washington, D.C. (submitted by ERG, Lexington, MA), 106 p. Available at https://www.epa.gov/caddis-vol2/metals

Lapham, W.W., F.D. Wilde and M.T. Koterba, 1997, Guidelines and Standard Procedures for Studies of Ground-Water Quality: Selection and Installation of Wells, and Supporting Documentation; U.S. Geological Survey Water-Resources Investigations Report 96-4233, 110 p.

Lappala, E.G, Healy, R.W., and Weeks, E.P., 1987. Documentation of computer program VS2D to solve the equations of fluid flow in variably saturated porous media, U.S. Geological Survey Water Resources Investigations Report 83-4099, 131 p.

Lappala, E.G., Healy, R.W., and Weeks, E.P., 1987. Documentation of computer program VS2D to solve the equations of fluid flow in variably saturated porous media. U.S. Geological Survey Water-Resources Investigations Report 83-4099, Denver, Colorado, 131 p.

Lawrence, S.J., 2006. Description, properties, and degradation of selected volatile organic compounds detected in ground water—a review of selected literature. U. S. Geological Survey, Open-File Report 2006-1338, Reston, VA, 62 p.

Lide, D.R., 2005. CRC handbook of chemistry and physics, 86th edition. CRC Press, Boca Raton, Florida, 2544 p.

Lee, K.K., and Risley, J.C., 2002. Estimates of ground-water recharge, base flow, and stream reach gains and losses in the Willamette River Basin, Oregon. U.S. Geological Survey Water-Resources Investigations Report 01-4215, Portland, Oregon, 52 p.

LeGrand, H.E., 1954. Geology and ground water in the Statesville area, North Carolina: North Carolina Department of Conservation and Development Bulletin 68, 68 p.

LeGrand, H.E., 1958. Chemical character of water in the igneous and metamorphic rocks of North Carolina: Economic Geology, v. 53, no. 12, p. 179-189.

LeGrand, H.E., 1967. Ground water of the Piedmont and Blue Ridge provinces in the southeastern states. U.S. Geological Survey Circular 538.

LeGrand, H.W, Sr., 2007. A master conceptual model for hydrogeological site characterization in the Piedmont and Mountain Region of North Carolina; A Guidance Manual. North Carolina Department of Environment and Natural Resources, Division of Water Quality, Groundwater Section. 40 p. + Appendices

Levinson, A.A., P.M.D. Bradshaw, and I. Thomson. 1987. Practical exploration geochemistry. Applied Publishing Ltd., Wilmette, IL, 269 p.

Lindsay, A.S., Mesko, T.O., and Hollyday, E.F., 1991. Summary of the hydrogeology of the Valley and Ridge, Blue Ridge, and Piedmont physiographic provinces in the eastern United States. Regional Aquifer System Analysis—Appalachian Valley and Piedmont, U.S. Geological Survey Professional Paper 1422-A, Reston, VA, 23 p.

Lindsey, D.A., Langer, W.H., and Knepper, D.H., Jr., 2005. Stratigraphy, lithology, and sedimentary features of Quaternary alluvial deposits of the South Platte River and some of its tributaries east of the Front Range, Colorado: U.S. Geological Survey Professional Paper 1705, 70 p.

Linsley, R.K., Kohler, M.A., and Paulhus, J.L.H., 1975. Hydrology for Engineers. McGraw-Hill, New York, 482 p.

Linsley, R.K., and Franzini, J.B., 1979. Water-resources engineering, Third edition. McGraw-Hill Book Company, New York, 716 p.

Logan, A. and Sealey, K.S., 2013. The Reefs of the Turks and Caicos Islands. In: C.R.C. Sheppard (ed.), Coral Reefs of the United Kingdom Overseas Territories, Coral Reefs of the World 4, 97 DOI 10.1007/978-94-007-5965-7_9, Springer Science+Business Media, Dordrecht, pp. 97-114

Lohman, S.W., 1972. Ground-water hydraulics. U.S. Geol. Survey Professional Paper 708, 70 p.

Lohman, S.W., et al., 1972. Definitions of selected ground-water terms - revisions and conceptual refinements. U.S. Geological Survey Water-Supply Paper 1988, 21 p.

Loos, R., Locoro, G., Comero, S., Contini, S., Schwesig, D., Werres, F., Balsaa, P., Gans, O., Weiss, S., Blaha, L., Bolchi, M., Gawlic, and Manfred, B., 2010. Pan-European survey on the occurrence of selected polar organic persistent pollutants in ground water. *Water Research* 44:4115-4126.

Lovelock, J.E., and Margulis, L., 1974. Atmospheric homeostasis by and for the biosphere: the gaia hypothesis, Tellus, 26:1-2, 2-10, DOI: 10.3402/tellusa.v26i1-2.9731

Lutgens, F.K., Tarbuck, E.J., Herman, R., 2018. The Atmosphere: An Introduction to Meteorology. 14th Edition. Pearson, Hoboken, NJ, 528 p.

Lyford, F.P., 1986. Northeast glacial regional aquifer-system study. In: Sun, R.J. (ed.), Regional aquifer-system analysis program of the U.S. Geological Survey – Summary of projects, 1978-1984, U.S. Geological Survey Circular 1002, p. 162-167.

Lyman, W.J., Reehl, W.F., and Rosenblatt, D.H., 1982. Handbook of Chemical Property Estimation Methods, Environmental Behavior of Organic Compounds. McGraw-Hill Book Co., New York, 500 p.

References and Select Readings

Margat, J., and J. van der Gun. 2013. Groundwater around the World. A Geographic Synopsys. CRC Press/Balkema, Boca Raton, FL, London, New York, Leiden 341 p. Available for download at:

https://www.un-igrac.org/sites/default/files/resources/files/Groundwater_around_world.pdf

Maslansky, S.P., and Maslansky, C.J., 1997. Health and Safety at Hazardous Waste Sites—An Investigators and Remediators Guide to HAZPOWER. John Willey and Sons, Inc., New York, NY

Maslansky, S.P., and Maslansky, C.J., 2006. Health and Safety Considerations in Ground-Water Monitoring Investigations. In: Nielsen, D.M. (editor), Practical Handbook of Environmental Site Characterization and Ground-Water Monitoring, Second Edition. CRC Taylor & Francis, Boca Raton, FL, pp. 1219-1261.

Maslia, M.L. and Randolph, R.B., 1986. Methods and computer program documentation for determining anisotropic transmissivity tensor components of two-dimensional ground-water flow. U.S. Geological Survey Open-File Report 86–227, 64 p.

Matthess, G., 1982. The properties of groundwater. John Willey & Sons, New York, 406 p.

Maupin, M.A., and N.L. Barber, 2005. Estimated withdrawals from principal aquifers in the United States, 2000. U.S. Geological Survey Circular 1279, Reston, Virginia, 46 p.

McGuire, V.L., Johnson, M.R., Schieffer, R.L., Stanton, J.S., Sebree, S.K., and I.M. Verstraeten, 2003. Water in storage and approaches to ground-water management, High Plains aquifer, 2000. U.S. Geological Survey Circular 1243, Reston, Virginia, 51 p.

McMahon, P.B., Dennehy, K.F., Michel, R.L., Sophocleous, M.A., Ellett, K.N., and Hurlbut, D.B., 2003. Water movement through thick unsaturated zones overlying the Central High Plains Aquifer, Southwestern Kansas, 2000–2001. U.S. Geological Survey Water-Resources Investigations Report 03–4171, Reston, Virginia, 32 p.

McNeill, D., 1998. Water as an economic good. Natural Resources Forum, vol. 22, no. 4, pp. 253–261.

Medema, G.J., and Stuyzand, P.J., 2002. Removal of micro-organisms upon recharge, deep well injection and river bank infiltration in the Netherlands. In: Management of Aquifer Recharge for Sustainability. A.A. Balkema Publishers, Lisse, the Netherlands, pp. 125–131.

Meinzer, O.E., 1923a. The occurrence of ground water in the United States with a discussion of principles. U.S. Geological Survey Water-Supply Paper 489, Washington, D.C., 321 p.

Meinzer, O.E., 1923b. Outline of ground-water hydrology with definitions. U.S. Geological Survey Water-Supply Paper 494, Washington, D.C., 71 p.

Meinzer, O.E., 1927a. Plants as indicators of ground water. U.S. Geological Survey Water-Supply Paper 577, Washington, D.C., 95 p.

Meinzer, O.E., 1927b. Large springs in the United States. U.S. Geological Survey Water-Supply Paper 557, Washington, D.C., 94 p.

Meinzer, O.E., 1932 (reprint 1959). Outline of methods for estimating ground-water supplies. Contributions to the hydrology of the United States, 1931. U.S. Geological Survey Water-Supply Paper 638-C, Washington, D.C., pp. 99-144

Meinzer, O.E., 1940. Ground water in the United States: a summary of ground-water conditions and resources, utilization of water from wells and springs, methods of scientific investigation, and literature relating to the subject. U.S. Geological Survey Water-Supply Paper 836-D, Washington, D.C., pp. 157-232

Metai, E., 2002. Vulnerability of freshwater lens on Tarawa – the role of hydrological monitoring in determining sustainable yield. Presented at Pacific Regional Consultation on Water in Small Island Countries, 29 July-3 August, 2002. Sigatoka, Fiji, 17 p.

Milanović, P., 1979. Hidrogeologija karsta i metode istraživanja (in Serbian; Karst hydrogeology and methods of investigations). HE Trebišnjica, Institut za korištenje i zaštitu voda na kršu, Trebinje, 302 p.

Milanovic, P.T., 1981. Karst Hydrogeology. Water Resources Publications, Littleton, CO, 434 p.

Milanovic, P.T., 2004. Water Resources Engineering in Karst. CRC Press, Boca Raton, FL, 312 p.

Miller, J.A., 1999. Introduction and national summary. In: Ground-Water Atlas of the United States. United States Geological Survey, A6. Available at: http//caap.water.usgs.gov/gwa/index.html.

Milojević, N., 1967. Hidrogeologija (Hydrogeology, in Serbian). Univerzitet u Beogradu, Zavod za izdavanje udžbenika Socijalističke Republike Srbije, 279 p.

Ministry of the Environment, 2004. Model project to combat desertification in Nare village, Burkina Faso. Technical report of the subsurface dam. Overseas Environmental Cooperation Center, Government of Japan, 77 p.

Modica, E., Buxton, H.T., and Plummer, L.N., 1998. Evaluating the source and residence times of ground-water seepage to headwaters streams, New Jersey Coastal Plain. *Water Resources Research*, v. 34, pp. 2797-2810.

Moench, A.F., 1996. Flow to a well in a water-table aquifer: an improved Laplace transform solution: *Ground Water*, v.34, no. 4, pp. 593-596.

Molz, F.J., Güven, O., and Melville, J.G., 1983. An examination of scale-dependent dispersion coefficients. *Ground Water*, Vol. 21, No. 6, pp. 715-725.

Molz, F. J., Güven, O., and J. G. Melville, (with contributions by I. Javandel, A. E. Hess, and F. L. Paillet), 1990. A new approach and methodologies for characterizing the hydrogeologic properties of aquifers, EPA/600/2-90/002, U.S. Environmental Protection Agency, Ada, Oklahoma.

Moody, L.F. 1944. Friction Factors for Pipe Flow. *Transactions of the ASME* 66 (8), pp. 671–684

Moorman, J.J., 1867. The mineral waters of the United States and Canada. Kelly & Piet, Baltimore, 507 p.

Morris, B. L., Lawrence, A.R.L., Chilton, P.J.C., Adams, B., Calow, R.C., and B.A. Klinck, 2003. Groundwater and its susceptibility to degradation: a global assessment of the problem and options for management. Early Warning and Assessment Report Series, RS. 03-3. United Nations Environment Programme, Nairobi, Kenya, 126 p.

Mozley, P.S. et al., 1996. Using the spatial distribution of calcite cements to infer paleoflow in fault zones: examples from the Albuquerque Basin, New Mexico [abstract]. American Association of Petroleum Geologists 1996 Annual Meeting.

Mualem, Y., 1976. A new model predicting the hydraulic conductivity of unsaturated porous media. *Water Resour. Res*. 12:513-522

Mueller, D.K., Hamilton, P.A., Helsel, D.R., Hitt, K.J., and B.C. Ruddy, 1995. Nutrients in ground water and surface water of the United States–An analysis of data through 1992. U.S. Geological Survey Water Resources Investigations Report 95-4031

Mull, D. S., Liebermann, T. D., Smoot, J. L., and Woosley Jr., L. H., 1988. Application of dye-tracing techniques for determining solute-transport characteristics of ground water in karst terranes. U.S. Environmental Protection Agency, EPA 904/6-88-001, Atlanta, GA, 103p.

Musgrove, M., and Crow, C.L., 2012. Origin and characteristics of discharge at San Marcos Springs based on hydrologic and geochemical data (2008–10), Bexar, Comal, and Hays Counties, Texas: U.S. Geological Survey Scientific Investigations Report 2012–5126, 94 p.

NASA (National Aeronautics and Space Administration), 2022. Visible Earth: a catalog of NASA images and animations of our home planet. http://visibleearth.nasa.gov; accessed April 10, 2022.

NASA (National Aeronautics and Space Administration), 2022a. Groundwater and Soil Moisture Conditions from GRACE-FO Data Assimilation for the Contiguous U.S. and Global Land. Available at: https://nasagrace.unl.edu/Default.aspx

National Academies of Sciences, Engineering, and Medicine, 2019. Manual on Subsurface Investigations. Washington, DC: The National Academies Press. https://doi.org/10.17226/25379.

References and Select Readings

National Research Council, 1994. Ground Water Recharge Using Waters of Impaired Quality. National Academy Press, Washington, DC, 382 p.

NDMC (National Drought Mitigation Center), 2022. U.S. Drought Monitor. Data Download. Available at: https://droughtmonitor.unl.edu/DmData/DataDownload.aspx

Nelson, P.H., and J.E. Kibler, 2003. A catalog of porosity and permeability from core plugs in siliciclastic rocks. U.S. Geological Survey Open-file Report 03-420. Denver, Colorado.

Neuman, S.P., 1972. Theory of flow in unconfined aquifers considering delayed response to the water table. *Water Resources Research*, Vol. 8, No. 4, p. 1031-1045.

Neuman, S.P., 1974. Effects of partial penetration on flow in unconfined aquifers considering delayed gravity response: *Water Resources Research*, v. 10, no. 2, p. 303-312.

Neuman, S.P., 1975. Analysis of pumping test data from anisotropic unconfined aquifers considering delayed gravity response. *Water Resources Research*, Vol. 11, No. 2, p. 329-342.

Newell, C.J., et al., 1995. Light nonaqueous phase liquids. *Ground Water Issue*, EPA/540/S-95/500, Robert S. Kerr Environmental Research Laboratory, Ada, Oklahoma, 28 p.

Newell, C.J., et al., 2002. Calculation and use of first-order rate constants for monitored natural attenuation studies. Ground Water Issue, EPA/540/S-02/500, U.S. Environmental Protection Agency, National Risk Management Research Laboratory, Cincinnati, Ohio, 27 p.

NFWMD (Northwest Florida Water Management District), 2022. Wakulla Spring. https://nwfwater.com/Water-Resources/Springs/Featured-Springs/Wakulla-Springs

NICOLE (Network for Industrially Contaminated Land in Europe), 2010. Road Map for Sustainable Remediation. https://nicole.org/uploadedfiles/2010-wg-sustainable-remediation-roadmap.pdf

Nielsen, D.M. (editor), 2006. Practical Handbook of Environmental Site Characterization and Ground-Water Monitoring, Second Edition. CRC Taylor & Francis, Boca Raton, FL, 1318 p.

Nielsen, D.M., Nielsen, G.L., and Preslo, L.M., 2006. Environmental Site Characterization. In: Nielsen, D.M. (editor), Practical Handbook of Environmental Site Characterization and Ground-Water Monitoring, Second Edition. CRC Taylor & Francis, Boca Raton, FL, pp. 35-205.

Nimmo, J.R., Deason, J.A., Izbicki, J.A., and Martin, P., 2002. Evaluation of unsaturated zone water fluxes in heterogeneous alluvium at a Mojave Basin site. *Water Resources Research*, Vol. 38, No. 10, 1215, doi:10.1029/2001WR000735, 2002

Nimmo, J.R., 2007. Simple predictions of maximum transport rate in unsaturated soil and rock. *Water Resources Research* vol. 43, W05426, doi:10.1029/2006WR005372.

NNPSMP (National Nonpoint Source Monitoring Program), 2008. Surface water flow measurements for quality monitoring projects. Technotes 3. Available at: https://319monitoring.wordpress.ncsu.edu/

NOAA (National Centers for Environmental information), Climate at a Glance: Statewide Time Series, Average Temperature, published October 2022, retrieved on October 17, 2022, at https://www.ncdc.noaa.gov/cag/

Nueces River Authority, 2007. Edwards Aquifer recharge dams.

Nutter, L.J., and Otton, E.G., 1969. Ground-water occurrence in the Maryland Piedmont: Maryland Geological Survey Report of Investigations no. 10, 56 p.

Olmstead, Alan L., and Paul W. Rhode. "A history of California agriculture." *Giannini Foundation of Agricultural Economics, University of California* (2017).

Opie, J, 2000. Ogallala, Water for a dry land, 2nd edition. University of Nebraska Press Lincoln, Nebraska, 475 p.

Osborne, P.S. 1993. Suggested operating procedures for aquifer pumping tests. Ground Water Issue, United States Environmental Protection Agency, EPA/540/S-93/503, 23 p.

OSHA (Occupational Safety and Health Administration), 2023. Recommended Practices for Safety and Health Programs. www.osha.gov

OSU (Oregon State University), 2023. Safety Instructions, Site Health and Safety Plan (HASP). OSU Environmental Health and Safety, www.ehs.oregonstate.edu

Ovchinikov, M.A., 1955. Obschaja gidrogeologia (General hydrogeology, in Russian). Nedra, Moskva.

Ovchinikov, M.A., 1970. Gidrogeohimia (Hydrogeochemistry, in Russian). Nedra, Moskva.

Owen, D., 2009. Green Metropolis: Why Living Smaller, Living Closer, and Driving Less are the Keys to Sustainability. Riverhead Books, New York, 368 p.

Paillet, F.L., 1989. Analysis of geophysical well logs and flowmeter measurements in boreholes penetrating subhorizontal fracture zones, Lac du Bonnet Batholith, Manitoba, Canada. U.S. Geological Survey Water-Resources Investigations Report 89-4211, Lakewood, Colorado, 30 p.

Paillet, F.L., 1994. Application of borehole geophysics in the characterization of flow in fractured rocks. U.S. Geological Survey Water-Resources Investigations Report 93-4214, Denver, Colorado, 36 p.

Paillet, F.L., 1998. Flow modeling and permeability estimation using borehole flow logs in heterogeneous fractured formations: *Water Resources Research*, v. 34, no. 5, p. 997-1010.

Paillet, F.L., 2000. A field technique for estimating aquifer parameters using flow log data. *Ground Water*, v. 38, no. 4, p. 510-521.

Paillet, F.L., 2001. Hydraulic head applications of flow logs in the study of heterogeneous aquifers. *Ground Water*, v. 39, no. 5, p. 667-675.

Paillet, F.L., and A.E. Hess, 1987. Geophysical well log analysis of fractured granitic rocks at Atikokan, Ontario, Canada, U.S. Geological Survey Water Resources Investigations Report 87-4154, Reston, Virginia.

Paillet, F.L., and R.S. Reese, 2000. Integrating borehole logs and aquifer tests in aquifer characterization. *Ground Water*, v. 38, no. 5, p. 713-725

Palmer, A.N., 1985. The Mammoth Cave region and Pennyroyal Plateau. In: P.H. Dougherty (ed.), Caves and Karst of Kentucky, Kentucky Geological Survey Special Publication 12, Series XI, p. 97-118.

Palmer, A.N. 1991. Origin and morphology of limestone caves. *Geol. Soc. Am. Bull.* 103: 1-21.

Palmer, A.N, 2007. Cave Geology. Cave Books, Trenton, NJ, 454 p.

Panday, S., 2020. Block-Centered Transport (BCT) Process for MODFLOW-USG Version 1.5.0. GSI Environmental, https://www.gsi-net.com/en/software/free-software/modflow-usg.html.

Panday, S., Langevin, C.D., Niswonger, R.G., Ibaraki, M., and Hughes, J.D., 2013. MODFLOW-USG version 1: An unstructured grid version of MODFLOW for simulating groundwater flow and tightly coupled processes using a control volume finite-difference formulation: U.S. Geological Survey Techniques and Methods, book 6, chap. A45, 66 p.

Pankow, J.F., and Cherry, J.A., 1996. Dense chlorinated solvents and other DNAPLs in groundwater. Waterloo Press, Guelph, Ontario, Canada, 522 p.

Papadopulos, I.S., 1965. Nonsteady flow to a well in an infinite anisotropic aquifer: Proc. Dubrovnik Symposium on the Hydrology of Fractured Rocks. International Association of Scientific Hydrology, pp. 21-31.

Parsons (Parsons Corporation), 2004. Principles and practices of enhanced anaerobic bioremediation of chlorinated solvents. Air Force Center for Environmental Excellence (AFCEE), Brooks City-Base, Texas; Naval Facilities Engineering Service Center Port Hueneme, California; Environmental Security Technology Certification Program, Arlington, VA

Pereira, L.S., Cordery, I., and Iacovides, I., 2002. Coping with Water Scarcity. International Hydrological Programme VI, Technical Documents in Hydrology No. 58, UNESCO, Paris, 269 p.

References and Select Readings

Perlmutter, N.M., et al., 1963. Movement of waterborne cadmium and hexavalent chromium wastes in South Farmingdale, Nassau County, Long Island, New York. In: Short papers in geology and hydrology, U.S. Geological Survey Professional Paper 475-C, p. C179-C184.

Perry, W.C., Costain, J.K., and Geiser, P.A., 1979. Heat flow in western Virginia and a model for the origin of thermal springs in the folded Appalachians. *Journal of Geophysical Research*, v. 84, no. B12, pp. 6875-6883.

Peterson N.V., and E.A. Groh. 1972. Geology and Origin of the Metolius Springs, Jefferson County, Oregon. The Ore Bin, Vol 34, No 3, Oregon Department of Geology and Mineral Industries, Portland, Oregon.

Petrusevski, B., Sharma, S., Schippers, J.C., and Shordt, K., 2007. Arsenic in drinking water. IRC International Water and Sanitation Centre, Thematic Overview Paper 17, Delft, the Netherlands, 57 p.

Phillips, C.S.H., and R.J.P. Williams. 1965. Inorganic chemistry. Vol. 2: Metals. Oxford University Press, New York.

Pierce, B., 2004. Comments & Recommendations from the Draft Ground Water Use and Vulnerability Discussion Paper. Memorandum to Guy Tomassoni, USEPA, Ken Lovelace, USEPA, September 30, 2004, Georgia Department of Natural Resources, Environmental Protection Division, Atlanta, Georgia, 4 p.

Pinder, G.F., and Jones, J.F., 1969. Determination of the groundwater component of peak discharge from the chemistry of total runoff. *Water Resources Research*, 5 (2), p. 438-445.

Piper, A.M., 1944. A graphic procedure in the geochemical interpretation of water analyses. *American Geophysical Union Transactions*, v. 25, pp. 914-923.

Plan, L., Kuschnig, G., and Stadler, H., 2010. Case Study: Klaffer Spring—the major spring of the Vienna water supply (Austria), In: Kresic, N., and Stevanovic, Z. (eds.), 2010. Groundwater Hydrology of Springs; Engineering, Theory, Management, and Sustainability. Elsevier, Butterworth-Heinemann, Amsterdam, pp. 411-427.

Plummer, L.N., and Friedman, L.C., 1999. Tracing and dating young ground water. U.S. Geological Survey Fact Sheet-134-99, 4 p.

Plummer, L.N., Michel, R.L., Thurman, E.M., and Glynn, P.D., 1993. Environmental tracers for age-dating young ground water. In: Alley, W.M., (ed.), Regional ground-water quality: Van Nostrand Reinhold, New York, , p. 255–294.

Plummer, L.N., and Busenberg, E., 2007. Chlorofluorocarbons. Excerpt from environmental tracers in subsurface hydrology, Peter Cook and Andrew Herczeg (eds.), Kluwer Academic Press. The Reston Chlorofluorocarbon Laboratory, U.S. Geological Survey.

Pohlmann, K.F. and J.W. Hess, 1988. Generalized Ground Water Sampling Device Matrix. Ground-Water Monitoring Review, Fall, pp. 82-84.

Post, V.E.A., and Kooi, H., 2003. On rates of salinization by free convection in high-permeability sediments; insights from numerical modelling and application to the Dutch coastal area. *Hydrogeology Journal*, v. 11, pp. 549-559.

Pruitt, W.O., and Lourence, F.J., 1985. Experiences in lysimetry for ET and surface drag measurements 51 69 In: Advances in evapotranspiration: Proc. National Conf. on Advances in Evapotranspiration. ASCE Publ. No. 14–85. St. Joseph, MI.

Pryor, W.A., 1973. Permeability-porosity patterns and variations in some Holocene sand bodies. *American Association of Petroleum Geologists Bulletin*, 57 (1), pp. 162-191.

Puls, R.W., J.H. Eychaner, and R.M. Powell, 1990. Environmental Research Brief: Colloidal Facilitated Transport of Inorganic Contaminants in Ground Water: Part I. Sampling Considerations; U.S. Environmental Protection Agency, EPA/600/M-90/023, 12 p.

Puls, R.W. and R.M. Powell, 1992. Acquisition of Representative Ground Water Quality Samples for Metals; Ground Water Monitoring Review, Vol. 12, No. 3, pp. 167-176.

Puls, R.W., D.A. Clark, B. Bledsoe, R.M. Powell and C.J. Paul, 1992. Metals in Ground Water: Sampling Artifacts and Reproducibility; Hazardous Waste and Hazardous Materials, Vol. 9, No. 2, pp. 149-162.

Puls, R.W., and M.J. Barcelona, 1996. Ground-Water Issue Paper: Low-Flow (Minimal Drawdown) Ground-Water Sampling Procedures; U.S. Environmental Protection Agency, EPA/540/S-95/504, 12 p.

Puls, R.W., and M.J. Barcelona, 1989a. Filtration of Ground Water Samples for Metals Analysis. Hazardous Waste and Hazardous Materials, v. 6, No. 4.

Puls, R.W., and M.J. Barcelona, 1989b. Ground Water Sampling for Metals Analyses. USEPA Superfund Ground Water Issue, EPA/504/4-89/001, 6 p.

Puri, S., Margat, J., Yurtsever, Y., and B. Wallin, 2006. Aquifer characterization techniques. In: Foster, S. and D.P. Loucks (Eds.), Non-renewable groundwater resources; A guidebook on socially-sustainable management for water-policy makers. IHP-VI, Series on Groundwater No. 10, UNESCO, Paris, pp. 35-47.

Putnam, L.D., Long, A.J., 2007. Analysis of ground-water flow in the Madison aquifer using fluorescent dyes injected in Spring Creek and Rapid Creek near Rapid City, South Dakota, 2003–04: U.S. Geological Survey Scientific Investigations Report 2007–5137, 27 p.

Pyne, R.D.G., 1995. Groundwater Recharge and Wells: A Guide to Aquifer Storage Recovery. Lewis Publishers, Boca Raton, FL, 375 p.

Quinlan, J.F. 1990. Special Problems of Ground-Water Monitoring in Karst Terranes, in D.M. Nielsen and A.I. Johnson, eds., Ground Water and Vadose Zone Monitoring. ASTM STP 1053, American Society for Testing and Materials, Philadelphia, pp. 275-304.

Quinlan, J.F. 1989. Ground-Water Monitoring in Karst Terranes: Recommended Protocols and Implicit Assumptions. USEPA EPA/600/X-89/050, 79 p.

Quinlan, J.F. 1987. Qualitative Water Tracing with Dyes in Karst Terranes, in J.F. Quinlan, ed., Practical Karst Hydrogeology with Emphasis on Ground-Water Monitoring (Course Manual): National Water Well Association, Dublin, Ohio, v. 6, p. E1-E24.

Quinlan, J.F., and E.C. Alexander, Jr. 1987. How Often Should Samples be Taken at Relevant Locations for Reliable Monitoring of Pollutants from an Agricultural, Waste Disposal, or Spill Site in a Karst Terrane? A First Approximation, in B.F. Beck and W.L. Wilson, eds., Proceedings of the 2nd Multidisciplinary Conference on Sinkholes and the Environmental Impacts of Karst, Orlando, Florida, pp. 277-286.

Quinlan, J.F., and R.O. Ewers. 1985. Ground-Water Flow in Limestone Terranes: Strategy Rationale and Procedure for Reliable, Efficient Monitoring of Ground-Water Quality in Karst Areas. Proceedings of the National Symposium and Exposition on Aquifer Restoration and Ground-Water Monitoring (5th, Columbus, Ohio), National Water Well Association, Worthington, Ohio, pp. 197-234

Radovanović, S., 1897. Podzemne vode; izdani, izvori, bunari, terme i mineralne vode (Ground waters; aquifers, springs, wells, thermal and mineral waters; in Serbian). Srpska književna zadruga, v. 42, 152 p.

Rai, D., Sass, B.M., and D.A. Moore, 1987. Chromium (III) hydrolysis constants and solubility of chromium (III) hydroxide. *Inorg. Chem.,* v. 26, pp. 345–349.

Raffensperger, J.P., Baker, A.C., Blomquist, J.D., and Hopple, J.A., 2017, Optimal hydrograph separation using a recursive digital filter constrained by chemical mass balance, with application to selected Chesapeake Bay watersheds: U.S. Geological Survey Scientific Investigations Report 2017–5034, 51 p., https://doi.org/10.3133/sir20175034.

Ransley, T., Radke, B., Feitz, A., Kellett, J., Owens, R., Bell, J. and Stewart, G., 2015. Hydrogeological Atlas of the Great Artesian Basin. Geoscience Australia. Canberra. [available from www.ga.gov.au using catalogue number 79790]

Raucher, R.S., et al., 2005. The Value of Water: Concepts, Estimates, and Applications for Water Managers. American Water Works Association Research Foundation (AwwaRF), Denver, CO, 286 p.

Rawls, W.J., Lajpat, R.A., Brakensiek, D.L., and Shirmohammadi, A., 1993. Infiltration and soil water movement. In: Maidment, D.R. (ed.), Handbook of hydrology. Mc-Graw Hill, Inc., New York, 5.1-5.51.

Reed, M.J. (editor), 1983. Introduction & Summary. Assessment of Low-Temperature Geothermal Resources of the United States-1982. Geological Survey Circular 892, United States Department of the Interior, pp. 31-50.

Rees, T.F., Bright, D.J., Fay, R.G., Christensen, A.H., Anders, R., Baharie, B.S., and M.T Land, 1995. Geohydrology, water quality, and nitrogen geochemistry in the saturated and unsaturated zones beneath various land uses, Riverside and San Bernardino Counties, California, 1991-93. U.S. Geological Survey Water-Resources Investigations Report 94-4127

Reese, R.S., 2002. Inventory and review of aquifer storage and recovery in southern Florida. U.S. Geological Survey Water-Resources Investigations Report 02–4036, Tallahassee, FL, 56 p.

Reichards, E.G., et al., 2003. Geohydrology, Geochemistry, and Ground-Water Simulation-Optimization of the Central and West Coast Basins, Los Angeles County, California. U.S. Geological Survey Water–Resources Investigations Report 03-4065, Sacramento, CA

Renner, J.L., White, D.E., and Williams, D.L, 1975. Hydrothermal Convection Systems. In: White, D.E., and Williams, D.L., (editors), Assessment of Geothermal Resources of the United States—1975. Geological Survey Circular 726, United States Department of the Interior, Washington, D.C., pp. 5-57 p.

Renken, R.A., Dixon, J., Koehmstedt, J., Ishman, S., Lietz, A.C., Marella, R.L., Telis, P., Rogers, J., and Memberg, S., 2005. Impact of Anthropogenic Development on Coastal Ground-Water Hydrology in Southeastern Florida, 1900-2000: Reston, Va., U.S. Geological Survey Circular 1275, 77 p.

Rehtlane, E.A. and Patton, F.D., 1982. Multiple port piezometers vs. standpipe piezometers: an economic comparison; Proceedings of the Second National Monitoring, National Water Well Association, Worthington, Ohio, pp. 287-295.

Reynolds, O., 1883. An experimental investigation of the circumstances which determine whether the motion of water shall be direct or sinuous, and of the law of resistance in parallel channels. *Proceedings of the Royal Society of London*. **35**(224–226): 84–99

Reynolds, O., 1894. On the dynamical theory of incompressible viscous fluids and the determination of criterion. *Proceedings of the Royal Society of London*. 56(336–339): 40-45

Richards, L.A. 1931. Capillary conduction of liquids through porous mediums. *Physics*, 1:3 18-333.

Risser, D.W., Gburek, W.J. and Folmar, G.J., 2005a. Comparison of methods for estimating ground-water recharge and base flow at a small watershed underlain by fractured bedrock in the eastern United States. U.S. Geological Survey Scientific Investigations Report 2005-5038, Reston, Virginia, various pages.

Risser, D.W., Conger, R.W., Ulrich, J.E. and Asmussen, M.P., 2005b. Estimates of ground-water recharge based on streamflow-hydrograph methods: Pennsylvania. U.S. Geological Survey Open File Report 2005-1333, Reston, Virginia, 30 p.

Rivet, M., Drewes, J., Barrett, M., Chilton, J., Appleyard, S., Dieter, H.H., Wauchope, D., Fastner, J., Schmoll, O., and G. Howard, 2006. Chemicals: health relevance, transport and attenuation. In: Schmol, O., Howard, G., Chilton, J., and Fastner, R. (eds.), Protecting Groundwater for Health: Managing the Quality of Drinking-water Sources. IWA Publishing, London, UK, pp. 81-137.

Robertson, F.N., 1975. Hexavalent chromium in the groundwater in the Paradise Valley, Arizona, *Ground Water,* v. 13, p. 516–527.

Robson, S.G., and E. R. Banta, 1995. Rio Grande aquifer system. In: Ground Water Atlas of the United States, Arizona, Colorado, New Mexico, Utah, HA 730-C.

Rogers, P., and Hall, A.W., 2003. Effective water governance. TEC Background Papers No. 7, Global Water Partnership Technical Committee (TEC), Global Water Partnership, Stockholm, Sweden, 44 p.

Ronen, D., Sorek, S. and Gilron, J., 2011. Rationales behind Irrationality of Decision Making in Groundwater Quality Management. Ground Water. doi:10.1111/j.1745-6584.2011.00823.x

Rorabaugh, M.I., 1964. Estimating changes in bank storage and g round-water contribution to streamflow. Extract of publication no. 63 of the I.A.S.H. Symposium Surface Waters, p. 432-441.

Rorabaugh, M.I., 1953. Graphical and theoretical analysis of step-drawdown test of artesian well. *Proc. Am. Soc. Civi Eng*., v 79, separate no. 362, 23 p.

Roscoe Moss Company, 1990. Handbook of Ground Water Development. John Wiley & Sons, New York, 493 p.

Rosenau, J.C., Faulkner, G.L., Hendry, C.W. Jr., and Hull, R.W., 1977. Springs of Florida. Geological Bulletin No. 31, revised, Florida Geological Survey, Tallahassee, Florida.

Rosenshein, J.S., and Hickey, J.J., 1977. Storage of treated sewage effluent and storm water in a saline aquifer, Pinellas Peninsula, Florida. Ground Water, vol. 15, no. 4, pp. 289–293

Rostad, K., 2002. Fate of disinfection by-products in the subsurface. In: U.S. Geological Survey Artificial Recharge Workshop Proceedings, April 2–4, 2002, Sacramento, CA, Aiken, G.R., and Kuniansky, E.L., editors. U.S. Geological Survey Open-File Report 02–89, pp. 27–30.

Rowe, G.L.Jr., Shapiro, S.D., and Schlosser, P., 1999. Ground-water age and water-quality trends in a Buried-Valley aquifer, Dayton area, Southwestern Ohio. U.S. Geological Survey Water-Resources Investigations Report 99-4113. Columbus, Ohio, 81 p.

Ruda, T., and Farrar, J., 2006. Environmental Drilling for Soil Sampling, Rock Coring, Borehole Logging, and Monitoring Well Installation. In: Nielsen, D.M. (editor), Practical Handbook of Environmental Site Characterization and Ground-Water Monitoring, Second Edition. CRC Taylor & Francis, Boca Raton, FL, pp. 297-344.

Runnells, D.D., T.A. Shepherd, and E.E. Angino. 1992. Metals in water: Determining natural background concentrations in mineralized areas. *Envir. Sci. Technol*. 26(12):2316-2322.

Rutledge, A.T., 1993. Computer programs for describing the recession of ground-water discharge and for estimating mean ground-water recharge and discharge from streamflow records. U.S. Geological Survey Water-Resources Investigations Report 93-4121, 45 p.

Rutledge, A.T., 1998. Computer programs for describing the recession of ground-water discharge and for estimating mean ground-water recharge and discharge from streamflow records – update. U.S. Geological Survey Water-Resources Investigations Report 98-4148, 43 p.

Rutledge, A.T., 2000, Considerations for use of the RORA program to estimate ground-water recharge from streamflow records. U.S. Geological Survey Open-File Report 00-156, Reston, Virginia, 44 p.

Rügner, H., and Bittens, M., 2006. Revitalization of contaminated land and groundwater at megasites; SAFIRA II Research Program 2006 – 2012, UFZ Center for Environmental Research Leipzig-Halle GmbH, Germany.

Ryan, S., 2010. Dense Nonaqueous Phase Liquid Cleanup: Accomplishments at Twelve NPL Sites. National Network of Environmental Management Studies Fellow. Published by the U.S. EPA on-line at http://cluin.org, 84 p.

Salem, O. and P. Pallas, 2001. The Nubian Sandstone Aquifer System (NSAS). In: Puri *et al.* (eds.), Internationally shared (transboundary) aquifer resources management: their significance and sustainable management; A framework document. IHP-VI, Series on Groundwater 1, IHP Non Serial Publications in Hydrology, UNESCO, Paris, pp. 41-44.

Salminen, R., and V. Gregorauskiene. 2000. Considerations regarding the definition of a geochemical baseline of elements in the surficial materials in areas differing in basic geology. *Appl. Geochem*. 15:647-653.

References and Select Readings

Salminen, R. and T. Tarvainen. 1997. The problem of defining geochemical baselines: case study of selected elements and geological materials in Finland. *J. Geochem. Explor*. 60:91-98.

Sander, R, 1999. Compilation of Henry's Law constants for inorganic and organic species of potential importance in environmental chemistry (Version 3). Air Chemistry Department, Max-Planck Institute of Chemistry, Mainz, Germany.

Scanlon, B.R., Healy, R.W., and Cook, P.G., 2002. Choosing appropriate techniques for quantifying groundwater recharge. *Hydrogeology Journal,* v. 10, no. 1, pp. 18–39.

Schaap, M.G., F.J. Leij, and M.Th. van Genuchten, 2001. Rosetta: a computer program for estimating soil hydraulic parameters with hierarchical pedotransfer functions. *Journal of Hydrology*, 251:163-176

Schendler, A., and Udall, R., 2005. LEED is Broken; Let's Fix It. *Grist*, October 26, 2005.

Scherer, T., Carroll, N., Frankenberger, J., Jones, D., and Powell, G.M., 2009. Private Water Systems Handbook. Midwest Plan Service, Iowa State University, Ames, IA, MWPS 14, 144 p.

Schwarzenbach, R.P., Gschwend, P.M., and Imboden, D.M., 2003. Environmental Organic Chemistry, 2nd ed. Wiley Interscience, Hoboken, NJ

Scott, T.M., Means, G.H., Meegan, R.P., Means, R.C., Upchurch, S.B., Copeland, R.E., Jones, J., Roberts, T., and A. Willet, 2004. Springs of Florida. Florida Geological Survey Bulletin No. 66, Version 1.1, Tallahassee, Florida, 658 p.

Serne, R.J. et al., 2002. Characterization of vadose zone sediment: borehole 299-W23-19 [SX-115] in the S-SX Waste Management Area. PNNL-13757-2, Pacific Northwest National Laboratory, Richland, Washington.

Shapiro, A. M., 2001, Characterizing Ground-Water Chemistry and Hydraulic Properties of Fractured Rock Aquifers Using the Multifunction Bedrock-Aquifer Transportable Testing Tool (BAT[3]): *U.S. Geological Survey Fact Sheet* FS-075-01, 4 p.

Shapiro, A.M. and Greene, E.A., 1995, Interpretation of prematurely terminated air-pressurized slug tests. *Ground Water*, v. 33, No. 5, 539-546.

Sheets, R.A., Bair, E.S., and Rowe, G.L., 1998. Use of $^3H/^3He$ ages to evaluate and improve groundwater flow models in a complex buried-valley aquifer. *Water Resources Research*, v. 34, no. 5, p. 1,077–1,089.

Shiklomanov, I. A., editor, 1999. World water resources: Modern assessment and outlook for the 21st century. (Summary of: World water resources at the beginning of the 21st century; prepared in the framework of the IHP UNESCO). Federal Service of Russia for Hydrometeorology & Environment Monitoring, State Hydrological Institute, St. Petersburg. Available at: http://espejo.unesco.org.uy/index.html).

Shook, G.M., Ansley, S.L., and Wylie, A., 2004. Tracers and Tracer Testing: Design, Implementation, and Interpretation Methods. Idaho National Engineering and Environmental Laboratory, Bechtel BWXT Idaho, LLC. INEEL/EXT-03-01466, Idaho Falls, Idaho, 30 p.

Showcaves, 2022. http://www.showcaves.com/english/fr/springs/Vaucluse.html, accessed in May 2022.

Shuttleworth, W.J., 1993. Evaporation. In: Maidment, D.R. (ed.), Handbook of hydrology. Mc-Graw Hill, Inc., New York, 4.1-4.53.

Simmons, C.T., et al., 2007. Variable density groundwater flow: From modelling to applications. In: G-WADI 2007. International Training Workshop on Groundwater Modeling in Arid and Semi-arid Areas, Course Material, 11-15 June 2007, Lanzhou, China, UNESCO, Asian G-WADI Network, Cold and Arid Regions Environmental Research Institute, Chinese Academy of Sciences, pp. 85-152.

Simon, J. A., 2011. Editor's Perspective—US Sustainable Remediation Forum Pushes Forward with Guidance on the State of the Practice. Remediation Journal, 21:1–5. doi:10.1002/rem.20287.

Singh, V.P., 1993. Elementary hydrology. Prentice Hall, Englewood Cliffs, New Jersey, 973 p.

Skinner, B.H., and Shaw, R.J., 1992. Technical Brief No.34: Protecting Springs - An Alternative to Spring Boxes, *Waterlines: Journal of Appropriate Technologies for Water Supply and Sanitation*, 11(2), pp.15-18, ISSN: 0262-8104.

Slichter, C.S., 1902. The motions of underground waters. U.S. Geological Survey WaterSupply and Irrigation Papers 67, Washington, DC, 106 p.

Slichter, C.S., 1905. Field measurements of the rate of movement of underground waters. U.S. Geological Survey Water-Supply and Irrigation Paper 140, Series 0, Underground waters, 43, Washington, D.C., 122 p.

Smart, C.C., 1983. Hydrology of a glacierized alpine karst. Ph.D. thesis, McMaster University, Hamilton, Ontario, 343 p.

Smart, C. C., 1988. Artificial tracer techniques for the determination of the structure of conduit aquifers. *Ground Water*, 26: 445–453.

Smart, C. C., and Karunaratne, K. C., 2001. Statistical characterization of natural background fluorescence as an aid to dye tracer test design. In: Beck, B.F., and Herring, J.G. (eds.), Proceedings of the Eighth Multidisciplinary Conference on Sinkholes and the Engineering and Environmental Impacts of Karst, Geotechnical and Environmental Applications of Karst Geology and Hydrology, Balkema, Rotterdam, the Netherlands, pp. 271–276.

Smart, C. C, and Simpson, B., 2001. An evaluation of the performance of activated charcoal in detection of fluorescent compounds in the environment. In: Beck, B.F., and Herring, J.G. (eds.), Proceedings of the Eighth Multidisciplinary Conference on Sinkholes and the Engineering and Environmental Impacts of Karst, Geotechnical and Environmental Applications of Karst Geology and Hydrology, Balkema, Rotterdam, the Netherlands, pp. 265–270

Smerdon, B.D., Ransley, T.R., Radke, B.M., and Kellett, J.R., 2012. Water resource assessment for the Great Artesian Basin. A report to the Australian Government from the CSIRO Great Artesian Basin Water Resource Assessment. CSIRO Water for a Healthy Country Flagship, Australia.

Smith, D.B. 2003. Verbal communication. U.S. Dept. of Interior, U.S. Geological Survey, Denver CO. dsmith@usgs.gov.

Smith, R.L., and Shaw, H.R., 1975. Igneous-Related geothermal Systems. In: White, D.E., and Williams, D.L., (editors), Assessment of Geothermal Resources of the United States—1975. Geological Survey Circular 726, United States Department of the Interior, Washington, D.C., pp. 58-83 p.

Snow, D.T., 1968. Rock fracture spacings, openings, and porosities. *J. Soil Mech*. Found. Div., Amer. Soc. Civil Engineers 94, pp. 73-91

Sophocleous, M., 2004. Ground-water recharge and water budgets of the Kansas High Plains and related aquifers. Kansas Geological Survey Bulletin 249, Kansas Geological Survey, the University of Kansas, Lawrence, Kansas, 102 p.

Sorey, M.L., Natheson, M., and Smith, C., 1983a. Methods for Assessing Low-Temperature Geothermal Resources. In: Reed, M.J. (editor), Assessment of Low-Temperature Geothermal Resources of the United States-1982. Geological Survey Circular 892, United States Department of the Interior, pp. 17-30.

Sorey, M.L., Reed, M.J., Foley, D., and Renner, J.L., 1983b. Low-Temperature Geothermal Resources in the Central and Eastern United States. In: Reed, M.J. (editor), Assessment of Low-Temperature Geothermal Resources of the United States-1982. Geological Survey Circular 892, United States Department of the Interior, pp. 51-65.

Sposito, G. 2016. The Chemistry of Soils, 3rd Edition. Oxford University Press, New York, 272 p.

St. Johns River Water Management District (SJRWMD), 2022. Silver Springs. https://www.sjrwmd.com/minimumflowsandlevels/silver-springs/

References and Select Readings

Stallman, R.W., 1971. Aquifer-test, design, observation and data-analysis: U.S. Geological Survey Techniques of Water-Resources Investigations, book 3, chap. B1, 26 p.

Stanin, F.T., 2005. The transport and fate of chromium (VI) in the environment. In: J. Guertin, J.A. Jacobs, and C.P. Avakian (eds.), Chromium(VI) Handbook, CRC Press, Boca Raton, Florida, pp. 165-214.

Stearns, N.D., Stearns, H.T., and G.A. Waring, 1937. Thermal springs in the United States. U.S. Geological Survey Water-Supply Paper 679-B, Washington, D.C.

Stephens, D.B., et al., 1998. A comparison of estimated and calculated effective porosity. *Hydrogeology Journal*, v. 6, pp. 156-165.

Stevanovic, Z., 2010. Utilization and regulation of springs. Chapter 9. In: Kresic, N., and Stevanovic, Z. (eds.), 2010. Groundwater Hydrology of Springs; Engineering, Theory, Management, and Sustainability. Elsevier, Butterworth-Heinemann, Amsterdam, pp. 339-388.

Stevanovic, Z., 2018. Global distribution and use of water from karst aquifers. Geological Society, London, Special Publications, 466, 217-236, 4 January 2018, https://doi.org/10.1144/SP466.17

Stowe, S., 2009. Collector Wells. In: Kresic, N., Groundwater Resources. Sustainability, Management, and Restoration. McGraw Hill, New York, pp. 515-522

Strack, O.D.L., 1976. A single-potential solution for regional interface problems in coastal aquifers. *Water Resources Research*, v. 12, no. 6, pp. 1165-1174.

Strahler, A.N., and Strahler, A.H., 1978. Modern physical geography. John Wiley & Sons, New York, 502 p.

Stumm, W. 1992. Chemistry of the solid-water interface: Processes at the mineral-water and particle-water interface. Wiley Inter-Science, New York, 428 p.

Sukhodolov, A. N., Nikora, V. I., Rowioski, P. M., and Czernuszenko, W., 1997. A case study of longitudinal dispersion in small lowland rivers. *Water Environ Resour*, 97: 1246–1253

SURF (U.S. Sustainable Remediation Forum), 2009. Sustainable Remediation White Paper—Integrating Sustainable Principles, Practices, and Metrics into Remediation Projects. Remediation Journal, 19:5–114. doi:10.1002/rem.20210

Sutherland, A.B., Freese, R., Slater J.B., Gordu, F., Di, J., and Hall, G.B., 2017. Minimum Flows Determination for Silver Springs, Marion County, Florida. Technical Publication SJ2017-2. Bureau of Resource Evaluation and Modeling, St. Johns River Water Management District, Palatka, Florida, 138 p. + Appendices

Swezey, C.S., Haynes, J.T., Lucas, P.C., and R.A. Lambert, 2017. Geologic controls on cave development in Burnsville Cove, Bath and Highland Counties, Virginia. In: Bailey, C.M., Shelley, J. (Eds), From the Blue Ridge to the Beach: Geological Field Excursions across Virginia. The Geological Society of America Field Guide 47, pp. 89-123

Szabo, Z., Rice, D.E., Plummer, L.N., Busenberg, E., Drenkard, S., and Schlosser, P., 1996. Age dating of shallow groundwater with chlorofluorocarbons, tritium/helium-3, and flowpath analyses, southern New Jersey coastal plain. *Water Resources Research*, v. 32, pp. 1,023–1,038.

Šimůnek, J., Šejna, M., and van Genuchten, M.Th., 1999. The Hydrus-2D software package for simulating the two-dimensional movement of water, heat, and multiple solutes in variably-saturated media, Version 2.0. U.S. Salinity Laboratory, U.S. Department of Agriculture, Riverside, California, 227 p.

Šimůnek, J., van Genuchten, M.Th., and M. Šejna, 2022. The HYDRUS Software Package for Simulating One-, Two-, and Three-Dimensional Movement of Water, Heat, and Multiple Solutes in Variably-Saturated Porous Media, Technical Manual II, Hydrus 2D/3D, Version 5.x, PC Progress, Prague, Czech Republic, 283 p.

Tai, D.Y., K.S. Turner and L.A. Garcia, 1991. The Use of a Standpipe to Evaluate Ground Water Samplers. *Ground-Water Monitoring Review*, Winter, pp. 125-132

Taylor, C.J. and Alley, W.M., 2001. Ground-water-level monitoring and the importance of long-term water-level data. U.S. Geological Survey Circular 1217, Denver, CO, 68 p.

Taylor, C.J., and E.A. Greene, 2008. Hydrogeologic Characterization and Methods Used in the Investigation of Karst Hydrology. Chapter 3 of Rosenberry, D.O., and J.W. LaBaugh (eds.), Field Techniques for Estimating Water Fluxes Between Surface Water and Ground Water, U.S. Geological Survey Techniques and Methods 4–D2, pp. 75-114.

Teeple, A.P., Kress, W.H., Cannia, J.C., and Ball, L.B., 2009. Geophysical characterization of the Quaternary-Cretaceous contact using surface resistivity methods in Franklin and Webster Counties, south-central Nebraska: U.S. Geological Survey Scientific Investigations Report 2009–5092, 35 p.

The California Environmental Protection Agency (Cal/EPA), 1995. Drilling, Coring, Sampling and Logging at Hazardous Substance Release Sites. Guidance Manual for Ground Water Investigations. 27 p.

The U.S. Salinity Laboratory Staff, 1954. Diagnosis and improvement of saline and alkali soils. U.S. Department of Agriculture Handbook 60, 160 p.

Theis, C.V., 1935. The lowering of the piezometric surface and the rate and discharge of a well using ground-water storage. *Transactions, American Geophysical Union*, Vol. 16, p. 519-524.

Thiem, G., 1906. Hydrologische methoden. Leipzig: Gebhardt, 56 p.

Thornthwaite, C.W., 1946. The moisture factor in climate. *Trans. Am. Geophys. Union*, vol. 27, pp. 41-48.

Thornthwaite, C.W., 1948. An approach toward a rational classification of climate. *The Geological Review*, January, pp. 55-94.

Tiemann, M., 1996. 91041: Safe Drinking Water Act: Implementation and Reauthorization. National Council for Science and the Environment, Congressional Research Service Reports.

Toze, S., and Hanna. J., 2002. The Survival Potential of Enteric Microbial Pathogens in a Reclaimed Water ASR Project. In: Management of Aquifer Recharge for Sustainability. A. A. Balkems Publishers, Lisse, the Netherlands, pp. 139–142

Trapp, H. Jr. and M.A. Horn, 1997. Delaware, Maryland, New Jersey, North Carolina, Pennsylvania, Virginia, West Virginia. Ground Water Atlas of the United States, United States Geological Survey, HA 730-L.

Trček, B., and Zojer, H., 2010. Recharge of Springs. In: Kresic, N., and Stevanovic, Z. (eds.), Groundwater Hydrology of Springs; Engineering, Theory, Management and Sustainability. Elsevier, New York, pp. 87-127.

Tuinhof, A., Dumars, C., Foster, S., Kemper, K., Garduño, H., and Nanni, M., 2002-2005a. Groundwater resource management; an introduction to its scope and practice. Sustainable Groundwater Management: Concepts and Tools, Briefing Note Series Note 1, GW MATE (Groundwater Management Advisory Team), The World Bank, Washington, D.C., 6 p.

Tuinhof, A., Foster, S., Kemper, K., Garduño, H., and Nanni, M., 2002-2005b. Groundwater monitoring requirements for managing aquifer response and quality threats. Sustainable Groundwater Management: Concepts and Tools, Briefing Note Series Note 9, GW MATE (Groundwater Management Advisory Team), The World Bank, Washington, D.C., 10 p.

UNESCO (United Nations Educational, Scientific and Cultural Organization with WWAP-World Water Assessment Program), 2003. Water for people, water for life: The UN world water development report. UNESCO Publishing and Berghahn Books, Barcelona.

UNESCO, 2004. Submarine groundwater discharge. Management implications, measurements and effects. IHP-VI, Series on Groundwater No. 5, IOC Manuals and Guides No. 44, Paris, 35 p.

UNESCO, 2006. Recharge systems for protecting and enhancing groundwater resources. Proceedings of the 5th International Symposium on Management of Aquifer Recharge ISMAR5, Berlin, Germany, 11–16 June 2005 United Nations Educational, Scientific and Cultural Organization, Paris, France, 913 p.

UNEP (United Nations Environment Programme), 2007. Vital water graphics. An overview of the state of the World's fresh and marine waters.

USACE (U.S. Army Corps of Engineers), 1984. Grouting technology. Engineer Manual 110-2-3506, Washington, DC.

USACE, 1995. Engineering and design: Chemical grouting. Engineer Manual 110-2-3500, Washington, DC.

USACE, 1999. Engineering and design: Multi-phase extraction. Engineering Manual 1110-1-4010, Washington, DC.

USACE, 1999a. Groundwater hydrology. Engineer Manual 1110-2-1421, Washington, D.C., var. pages.

USACE, 2006. Design: In situ thermal remediation. UFC 3-280-05. Unified Facilities Criteria (UFC). U.S. Army Corps of Engineers, Naval Facilities Engineering Command (NAVFAC), Air Force Civil Engineer Support Agency (AFCESA).

USACE, 2008. Engineering and design; In-situ air sparging. Manual No. 1110-1-4005, Washington, DC, various pages.

USAID (United States Agency for International Development), 1982. WFTW (Water for the World), Constructing Structures for Springs. Technical Note No. RWS. 1.C.1., Washington, D.C. Available at www.sswm.info/node/4384

USBR (United States Bureau of Reclamation), 1977. Ground water manual. U.S. Department of the Interior, Bureau of Reclamation, Washington, D.C., 480 p.

USDA (United States Department of Agriculture), 2022. Cash Receipts by Commodity, State Ranking, 2021 Nominal (Current Dollars). Available at: https://data.ers.usda.gov/reports.aspx?ID=17844

USDA (United States Department of Agriculture), Soil Science Division Staff. 2017. Soil survey manual. C. Ditzler, K. Scheffe, and H.C. Monger (eds.). Handbook 18. Government Printing Office, Washington, D.C. Available at http://soils.usda.gov/technical/manual/

USDA (United States Department of Agriculture), 2013. Farm and Ranch Irrigation Survey (FRIS), Table 36.

USDA, 2009. Small Watershed Hydrology. WinTR–55 User Guide. United States Department of Agriculture, Natural Resources Conservation Service, 47 p. + Appendices; User Guide and Computer Program available at https://www.nrcs.usda.gov/wps/portal/nrcs/detailfull/national/water/?cid=stelprdb1042901

U.S. EPA (United States Environmental Protection Agency), 1975. Manual of Water Well Construction Practices. EPA-570/9-75-001. Office of Water Supply, Washington, DC, 156 p.

U.S. EPA, 1977. The report to Congress: waste disposal practices and their effects on ground-water. EPA 570977001, 531 p.

U.S. EPA, 1985. Guidelines for Remedial Investigations under CERCLA. EPA/540/G-85/002, Office of Solid Waste and Emergency Response, Washington, D.C.

U.S. EPA, 1986. RCRA Ground-water Monitoring Technical Enforcement Guidance Document. Office of Waste Programs Enforcement, Office of Solid Waste and Emergency Response, OSWER-9550.1.

U.S. EPA, 1989. Health and Safety Audit Guidelines. EPA/540/G-89/010, Office of Solid Waste and Emergency Response, Washington, D.C.

U.S. EPA, 1991. Manual of Small Public Water Supply Systems. EPA 570/9-91-003. Office of Water, Washington, DC, 211 p.

U.S. EPA, 1991a. Seminar Publication -- Site Characterization for Subsurface Remediation. EPA/625/4-91/026, 259 p.

U.S. EPA, 1991b. Handbook – Ground Water, Volume II: Methodology. EPA/625/6- 90/016b, 144 p.

U.S. EPA, 1991c. Manual of Individual and Non-Public Water Supply Systems, Office of Water, WH-550, EPA 570/9-91-004, Washington, DC.

U.S. EPA, 1992. RCRA Ground-Water Monitoring. Draft Technical Guidance. Office of Solid Waste, Washington, D.C.

U.S. EPA, 1993. Guidance for Evaluating the Technical Impracticability of Ground-Water Restoration, OWSER Directive 9234.2-5, EPA/540-R-93-080, September 1993.

U.S. EPA, 1993a. Subsurface Characterization and Monitoring Techniques: A Desk Reference Guide: Volume I: Solids and Ground Water Appendices A and B; EPA/625/R-93/003a

U.S. EPA, 1993b. Use of Airborne, Surface, and Borehole Geophysical Techniques at Contaminated Sites: A Reference Guide. EPA/625/R-92/007, Office of Research and Development, Washington, D.C.

U.S. EPA, 1994. EPA Superfund Record of Decision: Southern California Edison, Visalia Pole Yard Superfund Site, Visalia, California. EPA ID: CAD980816466.

U.S. EPA, 1995. Use of Risk-Based Decision Making in UST Corrective Action Programs, OWSER Directive 9610.17, Office of Solid Waste and Emergency Response, 20 p.

U.S. EPA, 1995a. Ground Water Sampling - A Workshop Summary, Dallas, Texas, November 30-December 2, 1993; EPA/600/R94/205, 146 p.

U.S. EPA, 1996. Presumptive Response Strategy and Ex-Situ Treatment Technologies for Contaminated Groundwater at CERCLA Sites. OSWER Directive 9283.1-12.

U.S. EPA, 1996a. A Citizen's guide to bioremediation. EPA 542-F-96-007, Solid Waste and Emergency Response, 4 p.

U.S. EPA, 1996b. A Citizen's guide to natural attenuation. EPA 542-F-96-015, Solid Waste and Emergency Response, 4 p.

U.S. EPA, 1996c. Soil screening guidance: User's guide, Second edition. Publication 9355.4-23, Office of Emergency and Remedial Response, Washington, D.C.

U.S. EPA, 1996d. Pump-and-Treat Ground-Water Remediation: A Guide for Decision Makers and Practitioners. Office of Research and Development, EPA/625/R-95/005, Washington, DC, 90 p.

U.S. EPA, 1997. Treatment technology performance and cost data for remediation of wood preserving sites. Washington, DC, EPA Office of Research and Development. EPA/625/R-97/009

U.S. EPA, 1997a. Analysis of Selected Enhancements for Soil Vapor Extraction. OSWER. September. EPA 542-R-97-007.

U.S. EPA, 1997b. Presumptive Remedy: Supplemental Bulletin Multi-Phase Extraction (MPE) Technology for VOCs in Soil and Groundwater. OSWER. April. EPA 540-F-97-004.

U.S. EPA, 1998a. Evaluation of subsurface engineered barriers at waste sites. EPA 542-R-98- 005, Office of Solid Waste and Emergency Response, U.S. Environmental Protection Agency, Washington, DC, 102 p. + appendices.

U.S. EPA, 1998b. Permeable reactive barrier technologies for contaminant remediation. EPA/600/R-98/125, Office of Solid Waste and Emergency Response, U.S. Environmental Protection Agency, Washington, DC, 94 p.

U.S. EPA and NARUC (National Association of Regulatory Utility Commissioners), 1999. Consolidate water rates: Issues and practices in single-tariff pricing. U.S. Environmental Protection Agency, Office of Water, Washington, DC., 110 p.

U.S. EPA, 1999a. Understanding variation in partition coefficient, Kd, values; Volume I: The Kd model, methods of measurements, and application of chemical reaction codes. EPA 402-R-99-004A, U.S. Environmental Protection Agency, Office of Air and Radiation, Washington, D.C.

U.S. EPA, 1999b. Understanding variation in partition coefficient, Kd, values; Volume II: Review of geochemistry and available Kd values for cadmium, cesium, chromium, lead, plutonium, radon, strontium, thorium, tritium (^{3}H), and uranium. EPA 402-R-99-004B, U.S. Environmental Protection Agency, Office of Air and Radiation, Washington, D.C.

U.S. EPA, 1999c. Use of monitored natural attenuation at Superfund, RCRA corrective action, and underground storage tank sites. OSWER Directive 9200.4-17P, April 21, 1999, 32 p.

U.S. EPA, 1999d. A Guide to Preparing Superfund Proposed Plans, Records of Decision, and Other Remedy Selection Decision Documents. EPA 540-R-98-031

U.S. EPA, 1999e. EPA Superfund Record of Decision: MONTROSE CHEMICAL CORP. and DEL AMO. EPA ID: CAD008242711 and CAD029544731 OU(s) 03 & 03, LOS ANGELES, CA 03/30/1999. Dual Site Groundwater Operable Unit. II: Decision Summary, page 11-7. EPA/ROD/R09-99/035

U.S. EPA, 2000. Engineered Approaches to *In Situ* Bioremediation of Chlorinated Solvents: Fundamentals and Field Applications. EPA 542-R-00-008

U.S. EPA, 2000a. National Water Quality Inventory; 1998 Report to Congress; Ground Water and Drinking Water Chapters. EPA 816-R-00-013, Office of Water, Washington, DC.

U.S. EPA, 2001. Use of Bioremediation at Superfund Sites. EPA 542-R-01-019

U.S. EPA, 2002. Guidance on Choosing a Sampling Design for Environmental Data Collection for Use in Developing a Quality Assurance Plan. EPA QA/G-5S. EPA/240/R-02/005, Office of Environmental Information, Washington, D.C., 168 p.

U.S. EPA, 2004. In situ thermal treatment of chlorinated solvents; Fundamentals and field applications. EPA 542/R-04/010. Office of Solid Waste and Emergency Response, Washington, DC.

U.S. EPA, 2004a. Guidelines for water reuse. EPA/625/R-04/108, U.S. Environmental Protection Agency, Office of Wastewater Management, Office of Water, Washington, DC, 460 p.

U.S. EPA, 2005. Groundwater Sampling and Monitoring with Direct Push Technologies. OSWER No. 9200.1-51. EPA 540/R-04/005, 67 p.

U.S. EPA, 2006. In Situ Treatment Technologies for Contaminated Soil: Engineering Forum Issue Paper. EPA 542-F-06-013

U.S. EPA, 2007. Terms of environment: Glossary, abbreviations, and acronyms. http://www.epa.gov/terms/

U.S. EPA, 2008. A Systematic Approach for Evaluation of Capture Zones at Pump and Treat Systems; Final Project Report. Office of Research and Development, EPA 600/R-08/003, Washington, DC, 38 p. + appendices.

U.S. EPA, 2009a. DNAPL Remediation: Selected Projects Where Regulatory Closure Goals Have Been Achieved. Office of Solid Waste and Emergency Response, EPA 542/R-09/008, 52 p. Available at http://www.clu-in.org/s.focus/c/pub/i/1719/. Accessed July 25, 2011.

U.S.EPA, 2009b. Amendment #2 to the Record of Decision for the Commencement Bay–South Tacoma Channel Superfund Site, Operable Unit 1, Well 12A, EPA Region 10.

U.S. EPA, 2009c. Final Close Out Report: Southern California Edison Visalia Pole Yard Superfund Site, Visalia, Tulare County, California. EPA Region 9.

U.S. EPA, 2010. Superfund Remedy Report, Thirteenth Edition. Office of Solid Waste and Emergency Response, EPA-542-R-10-004, 36 p. + appendices.

U.S. EPA, 2011b. Green Power Equivalency Calculator Methodologies.
Available at http://www.epa.gov/greenpower/pubs/calcmeth.htm.

U.S. EPA, 2011c. Beneficial Effects of the Superfund Program. Office of Superfund Remediation and Technology Innovation. EPA Contract EP W-07-037.

U.S. EPA, 2011d. US and EU Perspectives on Green and Sustainable Remediation Part 2. CLU-IN Internet Seminar delivered March 15, 2011. https://clu-in.org/conf/tio/grconsoil2_031511/

U.S. EPA, 2011e. Introduction to Green Remediation. Office of Superfund Remediation and Technology Innovation. Quick Reference Fact Sheet. Available at https://www.epa.gov/remedytech/introduction-green-remediation

U.S. EPA, 2015. Use of Monitored Natural Attenuation for Inorganic Contaminants in Groundwater at Superfund Sites. Office of Solid Waste and Emergency Response, Directive 9283.1-36, 56 p. + Appendices

U.S. EPA, 2017. Groundwater Sampling. Operating Procedure, SESDPROC-301-R4. U.S. EPA Region 4, 34 p.

U.S. EPA, 2018. Design and Installation of Monitoring Wells. SESDGUID-101-R2, U.S. EPA Region 4, 33 p.

U.S. EPA, 2020. Superfund Remedy Report, 16th Edition. Office of Land and Emergency Management. EPA-542-R-20-001, 38 p. + Appendices

U.S. EPA, 2022a. http://www.clu-in.org/contaminantfocus/default.focus/sec/arsenic/

U.S. EPA, 2022b. http://www.clu-in.org/contaminantfocus/default.focus/sec/chromium/

U.S. EPA, 2022c. Contaminant Candidate List (CCL) and Regulatory Determination. https://www.epa.gov/ccl/basic-information-ccl-and-regulatory-determination

U.S. EPA, 2022d. Safe Drinking Water Act (SDWA). Available at https://www.epa.gov/sdwa

U.S. EPA, 2022e. Community Guide to Vapor Intrusion Mitigation. EPA-542-F-21-025

USGS (United States Geologic Survey), 1995. Springs of Florida. Fact Sheet FS-151-95, 2 p.

USGS, 2000. Interagency Field Manual for the Collection of Water-Quality Data. In cooperation with the U.S. Environmental Protection Agency. U.S., Geological Survey Open-File Report 00-213, Austin, TX,

USGS, 2004. Natural remediation of arsenic contaminated ground water associated with landfill leachate. U.S. Geological Survey Fact Sheet 2004-3057, 4 p.

USGS, 2004a. Vertical Flowmeter Logging. Office of Ground Water, Branch of Geophysics. Available at: http://water.usgs.gov/ogw/bgas/flowmeter/

USGS, 2005. U.S. Geological Survey Streamgaging. Fact Sheet 2005-3131. Available at: https://pubs.usgs.gov/fs//2005/3131/

USGS, 2007. Water science glossary of terms. http://ga.water.usgs.gov/edu/dictionary.html;

USGS, 2009a. Geysers, Fumaroles, and Hot Springs. http://pubs.usgs.gov/gip/volc/geysers.html

USGS, 2009b. USGS Multimedia Library. http://gallery.usgs.gov/

USGS, 2014. Estimated Use of Water in the United States in 2010. Circular 1405. Available at: https://pubs.er.usgs.gov/publication/cir1405

USGS (United States Geologic Survey), 2016. Groundwater and Drought. Available at: https://water.usgs.gov/ogw/drought/

USGS, 2021. Handheld Thermal Imaging for Groundwater/Surface-water. https://www.usgs.gov/media/galleries/handheld-thermal-imaging-groundwatersurface-water

USGS, 2022a. https://www.usgs.gov/mission-areas/water-resources/science/science-topics/groundwater-aquifers-wells-and-springs

USGS, 2022b. Unsaturated Flow Processes. https://wwwrcamnl.wr.usgs.gov/uzf/

US Forest Service Intermountain Region, 2008. Geologic Points of Interest by Activity; Springs/Falls. http://www.fs.fed.us/r4/resources/geology/geo_points_interest/activities/springs_falls.shtml

References and Select Readings

van der Perk, M., 2006. Soil and water contamination from molecular to catchment scale. Taylor & Francis/Balkema, Leiden, The Netherlands, 389 p.

van der Zaag, P., and Savenije, H.H.G., 2006. Water as an economic good: The value of pricing and the failure of markets. Value of Water Research Report Series No. 19. UNESCO-IHE Institute for Water Education, Delft, the Netherlands, 28 p.

van Genuchten, M.Th. 1980. A closed-form equation for predicting the hydraulic conductivity of unsaturated soils. *Soil Sci. Am. J*. 44:892-898.

van Genuchten, M.Th., Leij, F.J., and S. R. Yates, 1991. The RETC code for quantifying the hydraulic functions of unsaturated soils. EPA/600/2-91/065, Ada, Oklahoma, 83 p.

Vernadsky V.I., 1926. Biosphera (The Biosphere). Nauchnoe khimiko-technicheskoye izdatel'stvo (Scientific Chemico-Technical Publishing), Leningrad, 200 p.

Vernadsky, V.I., 1929. La Biosphere. Félix Alcan, Paris.

Vernadsky, V.I., 1997. The Biosphere. Completed Annotated Edition. A Peter Nevraumont Book. Copernicus/Springer-Verlag, New York, 1997. 192 p.

Vineyard, J.D. and Feder, G.L., 1982. *Springs of Missouri*. Water Resources Report No. 29, Missouri Department of Natural Resources, Division of Geology and Land Survey, 212 p.

Virginia Water Resources Research Center, 1999. A homeowner's guide to the development, maintenance, and protection of springs as a drinking water source. Virginia Polytechnic Institute and State University, Blacksburg, Virginia, 83 p.

Vordzorgbe, S.D., 2003. Managing water risks in Africa. In: Reports and Proceedings of the Pan-African Implementation and Partnership Conference on Water (PANAFCON), December 8–13, 2003, Addis Ababa. UN-Water/Africa, Economic Commission of Africa, Addis Ababa, Ethiopia, pp. 3–27.

VSF-Belgium, 2006. Subsurface Dams: A Simple, Safe and Affordable Technology for Pastoralists. A Manual on Subsurface Dams Construction Based on an Experience of Vétérinaires sans Frontières in Turkana District (Kenya). VSF-Belgium, Brussels, Belgium, 51 p.

Vuković, M., and Soro, A., 1985. Osnovi hidraulike. Drugo izdanje (Fundamentals of Hydraulics. Second Edition; in Serbian). University of Belgrade, School of Mining and Geology, Dept. of Hydrogeology, Belgrade, 232 p.

Walton, W.C., 1962. Selected analytical methods for well and aquifer evaluation. Illinois State Water Survey Bulletin, vol. 49, 81 p.

Water Replenishment District of Southern California (WRD), 2004. Technical Bulletin – An Introduction to the Central and West Coast Groundwater Basins.

Weary, D.J., and Doctor, D.H., 2014, Karst in the United States: A digital map compilation and database: U.S. Geological Survey Open-File Report 2014–1156, 23 p., http://dx.doi.org/10.3133/ofr20141156.

Welch, A.H., *et al.*, 2000. Arsenic in ground water of the United States-- occurrence and geochemistry. *Ground Water* v.38 no.4, p.589-604.

Wenzel, L.K., 1936. The Thiem method for determining permeability of water-bearing materials and its application to the determination of specific yield; results of investigations in the Platte River valley, Nebraska. U.S. Geological Survey Water Supply Paper 679-A, Washington, D.C., 57 p.

Werner, A.D., and Gallagher, M.R., 2006. Characterisation of sea-water intrusion in the Pioneer Valley, Australia using hydrochemistry and three-dimensional numerical modelling. *Hydrogeology Journal,* v. 14, pp. 1452-1469.

Werner, A.D., and Lockington, D.A., 2006. Tidal impacts on riparian salinities near estuaries. *Journal of Hydrology*, v. 328, pp. 511-522.

White, D.E., 1965. Geothermal Energy. Geological Survey Circular 519, United States Department of the Interior, Washington, D.C., 17 p.

White, W.B., 1988. Geomorphology and hydrology of karst terrains. Oxford University Press, New York, 464 p.

White, W.B., 2015. Geology of the Butler Cave–Sinking Creek System. In White, W.B., ed., The Caves of Burnsville Cove, Virginia. Springer International Publishing, Cham, Switzerland, p. 365–384

Whitehead, R.L., 1994. Ground Water Atlas of the United States—Segment 7: Idaho, Oregon, Washington: U.S. Geological Survey Hydrologic Investigations Atlas HA–730–H, 31 p.

Wiedemeier, T. H., et al., 1998. Technical Protocol for Evaluating Natural Attenuation of Chlorinated Solvents in Ground Water. EPA/600/R-98/128, U.S. Environmental Protection Agency, Office of Research and Development, Washington, D.C.

Wiedemeier, T. H., et al., 1999. Technical protocol for implementing intrinsic remediation with long-term monitoring for natural attenuation of fuel contamination dissolved in groundwater; Volume I (Revision 0), Air Force Center for Environmental Excellence (AFCEE), Technology Transfer Division, Brooks Air Force Base, San Antonio, Texas.

Williams, A.P., Cook, B.I., and Smerdon, J.E., 2022. Rapid intensification of the emerging southwestern North American megadrought in 2020–2021. *Nat. Clim. Chang.* **12**, 232–234 (2022). https://doi.org/10.1038/s41558-022-01290-z

Williams, J. H., and Lane, J. W., 1998. Advances in Borehole Geophysics for Ground-Water Investigations: U.S. Geological Survey Fact Sheet 002–98, U.S. Geological Survey, 4p.

Williams, S.D., and Farmer, J.J., 2003. Volatile organic compound data from three karst springs in middle Tennessee, Feb 2000 to May 2001. U.S. Geological Survey Open-File Report 03–355, Nashville, TN, 69 p.

Williams, J.H., Lane, J.W. Jr., Singha, K., and F.P. Haeni, 2002. Application of advanced geophysical logging methods in the characterization of a fractured-sedimentary bedrock aquifer, Ventura County, California. U.S. Geological Survey Water-Resources Investigations Report 00-4083, 28 p.

Williams, L.J., Kath, R.L., Crawford, T.J., and Chapman, M.J., 2005. Influence of geologic setting on ground-water availability in the Lawrenceville area, Gwinnett County, Georgia. U.S. Geological Survey Scientific Investigations Report 2005-5136, Reston, Virginia, 50 p.

Wilson, J. F., Jr, Cobb, E. D., and Kilpatrick, F. A., 1986. Fluorometric procedures for dye tracing. U.S. Geological Survey Techniques of Water Resources Investigations, Reston, VA, Book 3, Chapter A12, 34p

Wilson, J.L. and Guan, H., 2004. Mountain-block hydrology and mountain-front recharge. Preprint of paper to be published in Groundwater recharge in a desert environment: the Southwestern United States, edited by F.M. Phillips, Hogan, J., and B. Scanlon, 2004, American Geophysical Union, Washington, D.C. Accessed on-line September 2007, http://www.utsa.edu/LRSG/Staff/Huade/publications/

Wilson, J.T. et al., 2001. An Evaluation of Borehole Flowmeters Used to Measure Horizontal Ground-Water Flow in Limestones of Indiana, Kentucky, and Tennessee, 1999. U.S. Geological Survey Water-Resources Investigations Report 01-4139, Indianapolis, Indiana, 129 p.

Winpenny, J., 2003. Financing water for all. Report of the World Panel on Financing Water Infrastructure. World Water Council, 3rd World Water Forum, Global Water Partnership, 54 p.

Witherspoon, P.A., 2000. Investigations at Berkeley on fracture flow in rocks: from the parallel plate model to chaotic systems; in: Dynamics of Fluids in Fractured Rock, B. Faybishenko, P.A. Witherspoon and S.M. Benson (eds.), Geophysical Monograph 122, American Geophysical Union, Washington, D.C., p. 1-58.

WMO (World Meteorological Organization), 1997. Comprehensive Assessment of the Freshwater Resources of the World. WMO, Geneva, p.9.

References and Select Readings

Wolff, R.G., 1982. Physical properties of rocks—Porosity, permeability, distribution coefficients, and dispersivity: U.S. Geological Survey Open-File Report 82–166, 118 p.

World Health Organization (WHO), 2022. Drinking-water. https://www.who.int/news-room/fact-sheets/detail/drinking-water

WRI (World Resources Institute), 1998. World resources 1998–99. A guide to the global environment. Oxford University Press, New York, 384 p.

Wyckoff, R. D., Botset, H.G., Muskat, M., and D.W. Reed, 1934. Measurement of permeability of porous media. *Am. Assoc. Petroleum Geologists Bulletin*, 18 (2): 161–190

Xu, M., and Eckstein, Y., 1995. Use of weighted least-squares method in evaluation of the relationship between dispersivity and field scale. *Ground Water*, v. 33, no. 6, pp. 905-908.

Yeskis, D., and Zavala, B., 2002. Ground-Water Sampling Guidelines for Superfund and RCRA Project Managers. Ground Water Forum Issue Paper. EPA 542-S-02-001, 53 p.

Yobbi, D.K., 1997. Simulation of subsurface storage and recovery of effluent using multiple wells, St. Petersburg, Florida. U.S. Geological Survey Water-Resources Investigations Report 97–4024, Tallahassee, FL, 30 p.

Young, H.L., 1992. Summary of ground-water hydrology of the Cambrian-Ordovician aquifer system in the northern midwest, United States. U.S. Geological Survey Professional Paper 1405–A, 55 p.

Young, S.C. et al., 1998. Application of the electromagnetic borehole flowmeter. U.S. Environmental Protection Agency, Office of Research and Development, Washington, D.C., EPA/600/R-98/058, 60 p.

Zaidi, F.K., Ahmed, S., Dewandel, B., and Maréchal, J-C., 2007. Optimizing a piezometric network in the estimation of the groundwater budget: a case study from a crystalline-rock watershed in southern India. *Hydrogeology Journal*, v. 15, pp. 1131-1145.

Zemansky, G.M. and C.D. McElwee, 2005. High-resolution slug testing. *Ground Water*, v. 43, no. 2, pp. 222-230.

Zimmerman, R.W. and I.W. Yeo, 2000. Fluid flow in rock fractures: from the Navier-Stokes equations to cubic law; in: Dynamics of Fluids in Fractured Rock, B. Faybishenko, P.A. Witherspoon and S.M. Benson (eds.), Geophysical Monograph 122, American Geophysical Union, Washington, D.C., p. 213-224.

Hydrogeology 101

APPENDIX A
UNIT CONVERSION TABLES

Length				Area		
To convert from	To	Multiply by		To convert from	To	Multiply by
feet (ft)	meters (m)	0.3048		ft^2	m^2	0.0929
ft	centimeters (cm)	30.48		ft^2	hectares (ha)	9.29×10^{-6}
ft	millimeters (mm)	304.8		ft^2	in^2	144
ft	inches (in)	12		acres	ft^2	43560
ft	yards (yd)	0.333		acres	m^2	4046.86
inches (in)	ft	0.083		acres	ha	0.4047
in	m	0.0254		mi^2	acres	640
in	cm	2.54		mi^2	ft^2	2.788×10^7
miles (mi)	kilometers (km)	1.609		mi^2	ha	259
mi	m	1609		mi^2	km^2	2.59
mi	ft	5280		m^2	ft^2	10.764
mi	yd	1760		m^2	yd^2	1.196
meters (m)	feet (ft)	3.281		m^2	in^2	1550
m	in.	39.37		m^2	cm^2	10000
m	yd	1.094		hectares (ha)	acres	2.471
m	mm	1000		ha	m^2	10000
m	cm	100		km^2	ft^2	1.076×10^7
m	km	0.001		km^2	acres	247.1
kilometers (km)	m	1000		km^2	m^2	1×10^6
km	mi	0.6215		km^2	mi^2	0.3861
km	ft	3281				

Volume		
To convert from	To	Multiply by
ft^3	m^3	0.02832
ft^3	liters (L)	28.32
ft^3	gallons (gal)	7.48
ft^3	in^3	1728
acre-feet	ft^3	4.354×10^4
acre-feet	m^3	1233.48
gallons (gal)	m^3	0.003785
gal	L	3.785
gal	ft^3	0.134
liters (L)	ft^3	0.035
L	gal	0.2642
L	in^3	61.02
L	cm^3	1000
L	milliliter (mL)	1000
cm^3	mL	1
m^3	gal	264.2
m^3	ft^3	35.31
km^3	m^3	1×10^9
km^3	mi^3	0.24

Flow Rate		
To convert from	To	Multiply by
Cubic feet per second (ft^3/s; cfs)	Cubic meters per second (m^3/s)	0.0283
ft^3/s	Liters per second (L/s)	28.32
ft^3/s	Cubic meters per day (m^3/d)	2446.6
ft^3/s	Cubic feet per day (ft^3/d)	8.64x10^4
ft^3/s	Gallons per minute (gal/min)	448.8
ft^3/s	Gallons per day (gal/d)	6.46x10^5
ft^3/s	Acre-feet per day (acre-ft/d)	1.984
Gallons per minute (gal/min)	m^3/s	6.3x10^{-5}
gal/min	m^3/d	5.451
gal/min	L/s	0.0631
gal/min	ft^3/s	0.00223
gal/min	ft^3/d	192.5
gal/min	acre-ft/d	0.00442
Acre-feet per day (acre-ft/d)	m^3/s	0.0143
acre-ft/d	m^3/d	1233.5
acre-ft/d	ft^3/s	0.5042
acre-ft/d	ft^3/d	43,560
Cubic meters per second (m^3/s)	ft^3/s	35.31
m^3/s	ft^3/d	3.051x10^6
m^3/s	gal/min	1.58x10^4
m^3/s	L/s	1000
m^3/s	m^3/d	8.64x10^4
m^3/s	acre-ft/d	70.05
Liters per second (L/s)	ft^3/s	0.0353
L/s	ft^3/d	3051.2
L/s	acre-ft/d	0.070
L/s	gal/min	15.85
L/s	m^3/s	0.001
L/s	m^3/d	86.4

Hydraulic Conductivity, Transmissivity		
To convert from	To	Multiply by
Feet per day (ft/d)	Centimeters per second (cm/s)	3.53×10^{-4}
ft/d	Meters per second (m/s)	3.53×10^{-6}
ft/d	Meters per day (m/d)	0.305
Centimeters per second (cm/s)	ft/d	2835
cm/s	m/d	864
Meters per day (m/d)	ft/d	3.28
m/d	cm/s	0.00116
Square feet per day (ft^2/d)	Square meters per day (m^2/d)	0.0929
ft^2/d	Liters per foot per day (L/m-d)	92.903
ft^2/d	Gallons per foot per day (gal/ft-d)	7.4805
Square meters per day (m^2/d)	ft^2/d	10.764

| Temperature |
|---|
| To Convert Degrees of Fahrenheit (^{o}F) to Degrees of Celsius (^{o}C) |
| $^oC = (^oF - 32)\ /\ 1.8$ |
| To Convert Degrees of Celsius (^{o}C) to Degrees of Fahrenheit (^{o}F) |
| $^oF = {}^oC \times 1.8 + 32$ |

Other Books by Neven Kresic
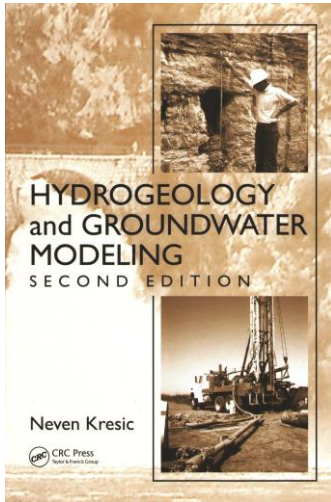
Coupling the basics of hydrogeology with analytical and numerical modeling methods, *Hydrogeology and Groundwater Modeling, Second Edition* provides detail coverage of both theory and practice. Written by a leading hydrogeologist who has consulted for industry and environmental agencies and taught at major universities around the world, this unique books fills a gap in the literature on groundwater studies.

Reflecting nearly ten years of new scholarship since the publication of the bestselling first edition, this second edition is wider in focus with added and updated examples, figures, and problems, yet still provides information in the author's trademark, user-friendly style. No other books offers such carefully selected examples and clear, elegantly explained solutions. The inclusion of step-by-step solutions to real problems builds a knowledge base for understanding and solving groundwater issues.

2007, CRC Press Taylor & Francis Group, ISBN 978-0-8493-3348-4
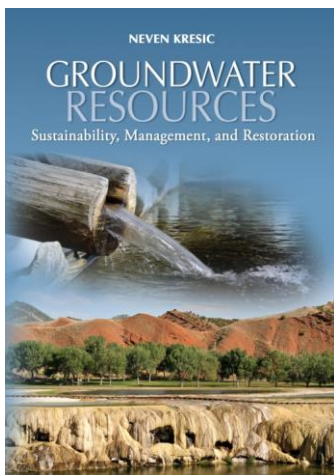
Groundwater Resources is a reliable, one-stop guide providing all the information needed to succeed in groundwater management and development projects. It covers virtually every aspect of the subject, from how to characterize groundwater and evaluate its resources to determining the interactions between surface water and groundwater.

Packed with hundreds of illustrations, this expansive guide reviews both established and innovative aquifer restoration techniques and technologies, including the control and remediation of contaminant sources and groundwater contaminant plumes.

Written by a recognized expert in the field, *Groundwater Resources* provides the last word on the all-important subject of how to evaluate and manage the most precious natural resource.

2009, McGraw-Hill Companies, ISBN 978-0-07-149273-7
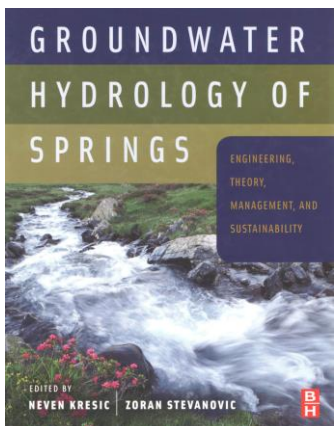
Edited by two world-renowned hydrogeologists, *Groundwater Hydrology of Springs: Engineering, Theory, Management, and Sustainability* will provide civil and environmental engineers with a comprehensive reference for managing and sustaining the water quality of springs. With contributions from experts from around the world, this book covers many of the world's largest springs, providing a unique global perspective on how engineers around the world are utilizing engineering principles for coping with problems such as mismanagement and overexploitation and their impacts on both water quantity and quality. This book will explain the theory and principles of hydrology as they apply to springs and will provide a rare look into the engineering practices used to manage some of the most important springs from around the world.

2010, Elsevier Butterworth-Heinemann, ISBN 978-1-85617-502-9
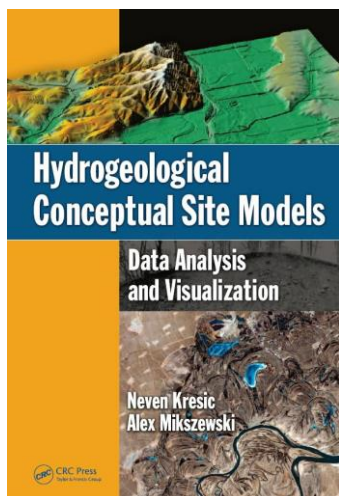
A reference for students, researchers, and environmental professionals, *Hydrogeological Conceptual Site Models: Data Analysis and Visualizations* covers conceptual site model development, spatial data analysis, and visual data presentations for hydrogeology and groundwater remediation. Written by expert practitioners, this **full-color** book demonstrates how fundamental hydrogeological concepts are translated into quantitative, high-resolution graphics. The authors explain analytical methods such as kriging, geospatial processing with GIS, and groundwater modeling through practical real-life examples. Data-rich case studies in groundwater remediation and water resources illustrate the controversial connections between conceptual site models and environmental policy. This visually powerful text contains over 500 illustrations and includes a companion DVD with animations, references, modeling software, and more.

2013, CRC Press Taylor & Francis Group, ISBN 978-1-4398-5222-4
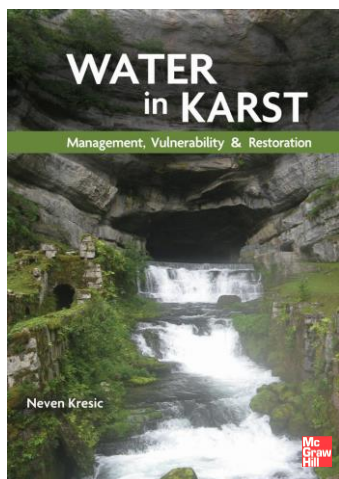
A complete guide to the management and restoration of water in karst environments.

Written by the former co-chair of the Karst Commission of the International Association of Hydrogeologists, this book addresses the unique challenges related to characterization, management, and protection of karst aquifers, which are present on all continents and numerous oceanic islands. *Water in Karst* describes karst hydrogeology and hydrology, surface water-groundwater interactions, site investigation, data collection, delineation of drainage areas, groundwater extraction, regulatory issues, and water vulnerability and restoration. Predictive modeling methods and solutions to restore contamination and overexploitation are included. Photos, diagrams, and an eight-page color insert illustrate the concepts presented in this practical, comprehensive reference.

2013, McGraw-Hill Companies, ISBN 978-0-07-175333-3
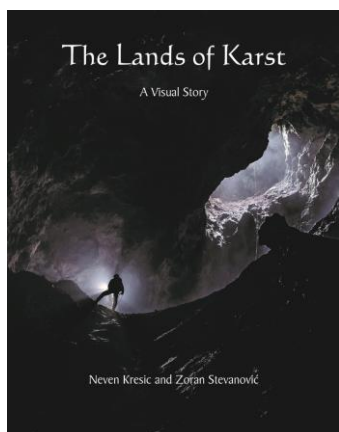
This story of the "Lands of Karst", where the term karst originated, includes hundreds of color photographs contributed by over 70 karst enthusiasts from Slovenia, Croatia, Bosnia and Herzegovina, Montenegro, Serbia, and North Macedonia.

Featured are all types of fascinating landscapes and life: Wild Mountains, Noisy Rivers, Silent Lakes, The Sea, Limestone Walls, Rough Surfaces, Fountains of Life, Windows to Unknown, Magic Chambers, Underground Creatures, Wildlife, and Human Inhabitants in the Past and Present.

The long-awaited visual story, never told before, is finally here.

2021, Blue Ridge Press, ISBN 978-0-578-32045-8

Hydrogeology 101 is a college textbook introducing basic concepts in groundwater science and engineering with 16 lectures, the duration of a typical one or two-semester course at American universities. It covers Introduction to Hydrogeology, Groundwater Use, Principles of Groundwater Flow, Aquifers and Aquitards, Groundwater Recharge and Discharge including Springs, Groundwater Chemistry, Groundwater Contamination and Remediation, Field Investigations, Groundwater in Water Supply, and guest lecture on Groundwater Drought in California by Alex Mikszewski. The textbook includes hundreds of full color illustrations and photographs.

Written by a leading international expert, author of several best-selling books on groundwater, this college textbook is available as pdf file on various web pages, free for download, reposting by academic institutions, and unrestricted dissemination for non-profit uses.

BLUERIDGE.press